NUCLEAR SCIENCE ABSTRACTS

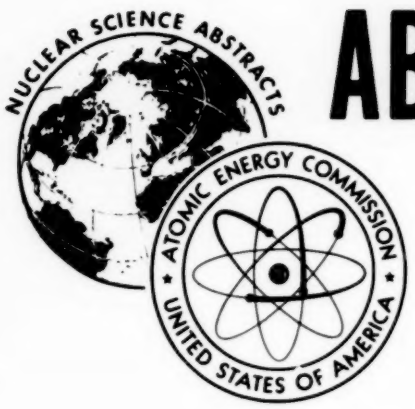

Volume 25 Number 3

Abstracts 4008-6257

February 15, 1971

UNITED STATES ATOMIC ENERGY COMMISSION
Division of Technical Information

REPORT COLLECTIONS IN THE UNITED STATES

The libraries listed below purchase and maintain microfiche collections of USAEC and foreign reports that are abstracted in *NSA*. Their collections also include *NSA* and its indexes, AEC's Technical Progress Reviews, AEC-sponsored translations, conference proceedings published by AEC, and various bibliographic tools. Most of these libraries have microfiche reader-printers or other photocopy facilities with which to reproduce enlarged copies from microfiche. Charges for reproduction services vary.

ALABAMA
Auburn, Auburn University
ALASKA
College, University of Alaska
ARIZONA
Tucson, University of Arizona
ARKANSAS
Fayetteville, University of Arkansas
CALIFORNIA
Davis, University of California
Los Angeles, University of California
COLORADO
Boulder, University of Colorado
DISTRICT OF COLUMBIA
Washington, Library of Congress (by deposit)
FLORIDA
Gainesville, University of Florida
GEORGIA
Atlanta, Georgia Institute of Technology
HAWAII
Honolulu, University of Hawaii
IDAHO
Pocatello, Idaho State University
ILLINOIS
Evanston, Northwestern University
Urbana, University of Illinois
INDIANA
Lafayette, Purdue University
IOWA
Ames, Iowa State University
KANSAS
Manhattan, Kansas State University
KENTUCKY
Lexington, University of Kentucky
Louisville, University of Louisville
LOUISIANA
Baton Rouge, Louisiana State University
New Orleans, Tulane University
MARYLAND
Baltimore, Johns Hopkins University
College Park, University of Maryland
MASSACHUSETTS
Cambridge, Massachusetts Institute of Technology
MICHIGAN
Ann Arbor, University of Michigan
MISSISSIPPI
State College, Mississippi State University
MISSOURI
Kansas City, Linda Hall Library
NEVADA
Las Vegas, University of Nevada
Reno, University of Nevada
NEW JERSEY
Princeton, Princeton University
NEW MEXICO
Albuquerque, University of New Mexico
NEW YORK
Albany, New York State Library
Buffalo, State University of New York at Buffalo
Ithaca, Cornell University
New York, Columbia University
Rochester, University of Rochester
Syracuse, Syracuse University
Troy, Rensselaer Polytechnic Institute
NORTH CAROLINA
Raleigh, North Carolina State University
OHIO
Cincinnati, University of Cincinnati
Columbus, Ohio State University
Toledo, University of Toledo
OKLAHOMA
Norman, University of Oklahoma
PENNSYLVANIA
Philadelphia, University of Pennsylvania
Pittsburgh, Carnegie Library
University Park, Pennsylvania State University
PUERTO RICO
San Juan, University of Puerto Rico
SOUTH CAROLINA
Columbia, University of South Carolina
TENNESSEE
Knoxville, University of Tennessee
Nashville, Joint University Libraries
Oak Ridge, Oak Ridge Associated Universities
TEXAS
Austin, University of Texas
College Station, Texas A & M University
Houston, Rice University
UTAH
Salt Lake City, University of Utah
VIRGINIA
Blacksburg, Virginia Polytechnic Institute
Charlottesville, University of Virginia
WASHINGTON
Pullman, Washington State University
Seattle, University of Washington
WEST VIRGINIA
Morgantown, West Virginia University
WISCONSIN
Madison, University of Wisconsin
WYOMING
Laramie, University of Wyoming

The following governmental and international organizations offer for sale USAEC reports abstracted in *Nuclear Science Abstracts*:

National Technical Information Services, U. S. Department of Commerce
Springfield, Virginia 22151
International Atomic Energy Agency, Vienna, Austria
National Lending Library, Boston Spa, England

XUM

Volume 25, Number 3, February 15, 1971

NUCLEAR SCIENCE ABSTRACTS

A semimonthly publication of the USAEC Division of Technical Information, Edward J. Brunenkant, Director,
Published by the USAEC Division of Technical Information Extension, Robert L. Shannon, Extension Manager.

Nuclear Science Abstracts provides the only comprehensive abstracting and indexing coverage of international nuclear science literature. *Nuclear Science Abstracts* covers scientific and technical reports of the U. S. Atomic Energy Commission and its contractors, other U. S. Government agencies, other governments, universities, and industrial and research organizations. In addition, books, conference proceedings, individual conference papers, patents, and journal literature on a worldwide basis are abstracted and indexed. Each issue of *Nuclear Science Abstracts* includes four indexes: subject, personal author, corporate author, and report number.

The following organizations scan and abstract the nuclear science literature in their respective countries:

Atomic Energy of Canada Limited
Australian Atomic Energy Commission
Danish Atomic Energy Commission
Finnish Atomic Energy Commission
French Atomic Energy Commission
Japan Atomic Energy Bureau–Atomic Energy Research Institute
Institutt for Atomenergi (Norway)
Aktiebolaget Atomenergi (Sweden)
United Kingdom Atomic Energy Authority

Numerous organizations, societies, and publishers throughout the world provide *Nuclear Science Abstracts* with advance page-proof copy of their publications, e.g., in the United States the American Institute of Physics provides page-proof copy of its publications.

A list of the journals scanned regularly and the abbreviations used appears in Issue 1 (January 15) of each volume of *Nuclear Science Abstracts* and is supplemented in Issues 7, 13, and 19. Issue 1 of each volume also describes the scope and arrangement of the subject matter covered in *Nuclear Science Abstracts*. The subject matter covered is also described in TID-4552, *Subject Scope of Nuclear Science Abstracts*, available free from the USAEC Division of Technical Information Extension, P.O. Box 62, Oak Ridge, Tennessee 37830. An outline of the subject categories appears in the Contents of each issue.

AVAILABILITY OF PUBLICATIONS ABSTRACTED

Public availability of all U. S. Atomic Energy Commission reports is indicated in the report number indexes. The availability of other reports, when known, is also indicated. The availability of some unnumbered reports is given in the abstract.

Dissertations abstracted in *Dissertation Abstracts* and included in *Nuclear Science Abstracts* are available from University Microfilms, Inc., 315 N. First Street, Ann Arbor, Michigan 48103.

Information on the availability of the published literature and unpublished conference papers abstracted in *Nuclear Science Abstracts* can be obtained from the USAEC Division of Technical Information Extension, P.O. Box 62, Oak Ridge, Tennessee 37830.

HOW TO OBTAIN NUCLEAR SCIENCE ABSTRACTS

Nuclear Science Abstracts is available to the public on a subscription basis from the Superintendent of Documents, U. S. Government Printing Office, Washington, D. C. 20402.

For the 24 regular issues, the yearly rate is $42.00 for domestic subscribers and $52.50 for foreign subscribers. A single issue costs $1.75, domestic rates, or $2.19, foreign rates. Domestic rates apply to the United States, Canada, Mexico, and Central and South American countries except Argentina, Brazil, Guyana, French Guiana, Surinam, and British Honduras.

For a yearly subscription to the cumulative indexes, the rates are $38.00 for domestic subscribers and $47.50 for foreign subscribers.

The following cumulative indexes are available:

From Johnson Reprint Corporation, 111 Fifth Avenue, New York, N. Y. 10003:
Vols. 1–4, Subjects and Authors (1948–1950), $30.00.

From Superintendent of Documents, U. S. Government Printing Office, Washington, D. C. 20402:

Vols. 5–10, Subjects and Authors (1951–1956), $5.25.

Vols. 11–15, Subjects (1957–1961), $19.00.
Vols. 11–15, Personal Authors (1957–1961), $14.25.
Vols. 11–15, Corporate Authors (1957–1961), $2.50.

Vols. 16–20, Subjects (1962–1966), $36.00.
Vols. 16–20, Personal Authors (1962–1966), $22.50.
Vols. 16–20, Corporate Authors (1962–1966), $3.75.

Vol. 21, Subjects and Authors (1967), $16.00.
Vol. 22, Subjects and Authors (1968), $26.00.
Vol. 23, Subjects and Authors (1969), $25.75.

Cumulative Report Number Index, Vols. 1-15 Revised, $4.00.
Cumulative Report Number Index, Vols. 16-20 Revised, $5.50.
Cumulative Report Number Index, Vols. 21-23, $4.25.

Nuclear Science Abstracts is available on an exchange basis to universities, research institutions, industrial firms, and publishers of scientific information. Government agencies may obtain *NSA* free of charge. Inquiries should be directed to the USAEC Division of Technical Information Extension, P. O. Box 62, Oak Ridge, Tennessee 37830.

INDEXES TO NSA

Comprehensive indexes appear in each issue and are cumulated quarterly and annually. Multivolume cumulations have been issued as indicated above.

All documents abstracted are indexed by subjects and personal authors. Report literature is indexed also by corporate author and report number. Each of these indexes in every issue is preceded by an introduction explaining in detail the organization of the index and the principles by which it is compiled. The reader is referred to these explanations for information not found in the brief summary below.

Personal Authors

Each author's name is indexed in the form appearing on the document abstracted:

ISHIHARA, T., Accumulation of fallout ^{137}Cs in newborn infants, 23:50538
ISHIHARA, Toyokuki, Shielding effect of paraffin, water, soil, concrete, Fe, and Pb for high-energy neutrons, 23:51748

Subjects

The subject index consisting of specific materials, objects, and processes is arranged alphabetically. Modifying phrases specific to these subjects in turn are arranged alphabetically under the subjects.

MELPHALAN
  effects on proliferation of cultured antigen-stimulated spleen cells from mice, dose-response curve for, 23:50820
MEMBRANE FILTERS
  design for removal of cell-free Streptococcus faecalus from bacteria cultures in fermentation tank, 23:49996 (UCRL-18667, pp 322-9)
MENDELEVIUM
  separation from einsteinium and fermium by electrolysis, 23:49772 (UCRL-18667, pp 277-312)
  separation from sodium acetate solutions by solvent extraction using sodium amalgam, 23:49772 (UCRL-18667, pp 277-312)
  stability of divalent state of, 23:49772 (UCRL-18667, pp 277-312)

Corporate Authors

Technical report literature is indexed from the name of the organization or institution responsible for the issuance of the report.

51093 (LA-4164) FABRICATION OF BORON CARBIDE RINGS AND DISKS. Sheinberg, H.; Herrera, T.; Kostacopoulos, J. **(Los Alamos Scientific Lab., N. Mex.).** Apr. 25, 1969. Contract W-7405-eng-36. 11p. Dep. CFSTI.

is indexed as:

LOS ALAMOS SCIENTIFIC LAB., N. MEX.
  Fabrication of boron carbide rings and disks, 23:51093 (LA-4164)

Report Numbers

Technical report literature is also indexed by report numbers. This index includes information on where individual reports may be obtained. While not reports, patents and conference papers are indexed here as a matter of convenience.

JPRS-	**(Non-AEC)**	
46949	23-51587	CFSTI
48330	23-52305	CFSTI
48331	23-52451	CFSTI
48481	23-50889	CFSTI
48743	23-51034	CFSTI
49025	23-51706	CFSTI (U. S. Sales Only)
JUL-	**(German)**	
571-RG	23-52269	Dep
578-PP	23-51624	Dep. CFSTI (U. S. Sales Only)
581-FN	23-51079	Dep. CFSTI (U. S. Sales Only)
584-RG	23-52313	Dep
586-FN	23-51035	Dep. CFSTI (U. S. Sales Only)
K-		
1777	23-50987	Dep. CFSTI
1778	23-50988	Dep. CFSTI
KFK-	**(German)**	
743	23-52461	Dep
743	23-52447	For translation see EURFNR-613
781/I	23-52462	Dep
824	23-52397	Dep. CFSTI (U. S. Sales Only)

XUM

TABLE OF CONTENTS

Volume 25, Number 3, February 15, 1971

Category	Page
CHEMISTRY	387
Analytical Chemistry	387
Chemical and Spectral Procedures	387
Isotope Dilution Procedures	389
Radiometric and Radiochemical Procedures	389
Activation Procedures	390
Inorganic, Organic, and Physical Chemistry	390
Chemical Properties	391
Isotope Effects and Exchange	391
Physical Chemistry	392
Radiation and Nuclear Chemistry	394
Radiation Effects	394
Radiation Processes	395
Radiolysis	396
Radioisotope Production	398
Recoil Production and Reactions	398
Radiochemistry	398
Separation Processes	399
EARTH SCIENCES	401
Geology and Hydrology	401
Meteorology	402
Mineralogy and Exploration	402
Oceanography	402
ENGINEERING	403
Nuclear Explosions	403
Facilities and Equipment	403
Heat Transfer and Fluid Flow	405
Isotope Technology	406
Materials Testing	407
Protective Structures	408
Radioactive Material Handling	408
INSTRUMENTATION	412
Radiation Detection Instruments	412
General Detectors and Monitors	412
Nuclear Spectroscopic Instrumentation	414
High Energy Physics Instrumentation	415
Radiation Dosimeters	415
Radiometric Instruments	416
Miscellaneous Instruments and Components	416
Radiation Effects on Instruments and Instrument Components	417
LIFE SCIENCES	419
Biochemistry, Physiology, and Molecular Biology	419
Basic Processes	419
Metabolism, Physiology, and Toxicology	420
Radiation Effects	423
Immunology	424
Ecology	425
Genetics and Cytogenetics	426
Health Physics and Safety	428
Radioactive Contamination and Decontamination	428
Dosimetry and Monitoring	428
Radiation Protection	430
Safety Procedures	430

Category	Page
LIFE SCIENCES (Cont'd.)	
Legal Aspects	431
Medicine	431
Protective Substances	431
Radiation Sickness and Injuries	441
Radiodiagnosis	441
Radiotherapy	450
Radiation Effects on Animals	451
Invertebrates	451
Vertebrates	451
Man	453
Radiation Effects on Plants	454
Radiation Effects on Microorganisms	455
Radiosterilization and Radiopreservation	455
METALS, CERAMICS, AND OTHER MATERIALS	457
Metals and Alloys	457
Corrosion and Erosion	457
Preparation and Fabrication	457
Properties Evaluations	458
Structure and Phase Studies	462
Radiation Effects	464
Ceramics and Cermets	466
Corrosion and Erosion	466
Preparation and Fabrication	466
Properties Evaluations	467
Structure and Phase Studies	469
Radiation Effects	470
Plastics and Other Materials	472
PHYSICS (GENERAL)	473
Astrophysics and Cosmology	473
Cosmic Ray Exposure Ages	473
Stars	473
Quasi-Stellar, Radio, and X-Ray Sources	474
Solar Phenomena	475
Galaxies	475
Cosmology	476
Planetary Phenomena	476
Atomic and Molecular Physics	476
Atomic, Electron, Ion, and Molecular Beams and Their Reactions	476
Atomic and Molecular Properties	477
Positronium, Muonium, and Mesic Atoms and Molecules	478
Collision Phenomena	478
Atomic Theory	480
Cosmic Radiation	480
Direct Energy Conversion	481
Fluid Physics	482
Geophysics (Upper Atmosphere)	483
Low-Temperature Physics and Cryogenic Equipment	486
Superconductivity	486
Equipment and Devices	488
Plasma and Thermonuclear Physics	489
Confinement and Heating	489
Diagnostics	490

TABLE OF CONTENTS (continued)

Category	Page
PHYSICS (GENERAL) (Cont'd.)	
Kinetics (General)	491
Kinetics (Experimental)	492
Kinetics (Theoretical)	492
Production	493
Stability	493
Thermonuclear Processes	494
Wave Phenomena	495
Shielding	496
Solid-State Physics	496
Radiation Effects	497
Physical Properties	498
Moessbauer Effects and NMR	504
Theory	506
Theoretical Physics	506
PHYSICS (HIGH-ENERGY)	508
Particle Interactions and Properties (Experimental)	508
Electromagnetic	508
Weak	509
Strong (Baryon-Induced)	510
Strong (Meson-Induced)	511
Particle Interactions and Properties (Theoretical)	513
General	513
Electromagnetic	514
Weak	516
Strong (General)	517
Strong (Baryon No. = 0)	518
Strong (Baryon No. = 1)	518
Strong (Baryon No. ≥ 2)	520
Particle Invariance Principles and Symmetries	521
General	521
Applications (Electromagnetic and Weak)	522
Applications (Strong)	522
Field Theories	522
General	522
Quantum Field Theory	522
Gravitation and General Relativity	523
Scattering Theory	524
Particle Accelerators	526
PHYSICS (NUCLEAR)	529
Neutron Interactions with Matter	529
Nuclear Properties and Reactions, A ≤ 5	532

Category	Page
PHYSICS (NUCLEAR) (Cont'd.)	
Nuclear Properties and Reactions, 6 ≤ A ≤ 19	535
Nuclear Properties and Reactions, 20 ≤ A ≤ 89	540
Nuclear Properties and Reactions, A ≥ 90	546
Nuclear Theory	557
REACTOR TECHNOLOGY	564
Commercial Power Reactors	564
Operation and Economics	564
Safety and Siting	565
Power Reactor Development	567
Kinetics and Dynamics	567
Control Systems	568
Shielding	568
Cooling Systems	569
Fuels	569
Auxiliary and Emergency Systems	572
Operation and Economics	573
Safety and Siting	573
Research and Test Reactors	575
Rocket and Space Reactors	576
Process Heat and Desalination Reactors	577
Marine and Portable Power Reactors	577
Production Reactors	577
Kinetics	577
Dynamics	579
Experimental Applications	579
Reactor Components, Fuels, and Accessories	580
GENERAL	582
CORPORATE AUTHOR INDEX	INDEX-1
PERSONAL AUTHOR INDEX	INDEX-10
SUBJECT INDEX	INDEX-58
REPORT NUMBER INDEX	INDEX-148

XUM

STAFF OF NUCLEAR SCIENCE ABSTRACTS

John W. Norris
Managing Editor

Donald D. Davis
Assistant Managing Editor

David E. Bost
Production Manager

Sidney F. Lanier
Subject Heading Specialist

J. Paul Meredith
Descriptive Cataloging Specialist

Frederick E. Marsh, Jr.
Computer Index Coordinator

Clara L. Fox
Corporate Author Specialist

Helen W. White
Report Number Specialist

Evaluators

Thomas S. Chapman
Rose V. Jermain
John H. Mitchell
Mary H. Newman
Polly C. Summers

Abstractors

F. S. Armstrong*
Ellis R. Bedford
Mary M. Brown
Jane G. Buchanan
D. Lamar Cason
Gloria M. Caton
David C. Cunningham
James R. Dulaney
Helga B. Gerstner
Mary C. Grissom
Phyllis C. Hansen
Carolyn D. Houston
Elaine E. Huber
Rose V. Jermain
W. Hugh Kinser, Jr.
Lisbeth C. Lieberman
Betty L. McDowell
Patricia B. McEwen
Fay M. Martin
William D. Matheny
Dora H. Moneyhun
Jean F. Peckham
Henry D. Raleigh
Mona H. Raridon
Julia S. Redford
Jessie W. Rushing
Robert W. Rutkowski
Francis L. Sachs
Lila B. Smith
Anne G. Ward
Helen L. Ward
Milton O. Whitson
Juanita Wilson

*Atomic Energy of Canada, Ltd.

Section Editors

Everett J. Hoffman
Chemistry

Robert C. Kelly
Engineering; Earth Sciences; Metals, Ceramics, and Other Materials

Lee M. Thompson
General Physics

Charles E. Stuber
High Energy Physics; Instrumentation

Helen G. Donald
Life Sciences

Lawrence T. Whitehead
Nuclear Physics

James M. Jacobs
Reactor Technology

Charles R. Bruce
Publishing Coordinator

Communication concerning the editorial policy and content of *Nuclear Science Abstracts* should be addressed to the Managing Editor, *Nuclear Science Abstracts*, USAEC Division of Technical Information Extension, P. O. Box 62, Oak Ridge, Tennessee 37830.

Use of funds for printing this publication approved by the Director of the Bureau of the Budget, June 26, 1969.

Volume 25, Number 3 February 15, 1971

NUCLEAR SCIENCE ABSTRACTS

CHEMISTRY

Analytical Chemistry

Refer also to abstracts 4310 and 4736.

4008 (BNWL-SA-3341) AUTOMATION IN ANALYTIC CHEMISTRY: METHODS AND MOTIVATION. Mahan, R. E. (Battelle-Northwest, Richland, Wash. Pacific Northwest Lab.). 8 Jun 1970. Contract AT(45-1)-1830. 8p. (CONF-700542-2). Dep. NTIS.

From Conference on Electronic Instrumentation, Moscow, Idaho.

Methods of automating analytical chemistry include three major systems design approaches: time-sharing large computers, time-sharing small computers, and dedicated computers. These are discussed along with programming sources and motivation. (M.C.G.)

4009 (TID-25190) ANALYSIS OF ELEMENTAL BORON. Lerner, Morris W. (New Brunswick Lab. (AEC), N. J.). 1970. 125p. Dep. NTIS.

Methods for determination of boron and its impurities are reviewed. Topics covered include: standards; dissolution of elemental boron and boron carbide; separations, losses, and contamination; determination of boron; isotopic analysis; impurities in elemental boron; determination of C, O, N, and H; emission spectrographic determination of impurities; flame-emission and atomic-absorption spectroscopic determination of impurities; x-ray spectrographic determination of impurities; polarographic determination of impurities; spark-source mass-spectrographic determination of impurities; neutron-activation determination of impurities; spectrophotometric determination of impurities; and a cooperative boron-analysis study. (M.C.G.)

4010 MODERN PHYSICAL METHODS FOR THE ANALYTICAL DETERMINATION OF IRON. Berenyi, Denes (Nuclear Research Inst., Debrecen, Hungary). Atomtech. Tajek.; 13: 170-4(1970). (In Hungarian).

Neutron activation is an important physical method for determining iron. Use of low-energy thermal neutrons, involving irradiation of the specimen in a reactor, is preferable to fast neutrons; on the other hand, the fast-neutron generators are flexible, mobile, and relatively inexpensive. Recent development of semiconductor-type x-ray detectors resulted in the widespread application of the x-ray fluorescence method; the less sensitive but very precise crystal x-ray spectrometers are still in use, because there are indications that their precision exceeds that of emission spectroscopy. The mass-spectrometric technique presents the advantage of very high sensitivity of the order of 0.05 nanogram but problems encountered in the ionization of the samples limit its application. In certain special cases β and γ backscattering and isotopic tracer techniques have yielded excellent results. More recently, the use of Moessbauer spectroscopy and inelastic scattering has been reported in the literature. (Review article, 44 references) (TTT)

Chemical and Spectral Procedures

Refer also to abstracts 4126, 4218, 4412, 4425, 4443, 4612, 4622, and 4798.

4011 (CEA-N-1340) ELECTRON PROBE MICROANALYSIS OF HIGHLY RADIOACTIVE MATERIALS: EQUIPMENT AND TECHNIQUES. Bazin, Jean; Conty, Claude; Guernet, Jacques; Lauger-Hache, Michel; Leleux, Achille; Roussel, Emile; Vignesoult, Nicole (Commissariat a l'Energie Atomique, Saclay (France). Centre d'Etudes Nucleaires). Sep 1970. 34p. (In French). Dep. NTIS (U. S. Sales Only).

A shielded electron microprobe for samples with a maximum activity of 4 Ci at 0.75 MeV was designed and constructed. This equipment was developed from the CAMECA MS 46 microprobe in accordance with the following conditions; total security for operators (irradiation intensity at the surface of equipment lower than 2.5 mrad/h), and easy maintenance of the shielded microprobe. (France)

4012 (DP-Report-443) DIFFERENTIAL CONCENTRATION GAS CHROMATOGRAPH FOR THE ANALYSIS OF LOW LEVELS OF IMPURITIES IN HELIUM. Project DRAGON. Gray, P. S.; Owens, D. R.; Green, L. O. (Atomic Energy Establishment, Winfrith (England)). Jul 1966. 21p. Dep. NTIS.

The development of a differential concentration gas chromatograph is described from a basic principle to an on-line plant instrument capable of analyzing helium for O_2, N_2, CO, CO_2, and CH_4 to better than 0.1 vpM with a high degree of reliability. Full details of construction are given together with an account of the performance of the instrument. (auth)

4013 (JUL-671-RW) PROCEDURE FOR IDENTIFICATION OF FUEL ELEMENT SPHERES OF HIGH-TEMPERATURE REACTORS WITH THE HELP OF EMISSION SPECTRAL ANALYSIS AT 40 ATMOSPHERES OF HELIUM. Lingen, Peter Ralf (Kernforschungsanlage, Juelich (West Germany). Institut fuer Reaktorwerkstoffe). Jul 1970. 89p. (In German). Dep. NTIS (U. S. Sales Only).

For emission spectrometry under 40 atm helium, the optimal combustion conditions were determined. Operating voltage characteristics, temperature determinations, burning off of the cathode and anode, radiation strength, and dependence of line and continuum intensity on pressure are discussed. The possibility of the sorting of graphite fuel spheres with broken coated particles and detection of labeled spheres for charge identification is considered. A completely automatic spark chamber for rapid analysis of spherical elements is being built. (M.C.G.)

4014 (NLCO-1072) AUTOMATIC DETERMINATION OF THORIUM IN AQUEOUS AND ORGANIC SOLUTIONS. Prall, J. R. (National Lead Co. of Ohio, Cincinnati). Oct 1970. Contract AT(30-1)-1156. 19p. Dep. NTIS.

A procedure was developed for the determination of thorium in aqueous solutions and organic solutions such as diamyl amylphosphonate diluted with ethyltoluene. A mixture of methanol and 1-butoxyethanol is used to dilute samples. The dye, thorin (1-(o-arsonophenylazo)-2-naphthol-3,6-disulfonic acid, sodium salt), is employed as the chromogenic reagent. Absorbance is measured in a 6- or 15-mm tubular flowcell at 540 nm. Data indicate that thorium in aqueous samples is absorbed on the pump tube unless the samples are acidified with nitric acid. The sensitivity of the method is about 20% lower for organic samples; however, this is due to a difference in the volume of liquid pumped rather than to any effect of the organic material on the determination. The effect of 20 diverse anions and 3 cations was studied. The most serious interferences were caused by vanadium, titanium, zirconium, and rare earths, which caused positive errors, and by fluoride, which bleached the thorium–thorin color. At a thorium concentration of 150 μg/ml the standard deviation was calculated to be ±1.1 ppM. The relative standard deviation was 0.7%. Agreement between the

automatic and routine procedures on production samples was good. (auth)

4015 (NUMEC-3524-76) SPECTROGRAPHIC ANALYSIS RESPONSE OF A CARRIER TO PLUTONIUM–URANIUM MIXED OXIDES. Murray, A. J.; Marley, J. L.; Scott, J. E. (Nuclear Materials and Equipment Corp., Apollo, Pa.). 2 Nov 1970. Contract AT(30-1)-3524. 21p. Dep. NTIS.

A study was made of the spectrographic analysis of plutonium–uranium mixed oxides. A silver chloride–barium fluoride–graphite carrier was used. Significant changes in spectral line intensity for the same element concentration levels were demonstrated among the elements studied as the plutonium oxide to uranium oxide ratio was changed. (auth)

4016 (UCLA-12-782, pp 83-8) BIOPHYSICS. (California Univ., Los Angeles. Lab. of Nuclear Medicine and Radiation Biology).

From annual progress report for the period ending June 30, 1970.

A rapid emission spectrometric procedure was developed for the determination of some 25 elements in biological tissues. Over 13,000 samples of animal and plant tissues have been analyzed. The development of a group of computer programs for data processing and display is reported. (C.H.)

4017 USE OF SODIUM BUTYLDITHIOCARBAMINATE IN THE SPECTROPHOTOMETRIC DETERMINATION OF NIOBIUM. Uvarova, K. A.; Usatenko, Yu. I.; Klopova, Zh. G. (Donetsk Polytechnic Inst., Stalino, USSR). Zavod. Lab.; 36: 909-11 (1970). (In Russian).

The interaction of niobium with sodium butyldithiocarbaminate in acid solutions results in the formation of colored products. The extraction of these compounds was studied. Absorption spectra are given. The reaction was used in the spectrophotometric determination of niobium. The effects of Ti, Zr, Ta, and F^- on the determination were studied. The method was examined using semiconductors of TiO_2 and lead titanium zirconate. (tr-auth)

4018 PHOTOMETRIC DETERMINATION OF NIOBIUM WITH THE REAGENT PAR IN COMPLEX COPPER-BASE ALLOYS. Elinson, S. V.; Pyatiletova, N. M.; Novikova, I. S. Zavod. Lab.; 36: 659-60(1970). (In Russian).

A method was developed for the photometric determination of Nb in Cu-base alloys with Ti, Zr, Cr, Fe, and Ni. The method is based on the fact that Nb forms a ternary colored complex with the reagent PAR (4-(2-pyridylazo)resorcinol) in 75 N HCl. The Cu is combined with thiourea and the other elements by Complexone III. The coefficient of variation for small amounts of Nb was equal to ±2.05. (auth)

4019 ACCURACY AND SENSITIVITY IN OPTICAL ^{15}N-ANALYSIS. Middelboe, Victor (Royal Veterinary and Agricultural Univ., Copenhagen). Appl. Spectrosc.; 24: 608-9 (Nov-Dec 1970).

Spectral determination of ^{15}N in nitrogen samples of low enrichment is discussed. The accuracy-limiting factors, methods of improving the accuracy, and comparison with other methods are discussed. (M.C.G.)

4020 SPECTROPHOTOMETRIC DETERMINATIONS OF TITANIUM AND NIOBIUM WITH N-CINNAMOYL-N-PHENYLHYDROXYLAMINE AND TITANIUM WITH N-BENZOYL-N-p-TOLYLHYDROXYLAMINE. Dutt, N. K.; Seshadri, T. (Indian Association for the Cultivation of Science, Calcutta). Indian J. Chem. 6: 741-2(Dec 1968).

N-Cinnamoyl-N-phenyl- and N-benzoyl-N-p-tolylhydroxylamines were used for the spectrophotometric determination of Ti and the former reagent for Nb by making use of the golden yellow complex formed with these reagents in 8 to 9 N HCl in the presence of NH_4CNS. The colored complex can be extracted with chloroform. The color intensity is measured at 410 mμ for N-cinnamoyl-N-phenyl- and at 370 mμ for N-benzoyl-N-p-tolylhydroxylamine with Ti and at 420 mμ for N-cinnamoyl-N-phenylhydroxylamine with Nb. All the systems obey Beer's law from 0.25 to 6 ppM. N-Cinnamoyl reagent appears to be very sensitive for Nb at dilutions below 0.3 ppM. (auth)

4021 CHEMICAL SEPARATION AND SPECTROGRAPHIC DETERMINATION OF TRACE AMOUNTS OF RARE EARTHS IN URANIUM USING LiF–AgCl CARRIER. Joshi, B. D.; Patel, B. M. (Bhabha Atomic Research Centre, Trombay, India). Appl. Spectrosc.; 24: 573-6(Nov-Dec 1970).

An emission spectrographic method is described for the determination of certain rare earths (Ce, Sm, Eu, Gd, Dy, Ho, Er, Yb, and Lu) at fractions of ppM concentration in uranium samples using LiF–AgCl–graphite powder mixture as carrier. The rare earths chemically separated from uranium were excited in a dc arc. Thulium was used as an internal standard. The detection limits in ppM on the basis of 5 g uranium sample are: Yb 0.004; Eu, Gd, Er 0.02; Dy, Lu 0.05; Sm, Ho, 0.2; and Ce 0.5. The precision of the method expressed as a coefficient of variation is estimated to be ±9%. The effect of 14 nonrare earth elements on the intensity of analysis lines was investigated. (auth)

4022 DETERMINATION OF OXYGEN, WATER, AND NITROGEN IN REFRACTORY METALS. V. COMPARATIVE INVESTIGATIONS ON OXYGEN AND NITROGEN DETERMINATION IN NIOBIUM AND TANTALUM. Friedrich, K. (Institutsteil fuer Metall-Physik und Reinstmetalle, Dresden); Lassner, E.; Paesold, G. J. Less-Common Metals; 22: 429-38(Dec 1970). (In German).

Determination of oxygen by means of vacuum fusion in powdered niobium and tantalum samples can be carried out using different flux methods, for example Pt, Ni, and Fe fluxes and does not entail any special difficulties. For the oxygen determination in compact pieces of tantalum, the Ni–Fe–Sn bath at 1700°C is quite useful, whereas for niobium it is suitable only at higher oxygen contents, when the blank is relatively less important. Determination of nitrogen by the nickel–magnesium–cerium method is possible in tantalum above a nickel–tantalum ratio of 8:1. A suitable method for nitrogen determination in niobium has not yet been found. (auth)

4023 ATOMIC ABSORPTION SPECTROPHOTOMETRY. Amer. Ind. Hyg. Ass. J.; 31: 525-8(Jul-Aug 1970).

A review is presented on the history, advantages, disadvantages, and uses of atomic absorption spectrophotometry in industrial hygiene. Data on detection capabilities of atomic absorption instruments, absolute detection limits by photometric and atomic absorption methods, and comparison of detection limits by boat and nebulizer techniques are tabulated. (P.C.H.)

4024 KOLICHESTVENNYI RENTGENOSPEKTRAL'NYI FLUORESTSENTNYI ANALIZ. (Quantitative X-Ray Spectrofluorescence Analysis). Losev, N. F. Moscow; Izdatel'stvo Nauka Glavnaya Redaktsiya Fiziko-Matematicheskoi Literatury (1969). 336p.

X-ray spectra fluorescence analysis used in geology, metallurgy, and chemistry for the determination of many elements in various materials is described. The method is characterized by high accuracy and speed, which allows the x-ray spectrometer to be used as recorders of chemical composition in control–check systems and in the regulation of technological operations. 254 references. (tr-auth)

4025 COULOMETRIC DETERMINATION OF URANIUM WITH A PLATINUM WORKING ELECTRODE. Davies, W.; Gray, W.; McLeod, K. C. (United Kingdom Atomic Energy Authority, Dounreay, Scotland). Talanta; 17: 937-44(Oct 1970).

Experimental conditions were established which enable uranium to be determined coulometrically by the reduction of uranium(VI) to uranium(IV) at a platinum working electrode, by controlled-potential or controlled-potential-limit techniques. The procedure was used successfully as a subsidiary method in the routine determination of uranium in pure uranyl nitrate solutions. The platinum electrode has several important practical advantages over the well-established mercury-pool electrode for the coulometric determination of uranium. The consecutive determination of iron(III) and uranium(VI), or plutonium(IV) and uranium(VI) can be carried out with the same working electrode in the same solution and the coulometric oxidation of uranium(IV) to uranium(VI) is practicable. The rate of stirring of the cell liquor is much less critical in the case of the platinum electrode. Two main problems had to be overcome before a practical procedure could be achieved; hydrogen evolution during the uranium(VI)-(IV) reduction had to be eliminated so that 100% current efficiency could be obtained for the desired reaction and electrode-surface poisoning phenomena had to be controlled so that reaction times could be kept reasonably short. It was found that selection of a hydrochloric acid base solution containing a small amount of bismuth(III) enabled hydrogen evolution to be avoided: also electrode-surface poisoning with this base solution was not particularly serious and could be maintained at a satisfactorily low level by occasionally anodizing the electrode in dilute sulphuric acid. Bismuth(III) forms a complex with chloride ions and its presence increases the hydrogen overvoltage at the working electrode: no visible deposit of bismuth metal forms on the electrode during the uranium reduction. Samples containing nitrate can be analyzed provided sulphamic acid is added to this hydrochloric acid base solution. (auth) (UK)

4026 PHOTOCHEMICAL PRECIPITATION OF THORIUM AND CERIUM AND THEIR SEPARATION FROM OTHER IONS

IN AQUEOUS SOLUTION. Das, M.; Heyn, Arno H. A.; Hoffman, Morton Z.; Agarwal, R. P. (Boston Univ.). Talanta; 17: 925-35 (Oct 1970).

Thorium was precipitated from homogeneous solution by exposing solutions of thorium and periodate in dilute perchloric acid to 253.7 nm radiation from a low-pressure mercury lamp. Periodate is reduced photochemically to iodate which causes the formation of a dense precipitate of the basic iodate of thorium(IV). The precipitate was redissolved, the iodate reduced, the thorium precipitated first as the hydroxide, then as the oxalate and ignited to the dioxide for weighing. Thorium(IV) solutions containing 8 to 200 mg of ThO_2 gave quantitative results with a standard deviation (s) of 0.2 mg. Separations from 25 mg each of iron, calcium, magnesium, 50 mg of yttrium, and up to 500 mg of uranium(VI) were quantitative (s = 0.25 mg). Separations from rare earths, except cerium, were accomplished by using hexamethylenetetramine rather than ammonia for the precipitation of the hydroxide. Cerium(III) was similarly precipitated and converted into CeO_2 for weighing. Quantitative results were obtained for 13 to 50 mg of CeO_2 with a standard deviation of 0.2 mg. Separations from 200 mg of uranium were quantitative. Other rare earths and yttrium interfered seriously. The precipitates of the basic cerium(IV) and thorium iodates obtained are more compact than those obtained by direct precipitation and can be handled easily. Attempts to duplicate Suzuki's method for separating cerium from neodymium and yttrium were not successful. (auth) (UK)

Isotope Dilution Procedures

4027 RADIOELECTROCHEMICAL DETERMINATION OF MICROGRAM IODIDE. Nilsson, A.-M.; Holmgren, A.; Beronius, P. (Univ. of Umea, Sweden). Radiochem. Radioanal. Lett.; 5: 125-9(6 Nov 1970).

Electrochemical isotopic dilution analysis as a means of determining microgram amounts of iodide is described. In the test run reported, an ethanolic sodium iodide solution containing 2.62 μg ml^{-1} of I^- was analyzed by this method and the value 2.64 μg ml^{-1} found. (auth)

4028 SIMPLIFIED EQUATIONS FOR DOUBLE-SPIKED ISOTOPIC ANALYSES. Dodson, M. H. (Univ. of Leeds, Eng.). Geochim. Cosmochim. Acta; 34: 1241-4(Nov 1970).

Relationships between fractionation correction coefficients, spike/sample ratio and observed isotope ratios were reduced to a set of linear simultaneous equations in three unknowns, whose coefficients are simple functions of isotope ratios and mass differences. Solutions are quickly and conveniently obtained by elimination and back-substitution. (auth) (UK)

Radiometric and Radiochemical Procedures

Refer also to abstracts 4151, 4291–4294, 4297, 4358, 4513, and 4631.

4029 (CISE-N-119) BETA DETECTION EFFICIENCY CURVES FOR ^{40}K, ^{90}Y, ^{90}Sr–^{90}Y, ^{137}Cs, ^{144}Ce–^{144}Pr, ^{147}Pm, ^{155}Eu, ^{204}Tl IN SOURCES OF DEFINITE CHEMICAL FORM AS A FUNCTION OF THEIR THICKNESS. Battaglia, A.; Bonfanti, G.; Triulzi, C. (Centro Informazioni Studi Esperienze, Milan (Italy)). Sep 1970. 36p. (In Italian). Dep. NTIS (U. S. Sales Only).

Beta detection efficiency curves for some radionuclides of interest (^{40}K, ^{90}Y, ^{90}Sr + ^{90}Y, ^{137}Cs, ^{144}Ce + ^{144}Pr, ^{147}Pm, ^{155}Eu, and ^{204}Tl) contained in sources of a suitable material and with a superficial density ranging from 3 to 110 mg/cm^2 are reported. They were experimentally drawn by measuring reference sources in different geometries by means of three G-M window detectors (one of low background) and of a 2π flow proportional counter. These curves have been used to determine such radionuclides in different thickness sources obtained by specific radiochemical separations carried out on various environmental samples. (auth)

4030 RAPID SIMULTANEOUS ELUTION AND ELECTRODEPOSITION OF RADIOACTIVE NUCLIDES ADSORBED ON PAPER. Parker, W.; Riedl, H. (Chalmers Univ. of Tech., Goteborg). Radiochem. Radioanal. Lett.; 5: 107-11(6 Nov 1970).

A device is described, which enables the rapid and simultaneous elution and electrodeposition of radioactive nuclides that were previously separated by means of paper chromatography or paper electrophoresis. This method can be applied to most elements and, provided that optimum conditions are established, requires less than 60 min. Elution and deposition yields are quantitative and the electroplated samples are ideal for α and β counting. (auth)

4031 SPECTROMETRY FOR DETERMINATION OF ISOTOPIC MIXTURES WITH SPECIAL REGARD TO BIOLOGICAL AND CLINICAL INVESTIGATIONS. Sjoestrand, U.; Lyttkens, L.; Oeberg, P. Aa.; Oestling, S. G. (Uppsala Univ.). Acta Soc. Med. Upsal.; 74: 219-46(1969).

Some practical and theoretical aspects of spectrometry of radioactive isotopic mixtures are summarized. On analysis of radioactive isotopic mixtures the error of the method was found to be small and the recovery good. A test procedure is presented by which the electronic stability of the analysis equipment can be studied. The values obtained in the analysis of a mixture of two isotopes were highly dependent on the electronic stability of the equipment and volumes and chemical compositions of the samples. A computer program for treatment of the data is briefly discussed. (auth) (Sweden)

4032 ASHING TECHNIQUE AS A MORE PRECISE METHOD FOR THE RADIOASSAY OF ^{51}Cr IN FECES. Kuiper, Donald H.; Fall, Daniel J.; Pollard, H. Marvin (Univ. of Michigan, Ann Arbor). J. Nucl. Med.; 11: 527-9(Sep 1970).

Two methods for the radioassay of stool for blood loss using ^{51}Cr-tagged erythrocytes were compared. One method assayed a sample of the 24-hr stool homogenate, while the other method assayed the ash of the entire 24-hr fecal collection. The ashing technique revealed better precision in recovery as shown by a s.d. of 3.0 as compared to a s.d. of 32.0 using the wet technique. The ashing method concentrates a large volume of stool, thereby yielding higher counts per sample and thus reducing the error in counting. (auth)

4033 SILICA GEL AS A SUPPORT FOR INORGANIC ION-EXCHANGERS FOR THE DETERMINATION OF ^{137}Cs IN NATURAL WATERS. Terada, Kikuo; Hayakawa, Hironobu; Sawada, Kiyoshi; Kiba, Toshiyasu (Kanazawa Univ., Japan). Talanta; 17: 955-63(Oct 1970).

The preparation and characteristics of ammonium molybdophosphate and potassium or ammonium hexacyanocobalt ferrate supported in silica gel, and their application to the determination of ^{137}Cs in natural waters are described. Use of columns of these materials gives better recovery of ^{137}Cs from natural waters (in comparison with co-precipitation with ammonium molybdophosphate), requires less exchanger, so raising the γ-counting efficiency of ^{137}Cs, and permits elimination of other radionuclides by washing with hydrofluoric acid. (auth) (UK)

4034 ALPHA-SCATTERING TECHNIQUE OF CHEMICAL ANALYSIS. Economou, Thanasis E. (Univ. of Chicago); Turkevich, Anthony L.; Sowinski, Kenneth P.; Patterson, James H.; Franzgrote, Ernest J. J. Geophys. Res.; 75: 6514-23(10 Nov 1970).

The α-scattering technique of chemical analysis as used on the Surveyor lunar missions is described. Improved α sources and methods of data analyses lead to appreciably better results than those achieved previously by this technique. The accuracy of the α-scattering method was tested through the analysis of eleven rocks of known composition using a space Surveyor instrument. These results provided the basis of estimation of the errors of the lunar surface analyses on Surveyors 5, 6, and 7. Some nonstandard geometrical relationships of sample to instrument, such as were encountered on the Surveyor missions, were studied and their effects estimated. As a by-product of this work, chemical analyses of five rocks of unknown composition were obtained. (auth)

4035 SLOW-NEUTRON TRANSMISSION ANALYSIS. Mott, William E. (Atomic Energy Commission, Washington, D. C.). Trans. Amer. Nucl. Soc.; 13: 488(Nov 1970).

From Meeting of the American Nuclear Society, Washington, D. C. See CONF-701102.

4036 DETECTION AND ANALYSIS OF A TITANIUM ORE USING ^{252}Cf. Wiggins, P. F. (Naval Academy, Annapolis); Duffey, Dick; Senftle, F. E. Trans. Amer. Nucl. Soc.; 13: 490(Nov 1970).

From Meeting of the American Nuclear Society, Washington, D. C. See CONF-701102.

4037 NEW BORON ANALYSIS METHOD. Weitman, J.; Daverhoeg, N.; Farvolden, S. (Aktiebolaget Atomenergi, Studsvid, Sweden). Trans. Amer. Nucl. Soc.; 13: 545-6(Nov 1970).

From Meeting of the American Nuclear Society, Washington, D. C. See CONF-701102.

4038 ISOTOPIC SOURCE ASSAY SYSTEM FOR NUCLEAR MATERIALS. Gozani, T.; Costello, D. G. (Gulf Energy and Environmental Systems, Inc., San Diego, Calif.). Trans. Amer. Nucl. Soc.; 13: 746-7(Nov 1970).

From Meeting of the American Nuclear Society, Washington, D. C. See CONF-701102.

4039 EXPRESS-METHOD FOR DETERMINING ^{90}Sr IN PLANTS. Saparlyev, Ch.; Zatsepina, L. N.; Kalishina, L. N. (Inst. of Botany, Ashkhabad, USSR. Inst. of Soil Science, Alma-Ata, USSR). Izv. Akad. Nauk Turkm. SSR, Ser. Biol. Nauk; No. 6, 19-22(1969). (In Russian).

An express method of determining ^{90}Sr in plants that excludes the determination of yield of stable strontium carrier from duty cycle is described. It reduces considerably time wastes and provides accuracy. (auth) (C.O.)

4040 MODIFICATION OF THE TSIVOGLOU METHOD FOR RADON DAUGHTERS IN AIR. Thomas, J. W. Health Phys.; 19: 691-2(Nov 1970).

The original Tsivoglou method, (NSA 7: 5695) is discussed. Improvements in the accuracy of the method by using the total alpha counts during selected time intervals after the end of sampling rather than the count rates at 5, 15, and 30 minutes after the end of sampling are considered. Air concentration equations for RaA, RaB, and RaC written directly in terms of alpha activities to make the method more convenient, are given. These give good agreement with the original, less accurate and more cumbersome, Tsivoglou method. (UK)

Activation Procedures

Refer also to abstracts 4133, 5472, and 5685.

4041 (AD-709901) SURVEY ON PHOTON ACTIVATION ANALYSIS USING THE NRL LINAC. Bendel, Warren L.; Numrich, Susan K. (Naval Research Lab., Washington, D. C.). 29 Jun 1970. 22p. (NRL-7109). NTIS.

Experiments show that microgram to nanogram quantities of carbon, nitrogen, oxygen, or fluorine can be detected using photon activation analysis. Irradiation with Linac bremsstrahlung is followed by coincidence counting of annihilation radiation. The minimum detectable amount of an element is strongly dependent on the material involved and the irradiation energy. Similar amounts of some other elements can be detected. (auth) (USGRDR)

4042 (CONF-680211-, pp 496-516) IN VIVO NEUTRON ACTIVATION ANALYSIS OF TOTAL BODY BONE MASS. Palmer, H. E.; Pailthorp, K. G. (Battelle-Northwest, Richland, Wash. Pacific Northwest Lab.); Nelp, W. B.; Murano, R.; Rich, C. (Washington Univ., Seattle. School of Medicine).

From Progress in methods of bone mineral measurements.

Measurements of the gamma rays emitted from human cadavers and phantoms after exposure to relatively low levels of fast neutrons show that several elements of body composition can be determined by this procedure. These elements include calcium, sodium, chlorine, nitrogen, and phosphorus. The determination of total body calcium may be one of the most important applications of this method. The results of this study show that the calcium content in man can probably be measured to an accuracy of ±8%, and that a change of 3% or more in the calcium content in the same person over a period of time can be detected. These results can be obtained with neutrons produced at a cyclotron and with radiation doses to the subject of 0.1 rad or less. The problems of obtaining a uniform neutron irradiation throughout the entire body and the methods used to overcome these problems are discussed. A sensitive method for measuring the induced radioactivity is described. The feasibility of measuring the relative bone mass of particular bone sections such as single vertebra by the use of collimated fast neutrons are also discussed. (auth)

4043 (GA-10125) MICRODETERMINATION OF FLUORINE IN HIGH-PURITY TUNGSTEN METAL BY PHOTOACTIVATION ANALYSIS. Buzzelli, G.; McDonald, K. (Gulf General Atomic, Inc., San Diego, Calif.). 4 Nov 1970. Contract AT(04-3)-167. 9p. Dep. NTIS.

A nondestructive method for determination of fluoride in assemblies of high-purity tungsten by photoactivation analysis was investigated. The samples were irradiated using the Gulf General Atomic 45-MeV linear accelerator and counted over an 8-hr period. The precision of the method appeared to be within ±10%, even at the 5-ppM level. (M.C.G.)

4044 REMOVAL OF ^{24}Na FROM NEUTRON-ACTIVATED SAMPLES. Bowen, H. J. M.; Cook, J. A. (Reading Univ., Eng.). Radiochem. Radioanal. Lett.; 5: 103-6(6 Nov 1970).

^{24}Na can be removed from neutron-activated samples by dissolving them in perchloric acid, diluting with an organic solvent, and passing the solution through a column of either sodium chloride or sodium perchlorate, using suction. The fractionation of several elements between column and eluate was tested. (auth)

4045 ACTIVATION ANALYSIS OF TRACE IMPURITIES IN THIN LAYERS OF SiO_2 AND Si_3N_4 ON SILICON. Kotas, P.; Kukula, F. Radiochem. Radioanal. Lett.; 5: 137-43(6 Nov 1970).

Neutron activation analysis was used for determination of trace impurities in thin layers of SiO_2 and Si_3N_4 on silicon. The layers were etched by hydrofluoric acid and silicon was removed in the form of volatile silicon fluoride. The residue was measured on a γ-spectrometer with a Ge(Li) detector. The series of analyses resulted in the determination of sodium in the range 2 to 5 ppM, copper 0.4 to 0.7 ppM, and arsenic 2 to 3 ppM. The relative error of the determination was 10 to 15%. The weight of the analyzed layer was about 5×10^{-5} g. (auth)

4046 DETERMINATION OF OXYGEN CONTENT IN SILICON BY MEANS OF PHOTONUCLEAR REACTION. Kasymov, A. K.; Masagutov, V. S.; Daminov, G. (Tashkent State Univ.). Dokl. Akad. Nauk Uzb. SSR; No. 1, 24-5(1970). (In Russian).

A method is described for the determination of oxygen in silicon by gamma activation in a betatron at a radiation dose of 7000 R/min. It was found that photon activation analysis exhibits high sensitivity and was in agreement with the data obtained by ir absorption. The oxygen content in silicon was 3 to 10^{-6} %. (R.V.J.)

4047 NON-DESTRUCTIVE NEUTRON ACTIVATION ANALYSIS FOR SOME TRANSITION ELEMENTS IN ROCKS. Dale, I. M.; Henderson, P.; Walton, A. (Univ. of Glasgow). Radiochem. Radioanal. Lett.; 5: 91-101(6 Nov 1970).

The Sc, Cr, Mn, Fe, and Co contents of ten standard rock samples were determined by instrumental neutron activation analysis. A comparison between these new results with those obtained by similar techniques and other methods was made. (auth)

4048 ALUMINUM AND SILICON ABUNDANCES OF SOME ITALIAN METEORITES AS DETERMINED BY INSTRUMENTAL ACTIVATION ANALYSIS. Meloni, Sandro; Maxia, Vera; Buzzi, Silvano (Univ., Pavia, Italy). Geochim. Cosmochim. Acta; 34: 1245-8(Nov 1970).

An instrumental pile neutron activation method for aluminum and silicon analysis in chondrites is described. Aluminum was first determined by irradiating the samples in a well-thermalized neutron flux through the reaction $^{27}Al(n,\gamma)^{28}Al$. Silicon was then determined by irradiating the samples in an in-core position where a high fast neutron flux was available. The relevant nuclear reaction was $^{28}Si(n,p)^{28}Al$. Corrections were applied for the interfering thermal activation of aluminum. (auth) (UK)

4049 NEUTRON ACTIVATION ANALYSIS OF TRACE ELEMENTS IN SKIN. IV. REGIONAL VARIATIONS IN COPPER, MANGANESE, AND ZINC IN NORMAL SKIN. Molokhia, Mohamed M.; Portnoy, Benjamin (Manchester and Salford Hospital for Skin Diseases, Manchester, Eng.). Brit. J. Dermatol.; 82: 254-5 (Mar 1970).

Levels of the trace metals copper, manganese and zinc in skin were found to vary in the same individual from one region of the body to another. The lowest concentrations were found in plantar epidermis while the highest levels were found in the epidermis of the foreskin. It is possible that these variations are related to dendritic cell populations in these areas. The separated epidermis and dermis were analyzed for copper, manganese, and zinc, using neutron activation techniques. (auth)

4050 ROLE AND HALF-LIFE IN ACTIVATION ANALYSIS. Guinn, Vincent P. (Univ. of California, Irvine). Trans. Amer. Nucl. Soc.: 13: 544-5(Nov 1970).

From Meeting of the American Nuclear Society, Washington, D. C. See CONF-701102.

Inorganic, Organic, and Physical Chemistry

Refer also to abstracts 4133 and 4732.

4051 (AI-AEC-12972) AEC UNCLASSIFIED PROGRAMS GFY 1970. Annual Technical Progress Report. (Atomics International, Canoga Park, Calif.). Contract AT(04-3)-701. 18p. Dep. NTIS.

Several attempts were made to prepare polywater, but without success. Thermal properties of superconductors are being studied. Void formation in nickel during high-temperature proton irradiation was investigated. (M.C.G.)

4052 (NYO-2043-216, pp 48-73) SOIL CHEMISTRY. (Inter-American Inst. of Agricultural Sciences, Turrialba (Costa Rica)).

From application of nuclear energy to agriculture. Annual report.

XUM

The uses of tracer techniques to study various chemical properties and reactions of soils are discussed. (M.C.G.)

Chemical Properties

Refer also to abstracts 4132, 4792, 4855, and 5154.

4053 (ANL-Trans-861) ADSORPTION OF MONOVALENT ASTATINE CATION BY CESIUM PHOSPHOTUNGSTATE AND HYDRATED TUNGSTEN OXIDE FROM NITRIC ACID SOLUTIONS. Norseev, Yu. V.; Khalkin, V. A.; Chao, Tao-nan. Translated for Argonne National Lab., Ill., from Izv. Sib. Otd. Akad. Nauk SSSR, Ser. Khim. Nauk; No. 3, 21-7(1965). 11p. Dep. NTIS.

Experimental data were obtained concerning the adsorption of astatine cation onto cesium phosphotungstate from nitric acid solutions. The astatine adsorption onto Cs_3PW is a reversible process. The distribution coefficient in 3M HNO_3–2×10^{-2}M $CsNO_3$–5×10^{-3}M $H_2Cr_2O_7$ at 15°C equals 420 ± 60. The quantity of astatine adsorbed onto Cs_3PW decreases sharply with an increase in temperature. Increasing acidity over the range of 1 to 5M HNO_3 has little effect on the adsorption process. It was found that in 1M HNO_3, bismuth readily destroys the H_3PW molecule. Information concerning the adsorption of astatine cation onto hydrated tungsten oxide is presented. (auth)

4054 (IS-Trans-83) THERMODYNAMICS OF THE REDUCTION OF THORIUM DIOXIDE BY CALCIUM. Zarembo, Yu. I. Translated from At. Energ. (USSR); 11: 185-6(1961). 4p. Dep. NTIS.

Initial thermodynamic data for calculating ΔZ^0_T and log K of the reaction for reducing thorium dioxide using calcium are shown. The results of calculations in the form of equations of the variation of the isobaric–isothermic potential of the reaction are given and the relationship between ΔZ^0, log K, R_{C_a} and temperature illustrated. The results of thermodynamic calculation show that at 1000 to 1100°K (optimum temperature of the process of calcium-thermal reduction) the reaction in which thorium and calcium oxide are formed is practically complete since the equilibrium calcium vapor pressure is very low at these temperatures. The reduction of thorium dioxide bicalcium is possible in this case only at temperatures below 1760°K (boiling point of calcium). (auth)

4055 MANDELATES OF LANTHANUM, PRASEODYMIUM, NEODYMIUM, AND URANIUM. Dubey, S.; Bhandari, A. M.; Misra, S. N.; Kapoor, R. N. (Univ. of Jodhpur, India). Indian J. Chem.; 7: 701-5(Jul 1969).

The reactions of the lanthanon (La, Pr, and Nd) alkoxides with mandelic acid were carried out in different molar ratios to yield products of the type: $M(OC_3H_7^i)[OOC \cdot CH(O)C_6H_5]$, $M[OOC \cdot CH(O)C_6H_5][OOC \cdot CH(OH)C_6H_5]$ and $M[OOC \cdot CH(OH)C_6H_5]_3$. Uranium pentaethoxide on treatment with mandelic acid yielded $U(OEt)_3[OOC \cdot CH(O)C_6H_5]$, $U(OEt)[OOC \cdot CH(O)C_6H_5]_2$ and $U[OOC \cdot CH(O)C_6H_5]_2[OOC \cdot CH(OH)C_6H_5]$. A detailed study of the complexation reaction of uranyl ion with mandelic acid was also made by the potentiometric method. The formation of 1:1 and 1:2 complexes was confirmed by preparative studies. Four compounds, viz. $(C_5H_6N)_2UO_2(O_3C_8H_6)_2$, $(NH_4)_2UO_2(O_3C_8H_6)_2$, $Na_2UO_2(O_3C_8H_6)_2$ and $K_2UO_2(O_3C_8H_6)_2$, were isolated. (auth)

4056 STUDIES IN CARBOXYLATES OF METALS. PART II. THORIUM CARBOXYLATES. Paul, R. C.; Saran, Mohan Singh; Bains, M. S. (Panjab Univ., Chandigarh, India). Indian J. Chem.; 7: 384-6(Apr 1969).

A number of new carboxylates of thorium were prepared in quantitative yield by an acid interchange method in which thorium acetate is refluxed with an excess of the higher boiling carboxylic acid and the liberated acetic acid is removed under suction. Thermogravimetric analysis of these carboxylates was carried out to throw light on their stability and mode of decomposition. (auth)

4057 STUDIES IN CARBOXYLATES OF METALS. PART I. URANIUM(IV) CARBOXYLATES. Paul, R. C.; Saran, Mohan Singh; Ghotra, J. S.; Bains, M. S. (Panjab Univ., Chandigarh, India). Indian J. Chem.; 7: 381-3(Apr 1969).

A new method for the preparation of uranium(IV) acetate in almost quantitative yield is described. Uranyl chloride and uranyl acetate are reduced with zinc amalgam in glacial acetic acid. On refluxing the reduced solutions with acetic anhydride, uranium(IV) acetate and zinc hexaacetato uranate(IV), respectively, are obtained. The latter on treatment with hydrochloric acid followed by refluxing with acetic anhydride also yields uranium(IV) acetate. Other uranium(IV) carboxylates were also prepared by an acid interchange method where uranium(IV) acetate is refluxed with an excess of higher boiling carboxylic acid and the liberated acetic acid is removed under suction. Thermogravimetric analyses of these carboxylates were also carried out. (auth)

4058 PREPARATION OF SOME URANIUM(IV) FLUORIDE COMPLEXES. Sahoo, B. (Indian Inst. of Tech., Kharagpur, India); Satpathy, K. C. Indian J. Chem.; 6: 460-1(Aug 1968).

A new hydrazine uranium(IV) fluoride complex, $UF_4(N_2H_4HF)_2$, was isolated. The complex on thermal decomposition at 400°C yields anhydrous uranium tetrafluoride. Uranium tetraformate, $U(HCOO)_4$, was prepared by refluxing uranium(IV) oxyformate, $UO(HCOO)_2 \cdot 1.5H_2O$, with formic acid. It reacts with ammonium bifluoride at 250°C to yield the anhydrous complex, UF_4NH_4F. Fluoride complexes of uranium(IV) with methylamine, diethylamine and tetramethylammonium ion were also prepared by photolytic process. The compounds prepared are $UF_4CH_3NH_2HF$, H_2O, $UF_4[(C_2H_5)_2NHHF, H_2O]_{\frac{1}{2}}$ and $UF_4[(CH_3)_4NF]_{\frac{1}{2}}$ respectively. Controlled thermal decomposition of these compounds does not afford anhydrous UF_4, since considerable decomposition to oxides of uranium takes place. (auth)

4059 URANIUM SULFIDE TRANSPORT. Slovyanskikh, V. K.; Sevast'yanov, V. G.; Ellert, G. V. Zh. Neorg. Khim.; 15: 2064-6 (Aug 1970). (In Russian).

The mechanism of transport of uranium sulfides through a gas phase in a closed volume was studied. The relation of the yield of monocrystals to the ratio of sulfur and uranium in the initial composition is given. Characteristic photographs of crystals grown are shown. (tr-auth)

4060 TWENTY-FIRST FARKAS MEMORIAL SYMPOSIUM ON PHOTOCHEMISTRY OF AQUEOUS AND POLAR SYSTEMS HELD IN JERUSALEM, 29–30 DECEMBER, 1969. Israel J. Chem.; 8: 103-279(1970). (CONF-691221).

Fourteen papers were presented and a separate abstract was prepared for one. (D.H.M.)

For an abstract of one paper see: 4132.

Isotope Effects and Exchange

Refer also to abstracts 4124 and 5172.

4061 BOND POLARIZABILITY INTERPRETATION OF THE RAMAN INTENSITIES OF CYCLOHEXANE AND CYCLOHEXANE-d_{12}. Snyder, R. G. (Shell Development Co., Emeryville, Calif.). J. Mol. Spectrosc.; 36: 204-21(Nov 1970).

The Raman intensities of cyclohexane and cyclohexane-d_{12} are interpreted in terms of a modified bond polarizability model. The main emphasis is on the vibrations below 1500 cm^{-1}. Both the spherical and anisotropic parts of the derived polarizability tensors are considered. The observed values of the derived mean polarizabilities were used to evaluate three parameters $\bar{\alpha}'_{CC}$, $\bar{\alpha}'_{HCH}$, and $\bar{\alpha}'_{CCC}$ while in a less satisfactory but nonetheless illuminating calculation the derived anisotropies were used to evaluate three more parameters $\bar{\beta}'_{CC}$, $\bar{\beta}'_{CH}$, and $\bar{\beta}'_{CC}$. Uncertainties in the data, the normal coordinates, and the model are discussed. (auth)

4062 INTERPRETATION OF THE RAMAN SPECTRUM OF POLYETHYLENE AND DEUTEROPOLYETHYLENE. Snyder, R. G. (Shell Development Co., Emeryville, Calif.). J. Mol. Spectrosc.; 36: 222-31(Nov 1970).

The Raman spectrum of polyethylene and deuteropolyethylene was calculated using polarizability parameters from cyclohexane. It was found that the spectrum of the stretched polymer measured by Hendra and Willis is not in conflict with the previously established assignments. From this spectrum the sign relationship between the spherical part and the anisotropy of the derived polarizability tensor can be determined. Polarizability components for CH and CC bonds are reported. It is concluded that the quantity $\Gamma_{CC}(=\bar{\beta}_{CC} - 2\bar{\beta}_{CH})$ is negative, contrary to general opinion. (auth)

4063 $^2\Pi - X\ ^2\Pi$ SYSTEM OF $^{14}N^{80}Se$ AND $^{14}N^{78}Se$. Subbaram, K. V.; Ramachandra Rao, D. (Indian Inst. of Tech., Kanpur). J. Mol. Spectrosc.; 36: 163-82(Nov 1970).

Vibrational and rotational analyses were carried out for some of the intense emission bands recorded in the region 3950 to 5675 Å for $^{14}N^{80}Se$ and $^{14}N^{78}Se$. The analyses yield the molecular constants indicating the electronic transition involved as $^2\Pi(a)$ to $X^2\Pi(a)$. It was possible to estimate the Λ-doubling coefficients for the upper and lower states in the $^2\Pi_{\frac{1}{2}}$ to $^2\Pi_{\frac{1}{2}}$ component from the observed large Λ-splittings. (auth)

4064 INFRARED DISPERSION IN LIQUID BENZENE AND BENZENE-d_6. Zelano, A. J.; King, W. T. (Brown Univ., Providence). J. Chem. Phys.; 53: 4444-50(15 Dec 1970).

The intensities of the major infrared absorption bands in liquid C_6H_6 and C_6D_6 were measured by an interferometric method. The

intensities of the very intense a_{2u} modes were found to be 14,450 ± 110 and 8600 ± 110 cm^{-1} cm^2/mM for C_6H_6 and C_6D_6, respectively. Small, but significant deviations from the predictions of the "oriented gas model," used to interpret these measurements, were observed. (auth)

4065 LONGITUDINAL MODES IN HYDROGEN AND DEUTERIUM HALIDE CRYSTALS. Friedrich, H. B.; Carlson, R. E. (Univ. of Iowa, Iowa City). J. Chem. Phys.; 53: 4441-3(15 Dec 1970).

The observation of four bands in the Raman spectra of the internal modes of crystalline HCl, DCl, HBr, and DBr was previously explained either by assuming a four-molecule primitive cell, which is different than the structure suggested by diffraction studies, or by assuming that two of the bands were due to longitudinal modes. Experimental infrared intensities with a dipolar coupling model appropriate to the cell symmetry were used to compute the LO frequencies. The calculated frequencies are in excellent agreement with those observed in the hydrogen and deuterium halide crystals. (auth)

4066 MATRIX-ISOLATION SPECTRA OF H_2S AND D_2S: AN EXAMPLE OF THE APPLICATION OF THE UNCOUPLED OSCILLATOR APPROXIMATION. Pacansky, Jacob; Calder, V. (Iowa State Univ., Ames). J. Chem. Phys.; 53: 4519-24(15 Dec 1970).

The first direct observation of the ν_3 vibration of H_2S and D_2S is reported. The location of this fundamental in the matrix spectra is constant with the band center calculated from the overtone-combination frequencies in the gas phase. General, quadratic, valence force constants are calculated from the isotopic shifts using simple equations based on the uncoupled oscillator approximation. (auth)

4067 METAL ISOTOPE AND HIGH PRESSURE EFFECTS ON THE INFRARED ACTIVE SKELETAL VIBRATIONS IN METAL SANDWICH COMPOUNDS. Nakamoto, K.; Udovich, Carl; Ferraro, John R.; Quattrochi, A. (Argonne National Lab., Ill.). Appl. Spectrosc.; 24: 606-8(Nov-Dec 1970).

Results are reported on metal isotope and high-pressure effects on skeletal vibrations in several metallocenes. The effects of ^{54}Fe and ^{57}Fe on the spectra of ferrocene were determined. (M.C.G.)

4068 INFRARED AND RAMAN SPECTRA OF PYRAZINIUM HALIDES. Foglizzo, R.; Novak, A. (CNRS, Paris. Faculte des Sciences, Paris). Appl. Spectrosc.; 24: 601-5(Nov-Dec 1970).

The ir and Raman spectra of pyrazinium chloride and bromide and their ND deuterated derivatives were obtained in the 4000 to 300 cm^{-1} range. Twenty-six fundamentals of the pyrazinium ion were identified and compared to those of the pyrazine molecule. Frequency shifts on protonation of pyrazine are discussed. (auth)

4069 EFFECT OF SUBSTITUENTS ON HYDROGEN EXCHANGE REACTION OF SOME FERROCENE DERIVATIVES. Kursanov, D. N.; Setkina, V. N.; Fedin, E. I.; Nefedova, M. N.; Khatami, A. I. Dokl. Akad. Nauk SSSR; 192: 339-41(11 May 1970).

The influence of substitutes with oppositely directed induced effects and with a conjugated effect (conditions under which the properties of ferrocene were easily distinguished from other aromatic systems especially from benzene) was studied in order to determine the rate of hydrogen exchange in $FSCH_3$ and $F(SCH_3)_2$. (R.V.J.)

4070 CHEMICAL ACTION OF LASER RADIATION ON ACETYLENE. Yampolskii, Yu. P.; Maksimov, Yu. V.; Novikov, N. P.; Lavrovskii, K. P. (Inst. of Petrochemical Synthesis, Moscow. Inst. of Problems of Mechanics, Moscow). Khim. Vys. Energ.; 4: 283-4(May-Jun 1970). (In Russian).

The effects of neodymium laser radiation on gaseous acetylene were investigated using acetylene, deuteroacetylene, and equimolar mixtures of C_2H_2 and C_2D_2. The irradiation of C_2D_2 yielded chiefly ethane, and the irradiation of C_2H_2, ethylene. The irradiation of C_2H_2 resulted also in the formation of a considerable amount of C_4H_2 whereas it was absent in the products obtained from C_2D_2. Mass spectrometric analysis of the isotopic composition of irradiation products of an equimolar $C_2H_2-C_2D_2$ mixture showed that under these conditions an intensive isotope exchange takes place resulting in the formation of C_2HD. (D.H.M.)

4071 ELECTROLYTE EFFECT IN THE ISOTOPIC EXCHANGE REACTION BETWEEN AMMONIUM BROMIDE AND BUTYL BROMIDE IN ACETONE. Beronius, P.; Holmgren, A.; Nilsson, A.-M.; Wikander, G. (Univ. of Umea, Sweden). Radiochem. Radioanal. Lett.; 5: 131-5(6 Nov 1970).

A strong dependence of the second-order rate constant on the electrolyte concentration in the exchange reaction, $NH_4{}^{82}Br + BuBr \rightleftharpoons NH_4Br + Bu^{82}Br$, in acetone as solvent was observed. Increasing the concentration of ammonium bromide from 1×10^{-4} to 3×10^{-4} M results in a nearly twofold decrease in the rate constant. This effect is interpreted in terms of the Acree hypothesis, which indicates that only the unpaired bromide ions undergo any measurable exchange with the organic bromide. (auth)

4072 ISOTOPIC EXCHANGE LAWS. VII. THERMODYNAMIC ISOTOPIC EFFECTS OF HYDRIDES. Knyazev, D. A.; Bantysh, A. N.; Ivlev, A. A. (Moscow Physical-Technical Inst.). Zh. Fiz. Khim.; 44: 1497-1503(Jun 1970). (In Russian).

Precise calculations were made of the ratios of statistical sums for states of the isotopic forms (beta factors) of several hundred normal and substituted hydrides. Corrections for anharmonicity were very significant in the case of the hydrogen isotope effect. The temperature relations of the beta factors of normal and substituted hydrides were studied. It is shown that the derived d ln $\beta/d(1/T)$, the analog of increasing enthalpy, is constant in the range 100 to 500°K. The magnitudes of these derivatives within the limits of the subgroup of related compounds are directly proportional to the magnitudes of beta. (tr-auth)

4073 EFFECT OF THE PARTICIPATION OF THE ACID IN FORMING THE HYDROGEN BOND DURING ELECTROPHILIC DEUTERIO-EXCHANGE. Zvyagintseva, E. N.; Gorbenko-Germanov, D. S.; Shatenshtein, A. I. (Inst. of Physical Chemistry, Moscow). Zh. Obshch. Khim.; 40: 1152-6(May 1970). (In Russian).

Rate constants are given for the deuterio-exchange reaction for 2.5-di-tert-butyl-3,4-dideuteriothiophene in trifluoroacetic acid. Addition of acetic acid decreased the rate constant by 3 or 4 orders of magnitude at molar ratios of 1:1 or 1:2, respectively. Infrared spectra confirmed the role played by the acid in the kinetics of electrophilic deuterio-exchange with respect to hydrogen bond formation. (M.C.G.)

Physical Chemistry

Refer also to abstracts 4754, 4760, and 4843.

4074 (UCRL-19685) VAPORIZATION MECHANISM OF GALLIUM ARSENIDE SINGLE CRYSTALS. Lou, Catherine Yuen-Chien (California Univ., Berkeley. Lawrence Radiation Lab.). Sep 1970. Contract W-7405-eng-48. 104p. Dep. NTIS.

The kinetics of vaporization of gallium arsenide single crystals into vacuum were investigated using microbalance and mass spectrometric techniques in the temperature range 700 to 900°C. It was found that gallium arsenide vaporized incongruently to give liquid gallium and arsenic vapor molecules. The total evaporation rates and the activation energies were found to be the same for both (111) and $(\bar{1}\bar{1}\bar{1})$ faces. The initial vacuum vaporization rate of gallium arsenide single crystals is lower than the maximum rate calculated from equilibrium vapor pressures by about a factor of two but the activation energy is the same (90 kcal/mole) as the heat of sublimation (per mole of GaAs). When excess gallium liquid was placed on top of the vaporizing surface, the rate was found to be increased by a factor of two compared to the calculated maximum rate, while the activation energy remained unchanged. Both Te-doped and Zn-doped GaAs samples give lower evaporation rates. The activation energy for Te-doped samples is 90 kcal/mole, the same as that found for pure samples. However the activation energy of vaporization is lower for the Zn-doped samples (76 kcal/mole). When excess gallium liquid was placed on top of the surface of these samples, the vaporization rate was found again to have increased to the maximum rate, with the activation energies remaining the same as those without the excess liquid gallium on top. The vapor compositions for the (111) and $(\bar{1}\bar{1}\bar{1})$ faces were found to be different from mass-spectrometric studies. Vaporization of the (111) or Ga face, yielded only tetramers (As_4). However, during the vaporization of the $(\bar{1}\bar{1}\bar{1})$ or As face both the tetramers (As_4) and the dimers (As_2) were detected. Excess gallium liquid on top of the crystal surfaces does not seem to affect the vapor compositions significantly. On the basis of these experimental results, a model for the vaporization mechanism of gallium arsenide single crystals is proposed. (auth)

4075 STUDIES OF MALEIC ACID COMPLEXES OF RARE EARTHS AND OTHER METALS. PART I. PREPARATION AND THERMAL BEHAVOIR. Bhat, T. R.; Mathur, B. S.; Shankar, J. (Bhabha Atomic Research Centre, Bombay). Indian J. Chem.; 8: 275-81(Mar 1970).

The preparation and thermal behavior of maleic acid complexes of the rare earths, Y, Ca, Mn, Co, Ni, Cu, Zn, Cd, U, and Th, were investigated. In all the cases (except Th) two types of complexes are formed: (i) normal complexes of the type $M_2L_n \cdot XH_2O$, and (ii) acido complexes of the type $M(LH)_n \cdot XH_2O$, where n is the

charge of the metal ion. Thorium forms only the normal complex. In the acido complexes the dibasic acid acts as a monodentate ligand. The normal complexes undergo hydrolytic disproportionation of the type, $M_2L_n + nH_2O \rightleftharpoons M(OH)_n + M(LH)$, on heating in aqueous solution, indicating their strong tendency to form acido complexes. The thermal behavior of the normal complexes is similar to that of oxalates. However, in the case of the acido complexes, a part of the ligand is volatilized before thermal degradation, indicating reaction of the type, $2M(LH)_n \rightleftharpoons M_2L_n + nLH_2$. The strong tendency of maleic acid, unlike other dibasic acids, to act as a monodentate ligand is attributed to its structure, which favors the formation of intramolecular hydrogen bonds. (auth)

4076 AQUOLUMINESCENCE FROM GAMMA-IRRADIATED HALIDES. Arnikar, H. J.; Damle, P. S.; Chaure, B. D.; Rao, B. S. M. (Univ. of Poona, India). Nature (London); 228: 357-8(24 Oct 1970).

The observation of a faint bluish-green glow, with a peak ~5000 Å, is reported when γ-irradiated NaCl, NaBr, KCl or KBr is dissolved in distilled water. A high speed photographic film was blackened within about 10 min by direct exposure to the glow, and the glow could be received on a photomultiplier and the output displayed on an oscilloscope. The maximum intensity developed in ~0.1 sec, and the decay time was 2 to 3 sec. The following mechanism is proposed: e^- (trapped in lattice) + water → e^- aq.; and e^- aq + Cl^0 → Cl^- aq + hν. The emission of a photon in a reaction of this type does not appear to have been hitherto reported. Data were obtained for the energy barrier for the trapped electron (1.1eV for NaCl), the first order rate constant for thermal annealing (3.5×10^{-2} sec^{-1} at 423°K), and the maximum number of defects producible by γ irradiation (2×10^{19}/mole in NaCl). It was concluded that the effect appears to offer a relatively simple method for studying irradiation effects in crystals. (UK)

4077 THERMOCHEMICAL STUDIES OF THORIUM(IV) AND URANIUM(IV) CHLORIDES. Smith, B. C.; Thakur, Lambodar; Wassef, Marguerite A. (London Univ.). Indian J. Chem.; 7: 1154-7(Nov 1969).

The standard heats of formation of crystalline thorium tetrachloride and uranium tetrachloride were redetermined, and the values agree well with the values recorded in literature. The bond energy terms for the gaseous tetrachlorides are: E{Th[4]–Cl} 118.4 kcal/mole [496 kJ $mole^{-1}$]; E{U[4]–Cl} 108.1 kcal/mole [452 kJ $mole^{-1}$]. The standard heats of formation of the crystalline uranium tetrachloride tetrakisalcohols, $UCl_4.4ROH$ (R = Me, Et, Pr^i), are −510.3, −546.8, and −587.9 kcal/mole [−2135, −2288, and −2460 kJ $mole^{-1}$] respectively. A comparison of the related bond energy terms and internuclear distances for thorium and uranium tetrachlorides in the gaseous and crystalline state reveals that the bonds are longer and stronger in $ThCl_4$ as compared to UCl_4. In the case of uranium tetrachloride tetrakisalcohol complexes of MeOH, EtOH, and iso-PrOH the coordinate bonds from oxygen appear to be stronger than the coordinate bonds from chlorine. The strengths of oxygen–uranium bonds increase along the series MeOH < EtOH < iso-PrOH. (auth)

4078 COMPLEXES BETWEEN URANIUM(VI) AND DIOXYDIQUINONE. Banerjee, Amitav; Mandal, Sukumar; Singh, Tej; Dey, Arun K. (Univ. of Allahabad, India). Indian J. Chem.; 7: 733-4(Jul 1969).

Complex formation between uranium(VI) and dioxydiquinone was studied using the Bjerrum–Calvin pH-titration technique. The protonation constant log K_1^H of the ligand is 5.06 and the stepwise formation constants of the complexes are: log K_1 = 5.57; and log K_2 = 3.09, determined at 25°C and at a constant ionic medium of 0.1M ($NaClO_4$). (auth)

4079 SATURATED VAPOR PRESSURE OF SOLID UF_4. Chudinov, E. G.; Choporov, D. Ya. Zh. Fiz. Khim.; 44: 1955-61 (Aug 1970). (In Russian).

The vapor pressure of solid UF_4 was measured by the effusion method at 555 to 1007°C. The data obtained are described by the equation $\lg P = 28.539 - 16504.9/T - 4.876 \lg T$. (tr-auth)

4080 POTENTIOMETRIC INVESTIGATION OF METAL COMPLEXES WITH PHENANTHRENEQUINONE MONOXIME. Trikha, K. C.; Dutt, Yag; Singh, R. P. (Univ. of Delhi). Indian J. Chem.; 6: 376-8(Jul 1968).

Dissociation constant of phenanthrenequinone monoxime and formation constants of some of its metal complexes were determined potentiometrically in 75% dioxane at constant ionic strength (0.1M) maintained by adding sodium perchlorate. The order of stability of the complexes is Cu > UO_2 > Ni > Be > Pb > Zn > Cd > Mn > Mg. (auth)

4081 PROTON NMR STUDIES OF 8-QUINOLINOL AND SEVERAL OF ITS METAL CHELATES AND ELECTROCHEMISTRY OF URANIUM–EDTA COMPLEXES. Baker, Blair Coleman. Riverside, Calif.; Univ. of California (1969). 147p. University Microfilms Order No. 70-11,978.

Thesis.

The proton NMR spectrum of 8-quinolinol (oxine, HOx) has been analyzed and assigned using computer techniques and substituted derivatives of oxine. Substituent effects for the ring-nitrogen and hydroxyl group have been studied by comparing the NMR spectra of ozine, quinoline, and naphthol with that of naphthalene. A definite correlation between the NMR spectra of these compounds and Extended Huckel calculations of total electron densities has been established. The metal-oxine chelates of Ba(II), Ca(II), Hg(II), Mg(II), Pb(II), Pd(II), Pt(II), Sn(II), Al(III), Bi(III), Co(III), Rh(III), Tl(III), Y(III), Th(IV), and U(VI) have been investigated by NMR methods. Consideration of chemical shift changes of the phenolic-ring and hetero-ring protons of the oxine ligand in the metal chelates relative to their position for the free ligand provides a measure of the strength (or lability) of the coordinate bonds to the oxygen and nitrogen atoms of the ligand. Structures are proposed which are consistent with the experimental data. In addition, the "solvated" oxinates of thorium(IV) and uranium(VI) have been examined. The data establish that the extra oxine in $ThOx_4 \cdot HOx$ and $UO_2Ox_2 \cdot HOx$ is only bound in the solid state and is completely removed in solution. The complex anion $UO_2Ox_3^-$ was found to be stable in solution with all three ligands equivalently bound. The red form of $UO_2Ox_2 \cdot HOx$ and the trihydrate, $UO_2Ox_2 \cdot 3H_2O$, can be dried to constant weight at 150°. The electrochemistry of the 1:1 uranium(VI)–EDTA complex has been investigated by cyclic voltammetry, controlled potential coulometry, and chronopotentiometry at mercury and platinum electrodes. Between pH 5 and 7 the complex is reduced by two irreversible one-electron steps with a chemical step between them (an ECE mechanism) to a stable uranium(VI)–EDTA species. At pH 6.4 and a scan rate of 0.02 V/sec the peak potential for reduction of the complex is −0.87 V vs SCE. On the basis of the electrochemical data and pH studies the electroactive species is UO_2YH^- (Y represents the tetraanion of EDTA); its diffusion coefficient at 25° is 5.5×10^{-6} cm^2/sec. The electron transfer kinetic parameters, n_a and k_{fb}°, have values of 0.2 and 2.1×10^{-5}, respectively. (Diss. Abstr. Int., B)

4082 THERMAL STABILITY OF AMMONIUM URANYL FLUORIDES. Davidovich, R. L.; Epov, D. G.; Buslaev, Yu. A. (Inst. of General and Inorganic Chemistry, Moscow). Dokl. Akad. Nauk SSSR; 193: 822-5(1 Aug 1970). (In Russian).

In previous studies on the decomposition of $(NH_4)_3UO_2F_5$, it was not possible to establish unequivocally that the pentafluoride is decomposed into the trifluoride $NH_4UO_2F_3$. Tests were therefore carried out on the decomposition of this compound and of the $(NH_4)_2(UO_2)_3F_8 \cdot 4H_2O$ complex. Thermogravimetric results indicated that the pentafluoride starts to decompose at 180°C and continues to lose up to 2.5 NH_4F molecules between 200 and 300°C. The thermogram also indicated that further decomposition results in an exothermic reaction with a maximum at 420°C. The overall reaction included the following steps:

$$2(NH_4)_3UO_2F_5 \xrightarrow[-5NH_4F]{400^\circ} NH_4(UO_2)_2F_5 \xrightarrow[-NH_4F]{400^\circ} 2UO_2F_2 \xrightarrow{600^\circ} U_3O_8.$$

The corresponding thermal decomposition of the complex goes through the following steps:

$$2(NH_4)_2(UO_2)_3F_8 \cdot 4H_2O \xrightarrow[-8H_2O]{105^\circ} 2(NH_4)_2(UO_2)_3F_8 \xrightarrow[-NH_4F]{250^\circ} 3NH_4(UO_2)_2F_5$$
$$\xrightarrow[-3NH_4F]{400^\circ} 6UO_2F_2 \xrightarrow{600^\circ} U_3O_8$$

Removal of 4 molecules of water is accompanied by a weight loss of 6.72%. A second endothermic effect at 280°C relates to the decomposition of the dehydrated salt, corresponding to the splitting off of 0.5 molecule of NH_4F from $(NH_4)_2(UO_2)_3F_8$. An intermediate complex, $(NH_4)(UO_2)_2F_5$ is formed during the thermal decomposition of ammonium unanyl fluoride complexes; its identity was confirmed by chemical, roentgenographic, thermogravimetric, and infrared spectroscopic analyses. The final decomposition yields UO_2F_2 which is hydrolyzed at high temperatures by moist air. (TTT)

4083 STABILITIES OF DIVALENT AND TRIVALENT METAL COMPLEXES OF HYDROXAMIC ACIDS. Seshadri, T. (Indian Association for the Cultivation of Science, Jadavpur, India). Indian J. Chem.; 8: 282-3(Mar 1970).

The formation constants of several metal complexes of hydroxamic acids, viz. benzohydroxamic, nicotinohydroxamic, salicylhydroxamic, and oxalodihydroxamic acids, were determined by pH-metric titration method at 30° ± 0.5°C maintaining ionic strength at 0.1M with respect to sodium perchlorate. The calculated values of solubility products of copper complexes with benzohydroxamic, nicotinohydroxamic and salicylhydroxamic acids suggest that these reagents can be used for the gravimetric estimation of copper. (auth)

4084 SPECTROSCOPIC INVESTIGATIONS IN THE SYSTEM $MeUO_4$–ThO_2 WITH Me = Nd, Dy, Ho, Yb, AND Y. Kemmler-Sack,

Sibylle; Ruedorff, Walter (Univ., Tuebingen, Ger.). Z. Naturforsch.; 25b: 905-10(Sep 1970). (In German).

Spectroscopic investigations in the system $(Me_{0.5-x/2}U_{0.5-x/2} \times Th_x)O_2$ with Me = Nd, Gd, Dy, Ho, Yb, and Y showed that the level splitting of uranium can not be reconciled with the existence of a cubic oxygen coordination. As a possible explanation of the experimental material, the assumption of a uranyl group, UO_2^+, is discussed. (tr-auth)

4085 IONIC RADII FOR USE IN GEOCHEMISTRY. Whittaker, E. J. W.; Muntus, R. (Oxford Univ.). Geochim. Cosmochim. Acta; 34: 945-56(1970).

The ionic radii proposed by Shannon and Prewitt (1969, 1970) as the effective values in oxides and fluorides were analysed for their conformity with the radius ratio principles of crystal chemistry. It is shown that a set of values intermediate between the "IR" and "CR" values of Shannon and Prewitt provides the best conformity in this respect, and a table of the values adopted is provided in periodic form. These values correspond to a VI coordinate oxygen radius of 1.32 Å and a VI coordinate fluorine radius of 1.25 Å, and the radii of the cations are therefore appreciably larger than those previously accepted, although not as large as Shannon and Prewitt's "CR" values. It is suggested that the radii obtained are most suitable for use in silicate geochemistry, and constitute a major improvement over previous values for this particular purpose. Although it is impossible to maintain the accuracy with which radius sums represent interatomic distances and at the same time to extend the range of the radii to other anions, it seems desirable to provide compatible (although only very approximate) values of radii for Cl, Br, I, S, and Se anions. Use of the new cation radii with these anion radii cannot be expected to be an improvement over the use of older radii, but should be about as satisfactory. The changes of cation radii relative to one another, as compared with Ahrens' radii, are tabulated in order to draw attention to their possible geochemical significance, and the implications are discussed in the case of scandium. (auth) (UK)

4086 DETERMINATION OF THE ACTIVITY COEFFICIENTS OF URANYL PERCHLORATE IN AQUEOUS SOLUTIONS. Schwabe, K.; Kretschmar, R.; Gaertner, R.; Rottenbach, R. (Technische Univ., Dresden). Z. Phys. Chem. (Leipzig); 238: 391-9(1968). (In German).

An attempt was made to find a method for determination of the activity coefficients in which the calculations are not made incorrect by hydrolysis. The activity coefficient decreased with decreasing concentration from f = 1 at c = 0 to f = 0.30 at c = 2.1 m; it then increased again to a value f = 3.9 at c = 5.3 m. The discrepancies between the values obtained from vapor pressure measurement and with the help of diffusion coefficients and from sedimentation equilibrium values are discussed. (M.C.G.)

4087 ANTIPYRINE COMPLEXES OF TITANIUM(IV), ZIRCONIUM(IV), THORIUM(IV), AND URANIUM(VI) PERCHLORATES. Savant, V. V.; Ramamurthy, P.; Patel, C. C. (Indian Inst. of Science, Bangalore). J. Less-Common Metals; 22: 479-86(Dec 1970).

Antipyrine complexes of TiO^{2+}, ZrO^{2}, Zr^{4+}, Th^{4+}, and UO_2^{2+} perchlorates with molecular formulas $TiO(Apy)_4(ClO_4)_2$, $ZrO(Apy)_3(ClO_4)_2$, $Zr(Apy)_5(ClO_4)_4$, $Th(Apy)_7(ClO_4)_4$, and $UO_2(Apy)_5(ClO_4)_2$ have been prepared and characterized. The complexes are stable in air at room temperature and decompose exothermally at ~300°C. The ir study indicated the bonding of the antipyrine to the metal ion through its carbonyl oxygen. The nature of the bonding of the perchlorate and the stereochemistry of the complexes are discussed in the light of infrared spectra, conductivity in solvents of different polarity, and molecular weight measurements. From the UO_2^{2+} group frequencies, the force constant K and r_{U-O} are found to be 6.29×10^5 dynes/cm^{-1} and 1.74 Å, respectively. (auth)

Radiation and Nuclear Chemistry

4088 (NP-18528) REPORT AND ACCOUNTS OF THE UNITED KINGDOM ATOMIC ENERGY AUTHORITY FOR THE YEAR ENDED 31st MARCH 1970 TOGETHER WITH THE COMPTROLLER AND AUDITOR GENERALS REPORT ON THE ACCOUNTS. Sixteenth Annual Report and Accounts, 1969–70. (United Kingdom Atomic Energy Authority, London (England)). 22 Jul 1970. 118p. Dep. NTIS (U. S. Sales Only). UK 17s.

The report is presented under the following headings; general survey, finance, accounts and contracts; trading fund report, production factories and the Radiochemical Center Amersham, the reactor program, nuclear fusion and plasma physics research, applied nuclear research and development, non-nuclear research and development, scientific and technical support, underlying research, major equipment, health and safety, international relations, information services, and the Authority's organization and staff. (UK)

Radiation Effects

Refer also to abstracts 4384, 4546, and 4547.

4089 EFFECT OF VARIOUS DRY ELECTRON SCAVENGERS ON THE RADIOLUMINESCENCE OF INDOLE IN POLAR SOLUTION. Steen, H. B. (Norsk Hydro's Inst. for Cancer Research, Oslo). J. Phys. Chem.; 74: 4059-61(12 Nov 1970).

The electron scavengers H_2O_2, $ClCH_2COOH$, CCl_3COOH, and $NaNO_3$ were found to reduce significantly the yield of the x-radioinduced phosphorescence of indole in ethylene glycol–water glass at 77°K when present in concentrations >0.1M. The reactions involved obey homogeneous competition kinetics. Since the major fraction of this phosphorescence is supposedly due to the geminate recombination between positive indole ions and nonhydrated electrons (e^-), this effect is attributed to the reaction between the electron scavengers and e^-. No effect of HCl was found. This is in agreement with the hypothesis of Hamill that $H_3O^+_{aq}$ is unreactive toward e^-. The relative scavenging constants determined by the present experiments agree with those obtained for what is believed to be e^- by picosecond pulse radiolysis of aqueous solutions, while they are significantly different from the scavenging constants reported both for "mobile electrons" in strongly acidic glasses as well as for e^-_{aq} in water. (auth)

4090 OXIDES AND OXYIONS OF THE NON-METALS. PART XIV. STRUCTURE AND REACTIVITY OF THE OXYANIONS OF TRANSITION METALS. PART XIX. ELECTRON SPIN RESONANCE STUDY OF THE RADICALS AsO_4^{2-} AND VO_4^{2-} FORMED BY γ-IRRADIATION OF ARSENATE AND VANADATE IN CALCIUM TUNGSTATE. Subramanian, S.; Symons, M. C. R. (Univ. of Leicester, Eng.). J. Chem. Soc., A; No. 14, 2367-70 (1970).

Hyperfine coupling to A for a range of X_2AO and X_3AO radicals with one electron less than the closed-shell species is reported and discussed, where X is $-O^-$, $-OH$, or $-OA$, and A is either metallic or nonmetallic. It is concluded that spin polarization of the A–O σ-electrons provides the major source of spin-density on A, and that the extent of this polarization depends strongly on the extent of p–s or d–s hybridization for A, and weakly upon the ionic character of the ligands. (auth) (UK)

4091 PHOTOCHEMICAL CONVERSIONS OF PARAMAGNETIC CENTRES IN γ-IRRADIATED MONOCRYSTAL OF L-CYSTINE DIHYDROCHLORIDE. Krivenko, V. G.; Kayushin, L. P.; Pulatova, M. K. (Inst. of Biological Physics, Moscow). Biophysics (USSR) (Engl. Transl.); 14: 650-65(1969).

Translated from Biofizika; 14: 615-27(1969).

On γ-irradiation of the monocrystal of L-cystine dihydrochloride at 77°K two processes of formation of paramagnetic centers occur: photo-ionization of the molecule with formation of the cation-radical and anion-radical (α_1) and rupture of the S–C bond of the molecule leading to the formation of the radical R–S–S · (β_1). On exposure of the sample to light ($340 < \lambda < 450$ mμ) and with change in temperature, physicochemical conversions of the paramagnetic centers occur leading to the destruction of some and appearance of other radicals. The electron structure, and the nature and orientation for all the radicals observed (α_1, α_2, α_3, β_1, β_2) in the elementary cell of the monocrystal of L-cystine dihydrochloride were determined and their thermo-physicochemical properties were investigated. In particular, it was shown that the α- and α_2-radicals adsorb light in the region $340 < \lambda < 450$ mμ while the β_1-, β_2- and α_3-radicals are stable on exposure of the monocrystal to light. (auth) (UK)

4092 EPR SPECTRA AND STRUCTURE OF THE FREE RADICALS IN IRRADIATED MONOCRYSTALS OF L-LEUCINE HYDROCHLORIDE. Almanov, G. A.; Tsvetkov, Yu. D. (Tbilisi State Univ., Moscow). Biophysics (USSR) (Engl. Transl.); 14: 788-90(1969).

Irradiated monocrystals were obtained at 77°K using a ^{60}Co γ-source at a dose of ~10M Rad. The EPR spectra were recorded in the form of the second derivative of the absorption line with an EPR spectrometer with modulation of the magnetic field at a frequency of 10 kc/s. The distribution of the intensities, the number of components, and their position in the spectrum could be explained by the ultrafine interaction of an unpaired electron with the protons of two methyl groups and two β-protons. Experimental data on the constants of ultrafine interaction and their anisotropy, measured for the directions of the magnetic field along the main axes, were obtained and the angle of rotation for the CH_2 group calculated. For the radicals formed on irradiation of L-leucine hydrochloride, the structure $(CH_3)_2CCH_2(NH_3^+)CO_2^-$-(III) satisfied the experimental data. (UK)

XUM

4093 ELECTRON SPIN RESONANCE STUDIES OF FREE RADICALS FORMED FROM OROTIC ACID. Huettermann, Juergen; Ward, John F.; Myers, L. S. Jr. (Univ. of California, Los Angeles). Contract AT(04-1)-Gen-12. J. Phys. Chem.; 74: 4022-9(12 Nov 1970).

The paramagnetic species produced in orotic acid (uracil-6-carboxylic acid) by γ irradiation of single crystals and polycrystalline material as well as by reaction with hydroxyl free radicals in an aqueous system were studied by electron spin resonance (ESR) spectroscopy. Three species were observed in the spectra of the crystals, two of them free radicals associated with the orotic acid molecule and the third, cupric ions resulting from radiation effects on crystal impurities. The spectra of the latter were not investigated in full detail. One of the free radicals is formed by hydrogen addition in the 5 position of the pyrimidine ring, leaving an unpaired electron in a $2p_z$ orbital of carbon atom $C_{(6)}$. The couplings of the two β-hydrogen atoms at the 5 position are 22.8 and 34.2 G, respectively. The principal values of the g tensor are 2.0023, 2.0066, and 2.0031. The second radical results from a hydrogen added to an oxygen of the carboxyl group, giving rise to interaction of the radical electron on carbon $C_{(7)}$ with two hydroxyl protons. The hyperfine couplings of the latter are almost axially symmetrical with one $A_{||} \simeq 12$, $A_{\perp} \simeq 0$ G, and the other $A_{||} \simeq 6$, $A_{\perp} \simeq 0$ G. The g tensor of this radical has principal values of 2.0022, 2.0090, and 2.0047. The spectra obtained from irradiated polycrystalline orotic acid can be explained on the basis of the same two radicals. Hydroxyl free radicals produced by the $Ti(III)-H_2O_2$ reaction add to the 5 position of orotic acid in acidic aqueous solution. The unpaired electron on carbon $C_{(6)}$ interacts with the β proton on $C_{(5)}$ to produce a doublet of 11.8-G spacing. Each doublet line is further split into three main lines with component spacing of 2.3 G by interaction with the ^{14}N nucleus in 1 position. (auth)

Radiation Processes

4094 STUDIES ON POLYVINYL ACETATE SOLUTIONS BY MEANS OF RADIATION-INDUCED CROSSLINKING. Gundiah, S.; Kawai, T. (Tokyo Inst. of Tech.). Indian J. Chem.; 7: 1125-9(Nov 1969).

Benzene solutions of three samples of poly(vinyl acetate) were irradiated from a ^{60}Co source for different doses and at different concentrations. Charlesby-Pinner plots constructed show that the ratio of chain scission to crosslinking indices remains constant for solutions of different concentrations. The large increase of gel dose at lower concentration is thus due to the increase in the proportion of intramolecular crosslinks formed at lower concentrations. The proportion of the intra- and intermolecular crosslinks formed by the irradiation of solutions of varying concentrations indicates the extent of overlapping of the molecular coils in solutions. The gel dose-concentration plots show that energy transfer processes are absent and that the segment density distribution becomes homogeneous and continuous throughout the solution at concentrations of about 10%. The critical concentrations below which no gel is formed in the solution irrespective of the radiation dose are in the range of Bueche's entanglement concentrations. The equilibrium swelling ratios for the gel fractions correlate well with radiation dose as $Q \propto D^{-0.6}$. Intrinsic viscosities of solutions of one of the samples irradiated at 4% concentration to doses below the gel dose show two minima and a maximum at doses which are approximate multiples of the gel doses of the concentrated solutions. (auth)

4095 RADIATION-CURABLE-VINYL RESIN PAINTS AND COATED ARTICLE. Burlant, William J.; Taylor, Clement R. (to Ford Motor Co.). U. S. Patent 3,528,844. 15 Sep 1970. Filed 21 Mar 1969.

An article of manufacture having a coating of paint adhered to an external surface of the article is prepared by applying to a substrate a liquid coating of film-forming solution of vinyl monomers and a unique copolymer of vinyl monomers and then crosslinking the vinyl monomers with this copolymer by ionizing radiation. The copolymer is an alpha-beta olefinically unsaturated polymer in which the concentration of alpha-beta olefinic unsaturation units is limited to the range of about 0.5 to about 5, preferably about 0.5 to about 3 per 1,000 units molecular weight. (Offic. Gaz.)

4096 ENERGY TRANSFER IN ALKALI HALIDE MATRICES. Khare, Mohan; Johnson, Everett R. (Univ. of Maryland, College Park). Contract AT(40-1)-3660. J. Phys. Chem.; 74: 4085-91 (12 Nov 1970).

The γ radioinduced decomposition of KNO_3 dispersed in a KBr matrix was studied to determine the mechanism of energy transfer in these systems. It is observed that $-G(NO_3^-)$ is as much as 100 times that for the pure salt depending on the concentration of KNO_3 in the system. The enhanced decomposition of the KNO_3 in these systems is due to the transfer of energy, but the matrix material with an energy gap less than 4.0 eV is ineffective in causing enhanced decomposition, indicating the importance of the role of excitons in the energy transport process. Further support for exciton mechanism was found in temperature dependence studies and preirradiation of the matrix material. (auth)

4097 RADIATION INDUCED CHAIN REACTION AND ITS APPLICATION TO POLYMER CHEMISTRY. Kagiya, Tsutomu; Mitsui, Hiroshi; Hagiwara, Miyuki (Japan Atomic Energy Research Inst., Takasaki). Kagaku No Ryoiki; 23: 1127-32(Dec 1969). (In Japanese).

The use of radioinduced chain reactions with polymer chemistry was investigated. Ions and radicals formed by the interaction of radiation with matter and the conditions under which specific ions or radicals were formed were considered. Conditions needed to induce chain reactions were also studied. The most important factor is the reactivity of active intermediates. The quantity "chain length energy factor" was introduced to signify the energy factor which determines the chain length of reaction. Radiation chemistry was considered in terms of the chain length energy factor. Application to radioinduced polymerization and crosslinking is discussed. (Japan)

4098 PRODUCTION OF POLYACETAL RESIN BY RADIATION POLYMERIZATION. Iwai, Tadashi (Ube Industries, Ltd., Yamaguchi, Japan). FAPIG (Tokyo); No. 55, 200-4(Dec 1969). (In Japanese).

The production of polyacetal resin by radioinduced solid-phase polymerization of trioxane is discussed. The process, results of the pilot-scale test, and prospects for the future are described. The product is attracting interest as a plastic for engineering purposes. The radioinduced polymerization takes place at 55°C for a period of 5 hours using 1 Mrad of electrons. The stabilizing treatment consists of acetylating the polymer end using acetic anhydride. The cost of producing polyacetal resin by the method is comparable with those by conventional methods. (Japan)

4099 RADIATION AND CATALYSIS: THE DECOMPOSITION OF HYDROGEN PEROXIDE AT THE SURFACE OF SOME REACTOR IRRADIATED OXIDES. Venkateswarlu, K. S.; Virmani, Y. P.; Shankar, J. (Bhabha Atomic Research Centre, Bombay). Indian J. Chem.; 6: 495-501(Sep 1968).

A detailed study was made of the catalytic decomposition of H_2O_2 on the surface of a number of semiconductor metal oxides, viz., transition metal oxides and rare earth oxides. With transition metal oxides, the activation energy is low for p-type oxides as compared to n-type. Reactor irradiation lowers the activation energy, which is partly reversed by thermal treatment. In a set of rare earth oxides the activation energy follows qualitatively an inverse pattern as compared to their magnetic susceptibilities. A compensation effect is noticed in the kinetic studies. Electric conductivity measurements in some oxides revealed changes on reactor irradiation. The magnitude of the change was more marked in the case of lanthanum oxide and was due to the presence of trapped electrons. This was confirmed by the ESR spectra of irradiated La_2O_3. Experiments such as the study of the heterogeneous decomposition of D_2O_2 at a few oxide surfaces, and a study of the H_2O_2 decomposition at NiO surface under irradiation in the d-d-region (730 mμ) of nickel, were also carried out and they establish the migration of a H atom and desorption of oxygen as intermediate steps. The irradiation effects were interpreted as partly a result of the generation of donor impurities effecting the Fermi level in the oxides and to the formation of charge carriers, besides the surface charging phenomenon due to the radioactivity of the samples. (auth)

4100 PROCESS FOR THE PRODUCTION OF CROSS-LINKED POLYMERS. (to Badische Anilin and Soda-Fabrik AG). French Patent 1,571,848. 12 May 1969. Priority date 11 Jul 1967, Germany. (In French).

A procedure is described for the preparation of cross-linked polymers by irradiation of a mixture of monomers containing 10 to 90% by weight of polymerizable halogen-containing unsaturated acids. (tr-auth)

4101 CALORIMETRIC STUDY OF THE RADIATION CROSS-LINKAGE OF POLYISOBUTYLENE IN THE PRESENCE OF MONOMER ADDITIONS. Kim, I. P.; Kaplan, A. M.; Barkalov, I. M.; Gol'danskii, V. I. (Inst. of Chemical Physics, Moscow). Dokl. Akad. Nauk SSSR; 193: 855-7(1 Aug 1970). (In Russian).

Preliminary experiments indicated that addition of acrylonitrile (AN) to polyisobutylene (PIB) leads to a cross-linked structure when the mixture is exposed to ionizing radiation. The mechanism of the cross-linkage process in the PIB–monomer system was

studied by means of a previously described calorimetric method. The stabilizer-free monomer was added by allowing the polymer to swell when exposed to the monomer vapors. The polymorphic transformation of AN and p-divinylbenzene (DVB) was also examined. Exposure of DVB to a total dose of 5 Mrad of γ radiation at 77°K did not lead to the formation of the polymer. Warming up of PIB in the calorimeter to 200 to 220°K led only to the transformation of the polymer from the vitreous to a viscoelastic state which resulted in the change of its heat capacity. The cross-linkage was studied in the PIB–AN and PIB–DVB systems exposed to γ radiation at 77°K. It was found that the thermal effect increased strongly with the dose up to 2 Mrad, after which it increased only slightly. A three-dimensional network was formed by the cross-linkage or by recombination of the growing chains with double bond formed by the radiolysis of the polymeric macromolecule. The polymerization was accelerated after devitrification of the polymer matrix. (TTT)

4102 NUCLEAR MAGNETIC RESONANCE OF TETRAFLUOROETHYLENE–ISOBUTYLENE COPOLYMERS OBTAINED BY γ-RAY IRRADIATION. Ishigure, Kenkichi; Tabata, Yoneho (Tokyo Univ.). Macromolecules; 3: 450-4(Jul-Aug 1970).

Fluorine and proton NMR spectra of tetrafluoroethylene–isobutylene copolymers obtained by γ irradiation were measured at 100 MHz (94 MHz for fluorine) and at 60 MHz (56.4 MHz). Methyl and methylene resonances were interpreted successfully in terms of triads. On the other hand, fluorine resonances were explained clearly in terms of tetrads, and it was found that the effect due to substituents at the third nearest carbon atoms should also be taken into account to explain fluorine resonances. It was confirmed that an alternating copolymer is obtained at high concentrations of tetrafluoroethylene in the monomer mixtures. (auth)

4103 EFFECTS OF RADIATION ON CATALYTIC PROPERTIES OF COMPLEXES OF AZOMETHANES AND IONS OF TRANSITION METALS. Movchan, L. A.; Savich, I. A.; Kudryavtsev, A. S. (Moscow State Univ.). Zh. Fiz. Khim.; 44: 1567-9(Jun 1970). (In Russian).

The effects of gamma radiation on the catalytic properties of certain complexes in the decomposition of hydrogen peroxide were studied. Irradiation led to increased activity for certain chelates. The chelates studied were formed by salicylaldehyde and o-aminophenol, picolinic acids, α-aminopyridine, phenylhydrazine, and copper and nickel ions. (tr-auth)

4104 POLYMERIZATION INDUCED BY GAMMA RADIATION OF STYRENE UNDER PRESSURE. Guarise, G. B.; Palma, G.; Siviero, E.; Talamini, G. (Univ., Padua). Polymer; 11: 613-25(Nov 1970).

The radioinduced polymerization of styrene in both liquid and solid states was investigated at high pressure in the temperature range 20 to 50°C. In the liquid phase pressure increased the polymerization rate as well as the molecular weight of the polymer in agreement with the results for chemically initiated polymerization. In particular, activation volume and energy are consistent with literature values. When the monomer has undergone the liquid-solid transition a sudden increase in the polymerization rate takes place. However the latter falls again to negligible values for a comparatively small pressure excess above the solidification point. The mechanism of the solid-state polymerization in the high-rate region is considered in the light of existing theories. (auth) (UK)

4105 STRUCTURAL AND KINETIC FACTORS IN RADIATION GRAFT-COPOLYMERIZATION. Dobo, Janos Magy. Kem. Lapja; 25: 368-74(Jul 1970). (In Hungarian).

In investigating graft-copolymerization paradoxical phenomena are often encountered. Thus, e.g., polytetrafluorethylene undergoes graft-copolymerization more readily than does poly(vinyl-alcohol); with some systems the degree of copolymerization is higher at smaller radiation intensities than at greater ones; the rate of grafting is some orders of magnitude greater than that of homopolymerization under similar conditions; thick polyethylene foils can be grafted more quickly than thin ones. In most cases these phenomena can be traced back to the interaction of two factors. The rate of graft-copolymerization in a high-viscosity medium first of all depends on the reduction in the rate of chain-closing reactions, that is, on the viscosity of the medium. On the other hand, the rigidity of the chains in the polymer matrix, the cohesion between the chains may prohibit grafting in the inside of the polymer matrix. (auth)

4106 GRAFTING OF ORGANIC POLYMERS ONTO INORGANIC SUBSTRATES BY GAMMA IRRADIATION. Raff, R. A. V.; Subramanian, R. B.; Schecter, D. J. (Washington State Univ., Pullman). Trans. Amer. Nucl. Soc.; 13: 511(Nov 1970).

From Meeting of the American Nuclear Society, Washington, D. C. See CONF-701102.

4107 KINETICS OF GAMMA-INDUCED POLYMERIZATION OF METHYL METHACRYLATE-CLAY COMPOSITES. Beeson, J. J.; Mayhan, K. G. (Univ. of Missouri, Rolla). Trans. Amer. Nucl. Soc.; 13: 511-12(Nov 1970).

From Meeting of the American Nuclear Society, Washington, D. C. See CONF-701102.

4108 RADIATION-CURING OF COMPOSITES OF METALS AND POLYMERS. Malliaris, A.; Kusy, R. P.; Turner, D. T. (Drexel Univ., Philadelphia). Trans. Amer. Nucl. Soc.; 13: 512 (Nov 1970).

From Meeting of the American Nuclear Society, Washington, D. C. See CONF-701102.

4109 ECONOMICS OF RADIATION VERSUS HEAT-CATALYST CURING FOR WOOD-PLASTIC FLOORING PLANT. Taylor, G.; Wei, L.; Dietz, G.; Duff, R. (Radiation Machinary Corp., Parsippany, N. J.). Trans. Amer. Nucl. Soc.; 13: 513(Nov 1970).

From Meeting of the American Nuclear Society, Washington, D. C. See CONF-701102.

Radiolysis

Refer also to abstracts 4398, 4425, 4458, and 4459.

4110 (AD-710231) ELECTRON SPIN RESONANCE STUDIES ON γ-IRRADIATED $KMnO_4$. White, Kevin J. (Ballistic Research Labs., Aberdeen Proving Ground, Md.). May 1970. 63p. (BRL-1482). NTIS.

Electron spin resonance (ESR) studies were carried out on the radicals produced by the gamma-irradiation of single crystals of $KMnO_4$. A crystal holder has been designed which allows an accurate orientation of the crystal. Analysis of the data yields at least two paramagnetic species. The first radical is produced by room-temperature irradiation and gives a single line for each of two inequivalent magnetic sites. There is no resolvable hyperfine structure. The spectrum is tentatively assigned to the MnO_2 or the MnO_4 radical. The second radical is produced by irradiation at 77°K and the spectrum disappears irreversibly at slightly higher temperatures. This spectrum is assigned to the MnO_4^{2-} radical. The relationship of the radicals observed to the effect of high-energy radiation on the decomposition of $KMnO_4$ in the light of current solid state theory is discussed. (auth) (USGRDR)

4111 (ORO-3909-2) SYNTHESIS, IDENTIFICATION, AND PURIFICATION OF C_6 AND C_7 FLUOROCARBONS FROM RADIOLYSIS. Annual Progress Report. Askew, W. C.; Ward, C. H.; Carey, G. W. (Auburn Univ., Ala. Dept. of Chemical Engineering). Nov 1970. Contract AT(40-1)-3909. 26p. Dep. NTIS.

Progress is reported on analytical techniques used for perfluoroheptane isomers; measurement of absorbed dose rate distribution in the Auburn University ^{60}Co pool source by benzene–water dosimetry; neutron irradiation of $n-C_4F_{10}$ and $n-C_4F_{10}$ with carbon granules; and spectrographic methods of identification of perfluoroalkane mixtures (including ir, Raman, ^{19}F NMR, and mass). (D.H.M.)

4112 PULSE RADIOLYSIS STUDIES OF AROMATIC RADICAL CATIONS IN 1,2-DICHLOROETHANE. Shank, Norman Eugene. Columbus, Ohio; Ohio State Univ. (1969). 117p. University Microfilms Order No. 70-14,096.

Thesis.

The rate of formation and subsequent decay of certain aromatic radical cations, produced by pulse irradiation of 1,2-dichloroethane solutions of the parent aromatic compound, were studied in an effort to learn the mechanisms of these processes. The aromatic cation was observed spectrophotometrically. The rate of biphenyl and para-terphenyl cation formation was found to be faster than the rate at which the radiation produced solvent cation and the neutral aromatic compound can diffuse together. This high rate is explained by a resonance charge transfer from a neutral solvent molecule to a solvent cation, which makes the positive charge more highly mobile than the molecular solvent cation. The subsequent decay of the biphenyl cation in the irradiated, aerated system exhibited mixed order kinetics and is explained as due to reaction with other radiolysis products, primarily the counter ion, which is suggested to be chloride ion. For three aromatic pairs the rate constant was measured for charge transfer from one neutral aromatic solute to the cation of the second aromatic compound. The rate constants were those of a diffusion controlled reaction in those cases where the reaction was highly exothermic. (Diss. Abstr. Int.)

4113 KINETICS OF ELECTRON AND ION REACTIONS DURING THE γ RADIOLYSIS OF LIQUID NEOPENTANE; DEPENDANCE OF CHARGE SCAVENGING KINETICS ON HYDROCARBON MOLECULAR STRUCTURE. Horacek, K.; Freeman,

G. R. (Univ. of Alberta, Edmonton). J. Chem. Phys.; 53: 4486-9(15 Dec 1970).

The large free ion yield in neopentane was confirmed by chemical measurement. For nitrous oxide solutions at 23°C $g(N_2)_{fi} = 0.95$ and $g(N_2)_{max} \approx 4.7$. The average number of nitrogen molecules formed per electron scavenged appears to be 1.1 ± 0.1 at all nitrous oxide concentrations. Thus $g_{fi} = 0.9$ in neopentane, which is sevenfold larger than that in n-hexane. The median range of the secondary electrons in liquid neopentane is about fourfold greater than that in n-hexane. The greater range in neopentane correlates with the more sphere-like shape of the molecules. In spite of the larger median electron range in neopentane, the ease with which electrons and ions can be scavenged in spurs in that liquid is similar to that in hydrocarbons with distinctly nonspherical molecules. Furthermore, the ratio of efficiencies of electron to positive ion scavenging (β_-/β_+) is 17 in neopentane, similar to the value 13 in the nonspherical methylcyclopentane. During the radiolysis of pure neopentane two types of ions were formed: $G(PH^+) = 1.7$ and $G(N^+) = 3.0$. PH^+ yielded hydrogen when neutralized by an electron, but not when neutralized by a massive negative ion. PH^+ can also donate a proton to ammonia. N^+ did not yield hydrogen upon neutralization, nor did it donate a proton to ammonia. In pure neopentane $G(H_2) = 2.5 \pm 0.1$ and $G(CH_4) = 3.9 \pm 0.2$ at a dose of 1.5×10^{18} eV/g. Scavenging the free ions by either N_2O or ND_3 reduced $g(H_2)$ by about 0.35, but had no effect on the methane yield. (auth)

4114 X- AND γ-RADIOLYSIS OF SOME TRYPTOPHAN DIPEPTIDES. Winchester, R. V.; Lynn, K. R. (National Research Council of Canada, Ottawa). Int. J. Radiat. Biol.; 17: 541-8(1970).

Irradiation of the dipeptides tryptophyl-glycine, -alanine, -leucine, -tryptophan, -tyrosine, and -phenylalanine in aerated solution gave essentially the same products in each case. The major products are those known to arise from the radiolysis of tryptophan, which is therefore proposed as the initial product of hydroxyl radical attack on the α-carbon atom adjacent to the peptide nitrogen. The presence of an aromatic ring in the C-terminal acid (try-tyr, try-phe) results also in hydroxyl radical attack on this ring. Results agree qualitatively with the mechanisms proposed for peptide radiolysis by Liebster and Kopoldova (1966) and Garrison (1968). (auth) (UK)

4115 PULSE RADIOLYSIS OF SELENIUM-CONTAINING RADIOPROTECTORS. I. SELENOUREA. Badiello, Roberto; Fielden, E. Martin (Inst. of Cancer Research, Sutton, Eng.). Int. J. Radiat. Biol.; 17: 1-14(1970).

The reactivity of the protective agent, selenourea, towards the primary radicals of water radiolysis, OH, H, and the hydrated electron, has been measured by the pulse-radiolysis technique. The radical reactivity of the selenium-, sulphur-, and oxygen-containing areas was compared with the radioprotective efficiencies of these compounds: the most efficient radical scavenger, selenourea, is the most efficient protective agent. Both the OH radical and the hydrogen atom give rise to the same radical species when reacting with selenourea. The radical formed by this reaction has a strong absorption band at 410 nm, and it was found to be a charged complex involving two selenourea molecules. The formation and decay kinetics of this radical ion have been measured together with the association/dissociation constant of the complex. On a radical-scavenging mechanism, the ability of a secondary radical to form a complex may have some bearing on the protective efficiency of the parent compound. The selenourea system has proved to be a useful source of data on OH radical reactivity and this is discussed. (auth) (UK)

4116 EFFECT OF ADDITIONS OF AROMATIC HYDROCARBONS ON THE CHEMICAL RADIATION STABILITY OF TRIBUTYL PHOSPHATE IN DODECANE SOLUTION. Barelko, E. V.; Solyanina, I. P.; Tsvetkova, Z. H. (Physical-Technical Inst., Moscow). Khim. Vys. Energ.; 4: 229-34(May-Jun 1970). (In Russian).

Solutions of tributyl phosphate (TBP) are used as extraction systems in nuclear fuel technology. The influence of aromatic additives on radiolysis of a dodecane solution of TBP was studied, with monoisopropylbiphenyl as the example. The yields of acid esters and hydrogen were measured, along with the changes in the distribution coefficients of ^{239}Pu and ^{95}Zr between the irradiated organic phase and an aqueous phase containing 2M HNO_3 and the nitrates of these metals. The relationships obtained for the product yields as functions of the aromatic-additive concentration indicate an increase in the radiochemical stability of TBP in the presence of the additive. In this example there appears to be the first observation of a synergistic effect in which the protective action in the ternary system is substantially stronger than would be calculated by the Stern–Vollmer equation and experimental data for binary systems, although these data are described quite satisfactorily by that equation. (auth)

4117 RADIATION CHEMISTRY OF FOODS. PART 4. MEASUREMENT OF RADIATION RATES OF FOOD AND BIOLOGICAL TISSUE EXTRACTS WITH HYDRATED ELECTRONS. Morita, Makio; Eguchi, Hiroshi; Tajima, Makoto; Fujimaki, Masao (Tokyo Univ.). Agr. Biol. Chem. (Tokyo); 34: 547-52(Apr 1970).

Reaction rates of extracts from foods and biological tissues with hydrated electrons were measured by using competition with N_2O. Water and 3% Na_2SO_4 aqueous extracts of pork and water extract of onion gave results that conformed to the simple relationship of competition. An additional test of the onion with acetone and nitrate suggested that their reactivities were simply additive, but the additive effect of cysteine was complicated. (auth) (Japan)

4118 SPECTROSCOPIC INVESTIGATION OF THE LOW-TEMPERATURE RADIOLYSIS OF SOME POLYOLEFINS. Dzhibgashvili, G. G.; Slovokhotova, N. A.; Leshchenko, S. S.; Karpov, V. L. (Inst. of Physical Chemistry, Moscow). Khim. Vys. Energ.; 4: 281-2(May-Jun 1970). (In Russian).

The low-temperature radiolysis of high-density polyethylene (HDPE) and ethylene copolymers with 7 mole % of propylene (ECP-7) and with 3 mole % of α-butylene (ECB-3) was investigated by ir spectrometry. Absorption bands corresponding to trans-vinylene double bonds at 970 cm^{-1}, to conjugated dienes at 985 cm^{-1}, and to vinyl double bonds at 910 cm^{-1} appeared in the ir spectrum of ECP-7 and ECB-3, which were irradiated at −180°C, as they did in the spectra of HDPE measured at the same temperature without intermediate heating; while the band at 910 cm^{-1} already existed in the spectrum of HDPE measured prior to irradiation, its intensity increased after irradiation. (D.H.M.)

4119 GAS PHASE RADIOLYSIS OF HYDROGEN SULFIDE AND PROPANE UNDER THE INFLUENCE OF THE PARTICLES FORMED IN THE REACTION $^{10}B(n,\alpha)^7Li$. Ezerska, K.; Forys, M.; Taube, M. (Univ. of Warsaw). Khim. Vys. Energ.; 4: 280-1 (May-Jun 1970). (In Russian).

Yields of hydrogen from the gas-phase radiolysis of hydrogen sulfide and yields of methane, ethane, and hydrogen from the gas-phase radiolysis of propane using α particles from the reaction $^{10}B(n,\alpha)^7Li$ are reported. The data indicated that the radiolysis of these compounds is independent of the type of radiation. (D.H.M.)

4120 MECHANISM OF FORMATION OF PRODUCTS OF THE RADIOLYSIS OF WATER. Byakov, V. M.; Kalyazin, E. P. (Moscow State Univ.). Khim. Vys. Energ.; 4: 255-9(May-Jun 1970). (In Russian).

On the basis that the scheme for molecular product formation in the radiolysis of water, X + X → M, is in good agreement with experimental relationships for the yield of molecular products as a function acceptor concentration at both low and high concentrations, it is concluded that molecular products are formed by a bimolecular reaction. However, the modern recombination model, which assumes that hydrated electrons are the precursors of molecular hydrogen, runs into a number of difficulties which are readily avoided if it is assumed that neutral particles are the precursors of the molecular products. The latter assumption is supported by the fact, obtained from an analysis of the experimental data, that the hydrated electron yield is equal to the hydroxyl radical yield for LET values from 0.02 to 15 eV/Å. The formation of OH radicals and hydrated electrons in the radiolysis of water is due to the acid–base dissociation of excited water molecules. (auth)

4121 RELATION OF CONCENTRATION TO YIELD OF HYDROGEN IN THE γ RADIOLYSIS OF MIXTURES OF CYCLOHEXANE AND BENZENE. Avdonina, E. N. (Moscow State Univ.). Khim. Vys. Energ.; 4: 226-8(May-Jun 1970). (In Russian).

On the basis of investigations on reactions of liberated tritium atoms in liquid mixtures of cyclohexane with benzene, an attempt was made to assess the contributions of the molecular splitting-off of hydrogen H_2, and of reactions of thermal and high-energy hydrogen atoms to the total radiation yield of hydrogen molecules determined during the radiolysis of liquid mixtures of cyclohexane with benzene. (auth)

4122 GAS-PHASE RADIOLYSIS OF ETHYLENE IN THE PRESENCE OF HYDROGEN SULPHIDE. REACTIONS OF HOT RADICALS. Niedzielski, J.; Gawlowski, J. (Warsaw Univ.). Radiochem. Radioanal. Lett.; 5: 159-64(6 Nov 1970).

The effect of hydrogen sulfide on the yields of some straight chained paraffins in the radiolysis of gaseous ethylene was examined. n-Butane and propane are not readily scavenged by H_2S; their persistence at concentrations of H_2S below 7 mole was explained in terms of reactions of hot methyl and ethyl radicals, added to ethylene to yield n-propyl and n-butyl radicals, subsequently scavenged by H_2S. The yields of hot methyl and ethyl radicals were de-

termined as equal to 0.1 and 0.4 radicals/100 eV, respectively. (auth)

4123 RADIATION CHEMISTRY OF ALCOHOLS. XII. METHANE FORMATION IN THE γ RADIOLYSIS OF ISOPROPANOL. von Sonntag, C. (Kernforschungszentrum, Karlsruhe, Ger.). Z. Naturforsch.; 25b: 654(Jun 1970). (In German).

In the γ radiolysis of liquid 2-propanol, methane originates with a G-value of 1.6. It is therefore, after hydrogen, the most important gaseous radiolytic product. The chief part of the methane, or its precursor the methyl radical, must originate from the electronic decay of highly excited 2-propanol molecules. (M.C.G.)

4124 ESR OF SO_2^-. Reuveni, A. (Weizmann Inst. of Science, Rehovoth, Israel); Luz, Z.; Silver, Brian L. J. Chem. Phys.; 53: 4619-23(15 Dec 1970).

The ESR spectrum of normal and ^{17}O labeled SO_2^- in aqueous solutions of $Na_2S_2O_4$ and in γ-irradiated $K_2S_2O_5$ was studied. The ^{33}S and ^{17}O hyperfine tensors were very nearly axially symmetric with parallel and perpendicular principal values of 58.0 ± 0.5 and 4 ± 4 G for ^{33}S and 30.0 ± 0.5 and 3 ± 3 G for ^{17}O. The principal values of the g tensor are 2.0057 ± 0.0005, 2.012 ± 0.003, and 2.0019 ± 0.0020 where the smallest component is parallel to the major ^{33}S and ^{17}O hyperfine components. The results are consistent with the unpaired electron occupying a $2b_1$ π molecular orbital for which semiempirical coefficients are derived. (auth)

4125 REACTIONS OF PHOTOEXCITED RADICALS OF THE ALLYL TYPE WITH THE HYDROCARBON MOLECULES IN THE SOLID PHASE. Roginskii, V. A.; Pshezhetskii, S. Ya. (Inst. of Physical Chemistry, Moscow). Khim. Vys. Energ.; 4: 240-5 (May-Jun 1970). (In Russian).

The reversible photoreactions of free radicals of the allyl type obtained by the γ-radiolysis of hex-1-ene, hept-1-ene, and pent-2-ene, and also of solutions of olefins in 3-methylpentane at 77°K were studied by EPR and gas chromatography. The radicals $\sim CH_2 - CH \dot{-} CH \dot{-} CH_2$ are characterized by an EPR spectrum of five (or seven) HFS lines with a separation of 14.5 Oe. When they are excited with light having λ ≤ 410 nm they disappear with the formation of equivalent amounts of alkyl radicals of the matrix as a result of the reaction: $(\sim CH_2 - CH \dot{-} CH \dot{-} CH_2)^* + RH \rightarrow \sim CH_2CH_2CH = CH_2 + R$. In the dark at 77°C the reverse transformations take place, probably as a result of the reaction: $CH_2CH_2CH = CH_2 + R \rightarrow \sim CH_2 - CH \dot{-} CH \dot{-} CH_2 + RH$. The kinetics of the forward and reverse reactions in γ-irradiated solutions of hex-1-ene in 3-methylpentane was studied. The possible causes of the predominant occurrence of reactions of photoexcited allyl radicals with neighboring molecules and not the migration of the free valence within the radical are discussed. (auth)

Radioisotope Production

Refer also to abstract 5756.

4126 (UJV-2431-Ch) PRODUCTION OF CARRIER-FREE RADIOSTRONTIUM ^{85}Sr. Hruby, J.; Knobloch, V.; Mudrova, B.; Svoboda, K. (Ceskoslovenska Akademie Ved, Rez. Ustav Jaderneho Vyzkumu). Sep 1970. 70p. (In Czech). Dep. NTIS (U. S. Sales Only).

Studies undertaken in order to find optimal methods of ^{85}Sr production by irradiation in the U-120 cyclotron are described. Methods of irradiating rubidium in a suitable chemical form by deuterons, as well as methods of isolation of the radioisotope produced from the bulk amount of rubidium, its purification, and methods of impurity determinations are specified. The most suitable way of target preparation proved to be layers of rubidium chloride (the properties of the layer being improved by an addition of 2 to 4% of rubidium sulfate) melted in argon on copper or silver supporting discs. By preirradiational vacuum annealing of the targets their properties can be significantly improved. The practical thick target yields are in the range 14 to 15.3 μCi/μA h. The most suitable method for separation of Sr from impurities is the chromatographic separation on the cation-exchanger Dowex 50×8 in 0.8 M hydrochloric acid or 1 M ammonium acetate. The efficiency of the separation is about 95%. Polarographic methods of analysis adjusted for the determination of chemical impurities in the ^{85}Sr preparation, e.g., Cu, Zn, Cd, and Pb, are discussed. (auth)

4127 SEPARATION OF NUCLEAR ISOMERS OF ^{80}Br ON METAL SURFACES. Redlich, J.; Dreyer, R. (Zentralinstitut fuer Kernforschung, Rossendorf, Ger.). Z. Phys. Chem. (Leipzig); 239: 406-10(1968). (In German).

In a vacuum apparatus and with high voltage, studies were made on the separation of nuclear isomers of ^{80}Br on bromide-covered metal surfaces. With this physical separation method the yield of ^{80g}Br depended on the surface condition of the metal sample. Separation was possible with Zr, Ti, and Ni samples, which contained solid adhesive layers formed by water and oxygen. Most of the Br was absorbed physically instead of chemically. On metal surfaces, where barrier layers did not occur, separation of nuclear isomers of ^{80}Br was impossible. (tr-auth)

4128 PRODUCTION AND MUTUAL DELIVERY OF ISOTOPES, LABELED COMPOUNDS, AND SEALED RADIATION SOURCES IN COMECON MEMBER STATES. Ertel, G. Isotopenpraxis; 6: 201-3(Jul 1970). (In German).

The development of the assortment of radioactive and stable isotopes, labeled compounds, and sealed radiation sources produced in the COMECON member countries, as well as the mutual supply of such products, are reviewed. (auth)

4129 ^{128}Xe PRODUCTION PROCESS DEVELOPMENT. Haase, D. W. (Douglas United Nuclear, Inc., Richland, Wash.). Trans. Amer. Nucl. Soc.; 13: 495(Nov 1970).

From Meeting of the American Nuclear Society, Washington, D. C. See CONF-701102.

Recoil Production and Reactions

Refer also to abstracts 4957 and 5153.

4130 ANNEALING OF ^{60}Co RECOIL ATOMS IN ALPHA AND BETA COBALT PHTHALOCYANINE. Mathur, P. K. (Bhabha Atomic Research Centre, Bombay). Indian J. Chem.; 7: 820(Aug 1969).

Thermal annealing was studied for neutron-irradiated α- and β-forms of cobalt phthalocyanine. It is shown that molecular symmetry has a considerable influence on the initial retention (α-form 2% and β-form 4%) and annealing which is faster in the β-form than in the α-form. (auth)

4131 RECOIL TRITIUM REACTIONS WITH METHYL ISOCYANIDE AND METHYL CYANIDE. ESTIMATES OF ENERGY DEPOSITION FOR THE T-FOR-H REACTION. Ting, C. T.; Rowland, F. S. (Univ. of California, Irvine). Contract AT(11-1)-34. J. Phys. Chem.; 74: 4080-4(12 Nov 1970).

The substitution of energetic T* for H in CH_3NC produces such energetic molecules of CH_2TNC^* that none (<1 in 300) are stabilized by gas phase collision prior to isomerization to CH_2TCN or decomposition to CH_2T plus CN. From experiments at 5 atm pressure of argon, it is concluded that less than 1% of the CH_2TNC^* molecules have 3.8-eV excitation energy or less. Substitution trajectories corresponding to excitation energies of less than 2 to 3 eV are apparently forbidden by the detailed dynamics of the substitution process. The substitution of T* for H in CH_3CN forms molecules of CH_2TCN^* sufficiently energetic to undergo the thermally unobserved reverse isomerization to CH_2TNC^* in small yield. This yield is only observed experimentally under the rapid collisional stabilization conditions of liquid phase densities. Estimates of level densities for CH_2TNC^* and CH_2TCN^* at energies high enough for rapid isomerization predict a nonzero experimental yield for CH_2TNC in the gas phase, in disagreement with the observations. (auth)

4132 HOT H ATOMS IN GAS-PHASE PHOTOCHEMISTRY. Vermeil, C. (ESPCI, Paris). Israel J. Chem.; 8: 147-64 (1970).

From 21st Farkas Symposium on Photochemistry of Aqueous and Polar Systems, Jerusalem, Israel. See CONF-691221.

By photolyzing hydrogenated molecules, H or D atoms with kinetic energies in the range of about 0.5 to 5 eV are produced. The special features of their chemical properties are reviewed and compared with recoil tritium atom reactions on the one hand and with systems in thermal equilibrium on the other. Although the mechanism of reactive and non-reactive collisions are by no means well known, hot hydrogen atom chemistry is, in first approximation, rather similar to high temperature chemistry. However, energy losses by energy transfer to molecules and even to rare gases are much smaller than expected from classical hard-sphere models. (auth)

Radiochemistry

4133 (NAS-NS-3026(Rev.)) RADIOCHEMISTRY OF MERCURY. Roesmer, Josef (Westinghouse Electric Corp., Pittsburgh, Pa. Astronuclear Lab.). Sep 1970. 202p. Dep. NTIS.

Topics covered include: isotopes of mercury, review of features of mercury chemistry of chief interest to radiochemists, ion exchange behavior of mercury, nuclear methods of mercury analysis, dissolution methods, and collection of detailed radiochemical procedures for mercury. (228 references). (M.C.G.)

XUM

Separation Processes

Refer also to abstracts 4026, 4044, 4116, 4129, 4133, 4153–4156, 4263, 4437, 5722, and 5882.

4134 (AEC-tr-7198) PROCESSING OF IRRADIATED MIXED PLUTONIUM AND URANIUM OXIDES. Faugeras, P. (Commissariat a l'Energie Atomique, Fontenay-aux-Roses (France). Centre d'Etudes Nucleaires). Translated from 2nd Spanish-French Sympsoium on Fuel Reprocessing and Plutonium Chemistry, Madrid, Spain, November 17–19, 1969. 31p. Dep. NTIS.

An abstract of this paper, prepared from the original language, appeared as NSA 24: 29357.

4135 (CEA-R-4097) COUNTER CURRENT EXTRACTION OF NEPTUNIUM BY TRIBUTYLPHOSPHATE SOLUTIONS FROM AQUEOUS NITRIC–NITROUS ACID SOLUTIONS. Gourisse, Daniel (Commissariat a l'Energie Atomique, Fontenay-aux-Roses (France). Centre d'Etudes Nucleaires). Oct 1970. 22p. (In French). Dep. NTIS (U. S. Sales Only).

Three schemes for multistage countercurrent extraction of neptunium by TBP solutions from nitrous acid–nitric acid solutions were studied. The comparison between the apparent values of the neptunium distribution coefficient in each stage and the values calculated from oxidation equilibrium showed that the oxidation and extraction increase with temperature and the oxidation increases with nitrous acid concentration. (France)

4136 (GAMD-9260(Pt.2)) HTGR FUEL REPROCESSING: HEAD-END TREATMENT OF EXPERIMENTAL SMALL-SCALE HTGR FUEL ELEMENTS. Brooks, L. H. (Gulf General Atomic, Inc., San Diego, Calif.). 13 Oct 1970. Contract AT(04-3)-167. 31p. Dep. NTIS.

Research and development work on the grind-burn-leach process has continued. A jaw crusher was designed and built for crushing 12-rod fuel elements. Experiments indicated that a jaw crusher breaks the fuel to an acceptable size range without breaking an unacceptable fraction of fuel particles. Tumbling and screening was shown to be a good method of separating the crushed material into two streams: a graphite-rich and a fuel particle-rich stream. This operation allows the utilization of two fluidized bed burners, a large one for graphite and a smaller one for fuel particles. Tumbling is fast and easy, but trials on irradiated fuels must be carried out before final conclusions can be drawn. Burning was carried out in fluidized beds. All types of fuel and graphite were tested and present no insoluble difficulties. Leaching trials were carried out in a 1-liter leacher. Burned BISO and ground, burned TRISO fuel particles were successfully leached. Although the rate of dissolution is acceptably high, work must be done on irradiated fuel before final conclusions can be drawn. (auth)

4137 (IS-T-377) ANION EXCHANGE SEPARATIONS OF METAL IONS IN THIOCYANATE MEDIA. Kaminski, Edward Eugene Jr. (Ames Lab., Iowa). Oct 1970. Contract W-7405-eng-82. 101p. Dep. NTIS.

Thesis.

Alamine 336, a weak base liquid ion exchanger, and Amberlyst A-21, a macroreticular weak base anion exchange resin were investigated to determine their analytical potential for the quantitative separation of metal ions in thiocyanate media. The study was organized into essentially three parts: the investigation of Alamine 336 as a liquid ion exchanger dissolved in a diluent, the investigation of Alamine 336 as the sorbed liquid phase in reversed-phase column chromatographic separations, and the investigation of uptake of metal ions by Amerlyst A-21 both by batch and column techniques. Alamine 336 was dissolved in toluene, converted to its thiocyanate form, $R_3NH^+SCN^-$, and used in a conventional solvent extraction procedure. Distribution ratios were determined for some 32 metal ions using 0.4 M $R_3NH^+SCN^-$. The aqueous phase consisted of metal ions, 0.5 M hydrochloric acid, and a thiocyanate concentration of either 0.0 M or 0.06 M. Two large scale separations of interest were the removal of interferences such as copper (II), cobalt(II), and iron (III) from hard water samples prior to the determination of water hardness and removal of cobalt(II) from nickel(II). Alamine 336 was applied as the liquid phase to inert chromatographic supports in two ways. Pure amine was coated onto Chromosorb W and the elution of metal ions with aqueous thiocyanate solutions, 1.0 M or less in thiocyanate and 0.5 M in hydrochloric acid, was studied. An analytical separation of interest was that of aluminum(III), gallium(III), and iron(III) (given in order of elution from the column). An interesting sidelight of this work was the development of atomic absorption methods of analysis for cobalt(II) or copper(II) after stripping them and the amine from a column with methanol. An analysis of an NBS standard sample for nickel(II) was also performed. Alamine 336 in toluene was sorbed onto XAD-2 support and based on the solvent extraction batch distribution ratios, the elution behavior of metal ions was studied. Distribution data were obtained for some 25 metal ions between aqueous solutions, ranging from 0.03 M to 1.0 M in thiocyanate ion and 0.5 M in hydrochloric acid, and Amberlyst A-21 in the thiocyanate form. Again, batch distribution data were used to determine column separation possibilities. By proper choice of eluents a separation of scandium(III) from thorium(IV) and rare earths(III) was accomplished. Other representative separations performed were nickel(II) from vanadium(IV), rare earths(III) from iron(III) and uranium(VI), and thorium(IV) from titanium(IV). (73 references). (auth)

4138 (ORNL-TM-3053) ENGINEERING DEVELOPMENT STUDIES FOR MOLTEN-SALT BREEDER REACTOR PROCESSING NO. 1. McNeese, L. E. (Oak Ridge National Lab., Tenn.). Nov 1970. Contract W-7405-eng-26. 85p. Dep. NTIS.

Equipment was installed in Bldg. 3592 to permit engineering studies on reductive extraction in countercurrent contactors. The system will allow countercurrent contact of up to 15 liters each of molten salt and bismuth at flow rates of 0.05 to 0.5 liter/min. The contactor presently being studied is a 0.82-in.-ID, 2-ft-long column (excluding end sections) that is packed with solid ¼-in. right circular cylinders of molybdenum. The flowsheet under consideration for processing fuel from the proposed MSBR uses an electrolytic cell. Fluorides of thorium or lithium in a molten-salt stream are reduced at the bismuth cathode, while metals that are extracted into bismuth are oxidized at the bismuth anode. The feasibility of separating rare earths from thorium in a bismuth solution by fractional crystallization of $ThBi_2$ was examined. A possible equipment configuration was considered, and an analysis was made of factors affecting the fraction of $ThBi_2$ that could be potentially recovered. A computer code, MATADOR, was developed to perform steady-state material-balance calculations that describe the nuclear, chemical, and physical processes occurring in the fuel stream of an MSBR. This code allows the effects of chemical processing on the nuclear performance of an MSBR to be investigated, fission-product inventories and heat-generation rates to be determined, flow rates of streams in the chemical processing plant to be specified. The buildup of transuranium isotopes, the production of activation products by neutron capture in the carrier salt, and chain-branching in the decay fission products are considered. The MATADOR code was used to compute inventories and heat-generation rates in the fuel stream of a 1000-Mw(e) single-fluid MSBR; this information is summarized for the reference reactor. (auth)

4139 APPLICABILITY OF ANION EXCHANGE WITH MIXTURES OF NITRIC ACID AND METHANOL FOR THE SEPARATION OF RARE EARTHS. Ross, R.; Beulich, H.; Hueller, J. (Zentralinstitut fuer Kernforschung, Rossendorf, Ger.). Isotopenpraxis; 6: 229-32(Jul 1970). (In German).

Anion exchange with nitric acid–methanol mixtures may be used for production of many pure elements. The possibilities of the practical application of this mixture for separation of light lanthanides, for the purification of the lanthanides from Zr and Hf, and for production of radioactive isotopes are described. (auth)

4140 SAFETY AND RADIATION PROTECTION. Herrmann, G.; Hunzinger, W. Neue Tech., B; 11: 33-8(1969). (In German).

Operation of the Eurochemic reprocessing plants in Belgium is described with respect to type and amount of radioactive and fissionable material, shielding against penetrating radiation, containment and control of contamination, monitoring of environment, and prevention of criticality accidents. Operation experience since 1966 proved that all safety procedures were satisfactory. No personnel received radiation in excess of permissible doses and incorporation of radioactive material was less than $\frac{1}{10}$ of permissible amounts. Monitoring of stack gases and environment revealed no case where permissible activities were exceeded. (tr-auth)

4141 OSVETLENIE I DEZAKTIVATSIYA STOCHNYKH VOD PENNOI FLOTATSIEI. (Clarification and Deactivation of Waste Waters by Frothing Flotation). Pushkarev, V. V.; Egorov, Yu. V.; Khrustalev, B. N. Moscow; Atomizdat (1969). 144p.

The theory of froth flotation of colloids as carriers of radioactive isotopes and problems of sorption of radioactive microcomponents by inorganic collectors are discussed. Processes and flotation methods for the surface active substances, ions, colloids, precipitants, and radioisotopes are described. Clarification and deactivation of waste waters by means of mechanical air dispersion and aspects of froth flotation for deactivation of waste water in radiochemical laboratories are analyzed. (R.V.J.)

4142 REMOVAL EFFICIENCY OF CHARCOAL FILTER FOR REMOVING RADIOACTIVE IODINE. Murata, Toshifumi;

Kamiya, Kunio (Hitachi Ltd., Ibaraki, Japan). Hitachi Hyoron; 52: 368-72(Apr 1970). (In Japanese).

The efficiency of a charcoal filter used in conjunction with the emergency gas treatment system of a light water reactor was evaluated. The effects of temperature, relative humidity, and velocity of the gas ventilating the charcoal filter on the efficiency of the filter for removing iodine and methyl iodide were measured. Scale-up on the filter was also investigated. It was concluded that the efficiency of the charcoal filter was adequate, and that scale-up did not bring about the lowering of the efficiency. The efficiency of a charcoal filter for removing iodine and methyl iodide can be evaluated from their absorption coefficients. (Japan)

4143 RADIOCHEMICAL SEPARATION OF MICROAMOUNTS OF In–Cd, In–Sn–Te, AND Sb–Sn BY EXTRACTION CHROMATOGRAPHY IN THE AMBERLITE LA-2–HYDROCHLORIC ACID SYSTEM. Stronski, I. (Lab. of Chemistry and Radiochemistry, Krakow). Radiochem. Radioanal. Lett.; 5: 113-17(6 Nov 1970).

Mixtures of tracer quantities of In(III)–Cd(II), In(III)–Sn(IV)–Te(IV), and Sb(V)–Sn(IV) were separated by column reversed-phase extraction chromatography in the liquid secondary long-chain amine Amberlite LA-2–hydrochloric acid system. (auth)

4144 PROCESS FOR THE RECOVERY OF NEPTUNIUM AS WELL AS OF URANIUM AND PLUTONIUM FROM NUCLEAR FUELS AND/OR IRRADIATED RAW MATERIAL. (to Gesellschaft fuer Kernforschung mbH). French Patent 1,569,268. 21 Apr 1969. Priority date 16 Jun 1967, Germany. (In French).

A process is described for the recovery of neptunium as well as uranium and plutonium from nuclear fuels or from irradiated raw materials by treatment with acid and subsequent extraction from the aqueous phase and acid by organic extraction agents. The process is characterized by the fact that neptunium and the plutonium are oxidized before the extraction by means of a solid oxidizing agent, not being in solution, for the purpose of obtaining the appropriate higher valence for the organic extraction agent utilized, which makes it possible to increase the recovery yield while simplifying the operation. (tr-auth)

4145 PROCESS FOR THE ELIMINATION OF RADIOACTIVE COMPONENTS IN A GAS CURRENT, AND SELECTIVE FILTERS FOR CARRYING OUT THIS PROCESS OR A SIMILAR ONE. (to CEAG Concordia Elektrizitaets AG). French Patent 1,569,103. 21 Apr 1969. Priority date 19 Apr 1967, Germany. (In French).

A procedure is described for the removal of radioactive compounds from a gas stream, especially for the removal of radioactive bromine contained in a gas stream in the form of a derivative. The gas contaminated by radioactive bromine is passed over a very porous material impregnated with nonradioactive bromine, which makes possible the fixation and rendering harmless of the labeled bromine derivative, particularly methyl bromide. (tr-auth)

4146 REPROCESSING OF OXIDE FUEL AT WINDSCALE. Hughes, T. G.; Kemp, E. F. (United Kingdom Atomic Energy Authority, Windscale, Eng.). Atom (London); No. 168, 206-11 (Oct 1970).

The reprocessing of irradiated fuel at Windscale is described. The advent of stainless steel-and zirconium-clad oxide fuel necessitated a new approach to the initial stages of reprocessing and it was decided to use the original Butex building as a site for a suitable head-end facility for a new complex. The head-end plant design and construction problems encountered both in the decontamination of the active cells of the old chemical plant and in the development and procurement of a fuel shear are discussed. A full description of the plant is given. The special features of the oxide fuel reprocessing arrangements at Windscale, which enable a variety of fuels to be reprocessed are considered, and future developments indicated. The current head-end unit is expected to cope with the oxide fuel load until the mid 1970's. (UK)

4147 TWO OCTYL PHENYL PHOSPHINIC ACIDS, $(R)(C_6H_5)PO(OH)$, AS EXTRACTANTS FOR SELECTED M(III) AND M(VI) METALLIC CATIONS. Mason, G. W.; Schofer, N. L.; Peppard, D. F. (Argonne National Lab., Ill.). J. Inorg. Nucl. Chem.; 32: 3375-86(Oct 1970).

The extraction of Y(III), selected lanthanides(III), selected actinides(III), and U(VI) from an aqueous chloride phase into a benzene solution of $(R)(C_6H_5)PO(OH)$ where R is n-octyl or cyclooctyl was studied. The stoichiometries of extraction were found to be $M^{3+} + 2.5(HY)_2 \rightleftharpoons MY(HY_2)_2 + 3H^+$ and $UO_2^{2+} + 2(HY)_2 \rightleftharpoons M(HY_2)_2 + 2H^+$ where $(HY)_2$ represents the dimeric extractant. Under a given set of conditions, the M^{3+} the n-octyl compound was the better extractant, but for UO_2^{2+} the cyclo-octyl extractant was the better. In no case was the effect large. In a comparison of the effectiveness of $(n\text{-octyl})(C_6H_5)PO(OH)$ and $(n\text{-octyl})_2PO(OH)$, an extractant previously reported, the former, which is the more strongly acidic, was by far the more effective extractant for the M^{3+} cations. For UO_2^{2+} the two extractants were equally effective. Plots of log K vs Z for the 15 lanthanides(III) in the two $(R)(C_6H_5)PO(OH)$ vs aqueous chloride systems were interpreted in terms of the tetrad hypothesis. On these plots, the value of yttrium places it at the Z position 67 to 68 as a pseudolanthanide(III). (auth)(UK)

4148 VERSATILITY IN REPROCESSING IRRADIATED FUELS. Leclercq-Aubreton, M. Y.; Detilleux, E. (EUROCHEMIC, Mol, Belgium). Trans. Amer. Nucl. Soc.; 13: 473-4(Nov 1970).

From Meeting of the American Nuclear Society, Washington, D. C. See CONF-701102.

4149 APPLICATION OF NITRIDE-FORMING REACTIONS TO REPROCESSING OF SPENT NUCLEAR FUELS. Anderson, R. N.; Parlee, N. A. D. (Stanford Univ., Calif.). Trans. Amer. Nucl. Soc.; 13: 474(Nov 1970).

From Meeting of the American Nuclear Society, Washington, D. C. See CONF-701102.

4150 EXTRACTION OF TRACES OF RARE-EARTH ELEMENTS FROM AQUEOUS SOLUTIONS OF NITRIC ACID WITH TOLUENE SOLUTIONS OF DI-2-ETHYLHEXYL PHOSPHORIC ACID 0.02 M IN URANIUM(VI). Tomazic, B. (Inst. Rudjer Boskovic, Zagreb). J. Less-Common Metals; 22: 495-502(Dec 1970).

The extraction of 10 rare earth traces into solutions of HDEHP in toluene, containing a macroquantity of uranium(VI), from aqueous solutions of nitric acid has been investigated in order to check the mechanism. Under the condition that the concentration of HDEHP is many times that of uranium(VI) (HDEHP/U(VI) ≥5), the mechanism of rare earth extraction is the same as in uranium(VI)-free systems. This is indicated by the third-order dependence of the distribution ratios upon the extractant concentration, which has to be corrected for the preferential complexing of uranium(VI). The tetrad effect, which characterizes extraction and partition chromatographic behavior of rare earths was observed in this complex system. (auth)

EARTH SCIENCES

Geology and Hydrology

Refer also to abstracts 4176, 4178, 4179, 4374, and 5493.

4151 (CEA-CONF-1500) DEVICES AND TECHNIQUES FOR CHARACTERIZATION OF MINERALS. CHARACTERIZATION OF COMPOUNDS AND MATERIALS BY NEUTRON DIFFRACTION. Delapalme, A.; Bertaut, E. F. (Commissariat a l'Energie Atomique, Grenoble (France). Centre d'Etudes Nucleaires). [1969]. 21p. (In French). (CONF-691213-1). Dep. CFSTI (U. S. Sales Only).

From Conference on Chemistry of the Solid State, Grenoble, France.

The properties of the neutron and the different reactions that it produces with a non-negligible probability are summarized briefly as an introduction to the characterization of minerals by neutron diffraction. The characterization of compounds and materials is illustrated by concrete examples of the location of light atoms with great precision, the determination of the magnetic order, characterization of the ionic or covalent state of a chemical bond, and the determination of the charge transfer in such bonds, and spin density. (J.S.R.)

4152 (CSIRO-Trans-10083) CALCULATION BY A MONTE CARLO METHOD OF THE DISTRIBUTION OF PHOTONEUTRONS FROM A BEAM OF GAMMA RADIATION WITH INITIAL ENERGY OF 4.1 MeV. Berzin, A. K.; Denisik, S. A.; Lukhminskii, B. E. Translated by B. Bergmanis (Commonwealth Scientific and Industrial Research Organization, Melbourne, Australia), from Tr. Vses. Nauch.-Issled. Inst. Yadern. Geofiz. Geokhim.; No. 1, 234-41(1968). 14p. Dep. NTIS (U. S. Sales Only).

An abstract of this article, prepared from the original, appeared as NSA 24: 9514 (1970). (Australia)

4153 (DOCKET-50201-51) WEST VALLEY REPROCESSING PLANT. Site Investigation: Proposed Spent Nuclear Fuel Processing Plant, Near Springville, New York. (Dames and Moore, San Francisco, Calif.). 8 May 1963. 53p. Dep. NTIS.

For Nuclear Fuel Services, Inc., West Valley, N. Y.

Results of an investigation of the site with reference to soil conditions at the proposed plant foundations are presented. Information is included on general soil conditions, soil data directly relevant to foundation design, and construction, and details of field and laboratory work used as the basis of recommendations concerning the site. (J.R.D.)

4154 (DOCKET-50201-52) WEST VALLEY REPROCESSING PLANT. Foundation Investigation: Proposed Plutonium Fuel Plant, West Valley, New York. (Dames and Moore, New York). 2 Sep 1970. 35p. Dep. NTIS.

For Nuclear Fuel Services, Inc., West Valley, N. Y.

Results of laboratory testing and engineering analyses carried out for a proposed Pu fuels plant are presented. Construction of the proposed waste lagoon, pickling pits, appurtenant structures, and roadways are summarized. (J.R.D.)

4155 (DOCKET-50201-53) WEST VALLEY REPROCESSING PLANT. Soils and Foundation Investigation: Proposed Iodine Recovery Building, West Valley, New York. (Dames and Moore, New York). 29 Sep 1970. 26p. Dep. NTIS.

For Nuclear Fuel Services, Inc., West Valley, N. Y.

Results of investigat.ons of soils and the site for foundations of a proposed iodine recovery building in the existing spent fuels reprocessing facility area are presented. Details of site conditions are included along with recommendations concerning the building. (J.R.D.)

4156 (DOCKET-50201-54) WEST VALLEY REPROCESSING PLANT. Topographical Map Showing Existing and Proposed Facilities. (Nuclear Fuel Services, Inc., West Valley, N. Y.). 11 Nov 1970. 3p. Dep. NTIS.

A topographic map is presented that shows the location of all buildings and facilities of the West Valley Reprocessing Plant. (R.C.K.)

4157 RADIOACTIVE POLLUTION OF RIVERS IN CZECHOSLOVAKIA. Havlik, Borivoj (Inst. of Hygiene, Prague). Health Phys.; 19: 617-24(Nov 1970).

One of the oldest uranium mining areas in the world is the spa Jáchymov in Bohemia. A study of environmental contamination began there when uranium mining was at a maximum, and continued until mining ceased 6 years later. Content of ^{226}Ra and total beta activity of water, river sediments and water plants were estimated in the streams of this area and from the other uranium ore area, where mining reached its maximum during the study period. Radioactive pollution of the major Czechoslovak rivers during 1964 to 67 is described. (auth) (UK)

4158 IMPORTANCE OF PULSE-HEIGHT ANALYSIS IN THE GAMMA-RAY ATTENUATION TECHNIQUE FOR MEASUREMENT OF SOIL MOISTURE. Saxena, G. S.; Franklin, R. E.; Taylor, George S. (Ohio State Univ., Columbus). Soil Sci.; 110: 283-6(Oct 1970).

In research on gamma-ray attenuation method of measuring soil moisture, the need for pulse height analyzers in counting systems was evaluated. Tests were made using dry and moist soil columns. It was found that there are advantages in not using pulse height analyzers. It is also noted that pulse height analyzers are not always available and are expensive. Te st data are included and evaluated. (J.R.D.)

4159 SPACE-ENERGY AND TIME DISTRIBUTION OF NEUTRONS IN BORON-CONTAINING MEDIA. Lebedev, V. E.; Rezvanov, R. A.; Fel'dman, I. I.; Perevalov, A. V. Tr., Vses. Nauch.-Issled. Inst. Yader. Geofiz. Geokhim.; No. 3, 55-67(1968). (In Russian).

The Monte Carlo method was used for idealizing the modeling of energy, spa<e, and time distribution of neutrons, in order to improve the neutron logging technique in wells drilled in strongly neutron-absorbing media. The initial energy of the neutrons emitted by a point source was assumed to be 2.45 MeV. A "quasi-water," $H_2B'O$ was used as basis for the calculations, assuming that part of the oxygen nuclei were replaced with the nuclei of a fictitious element, B', which combines the slowing-down ability of oxygen with the absorbing ability of boron. The elastic neutron scattering by oxygen and the fictitious B' nuclei was assumed to be 3.75 barns; the inelastic scattering was neglected. The energy range was divided into 8 areas, based on a 16-base logarithmic base. From the results of the calculations based on the trajectories of the neutrons as affected by the boron and hydrogen nuclei, the space-time and energy distribution of the neutron collision density could be obtained. The main result of the study was the establishment of a reliable correlation between the neutron logging readings and the boron content, under consideration of the well diameter for industrial-grade ores containing borates. The thermal neutron density was plotted as a function of the B_2O_3 content. The method may be used to evaluate the boron reserves in an area. (TTT)

4160 CATION EXCHANGE SELECTIVITY AND MINERALOGY OF SOIL CLAY MATERIALS. Dolcater, David Lee. Madison, Wis.; Univ. of Wisconsin (1970). 123p. University Microfilms Order No. 70-8279.

Thesis.

Interactions involving structural and charge properties of layer silicate exchangers and cation properties such as valence, size, and hydration gave rise to variations in cation exchange equilibria. Cation exchange selectivity values were determined as the ratio of exchangeable cation equivalents displaced from an exchanger which had been equilibrated with a solution 0.005 N with respect to each of two competing cations. When Na saturated initially, biotite and muscovite gave KX/CaX values ranging from 0.9 to 1.7, compared to 0.1 to 0.3 for montmorillonite, micaceous vermiculite, and soil clays. The differences were attributed to the presence of varying amounts of interlayer wedge sites and varying layer charge density. Selectivity values with coarse clay muscovite ranged from KX/CaX = 1.7, through KX=SrX = 1.3, to KX=BaX = 0.4, varying with the degree of hydration of the cations, decreasing in the order Ca, Sr, and Ba. Vermiculite, as a result of limited expansion, selectively adsorbed the divalent cation having the smallest unhydrated diameter (MgX/CaX = 2.7, SrX/CaX = 0.76, and BaX/CaX = 0.42). Potassium saturation and drying of the samples resulted in decreased basal spacing of the expansible materials, lowered cation exchange capacity, and doubled KX/CaX selectivity values relative to those obtained for Na saturated, undried materials. These results indicated that the number of interlayer wedge sites was increased by K saturation and drying. After these treatments, the cation exchange capacities of micaceous vermiculite, biotite, and muscovite were similar (9.5, 7.7, and 9.7 meq/100 g, respectively); however, the KX/CaX selectivity values (0.4, 1.7, and 4.0, respectively) still varied widely. The differences in selectivity were attributed to the high layer charge density of mica relative to that of vermiculite. The higher KX/CaX selectivity of muscovite

relative to biotite was explained by the smaller ditrigonal holes and the oblique orientation of hydroxyl groups in the muscovite structure. Titanium in the crystalline TiO_2 minerals, anatase and rutile, was differentiated from that isomorphously substituted into minerals dissolved by dihydrogen hexafluorotitanate (H_2TiF_6). Analyses of the original samples and the residues, by both wet chemical (Tiron) and neutron activation methods showed that 100% of the Ti in the synthetic anatase and 92% of the Ti in coarse clay sized rutile was in the residence. The latter value suggested that about 8% amorphous TiO_2 was removed from the mechanically dry ground rutile by the H_2TiF_6 reagent. An average of 86% of the titanium in seven kaolinite samples was present in the residue, largely anatase with some rutile as shown by x-ray diffraction. Only 28% of the Ti in two bentonites was present in the free TiO_2 form. The Ti present as crystalline TiO_2 in 40 soils and sediments ranged from 0 to 100%. Lyotropic cation exchange selectivity was greatly influenced by the number of interlayer wedge sites but also by variations in layer charge density. The combined effect resulted in the adsorption of 10 times as much K as Ca by muscovite compared to vermiculite and 40 times as much compared to montmorillonite. The layer charge density and cation exchange properties of minerals would be influenced by Ti isomorphously substituted into phyllosilicate layers. The several cation exchange factors of micaceous materials investigated undoubtedly influence their reaction with radioactive fallout products such as ^{137}Cs and ^{90}Sr, and with radioactive wastes and other pollutants entering soils. (Diss. Abstr. Int., B)

Meteorology

Refer also to abstracts 4478 and 5082.

4161 (ANL/ES-CC-7) MULTIPLE-SOURCE URBAN ATMOSPHERIC DISPERSION MODEL. Roberts, J. J.; Croke, E. J.; Kennedy, A. S.; Norco, J. E.; Conley, L. A. (Argonne National Lab., Ill. Chicago Dept. of Environmental Control, Ill. National Air Pollution Control Administration, Washington, D. C.). May 1970. Contract W-7405-eng-38. 148p. Dep. NTIS.

The dispersion-model development phase of the Chicago Air Pollution Systems Analysis Program is described in detail. A multiple-source, urban atmospheric dispersion model was developed which describes transients such as morning transitions in atmospheric stability and mixing layer height. The dispersion model has been validated by comparison with over 10,000 hourly averages of sulfur dioxide monitored by the Department of Environmental Control of the City of Chicago. For example, the model accounts for 50% of the variance in 6-hr averages of observed data and 70% of the variance in 24-hr averages. Of particular significance is the capability of the model to describe "area sources" as volumetric clouds of pollutant and thus to evaluate the effect of these sources on dose points within, as well as external to, the area. The atmospheric transport kernel in the model describes the instantaneous release (delta function) of pollutant, advection according to piecewise constant hourly wind vectors, and Gaussian diffusion about the centroid. Continuous plumes are simulated by integration in time of this point-source Green's function. The transport theory and all other computerized algorithms that influence the dispersion problem are described and statistical results of extensive validation studies are presented. (auth)

4162 (BNWL-SA-3450) SCAVENGING IN PERSPECTIVE. Fuquay, J. J. (Battelle-Northwest, Richland, Wash. Pacific Northwest Lab.). 14 Jul 1970. Contract AT(45-1)-1830. 11p. (CONF-700601-2). Dep. NTIS.

From Precipitation Scavenging Meeting, Richland, Wash.

Mechanisms of precipitation scavenging in the atmosphere are reviewed. It is noted that precipitation scavenging is usually thought of as being in major divisions including transport of the material to the scavenging site, in-cloud scavenging and precipitation, and below-cloud scavenging by the precipitation. Discussions are included concerning various metallic and nonmetallic pollutants. (J.R.D.)

4163 RADIOACTIVE STRONTIUM AND BARIUM FALLOUT. Cooper, W. W.; Beck, J. N.; Chen, T. S.; Kuroda, P. K. (Univ. of Arkansas, Fayetteville). Health Phys.; 19: 625-32 (Nov 1970).

Radiostrontium and radiobarium data in rain indicate that the radioisotopes injected into the troposphere generally travel eastward and circle the earth a number of times before being completely washed out by rain, and the ^{90}Sr inventory in the northern stratosphere appears to have decreased during the past several years at a rate corresponding to the stratospheric mean residence time of 1.1 yr. The paths of the radioisotopes injected into the lower atmosphere were traced by 300 mb and 500 mb air trajectories. During a period of two to three tropospheric mean residence times (60 to 90 days), the fallout particles seem to circle the earth three to four times. In calculating the stratospheric mean residence time, corrections were applied for the fresh injections of ^{90}Sr into the atmosphere by the Chinese nuclear explosions. (auth) (UK)

Mineralogy and Exploration

Refer also to abstracts 4085 and 4157.

Oceanography

4164 URANIUM, THORIUM, POTASSIUM, AND ARGON IN MARINE PHILLIPSITES. Bernat, Michel; Bieri, Rudolf H.; Koide, Minoru; (and others) (Univ. of California, San Diego, La Jolla). Geochim. Cosmochim. Acta; 34: 1053-71(Oct 1970).

Analyses of elements at trace levels in phillipsites from Pacific Ocean deposits indicate the mineral continues to grow within the sedimentary column. The thorium and uranium concentrations decrease while the mineral concentrations increase with depth in the deposit. This observation can be explained by a continuous growth of the phillipsite within the deposits. The varying concentrations of uranium and thorium in phillipsite, fish teeth and clay minerals from given levels of the core indicate a competition by such substances for the dissolved phases of these elements. Phillipsites from the surface layers (upper 20 cm) of widely separated deposits have apparent K–Ar ages $> 10^8$ yr. Systematic variations in this ratio occur with depth. At three levels a differentiation of the $^{40}Ar/^{40}K$ ratio with respect to size is observed, the larger crystals having smaller ratios and vice versa. Treatment of three samples with HCl, presumably removing about 40 per cent of the outer layers of the crystals, increased the concentration of radiogenic argon by almost a factor of two. Heating experiments indicate that loss of argon by diffusion is of minor importance. Idealized models of continuous spherical growth of the mineral over long time intervals, and assuming dr/dt = constant, indicate the time dependence of the $^{40}Ar/^{40}K$ ratios for a growing crystal. Most of the results can be explained by modified versions of such models. Without additional knowledge about the many parameters involved in marine phillipsite formation, however, these minerals are not suitable for dating by the K–Ar method. (auth) (UK)

ENGINEERING

Nuclear Explosions

Refer also to abstracts 4279, 4525, and 5311.

4165 (CONF-691051) WORLD SECURITY, DISARMAMENT AND DEVELOPMENT. Proceedings of the Nineteenth Pugwash Conference on Science and World Affairs, Sochi, U.S.S.R., October 22–27th, 1969. 374p.

Separate abstracts were prepared for five papers presented at the conference. Approximately fifty additional papers were presented on disarmament, reduction of nuclear weapons, scientific manpower, biological weapons, and other topics. (H.L.W.)

For abstracts of individual papers see: 4166, 4167, 4213, 4214, and 4505.

4166 (CONF-691051–, pp 24–8) REDUCTION AND ELIMINATION OF NUCLEAR WEAPONS AND DELIVERY SYSTEMS.

From World security, disarmament and development.

The problems of limiting the strategic arms race were discussed with emphasis on the political as well as technical difficulties. Conclusions relative to the dangers of nuclear proliferation, the necessity for prohibiting the seabed emplacement of weapons of mass destruction, the desirability of including underground testing in the nuclear test ban treaty, the hazards of accidental or unauthorized launching of any of the very large number of nuclear weapons deployed throughout the world, and the social responsibility of scientists and their obligation through their governments to disseminate information on the consequences of using biological, chemical, and nuclear weapons, are presented. (L.C.L.)

4167 (CONF-691051–, pp 192–8) OFFENSIVE WEAPONS AND MEANS OF PROTECTION. Emelyanov, V. S.

From World security, disarmament and development.

A Russian scientist's view of the motives behind the development of offensive and defensive (ABM) weapons systems in the USA and USSR is presented. (L.C.L.)

4168 (PNE–320) CLOSE-IN AIRBLAST FROM THE BUGGY EVENT. Project BUGGY I. Vortman, L. J. (Sandia Labs., Albuquerque, N. Mex.). 6 Nov 1970. 84p. Dep. NTIS.

Airblast measurements from the Buggy I nuclear row-charge cratering detonation were made at five ground-level stations to distances of about two miles, along each of four lines placed on axes of the row. No appreciable effects of terrain on airblast propagation were observed, even though terrain relief was pronounced. Peak ground-shock-induced overpressures measured perpendicular to the row were up to 3.7 times those measured off the ends. Differences were not constant because peaks attenuated with distance differently in the two directions. Ground-shock-induced peak overpressures were about equal to gas-venting peak overpressures off the ends of the row, while perpendicular to the row, ground-shock-induced peaks were decidedly larger. Peak ground-shock-induced and gas-venting overpressures were up to 3.7 and 2.8 times, respectively, those of the Cabriolet nuclear single-charge cratering event. (auth)

4169 (UCRL-Trans–10477) PROSPECTIVE APPLICATIONS OF UNDERGROUND NUCLEAR EXPLOSIONS IN THE NATIONAL ECONOMY OF THE USSR. Kedrovskii, O. L. Translated for Univ. of California Lawrence Radiation Lab., Livermore, from Perspektivy Primeneniya Podzemnykh Vzryvov v Narodnom Khozyavstve Sovetskovo Soyuza USSR State Committee on the Uses of Atomic Energy, Moscow, 1970. 48p. (CONF-700305–6). Dep. NTIS.

From Meeting on Technical Aspects of Peaceful Uses of Nuclear Explosives, Vienna, Austria.

Possible industrial uses of both contained and cratering underground nuclear explosions in the USSR are discussed with reference to the radiological and seismic safety of such explosions. Particular applications include petroleum and natural gas production stimulation, creation of underground reservoirs, underground ore crushing, water reservoir construction and river flow diversion, and rock and soil displacement. Specific further tests and studies to determine the feasibility of industrial uses of underground nuclear explosions are recommended. (L.C.L)

4170 REVIEW OF THE SOVIET PROGRAM ON NUCLEAR EXPLOSIVES FOR THE NATIONAL ECONOMY. Werth, Glenn C. (Univ. of California, Livermore). Trans. Amer. Nucl. Soc.: 13: 632(Nov 1970).

From Meeting of the American Nuclear Society, Washington, D. C. See CONF-701102.

4171 PLOWSHARE AND THE ENVIRONMENT. Holzer, Fred (Univ. of California, Livermore). Trans. Amer. Nucl. Soc.: 13: 632-3(Nov 1970).

From Meeting of the American Nuclear Society, Washington, D. C. See CONF-701102.

4172 METHOD FOR ESTIMATING THE RISK FROM A PLOWSHARE DETONATION. Otway, Harry J.; Lohrding, Ronald K. (Los Alamos Scientific Lab., N. Mex.). Trans. Amer. Nucl. Soc.: 13: 633-4(Nov 1970).

From Meeting of the American Nuclear Society, Washington, D. C. See CONF-701102.

4173 USE OF MULTIPLE EXPLOSIVES FOR NUCLEAR GAS STIMULATION. Nordyke, Milo D. (Univ. of California, Livermore). Trans. Amer. Nucl. Soc.: 13: 634(Nov 1970).

From Meeting of the American Nuclear Society, Washington, D. C. See CONF-701102.

4174 RECOVERY OF HIGH-VISCOSITY PETROLEUM BY STEAM FROM GEOTHERMAL HEAT. Paz-Castillo, Fernando; Kruger, Paul (Stanford Univ., Calif.). Trans. Amer. Nucl. Soc.: 13: 634-5(Nov 1970).

From Meeting of the American Nuclear Society, Washington, D. C. See CONF-701102.

4175 PLOWSHARE EXPLOSIVE SHIELDING. Green, Joseph B. Jr. (Lawrence Radiation Lab., Livermore, Calif.); Lessler, Richard M. Trans. Amer. Nucl. Soc.: 13: 636(Nov 1970).

From Meeting of the American Nuclear Society, Washington, D. C. See CONF-701102.

4176 POSSIBILITIES OF RECOVERING COPPER FROM CHALCOPYRITE BY NUCLEAR UNDERGROUND LEACHING IN SITU. Munoz Ribadeneira, F. J. (Puerto Rico Nuclear Center, Mayaguez); Gomberg, Henry J. Trans. Amer. Nucl. Soc.: 13: 636-7(Nov 1970).

From Meeting of the American Nuclear Society, Washington, D. C. See CONF-701102.

4177 MARVEL EXPERIMENT. Crowley, B. K.; Glenn, H. D. (Univ. of California, Livermore). Trans. Amer. Nucl. Soc.: 13: 637(Nov 1970).

From Meeting of the American Nuclear Society, Washington, D. C. See CONF-701102.

4178 MICROFRACTURING IN POSTSHOT GASBUGGY ROCKS. Borg, I. Y. (Univ. of California, Livermore). Trans. Amer. Nucl. Soc.: 13: 638(Nov 1970).

From Meeting of the American Nuclear Society, Washington, D. C. See CONF-701102.

4179 INFLUENCE OF WATER IN ROCKS ON UNDERGROUND NUCLEAR EXPLOSION EFFECTS. Butkovich, Theodore R. (Univ. of California, Livermore). Trans. Amer. Nucl. Soc.: 13: 638(Nov 1970).

From Meeting of the American Nuclear Society, Washington, D. C. See CONF-701102.

4180 RADIONUCLIDE DISTRIBUTION IN THE PARTICLES PRODUCED BY THE SCHOONER EVENT. Heft, Robert E.; Phillips, William A.; Steele, William A. (Univ. of California, Livermore). Trans. Amer. Nucl. Soc.: 13: 640-1(Nov 1970).

From Meeting of the American Nuclear Society, Washington, D. C. See CONF-701102.

4181 TRITIUM DISTRIBUTION, RESIDENCE TIME, AND INVENTORY IN SEDAN CRATER EJECTA. Martin, J. R.; Koranda, J. J. (Univ. of California, Livermore). Trans. Amer. Nucl. Soc.: 13: 642(Nov 1970).

From Meeting of the American Nuclear Society, Washington, D. C. See CONF-701102.

Facilities and Equipment

Refer also to abstracts 4218, 4302, 4303, 4851, 5064, 5163, and 6062.

4182 (AAEC/E–207) FLOW OF SPHERES IN CYLINDRICAL VESSELS. PART II. PEBBLE TRANSIT IN RECIRCULATED RANDOM PACKINGS. Gatt, F. C. (Australian Atomic Energy Commission Research Establishment, Lucas Heights). Jun 1970. 30p. Dep. NTIS (U. S. Sales Only).

An experimental and statistical investigation was made of the transit of individual pebbles in recirculated random packings of equal spherical pebbles. Slightly aspherical pebbles were also studied. Pebbles of 1.00 in. or 0.75 in. nominal dia were used to form 30 in. deep beds in a 30 in. dia vessel with a concave base in the form of a cone with 25° slope. The pebbles flowed downwards under the influence of gravity. The independent variables whose effects were studied were the radial position of the pebble, the number of pebbles in the bed situated beneath the seeding position, the pebble size and sphericity, and the amount of recirculation. Both transient and equilibrium conditions were considered. An estimate was made of the mean amount of recirculation required to reach equilibrium from an initially random packing. For spherical pebbles this was approximately 1.6 times the number of pebbles in the bed, and for aspherical pebbles it was 2.8 times the number. Formulas are given for predicting the amount of recirculation required for a particular pebble to emerge from the bed. (auth) (Australia)

4183 (DP-Report-484) LABORATORY EXPERIMENTS CARRIED OUT ON CLAM SEALS. Project DRAGON. Woodley, H. J. (Atomic Energy Establishment, Winfrith (England)). Oct 1966. 24p. Dep. NTIS.

Experiments have been made with four different sizes of clam seal manufactured from hardenable stainless steel. Minimum loads required for sealing have been measured and it has been shown that the upper working temperature limit is in the region of +300°C. A limited number of experiments indicate that it is possible to use the seals with liquid nitrogen. There is a limit to the number of times that joints may be broken and remade without causing damage to the sealing faces but experiments show that it should be possible in some cases to remachine damaged faces in situ and make them suitable for resealing. (auth)

4184 (LA-4404-TR) FISHER APPARATUS MEASUREMENT OF AVERAGE PARTICLE DIAMETER IN POWDER METALLURGY. Bukowiecki, Jerzy. Translated by A. D. Cernicek (Los Alamos Scientific Lab., N. Mex.), from Rudy Metale Niezelaz.; 13: 193-9(1968). 10p. Dep. NTIS.

The use and advantages of the Fisher apparatus in quickly identifying the average diameter of powder particles are discussed. Theoretical bases for measuring average particle diameters by the permeability method are presented. It is shown that when using the Fisher apparatus in research correcting coefficients must be introduced. (auth)

4185 (NYO-3930-8) LIQUID METAL BEARINGS TECHNOLOGY FOR LARGE, HIGH TEMPERATURE SODIUM ROTATING MACHINERY. Progress Report, May 1, 1970–July 31, 1970. (Mechanical Technology, Inc., Latham, N. Y.). Contract AT(30-1)-3930. 53p. (MTI-70-TR-64). Dep. NTIS.

Activities in programs directed toward design and development of Na-lubricated bearings for high capacity Na pumps used in fast breeder reactors are summarized. During the report period check-out of the computer program for calculation of the performance of large, turbulent, externally-pressurized bearings was completed. Optimization calculations to establish bearing and restrictor geometry that provide maximum fluid film stiffness and maximum film damping were conducted. Calculations of fluid film stiffness, damping, and flow for both optimum and off-optimum bearing designs were completed. Initiation of production calculations to generate the bearing performance tables for inclusion in the design handbook is reported. Work was continued on installation of the 12 in. diameter, self-acting sodium lubricated bearing test rig. Analyses of the results of the screening-type corrosion tests of bearing surface materials after exposure to 1100°F sodium were completed. (J.R.D.)

4186 (ORNL-TM-2995) HYDRAULIC PERFORMANCE AND CAVITATION CHARACTERISTICS OF AN ELECTROMAGNETIC HELICAL INDUCTION PUMP OPERATING WITH POTASSIUM AND PREDICTION OF PERFORMANCE WITH LITHIUM AT 2200°F. Young, H. C.; Clark, D. L. (Oak Ridge National Lab., Tenn.). Nov 1970. Contract W-7405-eng-26. 55p. Dep. NTIS.

An electromagnetic helical induction pump with a cell fabricated from the high-temperature refractory tantalum alloy T-111 was operated with potassium at temperatures up to 1500°F and at flow rates from 0 to 6 gpm. The hydraulic performance of the test pump with potassium was used as the basis for predicting performance at 2200°F with lithium. Data obtained during subsequent successful operation with lithium showed the prediction to be slightly conservative. Data taken during operation with potassium indicated a reduction in the net positive suction head required to suppress cavitation inception for operation with degassed potassium in comparison with operation with argon in the system surge tank. (auth)

4187 (RISO-214, pp 21-40) THEORETICAL RELIABILITY ASSESSMENT OF A FIRE PROTECTION SYSTEM. Antocicco, S.; Tenaglia, G.; Valeri, A. (Comitato Nazionale per l'Energia Nucleare, Rome (Italy)).

From Proceedings of the meeting of specialists on the reliability of mechanical components and systems for nuclear reactor safety, Risoe, September 24–26, 1969.

A quantitative prediction is made of the reliability of a fire protection system for a plutonium handling facility. On the basis of component failure data the system fractional deadtime is calculated by means of a NOTED computer programme and the most critical components are identified. (7 references) (Denmark)

4188 (TID-25553) SURVEY REPORT ON STRUCTURAL DESIGN OF PIPING SYSTEMS AND COMPONENTS. Rodabaugh, E. C. (Battelle Memorial Inst., Columbus, Ohio); Pickett, A. G. (Southwest Research Inst., San Antonio, Tex.). Dec 1970. Subcontracts 2913; 3056. 561p. Dep. NTIS.

For Oak Ridge National Lab., Tenn.

A summary of design practices, service experience, and research work on the structural design of piping components and systems is presented to provide a background and direction for future work. The analysis is restricted to structural design aspects of metal piping systems. The information is presented in chapters on factors involved in structural design, analytical methods, failures, standards, straight pipe welds, curved pipes and miters, connections, reducers, valves and pumps, supporting elements, thermal stresses, and dynamic effects. (J.R.D.)

4189 (UCRL-19764) SIMPLIFIED HELIUM CRYOSTATS FOR SUPERCONDUCTING DIPOLES AND QUADRUPOLE MAGNETS. Green, Michael A. (California Univ., Berkeley. Lawrence Radiation Lab.). 29 Jul 1970. Contract W-7405-eng-48. 18p. Dep. NTIS.

The most expensive part of a superconducting magnet installation is often the magnet cryostat. Extensive use of superconducting dipole and quadrupole magnets requires study of the cryostat problem from a systems viewpoint. A number of suggestions that should lead to magnet cryostats of minimum cost are presented. The interaction of the cryostat with the refrigeration system is discussed. Basic cryostat design parameters are treated and design conditions for three types of superconducting dipole and quadrupole cryostats are presented. (auth)

4190 (UCRL-50923) PLUGGING OF HIGH EFFICIENCY FILTERS BY WATER SPRAY. Murrow, Jack (California Univ., Livermore. Lawrence Radiation Lab.). Aug 1970. 9p. Dep. NTIS.

Opinions about system performance should be verified during reevaluation of critical components. Those which are not supported during testing must be discarded. Water droplets plug high efficiency filters is an opinion which was proved by a series of filter plugging tests using various spray droplet sizes and water volumes. A coarse spray generated by an automatic sprinkler spray-head eroded the filter until it was breached. Tests were performed on new clean filters. Used filters, with dusts and chemicals adhered to their surfaces, would probably be affected to a greater degree. (auth)

4191 SODIUM TEST FACILITY. Matsuda, Masamichi (Fuji Electric Co. Ltd., Tokyo). FAPIG (Tokyo); No. 57, 49-53(May 1970). (In Japanese).

The Sodium Test Facility was constructed to test devices used in a sodium-cooled fast breeder reactor. In the facility, sodium is stored in a tank during shutdown; when test is made, it is melted and charged to the pre-heated loop. The loop consists of test and Na purification sections, sodium being circulated with one electromagnetic pump. The test section is made up of a testing vessel, heater, and cooler. Cover gas fills the portion above the sodium level in the vessel. The purification loop consists of cold-trap circuit to purify the sodium, and plugging-meter circuit to measure Na equivalent purity. The facility has a Na inventory 3,000 kg; test temperature from 250 to 550°C; and a Na circulation 30 t/min. The structural material is SUS32. (Japan)

4192 CONSTRUCTION AND OPERATION OF THE (ATR) COMPONENT TEST LOOP. Ishikawa, Masashi (Kawasaki Heavy Industries, Ltd., Kobe, Japan). FAPIG (Tokyo); No. 57, 18-27(May 1970). (In Japanese).

The Component Test Loop (CTL) was constructed to test the endurance of various components of an ATR such as fuel assembly, the junction between different materials, and seal plugs. The design of CTL is similar to that of a primary cooling system of the ATR, including pressure, temperature, and flow-rate. The position of a test component within CTL is not heated, but the temperature is achieved by inlet steam heated outside the loop.

XUM

The fabrication and operation of the loop and aspects leading to its completion are discussed. (Japan)

4193 FIRE PREVENTION AND PROTECTION IN HOT CELLS. Hill, A. J. Jr. (Savannah River Lab., Aiken, S. C.). Trans. Amer. Nucl. Soc.; 13: 840(Nov 1970).
From Meeting of the American Nuclear Society, Washington, D. C. See CONF-701102.

4194 FIRE PROTECTION CRITERIA FOR NUCLEAR FACILITIES. Patterson, D. E. (Atomic Energy Commission, Washington, D. C.). Trans. Amer. Nucl. Soc.; 13: 840-1(Nov 1970).
From Meeting of the American Nuclear Society, Washington, D. C. See CONF-701102.

4195 RECENT IMPROVEMENTS IN FIRE SUPPRESSION AND CONTROL FOR GLOVE-BOX OPERATIONS AT ROCKY FLATS. Williams, A. K. (Dow Chemical Co., Golden, Colo.). Trans. Amer. Nucl. Soc.; 13: 841(Nov 1970).
From Meeting of the American Nuclear Society, Washington, D. C. See CONF-701102.

4196 FIRE PREVENTION AND CONTROL IN NUCLEAR AIR CLEANING SYSTEMS. Burchsted, C. A. (Oak Ridge National Lab., Tenn.). Trans. Amer. Nucl. Soc.; 13: 841-2(Nov 1970).
From Meeting of the American Nuclear Society, Washington, D. C. See CONF-701102.

4197 ARGON ATMOSPHERE FILTER SYSTEM IN HFEF HOT CELL. Swanstrom, R. H.; Hirsch, P. R. (Argonne National Lab., Ill.). Trans. Amer. Nucl. Soc.; 13: 849-50(Nov 1970).
From Meeting of the American Nuclear Society, Washington, D. C. See CONF-701102.

4198 LOW-COST TELEOPERATORS: A NEW INDUSTRIAL CONCEPT. Johnsen, Edwin G. (Atomic Energy Commission, Washington, D. C.). Trans. Amer. Nucl. Soc.; 13: 852-3(Nov 1970).
From Meeting of the American Nuclear Society, Washington, D. C. See CONF-701102.

4199 EXPERIMENTAL MOBILE AUTOMATION. Rosen, Charles A. (Stanford Research Inst., Menlo Park, Calif.). Trans. Amer. Nucl. Soc.; 13: 853-4(Nov 1970).
From Meeting of the American Nuclear Society, Washington, D. C. See CONF-701102.

4200 CAN MANKIND BENEFIT FROM MAN EXTENSION SYSTEMS. Flatau, Carl R. (Brookhaven National Lab., Upton, N. Y.). Trans. Amer. Nucl. Soc.; 13: 854(Nov 1970).
From Meeting of the American Nuclear Society, Washington, D. C. See CONF-701102.

4201 MECHANICAL SODIUM PUMP FOR LIQUID METAL COOLED FAST BREEDER REACTOR. Sagawa, Norihiko (Hitachi Ltd., Ibaraki, Japan); Kobayashi, Shigeaki; Ito, Yoshio. Hitachi Hyoron; 52: 419-24(May 1970). (In Japanese).

The results of construction of mechanical sodium pumps and problems when the size is increased in the future are described; these pumps are for the primary coolant circuit for a liquid-metal-cooled fast breeder reactor. The pump constructed in trial has operated satisfactorily with a total of about 3,000 operation hours, with various experiments done during the period. Subsequently to this, a pump was constructed in 1969 for use in an Na flow heat-transfer test facility of the Power Reactor and Nuclear Fuel Development Corporation (PNC). In the PNC, detailed designs were nearly completed for the experimental fast reactor, and conceptual designs were submitted to the prototype reactor firms. Problems for the pumps to be used in the practical reactors in future of output 1,000 to 3,000 MW(e) are discussed. (Japan)

Heat Transfer and Fluid Flow

Refer also to abstracts 4185, 4188, 4190, 4221, 4896, 5969, 6028, 6067, 6083, 6085, and 6199.

4202 (BNL-tr-365) BOILING OF LIQUID ALKALI METALS IN TUBES. Petukhov, B. S.; Zeigarnik, Yu. A. Translated by S. J. Amoretty (Brookhaven National Lab., Upton, N. Y.), from Teplofiz. Vys. Temp.; 8: 309-18(1970). 22p. Dep. NTIS.

An analysis of the state of the art in boiling alkali metal technology is presented which shows that investigation in this area is in its initial stages. A comparison of data on heat transfer to boiling alkali metals in tubes with calculated values for this phenomenon is included and examined. (J.R.D.)

4203 (DP-Report-578) ANALYTICAL TREATMENT OF A TRANSIENT METHOD FOR DETERMINATION OF THE THERMAL CONDUCTIVITY OF A HOLLOW RIGHT CYLINDER OF SOLID MATERIAL. Project DRAGON. Von Bonsdorff, M. (Atomic Energy Establishment, Winfrith (England)). Jun 1967. 9p. Dep. NTIS.

An analytical method is described for estimating the thermal diffusivity of solids in the shape of a hollow right cylinder. The thermal diffusivity of Dragon reactor annular fuel cartridges can be estimated using this method. (J.R.D.)

4204 (HASL-238) MASS TRANSFER OF AEROSOLS WITH AXIAL DIFFUSION IN CIRCULAR TUBES. Tan, C. W. Oct 1970. 57p. Dep. NTIS.
For Health and Safety Lab., New York Operations Office, N. Y.

A mathematical analysis of the diffusion of particles flowing in a circular tube has been done taking into account axial as well as radial diffusion. Both the case of particles entering the inlet, without formation in the channel, and the case of particles forming uniformly within the tube were considered for the two conditions of slug flow and Poiseuille flow. For slug flow, closed analytical solutions of the basic differential equations are presented. For Poiseuille flow, solutions were obtained with the aid of a high speed digital computer. Two detailed tables are given which permit calculation of aerosol diffusion constants from experimental parameters, with or without formation of aerosols within the diffusion tube. (auth)

4205 MEASUREMENT OF FLOW RATE USING TEMPERATURE FLUCTUATION CAUSED BY VORTEX STREET. Michiyoshi, Itaru; Ohtsubo, Akira (Kyoto Univ.). J. Nucl. Sci. Technol. (Tokyo); 7: 511-17(Oct 1970).

Vortexes are shed behind an obstructing rod standing in a stream. The shedding frequency of the vortexes is proportional to the velocity of the stream. To detect its frequency, measurement of the temperature fluctuations of the fluid caused by the vortexes behind a heated rod is proposed. By adopting this method, it should be possible to measure the flow rate of high-temperature fluids passing through a tube. (auth)

4206 ASYMMETRY EFFECTS ON HEAT TRANSFER AND FLUID FLOW IN ROD BUNDLES. Chen, Ka Wei; Fulford, P. J. (Purdue Univ., Lafayette, Ind.). Trans. Amer. Nucl. Soc.; 13: 808-9(Nov 1970).
From Meeting of the American Nuclear Society, Washington, D. C. See CONF-701102.

4207 VELOCITY PROFILE AND PRESSURE DROP MEASUREMENTS IN FULLY DEVELOPED MERCURY PIPE FLOW. Hochreiter, L. E.; Sesonske, Alexander (Purdue Univ., Lafayette, Ind.). Trans. Amer. Nucl. Soc.; 13: 809-10(Nov 1970).
From Meeting of the American Nuclear Society, Washington, D. C. See CONF-701102.

4208 HYDRODYNAMIC STABILITY IN CURVED STEAM GENERATOR TUBES. Malek, G. J.; Schlueter, G. (Gulf General Atomic, Inc., San Diego, Calif.). Trans. Amer. Nucl. Soc.; 13: 810-11(Nov 1970).
From Meeting of the American Nuclear Society, Washington, D. C. See CONF-701102.

4209 FILM AND TRANSITION BOILING AROUND SPHERES. Stevens, J. W.; Witte, L. C. (Univ. of Houston, Tex.). Trans. Amer. Nucl. Soc.; 13: 816(Nov 1970).
From Meeting of the American Nuclear Society, Washington, D. C. See CONF-701102.

4210 TIME-DEPENDENT NUCLEATE BOILING REQUIREMENTS FOR LIQUID SODIUM. Nystrom, R. E. (Naval Ship Research and Development Lab., Panama City, Fla.); Hammitt, F. G. Trans. Amer. Nucl. Soc.; 13: 818-19(Nov 1970).
From Meeting of the American Nuclear Society, Washington, D. C. See CONF-701102.

4211 CRITICAL AND LEIDENFROST POINT HEAT FLUXES IN A SODIUM-HEATED STEAM GENERATOR. Cho, S. M. (Atomics International, Canoga Park, Calif.). Trans. Amer. Nucl. Soc.; 13: 819-20(Nov 1970).
From Meeting of the American Nuclear Society, Washington, D. C. See CONF-701102.

4212 FURTHER STUDY OF THE PRESSURE-TEMPERATURE HISTORY MODEL OF LIQUID-METAL BOILING INCEP-

TION. Singer, Ralph M.; Holtz, Robert E. (Argonne National Lab., Ill.). Trans. Amer. Nucl. Soc.; 13: 820-1(Nov 1970).
From Meeting of the American Nuclear Society, Washington, D. C. See CONF-701102.

Isotope Technology

Refer also to abstracts 4128, 4253, 4259, 4304, 4329, 4349, 4350, 4356, 4409, 4517, 4631, 4634, 4635, and 4772.

4213 (CONF-691051–, pp 145-53) THE GAS CENTRIFUGE PROBLEM, THE MOMENTUM OF TECHNOLOGY AND INTERNATIONAL COLLABORATION IN NUCLEAR ENERGY. Barnaby, C. F.
From World security, disarmament and development.
The economic and political implications of developing gas centrifuges for U enrichment are discussed. It is concluded that: gas centrifuges do represent a real threat to world security, specifically as a means for producing fissile material clandestinely for nuclear weapons; the development of this technology would have adverse effects on the arms control negotiations; international collaboration in the development of gas centrifuges is the best security measure; and, if a gas centrifuge plant is constructed, it should be owned and operated by the IAEA. (L.C.L.)

4214 (CONF-691051–, pp 354-61) CENTRIFUGAL URANIUM ISOTOPE SEPARATION AND NUCLEAR WEAPON PROLIFERATION. Watson, C. J. H.
From World security, disarmament and development.
The possible threat to world peace represented by an imminent technological development, the separation of U isotopes by the ultracentrifuge, is examined, and suggestions are made for an international control system which would attempt to prevent the proliferation of nuclear weapons in the coming decades. (L.C.L.)

4215 (NUMEC–3731-23) SAFETY AND RADIATION REPORT. PHASE I SUMMARY. RADIOISOTOPE POWERED CARDIAC PACEMAKER PROGRAM. (Nuclear Materials and Equipment Corp., Apollo, Pa.). 29 Jun 1970. Contract AT(30-1)-3731. 183p. Dep. NTIS.
Safety and radiation results were developed during Phase I of the Radioisotope Powered Cardiac Pacemaker Program. These results include both analyses and testing related to the plutonium-238 fuel capsule. In the preparation of a preliminary safety analysis and test plan, credible accident conditions were assessed. Elevated temperature and pressure tests were performed on the experimental model and prototype capsule configurations to demonstrate that the capsules can sustain a maximum industrial fire-rated condition of a 1900°F temperature and the corresponding helium build-up pressures for a 50 year design life. Part of these efforts called for the development of an ultrasonic technique for detecting microcrack defects in the inner capsule material. Thirty prototype safety capsules, consisting of inner, middle and outer capsules and plugs, were used in the following types of tests: elevated temperature tests, crush tests, impact tests, bullet tests and power tool tests. During the impact tests, the capsule was shown to survive impact at a velocity of 242 ft/sec, a factor of 2.3 greater than the tumbling terminal velocity. During the elevated temperature tests, capsules were tested in an oxidizing atmosphere along the standard fire curve to 1900°F and higher, as well as in a fire debris test. A simulated cremation test of an unfueled pacemaker was performed in which a maximum temperature of 2070°F was reached. In order to sustain this increased temperature, several potential material design changes were suggested. The crush tests completed included forge press, cold roll, sledge hammer, and penetration tests. A series of hand-held power tool tests was also performed on the capsule using an industrial-type drill, saw and disc grinder. Firearm projectile penetration tests were performed to determine the capability of a capsule for sustaining firearm accidents. Analysis and measurement of the radiological emissions from fueled devices have also been presented. Dose levels at contact have been found to be less than the RPCP program objective of 5 mrad/hr. (auth)

4216 (SC-PR-70-682) AEROSPACE NUCLEAR SAFETY PROGRAM QUARTERLY REPORT, JULY 1–SEPTEMBER 30, 1970. Illing, R. G. (comp.) (Sandia Labs., Albuquerque, N. Mex.). Oct 1970. 47p. Dep. NTIS.
Research progress is reported on SNAP 27, Transit/Pioneer, isotope Brayton systems, fuel safety, Flintstone-1, and computer codes. (J.R.D.)

4217 RADIOISOTOPE HEAT SOURCE. Botts, William V.; Parkinson, Ronald Y.; Williams, John S. (to North American Rockwell Corp.). U. S. Patent 3,533,913. 13 Oct 1970. Filed 6 Feb 1967.
A thermal power radioisotope heat source characterized by low radiation dose rates and by uniquely high power density, reliability, safety, and passivity, which utilizes a low-weight depleted uranium structural radiation shield in combination with selected materials so that the uranium shield may be utilized at elevated temperatures, is described. Exemplary and preferred is a 5-watt (thermal) heat source having a power density of at least 2 watts/lb and a power-to-volume ratio of at least 1 watt/in.^{3} containing $^{147}Pm_2O_3$ as radioisotopic fuel enclosed in a first capsule of tantalum–tungsten alloy, which is then enclosed in a second capsule of depleted uranium material outwardly wrapped in a tantalum foil, and then enclosed in a third outer capsule of stainless steel. (auth)

4218 ^{252}Cf PROGRESS. Californium-252 Progr.; No. 4, 1-33(Aug 1970).
ATMOSPHERE — sulfur content of, performance of californium-252 source for measurement of
CALIFORNIUM-252 — availability in 1971
— evaluation of uses of
— handling, shipping, and storage of sources of
— shielding of, materials for
MINERAL DEPOSITS — prospecting by in situ neutron activation using californium-252 source
NEUTRON SOURCES — evaluation of californium-252
— availability of californium-252, in 1971
— handling, shipping, and storage of californium-252
— shielding of californium-252, materials for
RADIOGRAPHY, INDUSTRIAL — neutron source for, evaluation of californium-252
RADIOTHERAPY — neutron source for, evaluation of californium-252
SULFUR — content in atmosphere, performance of californium-252 source for measurement of
WELL LOGGING — neutron source for, evaluation of californium-252

4219 RADIOISOTOPE-FUELED THERMOELECTRIC MILLIWATT POWER SUPPLIES. Ream, Joseph T. (Gulf General Atomic, Inc., San Diego, Calif.). Trans. Amer. Nucl. Soc.; 13: 448(Nov 1970).
From Meeting of the American Nuclear Society, Washington, D. C. See CONF-701102.

4220 REVIEW OF THE NUCLEAR SAFETY PROGRAM ON THE SNAP-23A POWER SYSTEM. Menchen, William R. (Hittman Associates, Inc., Columbia, Md.); Vachon, Lawrence J. Trans. Amer. Nucl. Soc.; 13: 448-9(Nov 1970).
From Meeting of the American Nuclear Society, Washington, D. C. See CONF-701102.

4221 PROMPT AND MULTIORBITAL REENTRY OF SMALL RADIOISOTOPE HEATERS AT SUPERORBITAL VELOCITIES. Barsell, A. W.; Smith, T. H.; Warner, E. E. (Donald W. Douglas Labs., Richland, Wash.). Trans. Amer. Nucl. Soc.; 13: 449-50 (Nov 1970).
From Meeting of the American Nuclear Society, Washington, D. C. See CONF-701102.

4222 PASSIVE NUCLEAR ATTITUDE CONTROL SYSTEM FOR SOLAR PROBES. Choong, Philip T. (United Nuclear Corp., Elmsford, N. Y.); Mason, Edward A. Trans. Amer. Nucl. Soc.: 13: 450(Nov 1970).
From Meeting of the American Nuclear Society, Washington, D. C. See CONF-701102.

4223 HIGH-ENERGY CALIBRATION USING ^{252}Cf NEUTRON SOURCE. Trombka, J. I.; Eller, E. L.; King, K. J.; Fine, I. T. (Goddard Space Flight Center, Greenbelt, Md.). Trans. Amer. Nucl. Soc.; 13: 490-2(Nov 1970).
From Meeting of the American Nuclear Society, Washington, D. C. See CONF-701102.

4224 AEC ^{60}Co HEAT SOURCE PROGRAMS. Ross, C. P. (Savannah River Lab., Aiken, S. C.). Trans. Amer. Nucl. Soc.; 13: 492-3(Nov 1970).
From Meeting of the American Nuclear Society, Washington, D. C. See CONF-701102.

4225 2- TO 10-kW(e) RADIOISOTOPE-FUELED ORGANIC RANKINE POWER SYSTEM. Fink, Charles R. (Sanders Nuclear Corp., Nashua, N. H.); Krueger, Earl C. Trans. Amer. Nucl. Soc.; 13: 493-4(Nov 1970).
From Meeting of the American Nuclear Society, Washington, D. C. See CONF-701102.

4226 MAPLE IB: A ^{60}Co-FUELED THERMOELECTRIC GENERATOR. Hare, G. E.; Daughtrey, S. P.; Round, K. J.

(Atomic Energy of Canada Ltd., Ottawa). Trans. Amer. Nucl. Soc.; 13: 494-5(Nov 1970).
From Meeting of the American Nuclear Society, Washington, D. C. See CONF-701102.

4227 PRODUCTION OF ^{238}Pu WITH MINIMUM ^{236}Pu CONTAMINATION. Lindsey, W. J. (Atomic Energy Commission, Washington, D. C.); Roggenkramp, P. L.; Woods, W. K. Trans. Amer. Nucl. Soc.; 13: 496(Nov 1970).
From Meeting of the American Nuclear Society, Washington, D. C. See CONF-701102.

4228 PURIFICATION, ENCAPSULATION, AND CHARACTERIZATION OF ^{238}Pu FOR IMPLANTATION PURPOSES. Mullins, L. J.; Leary, J. A. (Los Alamos Scientific Lab., N. Mex.). Trans. Amer. Nucl. Soc.; 13: 496-7(Nov 1970).
From Meeting of the American Nuclear Society, Washington, D. C. See CONF-701102.

4229 DESIGN OF RADIOISOTOPE HEAT SOURCES FOR HUMAN IMPLANTATION. Cole, Donald W.; Mott, William E. (Atomic Energy Commission, Washington, D. C.). Trans. Amer. Nucl. Soc.; 13: 497-8(Nov 1970).
From Meeting of the American Nuclear Society, Washington, D. C. See CONF-701102.

4230 DESIGN OF RADIOISOTOPE HEAT SOURCE SUBSYSTEMS FOR HEART DEVICES. Bustard, Thomas S.; Princiotta, Frank T. (Hittman Associates, Inc., Columbia, Md.). Trans. Amer. Nucl. Soc.; 13: 501(Nov 1970).
From Meeting of the American Nuclear Society, Washington, D. C. See CONF-701102.

4231 RESULTS OF BENCH MODEL TESTING OF RADIOISOTOPE HEAT SOURCE SUBSYSTEMS FOR HEART DEVICES. Princiotta, Frank T.; Bustard, Thomas S. (Hittman Associates, Inc., Columbia, Md.). Trans. Amer. Nucl. Soc.; 13: 501-3(Nov 1970).
From Meeting of the American Nuclear Society, Washington, D. C. See CONF-701102.

4232 DESIGN OF A ^{238}Pu-POWERED IMPLANTABLE THERMAL ENGINE FOR HEART ASSIST DEVICES. Rudnicki, M. I. (Aerojet Nuclear Systems Co., Azusa, Calif.); Chesworth, R. H.; Harmison, L. T. Trans. Amer. Nucl. Soc.; 13: 503-4 (Nov 1970).
From Meeting of the American Nuclear Society, Washington, D. C. See CONF-701102.

4233 RADIOISOTOPE-FUELED STIRLING ENGINE ARTIFICIAL HEART POWER SYSTEM. Martini, W. R. (Donald W. Douglas Labs., Richland, Wash.); Riggle, P.; Harmison, L. T. Trans. Amer. Nucl. Soc.; 13: 504(Nov 1970).
From Meeting of the American Nuclear Society, Washington, D. C. See CONF-701102.

4234 RADIOISOTOPE-FUELED VAPOR CYCLE POWER SUPPLY FOR AN ARTIFICIAL HEART. Huffman, F. N. (Thermo Electron Corp., Waltham, Mass.); Bornhorst, W. J.; Harmison, L. T. Trans. Amer. Nucl. Soc.; 13: 504-5(Nov 1970).
From Meeting of the American Nuclear Society, Washington, D. C. See CONF-701102.

4235 IMPLANTABLE ELECTRICAL POWER SOURCE FOR AN ARTIFICIAL HEART SYSTEM. Altieri, F. D.; Kudrick, J. A. (Hittman Associates, Inc., Columbia, Md.). Trans. Amer. Nucl. Soc.; 13: 505(Nov 1970).
From Meeting of the American Nuclear Society, Washington, D. C. See CONF-701102.

4236 POPULATION SAFETY CONSIDERATIONS OF AN IMPLANTABLE ISOTOPIC POWER SOURCE. Perez, Lawrence J. Jr.; Coleman, James R. (Nuclear Utility Services, Inc., Rockville, Maryland). Trans. Amer. Nucl. Soc.; 13: 506-7(Nov 1970).
From Meeting of the American Nuclear Society, Washington, D. C. See CONF-701102.

4237 THERMIONIC AND BETAVOLTAIC NUCLEAR POWER SOURCES FOR PACEMAKING. Knapp, D. E. (Donald W. Douglas Labs., Richland, Wash.). Trans. Amer. Nucl. Soc.; 13: 507 (Nov 1970).
From Meeting of the American Nuclear Society, Washington, D. C. See CONF-701102.

4238 ANIMAL-IMPLANTED NUCLEAR POWERED PACEMAKERS. Pennington, W. Herbert (Atomic Energy Commission, New York); Hursen, Thomas F.; Frommer, Peter L.; Morrow, Andrew G. Trans. Amer. Nucl. Soc.; 13: 507-8(Nov 1970).
From Meeting of the American Nuclear Society, Washington, D. C. See CONF-701102.

4239 FRENCH NUCLEAR-POWERED PACEMAKER PROGRAM. Laurens, Paul (Institut National de la Sante et de la Recherche Medicale, Paris). Trans. Amer. Nucl. Soc.; 13: 508 (Nov 1970).
From Meeting of the American Nuclear Society, Washington, D. C. See CONF-701102.

4240 MINIATURE NUCLEAR BATTERIES: A REVIEW OF WORK IN THE UK. Poole, M. J.; Myatt, J.; Penn, A. W.; Brown, M. H. (Atomic Energy Research Establishment, Harwell, Eng.). Trans. Amer. Nucl. Soc.; 13: 508-9(Nov 1970).
From Meeting of the American Nuclear Society, Washington, D. C. See CONF-701102.

4241 ISOTOPE-POWERED, INDWELLING INTRACRANIAL PRESSURE SENSOR. Bloom, Gerald; Murphy, Kenneth; Cox, Thomas (Hittman Associates, Inc., Columbia, Md.). Trans. Amer. Nucl. Soc.; 13: 509-10(Nov 1970).
From Meeting of the American Nuclear Society, Washington, D. C. See CONF-701102.

4242 TOPS RTG NUCLEAR RADIATION ENVIRONMENT ANALYSIS. Anno, George H. (ART Research Corp., Los Angeles); Wolf, Fred. Trans. Amer. Nucl. Soc.; 13: 535-6 (Nov 1970).
From Meeting of the American Nuclear Society, Washington, D. C. See CONF-701102.

4243 RTG EFFECTS OF CCEM DETECTORS IN A PLASMA ANALYZER FOR PIONEER F/G. Zaviantseff, V. T. (Ames Research Center, Moffett Field, Calif.). Trans. Amer. Nucl. Soc.; 13: 536(Nov 1970).
From Meeting of the American Nuclear Society, Washington, D. C. See CONF-701102.

4244 NEUTRON EMISSION CHARACTERISTICS OF A PuO_2 SOURCE. Taherzadeh, M. (Jet Propulsion Lab., Pasadena, Calif.). Trans. Amer. Nucl. Soc.; 13: 537(Nov 1970).
From Meeting of the American Nuclear Society, Washington, D. C. See CONF-701102.

4245 GAMMA-RAY SOURCE CHARACTERISTICS OF PuO_2. Dore, Michael A. (Jet Propulsion Lab., Pasadena, Calif.). Trans. Amer. Nucl. Soc.; 13: 537-8(Nov 1970).
From Meeting of the American Nuclear Society, Washington, D. C. See CONF-701102.

4246 RTG/RADIOISOTOPE HEATER SHIELDING FOR SENSITIVE SCIENCE INSTRUMENTS ON SPACECRAFT. Dore, Michael A.; Noon, Edward L. (Jet Propulsion Lab., Pasadena, Calif.). Trans. Amer. Nucl. Soc.; 13: 539-40(Nov 1970).
From Meeting of the American Nuclear Society, Washington, D. C. See CONF-701102.

4247 INTERPLANETARY SPACECRAFT: RTG RADIATION ANALYSIS. Campe, Kazimieras M. (Hittman Associates, Inc., Columbia, Md.); Harris, Dale W. Trans. Amer. Nucl. Soc.; 13: 540-1(Nov 1970).
From Meeting of the American Nuclear Society, Washington, D. C. See CONF-701102.

4248 PORTABLE LOW-ENERGY PHOTON CALIBRATION SOURCE. Boggs, J. Vincent (Univ. of California, Livermore). Trans. Amer. Nucl. Soc.; 13: 880(Nov 1970).
From Meeting of the American Nuclear Society, Washington, D. C. See CONF-701102.

Materials Testing

Refer also to abstracts 4038, 4215, 4346, 4348, 4404, 4875, and 6033.

4249 CONTROL OF REINFORCED CONCRETE CONSTRUCTION BY MEANS OF FAST NEUTRONS. Gorbunov, V. I.; Blagin, V. B.; Pekarskii, G. Sh.; Yaroslavtsev, V. D. Izv. Vyssh. Ucheb. Zaved., Fiz.; No. 3, 139-41(1970). (In Russian).

In concrete construction work it was found that neutron defectoscopy could be satisfactorily used to detect air cavities around the reinforcing steel. The discrimination threshold and sensitivity were better for the neutron method than for gamma transmission methods. A unit developed at Tomsk Polytechnic University is described. The polonium-beryllium neutron source yielded 10^7 neutrons/sec. The scanning rate was 0.5 m/min for a concrete thickness of 400 mm. The width of the control section

was 30 mm. Air cavities having a size 15 × 15 × 15 mm could be detected in concrete 30 cm thick. The transmitted neutrons were picked up by means of a scintillation crystal and a photomultiplier. This part of the equipment was portable, and was connected to the measuring panel by a cable 25 m long. (TTT)

4250 METHOD FOR PRODUCING MICROAUTORADIOGRAMS OF THE SURFACE OF IRRADIATED ALUMINUM. Pshenichnov, Yu. P.; Yurish, M. (Inst. of Steel and Alloys, Moscow. Inst. of Science of Metals and the Tests of Materials, Freiburg, Ger.). Zavod. Lab.; 36: 956-9(1970). (In Russian).

Conditions were determined for obtaining high quality microautoradiograms of the surfaces of thermal-neutron irradiated aluminum. Calculations were made for the selection of parameters necessary for precise microautoradiograms, taking into consideration conditions of irradiation, and concentration of alloying element in the aluminum.

4251 ANALYTICAL MODEL OF THE RECORDING PROCESS IN NEUTRON RADIOGRAPHY. Harms, A. A.; Garside, B. K. (McMaster Univ., Hamilton, Ont.). Trans. Amer. Nucl. Soc.; 13: 542(Nov 1970).

From Meeting of the American Nuclear Society, Washington, D. C. See CONF-701102.

4252 NEUTRON RADIOGRAPHY DEVELOPMENT PROGRAM FOR SNAP-8 FUEL ELEMENTS. Hillig, O. R.; Golliher, K. G.; Swanson, V. A. (Atomics International, Canoga Park, Calif.). Trans. Amer. Nucl. Soc.; 13: 542-3(Nov 1970).

From Meeting of the American Nuclear Society, Washington, D. C. See CONF-701102.

4253 RADIOGRAPHIC INSPECTION OF A DEVELOPMENTAL ^{244}Cm–Be NEUTRON SOURCE. Barton, John P.; Buzzell, John; Berger, Harold (Argonne National Lab., Ill.). Trans. Amer. Nucl. Soc.; 13: 543-4(Nov 1970).

From Meeting of the American Nuclear Society, Washington, D. C. See CONF-701102.

4254 NEUTRON RADIOGRAPHY OF MIXED-OXIDE FUELS. Dahlke, L. W.; Robkin, M. A. (Univ. of Washington, Seattle). Trans. Amer. Nucl. Soc.; 13: 544(Nov 1970).

From Meeting of the American Nuclear Society, Washington, D. C. See CONF-701102.

Protective Structures

4255 (ORNL-TM-3016) TRANSPORTATION SYSTEMS AND DUAL PURPOSE BLAST SHELTERS. A Progress Report. Cristy, G. A. (Oak Ridge National Lab., Tenn.). Jul 1970. Contract W-7405-eng-26. 144p. Dep. NTIS.

A first step toward a full blast shelter oriented civil defense program could involve a change in priority of selection of existing shelters to utilize the inherent blast resistance of the 13 million PV 71-81 shelters (i.e., underground shelters) already located by the National Fallout Shelter Survey (NFSS). Minor modifications could be made in the design of structures to be built for new or expanded transportation facilities in and around the major cities, which would make it possible to provide additional blast shelters. This would include stations and tunnels of rapid transit systems, underground garages, highway and railway tunnels and the abutments of the interchange and grade separations of interstate highways. The availability of these types of shelters to the population of major cities is evaluated. The procedure used for evaluating and comparing the data is described. Of the 54 Standard Metropolitan Statistical Areas with populations over one-half million in 1960, 31 have provided data on new transportation systems being planned for the next decade. These planned structures could provide at least 5½ million blast shelters if the proper changes in design were accomplished before construction starts. In the largest (1960 census basis) SMSA, there are 8½ million PV 71-81 shelters located by the NFSS. Approximately 70% of this capacity could be filled by persons living within a 15-minute walk of the shelters. The potential shelter spaces within the 31 SMSA's could be filled to 80% capacity by persons living within a 30-minute walk. The program for matching shelters and population geographically is operational and can be used for any assignment problem provided that geographical distribution of the potential shelters is known. (auth)

4256 STUDY OF THE COMPONENTS OF THE EXPOSURE IN CYLINDRICAL STRUCTURES. Hinkley, D. E. (Radiation Research Associates, Inc., Fort Worth, Tex.). Trans. Amer. Nucl. Soc.; 13: 859(Nov 1970).

From Meeting of the American Nuclear Society, Washington, D. C. See CONF-701102.

Radioactive Material Handling

Refer also to abstracts 4193–4197, 4248, 4341, 4344, and 4515.

4257 (BNWL-SA-3304) ^{235}U DEPLETION AS A POTENTIAL INDEPENDENT CROSS-CHECK OF THE PLUTONIUM CONTENT OF SPENT POWER REACTOR FUELS. Schneider, R. A.; Christensen, D. E.; Granquist, D. P. (Battelle-Northwest, Richland, Wash. Pacific Northwest Lab.). 28 May 1970. Contract AT(45-1)-1830. 20p. (CONF-700541-1). Dep. NTIS.

From 11th Annual Meeting of the Institute of Nuclear Materials Management, Gatlinburg, Tenn.

Small and gross material sample data for the Yankee Reactor spent fuel were evaluated in a search for relations which would provide an independent cross-check of Pu content. The relation of ^{235}U depletion versus Pu content was examined. It was found that a linear function fits the data. These data are used to establish a technique applicable to individual input batches or the input to an entire campaign when a core of a single or uniform initial enrichment is being processed. It is also applicable to the entire input to a campaign when the core is of various initial enrichments. (J.R.D.)

4258 (BNWL-SA-3379) AMOUNT AND CHARACTERISTICS OF PLUTONIUM MADE AIRBORNE UNDER THERMAL STRESS. Mishima, J.; Schwendiman, L. C. (Battelle-Northwest, Richland, Wash. Pacific Northwest Lab.). 20 Oct 1970. Contract AT(45-1)-1830. 10p. (CONF-701106-1). Dep. NTIS.

From Symposium of the Health Physics Society, Idaho Falls, Idaho.

The quantity and nature of the particles airborne when plutonium metal or compounds are subjected to thermal stresses are under study. A retrospective review of incidents that have occurred in operations involving plutonium helped orient the investigation towards situations which may be most productively studied. An analysis was made of circumstances surrounding 46 incidents occurring in the nuclear industry from 1952 to 1967, and the incidents cataloged as to nature of the material involved, initiating event, and consequences. A series of laboratory studies was conducted to investigate the behavior of plutonium and its compounds when subjected to thermal stresses which might occur in overheating situations. Fractional release rate was measured for plutonium metal, plutonium nitrate, plutonium fluoride, and plutonium oxide when subjected to temperatures up to 1000°C. Release from heated solutions of plutonium nitrate was measured for several heating rates. Rate of release from combustion of small samples of four materials impregnated with powder or with nitrate was measured. The range of release rates is presented. Large scale experiments are planned using uranium compounds as simulants for plutonium. Conditions which reflect the type of thermal stresses typical of those postulated for some serious incidents will be imposed. Emphasis is to be given to those situations currently regarded as potentially serious when plutonium or its compounds in shipment are involved in a petroleum fire. The information gathered has given insight into the potential for release of plutonium and its compounds under various conditions. (auth)

4259 (BNWL-SA-3609) MODIFICATIONS OF A TRIODE SPUTTERING UNIT TO PROVIDE MAXIMUM FLEXIBILITY FOR USE IN A RADIOACTIVE GLOVE BOX ENVIRONMENT. Coleman, W. J. (Battelle-Northwest, Richland, Wash. Pacific Northwest Lab.). [nd]. Contract AT(45-1)-1830. 20p. (CONF-701011-2). Dep. NTIS.

In the development of a method to contain polonium as an isotopic heat source the hollow microsphere concept was originated. The process of modification and installation of a sputtering system for deposition of a protective coating onto microsphere heat sources is described. To make the heat source work many new fabrication processes were required. Deposition of activation layer (or direct deposition of alpha emitter) and deposition of compatibility cladding in this process involves sputtering and vacuum evaporation techniques. The process described is the modification and installation of a sputtering system to deposit a protective coating over the 150 μ diameter fueled microsphere in preparation for chemical vapor deposition of the containment shell. The substrate area consisted of microsphere container dishes located in a circular pattern, connected to two electromagnets. The power supply was designed to provide amplitude, frequency, and phase control to provide random movement of the microspheres for deposition of a uniform spherical coating. (auth)

4260 (CEA-Bib-184) SEPARATION METHODS OF NOBLE FISSION GASES FROM GASEOUS EFFLUENTS. Cardinale, Antonio (Commissariat a l'Energie Atomique, Saclay (France). Centre d'Etudes Nucleaires). Aug 1970. 64p. Dep. NTIS (U. S. Sales Only).

The physical principles of the various methods used for the separation of noble fission gases from gaseous effluents are reviewed. Diffusion through permselective membranes, thermal diffusion, absorption and fractional extraction into solvents, clathrate formation, low temperature distillation, and adsorption in solids are described. A description is also given of the main applications made up in the nuclear industry. Price estimates are presented for installations based on these principles and the advantages and disadvantages of each installation are listed. (auth) (France)

4261 (CEA-R-4067) REMOTE HANDLING IN OPERATION OF THE INSTALLATION "ATTILA". Rochedereux, Y.; Jeantet, E.; Bourgeois, M.; Perrot, M. (Commissariat a l'Energie Atomique, Fontenay-aux-Roses (France). Centre d'Etudes Nucleaires). Oct 1970. 41p. (In French). Dep. NTIS (U. S. Sales Only).

A description is made of the remote handling equipment and of the remotely operated systems used in the ATTILA facility. Experience obtained during 18 months of cell operation in the field of nonaqueous reprocessing is presented and discussed. (auth) (France)

4262 (DP-Report-446) FACILITIES AT RESEARCH ESTABLISHMENT RISOE FOR POST-IRRADIATION EXAMINATION OF DRAGON PROJECT EXPERIMENTS. Project DRAGON. Larsen, F. Bundgaard; Soerensen, Arne (Atomic Energy Establishment, Winfrith (England)). Jul 1966. 13p. Dep. NTIS.

This report contains a brief, general description of the hot cell facility at Research Establishment Risoe, Denmark, and a detailed description of equipment and working methods used in connection with post-irradiation examinations of Dragon Project experiments. (auth)

4263 (KFK-1102) DEVELOPMENT OF SAFEGUARDS PROCEDURES FOR A REPROCESSING PLANT SIMILAR TO THE WAK TYPE. Hagen, A.; Nentwich, D.; Kraemer, R.; Gupta, D.; Haefele, W. (Kernforschungszentrum, Karlsruhe (West Germany). Institut fuer Angewandte Reaktorphysik). Apr 1970. IAEA Contract 712/RB. 75p. Dep. NTIS (U. S. Sales Only).

An analysis of the WAK plant layout and process steps is presented along with descriptions of the plant operation and areas which are relevant to a rational safeguards system. Strategic areas in the plant at which the information required for safeguards can be obtained in a non-intrusive manner and without hampering the normal operation of the plant are discussed. The safeguards measures at these strategic areas have been developed and the procedures for carrying out such measures have been implemented. Error propagation mechanisms, including random and systematic components of measurement error, were analyzed and their effects on the establishment of a material balance are shown with the help of a numerical example. An effort has also been made to estimate the costs to be expected for the proposed safeguards system. It is shown that they may be about 3% of the reprocessing costs at the plant. Chemical analyses form a major part of the total costs. Means of reducing these costs are discussed. A number of possible improvements with regard to safeguards methods instrumentation and techniques are discussed. Estimates on workloads were also made. Relevant features in reprocessing plants which may be of interest for safeguards are described with the help of a reference plant layout. (auth)

4264 (NP-18527) ESTABLISHMENT OF HIGH-LEVEL RADIOACTIVE MATERIALS MANAGEMENT CENTERS IN SALT DOME STRUCTURES. (Gilbert and Pilcher, Inc., Baton Rouge, La.). Mar 1970. 64p.

For Southern Interstate Nuclear Board, Atlanta, Ga.

This study determined that the use of a salt dome as a repository for high-level radioactive materials is feasible. The salt dome being underground and isolated from man's environment presents an almost ideal means of permanent disposal. Domal salt properties, such as plasticity, thermal conductivity, porosity, permeability and structural strength, further substantiated the theory that salt domes should be given prime consideration in the waste management field. A preliminary design of a salt dome waste facility is described. Both topside facilities and mine-level facilities are presented. Although the overall mine-level facility is flexible and can be made almost any size within reason, the one proposed is approximately one square mile. Until certain regulations are established such as age of waste at the time of disposal, the size of the waste containers, and the types of wastes being disposed, it will be almost impossible to predict the life of the proposed repository as presented. Estimates are given of the initial investment and annual operating costs. (auth)

4265 (ORNL-TM-3130) DISSOLUTION OF CALCIUM-STRONTIUM CARBONATE AND ITS SUBSEQUENT MOVEMENT IN THE GROUND. Varga, Judith A.; Jacobs, D. G. (Oak Ridge National Lab., Tenn.). Nov 1970. Contract W-7405-eng-26. 14p. Dep. NTIS.

A series of laboratory experiments was performed to determine the relative behavior of strontium and calcium in the dissolution of strontium-contaminated calcium carbonate and subsequent movement through a mineral exchange system. The behavior of the two elements was found to be similar, and their release from the system was directly related to the amount of hydrochloric acid used in the leaching process. (auth)

4266 FISSIONABLE MATERIAL BALANCE AND SAFEGUARDS. Frenzel, W.; Heinz, W.; Moeken, H. Neue Tech., B; 11: 28-32(1969). (In German).

The handling of fissionable material by the Eurochemic reprocessing plant is discussed with respect to bookkeeping, quantitative measurements, sampling, analytical methods, balance analysis, quality control, random errors, systematic errors, and counterchecks. Eurochemic is monitored by two independent organizations, the European nuclear energy agency and Euratom. Euratom continuously has at least one inspector at the installations, while the European nuclear energy agency surveys monthly bookkeeping and conducts one or two annual inspections. (H.B.G.)

4267 PACKAGING ASSEMBLY FOR RADIOACTIVE MATERIALS. Koster, Curtis P. (to Mallinckrodt Chemical Works). U. S. Patent 3,531,644. 29 Sep 1970. Filed 31 Jan 1967.

A packaging assembly for radioactive materials is described. It consists of an outer container and cap, an inner radioactive shielding receptacle and cap, and a vessel retained within the receptacle for radioactive material. (auth)

4268 PROBLEMS OF RADIOACTIVE WASTE MANAGEMENT. Williams, I. G. K. (European Nuclear Energy Agency, Paris). Trans. Amer. Nucl. Soc.; 13: 466-7(Nov 1970).

From Meeting of the American Nuclear Society, Washington, D. C. See CONF-701102.

4269 NEW ERA FOR INTERNATIONAL SAFEGUARDS. Kratzer, Myron B. (Atomic Energy Commission, Washington, D. C.). Trans. Amer. Nucl. Soc.; 13: 475-6(Nov 1970).

From Meeting of the American Nuclear Society, Washington, D. C. See CONF-701102.

4270 SAFEGUARDS IN THE USA: AN UPDATING. Crowson, D. L. (Atomic Energy Commission, Washington, D. C.). Trans. Amer. Nucl. Soc.; 13: 476(Nov 1970).

From Meeting of the American Nuclear Society, Washington, D. C. See CONF-701102.

4271 ADAPTATION OF THE AGENCY'S SAFEGUARDS WORK TO THE NEW TASKS IN CONNECTION WITH NPT. Rometsch, R. (International Atomic Energy Agency, Vienna). Trans. Amer. Nucl. Soc.; 13: 476-7(Nov 1970).

From Meeting of the American Nuclear Society, Washington, D. C. See CONF-701102.

4272 TECHNICAL PROGRESS IN NUCLEAR MATERIALS SAFEGUARDS. Kouts, Herbert (Brookhaven National Lab., Upton, N. Y.). Trans. Amer. Nucl. Soc.; 13: 477(Nov 1970).

From Meeting of the American Nuclear Society, Washington, D. C. See CONF-701102.

4273 STOCHASTIC MODEL FOR SAFEGUARDS INSPECTIONS. Servais, F.; Goldschmidt, P. (Belgonucleaire, Brussels). Trans. Amer. Nucl. Soc.; 13: 478(Nov 1970).

From Meeting of the American Nuclear Society, Washington, D. C. See CONF-701102.

4274 ANALYSIS OF ACCOUNTABILITY DATA IN SAFEGUARDS. Goldstein, Rubin (Brookhaven National Lab., Upton, N. Y.). Trans. Amer. Nucl. Soc.; 13: 478-9(Nov 1970).

From Meeting of the American Nuclear Society, Washington, D. C. See CONF-701102.

4275 CURRENT STATUS OF U.S. WASTE MANAGEMENT PROGRAMS. Belter, W. G. (Atomic Energy Commission, Washington, D. C.). Trans. Amer. Nucl. Soc.; 13: 480-1(Nov 1970).

From Meeting of the American Nuclear Society, Washington, D. C. See CONF-701102.

4276 STATUS OF THE WASTE SOLIDIFICATION DEMONSTRATION PROGRAM. Blasewitz, Albert G.; McElroy, Jack L.; Schneider, Kenneth J. (Battelle-Northwest Labs., Richland, Wash.). Trans. Amer. Nucl. Soc.; 13: 481-3(Nov 1970).

From Meeting of the American Nuclear Society, Washington, D. C. See CONF-701102.

XUM

4277 DEMONSTRATIONAL REPOSITORY FOR SOLID RADIOACTIVE WASTES. Blomeke, J. O. (Oak Ridge National Lab., Tenn.). Trans. Amer. Nucl. Soc.; 13: 483-4(Nov 1970).
From Meeting of the American Nuclear Society, Washington, D. C. See CONF-701102.

4278 DESIGN AND SAFETY CONSIDERATIONS IN THE SHIPMENT OF SOLIDIFIED WASTES. Perona, J. J. (Univ. of Tennessee, Knoxville); Blomeke, J. O.; Dillon, R. S. Trans. Amer. Nucl. Soc.; 13: 484-5(Nov 1970).
From Meeting of the American Nuclear Society, Washington, D. C. See CONF-701102.

4279 DISPOSAL OF RADIOACTIVE WASTES IN NUCLEAR CHIMNEYS. Lombard, David B. (Atcor, Inc., Elmsford, N. Y.); Wethington, John A. Jr. Trans. Amer. Nucl. Soc.; 13: 485(Nov 1970).
From Meeting of the American Nuclear Society, Washington, D. C. See CONF-701102.

4280 CRITICAL APPROACH AND EXPONENTIAL EXPERIMENTS WITH PROTOTYPE FFTF DRIVER FUEL PINS IN WATER. Brown, C. L. (Battelle-Northwest, Richland, Wash.); Rogers, C. A. Trans. Amer. Nucl. Soc.; 13: 663-4(Nov 1970).
From Meeting of the American Nuclear Society, Washington, D. C. See CONF-701102.

4281 CRITICALITY OF PLUTONIUM NITRATE SOLUTIONS CONTAINING RASCHIG RINGS. Lloyd, R. C.; Clayton, E. D. (Battelle-Northwest, Richland, Wash.). Trans. Amer. Nucl. Soc.; 13: 664-5(Nov 1970).
From Meeting of the American Nuclear Society, Washington, D. C. See CONF-701102.

4282 EFFECT OF WATER SPRINKLERS ON ARRAY CRITICALITY SAFETY ANALYSES. Handley, G. R. (Union Carbide Corp., Oak Ridge, Tenn.). Trans. Amer. Nucl. Soc.; 13: 665-6(Nov 1970).
From Meeting of the American Nuclear Society, Washington, D. C. See CONF-701102.

4283 CALCULATED CRITICAL ARRAYS OF FISSILE MATERIALS. Ridgway, K. R. (Atlantic Richfield Hanford Co., Richland, Wash.). Trans. Amer. Nucl. Soc.; 13: 666-7(Nov 1970).
From Meeting of the American Nuclear Society, Washington, D. C. See CONF-701102.

4284 SURFACE DENSITY AS A USEFUL PARAMETER IN THE STORAGE AND HANDLING OF FISSILE METAL. Altschuler, S. J.; Schuske, C. L. (Dow Chemical Co., Golden, Colo.). Trans. Amer. Nucl. Soc.; 13: 667-8(Nov 1970).
From Meeting of the American Nuclear Society, Washington, D. C. See CONF-701102.

4285 SAFE FISSILE MATERIAL SPACING IN WATER. Carter, R. D. (Atlantic Richfield Hanford Co., Richland, Wash.). Trans. Amer. Nucl. Soc.; 13: 668(Nov 1970).
From Meeting of the American Nuclear Society, Washington, D. C. See CONF-701102.

4286 CRITICALITY SAFETY SPECIALIST'S VIEWS [ON IMPLICATIONS OF ANSI CRITICALITY SAFETY STANDARD N16.1]. Geiger, W. S. (Westinghouse Electric Corp., Cheswick, Pa.). Trans. Amer. Nucl. Soc.; 13: 684(Nov 1970).
From Meeting of the American Nuclear Society, Washington, D. C. See CONF-701102.

4287 PROCESS ENGINEER'S VIEWS [ON IMPLICATIONS OF ANSI CRITICALITY SAFETY STANDARD N16.1]. Orth, D. A. (Savannah River Lab., Aiken, S. C.). Trans. Amer. Nucl. Soc.; 13: 684-5(Nov 1970).
From Meeting of the American Nuclear Society, Washington, D. C. See CONF-701102.

4288 GOVERNMENT REGULATOR'S VIEWS [ON IMPLICATIONS OF ANSI CRITICALITY SAFETY STANDARD N16.1]. McCreless, Thomas, G. (Atomic Energy Commission, Washington, D. C.). Trans. Amer. Nucl. Soc.; 13: 685-6(Nov 1970).
From Meeting of the American Nuclear Society, Washington, D. C. See CONF-701102.

4289 MANAGER'S VIEWS [ON IMPLICATIONS OF ANSI CRITICALITY SAFETY STANDARD N16.1]. Zahn, Lyle L. (Atlantic Richfield Hanford Co., Richland, Wash.). Trans. Amer. Nucl. Soc.; 13: 686(Nov 1970).
From Meeting of the American Nuclear Society, Washington, D. C. See CONF-701102.

4290 PHYSICS AND NUCLEAR MATERIAL SAFEGUARDS. Gozani, T. (Gulf Energy and Environmental Systems, Inc., San Diego, Calif.). Trans. Amer. Nucl. Soc.; 13: 706-7(Nov 1970).
From Meeting of the American Nuclear Society, Washington, D. C. See CONF-701102.

4291 USE OF FISSION PRODUCT GAMMA RAYS FOLLOWING PHOTOFISSION FOR NONDESTRUCTIVE ASSAYS OF NUCLEAR MATERIALS. Rundquist, D. E.; Bramblett, R. L.; Ginaven, R. O. (Gulf Energy and Environmental Systems, Inc., San Diego, Calif.). Trans. Amer. Nucl. Soc.; 13: 747-8(Nov 1970).
From Meeting of the American Nuclear Society, Washington, D. C. See CONF-701102.

4292 PLUTONIUM WASTE COUNTER. Lawless, J. L.; Chanda, R. N. (Dow Chemical Co., Golden, Colo.). Trans. Amer. Nucl. Soc.; 13: 748-9(Nov 1970).
From Meeting of the American Nuclear Society, Washington, D. C. See CONF-701102.

4293 NONDESTRUCTIVE GAMMA ASSAY OF PLUTONIUM-CONTAMINATED SOLID WASTE IN DRUMS. Dukat, Alexander J.; Gonser, John; James, Dean B. (Nuclear Materials and Equipment Corp., Lewiston, N. Y.). Trans. Amer. Nucl. Soc.; 13: 749-50(Nov 1970).
From Meeting of the American Nuclear Society, Washington, D. C. See CONF-701102.

4294 DUAL SPECTRUM CONCEPT FOR LMFBR FUEL ASSAY. Kelber, Charles (Argonne National Lab., Ill.). Trans. Amer. Nucl. Soc.; 13: 750(Nov 1970).
From Meeting of the American Nuclear Society, Washington, D. C. See CONF-701102.

4295 OPERATING COMPUTERIZED SAFEGUARD AND CRITICALITY SYSTEM FOR PLUTONIA AND URANIA. Hagie, Laird T. (General Electric Co., Pleasanton, Calif.). Trans. Amer. Nucl. Soc.; 13: 750-1(Nov 1970).
From Meeting of the American Nuclear Society, Washington, D. C. See CONF-701102.

4296 INPUT ACCOUNTABILITY BY REMOTE WEIGHING OF PROCESSING PLANT TANKS. Booman, Glenn L. (Idaho Nuclear Corp., Idaho Falls). Trans. Amer. Nucl. Soc.; 13: 751-2(Nov 1970).
From Meeting of the American Nuclear Society, Washington, D. C. See CONF-701102.

4297 TESTING OF INSTRUMENTS AND MATERIAL BALANCE METHODS FOR PLUTONIUM SAFEGUARD CONTROL. Kurtz, Edward F.; Bishop, D. M.; Martin, C. G.; Simpson, J. L. (General Electric Co., Pleasanton, Calif.). Trans. Amer. Nucl. Soc.; 13: 752(Nov 1970).
From Meeting of the American Nuclear Society, Washington, D. C. See CONF-701102.

4298 PRESENT STATUS OF POSTIRRADIATION EXAMINATION FACILITY OF JAPAN ATOMIC ENERGY RESEARCH INSTITUTE. Homma, S.; Ito, H.; Yoshida, H.; (and others) (Japan Atomic Energy Research Inst., Tokai). Trans. Amer. Nucl. Soc.; 13: 836(Nov 1970).
From Meeting of the American Nuclear Society, Washington, D. C. See CONF-701102.

4299 ENTERING A HOT CELL AFTER SIX YEARS OF REMOTE SPENT-FUEL PROCESSING. Paige, D. M.; Kinkade, K. H. (Argonne National Lab., Idaho Falls, Idaho). Trans. Amer. Nucl. Soc.; 13: 836-7(Nov 1970).
From Meeting of the American Nuclear Society, Washington, D. C. See CONF-701102.

4300 CONTACT MAINTENANCE AND EQUIPMENT EVALUATION AFTER SIX YEARS OF CONTINUOUS REMOTE OPERATION INSIDE A HOT CELL. Kinkade, K. H.; Paige, D. M. (Argonne National Lab., Idaho Falls, Idaho). Trans. Amer. Nucl. Soc.; 13: 837-8(Nov 1970).
From Meeting of the American Nuclear Society, Washington, D. C. See CONF-701102.

4301 INTERIM EXAMINATION OF EBR-II EXPERIMENTAL IRRADIATIONS AT THE FUELS AND EXAMINATION FACILITY. Hagmann, D. B.; Bacca, J. P.; Feldman, M. J. (Argonne National Lab., Idaho Falls, Idaho). Trans. Amer. Nucl. Soc.; 13: 838(Nov 1970).
From Meeting of the American Nuclear Society, Washington, D. C. See CONF-701102.

XUM

4302 WESTINGHOUSE PLUTONIUM FUELS DEVELOPMENT LABORATORY, DESIGN PHILOSOPHY, AND STARTUP EXPERIENCE. Olson, R. E.; Nardi, A. J. (Westinghouse Electric Corp., Cheswick, Pa.). Trans. Amer. Nucl. Soc.; 13: 838-9(Nov 1970).
From Meeting of the American Nuclear Society, Washington, D. C. See CONF-701102.

4303 IN-CELL CRANE, MANIPULATOR, AND TELEVISION SYSTEMS FOR THE THORIUM–URANIUM RECYCLE FACILITY (TURF). Beckers, R. M.; Shepherd, D. M. (Oak Ridge National Lab., Tenn.). Trans. Amer. Nucl. Soc.; 13: 843-4(Nov 1970).
From Meeting of the American Nuclear Society, Washington, D. C. See CONF-701102.

4304 DESIGN AND INSTALLATION OF THE TURF CALIFORNIUM FACILITY. Peishel, F. L.; Burch, W. D.; Jarvis, J. P. (Oak Ridge National Lab., Tenn.). Trans. Amer. Nucl. Soc.; 13: 844(Nov 1970).
From Meeting of the American Nuclear Society, Washington, D. C. See CONF-701102.

4305 TRANSFER OF CALIFORNIUM SOURCES BY PNEUMATIC RABBIT. Jarvis, J. P.; Burch, W. D.; Chandler, J. M. (Oak Ridge National Lab., Tenn.). Trans. Amer. Nucl. Soc.; 13: 844(Nov 1970).
From Meeting of the American Nuclear Society, Washington, D. C. See CONF-701102.

4306 PNEUMATIC TUBE TRANSFER SYSTEM FOR RADIOACTIVE SAMPLES. Ludlow, J. O. (Catalytic, Inc., Philadelphia); Slawecki, M. A.; Brown, H. L. Trans. Amer. Nucl. Soc.; 13: 845(Nov 1970).
From Meeting of the American Nuclear Society, Washington, D. C. See CONF-701102.

4307 DRILL CORE PROCESSING FACILITY. Moore, Philip F. (Los Alamos Scientific Lab., N. Mex.). Trans. Amer. Nucl. Soc.; 13: 845-6(Nov 1970).
From Meeting of the American Nuclear Society, Washington, D. C. See CONF-701102.

4308 SMALL HOT CELL CHEMISTRY PLANT. Barnes, John W. (Los Alamos Scientific Lab., N. Mex.). Trans. Amer. Nucl. Soc.; 13: 846(Nov 1970).
From Meeting of the American Nuclear Society, Washington, D. C. See CONF-701102.

4309 HOT CELL STEREOMACROSCOPE AND POSITIONING STAGE FOR VIEWING OBJECTS IN EITHER A HORIZONTAL OR VERTICAL PLANE. Carnes, M. D. (Argonne National Lab., Idaho Falls, Idaho). Trans. Amer. Nucl. Soc.; 13: 848(Nov 1970).
From Meeting of the American Nuclear Society, Washington, D. C. See CONF-701102.

4310 MOCKUP OF REMOTELY OPERATED, HIGH-PURITY, INERT-ATMOSPHERE SODIUM ANALYSIS FACILITY. Lust, L. F.; Scott, F. A.; Jarosch, J. F. (Hanford Engineering Development Lab., Richland, Wash.). Trans. Amer. Nucl. Soc.; 13: 848-9(Nov 1970).
From Meeting of the American Nuclear Society, Washington, D. C. See CONF-701102.

4311 SHIELDED NEUTRON SHIPPING CASK. Hanson, C. L. (Univ. of California, Livermore); Coops, M. S.; Arnold, E. D. Trans. Amer. Nucl. Soc.; 13: 850(Nov 1970).
From Meeting of the American Nuclear Society, Washington, D. C. See CONF-701102.

4312 TRIGGER-ACTUATED MOTION LOCKS FOR MASTER-SLAVE MANIPULATORS. Coops, M. S.; Stearns, E. H.; Hanson, C. L. (Univ. of California, Livermore). Trans. Amer. Nucl. Soc.; 13: 850-1(Nov 1970).
From Meeting of the American Nuclear Society, Washington, D. C. See CONF-701102.

4313 WHERE DO WE GO FROM HERE WITH MASTER-SLAVE MANIPULATORS. Jelatis, D. G. (Central Research Labs., Red Wing, Minn.). Trans. Amer. Nucl. Soc.; 13: 852 (Nov 1970).
From Meeting of the American Nuclear Society, Washington, D. C. See CONF-701102.

4314 REQUIREMENTS FOR RADIATION PROTECTION DURING HANDLING OF PLUTONIUM RECYCLE FUEL RODS AND ASSEMBLIES. Tomonto, James R.; Tulenko, James S. (United Nuclear Corp., Elmsford, N. Y.). Trans. Amer. Nucl. Soc.; 13: 883-4(Nov 1970).
From Meeting of the American Nuclear Society, Washington, D. C. See CONF-701102.

4315 DISPOSAL OF RADIOACTIVE WASTE IN TO GROUND. Inoue, Yoriteru (Kyoto Univ.). Genshiryoku Kogyo; 16: No. 7, 25-31(Jul 1970). (In Japanese).

The disposal of radioactive wastes from nuclear power generation is carried out in the ground and ocean, and as future possibilities in space. Underground disposal of radioactive wastes is described in the following. Underground disposal appears at first sight to be dangerous, because of the underground water, but the ion-exchange capacity to retain radioactive materials is considerably large. The techniques carried out in oversea countries are reviewed, including liquid, solid and gaseous wastes. Underground movement, suitable location, and also variables in the disposal ground-layers are explained. Labor cost is significant in the overall cost of the underground disposal. Practical costs of the disposal, in the United States are reviewed. (Japan)

4316 PROBLEMS OF MARINE DISPOSAL OF RADIOACTIVE WASTE. Ichikawa, Ryushi (National Inst. of Radiological Sciences, Chiba, Japan). Genshiryoku Kogyo; 16: No. 7, 20-4(Jul 1970). (In Japanese).

With the growth of nuclear power generation, the disposal of radioactive wastes from the plants is a significant problem. Their disposal in oceans is attractive, but the close association of humans and ocean cannot be overlooked, especially in the case of Japan with active fisheries. Release of low-level liquid wastes in the coastal area is considered. The state of release regulation and monitoring, especially in Japan, is described, with regard to marine life. Another possibility is deep-sea disposal of solid wastes. The ocean behavior, and integrity of the containers must be considered. In this connection, the situation about 100 years hence by continued ocean disposal, in Japan, is estimated. Several instances of the study on the influence on marine-life eggs are given. (Japan)

4317 RECENT TREND IN RADIOACTIVE WASTE MANAGEMENT IN JAPAN. Ishihara, Takehiko (Japan Atomic Energy Research Inst., Tokai). Genshiryoku Kogyo; 16: No. 7, 5-9(Jul 1970). (In Japanese).

Nuclear power generation in Japan is now entering its mature stage. A significant problem is the disposal of radioactive wastes, which is difficult to solve in connection with economic nuclear power generation. The move to re-study radioactive waste disposal methods is described. The studies in the past 12 years in Japan concerning the disposal of radioactive wastes are reviewed. Studies on the methods of disposal, and the problems encountered are reviewed. The study group set up in the Atomic Energy Bureau (the Science and Technology Agency) is described; the problem in power companies is indicated. Various disposal methods are briefly mentioned. Economics of radioactive waste disposal, in close connection with nuclear power generation, are considered. (Japan)

XUM

INSTRUMENTATION

Radiation Detection Instruments

Refer also to abstracts 4029, 4223, and 4292.

General Detectors and Monitors

Refer also to abstracts 4381, 4409, 4632, 4634, 4635, 4648, 4653, 4928, 5606, 5973, 6044, 6118, 6206, and 6207.

4318 (JINR–E1-5098) TIME-OF-FLIGHT AND COORDINATE MEASUREMENTS IN A 130 cm SCINTILLATION COUNTER. Astvatsaturov, R. G.; Khachaturyan, M. N.; Kolpakov, I. F.; Smirnov, V. A. (Joint Inst. for Nuclear Research, Dubna (USSR)). 1970. 12p. Dep. NTIS (U. S. Sales Only).

By measuring the time interval between the arrival of the light signals at two opposite ends of a scintillator, the accurate determination of a coordinate is achieved in a long scintillation counter. As one of the basic counters, this counter was simultaneously used for time-of-flight measurements. The counter is $8 \times 8 \times 130$ cm^2. The accuracies of the coordinate and time-of-flight determination obtained in the experiment for charged particles are equal to ±1.7 cm and ±0.38 sec, respectively. It is shown that the accuracies of time-of-flight measurements and of the coordinate determination depend on the counter geometry. (auth)

4319 (JINR–P13-5403) IONIZATION COUNTER "dE/dx" FILLED WITH LIQUID XENON. Kulikov, Yu. V.; Malashkevich, N. I.; Ryabtsov, V. D.; Silaev, E. A. (Joint Inst. for Nuclear Research, Dubna (USSR). Lab. of High Energy). 1970. 8p. (In Russian). Dep. NTIS (U. S. Sales Only).

The ionization counter "dE/dx" filled with liquid xenon is described. The sensitive area of the counter is equal to 50 cm^2, the depth of the recording layer of liquid xenon being $t = 2$ g/cm^2. The results of the counter testing in a π^--meson beam at 6 GeV are presented. (auth)

4320 (KURRI-TR-59) SECOND NEUTRON MEASUREMENTS SYMPOSIUM. Kanda, Keiji; Kobayashi, Keiji; Kimura, Itsuo (eds.) (Kyoto Univ. (Japan). Research Reactor Inst.). 1969. 85p. (In Japanese). (CONF-690224–(Absts.)). Dep. NTIS (U. S. Sales Only).

Abstracts of thirteen papers presented at the Second Neutron Measurements Symposium held on February 20, 1969 at the Research Reactor Institute of Kyoto University are presented. The subjects covered include: Standard thermal neutron field in the KUR heavy water facility; the spectrum of the KUR graphite thermal column; calibration of neutron measurements in the epithermal region; standard thermal and epithermal neutron fields by means of a neutron generator (preliminary report); measurement of intermediate neutron spectrum with LINAC; standard resonance region spectrum pile TAKIT-2; transmission experiment with fast, continuous-spectrum neutrons; fast neutron experiments with LINAC; wave form discrimination of ^{3}He proportional counter; measurement of fast neutron spectrum with ^{3}He proportional counter; analysis of pulse-height distribution; studies on the semiconductor proton recoil counter; proton-recoil counter with γ-discrimination; and error evaluation on multi-detector methods in neutron dose measurements. (TTT)

4321 (LA–4465, pp 31,1-2) IMPROVEMENTS IN PERFORMANCE OF A LIQUID HELIUM SCINTILLATION COUNTER. Martin, J. C.; Broste, W. B.; Simmons, J. E. (Los Alamos Scientific Lab., N. Mex.).

From LASL contributions to the 3rd international symposium on polarization phenomena in nuclear reactions, Madison, Wisconsin, August 31–September 4, 1970.

4322 (NP–18433) MEASUREMENT OF THE SPECTRA AND FLUX OF ELECTRONS AND PHOTONS AT ANY POINT IN AN IRRADIATED SYSTEM. (Toulouse Univ. (France). Centre de Physique Atomique et Nucleaire). 1 May 1970. 40p. (In French). Dep. CFSTI (U. S. Sales Only).

The Monte Carlo method, used to calculate the parameters associated with the slowdown of 2- to 60-keV electrons in the multiplate geometries of liquid ionization chambers, allows one to determine each step of the electron slowdown, its energy, coordinates, direction, and displacement. Thus the effects of various types of material interfaces on the behavior of electron beams are determined. The use of surface barrier detectors with internal amplification operating in the avalanche region is studied. The technological processes for obtaining low currents are explained, and current–voltage curves are shown. (J.F.P.)

4323 (NYO–4028-TA-1) APPLICATIONS OF AVALANCHE TYPE SEMICONDUCTOR RADIATION DETECTORS. Final Report, October 1968–November 1969. Johnston, Phillip A. (General Electric Co., Philadelphia, Pa. Space Div.). Dec 1969. Contract AT(30-1)-4028. 50p. Dep. NTIS.

The use of avalanche detectors in radioisotope applications where other detection systems may be compromised due to size, temperature, or fragility is described. The applications discussed include the development of a portable X-ray fluorescence analyzer for geochemical exploration of the moon, a Mars soil analysis experiment, a silver ore analyzer, an archeological X-ray fluorescence analyzer, a beta particle pressure gauge, a cloud buoyancy gauge, an eggshell thickness gauge, and a tooth enamel gauge. (auth)

4324 MEASUREMENT OF IN VIVO RADIOACTIVITY: THE COLLIMATOR PROBLEM. Harris, C. Craig; Goodrich, Jack K.; Buffaloe, Thomas S. (Duke Univ., Durham, N. C.). pp 90-105 of Pulmonary Investigation with Radionuclides. /Gilson, Albert J. (ed.). Springfield, Ill.; Charles C Thomas, Publisher (1970).

From 1st Annual Seminar on Pulmonary Investigation with Radionuclides, Miami, Fla. See CONF-690334.

Fundamental parameters to be considered in the design and operation of collimators for scintillation cameras are considered. Sensitivity, resolution, counting rate, geometry, modulation transfer functions, and the gamma energy parameter are discussed. (W.H.K.)

4325 IMAGING DEVICES: COMPARATIVE PHYSICAL PROPERTIES. Harris, C. Craig; Goodrich, Jack K. (Duke Univ., Durham, N. C.). pp 135-45 of Pulmonary Investigation with Radionuclides. /Gilson, Albert J. (ed.). Springfield, Ill.; Charles C Thomas, Publisher (1970).

From 1st Annual Seminar on Pulmonary Investigation with Radionuclides, Miami, Fla. See CONF-690334.

The design, operation, performance, advantages, and disadvantages of scintillation cameras and radioisotope scanners are compared. (W.H.K.)

4326 IMAGING DEVICES: COMPARATIVE CLINICAL ATTRIBUTES (ONE OPINION). Goodrich, Jack K.; Harris, C. Craig (Duke Univ., Durham, N. C.). pp 146-59 of Pulmonary Investigation with Radionuclides. /Gilson, Albert J. (ed.). Springfield, Ill.; Charles C Thomas, Publisher (1970).

From 1st Annual Seminar on Pulmonary Investigation with Radionuclides, Miami, Fla. See CONF-690334.

Advantages and disadvantages of four different radioisotope imaging devices for various clinical applications are discussed. The autofluoroscope, the single overhead detector rectilinear scanner, the dual opposing-detector rectilinear scanner, and the Auger scintillation camera are studied. (W.H.K.)

4327 ADVANCED AND RESEARCH IMAGING DEVICES. Ter-Pogossian, Michel M. (Washington Univ., St. Louis). pp 160-70 of Pulmonary Investigation with Radionuclides. /Gilson, Albert J. (ed.). Springfield, Ill.; Charles C Thomas, Publisher (1970).

From 1st Annual Seminar on Pulmonary Investigation with Radionuclides, Miami, Fla. See CONF-690334.

The advantages and disadvantages of magnacameras for pulmonary function studies are briefly discussed. (W.H.K.)

4328 THE "IDEALIZED" DATA HANDLING SYSTEM. Smith, Edward M.; Larrea, Pablo A. (Univ. of Miami, Fla.). pp 171-85 of Pulmonary Investigation with Radionuclides. /Gilson, Albert J. (ed.). Springfield, Ill.; Charles C Thomas, Publisher (1970).

From 1st Annual Seminar on Pulmonary Investigation with Radionuclides, Miami, Fla. See CONF-690334.

The development of data handling systems for Auger cameras and rectilinear scanners for pulmonary function studies is described. (W.H.K.)

4329 PARYLENE THIN FILMS FOR RADIATION APPLICATIONS. Spivack, M. A. (Union Carbide Corp., Bound Brook, N. J.). Rev. Sci. Instrum.: 41: 1614-16(Nov 1970).

Thin parylene films have been prepared and are available in thicknesses to 0.025 μ. The parylene polymers are shown to be extremely uniform in thickness, have good gas barrier properties, and are relatively nonabsorbing throughout the entire soft x-ray region. Comparisons are made with commercially available Mylar, polycarbonate, polypropylene, VYNS, and Formvar. (auth)

XUM

4330 SMALL TISSUE EQUIVALENT AUTOMATIC IONIZATION CHAMBER. Sims, C. S. (General Dynamics, Fort Worth, Texas). Rev. Sci. Instrum.: 41: 1617-20(Nov 1970).

A quartz fiber electrometer (QFE) dosimeter system has been designed, developed, and tested to demonstrate the applicability of small dosimeters of the Neher type for use as space qualified instruments. The electrometer consists of a 3 mm diam × 30 mm cylindrical quartz rod partially coated with Au, and a 10 μ diam quartz fiber coated with Signa-Kote to a resistance between 0.25 and 1.5 MΩ/cm. The 9 cm^3 tissue equivalent ionization chamber is filled with 1 atm of C_2H_4, and consists of the automatic recycling QFE inside a 112 mg/cm^2 Signa-Kote coated Delrin electrode and a 103 mg/cm^2 Al case. Eight design verification units with various electrometer properties were subjected to tests involving calibration with ^{60}Co for five decades of dose rate, temperature variation from −40 to +82°C, simulated mission vibration and shock, orientation in the earth's gravity field, and gas leakage. The performance of the instruments indicates that they can indeed be developed into meritorious space qualified radiation dosimeters. (auth)

4331 CHANNEL ELECTRON MULTIPLIERS IN MAGNETIC FIELDS. Barnett, C. F.; Ray, J. A. (Oak Ridge National Lab., Tenn.). Rev. Sci. Instrum.; 41: 1665(Nov 1970).

Results of a study to determine the change in counting rate or multiplier efficiency as an external magnetic field is applied are presented. Atomic hydrogen beams were used in magnetic fields up to 120 Oe. The results imply that a channel multiplier can be operated efficiently in modest magnetic fields if proper care is taken with respect to field orientation. (W.H.K.)

4332 IMPROVEMENTS IN DETECTION EFFICIENCY OF THE JOHNSTON MULTIPLIER. Barnett, C. F.; Ray, J. A. (Oak Ridge National Lab., Tenn.). Rev. Sci. Instrum.; 41: 1673-5(Nov 1970).

A study to increase the detection efficiency of a Johnston multiplier is described. The efficiency was increased to approximately 90% by placing a high transparency grid 3 mm in front of the first dynode. The grid at the multiplier entrance was isolated and a negative potential was applied to increase the proton detection efficiency to near 100%. Results are presented graphically. (W.H.K.)

4333 FAST FISSION CHAMBER AMPLIFIER-DISCRIMINATOR SYSTEM. Ingle, R. W.; Gillespie, F. E.; Weston, L. W. (Oak Ridge National Lab., Tenn.). Rev. Sci. Instrum.; 41: 1539-43(Nov 1970).

To measure the fission cross section of ^{233}U as a function of neutron energy, instrumentation with fast pulse risetime and short resolving time characteristics is required. The efficient detection of fission−fragment pulses in the presence of a high alpha background requires these characteristics. A fission detector with an electron collection time of 25 nsec and containing 1 g of ^{233}U, and an amplifier with a risetime of 7 nsec and an over-all gain of 1000 were developed for this measurement. This system, detecting the fast rising current pulse from a parallel plate ionization chamber, is an integral part of the instrumentation used by a group at ORNL engaged in the measurement of the neutron fission and capture cross sections as a function of neutron energy. With this system, the fission cross section of ^{233}U was successfully measured over a neutron energy range from 0.4 to 2000 eV. (auth)

4334 SIMPLE TIME-TO-AMPLITUDE CONVERTER FOR FAST COINCIDENCE MEASUREMENTS. Bialkowski, Jacek (Inst. of Nuclear Research, Swierk, Poland). Nukleonika; 15: 117-28(1970).

The time-to-amplitude converter based on the pulse overlap principle and designed for coincidence and life time measurements is described. The linear range of the converter is 90 ns at integral linearity less than ±1%. The machine time resolution is about 35 ps. The coincidence curves measured with two scintillation counters (photomultipliers EMI 6097 F), a scintillation counter with Ge(Li) detector, and a Si(Li) detector with Ge(Li) detector are presented. (auth)

4335 MONITORING INSTRUMENT FOR DETECTING BETA AND GAMMA RADIATION. Roulet, Roger (to Commissariat a l'Energie Atomique). British Patent 1,207,838. 7 Oct 1970. Priority date 19 Oct 1966, France.

A detector system for total body beta and gamma radiation monitoring of personnel is described. (W.H.K.)

4336 COMPUTER PROCESSING OF IMAGES IN NUCLEAR MEDICINE. Kuhl, David E. (Univ. of Pennsylvania, Philadelphia). Trans. Amer. Nucl. Soc.; 13: 520-1(Nov 1970).

From Meeting of the American Nuclear Society, Washington, D. C. See CONF-701102.

4337 SURVEY OF RECENT INSTRUMENTATION ADVANCES. Brownell, Gordon L. (Massachusetts General Hospital, Boston). Trans. Amer. Nucl. Soc.; 13: 521(Nov 1970).

From Meeting of the American Nuclear Society, Washington, D. C. See CONF-701102.

4338 CHARGE DETERMINATION OF COSMIC-RAY TRACKS IN POLYCARBONATE PLASTIC DETECTORS. Enge, W. (Univ., Kiel); Bartholomae, K. P.; Fukui, K. Trans. Amer. Nucl. Soc.: 13: 523(Nov 1970).

From Meeting of the American Nuclear Society, Washington, D. C. See CONF-701102.

4339 FAST-NEUTRON-INDUCED ETCH-PIT DISTRIBUTIONS IN MAKROFOL POLYCARBONATE FOIL. Tuyn, J. W. N. (Reactor Centrum Nederland, Petten, Netherlands). Trans. Amer. Nucl. Soc.; 13: 523-4(Nov 1970).

From Meeting of the American Nuclear Society, Washington, D. C. See CONF-701102.

4340 AUTOMATIC SYSTEM FOR COUNTING ETCHED HOLES IN THIN DIELECTRIC PLASTICS. Congel, F. J. (Macalester Coll., St. Paul); Roberts, J. H.; Strait, E. N.; (and others). Trans. Amer. Nucl. Soc.; 13: 524(Nov 1970).

From Meeting of the American Nuclear Society, Washington, D. C. See CONF-701102.

4341 FLUX MONITOR UTILIZING TRACK-ETCH FILM FOR UNATTENDED SAFEGUARDS APPLICATION. Weidenbaum, B.; Lovett, D. B.; Kosanke, H. D. (General Electric Co., Pleasanton, Calif.). Trans. Amer. Nucl. Soc.: 13: 524-6(Nov 1970).

From Meeting of the American Nuclear Society, Washington, D. C. See CONF-701102.

4342 COUNTING OF HEAVILY ETCHED FISSION FRAGMENT TRACKS IN POLYCARBONATE. Gilliam, D. M.; Knoll, G. F. (Univ. of Michigan, Ann Arbor). Trans. Amer. Nucl. Soc.; 13: 526(Nov 1970).

From Meeting of the American Nuclear Society, Washington, D. C. See CONF-701102.

4343 AUTOMATIC COUNTING OF SOLID-STATE FISSION TRACK RECORDERS. Oosterkamp, W. J. (Kernforschungszentrum, Karlsruhe, Ger.); Schaar, J.; Van Velze, P. L. Trans. Amer. Nucl. Soc.; 13: 526-7(Nov 1970).

From Meeting of the American Nuclear Society, Washington, D. C. See CONF-701102.

4344 USE OF CELLULOSE NITRATE FOR ALPHA AUTORADIOGRAPHY IN METALLOGRAPHY. Kegley, T. M. Jr. (Oak Ridge National Lab., Tenn.). Trans. Amer. Nucl. Soc.; 13: 528(Nov 1970).

From Meeting of the American Nuclear Society, Washington, D. C. See CONF-701102.

4345 TRACK-ETCH RESEARCH AND DEVELOPMENT AT GE VALLECITOS NUCLEAR CENTER. Weidenbaum, B.; Lovett, D. B.; Caputi, R. W. (General Electric Co., Pleasanton, Calif.). Trans. Amer. Nucl. Soc.; 13: 528-30(Nov 1970).

From Meeting of the American Nuclear Society, Washington, D. C. See CONF-701102.

4346 CONTRAST IMPROVEMENT OF IMAGES OBTAINED IN CELLULOSE NITRATE FILM BY TRACK-ETCH METHODS. Barbier, J. (Kodak-Pathe Research Labs., Vincennes, France). Trans. Amer. Nucl. Soc.; 13: 530(Nov 1970).

From Meeting of the American Nuclear Society, Washington, D. C. See CONF-701102.

4347 SOME APPLICATIONS OF NUCLEAR TRACK ETCHING IN POLYMERS. Becker, Klaus (Oak Ridge National Lab., Tenn.). Trans. Amer. Nucl. Soc.; 13: 530-1(Nov 1970).

From Meeting of the American Nuclear Society, Washington, D. C. See CONF-701102.

4348 USE OF SPARKING TECHNIQUES TO ENHANCE TRACK-ETCH RADIOGRAPHS. Oltman, B. G. (Argonne National Lab., Ill.); Congel, F.; Lapinski, N. P.; Berger, Harold. Trans. Amer. Nucl. Soc.; 13: 531-2(Nov 1970).

From Meeting of the American Nuclear Society, Washington, D. C. See CONF-701102.

4349 RESPONSE OF MINIATURE G-M TUBES TO MONOENERGETIC GAMMA RADIATION. Campbell, R. W. (Jet Propulsion Lab., Pasadena, Calif.); Anno, G. H. Trans. Amer. Nucl. Soc.; 13: 533-4(Nov 1970).

From Meeting of the American Nuclear Society, Washington, D. C. See CONF-701102.

4350 RESPONSE OF A SHIELDED 300-MICRON SILICON DETECTOR TO GAMMA RAYS. Reier, Melvin (Jet Propulsion

Lab., Pasadena, Calif.); Anno, George H. Trans. Amer. Nucl. Soc.; 13: 534-5(Nov 1970).
From Meeting of the American Nuclear Society, Washington, D. C. See CONF-701102.

4351 RESPONSE OF SOLID-STATE DETECTORS TO MONOENERGETIC NEUTRONS DETERMINED BY THE USE OF THE MONTE CARLO TECHNIQUE. Anno, G. (ART Research Corp., Los Angeles); Taherzadeh, M. Trans. Amer. Nucl. Soc.; 13: 535(Nov 1970).
From Meeting of the American Nuclear Society, Washington, D. C. See CONF-701102.

4352 ON-LINE MONITOR OF NATURAL GAS LINES FOR ^{3}H AND ^{85}Kr. Brundage, Robert S. (CER Geonuclear Corp., Las Vegas, Nev.); Motes, Bill G.; Gant, Preston. Trans. Amer. Nucl. Soc.; 13: 639(Nov 1970).
From Meeting of the American Nuclear Society, Washington, D. C. See CONF-701102.

4353 NON-PERTURBING FISSION COUNTER FOR USE IN PLATE-TYPE CRITICAL ASSEMBLIES. Long, A. B.; Bohn, E. M.; Kaiser, W. C. (Argonne National Lab., Ill.). Trans. Amer. Nucl. Soc.; 13: 762-3(Nov 1970).
From Meeting of the American Nuclear Society, Washington, D. C. See CONF-701102.

4354 NOVEL, HIGH COUNTING RATE NEUTRON DETECTION SYSTEM. Diaz, N. J.; Ohanian, M. J. (Univ. of Florida, Gainesville). Trans. Amer. Nucl. Soc.; 13: 792-3(Nov 1970).
From Meeting of the American Nuclear Society, Washington, D. C. See CONF-701102.

4355 GAS-FLOW METHOD FOR DETECTION OF FAST NEUTRONS IN REACTORS. Brown, Donald P.; Upton, Joseph W. Jr.; Spear, Ward G. (Battelle-Northwest, Richland, Wash.). Trans. Amer. Nucl. Soc.; 13: 795-6(Nov 1970).
From Meeting of the American Nuclear Society, Washington, D. C. See CONF-701102.

4356 RESPONSE OF SELECTED TOTALLY DEPLETED AND LITHIUM-DRIFTED SILICON DETECTORS TO MONOENERGETIC GAMMA AND NEUTRON RADIATION. Jones, T. D. (Hanford Engineering Development Lab., Richland, Wash.); Endres, G. W. R.; Haverfield, A. J. Trans. Amer. Nucl. Soc.; 13: 873-4(Nov 1970).
From Meeting of the American Nuclear Society, Washington, D. C. See CONF-701102.

4357 COMPARISON OF FOIL ACTIVATION TECHNIQUES AND OTHER METHODS IN FAST-NEUTRON SPECTRUM MEASUREMENTS. Pearson, Dale A. (Idaho Nuclear Corp., Idaho Falls). Trans. Amer. Nucl. Soc.; 13: 877-8(Nov 1970).
From Meeting of the American Nuclear Society, Washington, D. C. See CONF-701102.

4358 CURRENT STATUS OF LIQUID SCINTILLATION COUNTING. Symposium Held at Cambridge, Massachusetts, March 31–April 3, 1969. Bransome, Edwin D. Jr. (ed.). New York; Grune and Stratton, Inc. (1970). 411p. $19.75. (CONF-690346).

New developments of the past several years in the basic physics of the liquid scintillation process are intercalated with an explicit general treatment of the subject. The history of liquid scintillation instrumentation development is reviewed, and counting statistics and counting error are discussed. Double isotope counting, low-level counting, flow monitoring, Cherenkov counting of beta particles, chemiluminescence, and bioluminescence are discussed. Special problems with radioisotopically labeled samples are considered including lipophilic, hydrophobic samples; aqueous samples; solid samples and heterogeneous counting systems; solid samples and homogeneous counting systems; and specially prepared samples. Chemical and color quenching are discussed, and methods for quench correction are described including external standardization and quench compensation by gain restoration. The physical basis of chemiluminescence is described, and the detection and correction of chemiluminescence in liquid scintillation counting is discussed. Also, examples of the three general approaches to automatic handling of liquid counting data and appropriate source references are given. (W.H.K.)

4359 APPROACHES TO OPTIMAL DATA PROCESSING IN RADIOISOTOPE IMAGING. Tanaka, E.; Iinuma, T. A. (National Inst. of Radiological Sciences, Chiba, Japan). Phys. Med. Biol.; 15: 683-94(Oct 1970).

An optimal data processor for detecting a small lesion (target) in a large organ (background) is derived theoretically by maximizing the signal-to-noise (S/N) ratio. The highest S/N ratio is obtained with a "matched filter" which has the same response as that of the source-collimator-imaging detector system. The method is suitable when the S/N ratio is of prime importance but the resolving power is unimportant. A good compromise between S/N ratio and resolution can be attained with an "optimum filter" which yields the highest signal amplitude for a given "smoothing area" without over-enhancement for any frequency component of the source distribution pattern. The relation between the resolving power and the random noise is obtained quantitatively assuming a Gaussian collimator response. The condition for optimal choice of the collimator is also discussed. (auth) (UK)

4360 POCKET RADIATION DOSE INTEGRATOR AND MONITOR. Splichal, W. F. (Savannah River Lab., Aiken, S. C.). Health Phys.; 19: 692-3(Nov 1970).

A gamma radiation dose integrator and monitor designed to be carried in a pocket or worn on a belt is described. Dose over two ranges, 0 to 100 mR and 0 to 1 R, is integrated by a modified electronic watch movement. The monitor can be equipped to provide a distinctive chirp which increases in frequency proportional to dose rate to give an audible warning of dose rate changes. The integrating monitor is described in detail and a circuit diagram is given. The limitations are indicated and discussed. (UK)

4361 USABLE COUNT-RATE RANGE OF A HALOGEN QUENCHED GEIGER-MUELLER (G.M.) COUNTER. Chiang, Hai Hung (National Tsing Hua Univ., Hsinchu, Taiwan). Health Phys.; 19: 687-90(Nov 1970).

It is recommended that halogen quenched G-M counters are operated only in the appropriate count-rate range. Because of the slow-moving positive ions, the G-M counter is paralyzed during their migration and the scaler will not register the true counts. Coincidence corrections have to be made. The observed count rate r is related to the true count rate R by the relation $R = r/(r - rT)$, where T is the resolving time. (auth) (UK)

Nuclear Spectroscopic Instrumentation

Refer also to abstracts 5148, 5682, and 5736.

4362 (CEA-N-1314) ANALOG COMPUTER FOR CALCULATING THE RATIO OF AMPLITUDE OF TWO PULSES. Moroni, Max; Rogerieux, Marcellin (Commissariat a l'Energie Atomique, Cadarache (France). Centre d'Etudes Nucleaires). Jun 1970. 28p. (In French). Dep. NTIS (U. S. Sales Only).

This computer, including two logarithmic amplifiers connected at the terminal inputs of an adder, is used for neutron–gamma discrimination in a neutron spectrometer with a recoil proton proportional counter. The various electronic circuits and some experimental results are presented. (France)

4363 DELAYED COINCIDENCE SPECTROMETER FOR LIFETIME STUDIES. Rao, B. V. Narasimha; Ayyangar, K. M. M. S.; Jnanananda, Swami (Andhra Univ., Waltair, India). Indian J. Pure Appl. Phys.; 6: 358-60(Jul 1968).

A delayed coincidence spectrometer with electron–electron coincidence arrangement has been developed. The resolving time of the arrangement observed with ^{60}Co is 0.78 nsec and the slopes of the prompt resolution curve is 0.0812 nsec. The performance of the set-up is tested by measuring the lifetimes of the 279 keV level of ^{203}Tl and the 411 keV level of ^{198}Hg. (auth)

4364 DESIGN OF INTERMEDIATE-ENERGY NEUTRON SPECTROMETERS AND THEIR CALIBRATION WITH PHOTONEUTRONS. Binney, S. E.; Henninger, R. J.; Amster, H. J.; Mark, H. (Univ. of California, Berkeley). Trans. Amer. Nucl. Soc.; 13: 762(Nov 1970).
From Meeting of the American Nuclear Society, Washington, D. C. See CONF-701102.

4365 EXPERIMENTAL TEST OF PULSE-HEIGHT SPECTRUM UNFOLDING. Harris, L. Jr.; Kendrick, H. (Gulf Energy and Environmental Systems, Inc., San Diego, Calif.). Trans. Amer. Nucl. Soc.; 13: 874-5(Nov 1970).
From Meeting of the American Nuclear Society, Washington, D. C. See CONF-701102.

4366 SIMULTANEOUS FAST-NEUTRON SPECTRAL MEASUREMENTS BY TIME-OF-FLIGHT AND PULSE-HEIGHT UNFOLDING TECHNIQUES. Straker, E. A.; Burgart, C. E.; Love, T. A.; Freestone, R. M. Jr. (Oak Ridge National Lab., Tenn.). Trans. Amer. Nucl. Soc.; 13: 875(Nov 1970).
From Meeting of the American Nuclear Society, Washington, D. C. See CONF-701102.

4367 MONTE CARLO UNFOLDING OF NEUTRON SPECTRA. Sanna, Robert; O'Brien, Keran (Atomic Energy Commission, New York). Trans. Amer. Nucl. Soc.; 13: 882-3(Nov 1970).
From Meeting of the American Nuclear Society, Washington, D. C. See CONF-701102.

XUM

High Energy Physics Instrumentation

4368 (AEC-tr-7099(Pt.1)) CHERENKOV RADIATION IN HIGH-ENERGY PHYSICS. PART I. CHERENKOV RADIATION IN ISOTROPIC AND ANISOTROPIC MEDIA: THEORY AND EXPERIMENTAL VERIFICATION. Zrelov, V. P. Translation of Izluchenie Vavilova-Cherenkova i ego Primenenie v Fizike Vysokikh Energii, Atomizdat, Moscow, 1968. 244p. (TT-70-50003/1; IPST-Cat.-5651). Dep. NTIS.

A review on the theory of the Cherenkov effect is presented. The classical Tamm–Frank theory of the Cherenkov radiation in an isotropic medium is presented in detail. The quantum theory of Cherenkov radiation, first developed by Ginzburg, and the inverse Cherenkov effect, investigated by Tamm, are presented. The main features of the radiation in isotropic and anisotropic media and their experimental verification are discussed in detail, as are some problems of the radiation in anisotropic media. (auth)

4369 (IFVE-SPK-69-53) PROGRAM OF CONNECTION OF THE MEASURING MICROSCOPES PUOS WITH COMPUTER MINSK-2. Ammosov, V. V.; Gorichev, P. A.; Teplov, E. V.; Shmelev, O. A. (Gosudarstvennyi Komitet po Ispol'zovaniyu Atomnoi Energii SSSR, Serpukhov. Institut Fiziki Vysokikh Energii). 1969. 24p. (In Russian). Dep. NTIS (U. S. Sales Only).

A program for the computer Minsk-2, that provides a connection of 4 measuring microscopes PUOS with Minsk-2, is described. The program allows in a real time scale: 1) to control the sequence of measuring the bubble chamber pictures, 2) to detect various errors of the operators, as well as of the measuring system PUOS, and 3) to give a convenient representation (on the tape) of the measurement results. The program has been adjusted and tested at the Institute for High Energy Physics. (auth)

4370 (INS-TH-67) CONTROL AND READ OUT SYSTEM OF SCALER. (Tokyo Univ. (Japan). Inst. for Nuclear Study). 26 Jun 1970. 48p. (In Japanese and English). Dep. NTIS (U.S. Sales Only).

Measurements on the differential cross sections at 180° for the reactions $\gamma p \rightarrow \pi^+ n$ and $\gamma n \rightarrow \pi^- p$ were made recently. In this experiment 27 scalers were used in connection with three coincidence-counters, one veto-coincidence counter, and a hodoscope consisting of 10 elements. Since data were taken repeatedly in a short interval, an accurate and expedient read-out of scalers was required. An apparatus having the following functions was made; 1) it controls 27 scalers, 2) it reads out the data of the scalers to a printer and a perforator, 3) it controls a simple precision flux meter. This apparatus was successfully used all through the three-months experiment. A detailed description of the apparatus is given. (auth)

4371 (JINR-P13-5327) DYNAMICS OF VAPOUR BUBBLES IN LIQUID HYDROGEN AND ULTRASONIC BUBBLE CHAMBERS. Akulichev, V. A.; Alekseev, V. N.; Naugolnykh, K. A. (Joint Inst. for Nuclear Research, Dubna (USSR). Lab. of Nuclear Problems). 1970. 15p. (In Russian). Dep. NTIS (U. S. Sales Only).

The dynamics of vapor bubbles in liquid in the ultrasonic field is considered theoretically. A system of equations is formulated describing the pulsation of a single vapor bubble in the approximation of an incompressible liquid. It is shown that a vapor bubble increases under the influence of the ultrasonic field reaching the asymptotic size. The calculated results of the bubble dynamics in liquid hydrogen are presented for the thermodynamical parameter values corresponding to the characteristic modes of bubble chambers. (auth)

4372 (SJC-T-70-3) PROGRAM FOR ANALYSIS OF BUBBLE-CHAMBER PHOTOGRAPHS. Okabe, Hisataka; Ochiai, Fumio; Konishi, Takeharu (Tokyo Univ. (Japan). Inst. for Nuclear Study). Aug 1970. 31p. (In Japanese). Dep. NTIS (U. S. Sales Only).

A program for analysis of bubble-chamber photographs has been developed to analyze the phenomenon of multi-particle formation, which is difficult by usual methods. In this program, the information of an average interval between bubbles is incorporated. The program has the following features: (1) sub-program ARANGE is used to reduce the limitation on a measuring time and to minimize the determination process by an observer; and (2) sub-programs are introduced for correcting for the distortion of an image, which is a drawback of the image-plane type projector, and to check the mis-punches due to a noise in the measuring projector. (Japan)

4373 STUDY OF LOW-ENERGY, HEAVY COSMIC RAYS USING A PLASTIC CHARGED-PARTICLE DETECTOR. Peterson, David Dee. Troy, N. Y.; Rensselaer Polytechnic Inst. (1969). 111p. University Microfilms Order No. 70-11,329.

Thesis.

A new, high-resolution, charged-particle detector is used to study low-energy, heavy cosmic rays. The detector consists of thin films of Lexan polycarbonate plastic in which latent track images of penetrating charged particles can be developed to a size suitable for viewing in an optical microscope. The detector is a particular application of a discovery made near the beginning of this decade that nearly all dielectric materials have the ability to record and retain the damage produced by the passage of an energetic charged particle. Two important characteristics exist for these detectors. First, all track recording dielectric materials, including Lexan, are characterized by a threshold damage density below which charged particle tracks are not developed. The development of tracks in plastics occurs by a chemical etching process whereby the etchant preferentially attacks the damage region along a particle path and produces an etch pit. This leads to the second characteristic, which is that for some plastics, including Lexan, the track attack rate has been related to the damage density which thus forms a basis for charged particle identification. In this work, cosmic ray nuclei provided data for which the above relation was established. In regard to this, the etch pit length and residual range are shown to be a unique function of the charge and mass of the incident charged particle. Due to the recent development of these detectors, there has existed a need to more clearly define the limitations of the detector with regard to charged particle identification. Therefore, various environmental effects on the latent track images in Lexan have been studied in detail, including the effects of age, ultraviolet light, and temperature. The development of tracks by chemical etching processes is studied in detail as well as the development of a high resolution, high magnification, optical microscope system for measuring the length of etch pits. The Lexan detector was used to determine the first elemental abundance of low energy (150 to 250 Mev/nucleon) cosmic rays with $16 \leq Z \leq 30$, which was not done previously for lack of high resolution detectors. These detailed results are compared with the more general results of various investigators and found to be in excellent agreement. And finally, the results of this work form the basis for high-resolution charged-particle identification using plastic detectors, in particular, Lexan. (Diss. Abstr. Int., B)

4374 EVALUATION OF ENERGY SPECTRA OF NEUTRONS GENERATED IN THE EARTH. Glotov, V. I. Krat. Soobshch. Fiz.; No. 7, 75-80(Jul 1970). (In Russian).

Possible approximations of neutron energy spectra in a granite of average chemical composition were analyzed using the experimental data on neutron activity in rocks. The influence of the energy distribution of neutrons in the earth on the multigroup neutron shielding calculations was evaluated on the basis of spectra obtained. (R.V.J.)

4375 DEVELOPMENT OF A WATER CHERENKOV COUNTER. Pathak, K. M. (Cotton Coll., Gauhati, India). Indian J. Pure Appl. Phys.; 6: 634-6(1968).

A directional but non-focusing type of Cherenkov counter has been designed using water as the dielectric medium for investigating the Cherenkov loss of relativistic muons in the momentum range 0.5 to 100 GeV/c. It consists of a steel tank containing water and four light collectors, each viewed by a 53 AVP (Mullard) photomultiplier tube and filled with a solution of liquid paraffin and dimethyl popop. The counter has good directional property; the response of the counter for particles of slightly varying path lengths in water is uniform within 5 per cent. (auth)

Radiation Dosimeters

Refer also to abstracts 4248, 4322, and 4330.

4376 (AD-710007) DEVELOPMENT OF A PASSIVE SELF-READING PERSONNEL DOSIMETER. Final Report, November 1968-May 1970. Murphy, Preston V. (Thermo Electron Corp., Waltham, Mass.). Jul 1970. Contract DAHC20-69-C-0110. 100p. (TE-4109-138-70). NTIS.

A passive, self-reading dosimeter for high level gamma ray monitoring has been developed. The gamma ray detecting element uses energetic Compton and photoelectron scattering in a dielectric–electrode matrix to generate the charge necessary for dose read-out. The detecting element has been designed to provide a uniform response for photons of 0.08 to 2 MeV energy and to charge an inverse-reading fiber voltmeter full scale for total doses in the range of 200 to 600 R. Evacuated, inverse-reading fiber voltmeters of suitable range have been fabricated and assembled with detecting elements to give prototype dosimeters. All prototype units were free of batteries or chargers, could be read repeatedly while in a radiation field, and showed good accuracy and repeatability. (auth) (USGRDR)

4377 (AERE-R-6498) NUCLEAR ACCIDENT DOSIMETRY SYSTEMS; UK MEASUREMENTS AT THE FIRST I.A.E.A. INTER-COMPARISON AT VALDUC, FRANCE, JUNE 1970. Dennis, J. A.; Delafield, H. J.; Holt, P. D.; Boot, S. J. (Atomic Energy Research Establishment, Harwell (England)). Oct 1970. 23p. Dep. NTIS (U. S. Sales Only). UK 4s.

Teams from several countries simultaneously exposed criticality dosimeters to mixed pulses of neutron and gamma radiation produced by the CRAC reactor at Valduc. An account is given of the measurements made by the Harwell team, both in free air and on phantoms, using personnel criticality dosimeters and a threshold detector system. A surface absorbed dose of 266 rads due to heavy recoil particles and 467 rads due to gamma radiation was received by the man phantom in the unshielded exposure; in the shielded exposure the doses were 107 rads and 351 rads respectively. These doses are based on conventional interpretations of accident dosimeter and TLD gamma measurements. The threshold detector system exposed in free air position gave values for the neutron kerma ranging from 280 to 392 hectoergs gm^{-1} of standard man tissue in the unshielded exposure, and from 128 to 141 hectoergs gm^{-1} in the shielded exposure. The range of values is due to the different methods of interpretation that are possible with the system. (auth) (UK)

4378 (BNWL-CC-2633) EVALUATION OF HANFORD BASIC THERMOLUMINESCENCE DOSIMETER. Kathren, R. L. (Battelle-Northwest, Richland, Wash. Pacific Northwest Lab.). Jul 1970. Contract AT(45-1)-1830. 26p. Dep. NTIS.

The Hanford lithium-7 fluoride thermoluminescent dosimeter for personnel dosimetry is described and evaluated. The reader, structural and wear tests, and field tests are discussed. The range, linearity, sensitivity, precision, energy and angular dependence, extraneous radiation response, environmental effects, fading, annealing, and interrelationship of variables are evaluated. (W.H.K.)

4379 (SC-TM-69-298) CALORIMETERS FOR MEASURING HIGH-ENERGY, HIGH-INTENSITY, PULSED ELECTRON BEAMS. Schulze, J. F. (Sandia Labs., Albuquerque, N. Mex.). Jun 1969. 31p. Dep. NTIS.

Calorimetry represents a reliable method of defining high-intensity electron beams associated with pulsed machines such as Hermes I and Hermes II. Described here are methods and techniques sufficient for the design of both linear array and total stopping calorimeters. Additionally, experimental data obtained on Hermes I are presented to demonstrate the utility of the method. (auth)

4380 USE OF EXOELECTRON EMISSION (EE) FROM BeO IN DOSIMETRY OF IONIZING RADIATION. Kriks, H.-J. PTB Mitt.; 80: 250-4(Aug 1970). (In German).

An investigation of the thermally stimulated exoelectron emission (TSEE) from beryllium oxide irradiated with ^{60}Co-γ-rays is reported. It is shown that it is possible to obtain a response which is sufficiently proportional to exposure in a range from 2 mR up to 2 R with BeO without adding graphite. A mixture of 15% BeO and 85% graphite powder extends the range of exposure proportionality to 500 R. The combination of two dosimeters with different BeO-content allows to measure the exposure in the range from 2 mR up to about 400 R, the half lethal exposure for man. (auth)

4381 HELIUM ACCUMULATING DOSIMETERS FOR HIGH NEUTRON FLUENCES AND LONG IRRADIATION PERIODS. Weitman, J.; Daverhoeg, N.; Farvolden, S. (Aktiebolaget Atomenergi, Studsvik, Sweden). Trans. Amer. Nucl. Soc.; 13: 881-2(Nov 1970).

From Meeting of the American Nuclear Society, Washington, D. C. See CONF-701102.

4382 TLD 700 (^7LiF) RESPONSE TO REACTOR NEUTRONS. Leonard, B. E.; Bransford, C. L. (Armed Forces Radiobiology Research Inst., Bethesda, Md.). Trans. Amer. Nucl. Soc.; 13: 885(Nov 1970).

From Meeting of the American Nuclear Society, Washington, D. C. See CONF-701102.

4383 NAVY ADOPTS KODAK TYPE III FILM FOR CENTRALIZED PHOTODOSIMETRY PROGRAM. Odor, D. L.; Purdy, C. (National Naval Medical Center, Bethesda, Md.). Health Phys.; 19: 690-1(Nov 1970).

The Kodak Type III film tested showed improved sensitivity, acceptably low background fog, adequate range, and was comparatively stable under a variety of storage conditions. The firm has serialized this film and packet and coded it with a prefix letter and five digit number series. The characters show adequate clarity even with four density units or more of response darkening. (auth) (UK)

4384 FADING OF RADIATION-INDUCED OPTICAL DENSITY IN POLYMETHYLMETHACRYLATE ON OXYGEN DIFFUSION. Chadwick, K. H.; Leenhouts, H. P. (Inst. for Atomic Science in Agriculture, Wageningen, Netherlands). Phys. Med. Biol.; 15: 743-4(Oct 1970).

Analysis of the results of a previous experiment showed that the fading of oxygen sensitive portion of the radiation induced optical density (OD) in PMMA, stored in the dark at room temperature in air or oxygen, follows a purely exponential law. This effect may be used in practical dosimetry situations for doses above 0.5 M rad to make an accurate fading correction where it has been impossible to measure the initial OD. In most practical cases fading will occur in air, and in the case of PMMA without plasticizer where the oxygen diffusion is very slow, a slight initial increase of 7% in OD was observed. (UK)

Radiometric Instruments

Refer also to abstracts 4035, 4323, 4896, and 5493.

4385 GAMMA SPECTRA: DENSITY RELATIONSHIPS IN A GAMMA BACKSCATTER DENSITY GAUGE. Swift, Jerry J. (Catholic Univ. of America, Washington D. C.). Trans. Amer. Nucl. Soc.; 13: 546-7(Nov 1970).

From Meeting of the American Nuclear Society, Washington, D. C. See CONF-701102.

4386 ATOMIC NUCLEAR RESOLUTION OF BETA BACKSCATTERING GAUGES. Segal, Y.; Notea, A. (Technion-Israel Inst. of Tech., Haifa). Trans. Amer. Nucl. Soc.; 13: 547-8(Nov 1970).

From Meeting of the American Nuclear Society, Washington, D. C. See CONF-701102.

Miscellaneous Instruments and Components

Refer also to abstracts 4011, 4249, 4328, 4633, 5422, 6025, 6026, 6046, and 6047.

4387 (AEEW-M-986) COMPUTER INTERFACE METHODS AND STANDARDS. Collins, G. B. (Atomic Energy Establishment, Winfrith (England)). Jul 1970. 8p. Dep. NTIS (U. S. Sales Only).

The functions of a computer interface are reviewed, and the various levels at which interfaces arise are described. The basic principles of computer interfaces are discussed, and their similarity is contrasted with the wide variety of sensors and actuators, to which connection may be required. Conventional computer interface equipment using electro-mechanical multiplexers is mentioned, and attention is then focussed on recent developments which attempt to reduce interfacing costs. These include modulated data highways and interrogative systems. The requirements and applicability of interface standards are discussed. Two complementary standards, BS4421 (1969) and CAMAC are described, with examples of their wider application. (auth) (UK)

4388 (DP-Report-498) PULSED ULTRASONIC THERMOMETER. Project DRAGON. Mobsby, E. G. H. (Atomic Energy Establishment, Winfrith (England)). Feb 1967. 24p. Dep. NTIS.

The design of a pulsed ultrasonic thermometer for the Dragon reactor is described. Temperature is measured by exploiting the change in the modulus of elasticity of solids which occurs as a function of the absolute temperature. Miniaturization, shortening the probe without employing higher frequencies, the form of the magnetostrictive material, operation, calibration, materials, and transmission lines are discussed. (W.H.K.)

4389 (DP-Report-590) A RESONANT PROBE ULTRASONIC THERMOMETER. Project DRAGON. Mobsby, E. G. H. (Atomic Energy Establishment, Winfrith (England)). Oct 1967. 11p. Dep. NTIS.

The probe makes use of the changes in the velocity of sound in solids due to changes in Young's modulus with temperature. The system launches bursts of ultrasonic energy, containing many waves, and measures the resonant frequency of the probe. (W.H.K.)

4390 (HMI-B-100) GRAPHIC DISPLAY TERMINAL FOR NUCLEAR EXPERIMENTS WITH ON-LINE COMPUTER. PART 1. FUNCTION, CHARACTERISTICS, DESCRIPTION. Abend, P.; Bublitz, R.; Jackel, D.; Klessmann, H.; Kollbach, A.; Zahn, J. (Hahn-Meitner-Institut fuer Kernforschung, Berlin (West Ger-

XUM

many)). Jul 1970. 96p. (In German). Dep. NTIS (U. S. Sales Only).

The integration of on-line computers into nuclear experimental physics requires a display terminal for interaction of the physicist with the computer controlled experiment. Displays offer means for monitoring the data acquisition, for real-time control of the experimental equipment, and for presentation of analysis results. Data are displayed on a direct-view storage tube by six different graphic or alphanumeric display modes. Data input for dynamic interaction with the experiment is accomplished by means of a keyboard for functions and alpha-numeric characters and a cursor control with a tracking ball. (auth)

4391 (LA-4465, pp 17,1-6) PROPOSAL FOR A LAMB-SHIFT POLARIMETER. Brolley, J. E.; Lawrence, G. P.; Ohlsen, Gerald G. (Los Alamos Scientific Lab., N. Mex.).

From LASL contributions to the 3rd international symposium on polarization phenomena in nuclear reactions, Madison, Wisconsin, August 31-September 4, 1970.

4392 (LYCEN-7032) ADVANCE IN THE APPLICATION OF THE CROSS-CORRELATION METHOD IN NUCLEAR PHYSICS. Rotival, Michel (Lyon Univ. (France). Institut de Physique Nucleaire. Lyon Univ. (France)). Apr 1970. 67p. (In French). Dep. NTIS (U. S. Sales Only).

Thesis.

A theoretical study of the experimental method of cross-correlation showed that the pseudo random pulse method, for identical measurement times and experimental conditions, led to a statistical accuracy which was much greater than that obtained by conventional time of flight methods. The experimental problems arising from the correlation method were studied and it was shown that they were not insurmountable. (France)

4393 COMPUTER TECHNIQUES: VIEW AND OVERVIEW. Hidalgo, John U. (Tulane Univ., New Orleans). pp 186-93 of Pulmonary Investigation with Radionuclides. /Gilson, Albert J. (ed.). Springfield, Ill.; Charles C Thomas, Publisher (1970).

From 1st Annual Seminar on Pulmonary Investigation with Radionuclides, Miami, Fla. See CONF-690334.

The uses of computers in nuclear medicine laboratories are briefly reviewed including generation of radioactive decay tables, computation of radiation dose distributions, processing of radioisotope scan images, and statistical studies. (W.H.K.)

4394 AUTOMATICALLY CONTROLLED NEUTRON DIFFRACTION GONIOMETER. Tobisch, J. (Technische Univ., Dresden); Betzl, M.; Reichel, P. Exp. Tech. Phys.; 17: 391-9 (1970). (In German).

The building and method of operation of a diffraction goniometer are described, as well as the necessary control elements for automatic operation. (tr-auth)

4395 METHOD OF MEASURING THE MOBILITY OF RADIOACTIVE IONS. Huertas, M. L.; Marty, A. M.; Fontan, J.; Lanegrasse, L.; Blanc, D. (Centre de Physique Atomique et Nucleaire, Toulouse). Rev. Sci. Instrum.; 41: 1567-9(Nov 1970).

We have measured the mobility of ions in air. The method of measuring the mobility is a time-of-flight method. The time of flight of the ions is measured between two grids G_1 and G_2, as in Bradbury's method. We have improved the resolution of the apparatus, using a rectangular cyclic voltage, and we have eliminated harmonic peaks. Results with radioactive ions of ThC″ and ions created in air by the β rays of a tritium source are discussed. (auth)

4396 SELF-SWITCHING DAMPING CIRCUIT FOR REDUCING TRANSMITTER RINGDOWN TIME IN HIGH POWER PULSE NMR. Samuelson, Gary L.; Ailion, David C. (Univ. of Utah, Salt Lake City). Rev. Sci. Instrum.; 41: 1601-3(Nov 1970).

In this paper we describe a circuit for reducing the transmitter ringdown time and thereby improving the recovery time in pulse NMR experiments. The circuit uses only solid state devices and requires no external switching. For transmitter voltages less than 0.5 V peak to peak the effective resistance in parallel with the transmitter coil in a crossed coil spectrometer is only 6 Ω, whereas for larger voltages the shunting resistance is of the order of 1-2 kΩ. This circuit thus has the effect of significantly squaring the envelope of an rf pulse. It has the extra advantage of suppressing noise generated by the transmitter during the time interval between pulses. (auth)

4397 SPECTROGRAPH FOR THE SIMULTANEOUS MEASUREMENT OF VELOCITY SPECTRA AND CHARGE-TO-MASS RATIOS OF IONS. Green, T. S. (European Space Research Inst., Frascati, Italy). Rev. Sci. Instrum.; 41: 1533-6(Nov 1970).

The design of a new ion spectrograph is described. Using magnetic deflection, analysis can be made of the velocity spectrum of the ions. For a given entrance angle to the magnetic field the foci lie on a straight line and second order focusing can be obtained. Application of an electric field parallel to the magnetic field causes displacement of the focal line to an extent determined by the charge-to-mass ratio of the ion. The image on the focal plane is thus a set of lines one for each ion species, the velocity distribution being displayed along each line. (auth)

4398 GATED PHOTOMULTIPLIER TECHNIQUE FOR USE IN PULSE RADIOLYSIS. Klein, Nathan; Rock, Theodore J. (Army Aberdeen Research and Development Center, Aberdeen Proving Ground, Md.). Rev. Sci. Instrum.; 41: 1671-3(Nov 1970).

The design and characteristics of a gated photomultiplier detector for high-intensity laser detection for pulse radiolysis studies are described. (W.H.K.)

4399 LOW PASS FILTER WHICH DISCOUNTS LARGE INPUT FLUCTUATIONS. Gottschalk, Bernard (Northeastern Univ., Boston). Rev. Sci. Instrum.; 41: 1658-9(Nov 1970).

A linear low pass filter for inputs within a small adjustable range of the recent average input value, but which gives less than full weight to inputs outside this range (spurious fluctuations), is described. Use of this filter for averaging pulse heights from a scintillation detector which was being scanned for defects with a monochromatic proton beam is discussed. (W.H.K.)

4400 POLARIZATION EFFECTS IN OXIDE INSULATORS. Gordon, R. L.; Schemmel, R. R. (Battelle-Northwest, Richland, Wash.). Trans. Amer. Nucl. Soc.; 13: 799-800(Nov 1970).

From Meeting of the American Nuclear Society, Washington, D. C. See CONF-701102.

4401 INSULATION RESISTIVITY MEASUREMENTS AT HIGH TEMPERATURES. Schemmel, R. R.; Gordon, R. L.; Bates, J. L. (Battelle-Northwest, Richland, Wash.). Trans. Amer. Nucl. Soc.; 13: 800-1(Nov 1970).

From Meeting of the American Nuclear Society, Washington, D. C. See CONF-701102.

4402 NEW METHODS FOR MEASURING COMPACTION OF CERAMIC INSULATORS IN SHEATHED THERMOCOUPLES. Carr, K. R. (Oak Ridge National Lab., Tenn.). Trans. Amer. Nucl. Soc.; 13: 801(Nov 1970).

From Meeting of the American Nuclear Society, Washington, D. C. See CONF-701102.

4403 X-RAY SPECTRA CALCULATIONS FOR COMPLEX DETECTOR GEOMETRIES. Marshall, J. D. (Radiation Research Associates, Inc., Fort Worth, Tex.). Trans. Amer. Nucl. Soc.; 13: 873(Nov 1970).

From Meeting of the American Nuclear Society, Washington, D. C. See CONF-701102.

4404 THREE-DIMENSIONAL X-RAY PICTURES. Redman, J. D. (Atomic Weapons Research Establishment, Aldermaston, Eng.). Atom (London); No. 167, 186-91(Sep 1970).

A brief description of the technique of x ray photography is given and the principles of holography described. Holography is theoretically possible at all wavelengths, but at x ray wavelengths the tolerance on movement is severe and direct x ray holography is impractical. A two stage process for making 3D x ray reconstructions developed by AWRE in which a sequence of radiographs is taken from differing view points and then stored in one hologram plate is described. The disadvantages of the first system, designed at AWRE, arose from the small scale and the discontinuities due to inaccurate registration of frames relative to one another. An improved system is described which works with a 35mm. film and produces a 10 × 8 hologram plate. This semi-automatic system, which keeps the angle between the reference beam and the hologram constant while the plate is rotated, is capable of producing life size reconstructions. The advantages are described and a diagram of the apparatus given. (UK)

Radiation Effects on Instruments and Instrument Components

Refer also to abstracts 4349 and 4350.

4405 (N-70-32671) SPACE RADIATION HAZARDS TO PROJECT SKYLAB PHOTOGRAPHIC FILM. Final Report. Hill, C. W.; Davis, D. N.; Davis, J. H. (Lockheed-Georgia Co.,

XUM

Marietta). Jun 1970. Contract NAS8-245-14. 89p. (NASA-CR-61329; ER-10725). NTIS.

A mathematical model of the Skylab Project cluster geometry is constructed. A radiation dose rate survey of the model is given for trapped protons, trapped electrons, and galactic cosmic radiation. The results of an analytical ATM film vault verification study are presented. (auth) (STAR)

4406 (N-70-35843) RADIATION DEGRADATION OF SELECTED FILMS. Oran, William (National Aeronautics and Space Administration, Huntsville, Ala. George C. Marshall Space Flight Center). 22 Jun 1970. 26p. (NASA-TM-X-64524). NTIS.

The change in base fog caused by radiation damage was measured for the following film types: SO-180, EF7241, EFB7242, SO-246, SO-267, 2475, Plus-X, Tri-X, and 1N. The films were exposed to ^{60}Co gamma rays in addition to 51.1- and 130.6-MeV protons. Graphs of density change versus radiation exposure are included. Sensitometric curves are also given for SO-246, SO-267, 2475, 1N, Plus-X, and Tri-X films. (auth) (STAR)

4407 (N-70-35923) ANALYSIS OF THE EFFECT OF HIGH-ENERGY PROTONS ON ATM PHOTOGRAPHIC FILM. Shelton, Russell D. (National Aeronautics and Space Administration, Huntsville, Ala. George C. Marshall Space Flight Center). 16 Sep 1969. 10p. (NASA-TM-X-53929). NTIS.

Described is an analytical scheme for incorporating experimental data, in the form of measured film darkening associated with monoenergetic, monodirectional proton streams, into a method of predicting the effects of the space proton spectrum on photographic film. (auth) (STAR)

4408 RADIATION DAMAGE IN MINIATURE AVALANCHE DIODES. Samuelson, Reid Robert. Berkeley, Calif.; Univ. of California (1969). 216p. University Microfilms Order No. 70-13,157.

Thesis.

The damage to miniature n^+-p silicon avalanche diodes by high energy neutrons and electrons was studied. The effects were caused by emission of carriers from defects in the p type material. Emission occurred by thermal emission and by tunneling. The defects were tentatively identified as the oxygen-vacancy pair and the divacancy. The diodes were operated in a pulse mode in which the avalanche is self-quenching in a manner analogous to the operation of a Geiger–Mueller tube. The pulse rate due to a constant carrier generation rate was experimentally and theoretically shown to be proportional to the voltage pulse height. The pulse rate due to radiation induced defects increased more rapidly than linearly with voltage. This was in part attributable to carrier trapping effects. The occurrence of trapping was established by an increase in the pulse rate with capacitance. In some circumstances the pulse rate was attributable to trapped carriers which tunneled from defects. This was determined by the reduction of carrier emission with a reduction of the bias voltage. The voltage dependence of the pulse rate of heavily electron irradiated diodes was exponential, which was in accord with an elementary theory of tunneling from defects. However, there was significant quantitative disagreement which indicated that the theory was incomplete. Thermal annealing of the pulse rate showed a prominent stage near 380°C and a lesser stage near 250°C. These annealing stages may be attributed to the oxygen-vacancy pair and to the divacancy respectively. (Diss. Abstr.)

4409 SUMMARY PAPER ON THE NUCLEAR INTERACTION OF RTG'S WITH SCIENTIFIC INSTRUMENTS FOR DEEP SPACE PROBES. Truscello, Vincent (Jet Propulsion Lab., Pasadena, Calif.). Trans. Amer. Nucl. Soc.; 13: 533(Nov 1970).

From Meeting of the American Nuclear Society, Washington, D. C. See CONF-701102.

XUM

LIFE SCIENCES

Biochemistry, Physiology, and Molecular Biology

Refer also to abstract 5311.

4410 PHAGOCYTIC POTENTIAL OF PULMONARY ALVEOLAR EPITHELIUM WITH PARTICULAR REFERENCE TO SURFACTANT METABOLISM. Corrin, B. (St. Thomas's Hospital Medical School, London). Thorax; 24: 110-15(1969).

Finely divided thorium and carbon were injected into the rat lung via the trachea and their uptake was studied electron microscopically. Small amounts of thorium were found in the lamellar vacuoles of the granular pneumocytes. Their presence was maximal at 24 hours and they later disappeared from these cells. This phenomenon is thought to represent a passive inflow as the vacuoles open on to the alveolar surface to discharge their content of surfactant, rather than evidence that the granular pneumocyte is concerned in surfactant disposal. An explanation reconciling the secretory nature of the vacuoles with their previously demonstrated content of lysosomal enzymes is advanced. Small quantities of thorium dioxide were ingested by the squamous pneumocytes and a little transferred to interstitial macrophages, but this is a minor route of disposal, the bulk of the material being ingested by alveolar macrophages. The limited phagocytic potential of the alveolar epithelium contrasts with that of the alveolar macrophages and is not taken to support the concept of an epithelial derivation of alveolar macrophages. (auth)

Basic Processes

Refer also to abstracts 4032, 4042, 4612, 4614, 4616, 4617, 4681, 4693, and 4722.

4411 (CEA-R-4031) PHYSIOLOGICAL DATA ON SWINE FOR USE IN RADIOBIOLOGY: PLASMA AND BLOOD VOLUMES. Remy, Jacques; Perdereau, Bernard; Nizza, Pierre (Commissariat a l'Energie Atomique, Fontenay-aux-Roses (France). Centre d'Etudes Nucleaires). Jun 1970. 16p. (In French). Dep. CFSTI (U. S. Sales Only).

Plasma and blood volumes of Corsican swine were measured using dilution with EVANS blue (T 1824). A value for plasma volume of 50 ml/kg of live weight was found with a hematocrit of 38. The technique used was compared with those used by various authors and the results, after control for some of them with nuclear indicators, were compared with those published for swine and man. Blood volume in the animals used in this experiment was lower by one third than the one measured in humans of the same weight. Red blood cells were labeled with ^{51}Cr and ^{32}P for determinations of whole blood volume, and ^{131}I-labeled albumin was used for measuring plasma volume. (France)

4412 (CONF-680211-, pp 5-24) CHEMICAL AND PHYSICAL NATURE OF BONE MINERAL. Posner, Aaron S. (Hospital for Special Surgery, New York).

From Progress in methods of bone mineral measurements.

Bone mineral was shown to consist of two calcium phosphate pools, a noncrystalline and a crystalline (apatite) phase. Such techniques as x-ray diffraction, electron microscopy, infrared absorption spectrophotometry and electron spin resonance spectroscopy were employed to show that the noncrystalline apatite mineral phases in bone are chemically and physically different. Synthetic experiments showed an amorphous tricalcium phosphate phase to be the precursor of the poorly crystallized hydroxyapatite precipitated from solution. Parallel experiments on bone aging indicate early bone contains a greater amorphous content than mature bone. In addition, bone apatite increases in average crystal size with age, levelling off at adulthood. It was concluded that in bone formation the cells form amorphous calcium phosphate and, subsequently, part of this pool is stabilized, while part of it is transformed, by dissolution and reprecipitation, into the apatite constituent. There was evidence for an intimate morphological and chemical relationship between the collagen and the apatite crystals in bone. In this regard, it was felt that collagen may act as a nucleating agent for the formation of crystals but not the amorphous phase in bone mineral. (auth)

4413 ^{99m}Tc-TECHNETIUM DIOXIDE FOR LIVER SCANNING. Johnson, A. E.; Gollan, F. (Veterans Administration Hospital, Miami, Fla. Univ. of Miami, Fla.). J. Nucl. Med.; 11: 564-5(Sep 1970).

The $^{99m}TcO_2$ can be produced by chemical reduction of sodium pertechnetate to an insoluble precipitate of $^{99m}TcO_2$. This precipitate consists of uniform particles about 0.5 micron in diameter. After intravenous injection, 85% of the radioactive particles are deposited in the liver, and rapid scans with good resolution are obtainable. The $^{99m}TcO_2$ particles are oxidized in the liver to soluble $^{99m}TcO_4^-$ and excreted. The uniform particle size of $^{99m}TcO_2$ and the absence of soluble $^{99m}TcO_4^-$ may lead to more reliable blood-flow studies than have been possible with currently available colloidal radionuclides. (auth)

4414 ^{99m}Tc LABELING OF ERYTHROCYTES. Anghileri, Leopoldo J.; Lee, Jong I.; Miller, Esther S. (Univ. of Colorado, Denver. Veterans Administration Hospital, Denver). J. Nucl. Med.; 11: 530-3(Sep 1970).

A method is described for the labeling of erythrocytes that produces a yield of incorporated radioactivity (^{99m}Tc bound to the cells) 10 to 50 times higher than the previously proposed technique. A penetration into the cell of the ^{99m}Tc carried over by the chromate ion and the subsequent complexing by the reduced iron of the hemoglobin seems to be the mechanism involved in this tagging reaction. (auth)

4415 RESEARCH AND BIOMEDICAL APPLICATIONS. Wagner, Henry N. Jr. (Johns Hopkins Medical Institutions, Baltimore). Trans. Amer. Nucl. Soc.; 13: 522(Nov 1970).

From Meeting of the American Nuclear Society, Washington, D. C. See CONF-701102.

4416 BASIC NUCLEAR ASPECTS OF AUTOHISTORADIOGRAPHY (WITH SUGGESTIONS CONCERNING COLOR AUTORADIOGRAPHY). Van Der Borght, O. (Belgian Nuclear Center, Mol). Acta Histochem., Suppl.; No. 8, 15-21(1968).

When working with labeled compounds, it must be ensured that the radioactivity observed after autohistoradiography really indicates the presence in the living organism of that part of the nonradioactive compound in which one is interested, that is, that the tracer really traces and does not go its own way. (Excerpta Med.)

4417 METHOD FOR INCREASING THE SENSITIVITY OF RADIAL-IMMUNODIFFUSION ASSAY. Rowe, D. S. (Lausanne Univ., Switzerland). Lancet; 1: 1340(20 Jun 1970).

The sensitivity of radial immunodiffusion assay can permit the detection of proteins as antigens down to approximately 100 ng per ml. In a modification of the technique, the zone of precipitate in the agar is made radioactive by application of a second isotopically labelled antibody or by the use of isotopically labelled antiserum incorporated into the agar plate. Zones of radioactivity are visualized as autoradiographs by placing the dried agar plate in contact with photographic film. (UK)

4418 AUTORADIOGRAPHY OF LABELED AMINO ACIDS INJECTED IONTOPHORETICALLY INTO THE GIANT SQUID SYNPASE. Heuser, J.; Miledi, R. (University Coll., London). J. Physiol. (London); 208: 55P-7(Jun 1970).

The location of protein synthesis sites in giant squid nerve fibres was studied by autoradiography of labelled aminoacids. A piece of pre or post ganglionic nerve was immersed in 10 μc/ml of labelled aminoacid, and isolated from the rest of the preparation which was washed by seawater maintaining a concentration ratio of labelled material of at least 10^5 between the two compartments. The nerve accumulated 0.02-0.2 μc of amino acid and incorporated 20% into protein, autoradiography showing the labelled protein located mainly in the glial cells and connective tissue. After periods of up to 12 hrs with continuous stimulation of the nerve at 2Hz, labelled material in the giant axons was retained only by freeze substitution and removed by fixatives. In other experiments, 0.01-0.07 μc labelled leucine and glutamate were injected into unstimulated pre or post synaptic axons. Presynaptic axons severed from their cell bodies showed small label retention and spread of labelled material. Post synaptic axons connected to cell bodies less than 1mm from injection sites showed large label retention in axons and cell bodies, less spread into the glial cells and no evidence for movement across the synaptic contact. When injection was stopped before it could diffuse, retention of label occurred confined to injection site. (UK)

4419 RADIOIMMUNOASSAY OF ANGIOTENSIN II IN PLASMA. Sundsfjord, Johan A. (Aker Hospital, Oslo). Acta Endocrinol.; 64: 181-92(1970).

Specific antibodies were produced in rabbits with val^{5}angiotensin II amid (Hypertensin®, Ciba) attached to succinyl-poly-l-lysine. Hypertensin was labelled with iodine-125 (^{125}I) according to a modified Hunter-Greenwood procedure. Ion exchange chromatog-

XUM

raphy followed by antibody association-dissociation technique was used in the purification of the labelled hormone. The separation between bound and free hormone was performed on Sephadex G-25. Maximum binding of the labelled material to the antibody was achieved within one hour. The equilibrium between bound and free hormone was markedly influenced by temperature. It was found that Hypertensin and ileu^{5}angiotensin II exhibited equal immunological activities, whereas ileu^{5}angiotensin I displayed less than 1% of the affinity of angiotensin II towards the antibody. For the determination of angiotensin II in plasma, samples were collected in chilled tubes containing EDTA and BAL at pH 5.5, in order to inhibit any possible enzymatic generation and degradation of angiotensin II. Concentration was achieved on a column of Dowex 50W−X2(NH_4^+) resin followed by freeze-drying of the eluate. Dilution of the material obtained behaved as standard angiotensin II in the assay. The recovery of 0.5 to 10 ng of angiotensin II added to 10 ml of plasma was 85 to 111%. The normal range for young healthy adults was 2.7 ± 1.4 (SD) ng/100 ml, in agreement with reports by some other groups. (auth)

4420 EXTRACTION OF PLASMA INSULIN IN RADIOIMMUNOASSAY FOR REMOVAL OF NONSPECIFIC INHIBITOR AND OF CIRCULATING INSULIN ANTIBODY. Ohneda, Akira; Toyota, Takayoshi; Sato, Shinichiro; Yamagata, Shoichi (Tohoku Univ., Sendai). Tohoku J. Exp. Med.; 100: 75-84(1970).

In the two-antibody assay system for insulin, insulin-free human plasma and human globulin fraction reduced the percentage of precipitated insulin-^{131}I. Insulin antibody in plasma was partially absorbed by means of anti-human globulin rabbit serum, that was not available for the removal of endogenous insulin antibody. In order to remove the inhibiting factor as well as the circulating insulin antibody, a simple method for the extraction of plasma insulin was described. The method consists of extraction by acid-ethanol and precipitation in cold acetone. The recovery rate of insulin-^{131}I added to serum by the present method was 92%, and that of human insulin added to a pooled human plasma was in the range of 80 to 94%. The extract contained a small amount of albumin but not globulin. The extraction method completely separated the insulin from the insulin-antibody complex. The mean values of the fasting extractable insulin in human plasma were 20.5, 19.3, 22.6 and 10.0 μU per ml in normal subjects, mild, moderate and severe diabetic patients, respectively. In the latter group the insulin response to glucose load decreased. Extractable insulin in plasma of several diabetic patients with insulin antibody was found to be 10 to 32 μU per ml. The insulin level in plasma of insulin-dependent patient with antibody to insulin could be estimated by the present extraction method. (auth)

4421 A TECHNIQUE FOR THE RADIOAUTOGRAPHY OF GERM CELLS IN WHOLE MOUNTS OF SEMINIFEROUS TUBULES. Huckins, Claire; Kopriwa, Beatrix Markus (McGill Univ., Montreal). J. Histochem. Cytochem.; 17: 848-51(1969).

A technique is described for preparing radioautographs of germ cells in intact segments of seminiferous tubules from rat testis. Pieces of tubules were dissected from testes, fixed in Bouin's fluid and stained in Harris hematoxylin. For radioautography, rectangular coverslips were first dipped in liquid Kodak NTB_2 emulsion. The tubules were placed on the partially set emulsion, and thus became evenly coated on their viewing surface with a thin layer of emulsion. Following routine exposure and processing, the coverslips bearing these tubules were inverted onto microscope slides to give the final whole mount radioautographic preparation. (auth)

4422 APPLICATION OF TWO RADIO-IMMUNOLOGICAL METHODS TO THE ASSESSMENT OF GROWTH HORMONE. RELEVANCE IN VARIOUS DYSMORPHIC SYNDROMES. Mirouze, J.; Orsetti, A.; Vidal, F. (Hopital St-Eloi, Montpellier, France). Ann. Endocrinol. (Paris); 31: 237-46(Mar-Apr 1970). (In French).

Two methods for radioimmunoassay were used to determine content of growth hormone in normal subjects and those exhibiting dysmorphic conditions. One method results in the separation of the free hormone from the bound complex by means of rheophoresis and the other, by means of immunoprecipitation with double antibodies. The values obtained by these two methods are comparable. The double antibody method provided a more consistently accurate assessment and was preferred to the rheophoresis method which was adversely effected by the variable quality of the paper used for the migration. (E.E.H.)

Metabolism, Physiology, and Toxicology

Refer also to abstracts 4477, 4479, 4552, 4566, 4592–4598, 4600–4602, 4667, 4669, 4673, 4677, 4678, 4700, and 4720.

4423 (COO-1601-23) MOBILIZATION OF RADIOACTIVE EMITTERS FROM BONE. Final Report. (Illinois Univ., Chicago. Medical Center). Aug 1970. Contract AT(11-1)-1601. 18p. Dep. NTIS.

Studies on mechanisms of uptake and mobilization of radioactive emitters by bone included a comparison of dead and living bone tissue; correlation of balance and kinetic studies; bone density and morphological studies; and metabolic activity. Studies on factors affecting uptake and mobilization included effects of circulation, oxygen tension, vitamin D, diuretics, parathormone, and low phosphorus diet. Experiments on the effects of diuretics on mobilization of ^{85}Sr in parathyroidectomized and intact rats were conducted. The parathyroidectomized group showed no significant mobilization of ^{85}Sr following administration of the diuretic. (H.L.W.)

4424 (TID-25567) METABOLISM AND REMOVAL OF ^{90}Sr AND ^{226}Ra IN MAN. Progress Report, December 1, 1969–November 30, 1970. Spencer, Herta (Loyola Univ., Maywood, Ill. Stritch School of Medicine). 9 Sep 1970. Contract AT-(11-1)-1231. 33p. Dep. NTIS.

Studies on ^{90}Sr metabolism in man were continued under constant and strictly controlled dietary conditions. Strontium-90 and calcium balances were determined during the intake of milk and of calcium gluconate in persons of older age group. Results showed marked differences in the observed ratio of urine/diet when calcium was given as milk or as calcium gluconate, while the observed ratio of stool/diet was about 1 on either intake level of calcium when given in either form. The effectiveness of two additional dose levels of stable strontium on calcium excretion was investigated. The data showed a five-fold increase of the urinary calcium excretion when the 900 mg dose of stable strontium was infused as compared to a factor of increase in urinary calcium of 1.5 when the 300 mg dose was given intravenously. Aluminum phosphate gel given orally immediately prior to the oral dose of ^{85}Sr decreased the total body retention of ^{85}Sr by about 90% while decreasing the total body retention of ^{47}Ca by only 40 to 50%. Other studies were conducted on passage of radiostrontium and radiocalcium from the vascular space into the intestine in rats and in vitro determinations on mineral exchange in bone. It was shown that the passage of ^{85}Sr and ^{47}Ca from the vascular space into different segments of the intestine was about equal. (H.L.W.)

4425 (UCLA-12-782) ANNUAL PROGRESS REPORT FOR THE PERIOD ENDING JUNE 30, 1970. (California Univ., Los Angeles. Lab. of Nuclear Medicine and Radiation Biology). Contract AT-04-1-GEN-12. 125p. Dep. CFSTI.

Separate abstracts were prepared for five sections of this report. A list is included of 100 publications during the period covered. (C.H.)

For abstracts of individual sections see: 4016, 4458, 4459, 4477, and 4657.

4426 KINETICS OF LANTHANUM RETENTION AND TISSUE DISTRIBUTION IN THE BEAGLE DOG FOLLOWING ADMINISTRATION OF $^{140}LaCl_3$ BY INHALATION, GAVAGE, AND INJECTION. Cuddihy, R. G.; Boecker, B. B. (Fission Product Inhalation Labs., Albuquerque, N. Mex.). Health Phys.; 19: 419-26 (Sep 1970).

Lanthanum tissue distribution kinetics following inhalation and gavage of $^{140}LaCl_3$ and injection of ^{140}La in various chemical forms were studied in the Beagle dog. The solution of a kinetic model was presented describing the tissue distribution of ^{140}La after aerosol exposure. Tissue distribution patterns after injection of $^{140}LaCl_3$ in solutions at pH 3.5, 4.5, and 6.5 and ^{140}La-citrate were markedly different from those obtained after inhalation of aerosol particles containing $^{140}LaCl_3$. The results indicate that tissue distribution patterns are greatly influenced by the chemical nature of the La presented to the biological system and that injection studies involving ^{140}La are of limited value for interpreting the results or predicting the fate of inhaled La. The highest radiation dose following inhalation of $^{140}LaCl_3$–CsCl particles (activity median aerodynamic diameter of 1.8 μ) was received by the nasal turbinates followed in decreasing order by lung, gastrointestinal tract, liver, skeleton and bronchial lymph nodes. (auth) (UK)

4427 ON THE OCCURRENCE OF ^{90}Sr IN BIOLOGICAL MATERIALS. Keil, R. (Univ., Rostock, Ger.). Nahrung; 12: 399-405(1968). (In German).

Radiochemical studies on the bones of 3 yr old carp (caught between December 1961 and October 1962) from ponds in Mecklenburg yielded ^{90}Sr contents of nearly 5 pCi/g Ca, or 2 pCi/g ash, or 370 pCi/kg fresh matter. Bones of chickens raised during 1965 contained (mean values): 2.9 pCi ^{90}Sr/g ash, 725 pCi/kg fresh matter, or 7.7 strontium units. The respective values for chicken-meat were: 0.39, 3.9, and 10. Thus the contamination rate of bones was 186 times that of meat. The reasons for the

XUM

higher ^{90}Sr content of the meat of fresh-water fish, as compared with that of the meat of salt-water fish, warm-blooded animals, and chickens, and of the high per capita intake of radiostrontium from the consumption of fresh-water fish is discussed on the basis of the respective West German findings. (TSS) (auth)

4428 AIRWAY CLOSURE. Milic-Emili, J. (McGill Univ., Montreal); Ruff, F.; Leblanc, P. pp 282-90 of Pulmonary Investigation with Radionuclides. /Gilson, Albert J. (ed.). Springfield, Ill.; Charles C Thomas, Publisher (1970).

From 1st Annual Seminar on Pulmonary Investigation with Radionuclides, Miami, Fla. See CONF-690334.

The closure of airways with relation to pleural pressure in various parts of the lung is discussed. It is pointed out that in a young subject no airways are closed during normal breathing, but that at full expiration 40 to 50% of the airways are closed. In order to detect airway closure, the subject inhales air containing ^{133}Xe, and at full inspiration the regional count rates of xenon are measured by means of a series of scintillation counters placed at different levels of the lung. During expiration the concentration of ^{133}Xe in the expired air is measured continuously by means of a scintillation counter placed near the mouth. The lung volume at which there is a change in the expired xenon concentration indicates the lung volume at which the dependent airways begin to close. Experiments on subjects of ages from 20 to 82 years showed that the lung volume at which the airways begin to close increases progressively with age. (H.L.W.)

4429 WASHOUT OF ^{133}Xe AFTER INTRAMUSCULAR INJECTION AND DIRECT MEASUREMENT OF BLOOD FLOW IN SKELETAL MUSCLE. Toennesen, K. H.; Sejrsen, P. (Univ. of Copenhagen, Bispebjerg Hospital, Copenhagen). Scand. J. Clin. Lab. Invest.; 25: 71-81(1970).

The distribution of injected ^{133}Xe was studied in isolated cat gastrocnemius. A significant correlation was found between the results of the two methods for blood flow measurement over a wide range. The traumatic effect of i.m. injection was studied. (auth)

4430 THE ABSORPTION OF ^{45}Ca FROM THE INTESTINAL TRACT OF THE RAT. Moll, H.; Sauer, P. (Univ., Munich). Z. Gesam. Exp. Med., 149: 266-76(Feb. 20, 1969). (In German).

To study absorption of radiocalcium from the intestine of rats, male Sprague-Dawley rats weighing 300 to 350 g were given 35 to 60 μCi of ^{45}Ca in 1.0 ml of saline by intubation into the intestinal segment. Arterial blood was sampled and radioactivity measured at intervals. In the first 60 min the rate of absorption of ^{45}Ca was fastest in the jejunum and decreased towards the distal end of the intestinal tract. The amount absorbed was largest when a solution with low Ca concentration was used. An increasing concentration of the cation in the test solution was followed by a slower rate of ^{45}Ca absorption. The intestinal uptake followed the Michaelis-Menton equation in all segments studied. The influence of K^+ ions upon the absorption of ^{45}Ca ion was also considered. (BBB)

4431 EFFECT OF THE UNCOUPLING OF OXIDATIVE PHOSPHORYLATION ON SUBCELLULAR DISTRIBUTION OF ^{45}Ca AND ^{89}Sr IN THE RAT LIVER. Carafoli, E. (Univ., Modena, Italy). Sperimentale, 117: 31-51(Jan.-Feb. 1967). (In Italian).

The effect of the in vivo treatment with agents uncoupling oxidative phosphorylation on the distribution of injected ^{45}Ca and ^{89}Sr in the subcellular fractions of rat liver was studied. It was found that the pretreatment markedly decreased the amount of radioactivity associated with the mitochondrial fraction, and it eliminated the concentration of the isotopes that takes place normally in mitochondria in the unfractionated homogenate. The amount of radioactivity associated with the microsomal fraction and with the soluble hyaloplasm was found to be increased. These effects were present only when mitochondrial oxidative phosphorylation was completely uncoupled. The Ca content of mitochondria pretreated with uncouplers is sharply decreased with respect to controls. Treatment with p-dichlorophenol caused the loss of about ⅔ of the mitochondrial Ca, and it decreased to about 40 to 50% the amount of ^{45}Ca found in the total mitochondrial fraction. It is suggested that mitochondria contain two pools of Ca, of which only one is sensitive to uncouplers of oxidative phosphorylation. It is concluded that in the liver cells of the intact animal energy-linked movement of Ca and Sr takes place in mitochondria. (BBB)

4432 STUDIES ON DOGS WITH IMPLANTED ^{238}Pu SOURCES. Huffman, F. N. (Thermo Electron Corp., Waltham, Mass.); Sandberg, G. W.; Norman, J. C. Trans. Amer. Nucl. Soc.; 13: 499 (Nov 1970).

From Meeting of the American Nuclear Society, Washington, D. C. See CONF-701102.

4433 RADIOBIOLOGICAL EFFECTS OF SIMULATED NUCLEAR POWER SOURCES FOR ARTIFICIAL HEARTS: A PRELIMINARY REPORT. Kallfelz, F. A.; Comar, C. L.; Casarett, A. P.; Craig, P. H. (Cornell Univ., Ithaca, N. Y.). Trans. Amer. Nucl. Soc.; 13: 499-500(Nov 1970).

From Meeting of the American Nuclear Society, Washington, D. C. See CONF-701102.

4434 RADIOISOTOPE-INDUCED, NEGATIVE SURFACE CHARGE FOR THROMBUS RESISTANCE. Bloom, Gerald; Howard, Edgar (Hittman Associates, Inc., Columbia, Md.). Trans. Amer. Nucl. Soc.; 13: 500(Nov 1970).

From Meeting of the American Nuclear Society, Washington, D. C. See CONF-701102.

4435 BODY DISTRIBUTION AND BIOLOGICAL AVAILABILITY OF RADIONUCLIDES PRODUCED BY PROJECT SCHOONER. Chertok, Robert J.; Lake, Suzanne (Univ. of California, Livermore). Trans. Amer. Nucl. Soc.; 13: 639-40(Nov 1970).

From Meeting of the American Nuclear Society, Washington, D. C. See CONF-701102.

4436 FATE OF SCHOONER FALLOUT RADIONUCLIDES INGESTED BY THE DAIRY COW. Potter, G. D.; Vattuone, G. M.; McIntyre, D. R. (Univ. of California, Livermore). Trans. Amer. Nucl. Soc.; 13: 640(Nov 1970).

From Meeting of the American Nuclear Society, Washington, D. C. See CONF-701102.

4437 A STUDY IN PREPARATION OF ^{113m}In COLLOID AS SCANNING AGENT AND ITS ORGAN DISTRIBUTION IN RATS. Koh, Chang Soon; Rhee, Chong Hoen; Chang, Ko Chang; Hong, Chang Gi D. (Radiological Research Inst., Seoul. Capital Army Hospital, Seoul). J. Nucl. Sci. (Seoul); 9: No. 2, Pt. 2, 105-6 (Apr 1970). (In English and Korean).

A $^{113}Sn-^{113m}In$ cow generator (25 mCi) was used to produce ^{113m}In. The sizes of the particles produced under various conditions were studied, and the possibilities for use in scanning organs were explored. It was found that the pH was the most important factor in the particle size of colloidal indium, and hence in its distribution. The highest level for blood was 7.1% at a pH of 1.7; for liver it was 88.4% at pH 3.5; for spleen it was 3.1% at pH 6.0; and for lung it was 85.3% at pH 11.0. The activity of ^{113m}In eluted from the generator was over 90% in the first 4 ml and about 86 to 88% in the first 2 ml. (C.O.)

4438 TOXICOLOGY OF RADIOACTIVE SUBSTANCES. VOLUME 4. ^{232}Th AND ^{238}U. Letavet, A. A.; Kurlyandskaya, E. B. (eds.). Elmsford, N. Y.; Pergamon Publishing Company (1970). 147p. $9.50.

Translated from the Russian by A. Crozy.

Separate abstracts were prepared for all 12 of the papers appearing in this publication. (E.E.H.)

For abstracts of individual papers see: 4439–4447 and 4700–4702.

4439 CERTAIN ASPECTS OF THE TOXICOLOGY OF INSOLUBLE COMPOUNDS OF ^{232}Th AND ^{238}U. Kurlyandskaya, E. B. Toxicol. Radioactiv. Subst. (USSR) (Engl. Transl.); 4: 1-8(1969).

Translated from Mater. Toksikol. Radioaktiv. Veshchestv.; 4: 1-8(1964).

Experimental investigations of some aspects of the toxicology of insoluble compounds of thorium and uranic oxides are reviewed. These experiments were carried out at the laboratory of the Institute of Labor Hygiene and Occupational Diseases, U. S. S. R. Academy of Medical Science. (E.E.H.)

4440 COMPARATIVE TOXICITY OF SOLUBLE AND INSOLUBLE COMPOUNDS OF ^{232}Th. Yan; Syao-shan. Toxicol. Radioactiv. Subst. (USSR) (Engl. Transl.); 4: 9-19(1969).

Translated from Mater. Toksikol. Radioaktiv. Veshchestv.; 4: 9-19(1964).

A comparative study of the toxic properties of thorium nitrate, thorium chloride, and thorium oxide showed that thorium nitrate is the most toxic. The difference in their toxicities is determined by their degree of solubility and the higher toxicity of the NO_3 radical as compared to the Cl anion. Poorly soluble ThO_2 is the least toxic. The physical and physico-chemical properties of thorium are reviewed. (E.E.H.)

4441 ABSORPTION, DISTRIBUTION, AND EXCRETION OF CERTAIN SOLUBLE COMPOUNDS OF NATURAL THORIUM. Traikovich, Miodrag. Toxicol. Radioactiv. Subst. (USSR) (Engl. Transl.); 4: 20-9(1969).

Translated from Mater. Toksikol. Radioaktiv. Veshchestv.; 4: 20-9(1964).

The distribution and excretion of certain soluble compounds of natural thorium and thorium nitrate in rats were studied following single dose administration by various routes. Following intraperi-

toneal, intramuscular, and oral administration of thorium compounds, between 53% and 75% of the amount of thorium found in the body was in bone tissue. Intracardiac administration of thorium citrate and thorium nitrate resulted in thorium concentration in the liver (17%) and in the spleen (3%). Three days after intraperitoneal and intramuscular injection of thorium nitrate, only small amounts were excreted in the feces and urine. However, three days following intracardiac administration of thorium citrate about 22% of the amount administered was excreted. Of this amount, 19% was found in the urine. It was concluded that common physicochemical and biological mechanisms are involved in the absorption, distribution, and excretion of thorium following intraperitoneal, intramuscular, and oral administration. After intracardiac administration, however, certain special features were found in the distribution of thorium that are associated with the degree of dispersion of its compounds. (E.E.H.)

4442 BEHAVIOUR OF THORIUM DIOXIDE IN RATS AFTER INTRATRACHEAL AND INTRAPERITONEAL ADMINISTRATION. Yan; Syao-shan. Toxicol. Radioactiv. Subst. (USSR) (Engl. Transl.); 4: 30-41(1969).

Translated from Mater. Toksikol. Radioaktiv. Veshchestv.; 4: 30-41(1964).

The excretion and distribution of thorium compounds in the organs and tissues of rats were studied at 1, 3, 5, 7, and 10 days and 5 and 21 mos. after intratracheal administration. Thorium dioxide in the amounts of 2, 20, 200, 300, and 400 mg/kg body weight was injected. After 13 mos., the rats were killed and thorium retention in tissues and organs was determined by histoautoradiography. Another series of experiments were designed to establish how long the ThO_2 remained at the site of injection. In order to measure content of administered thorium, it was necessary to determine the natural content of thorium in rats. Despite highly sensitive methods, no thorium was found in the organs of normal rats. The following results were obtained. Up to 5 days after intratracheal administration, thorium dioxide was found in the lungs, trachea, bifurcation and cervical lymph nodes, the gastro-intestinal tract and contents, liver, bones, and kidneys. The largest amount of thorium was found in the lungs and in the early stages after administration this was 68 to 73% of the dose given. After 21 mos., the rat lungs still contained 15 to 30% of the thorium, indicating the prolonged retention of ThO_2 in the lungs. Histoautoradiography of the lymph nodes 13 mos. after intratracheal administration of ThO_2 showed accumulation of thorium alpha particle tracks were observed in the lymphoid tissue. Excretion of ThO_2 in the urine and feces was insignificant at late times after intratracheal administration. Following intraperitoneal administration, thorium dioxide was retained for a long time in the abdominal cavity. After 15 mos., 14.4 to 74.6% of the amount administered was found in the abdominal cavity and 0.33 to 0.51% was found in the femoral bone. (E.E.H.)

4443 PHOTOMETRIC DETERMINATION OF LOW AMOUNTS OF THORIUM IN BIOLOGICAL MATERIALS. Pavlovskaya, N. A.; Cherkashina, T. N. Toxicol. Radioactiv. Subst. (USSR) (Engl. Transl.); 4: 83-6(1969).

Translated from Mater. Toksikol. Radioaktiv. Veshchestv.; 4: 83-6(1964).

To determine small quantities of thorium in biological media, it was found that an assay could be made on the basis of its reaction with Arsenazo III. The minimum amount that could be detected was 2 μgm with an error of not more than 15%. Titanium, zirconium, or PO_4^{3-} in a 1500 : 1 ratio to thorium did not interfere with the assay. (E.E.H.)

4444 EFFECT OF URANOUS-URANIC OXIDE (U_3O_8) IN EXPERIMENTAL WORK. Rubanovskaya, A. A. Toxicol. Radioactiv. Subst. (USSR) (Engl. Transl.); 4: 87-100(1969).

Translated from Mater. Toksikol. Radioaktiv. Veshchestv.; 4: 87-100(1964).

An investigation of chronic poisoning with small amounts of U_3O_8 was made to study the excretion of uranium in the urine and feces, its distribution and deposition in the body, and pathomorphological changes in the organs of dogs and rabbits. It was found that ingested U_3O_8 was almost completely removed in the feces and did not affect the health of the animals. Single intratracheal injection into the lungs of dogs and rabbits produced severe intoxication but most of the U_3O_8 particles were removed through the air passages and only minor morphological changes occurred in the lungs and kidneys. Injections under the skin of large amounts of U_3O_8 had no toxic effect. Subcutaneous administration, however, produced severe intoxication. (E.E.H.)

4445 CHANGES IN THE PERIPHERAL BLOOD FOLLOWING CHRONIC AND ACUTE POISONING WITH U_3O_8. Beloborodova, N. L. Toxicol. Radioactiv. Subst. (USSR) (Engl. Transl.); 4: 101-8(1969).

Translated from Mater. Toksikol. Radioaktiv. Veshchestv.; 4: 101-8(1964).

Experiments were carried out to determine the effect of chronic and acute intratracheal and oral administration of U_3O_8 on the peripheral blood of dogs. Following 2 to 4 mos. of chronic oral administration, the blood changes were insignificant. Repeated low dose injection into the trachea produced marked absolute lymphopenia, periodic monocytosis and eosinophilia, moderate neutrophilic leukocytosis, and disturbances in leukopoiesis. With acute single dose poisoning with U_3O_8 given intratracheally, the animals developed leukocytosis, disturbance in leukopoiesis, and in the acute period of intoxication, depressed erythropoiesis was indicated. (E.E.H.)

4446 EFFECT OF U_3O_8 ON THE BODY OF THE PREGNANT FEMALE AND THE FOETUS. Kurlyandskaya, E. B. Toxicol. Radioactiv. Subst. (USSR) (Engl. Transl.); 4: 109-19(1969).

Translated from Mater. Toksikol. Radioaktiv. Veshchestv.; 4: 109-19(1964).

Experiments were carried out in female rabbits and dogs at different periods of pregnancy to study the permeability of the placenta in relation to U_3O_8, the possibility of its excretion by the mammary glands, and the effect of this compound on embryonic development in the intrauterine and early extrauterine period. Following oral or intratracheal administration to the pregnant animal, uranium was found in the placenta and tissues of the embryo, in the milk of lactating animals, and in the tissues and urine of the puppies and young rabbits fed on the milk of the poisoned mother. Chronic exposure of animals to U_3O_8 has an effect on their littering capacity and the intrauterine and extrauterine development of young rabbits and puppies. (E.E.H.)

4447 PATHOMORPHOLOGICAL CHANGES IN ANIMALS FOLLOWING ACUTE AND CHRONIC POISONING WITH U_3O_8. Tolgskaya, M. S. Toxicol. Radioactiv. Subst. (USSR) (Engl. Transl.); 4: 120-35(1969).

Translated from Mater. Toksikol. Radioaktiv. Veshchestv.; 4: 120-35(1964).

The pathohistological changes in the internal organs of dogs and rabbits on exposure to uranous–uranic oxide were studied. The investigations were conducted using acute poisoning with uranium by the intratracheal route and chronic poisoning with uranium by intratracheal, subcutaneous, and oral administration. Histological changes occurred in the tissues of the animals following both acute and chronic poisoning. (E.E.H.)

4448 EXPERIMENTS ON THE UPTAKE OF RADIOACTIVE PHOSPHORUS BY BIVALVES AND ITS SUBSEQUENT DISTRIBUTION WITHIN THE BODY. Allen, J. A. (Univ. of Newcastle upon Tyne, Eng.). Comp. Biochem. Physiol.; 36: 131-41(Sep 1970).

Radioactive phosphate ions are taken up from solution by Mytilus edulis at both full and half salinity. The total phosphorus uptake for specimens 3 cm total length is of the order of 1μg P/65 l. sea water filtered. Excretion of phosphorus occurs at a low rate and is possibly of the order of 1.5% per day of the total phosphorus held in the body. Tissue counts and autoradiography show that the main place of assimilation of labelled phosphorus is the digestive gland where it is held in a labile form. The concentration of labelled phosphorus in the digestive gland falls with time as it is dispersed to the tissues. Within 1 week from uptake, kidney tissue contains by far the greatest concentration of bound phosphorus; the gill, too, stores relatively large amounts of phosphorus. Little labelled phosphorus was recorded in mantle tissue and mature gonads. The distribution of phosphorus within the body tissues following uptake from solution is similar to that following assimilation from food. (auth)

4449 ABSORPTION AND DISTRIBUTION OF ^{137}Cs BY TRIFOLIUM PRATENSE. Bergamini, P. G.; Palmas, G.; Piantelli, F.; Rigato, M. (Univ., Siena, Italy). Health Phys.; 19: 521-8(Oct 1970).

Growths of Trifolium pratense were contaminated by means of three solutions of $^{137}CsSO_4$ having different concentrations. Each one of the three solutions was used for contamination at three distinct stages of the plant's development, in two different ways: contamination of the soil only and contamination by means of overhead irrigation. The specific radioactivity of the plants was followed from their contamination up to about 80 days after the first flowering. The concentration factor was calculated for each sample. Autoradiographs were also produced. (auth) (UK)

4450 RADIOCESIUM RETENTION BY RATS AS AFFECTED BY L-THYROXINE AND PROPYLTHIOURACIL. Lengemann, F. W. (Cornell Univ., Ithaca, N. Y.). Contract AT(30-1)-4039. Health Phys.; 19: 551-6(Oct 1970).

Results are presented on the possible relationship of the thyroid

XUM

to the whole-body retention of radiocesium. The procedure used was to follow the decline in the body burden of radiocesium with time when the animals were fed diets containing L-thyroxine or propylthiouracil. The results showed that L-thyroxine increased the decline of the radiocesium body burden while propylthiouracil slowed it. Thyroxine was found to interact with temperature increasing the loss of radiocesium by a factor of 5 when the rats were kept at 32°C and by about 2 when the rats were at 4°C. Propylthiouracil promoted the retention of radiocesium at 4° by a factor of 1.7 and 32° by a factor of 1.4. Adrenalectomy tended to counter the action of thyroxine administration and tended to supplement the action of propylthiouracil. (auth) (UK)

4451 RENAL CLEARANCE OF RADIOPHOSPHATE IN THYROID DISEASE. Gennari, C.; Palazzuoli, V.; Bencini, M.; Borrello, G. (Univ., Siena, Italy). J. Nucl. Biol. Med.; 13: 103-5(Jul-Sep 1969).

The renal clearance of radiophosphate was studied in hyperthyroid and hypothyroid patients. ^{32}P-labeled sodium orthophosphate was administered and the radioactivity in blood plasma and urine was later measured. The effects of medical and surgical treatment on radiophosphate clearance was also investigated and the results were compared with those from the creatinine clearance method. (F.M.M.)

4452 EFFECTS OF IRRADIATION OF THE PAROTID GLAND AND PANCREAS ON HUMAN ISOAMYLASES. Wolf, R. O.; Taylor, L. L.; Brace, K. (National Institutes of Health, Bethesda, Md.). Amer. J. Clin. Pathol.; 54: 214-18(Aug 1970).

Isoamylases of parotid saliva, serum, and urine were studied during incidental ^{60}Co irradiation of the parotid glands in three patients. Samples were obtained before, one day after, and the fourth day after irradiation. Polyacrylamide electrophoretic zymograms and total amylase concentrations were obtained for each sample. Parotid saliva flow rates were also obtained. Total amylase increased in saliva, serum, and urine after irradiation and then decreased by the fourth day post-treatment. In general, the salivary zymograms reflected these amylase concentration changes in each of the bands. Serum and urine zymograms increased in the banding nearer the anode after irradiation, indicating the salivary gland contribution to serum amylase. A fourth patient was subjected to ^{60}Co pancreatic radiotherapy for generalized lymphosarcoma. Only serum and urine were collected. The part of the serum zymogram nearer the cathode increased after irradiation, in contrast to the increase in the part nearer the anode when parotid glands were irradiated, demonstrating the pancreatic serum amylase. (auth)

4453 INCORPORATION OF ISOTOPIC CARBON ^{14}C INTO THE CEREBRAL GLYCOGEN OF NORMAL AND X-IRRADIATED RATS. Lundgren, P. R.; Miquel, J. (Ames Research Center, Moffett Field, Calif.). J. Neurochem.; 17: 1383-6(1970).

Maximal incorporation of ^{14}C from labeled glucose into cerebral glycogen of the rat occurred at 3 to 6 h following intravenous injection of the precursor. A reduction of the rate of glycogen breakdown is the most likely cause of the glycogen accumulation observed in rat brain following exposure to 10 krad of x radiation. (auth)

Radiation Effects

Refer also to abstracts 4534, 4540–4547, 4550, 4551, 4567, 4569, 4605, and 4731.

4454 (NYO-3240-55) EFFECT OF IRRADIATION ON THE BIOCHEMICAL CHANGES OF MAMMALIAN CELLS IN THE ABSENCE AND PRESENCE OF PARTICULATE MATERIAL. (Saint Margaret's Hospital, Boston, Mass.). Aug 1970. Contract AT(30-1)-3240. 126p. Dep. NTIS.

Peritoneal exudate PMN collected from X-irradiated guinea pigs show a metabolic and phagocytic defect. Administration of bacterial endotoxin or poly A–U complexes to the irradiated animals reverses the defect. PMN collected from X-irradiated and endotoxin or poly A–U treated animals have stimulated H_2O_2 production and glucose-1-^{14}C oxidation during phagocytosis similar to PMN collected from normal guinea pigs. Endotoxin administration causes a 5-fold increase in the total number of circulating PMN during leukocytosis. Repopulation may account for endotoxin restoration. Poly A–U administration does not induce a significant leukocytosis. This suggests a mechanism other than repopulation. (auth)

4455 (ORO-3329-7) [EFFECT OF RADIATION ON MUCOSAL PHOSPHOLIPASE ACTIVITY]. Comprehensive Report, 1967–1970. Bernheim, Frederick; Ottolenghi, Athos (Duke Univ., Durham, N. C. Dept. of Physiology and Pharmacology). Nov 1970. Contract AT(40-1)-3329. 35p. Dep. NTIS.

Aims of the research were to study the relationship between phospholipase B activity and the eosinophilic leukocytes and to correlate findings with biochemical and physiological changes in the intestine after x irradiation. Various approaches were developed including a specific histochemical method for phospholipase B, correlation studies of the number of eosinophils and the enzyme content of rat tissues and an analysis of the pattern of decay and recovery of the phospholipase B of the small intestine following exposure to x radiation or drug administration. Combined evidence from these studies supports the conclusion that the phospholipase B of spleen, bone marrow, peritoneal fluid, and uterus is localized in the eosinophilic leukocytes which are the sole source of the enzyme. In the small intestine histochemical evidence shows that the enzyme is present in the eosinophils but the quantitative data on enzyme activity of the homogenates are in excess of the number of eosinophilic leukocytes counted in histologic sections. Radiation studies show that decay and recovery of the activity in the intestine and spleen follow a time course compatible with the hypothesis that the cells containing phospholipase B originate in the hematopoietic tissue. An additional factor which is localized in the intestine is radiosensitive and is not fully restored to preradiation levels until the fourth week after exposure was found. Studies with cytoxic drugs show the feasibility of a differential action on various compartments of eosinophilic cells. The data confirm the relative insensitivity of the bone marrow compartment to the action of corticoids which are instead effective in reducing the eosinophilic population of other tissues. In contrast, bone marrow depressants reduce the bone marrow population to very low values, induce some loss in minor peripheral compartments, but have little effect on the intestinal compartment. The combined administration of corticosteroids and bone marrow depressants brings about a marked decrease in all compartments including the intestine thus mimicking the first response to x radiation. (H.L.W.)

4456 (ORO-3596-15) PROGRESS REPORT [ON RADIATION BIOLOGY], AUGUST 1, 1969–JUNE 30, 1970. (Florida Univ., Gainesville. Radiation Biology Lab.). 10p. Dep. CFSTI.

Results are reported from studies on the effects of uv and x irradiation on DNA synthesis and DNA replication in chromosomes of Bacillus subtilis and Escherichia coli. Macromolecular events following cellular irradiation were emphasized including the effects of uv or x radiation on the DNA replication cycles in B. subtilis and E. coli; the effects of uv and x radiation on the transmethylation of DNA in E. coli; the effects of B-mercaptoethylamine (MEA) on the frequency of x-radioinduced strand breaks in DNA in solutions; and the comparison of DNA replication patterns in an excision-deficient, uv-sensitive mutant of E. coli and its resistant parent; and the influence of physiological state of bacteria at the time of irradiation on survival. (C.H.)

4457 (UCB-34-P-82-9) ELECTROPHYSIOLOGICAL AND BIOCHEMICAL STUDIES OF THE EFFECTS OF RADIATION ON BRAIN ACTIVITY AND DEVELOPMENT. Progress Report, 1 August 1969–31 July 1970. Timiras, Paola S. (California Univ., Berkeley). Contract AT(04-3)-34. 38p. Dep. CFSTI.

Experiments were conducted on effects of x radiation administered at various stages of development on acetylcholinesterase and choline acetyltransferase activity in the rat brain. Results indicated that quantitative imbalances between cholinergic and noncholinergic elements may be induced by x radiation in CNS structures still developing at the time of radiation, and that additional changes of a qualitative nature may also be induced through the direct effects of x radiation on cholinergic aspects of neurotransmission. Studies on subcellular fractions of the rat brain indicated that neonatal x radiation changes the distribution and the specific activity of choline acetyltransferase in the subcellular fractions of both the cerebral cortex and the cerebellum. Effects of x radiation on free amino acid content of the developing rat brain were studied by whole-body exposure of two-day old rats to 450 R. Results showed an increase of γ-aminobutyric acid and alanine and a decrease in glycine and cystathionine. In vitro studies included effects of x radiation on ^{14}C-uridine incorporation into RNA of chick cerebellum and effects of x radiation on ^{14}C-uridine incorporation into RNA of rat neural tissue. Results indicate that early alterations in basic biochemical processes may underlie the differential response of nervous tissue to x radiation during development. (H.L.W.)

4458 (UCLA-12-782, pp 1-21) BIOCHEMISTRY. (California Univ., Los Angeles. Lab. of Nuclear Medicine and Radiation Biology).

From annual progress report for the period ending June 30, 1970.

Results are reported from studies on: the metabolism of polyunsaturated fatty acids by cultured hepatocytes; the uptake of long chain fatty acids by the brain of adult animals; compo-

sition of lipids of several species of bristlemouth fish, including Cyclothone acclinidens, Cyclothone signata, Danaphos occulatus, and Vinciguerria lucetia; the establishment and characterization of a cultured cell line (RLC) derived from normal rat liver; protein turnover in cultured rat heart cells; the γ radiolysis of fatty acids; and the biosynthesis of unsaturated fatty acids by Bacillus megaterium. (C.H.)

4459 (UCLA-12-782, pp 23-47) RADIOBIOLOGY. (California Univ., Los Angeles. Lab. of Nuclear Medicine and Radiation Biology).

From annual progress report for the period ending June 30, 1970.

Results are reported from studies on: the γ radiolysis of frozen aqueous thymine solutions; the γ radiolysis of DNA nucleosides, and nucleotides in aqueous solutions; the electron spin resonance of radioinduced free radicals in orotic acid; the macromolecular structure of the hen oocytes; the effects of x irradiation of the head of neonatal rats on lipid metabolism and the synthesis of glycerol phosphate dehydrogenase and lactate dehydrogenase in the brain; the effects of several hormones on protein metabolism in brain cells in cultures; and the effect of salt stress (2% NaCl as the only fluid offered) on tumor incidence in rats. (C.H.)

4460 DNA REPLICATION IN RADIATION-INDUCED THYMOMAS OF C57BL MICE. Lagerloef, B.; Takahashi, H. (Karolinska Institute, Stockholm). Acta Cytol.; 14: 6-10(1970).

The replication of DNA during cell cycle in normal thymus and in γ radiation-induced thymomas of C57Bl mice has been studied by Feulgen-microspectrophotometry combined with ^{3}H-thymidine-autoradiography on the same cells. The normal thymocytes have a narrow peak in the diploid region in the Feulgen-DNA-histogram and only few cells in the S- and G2-phases. Autoradiography demonstrates lower rate of DNA synthesis early and late during S-phase than during the midst of the S-phase. All the thymomas show broadening of the diploid peak in the DNA histograms and increased number of cells in S- and G2-phases. In some cells there is evidence of arrest of DNA synthesis during S-phase. The pattern of the histogram of the labeled cells of a highly differentiated thymoma is similar to that of normal thymocytes whereas that of an almost undifferentiated thymoma is shifted to the right, indicating hyperploidy. (auth)

4461 ENZYME INACTIVATION WITH ULTRAVIOLET LASER ENERGY (2650 ANGSTROMS). Berns, Michael W. (Univ. of Michigan, Ann Arbor); Matsui, Sei-ichi; Olson, Robert S.; Rounds, Donald E. Science; 169: 1215-17(18 Sep 1970).

Inactivation of rat heart lactate dehydrogenase was accomplished by irradiation of the enzyme in solution with a frequency quadrupled neodymium glass laser. (auth)

4462 MACROMOLECULAR SYNTHESIS IN IRRADIATED BACTERIA. Setlow, Richard B.; Setlow, Jane K. (Oak Ridge National Lab., Tenn.). Mutat. Res.; 9: 434-6(Apr 1970).

This paper is a critical analysis by Setlow and Setlow of Smith's methodology pertaining to uv radiation effects on DNA synthesis in bacterial cultures. The kinetics of macromolecular synthesis may be measured as incorporation of radioactive precursors, starting with unlabeled or fully labeled cells. The method more desirable depends on the type of information wanted. Smith recommends the use of semi-log paper. There are discrepancies in explanation between Smith and Setlow on the fact that extensive breakdown of DNA occurs in various strains of irradiated Escherichia coli. (P.B.M.)

4463 ENHANCED EFFICIENCY OF EXCISION REPAIR OF NON-REPLICATED UV-DAMAGED E. COLI DNA. Radman, Miroslav; Errera, Maurice (Free Univ., Brussels). Mutat. Res.; 9: 553-60(Jun 1970).

The efficiency of excision repair of uv-damaged Escherichia coli DNA is enhanced when DNA replication is temporarily blocked. This block, in the presence and absence of excision repair, was obtained in a strain of E. coli, thermosensitive for DNA replication and in its excision-deficient derivative. It is suggested that the regulation of DNA synthesis plays an important role in excision repair. (auth)

4464 EFFECT OF DEUTERIUM OXIDE ON THE GIBBERELLIC ACID-INDUCED α-AMYLASE IN GERMINATING BARLEY SEEDS. Bhandarkar, M. K.; Bhattacharya, S.; Gaur, B. K. (Bhabha Atomic Research Centre, Trombay, India). Z. Naturforsch.; 25b: 1066-7(Sep 1970).

During the course of our investigations on the effect of D_2O on the germination of barley, we have observed that the formation of sugars from starch is highly retarded at all the concentrations of D_2O. Although, earlier reports do not indicate any significant retardation of amylase activity by D_2O, subsequent studies on isotope rate ratio for porcine pancreatic α-amylase suggest that D_2O influences the rate of action of this enzyme. It was therefore thought worthwhile to investigate the effect of D_2O on amylase activity in germinating barley seeds variety Himalaya. The modifying influence of gibberellic acid (GA) on α-amylase of normal seeds as well as embryoless seed halves, incubated in various concentrations of D_2O and GA, was also studied. (auth)

4465 EFFECTS OF GAMMA IRRADIATION ON WHEAT GLUTEN. Doguchi, Masao (Tokyo Metropolitan Labs. for Medical Sciences). Tokyo Toritsu Eisei Kenkyusho Nempo; No. 20, 183-7(Jan 1970). (In Japanese).

The effects of γ irradiation on wheat gluten were studied by means of gel filtration on Sephadex G-100, starch gel electrophoresis, and analysis of amino acid composition. Analyses of gluten at a moisture content of 2% revealed no significant change in amino acid composition except for cystine which was decreased by about 8% with irradiation at 10 Mrad. Changes in the chromatogram from gel filtration were interpreted in terms of random depolymerization resulting from irradiation. The results of starch gel electrophoresis suggested that irradiation levels greater than 3 Mrad resulted in characteristic changes in the molecular configuration of gliadin components. (auth) (Japan)

4466 VARIATION IN ASCORBIC ACID CONTENT AND ASCORBATE-OXIDASE ACTIVITY DURING GERMINATION IN DARK OF γ-IRRADIATED CASTOR SEEDS. Thanki, R. J.; Patel, K. C.; Patel, R. D. (Sardar Patel Univ., Vallabh Vidyanagar, India). Indian J. Exp. Biol.; 7: 277-9(Oct 1969).

Irradiated and non-irradiated resting seeds contained no ascorbic acid and ascorbate oxidase (EC 1.10.3.3); these were produced only during germination. Ascorbic acid content was maximum at 5 days of germination while ascorbate oxidase activity was maximum at 7 days of germination. Ascorbic acid content increased with increasing doses of irradiation. Ascorbate oxidase activity was also affected by irradiation. The results suggest that the formation of ascorbic acid is associated with the formation of carbohydrate fragments and not with photosynthesis, and the stimulatory effect on growth is dependent not only on high ascorbic acid content but also on other metabolic products. (auth)

4467 RADIATION SENSITIVITY STUDIES OF PLANT PIGMENTS. I. IN VITRO LABILITY OF β-CAROTENE IN LIPID SOLVENTS. Kumta, U. S.; Sawant, P. L.; Ramakrishnan, T. V. (Bhabha Atomic Research Centre, Trombay, India). Radiat. Bot.; 10: 161-7(Apr 1970).

β-carotene in fat solvents, petroleum ether, and iso-octane is highly susceptible to radiation damage. The colored products formed mask the spectral characteristics of β-carotene retained. A precise value representing 90% destruction of the molecules (D_{10} value) of 0.4 Mrad is obtained for β-carotene remaining untransformed after irradiation as against three different values of 0.54, 0.61, and 0.75 Mrad for the absorbance of the irradiated solutions, respectively at the maxima 480, 450, and 426 mμ. The major cleavage products appear to be colorless since formation of two colored fractions did not account for the degradation of β-carotene. (auth) (UK)

Immunology

Refer also to abstract 4656.

4468 EFFECT OF BURSECTOMY AND THYMECTOMY ON CELLULAR IMMUNOLOGICAL REACTIONS IN CHICKENS. Marvanova, H. (Inst. of Microbiology, Prague). Folia Microbiol. (Prague); 14: 566-70(1969).

The effect of thymectomy plus irradiation and of bursectomy plus irradiation on the rejection of skin grafts and injected homologous spleen cells was studied. Prolonged skin graft survival was found in thymectomized and irradiated chickens. Bursectomy together with irradiation and isolated irradiation did not affect the rejection of these grafts. Surgical operations together with irradiation had no effect on the rejection of an allogeneic cellular graft. In one-day-old recipients, survival of the cells was prolonged in all the birds, while in 12-day-old recipients the cells were rejected at the normal time by both bursectomized and thymectomized birds. The possible explanations of these results are discussed. (auth)

4469 REGENERATION OF PERIPHERAL BLOOD IN THYMECTOMIZED MICE AFTER SUBLETHAL WHOLE-BODY IRRADIATION. Schneiberg, K.; Stiller-Winkler, R.; Jonecko, A. (Inst. of Oncology, Gliwice, Poland). Postepy Hig. Med. Dosw.; 20: 957-73(Nov-Dec 1966). (In Polish).

Thymectomy was carried out in 3-wk-old mice of both sexes of two inbred strains (C57Bl and BA). One month later the animals

were irradiated with a single dose of 500 R of x rays. Mortality was followed for 90 days and peripheral blood was periodically examined. These immature thymectomized mice showed an increased mortality of 67.5% as compared to 31.5% in control animals. Thymectomy in adult animals, however, did not impair resistance to ionizing radiation. In all animals which died, regeneration of granulocytes was low. Among the animals surviving 90 days after irradiation, the thymectomized group exhibited distinct lymphopenia. Thus, the thymus was found to be an important organ of lymphocytopoiesis throughout the whole life of the mouse; moreover, it seems to be indispensable for granulocytopoiesis in the young animal. This role of the thymus disappears later in life. Hematopoietic function of the thymus persists longer in mice born in winter or spring. (BBB)

4470 RADIOSENSITIVITY OF IMMUNE RESPONSES TO 2,2 GeV PROTONS, GAMMA-RADIATION, AND X-RADIATION. Stoner, R. D.; Straub, R. F.; Moore, W. H.; Jesseph, J. E. (Brookhaven National Lab., Upton, N. Y.). Radiat. Eff.; 2: 97-104(Jan 1970).

Mice were exposed to sublethal radiation with either 2.2-BeV protons, γ radiation or x radiation to compare radioinduced repression of primary and secondary antibody responses and radiation-enhanced susceptibility to fatal anaphylactic shock. Five animals at a time were exposed in tandem in a 2.5-cm ID Lucite tube to a parallel beam of protons from the Cosmotron. A comparison of doses required to produce 50% repression of normal primary tetanus antitoxin responses indicates that exposure to $1.15 \times 10^9/cm^2$ protons (38 rads) is as effective in repressing primary responses as 100 rads of γ radiation and x radiation. Proton doses of the order of $5 \times 10^9/cm^2$ (165 rads) and 300 rads of γ radiation and x radiation were needed to repress secondary antibody responses by 50% of normal. An average RBE of 2.5 (S.D., 0.58) was obtained for primary responses, whereas an average RBE of 1.5 (S.D., 0.22) was found for secondary responses. Exposure to $4 \times 10^9/cm^2$ protons (132 rads) and 350 rads of γ radiation resulted in a similar degree of radiation-enhanced susceptibility to fatal anaphylaxis with an RBE of 1.5. (auth)

4471 EFFECTS OF ESTRADIOL ON SPLENIC REPOPULATION BY ENDOGENOUS AND EXOGENOUS HEMOPOIETIC CELLS IN IRRADIATED MICE. Jenkins, V. K.; Upton, A. C.; Odell, T. T. Jr. (Oak Ridge National Lab., Tenn.). J. Cell. Physiol., 73: 149-58(Apr. 1969).

The effect of estradiol on hemopoietic cell growth and differentiation was assessed, and the hypothesis examined that inhibition of myelopoiesis may account in part for the inhibitory effects of estrogen on the development of granulocytic leukemia in RF mice. Eight-week-old RFM/Un mice were x-irradiated in a single, whole body dose of 350 to 550 R and their spleens harvested 6 to 9 days later. To study the growth and differentiation of transplanted hemopoietic stem cells, mice were exposed to 750 R, injected intravenously with syngeneic bone marrow cells, and their spleens examined 6 to 9 days later. Estradiol treatment of irradiated mice during repopulation of their spleens by endogenous hemopoietic cells reduced the number of myelocytic colonies and increased the numbers of erythropoietic and undifferentiated colonies. The inhibitory effects of the hormone on myelopoiesis were not dependent on stimulation of erythropoiesis, since they occurred in the absence of erythropoiesis in mice made polycythemic by hypertransfusion. Treatment of bone marrow donors with estradiol reduced the ability of their marrow cells to form spleen colonies, particularly myelopoietic colonies relative to the total number of all types. Conversely, erythropoietic colonies, though reduced in absolute number, were increased in relative number. Such treatment also decreased the volume and cell content of the marrow cavity through stimulation of endosteal bone formation. Estradiol treatment of lethally irradiated recipient mice did not detectably alter the total numbers or types of hemopoietic spleen colonies formed in these animals from transplanted marrow cells. The sex of the donor or recipient mouse did not affect the numbers or types of colonies formed. (BBB)

4472 STUDY OF THE DYNAMICS OF AUTOIMMUNE PROCESSES BY MEANS OF DETECTING PLAQUE FORMING CELLS. Klemparskaya, N. N. (Inst. of Biophysics, Moscow). Zh. Mikrobiol., Epidemiol. Immunobiol.; 46: 18-20(Aug 1969). (In Russian).

Detection of cells that produce autoantibodies in the peripheral blood is important for clinical diagnosis of autoimmune diseases. Caningham's method of free suspension was applied in experiments on dogs and mice. Following ^{60}Co γ irradiation, there was an increase in the number of autoantibody-forming cells in the spleen and the peripheral blood from 3 to 15 days later in mice and from 16 to 29 days later in dogs. There is a possibility that this method can be applied to the study of spleen cells that form hemolysins with sheep erythrocytes 3 to 9 days after immunization. (E.E.H.)

Ecology

Refer also to abstracts 4435, 4436, 4503, 4504, and 4711.

4473 (AECL-3687) RADIUM-226 CONTENT OF WATER AND PLANKTON FROM THE CHALK RIVER AREA. Havlik, B. (Atomic Energy of Canada Ltd., Chalk River (Ontario). Chalk River Nuclear Labs.). Aug 1970. 29p. Dep. NTIS (U. S. Sales Only). AECL $1.00.

The ^{226}Ra content of water and plankton of four lakes, the Ottawa River, and well water was measured from March 1969 until February 1970. The twelve localities are within the Chalk River Nuclear Laboratories area and samples were taken at monthly intervals. The results of all 480 analyses of water ranged from <0.1 to 6.2 pCi per liter. The lake plankton had radium levels from 0.1 to 11.1 pCi per gram of dry weight, with a mean value of 1.9 pCi/g. This radium concentration corresponds to the natural background level. (auth)

4474 (BNWL-1515) FALL CHINOOK SALMON SPAWNING IN THE COLUMBIA RIVER NEAR HANFORD, 1947-1969. Watson, D. G. (Battelle-Northwest, Richland, Wash. Pacific Northwest Lab.). Oct 1970. Contract AT(45-1)-1830. 47p. Dep. NTIS.

There was no evident relationship between the operation of the Hanford reactors and the numbers of fish spawning in the Hanford reach of the river. Recent increases in numbers of fall chinook spawners seemed more closely associated with the construction of dams downstream and immediately upstream from Hanford, and the probable displacement of fish from these areas. Water temperatures were less than 15°C during the peak of spawning, well within the upper tolerance limits for this species. (auth)

4475 (NYO-3554-8) EFFECTS OF RADIATION ON MIGRATORY ORIENTATION OF SALAMANDERS. Final Report. Shoop, C. Robert [Wellesley Coll., Mass. Dept. of Biological Sciences]. [1970]. Contract AT(30-1)-3554. 17p. Dep. NTIS.

Effects of radiation on migratory salamanders, Ambystoma maculatum, were studied in two areas. Fifty-two adult salamanders were x-irradiated in doses up to 500 R. Controls were handled in the same way but not irradiated. It was found that fewer irradiated animals returned to the breeding pond, and breeding activities were stopped by irradiation. Laboratory studies were conducted on effects of x radiation on juveniles and adults of Ambystoma maculatum. Survival of juveniles given doses up to 600 R was significantly greater than that of adults given the same dose. The roles of secondary infection and environmental conditions following irradiation are discussed. The amphibian species, Rana catesbeiana, R. clamitans, Bufo woodhousei, B. americanus, Scaphiopus bombifrons, and Plethodon cinereus were x-irradiated and correlations of survival with DNA per liver cell were studied. The most radioresistant species were those known to have the lowest DNA values and the shortest larval periods. Ecological implications of results are discussed. The role of environmental factors in survival of eggs and larvae of salamanders is discussed. Adult Ambystoma maculatum were tagged with ^{182}Ta for studies on breeding migrations. (H.L.W.)

4476 (RISO-221) ENVIRONMENTAL RADIOACTIVITY IN THE FAROES IN 1969. Aarkrog, A.; Lippert, J. (Danish Atomic Energy Commission, Risoe. Research Establishment). Jul 1970. 22p. Dep. NTIS (U. S. Sales Only).

Measurements of fallout radioactivity in the Faroes in 1969 are presented. Strontium-90 (and ^{137}Cs in most instances) was determined in regularly collected samples of precipitation, grass, milk, lamb, fish, bread, and drinking water. In addition, analyses of spot samples of potatoes, sea water, sea plants, birds, vegetables, eggs, and human bone were carried out. Estimates of the mean contents of ^{90}Sr and ^{137}Cs in human diet in the Faroes in 1969 are given. (auth) (Denmark)

4477 (UCLA-12-782, pp 49-81) ENVIRONMENTAL RADIATION. (California Univ., Los Angeles. Lab. of Nuclear Medicine and Radiation Biology).

From annual progress report for the period ending June 30, 1970.

Research on a natural desert community exposed to continuous low-dose γ radiation during the past six-year period was continued. Radioinduced changes in the function and composition of the ecosystem were observed. Heteromyid rodents continued to reproduce but the life span of pocket mice (Perognatus formosus) was found to be decreased slightly. Leopard lizards (Crotaphytus wislizendii)

and whiptail lizards (Cnedidophorus tigris) appear to be disappearing because of radioinduced female sterility. It was concluded that the life span is an extremely important factor in determining the response of animals to sublethal, chronic irradiation. Seed production by the gymnosperm Ephedra nevadensis was drastically reduced. Changes in desert vegetation in three areas of the Nevada Test Site damaged by fallout from Plowshare excavation tests are reported. Mixed grasses (Sitanion hystrix, Oryzopsis hymenoides, and Poa nevadensis) account for much of the revegetation of the areas. The original cover was predominantly Artemisia tridentata and in some areas Artemisia seedlings have become established at densities varying from 10 to 20 percent of the original shrub population. Shrubs in the area that were protected from fallout by plastic covers survived without damage. This indicated that fallout damage to vegetation is primarily caused by β irradiation from fallout debris deposited onto plant foliage. Data are included from a number of related studies including: the effects of nutrient phosphorus levels on growth and mineral content of Franseria dumosa plants; the effects of soil moisture content and temperature on the uptake of soil water by Russian thistle (Salsola kali) plants; the effects of root temperatures and availability of Ca and nitrate on the uptake of ^{137}Cs, ^{22}Na, and ^{86}Rb by bush bean (Phaseolus vulgaris) plants; the propagation of various desert shrubs (17 varieties) by seeds and (14 varieties) by rooted cuttings; the influence of the photosynthetic pathway (C_4-dicarboxylic acid or Calvin cycle) on the growth of 14 xerophytic species of desert plants; the physiological characteristics of the creosote bush (Larrea divaricata), a common desert shrub that often reaches an age of over 100 years; the associative distribution of animals and plants in desert ecosystems; the chemical and physical properties and nutrient content of desert soils at the Nevada Test Site; the response of desert plants to supplementary irrigation and fertilization; and a tracer study on the effects of ammonium nitrate fertilization on the uptake of ^{90}Sr by tomato plants grown in four soils having different amounts of free $CaCO_3$ or Ca. (C.H.)

4478 PERSISTENCE OF PLUTONIUM IN SOIL, PLANTS, AND SMALL MAMMALS. Romney, E. M.; Mork, H. M.; Larson, K. H. (Univ. of California, Los Angeles). Health, Phys.; 19: 487-91(Oct 1970).

Periodic surveys during a 10-yr period were made of the persistence of residual ^{239}Pu in soil, plants, and small mammals indigenous to fallout areas contaminated with ^{239}Pu dispersed by high-explosive detonations. Downward migration of fallout particles occurred in undisturbed soil profiles, and wind and water erosion accounted for some redistribution of the initial ^{239}Pu contamination. Long-term cropping experiments showed a relatively low degree of ^{239}Pu transfer from soil to plants, but there was a consistent increase in its accumulation in plant tissue during a 5-yr cropping sequence. Plant uptake of ^{239}Pu from soil was enhanced by DTPA chelating agent. Qualitative trends from these surveys indicate that the accumulation of residual ^{239}Pu in kangaroo rats and jackrabbits was highest in bone tissue; considerable amounts also were found in lung tissue. Inhalation is known to be the major pathway for plutonium deposition in lung and bone, but the high levels found in the gastrointestinal tracts indicate that ingestion is also an important route through which these small mammals maintained contact with the residual ^{239}Pu contamination in the environment. (auth) (UK)

4479 SOME EFFECTS OF NUCLEAR DETONATIONS ON AQUATIC ECOSYSTEMS. Harrison, Florence L. (Univ. of California, Livermore). Trans. Amer. Nucl. Soc.; 13: 641-2 (Nov 1970).

From Meeting of the American Nuclear Society, Washington, D. C. See CONF-701102.

Genetics and Cytogenetics

Refer also to abstracts 4524, 4604, 4717, and 4724.

4480 COMMON STEPS IN THE REPAIR OF ALKYLATION AND RADIATION DAMAGE IN YEAST. Brendel, M.; Khan, N. A.; Haynes, R. H. (York Univ., Toronto). Mol. Gen. Genet.; 106: 289-95(1970).

Radiation sensitive mutants of Saccharomyces cerevisiae were exposed to the action of nitrogen mustard (HN2) and methyl methanesulfonate (MMS). Sensitivity of HN2 was found to be correlated with sensitivity to ultraviolet light, whereas sensitivity to MMS was found to be correlated with sensitivity to x-rays. One mutant strain that is sensitive to both uv and x rays was found to be sensitive also to HN2 and MMS. The latter result shows that there exists a locus in yeast that controls the repair of DNA damaged by all four of these mutagens. (auth)

4481 COMPARISON OF THE BROOD PATTERN OF CROSSOVERS IN DROSOPHILA MALES INDUCED BY THREE METHYLNITROSOCOMPOUNDS AND RADIATION. Ondrej, M. (Inst. of Experimental Botany, Prague). Folia Biol. (Prague); 16: 225-9(1970).

The frequencies of crossovers in Drosophila males heterozygous for second chromosome loci dp b cn bw were tested after treatment with methylnitrosourethane, dimethylnitrosoamine, N-methyl-nitrosopiperazine and x-radiation. While the first two compounds were administered only by injections, N-methylnitrosopiperazine was sometimes applied in the food, and this way appeared to be much more effective. Meiotic and premeiotic cells were sampled in two-day broods. Radiation-induced crossovers appeared starting from the brood V, i.e., 9th–10th day after treatment. Methylnitrosourethane induced few crossovers, which were distributed almost equally over all six broods scored. Dimethylnitrosoamine and N-methylnitrosopiperazine induced low numbers of crossovers found entirely in the seventh and eighth brood. While 45% of crossovers after irradiation occurred in clusters of identical and complementary crossovers in the offspring of single males, no clusters were found after methylnitrosocompounds. On the basis of the results with radiation, VII and VIII broods should correspond to sampling of treated spermatogonia. The most probable interpretation of the results with methylnitrosocompounds is conditioned crossing over, i.e., induction of weak points on the chromosomes in spermatogonia, which are likely to lead to crossing over in spermatocytes. A great delay in sampling spermatocytes due to the toxicity of the compound used, and induction of crossovers only in spermatocytes is an alternative explanation. (auth)

4482 PRESENT STATE OF MUTATION BREEDING. Report of International Symposium, Mito, Japan, August 15–17, 1968. Gamma Field Symp.; No. 7, 1-136(1968). (CONF-680824).

Separate abstracts were prepared for the eight papers published in the report. Three oral presentations on the use of induced mutations for the improvement of plants were given but not included in the published report. (H.L.W.)

For abstracts of individual papers see: 4483–4489 and 4604.

4483 RADIATION-INDUCED INTERNAL DISBUDDING AS A TOOL FOR ENLARGING MUTATION SECTORS. Yamakawa, Kunio; Sekiguchi, Fumihiko (Inst. of Radiation Breeding, Ibaraki, Japan. Utsunomiya Univ., Japan). Gamma Field Symp.; No. 7, 19-39(1968).

From 7th Symposium on Gamma Field, Mito, Japan. See CONF-680824.

Total exposures of 0.5 to 60 kR γ radiation were administered to Antirrhinum majus plants for studies on meristem damage and somatic mutations. A decreasing order of radiosensitivity in three types of buds was found as follows: floret primordia, flower stem apex, and lateral shoot apex. It was found that at doses of 30 KR, 98% of total mutations were entire shoot mutations. High exposure rates administered over a short period were more efficient in producing large petal-color mutation sectors than low exposure rates given over a long period of time. Tomato seedlings were used for studies on internal disbudding by sublethal γ exposure. The size of mutation sectors in regenerated shoots was estimated by scoring recessive mutants in the next generation after radioinduced internal disbudding. A total of 25 mutants were found consisting of inviable chlorophyll mutants, viable chlorophyll mutants, and male sterile mutants. (H.L.W.)

4484 INDUCED VARIABILITY IN DIPLOID AND POLYPLOID AVENA SP. Frey, Kenneth J. (Iowa State Univ., Ames). Gamma Field Symp.; No. 7, 41-56(1968).

From 7th Symposium on Gamma Field, Mito, Japan. See CONF-680824.

A review of the literature on mutation induction in oats is presented. The cultivated species of oats, Avena sativa and Avena byzantina, are hexaploid, highly fertile and autogamous. At meiosis, chromosome pairing is preferential and highly regular. All hexaploid species of Avena can be intercrossed readily and the hybrids are fertile. Because there appeared to be limited sources of variability within and among hexaploid oat species, mutation breeding seemed to be a natural method for expanding the available spectrum of genetic variability available to plant breeders. Investigation of mutation breeding for cultivated oats began about 25 years ago. Many promising strains of oats were derived via direct selection in mutagen-derived programs, and two varieties, Florad and Alamo-X, are putative products of mutation breeding. It appears that with oats, the mean for a quantitatively inherited trait may or may not be shifted by mutagen treatment, and the shift, if it does occur, is unpredictable. The variability induced by mutagen treatment of oat seeds has proven

XUM

to be as heritable as that derived from hybridization, and it has been used successfully in hybridization schemes such as recurrent selection. By mutagen treating of hybrid seeds it is possible to compound the variabilities from hybridization and mutagenesis, but in most cases these two sources have been something less than additive. Likewise, the variability induced by repeated mutagen treatment of successive generations tends to diminish with successive treatments. This diminution can be alleviated somewhat by using different mutagens for the successive treatments. (auth)

4485 MUTATION STUDIES INVOLVING QUANTITATIVE TRAITS. Gardner, C. O. (Univ. of Nebraska, Lincoln). Gamma Field Symp.; No. 7, 57-77(1968). (COO-1512-11).

From 7th Symposium on Gamma Field, Mito, Japan. See CONF-680824.

Genetic variability studies on populations of corn and soybeans are reviewed. Little evidence of useful genetic variation in corn was found after treatment with thermal neutrons. Studies on effects of radiation, recombination, and selection on populations of corn developed from a single cross are discussed. A table is presented to show effects of thermal neutrons on six agronomic traits in four populations of corn. Grain yield components indicated that the thermal neutron treatment substantially increased additive genetic variance. Studies on effects of thermal neutrons on corn in a mass selection program showed that irradiation reduced yield drastically but selection quickly eliminated undesirable genotypes and rapid progress was made after the irradiation was discontinued. Experiments on x-ray selected populations show increased prolificacy. (H.L.W.)

4486 ADAPTABILITY OF MUTANT IN MULBERRY TREE. Hazama, Kazuo (Sericultural Experiment Station, Tokyo). Gamma Field Symp.; No. 7, 79-85(1968).

From 7th Symposium on Gamma Field, Mito, Japan. See CONF-680824.

In 1959 mulberry saplings were γ-irradiated with doses of 5, 7.5, and 10 kR; they were then planted and mutations of leaf characteristics were observed. Methods of selection of mutants for agricultural improvement of plants are described. The tabulated results show that the leaf yield of the mutant strain was about 12% more than the original and that the mutant strain was more susceptible to dwarf disease. The use of mutants for improving the commercial value of plants is discussed. (H.L.W.)

4487 BREEDING OF A NEW RICE VARIETY REIMEI BY GAMMA-RAY IRRADIATION. Futsuhara, Yuzo (Nagoya Univ., Japan). Gamma Field Symp.; No. 7, 87-109(1968).

From 7th Symposium on Gamma Field, Mito, Japan. See CONF-680824.

Dry dormant seeds of a rice variety, Fujiminori were exposed to 20 kR and 30 kR of gamma-rays, with the aim of breeding of short-culm variety with lodging resistance. In X_2, 46 plants were selected from 1467 ear progenies, approximately 50,000 plants, on the basis of short-culm length. From the results of the yield test which was started in X_3, two promising lines, Fukei No. 70 and Fukei No. 71 were selected in X_5. Fukei No. 70, released as Reimei, was similar to the original variety in all characteristics except culm length reduced by about 15 cm and showed the high yielding ability because of its improved lodging resistance. It was widely adaptable in all the districts where Fujiminori has been cultivated. Another line, Fukei No. 71, with extreme straw stiffness, showed a decrease of 46% in culm length and thereby the lodging resistance was extremely increased. (auth)

4488 MUTATION BREEDING OF PLANTS IN ITALY. Scarascia-Mugnozza, G. T. (CNEN, Rome). Gamma Field Symp.; No. 7, 111-21(1968).

From 7th Symposium on Gamma Field, Mito, Japan. See CONF-680824.

A review is presented of mutations induced in various agricultural plants by radiation and chemical mutagens. The use of mutations for improvements in plant breeding is discussed. Experiments on mutagenic effects of thermal neutrons on four varieties of tobacco are described. An analysis was made of mutations in plant height and leaf characteristics. A review of mutations in peas induced by x rays and chemical mutagens for improved agricultural characteristics is presented. Radioinduced mutations in Vicia for improved forage are discussed. Effects of mutagens and radiation on cytogenetics and breeding characteristics of wheat were studied; an increased yield was obtained in mutant varieties. Genetic variability in quantitative characters was obtained following x irradiation of seeds of Triticum durum and T. aestivum. The use of induced mutations for improvement of gourds, squash, pumpkins, artichokes, fruit trees, and flowers is discussed. (H.L.W.)

4489 PRESENT STATE OF MUTATION BREEDING IN USSR. Khvostova, V. V. (Inst. of Cytology and Genetics, Novosibirsk, USSR). Gamma Field Symp.; No. 7, 123-36(1968).

From 7th Symposium on Gamma Field, Mito, Japan. See CONF-680824.

A review of the literature on mutation breeding in the USSR is presented. Studies on sensitivity of corn and peas to fast neutrons and γ radiation are discussed. Studies on the mechanism of radiation effects indicated that chromosome damage was caused by the direct action of ionizing radiations and not by the action of free radicals. Other studies on pea seeds treated with x rays indicated a relationship between the quantity of free radicals and the degree of chromosome damage. A review of studies on chemical mutagenesis is presented with emphasis on the effects of ethylenimine on Drosophila melanogaster and Crepis capillaris. Studies on effectiveness, efficiency, and specificity of mutagenic action showed that chemical mutagens were more effective than ionizing radiation. A table is presented to show mutation rate in seven pea varieties after seed treatment with γ radiation, EMS, and NEM. Experimental results of studies on hybridization of mutants in various agricultural plants are reported. (H.L.W.)

4490 EFFECT OF GIBBERELLIC ACID ON GAMMA IRRADIATED BARLEY SEEDS. Kumar, Sudhir (Udaipur Univ., India). Indian J. Genet. Plant Breed.; 27: 154-6(1967).

Treatment of irradiated seeds for 1 hr with 1,000 ppM gibberellic acid reversed the injurious effect of gamma radiation on barley seedlings and of induced chromosome aberration. (Indian Sci. Abstr.)

4491 CHROMOSOMAL DAMAGES IN CIRCULATING LYMPHOCYTES INDUCED BY THERAPEUTIC IRRADIATION. Matsubara, Sho (Tokyo Medical and Dental Univ.). Bull. Tokyo Med. Dent. Univ.; 16: 261-88(Dec 1969).

The dose-response relationship of the chromosomal damage to the blood lymphocytes was obtained from the in vitro experiment, and an attempt of its use was made to evaluate possible clinical meanings of the chromosomal damages to the lymphocytes in patients given radiation therapy for malignant diseases. In the patients given single dose of gamma ray exposure, the chromosome analysis of the circulating lymphocytes showed that the production of chromosome aberrations in the irradiated region was grossly analogous to that of the in vitro exposure and that the overall frequency of the chromosome aberrations was determined by the irradiated volume, body weight, and radiation dose. After repeated doses of therapeutic radiation, it was found that the irradiated volume, body weight, and radiation dose were also among the important factors influencing the level of chromosome aberrations in the circulating lymphocytes. From the data obtained, other factors such as loss of lymphocytes due to death and recovery of the lymphocyte system were shown to play an important part in the determination of the level of chromosome aberrations in the blood lymphocytes, especially in the long-term fractionated radiation therapy. (auth) (Japan)

4492 EFFECT OF FRACTIONATED X IRRADIATION ON THE ROOT-TIP CELLS. Paribok, V. P.; Krupnova, G. F. (Inst. of Cytology, Leningrad). Tsitologiya; 12: 525-33(Apr 1970). (In Russian).

Additional x radiation with 400 R of the root-tip cells of Vicia faba previously (90 min before) irradiated with 100, 200, and 300 R produced fewer chromosome aberrations than in the case of non-irradiated cells. This decrease of two-hit aberrations may partly be due to some alterations in the chromosomal sensitivity caused by the irradiation. This phenomenon is used for the explanation of the decrease of the yield exchanges below the base line. (auth)

4493 ASSOCIATION OF THE MARKED CHROMOSOMES OF THE MONKEY (MACACA MULATTA) IN NORMAL AND IRRADIATED CULTURES OF PERIPHERAL BLOOD LEUCOCYTES. Dzhemilev, Z. A. (Inst. of Experimental Pathology and Therapy, Sukhumi, USSR). Tsitologiya; 12: 534-8(Apr 1970). (In Russian).

Associations of marked chromosomes were investigated in cultures of the monkey peripheral blood leukocytes. The monkeys ranged in age from 8 to 11 years. The cultures were irradiated by x rays (100 R) at various stages of the cell cycle. The data obtained showed that the number of cells with associations of marked chromosomes was 7.2% in control cultures; 50.4% in the cells irradiated at the G_0; 33.9% at the G_1; 24.2% at the S; 6.9% at the G_2. Thus the frequency of metaphases with associations of marked chromosomes depends on the stage of mitotic cycle at which the cells were irradiated. (auth)

4494 ULTRAVIOLET-MICROSCOPICAL STUDIES ON ACHROMATIC LESIONS (GAPS) INDUCED BY X-RAYS IN THE CHROMOSOMES OF VICIA FABA. Scheid, W.; Traut, H. (Univ., Muenster, Ger.). Mutat. Res.; 10: 159-61(Aug 1970).

The nature of achromatic lesions or gaps was investigated in x-irradiated chromosomes of Vicia faba. Gaps are induced mostly in late interphase. Feulgen technique was used to observe the gaps. Some gaps photographed at 265 nm reveal two parallel strands that cannot be seen in gaps visualized by the Feulgen technique. A comparison between the two-strand gaps and Feulgen stained chromosomes of Vicia faba revealed certain similarity. It is suggested that the structures observed are identical. (P.B.M.)

4495 INDUCED SYSTEMATIC MUTATIONS IN SORGHUM. Sree Ramulu, K. (Agricultural Coll. and Research Inst., Coimbatore, India). Mutat. Res.; 10: 77-80(Jul 1970).

The validity of classifications of Sorghum by systematic mutations is discussed. Seeds of three cultivated varieties of Sorghum subglabrascens and S. durra were subjected to treatment with γ rays and the chemical mutagens, diethylsulfate (DES), ethyl methane sulfonate (EMS), methyl methane sulfonate (MMS), N-nitrosoethylurea (NEU), and N-nitrosomethylurea (NMU). Gamma radiation was given from a 3500 Ci ^{60}Co source at an exposure rate of 3200 R/min. For the treatments with EMS, MMS, and DES, the required concentrations were freshly prepared in phosphate buffer pH 7 at 27°C, while NEU and NMU were prepared in water. The seeds, presoaked in water for 4 hr, were treated with the chemicals for 8 hr. The different types of systematic mutations include those with wrinkled glumes, awnless, and awned. (P.B.M.)

4496 FORMATION OF INCOMPLETE TRANSLOCATIONS IN ROOT MERISTEMS OF CREPIS CAPILLARIS AFTER X IRRADIATION DURING POSTSYNTHETIC PHASE OF THE MITOTIC CYCLE. Generalova, M. V. (Inst. of Developmental Biology, Moscow). Genetika; 6: No. 6, 70-4(Jun 1970). (In Russian).

This study was performed in order to establish the presence of x-radioinduced chromatid translocations of incomplete type at the early fixation time. The comparative analysis of the non-union frequency in the translocations 2 and 4 hours after irradiation (2nd metaphase) as well as 10 and 13 hours after irradiation (4th metaphase) was carried out. The coincidence of the incomplete translocation frequencies in the diploid and tetraploid cells was observed. The prolonged process of formation of aberrations is postulated. (auth)

4497 INVESTIGATION OF VICIA FABA SEEDLING CHROMOSOME DAMAGES BY SPLIT-DOSE METHOD IN THE G_2-STAGE OF THE CELL CYCLE. Aptikaeva, G. F.; Bregadze, I. F.; Ganassi, E. E.; Suikova, L. A.; Eidus, L. Kh. (Inst. of Biological Physics, Puschino, USSR). Genetika; 6: No. 6, 42-7(Jun 1970). (In Russian).

Appearance of chromatid aberrations produced by fractional doses of x rays in cells of Vicia faba lateral roots in the G_2 stage was studied. First, the constancy of radiosensitivity within the interval of fractionation (by fixation from 4 to 9 hours after irradiation) was established. Analysis of chromatid aberrations during anaphase and of exchanges during metaphase showed that the yield was proportional to the dose over the range from 50 to 100 R. Split dose affected neither general yield of chromatid aberrations nor yield of two hit aberrations. These results are indicative for the absence both of the reparation in the G_2 stage and the increase of radioresistance after the first dose to the second fraction of dose. (auth)

4498 CHROMOSOME DAMAGES INDUCED BY VARIOUS γ-RAY DOSES IN DORMANT SEEDS OF CREPIS CAPILLARIS. Kraevoi, S. Ya.; Khalikov, P. Kh.; Nemtseva, L. S.; Romanov, V. P. (Inst. of General Genetics, Moscow). Genetika; 6: No. 6, 59-69(Jun 1970). (In Russian).

The structural changes induced by various doses of ^{137}Cs γ-rays in dormant seeds of Crepis capillaris at moisture content ~3.5% were studied. It was found that the relation between dosage and chromosomal aberrations does not conform with the classical idea on formation of chromosomal breaks and aberrations. (auth)

4499 INFLUENCE OF POLLEN RADIATION ON CROSSING ABILITY AND VARIABILITY IN COTTON. Egamberdiev, A.; Abdullaev, T.; Mukhamedzhanova, D.; Tokhriya, N. (Inst. of Experimental Biology of Plants, Tashkent). Uzb. Biol. Zh.; No. 6, 48-50(1969). (In Russian).

The pollen radiation effects on infructescence and mature cotton seeds of 108-F variety are described. There is no correlation between vitality and fertilization ability in pollen. It was established that radiation affects the variability of characters in M_1 plants. (auth)

4500 CYTOGENETIC EFFECTS OF LOW DOSES OF IONIZING RADIATIONS ON HUMAN CELLS: THE FINDINGS AND THEIR IMPLICATIONS. Bloom, Arthur D. (Univ. of Michigan, Ann Arbor). Trans. Amer. Nucl. Soc.; 13: 515(Nov 1970).

From Meeting of the American Nuclear Society, Washington, D. C. See CONF-701102.

4501 GENETIC EFFECTS OF LOW-LEVEL RADIATION. Russell, W. L. (Oak Ridge National Lab., Tenn.). Trans. Amer. Nucl. Soc.; 13: 515(Nov 1970).

From Meeting of the American Nuclear Society, Washington, D. C. See CONF-701102.

4502 GENETIC AND BIOLOGICAL EFFECTS OF LOW-LEVEL RADIATION: CARCINOGENESIS. Upton, Arthur C. (State Univ. of New York, Stony Brook). Trans. Amer. Nucl. Soc.; 13: 516(Nov 1970).

From Meeting of the American Nuclear Society, Washington, D. C. See CONF-701102.

Health Physics and Safety

Radioactive Contamination and Decontamination

Refer also to abstracts 4165, 4172, 4181, 4473, 4476, and 4478.

4503 (BNL-50196) 1966 ENVIRONMENTAL MONITORING RADIATION LEVELS AT BROOKHAVEN NATIONAL LABORATORY. Hull, A. P.; Gilmartin, J. T. (Brookhaven National Lab., Upton, N. Y.). Sep 1969. 32p. Dep. CFSTI.

Data obtained during routine environmental monitoring in the vicinity of Brookhaven National Laboratory during 1969 are summarized. The data show that radiation levels attributable to laboratory operations were well below the established radiation protection standards of the AEC for external exposures and for concentrations of radioactivity in air and water. (C.H.)

4504 (BNWL-1472) TEMPERATURE, TIMING, AND SEAWARD MIGRATION OF JUVENILE CHINOOK SALMON FROM THE CENTRAL COLUMBIA RIVER. Becker, C. D. (Battelle-Northwest, Richland, Wash. Pacific Northwest Lab.). Jul 1970. Contract AT(45-1)-1830. 22p. Dep. NTIS.

A sizeable population of adult chinook salmon now spawns each fall in the free-flowing Hanford environs of the central Columbia River. This population has acquired significance because other vital spawning areas in the mainstem Columbia have been inundated by hydroelectric development. Studies conducted in 1969 show that the progeny of the Hanford population migrates seaward from April to July in the ancient pattern that correlates with favorable water temperatures and high discharge volumes. In contrast, the passage of juvenile chinooks that now issue from upriver reaches is known to be delayed until July and August when temperatures and discharge volumes are less favorable. Temperatures in the central Columbia are modified by discharges of heated effluent from plutonium production reactors at Hanford, in addition to largely seasonal changes in river flow, cooling or warming by the upriver reservoir complex, and summer heat input from the atmosphere. In 1968 and 1969, mean weekly water temperatures peaked in late July, August and early September with maximum daily temperatures briefly reaching 19.1 and 19.7°C, respectively, at Priest Rapids and 19.7 and 20.6°C at Richland. (auth)

4505 (CONF-691051--, pp 324-35) ^{90}Sr AND INFANT MORTALITY. Rotblat, J.; Lindop, Patricia J.

From World security, disarmament and development.

A discussion is presented of the probable risks of genetic and somatic damage from nuclear tests. The validity of the claims made by Sternglass concerning effects of ^{90}Sr on infant mortality is examined. The assumption that the increased infant mortality after 1950 is caused by a genetic effect of ^{90}Sr from nuclear weapons tests is criticized. It is concluded from the analysis of evidence of Sternglass that there is no justification for linking infant mortality with strontium fallout. (H.L.W.)

Dosimetry and Monitoring

Refer also to abstracts 4040, 4088, 4377, 4378, 4395, 4425, 4432, and 4657.

4506 (AD-703266) FALLOUT COMPUTATIONAL TECHNIQUES. Final Report. Lofton, D. B.; Ellis, C. F.; Wasson, T. L.; Wegner, K. E.; Wendland, D. E. (Data Dynamics, Inc., Los Angeles, Calif.). 17 Jun 1969. Contract N00228-68-C-2750. 180p. (DDI-16-100-1). CFSTI.

The investigation of fallout computational techniques has resulted in several improved computer programs. These programs were written in FORTRAN for the CDC 6600 and UNIVAC 1108 computers. A program was developed to compute the β radiation

dosage at a specified depth below the surface of the skin due to multiple fallout particles. Programs were prepared to plot dynamic dose rate contours for fallout from multiple nuclear bursts at up to fifty input values of time. In addition, programs were developed to plot peak dose rate contours and contours of the time at which the peak dose occurs. A study was made of methods of analytically combining fallout field measurements. A program was developed to fit a least-squares polynomial surface to a set of intensity measurements. (auth)

4507 (EUR-4506) DOSIMETRY IN MICROBIOLOGY. Final Report. (Gesellschaft fuer Strahlenforschung m.b.H., Munich (West Germany)). 9 Jul 1969. 54p. (In German). Dep. NTIS (U. S. Sales Only). EUR DM 5,10.

Methods were developed for the use of dosimetry in microbiology. In particular, they concern the development and testing of an irradiation plant, the development of suitable methods of measurement to ascertain the radiation energy absorbed in the medium in microbiological subjects and the development of a simple method for determining radiation quality for use in microbiology. (auth)

4508 (KURRI-TR-63) LOG OF THE RADIATION CONTROL PROGRAM AT THE RESEARCH REACTOR INSTITUTE OF KYOTO UNIVERSITY, 1968. Katsuraya, Yukimari (Kyoto Univ. (Japan). Research Reactor Inst.). 1969. 22p. (In Japanese). Dep. NTIS (U. S. Sales Only).

The records kept for the radiation control program at the Research Reactor Institute of Kyoto University during the year January through December 1968 are discussed. In this fourth annual report it is mentioned that during the past year, the power level of the reactor was increased to 5 MW, making it necessary to provide additional supervisory personnel and to broaden the control measures. The radiation levels encountered at the reactor room, hot laboratory, waste disposal building, and tracer laboratory are given, including also data on the monitoring of the waste water, surface contaminations found in various laboratories, water in the reactor loop, and monitoring of the exhaust gas and dust. Some of the newly introduced and installed monitoring equipment and its corrections are described. (TTT)

4509 (MDC-G-363) STATISTICAL ANALYSIS OF SOLAR COSMIC RAY PROTON DOSE. Yucker, W. R. (McDonnell Douglas Astronautics Co.-West, Huntington Beach, Calif.). Jun 1970. 66p.

The results of a statistical analysis of the radiation hazard to astronauts owing to solar cosmic ray protons are described. While several similar studies were conducted in the past, some objections to the use of this approach to determining shielding requirements were raised owing to the limited number of solar proton events for which data are available. More recent data are incorporated into the present analysis, including events from 1956 to 1969, in order to improve the accuracy of the predicted mission fluence and dose. Also, an attempt is made to present a unified and consistent view of the solar cosmic ray proton hazard and to justify the application of a statistical approach for mission planning purposes. Mission fluence and dose versus shield thickness data are presented for mission lengths up to 3 years during periods of maximum and minimum solar activity, and corresponding to various levels of confidence that the predicted hazard will not be exceeded. (auth)

4510 SPINAL CORD DOSIMETRY IN ^{131}I-IHSA CISTERNOGRAPHY. Harbert, John C. (Georgetown Univ. Hospital, Washington, D. C.); McCullough, David C.; Zeiger, Louis S.; Davidson, Jack D. J. Nucl. Med.; 11: 534-41 (Sep 1970).

A method is described for the calculation of both the β and γ radiation dose in spinal cord source and target tissues and the cumulated whole-body radiation dose during cisternography using ^{131}I-labeled human serum albumin administered by lumbar intrathecal injection as the tracer. A coaxial cylindrical model of the source and target was used, the mathematical treatment is described, and kinetic data were derived experimentally. Results of radiation dose measurements in 15 patients are summarized. The data show that the greatest contribution to the adsorbed radiation dose to the spinal cord is from β emissions and this dose falls off rapidly from the cord surface inward. The radiation dose is very dependent upon the cerebrospinal fluid volume and clearance of the tracer. Data on the radiation dose (rads) to lumbar nerve roots as a function of distance from cord surface and the surface dose are presented for normal, hydrocephalus, and cervical block patients. (C.H.)

4511 ABSORBED DOSE CONSIDERATIONS FOR RADIOPHARMACEUTICALS USED FOR PULMONARY STUDIES. Smith, Edward M. (Univ. of Miami, Fla.); Mozley, James M. Contract AT-(40-1)-3734. pp 69-80 of Pulmonary Investigation with Radionuclides. /Gilson, Albert J. (ed.). Springfield, Ill.; Charles C Thomas, Publisher (1970).

From 1st Annual Seminar on Pulmonary Investigation with Radionuclides, Miami, Fla. See CONF-690334.

A critical evaluation is given of the relationships of the radiopharmaceutical, the radionuclide, and the organ visualization instrumentation on the resultant absorbed dose to the patient. The method for calculating the absorbed dose follows the recommendations of the Medical Internal Radiation Dose Committee of the Society of Nuclear Medicine. Equations are given for expressing relations between average absorbed dose, cumulative concentration of the radionuclide, cumulative activity of the radionuclide, mass of the organ, equilibrium absorbed dose constant, and absorbed fraction. Biological data, nuclear data, and absorbed fractions for macroaggregated albumin labeled with ^{131}I or ^{99m}Tc, colloidal iron hydroxide labeled with ^{113m}In, and xenon gas labeled with ^{133}Xe are reviewed, and results of the absorbed dose calculations are given. The method for relating the absorbed dose to the radiopharmaceutical, the radionuclide, the instrumentation system, and the desired clinical information are reviewed, and the results for a dual opposed five-inch scanning system are presented. (H.L.W.)

4512 PROBLEMS OF RADIATION DOSIMETRY IN ENDOLYMPHATIC THERAPY WITH RADIOACTIVE ISOTOPES. Pfannenstiel, P.; Weissleder, H.; Hoffmann, G. (Univ., Freiburg i. B i. B.). Lymphology (Stuttgart); 2: 160-6(1969).

Radiation dosimetry after endolymphatic therapy of patients with Hodgkin's disease with ^{131}I and ^{32}P labeled oily contrast medium was performed in 30 patients. The total dose applied averaged 33 mCi ^{131}I and 4 mCi ^{32}P respectively. By measuring the changes in concentration of the radioactivity in different parts of the body with a specially equipped profile scanner during the first two or three weeks, the radiation doses were calculated approximately from the rate of decomposition of the radionuclide in the different parts of the body and from the volume of the tissue. Assuming homogenous distribution in the pelvic and paraortal lymphnodes, the dosage is massive, up to 700,000 rads. A rather high percentage of radioactive labeled contrast medium is received by the lungs and consequently high radiation doses may occur here. However, serious limitations have to be considered in the reported measurements because of the marked inhomogenity of dose ditribution in lymph nodes and lungs. (auth)

4513 A NEW THREE-GATE METHOD FOR MEASURING ^{51}Cr IN THE PRESENCE OF ^{59}Fe IN SOURCES IN A SCATTERING MEDIUM. Bell, T. K. (Royal Victoria Hospital, Belfast); Johnston, A. R.; Spiers, E. W. Phys. Med. Biol.; 15: 475-82 (Jul 1970).

A method of assessing the counts from ^{59}Fe in a gate set to detect the 0.32 MeV photopeak of ^{51}Cr when both isotopes are used together is described. In the "single photopeak" procedure comparison is made in the spectra from ^{59}Fe sources in a water phantom, of the count rate in a gate B set on the 1.1 MeV photopeak and the count rate in a gate C set on the 0.32 photopeak of ^{51}Cr normalized to the count rate in a gate A set on the 1.29 MeV peak. In the "double photopeak" procedure comparison is made of the count rate in a gate B, set on the 0.66 MeV photopeak of ^{137}Cs, with the count rate in gate C, both normalized to the count rate in a gate A set on both the 1.1 and 1.29 MeV photopeaks. It is shown that for certain gate widths there is a linear relationship to within ±3.3% between the count ratios C/A and B/A which is independent of the size, shape and depth of the ^{59}Fe source. The three-channel system was tested by using it to determine the count rate from ^{51}Cr in a source containing both ^{59}Fe and ^{51}Cr in a ratio similar to that used in haematological measurements. (auth) (UK)

4514 COMPUTER PROGRAMS FOR IRRADIATION PLANNING IN HIGH-ENERGY THERAPY. Dobry, H.; Benedetti, G. R. (Siemens AG, Erlangen, Ger.). Electromedica; 38: 264-70 (1970). (In German).

The output of data under the form of isodoses or of basic data for dosage, e.g. depth of pendulum center, relative dose in the depth and in the rotation center are described. The correlation between measured and calculated distributions was tested and the degree of error was determined. New irradiation techniques may be investigated theoretically using data processing. Examples are given. The programs are written in FORTRAN IV, developed by way of Siemens System 4004 and transcribed for Siemens System 305. The programs can however be transcribed for other types of computers. (INIS)

4515 HEALTH PHYSICS PRACTICES AND EXPERIENCES OF ISOTOPE PRODUCERS AND DISTRIBUTORS. New York; Atomic Industrial Forum, Inc. (1970). 7p. $5.00. (NP-18469).

A compilation of regulatory inspection information acquired from questionnaires sent to commercial facilities engaged in

the processing and distribution of radioactive materials is presented. Information is included on personnel monitoring devices, measurement of body burdens, types and quantities of radioisotopes handled, inspection agencies, frequency of inspection, duration of inspection, and cost of health physics programs. (W.H.K.)

4516 APPARATUS FOR TAKING SAMPLES OF POSSIBLY RADIOACTIVE SUBSTANCES. Levy, Francoise; Tonnelier, Claude; Zerbib, Jean-Claude (to Commissariat a l'Energie Atomique). British Patent 1,203,688. 3 Sep 1970. Priority date 28 Jun 1967, France.

A device for sampling substances from a surface so that their state of radioactivity can be measured is described. (W.H.K.)

4517 IN-PHANTOM DOSIMETRY OF ^{238}Pu HEAT SOURCES. Cross, F. T.; Sheppard, J. C. (Battelle-Northwest, Richland, Wash.). Trans. Amer. Nucl. Soc.; 13: 498-9(Nov 1970).

From Meeting of the American Nuclear Society, Washington, D. C. See CONF-701102.

4518 SOURCES OF EXPOSURE TO THE PUBLIC. Meinhold, Charles B. (Brookhaven National Lab., Upton, N. Y.). Trans. Amer. Nucl. Soc.; 13: 517-18(Nov 1970).

From Meeting of the American Nuclear Society, Washington, D. C. See CONF-701102.

4519 RELATION BETWEEN THE DEPOSITION OF LONG LIVED FISSION PRODUCTS AND THE TOTAL DIETARY INGESTION. Strackee, L.; Mattern, F. C. M. (National Inst. of Public Health, Utrecht). Health Phys.; 18: 641-8(Jun 1970).

The relation between the deposition of ^{90}Sr and ^{137}Cs and the quarterly means of the estimated daily dietary intakes of these nuclides by the general population in the Netherlands during 1962 to 1967 is described by an equation of the form $I = A\Sigma De^{-\lambda(t-s)} + B\Sigma D$ where I is the ingestion, D the deposition, and A, B, and λ experimental parameters. The meaning of these parameters is discussed in some detail. The principal result is the finding that the contribution of the soil, expressed by the second term in the model equation, is less important than previously supposed. This means that the future ingestions of ^{90}Sr and ^{137}Cs will be lower than formerly assumed. (auth) (UK)

4520 NEW METHOD OF DETERMINING ABSORBED DOSES OF GAMMA RADIATION. Generalova, V. V.; Kishinevskaya, M. B. At. Energ. (USSR); 27: 564(Dec 1969). (In Russian).

Diffuse reflection spectra of glucose, calcium gluconate and barium sulfate were measured on a SF-4 spectrophotometer equipped with a PDO-1 supplementary unit. The diffuse reflection coefficient R is given as a function of the absorbed energy in the interval from 1.10^4 to 1×10^9 rads. Samples were irradiated in the form of tablets 4 mm thick and 12 mm in diameter in plastic containers at dose rates of 100 to 2000 rads/sec. The simplicity of the method of determining the radiation change, the availability of equipment and standard materials, the wide range of absorbed dose, the absence of a post effect, the high stability of the unirradiated samples, and the good reproducibility of the results favor this method as a rapid method for determining the absorbed dose, particularly at high doses. (TTT)

4521 NEUTRON MICRODOSIMETRY FOR 15-MeV NEUTRONS AT THE MODEL OF THE RABBIT EYE. Krueger, H.; Jacobi, K. W.; Ruether, W.; Neubauer, H.; Graul, E. H. (Phillips-Univ., Marburg, Ger. Univ., Cologne). Arch. Klin. Exp. Ophthalmol.; 180: 134-9(1970). (In German).

Since neutron dosimetry cannot be carried out easily if a biological object is irradiated, a microdosimetric technique was developed for the measurement. A phantom of the rabbit eye filled with a tissue-equivalent solution was used. In order to measure in as many positions as desired inside the phantom without unduly disturbing the radiation field, a tissue-equivalent proportional counter was constructed. The results are described and discussed. (auth) (TSS)

Radiation Protection

Refer also to abstracts 4140, 4175, 4314, 4531, and 4608.

4522 (BRH/DEP-70-24) IN-PLANT SURVEY OF TELEVISION RECEIVERS FOR X-RADIATION EMISSION CAPABILITY. Smith, D. R.; Reiter, S. E.; Smith, T. M. (Bureau of Radiological Health, Rockville, Md. Div. of Electronic Products). Sep 1970. 71p. NTIS.

Visits were made to the facilities of 21 domestic television manufacturers and one retailer of foreign receivers to measure x-radiation emissions from television receivers considered typical of those being marketed since the effective date of the Radiation Control for Health and Safety Act of 1968. The test data obtained during these visits provided basic information on the capability of the receivers to emit x radiation under certain operating conditions, including various adjustments to the receivers that could result in x-radiation emission under conditions expected to be found during home use. The information was used in the development of the performance standard for television receivers and also in the development of recommendations for future programs of compliance testing under the performance standard. (auth)

4523 MEDICAL SUPERVISION OF WORKERS EXPOSED TO IONIZING RADIATIONS. Gillon, J.-J. Arch. Mal. Prof. Med. Trav. Secur. Sociale; 28: 601-4(Jul-Aug 1967). (In French).

The medical supervision of workers exposed to ionizing radiations should begin with an evaluation of the fitness of the worker for the particular job. The general risks of exposure in a given situation should be taken into consideration. Specific counter-indications for workers exposed to the risk of contamination and counter-indications relative to safety are cited. The prevention of medico-legal claims is briefly considered. (J.S.R.)

4524 BIOLOGICAL EFFECTS OF IONIZING RADIATION AND MEANS OF PROTECTION AGAINST IT. Hoyos, Jorge Meneses. Medicina (Mex.); 48: 645-50(25 Dec 1968). (In Spanish).

The importance of understanding the effects of ionizing radiations and means of protection against them are summarized. The units used for the measurement of radioactivity are defined. The variability of the effect according to the dose received and to the sensitivity of the tissue is illustrated. The types of lesions and the mechanism for the production of radiation lesions are described. Radiomutations are briefly considered. Protection against radiation and the treatment for exposed personnel are considered. (J.S.R.)

Safety Procedures

Refer also to abstracts 4195, 4196, 4220, 4236, 4258, 4435, and 4436.

4525 (ORNL-TM-3216) RADIOLOGICAL CONSIDERATIONS IN THE USE OF NATURAL GAS FROM NUCLEARLY STIMULATED WELLS. Jacobs, D. G.; Barton, C. J.; Kelly, M. J.; Struxness, E. G. (Oak Ridge National Lab., Tenn.). Nov 1970. Contract W-7405-eng-26. 19p. Dep. NTIS.

Various pathways through which radionuclides in nuclearly stimulated natural gas can reach users of the gas or gas by-product have been considered. At activity levels in the gas that can be achieved in large-scale exploitation of this peaceful use of nuclear explosives, the calculations performed to date show that maximum doses of a few milliRems per year can be expected for the exposure conditions considered. This dose level can be compared with a value of 170 milliRems per year established by the Federal Radiation Council. (auth)

4526 TWELVE YEARS OF HEALTH PHYSICS IN A PLUTONIUM PRODUCTION PLANT. Rodier, J.; Chassany, J.; Estournel, R.; Peyresblanques, H. (CEA, Chuscian, France). Arch. Mal. Prof. Med. Trav. Secur. Sociale; 31: 9-22(Jan-Feb 1970). (In French).

The radiation protection of the personnel was entrusted to the health physics division which is independent of various operational departments. The ways and means developed for the radiation protection of the personnel, as well as the role of the health physics agent (often appointed as a laboratory assistant or a technician) are reported. Health physics is studied under normal and accidental exposure conditions or under the emergency conditions where the dose rates are higher than 7.5 mrems/h. Plutonium production plants in Marcoule have been on operation for twelve years without any serious accidents. The dose rates never exceeded the maximum permissible dose. (France)

4527 THE DEVELOPMENT OF SAFETY MEASURES IN REPROCESSING PLANTS. Mamelle, J. (Saint-Gobain Techniques Nouvelles, Courbevoie, France). Bull. Inform. A.T.E.N. (Ass. Tech. Energ. Nucl.); No. 81, 21-8(Jan-Feb 1970). (In French).

The problem of safety in a fuel reprocessing plant is above all a battle against the permanent risk of contamination, and to a lesser degree against the danger of a critical excursion. Contamination as a result of corrosion may be countered by using apparatus of standard alloys and replacing it periodically, or by using elements of very long probable lifetime. The problem of pumps and sampling devices is examined by way of example. Protection against contamination is obtained by dividing up the plant into several zones. Criticality problems arise mainly in the final

XUM

stage of Pu purification. As soon as it is planned to process several tens of kg of fissile material per day, it is necessary to develop continuous processes which lead to greater safety for personnel and real economic benefits. The problem of the conditioning and storage of high- and medium-activity liquid effluent and of solid and gaseous effluent is then examined. A comparison is made between the safety costs of the NFS American plant (26 M $) and the projected Japanese plant (40 M $) which produce 1 t/d. A saving of 1 M $ in the second plant could be made by adhering to French safety concepts. (CEA, France)

4528 RADIATION SAFETY. Mendoza, A. (Ministry of Tech., Birmingham, Eng.). Non-Destruct. Test.; 3: 44-7(Feb 1970).

A brief history of radiation injuries to personnel is presented, and the development of an awareness to the dangers of uncontrolled exposure is discussed. Formation of the International X-ray and Radium Protection Committee and its recommendations for safe exposure levels for those working with x-rays and radioactive isotopes are also discussed. General safety measures to be taken by an operator and his supervisor when engaged in radiography are outlined and brief details of personal monitoring devices are given. (auth) (UK)

Legal Aspects

Refer also to abstract 4708.

4529 (AERE-R-6523) ASSESSMENT OF MEDICAL REQUIREMENTS FOR WORKERS IN NUCLEAR INSTALLATIONS. Stott, A. N. B. (Atomic Energy Research Establishment, Harwell (England)). Aug 1970. 6p. Dep. NTIS (U. S. Sales Only). UK 1s. 9d.

A review is made of the experience of twenty years of routine medical examinations (including blood counts) at A.E.R.E., Harwell. The reasons for initiating medical surveillance are described and examined in the light of this experience. Illustrative cases are described showing that exclusion from radiation work would not prevent the development of various illnesses, and the statistical probabilities relating to the development of such illnesses are also explored. Although there has been a trend away from the more intense form of medical examination, I.C.R.P. recommendations are still equivocal. Since legislatory requirements will be based on existing medical practice, no alteration in these can be expected until the medical advisors themselves show that there is no need for continued medical surveillance of radiation workers. (auth) (UK)

4530 INSURANCE OF ATOMIC RISKS. Maurer, A. (Schweizer Pools fuer die Versicherung von Atomrisiken, Zurich). Neue Tech., B; 11: 151-8(1969). (In German).

The historical development of legal liabilities in the case of nuclear accidents is discussed from both international and national standpoints. Several characteristic traits of existing laws are analyzed. Also discussed are organization of nuclear insurance as well as difficulties associated with its management. (tr-auth)

4531 RADIATION CONTROL IN DIAGNOSTIC ROENTGENOLOGY. Bushong, Stewart C. (Baylor Univ., Houston, Tex.). Health Phys.; 19: 557-61(Oct 1970).

Recommendations are made regarding the control of radiation exposure to operating personnel in departments of diagnostic roentgenology. These recommendations are summarized as follows: 1. A protocol for the proper conduct of a radiation control survey should be undertaken and published under the sponsorship of a professional society. 2. A form or forms based on flexibility of use and ease of data extraction should be developed and made available to consulting health physicists. 3. Protective lead curtains draping a fluoroscopic screen carriage should extend over the fluoroscopic table and across the side opposite to that of the radiologist where the technologist normally stands. 4. Protective lead gloves should be employed on both hands by examining fluoroscopists. 5. If only one film badge is worn by the examining radiologist, it should be worn on the front collar above the protective lead apron. 6. If the location of a film badge is not standard, it should be recorded as an integral part of an individual's personnel monitoring record. (auth) (UK)

4532 RADIATION STANDARDS. Bond, V. P. (Brookhaven National Lab., Upton, N. Y.). Trans. Amer. Nucl. Soc.: 13: 518-19(Nov 1970).

From Meeting of the American Nuclear Society, Washington, D. C. See CONF-701102.

Medicine

Refer also to abstracts 4229–4235, 4237–4241, and 5311.

Protective Substances

Refer also to abstracts 4115, 4726, and 4728.

4533 EFFECT OF THE BONE MARROW BREAKDOWN PRODUCTS ON HEMOPOIESIS. Gotsiridze, G. A.; Kevlishvili, G. E. Probl. Gematol. Pereliv. Krovi; 15: No. 7, 37-9(Jul 1970). (In Russian).

It was revealed that lyophilized bone marrow which contained the products of decomposition of the cells of the hemopoietic tissue retained its hemostimulating properties for a period of two years. Lyophilized bone marrow stimulated hemopoiesis of healthy dogs, facilitated the course of radiation sickness in the irradiated animals, and reduced the mortality rate to 40% (against 80% in control), prolonging the mean life span of the dogs by 12.12 ± 0.94 days, and also restored the red blood indices in anemic rabbits at earlier periods in comparison with control animals. (auth)

4534 RADIATION PROTECTION AND SENSITIZATION. Proceedings of the Second International Symposium on Radiosensitizing and Radioprotective Drugs, Rome, 6–8 May 1969. Moroson, Harold; Walker, Donald S.; Quintiliani, Marcello (eds.). New York; Barnes and Noble, Inc. (1970). 537p. $25.00. (CONF-690525).

Separate abstracts were prepared on 72 papers presented at this conference. One paper was abstracted previously and appeared in NSA. (C.H.)

For abstracts of individual papers see: 4535–4603, 4688, 4689, and 4709.

4535 MOLECULAR MECHANISMS OF CELLULAR RADIOSENSITIZATION AND PROTECTION. Adams, G. E. (Mount Vernon Hospital, Northwood, Eng.). pp 3-14 of Radiation Protection and Sensitization. /Moroson, Harold (ed.). New York; Barnes and Noble, Inc. (1970).

From 2nd International Symposium on Radiosensitizing and Radioprotective Drugs, Rome, Italy. See CONF-690525.

Molecular aspects of bacterial radioprotection and radiosensitization are discussed in the light of recent data from both cellular and radiation chemical model systems. Analysis of the molecular basis for sensitization reveal two basic mechanisms: biochemical, occurring by either suppression of natural protectors or inhibition of repair processes; and radiation chemical; characterized by the extracellular or intracellular formation of toxic products or the intracellular fixation of radiation damage. The fixation of radiation damage may occur directly or indirectly. In the indirect mechanism, free radicals undergo either oxidative or reductive reactions with the hydrated electron. The role of hydrogen transfer in repair processes is discussed as the mechanism behind the molecular processes of radioprotection. (E.R.B.)

4536 REPAIR OF DNA AND THE MODE OF ACTION OF SENSITIZERS AND PROTECTORS IN BIOLOGICAL SYSTEMS OF DIFFERENT COMPLEXITY. Alexander, P.; Dean, C. J.; Lehmann, A. R.; Ormerod, M. G.; Feldschreiber, P.; Serianni, R. W. (Chester Beatty Research Inst., Belmont, Eng.). pp 15-34 of Radiation Protection and Sensitization. /Moroson, Harold (ed.). New York; Barnes and Noble, Inc. (1970).

From 2nd International Symposium on Radiosensitizing and Radioprotective Drugs, Rome, Italy. See CONF-690525.

X rays produce single-strand breaks with approximately equal efficiency in the DNA of murine lymphoma cells and Micrococcus radiodurans (M.r.). Production of double-strand breaks is however 2½ times greater in lymphoma cells than in M.r. It is suggested that variations in cellular radiosensitivity are not determined by the magnitude of the primary lesions in DNA. Since the dose of x rays needed to produce a single break in the DNA of the cells studied is very similar to that found when isolated DNA is irradiated under conditions where the contribution of indirect action is minimal, it would appear that in the cells direct action is largely responsible for the observed damage to DNA. The presence of oxygen does not alter the efficiency of single-strand breakage, but studies on the rejoining of breaks in M.r. indicate that oxygen may alter the chemical nature of the ends at the radiation induced breaks. The limited available data on the effect of other dose-modifying procedures indicates their effect in radiosensitivity is not due to altering the efficiency of single-strand breakage but that at least some agents act at the level of repair. Both lymphona cells and M.r. are capable of repairing single-strand breaks and for M.r. it was demonstrated that there is both a fast and a slow enzymatic rejoining process and that irradiation in the presence of oxygen prevents repair at 0°C but not at 30°C. Repair of double-strand breaks was observed in M.r. but not yet in lymphoma cells. Post-irradiation degradation of DNA was extensively studied in M.r. and survival of the cell depends on its ability to control the extent of the degradation. Cysteamine facili-

tates the control of DNA breakdown. Interference with protein synthesis by addition of chloramphenicol after irradiation causes uncontrolled degradation and results in marked sensitization. Many of the chemical substances that sensitize bacteria do so by modifying the radiolysis products of water formed extra-cellularly. Such products only contribute significantly to cell death in the absence of radical scavengers and this explains why these sensitizers are much more effective when the cells are irradiated in simple buffers than in complex media and also why the same agents sensitize mammalian cells to a much smaller extent. (auth)

4537 RADIOSENSITIZATION BY THE HALOGENATED PYRIMIDINE ANALOGUES: LABORATORY AND CLINICAL INVESTIGATIONS. Kaplan, Henry S. (Stanford Univ., Calif.). pp 35-42 of Radiation Protection and Sensitization. /Moroson, Harold (ed.). New York; Barnes and Noble, Inc. (1970).

From 2nd International Symposium on Radiosensitizing and Radioprotective Drugs, Rome, Italy. See CONF-690525.

Following a brief review of the structure, metabolism, and selective incorporation of halogenated pyrimidine analogues into nucleic acids, the radiosensitizing effects of these compounds are discussed. The parameters of radiobiologic response are briefly reviewed and evidence that radiosensitization is due to incorporation of these analogues into DNA is presented. Previous work on the molecular mechanisms of radiosensitization by these halogenated analogues is cited and results of clinical pharmacologic and radiotherapeutic investigations of these compounds are given. (E.R.B.)

4538 CHEMICAL PROTECTION AGAINST IONIZING RADIATION BY SULPHUR-CONTAINING AGENTS. Pihl, A.; Sanner, T. (Norwegian Radium Hospital, Oslo). pp 43-55 of Radiation Protection and Sensitization. /Moroson, Harold (ed.). New York; Barnes and Noble, Inc. (1970).

From 2nd International Symposium on Radiosensitizing and Radioprotective Drugs, Rome, Italy. See CONF-690525.

The mechanisms of protection against ionizing radiation by sulfur-containing agents are grouped into two major categories. The radiochemical mechanisms of protection include radical scavenging, hydrogen transfer, and alteration of intrinsic radiosensitivity. The biochemical and physiological mechanisms of protection include release of endogenous protective agents, increase in cellular radioresistance, and increase in repair processes. These mechanisms are discussed and future research in the area of protective mechanisms is suggested. (E.R.B.)

4539 RADIOPROTECTIVE ACTION OF COMPOUNDS NOT CONTAINING SULPHUR. Semenov, L. F. (Inst. of Experimental Pathology and Therapy, Sukhumi, USSR). pp 57-61 of Radiation Protection and Sensitization. /Moroson, Harold (ed.). New York; Barnes and Noble, Inc. (1970).

From 2nd International Symposium on Radiosensitizing and Radioprotective Drugs, Rome, Italy. See CONF-690525.

There are two large classes of protectors that do not include the thiol group in their molecular structure: amines and hypoxic agents. Among the various amines, only biologically active amines with stimulating neurotropic properties protect the mammals. These compounds produce many different reactions in the living organism but before all they cause the lowering of the tissue oxygen (pO_2). This effect is a selective one. It develops in muscles, in lymphatic nodes, in bone marrow, and is accompanied by a second small lowering of the oxidoreductive potential (ORP, ΔEh) in these tissues. The dependence of the protective activity of amines upon the hypoxia of blood-forming organs is highly probable. The hypoxic agents block on various levels the transport of O_2 to tissues producing similar changes of pO_2 and ORP in every tissue. That is supposed to be the reason of their protective action. The connection of a protective effect of the narcosis with the tissue hypoxia was not confirmed. (auth)

4540 ELECTRON TRANSFER STUDIES OF NUCLEIC ACID DERIVATIVES IN SOLUTIONS CONTAINING RADIOSENSITIZERS. Greenstock, C. L.; Adams, G. E.; Willson, R. L. (Mount Vernon Hospital, Northwood, Eng.). pp 65-71 of Radiation Protection and Sensitization. /Moroson, Harold (ed.). New York; Barnes and Noble, Inc. (1970).

From 2nd International Symposium on Radiosensitizing and Radioprotective Drugs, Rome, Italy. See CONF-690525.

The technique of pulse radiolysis was used to observe directly electron transfer reactions between various nucleic acid derivatives and certain biological radiosensitizers in aqueous solution. The decay of the optical absorption of the electron adducts of the nucleic acid derivatives and the concomitant build-up of absorption of the acceptor radical-anions of the radiosensitizers was followed. The rate constants for electron transfer reactions from free bases, nucleosides, and nucleotides to N-ethyl maleimide (NEM) and menadione (the sodium bisulphite salt) (MD) are high, approaching a diffusion-controlled limit. There is no difference in transfer rates for purines or pyrimidines. The more complex the chemical structure, the slower is the transfer. Transfers to MD (pH 6.5) are slightly faster than those to NEM (pH 11.5). This is probably caused by the effect of ionic strength rather than a difference in electron transfer efficiency. (auth)

4541 REACTION OF TRIACETONEAMINE-N-OXYL WITH RADIATION-INDUCED RADICALS FROM DNA AND FROM DEOXYRIBONUCLEOTIDES IN AQUEOUS SOLUTION. Willson, Robin L. (Mount Vernon Hospital, Northwood, Eng.); Emmerson, Peter T. pp 73-9 of Radiation Protection and Sensitization. /Moroson, Harold (ed.). New York; Barnes and Noble, Inc. (1970).

From 2nd International Symposium on Radiosensitizing and Radioprotective Drugs, Rome, Italy. See CONF-690525.

The reactions between triacetoneamine-N-oxyl (TAN) and the free radicals produced by hydroxyl radical attack on DNA and on several deoxyribonucleotides have been studied in aqueous solution by pulse radiolysis. The bimolecular rate constant for the reaction of TAN with the DNA(OH)· radical was 2.1×10^8 M^{-1} sec^{-1} and values ranging from $1-2 \times 10^8$ M^{-1} sec^{-1} were obtained for the reactions with the hydroxy nucleotide radicals. The ability of other sensitizing agents to react with the hydroxy radical of thymidylic acid, dTMP(OH)· was also investigated. Apart from oxygen and TAN, only ferricyanide and menadione reacted readily. Reactions with diacetyl and p.nitroacetophenone could not be observed, giving an upper limit of 10^7 M^{-1} sec^{-1} for the corresponding bimolecular rate constants. (auth)

4542 EFFECT OF 5-BROMOURACIL INCORPORATION ON ENERGY TRANSFER IN IRRADIATED DNA. Fielden, E. M.; Lillicrap, S. C. (Inst. of Cancer Research, Belmont, Eng.). pp 81-6 of Radiation Protection and Sensitization. /Moroson, Harold (ed.). New York; Barnes and Noble, Inc. (1970).

From 2nd International Symposium on Radiosensitizing and Radioprotective Drugs, Rome, Italy. See CONF-690525.

The emission spectrum and kinetics following pulsed electron irradiation of DNA, DNA with various percentage incorporation of 5BU, and of 5-bromodeoxyuridine itself have been recorded over the time scale of 5 μsec to 1 sec and the results compared. It is found that the incorporation of 5BU dramatically affects the emission characteristics of the DNA by increasing the luminescence intensity and bringing the kinetics into coincidence with those of 5 BUdR alone after a post-irradiation time that is dependent on the percentage incorporation of the sensitizer. It is suggested that the more efficient localization of energy of 5 BUdR than by thymine in the DNA chain may lead to enhanced damage at the 5 BUdR sites, thus accounting for the radiosensitivity of living systems possessing 5 BUdR incorporated into their DNA. (auth)

4543 FAST INTERMEDIATE REACTIONS SENSITIZING ALCOHOL DEHYDROGENASE TO RADIATION. Davies, J. V. (Christie Hospital and Holt Radium Inst., Manchester, Eng.); Ebert, M.; Quintiliani, M. pp 87-93 of Radiation Protection and Sensitization. /Moroson, Harold (ed.). New York; Barnes and Noble, Inc. (1970).

From 2nd International Symposium on Radiosensitizing and Radioprotective Drugs, Rome, Italy. See CONF-690525.

The sensitization of alcohol dehydrogenase (ADH) to ionizing radiation by iodine compounds has been studied by the pulse radiolysis technique. The absorption spectra of transient species observed after a single pulse (0.1 to 1 μsec duration) have been measured in aqueous buffered solutions of ADH, 3-iodopropionic acid (IPA), and sodium iodide (NaI). Kinetic decay traces have been evaluated for these transient species in the separate solutions and also for the mixtures of ADH/IPA and ADH/NaI. It has been shown that, in the case of IPA, both unchanged ADH and the transient species ADH· react with IPA transient but not with unchanged IPA. Similarly for the ADH/NaI system it is clear that ADH and ADH· react with I_2^-. Some evidence has been provided suggesting that ADH reacts very rapidly with iodine atoms, I·, by competition with the reaction $I^- + I\cdot \rightarrow I_2^-$. (auth)

4544 RADIOPROTECTIVE EFFECT OF CYSTEINE ON LYSOZYME IN DILUTE AQUEOUS SOLUTION. Brustad, T.; Jones, W. B. G. (Norsk Hydro's Inst. for Cancer Research, Montebello, Norway). pp 95-101 of Radiation Protection and Sensitization. /Moroson, Harold (ed.). New York; Barnes and Noble, Inc. (1970).

From 2nd International Symposium on Radiosensitizing and Radioprotective Drugs, Rome, Italy. See CONF-690525.

Rapid mixing techniques are used to elucidate mechanisms by which cysteine protects lysozyme irradiated in dilute anoxic solutions. No protection is observed when cysteine is admitted to irradiated lysozyme 5 msec or longer after irradiation. Full protective effect is obtained when irradiation is performed 6 msec or longer after mixing of lysozyme and cysteine. The most likely

XU

mechanism by which cysteine exerts its protective effect appears to be by scavenging water radicals (presumably OH). Restitution of enzymatic activity by hydrogen donation from cysteine to radiation-induced enzyme transients having life times exceeding a few msec does not occur. Protection by mixed disulphide formation between unirradiated lysozyme and cysteine is not involved. (auth)

4545 RADIOPROTECTION BY SELENIUM-CONTAINING COMPOUNDS. Badiello, Roberto; Breccia, Alberto (Univ., Bologna). pp 103-7 of Radiation Protection and Sensitization. /Moroson, Harold (ed.). New York; Barnes and Noble, Inc. (1970).

From 2nd International Symposium on Radiosensitizing and Radioprotective Drugs, Rome, Italy. See CONF-690525.

The chemical radioprotection afforded by selenium-containing compounds in biological and chemical systems is reported. Radioprotection, in the biological experiments, was evaluated by the ability of compounds to alleviate the mortality and the leukopenia occurring in irradiated rats. As chemical model systems, amino acids, either in the solid state or in aqueous solutions, have been studied. The results, both in biological and in chemical systems, show that these compounds have a powerful radioprotective action. The order of reactivity of selenium compounds with radicals appears to parallel their known radioprotective ability in biological systems and emphasizes the need for an understanding of radiation chemical processes to aid the understanding of radiobiological ones. (auth)

4546 RADIATION CHEMISTRY OF SELENIUM-CONTAINING PROTECTIVE AGENTS. Badiello, Roberto; Fielden, E. Martin (Inst. of Cancer Research, Belmont, Eng.). pp 109-15 of Radiation Protection and Sensitization. /Moroson, Harold (ed.). New York; Barnes and Noble, Inc. (1970).

From 2nd International Symposium on Radiosensitizing and Radioprotective Drugs, Rome, Italy. See CONF-690525.

The reactivity of the protective agent selenourea towards the primary radicals of water radiolysis, OH, H, and the hydrated electron has been measured by the pulse radiolysis technique. The radical reactivity of the selenium, sulfur, and oxygen containing ureas is compared with the radioprotective efficiencies of these compounds and it is found that the most efficient radical scavenger, selenourea, is the most efficient protective agent. Both the OH radical and the hydrogen atom give rise to the same radical species when reacting with selenourea. The radical formed by this reaction has a strong absorption band at 410 nm and it is shown to be a charged complex involving two selenourea molecules. The formation and decay kinetics of this radical ion have been measured together with the association/dissociation constant of the complex. It is suggested that similar complex radicals may occur more frequently than has previously been suspected in radiation chemistry. On a radical scavenging mechanism, the ability of a secondary radical to form a complex may have some bearing on the protective efficiency of the parent compound. (auth)

4547 CHARGE TRANSFER COMPLEXES AND THE MECHANISM OF ACTION OF CYSTEAMINE AND PENICILLAMINE. Lohmann, Wolfgang (Univ. of Iowa, Iowa City. Institut fuer Strahlenschutz, Neuherberg, Ger.). pp 117-20 of Radiation Protection and Sensitization. /Moroson, Harold (ed.). New York; Barnes and Noble, Inc. (1970).

From 2nd International Symposium on Radiosensitizing and Radioprotective Drugs, Rome, Italy. See CONF-690525.

By means of electron spin resonance and optical absorption measurements it was found that copper ions form a charge transfer complex with cysteamine and penicillamine, respectively. The SH-containing substances act as an electron donor resulting in a reduction of the cupric form. This effect is reversed by the addition of oxygen, while nitrogen has no effect. From the results obtained, it might be concluded that the radioprotective effect of the two substances investigated is caused by their reducing abilities. (auth)

4548 STRUCTURE-FUNCTION STUDIES OF THE AMINOTHIOL RADIOPROTECTANTS. Swartz, H. M.; Richardson, E. C.; Copeland, E. S.; Lofberg, R. T.; Jandacek, R. J. (Walter Reed Army Inst. of Research, Washington, D. C.). pp 121-31 of Radiation Protection and Sensitization. /Moroson, Harold (ed.). New York; Barnes and Noble, Inc. (1970).

From 2nd International Symposium on Radiosensitizing and Radioprotective Drugs, Rome, Italy. See CONF-690525.

An extensive structure-function study of the aminothiols with the goal of obtaining information on basic radiation injury processes has been described. Structural analogues of MEA are being synthesized, purified, and tested under biological conditions that minimize pharmacological, physiological, and metabolic effects of the aminothiols. The results to date are consistent with a theory that aminothiols and disulfides act selectively on radiation induced radicals, accelerating their transformation and decay. The radical species observed in γ irradiated bacteria (Escherichia coli) were found to be affected by the presence of aminothiols, annealing temperature, and pH. (auth)

4549 INFLUENCE OF SULPHUR-CONTAINING PROTECTIVE AGENTS ON BACTERIOPHAGE SURVIVAL CURVE SHAPES. Dewey, D. L. (Mount Vernon Hospital, Northwood, Eng.). pp 140-5 of Radiation Protection and Sensitization. /Moroson, Harold (ed.). New York; Barnes and Noble, Inc. (1970).

From 2nd International Symposium on Radiosensitizing and Radioprotective Drugs, Rome, Italy. See CONF-690525.

Under the influence of ionizing radiation cysteine is oxidized to cystine and cystine is reduced to cysteine. Thus irrespective of the starting compound, the result of irradiation is to produce an equilibrious mixture of the two, the relative concentrations depending only on the oxygen tension at the time of irradiation. Cystamine does not protect bacteria from anoxic radiation damage, but it does protect bacteriophage. By measuring survival over many powers of ten, it was possible to study the effect on Serratia marcescens of γ radiation doses up to 80,000 rad. At these high anaerobic doses, in the presence of cystamine, no protection was observed, but a lowering in the extrapolation number. In the case of phage T_7 the protection afforded by disulfide compounds is the same as with sulfhydryl compounds even at doses well below 80,000 rad, either in absence or in presence of oxygen. With phage T_4 cystamine does not have much effect in oxygen and protects in nitrogen only at higher doses where there has been some reduction to SH by radiation. The results point to the conclusion that protection by cystamine cannot be explained by reduction of disulphide to sulphydril with high radiation doses. The major effect is the ability of different organisms to use disulfide compound for protection from radiation damage. (auth)

4550 MODIFICATION OF DNA IN ESCHERICHIA COLI EXPOSED TO X-RAYS BY TRIACETONEAMINE N-OXYL AND OXYGEN. Emmerson, Peter T. (Yale Univ., New Haven). pp 147-54 of Radiation Protection and Sensitization. /Moroson, Harold (ed.). New York; Barnes and Noble, Inc. (1970).

From 2nd International Symposium on Radiosensitizing and Radioprotective Drugs, Rome, Italy. See CONF-690525.

The ability of an x-irradiated $Flac^+$ (ura) strain of E. coli to produce Lac^+ (Ura^+) colonies when mated with F^- (Ura^+) strains carrying rec^+ or recA13 has been studied. The presence of triacetoneamine N-oxyl (TAN) during irradiation of the donor strain under anoxia increases the effectiveness of the radiation by a factor of 7.5 as measured by the production of Lac^+ colonies in the cross with the F^- carrying recA13. Similarly, oxygen was found to increase the effectiveness of the radiation by a factor of three. This shows that the episomal DNA is modified by the presence of TAN or oxygen during irradiation. In separate experiments it was shown by sedimentation studies in alkaline sucrose gradients that TAN increased the number of radiation-induced single-strand breaks or alkali labile bonds in phage λ superinfecting E. coli (λ) by a factor of only 1.5. This indicates that TAN modifies DNA predominantly in other ways than by producing single-strand breaks. (auth)

4551 MODIFICATION OF POST-IRRADIATION DNA DEGRADATION IN E. COLI B/r. Cramp, W. A. (Hammersmith Hospital, London). pp 155-8 of Radiation Protection and Sensitization. /Moroson, Harold (ed.). New York; Barnes and Noble, Inc. (1970).

From 2nd International Symposium on Radiosensitizing and Radioprotective Drugs, Rome, Italy. See CONF-690525.

Thiourea, glycerol, dimethyl sulfoxide, N-ethyl maleimide, and indane trione were used in the optimum concentrations for protection or sensitization of E. coli B/r. Two of the protective agents, thiourea 0.3 M, and dimethyl sulfoxide IM almost completely inhibited electron post-irradiation DNA breakdown, glycerol IM had little or no effect. Indane trione 8.10^{-4} M completely inhibited degradation but N-ethyl maleimide 5.10^{-4} M had only a slight inhibitory effect. With pre-irradiation washing procedure only indane trione still inhibited DNA degradation. None of these compounds affect post-irradiation survival after pre-irradiation washing. It is suggested that DNA is not the only or most important target for the killing of bacteria by ionizing radiation. (auth)

4552 MECHANISMS OF RADIOSENSITIZATION BY SOME SULPHYDRYL POISONS. Singh, B. B.; Shenoy, M. A.; Gopal-Ayengar, A. R. (Bhabha Atomic Research Centre, Trombay, India). pp 159-62 of Radiation Protection and Sensitization. /Moroson, Harold (ed.). New York; Barnes and Noble, Inc. (1970).

From 2nd International Symposium on Radiosensitizing and Radioprotective Drugs, Rome, Italy. See CONF-690525.

XUM

Some biochemical processes were investigated in Escherichia coli cells γ irradiated in the presence of the radiosensitizers, iodoacetic acid, vitamin K_5, and its analogues. Following iodoacetic acid treatment post-irradiation synthesis and degradation of DNA were affected, whereas no significant changes in the protein synthesis could be noticed. Treatment of cells with vitamin K_5 increased the cell generation time and inhibited DNA synthesis. Further inhibition of DNA synthesis was noticed in irradiated cells. (auth)

4553 CHELATION AND RADIATION PROTECTION. Block, Seymour S. (Univ. of Florida, Gainesville); Muligan, David D.; Weidner, James P.; Doherty, David G. pp 163-6 of Radiation Protection and Sensitization. /Moroson, Harold (ed.). New York; Barnes and Noble, Inc. (1970).

From 2nd International Symposium on Radiosensitizing and Radioprotective Drugs, Rome, Italy. See CONF-690525.

In a series of para substituted phenylthioacetic acids and a series of para substituted N-phenyldithiocarbamates the substituents changed the nature of the compound from x-radioprotectant to x-radiosensitizer in Escherichia coli tests. The effect, except in the case of the CH_3, was in the order of the Hammett constants for σ, with the strongest electron donating group giving the greatest protection and the strongest electron withdrawing group giving the greatest sensitization. In tests with mice, 8-mercaptoquinoline showed protection against x radiation. Although highly toxic by itself, when used in combination with AET it increased the protection afforded by the latter. (auth)

4554 ANALYSIS OF THE RADIOPROTECTIVE EFFECT OF CYSTEINE ON ESCHERICHIA COLI STRAINS. Hernadi, F.; Nagy, Zs.; Kovacs, Ps.; Kari, Cs. (Univ. Medical School, Debrecen, Hungary). pp 167-70 of Radiation Protection and Sensitization. /Moroson, Harold (ed.). New York; Barnes and Noble, Inc. (1970).

From 2nd International Symposium on Radiosensitizing and Radioprotective Drugs, Rome, Italy. See CONF-690525.

Log-phase cultures of Escherichia coli 15 T^- were supplemented with 2 mM L-cysteine. The growth, as well as the synthesis of protein and RNA ceased immediately after the addition of cysteine, while that of DNA proceeded for 30 min. The radioresistance of bacteria, as studied by x-irradiating the cells in cysteine-free buffer, increased precipitously in the 1st min of the cysteine treatment, then slowly to the 30th min. After return to normal growth conditions, i.e. removal of cysteine, growth, as well as the synthesis of protein and RNA began immediately while that of DNA was resumed only after 25 min. Simultaneously, the radioresistance of bacteria showed an immediate decline followed by a slow decrease. The instantaneous rise and fall in radioresistance prior to and subsequently to the cysteine treatment seems to be related to the alterations of the acid-soluble sulphydryl content of the cells, while the second, slow rise and decline to the repair capacity of the bacteria. (auth)

4555 X-RAY SENSITIVITY OF E. COLI B CELLS AS AFFECTED BY CYSTEINE. Nagy, Zs.; Quintiliani, M. (Istituto Superiore di Sanita, Rome). pp 171-6 of Radiation Protection and Sensitization. /Moroson, Harold (ed.). New York; Barnes and Noble, Inc. (1970).

From 2nd International Symposium on Radiosensitizing and Radioprotective Drugs, Rome, Italy. See CONF-690525.

The x-radiosensitivity of growing E. coli B was significantly decreased when actively metabolizing cells were incubated with a growth inhibiting concentration of cysteine, which was washed away before irradiation. In condition where cell metabolism was reduced, or when cysteine was added to metabolizing cells in concentration not interfering with growth, the radiosensitivity remained unchanged. No correlation has been found between the occurrence of radioprotection, the amount of cysteine incorporated in micro-organisms, and its distribution in the following cell fractions: cold TCA extract, ethanol–ether extract, hot TCA extract, and residue. (auth)

4556 INFLUENCE OF CYCLOHEXIMIDE ON THE RADIOSENSITIVITY OF SACCHAROMYCES CEREVISIAE. Stehlik, G.; Cabela, E. (Reactor Centre, Seibersdorf, Austria). pp 177-81 of Radiation Protection and Sensitization. /Moroson, Harold (ed.). New York; Barnes and Noble, Inc. (1970).

From 2nd International Symposium on Radiosensitizing and Radioprotective Drugs, Rome, Italy. See CONF-690525.

In order to reduce the radiation dose in fruit juice preservation a number of combination treatments using γ radiation and chemicals were investigated. The effectiveness of cycloheximide, which is antibiotically effective against yeasts and fungi, was proved on the very radioresistant yeast strain Saccharomyces cerevisiae var. ellipsoideus using a semi-synthetic culture medium. Cycloheximide in its aqueous solution was not destroyed by γ radiation in the investigated dose range up to 500 krad. Growth curves for Sacch. cerevisiae var. ellipsoideus in a semi-synthetic culture medium with different concentrations of cycloheximide and γ radiation treatment were investigated over a period of 72 hr. Normally a concentration of 5 ppm is necessary for a total growth-inhibition of this yeast strain within 72 hr. If the antibiotic treatment is combined with γ radiation a synergistic effect occurs whereby a concentration of 1 ppm and an irradiation dose of 200 krad is sufficient to inhibit growth completely for this period of time. (auth)

4557 RADIOSENSITIZATION OF BACTERIAL AND MAMMALIAN CELLS WITH CARBONYL COMPOUNDS AND KETOALDEHYDES WITH SPECIAL REFERENCE TO THE PROPERTIES OF PHENYLGLYOXAL. Ashwood-Smith, M. J.; Barnes, J.; Huckle, J.; Bridges, Bryn A. (Medical Research Council, Harwell, Eng.). pp 183-8 of Radiation Protection and Sensitization. /Moroson, Harold (ed.). New York; Barnes and Noble, Inc. (1970).

From 2nd International Symposium on Radiosensitizing and Radioprotective Drugs, Rome, Italy. See CONF-690525.

A variety of carbonyl compounds such as diacetyl, ninhydrin, isatin, acetylisatin, cyclohexane dione, and phthalimide have been tested for radiosensitization properties against bacteria and mammalian cells in tissue culture. Ninhydrin and isatin were excellent to radiosensitizers of Serratia marcescens under anoxic conditions. However when tested for activity with Chinese hamster cells in tissue culture they were without effect. Studies with phenylglyoxal (1×10^{-4} M) have shown that it preferentially sensitizes anoxic cells in tissue culture to the lethal effects of x rays. The sensitization factor is nearly 2 (normal oxygen factor is between 2 and 2.6 for these cells). Oxygenated cells show only a small sensitization with phenylglyoxal. Sensitization takes place in the presence of 10 per cent serum. Post-irradiation treatment of cells with phenylglyoxal is ineffective and irradiated solutions of phenylglyoxal given to irradiated cells are without effect. This chemical is non-toxic to cells at the concentration used. The approximate LD_{50} for mice is eighteen times (1.8×10^{-3} M) greater than the effective dose to anoxic tissue culture cells. Chemical studies indicate that phenylglyoxal reacts rapidly with cysteine but less rapidly with glutathione. It is not known if this reactivity is connected with the mode of action of phenylglyoxal. (auth)

4558 DRUG-RADIATION DAMAGE INTERACTION AND ITS RELEVANCE TO RADIOSENSITIZATION IN MAMMALIAN CELLS. Elkind, M. M.; Kano, E.; Sakamoto, K. (National Cancer Inst., Bethesda, Md.). pp 195-200 of Radiation Protection and Sensitization. /Moroson, Harold (ed.). New York; Barnes and Noble, Inc. (1970).

From 2nd International Symposium on Radiosensitizing and Radioprotective Drugs, Rome, Italy. See CONF-690525.

When untreated cultured Chinese hamster cells are x irradiated, division is suppressed probably because of damage registered in a particular set of primary sites. Damage caused by energy absorption is registered in other loci as well. In some situations, an enhanced radiation response might be effected if, because of drug treatment, residual damage in secondary sites becomes extensive enough to compete with residual damage in primary sites. A more direct approach to radiosensitization would seem to be to treat cells with agents known (or at least thought) to interact at the primary radiation sites. The antibiotic actinomycin D and the bifunctional alkylating agent nitrogen mustard [$CH_3N(C_2H_4Cl)_2$] are toxic drugs and are both known to bind to DNA in mammalian cells. If we assume that radiation cell killing is caused by genomic damage, we might expect that treatment with either drug would lead to radiation sensitization. Contrary to expectation, sensitization results only from actinomycin D. The dose dependence of nitrogen mustard cell killing suggests, however, that this drug and radiation could still be acting on the same sites but in a way that does not result in sensitization. Thus, the point emerges that even when a common locus of action of a drug and radiation is involved, this by itself may not be a sufficient condition to ensure sensitization. In a given instance, drug and radiation lesions may be registered in the same molecular species but they may be of such a nature that independent action results. (auth)

4559 SENSITIZATION BY HYDROXYUREA AND PROTECTION BY CYSTEAMINE OF CHINESE HAMSTER CELLS DURING THE CELL CYCLE. Sinclair, Warren K. (Argonne National Lab., Ill.). pp 201-10 of Radiation Protection and Sensitization. /Moroson, Harold (ed.). New York; Barnes and Noble, Inc. (1970).

From 2nd International Symposium on Radiosensitizing and Radioprotective Drugs, Rome, Italy. See CONF-690525.

Hydroxyurea inhibits DNA synthesis in Chinese hamster cells and is selectively toxic for cells in DNA synthesis (i.e., in S phase) at the time of exposure to the drug. The presence of hydroxyurea also sensitizes cells to x radiation in the following

way: synchronized cells in G_1 inhibited from entering S by hydroxyurea become steadily more sensitive for a period of about four hr and then recover about a normal G_1 sensitivity in approximately a further four hr. They never achieve the high survival level normally found for uninhibited cells in late S, but they will reach this level quite rapidly if the hydroxyurea is removed prior to exposure. The sensitization is, therefore, completely reversible. Hydroxyurea has no effect if present during exposure only. Additional sensitization is obtained however if the drug is also present after exposure. This post-irradiation sensitization is independent of the time in the cycle at which inhibited cells are irradiated. Cysteamine present during x irradiation protects synchronized Chinese hamster cells in culture against lethal damage at all stages of the cell cycle. The effect is greatest for cells irradiated at sensitive stages such as mitosis and least for resistant cells, for example, late S (dose-modifying factors ~5 and ~3 respectively). The effect of 50 mM cysteamine is to partially level off the normally varying x ray age response for lethality. This suggests that there may be two major components of x ray damage, only one of which is age dependent, and it is against this component that cysteamine protects the cells. Cystamine, however, has no protective effect upon these cells at any stage of the cell cycle. Cysteamine also protects partially against the sensitization induced by hydroxyurea in G_1 cells (i.e. the dose modifying factor for inhibited cells is greater than for uninhibited cells), the effect again being toward a levelling of the normal age response of inhibited cells. (auth)

4560 RADIATION PROTECTION BY DISULPHIDES IN TISSUE CULTURE. Vos, O. (National Defence Research Organization, Rijswijk, Netherlands); Grant, G. A.; Budke, L. pp 211-15 of Radiation Protection and Sensitization. /Moroson, Harold (ed.). New York; Barnes and Noble, Inc. (1970).

From 2nd International Symposium on Radiosensitizing and Radioprotective Drugs, Rome, Italy. See CONF-690525.

The protective capacity of a number of thiol and disulfide compounds was studied at the cellular level in tissue culture. Reproductive integrity was used as parameter for protection. Cysteamine (and other thiol compounds) provides protection against x radiation in the usual growth medium, whereas cystamine only protects when rat blood is added to the medium. The influence of the concentration of blood and pre-incubation times has been studied. The results are explained by the inference that rat blood cells contain a reductase that converts some disulfide compounds to thiols. (auth)

4561 COMPOSITE RADIOPROTECTIVE AND RADIOSENSITIZING EFFECT OF AN ORGANIC FREE RADICAL. Revesz, L.; Littbrand, B. (Karolinska Institutet, Stockholm). pp 217-24 of Radiation Protection and Sensitization. /Moroson, Harold (ed.). New York; Barnes and Noble, Inc. (1970).

From 2nd International Symposium on Radiosensitizing and Radioprotective Drugs, Rome, Italy. See CONF-690525.

The clonogenic survival of a Chinese hamster cell line was studied after exposure in vitro to different, single, or divided x ray doses in the presence of varying concentrations of Triacetoneamine-N-oxyl (TAN). When exposures were made under anoxic conditions in argon, the extrapolation number of the survival curve of TAN-treated cells was increased in comparison to the controls. When exposures were made under aerobic conditions, the extrapolation numbers remained unaltered. The split-dose ratio was changed by TAN in a way comparable to the change of the extrapolation number, being larger than unity when exposures were made in anoxia, and unaltered when they were performed aerobically. The slope of the anoxic survival increased by treatment with TAN at concentrations between 0.25–2 mM, but was unaffected when the concentration was 20 mM. The observations find an explanation in the hypothesis that TAN sensitizes by a similar mechanism as the sensitization caused by oxygen; substitutes for oxygen in the recovery process; and at high concentrations, scavenges radiation induced radicals. (auth)

4562 INDANETRIONE, MENADIONE, SYNKAVIT, AND N-ETHYLMALEIMIDE TESTED AS RADIOSENSITIZERS ON MURINE ASCITIC TUMOUR IRRADIATED IN VITRO AND GROWN IN VIVO. Di Vita, G.; Marrian, D. H. (Cambridge Univ., Eng.). pp 225-31 of Radiation Protection and Sensitization. /Moroson, Harold (ed.). New York; Barnes and Noble, Inc. (1970).

From 2nd International Symposium on Radiosensitizing and Radioprotective Drugs, Rome, Italy. See CONF-690525.

Mice with growing ascitic tumors show a standard increase in body-weight of at least five g in three days; the tumor time between day of inoculation and day of completed standard increase is inversely proportional to the logarithm of the number of viable cells inoculated. Suspensions of ascitic tumor cells were incubated in vitro with chemical compounds, x irradiated in vitro, and then inoculated intraperitoneally into mice; the tumor time was used to estimate the radiosensitizing effect of the compound. Indanetrione produced a marked radiosensitization; also N-ethylmaleimide and menadione bisulphite enhanced the effect of radiation; Synkavit did not show any radiosensitizing effect in this test. (auth)

4563 EFFECT OF POLYCATION ON TUMOUR CELLS IN VIVO. Furlan, M.; Moroson, H. (Sloan-Kettering Inst. for Cancer Research, Rye, N. Y.). pp 233-42 of Radiation Protection and Sensitization. /Moroson, Harold (ed.). New York; Barnes and Noble, Inc. (1970).

From 2nd International Symposium on Radiosensitizing and Radioprotective Drugs, Rome, Italy. See CONF-690525.

One of the chief obstacles to the cure of animal or human tumors has been lack of ability to selectively destroy cancer cells more than normal cells. Generalized cytotoxic effects limit most drug dosages. A physical feature distinguishing some cancer cells from normal cells is their greater surface membrane electronegativity, as shown by electrophoretic measurements, by reduced adhesiveness and by failure of contact inhibition in sarcoma cells (Easty, Easty, and Ambrose 1960; Ambrose 1966). It is postulated that polycations bound to tumor cells may upset the cellular radiation repair system. Results of experiments designed to test this possibility have shown positive effects with the ascitic and solid form of Ehrlich carcinoma in Swiss mice x irradiated in vivo in the presence and absence of nontoxic doses (60 to 120 mg/kg) of polyethyleneimine injected intraperitoneally or subcutaneously. (auth)

4564 RADIOSENSITIZING EFFECT OF L-ERYTHRO-α, β-DIHYDROXYBUTYRALDEHYDE ON EHRLICH ASCITES TUMOUR CELLS. CYTOKINETIC ANALYSIS OF TUMOUR GROWTH. Perin, A. (Univ., Milan); Arnaboldi, A.; Sessa, A.; Scalabrino, G.; Ciaranfi, E.; Castellani, A. pp 243-4 of Radiation Protection and Sensitization. /Moroson, Harold (ed.). New York; Barnes and Noble, Inc. (1970).

From 2nd International Symposium on Radiosensitizing and Radioprotective Drugs, Rome, Italy. See CONF-690525.

An in vivo/in vitro technique was used, measuring the kinetic of in vivo growth of adrenocarcinoma Ehrlich ascites cells in the ascitic fluid, injecting cells pretreated in vitro with dihydroxybutyraldehyde (DIBA), x rays, and DIBA plus x rays. The kinetics of untreated tumor cells growth in mice show an exponential increase of cell number up to the 3rd or 4th day from inoculation followed by a progressive decrease of growth. The treatment with DIBA or x rays leads to a slow-down or blockage of the tumor growth in relation to the concentration, length of treatment with DIBA, or x ray dose. The treatment with 5 mM DIBA at 37°C for 30 min or the irradiation with 750 rad lead, within the first three days, to a slowdown of the tumor growth, while the tumor afterwards develops in a similar way as the control. The combined action of DIBA and x rays leads to an immediate and progressive decrease of the number of tumor cells, followed by their total disappearance from the ascitic fluid. (auth)

4565 ^{60}Co GAMMA-RAY EFFECT ON MOUSE EHRLICH ASCITES TUMOUR CELLS IN THE PRESENCE OF SOME COUMARIN DERIVATIVES. Musajo, L.; Bordin, F.; Busulini, L.; Baccichetti, F.; Bevilacqua, R. (Univ. of Padua). pp 245-9 of Radiation Protection and Sensitization. /Moroson, Harold (ed.). New York; Barnes and Noble, Inc. (1970).

From 2nd International Symposium on Radiosensitizing and Radioprotective Drugs, Rome, Italy. See CONF-690525.

The influence of 5,9-dihydroxypsoralen on the transmissibility of Ehrlich ascites tumor cells following exposure to ^{60}Co γ rays has been studied. At concentrations non-toxic for cells the drug has shown a marked radiosensitizing activity. In fact, the animals after the injection of tumor cell suspensions irradiated in its presence have shown a decrease in mortality and an increase in the mean survival time in comparison with controls. This effect was greatly reduced or quite absent when the 5,9-hydroxypsoralen (also when separately pre-irradiated) was added after the irradiation of cell suspensions. Therefore, 5,8-dihydroxypsoralen can be considered a new radiosensitizing substance for Ehrlich ascites tumor cells. (auth)

4566 RADIOPROTECTION AND MODIFICATION OF GLYCOLYSIS IN EHRLICH ASCITES TUMOUR CELLS. Ciccarone, P.; Palitti, F. ; Seganti, L. (CNEN, Rome). pp 251-5 of Radiation Protection and Sensitization. /Moroson, Harold (ed.). New York; Barnes and Noble, Inc. (1970).

From 2nd International Symposium on Radiosensitizing and Radioprotective Drugs, Rome, Italy. See CONF-690525.

In order to investigate whether changes in carbohydrates metabolism induced by the administration of some radioprotective drugs may play a role in the mechanism of radiopro-

tection, the possible radioprotective action of oxamic acid, which inhibits lactic acid dehydrogenase, was investigated. Tests were carried out on diploid Ehrlich ascites tumor cells, the survival of which after x irradiation in the presence or absence of oxamic acid was evaluated by measuring the number of them which had to be injected in the brain of C 57Bl mice to cause the death of 50 per cent of animals at 30 days by brain tumor. The metabolic conditions of cells have also been evaluated and the assay of intermediate metabolites showed that glycolysis was deeply disturbed. Under such conditions evidence of a radioprotective effect of oxamic acid was obtained. (auth)

4567 METHYL HYDRAZINE RADIOSENSITIZED EHRLICH ASCITES TUMOUR CELLS. Moroson, H.; Furlan, M. (Sloan-Kettering Inst. for Cancer Research, Rye, N. Y.). pp 257-63 of Radiation Protection and Sensitization. /Moroson, Harold (ed.). New York; Barnes and Noble, Inc. (1970).

From 2nd International Symposium on Radiosensitizing and Radioprotective Drugs, Rome, Italy. See CONF-690525.

Methyl hydrazine (MH) is a reducing agent and electron donor previously found to sensitize bacterial cells to radiation killing. This agent has been investigated for its possible x radiosensitizing effect on Ehrlich ascites tumor cells in vivo. At a combined dosage of MH and x radiation not lethal to the host, an enhanced radiation killing of tumor cells in vivo over that resulting from the use of each agent alone is observed. When Ehrlich ascites cells labeled with tritiated thymidine and treated in vitro with MH are layered upon an alkaline sucrose density gradient and centrifuged for 15 min at 25,000 rpm the sedimentation behavior of cellular DNA resembles that obtained from cells receiving a very large dose of x radiation, i.e. appearance of a great many single-strand breaks. If MH is present during incubation of these cells, the apparent single-strand breakage effect is enhanced, while if MH is absent, the amount of single-strand breakage is decreased. Interpretation of density gradient profiles is difficult because of their polydispersity, but the apparent enhancement of DNA strand breakage by MH may explain the enhanced cell killing effect when combined with x radiation. (auth)

4568 CELL MEMBRANE CHARACTERISTICS OF EHRLICH ASCITES TUMOUR CELLS IRRADIATED WITH SMALL DOSES OF IONIZING RADIATIONS IN THE PRESENCE OF RADIOPROTECTIVE AND RADIOSENSITIZING DRUGS. Mehrishi, J. N. (Cambridge Univ., Eng.). pp 265-73 of Radiation Protection and Sensitization. /Moroson, Harold (ed.). New York; Barnes and Noble, Inc. (1970).

From 2nd International Symposium on Radiosensitizing and Radioprotective Drugs, Rome, Italy. See CONF-690525.

The effect of 210 kV x rays, 15 MeV x rays, and electron radiation from a linear accelerator on the permeability of Ehrlich ascites tumor cell membrane has been studied in vitro by measuring the loss of potassium ions from the cells. Cell suspensions in saline were irradiated with doses over the range 50 to 10,000 rad in the presence of air, excess oxygen, 2-methyl-1,4-naphthaquinol bis(disodium phosphate) (MNDP) (Synkavit), 2-amino-3-methyl butane thiol (AMBT) cysteamine, citraconic anhydride (CA), 2,3-dimethylmaleic anhydride (DMA), and diacetyl (10^{-3} M). The radiosensitizing effects of MNDP, oxygen, and the radioprotecting effects of cysteamine and AMBT are clearly demonstrated. Treatment with CA and DMA and diacetyl block the cell surface groups and modify the radiation damage to the cell membrane which appears to be the obvious site of biochemical damage. (auth)

4569 IN VITRO RADIOSENSITIZATION OF EHRLICH ASCITES TUMOUR CELLS AND PURE ENZYMES BY IODINE COMPOUNDS. Cancelliere, G.; Misiti-Dorello, P.; Shejbal, J. (Istituto Superiore di Sanita, Rome). pp 275-80 of Radiation Protection and Sensitization. /Moroson, Harold (ed.). New York; Barnes and Noble, Inc. (1970).

From 2nd International Symposium on Radiosensitizing and Radioprotective Drugs, Rome, Italy. See CONF-690525.

The radiosensitizing effect of several iodine compounds in dilute solution on two experimental models, Ehrlich ascites cells and SH-enzymes, was studied. The release of potassium ions from Ehrlich ascites tumor cells after the irradiation of suspensions by low doses of x rays (50 to 800 rad) was observed. Iodoacetic acid (IAA), sodium iodide, iodopropionic acid (IPA), and methyl iodide (MeI) in concentrations in the order of 10^{-4} M, enhanced post-irradiation potassium release from cells into the medium, their dose modifying effect diminishing in the order IAA > NaI > IPA > MeI. The dose modifying capacity of NaI, IPA, and MeI was further studied on four enzymes, alcohol dehydrogenase, lactic acid dehydrogenase, hexokinase, and glyceraldehyde phosphate dehydrogenase, in dilute solutions. X ray doses ranged from 600 to 20,000 rad. The dose modifying effect of the sensitizing compounds diminished in the same order as with Ehrlich ascites tumor cells. (auth)

4570 RADIOSENSITIZING EFFECT OF MITOMYCIN C ON HAEMATOPOIETIC COLONY FORMING CELLS. Duplan, J. F.; Fuhrer, J. (Institut du Radium, Paris). pp 281-7 of Radiation Protection and Sensitization. /Moroson, Harold (ed.). New York; Barnes and Noble, Inc. (1970).

From 2nd International Symposium on Radiosensitizing and Radioprotective Drugs, Rome, Italy. See CONF-690525.

The radiosensitizing activity of Mitomycin C (MC), 5-Fluorouracil (5-FU), and Actinomycin D (AD) (Dactinomycin) has been evaluated with the technique based on the ability of bone marrow cells to form spleen colonies following transplantation into syngenic mice. Dose-effect curves demonstrate that MC is a true radiosensitizer while both 5-FU and AD add only their lethal effect to that of x rays. The D_0 value which is 65R for controls is not significantly changed after a treatment with 5-FU (53R) or AD (59R) but goes down to 37R when the donors have received MC. With this last drug, the dose increment factor (DIF) is close to 1·7. It is noted that the shoulder of the curves seems to disappear when the CFC have been treated with one of these three chemicals. Further investigations have been carried out to study the early repair of radiosensitized CFC. These cells when irradiated with 100 R, have recovered 70 per cent of their normal radiosensitivity (early cell repair) 5 hr after exposure to x rays. Cellular alterations induced by MC alone do not show any spontaneous recovery (measured by a return to normal of their radiosensitivity) within the same period of time. Pretreatment with MC does not increase the cellular damage susceptible to spontaneous repair and does not inhibit the mechanism responsible for this. The surviving fraction of the CFC treated with MC and x radiation shows a decreased sensitivity to the lethal effect of a second dose of x rays. (auth)

4571 PROTECTIVE EFFECT OF PARA-AMINOPROPIOPHENONE AND PROPYLENE GLYCOL ON THE HAEMATOPOIETIC STEM CELLS OF MICE. Vacek, A.; Davidova, E. (Inst. of Biophysics, Brno). pp 289-93 of Radiation Protection and Sensitization. /Moroson, Harold (ed.). New York; Barnes and Noble, Inc. (1970).

From 2nd International Symposium on Radiosensitizing and Radioprotective Drugs, Rome, Italy. See CONF-690525.

The method of endogenous and exogenous spleen colony formation in syngenic mice was adopted for estimation of the protective effect of para-aminopropiophenone (PAPP) and propylene glycol (PG). The dose of PAPP was 50 mg/kg, and PG was injected in a dose 10 g/kg of body weight. The protective effect of PAPP and PG was established when injected intraperitoneally 15 min prior to exposure by x rays. Administration of PAPP in PG or PG alone, reduced the proliferative capacity of hematopoietic stem cells and 6 hr ^{59}Fe uptake in femur and spleen of non-irradiated mice. (C.H.)

4572 RADIOPROTECTIVE ACTION OF HAEMATOPORPHYRIN ON ENDOGENOUS SPLEEN COLONY-FORMING UNITS. Cittadini, G.; Lanfredini, L.; Mancini, G. (Univ., Siena, Italy). pp 295-8 of Radiation Protection and Sensitization. /Moroson, Harold (ed.). New York; Barnes and Noble, Inc. (1970).

From 2nd International Symposium on Radiosensitizing and Radioprotective Drugs, Rome, Italy. See CONF-690525.

Hematoporphyrin chlorhydrate (5 mg/kg i.p.) was administered to DBA/2 mice 72, 48, 24 hr, or 30 min before whole-body γ irradiation (^{60}Co; 750 and 850 rad). On the tenth day animals were bled, spleens removed, weighed, and fixed for hematopoietic colony counts. When administered 72, 48, or 24 hr hematoporphyrin induced no difference in spleen weights and colony counts in regard to control animals treated with saline. When administered 30 min before irradiation hematoporphyrin induced a significant increase in the number of colonies. This effect seems really expressive of a radioprotective action. The relation between the general radiosensitization demonstrated by survival tests and the radioprotection of hematopoietic stem cells is briefly discussed. (auth)

4573 SENSITIZATION OF ANOXIC FERN SPORES TO X-RAYS BY CHEMICALS KNOWN TO BE EFFECTIVE IN BACTERIA. Foster, J. L. (Christie Hospital and Holt Radium Inst., Manchester, Eng.). pp 299-303 of Radiation Protection and Sensitization. /Moroson, Harold (ed.). New York; Barnes and Noble, Inc. (1970).

From 2nd International Symposium on Radiosensitizing and Radioprotective Drugs, Rome, Italy. See CONF-690525.

Several drugs have been tested for their ability to sensitize anoxic spores of the fern Osmunda regalis to the cell killing effects of x rays. Spores were suspended in solutions of diacetyl

XUM

(10, 6, and 3 mM), indanetrione (1 mM), indanone (10 mM), isatin (10 mM), N-ethylmaleimide (100 μM), dehydroascorbic acid (10 mM), ethylpyruvate (10 mM), p-chloroacetophenone (300 μM), and tetramethylpiperidine N-oxide (10 mM) for periods of up to two hr before irradiation. Suspensions were made anoxic by bubbling with pure nitrogen for 30 min before and during irradiation. On a comparison of survival curves of treated and untreated spores only diacetyl and isatin showed a sensitizing effect (ratios of D_0 controls/treated 1.5 and 1.4 respectively). The ability of these compounds to sensitize anoxic fern spores is not clearly related to their ability to sensitize other systems. (auth)

4574 DOSE-MODIFYING FACTORS AND INHIBITORS OF REPAIR. Howard, Alma (Christie Hospital and Holt Radium Inst., Manchester, Eng.). pp 305-8 of Radiation Protection and Sensitization. /Moroson, Harold (ed.). New York; Barnes and Noble, Inc. (1970).

From 2nd International Symposium on Radiosensitizing and Radioprotective Drugs, Rome, Italy. See CONF-690525.

A radiation sensitizer is defined as an agent that increases a given radiation response when present during the radiation exposure. If we accept this definition, hypoxia must be regarded as a sensitizer if the radiation exposure is long enough (say 15 min) to allow time for significant repair, and if hypoxia blocks the repair process. Relevant experiments were performed with the green algae Oedogonium cardiacum. In this plant, split-dose x irradiation experiments show that survival does not increase if the cells are kept hypoxic (<0.01 μM O_2) after the first dose. On the other hand, survival increases promptly provided O_2 is present. Therefore hypoxia blocks repair. At low dose-rates, hypoxia during irradiation will therefore increase the lethal effect. Hypoxia thus acts as a sensitizer. This action will be difficult to demonstrate: a reduced OER is, however, expected. If potassium cyanide (KCN) is present between the two fractions of a split dose, survival is even lower than if hypoxia is present. Other experiments showed that KCN enhances the effect of single doses when given either before, during, or after irradiation. Potassium cyanide can be regarded as an inhibitor of repair of potentially lethal damage. (auth)

4575 CHEMICAL SENSITIZATION OF THE DAMAGING EFFECTS ON EMBRYOS PRODUCED BY LOW RADIATION DOSES: THE ROLE OF ENERGY METABOLISM AND IMMEDIATE REPAIR. Fritz-Niggli, Hedi; Michel, Chr. (Univ., Zurich). pp 311-17 of Radiation Protection and Sensitization. /Moroson, Harold (ed.). New York; Barnes and Noble, Inc. (1970).

From 2nd International Symposium on Radiosensitizing and Radioprotective Drugs, Rome, Italy. See CONF-690525.

Nine-day-old rat embryos in utero were x irradiated with 12.5, 25, 50, and 100 R. Iodoacetamide in a concentration of 0.925 mg/kg body weight was administered by intraperitoneal injection one hr before irradiation. The fetuses were examined microscopically and macroscopically four days after irradiation for signs of radiation damage. Special attention was paid to malformation in the head region. Malformations occurred at doses as low as 12.5 R. Reduced body size, microcephaly, brain hernias, anophtalmia, microphtalmia, and other anomalies in the development of the eyes and brain were observed. The injection of 0.925 mg/kg iodoacetamide (IA) one hr before irradiation increased the number of anomalies significantly. The results indicate that the injurious effects of small doses of radiation in embryo tissue can apparently be potentiated by chemical agents in otherwise innocuous concentrations. (C.H.)

4576 CHEMICAL PROTECTION OF MICE INFLICTED WITH IRRADIATION AND OPEN SKIN WOUNDS. Messerschmidt, Otfried; Birkenmayer, Eline (Univ., Freiburg i. B.). pp 319-23 of Radiation Protection and Sensitization. /Moroson, Harold (ed.). New York; Barnes and Noble, Inc. (1970).

From 2nd International Symposium on Radiosensitizing and Radioprotective Drugs, Rome, Italy. See CONF-690525.

Mice with open skin wounds were exposed to whole-body x irradiations (510 R). If wounds (causing a lethality of 6 per cent) were set at different intervals after irradiation, radiation lethality was increased from 20 up to 72 per cent. The lethality of irradiated animals and of those inflicted with combined injuries could be reduced to less than 10 per cent by pre-treatment with 5-hydroxytryptamine (serotonin) or cysteamine. (auth)

4577 RADIOPROTECTIVE EFFECT OF N-SUBSTITUTED AET-DERIVATIVES HAVING AMINO ACID STRUCTURE. Varteresz, V.; Sztanyik, B. L.; Nador, K. (Veterinary Univ., Budapest). pp 325-9 of Radiation Protection and Sensitization. /Moroson, Harold (ed.). New York; Barnes and Noble, Inc. (1970).

From 2nd International Symposium on Radiosensitizing and Radioprotective Drugs, Rome, Italy. See CONF-690525.

Substitution by amino acids or dipeptides in the isothiuronium group of AET molecule reduces the toxicity of the compound. The majority of such derivatives are still radioprotective, and the radioprotective activity of some of them is the same or only slightly less than that of the parent compound. However, to obtain a radioprotective effect equivalent to that of AET, the administered dose has to be increased roughly in proportion with the decrease of toxicity. Several experiments were performed on the duration of the radioprotective effect in mice exposed to doses of 630 to 1000 R x radiation. In these cases pretreatment was timed 10, 30, 60, and 120 min prior to the beginning of exposure. No significant differences were found compared to the duration of the radioprotective effect of AET. Accordingly, the substitutions introduced did not result in any prolongation of the protective activity. (C.H.)

4578 RADIOPROTECTION BY HYPOXIA AND SOME CHEMICAL PROTECTORS. Veninga, T. S.; Lemstra, W. (Univ., Groningen, Netherlands). pp 331-4 of Radiation Protection and Sensitization. /Moroson, Harold (ed.). New York; Barnes and Noble, Inc. (1970).

From 2nd International Symposium on Radiosensitizing and Radioprotective Drugs, Rome, Italy. See CONF-690525.

Hypoxic treatment affording protection against ionizing irradiation stimulates the anaerobic glycolysis as can be deduced from the observed increase of lactic acid in blood and urine and the elevation of the blood glucose level immediately after hypoxia. In contrast, alloxan-diabetis, known to cause a blockage of glycolysis, abolished the protective action of hypoxia in x-irradiated mice. These observations may indicate that the protection afforded by hypoxia elapses through a recovery mechanism which is brought into action by the hypoxic treatment. (auth)

4579 RADIOPROTECTIVE EFFECTS OF SODIUM FLUOROACETATE AND ITS PROBABLE MECHANISM OF ACTION. Novak, L. (Inst. of Biophysics, Brno). pp 335-41 of Radiation Protection and Sensitization. /Moroson, Harold (ed.). New York; Barnes and Noble, Inc. (1970).

From 2nd International Symposium on Radiosensitizing and Radioprotective Drugs, Rome, Italy. See CONF-690525.

Results of experiments carried out on mice irradiated at the age of 9 to 12 weeks with x rays (180 kV, 15 mA, 0.5 mm Cu, 0.5 mm Al, 43 R/min), showed that intraperitoneal administration of 5 or 7.5 mg/kg c (FA) in physiological saline affords a very marked protection against the effect of ionizing radiation, lasting roughly from 30 to 40 min till seven hr after application of the compound. The maximum effect was reached between one and two hr following FAc administration, when the value LD 50/30 shifts to 935 to 998 R, compared with 648 R in the control group. A comparison of these data with the results obtained with other radioprotectors, such as cysteine, cysteamine, AET, or serotonine, shows that FAc possesses a similar radioprotective effect as the listed compounds. The effect of FAc, however, depends primarily on the selective blockage of a single enzyme, i.e., aconitase. (auth)

4580 IMPORTANCE OF HYPOTHERMY IN THE MECHANISM OF THE PROTECTIVE ACTION OF SODIUM FLUOROACETATE. Misustova, J.; Novak, L. (Inst. of Biophysics, Brno). pp 343-7 of Radiation Protection and Sensitization. /Moroson, Harold (ed.). New York; Barnes and Noble, Inc. (1970).

From 2nd International Symposium on Radiosensitizing and Radioprotective Drugs, Rome, Italy. See CONF-690525.

The role of temperature in the mechanism of radioprotective action of sodium fluoroacetate (FAc), was studied on H-strain male mice, aged 9 to 12 weeks. After FAc application (5 mg/kg body weight) animals were kept at temperatures 17°, 23°, and 30°C and x irradiated at these temperatures with 800 R. Change of ambient temperature in the course of intoxication by FAc significantly influences the body temperature of experimental animals, but does not affect the degree of protection or its time course. These results correspond with the opinion that the degree of protection by FAc is determined by the consequences of blocking of aconitase, which is proportional to FAc dose, rather than hypothermy. (auth)

4581 PROTECTIVE EFFECT OF CYSTAMINE, AET, SEROTONIN, AND MEXAMINE AGAINST FRACTIONATED LETHAL GAMMA-IRRADIATION. Dostal, M. (Purkyne Medical Research and Postgraduate Inst., Hradec Kralove, Czech.). pp 349-53 of Radiation Protection and Sensitization. /Moroson, Harold (ed.). New York; Barnes and Noble, Inc. (1970).

From 2nd International Symposium on Radiosensitizing and Radioprotective Drugs, Rome, Italy. See CONF-690525.

The protection obtained by cystamine was found to be significant using lethality of rats, mid-lethal exposure, and fractionated ^{60}Co γ irradiation as criteria. In the mid-lethal and lethal expo-

sure level serotonin and mexamine surpassed the sulphur-containing compounds in ability to protect against lethality after fractionated irradiation. (auth)

4582 REDUCTION OF SHORT- AND LONG-TERM RADIATION EFFECTS BY MIXTURES OF CHEMICAL PROTECTORS. Maisin, J. R.; Mattelin, G.; Lambiet-Collier, M. (Centre d'Etude de l'Energie Nucleaire, Mol, Belg.). pp 355-61 of Radiation Protection and Sensitization. /Moroson, Harold (ed.). New York; Barnes and Noble, Inc. (1970).

From 2nd International Symposium on Radiosensitizing and Radioprotective Drugs, Rome, Italy. See CONF-690525.

Mixtures of chemical radioprotective drugs are known to increase markedly the short-time survival of x irradiated mice. In the present experiments a dose reduction factor of 2.8 has been observed for the LD 50/30 days of BALB/c^+ mice (LD 50/30 days: 576 R and LD 99/30 days: 750 R) treated with a mixture of 2-β-aminoethylisothiouronium-Br-HBr, mercapto-ethylamine, cysteine (cyst), glutathione and 5-hydroxytryptamine, prior to an x-ray exposure. Long-term survival after a single dose of x-rays is also improved significantly by administration of a mixture of chemical protectors. The total number of cancers and of leukaemia observed in the protected mice (1350 R) is about 2 to 3 times smaller than in the non-protected ones (650–700 R). On the other hand, many of the mice irradiated with 1350 R and most of the mice irradiated with a dose of 2000 R die of radiation pneumonitis. Survival after repeated doses at intervals of 15, 30, or 60 days was also studied in mice protected with AET alone or with a mixture of radioprotectors. Protected mice with a mixture of five radioprotectors and irradiated at an interval of 30 days die after a cumulative dose of 6000, 6400, 6000, and 4800 R, when the single doses are 600, 800, 1000, or 1200 R respectively. Non-protected mice exposed to doses of 400 or 600 R at an interval of 30 days, die after a cumulative dose of 3600 and 1200 R respectively. The beneficial value of mixtures of radioprotectors was limited by the incidence of chemical toxicity. Many of the mice which did not die of toxicity, show radiation pneumonitis. (auth)

4583 RADIOPROTECTIVE EFFECT OF A MIXTURE OF AET AND 5-METHOXYTRYPTAMINE IN X-IRRADIATED MICE. Sztanyik, B. L.; Varteresz, V. (Frederic Joliot-Curie National Research Inst. for Radiobiology and Radiohygiene, Budapest). pp 363-7 of Radiation Protection and Sensitization. /Moroson, Harold (ed.). New York; Barnes and Noble, Inc. (1970).

From 2nd International Symposium on Radiosensitizing and Radioprotective Drugs, Rome, Italy. See CONF-690525.

The toxicity and the radioprotective effect of mixtures containing various proportions of AET and 5-methoxytryptamine were found to be far higher than those of the single compounds alone. The radioprotective effects of the two compounds administered separately or simultaneously were evaluated on the basis of 30-day survival of x-irradiated mice. Adopting the pharmacological methods of investigation into the cooperative action of drugs, the synergism of both effects of the two compounds was quantitatively analyzed, and found to be of potentiating character. The knowledge of the isobole of synergism permits the selection of combinations of optimum proportion, having the least toxic effect with the highest radioprotective activity. (C.H.)

4584 ROLE OF THE CNS ON THE RADIOPROTECTIVE EFFECT OF 5-HYDROXYTRYPTAMINE. Streffer, Christian; Konermann, Gerhard (Univ., Freiburg i. B.). pp 369-73 of Radiation Protection and Sensitization. /Moroson, Harold (ed.). New York; Barnes and Noble, Inc. (1970).

From 2nd International Symposium on Radiosensitizing and Radioprotective Drugs, Rome, Italy. See CONF-690525.

From recent experiments it was concluded that the central nervous system (CNS) might be important for the radioprotective effect of 5-hydroxytryptamine (5-HT) x-irradiated in mice. When investigating the distribution and metabolism of the injected 5-HT-^{3}H and -^{14}C by chemical methods and by histo-autoradiography little radioactivity was found in the fore-, mid- and hindbrain. However, the activity was enhanced by a factor of 25 in some hypothalamic structures (infundibulum) as well as in the pituitary gland and by a factor of 75 in the liver and kidneys. The chemical analysis showed that most of the injected amine was metabolized to the sulphate esters of 5-HT and of 5-hydroxyindole acetic acid in the pituitary as well as in the other organs 15 min p.i. In further experiments it was found that the 5-HT was also radioprotective against whole-body irradiation when the amine was injected intracerebral instead of intraperitoneal. The distribution and the metabolism of the intracerebral applicated 5-hydroxytryptamine was investigated. The experimental data are discussed with respect to the mechanism of 5-HT in radioprotection of mammals. (auth)

4585 5-HYDROXYTRYPTAMINE PROTECTION OF RAT BONE-MARROW CHROMOSOMES AGAINST X-IRRADIATION IN VIVO. Chaudhuri, Jyoti P. (Univ., Ulm, Ger.); Langendorff, Hanns. pp 375-9 of Radiation Protection and Sensitization. /Moroson, Harold (ed.). New York; Barnes and Noble, Inc. (1970).

From 2nd International Symposium on Radiosensitizing and Radioprotective Drugs, Rome, Italy. See CONF-690525.

Optimally high frequency of chromosome aberrations in the rat bone-marrow was obtained 18 hr after 640 R x-irradiation (230 kVp, 12 mA) in vivo. Intraperitoneal pretreatment with 50 mg/kg of 5-hydroxytryptamine (5-HT) protected bone marrow chromosomes against chromatid breaks. (C.H.)

4586 SURVIVAL-PROMOTING EFFECTS OF ENDOTOXIN IN MICE, DOGS, AND SHEEP. Ainsworth, E. J.; Larsen, R. M.; Mitchell, F. A.; Taylor, J. F. (Naval Radiological Defense Lab., San Francisco). pp 381-8 of Radiation Protection and Sensitization. /Moroson, Harold (ed.). New York; Barnes and Noble, Inc. (1970).

From 2nd International Symposium on Radiosensitizing and Radioprotective Drugs, Rome, Italy. See CONF-690525.

A pre-irradiation injection of bacterial endotoxin increased survival of x-irradiated mice, dogs, and sheep. The post-irradiation leukocyte counts showed an accentuated abortive rise. The mechanism involves hematopoietic stimulation, and an earlier, although transient reappearance of leukocytes. Endotoxin does not change the D_0 for colony-forming units in the femur or spleen, but the amount of surviving hematopoietic tissue in the spleen is increased. Repopulation of colony-forming units in the femur and spleen is transiently promoted in endotoxin-treated mice. Speculations concerning the responses of the hematopoietic system to endotoxin are presented. (auth)

4587 INFLUENCE OF CHEMICAL RADIOSENSITIZING AGENTS ON ORGANS AND CELL STRUCTURES. Braun, Hildegard (Univ., Freiburg i. B.). pp 389-95 of Radiation Protection and Sensitization. /Moroson, Harold (ed.). New York; Barnes and Noble, Inc. (1970).

From 2nd International Symposium on Radiosensitizing and Radioprotective Drugs, Rome, Italy. See CONF-690525.

The cytotoxic and x-radiosensitizing effects of the thiol-binding agents iodoacetomide (IAA), N-ethylmaleimide (NEM), and iodoacetic acid (IA) on the crypt cells of the duodenum of mice were investigated. With regard to mortality and mitotic activity, IA and NEM were more effective than IAA, while IAA and IA showed identical ultrastructural changes, distension of the mitochondria, and unfolding of their inner membrane. The alterations produced by NEM were different and were observed in the mitochondrial cristae. The subcellular organelles in cells of pretreated and irradiated mice were more affected than after irradiation alone. (auth)

4588 RADIOSENSITIZING PROPERTIES OF SOME BARENES (ORTHO-1,2 DICARBACLOVODODECABORANE). Romantzev, E. F.; Stanko, V. I.; Romanova, E. A.; Anorova, G. A.; Kozyreva, E. V. (Inst. of Biophysics, Moscow). pp 398-400 of Radiation Protection and Sensitization. /Moroson, Harold (ed.). New York; Barnes and Noble, Inc. (1970).

From 2nd International Symposium on Radiosensitizing and Radioprotective Drugs, Rome, Italy. See CONF-690525.

Intraperitoneal administration of barenylacetic acid (BAA) (35 mg/kg) and methyl-o-barencarboxylic acid (MBA) (35 mg/kg) into mice caused increase in their radiosensitivity to fast neutrons or γ rays. The distribution of ^{14}C-barenylacetic acid in animal tissues and organs and also its intracellular distribution in liver nuclei, mitochondria, and ribosomes were investigated. (auth)

4589 PROTECTION OF MICE AGAINST IONIZING RADIATIONS BY ADRENOCHROME MONOGUANYLHYDRAZONE METHANSULPHONATE; A PROMISING AGENT FOR CLINICAL USE. Sugahara, T.; Tanaka, T.; Nagata, H. (Kyoto Univ.). pp 401-8 of Radiation Protection and Sensitization. /Moroson, Harold (ed.). New York; Barnes and Noble, Inc. (1970).

From 2nd International Symposium on Radiosensitizing and Radioprotective Drugs, Rome, Italy. See CONF-690525.

No agent with a definite protective effect and non-toxic enough to be applicable to man has yet been discovered except the one reported by us, adrenochrome monoguanylhydrazone methansulfonate (AMM). Sixty-day-old male dd/YF mice were irradiated with various doses of internal B, or external γ or x radiation after the treatment with AMM. The 30-day survival and survival time of lethally irradiated mice were used as criteria. Maximum protection was observed at 5 mg/kg when given 15 min prior to irradiation of 700 and 1000 R. The dose reduction factor was 1.32 at 5 mg/kg. A significant protection was observed when pellets

XUM

containing AMM 0.84 g/kg were given for 24 hr before irradiation. According to preliminary experiment, the agent seems to be protective against chronic irradiation with ^{60}Co γ rays and internally administered ^{32}P. Mice fed the AMM pellets showed longer survival time than the mice fed control pellets under continuous irradiation at 200 R/20 hr-day. Survival time of mice injected intravenously with ^{32}P 15 μCi/g body weight was increased when AMM 5 mg/kg was injected daily for two weeks after the injection. The LD_{50} of the agent for mice was estimated to be 1834 mg/kg when given subcutaneously and more than 3000 mg/kg when given per os. (auth)

4590 EFFECT OF 6-AZAURIDINE ON IRRADIATED TUMOURS. Magdon, E. (Robert-Roessle-Clinic, Berlin). pp 409-14 of Radiation Protection and Sensitization. /Moroson, Harold (ed.). New York; Barnes and Noble, Inc. (1970).

From 2nd International Symposium on Radiosensitizing and Radioprotective Drugs, Rome, Italy. See CONF-690525.

The effect of 6-azauridine on radiation-induced inhibition of the growth of Yoshida sarcomas, Ehrlich carcinomas, benzopyrene-induced carcinomas in mice or rats and of the growth and the transplantability of spontaneous mammary carcinomas was studied. The application of 6-azauridine (200 mg/kg body-weight) before x irradiation produced a significant increase of the radiation effect in solid Ehrlich carcinomas and spontaneous mammary carcinomas in strict dependence on the time interval between 6-azauridine application and irradiation. The maximum radiosensitizing effect was obtained when the substance was administered 24 hr prior to irradiation. Under these conditions the sensitizing factor (SF) was 1.56 and 1.84 for Ehrlich carcinomas and Yoshida sarcomas, respectively. It is suggested that the radiosensitizing effect of 6-azauridine is caused by a partial synchronization, during which the cells pass through a phase with maximum radiation sensitivity. (auth)

4591 RADIOSENSITIZING ACTION OF ANDROGEN ON THE OVARIES OF HETEROPNEUSTES FOSSILIS (BLOCH). Rathi, S. K. (Univ. of Rajasthan, Jaipur, India). pp 415-18 of Radiation Protection and Sensitization. /Moroson, Harold (ed.). New York; Barnes and Noble, Inc. (1970).

From 2nd International Symposium on Radiosensitizing and Radioprotective Drugs, Rome, Italy. See CONF-690525.

The effect of testosterone propionate on γ-irradiated Indian catfish, Heteropneustes fossilis (Bloch), ovaries was studied. While in control γ-irradiated fish, degenerative changes of ovaries were not accompanied by changes in weight; in those treated with γ rays and androgen, the ovaries showed a 25% decrease in weight and much more severe histological changes. (auth)

4592 BIOCHEMICAL MECHANISM OF RADIOPROTECTIVE ACTION OF AMINOTHIOLS. Romantzev, E. F.; Koshcheenko, N. N.; Filippovich, I. V. (Inst. of Biophysics, Moscow). pp 421-7 of Radiation Protection and Sensitization. /Moroson, Harold (ed.). New York; Barnes and Noble, Inc. (1970).

From 2nd International Symposium on Radiosensitizing and Radioprotective Drugs, Rome, Italy. See CONF-690525.

Experimental data in favor of the hypothesis of complex biochemical mechanism of action of radioprotectors in mammals are submitted. Aminothiols administration into rats at a radioprotective dose leads to temporary inhibition of nuclear RNA-synthesis in radiosensitive tissue of thymus. Simultaneously the system responsible for thymidine phosphorylation is also inhibited during the short time interval. The latter system is one of the powerful control mechanisms in DNA-biosynthesis. Radiosensitizers, like dl-penicillamine and β-mercaptoethanol, inhibit the process of thymidine phosphorylation in thymus for a relatively long time interval. The correlation between SH-protectors (AET and MEA) accumulation in radiosensitive tissues, their radioprotective action, and inhibition of radiosensitive biochemical processes was established. The possible biochemical mechanisms of radioprotective action of aminothiols are discussed. (auth)

4593 BLOOD REDOX POTENTIALS OF RATS AND MICE INJECTED WITH CYSTAMINE. Duyckaerts, Claire; Liebecq, Claude (Univ., Liege). pp 429-32 of Radiation Protection and Sensitization. /Moroson, Harold (ed.). New York; Barnes and Noble, Inc. (1970).

From 2nd International Symposium on Radiosensitizing and Radioprotective Drugs, Rome, Italy. See CONF-690525.

Rats injected with cystamine (68 mg/kg) develop hypotension, hypothermia, and a temporary increase in blood lactate. The lactate pyruvate ratios in the blood showed variations symptomatic of hypoxia with a maximum after 45 min, concomitant with the second peak of radioprotection afforded by cystamine to the rat. Blood glucose increased with a maximum after 90 min. The administration of β-adrenergic blocking agents provides evidence that these effects are probably mediated by catecholamines. (C.H.)

4594 RADIOPROTECTORS AND PLASMA ENZYMES. Plomteux, G.; Beaumariage, M. L.; Bacq, Z. M.; Heusghem, C. (Univ., Liege). pp 433-7 of Radiation Protection and Sensitization. /Moroson, Harold (ed.). New York; Barnes and Noble, Inc. (1970).

From 2nd International Symposium on Radiosensitizing and Radioprotective Drugs, Rome, Italy. See CONF-690525.

Cysteamine, 5-mercaptopyridoxine, and hypoxia (via reduction of partial oxygen pressure in the inhaled gases) produce an increase in the concentrations of various enzymes (lactate dehydrogenase, glutamate dehydrogenase, malate dehydrogenase, aspartate aminotransferase, and β-glucuronidase) in rat plasma. These treatments also protect against the effects of ionizing radiation. Treatment with β-mercaptoethanol and 4-mercaptopyridoxine, both non-radioprotectors, did not affect these plasma enzyme levels. (auth)

4595 METABOLIC EFFECTS OF SULPHUR-CONTAINING RADIOPROTECTIVE DRUGS. Betz, E. H.; Lelievre, P. (Univ., Liege). pp 439-44 of Radiation Protection and Sensitization. /Moroson, Harold (ed.). New York; Barnes and Noble, Inc. (1970).

From 2nd International Symposium on Radiosensitizing and Radioprotective Drugs, Rome, Italy. See CONF-690525.

The metabolic effects of cysteamine, cystamine, and cysteine have been studied in the rat. The three substances decrease the oxygen uptake, but cystamine is the most active in this regard. Cystamine, and in a lesser degree cysteamine, increase the respiratory quotient. This effect could be related to the tissular anoxia which is induced by these substances (measured by the intrasplenic oxygen tension). Metabolic disturbances were studied in tissues taken at various delays from injected animals and then incubated in vitro. All the results were negative. Studies were then performed on tissue homogenates or isolated mitochondria incubated in vitro in the presence of the various protectors. In these conditions, cystamine decreases the oxygen uptake and inhibits the oxidative phosphorylations. The latter are the most sensitive to cystamine. Pyruvic oxidase is inhibited by various SS compounds (cystamine, oxidized glutathione, GED) but is unaffected by SH substances (cysteamine, reduced glutathione, MEG). Aconitase is inhibited by the SH compounds tested but unaffected by the oxidized substances. Beta-mercapto-ethanol has no effect either on pyruvic oxidase nor on aconitase. None of the substances tested did affect the enzyme catalysing the formation of citrate from oxalo-acetate and coenzyme A. Cystamine inhibits also anaerobic glycolysis of tissue homogenates whereas cysteamine is ineffective. Phosphoglyceraldehyde dehydrogenase and hexokinase are the only enzymes inhibited by cystamine. PGDH is the most sensitive to this effect. (auth)

4596 ACTION OF SH-CONTAINING RADIOPROTECTORS ON NUCLEIC ACID METABOLISM. Goutier, R. (Univ., Liege. Centre d'Etudes de l'Energie Nucleaire, Mol, Belg.); Baugnet-Mahieu, L. pp 445-51 of Radiation Protection and Sensitization. /Moroson, Harold (ed.). New York; Barnes and Noble, Inc. (1970).

From 2nd International Symposium on Radiosensitizing and Radioprotective Drugs, Rome, Italy. See CONF-690525.

Inhibition of DNA synthesis is described in rat thymus and spleen after AET and MEA injection and in regenerating liver when AET is injected before partial hepatectomy. The delay in DNA synthesis and in mitotic activity observed in regenerating liver arises from a delay in the synthesis of the relevant enzymes: nuclear RNA-polymerase and thymidine-phosphorylating kinases. The importance of these observations for understanding the mechanisms of radioprotection is discussed, as well as the possible occurrence of a protection of the DNA repair mechanisms. (auth)

4597 FORMATION OF ATP IN NUCLEI AND MITOCHONDRIA AND THE INFLUENCE OF β-MERCAPTOETHYLAMINE. Zhulanova, Z. I.; Romantzev, E. F.; Kolesnikov, E. E.; Kozyreva, E. V. (Inst. of Biophysics, Moscow). pp 453-6 of Radiation Protection and Sensitization. /Moroson, Harold (ed.). New York; Barnes and Noble, Inc. (1970).

From 2nd International Symposium on Radiosensitizing and Radioprotective Drugs, Rome, Italy. See CONF-690525.

Some aminothiols have found a wide clinical use for the treatment of the radiation disease that may accompany roentgenotherapy of neoplasms. Action mechanism of radioprotective agents is to a large degree due to the most radiosensitive biochemical systems. To such systems belongs for example oxidative phosphorylation, which rapidly deteriorated following exposure to ionizing radiation. The action of one of the most effective radioprotectors, β-mercaptoethylamine (MEA), on respiration and oxidative phosphorylation in the liver mitochondria and respiration of thymus nuclei in rats was studied. It has been found that by adding MEA to mitochondria, acceleration in respiration of these organelles followed by its subsequent slowing down occurs. According to

the pattern of polarographic curves, MEA action is similar to the action of adenosine diphosphoric acid (ADP) on mitochondria. After addition of MEA during ADP phosphorylation, increase in ADP phosphorylation time and decrease in ATP synthesis have been observed. In isolated rat thymus nuclei, MEA causes reduction of ATP synthesis both in vitro and in vivo. Change in nuclei respiration under MEA action was found only in in vitro experiments. (auth)

4598 KINETIC INVESTIGATIONS ON THE INFLUENCE OF RADIOSENSITIZING VITAMIN K_3 ON THE HAEMOGLOBIN-METHAEMOGLOBIN EQUILIBRIUM. Cristea, Al.; Olinescu, R.; Thomas, E.; Nicolau, Cl. (Inst. of Inframicrobiology Stefan Nicolau, Bucharest). pp 457-65 of Radiation Protection and Sensitization. /Moroson, Harold (ed.). New York; Barnes and Noble, Inc. (1970).

From 2nd International Symposium on Radiosensitizing and Radioprotective Drugs, Rome, Italy. See CONF-690525.

Addition of vitamin-K_3 to a red cell suspension in concentrations lower than a certain threshold caused a temporary formation of methemoglobin, followed by a partial reduction of it; an increase of pyruvic acid concentration and a decrease of lactic acid concentration; and an enhancement of the glucidic metabolism, especially of the pentosic shunt. Oxygen and glucose consumptions were increased, as a result of a compensatory yield of NADH, NADPH, GSH oxidized by the added vitamin-K_3. An excess concentration of vitamin K_3 led to inhibition of glycolitic enzymes and to a continuous methemoglobinization. The processes, reduced to a complex interaction of the different redox systems, are described by a kinetic scheme containing the main reactions. The indirect mechanism of action of the radiosensitizer is discussed. (auth)

4599 CARDIOVASCULAR, BIOCHEMICAL, AND HAEMATOLOGICAL CHANGES AFTER THE APPLICATION OF AET. Dienstbier, Z.; Arient, M.; Pospisil, J.; Kourilek, K. (Charles Univ., Prague. Central Military Hospital, Prague). pp 467-70 of Radiation Protection and Sensitization. /Moroson, Harold (ed.). New York; Barnes and Noble, Inc. (1970).

From 2nd International Symposium on Radiosensitizing and Radioprotective Drugs, Rome, Italy. See CONF-690525.

Cardiovascular changes, the concentration of blood transaminases, bone marrow, and peripheral blood pictures were studied after the application of AET and x-irradiation of dogs and rats. It was found that the radioprotective effect of AET is caused to a great extent by the metabolic inhibition conditioned by toxic effects of this compound. (auth)

4600 PREVENTION BY CYSTEINE OF FATTY LIVER INDUCED BY CCl_4 AND ETHIONINE. Agostini, Cesare; Comi, Paola (Univ., Milan). pp 471-5 of Radiation Protection and Sensitization. /Moroson, Harold (ed.). New York; Barnes and Noble, Inc. (1970).

From 2nd International Symposium on Radiosensitizing and Radioprotective Drugs, Rome, Italy. See CONF-690525.

The influence of cysteine administration on fatty liver induced by CCl_4 and ethionine has been studied in rats. The liver triglyceride determinations have demonstrated that cysteine administration protects against fatty liver produced either by CCl_4 or ethionine. The effects of cysteine treatment on the thiobarbituric acid (TBAS) formation by liver and kidney homogenates of rats killed one hr and five hr after the administration of hepatotoxins were also investigated. No effects of cysteine on TBAS formation have been noted one hr after treatment with steatogenic poisons. After five hr there is an increase of TBAS formation by liver homogenates of CCl_4 and cysteine-treated rats compared with liver homogenates of rats treated with CCl_4 only. Therefore it has been postulated that cysteine does not act by an inhibition of TBAS formation in preventing fatty liver. (auth)

4601 DISORIENTATION RESPONSE OF CHICKS WHICH SURVIVED 2-β-AMINOETHYLISOTHIOURONIUM-Br-HBr (AET) ADMINISTRATION DURING EARLY EMBRYOGENESIS. Morgan, Walter (South Dakota State Univ., Brookings); Maisin, J. R.; Callebaut, M.; Mattelin, G. pp 477-81 of Radiation Protection and Sensitization. /Moroson, Harold (ed.). New York; Barnes and Noble, Inc. (1970).

From 2nd International Symposium on Radiosensitizing and Radioprotective Drugs, Rome, Italy. See CONF-690525.

During the course of assaying tolerance levels of radioprotectors, for chick embryos at ages ranging from four to eight days, it was observed that a disorientation syndrome resulted. Chicks, which otherwise appeared normal, were not able to maintain an upright posture. For the controls and for four of the radioprotectors, the chicks were normal. Only in one group, that is from embryos treated at seven days of age with AET, was disorientation observed. Thus, one more adverse effect of AET on the central nervous system is recorded. (auth)

4602 CLINICAL STUDIES OF INTRA-ARTERIAL INFUSION OF 5-BROMODEOXYURIDINE PLUS 5-FLUOROURACIL AND RADIATION. Tanaka, Yoshimasa; Takahashi, Masaji (Tenri Hospital, Japan). pp 485-9 of Radiation Protection and Sensitization. /Moroson, Harold (ed.). New York; Barnes and Noble, Inc. (1970).

From 2nd International Symposium on Radiosensitizing and Radioprotective Drugs, Rome, Italy. See CONF-690525.

Methods to increase the ratio of incorporation of 5-bromodeoxyuridine (BUDR) or 5-iododeoxyuridine (IUDR) into tumor DNA to normal tissue DNA were investigated in mice using tracer techniques and Ehrlich's transplanted tumors. Applications in increasing tumor radiosensitivity in patients with advanced untreated tumors of the head and neck are reported. The incorporation of IUDR was about six times greater when (5-FU) 5-fluorouracil was added. The most suitable doses of BUDR and 5-FU were 250 mg/day and 50 mg/day respectively. Tumor regression degrees were about 2-fold greater than with irradiation alone. Histological examination of biopsy samples revealed a remarkable effect on the tumor tissue, only scar tissue remaining in almost all cases, but findings on patients who were compelled to discontinue planned radiotherapy because of intense mucosal reaction showed remaining cancer cells. (C.H.)

4603 STUDIES ON RESTORATIVE EFFECT OF TAURINE IN RADIATION INJURY AND ITS CLINICAL APPLICATION. Abe, Mitsuyuki; Fukuda, Masasi (Kyoto Univ.). pp 503-9 of Radiation Protection and Sensitization. /Moroson, Harold (ed.). New York; Barnes and Noble, Inc. (1970).

From 2nd International Symposium on Radiosensitizing and Radioprotective Drugs, Rome, Italy. See CONF-690525.

It was demonstrated that there was a prominent increase in urinary taurine excretion in patients exposed to therapeutic doses of γ radiation at 200 R/day to a total dose of 5000 to 10,000 R who showed marked leukopenia, while no such taurinuria was found in patients whose leukopenia was not significant. Three g per day of taurine was given orally to patients beginning on the day when the leukocyte count was depressed below 4000 cells per mm^3. The leukocyte count was increased again soon after the administration of taurine and reached a maximum value about two weeks later. No further decrease in leukocytes was observed, although radiotherapy was continued with no change of dose. The effectiveness of taurine on leukopenia induced by radiotherapy was demonstrated clinically in a statistically controlled study. (auth)

4604 MODIFYING EFFECTS OF WATER CONTENT, OXYGEN, AND CYSTEINE ON GENETIC EFFECTS OF GAMMA AND FAST NEUTRON RADIATIONS IN BARLEY SEEDS. Mikaelsen, K. (International Atomic Energy Agency, Vienna). Gamma Field Symp.; No. 7, 1-17(1968).

From 7th Symposium on Gamma Field, Mito, Japan. See CONF-680824.

Seeds containing 13% and 5% water were used for studies on the effects of water content. Following γ radiation doses of 2.5 to 15 krad there was a higher frequency of chromosome aberrations and chlorophyll mutations in the seeds containing 5% water than in those containing 13%. Following fast neutron doses of 75 to 1200 rad there was little difference in the two groups of seeds. Seeds were hydrated in oxygen- and nitrogen-bubbled water for studies on the oxygen effect. Frequencies of chromosome aberrations and chlorophyll mutations were higher in oxygen-treated seeds following γ irradiation, but there was no difference in the two groups of seeds following fast neutron irradiation. A significant reduction in γ-radioinduced chromosome aberrations and chlorophyll mutations was observed after treatment with cysteine, but only a small reduction was observed following fast neutron treatment. (H.L.W.)

4605 EFFECT OF METHYLENE BLUE ON LACTIC DEHYDROGENASE LEVEL AND LACTIC DEHYDROGENASE ISOENZYMES OF RATS EXPOSED TO GAMMA-IRRADIATION. Nam, Sang Yul; Chang, Seung Haann (Kyung Hee Univ., Seoul). Annot. Zool. Jap.; 43: No. 2, 79-87(Jun 1970).

Albino rats were given 360 rads of single whole-body γ irradiation 28 to 32 minutes following an intraperitoneal injection of physiological saline or methylene blue (38 mg/kg). Lactic dehydrogenase (LDH) activity in serum and LDH isoenzymes in serum, liver, heart, and testis were determined at various time intervals after exposure. Methylene blue delayed the LDH rise at 15 and 64 hr after exposure. The exposure in the control and the methylene blue-treated rats resulted in an increase in the amount of the more electrophoretically mobile-anodal isoenzyme and a decrease in the last mobile-cathodal isoenzyme in serum, liver, heart, and testis at 40 and 116 hr, respectively. Methylene blue showed

XUM

a slight delay in heart tissue LDH isoenzyme patterns in alteration after irradiation. The increase in serum LDH level after exposure is a reflection of an immediate increase in the H·type, band 1 of LDH isoenzymes. Protective action of methylene blue against γ irradiation in rats is discussed. (auth)

4606 MEDIA AND SURVIVING FRACTION OF X-IRRADIATED HeLa S3 CELLS. Masuda, Koji (Kyushu Univ., Fukuoka). Nippon Igaku Hoshasen Gakkai Zasshi; 29: 1484-7(Mar 1970). (In Japanese).

The effect of serum on the reproductive capacity of x-irradiated HeLa S3 cells was studied, using single-cell culture method and Eagle MEM supplemented with 5% or 20% calf serum. It was found that the survival rate depended on the serum concentration within 24 hr after irradiation. Although the feeder layer (2×10^3 R irradiated 1×10^4 HeLa cells) changed the survival rate of cells cultured in 5% calf serum, no effect on the survival rate of cells cultured in 20% calf serum was observed. It was suggested that the serum affected the radiosensitivity of the cells by modifying the course of damage received by irradiated cells. (auth) (Japan)

4607 EFFECTS OF POST-TREATMENT WITH CAFFEINE ON THE SENSITIVITY OF ULTRAVIOLET LIGHT IRRADIATION OF TWO LINES OF HeLa CELLS. Wilkinson, Ray; Kiefer, J.; Nias, A. H. W. (Christie Hospital and Holt Radium Inst., Manchester, Eng.). Mutat. Res.; 10: 67-72(Jul 1970).

The effect of uv irradiation was investigated on a standard line of HeLa cells and on a line sensitive to methyl methanesulphonate (MMS). The MMS sensitive line was found to be more sensitive to uv irradiation than the parent line. When the two cell lines were plated in caffeine-containing medium immediately after uv irradiation, there was no reduction in the surviving fraction of cells of either line even when toxic concentrations of caffeine were used. (auth)

4608 CLINICAL TRIAL OF TWO SUNSCREENING CREAMS. Abbott, L. G.; Deakin, M. J.; Langley, R. A.; Tipping, R. M. Med. J. Aust.; 1: 1094-5(30 May 1970).

Under natural conditions of summer sun exposure, the uv radiation filter creams Uvistat, and Maxafil Cream 124CX.1, were subjected to a clinical trial. The results indicate that both creams are effective uv ray filtering preparations, but that one is superior to the other. (Australia)

4609 USE OF COMBINED RADIATION PROTECTION COMPOUNDS. Vasin, M. V.; Saksonov, P. P.; Shashkov, V. S. Farmakol. Toksikol. 33: 501-7(Jul-Aug 1970). (In Russian).

A brief review of results obtained in studies of pharmacological properties of various radioprotective and compensatory elements used in various combinations revealed variable reactions of organisms to the pharmacological compounds. Efficient combinations of various radioprotectors offer wide possibilities in development of future effective means of radiation protection. Extensive references are included. (R.V.J.)

Radiation Sickness and Injuries

Refer also to abstracts 4472 and 4524.

4610 HOT SPRING THERAPY OF RADIATION INJURY. XXVI. EXPERIMENTAL STUDIES ON THE HOT SPRING EFFECTS FOR THE IRRADIATION INJURY DUE TO NEUTRON AND γ-RAY. Hatta, Osamu; Arima, Masashi. Oita-ken Onsen Chosa Kenkyu-kai Hokoku; No. 20, 86-7(Mar 1969). (In Japanese).

The therapeutic effects of baths in hot springs on radiation injury were investigated histologically. Thirty mice of ddN pure strain were put in one group, and five mice each were killed on 1st, 3rd, 10th, 15th, and 21st day after irradiation. Stomachs, small intestines, liver, testes, spleen, and kidneys were examined histologically. Mice were bathed in fresh water, A-bomb Center Spring, Yanagi Bath, Umijigoku Hot Spring, and the modified spring at 380 once a day, from 1 to 20 days after irradiation. The spleen was affected the most effectively by bathing. Almost no histological difference between groups was observed until the 5th day. Histological differences were observed between the groups on the 10th day; the 15th day, about 80% of those bathed returned to normality, especially those in the modified bath group, the A-bomb Center Bath group, and the Yanagi Bath group; on the 21st day, the bathing groups were normal, while the recovery in the control group was delayed. Histological recovery of the control group corresponded on the 21st day to that of the bathing group on the 15th day after irradiation. (TSS)

Radiodiagnosis

Refer also to abstracts 4324–4328, 4336, 4337, 4359, 4411–4413, 4415, 4425, 4437, 4510, 4511, 4531, and 4716.

4611 (CEA-R-3920) MATHEMATICAL PROCESSING OF SCINTIGRAPHIC IMAGES. Ottavi, Henri (Commissariat a l'Energie Atomique, Cadarache (France). Centre d'Etudes Nucleaires). Dec 1969. 34p. (In French). Dep. CFSTI (U. S. Sales Only).

A scintigraphic image always lacks sharpness, whether it be obtained using a stenopaeic cine-camera, a collimating grid, or by scanning. If the object is planar, the image can be deduced from the object by a linear transformation. A method for the inversion of this transformation is presented taking into account random changes in the image. From this is deduced the order of magnitude of the sharpness which one can hope to obtain from a mathematical processing of the image, taking into account the three parameters: object activity, exposure time, object distance. (auth) (France)

4612 (CONF-680211) PROGRESS IN METHODS OF BONE MINERAL MEASUREMENT. Conference held in Bethesda, Maryland, February 15–17, 1968. (National Inst. of Arthritis and Metabolic Diseases, Bethesda, Md.). 579p. GPO $4.00.

Twenty-seven papers were presented. Separate abstracts were prepared for 19 papers. The papers that were not included deal with routine studies of minerals and density of bones. (H.B.G.)

For abstracts of individual papers see: 4042 and 4412–4629.

4613 (CONF-680211–, pp 27-80) ASSESSMENT OF BONE MASS BY ROENTGENOGRAPHIC DENSITY TECHNIQUES. Mack, Pauline Beery (Texas Woman's Univ., Denton); Vogt, Fred B. (Texas Univ., Houston. Graduate School of Biomedical Sciences).

From Progress in methods of bone mineral measurements.

The optical density of a roentgenographic bone image can be related to the mass of bone present if conditions of exposure and development of the film are standardized and kept constant. Changes in x-ray density measurements of a given bone thus can be used to express dynamic alterations in the bone as a result of experimental or environmental conditions. The significance of changes in bone mass under specified conditions depends upon a consideration of the reproducibility of the results obtained in following the assessment procedure carefully, taking into account the biological variability in bone mass which occurs from day to day in persons undergoing similar types of physical activity and experiencing a controlled dietary intake. The status of methodology and instrumentation presently in use in our laboratory at the Texas Woman's University is presented. Results of day-to-day variability in bone mass measurements are given for the following groups of subjects in selected anatomical sites as follows: ambulatory subjects on constant controlled dietary intakes undergoing similar types of physical activity; subjects consuming non-controlled diets and engaging in various types of physical activity; subjects on controlled diets in all respects except calcium and phosphorus, but with step-wise changes in the intake of these nutrients; and subjects whose level of calcium intake in a controlled diet is changed by different amounts in going from ambulation to horizontal bed rest. The present densitometric assembly at the Texas Woman's University includes a small digital computer which is used to provide the calibration and automatic calculations of the information obtained from optically scanning a roentgenogram. A printout from the computer presents identification of the film and the results of the analysis. (auth)

4614 (CONF-680211–, pp 80-95) BONE MINERAL MEASUREMENTS FROM X-RAY IMAGES. Colbert, Charles (Fels Research Inst., Yellow Springs, Ohio).

From Progress in methods of bone mineral measurements.

A simplified mathematical model serves as the basis for a technique to determine bone mineral content from x ray film images. A microdensitometer scan of a reference wedge image is used to establish the background film density contributed by scattered radiation, chemical fog, emulsion and film base. Since this background optical density does not contribute meaningful information about the specimen, it is subtracted from all optical density readings subsequently made while scanning the bone image. Electrical signals corresponding to the optical density data produced by the microdensitometer are fed directly from the microdensitometer into a LINC-8 computer which first computes background from the wedge image, and then computes a numerical parameter proportional to the mineral concentration in the bone specimen. Scanning of an image and computations are completed within a matter of minutes. The formulas used for these computations make certain assumptions about the behavior of polychromatic x rays which demand substantiation. The assumptions made in devising the simplified mathematical model seem to be in accord with the actual behavior of the physical system. (auth)

4615 (CONF-680211–, pp 95-115) X-RAY BONE DENSITOMETRY IN SHORT AND LONG DURATION STUDIES. Vose, George P. (Texas Woman's Univ., Denton).

From Progress in methods of bone mineral measurements.

Radiographic densitometry of x ray films exposed simultaneously with a suitable standard absorber was used to detect more subtle changes in bone mineral content than those observed by assessment, often described as requiring a loss of 30% of the total skeletal mineral before a density decrease is visually conspicuous. Although bone mass losses associated with metabolic bone diseases were reported with increasing frequency, it is very infrequent that positive gains were reported. In a current, long-duration study involving 140 permanently bedfast institutionalized children divided into a control group and three treatment groups, including fluoride, oral phosphate, and hormones, densitometric studies of the os calcis indicated that the fluoride and hormone groups increased in bone mass faster than the controls. After 18 months of treatment no significant difference was observed between the control group and those on phosphate treatment of .18 mg/kilo/day administered during alternating six-week periods. All of the patients selected for the study exhibited prior radiographic evidence of osteoporosis of disuse. (auth)

4616 (CONF-680211–, pp 115-35) AGE-RELATED BONE CHANGES IN WOMEN. Doyle, Frank H. (Royal Postgraduate Medical School, London (England). Hammersmith Hospital, London (England)).

From Progress in methods of bone mineral measurements.

Bone mineral was measured in the distal third of the left ulna by a method using x-rays and photometric comparison of the bone mineral in the ulna with an aluminium standard. The technical requirements, advantages and limitations of the method were briefly mentioned. Measurements of ulnar bone mineral, cortical thickness and derived quantities in 180 normal women aged 15 to 79 were presented. Differences in external dimensions of the ulna are discussed. (auth)

4617 (CONF-680211–, pp 135-59) INTERRELATIONSHIPS BETWEEN CORTICAL BONE THICKNESS, MINERAL MASS, AND MINERAL DENSITY IN HUMAN RADIUS: A ROENTGENOLOGIC-DENSITOMETRIC STUDY. Meema, H. E.; Meema, Silvia (Toronto Western Hospital (Ontario)).

From Progress in methods of bone mineral measurements.

A roentgenologic-densitometric technique for cortical bone analysis using the proximal end of the shaft of the radius allows the determination of three parameters of cortical bone: mineral mass, bone thickness, and mineral density. By differential use of all three parameters, abnormalities in cortical bone mineral content may be detected more frequently than by the use of any of the parameters separately. Results are reported for measurements on 211 normal men and 309 normal women in the age range of 21 to 91 years. Each sex was divided into three age groups. Using the young male and premenopausal female groups as baselines, losses in bone mineral mass with aging were found to be more marked in women than in men. Although the measurement of bone mineral mass gives the best overall diagnostic results, determination of bone mineral density adds another dimension to the knowledge of the mineralization of cortical bone and is not infrequently the only abnormality found, especially in the early stages of developing osteoporosis. Particularly low values of all parameters were found in persons with vertebral compressions, and in those suffering from osteomalacia and hyperparathyroidism. (auth)

4618 (CONF-680211–, pp 159-77) BONE PATTERNS IN AGING AND OSTEOPOROSIS. Nordin, B. E. C. (Medical Research Council, Leeds (England). Mineral Metabolism Unit).

From Progress in methods of bone mineral measurements.

X-ray densitometry was used to measure bone mineral content of the human metacarpal, radius, ulna, and the lumbar spine and simple morphological measurements were applied to the metacarpal and the femur. All results were converted into mg. of bone ash per unit volume of bone, which shows that the vertebrae have the lowest mineral content per unit volume of the bones studied followed by the radius, the ulna, and the metacarpal. The seven measurements were performed in normal and osteoporotic men and women and in females following an artificial menopause. The internal correlations between the different bone measurements were established in each group, some of them being highly significant and some of them less so. No single bone measurement was found that satisfactorily distinguished between clinical spinal osteoporosis and the normal state but it is possible that certain combinations of bone measurements will be found to provide the desired discrimination. There was no striking difference in bone distribution between age-dependent bone loss and pathological osteoporosis; the latter appeared to be an exaggeration of the normal trend. (auth)

4619 (CONF-680211–, pp 177-91) MINERAL AND DENSITY CHANGES IN BONE WITH AGE IN NORMAL AND PATHOLOGICAL STATES. Smith, Deryk A.; Anderson, J. B.; Shimmins, J.; Speirs, C. F.; Barnett, E. (Western Infirmary, Glasgow (Scotland)).

From Progress in methods of bone mineral measurements.

A radiographic technique for measuring the mineral content and density of the third metacarpal was used in men during normal and pathological states. The measurements were analyzed in relation to age. Two measurements were used. The first was the Aluminium Equivalent that measures the amount of mineral at the midpoint of the third metacarpal. This was divided by the width of the metacarpal to allow for differences in size and termed the Standardised Aluminum Equivalent (S.A.E.). The second was a measurement of density and was a measure of the mineral per unit volume of cortex. Normal male subjects showed a rise in S.A.E. with age that reached a maximum at the age of 34 and declines slowly thereafter. The normal female subjects showed a rise to a maximum at the age of 36 and a slow fall to the age of 50 years after which a much more rapid fall occurred. Density rose throughout the age range from 5 to 75 years in the normal male. In the female subjects, it rose to a maximum at 40 years and declined slowly thereafter. Since both S.A.E. and density are very dependent upon age, a third polynomial was fitted to the data to represent the lines of best fit. The cumulative percentile lines ranging from the 5 to the 50 percentile line were derived (i.e., these indicate that 5% or 50% respectively of the normal population lie below these lines). These percentile lines were used to evaluate mineralization in patients with metabolic bone disease in relation to the normal population. The relation between the measurements of spinal and metacarpal mineral content is discussed. (auth)

4620 (CONF-680211–, pp 191-203) HIGH-SPEED AREA-MEASURING SCANNING DENSITOMETER. Ledley, Robert S. (National Biomedical Research Foundation, Silver Springs, Md.).

From Progress in methods of bone mineral measurements.

To measure the mineral content of bone, x-ray films are taken. For evaluation of the films a high-speed area-measuring densitometer was developed and is described. The equipment can scan and sample 350,000 points on a film within 0.35 sec, with the density of each sample point distinguished as one of sixteen grey levels. This means that points on the picture are sampled at the rate of 10^6/sec. The information from the sample points is fed directly into the high-speed core memory of a digital computer. (H.B.G.)

4621 (CONF-680211–, pp 204-15) IN VIVO MEASUREMENT OF THE MINERAL CONTENT OF A SECTION OF THE RADIUS. Goodman, Leonard S. (Argonne National Lab., Ill.); Bertram Levin (Michael Reese Hospital, Chicago, Ill.).

From Progress in methods of bone mineral measurements.

The in vivo measurement of the mineral content (in units of grams of $Ca_3(PO_4)_2$ equivalent) of a section of the radius is performed by monoenergetic x-ray transmission studies for both a sample of 373 normal young and middle-age adults and a sample of 110 aged people. The significance and value of interpreting these measurements on the basis of a simple cylindrical model of the radius is discussed. The comparisons between the measured values within the younger and older age groups and between these groups are discussed. The elementary physics of the photometric measurement of roentgenograms for the purpose of estimating the mineral content of tissue is reexamined. A roentgenographic photometric in vivo technique of measurement of mineral content is designed that is in principle equivalent to transmission measurements made with radioactive sources and scintillation counter detectors. The details and rationale of the technique are discussed. (auth)

4622 (CONF-680211–, pp 216-49) QUANTITATIVE MEASUREMENTS OF BONE MINERAL CONTENT BY DENSITOMETRIC METHODS. Heuck, Friedrich (Katharinenhospital der Stadt Stuttgart (West Germany). Zentralroentgeninstitut).

From Progress in methods of bone mineral measurements.

The necessity for quantitative measurements of the mineral content of bone is considered. The different methods used for achieving objective radiological bone density figures are discussed. The method of quantitative radiometric measurement in vivo, developed by HEUCK and SCHMIDT, for estimating comparable and reproducible values for total mineral content in each bone area, the so-called apatite value, is described. The percentage inaccuracy of the method and the discrepancy between the values found radiologically and those obtained by chemical analysis are discussed. The differences between values found in healthy persons and in patients with localized and generalized bone lesions of the neck of the femur, the os calcis, and the radius metaphysis are analyzed. The practicality of this simple densitometric method in clinical medicine is discussed. (auth)

XUM

4623 (CONF-680211–, pp 253-68) MEASUREMENT OF BONE MINERAL BY THE DIRECT PHOTON ABSORPTION METHOD: PRINCIPLES AND INSTRUMENTATION. Cameron, John; Sorenson, James A. (Wisconsin Univ., Madison. Dept. of Radiology).

From Progress in methods of bone mineral measurements.

The basic principles of the technique of γ of x radiation transmission scanning for measurements of bone mineral content in vivo are reviewed. Factors that limit its present accuracy and reproducibility to about 2 percent are discussed. Also discussed are the choice of monoenergetic photon sources in relation to the bones to be measured, choice of beam and detector collimation size for a given bone, designs of different scanning mechanisms that can scan any bone of the appendicular skeleton, choice of data output modes from the scanner, and techniques for the evaluation of the data. Methods for extending the technique to the axial skeleton using the double photon technique are discussed. (auth)

4624 (CONF-680211–, pp 283-96) MEASUREMENT OF BONE MASS IN THE RADIUS. Johnston, C. Conrad Jr. (Indiana Univ., Indianapolis. Medical Center).

From Progress in methods of bone mineral measurements.

The method of photon transmission scanning was utilized to measure bone mass in the human radius. Iodine-125 was used as the γ photon source. Scans were performed at 3 cm from the distal end, an area of cancellous bone, and 8 cm, an area of cortical bone. The coefficient of variation for repeated measurements in a single individual was approximately 2.5%. This was confirmed by a reliability estimate that showed that the principal source of variation was caused by individual difference rather than instrumentation error. It was demonstrated by this method that males have higher bone mass than females and Negroes higher bone mass than Caucasians. A group of 157 Caucasian females of varying age was scanned and it was found that bone mass fell significantly after age 50. A smaller group of males (66) was scanned and a significant decrease occurred after age 60. The radial bone mass was compared in the group of women with and without lumbar vertebral collapse. A significantly lower figure was found in the 3 cm scans of those with fracture; however, there was no difference at 8 cm. In a small group of post-menopausal women the bone mass of patients on estrogen replacement (15) was compared to those on no replacement (57). Those on therapy had significantly greater mass at the 3 cm scan distance. However, no definitive conclusion can be drawn, since the bone mass in the two groups before menopause is unknown. Other data showed that women with post-menopausal hot-flushes have significantly higher bone mass than those without this symptom, and these patients would be the ones treated with estrogen. (auth)

4625 (CONF-680211–, pp 296-308) CLINICAL USE OF AN IN-VIVO MEASUREMENT OF BONE MINERAL CONTENT. Evens, Ronald G.; Pak, Charles Y. C.; Bartter, Frederic C. (National Heart Inst., Bethesda, Md.); Ashburn, William (National Institutes of Health, Bethesda, Md.).

From Progress in methods of bone mineral measurements.

Determinations of bone mineral content were made in normal subjects and in patients with bone disease using photon transmission scanning methods. A photon source (^{125}I-27.4 keV photon) was mechanically passed under the forearm, which was immersed in water, and the collimated beam was counted by a 0.5 in. by 2 mm NaI (Tl) crystal. The number of photons reaching the crystal each 0.5 sec was tabulated and an integral determination of absorption by bone mineral was computed. The determination was made on the left radius and ulna, 4.5 inches from the metacarpal-phalongeal joint. Repeat determinations, performed on the same day after repositioning the arm, were reproducible with a mean difference of 0.2% ± 1% (S.E.D.) in 50 subjects. A dog femur, embedded in lucite, was counted 11 times during a three month period, with a 2% standard deviation. Eight normal subjects and two patients without active bone disease had repeated determinations, at intervals of one to ten weeks, with a mean difference of 1% ± 1% (S.E.D.). Measurements were performed on patients with osteoporosis, osteogenesis imperfecta, osteomalacia, hyperparathyroidism, hypoparathyrodism, renal failure, and osteopetrosis with excellent correlation between bone mineral content and clinical state. This technique was used to assess the clinical response to various therapeutic measures in patients with bone disease, and results are discussed. (auth)

4626 (CONF-680211–, pp 308-19) BONE DENSITOMETRY: CLINICAL APPLICATIONS. Strandjord, Nels M.; Forland, Marvin; Lanzl, Lawrence; Cox, Anna (Chicago Univ., Ill. Dept. of Radiology).

From Progress in methods of bone mineral measurements.

Bone density measurements made by ^{125}I γ transmission scanning of a finger phalanx and expressed as a linear coefficient of absorption were used to study the mineral content of bones in a variety of patients. Normal males demonstrated a decrease in bone density with advancing age. Normal females also show diminished bone density with aging. Females given estrogens postmenopausal (up to 25 years) demonstrated less loss of bone with advancing age as compared to untreated females. Densitometry measurements were performed on 20 patients with surgically proven hyperparathyroidism. In all but three patients the bone density was significantly below normal. Several patients were measured postsurgical and demonstrated a slight increase in density. (auth)

4627 (CONF-680211–, pp 319-28) BONE DENSITOMETRY USING A SINGLE BEAM FROM A RADIONUCLIDE SOURCE. Nilsson, Bo E. (Malmo General Hospital. (Sweden). Dept. of Orthopedic Surgery).

From Progress in methods of bone mineral measurements.

Post-traumatic osteopenia in the knee region following fracture of the shaft of the tibia was studied in patients using γ transmission scanning for measurements of bone mineral content. A measuring device was constructed, consisting of a γ radiation source using ^{241}Am and a scintillation detector. The bone mineral content was evaluated from the photon attenuation in the bone of a single wide beam. Although the method was blind as regards localization of the bone and therefore has a relatively poor precision, the simplicity of the device offered some advantages. Results were presented from studies of post-traumatic osteopenia and from bone densitometry of the head of the humerus in cases of frozen shoulder. Results of bone densitometry of the distal end of the femur in population studies of individuals from areas with high and low water fluoride concentrations, and from comparisons of diabetic and non-diabetic females, were also presented. (auth)

4628 (CONF-680211–, pp 331-51) RADIOGRAPHIC TRABECULAR QUANTITATION OF HUMAN LUMBAR VERTEBRAE IN SITU: PROGRESS IN DEVELOPMENT OF METHOD AND DIGITAL COMPUTER ANALYSIS. Rockoff, S. David; Selzer, Robert (Yale Univ., New Haven, Conn. School of Medicine).

From Progress in methods of bone mineral measurements.

A scanning microdensitometer-analog computer system was devised that permits quantitation of vertically and horizontally oriented radiographic trabecular shadows. The method, that is relatively independent of the degree of film blackening, was applied to radiographs of in situ human lumbar vertebrae. The trabecular quantitation was shown to be directly related to the quantity of bone present, the compressive bone strength, and the calcium, phosphorus, and magnesium content. A relatively constant relationship exists between the data obtained from the in situ and from the in vitro radiographs. A digital computer method was developed to measure changes in trabecular bone architecture from radiographic film. Pictorial data were fed into the computer by means of a film scanning and digitizing system. Once in the computer, two-dimensional digital filters were applied to the pictures for smoothing and then a one-dimensional peak connecting algorithm was applied to each picture line in order to locate trabecular shadows. From this data three parameters (mean trabecular width, mean trabecular frequency, and mean trabecular separation) were calculated. Typically, 600 scan lines, spaced 25 microns apart, were taken and average parameters calculated. Initial results seemed to indicate that the computer can satisfactorily locate the trabecular shadows. (auth)

4629 (CONF-680211–, pp 411-21) MINERAL DENSITY IN NORMAL AND OSTEOPOROTIC BONE. Jowsey, Jenifer; Phil, D. (Mayo Clinic, Rochester, Minn.).

From Progress in methods of bone mineral measurements.

Mineral can be released from the skeleton by the process of resorption of bone tissue. In this process both the mineral and organic fraction are removed simultaneously on bone surfaces. Mineral exchange, on the other hand is a process that was shown to involve only the mineral phase of bone, specifically the calcium, and to take place throughout mineralized tissue. The disorder, osteoporosis, is related to calcium loss by the body and is characterized by increased resorption of bone. It is also possible that mineral may be lost from the skeleton by the mechanism of long-term exchange. Quantitative densitometry of normal and osteoporotic bone was carried out using a dye precipitation method and microradiographs of cross-sections of cortical bone. The results represented the density of bone analyzed in units of one osteone or pooled interstitial lamellae samples; and the volumes included lacunae and canaliculi, but excluded larger soft-tissue spaces such as Haversian canals. The density values suggested that bone from individuals with osteoporosis has an overall lower calcium content than bone from normal individuals. (auth)

4630 (CONF-700515) PROCEEDINGS OF BONE MEASUREMENT CONFERENCE, CHICAGO, ILLINOIS, MAY 22–23,

XUM

1970. Cameron, J. R. (ed.) (Wisconsin Univ., Madison. Bone Mineral Lab.). 441p. Dep. CFSTI.

Separate abstracts were prepared on 24 papers. Fourteen additional papers discuss the mechanical properties of bones and applications of bone mineral measurements in the treatment of patients with various disease conditions. (C.H.)

For abstracts of individual papers see: 4631–4654.

4631 (CONF-700515–, pp 1-21) THEORETICAL ACCURACY AND PRECISION IN THE PHOTON ATTENUATION MEASUREMENT OF BONE MINERAL. Judy, Philip F. (Wisconsin Univ., Madison). (COO–1422–68).

From Proceedings of bone measurement conference, Chicago, Illinois, May 22–23, 1970.

The accuracy and precision of the measurement of the bone mineral content by photon attenuation methods depend on a number of factors. Among these factors are: photon energy; non-monochromaticity; photon source size; source intensity; bone-source distance; and detector collimation. As an example of some of these effects, theoretical calculations using experimental beam profiles from ^{125}I and ^{241}Am sources were made. To obtain adequate intensity to scan with ^{241}Am, the source has to be larger in diameter than the ^{125}I source and consequently larger detector collimation has to be used. Theoretical estimates of the counting precision were made using the Poisson probability distribution. (C.H.)

4632 (CONF-700515–, pp 22-7) PRELIMINARY REPORT ON A DIRECT DIGITAL READOUT SYSTEM FOR ABSORPTIOMETRIC DETERMINATION OF BONE MINERAL CONTENT. Mazess, R. B.; Cameron, J. R. (Wisconsin Univ., Madison. Dept. of Radiology); Miller, H. (Wisconsin Univ., Madison. Instrumentation Center). (COO–1422–69).

From Proceedings of bone measurement conference, Chicago, Illinois, May 22–23, 1970.

A portable system for absorptiometric (photon transmission) scanning of bone mineral content was developed. The new portable system uses analog rather than digital techniques; immediate direct digital readout of bone mineral content and bone width is provided. The portable electronics system consists of a high voltage supply for the photomultiplier tube, preamplifier-amplifier, and single channel analyzer. Instead of a scaler/timer, however, the analyzer output goes to a ratemeter and then to a novel logarithmic converter-integrator unit. This unit provides a logarithmic conversion of the ratemeter signal. An initial adjustment is made for each bone scan to compensate for the varying baseline level (reflecting soft-tissue absorption). (C.H.)

4633 (CONF-700515–, pp 28-32) PRECISION OF THE NORLAND INSTRUMENTS BONE MINERAL ANALYZER. Rose, F. A. (Norland Instruments, Fort Atkinson, Wis.).

From Proceedings of bone measurement conference, Chicago, Illinois, May 22–23, 1970.

The precision of one commercially-available bone mineral analyzer that employs γ transmission scanning is discussed. This analyzer is completely automated and utilizes analog computation and digital control techniques to produce a final digital result of bone mineral directly in grams per centimeter and bone width in centimeters. The machine is calibrated by measuring a known phantom standard. Hence the absolute precision of clinical measurements is determined by the variability of sequentially obtained results. The variability of individual results as compared to the mean of a series of measurements is discussed. (C.H.)

4634 (CONF-700515–, pp 33-47) ADDITIONAL SYSTEM FOR BONE DENSITOMETRY STUDIES. Lanzl, L. H.; Cox, A.; Dobben, G. (Argonne Cancer Research Hospital, Chicago, Ill. Chicago Univ., Ill. Dept. of Radiology); Olson, R.; Toman, J.; Schrodt, A. (Packard Instrument Co., Downers Grove, Ill.).

From Proceedings of bone measurement conference, Chicago, Illinois, May 22–23, 1970.

The design features of a commercially-available combined source-detector assembly for use in γ transmission scanning of human bones for measurement of mineral content are described. The assembly is linked to an electronics printout assembly. Americium-241, ^{125}I, or other isotope γ sources can be used in the unit. The unit allows a variety of positioning of arm and leg bones, rapid adjustment of the source-collimator system, and uses a small scintillation detector and source shielding that keeps the radiation dose at the surface of the unit below background levels. The unit gave good performance during bone mineral measurements on several hundred patients with bone demineralization diseases. (C.H.)

4635 (CONF-700515–, pp 48-57) FEATURES AND PERFORMANCE CHARACTERISTICS OF THE PACKARD OSTEODENSITOMETER. Schrodt, A. G.; Schavey, R. E.; Kus, J. E. (Packard Instrument Co., Downers Grove, Ill.).

From Proceedings of bone measurement conference, Chicago, Illinois, May 22–23, 1970.

The design features of an instrument for measurements of the mineral content of human bones by γ transmission scanning are described. Americium-241 or ^{125}I were used as the γ sources. The instrument may be used in all areas of bone mineral research and provides for the attachment of many different types of readout systems to analyze results obtained using a scintillation detector. (C.H.)

4636 (CONF-700515–, pp 169-87) SENSITIVE METHOD FOR SEPARATE CALCULATION OF MINERAL CONTENT IN CANCELLOUS AND COMPACT BONE OF THE FINGER BY A ^{125}I PROFILE SCANNER. EFFECT OF CALCIUM AND FLUORIDE THERAPY ON DEMINERALIZED BONE. Boerner, W.; Moll, E.; Rauh, E.; Reiners, Chr. (Wuerzburg Univ. (West Germany). Nuklearmedizinische Abt.).

From Proceedings of bone measurement conference, Chicago, Illinois, May 22–23, 1970.

A method for γ transmission scanning is presented which allows a separate estimation of mineral density for cancellous and compact bone. For measuring absorption across a phalanx in two planes, a profile scanner with a ^{125}I source was used. A simplified geometrical model of the finger was used for calculating simulated absorption curves with a computer. The data thus obtained served as the basis for diagrams used for practical evaluation. This sensitive method, which in no way affected the patient, was used to test the influence of long-term therapy with calcium and fluoride on the bone mineral content of elderly individuals who were suspected of having osteoporosis. Measurements before, during, and after therapy were carried out. The results of calcium and fluoride treatment on demineralized bone are discussed. (C.H.)

4637 (CONF-700515–, pp 188-94) AUTOMATIC SCANNER-COMPUTER ANALYSIS OF RADIOGRAPHIC BONE TRABECULAR ACTIVITY. Zacher, Richard; Scandrett, John; Rockoff, S. David (Washington Univ., St. Louis, Mo. Edward Mallinckrodt Inst. of Radiology).

From Proceedings of bone measurement conference, Chicago, Illinois, May 22–23, 1970.

An automatic scanner-computer system is described that, in the dried distal human radius, permits quantitation of the number and two-dimensional angular orientation of the trabecular shadows. Studies to determine the variables which may affect these calculations, the meaning of the trabecular data in terms of actual bone structure present, and the applicability of the method to the examination of radiographs of human bones for mineral content are discussed. (C.H.)

4638 (CONF-700515–, pp 195-8) MEASUREMENT OF BONE MINERAL USING COMPUTER ANALYSIS OF MICRORADIOGRAPHS. Lloyd, Elizabeth (Argonne National Lab., Ill.).

From Proceedings of bone measurement conference, Chicago, Illinois, May 22–23, 1970.

A technique for measuring bone mineral content is described that involves the automatic scanning of microradiographs on black and white 35 mm film exposed to give maximum contrast. Sections of bone are cut with a thickness of about 100μ from representative sites. The 35 mm film is scanned by a photomultiplier and cathode ray tube whose focal spot is under the control of a computer. The computer-scanner generates line segments over the areas of bone that are related to porosity or bone volume of the sample. (C.H.)

4639 (CONF-700515–, pp 199-204) NEW METHOD OF EVALUATING BONE LOSS IN OSTEOPOROSIS. Singh, Manmohan (Michael Reese Hospital, Chicago, Ill.); Riggs, B. Lawrence; Jowsey, Jenifer; Phil, D. (Mayo Clinic, Rochester, Minn. Mayo Foundation, Rochester, Minn.).

From Proceedings of bone measurement conference, Chicago, Illinois, May 22–23, 1970.

A method is described for the evaluation of bone mineral content in elderly patients with osteoporosis that involves the study of the trabecular pattern of the upper end of the femur in ordinary radiographs of the pelvis. The analysis of radiographs of 35 patients over 50 years of age showed that as normal bone deteriorates to severe osteoporosis, six different trabecular patterns can be observed in radiographs of the proximal femur. (C.H.)

4640 (CONF-700515–, pp 205-23) EVALUATION OF THE SIGNIFICANCE OF THE CONTRIBUTION OF COHERENT SCATTERING OF AN X RAY BEAM TO DARKENING OF RADIOGRAPHIC FILM. Moore, Richard (Minnesota Univ., Minneapolis); Ledley, Robert S. (National Biomedical Research Foundation, Silver Spring, Md.).

From Proceedings of bone measurement conference, Chicago, Illinois, May 22–23, 1970.

In the use of x rays for quantitative bone densitometry, the ac-

XUM

curacy of results obtained might be reduced by coherent scattering of the radiation in the specimen. To explore this possibility, a mathematical model was constructed of the absorption of x rays in a sample of bone. The model was used to calculate the darkening of x-ray film to be expected from the radiography of a sample of bone, with and without coherent scattering. The results indicated that the difference in the darkening of the film caused by the coherent scattering was negligible. This implies that coherent scattering is not a limitation to the use of x rays for quantitative bone densitometry. (auth)

4641 (CONF-700515–, pp 224-36) PHALANGEAL ATLAS: AN APPLICATION OF RADIOGRAPHIC PHOTODENSITOMETRY. Colbert, C.; van Hulst, H.; Spruit, J. J. (Fels Research Inst., Yellow Springs, Ohio).

From Proceedings of bone measurement conference, Chicago, Illinois, May 22–23, 1970.

A microdensitometer/computer system was used to scan radiographs of the human hand-wrist to estimate the weights of the phalangeal bones. A planimeter was used to estimate the bone sizes. Radiographically determined bone weights (bone indexes), bone sizes (bone areas), and paradensities (bone indexes/bone areas) were recorded for white urban Ohio subjects ranging in age from 1 to 90 years in relation to typical findings for various disease states. The data can be used to assess skeletal health and patient progress. (C.H.)

4642 (CONF-700515–, pp 237-42) BONE SALT DETERMINATION BY X-RAY SPECTROPHOTOMETRY. Jacobson, Bertil (Karolinska Institutet, Stockholm (Sweden)).

From Proceedings of bone measurement conference, Chicago, Illinois, May 22–23, 1970.

A multichannel recording x-ray spectrophotometer was developed for quantitative analysis of certain substances in vivo. When used for bone mineral determinations a special circuit was employed to eliminate errors caused by the presence of fat in the tissues. (C.H.)

4643 (CONF-700515–, pp 243-54) DETERMINATION OF BONE MINERAL CONTENT IN LUMBAR VERTEBRAE BY A DOUBLE GAMMA-RAY TECHNIQUE. Roos, Bengt; Rosengren, Bengt; Skoeldborn, Holger (Sahlgren Hospital, Goteborg (Sweden)).

From Proceedings of bone measurement conference, Chicago, Illinois, May 22–23, 1970.

The low accuracy of radiographic methods for determination of bone mineral content has, in recent years, caused the introduction of various methods utilizing isotopes. These methods have two main advantages, monochromatic radiation and constant intensity during the measurement. Methods utilizing a single, usually soft, γ-emitting isotope have been developed for both stationary transmission measurements and scanning procedures. Because of the disturbing influence of the soft tissue the single γ transmission methods are limited to the bones of the extremities. By using two γ energies it is possible to eliminate the influence of one extra attenuator, provided it has a known effective atomic number. Assuming that many skeletal changes become apparent more distinctly and earlier in the vertebrae, an apparatus to determine the mineral content of a vertebra, preferably a lumbar vertebra, was developed. Two separate γ energies must be measured simultaneously in order that the unknown amount of soft tissues in the path of the beam can be eliminated. Since a vertebra is highly irregular in all directions it is necessary to use an integration procedure, which takes into account several values determined along a path through the vertebra. The diameter of the beam should include an entire vertebra. An assembly that employs a ^{241}Am source and a ^{137}Cs source arranged so that both radiations are measured simultaneously is described. (C.H.)

4644 (CONF-700515–, pp 255-62) EFFECTS OF FAT ON BONE MINERAL MEASUREMENTS. Sorenson, James A.; Mazess, Richard B. (Wisconsin Univ., Madison). (COO–1422–75).

From Proceedings of bone measurement conference, Chicago, Illinois, May 22–23, 1970.

Errors in bone mineral measurements caused by fat in the medullary cavity are reviewed. Calibration techniques involving phantoms containing only bone mineral and muscle equivalent substances, e.g., hydroxyapatite and water, may be inaccurate because they do not include the fat and collagen found in real bones. As for medullary fat, approximate corrections could be applied if cortical thickness measurements (r_i and r_0) could be obtained, using correction curves. Calibration techniques which employ real bones, which are measured and subsequently ashed to determine mineral content, would already include some correction for collagen and fat, but only in an average sense, i.e., for bones of approximately the same size and composition as those involved in calibration. Further corrections such as by cortical thickness measurements would also be required in this case for measurements on bones of extreme or unusual dimensions, e.g., on a bone with an extremely thin cortex as may be found in severely demineralized individuals. (C.H.)

4645 (CONF-700515–, pp 263-71) TWO WAVELENGTH TECHNIQUE FOR THE MEASUREMENT OF BONE MINERAL CONTENT IN VIVO. Burch, William; Bloch, Peter (Pennsylvania Univ., Philadelphia. Dept. of Radiology).

From Proceedings of bone measurement conference, Chicago, Illinois, May 22–23, 1970.

The results of a study using dual beam γ transmission scanning and dipotassium hydrogen phosphate as a bone mineral substitute show that if the mass attenuation coefficients for bone mineral are known, the mineral content per unit cross-sectional area in a two component system can be determined to within 2 percent. The two wavelength technique described used Ra D and E (^{210}Pb and ^{210}Bi) and ^{241}Am with γ energies of 46.5 keV and 59.6 keV respectively as the γ sources. (C.H.)

4646 (CONF-700515–, pp 272-3) TWO PHOTON ABSORPTIOMETRIC ANALYSIS USING ^{109}Cd. Schmonsees, W. G.; Preuss, Luther E. (Edsel B. Ford Inst. for Medical Research, Detroit, Mich. Div. of Nuclear Spectroscopy and Radiation Physics).

From Proceedings of bone measurement conference, Chicago, Illinois, May 22–23, 1970.

Cadmium-109 and ^{241}Am–^{125}I have been evaluated for dual beam absorptiometry measurements of the lipid content of soft tissue. The former offers the advantages of being 2.6 times more sensitive to tissue composition than ^{125}I–^{241}Am as well as producing a low energy beam 3% more intense than ^{125}I filtered to equivalent monochromicity (99.9%). The 453 day half-life (compared to the 60 days of ^{125}I) and the single source of two beams further enhance cadmium's superiority. In vitro muscle analysis has been performed, using ^{109}Cd, with an accuracy of 2%. (auth)

4647 (CONF-700515–, pp 274-9) ^{244}Cm AND ^{145}Sm–^{145}Pm X-RAY SOURCES. Kastner, J.; Friedman, A. M.; Oltman, B. G.; Eckerman, Keith (Argonne National Lab., Ill.).

From Proceedings of bone measurement conference, Chicago, Illinois, May 22–23, 1970.

Curium-244 was tested as a source of L x rays for transmission scanning of small bones for measurements of mineral content. A source was prepared by encasing 90 mCi of ^{244}Cm in a brass holder with a thin Be window. Good scans of small finger bones were not obtained using NaI(Tl) or Si(Li) detectors. The possibility of using ^{145}Sm or ^{145}Pm as x-ray sources for transmission scanning of small bones was also investigated and preliminary data are reported. (C.H.)

4648 (CONF-700515–, pp 291-302) SPECIFICATIONS OF PHOTON ABSORPTIOMETER FOR BONE MINERAL MEASUREMENTS. (Sloan-Kettering Inst. for Cancer Research, New York).

From Proceedings of bone measurement conference, Chicago, Illinois, May 22–23, 1970.

The design specifications of an absorptiometer for use in measurements of bone minerals by dual beam γ transmission scanning are discussed. The instrument uses ^{241}Am and ^{125}I as sources, a scintillation detector, and computer data processing system. The collimator specification, electronic components, and modified Fortran IV program for IBM 1800 computer are included. The instrument gave good results when used for scanning arm or leg bones. (C.H.)

4649 (CONF-700515–, pp 308-12) ABSORPTIOMETRIC BONE MINERAL DETERMINATION USING ^{153}Gd. Mazess, R. B.; Ort, M.; Judy, P.; Mather, W. (Wisconsin Univ., Madison. Dept. of Radiology). (COO–1422–71).

From Proceedings of bone measurement conference, Chicago, Illinois, May 22–23, 1970.

Gadolinium-153 appeared to be a convenient source for dichromatic scanning of bones for measurement of mineral content, and the lower energy (43 keV) was useful by itself for conventional transmission scanning of long bones. The precision and accuracy of measurement appeared satisfactory in preliminary experiments. The major advantage of ^{153}Gd is probably in measurement of larger bones or bones with substantial soft-tissue cover. The use of this source for measurements of both mineral content and soft-tissue mass in humans and large animals is reported. (C.H.)

4650 (CONF-700515–, pp 314-31) POLYCHROMATIC X-RAY BEAM TO REPRESENT n MONOENERGETIC PHOTON SOURCES. I. LIMITATIONS AND CORRECTION FACTORS FOR PHOTON DETECTORS. Waggener, Robert G.; Rogers, Lee F.; Zanca, Peter (Texas Univ., San Antonio. Dept. of Radiology).

From Proceedings of bone measurement conference, Chicago, Illinois, May 22–23, 1970.

The idea of using a polychromatic x-ray beam as n monoenergetic photon sources for measurements of mineral content of bones by absorption analysis is discussed. An analysis of the difficulties reveals that they may be resolved by applying certain corrections to the x-ray spectrum and normalizing the x-ray output of individual runs. The true spectrum, $N_i(E)$, may be generated by the application of matrix methods utilizing experimentally measured correction factors. The technique of deriving these correction factors is well known and may be adapted for use with a NaI(Tl) crystal, or other detectors, to detect the x-ray spectrum. The x-ray method, when properly applied, will yield the same degree of accuracy in measuring the composition of substances utilizing x-ray absorption as that now provided by using monoenergetic photon sources. (C.H.)

4651 (CONF-700515–, pp 340-50) CLINICAL TRIAL OF THE ^{125}I ISOTOPE SCANNING DEVICE AS A SCREENING METHOD FOR THE EARLY DETECTION OF OSTEOPOROSIS. Johnston, James O.; Goldsmith, Naomi F. (Kaiser Foundation Research Inst., Oakland, Calif.).

From Proceedings of bone measurement conference, Chicago, Illinois, May 22–23, 1970.

Bone mineral content was measured in 3740 individuals ranging from 30 to 70 years of age. Women comprised 61% of the group and men 39% of the total, and 80% of the group were in their 50's. Radiography of the spine was used to evaluate bone mineral content in 2123 individuals and 1617 were evaluated for mineral content by γ transmission scanning of the distal radius using ^{125}I as the source. Results of γ transmission scanning showed the highest degree of correlation with spinal osteoporosis. The data were analyzed in relation to race (Caucasian, Negro, Oriental), sex, bone mass, bone mineral content, and history of bone fractures. (C.H.)

4652 (CONF-700515–, pp 365-82) INTERNAL RELATIONSHIPS BETWEEN SKELETAL PARAMETERS IN TWENTY-THREE MALE SKELETONS. Horsman, A.; Bulusu, L.; Bentley, H. B.; Nordin, B. E. C. (Medical Research Council, Leeds (England). Mineral Metabolism Unit).

From Proceedings of bone measurement conference, Chicago, Illinois, May 22–23, 1970.

Twenty-three male skeletons were examined using x-ray densitometric methods and contact radiography. The skeletal weight and volume were measured directly and the weight and weight/volume ratio used as the dependent variables in a multiple regression analysis of linear and densitometric measurements taken on the metacarpal, radius, ulna, femur and spine of each skeleton. The inter-relationships between variables were compared with those obtained in life in a group of normal male subjects.

4653 (CONF-700515–, pp 408-22) MINERAL CONTENT CHANGES IN THE OS CALCIS, ULNA, AND RADIUS INDUCED BY PROLONGED BED REST. Vogel, John M.; Friedman, Ronald J. (Public Health Service, San Francisco, Calif. Hospital).

From Proceedings of bone measurement conference, Chicago, Illinois, May 22–23, 1970.

A γ transmission scanning apparatus used for measurement of mineral content of the heel bone (os calcis) is described. It consists of a rectilinear scanner capable of performing scans across an area of bone by incrementing up or down after each horizontal row, and uses a 200 mCi ^{125}I source held in a housing with a narrow beam collimator ($\frac{1}{8}$") directly opposed and 5" distant from a similarly collimated 3mm × 1.5 cm, NaI crystal detector. These move synchronously and measure the beam attenuation caused by minerals in bone in any limb placed on a stationary platform between them. A mold is made of the subject's foot and housed in a plexiglass box with parallel sides which, when filled with water, provides a uniform tissue equivalence throughout the scan. Initial positioning is determined by a pre-study x-ray picture. A subsequent contour display of each scan can be compared with the x-ray picture to verify accurate repositioning. Each data point, 256 per row and 16 rows per scan, is modulated in intensity proportional to the magnitude of the count information. A similar device was constructed for scanning arm bones (radius and ulna). Applications of the scanning device for measurements of mineral content changes in the os calcis, radius, and ulna in patients during prolonged bed rest are reported. (C.H.)

4654 (CONF-700515–, pp 424-7) RESTRAINT DEVICE FOR SCANNING DOGS. Lee, Philip H.; Harris, William H. (Massachusetts General Hospital, Boston).

From Proceedings of bone measurement conference, Chicago, Illinois, May 22–23, 1970.

Studies on skeletal metabolism in mature dogs demanded an in vivo means of determining changes in bone mineral content periodically over the duration of a long term. The photon scan method has proved ideal for experimental work of this nature. The distal femur and distal tibia were scanned, primarily to facilitate reproducible placement. These sites are also reasonably representative of changes occurring in long bones elsewhere in the same skeleton. A restraint device was designed and fabricated that would ensure reproducible positioning of these two sites on dogs of various sizes. In all cases the dogs were immobilized with a general anesthetic given intravenously. The design of the restraint device is described. (C.H.)

4655 (COO–1762-6) [GROWTH OF UTERINE, PLACENTAL AND FETAL VASCULATURE]. Makowski, Edgar L. (Colorado Univ., Denver. Medical Center). [1970]. Contract AT(11-1)-1762. 37p. Dep. NTIS.

A method is described for measuring total and regional blood circulation in fetuses and in the uterus and placental tissues of pregnant mammals. Tissue samples obtained at various times following the injection of radioisotope-labeled plastic microspheres (^{141}Ce, ^{51}Cr, ^{125}I, ^{85}Sr, or ^{169}Yb) were counted in a well-type scintillation counter. Results are reported from studies of uterine blood flow and distribution in fetuses of Rhesus monkeys and sheep. The effects of biological stress induced by exercise, acidosis, hypotension, or hypoxia on the distribution of uterine blood in the fetuses in monkeys and blood circulation in the brain of fetuses in sheep were also studied. (C.H.)

4656 (ORNL–4615) MOLECULAR ANATOMY PROGRAM. (The MAN Program). First Semiannual Progress Report for Period March 1–August 31, 1970. (Oak Ridge National Lab., Tenn.). Oct 1970. Contract W-7405-eng-26. 82p. Dep. NTIS.

The discovery that irradiated fetal tissues can immunize adult animals against challenge with virus-induced tumor cells opens up a new era in oncology. Efforts are proceeding aimed at the isolation of the active principle and at the solubilization and characterization of tumor specific transplantation antigens from rodent and human cells transformed with SV40 virus, adenovirus 31, and polyoma virus. The mechanisms involved in native and immunogen stimulated rejection mechanisms are being delineated to define procedures which may be useful in human therapy. The development of methods for monitoring anti-TSTA antibodies in animals after surgical removal of tumors shows that when tumor removal is complete, circulating antibodies rapidly return to a fairly high level. When a very small amount of tumor remains, the level rises and then falls rapidly. This suggests the feasibility of similar measurements in man to determine whether extirpation is complete or whether chemotherapy and radiation should be employed to destroy small residual tumor masses. The discovery that ^{67}Ga localizes preferentially in many human tumors has led to renewed interest in the development of high resolution total-body scanning. Work is progressing rapidly on the development of precision focusing scanners and on computer storage, reduction, and display of scanning data to obtain high resolution images. The feasibility of combining radioactive and ultrasonic scanning as a method for reducing or eliminating blood vessels from radioactivity scans is continuing. (C.H.)

4657 (UCLA–12-782, pp 89-125) NUCLEAR MEDICINE. (California Univ., Los Angeles. Lab. of Nuclear Medicine and Radiation Biology).

From annual progress report for the period ending June 30, 1970.

Radioisotope inhalation and perfusion scanning were found to be effective for the evaluation of ventilation and perfusion abnormalities of lung transplants in dogs. Seventy-three patients with suspected pulmonary embolism were studied with combined inhalation and perfusion lung scanning using ^{99m}Tc- or ^{113m}In-albumin aerosol and ^{131}I- or ^{99m}Tc-macroaggregated albumin. A review of the results led to the conclusion that perfusion and radioaerosol inhalation scanning procedures help distinguish the regional ischemia of pulmonary embolism from that associated with obstructive airways disease. Studies in dogs indicated that the injection of sufficient doses of radioactive albumin macroaggregates for scanning regional myocardial blood flow does not interfere with heart function. The long-term retention of Ta, recently recommended as a promising bronchographic contrast agent, in the lungs of dogs was demonstrated. A comparative evaluation of ^{99m}Tc-pertechnetate scanning and cerebral angiography for the diagnosis of brain lesions in children showed good correlation for the diagnosis of most tumors and that the scan was of little value for the diagnosis of congenital and degenerative defects. A survey of results of ^{99m}Tc-pertechnetate brain scans performed on approximately 1500 patients showed that best diagnostic results were obtained when scans performed within one hour of injection of the tracer were followed by rescanning three to four hours later. The use of ^{99m}Tc-DTPA or ^{113m}In chelates as a substitute for ^{131}I-hippurate for scanning kidney transplants for functional changes is discussed. The use of a 3-dimensional phantom to study the variables that affect radioisotope scan images is described. Arterial and venous

XUM

blood circulation in the human liver was studied using a magna-camera and video quantifier following the rapid intravenous injection of ^{99m}Tc-labeled albumin solutions or microaggregates. The radiation dose to a human adult population (454 persons) attributable to fallout ^{137}Cs internal contamination during the past 10-year period was estimated to be between 8 and 10 mrad, or about 6% of the radiation dose delivered by natural ^{40}K continuously present in the body. The dose estimates were based on the results of 1052 whole-body measurements of ^{137}Cs content performed between 1960 and 1969 and calculations of absorbed radiation dose based on MIRD formulas. (C.H.)

4658 DISAPPEARANCE OF IODOALBUMIN FROM PERICARDIAL SAC IN A PATIENT WITH MYXEDEMA. Tauxe, W. Newlon; Broadbent, James C.; Thorsen, Helen C. (Mayo Clinic and Mayo Foundation, Rochester, Minn.). J. Nucl. Med.; 11: 554-8(Sep 1970).

The rate of disappearance of ^{131}I-labeled human serum albumin from the pericardium was determined in a patient with pericardial effusion which accompanied myxedema but which did not clear after appropriate thyroid replacement therapy. Sequential scintiscanning was performed, and the data were digitized and computer processed. The total counting rates over the pericardium were obtained from the computer plots of the scintiscan matrices. Net counts were corrected for decay and plotted against time on semi-logarithmic paper. A single exponential was obtained, the slope of which indicated a disappearance rate of 1.5%/day. It was not clear from our data whether the slow clearance of labeled albumin had been caused by or associated with a prior myxedematous state. (auth)

4659 TUMOR THROMBUS OF THE RIGHT ATRIUM DISPLAYED BY RAPID SEQUENCE SCINTIPHOTOGRAPHY. Staub, Roy T. (Veterans Administration Hospital, New Orleans). J. Nucl. Med.; 11: 559-60(Sep 1970).

Rapid sequence γ camera scintigraphy following the injection of a tracer dose of metastable ^{99}Tc-pertechnetate revealed a large space-occupying lesion in the right heart atrium of a patient with a kidney carcinoma that was demonstrated by ^{203}Hg-chlormerodrin and ^{131}I-hippuran scanning. It was concluded the tumor thrombus obstructed the inferior vena cava and extended into the right atrium. (C.H.)

4660 ^{99m}Tc BRAIN SCANNING IN HERPES VIRUS TYPE I ENCEPHALITIS. Halpern, S. E.; Smith, C. W. Jr.; Ficken, V. (Univ. of Oklahoma, Oklahoma City). J. Nucl. Med.; 11: 548-50(Sep 1970).

Abnormalities in metastable ^{99}Tc-labeled pertechnetate brain scans on one patient with Herpes simplex encephalitis are reported. The diagnosis was made by culture of brain tissue obtained by biopsy. A second scan made 55 days following the first one and after therapy showed some decrease in uptake of ^{99}Tc-pertechnetate. (C.H.)

4661 EFFECT OF CAPSULE CONTENT VARIATIONS ON THYROID UPTAKE RESULTS. Lawrence, Cynthia A.; Russell, Moses E.; Davis, Rachel P.; Johnson, Raleigh F. Jr.; Gorten, Ralph J. (Veterans Administration Hospital, Durham, N. C. Duke Univ., Durham, N. C.). J. Nucl. Med.; 11: 561-3(Sep 1970).

The customary method of measuring the thyroid uptake of iodide depends on the administration of a patient dose of ^{131}I of the same strength as the standard which is to be used as the basis of comparison. It is generally assumed that all capsules in a given lot from a commercial radiopharmaceutical supplier contain equal amounts of radioactive iodide. Thus they may be used for either the patient or the standard. Clinically important variations in capsule content of tracer have been found to occur on occasions. This is in spite of the diligent efforts of manufacturers to provide uniformity in every capsule lot. The analysis of these observations indicates that significant errors in thyroid uptakes may occur if the percent capsule difference in a lot is greater than 8% or the deviation from the mean or label exceeds ±4%. Therefore it is strongly recommended that precounting of every lot of capsules be made a routine procedure in every nuclear medicine laboratory. (auth)

4662 PULMONARY INVESTIGATION WITH RADIONUCLIDES. First Annual Nuclear Medicine Seminar, Miami, Florida, March 7–11, 1969. Gilson, Albert J.; Smoak III, William M. (eds.). Springfield, Ill.; Charles C Thomas, Publisher (1970). 384p. $21.50. (CONF-690334).

Separate abstracts were prepared for 26 of the 31 papers presented. The remaining five papers were not within the scope of NSA. (W.H.K.)

For abstracts of individual papers see: 4324–4328, 4393, 4428, 4511, and 4663–4680.

4663 RADIOACTIVE GASES. Milic-Emili, J. (McGill Univ., Montreal). pp 59-64 of Pulmonary Investigation with Radionuclides. /Gilson, Albert J. (ed.). Springfield, Ill.; Charles C Thomas, Publisher (1970).

From 1st Annual Seminar on Pulmonary Investigation with Radionuclides, Miami, Fla. See CONF-690334.

The measurement of regional lung function by external scanning using radioactive gases is discussed. Data are presented for half-life, γ energy emission, and solubility coefficients of ^{13}N, ^{15}O, ^{133}Xe, and ^{135}Xe. A closed circuit spirometer is described for obtaining the relationship between the intrapulmonary ^{133}Xe concentration and the external counting rate or the calibration factors. The gas-liquid partition coefficients of xenon for saline, plasma, red cells and whole blood are given. (H.L.W.)

4664 CYCLOTRON PRODUCTS. Ter-Pogossian, Michel M. (Washington Univ., St. Louis). pp 65-8 of Pulmonary Investigation with Radionuclides. /Gilson, Albert J. (ed.). Springfield, Ill.; Charles C Thomas, Publisher (1970).

From 1st Annual Seminar on Pulmonary Investigation with Radionuclides, Miami, Fla. See CONF-690334.

The production of short-lived radioactive nuclides for pulmonary function studies using a positive ion accelerator such as a cyclotron is discussed. The source of the deuteron for the cyclotron is a tank of deuterium gas. The beam goes through an aluminum window and escapes from the vacuum of the chamber. The deuteron path then hits a target chamber in which the target gases are irradiated. Radioisotopes produced by the cyclotron are ^{15}O, ^{11}C, and ^{13}N. Each of these decays with a rather short half-life and with the emission of positrons. The value of these isotopes in various fields of research as well as in lung scanning for pulmonary function is emphasized. (H.L.W.)

4665 ARCHAIC METHODS OF REGIONAL VENTILATION: PERFUSION ASSESSMENT. Marks, Asher (Univ. of Miami, Fla.). pp 83-9 of Pulmonary Investigation with Radionuclides. /Gilson, Albert J. (ed.). Springfield, Ill.; Charles C Thomas, Publisher (1970).

From 1st Annual Seminar on Pulmonary Investigation with Radionuclides, Miami, Fla. See CONF-690334.

The historical background of regional ventilation and perfusion is reviewed. A number of techniques have been used for quantitative assessments of maldistribution of ventilation. In the method of helium equilibration the individual was allowed to equilibrate with helium over a number of breaths; this method revealed more than one compartment of ventilation. The method of breathing oxygen and then monitoring the nitrogen washout is useful for measurement of residual volume. In the single-breath method the individual takes a single breath and breathes out through a nitrogen meter. Some regional estimation of flow is possible with angiography techniques. The first practical technique was that of bronchospirometry. Regional ventilation and perfusion are now measured safely and quickly using a multicrystal rectilinear scanner as a detector with ^{133}Xe for ventilation and iodine-labeled macroaggregated albumin for perfusion. (H.L.W.)

4666 USE OF RADIOACTIVE GAS IN THE INVESTIGATION OF PULMONARY FUNCTION. Milic-Emili, J. (McGill Univ., Montreal). pp 106-17 of Pulmonary Investigation with Radionuclides. /Gilson, Albert J. (ed.). Springfield, Ill.; Charles C Thomas, Publisher (1970).

From 1st Annual Seminar on Pulmonary Investigation with Radionuclides, Miami, Fla. See CONF-690334.

Methods for measuring the regional ventilatory function of the lung using ^{133}Xe consist of single breath and multiple breath tests. The multiple breath tests consist of analysis of wash-in curves of inhaled ^{133}Xe which can be done either by having the subject breathe from an open circuit or by having him rebreathe in a closed circuit. The ^{133}Xe that has been delivered into the lung by inhalation or by intravenous injection is measured for regional washout curves. A bolus of ^{133}Xe dissolved in saline is then injected into a vein and the washout of the injected xenon is followed. Analysis of the wash-in and wash-out curves is done by plotting count rates against time. In the single breath tests the bolus technique consists essentially of having subjects take a vital capacity. A small bolus of ^{133}Xe is then injected into the inspirate. The subject breathes all the way in and at the end of the inspiration count rates are measured by means of scintillation counters. In elderly subjects the distribution pattern is essentially the same as in younger subjects. However, in young subjects the point at which all airways reopen is lower than the functional residual capacity. Thus in young subjects airway closure is not present in the normal range of tidal volume breathing. A method for calculating ventilation per alveolus is described. (H.L.W.)

XUM

4667 DISTRIBUTION OF BLOOD FLOW AND VENTILATION WITH ^{15}O, ^{13}N, AND ^{11}C. West, John B. (Royal Postgraduate Medical School, London). pp 118-22 of Pulmonary Investigation with Radionuclides. /Gilson, Albert J. (ed.). Springfield, Ill.; Charles C Thomas, Publisher (1970).

From 1st Annual Seminar on Pulmonary Investigation with Radionuclides, Miami, Fla. See CONF-690334.

Studies were conducted on the clearance rate of CO_2 from alveolar gas into the pulmonary capillary bed. When the CO_2 is labeled with ^{15}O, the clearance rate is extremely rapid; however, when ^{11}C is used as a label, the clearance rate is much slower. Mechanisms involved in this difference are discussed. The use of information obtained from clearance rate studies in clinical practice is discussed. Clearance rates of radioactive carbon monoxide were obtained and the value of this gas for measuring the diffusing capacity of the lung is pointed out. The advantages of radioactive nitrogen over xenon for applications in measuring regional ventilation and blood flow are examined. The use of radioactive water vapor for clearance rate studies is discussed. (H.L.W.)

4668 DETERMINATION OF VENTILATION: PERFUSION RELATIONSHIPS. Gilson, Albert J. (Univ. of Miami, Fla. Mount Sinai Hospital, Miami, Fla. Jackson Memorial Hospital, Miami, Fla.). pp 123-8 of Pulmonary Investigation with Radionuclides. /Gilson, Albert J. (ed.). Springfield, Ill.; Charles C Thomas, Publisher (1970).

From 1st Annual Seminar on Pulmonary Investigation with Radionuclides, Miami, Fla. See CONF-690334.

A 10-crystal rectilinear scanner was developed for ^{133}Xe lung scanning. The counts from each radiation detector were fed into an electronic interface which assigned X and Y coordinates, located anatomic landmarks, and the count information recorded directly onto a computer-compatible format on magnetic tape. Ventilatory distribution was determined by having the subject breathe into a closed system spirometer containing ^{133}Xe. Operation of the scanner is begun simultaneously with ^{133}Xe breathing. Two successive wash-in scans are obtained in less than six minutes. At the beginning of the eighth minute of ^{133}Xe breathing, an equilibration scan is obtained for determination of the ventilated space. On completion of this study, the patient is switched into an open circuit oxygen breathing system and two successive washout scans are recorded. Following the last washout, 200 μCi of MAA labeled with ^{131}I are injected intravenously and a perfusion scan is recorded. The data are recorded on magnetic tape and then processed on the IBM 7040-1401. The equilibrated ventilation and perfusion scans are processed to give corrected numerical values for the collected counts. This method is valuable in the assessment of regional pulmonary function in normal subjects and in patients with a variety of pulmonary diseases. (H.L.W.)

4669 NEW FRONTIERS IN PULMONARY INVESTIGATION. Ter-Pogossian, Michel M. (Washington Univ., St. Louis). pp 205-9 of Pulmonary Investigation with Radionuclides. /Gilson, Albert J. (ed.). Springfield, Ill.; Charles C Thomas, Publisher (1970).

From 1st Annual Seminar on Pulmonary Investigation with Radionuclides, Miami, Fla. See CONF-690334.

A new technique for measuring regional oxygen metabolism in the lung is described. Radioactive oxygen and carbon dioxide are used to determine the integrity of the pathway supplying oxygen or hydrogen ions. A diagram is presented to show the components of metabolism and the role of the cytochrome system in oxygen and water metabolism. Another technique is described for measuring cerebral blood flow to the lung. Conventional methods using radioisotopes for labeling the blood provide only a two-dimensional picture of blood flow. It is suggested that with the development of electronic circuitry, positron emitters will give the third dimension. Another method using a nonradioactive element as an indicator is described. The element is localized by means of x rays and the resulting fluorescence is detected by means of a solid state radiation detector. This method provides a three-dimensional localization of the tracer, is extremely sensitive, and is capable of detecting extremely small amounts of the tracer. (H.L.W.)

4670 LUNG SCANS IN SPATIAL PERSPECTIVE. Hidalgo, John U. (Tulane Univ., New Orleans). pp 210-15 of Pulmonary Investigation with Radionuclides. /Gilson, Albert J. (ed.). Springfield, Ill.; Charles C Thomas, Publisher (1970).

From 1st Annual Seminar on Pulmonary Investigation with Radionuclides, Miami, Fla. See CONF-690334.

An attempt was made to extend the usefulness of multiple scan images. For this study, lung scanning procedures were selected and studied. This was an attempt to extract the maximum utilization of available data by using more than one scan image for viewing. Most of the scans studied were scans made from patients given macroaggregated albumin labeled with ^{131}I. Three data sets are available for comparative analysis in the lung scan procedure: anterior-posterior scan, posterior-anterior scan, and chest roentgenogram. (H.L.W.)

4671 FOUR QUANDRANT RADIOSPIROMETRY IN NORMAL AND DISEASED STATES. Arborelius, Mans Jr. (Univ. of Lund, Sweden); Mioerner, G.; Lindell, S. E.; Svanberg, L.; Swenson, Edward W. pp 216-26 of Pulmonary Investigation with Radionuclides. /Gilson, Albert J. (ed.). Springfield, Ill.; Charles C Thomas, Publisher (1970).

From 1st Annual Seminar on Pulmonary Investigation with Radionuclides, Miami, Fla. See CONF-690334.

The lung volume was visualized following administration of ^{133}Xe by eight external scintillation detectors coupled together in pairs, one in front and one behind the subject. The output from each channel was recorded by a multichannel tape recorder after passing a rate meter. After routine pulmonary function studies have been performed, a plastic catheter is passed from an antecubital vein to the right atrium. The detectors are placed over the patient, and ^{133}Xe is injected while the patient is told to hold his breath. The amplitude of the output from each of the four pairs of detectors over each region is directly proportional to the regional blood flow. Regional ventilation is measured, and the gas volume of the lung under each detector is measured after rebreathing of ^{133}Xe from a spirometer. Equations are presented for calculating the percentage of perfusion, ventilation, functional residual capacity, and vital capacity. It is stressed that radiospirometry is a supplementary study to the common lung function measurements and of little value without them. (H.L.W.)

4672 SIMPLE TECHNIQUE FOR PULMONARY INVESTIGATION USING ^{133}Xe. West, John B. (Royal Postgraduate Medical School, London). pp 227-30 of Pulmonary Investigation with Radionuclides. /Gilson, Albert J. (ed.). Springfield, Ill.; Charles C Thomas, Publisher (1970).

From 1st Annual Seminar on Pulmonary Investigation with Radionuclides, Miami, Fla. See CONF-690334.

The use of ^{133}Xe scanning for measuring distribution of ventilation and blood flow in the lungs is discussed. Three methods in use are: use of a battery of fixed counters, use of fast scanning, and use of the radiation camera. The use of computer programs in combination with scanning counters was found to be useful in sorting out the patterns of blood flow caused by heart and lung disease. Normal patterns of blood flow are compared with flow in a patient with severe mitral stenosis. The cause of inversion of blood flow in patients with a severe rise in pulmonary venous pressure was investigated using dogs as experimental animals. Dextran was injected to induce interstitial edema and an increase in pulmonary venous pressure was found. It was concluded that the edema exaggerated the normal reduction of blood flow at the bottom of the lung. Results of lung scanning of patients in the vertical and horizontal positions are described. (H.L.W.)

4673 FUNDAMENTAL ASPECTS IN THE STUDY OF LUNG FUNCTIONS WITH RADIONUCLIDES. Sternberg, Joseph (Univ. of Montreal). pp 241-59 of Pulmonary Investigation with Radionuclides. /Gilson, Albert J. (ed.). Springfield, Ill.; Charles C Thomas, Publisher (1970).

From 1st Annual Seminar on Pulmonary Investigation with Radionuclides, Miami, Fla. See CONF-690334.

The use of radioisotopes for lung function studies during pregnancy is reviewed. Problems encountered are the following: the irradiation of the fetus by a γ-emitting radionuclide administered to the mother and confined to the maternal compartment; and the placental transfer and subsequent fetal uptake of labeled compounds and the fetal radiation damage. Relative hazards from the use of macroaggregates labeled with ^{113m}In, ^{131}I, and ^{99m}Tc are discussed. Inhalation of radioactive gases during pregnancy following accidents such as the Windscale incident and placental transfer of gaseous decay products of ^{226}Ra and ^{234}Th are considered. The uptake of ^{133}Xe by the fetus following use for assessment of uterine blood flow is discussed. The application of the Fick equation of diffusion to placental transfer of inert gases is discussed. The excretion of volatile compounds such as acetone, alcohol, ammonia, and methyl mercaptan, from the lungs is discussed. The excretion of mercury salts by the lungs following the use of $^{203}HgCl_2$ for kidney studies is considered. Studies on pulmonary excretion of ^{75}Se showed that excretion occurred only after injection of selenite and was not detected after injection of selenate, ^{75}Se-labeled methionine, or ^{75}Se-labeled cystine. (H.L.W.)

4674 IMPORTANCE OF REPRODUCIBLE LUNG SCANNING. Goodrich, Jack K.; Harris, C. Craig (Duke Univ., Durham, N. C.). pp 260-70 of Pulmonary Investigation with Radionuclides. /Gilson, Albert J. (ed.). Springfield, Ill.; Charles C Thomas, Publisher (1970).

XUM

From 1st Annual Seminar on Pulmonary Investigation with Radionuclides, Miami, Fla. See CONF-690334.

The importance of reproducible scan recording techniques is discussed. The need is illustrated by the review of a case report on a patient with an embolus in a pulmonary artery on whom repeat ^{131}I-albumin macroaggregate lung scans were performed. (C.H.)

4675 PATHOPHYSIOLOGY OF PERFUSION IN PULMONARY DISEASE. Smoak III, William M.; Viamonte, Manuel Jr. (Univ. of Miami, Fla.). pp 271-4 of Pulmonary Investigation with Radionuclides. /Gilson, Albert J. (ed.). Springfield, Ill.; Charles C Thomas, Publisher (1970).

From 1st Annual Seminar on Pulmonary Investigation with Radionuclides, Miami, Fla. See CONF-690334.

Diagnostic problems in perfusion lung scanning and in chest radiography are discussed. The complementary use of these techniques is being investigated for differentiating between various lung diseases. The alterations of the blood supply to the lung in normal man and in various pathological conditions using pulmonary angiography, selective bronchial arteriography, and lung scanning are being studied. Obstructive ventilatory diseases and obliteration of both bronchial and pulmonary artery circulations in diseases such as panacinar pulmonary emphysema were demonstrated. Chest roentgenography, single and serial pulmonary perfusion and ventilatory scanographic examinations, and pulmonary angiography are used in combination for the best assessment of pathological changes in the lungs. (H.L.W.)

4676 EVALUATION OF PULMONARY DISEASE USING ^{133}Xe GAS AND THE SCINTILLATION CAMERA. Loken, Merle (Univ. of Minnesota, Minneapolis). pp 275-81 of Pulmonary Investigation with Radionuclides. /Gilson, Albert J. (ed.). Springfield, Ill.; Charles C Thomas, Publisher (1970).

From 1st Annual Seminar on Pulmonary Investigation with Radionuclides, Miami, Fla. See CONF-690334.

Scintiphotograms showing the distribution and washout of ^{133}Xe administered by inhalation or intravenous injection are presented for normal subjects and patients with emphysema, obstructive lung disease, cystic fibrosis, neonatal tetralogy of Fallot, and pulmonary emboli. Technetium-99m-labeled albumin was also used for long scanning. It was concluded that in the presence of a normal chest film and a macroaggregate scan showing areas of decreased perfusion, the diagnosis of pulmonary emboli may be in error, since other diseases, notably emphysema, may give similar findings. Emphysematous areas show decreased perfusion and abnormal ventilation with delayed clearance by the ^{133}Xe technique, while areas of embolization show decreased perfusion and essentially normal ventilation and clearance times. (H.L.W.)

4677 TECHNETIUM-INDIUM DOUBLE LUNG SCANNING IN THE STUDY OF THE REDISTRIBUTION OF PULMONARY BLOOD FLOW IN ACUTE LEFT VENTRICULAR FAILURE. Swenson, Edward W. (Univ. of Florida, Gainesville); Arborelus, Mans Jr.; Bruno, Fred P.; Williams, Clyde M. pp 291-5 of Pulmonary Investigation with Radionuclides. /Gilson, Albert J. (ed.). Springfield, Ill.; Charles C Thomas, Publisher (1970).

From 1st Annual Seminar on Pulmonary Investigation with Radionuclides, Miami, Fla. See CONF-690334.

Dogs were anesthetized and catheters were placed in the pulmonary artery, thoracic aorta, and left atrium. Left ventricular failure was induced by embolizing a branch of the left coronary artery. Either ^{113}In or ^{99}Tc was injected and cardiac output was determined during ventricular failure. The other tracer was then injected and the lungs were scanned with the gamma camera for distribution of blood flow with one tracer and then with the other. Graphs are presented to show changes in systemic and pulmonary arterial pressure before and during acute ventricular failure; changes in arterial oxygen and carbon dioxide before and during ventricular failure; changes in pulmonary compliance before and during ventricular failure; and changes in output dye, dilution curve method before and during left ventricular failure, and the amount of flow to the right lung as a percentage of the total pulmonary blood flow. (H.L.W.)

4678 RADIOAEROSOL INHALATION SCANNING. Taplin, George V.; Poe, Norman D.; Dore, Earl K.; Greenberg, A.; Isawa, T. (Univ. of California, Los Angeles). pp 296-317 of Pulmonary Investigation with Radionuclides. /Gilson, Albert J. (ed.). Springfield, Ill.; Charles C Thomas, Publisher (1970).

From 1st Annual Seminar on Pulmonary Investigation with Radionuclides, Miami, Fla. See CONF-690334.

The basic principles, test agents, techniques, and equipment for performing inhalation lung scintiscans are described. The current concepts regarding the mechanism and significance of abnormal aerosol inhalation scan patterns are presented and demonstrated in controlled animal experiments. The results of combined radioaerosol inhalation-perfusion lung scanning in more than eight hundred patients are condensed by presenting representative cases that illustrate the reproducibility and clinical value of both types of scintiscanning procedures in major pulmonary disorders. Emphasis is placed on the value of combined inhalation-perfusion scanning as practical methods for disclosing regional abnormalities of pulmonary function because of their unique capacity to disclose localized areas of pulmonary ischemia and/or sites of partial or complete airways obstruction. Scans, angiograms, and bronchograms are not competitive procedures. They provide different kinds of information, and when coordinated, each enhances the value of the other. Radioaerosol inhalation scanning has several important applications in chronic obstructive pulmonary disease. Both types of scanning procedures are valuable adjuncts to radiography and pulmonary function tests whenever assessment of regional arterial perfusion and airway patency is needed to guide the course of treatment. (auth)

4679 PATHOPHYSIOLOGIC ASPECTS OF PULMONARY EMBOLISM. Robin, Eugene (Univ. of Pittsburgh). pp 339-48 of Pulmonary Investigation with Radionuclides. /Gilson, Albert J. (ed.). Springfield, Ill.; Charles C Thomas, Publisher (1970).

From 1st Annual Seminar on Pulmonary Investigation with Radionuclides, Miami, Fla. See CONF-690334.

The following changes occurring as a result of pulmonary embolism are discussed: abnormalities of perfusion and ventilation, ventilation-perfusion relations, pulmonary infarction, blood gas and acid base changes, and unusual manifestations of pulmonary embolism. Problems associated with scanning consist of individual variations in ventilation-perfusion abnormalities, areas of resolution of clotting, non-specific alterations seen on scans, wide separation of changes in time and space, need for additional diagnostic measures, and limited prognostic value of diagnosis of pulmonary occlusion. (H.L.W.)

4680 PULMONARY SCANNING IN THE DIAGNOSIS OF PULMONARY THROMBOEMBOLISM. Quinn III, James L. (Northwestern Univ., Chicago). pp 349-55 of Pulmonary Investigation with Radionuclides. /Gilson, Albert J. (ed.). Springfield, Ill.; Charles C Thomas, Publisher (1970).

From 1st Annual Seminar on Pulmonary Investigation with Radionuclides, Miami, Fla. See CONF-690334.

The advantages of lung scanning, using ^{113m}In, ^{131}I, and ^{99m}Tc, as a diagnostic aid are pointed out. Results of lung scanning in cases of multiple perfusion defects and acute hemoptysis are described and illustrated. Laboratory experiments were conducted on dogs to study conditions that caused altered perfusion. Causes for nonuniform pulmonary perfusion are as follows: gravity, thromboembolism, pulmonary arterial wall disease, mediastinal mass, and excess free fluid. Conditions with abnormal chest films which showed normal perfusion lung scans included cardiac failure with pleural effusion and acute pulmonary edema. It is pointed out that the lung scan should be used in cases of unexplained deterioration in chronic lung disease, chest pain, hemoptysis, dyspnea, and left ventricular failure. (H.L.W.)

4681 REGIONAL CEREBRAL BLOOD FLOW IN ORGANIC DEMENTIA WITH EARLY ONSET. Ingvar, David H.; Gustafson, Lars (University Hospital, Lund, Sweden). Acta Neurol. Scand.; 46: Suppl. 43, 42-73(1970).

Regional cerebral blood flow (rCBF) was determined in 38 patients with organic dementia with early onset, by means of the ^{133}Xe-clearance technique, using an 8- or a 32-detector unit. Thirty-five of the patients were studied in the dominant hemisphere. The patients were diagnosed as suffering from Alzheimer-Pick's disease in 14 cases, and from dementia of the cerebrovascular type in 12 cases. In nine out of 12 further cases, a possible aetiology for the dementia could be identified (hydrocephalus, head injury, thyroid dysfunction, chronic encephalitis). The patients were studied from 2 to 5 years after the onset of symptoms. Mean rCBF variables were significantly reduced in the most demented cases, especially in the Alzheimer group, in which the severest forms of intellectual impairment were encountered. A number of local flow reductions were found in temporal and adjacent regions, a finding possibly related to the amnesic-agnosic symptoms, as well as to the predominance of the patho-anatomical changes in the same part of the brain. One patient, possibly suffering from an unknown form of chronic encephalitis, was found to have a very marked diffuse cerebral hyperaemia (confirmed 1 year later). She was largely neurologically normal, and the CSF did not show any abnormalities. There were also some other cases showing unexpectedly high rCBF values. Fourteen of the patients with severe dementia and low rCBF values showed diffuse EEG abnormalities with a slowing of

XUM

the background activity and bifrontal delta episodes. Many of these patients had suffered from vertigo, dizziness, fainting spells and/or regular drop attacks. These symptoms, in combination with the EEG abnormalities described, indicate that a brain-stem dysfunction of degenerative and/or cerebrovascular type may play a great role for the pathogenesis of organic dementia with early onset. It is concluded that rCBF measurements may be used to quantitate some of the cerebral consequences of organic dementia, and possibly also to localize the most affected brain regions to some extent. The rCBF technique is used to study the prognosis, as well as the effects of therapy, when available. (auth)

4682 IN VIVO DIAGNOSTIC APPLICATIONS OF EXTERNAL RADIOACTIVE SOURCES. Cameron, John R. (Univ. of Wisconsin, Madison). Trans. Amer. Nucl. Soc.; 13: 520(Nov 1970).

From Meeting of the American Nuclear Society, Washington, D. C. See CONF-701102.

4683 ROLE OF THE CYCLOTRON IN NUCLEAR MEDICINE. Laughlin, John S. (Sloan-Kettering Inst., New York). Trans. Amer. Nucl. Soc.; 13: 522(Nov 1970).

From Meeting of the American Nuclear Society, Washington, D. C. See CONF-701102.

4684 PHYSICAL ASPECTS OF SCINTISCANNING. Mallard, John R. (Univ. of Aberdeen, Scotland). Proc. Roy. Soc. Med.; 62: 787-94(Aug 1969).

Physical factors that affected the quality of ^{99m}Tc scintigraphy, and applications of recent instrumentation were discussed. A collimator effective for brain scanning using ^{99m}Tc was described. This collimator provides a comparatively well-defined acceptance region laterally where the counting rate was between 50 and 100% over a region 8 mm wide at 14 cm depth in tissue and the variation of response with depth was between 70 and 100% from 8 to 16 cm deep. The detector was the prime component that decided sensitivity, resolution and depth dependence from radioactivity in the body. The definition and physical measurement of sensitivity and resolution were discussed. The line spread function (LSF) provided a measure of sensitivity and resolution from which was derived a more complete description of the resolving properties of the collimator, the modulation transfer function. This was, in effect, a frequency response of the collimator. The physical characteristics of the γ camera were reviewed. The advantages of the line source method of determining a measure of sensitivity and resolution for a γ camera were discussed. The γ camera had a very rapid fall-off in sensitivity and resolution with increasing depth in the body. The worst defect of the γ camera was non-uniformity over the field of view. Overall performance of scintigraphic devices for detection and resolution of ^{99m}Tc was discussed and evaluated. (BBB)

4685 PULMONARY HEMOSIDEROSIS IN A 9-YEAR OLD CHILD WITH A TRISOMY 18. EXPLORATION WITH RADIOACTIVE ^{51}Cr AND ^{59}Fe. Orsini, A.; Stahl, A.; Sansot, M.; Giraud, F.; Perrimond, H.; Bernard, P. J.; Brusquet, Y.; Taramasco, H. (Hopital de la Conception, Marseille). Pediatrie; 24: 339-49(Apr-May 1969). (In French).

A polymalformed encephalopathic patient was hospitalized at the age of 8 years for a serious hyposideremic hypochromic anemia. The child was dyspneic. The pulmonary radiograms show a granulo-reticulated surcharge of the two pulmonary fields. The external isotopic countings made during evolution showed that the pseudohemolytic shortening of the life of the red blood cells is in fact due to intraalveolar hemorrhagic phenomena that are represented by an isotopic sequestration at the level of the pulmonary parenchyma. The chromosome study confirms the existence of a trisomy 18 responsible for the polymalformations this child has: low implantation of the ears, sternal shortness, single median palm crease, clubfooted with rudiments of a sixth toe, associated with encephalopathy. The evolution of the pulmonary hemosiderosis was made toward remission, but an acute relapse occurred within a few hours several months later. A postmortem pulmonary puncture confirmed the isotopic diagnosis. The association of a trisomy 18 and of pulmonary hemosiderosis does not appear fortuitous although the relation between these two afflictions remains uncertain: elastic dystrophy or correlation between immunologic illness and chromosome aberration. (tr-auth)

4686 DOUBLE CONTRAST EXAMINATION OF THE SMALL INTESTINE. PRELIMINARY COMMUNICATION OF A NEW TECHNIQUE. Pajewski, M.; Itzchak, Y.; Profis, A. (Univ. of Tel-Aviv Medical School, Zerifin, Israel). Clin. Radiol.; 21: 83-6(Jan 1970).

A method allowing the visualization of the small intestine by double contrast was described. The small bowel, containing an ingested opaque material, was inflated with air and its motility was depressed by pharmacological means (Probanthine or Paragon). Out of 20 unselected cases, excellent visualization of the small intestine was obtained in 15 instances. In three cases, only a part of the small intestine was satisfactorily seen. There were two failures. (auth)

4687 A STUDY OF LIVER SCAN USING ^{113m}In COLLOID. Koh, Chang Soon (Radiological Research Inst., Seoul); Rhee, Chong Hoen; Chang, Kochang; Hong, Chang Gi D. J. Nucl. Sci. (Seoul); 9: No. 2, Pt. 2, 109-10(Apr 1970). (Korean).

The dose of ^{113m}In for high diagnostic value in examination of each organ was determined and the diagnostic interpretability of liver scanning with the use of ^{113m}In was carefully evaluated in comparison with the results of the liver scanning by the conventionally applied radioisotopes. It was found that the liver uptake rate and clearance into peripheral blood were greater with ^{113m}In colloid than with ^{198}Au colloid. The interpretability of a space-occupying lesion in liver scanning with ^{113m}In was also superior to ^{198}Au. Liver scans with ^{113m}In colloid did not always correspond to the scan with ^{198}Au. This difference can be explained by differences of phagocytic ability of the reticuloendothelial system within liver. In liver scanning with ^{113m}In colloid, the spleen was visualized even in normal subjects. In cases of disturbed liver function, uptake was less for ^{113m}In colloid than ^{198}Au; in the spleen, however, it was greater. With use of ^{113m}In colloid, the time required for scanning could be shortened in comparison with ^{198}Au. The filtration of ^{113m}In colloid for scanning prior to human administration gives an expectation for better scans. (C.O.)

Radiotherapy

Refer also to abstracts 4218, 4512, 4514, 4683, 4705, 4712, and 4714.

4688 BROMOURIDINE (BUdR) AS A RADIOSENSITIZING AGENT OF MALIGNANT BRAIN TUMOURS. Hoshino, Takao (Univ. of California, San Francisco); Nagai, Masakatsu; Sato, Fumiaki; Sano, Keiji; Watari, Tsutomu pp 491-7 of Radiation Protection and Sensitization. /Moroson, Harold (ed.). New York; Barnes and Noble, Inc. (1970).

From 2nd International Symposium on Radiosensitizing and Radioprotective Drugs, Rome, Italy. See CONF-690525.

Radiotherapy has been applied widely to the treatment of malignant brain tumors but, as far as gliomas are concerned, it is usually of little benefit. However, the combination of radiotherapy with the administration of a radiosensitizing agent seems to be more promising. A regimen of BUdR-Antimetabolite-Continuous intra-arterial infusion-Radiation therapy, termed BAR therapy, was applied to patients with malignant brain tumors. 5-Bromo-2'-deoxyuridine (BUdR) is a radiosensitizing agent that is incorporated mainly into the DNA of dividing cells in place of thymidine and is degraded rapidly by the liver. The advantage of this BUdR therapy is that brain tumor cells are radiosensitized selectively, since nerve cells have no mitotic activity and are protected by an intact blood-brain barrier. Infusion via the internal carotid artery channels large amounts of BUdR directly to the tumor tissue before it can be degraded by the liver. A small amount of an antimetabolite, such as methotrexate or 5-fluorouracil, is administered simultaneously to enhance the incorporation of BUdR into tumor cells: such antimetabolites inhibit biosynthesis of thymidine and force the cells to use the exogenous thymidine (BUdR). This regimen was used for therapy in 70 patients, 29 with highly malignant gliomas. Survival in one has exceeded three years, 10 patients have survived for over 18 months. The side effects of this therapy are depilation, radiodermatitis on the catheterized side of the forehead, and onychomadesis of fingernails. (auth)

4689 RADIOSENSITIZATION BY PROCARBAZINE IN THE TREATMENT OF MALIGNANT MESOTHELIOMA. Falkson, Geoffrey; Falkson, H. C.; Fichardt, T. (Verwoerd Hospital, Pretoria, Univ. of Pretoria). pp 499-502 of Radiation Protection and Sensitization. /Moroson, Harold (ed.). New York; Barnes and Noble, Inc. (1970).

From 2nd International Symposium on Radiosensitizing and Radioprotective Drugs, Rome, Italy. See CONF-690525.

Forty-five patients with malignant pleural mesothelioma were treated. None of nine patients who received radiotherapy only responded favorably. Fourteen of 26 patients treated with procarbazine and various doses of irradiation showed objective improvement for up to 20 months. Repeated courses of the combined treatment were necessary to maintain remissions. In patients receiving procarbazine significant tumor shrinkage was usually confined to the areas irradiated. The prolongation of survival time of patients who responded was related to the duration of remission. (auth)

XUM

4690 APPLICATION OF FAST ELECTRONS TO THE TREATMENT OF DISEASES OF THE EYE BALL AND EYE SOCKET. Belletti, Sergio; Tunesi, Giuseppe. Radiaz. Alta Energ.; 9: 3-14(Jan 1970). (In Italian).

An irradiation method for the treatment of diseases of the eyeball and the eye socket is described. Two orthogonal fields of fast electrons are used, one in front, directed at the orbit region, and one on the side, on the temple region. Energy data of the two beams and geometric features of irradiation are provided. (auth)

Radiation Effects on Animals

Refer also to abstracts 4493 and 4606.

4691 A TWO-COMPARTMENT MODEL FOR CELL SURVIVAL AFTER IRRADIATION WITH IONIZING RADIATION. Gupta, P. C. (Inst. of Nuclear Medicine and Allied Sciences, Delhi). Bull. Math. Biophys., 31: 1-8(Mar. 1969).

A theory of cell survival after irradiation was developed, considering the cell as composed of two compartments with different sensitivities and taking into account recovery phenomena. The two compartments are identified as the nucleus and the cytoplasm, and an attempt is made to calculate the combined effects of nuclear and cytoplasmic damage. Expressions are obtained for the probabilities that the cell will be in a survival state or damaged state or will function with reduced efficiency. The following assumptions were made: of the two compartments C_1 and C_2 (C_1 identified with the nucleus and C_2 with cytoplasm), part C_1 is considered as a single entity for the purpose of radiation damage. The compartment C_2 is assumed to consist of n sensitive regions, and the damage to any of the n regions will contribute toward reducing the efficiency of the cell. As soon as the cell is damaged in either compartment, the repair process starts simultaneously. Three alternative states were postulated for the subsequent condition of the cell: survival state E_s (assumed to be indistinguishable from the normal state); damaged state E_d (the cell is not viable), and survival with reduced efficiency E_R (not correlated state with any particular functional characteristic of the cell, but intermediate between states E_s and E_d, with the possibility that given enough time, the state E_R may approach E_s). (BBB)

Invertebrates

Refer also to abstracts 4418 and 4735.

4692 (COO-1209-13) X-RADIATION EFFECTS ON THE BIOLOGY OF HETERAKIS GALLINARUM, CECAL WORM OF FOWL, AND A PATHOGENIC PROTOZOAN HISTOMONAS MELEAGRIDIS. Final Report. (Kansas State Univ., Manhattan). [1970]. Contract AT(11-1)-1209. 11p. Dep. NTIS.

Exposure of eggs of Heterakis gallinarum to x radiation doses of 4,000 to 120,000 R revealed that doses up to 64,000 retarded embryogenesis and 120,000 R appeared lethal. Morphological effects were abnormal cleavage and differentiation as well as vacuolation. Studies on effects of various doses of γ radiation on in vitro growth of Histomonas meleagridis showed that 50 Kr did not influence growth while doses of 150 to 200 Kr reduced growth. Gamma irradiation reduced the pathogenicity of H. meleagridis for turkeys. Studies on development of Ascaridia galli from x-irradiated embryonated eggs indicated that a complete absence of male worms was caused by their elimination rather than sex reversal. X irradiation of Ascaridia galli eggs before cleavage retarded development and increased mortality. Effects of Histomonas meleagridis on plasma enzymes in chickens and turkeys were studied. Serum protein changes in chickens subsequent to infection with H. meleagridis were investigated. Studies on effects of γ radiation on survival of Tribolium confusum infected with cysticercoids of Raillietina cesticillus showed that infected beetles were most susceptible to radiation. The relationship of plasma glutamic oxalacetic transaminase to liver lesions from histomoniasis in turkeys was studied. Factors affecting the in vitro cultivation of H. meleagridis are discussed. (H.L.W.)

4693 GAMETOGENESIS AND OVIPOSITION IN LYMNAEA STAGNALIS AS INFLUENCED BY γ-IRRADIATION AND HUNGER. Joosse, J.; Boer, M. H.; Cornelisse, C. J. (Free Univ., Amsterdam). Symp. Zool. Soc. London; No. 22, 213-35(1968).

From Symposium on Studies in the Structure, Physiology, and Ecology of Molluscs, London, England. See CONF-670340.

A study of some aspects of gametogenesis and oviposition in the freshwater snail Lymnaea stagnalis (Basommatophora, Pulmonata) reveals the phenomenon of resorption of gametes. The gametogenesis and the oviposition of adult pond snails are affected by γ-radiation with a cobalt-60 source at a dose rate of 10,000 r. As a result oviposition stops. The developing sex cells in the gonad degenerate within a period of about 30 days. However, gametogenesis starts again and at 78 days after exposure new ripe sex cells can be observed in the acini of the ovotestis. (auth) (UK)

Vertebrates

Refer also to abstracts 4425, 4427, 4432, 4433, 4440, 4444–4447, 4453, 4455, 4457, 4459, 4460, 4469–4471, 4475, 4477, 4501, 4533, 4534, 4536, 4539, 4545, 4553, 4557–4571, 4575–4591, 4599, 4605, and 4727.

4694 (UCLA-12-791) APPEARANCE OF A BRAIN-SPECIFIC ANTIGEN (S-100 PROTEIN) IN THE DEVELOPING RAT BRAIN. Herschman, Harvey R.; Levine, Lawrence; de Vellis, Jean (California Univ., Los Angeles. Lab. of Nuclear Medicine and Radiation Biology). [1970]. Contract AT(04-1)-Gen-12. 15p. Dep. NTIS.

The level of the S-100 protein, a brain-specific antigen, has been determined by quantitative complement fixation in the brain stem and cerebrum of the rat during postnatal maturation. The content was minimal at birth in the brain stem and rose to its adult value by day 25. Although S-100 protein could not be detected in the cerebrum of the 2-day-old rat, adult values were also present by the twenty-fifth day of age. Neither single dose x-irradiation with 750 R to the head at 2 days of age or single dose x-irradiation at 11 days of age affected the adult level of S-100 protein in the brain stem or cerebrum. Similarly, hypophysectomy at 20 days of age had no effect on the subsequent levels of S-100 protein. (auth)

4695 ABSORPTION OF LIPIDS BY CELLS OF DUODENAL EPITHELIUM ON EXPOSURE TO ^{144}Ce RADIATION. Tokin, I. B. (Inst. of Radiation Protection, Leningrad). Arkh. Anat., Gistol. Embriol.; 58: No. 6, 35-43(Jun 1970). (In Russian).

Electron microscopic studies are reported on the process of lipid absorption, as affected by low doses of internal irradiation. For 10 days, Wistar rats were given oral doses of 25μ Ci of ^{144}Ce chloride; two hours after the first and last isotope administration rats were fed 0.5 ml corn oil; at intervals from 30 minutes to 6 hours, specimens of duodenum were obtained for analysis. It is shown that under the effect of low doses of radiation lipid absorption becomes intensified, as compared to normal conditions, due to augmented permeability, as well as to activation of intracellular transport and enhanced enzymatic activity of acid and alkaline phosphatases and ATP-ase. At the same time, although there appears to be no significant morphologic injury, functional tests demonstrate that in addition to changes in membrane permeability these low doses of radiation also affect mechanisms responsible for close contacts between cells, their interconnection becomes much looser. In general, absorption of lipids proceeds according to the same pattern, as under normal conditions, with preliminary break down, passage across membranes of microvilli, resynthesis in apical vesicles of the endoplasmic reticulum, transportation to the region of Golgi complex, and reverse pinocytosis into the region of perinuclear intercellular spaces. Thus, throughout the whole process of lipid penetration of cells is isolated from cytoplasmic ground substance by intracellular membranes. (auth)

4696 EFFECT OF ADRENALECTOMY ON ACUTE CHANGES IN ERYTHROPOIESIS IN THE SPLEEN AND BONE MARROW OF MICE IRRADIATED WITH SUBLETHAL EXPOSURES. Pospisil, M.; Ptacek, V. (Inst. of Biophysics, Brno). Folia Biol. (Prague); 16: 264-72(1970).

The effect of adrenalectomy on the uptake of radioactive iron in the spleen and bone marrow of mice was studied one, two and four days after whole body irradiation with single x-ray exposures of 100, 200 and 300 R. The impairment of water balance induced by adrenalectomy was corrected by the administration of mineralocorticoids, which do not influence erythropoiesis in non-adrenalectomized irradiated animals. Adrenalectomy did not influence ^{59}Fe uptake in the spleen and bone marrow of nonirradiated fed animals. In the spleen of adrenalectomized and irradiated animals, however, ^{59}Fe uptake rose, indicating that the degree of postirradiation inhibition was lower and that the rate of postirradiation regeneration of erythroid differentiation was higher, or that regeneration started sooner. Postirradiation changes in ^{59}Fe uptake in the bone marrow were not affected by adrenalectomy. The daily administration of hydrocortisone to adrenalectomized animals irradiated with an exposure dose of 100 R depressed postirradiation erythropoiesis in the spleen, but not in the bone marrow. The results furnish evidence of the inhibitory effect of glucocorticoids on erythroid differentiation or the proliferation of stem cells in the mouse spleen in the early intervals after irradiation. (auth)

4697 CERTAIN MECHANISMS OF CHANGE IN VASOMOTOR FUNCTION IN NORMAL ANIMALS AND IN THE INITIAL STAGE OF DEVELOPMENT OF EXPERIMENTAL HYPERTENSION UNDER THE EFFECT OF SUNLIGHT AND ULTRAVIOLET RAYS. Baronenko, V. A. Vop. Kurortol., Fizioter. Lech. Fiz. Kul't.; 33: 331-7(Jul-Aug 1968). (In Russian).

During his previous study, the author observed that exposure to sunlight or artificial uv sources slows down the development of experimental hypertension. This problem was further investigated on rabbits by examining the role of the vagus nerve in the protective action caused by exposure to sunlight uv radiation in the development of artificially induced renal hypertension; the experimental work involved removal of one kidney and obstructing the flow of blood in the remaining renal artery. The results indicated that in the case of exposure to sunlight, the beneficial action is caused by the ultraviolet component. Exclusion of the nerve on the aortal-cardiac region in previously irradiated animals did not eliminate the effects of irradiation as far as the vasomotor pressure reaction to adrenalin is concerned; this effect was depressed with respect to the reaction to choline chloride during the initial stages of the development of renal hypertension. The results confirmed the author's earlier finding that the enhancement of the function of the vagus nerve is an important factor in slowing down the development of hypertension in animals previously exposed to sunlight or ultraviolet radiation. (TTT)

4698 CHANGE OF SODIUM POTASSIUM AND CALCIUM CONTENT IN THE HEART MUSCLE. Movsesyan, M. A.; Sarukhanov, A. G. Zh. Eksp. Klin. Med.; 8: No. 4, 7-14(1968). (In Russian).

Changes in the content of Ca, K, and Na of heart muscle, blood plasma, and erythrocytes were observed during the first hours following the exposure of rabbits to a single, lethal dose of x radiation. A decrease in Na content in plasma and a decrease in content of Ca, K, and Na in erythrocytes were noted. Irradiation did not cause marked changes in the content of Ca, K, and Na in heart muscle but the coefficient of Na to K was decreased. (C.H.)

4699 HISTOPATHOLOGY OF PRIMARY LUNG TUMOURS IN THE MOUSE. Amaral-Mendes, J. J. (St. Bartholomew's Hospital Medical Coll., London). J. Pathol.; 97: 415-27(Mar 1969).

Primary spontaneous lung tumors of the mouse were studied histopathologically in material from a number of experiments, every gradation from small foci to fully developed tumors being available. The findings are compared with findings in lung tumors occurring following exposure to whole-body ionizing radiation or whole-body irradiation combined with administration of chemical carcinogens. Two main tumor types are separated, arising in the alveolar cells (type A) and in the bronchiolar epithelium (type B), with a third intermediate type. The importance of chronic pneumonic processes and especially chronic leukemic deposits in the origin of these tumors was established. (auth)

4700 EFFECT OF THORIUM DIOXIDE ON THE PERIPHERAL BLOOD OF RATS. Yan, Shay-shan. Toxicol. Radioactiv. Subst. (USSR) (Engl. Transl.); 4: 42-57(1969).

Translated from Mater. Toksikol. Radioaktiv. Veshchestv.; 4: 42-57(1964).

Experimental study of the effects of intratracheal injections of thorium dioxide on hematopoiesis in rats indicated that changes in lymphopoiesis and thrombocytopoiesis occurred. Morphological changes in the nuclei of neutrophils indicated disturbance in granulocytopoiesis, although no quantitative changes in the number of neutrophils were observed. (E.E.H.)

4701 EFFECT OF THORIUM DIOXIDE ON ARTERIAL PRESSURE AND THRESHOLD OF STIMULATION OF THE NERVE-MUSCLE APPARATUS IN RATS. Yan, Syao-shan. Toxicol. Radioactiv. Subst. (USSR) (Engl. Transl.); 4: 58-65(1969).

Translated from Mater. Toksikol. Radioaktiv. Veshchestv.; 4: 58-65(1964).

The effect on arterial pressure in rats following intratracheal and intraperitoneal injection of thorium dioxide was investigated. Doses of 2, 20, 200, 300, 400, and 1000 mg/kg produced a sharp and persistent fall in pressure. The stimulation threshold of the muscle-nerve apparatus in the hind paws of rats treated with thorium dioxide was investigated using a combined electrometronome. No significant changes were seen during 18 mos. of observation. (E.E.H.)

4702 MORPHOLOGICAL CHANGES IN THE LUNGS AND OTHER ORGANS IN RATS ON INTRATRACHEAL ADMINISTRATION OF THORIUM DIOXIDE. Gaidova, E. S.; Yan, Syao-shan. Toxicol. Radioactiv. Subst. (USSR) (Engl. Transl.); 4: 66-82 (1969).

Translated from Mater. Toksikol. Radioaktiv. Veshchestv.; 4: 66-82(1964).

The effects of single-dose, intratracheal administration of thorium dioxide on rats were investigated. Histological changes observed in the lungs were the development of chronic suppurative lesions of the bronchi with sclerotic changes of peribronchial tissue, formation of bronchiectases, perifocal pneumonia, abscesses, and, in late stages, 13.6% developed sarcomas and squamous-cell carcinomas. In the liver, changes of the protein dystrophy type and focal micronecroses were observed. The kidneys showed protein dystrophy of the epithelium of the convoluted tubules and, in some cases, a large number of hyalin cylinders in the lumen of the tubules. The intensity of these changes was directly related to the dose of substance administered and the time of its action. (E.E.H.)

4703 INDUCTION OF CARCINOMA OF THE GLANDULAR STOMACH IN MICE BY WHOLE-BODY IRRADIATION. Upton, A. C.; Cosgrove, G. E.; Lushbaugh, C. C. (Oak Ridge Associated Universities, Tenn.). GANN Monogr., No. 8, 63-74(1969).

Carcinoma of the glandular stomach, a rare disease in laboratory mice, is increased in incidence by whole-body ionizing radiation. The increase varies as a function of the dose and quality of radiation, with neutrons being relatively more effective than x rays or γ rays. Even midlethal doses of neutrons, however, have not been observed to increase the incidence above 5%, although at the same dose level a large proportion of animals develop a hyperplastic gastritis. The latter is characterized by varying degrees of mucosal inflammation, ulceration, and scarring; nodular and polyploid glandular hyperplasia, disorganization and dilatation of the mucosal glands, penetration of mucosal glands through the muscularis, with subperitoneal adenosis, and progressive degeneration and sclerosis of small arteries and arterioles. These observations support the concept that radiation-induced neoplasia of the glandular stomach of the mouse is preceded by chronic gastritis, with atrophy, fibrovascular sclerosis, and atypical regenerative hyperplasia of the gastric mucosa. They also indicate that the glandular stomach is less susceptible to radiation-induced neoplasia than many other organs of the body in those strains of mice investigated to date. (auth)

4704 BURN INJURY AFTER CARBON DIOXIDE LASER IRRADIATION. Litwin, Martin S. (Tulane Univ., New Orleans); Fine, Samuel; Klein, Edmund; Fine, Ben S. Arch. Surg., 98: 219-22(Feb. 1969).

Various species of living anesthetized animals, including rabbits, dogs, and monkeys, were exposed to CO_2 laser radiation at varying levels of power and power density for varying lengths of time, and the effects were recorded. The well-localized areas of third-degree burn on canine skin were proportional in size to laser beam spot size. These burns granulated and healed by burn scar formation. Depth of penetration was directly related to power, power density, and exposure time. Rate of soft tissue penetration was about 0.001 cm/sec/w/cm^2. When the site of irradiation overlay vital body structures, they were penetrated, with death of the animal if exposure time, power, and power density were great enough. The ophthalmic effect of irradiation with the CO_2 laser beam was also that of intense, well-localized heat. Exposure of the eyes of rabbits for 1.0 sec at 5-w power caused severe corneal burns, which healed by secondary scar formation, but left disabling corneal opacities. When exposure of the eye of a monkey was carried out at 15 w-sec for 1.0 sec, the eyeball was penetrated, and the ocular media extruded. When the dog's scalp was irradiated at 24 w-sec for 10 sec, again the effects of intense and well-localized heat were evident. Underlying bone was rapidly exposed and subjected to sharply localized heat of such intensity that the bone was carbonized. A 1000-w CO_2 laser beam at a tissue penetration rate of 0.001 cm/sec/w/cm^2 can be expected to produce a localized soft-tissue burn 1 cm deep over an area of 1 cm^2 within one sec. Concussion injury, elastic propagation of shock waves, and overpressures in closed cavities were not problems with the CO_2 laser. (BBB)

4705 THE EFFECT OF TOTAL-BODY IRRADIATION ON WOUND HEALING AND THE HEMATOPOIETIC SYSTEM IN MICE. Zelman, Donald; Song, In Chul; Porteous, Donald D.; Bromberg, Bertram E. (State Univ. of New York, Brooklyn). Bull. N. Y. Med. Acad., 45: 293-300(Mar. 1969).

Experiments were performed to determine the optimum time for operative intervention following whole-body irradiation, with specific reference to wound healing. Immediately or 1, 2, or 3 wks after x irradiation with 200, 400, or 600 rad, mice were incised longitudinally over the dorsum. Tensile strength of the wound was measured and histological studies were performed 1 and 2 wks after incision. Irradiated animals demonstrated a decrease in tensile strength, the degree of which was directly

XUM

related to the dose of irradiation. Recovery of tensile strength was demonstrated when the incision was delayed 2 to 3 wks after irradiation. Leukocyte counts demonstrated an immediate depression, with recovery in all groups of irradiated mice at 21 days. The percentage of ^{59}Fe (as $FeCl_3$) incorporation showed a depression in the 400 and 600 R groups of mice at 7 days, with recovery occurring at 21 days. From an evaluation of the data presented concerning the effect of ionizing irradiation on the tensile strength of wounds and the hematopoietic system, it was concluded that operative intervention should be undertaken 2 to 3 wks after irradiation. (BBB)

4706 EFFECTS OF THORACIC IRRADIATION UPON CARDIOPULMONARY FUNCTION IN THE DOG. Schreiner, Bernard F. Jr.; Michaelson, Solomon M.; Yuile, Charles L. (Univ. of Rochester, N. Y.). Amer. Rev. Respirat. Dis., 99: 205-18(Feb. 1969).

A study was undertaken of the chronology of the postirradiation reaction in the lungs of dogs by ventilatory and cardiopulmonary hemodynamic parameters and to correlate these abnormalities with pathologic changes. Combined right and left heart catheterization and measurements of blood gas exchange were performed before, during, and after positive pressure breathing and electrically induced simulated exercise. The dogs received doses of 1000-KeV x rays of 2000 to 5000 R to the lungs. In the irradiated animals functional abnormalities consisting of an abnormally wide alveolar arterial oxygen gradient and a larger than normal ratio of shunt to total blood flow during positive pressure breathing were detectable 1 wk to 1 mon after irradiation. Although light microscopic changes were minimal at this time, electron microscopic results indicated that these functional abnormalities may reflect x-ray-induced depletion of pulmonary surfactant. Two to 4 months postirradiation, progressively abnormal responses to positive pressure breathing were noted. In addition, the response to simulated exercise strongly suggested progressive obstruction of the pulmonary vascular bed, which was confirmed by pathologic examination. Evidently, localized irradiation of the lung of the dog results in an irreversible syndrome of progressive pulmonary dysfunction, characterized by impaired alveolar arterial gas exchange, pulmonary hypertension, and progressive obliteration of the pulmonary vascular bed. (BBB)

4707 COMPARATIVE STUDY OF THE CHANGES IN THE ELIMINATION OF 17-KETOSTEROIDS IN MALE RATS AFTER SURGICAL AND RADIATION-INDUCED CASTRATION AND HISTOLOGIC STUDY OF THE TESTES IRRADIATED WITH SCALAR DOSES. Ferri, G. G.; Calzavara, F.; Bernardi, R. (Univ., Padua). Quad. Radiol.; 33: 139-50(Mar-Apr 1968). (In Italian).

The daily urinary elimination of 17-ketosteroids was examined in two groups of male-rats, 10, 20, 30 and 45 days after orchiectomy, and after submitting them to fractionated irradiation of the testicles with a global dose of 1000 R. Another four groups of rats were irradiated in the testicular region with doses of 200, 400, 600, and 800 R. At the end of the test all animals were submitted to autopsy, and the irradiated testicles were examined histologically. The loss of urinary 17-ketosteroids in the irradiated rats appeared less rapid, compared with the orchiectomized animals, but so continuous as to reach values lower in comparison with those ascertained in the latter animals, at the end of the experiment. The histological results show a significant range of damage in relation to the employed dose, and demonstrate that testicular structures are thoroughly destroyed after a dose of 800 to 1000 R. (auth)

Man

Refer also to abstracts 4452, 4502, 4524, 4603, 4607, and 4608.

4708 (UR-49-1256) BIOLOGICAL EFFECTS OF MICROWAVE EXPOSURE: AN OVERVIEW. Michaelson, Sol M. (Rochester Univ., N. Y. Dept. of Radiation Biology and Biophysics). [1970]. 14p. (CONF-701010-1). Dep. NTIS.

From Microwave Power Symposium, Scheveningen, Netherlands.

A review of the literature on the biological effects of microwaves is presented. Electrical and scattering properties of tissues are discussed with relation to effects of electromagnetic radiation on organisms. It is emphasized that effects of microwaves are a manifestation of thermal conversion, while the harmful effects of x or γ rays are caused by ionization. A discussion of the relative importance of thermal and non-thermal effects of microwaves is given. Studies on cataractogenic effects of microwaves on eyes of rabbits are reviewed. A review of studies on human populations exposed to microwaves includes radar operators and microwave personnel; comparisons of studies on Russian and United States workers are discussed. Studies on lenticular opacities in microwave workers showed that there were no clinically significant defects in terms of decreased visual acuity. Safety standards for human exposure to microwaves are discussed; a maximum exposure level 10 mW/cm^2 is recommended by the American National Standards Institute. Evaluation of hazards is discussed and the importance of a precise and accurate system of dosimetry is pointed out. (H.L.W.)

4709 DAMAGING RADIATION CHEMICAL EVENTS. Ebert, M. (Christie Hospital and Holt Radium Inst., Manchester, Eng.). pp 133-6 of Radiation Protection and Sensitization. /Moroson, Harold (ed.). New York; Barnes and Noble, Inc. (1970).

From 2nd International Symposium on Radiosensitizing and Radioprotective Drugs, Rome, Italy. See CONF-690525.

Comparison of the radiosensitivity of HeLa cells at 20°C and at −196°C suggests that 30 per cent of damage is caused by the direct effect. Radiation damage to dry fern spores allows us to describe the mode of action of O_2 on the direct effect. Molecular configuration of macromolecules and other factors determining radiation sensitivity are discussed. (auth)

4710 AN UNUSUAL HAZARD IN FORGERY DETECTION. Barnes, R. (Dept. of Public Health, New South Wales, Australia). Med. J. Aust.; 1-57th year (11): 540-1.

An investigation into possible eye and skin hazards for workers exposed to ultra-violet light used in the detection of forged $10 notes was made after complaints of eye and skin irritation were made. No clinical evidence of eye irritation or damage was found, but some evidence of erythemia of the forearms caused by the ultra-violet light was seen. Control of eye and skin exposure was relatively simple, and the complaints have since ceased. (auth) (Australia)

4711 CHEMICAL AND HYGIENIC STUDIES ON NATURAL RADIOACTIVE SPA. 4. MEASUREMENT OF EXTERNAL RADIATION AT MISASA AND MASUTOMI SPA AREAS. Kametani, Katsuaki; Hasegawa, Akira; Ikebuchi, Hideharu; Kido, Yasumasa; Urakubo, Goro (National Inst. of Hygienic Sciences, Tokyo). Eisei Kagaku; 16: No. 1, 28-31(Feb 1970). (In Japanese).

Dose rates of external radiation were measured with an ionization chamber equipped with vibrating reed electrometer at some spots in Misasa and Masutomi spa areas that are called strong radioactive fountains in Japan. At Misasa spa area, the maximum value of 25.0 μR/hr was recorded in a bathroom, and the minimum value was 13.0 μR/hr in a field. The maximum value recorded at Masutomi spa area was 24.5 μR/hr in a bathroom, and a minimum value recorded in a garden of the hotel was 5 μR/hr, which was equal to the average value measured in Tokyo. If the habitants in these spa areas are assumed to take a 30 min. bath every day, their radiation dose rates might amount to 116 mR/year at Misasa and 48 mR/year at Masutomi. (NSA of Japan)

4712 IRRADIATION GASTRITIS SIMULATING CARCINOMA. Lane, D. (Repatriation General Hospital, Brisbane). Med. J. Aust.; 2: 576-7(26 Sep 1970).

Attention is drawn to the problem of irradiation gastritis of severe degree. Two cases are presented to illustrate the difficulties of diagnosis. The possibility of other complications ensuing is mentioned. (auth) (Australia)

4713 BIOLOGICAL EFFECTS OF LOW-LEVEL RADIATION ON THE EMBRYO. Brent, Robert L. (Thomas Jefferson Univ., Philadelphia). Trans. Amer. Nucl. Soc.; 13: 515-6(Nov 1970).

From Meeting of the American Nuclear Society, Washington, D. C. See CONF-701102.

4714 FUNCTIONAL AND MORPHOLOGICAL STUDIES OF NEPHROPATHY SECONDARY TO IRRADIATION (COBALT THERAPY). Campanacci, L.; Romagnoli, G. F.; Patrese, P.; Mendola, R.; Okolicsanyi, L.; Casara, S. (Univ., Padua. Ospedale Civile, Padua). Minerva Nefrol.; 15: 184-94(May-Jun 1968). (In Italian).

The functional and morphological study of nephropathy secondary to cobalt therapy of the lumbar region with doses of 3000 to 4000 rads shows the appearance with relative frequency (incidence of 25% in cases studied) of a renal lesion evidenced by a clear functional defect. There is also a nephropathy in general asymptomatic or slightly symptomatic on the clinical plane and detectable only in renal function or the nephrobiopsis studies. In order to determine the extent of the kidney involvement better values must be obtained of the VFG, PRP, and some tubular functional indices. The medical report of a particularly severe unilateral renal lesion in which a relapse of a Hodgkin granuloma occurred could confirm the thesis that the increase of neoplastic mass favors the manifestation of radiation nephropathy. (tr-auth)

4715 PHYSIOLOGIC REACTIONS FOLLOWING LARGE DOSE INFRARED RADIATION. Kaderavek, F. Fysiat. Reumatol. Vestn.; 48: 24-8(Feb 1970). (In Czech).

Based on the investigation of 108 volunteers, the physiological reactions produced by increasing large doses of infrared radiation on the skin of the trunk were evaluated. The application induced characteristic changes in the pattern of internal body temperature, skin temperature, quantitative changes in perspiration and changes of some general circulatory reactions. As regards more detailed manifestations, attention was devoted to the initial decline of internal body temperature that, however, could be prevented by fanning. Great radiation stress produced so-called thermic equilibrium dynamic states. Terms used for such states are introduced from terms used in physical science. This applies to the so-called first dynamic balance, induced primarily by physiological responses. As regards the second dynamic balance, this process is mediated already chiefly by increments in conduction-convection gradients between the body and the environment. (auth)

4716 BILE DUCT CARCINOMAS AFTER THOROTRAST. Breining, H.; Yazdanbakhsch, I.; Helpap, B. (Univ., Bonn). Gastroenterologie; 8: No. 1, 44-8(1970). (In German).

After a bullet wound through the neck, angiography was performed with thorotrast. This fact remained unknown to the patient. Twenty years later, and three years prior to death, thorotrast depositions were uncovered accidentally in liver and spleen. At the age of 60 the patient died from bile duct carcinoma of the liver. Because angiography was performed for a service-connected injury, the liver carcinoma was also considered a service-connected disease. (tr-auth)

Radiation Effects on Plants

Refer also to abstracts 4425, 4464–4467, 4477, 4480, 4482–4490, 4492, 4494–4499, 4556, 4573, 4574, 4604, 4709, and 4732.

4717 (NYO-2043-216, pp 1-18) RADIATION BOTANY AND PLANT GENETICS. (Inter-American Inst. of Agricultural Sciences, Turrialba (Costa Rica)).

From application of nuclear energy to agriculture. Annual report.

Studies on 44 species of Leguminosae and 18 species of Convolvulaceae (morning glory family) showed that there was a wide range of radiosensitivity among the species of Leguminosae and that the Convolvulaceae were relatively radioresistant. The mutagenic effects of cycasin, a compound occurring naturally in the cycad plants, were studied in beans (Phaseolus vulgaris). The enzyme, β-glucosidase, which is required for cycasin to produce its effects, was found to be present in bean seeds. Seeds were exposed to various concentrations of cycasin solutions and mutation frequencies for chlorophyll and morphological characteristics, as well as survival rates, are tabulated. (H.L.W.)

4718 REVERSAL OF INHIBITORY EFFECTS OF γ-RAYS ON THE SEEDLING GROWTH OF WHEAT BY THE APPLICATION OF IAA, TRYPTOPHANE, AND ZINC. Abrol, Y. P.; Sirohi, G. S.; Sinha, S. K. (Indian Agricultural Research Inst., New Delhi). Indian J. Exp. Biol.; 7: 114-16(Apr 1969).

Seeds of Triticum vulgare variety Sonora 64 treated with increasing doses of γ rays (^{60}Co as source) showed progressive inhibition of growth of roots and shoots, inhibition being maximum at 40 Kr. The pre-sowing soaking treatment of irradiated seeds with IAA, tryptophane, and zinc induced recovery of inhibition of growth. The irradiation of seeds also decreased the α-amylase activity that was restored by the pre-sowing soaking treatment with IAA. (auth)

4719 EFFECT OF GAMMA RADIATION DOSAGES ON ROOTING OF PINEAPPLE CROWN SECTIONS, SHOOT EMERGENCE, AND GROWTH. Irizarry, H.; Velez Fortuno, J. (Univ. of Puerto Rico, Mayaguez). J. Agr. Univ. Puerto Rico; 54: 551-8(Jul 1970).

Longitudinal pineapple fruit crown sections were irradiated and studied for their rooting ability. Groups of 40 sections each were exposed to gamma ray doses of 500 to 32,000 rads in two separate experiments. The treated plant material was propagated, with checks, in sterilized soil in metal flats. The results indicate that at low doses of 500 to 4,000 rads no radiation effect was detected on the rooting of crown sections, proliferation of shoots and shoot stuntiness. Delayed germinal bud sprouting was observed above 3,000 rads. Exposures to 8,000 and 16,000 rads reduced rooting of crown sections, retarded sprouting of germinal buds, reduced proliferation of shoots, and caused stuntiness in the initial stage of shoot growth. Exposure to 32,000 rads resulted in killing pineapple vegetative tissue. (auth)

4720 EFFECT OF URANYL NITRATE ON SUCROSE PRODUCTION AND STORAGE IN CORN SCUTELLUM SLICES. Humphreys, T. E.; Garrard, L. A. (Univ. of Florida, Gainesville). Phytochemistry; 9: 1715-23(Aug 1970).

Uranyl nitrate (1.5×10^{-3} M) completely inhibited the storage of exogenous sucrose in slices of the corn scutellum, but had no effect on the storage of intracellularly synthesized sucrose. Sucrose production from glucose or fructose was inhibited by 15 and 35 per cent, respectively, and the inhibitions were not increased by a 10-fold greater uranyl ion concentration. Essentially the same degrees of inhibition were obtained when the slices were incubated with uranyl ion and sugar as when the slices were pretreated in uranyl ion and then washed and placed in sugar solutions. In the latter case, the inhibition was shown to be completely reversed by hydrogen ion or partially reversed by certain metal cations. Uranyl ion also strongly inhibited the exchange of sucrose between the bathing solution and the storage compartment of the cell. These results are consistent with a scheme which includes two sucrose transport membranes, one at the cell exterior for exogenous sucrose and the other at the cell interior between the sucrose synthesis and storage compartments and a membrane containing hydrophilic pores through which hexose molecules can freely diffuse from the cell exterior into the synthesis compartment. (auth)

4721 EFFECT OF ELECTRON RAYS ON THE STRENGTH OF THE EXOCARP OF CHERRIES. Penner, H. (Bundesforschungsanstalt fuer Lebensmittelfrischhaltung, Karlsruhe, Ger.). Ind. Obst- Gemueseverwert.; 55: 163-6(Mar 1970). (In German).

The strength of cherry exocarp was measured using the Wolodkewitsch testing instrument. With this method, the effects on the stability of cherries of ionizing radiation, storage time, and calcium chloride treatments were studied. The irradiation caused a decrease, while $CaCl_2$ and storage caused an increase of stability. (auth) (INIS)

4722 EVALUATION OF VARIOUS METHODS FOR STIMULATION OF SUGARBEET SEED. Zavadil, S. (Research Inst. of Beet Growing, Semcice, Czech.). Rostlinna Vyroba; 15: 673-80(Jul 1969). (In Czech).

Laboratory and field tests were performed to examine the following techniques of sugarbeet seed stimulation previous to sowing: treatment with pyrimidine derivatives, with a solution of the sodium salt of petroleum extracts, ultrasound at a frequency of 3 MHz and 30,000 Hz, ^{60}Co gamma radiation, and infraviolet rays of an infra-lamp (250 W) and of an electric field with intensity 2 kV/cm. Polished seed of the Dobrovická N sugar beet, polished seed of Dobrovická A, and the genetically monogerm seed of Bělocerkovská 6 of various years of harvest and of various germinating power were used for the tests. The experiments showed that the positive effects of certain kinds of seed stimulation upon the energy of germination, the germination power, and the sprouting capacity, found under laboratory conditions, did not prove to be stable in the further development of the sugarbeet plants. In particular under worse ecological conditions, the growth and the final yield in the affected variants became worse in most of the instances. The effects of individual methods varied unequally in experiments lasting several years. The tests proved that the investigated stimulation methods did not improve the value of seed with worse biological properties. Thus one cannot recommend any of the tested methods of stimulation of sugarbeet seed for practical use. (auth) (NSA of Czech.)

4723 GAMMA IRRADIATION STUDIES ON SEEDS, SEEDLINGS, AND CALLUS TISSUE CULTURES OF PHASEOLUS VULGARIS L. Bajaj, Y. P. S.; Saettler, A. W.; Adams, M. W. (Michigan State Univ., East Lansing. Dept. of Agriculture, East Lansing, Mich.). Radiat. Bot.; 10: 119-24(Apr 1970).

The effects of ^{60}Co γ radiation on seeds, seedlings, and callus tissue cultures of Phaseolus vulgaris L. var. Manitou were compared. Tissues were subjected to various doses (0.5 to 40 kilorad) of γ radiation at 200 rad/min and subsequently grown for 4 to 8 weeks. Seeds irradiated with 10 to 12 krad produced stunted seedlings that later exhibited delayed flowering, and poor seed set; although the seeds germinated, no normal seedlings were formed at 15 krad. However, when 8-day-old seedlings were irradiated, severe inhibition of growth occurred at 2 krad, followed by degeneration of the apical meristem and death at 5 krad. Callus grown in suspension cultures in a modified White's medium supplemented with 2, 4-D, kinetin, and yeast extract showed significant stimulation of growth ($P < 0.01$) at 0.5 krad followed by a gradual decrease from 1 to 10 krad. Cells in such cultures showed mitotic inhibition, degeneration of cytoplasm, increased polyploidy, and reduced plating efficiency. Callus growth at 20 to 30 krad was drastically reduced and ceased completely at 40 krad. The color of the callus continued to darken with increasing doses. There is a striking dif-

XUM

ference in the radiosensitivity of seeds, seedlings, and callus tissue; the young seedlings are most radiosensitive, followed by seeds, and callus tissue is most tolerant. (auth) (UK)

4724 STUDIES ON THE RADIATION BREEDING OF PERENNIAL PLANTS. I. RADIOSENSITIVITIES OF SOME ECONOMIC AND ORNAMENTAL TREE SPECIES IN KOREA. Kim, C. M. (Radiation Research Inst. in Agriculture, Seoul); Sohn, C. Y.; You, Y. S.; Yim, K. B. J. Nucl. Sci. (Seoul); 9: No. 2, Pt. 2 75-87(1970). (In Korean).

Seed irradiation of several economic and ornamental tree species in Korea was conducted by x or γ rays at a dose range of 0.5 to 40 kR. To determine radiosensitivity and to select the useful mutant lines the LD_{50} of germination or survival, morphological changes of leaf and twig, chlorophyll mutants, recovery from radiation damage, and height of growth were investigated in seedlings at 1 or 2 years of age. In Firmiana platanifolia, stimulating effect in germination was observed at doses below 10 kR x rays and in Hibiscus syriacus at doses that ranged 1 to 40 kR γ rays, while delayed or suppressed germination was observed at high doses in all the species tested. The LD_{50} of germination was estimated for several species. It ranged from 1.5 kR for Abies holophylla to over 4.0 kR for Hibiscus syriacus. The LD_{50} of survival was also estimated for a few species. In general, gymnosperms showed higher radiosensitivity than hardwood trees. At low doses, a slight stimulating effect on height growth appeared, whereas at high doses height growth was significantly suppressed in all the species tested. In Firmiana platanifolia leaf area showed a tendency to decrease linearly with the increase of doses. In 2-year-old seedling Hibiscus syriacus, chlorophyll deficiency like yellow or light green leaf, which is of ornamental value appeared. (15 Tables; 6 Figures) (C.O.)

Radiation Effects on Microorganisms

Refer also to abstracts 4456, 4462, 4463, 4507, 4536, 4548–4555, and 4557.

4725 INFLUENCE OF DNA REPLICATION ON THE X-RAY SENSITIVITY OF BACTERIA. Bhaumik, Gayaram; Bhattacharjee, S. B. (Saha Inst. of Nuclear Physics, Calcutta). Mutat. Res.; 9: 561-8(Jun 1970).

It was observed that upon incubation in a medium in which DNA synthesis was allowed but not protein and RNA syntheses (i.e. by incubating the cells in +T–AU medium), uv-irradiated Escherichia coli 15 T–A–U–M–Pr–Tr–Sm^r (requiring thymine, arginine, uracil, methionine, proline, and tryptophan and resistant to streptomycin) became more resistant to x rays compared to those cells that were irradiated but not incubated. A similar increase in resistance was also observed for uv-irradiated thymine-grown and 5-bromodeoxyuridine (BUdR)-grown cells incubated in +BUdR–AU medium. The results indicated that some of the uv-induced lesions could be repaired on incubation in such restricted media. However, such an increase in x ray resistance due to the incubation could not be related to the increase in viability; in some cases of incubation, where there was a decrease in viability, an increase in resistance was observed; in other cases, where there was an increase in viability, a decrease in resistance was observed. Incubation of the nonirradiated thymine-grown cells in +T–AU medium increased the shoulder of the x-ray-survival curve and also decreased the slope, while such cells, on incubation in +BUdR–AUmedium, became more sensitive to x rays than the control nonirradiated and nonincubated cells. For BUdR-grown cells, although there was a marked decrease in x-ray sensitivity due to incubation in +T–AU medium, no significant change in x-ray sensitivity was observed on subsequent incubation in +BUdR–AU medium as compared to the nonincubated cells. (auth)

4726 RADIATION RESISTANCE OF SPORES. Tallentire, A. (Univ. of Manchester, Eng.). J. Appl. Bacteriol.; 33: 141-6(Mar 1970).

The mechanism(s) of high resistance of bacterial spores to radiation is examined in the light of current experimental evidence on the effects of water content on the radiation resistance of cells, radiation protection by innate chemical substances, the presence of unique structures in spore DNA and the existence of spore-specific repair processes. (auth)

4727 ULTRAVIOLET LIGHT ENHANCED REACTIVATION OF A MAMMALIAN VIRUS. Bockstahler, Larry E.; Lytle, C. David (Bureau of Radiological Health, Rockville, Md.). Biochem. Biophys. Res. Commun.; 41: 184-9(9 Oct 1970).

When CV-1 mammalian cells are lightly uv-irradiated before infection with uv-irradiated herpes simplex virus, an increase in survival (uv-reactivation) of this virus was observed. The doses of uv to the cells necessary for maximizing uv-reactivation were a factor of about 10 lower than those previously reported for bacteriophage–bacteria systems. (auth)

4728 PHOTOREACTIVATION OF ESCHERICHIA COLI B_{s-3} AFTER INACTIVATION BY 313 nm RADIATION IN THE PRESENCE OF ACETONE. Mennigmann, Horst-Dieter; Wacker, Adolf (Univ., Frankfurt am Main). Photochem. Photobiol.; 11: 291-6(May 1970).

The colony-forming ability of Escherichia coli B_{s-3} can be inactivated by light of 313 nm wavelength in an acetone-sensitized photochemical reaction. This ability can subsequently be restored quantitatively by illumination with photoreactivating light. A small fraction of the population cannot be inactivated; this is assumed to be due to a complete dark repair of the lesions, whatever the dose of radiation was. Thus, such triplet energy transfer experiments can successfully be applied to whole cells. Since thymine dimers are formed almost exclusively, this suggests a new way of studying these lesions in relation to the biologically observable effects. (auth) (UK)

4729 GROWTH CHARACTERISTICS OF REOVIRUS TYPE 2: ULTRAVIOLET LIGHT INACTIVATED VIRION PREPARATIONS AND CELL DEATH. Loh, P. C.; Ote, H. K. (Univ. of Hawaii, Honolulu). Arch. Gesam. Virusforsch., 26: 197-208 (Feb. 1969).

A comparative study was made on the time of appearance and development of the morphological lesions induced in HeLa cells by the uv-inactivated virion and by the untreated virion. Ultraviolet light irradiation of reovirus type 2 samples was performed with a General Electric 15-w germicidal lamp (2537 Å). The uv-inactivated preparations of purified type 2 when added to monolayers of HeLa cells caused a cytotoxic effect (CTE). At multiplicities of 80 to 100 infectious units per cell (IU/cell) cellular death due to CTE was initially observed at 3 to 4 hr postinfection and reached maximum 9 to 10 hr after infection. The cell survival curves suggested that the rate of cell killing was dependent upon the multiplicity of infection and exhibited multiple hit type of kinetics. The CTE was preceded by marked alterations in the synthesis of cellular RNA, DNA, and protein, and not produced by uv-irradiated preparations of uninfected HeLa cell homogenates nor by uv-treated reovirus 2 preparations heated at 56°C for 30 min. When uv-treated preparations were subjected to ultracentrifugation (45,000 rpm, 1.5 hr), activity was restricted to the sediment only. In addition, CTE could not be serially transferred and could be prevented by addition of reovirus type 2 antiserum. Thus, the toxic factor is an intimate part of the uv-inactivated viral particle. (BBB)

4730 BIOLUMINESCENCE AND RADIATION RESPONSE OF PHOTOBACTERIUM FISCHERI H-2. Lerch, I. A. (Univ. of Chicago). Radiat. Res.; 43: 161-72(Jul 1970).

A strain of Photobacterium fischeri designated H-2 was employed for the purpose of conducting radiobiological studies with a pulsed linear accelerator electron beam. The bioluminescence of this organism was found to be an excellent determinant for the in vivo response of the luciferase enzyme system to various radiation protocols. Post-irradiation bioluminescent activity was measured with a phototube connected in series with a log amplifier and an x–y plotter for the recording of glow curves as a function of time. It was found that bioluminescence decayed exponentially with time immediately after exposure to a high dose rate primary electron beam with a rate constant varying linearly as dose. Bioluminescence survival curves were constructed utilizing measurements obtained one to two hours postirradiation upon stabilization of the light output. Clonogenic survival was found to be a much more radiosensitive function than bioluminescent survival. (auth)

4731 STUDY OF THE RELATIONSHIP BETWEEN SURVIVAL AND REPAIR SYNTHESIS OF DNA AFTER ULTRAVIOLET LIGHT EXPOSURE. Sedliakova, M.; Bilien, D.; Bruns, L. (Univ. of Florida, Gainesville). Photochem. Photobiol.; 11: 309-17(May 1970).

The influence of amino acid prestarvation on both the resistance to uy and the postirradiation repair synthesis of Escherichia coli 15 T^- 555-7 thy meth arg trp and E. coli B/r (HCR^+) was followed. Prestarvation increased the number of survivors about 30 to 100 fold in both strains at doses of 600 to 1200 ergs/mm^2. In contrast to survival, no increase in repair synthesis was observed. Thus, the increase in survival has to be brought about by a mechanism that seems to be independent of additional repair synthesis. (auth) (UK)

Radiosterilization and Radiopreservation

Refer also to abstracts 4556 and 4721.

XUM

4732 (NYO-2043-216) APPLICATION OF NUCLEAR ENERGY TO AGRICULTURE. Annual Report. Moh, Carl C. (Inter-American Inst. of Agricultural Sciences, Turrialba (Costa Rica)). 1 Jul 1970. Contract AT(30-1)-2043. 78p. Dep. CFSTI.

Separate abstracts were prepared for each of the three sections on radiation botany and plant genetics, entomology, and soil chemistry. (M.C.G.)

For abstracts of individual sections see: 4052, 4717, and 4733.

4733 (NYO-2043-216, pp 19-48) ENTOMOLOGY. (Inter-American Inst. of Agricultural Sciences, Turrialba (Costa Rica)). From application of nuclear energy agriculture. Annual report.

Studies on eradication of the Mediterranean fruit fly by radiosterilization using the sterile male technique included: mating competitiveness of males irradiated during pupal or adult stages; insemination frequency of males irradiated during pupal or adult stages; laboratory studies to evaluate sexual mating competitiveness of males irradiated at various doses; suppression of the reproductive potential of the flies by γ-irradiated males in caged coffee trees; effect of γ sterilization on the mating duration of the males; effect of γ sterilization on the sexual maturity of the males; effect of γ sterilization on the sperm transfer ability of the treated males; and induction of visible mutants. The sterile male technique was also used in studies on the biology and sterilization of the coffee leaf miner, Leucoptera coffeella. Effects of sterilization on the longevity of treated moths and dose-response curves of male and female moths were determined. (H.L.W.)

4734 (TID-25467) PREPARATORY EFFICACY STUDIES FOR THE APPLICATION OF IONIZING RADIATIONS TO THE EXTENSION OF THE REFRIGERATED STORAGE OF FRESHWATER PERCH (PERCA FLAVESCENS). Final Report, April 15, 1967-June 1, 1968. Graikoski, John T. (Bureau of Commercial Fisheries, Ann Arbor, Mich.). Sep 1970. Contract AT(49-11)-2954. 46p. Dep. CFSTI.

The objective of this study was to determine the storage time required for radiation-pasteurized yellow perch (Perca flavescens) fillets held at various temperatures to be totally rejected due to spoilage. Data obtained on six different lots of commercially produced fillets revealed a wide range in rejection times as determined by odor of the fillets. The range in rejection times was evident, both for the nonirradiated and irradiated fish. For the nonirradiated fish, the range in time for rejection for those stored at 50°F (10°C) was 3 to 12 days; for those at 42°F (5.6°C), 6 to 12 days; and for those stored at 36°F (2.2°C), 10 to 16 days. For fillets irradiated to 200 kilorads and stored at 50°F, the range in time for rejection was 8 to 19 days; for those stored at 42°F, 19 to 33 days; and for those stored at 36°F, 28 to 41 days. Microbial spoilage patterns obtained from total aerobic plate counts had a similar pattern as was observed from odor evaluations of the same fish. However, maximum counts of microorganisms were reached earlier than when the samples were rejected by odor. Microbial counts can, therefore, be employed in experimental procedures as a pre-indication of fish quality in regard to spoilage as assessed by odor of fish. (auth)

4735 STUDIES ON THE INSECT PEST CONTROL USING STERILE-MALE TECHNIQUE. I. ON THE RADIOSENSITIVITY OF FALL WEBWORM (HYPHANTRIA CUNEA DRURY). Lee, Chung Choo; Chung, Kyu Hoi; Park, Chang Kyu; Park, Seung Heui (Radiation Research Inst. in Agriculture, Seoul). J. Nucl. Sci. (Seoul); 9: No. 2, Pt. 2, 89-94(Apr 1970). (In Korean).

Fall webworm pupae, 2 to 3 days old, were irradiated with 3 kR to 200 kR by ^{60}Co γ rays. The results obtained were summarized as follows: The number of eggs laid per female was 443.1 in the control group, and the sex ratio of pupae was shown to be 100:178, with the male predominating. Sub-lethal dosage (LD_{50}) was 93.5 ± 1.2 kR in females and 83.7 ± 1.1 kR in males. Sterile dosage (SD_{50}) was 27.5 kR in males and such low dosages appear adequate for sterilization techniques. (auth)

METALS, CERAMICS, AND OTHER MATERIALS

Metals and Alloys

Refer also to abstracts 4184, 4188, and 4192.

Corrosion and Erosion

Refer also to abstracts 4186 and 5173.

4736 (ANL/ST-3) SODIUM TECHNOLOGY QUARTERLY REPORT APRIL, MAY, JUNE 1970. Kesser, G. M. (comp.) (Argonne National Lab., Ill.). Sep 1970. Contract W-31-109-eng-38. 77p. Dep. NTIS.

The research, development, and management activities are reported. Efforts devoted to initiation of a national meter program to characterize on-line instrumentation for monitoring oxygen, carbon, and hydrogen in sodium, for detecting leaks in steam generators, and to establish the commercial availability of such meters built to RDT standards are summarized. Implementation of a program to formulate standard analytical methods that meet the needs of the national sodium technology program, and development of methods for determining oxygen, carbon, nitrogen, and trace metals in sodium and radioisotopes in cover gases are described. Definition of problems created by radioactivity in primary sodium and cover gases, development of methods for detecting and characterizing fuel failures, and investigation of methods for measuring sodium aerosol in cover gases are reported. Results of studies of nitrogen-bearing species in sodium, examinations of phase relations in the sodium-rich region of the Na–O–H ternary system, and measurement of the solubility of xenon in sodium are reviewed. Development of methods for purifying primary coolant sodium, studies of the transport of carbon in sodium-steel systems, and evaluation of vanadium alloys as cladding for LMFBR fuels are described. (auth)

4737 (CISE-R-290) FURTHER EXPERIMENTS ON THE CORROSION RATE OF ZIRCALOY-2 IN STEAM–WATER MIXTURE UNDER REACTOR RADIATIONS. Topical Report No. 77. Cerrai, E.; Gadda, F.; Scaroni, A. (Centro Informazioni Studi Esperienze, Milan (Italy). Oct 1969. Contract 008.65.1-NTRI. 19p. Dep. NTIS (U. S. Sales Only).

Samples of Zircaloy-2 were tested in in-pile water loops for corrosion. One set of tests was conducted under neutral steam-water conditions and another set was conducted using ammoniated steam-water mixtures. Data and information on corrosion and the effects of radiation are included. (J.R.D.)

4738 (DP-Report-527) THE HIGH TEMPERATURE CORROSION OF NIMONIC-75 AND VARIOUS STEELS IN GASES AT LOW PARTIAL PRESSURES. Project DRAGON. Knutsen, A. B.; Conde, J. F. G.; Piene, K. (Atomic Energy Establishment, Winfrith (England)). Feb 1967. 59p. Dep. NTIS.

The reactions of Nimonic-75 in low partial pressures of CO_2, H_2O, CO, CH_4, N_2, and in various mixtures of these gases have been studied in the temperature range 750 to 1000°C. In addition a series of steels including two mild steels, three Cr–Mo steels and five different austenitic stainless steels have been reacted in the five component mixture $N_2 + CO + H_2 + H_2O + CH_4$ (1 : 3 : 3 : 0.5 : 0.5) at temperatures in the range 500 to 750°C and at pressures from 0.3 to 10 torr. The results of the kinetic and other complementary studies on Nimonic-75 in the various gases and of the ten steels in the five component mixture are presented together with preliminary data from the long term studies in the $CO + H_2 + H_2O$ environments. (auth)

4739 (JAERI-Memo-4132) PROCESS OF CARBURIZATION IN AUSTENITE STAINLESS STEEL. Nishio, Gunji; Shimokawa, Junichi (Japan Atomic Energy Research Inst., Tokyo). Sep 1970. 23p. Dep. NTIS (U. S. Sales Only).

The investigations were made to provide basic information on the compatibility between the carbide fuel and austenitic stainless steel cladding. The apparent volume and grain boundary diffusion coefficients for 304 stainless steel are measured by means of ^{14}C tracer with the instantaneous source model by the standard sectioning technique. The two apparent diffusion coefficients are represented as a function of temperature, as follows: $D_V = 0.351 \exp(-(55{,}300 \pm 700)/RT)$ at 900 ~ 1100°C, and $D_B = (3.85/\delta) \exp(-(61{,}800 \pm 4{,}300)/RT)$ at 600 ~ 1100°C. The high activation energies found may be due to the sink effect caused by the carburization of chromium in the stainless steel. Other studies are performed on the diffusion kinetics and mechanism of carburization in stainless steel. The penetration profiles obtained by ^{14}C monitoring at 650 to 830°C are relatively good agreement with the theory of grain boundary diffusion proposed by Fisher. By comparing results of experiments and theory, the carbon concentration between the graphite and polished surface of the stainless steel may be kept by the thermodynamic balance. The depth of carburization appeared to follow the logarithmic law as a function of the annealing time. (auth)

Preparation and Fabrication

Refer also to abstract 4259.

4740 (BM-RI-7455) CHARACTERISTICS OF ELECTROWON AND OF HYDROGEN-REDUCED MOLYBDENUM POWDER AND SHEET. Ferrell, E. F.; Iverson, H. G. (Bureau of Mines, Reno, Nev. Reno Metallurgy Research Center). Dec 1970. 29p.

Electrowon molybdenum powders and a commercial hydrogen-reduced powder, all with different minor impurities, were investigated with respect to inherent properties, to fabrication techniques, and to properties of the fabricated sheet. Compared with the commercial hydrogen-reduced powder, the electrowon powders had a larger particle size, a greater flow rate, a higher apparent density, and a lower oxygen content. Sheet materials prepared from the two types of powders showed similar mechanical properties, under the same conditions of heat treatments, except for low-temperature ductility. Yield strengths varied with carbon content, heat treatment, and test temperature. (auth)

4741 (BNWL-CC-491) INVENTION REPORT: PULSED CURRENT ELECTROPLATING. Stromatt, R. W.; Lundquist, J. R. (Battelle-Northwest, Richland, Wash. Pacific Northwest Lab.). 9 Feb 1966. Contract AT(45-1)-1830. 4p. Dep. NTIS.

Improvements in methods for electroplating thin protective coats on substrate metals by application of high-current rectangular shaped pulses are described. Merits of the method are supported by photomicrographs of deposits. (J.R.D.)

4742 FIBRE-REINFORCED ALLOY. Piatti, Giovanni (to European Atomic Energy Community). British Patent 1,211,467. 4 Nov 1970. Priority date 2 Nov 1967, Netherlands.

A fiber-reinforced Al alloy is described in which Al–Ce fibers are embedded in the Al matrix. This alloy has good ductility and strength at high temperature and has favorable properties as regards neutron economy. (J.R.D.)

4743 MANUFACTURE OF METALLIC URANIUM NUCLEAR FUELS: SOME INDUSTRIAL AND ECONOMIC ASPECTS. Jeanpierre, G.; Le Duigou, A.; Dumonteil, G. (CEA, Saclay, France). Bull. Inform. Sci. Tech. (Paris); No. 148, 81-7(May 1970). (In French).

Since 1955, the productivity of uranium nuclear fuel fabrication has been improved. The evolution of the manufacturing costs is analyzed. (auth) (France)

4744 REMOVAL OF VOLATILE IMPURITIES FROM VACUUM MELTS. Chernov, B. G.; Ageev, P. Ya. Izv. Vyssh. Ucheb. Zaved., Chern. Met.; No. 12, 16-18(1969). (In Russian).

The behavior of some non-ferrous metal impurities (Pb, Bi, Sb, and Sn) in Fe–Ni melts was investigated when varying the Ni content in the range 0 to 100% and when alloying separately and jointly with Cr, W, Mo, Al, and Ti. The heats were made in a vacuum induction furnace at a residual pressure of 0.5 and 10^{-3} torr. Lead and Bi were eliminated rapidly from Fe–Ni alloys, irrespective of the Ni content. The rate of removal of Pb, Bi, and Sb from melts alloyed with Cr, W, Mo, and up to 3% Al + Ti depended on the degree of evacuation, and was much greater at lower pressures. Sn remained unchanged. (Metals Abstr.)

4745 UNIQUE METHODS AND EQUIPMENT PRODUCE PRECISION TUBULAR PARTS. West. Mach. Steel World; 61: No. 2, 20-5(Feb 1970).

Titanium 6Al–4V alloy, Inco 625, Inco 718, unalloyed Ta, Waspaloy, Al and TD Ni are among the metals produced to precise tolerance at this installation for applications such as tank supports and trusses for the lunar module, control rods for aircraft and nuclear reactor components. One method used in fabricating the tubular parts is the Roll-Flo process, which deforms metal plastically by coaxial rolling over a hardened mandrel. It forms seamless variable-wall tubing in lengths to 45 ft and dia to 24 in. The Roto-Draw tapering process fabricates precise, small-dia tapered tubes from 304 stainless, Inconel X and Hastelloy. Rotary swaging and draw bench operations are also utilized. Quality control is extremely rigid, as illustrated by the production of tapered helicopter spar tubes from seamless

4340 steel stock and various engine parts for the lunar module and Saturn rockets. (Metals Abstr.)

Properties Evaluations

Refer also to abstracts 4183, 4203, 4841, 5055, 5152, 5169, 5170, 5184, and 6060.

4746 (AD–710275) SOME EFFECTS PRODUCED BY ADDING RHENIUM TO ALLOYS OF TUNGSTEN AND CARBON. Final Report, June 30, 1964–August 31, 1969. Owen, W. S. (Cornell Univ., Ithaca, N. Y. Dept. of Materials Science and Engineering). 1970. Contract DA-31-124-ARO(D)-228. 6p. (AROD–4917:5-MC). NTIS.

One aspect of the rhenium alloying effect in tungsten which has not been explored quantitatively to the extent which its potential importance warrants is the change in the jump frequency of an interstitial carbon atom in a tungsten lattice. The work was designed to study this phenomenon from two aspects; the effect of rhenium on the diffusivity of carbon in tungsten and the effect of an anelastic relaxation dependent upon the jumping of carbon in a stressed tungsten lattice. (auth) (USGRDR)

4747 (AWRE-O–63/70) INFLUENCE OF IMPURITIES ON THE PROPERTIES OF URANIUM. Wakelin, R. J. (Atomic Weapon Research Establishment, Aldermaston (England)). Sep 1970. 41p. Dep. NTIS (U. S. Sales Only). UK 7s. 0d.

The effects of Fe, Si, Al, Ni, Cr, and Zr impurities on the properties of uranium were investigated. The difficulties of making uniform and reliable U–C alloys is now appreciated. The main practical result of use in ^{235}U processing is that the iron content must be limited to 500 ppM maximum, the silicon and aluminium contents to 1000 ppM each. The effect of up to 2000 ppM of any of these impurities did not seriously affect the drawing characteristics. (auth)

4748 (DP-Report–537) MATERIALS FOR THE BOILER TUBES OF A HTGC POWER REACTOR. Project DRAGON. Conde, J. F. G. (Atomic Energy Establishment, Winfrith (England)). May 1967. 54p. Dep. NTIS.

The desirability of surveying the relative merits of materials for the steam plant with a view to their use in a HTGC power reactor system is indicated and the aspects which should receive attention are noted. Materials for conventional steam plant are discussed together with the characteristics which are of principal value in determining their suitability. A review of the available materials is followed by a discussion of creep and rupture properties, corrosion resistance, metallurgical stability, fabrication aspects, and physical properties. The properties relevant to HTGC reactor service are detailed and potential problems are outlined. Design criteria and economic aspects are discussed and in conclusion recommendations are made on the materials which should be used and the experimental program which should be carried out concurrently with power reactor assessment studies and the operation of the Dragon Reactor. (auth)

4749 (SC-DR–70-718) SURVEY OF FACTORS WHICH INFLUENCE STRESS CORROSION CRACK INITIATION IN SEVERAL URANIUM BASE ALLOYS. Stephenson, L. L. (Sandia Labs., Albuquerque, N. Mex.). Oct 1970. 25p. Dep. NTIS.

The effect of a number of metallurgical and electrochemical variables on the initiation phase of stress corrosion cracking in Mulberry (U-7½% Nb-2.5% Zr), U-4½% Nb, U-6½% Nb, and U-8½% Nb alloys was determined. A potentiostat was used to establish the passivation behavior of Mulberry in several different solutions. Bend specimens, immersed in aqueous solutions and held at constant potentials, were used to investigate the stress corrosion crack initiation characteristics of the various alloys. The effect of potential on the mode of crack growth in Mulberry in dilute KCl solutions was determined. (auth)

4750 (TEE–4125-2) SUBLIMED EMITTER AND COLLECTOR COATINGS. Ernst, D.; Meyers, R.; Poirier, V. (Thermo Electron Corp., Waltham, Mass.). Jun 1970. Contract AT(30-1)-4125. 64p. (TE–4122-2-71). Dep. NTIS.

Initial work on coating of planar W emitters with additional layers of W involved deposition in such a way that the surface of the added layer was a better cesiated emitter than the original substrate. It was found that the vacuum work function of polycrystalline W (4.5 to 4.6 eV) could be increased to the level of single-crystal (110) W (5.1 to 5.2 eV). Results of studies have indicated that under certain depositing conditions, the bounding planes on the new surface are predominantly (110), no matter what the orientation of the underlying substrate is; evidence suggests that it is this phenomenon that results in the improvement in work function. One such coated W emitter has been tested in a cesiated diode; its performance is described. Related work has also been done with niobium collectors, coating them with sublimed deposits of Mo, Ni, Nb, and W. Thermal cycling, metallography, x-ray diffraction, and surface contour studies have all been used to characterize these collector coatings. Diode performance studies are now under way. The coated collectors have been prepared at much lower substrate temperatures than the coated emitters and would probably not be as stable to very severe annealing, but it is anticipated that they will be stable in the temperature range normally encountered by a collector. Both the emitter and collector coating investigation results indicate promising methods of achieving improved thermionic performance. Use of the coatings allows the electrode surface characteristics to be selected primarily from thermionic considerations. Selection of the substrate materials can be based on strength or other structural properties to meet the requirements of the particular diode application. (auth)

4751 (TEE–4125-3) PERFORMANCE REPRODUCIBILITY OF CYLINDRICAL DIODES WITH CVD FLUORIDE TUNGSTEN–NIOBIUM ELECTRODES. Gunther, B.; Teagan, P. (Thermo Electron Corp., Waltham, Mass.). Jun 1970. Contract AT(30-1)-4125. 50p. (TE–4122-4-71). Dep. NTIS.

Activities in a program to fabricate and test 12 identical diodes to determine the performance reproducibility that could be expected among diodes of a given type are described. Cylindrical diodes with CVD fluoride tungsten emitters and niobium collectors were tested. These electrode pairs are typical of those considered for fission-heated thermionic converters. The converters were tested and are compared at common output current densities and cesium reservoir temperatures, such as may be present in a string of series-connected modules with a common cesium reservoir. The average performance of the converters was established and variations in performance of the individual converters from this average were quantified by a standard deviation. This standard deviation is a measure of the reproducibility of this type of converter. After the performance of each of the converters was established, they were operated under steady state conditions for 200 hours. The converters were then retested to determine the extent of possible short-term changes in performance of individual converters and to what extent such changes in individual diode performance affected the average performance and the standard deviation. (J.R.D.)

4752 (TEE–4125-4) EMITTER TEMPERATURE DEPENDENCE OF LOWER MODE CURRENT. Gunther, B. (Thermo Electron Corp., Waltham, Mass.). Jul 1970. Contract AT(30-1)-4125. 24p. (TE–4137-27-71). Dep. NTIS.

Measurement of the apparent saturation current in the extinguished mode has been suggested as a means of determining the emitter temperature. Data obtained from two converters with substantially different emitters ((110) and (100) tungsten) were in good agreement, showing that the emitter work function does not influence the deduced emitter temperature (within 25°K). Ignition current was essentially independent of collector temperature and, therefore, of collector work function, and was an inverse function of interelectrode spacings. It was found, however, that the ignition current is a linear function of emitter temperature. This is in contrast with the theoretical model which is the basis for predicting an exponential relation with inverse temperature. This difference corresponds to an error of 50°K in emitter temperature determinations. (J.R.D.)

4753 RELIABILITY EVALUATION OF BRITTLE MATERIALS AND OF WELDED STRUCTURES. Basile, D.; Musso, G.; Volta, G. (Joint Nuclear Research Center, Ispra, Italy). Met. Ital.; 52: No. 3, 99-109(1970). (In Italian).

The theory of reliability applied to material resistance is examined. A critical review is given of parameters used to characterize materials and structures including allowable stresses, elongations, impact properties, and fractures toughness under different load conditions. Methods for computation of safety factors are introduced. The theory is applied to a zirconium alloy pressure tube for a nuclear reactor in which peculiar brittleness problems exist due to the presence of welds, intermetallic joints and hydriding corrosion. (Euratom)

4754 THERMODYNAMIC STUDY ON THE ACTIVITIES OF BOTH COMPONENTS IN BINARY MOLTEN ALLOYS. Okajima, Kazuhisa; Sakao, Hiroshi (Nagoya Univ., Japan). Trans. Jap. Inst. Metals; 11: 217-24(Jul 1970).

The present study was undertaken to evaluate the activities of both components in binary molten alloys and also to investigate the relations existing between the activities. It was made clear that the activities of both components can be approximately calculated from the known thermodynamic values of the intermetallic

XUM

compounds on the assumption of partial molar free energies neglecting the Gibbs-Duhem relationship. A modified Gibbs-Duhem equation was then presented, which can be applied to the activities of both components measured by the TIE method. The modified equation can be represented by the form $\ln a_1 = k[-\int_1^{N_1} N_2/N_1 \, d \ln\gamma_2 + \ln N_1]$, where a_1 and γ_2 are the activity of component 1 and the activity coefficient of component 2, N_1 and N_2 are the mole fractions of components 1 and 2, respectively, and k is a factor which varies with composition. (auth)

4755 THERMODYNAMIC AND KINETIC ASPECTS OF CARBON TRANSPORT IN SODIUM–STEEL SYSTEMS. Natesan, K.; Kassner, T. F. (Argonne National Lab., Ill.). J. Nucl. Mater.; 37: 223-35(Nov 1970).

The thermodynamic activity and solubility of carbon in Fe–Cr–Ni alloys were calculated in the temperature range of 500 to 800°C by extrapolation of higher temperature data in the Fe–Cr–C and Fe–Ni–C systems. These results were used with phase-equilibria information and data for the solubility of carbon in sodium to obtain an equilibrium relationship between the total carbon concentration in the alloys and that in sodium. The calculations showed that the Fe–Cr–Ni alloys with nominal initial carbon concentrations may undergo carburization or decarburization depending upon the carbon concentration in sodium in the temperature range of 500 to 800°C. Computed carbon concentrations in sodium for incipient carbide formation in an 18-8 stainless steel were significantly lower (<1 ppM) than those commonly reported (15 to 30 ppM) for stainless steel-sodium systems operating at temperatures below 700°C. The phase equilibria and activity data were used to explain the observed phenomenon of transfer of carbon from austenitic steel to sodium when chromium depletion, due to mass transfer, occurs. In addition, the driving force for carbon transfer from ferritic to austenitic steel under isothermal conditions was calculated. (auth)

4756 HYDROGEN SUPERCHARGING DURING THERMAL CYCLING OF ZIRCONIUM. Westlake, D. G.; Ockers, S. T. (Argonne National Lab., Ill.). J. Nucl. Mater.; 37: 236-42 (Nov 1970).

Zirconium was coated with zirconium hydride and allowed to equilibrate at 689°K. Thermal cycling between 689 and 298°K caused supercharging, the same phenomenon reported by Westerman for Zircaloy-2, i.e., the hydrogen concentration of the core exceeded the terminal solubility at 689°K. It was demonstrated that impurities, grain boundaries and geometry played no role. The concentration of hydrogen (at. %) after n cycles was $C_H = (8.14 + 1.13\,n)^{\frac{1}{2}}$ for slow heating and cooling when the specimen was allowed to remain at 689°K long enough for equilibration. Supercharging is attributed to the transfer of hydrogen from the hydride surface layer to resaturate the solid solution at the core when precipitates fail to dissolve completely at 689°K because of irreversible plastic deformation. (auth)

4757 RECRYSTALLIZATION AND MECHANICAL BEHAVIOR OF ZIRCALOY-2 TUBING. Lee, D. (General Electric Research and Development Center, Schenectady, N. Y.). J. Nucl. Mater.; 37: 159-70(Nov 1970).

The effect of recovery and recrystallization treatment on the mechanical behavior of cold worked Zircaloy-2 tubing was examined. The structures of annealed specimens were identified by electron microscopy, and the tensile properties were determined by pulling the tubing along its circumferential direction in a specially designed fixture. For the specimens annealed over the range of temperatures, both the hardness and tensile strength changed abruptly over a narrow range of annealing temperatures, and these changes were associated with the appearance of new, strain-free recrystallized grains. It is concluded that the rapid rate of recrystallization was due to the excessively large amount of cold work present in the tubing. A maximum value of tensile ductility was achieved at the annealing temperature just high enough to achieve complete recrystallization. The ultrafine equiaxed structure so achieved also provided an optimum combination of strength and ductility at temperatures where an anomalously low ductility is known to occur. (auth)

4758 MIGRATION OF HELIUM BUBBLES IN A 20 PERCENT Cr/25 PERCENT Ni/Nb STABILISED STEEL. Walker, G. K. (Berkeley Nuclear Labs., Eng.). J. Nucl. Mater.; 37: 171-6 (Nov 1970).

Stainless steel foils were bombarded with He^+ ions to produce bubbles on subsequent heat-treatment. Using an electron microscope, bubble migration was observed after isothermal anneals at temperatures in the range 800 to 900°C. Mobility was a maximum at a bubble radius of $\approx 5.0 \times 10^{-3}$ μm, independent of annealing temperature. The movement of bubbles larger than this was characteristic of a migration process controlled by volume diffusion. (auth)

4759 INFLUENCE OF AN ELECTRIC FIELD ON A PHASE TRANSITION AND SWITCHING EFFECT IN V_2O_3. Andreev, V. N.; Aronov, A. G.; Chudnovskii, F. A. (Inst. of Semiconductors, Leningrad). Sov. Phys.-Solid State (Engl. Transl.); 12: 1230-1(Nov 1970).

Translated from Fiz. Tverd. Tela; 12: 1557-9(May 1970).

The effects of a strong electric field on the semiconductor–metal phase transition in V_2O_3 crystals of varying thickness were investigated. When the field reached a critical value of $\sim 10^4$ V/cm in the semiconductor state, the current increased rapidly. This critical field depended weakly on the thickness. Current oscillations were also observed, and their frequency could be varied from 10 to 1 MHz. The results can be explained by a reduction in the energy gap (forbidden band width) due to the piezoelectric effect which causes the phase transition because of increased excitation. (D.L.C.)

4760 THERMODYNAMICS OF RARE EARTH METALS AT LOW TEMPERATURES. I. HEAT CAPACITY C_p OF RARE EARTH ELEMENTS. Semenchenko, V. K.; Badra, Kh. M. (Moscow State Univ.). Zh. Fiz. Khim.; 44: 1925-31(Aug 1970). (In Russian).

Using the method of thermodynamic stability, experimental data were obtained on the heat capacity C_p of all the rare earth metals except Pm at low temperatures. The results obtained indicated that all observed phase transitions belong to the supercritical type. In four cases the thermal stability coefficient T/C_p passed through an extreme, indicating the presence of a supercritical transition at this point or near it. (tr-auth)

4761 DIFFUSIVITY AND ISOTOPE-EFFECT MEASUREMENTS IN EQUIATOMIC Fe–Co. Fishman, S. G.; Gupta, D.; Lieberman, D. S. (Univ. of Illinois, Urbana). Phys. Rev., B; 2: 1451-60(15 Sep 1970).

Several radioactive isotopes of Fe and Co were simultaneously diffused into an equiatomic FeCo alloy which exhibits fcc, bcc, and CsCl-type ordered phases with decreasing temperature. Penetration profiles were obtained by standard lathe sectioning and a grinding-sectioning technique which is described. From lnD-versus-1/T plots, activation energies of 68.5 and 55 kcal and frequency factors of 1.26 and 0.25 cm^2/sec were obtained for diffusion of ^{59}Fe in the fcc and bcc phases, respectively. From similar plots, activation energies of 69.4 and 60.0 kcal and frequency factors of 1.33 and 2.00 cm^2/sec were obtained for diffusion of ^{57}Co in the fcc and bcc phases of the FeCo alloy. The average isotope-effect parameters were 0.66 in the fcc phase and 0.52 in the bcc phase. Manning's theory for concentrated alloys was used to calculate correlation factors for the FeCo alloy. From these calculated values and experimentally measured isotope-effect parameters, ΔK was determined to be slightly larger in the fcc and bcc phases of the FeCo alloy than has been reported in pure Fe. The observed decrease in the isotope-effect parameter with increasing degree of order during the bcc-to-CsCl-type ordering transformation is explained in terms of an increase in atom-jump correlation with the onset of long-range order. (auth)

4762 HYDROGEN INDUCED SUSTAINED LOAD CRACK GROWTH IN Ti–6Al–4V. Pittinato, G. F.; Frederick, S. F. (McDonnell Douglas Astronautics Co., Santa Monica, Calif.). Met. Trans.; 1: 3241-3(Nov 1970).

Results of fatigue crack propagation tests conducted in helium and hydrogen on specimens of Ti–6Al–4V alloy are presented which show that hydrogen increases crack growth rate at 73 to −100°F. It was also found that hydrogen environments can induce sustained load crack growth in this alloy at 73°F. (J.R.D.)

4763 DIFFUSION OF ^{14}C IN TUNGSTEN AND TUNGSTEN–RHENIUM ALLOYS. Shepela, Adam. Ithaca, N. Y.; Cornell Univ. (1970). 274p. University Microfilms Order No. 70-12,649.

Thesis.

The diffusion coefficients of carbon-14 in randomly-oriented crystals of tungsten and tungsten-rhenium alloys (3.9 at. % Re, 6.8 at. % Re) have been measured over the temperature range 1500 to 1800°C: $D(^{14}C/W) = (3.45 \pm 0.12)\ 10^{-3} \exp(-37800 \pm 140/RT)$, $D(^{14}C/W - 3.9$ at. % Re$) = (3.00 \pm 0.26)\ 10^{-3} \exp(-37000 \pm 330/RT)$, $D(^{14}C/W - 6.8$ at. % Re$) = (2.24 \pm 0.09)\ 10^{-3} \exp(36100 \pm 170/RT)$. The values for the activation energy (cal/mole) and frequency factor (cm^2/sec) for carbon-14 in tungsten agree well with the values determined by Kovenskii (1800 to 2800°C): Q = 40400, $D_0 = 9.22 \times 10^{-3}$. Experimentally, a thin carbide layer formed at 900°C on one face of the sample by a reaction with carbon-14 (fine powder, 10 mc/mM), provided the source of carbon throughout the diffusion anneal. At the diffusion temperature the carbon concentration at the carbide-solid solution interface is the terminal solubility. The solution to the one-dimensional diffusion equation is $A(x) = A_L \operatorname{erfc}(x/2\sqrt{Dt})$ where A(x) is the activity at a distance x

from the interface, and A_L is the activity at the interface. A non-equilibrium redistribution of carbon occurred during cooling. Thus the concentration profile within 50 microns of the interface measured at room temperature was different from that established during the diffusion anneal. A computer iteration technique calculated a best fit value for D from the measured values of A(x), x, t and estimated values of A_L. The elastic strain model of Yang, which expresses the activation energy of diffusion in terms of the bulk elastic properties of the matrix, qualitatively predicts the decrease in the activation energy of carbon diffusion with increasing rhenium content which has been observed experimentally. The models of Beshers and Yang, which distinguish between octahedral and tetrahedral site occupancy, give diametrically opposed predictions when applied to the tungsten-carbon system. In all diffusion samples a zone of carbon depletion adjacent to the interface was observed as a result of carbon segregative to the interface. The extent of the depleted zone is a function of cooling rate. The driving force for the interface enrichment effect is the supersaturation of the solid solution with carbon as the sample temperature is decreased. A computer calculation was used to theoretically estimate the resultant concentration profiles after cooling. The appropriate solution of the one dimensional diffusion equation containing the time-dependent diffusion coefficient is $c(x,t) = c_L(t) * [x/2(\pi D(t)t^3)^{1/2}] \exp(-x^2/4 D(t)t)$, for the conditions $c(x,o) = o$, $c(o, t) = C_L(t)$, $dc(\infty,t)/dt = o$. This model assumes a supersaturation at the interface during cooling which is a numerical factor times the time-dependent equilibrium terminal solubility. The calculations were terminated at 1250°C during the cooling cycle since the eutectoid reaction $W_2C = WC + W$ invalidates the boundary conditions. Calculated concentration profiles with supersaturations of 1.42 and 1.44 agree well with experimental data for two tungsten samples cooled at different rates. (Diss. Abstr. Int., B)

4764 METHOD AND APPARATUS FOR MEASURING APPARENT DENSITY BY GAMMA RADIATION. Bretonniere, Serge; Chevrier, Jean-Pierre; Gabilly, Yves (to Etat Francais). U. S. Patent 3,531,643. 29 Sep 1970. Priority date 25 Nov 1966, France.

A method and apparatus for measuring the apparent density of a solid body by gamma rays are described. An emitter of an incident beam of gamma rays is mounted on a frame with an adjustable support for the sample to be measured placed on the axis of the emitted beam and a receiver for the emergent beam placed after the support on the same axis. Adjustable collimating means are placed between the emitter and the sample support for forming the incident beam into a narrow pencil of substantially parallel rays in the axis of the incident beam. A discriminating device is incorporated with the receiver to determine the energy of the photons received thereby. (auth)

4765 FRACTOGRAPHIC STUDY OF STAGE I FATIGUE CRACKING IN A NICKEL-BASE SUPERALLOY SINGLE CRYSTAL. Duquette, D. J.; Gell, M.; Piteo, J. W. (Pratt and Whitney Aircraft, Middletown, Conn.). Met. Trans.; 1: 3107-15(Nov 1970).

An electron fractographic study was made of opposing crystallographic (Stage I) fatigue fracture surfaces of specimens of a single crystal nickel-base superalloy, low carbon MAR-M200, that were tested at room temperature. In regions near the crack initiation site, features on both surfaces were the same. In regions at some distance from the initiation site significant differences in the type and extent of microfeatures were observed. For a crack propagating in an upward direction, irregular markings were observed on the upper fracture surface and regularly spaced slip offsets and slip band cracks were observed on the lower surface. These observations are explained by a consideration of the elastic stress field and the resultant glide forces on all possible slip systems surrounding a crack growing at an angle to the principal stress direction. Additionally the results are used to support a previously proposed model for Stage I fatigue crack propagation. (auth)

4766 LOCAL ORDERING AND THE RESISTIVITY OF Ni–W AND Pd–Co ALLOYS. Katsnel'son, A. A.; Alimov, Sh. A.; Dazhaev, P. Sh.; Silonov, V. M.; Stupina, N. N. (Moscow State Univ.). Phys. Metals Metallogr. (USSR) (Engl. Transl.); 26: No. 6, 26-35(1968).

Translated from Fiz. Metal. Metalloved.; 26: No. 6, 987-95 (1968).

On specimens treated in the same way, the short-range order parameters and resistivity ρ of Ni–W and Pd–Co alloys were measured. The annealing rise in ρ was found to be due to local ordering and secondary electron scattering on boundary regions of various compositions at various stages of order. (auth)

4767 STUDY OF OXIDATION OF YTTERBIUM AND HOLMIUM THIN FILMS IN THE ELECTRON MICROSCOPE. Kumar, Jitendra; Bist, B. M. S.; Srivastava, O. N. (Banaras Hindu Univ., India). Mater. Sci. Eng.; 6: 371-6(Dec 1970).

The oxidation behavior of thin films of the rare-earth metals ytterbium and holmium were studied. It was shown that the Pilling–Bedworth criterion did not hold good in the oxidation of these thin films. The oxidation always took place through the development of porous oxide film and reaction of oxygen with the metal film. This is at variance with the previous observations of Murr on erbium thin film oxidation. The oxidation characteristics observed in the present investigation were compared with the other available observations on the oxidation of rare-earth metals. (auth)

4768 TENSILE BEHAVIOR OF POLYCRYSTALLINE ZIRCONIUM AT 4.2°K. Ramachandran, V.; Baldwin, D. H.; Reed-Hill, R. E. (Univ. of Florida, Gainesville). Met. Trans.; 1: 3011-18(Nov 1970).

Tensile tests were conducted at 4.2°K on both longitudinal and transverse specimens machined from zirconium plate. In this plate the basal planes of the grains were strongly aligned parallel to and distributed nearly uniformly about the rolling direction. The metal had higher ductility at 4.2°K than at room temperature. Prestraining transverse specimens at 4.2°K produced higher room temperature damping capacity than prestraining at 77°K. All stress-strain curves for the 4.2°K tests exhibited characteristic sudden drops in the load. Transverse specimens showed a much higher incidence of twinning, greater strain hardening, more plastic deformation between serrations, and fewer serrations than longitudinal specimens. The experimental evidence is in agreement with Kula and DeSisto's conclusions that twinning per se is probably not responsible for the discontinuous yielding. The present observations are also consistent with Basinski's hypothesis that the load drops are related to thermal softening. A simple calculation shows that at temperatures near absolute zero, the heat generated in a specimen during deformation is much more than that necessary to cause an instability and consequent load drop. Hence it is concluded that all the heat generated is not retained in the specimen and a large fraction must be lost to the surroundings. An estimate of the magnitude of the temperature rise associated with a typical load drop was made. (auth)

4769 INFLUENCE OF GRAIN BOUNDARIES ON THE FRACTURE MODE OF ZIRCONIUM AND ZIRCALOY-2. Lee, D.; Koch, E. F.; Rogers, H. C. (General Electric Research and Development Center, Schenectady, N. Y.). Met. Trans.; 1: 3125-31(Nov 1970).

The mode of fracture was examined in Zircaloy-2 sheet specimens pulled in tension over a range of strain rates (10^{-5} to 10^{-1} min^{-1}) at 350°C. As the strain rate decreased from 10^{-1} to 10^{-4} min^{-1}, the mode of fracture changed from transgranular ductile shear to a mixed mode of intergranular and ductile shear failure. This was accompanied by the ridging of grain boundaries on the fracture surface. With decreasing grain size this ridging became more evident. It was not observed on the fractures of high purity iodide zirconium. This correlates with the earlier observation that the fracture strain decreases with decreasing strain rate for Zircaloy-2 but not for iodide zirconium. No direct evidence could be found for any grain boundary strengthening phenomenon. The microscopic fracture behavior was, however, found to correlate with the macroscopic fracture orientation. The ridging of the boundaries increases as the fracture path shifts from a direction with a high shear component to one that is nearly normal to the tensile axis. (auth)

4770 DEVELOPMENT OF STEELS FOR NUCLEAR POWER PLANT WITH SPECIAL REFERENCE TO THE REPORT OF STEEL IRRADIATION JOINT-COMMITTEE OF JAPAN. Hasegawa, Masayoshi; Yonezawa, Toshio (Waseda Univ., Tokyo). Tetsu To Hagane; 56: 446-62(Mar 1970). (In Japanese).

The present status of reactor steels, especially in connection with irradiation brittleness, is reviewed. The use of stainless steels in fast breeder reactors is also discussed. Mechanisms associated with irradiation brittleness and changes in the crystal structure leading to the brittleness are explained. The trend from ASTM 200 series to 500 series as the power capacity is increased is explained. The irradiation effects on A302B, HY-80, and on SIJC are examined in comparison with results obtained in the U. S. Metallurgical factors in irradiation brittleness such as alloying elements, dissolved gases, and prefabrication treatments are discussed. Stainless steel behavior in fast reactors with respect to atomic displacement, nuclear transformation gases, swelling, and Na reactions are examined. The results of studies by the Joint Committee are reported. (Japan)

4771 ELECTRICAL CONDUCTIVITY OF DYSPROSIUM THIN FILMS. Lodge, F. M. K.; Taylor, K. N. R. (Univ. of Durham, Eng.). pp 531-9 of Les Elements des Terres Rares. Tome II.

XUM

Paris; Centre National de la Recherche Scientifique (1970).
From International Symposium on Rare Earths, Paris, Grenoble, France. See CONF-690517.

Measurements were made of the electrical conductivity in the film plane of dysprosium films over a film-thickness range of 130 to 2500 Å. The films were deposited onto glass substrates by high-vacuum evaporation at pressures better than 10^{-6} torr and protected by an overcoating of SiO. The conductivity was examined between 4.2°K and room temperature and the magnetoresistance was studied in the presence of applied transverse and longitudinal fields up to 10 kG. The variation of resistance with temperature is similar in form to that obtained for bulk specimens for all film thicknesses (Legvold et al. 1960). However, in films less than 200 Å thick, the residual resistance is observed to rise rapidly while the magnetic spin contribution (ρ_{spin}) shows a decrease. The spin contribution was obtained by computing a "least squares" fit to the linear high temperature part of the resistance curve and extrapolating to 0°K. Even in the thickest films the derived values of the spin contribution are less than that of the bulk material. The results show that ρ_{spin} is proportional to T^2 over an appreciable temperature range in the ferromagnetic region, in agreement with the spin-wave model for a ferromagnetic metal. However, at low temperatures the experimental results depart from this simple model. In the antiferromagnetic region ρ_{spin} is proportional to T^5. The detailed shape of the resistance vs temperature curve was used to obtain the paramagnetic Curie temperature and the antiferromagnetic Neel point. Both are found to decrease slightly with decreasing thickness. (tr-auth) (France)

4772 CONSTRUCTION MATERIALS FOR NEUTRON CAPTURE GAMMA-RAY SPECTROSCOPY WITH ^{252}Cf SOURCES. Evans, A. G. (Savannah River Lab., Aiken, S. C.); Senftle, F. E.; Wiggins, P. F.; Duffey, D. Trans. Amer. Nucl. Soc.; 13: 488-9(Nov 1970).
From Meeting of the American Nuclear Society, Washington, D. C. See CONF-701102.

4773 INTERSTITIAL TRANSFER IN SODIUM SYSTEMS. Bagnall, C.; Miller, R.; Schrock, S.; Shiels, S. (Westinghouse Advanced Reactors Div., Madison, Pa.). Trans. Amer. Nucl. Soc.; 13: 577-8(Nov 1970).
From Meeting of the American Nuclear Society, Washington, D. C. See CONF-701102.

4774 RADIOCHEMICAL MEASUREMENT OF MASS TRANSFER COEFFICIENTS IN FORCED-CONVECTION SODIUM. Cooper, M. H.; Taylor, G. R. (Westinghouse Advanced Reactors Div., Madison, Pa.). Trans. Amer. Nucl. Soc.; 13: 579(Nov 1970).
From Meeting of the American Nuclear Society, Washington, D. C. See CONF-701102.

4775 NEW CANDIDATE LMFBR CLADDING ALLOY. Laidler, J. J. (Hanford Engineering Development Lab., Richland, Wash.). Trans. Amer. Nucl. Soc.; 13: 589-90(Nov 1970).
From Meeting of the American Nuclear Society, Washington, D. C. See CONF-701102.

4776 DEVELOPMENT OF TYPE 316 STAINLESS-STEEL TUBING FOR LMFBR FUEL ELEMENT CLADDING. Padden, T. R.; Ray, W. E.; Snyder, H. J.; Thomas, K. C. (Westinghouse Advanced Reactors Div., Madison, Pa.). Trans. Amer. Nucl. Soc.; 13: 590-1(Nov 1970).
From Meeting of the American Nuclear Society, Washington, D. C. See CONF-701102.

4777 DYNAMIC STRAIN AGING IN 304 STAINLESS STEEL. Paxton, M. M.; Steichen, J. M.; Ward, A. L. (Hanford Engineering Development Lab., Richland, Wash.). Trans. Amer. Nucl. Soc.; 13: 608-9(Nov 1970).
From Meeting of the American Nuclear Society, Washington, D. C. See CONF-701102.

4778 COLD-WORKING MAXIMUM OF INTERNAL FRICTION. Schlaet, F. Wiss. Z. Tech. Hochsch. Otto von Guericke Magdeburg; 13: 361-4(1969). (In German).

Investigations with the aim of elucidating the nature of cold-working damping maximum by measuring mechanical damping and the secondary after-effect are described. The investigations were made on Ta and Nb containing interstitial O and N. The maximum was caused by the movement of dislocations with their Cottrell atmospheres. The processes of dislocation re-ordering and their blocking by relatively immobile foreign atoms are of major importance in the occurrence and healing of the maximum on heating after plastic deformation. It is not known whether the mechanism described is also valid for α-Fe. (Metals Abstr.)

4779 HEAT RESISTING STEELS AND ALLOYS FOR HTGR. Yoshida, Heitaro (National Research Inst. for Metals, Tokyo). Genshiryoku Kogyo; 16: No. 7, 43-8(Jul 1970). (In Japanese).

The application of nuclear reactors for iron making and chemical industry is drawing increasing interest in recent years. And here high-temperature gas-cooled reactors emerged as a promising possibility for the purpose. The problems of heat-resistant materials in this connection are described, for the shell-and-tube type heat exchangers, with He gas temperatures of 800 to 1000°C as the primary coolant and CO and H_2 mixed as the secondary coolant for iron-making and chemical purposes. The problems include the following areas: high-temperature strengths of heat-resistant metal materials — interconnection between workability, strength and wall thickness are described, centered on the permissible stress and rupture strength; Cementation, briefly describing the case of heat-exchange tube cementation by CO in the mixed gas; and hydrogen brittleness and hydrogen penetration and solubility in the alloys. (Japan)

4780 CONSIDERATIONS IN THE EVALUATION OF ALUMINUM MASTER ALLOYS. Sevier, P. E.; Dore, J. E.; Peterson, W. S. (Olin Corp., New Haven). J. Metals; 22: No. 11, 37-46 (Nov 1970).

Master alloys are added to aluminum melts as a source of alloying elements and grain refining agents. The quality of these materials has an important effect on the quality and performance of wrought and cast aluminum end product. Frequently, however, this fact is not appreciated, and master alloys are purchased on the basis of price per lb only. This paper describes techniques used to evaluate master alloys from the user's standpoint. Particular attention was given to the development of methods to assess presence and amount of nonmetallic inclusions and the size and distribution of second phase particles such as TiB_2. These techniques include metallographic examination and physical separation of second phase particles from the aluminum matrix followed by a counting operation using a Coulter Counter. Examples of the use of these methods of evaluation are given for Al-Ti, Al-B and Al-Ti-B master alloys. Results obtained with commercial products demonstrate the wide variations observed in quality of these materials in respect to composition, oxide and/or dirt content, and nature and effectiveness of grain refining agents. (auth)

4781 BREAKING AT THE WELDS. Ogura, Nobukazu (Yokohama National Univ., Japan). Nippon Kikai Gakkaishi; 73: 677-83(May 1970). (In Japanese).

The nature of cracks in the welds of structures was reviewed. Accident countermeasures for nuclear piping in the United States are described. In connection with damages in the primary coolant system of nuclear power plant, the Pipe-rupture Project was carried out. In phase I the present state of the ruptures was studied, included the range of factors involved, rupture instances, the forms of rupture, and propriety of the existing standards. These, mainly the results of questionnaires, are explained, with appropriate considerations thereof. Instances of rupture in pressure vessels are described. Two in the U. K. are given: an ammonia-plant vessel at Imming-ham, a welding of ten steel cylinders, and a boiler drum at Cockenzie. Then, accidents in storage tanks in Japan are described, analyzing the causes. (Japan)

4782 PROPERTIES OF THE CHROMIUM–NICKEL ALLOYS CONTAINING NIOBIUM AND MOLYBDENUM. Nekhendzi, Yu. A.; Ionkina, E. M. (Leningrad Polytechnical Inst.). Izv. Vyssh. Ucheb. Zaved., Chern. Met.; No. 3, 148-51(Mar 1970). (In Russian).

Effects of 2 to 12% Nb and 5, 10, and 15% Mo on the microstructure and hardness of hot and cold states of Ni-15% Cr alloys were analyzed. Data obtained show that the hardness of the alloys increased with the increased amounts of Nb or Nb and Mo. With additions of 8% Nb or 5 to 7% Nb and 5 to 15% Mo the Ni-15% Cr alloy exhibited satisfactory heat resistance properties at 740°C during smelting in air. (auth) (IMS)

4783 STUDIES OF PLASTIC DEFORMATION IN THE ZINC–CADMIUM AND COPPER–ALUMINUM ALLOY SYSTEMS. Henry III, Leonard Francis. Charlottesville, Va.; Univ. of Virginia (1969). 362p. University Microfilms Order No. 70-8040.
Thesis.

The results of an investigation of the plastic deformation of single crystals of the zinc–cadmium alloys are presented. Single crystals of the pure materials and their dilute alloys with a standard orientation were subjected to tensile elongation. For small strains, the crystals yield locally through the formation of well defined glide bands. With the development of techniques for producing near optically flat surfaces on these crystals prior to tensile straining and for the post deformation etch pitting of the crystals, it was possible to establish the surface topography and

arrangements of retained dislocations associated with the bands of basal slip. The integrated shear displacement of the individual glide bands was found to account for the total elongation of the crystals. Comparison of the surface topographies of glide bands on the opposite crystal faces showed that the bands often extend completely through the deformed crystals. When crystals of the pure materials were re-strained, further glide occurred within the bands. For crystals of the alloys, etch pitting revealed that the bands were often well-defined and that the dislocations were contained in linear multipoles and regions of glide polygonization. Strong sub-boundaries were found to block the motion of the dislocations during tensile elongation. Analysis of the surface topography of the bands and the stress-strain curves indicated that sufficient energy was available for the high velocity propagation of dislocations in these soft crystals. A model of the deformation is proposed that qualitatively predicts the observed features of the glide bands. Results of an investigation of the temperature dependence of the deformation of Cu–13.2 at. % Al single crystals and the low temperature deformation of Cu-10.5 at. % Al single crystals are presented. Resistance to the motions of dislocations in these crystals varied markedly with temperature. At 4.2°K, discontinuous yielding occurred and depended on the stiffness of the tensile machine. The abrupt elongations took place in a time of several milliseconds and required an average dislocation velocity of about 10^3 cm/sec. From stress relaxation curves, it was found that dislocation velocities of the same magnitude must result in the crystals when they are subjected to tensile deformation at room temperature. The surface topography of the bands of deformation which form in these crystals was studied in detail. The bands of deformation formed at room temperature and 4.2°K were nearly identical and were qualitatively the same as those found in crystals of copper aluminum containing a lesser concentration of aluminum. The individual slip terraces within the bands of deformation were grouped into clusters which were often regularly distributed over the crystal surfaces. For deformation at 4.2°K, the terraces represented a greater shear displacement than for crystals elongated at room temperature. In both cases, the terraces represented slip on a single atomic plane. The occurrence of cross-slip within the bands was investigated and appeared to result from the direct transfer of dislocations from the primary system to the cross-slip system near the surface. The mechanism of deformation of Cu-Al single crystals involves the high velocity propagation of avalanches of dislocations. A model of the mechanism of yielding is discussed which accounts for the formation of bands of deformation through the successive generation of avalanches of edge dislocations at opposite crystal surfaces. (Diss. Abstr. Int., B)

4784 LOW-TEMPERATURE DEFORMATION CHARACTERISTICS OF HIGH-PURITY ZIRCONIUM SINGLE CRYSTALS. Goodrich, David George. Corvallis, Oreg.; Oregon State Univ. (1970). 111p. University Microfilms Order No. 70-14,130.

Thesis.

High purity single crystals of zirconium were produced and mechanically strained in the temperature range from 4.2 to 293°K. The crystals were produced by thermal treatment with a specially constructed electron beam zone refiner which provided the abrupt temperature gradient necessary for crystal growth. Specimens were electrolytically machined to have a reduced center section and chemically polished. Both examination under polarized light and Laue back reflection patterns were necessary to select specimens without alpha variants. Single crystals were tested at liquid helium temperature in cryostat which was constructed for this study. Intermediate test temperatures were obtained with the specimen immersed in the proper refrigerant. The flow stress was determined for strains of 0.02, 0.1, and 0.2%. Strain rate was cycled from 0.002 inches per minute to 0.02 inches per minute to obtain data for calculation of activation volumes. The flow stress versus temperature curve was found to level off at a temperature of approximately 120°K which is 330°K lower than the lowest temperature observed previously for the phenomena. A pronounced peak in the curve of activation volume versus temperature was found at 230°K. Two possible explanations are proposed for the peak in activation volume. Inverse strain rate sensitivity was observed in three specimens two of which were tested at room temperature and one in liquid nitrogen. No evidence of basal slip or twinning was found at any temperature. A complete description of the design and operation of the zone refiner and cryostat is given in separate appendixes. (Diss. Abstr. Int., B)

Structure and Phase Studies

Refer also to abstracts 4776 and 5181.

4785 (CEA-R-4092) STUDY OF THE α AND ϵ PHASES OF Pu BY USING HIGH-HYDROSTATIC PRESSURES. Cornet, Jean-Andre (Commissariat a l'Energie Atomique, Fontenay-aux-Roses (France). Centre d'Etudes Nuceaires). Nov 1970. 97p. (In French). Dep. NTIS (U. S. Sales Only).

Thesis. Submitted to Univ. of Paris, Orsay, France.

Large grains of Pu in the α phase were prepared by using high hydrostatic pressures. A mechanism is proposed in order to explain the self diffusion properties in the α phase. Under pressure, the phase change method is better than the discontinuous growth method to obtain large grains of the α phase (section $\simeq 9$ mm^2). However, the substructure remains important. The self diffusion coefficients in the ϵ phase increase exponentially with pressure; the activation volume is negative and of the order of 34 percent of the molar volume. This result is not very consistent with a vacancy mechanism, but it can be interpreted with a mechanism of activated interstitials with the same electron configuration as plutonium atoms in the liquid state. (auth) (France)

4786 (COO-1676-13) DISLOCATION-SOLUTE ATOM INTERACTIONS IN ALLOYS. Technical Progress Report. Gibala, R.; Ulitchny, M. G.; Klems, G. J.; Vasudevan, A. K.; Sagues, A. A. (Case-Western Reserve Univ., Cleveland, Ohio). 31 Oct 1970. Contract AT(11-1)-1676. 32p. Dep. NTIS.

The anelastic behavior of Fe–Ni–C and Fe–Cr–Ni–C austenites at 25 to 400°C was investigated by torsional pendulum methods. A bound-pair carbon peak observed in these alloys is interpreted as a stress-induced carbon-vacancy reorientation process. The internal friction of Fe–Ni–C martensites was studied. Results of this study were not clear enough to allow establishment of the role of dislocations in the dissolution of eta-phase carbide precipitates. Work on dislocation-solute atom interactions in bcc metals by measurements of dislocation damping was continued. Research on hardening and softening in bcc refractory metals was mainly directed to Nb. Results show that interstitial hardening is associated with the high strength of bcc metals and is thermally activated. Results of anelasticity experiments are included which are the basis for models of alloy softening. (J.R.D.)

4787 CONSTITUTIONAL INVESTIGATIONS ON THE MISCIBILITY GAP IN IRON–CHROMIUM AND IRON–CHROMIUM–VANADIUM SYSTEMS. Mima, Genjiro; Yamaguchi, Masaharu (Osaka Univ.). Trans. Jap. Inst. Metals; 11: 239-44(Jul 1970).

The effect of vanadium additions on the miscibility gap in the iron–chromium binary system was investigated by means of differential thermal analysis and Moessbauer effect measurements. The miscibility gap obtained experimentally in the iron–chromium–vanadium ternary system was qualitatively in agreement with that predicted from thermodynamical data on three binary systems of iron–chromium, iron–vanadium and chromium–vanadium. The ternary miscibility gap in the iron–chromium–vanadium system is considered to take the form of a mountain with the peak. The ternary tie-lines were determined by means of the Moessbauer measurements of the binary and ternary alloys aged at 480°C. In the aged ternary alloys the greater part of the vanadium content was dissolved in the iron-rich matrix. (auth)

4788 PHASE EQUILIBRIUMS IN Ni–Nb–W AND Ni–W SYSTEMS. Allibert, Colette; Wicker, Alain; Driole, Jean; Bonnier, Etienne (Ecole Nationale Superieure d'Electrochimie et d'Electrometallurgie, Grenoble, France). Compt. Rend., Ser. C; 271: 716-19(28 Sep 1970). (In French).

The study of two isothermal sections of the ternary system Ni–Nb–W at temperatures of 1,800 and 1,900°C led to a new phase diagram for the binary system Ni–W between 1,400 and 2,100°C. (auth) (France)

4789 METASTABLE PHASE OF THE TYPE Ni_3Mo IN NICKEL–25 AT. PERCENT TUNGSTEN ALLOY. Umanskii, Ya. S.; Dubrovina, A. N.; Arapova, L. P. Izv. Vyssh. Ucheb. Zaved., Chern. Met.; No. 9, 118-21(1969). (In Russian).

An investigation of the metastable phase Ni_3W in Ni–25% W alloy is described. During an isothermal anneal of Ni–25% W alloy at 1150°C, the new phase Ni_3W was precipitated in addition to existing α- and γ-phases. The amount of Ni_3W phase first increased with the isothermal annealing time, reached a max, and finally decreased. The metastable phase Ni_3W, isomorphous with the Ni_3Mo phase in the Ni–Mo system, was rhombic with the lattice parameters: a = 4.948 ± 0.001, b = 4.203 ± 0.001, and c = 4.621 ± 0.001 Å. (Metals Abstr.)

4790 INFLUENCE OF THE ALLOTROPIC TRANSFORMATION $\beta \rightleftharpoons \alpha$ AND OF OXYGEN ON THE DISTRIBUTION OF PLUTONIUM IN DILUTE ZrPu AND TiPu ALLOYS. Languille, A.; Remy, C.; Calais, D. (Centre d'Etudes Nucleaires, Fontenay-aux-Roses, France). J. Nucl. Mater.; 37: 139-52(Nov 1970). (In French).

In titanium and zirconium the allotropic α (hep) $\rightarrow \beta$ (bcc) transformations were of martensitic type. Nevertheless solute segrega-

tions appeared in the dilute Pu–Zr and Pu–Ti alloys after prolonged anneal above the transformation temperature of the pure metal. Anisotropic displacement of solute atoms cannot be explained in terms purely of thermal diffusion during transformation, when one takes into account the value of the diffusion coefficients and the rates of cooling. Two hypotheses are advanced to explain this phenomenon: an acceleration of diffusion during phase transformation and a contamination by oxygen, an element very favorable to the formation of α phase. Experiments on Ti–2.5 wt % Pu alloys showed that the magnitude of the segregations was a function of the temperature of anneal and of the rate of cooling. Oxygen contamination substantially increased the temperature interval of the two-phase $\alpha + \beta$ region which favored formation of segregations. The magnitude of these depended on the speed with which the two-phase domain was traversed. The anomalies observed in chemical diffusion in the Pu–Zr system can also be explained by the presence of oxygen. (auth)

4791 PREPARATION OF Th–Pa ALLOYS AND DETERMINATION OF THE SOLUBILITY OF Pa IN Th. Lorenz, R. (Technische Univ. Brunswick, Ger.); Scherff, H. L.; Toussaint, N.; Voss, G. J. Nucl. Mater.; 37: 203-8(Nov 1970).

Thorium-protactinium alloys were prepared in small quantities by the Van Arkel process, starting from mixed thorium-protactinium carbides. The wire specimens thus obtained were used directly for structure determination by the Debye–Scherrer method. The lattice parameter of the alpha-phase of thorium diminished according to a linear function with increasing protactinium content, according to Vegard's law. The solubility of protactinium in alpha thorium was 6.7 ± 0.3% at 1300 ± 30°C, and 4.5 ± 0.5% at room temperature. At higher protactinium concentrations a second phase precipitated; this was identified as having an analogous structure to body-centered tetragonal protactinium with slightly increased lattice parameters: $a_0 = 3.938 \pm 0.002$ and $c_0 = 3.245 \pm 0.002$ Å. The parameter increase is attributed to its saturation with thorium. (auth)

4792 USE OF THE POTENTIOSTAT IN THE MICROSTRUCTURAL EXAMINATION OF URANIUM. Kocik, J.; Mance, A.; Mihajlovic, A. (Boris Kidric Inst. of Nuclear Sciences, Vinca, Yugoslavia). J. Nucl. Mater.; 37: 243-7 (Nov 1970).

The electrochemical behavior of unalloyed uranium was studied in the electrolytes which were used for metallographic examination of α uranium. The polarization curves and the microstructures for optimal electrolytic etching condition are given. The most favorable potential interval for α-grain morphology is between +250 and +350 mV, i.e. the interval where an intensive anodic dissolution begins. (auth)

4793 URANIUM–OXYGEN SYSTEM AT HIGH PRESSURE. Hoekstra, Henry R.; Siegel, Stanley; Gallagher, Francis X. (Argonne National Lab., Ill.). J. Inorg. Nucl. Chem.; 32: 3237-48 (Oct 1970).

Phase relationships existing in the uranium–oxygen system at temperatures to 1600°C and pressures to 60 kb are reported. The compounds identified in the system include UO_2, U_4O_9, $U_{16}O_{37}$, U_8O_{19}, U_2O_5 and UO_3. Properties of new phases were studied by x-ray diffraction, thermal and i.r. analysis. Temperature and pressure stability ranges for three crystal forms of U_2O_5 are outlined. The crystal symmetry of α-U_2O_5 is unknown, β-U_2O_5 is hexagonal and γ-U_2O_5 is monoclinic. Marked changes in the relative stability of uranium oxides are shown to occur at high pressure, and are correlated with the respective oxide structure types. (auth) (UK)

4794 INVESTIGATION OF THE ALLOY NICKEL–25 AT. PERCENT TUNGSTEN AFTER ISOTHERMAL [HIGH-TEMPERATURE] ANNEALING. Umanskii, Ya. S.; Dubrovina, A. N.; Arapova, L. P. Izv. Vyssh. Ucheb. Zaved., Chern. Met.; No. 11, 129-31(1969). (In Russian).

The appearance of the intermediate metastable phase Ni_3W in Ni–25 at. % W during isothermal holding at 1150°C, observed in previous work, was studied by x-ray structural analysis of specimens heat-treated by three different schedules. After holding the alloy at 800°C a new metastable phase of the type Ni_3W is obtained. This phase is absent when alloy powders are furnace-cooled from 1550°C, when only lines of Ni_4W and γ are found. (Metals Abstr.)

4795 CRYSTAL STRUCTURE OF BERYLLIUM AT 77 TO 300° K. Finkel, V. A.; Papirov, I. I. (Physical-Technical Inst., Kharkov). Phys. Metals Metallogr. (USSR) (Engl. Transl.); 26: No. 6, 150-2(1968).

Translated from Fiz. Metal. Metalloved.; 26: No. 6, 1108-10 (1968).

An x-ray diffraction analysis was carried out on single crystals of 99.0 and 99.9% pure Be at low temperatures. The a and c parameters increase with impurities, which have an abnormal effect on the thermal expansion coefficients, increasing $\alpha_\perp$ and reducing $\alpha\|$. The axial ratio c/a decreases with temperature. (D.L.C.)

4796 VISUALIZING THE DISLOCATION STRUCTURE OF MOLYBDENUM BY ETCHING IN A HIGH-TEMPERATURE ARGON FLOW. Emel'yanova, L. I.; Mikhailov, S. K. Phys. Metals Metallogr. (USSR) (Engl. Transl.); 26: No. 6, 158(1968).

Translated from Fiz. Metal. Metalloved.; 26: No. 6, 1114 (1968).

The dislocation structure of Mo can be visualized by etching for 5 to 10 min in an Ar flow (4 to 6 g/sec) heated to 1800 to 2000°C. The specimen is heated to 1000 to 1500°C during the etch, and the etching is accomplished by the oxygen impurity in the Ar gas. (D.L.C.)

4797 CRYSTALLOSTRUCTURAL CHANGES IN THE WORK-HARDENED SURFACE LAYERS OF TUNGSTEN, NIOBIUM, AND MOLYBDENUM AS A RESULT OF ANNEALING IN A STEADY VACUUM. Kozyrskii, O. I.; Tikhonov, L. V. (Inst. of Metal Physics, Kiev). Phys. Metals Metallogr. (USSR) (Engl. Transl.); 26: No. 6, 126-31(1968).

Translated from Fiz. Metal. Metalloved.; 26: No. 6, 1084-90 (1968).

X-ray diffraction analysis was used to study the changes taking place during annealing, in a steady vacuum (2 to 4×10^{-4} mm Hg), in the thin surface layers (~5 μ) of tungsten, niobium, and molybdenum work-hardened as a result of grinding. The mechanism of elastic distortion relief on annealing and the behavior of the solute gases at different annealing temperatures are discussed. (auth)

4798 AUGER ELECTRON SPECTROSCOPY: METALLURGICAL APPLICATIONS. Dooley III, George J.; Haas, T. W. (Aerospace Research Labs., Wright-Patterson AFB, Ohio). J. Metals; 22: No. 11, 17-24(Nov 1970).

A relatively new tool in the field of metallurgy, namely Auger electron spectroscopy, has several potentially valuable uses for metallurgists. Areas of interest in which Auger electron spectroscopy studies are useful are corrosion, alloy formation, nucleation, diffusion, catalysis, epitaxy, thin film growth, and fractography. The actual experimental methods associated with the use of this technique are discussed in some detail, and where they are available, specific examples are given to illustrate usages in the above areas. One of the present major uses of Auger spectroscopy is the detection and identification of impurities segregating on the surfaces and at grain boundaries of both polycrystalline and single crystal metals. Several refractory metals were studied, and the surface impurites present on many of them were reported. Specific examples are given for two metals, namely zirconium and hafnium, with special emphasis upon surface cleaning and bulk purification. A new technique for the production of high purity zirconium and hafnium in small quantities is suggested as a result of an Auger electron spectroscopy study of these two metals. It is shown that zirconium atoms normally present to some extent even in high purity hafnium will segregate on the surface of hafnium which has been heated in ultra high vacuum. These zirconium atoms can then be removed from the hafnium surface by means of argon ion bombardment. (auth)

4799 POROSITY AND ANOMALOUS RECRYSTALLIZATION BEHAVIOR IN DOPED TUNGSTEN WIRE. Friedman, S.; Brett, J. (General Telephone and Electronics Labs., Bayside, N. Y.). Met. Trans.; 1: 3225-31(Nov 1970).

An anomalous recrystallization behavior was observed in 0.010 in. dia K-Si-Al doped tungsten wire. Recrystallization to relatively equiaxed grains occurred only in the core at temperatures of 1400 to 1600°C, but not at lower temperatures or higher temperatures up to 1900°C. The anomalous recrystallization reaction was suppressed when the wire was preannealed at 1700 to 1900°C, but not by preanneals at temperatures between 500 and 1100°C. Critically shadowed electron fractographs indicated that linear arrays of microporosity (~100 Å dia) were responsible for the stabilization of the fibrous structures. Recrystallization occurred when these strings of pores were absent. (auth)

4800 SLIP IN SINGLE CRYSTALS OF NIOBIUM–MOLYBDENUM ALLOYS DEFORMED IN COMPRESSION. Statham, C. D.; Vesely, D.; Christian, J. W. (Oxford Univ.). Acta Met.; 18: 1243-52(Dec 1970).

The slip geometry and morphology, and the hardening behavior in compression of single crystals of Nb–Mo alloys with up to 50 at. % Mo were investigated in the range 77 to 475°K; a few tensile experiments are also reported. Detailed results were obtained for Nb–5 at. % Mo and Nb–16 at. % Mo. The orientation dependence of the operative slip plane [the $\psi(\chi)$ curve] was changed by temperature or alloying mainly for orientations in the left half of the sterographic triangle, i.e., near [001], and this behavior cannot be fully explained by current

theories. The change in the morphology of the slip bands with temperature and molybdenum content appears to depend largely on the stress level, and is interpreted in terms of the ability of serew dislocations to cross-slip. Some results indicate that the yield point drop is connected with the beginning of cross-slip. From measurements of work hardening rates, it is concluded that the effect of adding solute atoms is to increase the yield stress, increase θ_I and decrease θ_{II}. The increase in θ_I is discussed in terms of present knowledge of dislocation structure in deformed crystals. (auth)

4801 CRYSTALLINE PARAMETER OF DELTA-PHASE Pu-Ga ALLOYS. Daumas, M. T. (CEA-DAM-Centre, Bruyeres-le-Chatel, France). J. Nucl. Mater.; 36: 108-9(Jul 1970). (In French).

The fcc delta phase of pure plutonium is stable in the temperature range from 310 to 450°C. This phase is stabilized at room temperature by the addition of 2 to 11 at. % gallium. An equation is given relating the parameter a, determined by the diffraction method using the Bragg angle, to the concentration of gallium in the alloy. (R.C.K.)

4802 COMPARISON OF THE SUBSTRUCTURES AND PROPERTIES OF NICKEL, TD-Ni, CHROMEL-A, INCONEL 600, AND TD-NiCr FOLLOWING EXPLOSIVE-SHOCK DEFORMATION. Murr, L. E.; Vydyanath, H. R.; Foltz, J. V. (Univ. of Southern California, Los Angeles). Met. Trans.; 1: 3215-23 (Nov 1970).

The substructures of Ni, TD-Ni, Chromel-A (80/20 NiCr), Inconel 600, and TD-NiCr following simultaneous explosive shock loading at pressures of 80, 180, 240, and 460 kbars were observed by transmission electron microscopy. Well defined dislocation cells having average diameters of 0.8, 0.3, 0.2, and 0.1 μ for the respective pressure level were observed in pure nickel, but were not developed to the same extent in annealed TD-Ni due to the presence of the ThO_2 particles having a mean particle diameter of 340 Å. Deformation microtwins having an average width of 175 Å occupied approximately 1 vol % of the nickel substructure at 460 kbars, while twinning was inhibited by the ThO_2 particle distribution in the TD-Ni. Planar dislocation arrays observed in the Chromel-A and Inconel 600 were generally not observed to form in TD-NiCr following shock loading at 80 and 180 kbars. In addition, deformation microtwins having an average width of 150 Å occupied 5% of the Chromel-A microstructure at the same pressure. At 460 kbars, twins occupied 18% of the Chromel-A and 24% of the Inconel 600 microstructure. No evidence of deformation twinning was observed in the TD-NiCr microstructure because of the inhibition afforded by the ThO_2 particle distribution having a mean particle diameter of 145 Å in the annealed material. A relationship was observed for the residual hardness and dislocation density; and stacking-fault energy and the character of the microstructures. (auth)

4803 TETRAGONAL AND TRIGONAL DISTORTIONS OF THE LATTICE OF SOME TRIVALENT COMPOUNDS OF RARE EARTHS. Busch, G.; Levy, F. (Swiss Federal Inst. of Tech., Zurich). pp 363-73 of Les Elements des Terres Rares. Tome II. Paris; Centre National de la Recherche Scientifique (1970). (In French).

From International Symposium on Rare Earths, Paris, Grenoble, France. See CONF-690517.

Results of measurements of the rhombohedral and the tetragonal distortions of the crystalline lattices of antiferromagnetic compounds of trivalent rare earths are given. These distortions give rise to an additional term of axial symmetry in the crystal field potential. The Stark splitting of the ground-state multiplet is given as a function of the distortion. The lowering of the ground-state level determines the axis of contraction of the crystal lattice, which is perpendicular to the directions of easy magnetization of the magnetic sublattices. (tr-auth) (France)

4804 MOLYBDENUM DISTRIBUTION IN IRRADIATED OXIDE FUELS. Lawrence, L. A.; Christensen, J. A. (Battelle-Northwest, Richland, Wash.). Trans. Amer. Nucl. Soc.; 13: 605-6(Nov 1970).

From Meeting of the American Nuclear Society, Washington, D. C. See CONF-701102.

4805 COMMENTS ON PHASE TRANSFORMATIONS IN BETA ISOMORPHOUS TITANIUM ALLOYS. Narayanan, G. Hari; Archbold, T. F. (Univ. of Washington, Seattle). Scr. Met.; 4: 873-6(Nov 1970).

Comments are given on a paper published previously concerning phase transformations in beta isomorphous titanium alloys. The paper was abstracted in NSA as 24: 32444. (G.M.C.)

4806 REPLY TO COMMENTS ON PHASE TRANSFORMATIONS IN BETA ISOMORPHOUS TITANIUM ALLOYS. Koul, M. K.; Breedis, J. F. (Massachusetts Inst. of Tech., Cambridge). Scr. Met.; 4: 877-80(Nov 1970).

A rebuttal is given to Narayanan and Archbold [Scr. Met., 4: 873-6 (1970)] concerning their comments on a paper dealing with phase transformations in beta isomorphous titanium alloys (previously published and abstracted in NSA as 24: 32444). (G.M.C.)

4807 MARTENSITE CRYSTALLOGRAPHY OF THE CUBIC TO ORTHORHOMBIC TRANSFORMATION IN Au-47.5 Cd. Ledbetter, H. M. (National Bureau of Standards, Boulder, Colo.). Scr. Met.; 4: 931-8(Nov 1970).

A complete set of crystallographic calculations was carried out for the β (cubic) $\rightarrow \beta'$ (orthorhombic) martensitic transformation in the Au-47.5 at. % Cd system. None of the usual parameters such as the habit plane provide a sufficiently sensitive index for distinguishing between Type I and Type II transformation twinning. New alternatives are proposed for effecting experimentally this distinction. (auth)

4808 STUDIES OF RECRYSTALLIZATION IN DILUTE ALLOYS OF MAGNESIUM. Hong, William Jong-jau. Salt Lake City; Univ. of Utah (1970). 95p. University Microfilms Order No. 70-14,447.

Thesis.

Experimental work was carried out to determine the recrystallization kinetics of magnesium-cadmium and magnesium-zirconium dilute alloys using an x-ray diffraction technique. A theory was developed to explain the linear variation of per cent recrystallization with log time as observed in these alloys. Free energies of activation for recrystallization in Mg-Cd and Mg-Zr were found to be 42 and 30 kilocalories per mole respectively. Pole figures were determined for Mg, Mg-Cd, and Mg-Zr alloys in the cold worked and annealed conditions. Inverse pole figures were determined for pure Mg in the cold worked and annealed state. Variations were measured in the a and c lattice parameters of Mg as a function of the amount of Zn, Cd, Zr, and Ni added. Possible causes for the observed effects of impurity additions were discussed. Those elements which have a limited solubility in Mg and a distribution coefficient less than one such as Zn, Cd, Ni had the greatest effect in increasing the recrystallization temperature. (Diss. Abstr. Int., B)

Radiation Effects

Refer also to abstracts 4051, 4250, 4775, 5948–5950, 5990, 6145, 6146, and 6191.

4809 (AD-710358) DISLOCATION CHANNELING IN IRRADIATED METALS. Smidt, Fred A. Jr. (Naval Research Lab., Washington, D. C.). 3 Jun 1970. 17p. (NRL-7078). NTIS.

The present understanding of the phenomenon of dislocation channeling, or the removal of defect aggregates from the slip plane by glide dislocations in irradiated or quenched metals, is reviewed. Channeling is a general feature of any system where penetrable defect aggregates are removed by the glide dislocations. The crystallography of the channels and their correspondence with surface slip traces is shown to be well established. It is shown that several areas of the problem require further research in order to gain an adequate understanding of the phenomenon. In particular the mechanism of initiation of the channels, the dislocation-defect interaction mechanism in which defects are annihilated or assimilated, and the mechanism of work hardening, which stops further deformation in a channel, require further study. In addition, a quantitative correlation between the microscopic parameters of channeling and the macroscopic properties of the work hardening coefficient and ductility is needed. (auth) (USGRDR)

4810 (BNWL-SA-3283) IRRADIATION INDUCED SWELLING AND CREEP IN FAST REACTOR MATERIALS. Claudson, T. T. (Battelle-Northwest, Richland, Wash. Pacific Northwest Lab.). 21 May 1970. 4p. (CONF-700920-2). Dep. NTIS.

From International Meeting on Fast Reactor Fuel and Fuel Elements, Karlsruhe, Germany.

The effects of fluence and temperature on metal swelling in fast neutron irradiation are examined as they affect the components of FFTF. Results of analyses on irradiated specimens of Types 304 and 316 stainless steels are included. (J.R.D.)

4811 (BNWL-SA-3300) OBSERVATIONS ON THE NUCLEATION AND GROWTH OF VOIDS IN NICKEL. Brimhall, J. L.; Kissinger, H. E.; Mastel, B. (Battelle-Northwest, Richland, Wash. Pacific Northwest Lab.). 18 May 1970. 2p. (CONF-701003-6). Dep. NTIS.

From 28th Meeting on Electron Microscopy Society of America, Houston, Tex.

Radiation effects on the microstructure of high purity Ni are described. Foils of Ni were exposed to fast neutrons at 300, 400, and 450°C. An explanation of void nucleation is included along with micrographs and data on density and size of voids. (J.R.D.)

4812 (BNWL-SA-3495) FUNDAMENTAL MATERIALS PROBLEMS IN NUCLEAR REACTORS. Bement, A. L. (Battelle-Northwest, Richland, Wash. Pacific Northwest Lab.). 27 Aug 1970. 29p. (CONF-700819-5). Dep. NTIS.

From 2nd International Conference on the Strength of Metals and Alloys, Pacific Grove, Calif.

Four general categories of materials behavior which are considered critical to reactor design and performance are discussed. The effects of radiation on hardening, fracture, swelling, and creep are examined. Fundamental investigations of these phenomena in metals are of relatively recent origin: strength and fracture behavior beginning about 1950, creep and growth beginning about 1960, and swelling due to voids beginning about 1967. However, work during the past three years, in addition to providing considerable insight into the physical nature of these processes, has created a number of ambiguities and unanswered questions for inquiry, consideration, and solution. A review of recent progress to identify some of the important fundamental problems uncovered is presented. (auth)

4813 (IN-1440) EFFECT OF FAST NEUTRON IRRADIATION ON THE MECHANICAL PROPERTIES OF HAFNIUM. Korth, G. E.; Brinkman, C. R.; Beeston, J. M. (Idaho Nuclear Corp., Idaho Falls). Oct 1970. Contract AT(10-1)-1230. 18p. Dep. NTIS.

Property changes of hafnium specimens irradiated to fast neutron exposures of 0.6 to 1.4×10^{21} n/cm^2 (E > 1 MeV) at 110°C have been measured utilizing tensile tests, immersion density, hardness, fractography, metallography, and transmission electron microscopy. The ultimate and yield strength increased significantly with increased exposure, reduction in area decreased slightly, but the total elongation remained unchanged as compared to unirradiated control specimens. Ultimate failure occurred by shear in all specimens. Comparison between the microstructure of unirradiated and irradiated hafnium in both the deformed and undeformed state is presented. (auth)

4814 (N-70-32313) THERMAL NEUTRON ABSORBER BUILDUP IN IRRADIATED BERYLLIUM. Peters, Lawrence E. Jr. (National Aeronautics and Space Administration, Cleveland, Ohio. Lewis Research Center). Jul 1970. 14p. (NASA-TM-X-2039; E-5473). NTIS.

The differential equations which describe the buildup of thermal neutron absorbers in beryllium have been solved. The solutions were used to calculate the change in the macroscopic absorption cross section of the Plum Brook Reactor as a result of the buildup of these poisons. This calculated value agrees within the experimental error of an actual observed change. The effects of variations in the factors on which the poison is dependent were studied and are presented in the form of graphs. (auth) (STAR)

4815 (RD/B/N-1722) PREDICTING THE HEAVY ELEMENT COMPOSITION OF IRRADIATED REACTOR FUELS. Clarke, R. H. (Central Electricity Generating Board, Berkeley (England). Berkeley Nuclear Labs.). Jun 1970. 22p. Dep. NTIS (U. S. Sales Only).

A method was developed which can be used to study the heavy element content of irradiated reactor fuels which have had any given rating history in the reactor followed by the desired subsequent cooling. The buildup and decay chains of all the probable isotopes from ^{230}Th to ^{250}Cm were considered. This covers the present range of interest and allows for extension to thorium or plutonium loaded fuels. The solution of the equations for the concentrations for all these isotopes were programmed into the code HYLAS which performs multi-energy group burnups providing number densities, activities and spontaneous fission rates as a function of time within the fuel. (auth) (UK)

4816 (WHAN-FR-19) UNIAXIAL AND BIAXIAL CREEP-RUPTURE OF TYPE 316 STAINLESS STEEL AFTER FAST REACTOR IRRADIATION. Lovell, A. J.; Barker, R. W. (WADCO Corp., Richland, Wash. Battelle-Northwest, Richland, Wash. Pacific Northwest Lab.). Sep 1970. Contract AT(45-1)-1830. 30p. (CONF-700630-1). Dep. NTIS.

From Symposium on Effects of Radiation on Structural Materials, Niagara Falls, Ontario, Canada.

The degradation in creep-rupture properties of Type 316 stainless steel after fast reactor irradiation was determined for both uniaxial and biaxial loading conditions. Uniaxial specimens (rod-type) and biaxial specimens (tube-type) were irradiated in the 7C4 position of the EBR-II to a total fluence of 1.2×10^{22} n/cm^2 (E > 0.1 MeV) at ~480°C. Postirradiation tests were performed over the temperature range 538 to 760°C. The results from both uniaxial and biaxial tests at 538°C showed significant losses in rupture life relative to unirradiated specimens when compared on the basis of initial true stress. Rupture life was reduced by factors down to 1/20 for uniaxial and by factors down to 1/40 for biaxial tests. The substantial loss in rupture life at 538°C was primarily a result of high creep rates, and the contribution from ductility loss was relatively small. Uniaxial test results at 593°C showed reductions in rupture life of a factor of 1/5 at high stresses and only small reductions at low stresses. The rupture life for both uniaxial and biaxial tests at 649°C showed only a factor of 1/2 decrease after irradiation. The decrease became more substantial again at 760°C with a factor of 1/10 to 1/7 reduction in life. The rupture life reductions at 593, 649, and 760°C were the results of reduced ductility, with no significant contributions from creep rate differences. The underlying cause of the low ductility at these higher temperatures is associated with helium embrittlement and defect structure. (auth)

4817 INFLUENCE OF THE NEUTRON FLUX ON THE PROPERTIES OF DISPERSION-HARDENING STEELS IN CONNECTION WITH PRELIMINARY HEAT TREATMENT. Kondrat'ev, Yu. A.; Nikolaev, V. A.; Patrikeev, Yu. I. Fiz. Khim. Obrab. Mater.; No. 5, 142-6(Sep-Oct 1970). (In Russian).

The changes in the mechanical properties and electric resistivity of the dispersion-hardening Kh18N22V2T2-type steel, caused by exposure to a neutron flux of 6.2×10^{18}, 7.8×10^{19} and 5.4×10^{20} n/cm^2 (E 1 MeV) were investigated. The specimens were subjected to various heat treatments before the irradiation. A correlation was found between the amount and the directions of the resistivity changes of the irradiated steel and its original state. The changes were lower than in the case of austenitic steels which cannot be easily dispersion-hardened. No dependence of the radiation-induced increase of the yield point and of the electrical resistivity on the previous heat treatment could be established. The data obtained do not agree with the theory of "superaging." There might be a correlation between the anomalous behavior of the steel and the radiation-induced stress release in the junction zone of the crystal lattices of the matrix and the segregations. The specimens were aged for 10 hours at 450 to 850°C after having been austenized at 1080°C. The results do not necessarily contradict the possible acceleration of the phase transformation as a result of the irradiation, although it is expected that the temperature must be quite high to achieve this in austenitic, dispersion-hardening steels. (TTT)

4818 VOIDS IN RE-IRRADIATED ALUMINUM. Packan, N. H. (Oak Ridge National Lab., Tenn.). J. Nucl. Mater.; 37: 251-4(Nov 1970).

Gases are produced as transmutation products during neutron irradiation, and this suggested an experiment to explore the effect of implanted gases on subsequent void formation. A piece of high-purity aluminum was irradiated with neutrons to create voids, dislocation loops, and transmutation impurities (helium, hydrogen, and silicon). It was then annealed to remove visible structural damage, and was re-irradiated to produce further voids, loops, and impurities. A distinct effect of the preirradiation was noted. (auth)

4819 VOID FORMATION IN NICKEL DURING IRRADIATION WITH 8-MeV SELENIUM IONS. Kulcinski, G. L.; Brimhall, J. L.; Kissinger, H. E. (Battelle-Northwest, Richland, Wash.). Trans. Amer. Nucl. Soc.; 13: 555(Nov 1970).

From Meeting of the American Nuclear Society, Washington, D. C. See CONF-701102.

4820 YIELD STRENGTH AND CREEP STRAIN ESTIMATES FOR IRRADIATED STAINLESS STEEL IN THERMAL AND FAST REACTORS. McElroy, W. N.; Simons, R. L.; Blackburn, L. D. (Hanford Engineering Development Lab., Richland, Wash.). Trans. Amer. Nucl. Soc.; 13: 555-7(Nov 1970).

From Meeting of the American Nuclear Society, Washington, D. C. See CONF-701102.

4821 ANOMALOUS HELIUM PRODUCTION IN NICKEL. Weitman, J.; Daverhoeg, N.; Farvolden, S. (Aktiebolaget Atomenergi, Studsvik, Sweden). Trans. Amer. Nucl. Soc.; 13: 557-8 (Nov 1970).

From Meeting of the American Nuclear Society, Washington, D. C. See CONF-701102.

4822 HELIUM PRODUCTION IN Fe, Cr, Ni, Ti, AND Cu DUE TO THE FISSION NEUTRON PART OF REACTOR SPECTRA. Weitman, J.; Daverhoeg, N.; Farvolden, S. (Aktiebolaget Atom-

energi, Studsvik, Sweden). Trans. Amer. Nucl. Soc.; 13: 558-9 (Nov 1970).
From Meeting of the American Nuclear Society, Washington, D. C. See CONF-701102.

4823 PERIODIC IN SITU ANNEALING TO REDUCE STAINLESS-STEEL SWELLING IN THE LMFBR. Fulford, P. J.; Huebotter, P. R. (Argonne National Lab., Ill.). Trans. Amer. Nucl. Soc.; 13: 559(Nov 1970).
From Meeting of the American Nuclear Society, Washington, D. C. See CONF-701102.

4824 EFFECT OF COLD WORK ON IRRADIATION-INDUCED SWELLING. Holmes, J. J.; Straalsund, J. L. (Hanford Engineering Development Lab., Richalnd, Wash.). Trans. Amer. Nucl. Soc.; 13: 559-60(Nov 1970).
From Meeting of the American Nuclear Society, Washington, D. C. See CONF-701102.

4825 METALLURGICAL PROPERTIES OF IRRADIATED COLD-WORKED Zr–2.5 WT. PERCENT Nb PRESSURE TUBES. Langford, W. J.; Mooder, L. E. J. (Atomic Energy of Canada Ltd., Chalk River, Ont.). Trans. Amer. Nucl. Soc.; 13: 563 (Nov 1970).
From Meeting of the American Nuclear Society, Washington, D. C. See CONF-701102.

4826 ROLE OF GRAIN BOUNDARIES IN THE SWELLING OF UN AT 1600 TO 1700°C. Hilbert, R. F.; Storhok, V. W.; Chubb, W. (Battelle Memorial Inst., Columbus, Ohio). Trans. Amer. Nucl. Soc.; 13: 564(Nov 1970).
From Meeting of the American Nuclear Society, Washington, D. C. See CONF-701102.

4827 SPUTTERING OF URANIUM BY FISSION. Laskiewicz, R. A.; Verghese, K. (North Carolina State Univ., Raleigh). Trans. Amer. Nucl. Soc.; 13: 565-6(Nov 1970).
From Meeting of the American Nuclear Society, Washington, D. C. See CONF-701102.

4828 UNUSUAL INTERSTITIAL AGGREGATES IN VANADIUM IRRADIATED AT 0.15 T_m. Smidt, F. A. Jr. (Naval Research Lab., Washington, D. C.). Trans. Amer. Nucl. Soc.; 13: 594-7(Nov 1970).
From Meeting of the American Nuclear Society, Washington, D. C. See CONF-701102.

4829 HEAVY-ION-BOMBARDED 20 PERCENT COLD-WORKED TYPE 316 STAINLESS STEEL. Brager, H. R. (Hanford Engineering Development Lab., Richland, Wash.). Trans. Amer. Nucl. Soc.; 13: 597-8(Nov 1970).
From Meeting of the American Nuclear Society, Washington, D. C. See CONF-701102.

4830 IRRADIATION CREEP BY LOOP UNFAULTING. Gilbert, E. R.; Holmes, J. J. (Hanford Engineering Development Lab., Richland, Wash.). Trans. Amer. Nucl. Soc.; 13: 609(Nov 1970).
From Meeting of the American Nuclear Society, Washington, D. C. See CONF-701102.

4831 SYSTEM FOR PREDICTING POSTIRRADIATION TENSILE PROPERTIES. Holmes, J. J.; Ward, A. L. (Hanford Engineering Development Lab., Richland, Wash.). Trans. Amer. Nucl. Soc.; 13: 609-10(Nov 1970).
From Meeting of the American Nuclear Society, Washington, D. C. See CONF-701102.

4832 DAMAGE THRESHOLD FOR PRESSURE VESSEL STEEL EMBRITTLEMENT LOWER THAN 1 MeV. Serpan, Charles Z. Jr. (Naval Research Lab., Washington, D. C.). Trans. Amer. Nucl. Soc.; 13: 610-11(Nov 1970).
From Meeting of the American Nuclear Society, Washington, D. C. See CONF-701102.

4833 NEUTRON IRRADIATION EMBRITTLEMENT CHARACTERISTICS OF A533-B ELECTROSLAG WELDMENTS. Hawthorne, J. Russell (Naval Research Lab., Washington, D. C.). Trans. Amer. Nucl. Soc.; 13: 613-14(Nov 1970).
From Meeting of the American Nuclear Society, Washington, D. C. See CONF-701102.

4834 DEPENDENCE OF NEUTRON RADIATION DAMAGE IN METALS ON CRYSTAL LATTICE GEOMETRY. Garner, Francis Albert. Charlottesville, Va.; Univ. of Virginia (1969). 257p. University Microfilms Order No. 70-8091.
Thesis.
Transmission electron microscopy was employed to study the nature and distribution of the damage produced by fast neutrons in nickel and copper. The major effort was directed towards the study of the distribution and density of the resultant dislocation loops in the vicinity of various crystal boundaries, particularly crystal surfaces and coherent twin boundaries. Bulk nickel, electrochemically thinned for observation, was employed in addition to a wide variety of vapor deposited thin films. The thin films were subjected to various deposition conditions and annealing treatments to yield films with a high density of coherent twin boundaries and a low density of strain imperfections. Some films were also produced that had internal surfaces such as voids and web holes. After irradiations varying from 8.6×10^{16} to 1.7×10^{19} nvt (E > 1.0 MeV) in the UVAR reactor, the films were observed in the JEM 6A and Siemens Elmiskop IA electron microscopes at 80 and 100 kV accelerating potentials. The neutron irradiation of thin film at 30 to 37°C appeared to yield essentially the same results as the neutron irradiations of bulk material. In the vicinity of coherent twin boundaries, there was a visible enhancement of damage which appeared to be 50 to 100% greater than that in the unfaulted bulk material. There did not appear to be any distribution of enhancement across the boundary; all enhanced spots appeared to be anchored to the boundaries. In copper the enhancement appeared to be solely of the larger variety of loops, which are currently believed to be interstitial loops. No statements can be made about the nature of the enhancement observed in nickel; the differences in the size of the loops do not appear to be as well defined as they are in copper. The phenomenon of enhancement at coherent twin boundaries was explained in terms of the interruption at crystal boundaries of the energy dissipation mechanisms required by the crystals' lattice structure. Normally, the crystal lattice partitions the incident energy into defect producing modes and non-defect producing modes. The presence of the boundary shifts the partition towards the defect producing modes, leading to enhancement. A model was proposed which includes the contributions to enhancement from channeling events and correlated collision sequences. The channeling contribution was found to be too small to be observed above background fluctuations in the damage density. Correlated collision sequences, however, were found to account for the observed enhancement, yielding up to a 40% increase in the probability of forming a Fenkel pair from the boundary atoms. (Diss. Abstr. Int., B)

Ceramics and Cermets

Corrosion and Erosion

Refer also to abstract 5985.

4835 (DP-Report-448) RECENT RESULTS FROM THE IN-PILE CARBON TRANSPORT LOOP. Project DRAGON. Van Massenhove, G. (Atomic Energy Establishment, Winfrith (England)). Jul 1966. 16p. Dep. NTIS.
Three experiments were performed in the loop in the BR2 Reactor in 1965: two tests in which corrosion was measured from weight losses of the graphite samples, and one test using ^{14}C tracer. Results of the tests are presented. (D.L.C.)

Preparation and Fabrication

Refer also to abstracts 5942 and 6007.

4836 SINTERING OF THORIA POWDERS. V. INFLUENCE OF TEMPERATURE, PRESSURE, AND NATURE OF POWDER DURING HOT PRESSING OF THORIA POWDERS. Moorthy, V. K.; Bahl, J. K. (Bhabha Atomic Research Centre, Trombay, India). Trans. Indian Ceram. Soc.; 26: No. 5, 111-15(1967).
The influence of temperature and pressure on the density attained by hot pressing of two types of thoria powders, one derived from oxalate and another from tannate, was studied. It was found that a rise either in temperature or pressure improved the densification in both types of powders, but much more so in the poorly crystalline powder derived from the tannate. Thoria powders derived from tannate could be hot pressed to a density of over 95% theoretical at 1200°C at 1.5 tsi. (Indian Sci. Abstr.)

4837 SINTERING OF BERYLLIA. III. STUDIES ON HOT PRESSING OF BERYLLIUM OXIDE DERIVED FROM HYDROXIDE. Moorthy, V. K.; Bhat, R. (Bhabha Atomic Research Centre, Bombay). Trans. Indian Ceram. Soc.; 26: No. 4, 75-81(1967).
The influence of experimental conditions on the hot pressing behavior of BeO powders derived from hydroxide was studied with a view to develop high density pellets with min grain growth. In the temperature range of 1000 to 1500°C and with applied pressure of 1 to 3 tsi both the temperature and pressure promoted densification. Grain growth and crystallinity development in the hot pressed pellets were more directly related to sintering temperature and not to the density attained. In this study BeO samples of density of

XUM

2.98 gm/cc (theoretical 3.01 gm/cc) and grain size of about 1 micron were prepared by hot pressing beryllium hydroxide powder at 1250°C and 3 tsi. (Indian Sci. Abstr.)

4838 DEVELOPMENT OF CONCRETE-POLYMER MATERIALS AND COMPOSITES. Steinberg, M.; Kukacka, L. E.; Colombo, P.; Manowitz, B. (Brookhaven National Lab., Upton, N. Y.). Trans. Amer. Nucl. Soc.; 13: 512-13(Nov 1970).

From Meeting of the American Nuclear Society, Washington, D. C. See CONF-701102.

Properties Evaluation

Refer also to abstracts 4764, 4780, 4838, 5176, 5179, 5942, and 6008.

4839 (KFK-1245) CHANGE IN THERMAL CONDUCTIVITY OF AN OXIDE FUEL ELEMENT DURING BURN UP. Kleykamp, H. (Kernforschungszentrum, Karlsruhe (West Germany). Institut fuer Material und Festkoerperforschung). Jul 1970. 15p. (In German). Dep. NTIS (U. S. Sales Only).

The change in thermal conductivity of mixed-oxide during burnup is discussed. The influence of the porosity and change in stoichiometry as well as the heat-transfer coefficient was estimated. The formation of the fission products during burnup led to a decrease in thermal conductivity. The latter fell by 25% after a burnup of 10% due to the solid solution formation (U,Pu)-oxide-rare earth oxides-zirconia. An increase of about 8% compared with the pure matrix is to be expected in the case of metallic and oxide inclusions in dispersion form. (auth)

4840 (LA-4526) CMF-13 RESEARCH ON CARBON AND GRAPHITE. Report No. 14. Summary of Progress from May 1-July 31, 1970. Smith, Morton C. (Los Alamos Scientific Lab., N. Mex.). Oct 1970. Contract W-7405-eng-36. 26p. Dep. NTIS.

Research and development on carbon and graphite were undertaken primarily to increase understanding of their properties and behavior as engineering materials, to improve the raw materials and processes used in their manufacture, and to learn how to produce them with consistent, predictable, useful combinations of properties. The approach taken is microstructural, based on study and characterization of natural, commercial, and experimental carbons and graphites by such techniques as x-ray diffraction, electron and optical microscopy, and porosimetry. Physical and mechanical properties are measured as functions of formulation, treatment, and environmental variables, and correlations are sought among properties and structures. Raw materials and manufacturing techniques are investigated, improved, and varied systematically in an effort to create specific internal structures believed to be responsible for desirable combinations of properties. Prompt feedback of information among these activities then makes possible progress in all of them toward their common goal of understanding and improving manufactured carbons and graphites. Results of research are included on Santa Maria coke, particle packing, binder chemistry, extruded graphite, graphite-carbide composites, effects of porosity on graphite properties, skin effects in graphite, and graphitization processes. (J.R.D.)

4841 (SRO-552-5) QUANTITATIVE DETERMINATION OF THE STRUCTURE-PROPERTY RELATIONSHIPS IN NUCLEAR FUEL ELEMENT MATERIALS. Quarterly Progress Report, June 15-September 15, 1970. Rhines, F. N.; DeHoff, R. T.; Whitney, E. D. (Florida Univ., Gainesville. Engineering and Industrial Experiment Station). Oct 1970. Contract AT(38-1)-552. 37p. Dep. NTIS.

An image analyzing computer was acquired, which permits the automatic measurement of the metric properties, volume, surface area, and total curvatures of porous structures. Metallographic technique suitable for preparing samples for this instrument has been devised and put into operation for nickel sinterings. Topological properties of loose stacks of powder have been made more accessible through the development of a procedure for estimating genus from observations made on fracture surfaces in scanning electron microscopy, and through the use of the Coulter Counter to determine the number of particles per gram of powder. Expansion of experimental results in all areas, including quantitative microstructural analysis, gas permeability, short time mechanical properties, creep behavior, and thermal conductivity, continues for both nickel and uranium dioxide sinterings. A significant advance in sample preparation procedure has begun to provide a steady supply of uranium dioxide samples for analysis. (auth)

4842 MECHANISM OF THE INTERACTION OF V_2O_5 WITH CARBON. II. Elyushin, V. P.; Pavlov, Yu. A.; Polyakov, V. P.; Sheboldaev, S. B. Izv. Vyssh. Ucheb. Zaved., Chern. Met.; No. 7, 5-7(1969). (In Russian).

Data obtained chromatographically on the influence of the flow of inert gas on the interaction process V_2O_5 with C are presented. The rate of reduction is determined in the initial stages of the process by the removal of the products CO and CO_2, desorbed from the surface of the solid reactants, and in the case of more extensive reduction, by diffusion phenomena in the solid phases. (Metal Abstr.)

4843 ENTHALPY-OF-FORMATION DATA ON COMPOUNDS OF URANIUM WITH GROUPS V A AND VI A ELEMENTS. Baskin, Y.; Smith, S. D. (Argonne National Lab., Ill.). J. Nucl. Mater.; 37: 209-22(Nov 1970).

Enthalpy-of-formation data (ΔH_f^0) were obtained by means of direct-reaction calorimetry on the following compounds: UP, $UP_{1.33}$, UAs, $UAs_{1.33}$, USb, $USb_{1.33}$, USb_2, US, $US_{1.5}$, USe, $USe_{1.33}$, UTe, and $UTe_{1.33}$. A preliminary value also was obtained for $UBi_{1.33}$. Within each group the ΔH_f^0 values showed a systematic decrease with increasing U-X distance and, given equivalent U-X distances, the UX(VI) compounds had higher ΔH_f^0 values than those of the UX(V) compounds. (auth)

4844 EFFECT OF POROSITY ON THE VARIATION OF THERMAL CONDUCTIVITY OF URANIUM DIOXIDE AS A FUNCTION OF TEMPERATURE. APPLICATION TO THE MIXED OXIDE $(UPu)O_{2.00}$ AT 20 PERCENT PuO_2. Van Craeynest, Jean Claude; Stora, Jean Pierre (Centre d'Etudes Nucleaires, Fontenay-aux-Roses, France). J. Nucl. Mater.; 37: 153-8 (Nov 1970). (In French).

With the aim of establishing a relationship for correcting the thermal conductivity for the effects of porosity in nuclear fuel elements, the thermal diffusivity of sintered UO_2 and of mixed UO_2-PuO_2 containing 20% of PuO_2 was measured at a temperature range from 50 to 1000°C, and for porosities ranging from 72.3 to 100% of theoretical density. The following correction law was established: $k_p = k_0[1-(2.58-0.58\times10^{-3}T)p]$. (auth)

4845 STUDY OF DIFFUSION BY TRACKS LEFT BY NUCLEAR REACTION PRODUCTS IN A SOLID DETECTOR. Geguzin, Ya. E.; Kaganovskii, Yu. S.; Solunskii, Yu. S.; Solunskii, V. I. (Kharkov State Univ.). Dokl. Akad. Nauk SSSR; 192: No. 1, 78-81(1970). (In Russian).

The concentration of a diffusing substance as a function of penetration depth can be determined by irradiating sections of a substance such as uranium with neutrons in contact with a material such as mica which will reveal tracks of fission fragments on development with hydrofluoric acid as an etching agent. The penetration of ^{235}U dioxide along defects in KCl was studied by means of this technique by sputtering uranium dioxide on a KCl surface. In investigating the results of a diffusion annealing (T = 600 to 690°C) the cleavage plane of the crystal perpendicular to the plane of sputtering was brought into contact with the mica detector. The combined sample was irradiated with neutrons in the thermal column of a reactor. The tracks in the mica were developed with HF, and the distribution was studied under a microscope. The results show preferential diffusion along dislocations. Experimental results on the diffusion of UO_2 in nickel metal are also presented. (TTT)

4846 STUDIES ON ULTRA-CLEAN CARBON SURFACES. IV. DECOMPOSITION OF CARBON-OXYGEN SURFACE COMPLEXES. Bansal, R. C.; Vastola, F. J.; Walker, P. L. Jr. (Pennsylvania State Univ., University Park). Carbon; 8: 443-8(Oct 1970).

Graphon was first activated by preoxidation to 16.6 wt. % loss at 625°C to introduce a desired amount of active surface area. Varying amounts of oxygen were then chemisorbed on this sample at 100°C by exposure to 0.10 torr O_2. After each chemisorption, the sample temperature was increased at a constant rate of 2°C/min to 950°C. Oxygen was released as CO and CO_2; these gases were allowed to remain in contact with the sample. The cumulative recovery of CO increases with increasing temperature. Recovery of CO_2, meanwhile, goes through a maximum because of its reaction at elevated temperatures with nascent carbon sites, produced primarily by the decomposition of the CO-producing complex. The plot of cumulative recovery of CO + CO_2 against temperature shows distinct linear regions, the amount recovered in each linear region showing close agreement with the amount of oxygen previously chemisorbed at different site configurations on the Graphon surface. (auth) (UK)

4847 OBTAINING OF THERMAL GRADIENTS PRODUCED IN UO_2 HEATED BY THE JOULE EFFECT. OBSERVATIONS ON BASALTIC RECRYSTALLIZATION. Kurka, Gerard (Centre d'Etudes Nucleaires, Grenoble, France). J. Nucl. Mater.; 37: 133-8(Nov 1970). (In French).

By passing an electric current through cylindrical UO_2 specimens it was possible to obtain thermal gradients up to 5000°C per cm. The temperature distribution in the interior of the sample

was calculated and the validity of this calculation was checked by means of optical pyrometry measurements. Under certain conditions of temperature and temperature gradient, columnar grains are formed; their diameter is of the same order as that deduced from models based on evaporation-condensation mechanisms. (auth)

4848 POSSIBLE CONTRIBUTION OF DIFFUSIVE GRAIN-BOUNDARY PORE GROWTH TO CREEP DEFORMATION OF CERAMIC MATERIALS. Nicholson, Patrick S.; Lloyd, David J. (McMaster Univ., Hamilton, Ont.). J. Amer. Ceram. Soc.; 53: 578-9(Oct 1970).

The possible contribution of grain-boundary porosity growth to high-temperature creep strain was calculated for several ceramics. (G.M.C.)

4849 DISCUSSION OF KINETICS OF THE GRAPHITE–URANIUM DIOXIDE REACTION FROM 1400° TO 1756°C. Rao, Y. K. (Columbia Univ., New York). J. Amer. Ceram. Soc.; 53: 580-1(Oct 1970).

Includes reply by T. B. Lindemer, M. D. Allen, and J. M. Leitnaker.

Comments are given on a paper published previously concerning the kinetics of the graphite–uranium dioxide reaction from 1400 to 1756°C. The paper was abstracted in NSA as 23: 30164. A rebuttal is given to the above comments. (G.M.C.)

4850 BINDING BETWEEN GAS BUBBLES AND GRAIN BOUNDARIES. Mackworth, A. J. (Battelle Memorial Inst., Columbus, Ohio). Mater. Sci. Eng.; 6: 391-2(Dec 1970).

A simple model, analogous to that employed by Nelson, was used to calculate the binding energy between a gas bubble and a planar grain boundary. The result was applied to loosely bound bubbles and the specific case of gas bubbles in uranium monocarbide was examined. (auth)

4851 DEVELOPMENT OF AN EXPERIMENTAL TECHNIQUE TO THERMALLY SHOCK GRAPHITES. King, Charles R. (Los Alamos Scientific Lab., N. Mex.). Carbon; 8: 479-84 (Oct 1970).

A method of producing thermal-shock failures in thin graphite disks was developed, which permits the ranking of experimental materials on the basis of their resistance to thermal shock. A radio-frequency power source was used to obtain the very large transient thermal gradient for this test. The test apparatus is simple, and results can be obtained quickly with excellent reproducibility. Representative experimental data are presented. (auth) (UK)

4852 VARIATIONS IN COEFFICIENT OF THERMAL EXPANSION AS A FUNCTION OF PRESTRESSING. Gazda, I. William (Great Lakes Carbon Corp., Niagara Falls, N. Y.). Carbon; 8: 511-15(Oct 1970).

The effects on the coefficient of thermal expansion, CTE, of applying an initial compressive stress to a graphite material was investigated. Three materials, representing fine, intermediate and coarse-grained commercial graphites, were chosen for the investigation. The results indicate that significant increases in the 0 to 75°C CTE can result from prestressing a graphite body to 80% or 90% of failure. By successively annealing these prestressed specimens to 500, 1000, 2000, and 2800°C, a gradual reduction in the CTE was attained. After the 2800°C anneal, the CTE of the material had returned to or was slightly lower than its original value before stressing. (auth) (UK)

4853 BUBBLE MIGRATION IN UO_2: A STUDY USING A LASER IMAGE FURNACE. Oldfield, W.; Brown, J. B. Jr. (Battelle Memorial Inst., Columbus, Ohio). Mater. Sci. Eng.; 6: 361-70(Dec 1970).

The migration rate of bubbles in UO_2 was studied. Migration was induced by a temperature gradient caused by a laser beam focused on one surface of the UO_2 sample. Temperatures within the specimen were computed from knowledge of the boundary conditions for heat flow and the temperature-dependent physical properties of the material. (The hot surface temperature was calculated from the rate of evaporation of the material, and the cold surface temperature was measured by a thermocouple.) The migration velocities were determined from the length of columnar grains lying behind lenticular bubbles. Bubble migration velocities were much slower than forecast by a diffusion-controlled migration mechanism. In the case of one bubble, we estimate that of a total driving force of 8.6°C, about 5.8°C was used to develop new ledges on the condensing surface, and only about 0.2°C was used to promote diffusion of UO_2 molecules across the bubble. From this study it is concluded that bubble migration in nuclear fuels is likely to be variable, and especially sensitive to impurities which might affect the processes involved in migration (particularly surface active materials, which grossly affect layer nucleation). Consequently, the response of the fuel to bubble migration under irradiation (swelling and gas release) is in principle subject to control. (auth)

4854 LATTICE THERMAL EXPANSION PERPENDICULAR TO THE LAYER PLANES OF PYROCARBONS PRODUCED IN A FLUIDIZED BED. Pellegrini, G. (European Atomic Energy Community, Petten, Netherlands). Carbon; 8: 497-502(Oct 1970).

The lattice thermal expansion perpendicular to the layer planes of various pyrocarbon structures produced in a fluidized bed was measured at 10 to 1200°C. It was found that the thermal expansion of this type of material is structure sensitive. The average expansion coefficient α_c over the considered temperature range varied from 18×10^{-6} for structures deposited at 1650°C with small crystallites and low density, up to 24×10^{-6} for pyrocarbons deposited at 2100°C with an apparent crystallite size of 150 Å and a relatively high density. (auth) (UK)

4855 MASS SPECTROMETRIC INVESTIGATION OF THERMAL DISSOCIATION OF SAMARIUM AND EUROPIUM CARBIDES. Kyshtobaeva, G. M.; Smagina, E. I.; Kutsev, V. S. (State Scientific-Research and Planning Inst. of the Rare Metals Industry, Moscow). Zh. Fiz. Khim.; 44: 1405-9(Jun 1970). (In Russian).

Mass spectrometric studies were made of the thermal dissociation of samarium and europium dicarbides, obtained by reduction of the sesquioxides by carbon. It is shown that samarium carbide at 1250°K and europium carbide at 1185°K and a vacuum of 10^{-6} mm Hg are thermodynamically unstable and decompose with the formation of atomic samarium, europium, and graphite vapors. Chemical and phase compositions were established and the lattice parameters of samarium carbide are a = 5.320 and c = 6.331 Å. The heats of decomposition (–62.7 ± 2.0 and –51.6 ± 1.5 kcal/mol) and the heats of formation (13.4 ± 2.0 and 9.0 ± 1.5 kcal) were determined for samarium and europium dicarbides, respectively. (tr-auth)

4856 PORE CHARACTERISTICS OF CARBONS. Turkdogan, E. T.; Olsson, R. G.; Vinters, J. V. (Edgar C. Bain Lab., Monroeville, Pa.). Carbon; 8: 545-64(Oct 1970).

The pore characteristics of carbons, e.g., graphites, coke, and charcoals, were investigated by utilizing x-ray and microscopic techniques and by measuring pore volume, pore surface area, and the corresponding effective diffusivities of $CO-CO_2$ and H_2-H_2O. The large surface area of carbons is shown to be due to the presence of micropores which become extensive in charcoals. A method is developed for the determination of surface areas from the BET technique using nitrogen (–195°C) and carbon dioxide (–78°C) adsorption isotherms at low relative pressures. Several techniques are used in determining the effective diffusivities of $CO-CO_2$ and H_2-H_2O. It is shown that over a wide temperature range (18 to 900°C) and at 1 atm pressure and above, the diffusive flux is that due primarily to normal (molecular) diffusion. The pore volume, pore surface area, and effective diffusivity increase with increasing weight loss during internal oxidation. These changes are not reflected in the measurements of the rate of oxidation. The results of present and previous investigations indicate that for a given type of carbon the effective surface area (due primarily to large pores of 1 μm dia or larger) does not change much with oxidation up to at least 20 per cent weight loss. The difference in the rate of oxidation between types of carbon is attributed essentially to the difference in the effective surface areas. (auth) (UK)

4857 MASS SPECTROMETRIC STUDIES OF THERMODYNAMIC PROPERTIES OF THE BINARY SYSTEM $NaF-MeF_3$(Me = Sc, Y, La). II. COMPOSITION-PRESSURE DIAGRAM. Sidorov, L. N.; Shcheredin, V. P.; Akishin, P. A. (Moscow State Univ.). Zh. Fiz. Khim.; 44: 1577-9(Jun 1970). (In Russian).

A composition-pressure diagram was established for the compounds NaF, Na_2F_2, Na_2F_3, ScF_3 and $NaScF_4$ at 1169°K. The change of initial component with composition in systems $NaF-YF_3$, (1321°K) and $NaF-LaF_3$ (1276°K) was determined. It is proposed that similar systems be characterized using diagrams of initial component partial pressure in like compositions and using the tables of constants for equilibrium gas reactions. (tr-auth)

4858 RESEARCH IN THE UNCERTAINTY OF OXIDE FUEL ELEMENT THERMAL CONDUCTIVITY DEPENDENCE UPON POROSITY. Mueller, Eva-Maria (INTERATOM, Bensberg, Ger.). Atomwirt., Atomtech.; 15: 434-5(Sep-Oct 1970). (In German).

Critical measurements and experiments were evaluated for determination of the dependence on porosity of the thermal conductivity of oxide fuels and to produce an optimal curve. Correction function for thermal conductivity in relation to porosity, are given. (M.C.G.)

4859 CONCRETE-POLYMER BUILDING BLOCKS. Welt, M.; Bernstein, B.; Hallman, D.; Rosen, S. (Radiation Tech. Inc., Rockaway, N. J.). Trans. Amer. Nucl. Soc.; 13: 513-14(Nov 1970).

From Meeting of the American Nuclear Society, Washington, D. C. See CONF-701102.

4860 CONCENTRATION DEPENDENCE OF THE DIFFUSION COEFFICIENT OF VOLATILE FISSION PRODUCT METALS IN GRAPHITE. Zumwalt, Lloyd R. (North Carolina State Univ., Raleigh). Trans. Amer. Nucl. Soc.; 13: 566-8(Nov 1970).

From Meeting of the American Nuclear Society, Washington, D. C. See CONF-701102.

4861 COMPRESSIVE CREEP OF UO_2–22 PERCENT PuO_2. Houston, M. D.; Kruger, O. L.; Pardue, W. M. (Battelle Memorial Inst., Columbus, Ohio). Trans. Amer. Nucl. Soc.; 13: 571 (Nov 1970).

From Meeting of the American Nuclear Society, Washington, D. C. See CONF-701102.

4862 THERMAL CONDUCTIVITY OF PHYSICALLY MIXED $(U_{0.8}Pu_{0.2})O_{2-x}$. Evans, S. K.; Bohaboy, P. E. (General Electric Co., Pleasanton, Calif.). Trans. Amer. Nucl. Soc.; 13: 571-2 (Nov 1970).

From Meeting of the American Nuclear Society, Washington, D. C. See CONF-701102.

Structure and Phase Studies

Refer also to abstracts 4802, 5190, 5224, 5992, and 5993.

4863 (DP-Report-574) SOME OBSERVATIONS OF FUEL PARTICLE COATINGS AT VERY HIGH MAGNIFICATION. Project DRAGON. Voice, Eric (Atomic Energy Establishment, Winfrith (England)). Jun 1967. 29p. Dep. NTIS.

A scanning-beam electron microscope, the Stereoscan, was used to look at the surface and sections of pyrocarbon and silicon carbide coatings on fuel particles. The principle of instrument operation and the mode of examination are described and a series of photographs is used to illustrate the nature of the deposited layers and the ways in which they are modified by different conditions of deposition and treatment. (auth)

4864 REACTION OF ZrO_2 WITH U_3O_8. Verbetskii, V. N.; Kovba, L. M. Zh. Neorg. Khim.; 15: 1728-30(Jul 1970). (In Russian).

X-ray phase analysis was used to establish the formation of solid solutions $ZrO_2 \cdot nU_3O_8$ in $ZrO_2 - U_3O_8$ systems and their parameters were determined. The $ZrO_2 \cdot nU_3O_8$ phase has a noticeable region of homogeneity. On oxidation of $ZrO_2 \cdot nU_3O_8$ phases by oxygen under pressure, the hexagonal phase $(Zr,U)O_x$, the rhombic phase $(Zr,U)O_x$, and $\alpha - UO_{3-x}$ were formed. The degree of oxidation of uranium $-$ O/U = 2.90 to 2.91. Pure U_3O_8 under the same conditions is oxidized to $\gamma - UO_3$. Lattice parameters of the new phases were determined. For the hexagonal phase $(Zr,U)O_x$, a = 4 × 3.958 and c = 4.157Å. In other cases subcell parameters were determined. (tr-auth)

4865 THEORETICAL AND EXPERIMENTAL INVESTIGATION OF THE GRAPHITE PHASE DIAGRAM AND GRAPHITE PROPERTIES IN THE LIQUID CORE NUCLEAR ROCKET PRESSURE–TEMPERATURE RANGE. Woods, Hugh Wilroy. Gainesville, Fla.; Univ. of Florida (1969). 118p. University Microfilms Order No. 70-11,759.

Thesis.

Graphite properties needed in the design of high-temperature, solid or liquid, graphite nuclear reactor cores were investigated. The graphite phase diagram solidus–liquidus interface was experimentally measured from the triple point up to 1000 atmospheres pressure. Techniques believed to be relatively free from systematic errors were used. The LANG grade graphite triple-point temperature measured was 7606 ± 60°R. The melting temperature increases with pressure until it reaches a measured value of 7821 ± 63°R at 1000 atmospheres pressure. A theoretical model was developed for the graphite thermodynamic functions at high temperatures. The measured phase diagram data, together with other data, were used to evaluate parameters in the theory and to apply the theory to liquid and solid graphite at higher pressures. The Debye solid graphite characteristic temperature obtained varies from 1470.0°K at one atmosphere pressure to 1473.7°K at 1000 atmospheres pressure, and the liquid graphite characteristic temperature varies from 546.2°K at 103 atmospheres pressure to 555.5°K at 1000 atmospheres pressure. (Diss. Abstr. Int., B)

4866 DENSITY AND STRUCTURAL DISTRIBUTIONS IN ARTIFICIAL GRAPHITES. Engle, G. B. (Gulf General Atomic Inc., San Diego, Calif.). Carbon; 8: 485-95(Oct 1970).

Densitometric separations were performed on a number of artificial graphites, and the apparent crystallite sizes of the density fractions were measured. Anisotropic porous artificial graphites are shown to consist of semigraphitic regions coexisting with highly graphitic regions. The transition of the structure from semigraphitic to highly graphitic is smooth, and the apparent crystallite size can be correlated with the apparent density of the fractions. The near-isotropic graphites have semigraphitic structures and are more uniform in apparent crystallite size than the anisotropic graphites. The mean apparent crystallite size $\overline{L}_c$ of the graphites shows a systematic correlation with the volume thermal expansivity of the samples. Materials that are nearly isotropic, such as Poco or Gilsonite graphites, have the highest thermal expansivities, the smallest apparent crystallite sizes, and the smallest range of crystallite sizes. (auth) (UK)

4867 EFFECT OF HOT-PRESSING ON THE STRUCTURE OF CARBON ARTIFACTS. Boeder, H.; Fitzer, E. (Univ., Karlsruhe, Ger.). Carbon; 8: 453-66(Oct 1970).

Polycrystalline carbon artifacts having different filler and binder composition as well as pyrolytic graphite and glasslike carbon were hot-pressed in graphite molds at temperatures up to 2900°C and pressures up to 700 kg/cm². In all cases pressurization caused an enhanced decrease of the c-spacing compared with graphitization without pressure. The effect of hot-pressing on the mean crystallite size depends on the direction of pressurization in its relationship to the preferred orientation of the crystallites prior to pressing. When the pressing direction is parallel to the c-direction, an increase in the $\overline{L}_c$ and $\overline{L}_a$ values and a reduction of the mean square fractional displacement is observed. In all other cases, hot-pressing leads to a reduction of the $\overline{L}_c$ and $\overline{L}_a$ values. Decisive effects depend on the nature of the starting material. The x-ray anisotropy as a function of the unidirectional strain and the sample properties are discussed. Investigations by optical and scanning microscopy revealed that the reduction in crystallite size, as well as the decrease of the mean c-spacing, are due to slip, kink formation, and polygonization. The observed densification and the enhancement of anisotropy are interpreted as being due to flow processes in layer stacks. In addition, there is a stress-induced graphitization of disordered carbons. (auth) (UK)

4868 TRANSMISSION ELECTRON MICROSCOPY OF POLYCRYSTALLINE GRAPHITE. Yust, C. S.; Morgan, C. S.; Gaddis, H. R. (Oak Ridge National Lab., Tenn.). Carbon; 8: 449-51(Oct 1970).

The preparation of polycrystalline graphite specimens for electron transmission microscopy is described. Examples of the results obtained with several different commercial graphites are presented. The observed structures are compared, and the influence of the preparation technique on the observations is discussed. (auth) (UK)

4869 LIQUIDUS CURVE OF THE ZrO_2–Y_2O_3 SYSTEM AS MEASURED BY A SOLAR FURNACE. Noguchi, Tetsuo; Mizuno, Masao; Yamada, Toyoaki (Government Industrial Research Inst., Nagoya, Japan). Bull. Chem. Soc. Jap.; 43: 2614-16(Aug 1970).

The freezing points of a composition in the ZrO_2–Y_2O_3 system were measured by specular reflection. The brightness temperature at the freezing point of the system was determined using the cooling curve. The spectral reflectivity of the specimens was measured and the spectral emissivity was estimated from these data. In this way the true freezing point temperature was calculated. (J.R.D.)

4870 APPLICATION OF INTERNAL FRICTION TO THE STUDY OF GRAPHITIZATION. Gobin, P. (Institut National des Sciences Appliquees, Lyon); Merlin, J.; Jouquet, G.; Rappeneau, J. J. Nucl. Mater.; 36: 113-15(Jul 1970). (In French).

The internal friction of various graphites was studied in the range from 900 to 2700°C. The behavior of these graphites was compared to nuclear graphites. The coefficient of internal friction appeared to be a parameter sensitive to the process of graphitization. Its measurement should allow classification of carbonaceous materials according to their degree of graphitization and as a function of crystallite size. (R.C.K.)

4871 RECONNAISSANCE OF THE SYSTEM BeO–Al_2O_3–SiO_2–H_2O. Ganguli, D.; Saha, P. (Central Glass and Ceramic Research Inst., Calcutta). Trans. Indian Ceram. Soc.; 26: No. 4, 102-10(1967).

The nature of the subsolidus phase relations in the system BeO–Al_2O_3–SiO_2–H_2O at 300 to 700°C was investigated at a water vapor pressure of 15,000 psi. Phases synthesized were beryl, chryso-

beryl phenacite, mullite, bertrandite, pyrophyllite, kaolinite, bromellite, and quartz. The curve for the reaction, beryl + H_2O ⇌ bertrandite + pyrophyllite, demarcating the lower thermal stability limit of beryl, was traced down to 3,000 psi. The hydrous compound bertrandite gave indications of a fairly wide range of solid solution, suggesting variability of the Be : Si ratio in its composition. (Indian Sci. Abstr.)

4872 SYSTEM MoO_3–CeO_2. Ustinov, O. A.; Novoselov, G. P.; Andrianov, M. A.; Chebotarev, N. T. Zh. Neorg. Khim.; 15: 2549-51(Sep 1970). (In Russian).

Roentgenographic analyses of this system revealed the existence of $CeMoO_2$, Ce_2MoO_3, and $CeMoO_{12}$ with Ce in tetravalent state. A phase diagram was prepared for CeO_2 contents up to 40 mole % which shows eutectic occurrence at approximately 22 mole % of CeO_2. (tr-auth)

4873 SYSTEM MoO_3–BaO. Ustinov, O. A.; Novoselov, G. P.; Andrianov, M. A.; Chebotarev, N. T. Zh. Neorg. Khim.; 15: 2552-4(Sep 1970). (In Russian).

Thermographic and roentgenographic methods were used to study the constitution diagram of MoO_3–BaO system at BaO content of O to 50 mole %. The existence of the compound BaO · $2MoO_3$ which melts incongruently at 715°C was established. The existence of the molybdate BaO · MoO_3 was also confirmed. A eutectic occurring at approximately 640°C with a BaO content of ~18.9 mole % was established. (tr-auth)

4874 MEASUREMENT OF PLUTONIUM HOMOGENEITY IN THERMAL RECYCLE FUELS PREPARED FOR EEI PROGRAM. Wadekamper, D. C.; Aitken, E. A.; Evans, S. K.; O'Neill, G. L. (General Electric Co., Pleasanton, Calif.). Trans. Amer. Nucl. Soc.; 13: 549(Nov 1970).

From Meeting of the American Nuclear Society, Washington, D. C. See CONF-701102.

4875 MEASURING PLUTONIUM HOMOGENEITY IN FAST REACTOR FUELS. . Aitken, E. A.; Evans, S. K.; Rosenbaum, H. S.; Wadekamper, D. C. (General Electric Co., Pleasanton, Calif.). Trans. Amer. Nucl. Soc.; 13: 602(Nov 1970).

From Meeting of the American Nuclear Society, Washington, D. C. See CONF-701102.

4876 EVALUATION OF PuO_2 HOMOGENEITY IN PuO_2–UO_2 FAST REACTOR FUEL BY SCANNING ELECTRON MICROPROBE. Stranik, D. A.; Powers, H. G.; Last, G. A. (Hanford Engineering Development Lab., Richland, Wash.). Trans. Amer. Nucl. Soc.; 13: 603(Nov 1970).

From Meeting of the American Nuclear Society, Washington, D. C. See CONF-701102.

4877 SOLUBILITY OF OXYGEN IN ZIRCONIUM CARBIDE. Sarkar, Satya Kinkar. Seattle; Univ. of Washington (1969). 88p. University Microfilms Order No. 70-14,786.

Thesis.

Heating zirconium carbide, various mixtures of zirconium oxide and carbon, and mixtures of zirconium oxide and zirconium carbide at 1800°C in a carbon monoxide atmosphere resulted in the formation of a fcc phase (ZrC_xO_y) with lattice parameter between 4.673 and 4.689 A°. The determination of composition indicated that the lattice parameter decreased linearly with the oxygen content. Lattice parameter varied non-linearly with C and sum of C and O_2. There was evidence of equilibrium being attained in some, if not in all, cases. Assuming the activity of carbon to be unity in ZrC_xO_y of composition $ZrC_{0.856}O_{0.07}$, the oxygen activity was calculated to be 1.36×10^{-15}. The standard free energy of formation of this composition was calculated to be –39.5 kcal/mole, assuming the activity of zirconium to be 10^{-3}. The final composition of ZrC_xO_y depended on the temperature and the superincumbent CO pressure. For the attainment of the equilibrium, the material transfer from the external environment is essentially through the CO phase. (Diss. Abstr. Int., B)

4878 UNFAMILIAR OXIDATION STATE OF ZIRCONIUM AND THE EFFECT OF OXYGEN ACTIVITY ON THE STRUCTURE OF ZrO_2. Nair, K. Manikantan. Seattle; Univ. of Washington (1969). 78p. University Microfilms Order No. 70-14,775.

Thesis.

The Zr–ZrO_2 system was investigated between 700 and 1600°C using controlled oxygen partial pressures. The system was approached from two directions; starting with pure metal powder and oxidizing it in argon and oxygen mixtures, and starting with pure ZrO_2 powder and reducing it in different mixtures of CO and CO_2. Two lower valence oxides of zirconium were observed by x-ray powder diffraction analysis. One of them had a fcc zinc blende (ZnS) type crystal structure with an $a_0 = 3.8956$ Å and ZrO composition is proposed. The second oxide, Zr_3O, had a hexagonal closed packed crystal structure similar to that of zirconium metal, with oxygen atoms occupying one third interstitial positions in an ordered manner. The stability of this oxide was determined. A series of reduced ZrO_{2black} samples were prepared at 1200 and 1470°C and varying oxygen partial pressures. Another set of ZrO_{2black} samples was prepared at 1000 to 1600°C and in hydrogen atmospheres. These reduced ZrO_2 samples were reoxidized to ZrO_{2white} at 1000°C in an air atmosphere. The d-spacings and relative intensities of ZrO_{2b} and ZrO_{2w} did not show any change with change in oxygen activity of temperature. A mechanism for the formation of reduced ZrO_{2black} is proposed. The apparent activity of free Zr atoms in the monoclinic ZrO_{2black} lattice is calculated. (Diss. Abstr. Int., B)

Radiation Effects

Refer also to abstracts 4815, 5166, 5994–5997, 6000–6004, 6008, 6012, 6197, and 6198.

4879 (CEA-CONF-1659) PARTIAL MELTING OF LOW DENSITY MIXED OXIDE $(U,Pu)O_2$ AT THE BEGINNING OF IRRADIATION. IN-PILE DISTRIBUTION OF THE FUSED OXIDE. Conte, Madeleine; Leclere, Jacques; Lhermenier, Andre; Mikailoff, Hubert (Commissariat a l'Energie Atomique, Fontenay-aux-Roses (France). Centre d'Etudes Nucleaires). 1970. 21p. (In French). (CONF-700920–3). Dep. NTIS (U. S. Sales Only).

From International Meeting on Fast Reactor Fuel and Fuel Elements, Karlsruhe, Germany.

During irradiation of mixed oxide UO_2–PuO_2 containing 15 to 20 percent of PuO_2, neutrographic examination shows the formation of a regularly shaped central hole during the first power rise at temperatures above 1950°C but below the melting point. The diameter of the hole becomes very irregular when the fuel core temperature reaches melting point, and two or three concentric zones of different structures are observed. Two experiments are described, GE_3 and GE_4, in which the displacement of matter was followed at the time of partial melting of the fuel and in the course of irradiation (rearrangement of the central hole). In GE_4, melting and rearrangement occur at a moderate power level; in GE_3, the rearrangement is produced after densification of a large volume of fuel, and partial melting obtained by a brief excursion at high power. It was observed that the radial distribution of fission products is affected by the presence of a fused zone, and that maintenance of a high temperature in the zones filled by the flow of molten oxide leads to a fast rearrangement of matter along the central hole. This rearrangement necessarily implies the transfer of some of the oxide. It was accepted that this transfer took place through the vapor phase owing to the existence of a longitudinal thermal gradient. The rearrangement process begins at a temperature above 2500°C, after an irradiation period of 12 days. (France)

4880 (CEA-N–1374) ELEMENTARY MODEL OF THE MACROSCOPIC EFFECTS OF NEUTRON IRRADIATION IN GRAPHITE. Genthon, J. P. (Commissariat a l'Energie Atomique, Saclay (France). Centre d'Etudes Nucleaires). Jun 1970. 46p. (In French). Dep. NTIS (U. S. Sales Only).

A study of a structural model in zones of displacements of the defects created in graphite by neutron irradiation shows that, before any random thermal annealing, these zones are made up of 4 stable atomic displacements: 4 vacancies in groups of two, three and four vacancies and 4 interstitials, isolated or in groups of two, three and four interstitials (single vacancies and groups of 5 interstitials are possible in small proportions). The effects of irradiation temperature on the dimensional changes in irradiated graphite, as established from published experimental data, are well illustrated from this model. In particular its application enables irradiation rate effects to be taken into account (problems of instantaneous flux or equivalent temperature correction). At low temperatures ($T \lesssim 300$°C) the treatment is equivalent to the empirical treatment used nowadays and extrapolates well to higher temperatures. As a general rule, and in a first approximation, it may be said that an increase in temperature (expressed in °K) of 7.5 compensates a multiplication by 10 of the flux, at given fluence. (auth) (France)

4881 (DP-Report-352) GRAPHITE OXIDATION UNDER IRRADIATION BY TRACES OF CO_2 IN A HIGH PRESSURE HELIUM CARRIER GAS. Project DRAGON. Valette, L.; Van Massenhove, G. (Atomic Energy Establishment, Winfrith (England)). Jun 1965. 42p. (CONF-651094–1). Dep. NTIS.

From Symposium on Basic Research, Harwell, Eng.

Work on graphite corrosion by traces of carbon dioxide in helium under irradiation in the BR2 Reactor is reviewed. The experiments covered the temperature range 250 to 900°C, in fast neutron

XUM

fluxes up to 5×10^{14} n/cm^2 s and γ fluxes up to 15 W/g. The observed corrosion rates were almost independent of temperature and carbon dioxide concentrations (>10 vpM). The rates were of the same order of magnitude as the rates of the thermal reaction at 1000°C and 10 cpM CO_2. Decomposition of the carbon dioxide, with the formation of oxygen and carbon monoxide, was observed; and the amounts of oxygen produced could account for the observed graphite corrosion rates. Hydrogen, carbon monoxide and methane were found to inhibit both the decomposition of the carbon dioxide and the radiolytically induced corrosion of the graphite. It was established that the observed radiolytic effects are largely due to energy transfer from the helium. (auth)

4882 (DP-Report-436) CORROSION EXPERIMENTS ON COATED FUEL PARTICLES USING THE "XENON RELEASE" TECHNIQUE. Project DRAGON. Pollitt, N. (Atomic Energy Establishment, Winfrith (England)). Jun 1966. 29p. Dep. NTIS.

Post-irradiation xenon release studies on PyC and PyC/SiC coated fuel particles, under inert and mildly oxidizing conditions, revealed no significant difference in the rate of release of ^{133}Xe It appears that good quality coated particles are resistant to oxidation. An exposure of 200,000 μ atm hours to carbon dioxide in helium at 1300°C resulted in a gas release value below the limit of sensitivity of the experiment. (auth)

4883 (DP-Report-473) DIMENSIONAL CHANGES IN GRAPHITE DURING HIGH-TEMPERATURE IRRADIATION IN THE HIGH FLUX REACTOR RCN, PETTEN. Project DRAGON. Blackstone, R.; Graham, L. W. (Atomic Energy Establishment, Winfrith (England)). Jul 1967. 74p. Dep. NTIS.

The dimensional changes observed in a range of graphitic materials following irradiation at 600, 900 and 1200°C are reported. The results are discussed in the light of current models for irradiation damage in graphite and it is concluded that for conventional materials the dimensional behavior can be related to the material properties. Further confirmation of the extreme dependence of the dimensional changes on the crystallite size has been obtained. The way in which the rate of dimensional change varies with temperature is compatible with this effect being caused by vacancy loss at crystallite boundaries. For a given crystallite size there appears to be a breakaway temperature above which the rate of dimensional change accelerates rapidly. (auth)

4884 (DP-Report-556(Pt.1)) DIMENSIONAL CHANGES OF GRAPHITE SPECIMENS IRRADIATED IN DRAGON FUEL ELEMENT 700. Project DRAGON. Everett, M. R.; Lamb, D. (Atomic Energy Establishment, Winfrith (England)). Nov 1967. 62p. Dep. NTIS.

Fuel element 700 was the first of the four elements in the first metallurgical series to be removed from the Dragon core, having received a fast neutron dose of $\sim 3 \times 10^{20}$ n cm^{-2}. The changes in physical properties of the graphite specimens, contained in the spines of this element, were measured and correlated with the available and derived data on temperature and neutron dose. (auth)

4885 (DP-Report-556(Pt.2)) DIMENSIONAL CHANGES OF GRAPHITE SPECIMENS IRRADIATED IN DRAGON FUEL ELEMENT 700. PART II. SOME COMMENTS ON THE IRRIDATION SHRINKAGE OF GRAPHITE. Project DRAGON. Everett, M. R.; Graham, L. W. (Atomic Energy Establishment, Winfrith (England)). Nov 1967. 23p. Dep. NTIS.

Although the qualitative mechanism of irradiation damage and dimensional change of graphite crystallites is quite well understood, the existing quantitative theories do not predict the irradiation shrinkage behavior of a range of graphites with very good accuracy. It is suggested that this is because the effects of crystallite height, crystallite diameter, crystallite shape, and crystallite mechanical properties such as the shear modulus are not considered with respect to the magnitude of crystallite/crystallite dimensional interactions. A model which takes into account these effects is developed and the associated physical property parameter correlated against the initial irradiation volume shrinkage rates of fourteen different graphites. It is considered more logical that the volume change of a graphite should be first understood and the anisotropy taken into account at a later stage. (auth)

4886 (GEAP-10204) ZIRCALOY-CLAD UO_2 FUEL ROD EVALUATION PROGRAM. Quarterly Progress Report No. 10, February–April 1970. Megerth, F. H. (comp.) (General Electric Co., San Jose, Calif. Reactor Fuels and Reprocessing Dept.). May 1970. Contract AT(04-3)-189. 42p. Dep. NTIS.

The two SA-1 subassemblies, which were received at Vallecitos Nuclear Center (VNC) in March were visually examined in the hot cells and found to be in generally good condition. All rods were removed from the subassembly structures and individually inspected. In general, the appearance of these more highly exposed fuel rods was similar to that observed after the first two cycles of Dresden operation, both in pool examinations at Dresden and in examinations of the ten removed rods conducted in the hot cells at VNC. The corrosion product, or crud, film that was deposited on the rods during operation generally gave most of the surface area a coloration best described as bluish-gray with varied amounts of reddish-brown. The reddish-brown portion of the film frequently was distributed in the form of speckles, and in such cases the surface usually appeared somewhat rough in texture. Metallographic examinations of fuel rod sections performed during the initial phase of the program indicate that this surface roughness is probably a consequence of an uneven, pitting type ZrO_2 corrosion layer. There were noticeable differences in the degree and extent of surface roughness among different rods, and along the length and around the circumference of a given individual rod. The axial variation in roughness tended to correspond with the axial power profile, but there were exceptions to this relationship. An increased deposition of brownish crud was observed on most rods at the three spacer locations along the fuel column. Spalling or cracking of the crud had occurred in several instances at these locations. A few rods showed spalling or cracking of the crud layer between the spacer locations. A corner rod that operated in the top subassembly and positioned at a wide-narrow water gap throughout its Dresden irradiation exhibited the greatest amount of crud spalling. Many of the rods were marked with fine longitudinal lines. These lines appeared to result from handling, but it is remotely possible that some of them might be hairline cracks. In addition to those rods with hairline markings, a few rods exhibited small pitlike penetrations, short jagged cracks, small blisters, or discolored areas. The depths of penetration and exact natures of these anomalies could not be determined solely by visual inspection of the external surfaces, and additional investigations with neutron radiography and possibly pressure testing are planned. Several thin slivers of irradiated UO_2 were examined by transmission electron microscopy with both the 100-keV and 650-keV machines. The slivers were extracted from a metallography specimen with an average burnup of 8.1×10^{20} fissions/cm^3 (29,700 MWd/t U), which was obtained from one of the initial ten rods removed from SA-1. Several small pores were visible at the edge of one of the slivers. Samples taken from regions relatively near the pellet periphery showed numerous defects. Rod or plate shaped inclusions were visible in a sliver from a peripheral location. Only a few defects were visible in two thin fuel chips taken from near the pellet center when examined in bright field. In the dark field image, on the other hand, the structure of one of the chips looked severely disrupted. (auth)

4887 (KFK-1215) PRODUCTION, DETECTION, ANNEALING OF CRYSTAL LATTICE POINT DEFECTS BY NEUTRON IRRADIATION OF CERAMIC MATERIALS. Dienst, W. (Kernforschungszentrum, Karlsruhe (West Germany). Institut fuer Material und Festkoerperforschung). 14 Jul 1970. 176p (In German). Dep. NTIS (U. S. Sales Only).

Methods of theoretically treating defects in the crystal lattice caused by neutron irradiation are described. The production of point defects and displacement spikes by collision processes is described as well as the corresponding lattice-site exchanges and the site exchanges due to ionization and temporary overheating in the neighborhood of fission fragment paths. Other subjects considered are the point-defect concentration in equilibrium between defect production and recovery and the formation of point-defect clusters. A survey of experimental results found in the literature with respect to lattice defects by neutron irradiation in non-fissile ceramic materials is included. The comparatively large number of results available for light-metal oxides such as BeO, MgO, Al_2O_3 is supplemented by data on the irradiation behavior of transition-metal carbides, SiC, Mo, and LiF. A comparison of all data suggests a dependence of the maximum lattice expansion (by irradiation) on the type of lattice bonding. The lattice expansion increases in the sequence of metallic → ionic → covalent bond. Conversely, the saturation dose, i.e., the neutron fluence at which the maximum lattice expansion is attained, depends mainly on the atomic weight of the lattice atoms. For compounds which consist of atoms with intermediate atomic weights it seems to be lower by approximately one decimal order of magnitude as compared to compounds of light atoms. These trends have been confirmed by x-ray diffraction analysis carried out on irradiated powder specimens of ZrO_2 (cubic stabilized), ZrN, and ZrC. The specimens were irradiated at temperatures below 150°C with neutron fluences up to about 5×10^{19} n/cm^2 (fast neutrons/cm^2) or uranium fission fragments up to 7 to 10×10^{17} f/cm^3 (apparent fissions/cm^3). Lattice expansion was nearly saturated after the indicated neutron fluence. It increased in the sequence ZrO_2, ZrN, ZrC. After fission fragment irradiation the differences of lattice expansions between the different Zr-compounds were smaller than after neutron irradiation. These differences were mainly attributed to differently ordered states of point-defect clusters depending on

the type of lattice bonding. In case of fission fragment irradiation a thermal recovery effect by the thermal rods (along the fission fragment paths) seems to improve the ordered state of clusters. Powder specimens of UN and UC were examined after irradiation at temperatures below 150°C up to fission densities of 4×10^{20} f/cm³ (fissions/cm³) at the maximum. The course of lattice expansion and distortion with increasing fission density in UN is similar to that in UO_2. However, it is characterized by stronger irradiation effects and higher specific fission densities. This leads to the conclusion that in UN the formation of large ordered point-defect clusters is more difficult than in UO_2 owing to the predominant covalent metal/non-metal bond. Lattice expansion and distortion in UC showed a course essentially different from that in UN. This may be due to a relatively weak metal/non-metal bond which facilitates the formation of point-defect clusters in the partial lattices of UC. Having attained a maximum linear lattice expansion of 2.1×10^{-3} after about 5×10^{17} f/cm³, a reversion of lattice expansion down to slightly negative values was observed for UN at higher fission densities. This course was interpreted as a consequence of different overlapping volumes for vacancy core and interstitial-atom zone of the displacement spikes. The irradiated specimens of Zr- and U-compounds were subjected to recovery annealings of 2 hours duration each at steps of 100°C. After each annealing step the percentage recovery of lattice expansion and distortion was measured. Recovery took place in temperature ranges which are clearly related to the melting point of the sample material. Steps of accelerated recovery of lattice expansion occurred at about 0.15 to 0.2 T_M and 0.3 to 0.35 T_M (T_M = melting point, °K). They can be attributed to the migration of isolated interstitial atoms and vacancies, respectively, produced under irradiation. An estimation of the enhancement of diffusion processes in the lattice caused by the increase in point defect concentration and the lattice-site exchange-frequency under irradiation is included. The estimate shows that a measurable increase in the diffusion rate as a result of irradiation can be expected especially for ceramic fuels. It could possibly result in an enhancement of diffusion-induced creep which might be described with a modified Nabarro–Herring-model. (auth)

4888 (TRG-Report-1937) SOME LIMITING ASPECTS OF UO_2 PERFORMANCE. Ainscough, J. B. (United Kingdom Atomic Energy Authority, Springfields (England). Reactor Group). 29 Sep 1969. 16p. Dep. NTIS (U. S. Sales Only). UK 3s.

Recent developments in aspects of UO_2 behavior such as fission gas release, fission product swelling, and UO_2 creep are examined. Fission gas release from UO_2 at temperatures below that necessary to cause columnar grain formation, is now believed to be at least a two-stage process involving first the movement of single atoms and very small bubbles to grain boundaries, and then the growth and link up of gas bubbles at the boundaries and their ultimate escape to the fuel-can interspace. The volume of these bubbles, and hence the swelling produced by them will be a function of the applied restraint of temperature insofar as this governs the rate of gas atom migration and also the deformation rate of the fuel, and also of the extent to which gas has escaped from the fuel altogether. Failure due to gas pressure build up is only likely in a reactor concept which uses short pins and the main danger from the fission gases is more likely to be due to their contribution to fuel swelling. Both the solid and the gaseous fission products contribute to swelling. The contribution of the first is fairly easily calculated from the fission yields and from a knowledge of the likely chemical form of each fission product, but the extent of the second, being dependent on burn-up, restraint and temperature is more difficult to assess since it will vary along the radius of a fuel pellet. There is now good evidence for believing that in addition to the thermal creep of UO_2 there is also an irradiation creep process which is temperature independent but a function of rating, so that from the creep point of view the oxide will behave as if no part of it were below some rating dependent and calculable temperature. Whether or not overall swelling of a fuel pin will occur is a fairly complex problem which will depend on the restraint available from clad and coolant, on the temperature dependent swelling rate of the UO_2 and on its creep rate, on the porosity of the original fuel and on the free space within the cladding both fuel-to-can clearances and dishes in pellet ends. (auth)

4889 (UNC-5263) FAST REACTOR MIXED-CARBIDE FUEL ELEMENT DEVELOPMENT PROGRAM. Twelfth Quarterly Progress Report, April–June 1970. (United Nuclear Corp., Elmsford, N. Y. Research and Engineering Center). 19 Aug 1970. Contract AT(30-1)-3415. 33p. Dep. NTIS.

Research directed toward development of clad PuC–UC fuel rods to perform at high burnup and high power levels is reported. Progress is reported on high-density pellet evaluation in EBR-II, annular and low-density pellet evaluation in EBR-II, fission gas release and fuel swelling, evaluation of sodium-bonded fuel, fabrication methods development for mixed oxides, evaluation of thermal properties of PuC–UC fuels, and TREAT evaluation of mixed carbides. (J.R.D.)

4890 RESISTOMETRIC INVESTIGATION ON SAP ALLOYS NEUTRON IRRADIATED AT 100°K. Audoly, S.; Bassani, C. (CCR-EURATOM, Ispra, Italy). J. Nucl. Mater.; 37: 125-32 (Nov 1970).

Results of a resistometric study on SAP alloys of different compositions, which were irradiated with fast neutrons at 100°K, showed that the amount of resistivity introduced by the irradiation strongly depended on the impurity content of each alloy. The defects introduced were investigated by isochronal and isothermal annealings. All the damage was recovered at room temperature, through a spectrum which was resolved in stages II-b and III. An activation energy of 0.60 ± 0.02 eV was determined for the defects migrating in stage III. The implications of these results on existing recovery models are discussed. (auth)

4891 MOLYBDENUM DISTRIBUTION IN IRRADIATED OXIDE FUELS. Lawrence, L. A.; Christensen, J. A. (Pacific Northwest Lab., Richland, Wash.). J. Nucl. Mater.; 37: 248-50(Nov 1970).

The distribution of fission product molybdenum in irradiated oxide fuel was studied. Molybdenum-99 activity profiles in several irradiated UO_2 – 25 wt % PuO_2 fuel pins were measured by gamma ray spectrometric methods. Concentration profiles showed movement of molybdenum outward from the fuel center. (G.M.C.)

4892 INFLUENCE OF SINGLE IRRADIATION AND HEAT TREATMENT ON THE PROPERTIES OF BeO. Buresch, F. E. (Max-Planck-Institut fuer Metallforschung, Stuttgart); Galikine, V.; Neef, N.; Roehrig, D. Atomwirt., Atomtech.; 15: 437-9 (Sep-Oct 1970). (In German).

The characteristics of various BeO samples after cyclic irradiation and heat treatment were investigated. The temperature of the BeO samples increased during their irradiation time of about 14 weeks from 300 to 900°C at a fast neutron dose of about 3×10^{20}n/cm². Data are presented in graphs. (M.C.G.)

4893 CONTINUOUS MEASUREMENT OF THE CREEP OF UO_2 UNDER IRRADIATION. Brucklacher, D.; Dienst, W. (Kernforschungszentrum, Karlsruhe, Ger.). J. Nucl. Mater.; 36: 244-7 (Aug 1970). (In German).

Creep studies were made on UO_2 with a relative theoretical density of 95 ± 1%. The creep rate for a fission rate of 2.5×10^{14}f/cm³ · sec and a pressure load of 2 kp/mm² was estimated at about 1×10^{-4}/hr. The effects of fission rate and temperature were studied. The irradiation dependence of creep rate increased with increasing temperature. (M.C.G.)

4894 POSTIRRADIATION OBSERVATIONS OF SODIUM-BONDED (U,Pu)C FUELS. Levine, P. J. (Westinghouse Advanced Reactors Div., Madison, Pa.); Harbourne, B. L.; Biancheria, A.; Latimer, T. W.; Neimark, L. A. Trans. Amer. Nucl. Soc.; 13: 606-7(Nov 1970).

From Meeting of the American Nuclear Society, Washington, D. C. See CONF-701102.

Plastics and Other Materials

Refer also to abstracts 4109, 4175, 4249, 4764, and 5990.

4895 METHOD OF RESTORING CRYSTALS DAMAGED BY IRRADIATION. Mayer, James W.; Marsh, Ogden J. (to Hughes Aircraft Co.). U. S. Patent 3,533,857. 13 Oct 1970. Filed 29 Nov 1967.

Silicon crystals damaged by particle irradiation are restored by annealing at lower temperatures than heretofore, by irradiation simultaneous with the annealing process. (auth)

4896 APPLICABILITY OF THE RADIOGAUGES FOR MEASURING THE DENSITY OF THE FLOWING SOLID–LIQUID MIXTURES. Korbel, K. (Inst. of Nuclear Physics, Krakow). Isotopenpraxis; 6: 222-4(Jul 1970).

The accuracy density measurements for flowing unhomogeneous solid–liquid mixtures by means of radiogauges is discussed. Based on results obtained in investigations being performed with use of the radiometric measuring methods. (auth)

XUM

PHYSICS (GENERAL)

Astrophysics and Cosmology

Cosmic Ray Exposure Ages

Refer also to abstract 4048.

Stars

Refer also to abstract 5419.

4897 MASS EXCHANGE IN BINARY STARS. Plavec, Miroslav (Ohio State Univ., Columbus). Publ. Astron. Soc. Pac.; 82: 957-95(Oct 1970).

The semidetached eclipsing binaries (similar to Algol) seem to contradict the theory of stellar evolution, since the less massive components appear to be more evolved. Besides, they are overluminous, fill their critical Roche lobes, and tend to lose mass. All these facts can be explained in terms of a large-scale mass exchange which interchanged the roles of the components. This successful interpretation of the Algol systems shows that the Roche limit plays an important role in the evolution of binary stars. If so, then mass exchange must occur in practically all eclipsing and spectroscopic binaries, and perhaps even in some visual binaries. The outcome of the process depends mainly on the physical constitution of the mass-losing component. Its final stage is a helium star or a white dwarf. It is hoped that mass exchange can explain a number of peculiar objects such as the Wolf–Rayet stars, novae, U Germinorum stars, and shell stars or at least some of them. (auth)

4898 PHOTOMETRY OF VISUAL BINARIES. McNamara, D. H.; Langford, W. R. (Brigham Young Univ., Provo, Utah). Publ. Astron. Soc. Pac.; 82: 1022-5(Oct 1970).

Photometric observations of the integrated light of 36 visual binaries are presented. The photometric indices are used to calculate intrinsic (b−y) values. A comparison of the observed (b−y) values with the intrinsic (b−y) values shows that binary stars do not introduce large systematic errors in color-excess determinations. (auth)

4899 SEARCH FOR ^{26}AlH IN THE SPECTRA OF TECHNETIUM STARS. Branch, David; Peery, Benjamin F. (Carnegie Institution of Washington, D. C. California Inst. of Tech., Pasadena, Calif.). Publ. Astron. Soc. Pac.; 82: 1060-4(Oct 1970).

The presence of unstable, long-lived ^{26}Al has been sought in the spectra of the long-period variable R Andromedae (S6,6e) and the irregular variable carbon star 19 TX Piscium (C6,2). The spectra of both stars show technetium. No isotope shift was found in the absorption lines of AlH and it was concluded that $^{26}Al/^{27}Al < 1/7$. (auth)

4900 THREE ECLIPSING BINARIES FOUND SPECTROSCOPICALLY. Bond, Howard E. (Louisiana State Univ. Observatory, Baton Rouge. Cerro Tololo Inter-American Observatory, La Serena, Chile). Publ. Astron. Soc. Pac.; 82: 1065-9(Oct 1970).

Six southern stars with diffuse or double lines noted on objective-prism plates were observed photoelectrically. HD 101799, HD 120734, and HD 123732 were found to be W Ursae Majoris systems, with periods of 0.37, 0.34, and 0.39 days, respectively. Four-color photometry of HD 120734 and HD 123732, if interpreted conventionally, indicates moderate metal deficiencies for these systems. (auth)

4901 PHOTOELECTRIC OBSERVATIONS OF NOVA SERPENTIS 1970. Borra, Ermanno F.; Andersen, Per H. (Univ. of Western Ontario, London). Publ. Astron. Soc. Pac.; 82: 1070-6(Oct 1970).

Thirty nights of observations in three color indices were obtained from shortly after maximum until the nova faded to magnitude 11.6 in the V band. The similarity of the light curve to that of XX Tauri is discussed. An estimate of the distance of the nova is given based on the decay time of the light curve. (auth)

4902 UBV PHOTOMETRIC STUDY OF IQ PERSEI. Hall, Douglas S. (Vanderbilt Univ., Nashville); Gertken, Richard H.; Burke, Edward W. Jr. Publ. Astron. Soc. Pac.; 82: 1077-92 (Oct 1970).

About 400 UBV photoelectric observations were obtained for IQ Persei, an eclipsing binary with a visual companion. The period, heretofore unknown, was found to be 1.7435673d. The primary eclipse is annular, and the secondary is total but displaced, falling at 0.542P. With the assumption of $x_1 = x_2 = 0.6$, a solution was secured that satisfactorily represented all three light curves. There were no photometric complications. The (U−B) and (B−V) of the hot component are consistent with a spectral type of B7 reddened by $E_{B-V} = 0.15$m. The (U−B) and (B−V) of the visual companion are consistent with a spectral type of A1 ± 1 if the same amount of reddening is assumed. Both photometrically inferred spectral types are in agreement with Meisel's (1968) spectral classifications. From the ratio of the depths of the two eclipses the spectral type of the cool component was found to be A2 ± 2. The differences in V among the three stars are consistent with the supposition that all three are main-sequence stars at the same distance. It would be worthwhile to obtain the spectroscopic orbital elements, to perform a least squares determination of the limb-darkening coefficients by the method of differential corrections, and to verify the predicted 70-year apsidal motion period. (auth)

4903 LIGHT VARIATION OF EM CEPHEI. Johnston, Kenneth (Georgetown Coll. Observatory, Ky.). Publ. Astron. Soc. Pac.; 82: 1093-1110(Oct 1970).

The light variation of EM Cephei was studied photoelectrically with an intermediate-band filter centered at Hβ. The period of the eclipsing binary, which consists of two early B-type stars, was found to be 0.806277d. From an analysis of the light curve and variations in this light curve, EM Cep probably consists of a contact system that is undergoing mass transfer between its component stars. (auth)

4904 RADIAL VELOCITY OBSERVATIONS OF μ^1 BOOTIS. Niehaus, R. J.; Scarfe, C. D. (Univ. of Victoria, B. C.). Publ. Astron. Soc. Pac.; 82: 1111-18(Oct 1970).

Thirty-eight coudé and 38 Cassegrain spectrograms of μ^1 Bootis obtained between 1963 and 1969 were measured for radial velocity. The data did not support Abt's (1965) orbital elements. Indeed, statistical tests revealed no evidence for variability in the radial velocity of the star whether the period is long or short. The velocities were found to scatter in a random manner about a mean value of −13 ± 2 km/sec. The large standard error arises chiefly from uncertainties in the adopted stellar wavelengths. (auth)

4905 MASS FUNCTIONS OF BINARIES WITH GIANT PRIMARIES. Scarfe, C. D. (Univ. of Victoria, B. C.). Publ. Astron. Soc. Pac.; 82: 1119-32(Oct 1970).

Data from the Sixth Catalogue of Spectroscopic Binary Orbits were collected for those binaries with giant primaries that are well separated from their companions. On the assumption that the primary is always more massive than its companion, the mean mass of the primary was found to be greater than one solar mass. The distribution of mass functions was very different from that predicted by means of a fixed mass ratio and a random distribution of orbit orientations. This distribution and the rarity of double-line binaries with giant primaries lead to the conclusion that companions of substantially lower mass than their primaries are common. (auth)

4906 NATURE OF BD + 17° 4708. Cohen, Judith G.; Greenstein, Jesse L. (Carnegie Institution of Washington, D. C. California Inst. of Tech., Pasadena). Publ. Astron. Soc. Pac.; 82: 1152-6(Oct 1970).

Oke, Greenstein, and Gunn (1966) called the G0 star BD + 17°4708 a field horizontal-branch star. They determined its effective temperature to be 6000°K and its surface gravity as log g = 3.0. In his study of field horizontal-branch stars, Newell (1969) found BD + 17°4708 to be the reddest such star, and it occupied a critical position in his plot of θ_e vs. log g, serving to separate more clearly the groups he calls disk horizontal-branch and halo horizontal-branch stars. It is the purpose of this note to indicate that BD + 17°4708 is a G subdwarf, possibly slightly evolved, rather than a field horizontal-branch star. (W.D.M.)

4907 NOTE ON THE LIGHT VARIATION OF GAMMA CORONAE BOREALIS. Tippets, R.; Wilcken, S. K. (Brigham Young Univ., Provo, Utah). Publ. Astron. Soc. Pac.; 82: 1156-7(Oct 1970).

Observations of γ Cr B made in yellow light, relative to θ Cr B, were obtained on July 7 and 12, 1970 with the 24-inch reflector at BYU. A refrigerated 1P21 photomultiplier and five ten-second integrations per observation were used. The differential magnitudes in the sense of θ Cr B minus γ Cr B are displayed and small differential magnitude corrections for atmospheric extinction were applied to the data points. (W.D.M.)

XUM

4908 NEAR-INFRARED SPECTRUM OF VY CANIS MAJORIS. Humphreys, Roberta M. (Vanderbilt Univ., Nashville. Cerro Tololo Inter-American Observatory, La Serena, Chile). Publ. Astron. Soc. Pac.; 82: 1158-61(Oct 1970).

The absorption-line spectrum of the peculiar star VY Canis Majoris shows a general line weakening in the near infrared. The veiled appearance of the absorption spectrum causes VY CMa in the near infrared to appear less luminous than a normal M supergiant. Continuous infrared emission may be responsible for the weakened absorption spectrum. New radial velocity measurements for the emission and absorption lines are given. (auth)

4909 RECENT SPECTROGRAM OF AG CARINAE. Humphreys, Roberta M. (Vanderbilt Univ., Nashville). Publ. Astron. Soc. Pac.; 82: 1161-5(Oct 1970).

A spectrogram of AG Carinae, a P Cygni-like star, obtained in February 1970 at Cerro Tololo shows considerable change from the spectrum shown by Bond and Landolt (1970) obtained just two years before. The mean velocity of the absorption relative to the emission components of the P Cygni profiles is 230 km/sec. (auth)

4910 INTERCOMPARISON OF THREE SPECTROSCOPIC LUMINOSITY CRITERIA. Lutz, Thomas Edward. Urbana, Ill.; Univ. of Illinois (1969). 96p. University Microfilms Order No. 70-13,403.

Thesis.

Visual binary stars were utilized to estimate the external errors of and systematic differences between three luminosity systems: 1) the K-line absolute magnitude system of Wilson and Bappu; 2) a line-ratio luminosity system which is developed here; and 3) Petrie's revised H_γ luminosity system. (TSS) (Diss. Abstr. Int., B)

4911 HELIUM CORE FLASH HYDRODYNAMICS. Tomasko, Martin George. Princeton, N. J.; Princeton Univ. (1969). 41p. University Microfilms Order No. 70-14,245.

Thesis.

The importance of hydrodynamical effects during the helium core flash phase of stellar evolution is investigated in two parts. First, the cores of hydrostatically computed stellar models at the peak of the helium flash are shown to be pulsationally stable having periods of approximately 30 seconds and damping times of from about 20 to more than 100 periods depending on peak flash height. This may indicate that hydrodynamical effects generally do not greatly alter the course of the flash. Second, the hydrodynamical consequences for the outer regions on the star are investigated based on the assumption that the core flash follows previous hydrostatic computations. Linearized numerical computations of the traveling wave launched by the expansion of the core occurring during the flash indicate that the wave loses most of its energy by lifting the passed over material to a new hydrostatic equilibrium, and can lead to a loss of less than some 10^{-5} of the star's mass when it reaches the surface. It is concluded that unless other effects result in a change of the basic time scale for the helium core flash, hydrodynamical effects seem unlikely to substantially alter post-flash evolution from that indicated by previous hydrostatic computations. (Diss. Abstr. Int., B)

4912 STELLAR ATMOSPHERES. Mihalas, Dimitri. A Series of Books in Astronomy and Astrophysics. San Francisco; W. H. Freeman and Company (1970). 475p. $16.00.

In this graduate-level textbook and monograph, the theory of radiative transfer is used to describe the flow of energy through the stellar atmosphere and to predict the spectrum emergent from the surface of the star. The main emphasis is on current theoretical developments, although a thorough account of the classical work is also given to provide background information. (W.D.M.)

4913 SPECTROSCOPIC ASTROPHYSICS. An Assessment of the Contributions of Otto Struve. Herbig, G. H. (ed.). Berkeley, Calif.; University of California Press (1970). 468p. $10.00.

Ten areas in which Struve either pioneered or made contributions of lasting significance are introduced directly from the pages of the original journals. Then, each area is taken up by a leading specialist who discusses the field as Struve left it, where it stands today, and where it may go next. (W.D.M.)

4914 NUCLEOSYNTHESIS IN STARS. Clayton, Donald D. (Rice Univ., Houston, Tex. Inst. of Theoretical Astronomy, Cambridge, Eng.). pp 21-39 of Proceedings of the 11th International Conference on Cosmic Rays, Budapest, 25 August-4 September, 1969. /Bozoki, G. (ed.). Budapest; Central Research Inst. for Physics (1969).

See CONF-690814.

The quantitative success of the theory that the elements owe their origin and natural abundances to thermonuclear reactions in stars has increased remarkably in the past two years. A brief survey of the overall picture is presented, followed by a detailed account of recent theoretical success in the region $10 \leq z \leq 28$. Gamma-ray astronomy now offers a possibility not only for confirming the theory, but of measuring the history of nucleosynthesis within the Universe as well. (21 references) (auth)

Quasi-Stellar, Radio, and X-Ray Sources

Refer also to abstracts 4920 and 4978.

4915 (LA-4542) PROPOSAL FOR THE DETECTION OF MOTHER MOLECULES IN COMETS BY THEIR MICROWAVE LINES. Huebner, Walter F. (Los Alamos Scientific Lab., N. Mex.). Oct 1970. Contract W-7405-eng-36. 37p. Dep. NTIS.

A general proposal is made for radio detection of molecular transitions in comets. The importance of detecting cometary molecules is outlined and past attempts to observe comets with radio telescopes are discussed briefly. Relevant points for choice and observation of a comet and selection of a radio telescope are summarized. Tables of pertinent data for interesting molecules with known transitions in the microwave range are suitably prepared for rapid access when a specific proposal for observation of a selected comet is to be made. (auth)

4916 UBV OBSERVATIONS OF 3C 273. III. Burkhead, Martin S.; Lee, Vincent J. (Indiana Univ., Bloomington). Publ. Astron. Soc. Pac.; 82: 1150-2(Oct 1970).

UBV observations of 3C 273 for 1970 are presented. The observations were obtained with the same equipment, techniques, and comparison stars as reported by Burkhead and Parvey (1968). The data indicate that the visual magnitude of 3C 273 was rather erratic with a total variation of about 0.1 magnitude. (W.D.M.)

4917 MASERS IN SPACE. Turner, B. E. (National Radio Astronomy Observatory, Green Bank, W. Va.). Publ. Astron. Soc. Pac.; 82: 996-1021(Oct 1970).

Of the seven molecules presently detected at radio wavelengths in the interstellar medium, OH and H_2O display spectacular emission properties attributed to maser action. The OH masers fall into three distinct classes, each of which is anomalously excited by a different pumping mechanism. Far-ir radiative pumping is applied to recent observations of anomalous OH emission in dust clouds. The excitation of OH by the collisional dissociation of water vapor is described and is shown to explain recent observations of microwave emission from excited states of OH. It also explains why the type of OH emission that it produces (Class I) is observed to occur in the same regions as anomalous H_2O emission. A pumping mechanism for the H_2O is also described which is expected to operate in any regions in which Class-I OH emission occurs. (auth)

4918 RADIO-ASTRONOMY OBSERVATIONS AT A FREQUENCY OF 35 GHz. Braun, Lorne David. Toronto; Univ. of Toronto (1968).

Thesis.

In 1965 a 35-GHz radio astronomy observational program was begun, utilizing the 10-meter radio telescope and then the newly completed 46-meter telescope at the Algonquin Radio Observatory. The antennas had not previously been used at frequencies above 6.6 and 10.6 GHz, respectively, so one of the principal aims of the program was to evaluate the performance of the antennas at 35 GHz. A further aim was to observe as wide a variety of radio sources as possible, including extended sources that could be resolved by the one-arc-minute beam of the 46-m antenna. The characteristics of the receiver and of the antennas are discussed as well as the problems and limitations involved in high-frequency radio observations. The planets Venus, Jupiter, and Saturn were observed as well as a variety of quasi-stellar sources, several galaxies and two H II regions. The source list includes 3C 84, 3C 120, 4C 39.25, 3C 273, 3C 345, VRO 42.22.01, 3C 446, 3C 454.3, DR 21, and NGC 7027. In addition, the supernovae remnants Taurus A and Cassiopeia A were mapped with the one-arc-minute beam of the 46-m antenna. (Diss. Abstr. Int., B)

4919 ABSORPTION LINES OF QUASI-STELLAR OBJECTS. Burbidge, E. Margaret; Lynds, C. Roger. Sci. Amer.; 223: No. 6, 22-9(Dec 1970).

Emission lines in the spectra of quasars are enormously shifted toward the red. Absorption lines in some of the spectra, however, are shifted by different amounts. An attempt is made to elucidate these variations in the absorption redshift. (W.D.M.)

XUM

Solar Phenomena

4920 (CSIRO-Trans-9897) INVESTIGATION OF CIRCUM-SOLAR PLASMA BY PULSAR TRANSLUCING. Vetkevich, V. V. Translated by M. A. Hintze (Commonwealth Scientific and Industrial Research Organization, Melbourne, Australia), from Astron. Tsirk.; No. 477, 1-2(Aug 1968). 4p. Dep. NTIS (U. S. Sales Only).

Mean electron concentrations and time lag of longer waves in relation to shorter ones for pulsars can be determined by the translucing method. The position of CP 0950 relative to the Sun is considered best suited for investigation. (Australia)

4921 ORIGIN AND DYNAMICAL EVOLUTION OF THE SOLAR SYSTEM. Hills, Jack Gilbert. Ann Arbor, Mich.; Univ. of Michigan (1969). 175p. University Microfilms Order No. 70-14,544.

Thesis.

It is shown that if the specific energy and angular momentum of the solar nebula have been conserved in the planets, the solar nebula could not have extended more than 11 AU from the Sun, which suggests that the three outermost planets were ejected into their present orbits by encounters with the inner planets. A model is developed for the growth of the planets in the solar nebula. This has for one of its consequences Jupiter and Saturn being the outermost planets to form in the nebula. This again suggests the dynamical evolution of planets after their formation. (TSS) (Diss. Abstr. Int., B)

4922 EARLY SOLAR SYSTEM ABUNDANCES OF ^{129}I AND ^{244}Pu FROM ANALYSIS OF XENON IN NEUTRON-IRRADIATED METEORITES. Podosek, Frank Anthony. Berkeley, Calif.; Univ. of California (1969). 72p. University Microfilms Order No. 70-13,137.

Thesis.

The results of mass-spectrometric analyses of the xenon released in several stages of heating of a group of neutron-irradiated meteorites are reported. Analysis of meteoritic xenon is useful for many reasons, but the primary interest here is the information such experiments provide about the early solar system abundances of two extinct radioactivities: ^{127}I (17 million year half-life) and ^{244}Pu (82 million year half-life), both of which decay to isotopes of xenon. The neutron-irradiation also produces isotopes of xenon from ^{127}I and ^{235}U present in the meteorite. Since ^{129}I and ^{127}I occupy the same crystal lattice sites, their xenon decay products will be released in constant proportion, at least from the more gas-retentive mineral locations. The initial abundance ratio $^{129}I/^{127}I$ can then be determined from isotopic ratio correlations, a method which is in several respects superior to separate measurements of total radiogenic ^{129}Xe and total ^{127}I. The same remarks apply to the determination of the abundance ratio $^{244}Pu/^{238}U$, although less forcefully, since plutonium and uranium have similar but not identical chemical behavior. Both abundance ratios are useful in considering the processes and chronology of nucleosynthesis and formation of meteorite parent bodies. The $^{129}I/^{127}I$ ratio is particularly valuable in establishing the relative formation times of various meteorites. The average value of the $^{129}I/^{127}I$ ratio is about 1×10^{-4}, indicating an interval of 60 to 200 million years between isolation of the solar nebula and formation of parent bodies, depending on the model of nucleosynthesis. Previously published data from similar experiments are examined and the $^{129}I/^{127}I$ ratio computed in the same way as for the data presented here. The relevance of iodine–xenon dating to theories of nucleosynthesis, early solar system chronology, and theories of meteorite parent body formation is discussed. Because of the longer half-life and the fact that ^{244}Pu cannot be produced locally within the solar system, the abundance ratio $^{244}Pu/^{238}U$ is important in considerations of the modes and chronology of galactic nucleosynthesis. For St. Severin, $^{244}Pu/^{238}U = 0.0127 \pm 0.0026$ at the onset of xenon retention. This value is compared to other values obtained by different means. (TSS) (Diss. Abstr. Int., B)

4923 SOLAR CYCLE VARIATION OF SOFT X-RAY EMISSION. Kreplin, Robert W. (Naval Research Lab., Washington, D. C.). Ann. Geophys.; 26: 567-74(Apr-Jun 1970).

X-ray monitoring of the Sun by the NRL Solrad Satellites has provided nearly continuous records from which the daily average emission levels in the bands 44 to 60 Å, 8 to 20 Å, and 1 to 8 Å have been obtained since January 1964. These records show increases of a factor of 20 in the 44 to 60 Å band between solar minimum in 1964 and solar maximum in 1969. For the same period an increase of a factor of 200 has been observed in the 8 to 20 Å band. Short-term fluctuations are observed to correspond to the presence of active regions on the disk. The x-ray emission history of one such region, McMath 8207, is examined in detail and it is seen that the emission levels vary with complexity of the magnetic fields of the spot group. Observation of x-ray emissions $1\frac{1}{2}$ days prior to the appearance of the active region on the limb indicates emission from altitudes as great as 50,000 km in the lower corona. (tr-auth) (France)

4924 SOLAR X RADIATION BELOW 25 A. Pounds, K. A. (Univ. of Leicester, Eng.). Ann. Geophys.; 26: 555-65(Apr-Jun 1970).

Much new solar x-ray data has been derived from a variety of rocket and satellite experiments in the last three or four years. The more-important results are reviewed and discussed in terms of the extremely hot and dense plasmas, which apparently are a common feature of the active corona. The correlation of x radiation with other indices of solar activity often used in diagnostic studies of the upper atmosphere, such as Hα flares, calcium plages, and microwave emission, is discussed. (tr-auth) (France)

4925 EXTREME ULTRAVIOLET SOLAR SPECTRUM AND ITS VARIATION DURING A SOLAR CYCLE. Hinteregger, H. E. (Air Force Cambridge Research Labs., Bedford, Mass.). Ann. Geophys.; 26: 547-54(Apr-Jun 1970).

Previously published data on the spectral intensity distribution of incident solar radiation in the range from about 1800 to 30 Å are re-examined in the light of results from more recent rocket and satellite experiments. Strictly applicable only to specific flight dates (generally conditions of a nonflaring Sun at a medium activity), these results are used to compose a reference table of solar x and ultraviolet fluxes recommended for aeronomical models for medium solar activity (say for $F_{10.7cm} \sim 130 - 170 \times 10^{-22} Wm^{-2}Hz^{-1}$). These fluxes should not be adopted without revision of previously recommended data for the past solar minimum. The aeronomical needs for an improved experimental program of absolute solar xuv spectrophotometry are re-emphasized. (tr-auth) (France)

4926 MAGNETIC STRUCTURE OF INTERPLANETARY SPACE. Ness, Norman F. (Goddard Space Flight Center, Greenbelt, Md.). pp 41-83 of Proceedings of the 11th International Conference on Cosmic Rays, Budapest, 25 August–4 September, 1969. /Bozoki, G. (ed.). Budapest; Central Research Inst. for Physics (1969).

See CONF-690814.

A brief summary and over-all view of the present understanding of the interplanetary magnetic field structure are presented. The field is discussed in terms of its micro-, meso-, and macrostructure. (60 references) (W.D.M.)

4927 SOLAR PARTICLES AND RELATED SOLAR PHENOMENA. Anderson, K. A. (Univ. of California, Berkeley). pp 315-39 of Proceedings of the 11th International Conference on Cosmic Rays, Budapest, 25 August–4 September, 1969. /Bozoki, G. (ed.). Budapest; Central Research Inst. for Physics (1969).

See CONF-690814.

Since the greatest development in the subject of solar cosmic rays and related solar phenomena over the last two years has been in the electron component and the lower energy fluxes, this summary report concentrates on those aspects of the subject. The discussion is presented in terms of energetic particles in the solar atmosphere, particle emission into interplanetary space by solar flares, and propagation of solar particles. (37 references) (W.D.M.)

4928 NUCLEAR PARTICLE DETECTION SYSTEM (NPDS) RESPONSE ANALYSIS. Liley, B. (North American Rockwell Corp., Downey, Calif.). Trans. Amer. Nucl. Soc.; 13: 451-2 (Nov 1970).

From Meeting of the American Nuclear Society, Washington, D. C. See CONF-701102.

Galaxies

4929 (N-70-33057) DYNAMICAL EVOLUTION OF DISK GALAXIES. Hohl, Frank (National Aeronautics and Space Administration, Langley Station, Va. Langley Research Center). Jul 1970. 110p. (NASA-TR-R-343; L-7110). NTIS.

A computer model for isolated disks of stars is presented and is used to study the self-consistent motion of large numbers of point masses as they move in the plane of the galactic disk. Most disks investigated were found to be unstable against slowly growing long-wavelength modes, and after about two rotations the disks tended to assume a bar-shaped structure. It was also found that the final mass distribution for most disks could be closely approximated by an exponential variation irrespective of the initial mass distribution. To study the development of spiral structure, the model was modified to include a fixed central force similar to that in the Schmidt model of the Galaxy. The mass of the stars

in the disk was taken to be from 5 to 50% of the total mass of the Galaxy. The evolution of a number of initial distributions of the stars was investigated. Results of the calculations gave a velocity dispersion for the disk stars that was about 50% larger than the value of about 30 km/sec found from observation of stars in the solar neighborhood. For some of the disks investigated, a pronounced spiral structure remained even after 8.5 rotations. (auth) (STAR)

4930 FAINT BLUE OBJECTS IN cD CLUSTERS OF GALAXIES. Sastry, Gummuluru N. (Wesleyan Univ., Middletown, Conn.). Publ. Astron. Soc. Pac.; 82: 1051-9(Oct 1970).

During a study with Palomar Sky Survey print and plate reproductions of the distribution of galaxies in clusters associated with supergiant (cD) galaxies, a number of "blue objects" were found. A preliminary survey of these blue objects suggests that there is a definite tendency for them to cluster around radio-cD galaxies. (auth)

4931 DIAMETER–LUMINOSITY RELATION AND DISTANCE OF THE VIRGO GALAXY CLUSTER. Heidmann, Jean (Observatoire de Paris, Meudon, France). Compt. Rend., Ser. B; 271: 658-60(28 Sep 1970). (In French).

New corrections taking into account inclination and absorption effects on the magnitudes and apparent diameters of galaxies were introduced into the relation between the diameter (A) and the optical luminosity (L) of spiral galaxies. The study of the spirals of the Virgo cluster showed the relation $L = kA^{2.6\pm0.1}$ with a correlation coefficient of −0.975 on a 4.5 magnitude scale. The precision of this relation for measuring distances is comparable to other methods and this relation may be used over a large range. When calibrated with six close spirals of known distances, a distance modulus of 30.7 ± 5 was obtained for the spirals of the Virgo cluster. (France)

Cosmology

4932 COSMIC DENSITY. Noonan, Thomas W. (Brockport State Coll., N. Y.). Publ. Astron. Soc. Pac.; 82: 1038-50(Oct 1970).

An assumption regarding the randomness of the selection of galaxies in a redshift catalog is used to bypass the need for a specific luminosity function in arriving at the mean cosmic density. Application of the method to the Humason–Mayall–Sandage catalog, with the use of published mass–luminosity ratios, gives a mean density of $(11 \pm 6) \times 10^{-31}$ gm cm^{-3}. A by-product of the analysis is the denial of the principle that outlying galaxies near a cluster, which show the same average redshift as the cluster, are cluster members. (auth)

4933 RELATIVITY AND THE QUESTION OF DISCRETIZATION IN ASTRONOMY. Edelen, Dominic G. B.; Wilson, Albert G. Springer Tracts in Natural Philosophy, Volume 20. New York; Springer-Verlag, New York, Inc. (1970). 198p. $10.50.

This volume approaches the problem of large-scale discretization through mathematical modeling of an entitation process of importance in the theory of levels: The derivation of the large-scale properties of an aggregate when the local properties of the constituent elements are known. Topics discussed include the environment for cosmic structures, equilibrium theory of galactic isopleths, galactic morphology and scale, observational problems of macroscale discretization, and observational evidence for discretization phenomena. (W.D.M.)

4934 EXTRAGALACTIC RADIO SOURCES IN UNIFORM MODEL UNIVERSES. Ringenberg, Richard Ray. Urbana, Ill.; Univ. of Illinois (1969). 101p. University Microfilms Order No. 70-13,456.

Thesis.

Several formulae are derived in zero-pressure uniform model universes. These formulae pertain to the distribution of extragalactic radio sources in space. The source count formula, which applies in any model universe, is derived. The sources have an arbitrary dispersion in luminosity and a general evolution function. Several additional theoretical relationships are then worked out. These give the formulae for the background radiation, the background radiation of certain classes of sources, the confusion noise, the luminosity distribution, and the fraction of distant sources in certain regions in flux density. Observational data are introduced and previous analyses of the source counts are examined. It is then shown that it is possible to find solutions for the evolution function for certain types of evolution. These solutions are expressed in terms of several cosmological quantities, some of which are known, and some only roughly known from observation. Numerical solutions are found by computer using the most probable value of the known quantities and several values of some of the lesser known quantities. Once numerical solutions for the evolution function are found, several auxiliary calculations are made which relate to other observable quantities. The errors and uncertainties and the conclusions resulting from the calculations are discussed. (Diss. Abstr. Int., B)

Planetary Phenomena

4935 (ORNL-TM-3131) RESEARCH ON STIMULATED EXOELECTRON EMISSION FROM LUNAR MATERIALS. Gammage, R. B.; Becker, Klaus (Oak Ridge National Lab., Tenn.). 28 Aug 1970. Contracts W-7405-eng-26; NASA-T-90269. 33p. Dep. CFSTI.

Preliminary results on the thermally stimulated exoelectron emission (TSEE) from Apollo 12 fines and rocks show little emission from virgin materials, but intense TSEE at various temperatures between ~130 and ~550°C can be induced by (a) oxidation of the surface, (b) adsorption of O_2, and perhaps (c) the release of trapped solar wind. The TSEE characteristics of differently treated samples are a sensitive indicator of changes occurring on the surface and have, therefore, been studied in some detail. Further experimental plans are outlined. (auth)

4936 IONIZATION PROCESSES IN THE ATMOSPHERES OF VENUS AND MARS. McElroy, Michael B. (Kitt Peak National Observatory, Tucson, Ariz.). Ann. Geophys.; 26: 643-52(Apr-Jun 1970).

Physical and chemical processes in the upper atmospheres of venus and Mars are reviewed with special emphasis on processes which affect the height distribution of ionization. The Venus ionosphere below 200 km is adequately accounted for by a photochemical equilibrium theory if the neutral atmosphere in this height range is dominated by CO_2. Light constituents such as H_2, He, or O are required to account for the ionization observed at higher altitudes. The ionosphere terminates rather abruptly above 500 km, presumably due to an interaction with the solar wind. The precise mechanism for this interaction is not yet understood. Interpretation of the observed Martian ionosphere is controversial. One model invokes an interaction with solar wind, the consequence of which is a reduction in ionospheric scale height by an approximate factor of 2 over results derived with photochemical equilibrium. The exospheric temperature for this model is approximately 500°K at solar minimum. The second model favors an exospheric temperature of 250°K and accounts for the ionosphere on the basis of static photochemistry. A low exospheric temperature for Mars may be indicative of important dynamical effects in the upper atmosphere. Tidal motions in particular are expected to play a more important role for Mars than they do for either Venus or Earth. (tr-auth) (France)

Atomic and Molecular Physics

Atomic, Electron, Ion, and Molecular Beams and Their Reactions

Refer also to abstract 5155.

4937 (IS-T-380) ELECTRON ENERGY LOSS TO SURFACE EXCITATIONS IN THIN FILMS. Chase, Jay Benton (Ames Lab., Iowa). Nov 1970. Contract W-7405-eng-82. 144p. Dep. NTIS.

Thesis.

The energy lost by fast electrons passing through thin films is calculated using classical electrodynamics including retardation and a small scattering angle approximation. An energy-loss theory is developed for 25-keV electrons incident perpendicular to a film of LiF crystal described by a local dielectric function, $\epsilon = \epsilon(\omega)$. It is shown that a large loss peak occurs corresponding to the low-frequency surface phonon and that the high-frequency surface phonon is not observable in very thin samples. The energy loss distribution is integrated over appropriate scattering-angle and energy-resolution functions and compared to the experiment of Boersch, Geiger, and Stickel (Z. Phys., 212: 130(1968)). All the features of the experimental energy loss distribution are represented very well by the theory. The effects of using a poor conductor (amorphous carbon) as a film substrate are shown to be negligible. A nonlocal representation $[\epsilon = \epsilon(\vec{q},\omega)]$ must be used to describe the response of a metal to electromagnetic excitation. Assuming specular reflection of the electrons of the metal which strike the surface, a theory for the energy loss is developed in which the incident angle of the fast electron is arbitrary. Setting the denominator of the resulting energy loss distribution equal to zero yields equations for the surface plasmon dispersion relations.

XUM

The resulting dispersion curves are unusual in that they involve a complex frequency as a function of the wave vector. Surface plasmon dispersion curves are obtained for a variety of thicknesses, materials, and phenomenological relaxation times (damping factors). It is shown that the real part of the frequency, as a function of the component of the wave vector parallel to the film, $Q_\parallel$, has two different values for small wave vector (two nondegenerate modes). For such values of $Q_\parallel$, the dispersion relations can also be obtained using the local dielectric function. For large $Q_\parallel$, the real parts of the two modes become degenerate and exhibit pronounced nonlocal behavior. The real part of the frequency for large $Q_\perp$ is independent of the film thickness, in contrast to the imaginary part of the frequency (which gives the line width or mode lifetime). For very thin films (~100 Å) there is an oscillation of the line width as a function of $Q_\parallel$, which disappears as the thickness increases. (auth)

4938 PASSAGE OF ELECTRONS THROUGH MATTER. Baranov, V. F.; Pavlovskii, O. A. This paper was summarized in At. Energ. (USSR); 25: 317(Oct 1968) as paper No. 236. (In Russian).

The method of statistical trials is used to calculate the energy and angular distribution of electron radiation scattered in an aluminum barrier in the case of normal incidence of monoenergetic electrons on the barrier surface. For each initial electron energy E_0, which was equal to 0.4, 0.8, 1.0, 1.25, 1.5, and 2.0 MeV, the thickness d of the barrier was chosen equal to 0.05, 0.1, 0.15, 0.2, 0.3, 0.4, and 0.6 of the maximum range R_0 of electrons with an energy E_0. In the calculations it is assumed that the energy losses of the electrons in the substance are determined by the Bethe–Bloch relationship, and that the probability of elastic scattering at a specified angle on an elementary segment of the path traversed in the substance is given by the Moliére relationship; the bremsstrahlung energy losses and the spread in the energy losses are neglected. (M.H.R.)

4939 ANISOTROPY IN EJECTION PATTERNS DUE TO GENERATION OF FOCUSING COLLISIONS BY CHANNELED PARTICLES. Elich, J. J. Ph.; Roosendaal, H. E. (FOM-Instituut voor Atoom- en Molecuulfysica, Amsterdam). Phys. Lett.; 33A: 235-6(2 Nov 1970).

The ejection pattern of copper after bombardment by 20-keV Ne^+ under well-defined circumstances shows a structure that can be described in terms of momentum transferred to string atoms by channeled particles. (auth)

4940 CALCULATION OF PATH LENGTHS OF LIGHT IONS IN SOLID BODIES. Kessel'man, V. S. This paper was summarized in At. Energ. (USSR); 26: 60(Jan 1969) as paper No. 261. (In Russian).

In an earlier paper (At. Energ. (USSR), 24: 557(1968)) the author obtained analytic expressions for the calculation of the depth of penetration of ions into matter. These equations only gave a good description of the experimental results in the case of heavy ions, i.e., when $\mu = M_1/M_2 \ll 1$(M_1, M_2 are the mass of the ions and the stopping atom of the matter, respectively). In this case the mean path length $\bar{R}$ of the ion in the matter and the mean path length along the direction of the original motion (projective path) $\bar{R}_p$ are similar. The ratio R/R_p deviates particularly strongly from unity at large values of μ and small energies of the incident ion. Using the expressions for the stopping forces in elastic collisions obtained in the earlier paper, analytic expressions were found for the calculation of the path lengths of light ions, when $\mu \lesssim 7$. The results of calculations for ^{15}N ions in Ag and Au, according to the exact and the approximate formulas, are compared with various experimental results and it is shown that, even at high ion energies, $\bar{R}_p$ can be considerably smaller than $\bar{R}$. It is also demonstrated that, for $\mu \gg 1$, the expressions can be simplified and used for the calculation of the path length of protons. (L.M.T.)

4941 ATOMIC-BEAM DEFLECTION BY RESONANCE-RADIATION PRESSURE. Ashkin, A. (Bell Telephone Labs., Holmdel, N. J.). Phys. Rev. Lett.; 25: 1321-4(9 Nov 1970).

It is proposed to use the saturated value of the radiation pressure force on neutral atoms to produce a constant central force field to deflect atoms in circular orbits and make a high-resolution velocity analyzer. This is useful for studying the interaction of atoms with high-intensity monochromatic light, and to separate, velocity-analyze, or trap neutral atoms of specific isotopic species or hyperfine level. (auth)

4942 INTERPRETATION ERROR IN MOLECULAR BEAM EXPERIMENTS. Klavins, Andrew; Sentman, Lee H. (Univ. of Illinois, Urbana). Rev. Sci. Instrum.; 41: 1560-7(Nov 1970).

This study is concerned with the interpretation of the ionization gauge detector signal in a molecular beam experiment as a particular functional of the reflected molecule distribution function, called the nominal value of the detector signal. The detector configurations examined are those used to measure number density and time-of-flight velocity distributions. Expressions for the actual detector signals are established on the basis of the apparatus geometry; the nominal expressions are derived as approximations to the actual signal. Differences between these actual and nominal functionals are examined quantitatively, using the Nocilla reflection model. It is found that, in the density case, the significant apparatus parameter is the solid angle subtended at the detector by the illuminated target area. If this solid angle is large, the error introduced by assuming the detector signal to be represented by the nominal expression becomes significant when the reflection is highly anisotropic. In the velocity distribution measurement, the significant factor is the shutter function. For slow shutter speeds, differences between the actual and nominal expressions for the detector signal increase rapidly as the error in the time the shutter is open increases. (auth)

4943 INTERACTION OF LOW-ENERGY ATMOSPHERIC IONS WITH CONTROLLED SURFACES. Prince, Robert Harry. Toronto; Univ. of Toronto (1968).

Thesis.

The ejection of electrons associated with the Auger neutralization of N_2^+, H_2^+, and N^+ ions at the (100) face of a tungsten single crystal and a polycrystalline molybdenum surface was studied for the first time in the energy range 10 to 30 eV under controlled surface conditions. The dependence of the electron yields and energy distributions on ion energy was investigated in detail for the above ion–surface combinations. A detailed description is given of the ion beam used in these studies. The combination of ultrahigh vacuum techniques to lengthen the time required to reach adsorption equilibrium after flashing and special guarding and analog data-reduction techniques to reduce instrumentation time response permitted the study of transient adsorption effects as well as the more usual equilibrium studies. Surface structure was established by optical and electron-transmission microscopy and by x-ray back-diffraction. Surface contamination was inferred using the retarding-field diode technique, permitting measurement of the work function, which is sensitive to surface adsorption levels. The fact that the electron yields for diatomic ions are considerably lower than those for the inert gas ions treated by Hagstrum's theory led Propst and Lüscher to propose that the neutralized ion may be vibrationally excited as a consequence of the interaction. They suggested a qualitative procedure by which the inert-gas theory could be modified. In the present report, a quantitative calculation was performed in this low-energy regime for which kinetic broadening effects may be safely neglected. The simplified theoretical treatment provides good agreement with Propst and Lüscher's data for 50-eV N_2^+ ions on polycrystalline tungsten, using a value of the escape parameter f (the anisotropy of excited metal electrons) taken from Hagstrum's work. A slightly larger anisotropy permits good agreement with the present data for the (100) face of a tungsten single crystal, indicating a stronger focussing of electrons towards the surface normal, a result found by Hagstrum for the case of single-crystal semiconductor surfaces. This observation is further substantiated by data for the H_2^+ ion, which was chosen because of its great similarity to N_2^+. (Diss. Abstr. Int., B)

Atomic and Molecular Properties

Refer also to abstract 4063.

4944 RADIATIVE LIFETIME OF THE METASTABLE 2^1S_0 STATE OF HELIUM. Van Dyck, R. S. Jr.; Johnson, C. E.; Shugart, H. A. (Univ. of California, Berkeley). Phys. Rev. Lett.: 25: 1403-5(16 Nov 1970).

Two fixed, spatially separated detectors are used to measure the decay in flight of a cooled, thermal beam of pulsed metastable helium atoms. The preliminary value obtained for the radiative lifetime of the metastable 2^1S_0 state of helium is 20 ± 2 msec. (auth)

4945 AVERAGE ENERGIES OF GROUND, SINGLY, AND DOUBLY EXCITED CONFIGURATIONS IN HIGHLY IONIZED ATOMS, FOR ELECTRON NUMBERS N = 3 TO N = 46 AND ATOMIC NUMBERS Z = 6 TO Z = 92. Shadmi, Yehuda; Kastner, Sidney O. (Goddard Space Flight Center, Greenbelt, Md.). J. Chem. Phys.; 53: 4710-11(15 Dec 1970).

A calculation of the average energies of many configurations of spectroscopic interest is described briefly. A basis of orthogonalized screened hydrogenic radial functions was used. The energy of a "core" was calculated in zero-order approximation (electronic interactions included implicitly through the screening parameters), and the energy of all other electrons was calculated in first-order approximation (electronic interactions included explic-

itly as a perturbation). Configuration interactions and correlation energy contributions as well as relativistic contributions were not included. The detailed results will be published in a NASA report bearing the same title as this paper. (A.G.W.)

4946 BOUNDS FOR OSCILLATOR-STRENGTH SUMS FROM APPROXIMATE QUADRATURES. Yates, A. C.; Langhoff, P. W. (Indiana Univ., Bloomington). Phys. Rev. Lett.; 25: 1317-20(9 Nov 1970).

Rigorous upper and lower bounds are prescribed in the form of approximate quadratures for a variety of oscillator-strength sums. The required integration points and weights are determined from continued-fraction approximants and linear programming techniques, employing oscillator-strength moments as inputs to the method. Illustrative bounds are provided in the cases of atomic hydrogen, helium, and neon, for odd-integer sums and for the mean energies associated with stopping, straggling, excitation, and the Lamb shift. (auth)

4947 L-SHELL FLUORESCENCE IN ^{238}Pu. Byrne, J.; Beattie, R. J. D.; Benda, S.; Collingwood, I. (Univ. of Sussex, Brighton, Eng.). J. Phys., B (London); 3: 1166-74(Aug 1970).

The number F of ^{238}Pu L x rays per alpha disintegration of ^{242}Cm was determined using fast coincidence techniques. The result F = (9.70 ± 0.14)% is in accord with the one value previously reported. The disagreement between the measured values for the L_2 subshell yields in ^{240}Pu and ^{238}Pu is therefore not resolved and an explanation is suggested for the observed discrepancies. (auth) (UK)

4948 CORRELATED WAVE FUNCTIONS FOR THE GROUND STATE OF H^-, He, AND Li^+. Carlton, Terry S. (Oberlin Coll., Ohio). J. Chem. Phys.; 53: 4234-7(1 Dec 1970).

Energies are calculated variationally using a closed-shell orbital product times the correlation function $g_a = [1 + \lambda r_{12} + \mu(r_1 - r_2)^2 + \nu r_{12}^2(r_1 + r_2)^{-n}]^{\frac{1}{2}}$ (n = 1 or 2). Energy errors for H^-, He, and Li^+, respectively, are 0.00193, 0.00019, and 0.00021 a.u. when n = 1 and 0.00229, 0.00025, and 0.00064 a.u. when n = 2 or ν = 0. An explanation is proposed for the fact that g_a is much more accurate for He and Li^+ than for H^-, whereas the opposite is true for the correlation function $g_b = 1 + \lambda r_{12} + \mu(r_1 - r_2)^2$. For He, expectation values other than the energy are typically accurate to four figures. (auth)

4949 ELECTRIC POLARIZABILITY OF MOLECULAR HYDROGEN AS CALCULATED BY USE OF THE NONSYMMETRICAL WAVE FUNCTION. Saika, A. (Yeshiva Univ., New York); Musher, Jeremy I.; Ando, Toshihiko. J. Chem. Phys.; 53: 4137-40(1 Dec 1970).

The nonsymmetrical (NS) wave function was employed to calculate the static electric dipole polarizability of the hydrogen molecule. It has been found that the double perturbation calculations carried through first order in electron correlation give results much better than those by zeroth-order Hartree–Fock (HF) calculations and comparable to first-order HF results with much less labor. Thus it appears better to obtain corrections to a starting wave function, even if it is exceedingly crude, rather than to find the best possible zeroth-order approximation and stop there. (auth)

4950 HIGH-RESOLUTION STUDY OF THE He II 6560- AND 10124-A TRANSITIONS. Kessler, Ernest George Jr. Madison, Wis.; Univ. of Wisconsin (1969). 153p. University Microfilms Order No. 70-3579.

Thesis.

The first high-resolution study of the He II 6560-Å (n = 6 to n = 4) and 10124-Å (n = 5 to n = 4) line complexes as observed in a liquid-nitrogen-cooled hollow cathode was made with a pressure-scanned double Fabry–Perot spectrometer. All signals were photoelectrically detected and the data were digitally recorded and analyzed with a computer. The relative separations, relative intensities, line widths, and isotope shift of the more intense isolated components were measured. The theoretical component separations were confirmed to within 0.002 cm^{-1} for the best measured components. Lamb shifts for the 4S, 5S, and 6S levels for He II were determined from the measured separations of the components. The observed relative intensities were characteristic of a gas at low pressure: components arising from S and P states were considerably more intense than statistical theory predicts. The widths of the lines were appreciably greater than the widths of He II lines and the ionized-helium line profiles exhibited an extended wing. The data indicate that several processes were active in the excitation of the n = 5 and n = 6 levels including ionization–excitation of the neutral helium ground state, excitation of the helium ion ground state, and processes involving cascades from higher levels. A small anode drift shift was observed and attributed to a residual electric field in the discharge. The interferometric calibration of scanning polyetalon spectrometers was studied and perfected so that accuracies of 0.01% are now possible. Using the improved calibration system, scans of the He II 4686-Å (n = 4 to n = 3) transition were recorded with the primary objective of obtaining precise component positions. The measured positions confirm the quantum electrodynamic predictions. (Diss. Abstr. Int., B)

4951 MEASUREMENT OF THE $2^2S_{\frac{1}{2}}-2^2P_{\frac{1}{2}}$ ENERGY SEPARATION, (ΔE-S), IN HYDROGEN (n = 2). Shyn, Tong Wha. Ann Arbor, Mich.; Univ. of Michigan (1969). 94p. University Microfilms Order No. 70-14, 642.

Thesis.

The $2S_{\frac{1}{2}}-2P_{\frac{1}{2}}$ energy separation (ΔE-S) in the n = 2 state of atomic hydrogen was measured by an atomic-beam radio-frequency method. A beam of metastable atoms in the single hyperfine state β_A (F, m_F = 0,0) was used. The electric dipole transitions β_A – b(F,m_F = 1,+1) and β_A – d(F,m_F = 1,–1) were observed at fixed frequencies by sweeping the Zeeman magnetic field parallel to the beam axis. Measurements of the frequencies of the rf field used to drive the transitions and the magnetic fields at the line centers of the resonance curves along with theory of Zeeman splitting were used to determine the zero-field splitting (ΔE–S). The final value of the (ΔE–S) is 9911.250 ± 0.063 MHz where the quoted uncertainty is one average deviation from the mean. By using the average of the Lamb and Robiscoe experimental values of the Lamb shift, S_H = 1057.82(10) MHz, the value ΔE = (10969.070 ± 0.163) MHz was obtained. The corresponding value for α^{-1} is 137.0360 ± 0.0008. (Diss. Abstr. Int., B)

Positronium, Muonium, and Mesic Atoms and Molecules

Refer also to abstracts 5254, 5288, 5576, 5794, and 5866.

4952 (JINR–P4-5039) SLOW COLLISIONS IN THE SYSTEM OF THREE BODIES INTERACTING ACCORDING TO THE COULOMB LAW. IV. MESIC ATOM PROCESSES IN HYDROGEN. Matveenko, A. V.; Ponomarev, L. I. (Joint Inst. for Nuclear Research, Dubna (USSR)). 1970. 36p. (In Russian). Dep. NTIS (U. S. Sales Only).

A general approach, developed for solution of the problem of three bodies interacting according to the Coulomb law, was used for calculations of specific reactions involving μ^- mesons and the hydrogen isotopes. The cross sections and the constants of interception are obtained for μ^--meson transitions between hyperfine-structure levels and for the isotope exchange reactions $p\mu^- + d \rightarrow p + d\mu^-$, $p\mu^- + t \rightarrow p + t\mu^-$, and $d\mu^- + t \rightarrow d + t\mu^-$. The calculated results are compared with previous calculations and experimental data. (auth)

4953 ELECTRIC QUADRUPOLE TRANSITIONS IN MUONIC ^{208}Pb. Martin, P. (Coll. of William and Mary, Williamsburg, Va.); Miller, G. H.; Welsh, R. E.; Jenkins, D. A.; Powers, R. J. Phys. Rev. Lett.; 25: 1406-9(16 Nov 1970).

Electric quadrupole (4f → 2p and 3d → 1s) atomic transitions were observed in muonic ^{208}Pb. An identification based upon energy and relative intensity determination provides good agreement with theoretical predictions. (auth)

Collision Phenomena

4954 VIBRATIONAL EXCITATION OF A MORSE OSCILLATOR. Lin, Jeong-long (Boston Coll., Chestnut Hill, Mass.). J.Chem. Phys.; 53: 4567-74(15 Dec 1970).

Vibrational excitation in the system He + H_2 is studied theoretically by considering H_2 as a rotating Morse oscillator. The anharmonicity of molecular vibration is found to have only a small effect on the 0 → 1 transitions. Vibrational transition probabilities are also found to be insensitive to the rotational energy of the diatom. Following the approach of Mies and Shuler, based on the modified wave-number approximation, three-dimensional transition probabilities are calculated from one-dimensional results and the steric factor is obtained as a function of the collision energy. (auth)

4955 VARIATIONAL FORMULATION OF THE HARRIS EXPANSION TECHNIQUE. Kolker, H. J. (United Aircraft Research Labs., East Hartford, Conn.). J. Chem. Phys.; 53: 4697-4704(15 Dec 1970).

The Harris expansion technique for calculating elastic scattering phase shifts is studied within the context of the Kohn variational principle. It is shown that Harris' method is capable of yielding upper and lower bounds for the tangent of the phase shift. (auth)

4956 EXPERIMENTAL RELATIVE ELECTRON IMPACT CROSS SECTIONS FOR GROUP-III METAL ATOMS AND COM-

XUM

PARISON WITH THEORIES. Gingerich, Karl A. (Texas A and M Univ., College Station); Blue, Gary D. J. Chem. Phys.; 53: 4713-14(15 Dec 1970).

Measured values of the electron-impact ionization cross sections of Ga and In with respect to Ag and Al with respect to N_2 are reported. Comparison of these values with values calculated by two different methods shows that the experimental relative cross sections are consistently higher than the corresponding ones calculated by either method. Reasons for the discrepancies and suggestions for improving the agreement are discussed briefly. (A.G.W.)

4957 SCATTERING OF ATOMS OF HYDROGEN IN NOBLE GASES. Belyaev, Yu. N.; Kamyshov, N. V.; Leonas, V. B. (Moscow State Univ.). Khim. Vys. Energ.; 4: 260-2(May-Jun 1970). (In Russian).

On the basis of a study of the elastic scattering of a beam of H atoms by the noble gases, the interaction potentials of these atoms were obtained. The potentials found are used to calculate the mean logarithmic elastic losses of energy in the retardation of recoil T atoms in a substance. (auth)

4958 CALCULATIONS ON HIGH-ENERGY CHARGE TRANSFER WITH THE CONTINUUM DISTORTED-WAVE METHOD. Salin, A. (Observatoire de Paris, Meudon, France). J. Phys., B (London); 3: 937-51(Jul 1970).

The available theories of charge exchange in high-energy collisions are discussed. Attention is drawn to the utility of the continuum distorted-wave method of Cheshire (1963 and 1964). Results of calculations with this method are presented for electron capture by protons in atomic hydrogen and helium. (auth) (UK)

4959 GENERALIZED OSCILLATOR STRENGTHS FOR THE 1^1S yields 2^1S TRANSITION IN HELIUM BY ELECTRON IMPACT. Peresse, J.; Le Nadan, A.; Pochat, A. (Faculte des Sciences, Brest, France). Phys. Lett.; 33A: 317-18(16 Nov 1970). (In French).

Angular and energy dependences of generalized oscillator strengths were determined for the $1^1S \rightarrow 2^1S$ transition in helium in the range 35 to 150 eV for scattering angles between 0° and 20°. The results are compared with the theoretical oscillator strengths obtained by Kim and Inokuti. (auth)

4960 SPIN CONSERVATION IN IONIZING COLLISIONS BETWEEN He(2^3S_1) METASTABLE ATOMS. Schearer, L. D.; Riseberg, L. A. (Texas Instruments Inc., Dallas). Phys. Lett.; 33A: 325-6(16 Nov 1970).

By a direct observation of the electron density in a flowing afterglow, the spin dependence of the process $He(2^3S_1) + He(2^3S_1) \rightarrow He(1^1S_0) + He^+ + e$ was demonstrated. When the metastable He atoms are optically oriented, the process violates spin conservation, and a decrease of 5% in the electron density is observed. (auth)

4961 SOME INTERESTING ANOMALIES IN THE SCATTERING OF ELECTRONS FROM HELIUM. Labahn, R. W. (Louisiana State Univ., Baton Rouge). Phys. Lett.; 33A: 327-8(16 Nov 1970).

Elastic s-wave scattering of electrons from helium is examined in a single-channel open-shell calculation. The behavior of the phase shift about the resonance in this system at 73.5 eV as reported by Herzenberg and Lau is examined. (auth)

4962 δ-FUNCTION SCATTERING. MOLECULAR COLLISIONS. Locker, David J. (Vanderbilt Univ., Nashville). J. Chem. Phys.; 53: 4333-9(1 Dec 1970).

Molecular interactions are examined in which the intermolecular potential energy surface is approximated by a series of δ functions of appropriate integrated areas. The method is verified by comparisons with the results of other procedures. The δ-function technique is found to require little computation time even for potentials approximated by 60 δ functions. The dependence of flux conservation upon atomic masses is explored. The procedure is extended to include four-body collinear interactions. (auth)

4963 PRODUCTION OF POSITIVE IONS AND ELECTRONS IN COLLISIONS OF 1- TO 25-keV PROTONS AND HYDROGEN ATOMS WITH CO, CO_2, CH_4, AND NH_3. McNeal, R. J. (Aerospace Corp., El Segundo, Calif.). J. Chem. Phys.; 53: 4308-13 (1 Dec 1970).

Cross sections are reported for the production of slow, positive ions (σ_+) and electrons (σ_-) in collisions of 1- to 25-keV protons and hydrogen atoms with CO, CO_2, CH_4, and NH_3. For H^+ bombardment σ_- is the total ionization cross section and $\sigma_+ - \sigma_-$ is the total electron-capture cross section, σ_{10}. For H^0 bombardment σ_+ is a good approximation to the total ionization cross section. The results are compared with other results in different, overlapping energy ranges, and their application to the physics of planetary atmospheres is discussed. (auth)

4964 COLLISIONAL DEACTIVATION OF $H(2^2P)^*$ FLUORESCENCE. Braun, Walter (National Bureau of Standards, Washington, D. C.); Carlone, Cosmo; Carrington, Tucker; Van Volkenburgh, Gregg; Young, Robert A. J. Chem. Phys.; 53: 4244-8 (1 Dec 1970).

Collision cross sections for deactivation of $H^*(n = 2)$ at 300°K were measured by observations of the quenching of Lyman-α fluorescence in a discharge flow system. The quenchers (with cross section in Å²) are $H_2(84 \pm 8)$, $D_2(84 \pm 8)$, $N_2(62 \pm 6)$, He(<3). For $H^* + H_2$, less than 1% of the total quenching produces ions. Care has been taken to work with systems optically thin in Lyman-α so that the rate of escape of radiation, which is the reference to which the quenching rate is compared, is not reduced by resonance trapping. (auth)

4965 VELOCITY DEPENDENCE OF THE RELATIVE TOTAL CROSS SECTION FOR He + He FROM 2070 TO 2750 m/sec. McArdle, K. T.; Skofronick, J. G. (Florida State Univ., Tallahassee). J. Chem. Phys.; 53: 4403-4(1 Dec 1970).

The relative total cross section for He on He as a function of relative velocity was measured over the velocity range of 2070 to 2750 m/sec. Experimentally two nozzle beams were crossed at 90° and the attenuation of one by the other was measured. The results are compared with the total cross section in relative coordinates, calculated by solving Schroedinger's equation for the potential suggested by Beck (Mol. Phys., 14: 311 (1968)). (A.G.W.)

4966 SINGLE-PARTICLE FORMULATION OF ELECTRON–ATOM SCATTERINGS WITH STRONG CORRELATION EFFECTS. Hahn, Yukap (Univ. of Connecticut, Storrs). Ann. Phys. (N. Y.); 58: 137-56(May 1970).

The continuum shell model with configuration interactions is reformulated in terms of the commuting single-particle projection operators. Diagonalization of the energy submatrix for the target-state configurations constructed from the single-particle basis provides improved threshold energies and allows a simple form of open-channel projection operators. The continuum electron is treated by solving a set of coupled integro-differential equations with complete exchange symmetry. The correlation effect is included as an effective distortion potential to be estimated variationally using either the single-particle or the Hylleraas form of wave functions. The nonorthogonality of the exchange channel wave functions, the calculation of resonance energies and their widths, and approximate bounds on scattering parameters are discussed. Two- and three-electron scattering systems are considered in some detail. (auth)

4967 STUDY OF THE ENERGY-LOSS SPECTRA INDUCED BY IMPACT OF 25- TO 125-keV PROTONS ON HELIUM ATOMS. Schowengerdt, Franklin Dean. Rolla, Mo.; Univ. of Missouri (1969). 191p. University Microfilms Order No. 70-11,761. Thesis.

Results of a study of the inelastic energy-loss spectra induced by the impact of protons on gaseous helium at energies of 25 to 125 keV are reported. The spectra were obtained by sending an accelerated beam of protons through a chamber containing the helium target gas, mass-analyzing the forward-scattered beam, then decelerating the beam to a low, well-defined energy for energy analysis and detection. The accelerating potential was varied to produce the spectra. An energy resolution of 2 eV was obtained. Apparent differential cross sections and absolute total cross sections were obtained from the spectra. Total cross sections for the sum of the 1^1S-2^1S and 1^1S-2^1P excitations in the helium atom are reported, along with estimates of the relative contributions of each. Total ionization cross sections, total cross sections for inelastic scattering, apparent energy distributions of ejected electrons, and partial ionic stopping powers are also reported. The excitation cross sections show excellent agreement with recent calculations on the coupled-state approximation, but show little or no agreement with calculations on the distortion and first Born approximations. No other experimental data on these excitation cross sections are available for comparison. The ionization cross sections show good agreement with results obtained by other methods and show fair agreement with the first Born approximation at high impact energies. The apparent energy distributions of ejected electrons fall below the results of direct measurements and show poor agreement with the available Born and classical theories. The total cross sections for inelastic scattering show agreement with theory similar to that found in the case of ionization. No other experimental data on total inelastic cross sections are reported in the literature. The partial ionic stopping powers fall below the total stopping

powers, the differences increasing at lower impact energies, where charge exchange is more probable. This behavior is consistent with the difference in definition of the two quantities. (Diss. Abstr. Int., B)

4968 ANGULAR DISTRIBUTION OF FAST ELECTRONS EMITTED FROM INNER ATOMIC SHELLS BY PROTON IMPACT. Choi, Byung-ho. Chapel Hill, N. C.; Univ. of North Carolina (1969). 38p. University Microfilms Order No. 70-3214.

Thesis.

Time-dependent perturbation theory was used to evaluate the angular distribution of electrons (delta rays) emitted from heavy atoms in collisions of protons and other heavy charged particles. The incident particle was assumed to move on a classical straight-line trajectory. Hydrogenic wave functions were used for the initial electron state and continuum Coulomb wave functions for the final electrons. Comparison was made between the angular distributions of electrons emitted from K and L shells at the same incident energy. At not too small angles and at sufficiently high kinetic energies of the electrons, the K-electrons contribute predominantly. The separate contributions of the L-subshells to the angular distributions were also calculated. (Diss. Abstr. Int., B)

4969 PRODUCTION AND LOSS OF FAST METASTABLE HELIUM ATOMS DURING CHARGE CHANGING COLLISIONS WITH PERMANENT GASES. Miers, Richard Ernest. Madison, Wis.; Univ. of Wisconsin (1970). 98p. University Microfilms Order No. 70-8317.

Thesis.

The cross sections for production and destruction of fast neutral He atoms in the metastable triplet state in gas targets of Xe, Kr, H_2, Ar, Ne, and He were measured for energies of the incident He^+ ion between 10 and 30 keV. A He^+ beam is passed through two targets. In the first target containing one of the permanent gases the He^+ beam is partially neutralized by charge exchange. The charged particles are deflected from the beam, and the neutral particles are allowed to pass into a second target containing Cs vapor. The intensity of the He^0, He^+, and He^- beams emerging from the Cs target is measured. Since the production of He^+ and He^- from a fast He^0 beam is sensitive to the fraction of metastable triplet atoms in the He^0 beam, the Cs target makes a very useful analyzer for the fraction of triplets in the fast He^0 beam emerging from the first gas target. Values of the fraction of neutral He atoms in the metastable triplet state emerging from thin gas targets of Xe, Kr, H_2, N_2, Ar, Ne, and He are 0.21, 0.12, 0.09, 0.06, 0.06, 0.02, and <0.02, respectively, for incident He^+ energies of 30 keV. By analyzing the fraction of He atoms in the metastable triplet state emerging from the first target as a function of the density of the first target the cross sections for loss of fast He^0 in the triplet metastable state are also determined. Subsequently, each of the permanent gases was used as the second target. Selected gases such as Xe, Kr, H_2, N_2, or He were used at low densities in the first target to produce known fractions of triplet metastable atoms. The charged particles are deflected leaving only the neutral particle to enter the second target. The fraction of fast He^+ emerging from the second target is analyzed as a function of the density of the gas target, and the cross sections for ionization of He atoms from the metastable triplet state in the gas are determined. (Diss. Abstr. Int., B)

Atomic Theory

Refer also to abstract 5832.

4970 RELATION OF THE FUNDAMENTAL EQUATION OF STATISTICAL ATOMIC MODELS AND THE SCHROEDINGER EQUATION. Gombas, P. (Univ., Budapest). Acta Phys. Acad. Sci. Hung.; 28: 225-8(1970). (In German).

It is shown that the fundamental equation of statistical atomic models expanded with the Weizsäcker correction is equivalent to the Schroedinger equation for the electrons in the highest energy state of the atom. (tr-auth)

4971 EFFECT OF SECOND-ORDER RELATIVISTIC CORRECTIONS IN THE CASES OF COMPLEX ELECTRONIC CONFIGURATIONS. Rudzikas, Z. B.; Karaziya, R. I. (Inst. of Physics and Mathematics, Vilnyus, USSR). Liet. Fiz. Rinkinys, Liet. TSR Mokslu Akad., Liet. TSR Aukst. Mokyklos; 10: No. 1, 13-26 (1970). (In Russian).

The expressions for matrix elements of the second-order relativistic corrections to the atom energy in the cases of two nonequivalent electrons and two incomplete shells are given. Algebraic tables for coefficients of the radial integrals in two-electron matrix elements are presented. The coefficients are expressed in terms of orbital quantum number of one electron. Numerical values of analyzed corrections for several atoms and ions of the iron group are calculated. (auth)

4972 CAN MACROSCOPIC TESTS OF COULOMB'S LAW RESULT IN A REVISION OF PRESENT ATOMIC THEORY? Zygan, H. (Farbenfabriken Bayer AG, Leverkusen, Ger.). Phys. Lett.; 33A: 293-4(16 Nov 1970).

Measurements on atomic systems prove to an accuracy exceeding 10 ppM only the combination of the exact Coulomb's law and the accepted atomic theory. Estimates show the feasibility of concentric-hollow-spheres experiments testing Coulomb's potential for atomic distances to 1 ppM. (auth)

4973 GAUSSIAN GEMINALS FOR ELECTRON PAIR CORRELATION. Pan, Kee-chuan; King, Harry F. (State Univ. of New York, Buffalo). J. Chem. Phys.; 53: 4397-9(1 Dec 1970).

Second-order pair correlation energies were calculated using Gaussian-type geminals. Initial calculations on He, Be, and Ne were restricted to very short geminal expansions, usually to only three or four terms, but gave surprisingly good results. It is concluded that Gaussian geminals not only have convenient computational properties, but also they are well suited to describe correlation effects. (A.G.W.)

Cosmic Radiation

Refer also to abstracts 4338, 4373, 5257, 5273–5275, and 5340.

4974 (AD-710278) PRODUCTION OF LOW-ENERGY MUONS BY NEUTRAL COMPONENTS OF THE COSMIC RADIATION AT SEA LEVEL. Final Report. Cowan, Clyde L. (Catholic Univ. of America, Washington, D. C. Dept. of Physics). 31 May 1970. 30p. (AFOSR-70-1646-TR). NTIS.

Reactions at sea level produced by neutral components of the cosmic radiation that result in at least one muon of either sign, and with energy lying between a few tens and a few hundreds of MeV, were investigated. Reactions produced by incident neutrons (via pion production and decay) and by gamma radiation were observed and measured in the course of the work. A component of the total production process was observed that seems to be inconsistent with either the neutron or gamma production mode. It is, apparently, strongly correlated with sidereal time and goes via the single negative muon channel only. The value of incident flux times cross section per target nucleon is $\sim 3 \times 10^{-33}$ per second per steradian. The change ratio μ^-/μ^+ of the muons produced is about 1.15 for a 50% confidence interval obtained from 76 events collected in 2,475 hours of run time, where these 76 events include single negative pion production and in-flight decay events as well. (auth) (USGRDR)

4975 (AECL-3736) COSMIC RAY NM-64 NEUTRON MONITOR DATA. XVI. Monthly Graphs, May 1970–August 1970. Steljes, J. F. (Atomic Energy of Canada Ltd., Chalk River (Ontario)). Oct 1970. 69p. Dep. NTIS (U. S. Sales Only). AECL $1.50.

Uncorrected and barometer-corrected results from the cosmic-ray stations in Canada using equipment maintained by AECL are given in tabular form for the period from May to August 1970. Normalized graphs are given for the same period. Correction factors for the constant rates of drift of the barometers at each of the four stations are given. (auth)

4976 PROCEEDINGS OF THE 11th INTERNATIONAL CONFERENCE ON COSMIC RAYS, BUDAPEST, 25 AUGUST–4 SEPTEMBER, 1969. Invited Papers and Rapporteur Talks. Bozoki, G.; Gombosi, E.; Sebestyen, A.; Somogyi, A. (eds.). Budapest; Central Research Institute for Physics (1969). 620p. (CONF-690814).

Separate abstracts were prepared for the six invited papers and fourteen rapporteur papers. The full texts of the 485 original papers will be published in four volumes as Supplementa to the Acta Physica Hungarica in 1970. (W.D.M.)

For abstracts of individual papers see: 4914, 4926, 4927, 4977–4989, 5033, and 5272–5274.

4977 NATURE OF THE PRIMARY COSMIC RADIATION. Powell, C. F. (Univ. of Bristol, Eng.). pp 3-16 of Proceedings of the 11th International Conference on Cosmic Rays, Budapest, 25 August–4 September, 1969. /Bozoki, G. (ed.). Budapest; Central Research Inst. for Physics (1969).

See CONF-690814.

An attempt is made to trace the development of the present understanding of cosmic radiation and to show how it now bears on many of the central problems of astrophysics and on the existence and production of very heavy elements. (W.D.M.)

XUM

4978 PULSARS AND THE ORIGIN OF HIGH ENERGY PARTICLES. Gold, Thomas (Cornell Univ., Ithaca, N. Y.). pp 163-75 of Proceedings of the 11th International Conference on Cosmic Rays, Budapest, 25 August–4 September, 1969. /Bozoki, G. (ed.). Budapest; Central Research Inst. for Physics (1969).
See CONF-690814.

Information now available on pulsars gives a strong suggestion that they are a source of relativistic gas, and thus, a possible candidate for emission of high-energy cosmic particles. This theme is briefly expanded, and the properties of neutron stars are discussed in some detail. (W.D.M.)

4979 ORIGIN AND ACCELERATION MECHANISMS. Syrovatskii, S. I. (Lebedev Inst. of Physics, Moscow). pp 233-9 of Proceedings of the 11th International Conference on Cosmic Rays, Budapest, 25 August–4 September, 1969. /Bozoki, G. (ed.). Budapest; Central Research Inst. for Physics (1969).
See CONF-690814.

In summarizing the situation concerning the suggested cosmic-ray acceleration mechanisms, it is seen that there are reliable dimensional and energetic estimations in favor of the acceleration of the bulk of cosmic-ray particles near pulsars, but to recognize the real mechanism of acceleration, both observational and theoretical efforts need to be intensified. (W.D.M.)

4980 ELECTRON–PHOTON COMPONENT OF COSMIC RAYS. Pal, Yash (Tata Inst. of Fundamental Research, Bombay). pp 241-74 of Proceedings of the 11th International Conference on Cosmic Rays, Budapest, 25 August–4 September, 1969. /Bozoki, G. (ed.). Budapest; Central Research Inst. for Physics (1969).
See CONF-690814.

Some sixty papers in this field were presented at the conference, which for the purpose of discussion were divided into four broad areas, namely: γ rays in the energy range ~100 MeV; search for γ rays of 100 to 1000 GeV; low-energy electrons of energy less than ~3 GeV; and high-energy electrons of energy up to ~600 GeV. In addition, some theoretical papers were presented that dealt with the origin of, and the correlations between, various electromagnetic components. (48 references) (W.D.M.)

4981 PROTONS AND NUCLEI IN THE GALACTIC RADIATION. CHARGE COMPOSITION AND ENERGY SPECTRA. Webber, W. R. (Univ. of New Hampshire, Durham). pp 275-311 of Proceedings of the 11th International Conference on Cosmic Rays, Budapest, 25 August–4 September, 1969. /Bozoki, G. (ed.). Budapest; Central Research Inst. for Physics (1969).
See CONF-690814.

A total of 45 papers were presented on various topics in the sessions on protons and nuclei in the galactic radiation. About 20 of the papers were concerned with charge composition. Approximately 10 papers were given under the general topic of energy spectra. Ten or twelve papers could be classified as mainly theoretical in nature. There were four papers presented on the sidereal variation of galactic cosmic-ray nuclei in the energy range $\gtrsim$100 GeV. (W.D.M.)

4982 REPORT ON QUASI-STATIONARY MODULATION PAPERS. Parker, E. N. (Univ. of Chicago). pp 341-56 of Proceedings of the 11th International Conference on Cosmic Rays, Budapest, 25 August–4 September, 1969. /Bozoki, G. (ed.). Budapest; Central Research Inst. for Physics (1969).
See CONF-690814.

The papers covered in this summary deal with detailed and/or quantitative questions concerning the propagation of galactic cosmic rays and energetic solar particles in the solar wind. There are a number of distinct questions and problems which the papers pursue, and the papers have been grouped in this way. (W.D.M.)

4983 MODULATION DYNAMICS. Somogyi, A. (Central Research Inst. of Physics, Budapest). pp 357-80 of Proceedings of the 11th International Conference on Cosmic Rays, Budapest, 25 August–4 September, 1969. /Bozoki, G. (ed.). Budapest; Central Research Inst. for Physics (1969).
See CONF-690814.

This summary report deals with the nonstationary features of the modulation of galactic cosmic radiation as reflected in the 31 papers submitted. The papers are grouped for the purpose of discussion into 11-year variation, 27-day variation, short-term variations, and Forbush decreases. (14 references) (W.D.M.)

4984 GEOPHYSICAL EFFECTS AND PROPERTIES OF THE VARIOUS COMPONENTS OF THE COSMIC RADIATION IN THE ATMOSPHERE. Dorman, L. I. (Inst. of Terrestrial Magnetism, Ionosphere, and Radio-Wave Propagation, Moscow). pp 381-442 of Proceedings of the 11th International Conference on Cosmic Rays, Budapest, 25 August–4 September, 1969. /Bozoki, G. (ed.). Budapest; Central Research Inst. for Physics (1969).
See CONF-690814.

A large variety of problems concerning the properties of the secondary components in the atmosphere and their geophysical effects was dealt with during this conference. The papers were grouped under meteorological effects, cosmic rays in the geomagnetic field, coupling coefficients and integral multiplicity, and the various secondary components in the atmosphere and albedo phenomena. (39 references) (W.D.M.)

4985 EXTENSIVE AIR SHOWERS (EXPERIMENT). Truemper, J. (Univ., Kiel). pp 497-518 of Proceedings of the 11th International Conference on Cosmic Rays, Budapest, 25 August–4 September, 1969. /Bozoki, G. (ed.). Budapest; Central Research Inst. for Physics (1969).
See CONF-690814.

About 50 papers concerning experimental results on extensive air showers were presented. The main results from these papers are briefly summarized. (20 references) (W.D.M.)

4986 EXTENSIVE AIR SHOWERS (THEORY). Feinberg, E. L.; Ivanenko, I. P. (Lebedev Inst. of Physics, Moscow. Moscow State Univ.). pp 519-52 of Proceedings of the 11th International Conference on Cosmic Rays, Budapest, 25 August–4 September, 1969. /Bozoki, G. (ed.). Budapest; Central Research Inst. for Physics (1969).
See CONF-690814.

Some seventy papers dealing with the theory of extensive air showers are summarized under the broad groupings of Cherenkov light, theory of electromagnetic cascades, and nuclear cascades. (15 references) (W.D.M.)

4987 EAS: RADIO PULSES. Allan, H. R. (Imperial Coll. of Science and Tech., London). pp 553-64 of Proceedings of the 11th International Conference on Cosmic Rays, Budapest, 25 August–4 September, 1969. /Bozoki, G. (ed.). Budapest; Central Research Inst. for Physics (1969).
See CONF-690814.

Highlights from papers dealing with radio emission from extensive air showers are briefly summarized. Experimental problems inherent in detecting the radio pulses are discussed. (W.D.M.)

4988 MUONS. Wolfendale, A. W. (Univ. of Durham, Eng.). pp 567-90 of Proceedings of the 11th International Conference on Cosmic Rays, Budapest, 25 August–4 September, 1969. /Bozoki, G. (ed.). Budapest; Central Research Inst. for Physics (1969).
See CONF-690814.

Some fifty papers were presented in the muon sessions, along with others in the EAS field, which relate to the interesting information that muon measurements are providing on the nature of the primary cosmic rays, with regard both to energy spectra and mass composition. Highlights of these papers are summarized (9 references) (W.D.M.)

4989 NATURAL NEUTRINOS. Marx, G. (Roland Eoetvoes Univ., Budapest). pp 591-612 of Proceedings of the 11th International Conference on Cosmic Rays, Budapest, 25 August–4 September, 1969. /Bozoki, G. (ed.). Budapest; Central Research Inst. for Physics (1969).
See CONF-690814.

The production, propagation, reactions, and detection of natural neutrinos are considered in terms of available data and experimental arrangements. (15 references) (W.D.M.)

4990 NEW COSMIC-RAY IONIZATION MEASUREMENTS AT BALLOON ALTITUDES. Raft, P. D.; Negro, V. (Atomic Energy Commission, New York). Trans. Amer. Nucl. Soc.; 13: 451(Nov 1970).
From Meeting of the American Nuclear Society, Washington, D. C. See CONF-701102.

Direct Energy Conversion

Refer also to abstracts 4750–4752.

4991 (INR–1199) NUMERICAL CALCULATIONS OF THE ELECTRICAL PARAMETERS IN A FARADAY-TYPE MHD GENERATOR WITH TWO-DIMENSIONAL GAS FLOW. Celinski, Z. (Institute of Nuclear Research, Warsaw (Poland)). 1970. 34p. Dep. NTIS (U. S. Sales Only).

The two-dimensional electrical network was assumed as a model of the two-dimensional gas flow in MHD channels. Applying the calculated velocity and temperature profiles, the net-

work was solved using the GIER computer. All electrical values, the terminal ones as well as local, were calculated. The constant channel cross section, the subsonic gas flow, and the uniform distribution of the gas parameters along the channel were assumed in the calculations. The distribution of the gas parameters was assumed to be independent of the generator loading. The channel end effects were neglected. (auth)

4992 (N-70-34006) DESIGN STUDY FOR A MAGNETOHYDRODYNAMIC POWER SYSTEM FOR A NUCLEAR ELECTRIC PROPELLED UNMANNED SPACECRAFT. Final Report, May 26, 1969–May 25, 1970. (General Electric Co., Philadelphia, Pa. Missile and Space Div.). Jul 1970. Contract JPL-952415. 305p. (NASA-CR-109851; GESP-7041). NTIS.

For Jet Propulsion Lab., Pasadena, Calif.

The progress made in a one-year design study of nuclear-electric propelled unmanned spacecraft using a liquid metal magnetohydrodynamic (MHD) power system is discussed. The study guidelines and approach are defined, and the characteristics of the launch vehicle, the thruster subsystem, and the payload and communications system are presented. The MHD power conversion system is described, and methods used to calculate MHD-system parameters are discussed. A discussion of the arrangement and structural arguments used to select the system configuration is included. The system startup technique is identified, and the detailed design and weight summaries are presented for systems of 100 kWe to 3 MWe power rating. (auth) (STAR)

4993 (TEE-4125-1) THERMIONIC PERFORMANCE OF FLUORIDE CVD TUNGSTEN-NIOBIUM CONVERTER. Rufeh, F.; Lieb, D. (Thermo Electron Corp., Waltham, Mass.). Jun 1970. Contract AT(30-1)-4125. 69p. (TE-4122-12-71). Dep. NTIS.

Fluoride vapor-deposited tungsten has been shown to form a mechanically stable and easily fabricated thermionic emitter structure. Parametric data are obtained in a research, variable-spacing thermionic converter for a wide range of converter parameters. Attempts were also made to measure the cesiated work function of the electrodes. The transient effects observed showed that, unlike other materials, the emission characteristics of this emitter depend on its temperature history preceding the test. This dependence was attributed to the diffusion of an impurity element, possibly carbon, in the fluoride tungsten material to the emitter surface. It is known that the performance of fluoride tungsten emitters is considerably lower than that of other emitters (e.g., chloride tungsten). The present data indicate that the performance at low temperatures (less than 1800°K) would have been even lower if additives were not diffusing through the emitter. The data presented are believed to be representative of fluoride tungsten emitters. (M.O.W.)

4994 THERMIONIC CONVERTER. Schutt, Paul F. (to Babcock and Wilcox Co.). U. S. Patent 3,534,202. 13 Oct 1970. Filed 24 Aug 1967.

An arrangement for controlling a thermionic converter having a cathode heated by the thermal energy developed in a nuclear reactor is described. The converter comprises a container within which a pair of electrodes is disposed, including a cathode surrounded by an anode for collecting electrons thermionically emitted from the cathode. The container is insulated from the anode by a gas and/or gas permeable substance. A pressure regulating device is connected in gas flow communication with container for increasing and decreasing the pressure of the gas between the anode and container thus changing the heat transfer characteristic of the gas. (Offic. Gaz.)

4995 MODELING OF THE CHANNEL CHARACTERISTICS OF A CONDUCTION-TYPE DIRECT-CURRENT MAGNETOHYDRODYNAMIC MACHINE. Kovner, D. S. (Aviation Inst., Moscow). High Temp. (USSR) (Engl. Transl.); 8: 177-80(Jan-Feb 1970).

Translated from Teplofiz. Vys. Temp.; 8: 189-92(Jan-Feb 1970).

Under the assumption of a linear relationship between the criteria that determine the operation of a channel for the case of flow which is self-similar with respect to viscosity, formulas are obtained in the inductionless approximation that describe the characteristics of a channel with a pump and a generator. The use of formulas connecting parameters proportional to the determining criteria permits simple conversion of the experimental calculating characteristics to other working fluids, channel dimensions, and conductivity of the walls. (auth)

Fluid Physics

Refer also to abstract 5105.

4996 TRANSPORT EQUATIONS OF UNIPOLAR MEDIUM. ION OSCILLATIONS IN ELECTROGASDYNAMIC FLOW IN CHANNELS. Brunne, M.; Malaczynski, G. (Inst. of Fluid-Flow Machines, Danzig). Pr. Inst. Masz. Przeply.; 48: 63-90(1969). (In Polish).

The equations of electrogasdynamics for a two-fluid and single-fluid model of isothermal transport of a unipolar medium are considered. Use is made of several earlier publications. A discussion of plane-wave propagation is given in an infinite Cartesian space filled with a medium, the behavior of which is analyzed on the grounds of the laws of electrogasdynamics. It is proved that the coupling between ion waves and sound waves in a dissipative (viscid and heat-conducting) medium is represented solely by the effects connected with the convection of charges in the velocity field of their neutral carrier. This proof is based on the single-fluid model of the medium. The solutions obtained for the one-dimensional Poiseuille flows in axisymmetric channels are taken as a state of stable equilibrium. This allows one to linearize the equations describing ion waves in such flows by using the perturbation method. Some particular cases of ion waves behavior are specified and discussed, including the equations of dispersion given in form rendering itself to numerical solution. Finally, the forced oscillations of ions are considered with initial disturbance of concentration assumed in form corresponding to the disturbances of a source of charges in channels of electrogasdynamic conversion. Moreover, the relaxation times of forced oscillations are discussed. (auth) (NSA of Poland)

4997 ELECTROHYDRODYNAMIC STABILITY: FLUID CYLINDERS IN LONGITUDINAL ELECTRIC FIELDS. Saville, D. A. (Princeton Univ., N. J.). Phys. Fluids; 13: 2987-94 (Dec 1970).

The stability of a fluid cylinder stressed by an axial electric field has heretofore been studied, assuming that the cylinder and its surroundings behave as perfect dielectrics and viscous effects being ignored. With many fluids this is unrealistic since the existence of even a small conductivity implies that the deformed interface carries an electric charge. Upon deformation of the interface the charge interacts with the field to produce an electrical shearing stress. Thus, to avoid singular behavior, viscous shear must be considered from the outset. The analysis is applicable to situations where the relaxation time for free charges is short compared with the time scale for fluid motion. It is found that electrical shearing forces can, under some conditions, completely stabilize the cylindrical interface to axisymmetric deformations. On the other hand, the conditions under which these same forces produce instability are delineated. In instances where both fluids have low viscosities, a boundary layer effect produces additional damping and, in the presence of an axial electric field, electrical shearing stresses in this boundary layer may render an otherwise stable oscillation unstable. (auth)

4998 GENERAL SOLUTION FOR THE LINEARIZED EKMAN-HARTMANN LAYER ON A SPHERICAL BOUNDARY. Loper, David E. (Florida State Univ., Tallahassee). Phys. Fluids; 13: 2995-8(Dec 1970).

A general solution for the linearized, hydromagnetic Ekman-Hartmann boundary layer on a spherical boundary is presented. The fluid is assumed to be incompressible, viscous, electrically conducting, and in a state of motion close to rigid-body rotation. The conductivity of the boundary is unspecified and an arbitrary magnetic field permeates the fluid and boundary. The solution obtained is found to be independent of both the conductivity of the boundary and the magnetic field components parallel to the boundary. If the magnetic field is assumed to be frozen into the fluid outside the boundary layer, the general solution may be integrated for large time to obtain a stationary solution. It is found that hydromagnetic effects preclude the possibility of boundary-layer breakdown whenever a local normal magnetic field exists. (auth)

4999 STEADY HYDROMAGNETIC BOUNDARY LAYER NEAR A ROTATING, ELECTRICALLY CONDUCTING PLATE. Loper, David E. (Florida State Univ., Tallahassee). Phys. Fluids; 13: 2999-3002(Dec 1970).

Gilman and Benton's study of the steady fluid motions and magnetic fields induced by a differentially rotating, electrically insulating infinite flat plate in the presence of a uniform magnetic field is generalized by allowing the electrical conductivity of the plate to be an arbitrary function of distance from the fluid-plate interface. It is found that the important measure of the conductivity of the plate is the ratio of plate conductance to conductance of a layer of fluid whose thickness is one Ekman depth. The form of the steady Ekman-Hartmann layer is found to be completely independent of the conductivity of the plate. The steady perturbation magnetic field within the plate is found to be entirely azimuthal and its magnitude is directly proportional to the conductance ratio.

XUM

For values of parameters approximating conditions within the earth, the perturbation field may not be small. This azimuthal field causes an axial electric current to be drawn into the plate from the fluid, effectively strengthening the coupling between fluid and plate. If the conductance ratio is large, as it is within the earth, spin-up is accomplished primarily by this current and the Ekman–Hartmann layer no longer plays a dominant role in coupling the fluid with its boundary. (auth)

5000 THEORETICAL STUDY OF A FORCED VORTEX IN AN ELECTROCONDUCTING VISCOUS LIQUID PLACED IN AN AXIAL MAGNETIC FIELD. Chambarel, Andre; Dorlhac, Francois (College Scientifique Univ., Avignon, France). Compt. Rend., Ser. A; 271: 515-18(14 Sep 1970). (In French).

A viscous and electrically conducting liquid, driven into vortex motion by the walls of two coaxial cylinders and placed in an axial uniform magnetic field, is studied. The equations giving the radial distribution of the velocities are developed, and the shape of the free surface resulting from the rotation was determined. (tr-auth) (France)

Geophysics (Upper Atmosphere)

5001 (AD-710426) TECHNIQUE FOR USING THE DISTURBING BEFORE-WANTED INTERACTION EXPERIMENT TO OBTAIN THE EXCESS ELECTRON ENERGY LOSS FACTOR. Kissick, W. A. (Pennsylvania State Univ., University Park. Ionosphere Research Lab.). 10 Aug 1970. Contract Nonr-656(35). 72p. NTIS.

The development of the electron energy balance equation, as it is used in D-region interaction studies, is examined. It is proposed to experimentally find the excess electron energy loss factor, G, that appears in this equation. G represents the fraction of excess energy (above ambient) that an electron loses per collision with a neutral particle. An experiment in which the disturbing pulse is transmitted before the wanted pulse is described, and the necessary theory is derived. The interaction equations are then programmed on a digital computer to examine the effects of ionospheric parameters. It is shown that the Disturbing-Before-Wanted experiment is sensitive to G. A graphical technique for the reduction of experimental data is developed, and some preliminary results are shown in the form of the seasonal variation of G. (auth) (USGRDR)

5002 (AD-710604) RADIAL DIFFUSION OF OUTER-ZONE ELECTRONS: AN EMPIRICAL APPROACH TO THIRD-INVARIANT VIOLATION. Schulz, Michael; Lanzerotti, L. J.; Maclennan, C. G. (Aerospace Corp., El Segundo, Calif.). 31 Jul 1970. Contract F04701-70-C-0059. 66p. (TR-59(6260-20)-6; SAMSO-TR-70-277). NTIS.

The near-equatorial fluxes of outer-zone electrons (E > 0.5 MeV and E > 1.9 MeV) measured by an instrument on the satellite Explorer 15 following the geomagnetic storm of December 17–18, 1962, are used to determine the electron radial diffusion coefficients and electron lifetimes as functions of L for selected values of the conserved first invariant μ. For each value of μ the diffusion coefficient is assumed to be time-independent and represented in the form $D = D_n L_n$. The diffusion coefficients and lifetimes are then obtained simultaneously by requiring that the L-dependent reciprocal electron lifetime, as determined from the Fokker–Planck equation, deviate minimally from a constant in time. Applied to the data, these few assumptions yield a value of D that is smaller by approximately a factor of ten than the value obtained recently by Newkirk and Walt in a separate analysis of 1.6-MeV electron data obtained during the same time period on another satellite. The electron lifetimes are found to be strong functions of L, with 4–6 day lifetimes observed at the higher L values (4.6 to 4.8). (auth) (USGRDR)

5003 SPATIAL EXTENT OF THE RETURN CURRENT OF THE AURORAL-ZONE ELECTROJET. PART II. Kamide, Yohsuke; Fukushima, Naoshi (Tokyo Univ.). Rep. Ionosphere Space Res. Jap.; 24: 115-26(Jun 1970).

Geomagnetic field variation in low latitudes during polar magnetic substorms was quantitatively examined and compared with a model ionospheric current distribution produced by model electrojets along the auroral ovals in the northern and southern hemispheres. It is shown that the observed current pattern and its latitudinal intensity gradient at least in the night hours are in general agreement with the theoretical model. The increase of several tens of gammas in the H-component at the developed stage of geomagnetic bays in the night hours, seems to be attributable to the return flow of the intense auroral-zone electrojets, if the latitudinal width of the jet is greater than 10 degrees. (auth)

5004 EVOLUTION OF CHARGED PARTICLES FROM THE POINT SOURCE IN THE FIELD OF MAGNETIC DIPOLE. Kolesnikov, E. K.; Filippov, B. V. Vestn. Leningrad. Univ., Mat., Mekh., Astron.; No. 7, 88-120(Apr 1970). (In Russian).

The spreading of charged particles from the point source in the field of a magnetic dipole is investigated. This work is based on the study of two famous integrals for the movement of charged particles in dipole fields. The equatorial injection of electrons and zones is investigated, the independence of boundaries of this zone on the value of magnetic dipole moment, on the charge and the mass of injecting particles is proven. (auth)

5005 MICROPULSATION Pc-1 PHASE AND POLARIZATION COMPARISONS BETWEEN COLLEGE AND KOTZEBUE, ALASKA. Heacock, R. R. (Univ. of Alaska, College). Ann. Geophys.; 26: 653-60(Apr-Jun 1970).

Pc1-micropulsation data for July–October 1969 were telemetered from Kotzebue to College, Alaska, and recorded in fm mode on three channels of the College data recorder. Polarization and phase comparisons were made by playing the data back into a dual trace x–y oscilloscope. Several large-amplitude events were analyzed and were found consistent with a model in which a primary packet of L waves couples into R waves in the ionosphere. The waves were found to be approximately in phase at the two sites. The accuracy of the phase comparisons was limited, owing to the different shapes of the polarization configurations at the two sites. The nighttime events showed about as much R polarization as the day events, suggesting that L– to –R wave coupling is strong even at times when the normal E layer is minimal. (auth)

5006 ANOMALIES OF LOWER IONOSPHERE IONIZATION IN MEDIUM LATITUDES. Lauter, E. A.; Taubenheim, J. (Zentralinstitut fuer Solar-Terrestrische Physik, Berlin). Ann. Geophys.; 26: 631-41(Apr-Jun 1970).

The experimental evidence and interpretation of sunrise effects, the winter anomaly of absorption and the effects observed during stratospheric warmings, and the after-effects of severe magnetic storms were reviewed. (tr-auth) (France)

5007 IONIZING EFFECT OF BREMSSTRAHLUNG ASSOCIATED WITH PRECIPITATING ELECTRONS. Kamiyama, Hiroshi (Tohoku Univ., Sendai). Ann. Geophys.; 26: 625-30 (Apr-Jun 1970).

An estimate is given of the emissivity of bremsstrahlung x rays caused by energetic electrons precipitating into the upper atmosphere. The spectrum of the bremsstrahlung flux at any given altitude is characterized by an incident electron energy and the atmospheric absorption, depending on the direction of the flux. The rate of ionization produced through the absorption of bremsstrahlung x rays in various energy ranges is calculated as a function of the altitude. The photoionization rate is found to be maximum at about 170 km for the incident energy E_0 = 10 keV, at about 100 km for E_0 = 10 keV, and at about 45 km for E_0 = 100 keV. (tr-auth) (France)

5008 IONIZATION PROCESSES IN THE POLAR CAP. Sandford, Brian P. (Air Force Cambridge Research Labs., Bedford, Mass.). Ann. Geophys.; 26: 619-24(Apr-Jun 1970).

A brief review is given of polar cap ionization relating to the problems of the maintenance of the winter F region at latitudes higher than the auroral oval. Particle precipitation, horizontal drifts, the polar wind, distortions of the magnetospheric tail, and meteorological factors are all important in this problem. (tr-auth) (France)

5009 IONIZATION IN AURORAS DETECTED BY ATOMIC OXYGEN AND NITROGEN LINES. Omholt, A. (Univ. of Oslo). Ann. Geophys.; 26: 615-7(Apr-Jun 1970).

The excitation of the N II and O II lines in aurora is discussed. It is concluded that the intensities of these lines give little quantitative information about the ionization rates in aurora. However, important intensity variations occur, and a better knowledge about the excitation and deactivation processes involved may ultimately make it possible to use these lines for quantitative studies of the primary particles and their effects on the atmosphere, including ionization. (tr-auth) (France)

5010 IONIZATION PRODUCED BY AURORAL PROTON PRECIPITATION. Eather, R. H. (Lockheed Palo Alto Research Lab., Palo Alto, Calif.). Ann. Geophys.; 26: 609-13(Apr-Jun 1970).

Ionization rate and electron density height profiles are presented for a typical auroral proton energy spectrum. Associated radio-noise absorption, sporadic-E, and radio aurora are discussed briefly. (tr-auth) (France)

5011 METASTABLE SPECIES IN THE IONOSPHERE. Dalgarno, A. (Harvard Coll. Observatory, Cambridge, Mass. Smithsonian Astrophysical Observatory, Cambridge, Mass.). Ann. Geophys.; 26: 601-7(Apr-Jun 1970).

The role of metastable species in the ionization balance of the upper atmosphere is reviewed. The metastable $O_2(a^1\Delta_g)$ molecule is an important source of O_2^+ ions in the D region, the $N(^2D)$ atom is an important source of NO and possibly of N^+ ions in the E region and the $O^+(^2D)$ ion is an important source of N_2^+ ions in the F region. The $N_2(A^3\Sigma_u^+)$ molecule may significantly modify the atmospheric chemistry during auroral bombardment. (tr-auth) (France)

5012 IONIC REACTIONS FOR METEORIC ELEMENTS. Swider, W. (Air Force Cambridge Research Labs., Bedford, Mass.). Ann. Geophys.; 26: 595-9(Apr-Jun 1970).

Ionization and loss processes for meteoric constituents in the lower ionosphere are reviewed. Loss processes for the alkali metal ions remain obscure, although it is suggested that their depletion may occur through the formation of hydrates. It is emphasized that the measurements of Narcisi support a meteoric origin for most, if not all, of the metallic species observed in the lower ionosphere. (tr-auth) (France)

5013 RECENT RESULTS ON ION CHEMISTRY OF THE D REGION OF THE IONOSPHERE. Ferguson, E. E. (Environmental Science Services Administration, Boulder, Colo.). Ann. Geophys.; 26: 589-94(Apr-Jun 1970).

The most important recent advances in D-region laboratory ion chemistry were summarized. These include new measurements on three-body reactions, the reaction scheme for production of the water cluster ions, H_3O^+, $H_5O_2^+$, etc., and new results on negative ion reaction rate constants. Reactions of cluster ions in which the neutral molecule attached to an ion is exchanged in a binary collision are described. (auth)

5014 VERTICAL DISTRIBUTION OF IONIZATION AT THE F2 PEAK RELATED TO IONIC PRODUCTION AND TRANSPORT PROCESSES. Yonezawa, T. (SRC Radio and Space Research Station, Slough, Eng.). Ann. Geophys.; 26: 581-8(Apr-Jun 1970).

Electron density profiles in a steady state were calculated for CIRA 1965 Model Atmospheres and others on the assumption that their temperature distributions with height above and below the 300-km level can be well approximated by linear functions of height, respectively, as well as on other conventional assumptions. It was found that the calculated peak electron density, N_m, and the height of the peak, h_m, of the F2 layer increase linearly with the intensity of solar 10.7-cm radiation and each of these solar cycle variations in N_m or h_m can be expressed in a simple form in terms of solar zenith angle, magnetic dip, and the values at 300 km of such parameters as the scale height for atomic oxygen, the ambipolar diffusion coefficient and the electron loss coefficient. When the model atmosphere is fixed and the values of the parameters only are changed, h_m can be expressed in a similar form as above, but an expression of somewhat different form is obtained for N_m. It was also shown that, under normal conditions, an influx or efflux of electrons and ions from or to the exosphere is not likely to have any very great influence on the electron density profile, that varying degrees of difference between the plasma and neutral scale height have practically no effect on an electron density profile on the bottomside of the F2 layer but may have considerable influence on the topside, and that, if the value of the electron loss coefficient at the 300-km level is the same, it does not matter to any great extent for the calculation of electron density profiles whether the loss coefficient is assumed to be proportional to the number density of O_2 or N_2, in particular on the topside of the layer. (tr-auth) (France)

5015 COMPARISON BETWEEN THE UPPER ATMOSPHERIC IONIZATION DUE TO PHOTOIONIZATION AND IONIZATION BY COLLISION OF CHARGED PARTICLES. Ivanov-Kholodnyi, G. S. (Inst. of Applied Geophysics, Moscow). Ann. Geophys.; 26: 575-9(Apr-Jun 1970).

A review of calculations of the upper atmosphere photoionization by extreme ultraviolet solar radiation is presented. Approximate formulae for the rate of ion production and heights of maximum ionization caused by a flux of charged particles are given. A comparison of ionospheric observations and rocket measurements is made which refer to the existence of corpuscular ionization in the upper atmosphere. (tr-auth) (France)

5016 THERMOSPHERIC DENSITY VARIATIONS AS AN OSCILLATOR CIRCUIT SYSTEM. Volland, H. (Goddard Space Flight Center, Greenbelt, Md.). Ann. Geophys.; 26: 523-30 (Apr-Jun 1970).

The in situ generation of neutral air waves within the thermosphere by an external heat source is calculated using an approximate approach by neglecting the transmission quality of the waves. The energy equation can be transformed in such a way that it formally is equivalent to the equation of an electric circuit system in series in which the density amplitude represents the electric current and the heat source replaces the electric voltage. The inductance of the circuit is related to internal heat of the wave and to vertical heat advection. The capacitance is related to horizontal and vertical heat advection. The resistance is related to ion drag and vertical heat conduction. Numerical calculations depending on frequency, collision number, and horizontal wave number agree sufficiently well with exact full-wave calculations. They are applied to the diurnal and semidiurnal tidal density variations, to the geomagnetic activity effect, the 27-day variation, and the semiannual effect within thermospheric heights. (tr-auth) (France)

5017 VERTICAL DISTRIBUTION OF ATMOSPHERIC OZONE FROM ANALYSIS OF DIRECT SOLAR RADIATION. Vigroux, E. (CNRS, Paris). Ann. Geophys.; 26: 511-21(Apr-Jun 1970).

A new interpretation of the observations made at Arosa to determine the vertical distribution of atmospheric ozone was given. This interpretation was tested from measurements performed with chemical probes and by ir and uv analysis. The agreement between the distributions obtained from these two methods is satisfying. When the ozone distribution curve exhibited several density maxima, preliminary investigations made by Dutsch, at Boulder, in the spring of 1964 were used, and a mean distribution curve having a single density maximum was determined. (France)

5018 EXCITATION MECHANISM OF SODIUM D LINES IN NIGHTGLOW. Srivastava, A. N.; Shukla, R. V. (Allahabad Univ., India). Ann. Geophys.; 26: 501-4(Apr-Jun 1970).

Various processes responsible for the excitation of sodium atoms in the nightglow are considered. The coefficients of several reactions involved are discussed, and values of some of them are obtained. A comparison of the volume emission rates determined from all the processes shows that the Chapman mechanism is mainly responsible for the emission of Na–D lines in the Earth's atmosphere. (tr-auth) (France)

5019 BREMSSTRAHLUNG X-RAY FLUX AND ITS IONIZING EFFECT IN THE LOWER IONOSPHERE. Prasad, R. Y.; Singh, R. N. (Banaras Hindu Univ., India). Ann. Geophys.; 26: 493-9(Apr-Jun 1970).

The bremsstrahlung x-ray flux produced by an incoming energetic electron flux in the lower ionosphere was studied. The x-ray flux produced by electron atom collisions is more important than the corresponding flux produced by electron ion–collisions. The total x-ray flux calculated at 100 km is more important than the unattenuated measured x-ray flux. The electron–ion pair production rate obtained from calculated x-ray flux data is found to be as significant as the rate of ionization by solar x and ultraviolet radiations. The discrepancies between calculated and measured results are discussed. (tr-auth) (France)

5020 PHASE AND AMPLITUDE CHANGES OF VLF SIGNALS ASSOCIATED WITH PCA EVENTS WITH REFERENCE TO THE SOUTH ATLANTIC GEOMAGNETIC ANOMALY. Mendes, A. M.; Ananthakrishnan, S.; Paes de Barros, M. H. (Mackenzie Univ., Sao-Paulo, Brazil). Ann. Geophys.; 26: 483-92(Apr-Jun 1970).

Thirteen PCA events were analyzed in terms of phase and amplitude changes on vlf signals received at Camposdo-Jordano, Sao-Paulo (Brazil). The events occurred between July 7, 1966, and December 12, 1968, and were observed on seven different propagation paths situated at different geographic latitudes. All the propagation paths crossed the South Atlantic Geomagnetic Anomaly. The effects of trapped particles inside the anomaly and particles in the polar zone on the vlf signals were studied, and it was shown that, even for a relatively low-latitude path, well-defined phase advances are observed within a few hours of the onset of the PCA. A qualitative interpretation of the results is given in terms of the electron precipitation into the anomaly from the radiation belts. (tr-auth) (France)

5021 IMPACT IONIZATION BY NEUTRAL INTERPLANETARY PARTICLES. Blum, P. W.; Fahr, H. J. (Univ., Bonn). Ann. Geophys.; 26: 475-81(Apr-Jun 1970).

There exists conflicting evidence about the density of the neutral interstellar medium in the vicinity of the solar system. While from Ly-α scattering measurements low densities can be inferred, radioastronomical and other measurements point to densities in the order of 1 to 5 particles/cm^3. Owing to a mean

XUM

relative velocity of the order of 20 km/sec between this interstellar gas and the Sun, interstellar particles succeed in penetrating into the inner regions of the solar system. Fast neutral hydrogen corresponding to a kinetic energy of 1000 eV will be produced by charge exchange processes with solar wind protons. The effect on the ionosphere of these neutrals when they are intercepted by the Earth is studied. Based on the assumption that $n_0 \sim 1$ to 5 it is shown that above 300 km these neutrals constitute an additional source of ionization besides the far uv radiation of the Sun. Interstellar helium that amounts to about 10% of the density of the interstellar gas penetrates into the Earth's orbit almost without being attenuated. During part of the year these helium atoms enter the terrestrial atmosphere mainly from the antisolar direction and thereby may contribute to the maintenance of the residual nighttime E-layer. (auth)

5022 SOLAR AND GEOMAGNETIC EVENTS OF THE YEAR 1968. Ballario, M. C. (Osservatorio Astrofisico di Arcetri, Florence). Ann. Geophys.; 26: 459-73(Apr-Jun 1970).

The solar and geomagnetic events of the year 1968, were examined. It results that geomagnetic storms and disturbances are generally correlated with the central meridian passages of plages of low or moderate activity that, before the meridian transit, are never associated with spot-groups type C or greater, and/or with the occurrence of specific flares. The data referring to probably identified M solar regions (Bartels) are also given. (tr-auth) (France)

5023 DIAGNOSTICS OF THE MAGNETOSPHERE USING GEOMAGNETIC, AURORAL, AND AIRGLOW PHENOMENA. Akasofu, S.-I. (Univ. of Alaska, College). Ann. Geophys.; 26: 443-57(Apr-Jun 1970).

Various geomagnetic, auroral, and airglow parameters which could be used for diagnosing magnetospheric conditions are critically examined. It is pointed out that most of the presently available and potentially useful parameters have not been calibrated carefully enough by satellite observations to be useful for the diagnosis. Some organized efforts between satellite and ground workers are suggested to accomplish this calibration. (tr-auth) (France)

5024 SOLAR WIND PROPERTIES AND THE STATE OF THE MAGNETOSPHERE. Hundhausen, A. J. (Los Alamos Scientific Lab., N. Mex.). Ann. Geophys.; 26: 427-42(Apr-Jun 1970).

The observational evidence bearing on the relationship between the state of the solar wind and geomagnetic activity is reviewed. Correlations were established between numerous solar wind properties and the general level of geomagnetic activity. In attempting to understand the physical implications of the correlations, specific patterns of change in the solar wind are identified and the detailed geomagnetic response examined. The relation between interplanetary discontinuities, shock waves, and flare-associated disturbances, and the sequence of geomagnetic activity making up a geomagnetic storm is discussed in some detail. In general, the influence of the solar wind on magnetospheric properties related to the gross size and shape of the geomagnetic cavity (or currents at the magnetopause) is fairly well understood; the influence of the solar wind on magnetospheric properties related to internal current or plasma motion is, in contrast, quite poorly understood. (tr-auth) (France)

5025 SATELLITE INFORMATION ON THE ORIGIN OF GEOMAGNETIC VARIATIONS. Nishida, Atsuhiro (Tokyo Univ.). Ann. Geophys.; 26: 401-16(Apr-Jun 1970).

With the information made available by the advent of space probes, the origins of SI (and SSC) and DR were identified. SI's are due to sudden expansions or contractions of the entire magnetosphere, that in turn are caused by impacts of the interplanetary shock waves or discontinuity surfaces with the magnetosphere. The DR field is due to the motion of the energetic protons forming the radiation belt, and quantitative agreement was found between observations and the model based on this idea. The nature of DP still remains a problem, and it is investigated by combining satellite data, that can yield intimate information on processes taking place in the vicinity of the origin, and ground data, that can give synoptic information on processes taking place in the entire magnetosphere. The fluctuations in the DP 2 field is highly correlated with variations in the north–south component of the interplanetary magnetic field, and thus they seem to be driven by the electric field $E = -u \times B$ in the interplanetary space. The activity of the DP 1 field also shows significant correlation with variations in the interplanetary magnetic field, but in this case the energy seems stored in the near-tail region of the magnetosphere, before it is suddenly released to give DP 1 and associated phenomena. (tr-auth) (France)

5026 INTERRELATION BETWEEN PARAMETERS OF THE SOLAR WIND AND THE STATE OF THE GEOMAGNETIC FIELD. Pudovkin, M. I.; Raspopov, O. M.; Dmitrieva, L. A.; Troitskaya, V. A.; Shepetnov, R. V. (Inst. of the Physics of the Earth, Moscow). Ann. Geophys.; 26: 389-96(Apr-Jun 1970).

The interaction between the intensity and orientation of the magnetic field of the solar wind and the intensity of geomagnetic distrubances and geomagnetic pulsations Pi2 at the Earth's surface is considered. It is shown that geomagnetic disturbances with periods of about 1 hour or more lag behind the corresponding variations in the magnetic field of the solar wind by 1.0 to 3.0 hours and that this correlation exists only when the interplanetary magnetic field is in a southerly direction. The same correlation is observed for the Pi2 pulsations except when they occur simultaneously with an abrupt change in sign of the vertical component of the magnetic field of the solar wind. This delay may result from the drift of the plasma irregularities in the tail of the magnetosphere toward the Earth up to the auroral zone. If the value of this delay is known, it is possible to estimate the intensity of the large-scale electric field responsible for the drift of the plasma. (tr-auth) (France)

5027 DETERMINATION OF SOME MAGNETOSPHERE PARAMETERS BASED ON DATA FROM GROUND OBSERVATIONS OF Pc-1 TYPE MICROPULSATIONS. Feyguin, F. Z.; Gokhberg, M. B.; Troitskaya, V. A.; (and others) (Inst. of Terrestrial Physics, Moscow. Moscow State Univ. CNRS, Saint-Maur-des-Fosses, France). Ann. Geophys.; 26: 383-8(Apr-Jun 1970).

Knowing the carrier frequency of Pc1-type micropulsations, the inclination of structured elements of dynamical characteristics (sonograms) of micropulsations, and the change of this inclination with time, it is possible to determine the magnitude of the magnetic field at the top of the geomagnetic force line along which the wave packet is traveling. The corresponding L shell is determined from this data. Knowing the parameter, L, and the signal repetition time, T, it is possible to evaluate the cold plasma density of this shell and then the energy of the hot protons. The flux of these hot particles is deduced from the measurements on wave-packet broadening. All these calculations were carried out assuming that thePc1 micropulsations are due to cyclotron instability in the radiation belt plasma. (tr-auth) (France)

5028 MICROPULSATIONS: A DIAGNOSTIC TOOL. Kenney, J. F.; Knaflich, H. B. (Boeing Scientific Research Labs., Seattle). Ann. Geophys.; 26: 371-81(Apr-Jun 1970).

Existing reviews on micropulsation research are updated by an inclusion of the most recent results in the Pc1- and Pi1-range. The applicability of using micropulsations as a diagnostic tool for magnetospheric research is treated. The differences between ulf and vlf results are explained in terms of different source and amplification mechanisms. Fine structure of Pc1 and falling tones are also treated in terms of triggered emissions and possible R-mode propagation. (tr-auth) (France)

5029 REMARKS ON THE GROUND-BASED WHISTLER METHOD OF STUDYING THE MAGNETOSPHERIC THERMAL PLASMA. Carpenter, D. L. (Stanford Univ., Calif.). Ann. Geophys.; 26: 363-70(Apr-Jun 1970).

A whistler receiver at Eights, Antarctica is capable of viewing a region of the magnetosphere extending from $L \sim 2.5$ to $L \sim 6$ and roughly $\pm 15°$ around the longitude of the station. Multicomponent whistlers propagating on paths distributed over a significant fraction of this region may be used to identify radial and longitudinal irregularities in electron density, bulk motions of the plasma, and the position and displacements of the plasmapause. (tr-auth) (France)

5030 DIAGNOSTICS OF THE MAGNETOSPHERE FROM GROUND-BASED MEASUREMENTS OF ELECTROMAGNETIC WAVES. Aubry, M. P. (CNRS, Saint-Maur-Des-Fosses, France). Ann. Geophys.; 26: 341-62(Apr-Jun 1970).

Three methods using the propagation of electromagnetic waves for ground studies of the magnetosphere are presented. In the hf range (freq. $\geq$ 20 MHz), the integrated electron density in the magnetosphere and the ionosphere was measured, using lunar radar echoes, but it was impossible to measure the local electron density accurately, as the waves pass through so many different regions. For very low frequencies (1 kHz $\leq$ freq. $\leq$ 40 kHz) the electron density profiles and plasma convection velocities in the equatorial plane inside the plasmapause were determined from the analysis of whistlers. In the ultra low-frequency range (10^{-3} Hz $\leq$ freq. $\leq$ 5 Hz), the proton density beyond the plasmapause was obtained from the processing of various micropulsation data. An empirical relation between the period T of the micropulsations in the eigenmode frequency range (freq. $\leq$ 0.1 Hz) and the geocentric distance of the magnetopause was shown to exist. (France)

5031 NONLINEAR MECHANISMS ASSOCIATED WITH WAVE PARTICLE INTERACTIONS IN THE MAGNETOSPHERE. Roux, A.; Solomon, J. (CNRS, Saint-Maur-des-Fosses, France). Ann. Geophys.; 26: 279-97(Apr-Jun 1970). (In French).

From the Maxwell–Vlasov coupled equations, a nonlinear theory was deduced, which is exact to the second order; it describes the interaction of an infinite homogeneous plasma with a transverse electromagnetic wave, circularly polarized, propagating along the static magnetic field. Validity conditions for the quasi-linear theory are then stated; they are expressed as functions of the spectrum width, and maximum amplitude of the emitted waves. It was shown that the vlf noise with a large bandwith of the hiss-type can be explained by the quasi-linear theory, but that the ultra low-frequency emission in the Pc1 range (the so-called pearls) must be described by a different theory: the monochromatic theory. The saturation amplitude of the waves in both cases was calculated; the orders of magnitude are in good agreement with experimental data. (tr-auth) (France)

5032 ROLE OF AN EXTRATERRESTRIAL RING CURRENT IN DYNAMICS OF AURORA. Wang, Chung-shan. Moscow, Idaho; Univ. of Idaho (1969). 94p. University Microfilms Order No. 70-10,713.

Thesis.

The existence of an extraterrestrial ring current in the magnetosphere is considered to have a profound influence on the trajectories of the charged particles responsible for the production of an auroral display. A change in the intensity of the ring current can thus provide a convenient and physically meaningful parameter for an investigation of certain dynamical features of auroras. There is evidence that the source of the auroral particles is located in the equatorial plane at a distance of at least 3.5 Earth radii. A variation of the conditions in the source region is then related to the auroral phenomena by the magnetic flux conservation theorem. The equation of the magnetic lines of force is derived for the combined system of the Earth's dipole and the ring current. Moreover, by imposing a constraint on the injection of the charged particles, namely by requiring the location of the source region to move in such a way that the field intensity at its position remains constant, an analytic expression relating the latitude and the change of the current intensity is obtained. As a consequence, the results are then used to explain the shift of the auroral oval, to evaluate the speeds of the north–south motion of auroral arcs, and evaluate the speeds of monochromatic mid-latitude auroral arcs of 6300A-(O I). (Diss. Abstr. Int. B)

5033 EARTH'S RADIATION BELTS. Vernov, S. N. (Moscow State Univ.). pp 85-162 of Proceedings of the 11th International Conference on Cosmic Rays, Budapest, 25 August-4 September, 1969. /Bozoki, G. (ed.). Budapest; Central Research Inst. for Physics (1969).

See CONF-690814.

The proton component of the radiation belts is considered in terms of high-energy protons (inner belt), time variations of energetic protons, fluxes and spectra of low-energy protons, and time variations of low-energy protons. Under the main heading of radiation-belt electrons, discussions are given on the outer radiation belt and unstable reaction zone, outer belt during magnetic storms, and the inner radiation belt. (137 references) (W.D.M.)

Low-Temperature Physics and Cryogenic Equipment

Refer also to abstract 4189.

5034 (TID-25601) STRUCTURE OF ELECTRON BUBBLES IN LIQUID HELIUM FROM PHOTO-EJECTION UNDER PRESSURE. Zipfel, Christie Lewis (Michigan Univ., Ann Arbor). 1969. 80p. Dep. NTIS.

Thesis.

As a test of the bubble model of the unusual electron behavior in liquid He, cross sections for photoinduced transitions of electrons from bubble-bound to quasi-free states were measured at 0.5 to 2.5 eV and 10 to 250 psi pressures. Comparison of the experimental cross sections with theory was used to derive the bubble radius and well depth for each pressure. The results confirm the bubble model, although the anomalous structure remains unexplained. (D.L.C.)

5035 (UCSD-34-P-143-30) EXPERIMENTS OF THE FUTURE AT ULTRA-LOW TEMPERATURES (<0.3°K). Wheatley, J. C. (California Univ., La Jolla, San Diego. Dept. of Physics). [1970]. 30p. Dep. NTIS.

Four major technical advances in ultra-low temperature physics in the 1960's are catalogued. An attempt is made to list some areas that will be dominant in the 1970's: quantum fluids and solids, polarized or oriented nuclei, magnetism, noise, electrical phenomena, third law of thermodynamics, thermometry, thermal contact, materials, cooling methods, and lower temperatures. Some of the ideas, concepts, and possible experiments are discussed. (D.L.C.)

Superconductivity

Refer also to abstract 4051.

5036 (NYO-4060-5) STUDY OF THE INTERACTION BETWEEN MAGNETIC FLUXOIDS AND CRYSTAL DEFECTS IN TYPE II SUPERCONDUCTORS. Informal Progress Report. Kramer, Edward J. (Cornell Univ., Ithaca, N. Y. Dept. of Materials Science and Engineering). 31 Oct 1970. Contract AT-(30-1)-4060. 27p. Dep. NTIS.

LEAD ALLOYS & SYSTEMS — In–Pb-base, stress relaxation induced by magnetic field reduction in superconducting
NIOBIUM — superconducting fluxoid pinning near surfaces in single crystals of
— dislocation motion in superconducting (D.L.C.)

5037 SUPERCONDUCTOR/NORMAL METAL/SUPERCONDUCTOR POINT CONTACTS. Bondarenko, S. I.; Dmitrenko, I. M.; Balanov, E. I. (Physical-Technical Inst. of Low Temperatures, Khar'kov). Sov. Phys.-Solid State (Engl. Transl.); 12: 1113-17(Nov 1970).

Translated from Fiz. Tverd. Tela; 12: 1417-22(May 1970).

An experimental study was made of the stationary and nonstationary Josephson effects in superconductor/normal metal/superconductor Ta/Ag/Sn and Sn/Ag/Sn point contacts. The relation between the critical current I_c of the contact and its normal resistance R_N, the temperature T, and the thickness d of the normal metal layer was studied. The effect of resistance and film thickness on the critical contact temperature T_c, and the conditions for observing intrinsic current steps in the volt–ampere characteristics of a contact in a superconducting strip resonator was investigated. The empirical equation was found $I_c \simeq 3.6 \times 10^{-3}\left(1-\frac{T}{T_c}\right)^2 \frac{\exp(-(d/770))}{R_N}$ for the critical current (I_c in amperes, d in Å, and R_N in ohms) if $R_N \leq 10^{-2}$ ohm, $d < 2000$Å, and $(T/T_c) \simeq 0.95$ to 0.58. The relation agrees well with the theory of the proximity effect in systems in the limit $l \ll \xi_0$ (l is the mean free path, $\xi_0 = \hbar v_F/2\pi kT_c$, and v_F is the Fermi velocity). $T_c(R_N, d)$ = constant while T_c decreases if the given restrictions (for R_N and d) are violated. The latter fact may be related to a growing role of fluctuations. The voltage V_n for which current steps appear is given by the equation $V_n = (\hbar c/2e)(\pi n/b)[t^*/\epsilon(t + \lambda_1 + \lambda_2 + d)]^{1/2}$, where n = 1, 2, 3, ..., b is the length of the strip, t is the thickness of the dielectric in the resonator, ϵ is the electric permittivity of the dielectric, and $\lambda_{1,2}$ are the superconducting penetration depths. This confirms the nonstationary Josephson properties of a superconductor/normal metal/superconductor contact which radiates electromagnetic waves with a frequency $\nu = 2eV/h$. Resonance (in the form of a current step) corresponds to the condition $n(\lambda^*/2) = b$ (λ^* is the wavelength in the resonator). (auth)

5038 SUPERCONDUCTIVITY OF TITANIUM CARBIDE. Klimashin, G. M.; Neshpor, V. S.; Nikitin, V. P.; Novikov, V. I.; Shalyt, S. S. (Semiconductor Inst., Moscow). JETP Lett. (USSR) (Engl. Transl.); 12: 102-3(5 Aug 1970).

Translated from Zh. Eksp. Teor. Fiz., Pis'ma Red.; 12: 147-9(5 Aug 1970).

The electric conductivity of several homogeneous titanium carbides, with compositions ranging from $TiC_{0.91}$ to $TiC_{0.46}$, was measured at low temperatures. The results show that $TiC_{0.52}$ and $TiC_{0.46}$ become superconducting at 3.42 and 3.32°K. The critical fields H_{c2} are 48 and 45 kOe at 1.6°K. (D.L.C.)

5039 SUPERCONDUCTIVITY AND NORMAL-STATE CONDUCTION MECHANISM IN OXIDIZED THIN ALUMINUM FILMS. Strongin, Myron; Dickey, J. M.; Crow, J. E. (Brookhaven National Lab., Upton, N. Y.). Solid State Commun.; 8: 1647-51 (15 Oct 1970).

Measurements are presented which show that, as thin Al films are oxidized more and more, there is an increasing negative temperature coefficient of resistance below about 50°K. These increases in resistance with decreasing temperature can be significant in heavily oxidized films, and a discussion is given of how this increasing normal state resistance influences the paraconductivity above T_c and affects estimates of the parameter τ_0 of the Aslamazov–Larkin theory. (auth) (UK)

XUM

5040 NONLINEAR EXCESS CONDUCTIVITY IN SUPERCONDUCTING ALUMINUM FILMS ABOVE THE TRANSITION TEMPERATURE. Kajimura, K.; Mikoshiba, N. (Electrotechnical Lab., Tokyo). Solid State Commun.; 8: 1617-19(15 Oct 1970).

Experimental results on the nonlinear excess conductivity in Al films are presented. The results are not consistent with the existing theories. An empirical relation is found for the temperature dependence of the characteristic electric field where the nonlinearity occurs. (auth) (UK)

5041 ENERGY SPECTRUM OF SUPERCONDUCTORS WITH OVERLAPPING BANDS. Fal'ko, Igor I. (Kharkov State Univ.). Solid State Commun.; 8: 1615-16(15 Oct 1970).

Interband pairing between electrons in a two-band superconductor leads to the formation of a united energy spectrum with two branches, depending on the topology characteristics of the two bands. (auth) (UK)

5042 TEMPERATURE DEPENDENCE OF SUPERCONDUCTING ENERGY GAP OF AMORPHOUS Bi. Vashishta, P.; Carbotte, J. P. (McMaster Univ., Hamilton, Ont.). Solid State Commun.; 8: 1661-4(15 Oct 1970).

The temperature variation of the energy gap in amorphous Bi was calculated from the Eliashberg kernels, which have recently been inferred from low-temperature quasi-particle tunneling data. The gap is found to exhibit important departures from a BCS temperature variation. These deviations are a result of strong-coupling effects, and are considerably larger than those expected in Pb. They should be easily measurable. (auth) (UK)

5043 EFFECT OF MICROWAVE PHONONS ON SUPERCONDUCTIVE TUNNELING. Cohen, R. W. (RCA Labs., Princeton, N. J.). Phys. Lett.; 33A: 271-2(16 Nov 1970).

The effect of externally applied longitudinal microwave phonons on the complex energy gap of superconductors was calculated. The resulting change in the tunneling current of superconducting junctions accounts for some discrepancies between experiment and previous theory. (auth)

5044 MEASUREMENT OF ENERGY DISSIPATED IN SUPERCONDUCTORS DURING FLUX JUMPS. McFarlane, I. D.; Dew-Hughes, D. (Univ. of Lancaster, Eng.). J. Phys., D (London); 3: 1423-9(Oct 1970).

The energy dissipated during field cycling and during flux jumps was calculated from measurements of specimen temperature on samples of Pb–Bi eutectic alloy. The dissipation thus calculated is compared with that obtained directly from the area of the magnetization curves. The agreement is well within experimental error. The energy dissipated ΔW during three types of flux jump was measured. For complete flux jumps with no flux penetration of the sample between jumps, ΔW is found to be equal to $\frac{1}{2}\Delta B\Delta H$. For complete flux jumps with flux penetration between successive jumps, ΔW is found to be equal to $\frac{3}{4}(\Delta B)^2$. For partial flux jumps ΔW is equal to between $(H - B)\Delta B$ and $2.5(H - B)\Delta B$, showing that much of the extra flux introduced during the jump is concentrated near the center of the sample. These results are entirely consistent with the description of flux jumps in terms of the critical-state model of irreversible Type-II superconductors. (auth) (UK)

5045 QUANTUM OSCILLATIONS AND THE ORDER OF THE PHASE CHANGE IN A LOW-κ TYPE II SUPERCONDUCTING MICROCYLINDER. I. McLachlan, D. S. (Univ. of the Witwatersrand, Johannesburg). Solid State Commun.; 8: 1589-93(15 Oct 1970).

Reversible susceptibility curves show the entry and exit of single fluxoids measured close to T_c. At lower temperatures, hysteresis is observed. Good agreement with the Ginsburg–Landau theory is obtained and the theoretical predictions, based on this theory, enable reasonable values of $\lambda(0)$ and $\xi(0)$ to be calculated. (auth) (UK)

5046 QUANTUM OSCILLATIONS, PINNING, AND THE SUPERHEATING AND OTHER CRITICAL FIELDS IN A LOW-κ TYPE II SUPERCONDUCTING MICROCYLINDER. II. McLachlan, D. S. (Univ. of the Witwatersrand, Johannesburg). Solid State Commun.; 8: 1595-9(15 Oct 1970).

Ac susceptibility measurements show the pinning and unpinning of individual fluxoids by the alternating magnetic field. The following critical fields can be identified: H_{c1}, H_{c2}, H_{c3}, and H_s (the superheating field). H_{c2} and H_s give consistent κ values while H_{c1} indicates a size effect or supercooling. In accord with theory the ratio H_{c3}/H_{c2} is greater than 1.7. (auth) (UK)

5047 TRANSITION METALS AND THE FROEHLICH MECHANISM FOR SUPERCONDUCTIVITY. Rothwarf, Allen (RCA Labs., Princeton, N. J.). Phys. Rev., B; 2: 3560-71(1 Nov 1970).

The properties of screened plasma oscillations of the d band, which Froehlich first suggested could lead to superconductivity, are investigated. Specific-heat anomalies in the normal and superconducting states, normal-state resistivities, pressure-induced and pressure-dependent superconductivity, Moessbauer-effect studies, lattice transformations, and the occurrence of superconductivity in transition metals are compared with the theory. These diverse properties indicate that the Froehlich mechanism is operative in high-T_c transition elements and constitutes a new mechanism for superconductivity. (auth)

5048 CORRELATION OF THE SUPERCONDUCTING TRANSITION TEMPERATURE WITH AN EMPIRICAL PSEUDOPOTENTIAL DETERMINED FROM ATOMIC SPECTRA. Gambino, R. J.; Seiden, P. E. (IBM Watson Research Center, Yorktown Heights, N. Y.). Phys. Rev., B; 2: 3571-7(1 Nov 1970).

A correlation was observed between the superconducting transition temperature and the energy of the first excited electronic configuration of the atom as determined from the optical spectra. This led to the formulation of an empirical pseudopotential using atomic spectral data. Using this pseudopotential it was shown to be the dominant factor in accounting for the cohesive energy, melting temperature, Debye temperature, thermal expansion coefficient, and superconducting transition temperature. (auth)

5049 HEALING LENGTH OF THE SUPERCONDUCTING ORDER PARAMETER. Cleary, Robert M. (Univ. of Illinois, Urbana). Phys. Rev., B; 2: 3577-9(1 Nov 1970).

Using the Bardeen–Kuemmel–Jacobs–Tewordt approach to the BCS theory of a nonuniform superconductor, the problem of a semi-infinite superconductor with a rigid potential barrier at the interface is studied. Very close to T_c, the spatial variation of the order parameter is given by the Ginzburg–Landau formula $\Delta(z,T)/\Delta_\infty(T) = \tanh[z/\sqrt{2}\,\xi_{GL}(T)]$. At decreasing temperatures, however, the order parameter heals much more rapidly than $\xi(T) = v_F/\pi\Delta_\infty(T)$, where $\xi_{GL}(T) = \lim 0.74\,\xi(T)$ as $T \to T_c$; and, at low and intermediate temperatures, does so over atomic distances. (auth)

5050 MOTION OF THE ORDER PARAMETER IN TYPE-II TRANSITION-ELEMENT SUPERCONDUCTORS IN A HIGH MAGNETIC FIELD. Tang, I-ming (Reed Coll., Portland, Oreg.). Phys. Rev., B; 2: 3582-7(1 Nov 1970).

The resistive state of type-II transition-element superconductors in a high magnetic field is studied, using a technique due to Maki et al. The order parameters for the individual bands have similar Abrikosov-type solutions. Assuming a common upper critical field for the two bands, it is seen that the motions of the s- and d-electron pairs are controlled by different diffusion equations. The diffusion constants for the s- and d-pair motions are obtained for a typical transition-element superconductor. It is found that the s-band diffusion constant is not affected by the presence of the second band, but that the d-band diffusion constant is affected. (auth)

5051 THEORY OF AN ISOLATED VORTEX IN A PURE SUPERCONDUCTOR NEAR $T = T_c$. Jacobs, A. E. (Univ. of Toronto). Phys. Rev., B; 2: 3587-93(1 Nov 1970).

It is demonstrated that the theory of Bardeen, Klimmel, Jacobs, and Tewordt for an isolated vortex in a pure type-II superconductor at arbitrary temperatures is in agreement with the theory of Neumann and Tewordt near $T = T_c$, if nonanalytic terms of odd order in $(1 - T/T_c)^{\frac{1}{2}}$ in the free energy are assumed to vanish. The leading nonanalytic term is examined by the use of perturbation theory to see if it vanishes, but no definite conclusion can be drawn. The approximations used in deriving these results should prove useful in the application of the method of Bardeen et al. to other problems involving pure inhomogeneous superconductors. (auth)

5052 BOSON METHOD IN SUPERCONDUCTIVITY: APPLICATION TO THE STUDY OF VORTEX LINES. Leplae, L.; Mancini, F.; Umezawa, H. (Univ. of Wisconsin, Milwaukee). Phys. Rev., B; 2: 3594-3605(1 Nov 1970).

The boson method in superconductivity, developed in previous articles, is extended and applied to the problem of vortices in neutral and type-II superconductors. In the approximation considered, the distributions of current and magnetic field of a single vortex are given in the whole domain, up to the center of the flux line. Expressions for the vortex self-energy and the interaction energy between two vortices are also derived. In the limiting case, in which $\kappa \gg 1$ (where κ is the Ginzburg–Landau parameter) and the structure of the core is approximated by a δ function, the results agree with those of Abrikosov's theory, based on the Ginzburg–Landau equations. (auth)

5053 CURRENT-PULSE EFFECT IN THE INTERMEDIATE STATE OF SUPERCONDUCTING LEAD FILMS. Huebener, R. P.

(Argonne National Lab., Ill.). Phys. Rev., B; 2: 3540-5(1 Nov 1970).

The enhancement of the resistive voltage in the intermediate state of superconducting lead films due to a high current pulse was studied at 4.2°K as a function of the width of the pulse τ, the magnetic field H, and the film thickness. The film thickness ranged between 1 and 7 μm. The resistive voltage increment after the current pulse, plotted versus τ, yields S-shaped curves that saturate at high values of τ. The half-time τ^* decreases strongly with increasing H. Assuming that the voltage increment is caused by the formation of a laminar flux structure perpendicular to the current during the pulse, the product of τ^* and the flux-flow velocity v_φ during the pulse can be expected to be of the order of the periodicity length of the laminar flux structure. Estimating v_φ at the pulse current from the flux-flow resistivity at small currents, the product $\tau^* \times v_\varphi$ increases with increasing film thickness and is in reasonable agreement with the value expected from Landau's model of the intermediate state. The current-pulse effect disappears below a film thickness between 1 and 2 μm. This can be understood from the experiments of Cody and Miller, which suggest that below a film thickness of about 1.5 μm lead films behave like type-II material. (auth)

5054 BULK UPPER CRITICAL FIELD OF CLEAN TYPE-II SUPERCONDUCTORS: V AND Nb. Williamson, S. J. (North American Rockwell Corp., Thousand Oaks, Calif.). Phys. Rev., B; 2: 3545-56(1 Nov 1970).

The bulk upper critical field H_{c2} of single crystals of Nb and V has been measured for various crystallographic orientations within the temperature range between the respective critical temperature and T ≈ 0.06°K. The normalized critical field averaged over all crystallographic directions $\langle h(t)\rangle = \langle H_{c2}(t)\rangle / (-dH_{c2}/dt)_{t=1}$, where $t = T/T_c$, and the relative anisotropy of H_{c2} for the two metals are found to be similar. The measurements support predictions of the Hohenberg–Werthamer calculation that attributes the observed anisotropy of H_{c2} to the effects of an anisotropic Fermi surface. Some differences in the behavior of $H_{c2}(t)$ for the present samples can be understood qualitatively to arise from the effects of a shorter electron-collision time τ for the less pure V specimen. At very low temperatures, $H_{c2}(0) - H_{c2}(t)$ for V does not follow a $t^2 \ln(t)$ temperature dependence, previously observed for Nb, but can be characterized by an empirical formula $t^2 \ln(t + \alpha)$ in which the constant α is conjectured to be inversely proportional to τ. (auth)

5055 THERMAL CONDUCTIVITY OF NORMAL AND SUPERCONDUCTING INDIUM–LEAD ALLOYS. Giedd, Ronald E.; Reynolds, C. A. (Univ. of Connecticut, Storrs). Phys. Rev., B; 2: 3533-40(1 Nov 1970).

Twelve In–Pb alloy samples with 3.00 to 8.00 at.% Pb concentrations were studied. These were divided into two sets, each consisting of six samples, one set with their c axis oriented approximately at 81°, and the other at approximately 14°, with respect to the sample axis. The electrical resistivities ρ at 4.2, 77, and 273°K were measured, yielding the electrical anisotropies a(4.2), a(77), and a(273), where $a = \rho_\perp/\rho_\parallel$. These verified the earlier findings of Carriker. For the pure In, a(77) = 0.986 ± 0.003 and a(273) = 1.041 ± 0.003, showing the same shift in maximum resistivity from the c to the a direction as the temperature is increased from 77 to 273°K. Also, the anomalies at 3.50 and 7.00 at.% Pb were again seen. The thermal conductivities were measured for all samples in both the normal and the superconducting state. In the normal thermal conductivities at 3°K, the anisotropy was a = 1.077 for the 3.00-at.%–Pb samples, and a = 1.054 for the 8.00-at.%–Pb samples where $a = K_\parallel/K_\perp$. The anomalies at 3.50 and 7.00 at.% Pb were evident. A temperature minimum existed in the superconducting thermal conductivity for all samples and was a linear function of Pb concentration for both sets, slowly increasing with increasing concentration from a temperature of 1.66 to 2.1°K. The normal lattice thermal conductivity was never more than 10% of the total thermal conductivity; it is accounted for by phonon–electron interaction scattering, mass-defect scattering, and scattering due to distortion of the lattice around the mass defect; and it was anisotropic. It was found that adding the squares of the strengths of the scattering mechanisms gave a better fit than adding the mean square-root values and then squaring, since the phases of the scattering mechanisms were not known. The ratio K_{gs}/K_{gn} was plotted as a function of the reduced temperature and compared with the Klemens–Tewordt theoretical expression. (auth)

5056 ENHANCED SUPERCONDUCTIVITY IN ULTRA-RAPIDLY QUENCHED BULK ALUMINUM–COPPER ALLOY. Babic, E.; Krsnik, R.; Leontic, B.; Zoric, I. (Univ., Zagreb). Phys. Rev., B; 2: 3580-2(1 Nov 1970).

Transition temperatures T_c of up to 2.95°K were obtained in bulk samples of an aluminum–copper alloy containing 0.85 at.% Cu that had been subjected to the process of ultrarapid quenching. The samples were obtained by a new method of ultrarapid quenching, which secures large thin samples that had undergone cooling rates from the melt of about 10^6°K sec^{-1}. At the same time, samples conventionally prepared from the same melt showed the normal behavior expected from such an alloy. The rise of T_c is linked to the quenching speed and is proportional to the residual resistance. A possible explanation of the phenomenon is offered by evoking a phonon surface-mode mechanism. (auth)

5057 CRITICAL MAGNETIC FIELD CURVES OF SUPERCONDUCTING MOLYBDENUM AND CADMIUM ABOVE 0.03°K. Hamblen, David Gordon. Urbana, Ill.; Univ. of Illinois (1969). 87p. University Microfilms Order No. 70-13,340.

Thesis.

The critical magnetic field curves of molybdenum and cadmium were measured from T_c to 0.03°K, using the critical field curve of aluminum as a thermometer. The data, when extrapolated to T = 0, yield values of H_0 = 96.24 gauss and γ = 1.835 mJ/(mole°K^2), for Mo, and H_0 = 28.05 gauss and γ = 0.685 mJ/(mole°K^2) for Cd. The extrapolation to $H_c = 0$ yields T_c values of 0.9134°K and 0.515°K for Mo and Cd, respectively. These values, together with the experimental data, are used to calculate the superconducting electronic entropy and the deviation of the critical field curve from parabolicity over the entire temperature range. The results show satisfactory agreement with previous measurements and with Clem's theory of anisotropy. (Diss. Abstr. Int., B)

5058 EFFECTS OF THE SUPERCONDUCTING TRANSITION ON THE PURE QUADRUPOLE RESONANCE FREQUENCIES IN DHCP LANTHANUM METAL. Poteet, Wade Martin. Blacksburg, Va.; Virginia Polytechnic Inst. (1970). 76p. University Microfilms Order No. 70-13,694.

Thesis.

Measurements of the pure nuclear quadrupole resonance (PQR) frequencies of ^{139}La in dhcp La metal in both its superconducting and normal states were made, using superregenerative spectrometer techniques. PQR associated with the $3/2 - 5/2$ and $5/2 - 7/2$ transitions in the spin-$7/2$ ^{139}La nucleus was observed at both inequivalent sites in the dhcp structure over the temperature range 4.2 to 12°K, and the results for both sets of PQR frequencies show a definite shift on passing through T_c, the superconducting transition temperature. It is of course impossible to say which set is associated with the A-site resonance and which with the equivalent B and C sites (in the ABAC stacking sequence for the dhcp structure), since there exists no sufficiently accurate information on the relative electronic contributions to the electric field gradient (EFG) at these sites. The results for the $3/2 - 5/2$ and $5/2 - 7/2$ PQR frequencies in the normal state give the values 7.700(2) MHz and 6.798(4) MHz for the quadrupole coupling constant $|e^2qQ/h|$ at the two sites (a difference of about 13%). The corresponding shifts in the magnitude of the total EFG, on passing from the normal to the superconducting state, are +0.10% and +0.14% and occur at about 4.5°K, coinciding with the observed T_c for the sample used. These results show that the new mechanism for superconductivity proposed by Hamilton and Jensen does not contribute significantly to the superconductivity in dhcp lanthanum, since the theory associated with this mechanism predicts an appreciable shift in the electric field gradient due to an f-band condensation process. (Diss. Abstr. Int., B)

5059 TRANSMISSION OF FAR-INFRARED RADIATION THROUGH THIN FILMS OF SUPERCONDUCTING AMORPHOUS BISMUTH AND GALLIUM. Harris, Richard Elgin. Urbana, Ill.; Univ. of Illinois (1969). 138p. University Microfilms Order No. 70-13,342.

Thesis.

The ratio T_s/T_n of the far-infrared radiation transmitted through a thin film in the superconducting state to that transmitted through it in the normal state was measured for several samples of amorphous bismuth and gallium. The transition temperature T_c of each film was also measured. Thicknesses were approximately in the range 50 to 200 Å. Numerical calculations based on the strong-coupling theory of superconductivity and on tunneling data produced theoretical values of T_s/T_n for comparison with the data, showing moderately good agreement. For each sample, the energy gap $2\omega_g$ was determined. For bismuth and gallium, T_c and $2\omega_g$ decrease with increasing film resistance. It was also noted that for both materials, the abrupt resistance change at about 15°K, characteristic of thicker amorphous films, appeared instead as a gradual change in resistance beginning at temperatures higher than 20°K. (Diss. Abstr. Int., B)

Equipment and Devices

Refer also to abstracts 5456 and 5459.

5060 (NP-18484) SEARCH FOR EXCESS ELECTRON PHOTO-EJECTION IN LIQUID HELIUM. Note No. 263. Mazzacurati, V.; Moss, F. E.; Sampoli, M. (Rome Univ. (Italy). Istituto di Fisica). 4 Jul 1970. 16p. Dep. NTIS (U. S. Sales Only).

An attempt was made to detect the photo-ejection cross section of the excess electron in liquid helium, in the wave-length region between 0.5 and 1.5 μ, and a lower limit of about 2.0×10^{-15} cm^2 was obtained. This result is far from the subsequent theoretical calculation (2.0×10^{-18} cm^2). On the basis of recent theory of the bubble model, the possibility of a new absorption experiment in the wavenumber region of 800 to 2,500 cm^{-1} is suggested, using an unconventional technique. (auth)

5061 (UCSD-34-P-143-31) CONTINUOUSLY OPERATING ^{4}He EVAPORATION REFRIGERATOR. DeLong, L. E.; Symko, O. G.; Wheatley, J. C. (California Univ., La Jolla, San Diego, Dept. of Physics). [1969]. Contract AT(04-3)-34. 19p. Dep. NTIS.

A simple and compact device was developed to provide continuous, self-regulating refrigeration at approximately 1.3°K. The temperature of the device remains nearly constant, independent of external power, up to a critical power. For a flow rate of 10^{-4} moles/sec, the refrigerator can absorb 4.5 mW. Such a refrigerator should be suitable for condensing ^{3}He in a ^{3}He–^{4}He dilution refrigerator. (auth)

5062 (UCSD-34-P-143-32) PRINCIPLES AND METHODS OF DILUTION REFRIGERATION. II. Wheatley, John C.; Rapp, R. E.; Johnson, R. T. (California Univ., La Jolla, San Diego, Dept. of Physics). [1970]. Contract AT(04-3)-34. 71p. Dep. NTIS.

Some important fundamental questions that lead to degradation in the performance of a dilution refrigerator are considered: namely, convection on the dilute side and superfluid on the concentrated side. Experimental results are presented for a film suppressing still used in conjunction with a continuous heat exchanger (several designs are considered) and a variable number (0 to 6) of step heat exchangers of a copper foil type with a high surface area to a viscous impedance ratio. The first quantitative measurements of viscous heating on the dilute side are presented as well as measurements of thermal resistance on the dilute and concentrated side. Finally, the properties of the refrigerator under external heat load are considered. (auth)

5063 CHANGE OF EIGENSTATE IN A SUPERCONDUCTING rf CAVITY DUE TO A NONLINEAR RESPONSE. Halbritter, J. (Univ., Karlsruhe, Ger. Kernforschungszentrum, Karlsruhe, Ger.). J. Appl. Phys.; 41: 4581-8(Oct 1970).

The studies on superconducting rf cavities have shown phenomena not familiar to normal conducting cavities. Therefore, the phenomenological description of rf cavities at low- and high-field levels, especially nonlinear effects accompanied with high rf field strength, is rediscussed. To handle nonlinear effects, an appropriate perturbation theory is developed. Together with knowledge on the surface impedance in the superconducting state and on field-emitted electrons in the cavity, this theory is solved in lowest approximation. The resulting frequency shift and the nonlinear rf losses are compared with published experimental data. This comparison shows that, at present, nonideal effects define the results. The intrinsic fast superconducting mechanisms causing harmonics are overshadowed by slow nonideal effects. (auth)

5064 SUPER CONDUCTOR MAGNETIC ENERGY STORAGE SYSTEM. Schweitzer, Donald G. (to United States Atomic Energy Commission). U. S. Patent 3,518,496. 30 Jun 1970. Filed 24 Jan 1968.

A system for selectively storing and releasing magnetic energy in a superconductor without external connections to a power supply is described. The superconductor is cooled to a first temperature below its critical temperature and exposed to hysteretic magnetic field cycle selectively to reduce the magnetic moment of the superconductor to zero in the absence of an externally applied magnetic field thereby to store residual magnetic energy in the superconductor mass which can be selectively released from the superconductor by the warming thereof. (AEC)

5065 SORPTION PUMPED ^{4}He II CRYOSTAT FOR SUSTAINING TEMPERATURES BELOW 1°K FOR LONG PERIODS. Hanley, P. E. (Oxford Instrument Co. Ltd.). J. Phys., E (London); 3: 830-2(Oct 1970).

A He II cryostat was constructed that maintained a temperature of 0.9°K for 75 hours by means of an internal sorption pump. A wide-aperture low-temperature valve was used to shut off or throttle the sorption pump in order to obtain temperatures between 0.9 and 4.2°K. (auth) (UK)

Plasma and Thermonuclear Physics

5066 (NP-18495) ANNUAL REPORT, 1968. (Institut fuer Plasmaphysik, G.m.b.H., Garching (West Germany)). 185p. (In German). Dep. NTIS (U. S. Sales Only).

Experimental and theoretical research is presented on the following: (1) linear theta pinch, (2) shock-free compression and turbulent heating of plasma densities between 10^{12} and 5×10^{14} cm^{-3}, (3) special measuring methods and investigation of hot plasmas, (4) toroidal confinement, (5) thermal plasmas and probe diagnostics, (6) stationary heating of high-density plasmas, (7) plasma production with laser beams, (8) magnetoplasma dynamics, (9) plasma waves, (10) theoretical studies of plasma dynamics, and (11) other related topics. (M.O.W.)

5067 TECHNOLOGY INDEX FOR PLASMAPHYSICS RESEARCH AND FUSION REACTORS. VOLUME 4, NO. 9, 1970. Bibliography, Author Index, Subject Index, Appendix. Frankfurt am Main; Zentralstelle fuer Atomkernenergie-Dokumentation (1970). 43p.

This listing includes 220 articles on various aspects of plasma physics and fusion reactors. (M.O.W.)

Confinement and Heating

Refer also to abstract 4088.

5068 (AD-710318) TURBULENT HEATING IN PLASMAS. Koch, Paul (Innsbruck Univ. (Austria). Institut fuer Theoretische Physik). 25 Apr 1970. Contract F61052-70-C-0014. 25p. (UNICP-SR-70; AFOSR-70-2095-TR). NTIS.

The results of a Lagrangian analysis of homogeneous plasma turbulence were used to justify the assumption that trapped-particle modes are instrumental in the turbulent heating of plasma, and a set of equations was derived that describes the behavior of individual waves of that type. The usual probabilistic assumptions of homogeneous turbulence are applied to the basic equations of a Vlasov plasma. A simple mixing-length approximation is used to achieve closure of the resulting set of equations. Some basic principles of Lagrangian plasma turbulence are outlined. Trapped-particle modes are examined and the results of Bohm and Gross are extended so that the exact nonlinear equations that govern them can be derived. (auth) (USGRDR)

5069 CURRENT-INDUCED ION HEATING IN A TOROIDAL PLASMA. Mah, S. Q.; Skarsgard, H. M.; Strilchuk, A. R. (Univ. of Saskatchewan, Saskatoon). Phys. Rev. Lett.; 25: 1409-13 (16 Nov 1970).

Time-resolved measurements of plasma temperatures, current, and density were made in a turbulent heating experiment. Rapid ion heating ceases at the instant the mean electron velocity falls below the critical value for generation of ion-acoustic waves. (auth)

5070 PLASMA CONFINEMENT IN A HIGH MAGNETIC FIELD TOROIDAL QUADRUPOLE. Lubin, M. J. (Univ. of Rochester, N. Y.); Friedman, W.; Roberts, M.; Alexeff, I. Phys. Fluids; 13: 3054-6(Dec 1970).

Plasma ($n < 10^{11}$ cm^{-3}, $T_e < 100$ eV) in the $\oint dl/B$ stable region shows two decay times, τ_{fast} (20 μsec) followed by τ_{slow} (120 μsec, at constant T_e). Where Debye length exceeds electron Larmor radius, $\tau \sim B^2$ with particle loss mainly radial below that field, $\tau \sim B^4$. (auth)

5071 DRIFT OF UNTRAPPED PARTICLES IN A TOKAMAK. Klima, R. (International Centre for Theoretical Physics, Trieste, Italy). Phys. Lett.; 33A: 267-8(16 Nov 1970).

It was shown earlier that the drifts of particles due to the E_φ field are important for the containment of plasma in a tokamak. The influence of an electrostatic field on these drifts is derived here, considering the untrapped particles. (M.O.W.)

5072 ELECTRON HEATING BY ION-WAVE TURBULENCE. Gary, S. P. (Institut fuer Plasmaphysik, Garching, Ger.). Phys. Lett.; 33A: 301-2(16 Nov 1970).

The equations of motion of electrons subject to simulated ion wave turbulence are integrated numerically in one dimension. There is no significant heating unless either the "trapping range" or the "stochastic range" is greater than the electron thermal velocity. (auth)

5073 INVESTIGATION OF ION HEATING DURING DEVELOPMENT OF HIGH-FREQUENCY CLUSTER CENTRIFUGAL INSTABILITY. Marinin, V. G. (Physical-Technical Inst., Kharkov). Ukr. Fiz. Zh.; 15: 1031-3(Jun 1970). (In Russian).

An earlier investigation of the interaction of a beam with plasma

in a magnetic trap showed that the beam–plasma system can be in one of two regimes. Transition from one regime to the other was related to the change of character of the beam–plasma interaction, in particular, to the development of the hf cluster-centrifugal instability. It originates in the system of strong radial electric and longitudinal magnetic fields. Development of this instability is discussed here, noting the heating of the ion component. The transverse energy of the ions was recorded by the delayed-potential method, using a flight analyzer and a probe, which analyze the energy of Larmor precession. It was found that the transverse energy of ions increases linearly with the increase of magnetic field and discharge current. The maximum value of transverse ion energy was 1.8 keV. (tr-auth)

5074 METHOD FOR MAPPING A TOROIDAL MAGNETIC FIELD BY STORAGE OF PHASE STABILIZED ELECTRONS. Sinclair, R. M.; Hosea, J. C.; Sheffield, G. V. (Princeton Univ., N. J.). Rev. Sci. Instrum.; 41: 1552-9(Nov 1970).

A method is described for measuring the shape of a toroidal magnetic field (such as in a stellarator) to demonstrate the existence and nature of magnetic surfaces. The successive circuits of a pulse of low-energy, phase-stabilized electrons injected parallel to the field and stored for many thousands of circuits are detected. It is found that the cumulative effect of various field perturbations alters the parameters of the surfaces significantly, but does not destroy them. In certain special cases, there is excellent agreement between the measured and computed field shapes for the specific device. These results and methods are of immediate application to a broad class of magnetic (or other area preserving) mappings. The same experimental technique can also be used for the long-term storage of low-energy ions. (auth)

5075 ION HEATING IN A PENNING DISCHARGE. Fumelli, M.; Dei-Cas, R.; Girard, J. P.; Valckx, F. P. G. (Centre d'Etudes Nucleaires, Fontenay-aux-Roses, France). Plasma Phys.; 12: 423-33(Jun 1970). (In French).

Ion heating by self-excited plasma oscillations was observed under particular conditions in a lithium plasma column produced by a Penning discharge in a magnetic mirror geometry. With a lithium flow of 10^{19} atoms/sec, and for a discharge power exceeding 2 kW, an unstable mode develops in which ions are accelerated at approximately right angles to the magnetic field lines. A plasma density of 10^{11} cm^{-3} was measured at the center of the magnetic configuration in a volume of 250 cm^3. Fast charge-exchange neutrals show a very broad energy spectrum extending from some hundred eV to 30 keV. The electron temperature is about 40 eV. Important ion losses can be attributed to a m = 2 flute-like instability, observed at 10 cm from the axis. Strong axial symmetrical oscillations near the ion cyclotron frequency were observed, to which the ion heating is attributed. (auth) (UK)

5076 ION CYCLOTRON HEATING OF HYDROGEN PLASMA BY TWO-PHASE EXCITATION. Bashir, Abdul Kabir Abdul, Columbus, Ohio; Ohio State Univ. (1969). 100p. University Microfilms Order No. 70-13,976.

Thesis.

A two-phase excitor coil system was designed and constructed. The system is energized by two 30-kW amplifiers operated at 4.225 MHz in quadrature. A static magnetic field, in the form of a "mirrow machine" is used to confine plasma. The excitor coil system placed at the center of the mirror machine, produces a revolving magnetic field and a rotating induced electric field. In the central plane of the magnetic bottle, strength of the magnetic field produced by the two-phase excitor coil system has a maximum strength of about 3.0 gauss at the edge of the vacuum chamber and zero strength on the axis of the bottle. The rotating induced electric field has a maximum strength on the axis of about 1.28 volt/cm. Ion angular acceleration occurs because the induced electric field is always in the direction of the ion motion. An element of stability is achieved because an ion in resonance always experiences a stronger magnetic field whenever motion is away from the axis of the bottle. The energy gained by the hydrogen plasma from a 4.225-MHz rf field was studied experimentally. The frequency 4.225 MHz corresponded to the cyclotron resonance frequency for atomic hydrogen at 2792 gauss. The existence and extent of the resonance effect was found by measuring the light output from plasma by using a CdS resistive photocell and a photomultiplier as detectors. At resonance conditions, the intensity of the light was found to be increased markedly. The cyclotron resonance is very sharp over a pressure range from 2 to 10 μ. The maximum optical response occurred at 4 μ. Photographic studies of the plasma confirmed the above findings. The energies of the positive ions emitted from the neck of the magnetic bottle and measured by a Faraday cup indicate that ions in the plasma had a peak energy of about 500 eV perpendicular to the bottle field prior to a 90° scatter. The current density estimate is 5×10^{12} cm^{-3}. The plasma was also studied spectroscopically. (Diss. Abstr. Int., B)

Diagnostics

5077 (AD–710597) TIME-RESOLVED ENERGY DISTRIBUTIONS IN A STRIATING DISCHARGE. Final Report. Weber, R. F.; Garscadden, A. (Aerospace Research Labs., Wright-Patterson AFB, Ohio). May 1970. 28p. (ARL–70–79). NTIS.

Preliminary results are reported for time-resolved Langmuir probe measurements made in a striating neon discharge. The presence of large-amplitude moving striations of frequencies of a few kHz required the use of a recently developed sample-and-hold diagnostic system for analysis. This system allows one to obtain digital probe current data with an accuracy greater than 0.3% and compatible with computer reduction. Numerical analysis of the data provides the second-derivative and also determines the electron energy distribution, having identified space potential from the second derivative. The measurements show that the distribution is non-Maxwellian; in particular, preceding the peak of the light intensity fluctuation, there exists a high-energy group of electrons. The relaxation of this group through the phase of the striation is demonstrated and examples of the dependence on other discharge parameters are given. Measurements were made for two wave types distinguished by their products Eλ where E is the longitudinal electric field and λ the wavelength of the striation. (auth) (USGRDR)

5078 (CEA-R–3998) THOMSON SCATTERING AND RAYLEIGH SCATTERING IN AN ARGON PLASMA JET. Decroisette, Michel (Commissariat a l'Energie Atomique, Limeil-Brevannes (France). Centre d'Etudes). Aug 1970. 100p. (In French). Dep. NTIS (U. S. Sales Only).

Experimental determination of electron density in the jet nozzle of an argon plasma torch by Thomson scattering of a ruby laser beam is reported. The results are compared with those obtained from other processes (absolute continuum, absolute intensity of the ArI 4044 Å line). The experimental set up makes it possible to determine the absolute value of the differential scattering cross section: it is found to be in agreement with the theoretical value of: $\sigma' = 0.47 \times 10^{-26}$ cm^2. (auth) (France)

5079 (CLM-R–107) MEASUREMENT OF THE PLASMA PARAMETERS IN TOKAMAK T3-A BY THOMSON SCATTERING. Forrest, M. J.; Peacock, N. J.; Robinson, D. C.; Sannikov, V. V.; Wilcock, P. D. (United Kingdom Atomic Energy Authority, Abingdon (England). Culham Lab.). Jul 1970. 42p. Dep. NTIS (U. S. Sales Only). UK 7s. 0d.

The electron temperature and density in Tokamak T3-A are established from an analysis of the spectral intensity of the scattered photons from a pulsed ruby laser. Electron temperatures up to 2 keV are measured over a range of densities from 1 to 4.5×10^{13} cm^{-3} and ohmic heating currents up to 150 kA. Radial measurements show the pressure profile to be practically flat over the central half of the plasma. The total energy in the plasma column agrees with that measured from the diamagnetic signal. The dependence of the temperature on the discharge parameters is expressed by the relation $I^2\beta_\theta = 200\ Nk(T_e + T_i)$, where β_θ with respect to the heating current is 0.5 in the middle of the current pulse. The value of β_θ reaches 2, which is close to the limit set by classical diffusion, when dI/dt is negative, late in the current pulse. The local temperature rise in the outer region of the discharge due to skin currents is weak, and after the initial increase of the current, is negligible. The resistivity is always anomalous except late in the current pulse and is associated with a critical value for the ratio of the drift to sound speed. The measured particle loss time (which has almost the classical value) is always 3 or 4 times the energy loss time. It is shown by considering the energy balance, taking into account the anomalous factor in the heating, that the main energy loss is by heat conduction, which is anomalously large for all but the highest densities. (auth)

5080 (LA–4520-TR) CONFERENCE ON DIAGNOSIS OF HIGH-TEMPERATURE PLASMA HELD MAY 13–20, 1970 AT THE PHYSICO-TECHNICAL INSTITUTE, SUKHUMI, USSR. Program and Abstracts of Reports. (Gosudarstvennyi Komitet po Ispol'zovaniyu Atomnoi Energii SSSR, Sukhumi. Fiziko-Tekhnicheskii Institut). Translated for Los Alamos Scientific Lab., N. Mex., from Soveshchaniia po Diagnostike Vysokotemperaturnoi Plazmy, Sukhumi, Mai 13–20, 1970. 157p. (CONF-700543–(Absts.)). Dep. NTIS.

Abstracts are given of 102 papers presented at the conference. The papers are given under the following sections: (1) correlation method of analyzing results of a plasma experiment, (2) probe and other methods of plasma diagnostics, (3) laser applications (interferometry), (4) corpuscular method, (5) microwave methods,

XUM

(6) methods of automatic processing of results, (7) laser application (scattering), (8) spectroscopic methods, and (9) ultraviolet and soft x radiation. (M.O.W.)

5081 (N-70-32493) DOUBLE LANGMUIR PROBE MEASUREMENTS IN A MAGNETIZED POSITIVE COLUMN. Dunham, V. C. (Pennsylvania State Univ., University Park. Ionosphere Research Lab.). 15 May 1970. 78p. (NASA-CR-110646; SR-356). NTIS.

The positive column of a cold-cathode, cylindrical glow discharge in nitrogen (.2 and 1.0 torr) under the influence of a small, approximately uniform, longitudinal magnetic field (0 to 200 gauss) was studied. To supply a background for the study, the theories of glow discharges and both single and double probes with and without magnetic fields were surveyed. Using double cylindrical probes, measurements were made in the positive column to determine the effect of the magnetic field on the electron temperature and density. For B = 0, the temperature and density are shown to agree with the theory, the former being constant across the column, and the profile of the latter being described by the zero-order Bessel function. For B > 0, the temperature decreases more rapidly than the theory predicts for increasing B, but becomes constant for B = 100 to 200 gauss. The axial density is shown to increase nearly at the rate predicted by the theory. (auth) (STAR)

5082 (N-70-33122) LINE BROADENING OF THE TRIPLET DIFFUSE SERIES OF HELIUM IN AN ARC-JET PLASMA. Scott, Carl Douglas (National Aeronautics and Space Administration, Houston, Tex. Manned Spacecraft Center). Jul 1970. 122p. (NASA-TM-X-58050). NTIS.

Thesis. Submitted to Univ. of Texas, Austin.

Established spectroscopic techniques were used to determine the electron density and temperature in a helium arc-jet plasma. The measured parameters were used to calculate the Stark broadening of spectral lines in the triplet-diffuse series of helium. These calculations were made by use of the quasi-static approximation for ions and electrons, and were compared with measured profiles in a plasma where the center-line electron density $1.4 \times 10^5 \pm 13\%$ cm^{-3} and the center-line temperature was $7800 \pm 17\%$ K. (auth) (STAR)

5083 OPTICAL INVESTIGATIONS OF ELECTROSTATIC TURBULENCE IN PLASMA. Ben-Yosef, N.; Rubin, A. G. (Air Force Cambridge Research Labs., Bedford, Mass.). Phys. Lett.; 33A: 222-3(2 Nov 1970).

A new method of measuring turbulent electric fields and electron temperatures from broadening of hydrogen Balmer lines is presented. (auth)

5084 ELECTROSTATIC PROBE IN A REACTING GAS. Carrier, G. F. (Harvard Univ., Cambridge, Mass.); Fendell, F. E. Phys. Fluids; 13: 2966-82(Dec 1970).

A spherical perfectly catalytic conductor with negative potential bias lies in a quiescent slightly ionized gas whose density is large enough to warrant the use of continuum theory. The Debye number ϵ, the ratio of the Debye length to the conductor radius, is small. Principal attention is given to the case, amenable to asymptotic analysis, of probe potential $\psi_p > O(\ln \epsilon)$. The relation between the current collected by the probe and the electrode potential is sought; the current virtually saturates (increases very slowly relative to increases in applied potential difference) for $\psi_p \gg O(\ln \epsilon)$. A reconstruction of the chemically frozen case with three novel features is furnished: a transformation of variables that renders the transition-zone equations almost uniformly valid; a very accurate, easily obtained closed-form approximation to the solution of the resulting boundary-value problem; and a current-potential relationship that is derived on the basis of the gross behavior of this approximate closed-form solution. Then the increase in current is determined for the case of finite-rate gas-phase ionization and recombination in which the negative-charge carrier is an electron and in which an electron does not serve as the third body for recombination. It is found that ionization can play a role in a thick sheath in addition to the more conventional effect of both ionization and recombination in the quasineutral region. When an electron serves as the third body for recombination, the sheath is frozen. (auth)

5085 DETERMINATION OF THE PRESSURE ANISOTROPY IN A MIRROR-CONFINED PLASMA. Jacquinot, J.; Waelbroeck, F. (Centre d'Etudes Nucleaires, Fontenay-aux-Roses, France). Plasm Phys.; 12: 447-57(Jun 1970).

An external method is proposed for measuring the pressure anisotropy in a mirror-confined plasma. From a theory based on the adiabatic motion of particles, the variation of characteristic plasma parameters along the axis of a magnetic bottle is derived. The calculations are made with several angular distribution functions and show the dependence on the pressure anisotropy. As an example, the measurement of the diamagnetic profile of a hot electron plasma with a set of magnetic loops allows a quantitative determination of the plasma pressure anisotropy. The method also permits the time variation in both stable and unstable regimes to be measured. (auth) (UK)

5086 LASER LIGHT-SCATTERING MEASUREMENT OF PLASMA TEMPERATURE, DENSITY, AND CORRELATION SPECTRUM. Anderson, Oscar Albin. Berkeley, Calif.; Univ. of California (1969). 152p. University Microfilms Order No. 70-13,009.

Thesis.

The experimental apparatus consisted of a plasma generator, a light source, a scattered-light analyzer, and an optical system for transferring light to the analyzer. The sheet-pinch plasma generator is discussed; it is shown to have particular advantages for studying correlated scattering. Problems of designing a 1-joule giant-pulse ruby laser with suitable line width, wavelength stability, and pulse length are presented, along with the solutions which were found. The scattered spectrum was analyzed by a polychromator based on a readily available Ebert-type spectrometer designed for curved slits. A novel application of crossed cylindrical lenses was discovered which yielded diffraction-limited resolution with a conveniently straight input slit. Because the full slit length was usable, optimum collection of scattered light was achieved: 2×10^6 photons into the 0.01 solid angle of the spectrometer for a moderately dense plasma ($n_e \approx 2 \times 10^{16}$). Thus, adequate photon statistics were obtained from single shots with the 1-joule laser. Because the Thomson cross section is extremely small, stray scattering must be minimized. A negative parallax doublet lens arrangement for imaging the plasma-scattered light onto the spectrometer slit helped to give a stray-light rejection ratio of almost 10^{14}. The scattering measurements showed that the spectrum of light scattered by sheet pinch plasma is smooth and reproducible during the early part of the pinch. Later, instabilities cause irregular nonreproducible spectra. The spectrum from the early quiescent pinch agrees with the theoretical spectrum for thermal equilibrium, displaying strong ion-controlled scattering, and a broad weak electron-controlled plateau bounded by a Landau-damped electron-wave peak. (Diss. Abstr. Int., B) (TSS)

5087 DIAGNOSTIC STUDIES OF HYDROGEN PLASMAS HEATED BY TWO-PHASE EXCITATION AT THE CYCLOTRON FREQUENCY. Kemppel, Roger Raymond. Columbus, Ohio; Ohio State Univ. (1969). 85p. University Microfilms Order No. 70-14,051.

Thesis.

A hydrogen plasma, confined by a magnetic mirror field, and heated by ion-cyclotron resonant heating was produced. Radio-frequency exciter coils were designed that produce rotating electric and revolving magnetic fields, rotating and revolving at a frequency of 4.255 MHz, which corresponds to the hydrogen ion cyclotron frequency at a magnetic field strength of 2790 gauss. The theory of the motion of an ion in rotating electric and revolving magnetic fields is presented. Charged particles escaping from the ends of the magnetic mirror were detected through the use of a Faraday cup used as a retarding-field energy analyzer. A method is presented by which an estimate of the atomic hydrogen ion density of the plasma of 1.88×10^{12} ions/cm^3 was obtained. The energy of the atomic hydrogen ion present in the plasma in the greatest number was shown to be 385 eV. The maximum energy of the H ions was shown to asymptotically approach 930 eV. The energy of the atomic hydrogen ions was shown to increase with increased rf power applied to the exciter coils and to be approximately inversely proportional to the filling pressure. Atomic ion cyclotron resonance was clearly evidenced by a peak, 100 above background, in the current collected by the Faraday cup as the magnetic field B_z was swept through its range. (Diss. Abstr. Int., B)

Kinetics (General)

5088 (AD-710218) ABSORPTION CORRECTIONS FOR OPTICALLY THICK PLASMAS. Final Report. Olsen, H. N. (Plasma Sciences Labs., Inc., Van Nuys, Calif.). Mar 1970. Contract F33615-67-C-1071. 69p. (ARL-70-48). NTIS.

A self-consistent, iterative method was developed for inverting spatially integrated spectral intensities of spectral lines to local emission coefficients with correction for self-absorption. The method is applicable to plasmas that are axisymmetric, exhibit local thermodynamic equilibrium, and whose total absorption along the plasma diameter does not exceed ~20%. As wavelength profiles of the spectral lines need not be measured, the method can be used to correct existing experimental data obtained, with no special consideration having been given to the possibility of a

significant self-absorption. A Fortran 4 computer program is included that has been applied to experimental data obtained with the free-burning argon arc plasma at pressures of 0.5, 1.1, and 2 atm. Corrected values for some argon transition probabilities are used to judge the accuracy of the method. (auth) (USGRDR)

5089 BEHAVIOR OF AN IONIZED GAS IN A HOMOPOLAR DEVICE. Diamond, Stephen Alan. Ithaca, N. Y.; Cornell Univ. (1969). 171p. University Microfilms Order No. 70-5764. Thesis.

The behavior of an ionized gas in a homopolar device is studied. The positive column of a glow discharge constitutes the ionized medium. The influence of a magnetic field and the homopolar geometry upon the discharge is determined. The rotation of the discharge is studied, with emphasis on determining what species in the lightly ionized gas are in motion and what is the mechanism causing rotation of the discharge. Argon and helium data were taken over a pressure range of 1 to 50 torr, with magnetic field strengths up to 3 kG. An externally imposed radial flow was necessary to combat the sputtering of impurities from the cathode. Rotational data was acquired by measuring the time between consecutive arrivals of the leading edge of the discharge at a fixed electrostatic probe. Magnetic fields and high pressures constrain the discharge in an azimuthal direction. High-pressure argon discharges contracted severely, both in azimuth and away from the homopolar walls. The discharge parameter E/p increases with decreasing current, increasing magnetic field strength, and decreasing pressure. Curvature of the discharge is caused by the Hall currents. The neutrals in a helium glow discharge rotate with a velocity less than that of the ions. The charged species define the rotating helium discharge. The neutrals in a high-pressure (greater than 25 torr) argon glow discharge rotate with a velocity equal to that of the ions. The low-pressure argon discharges rotate at a rate greater than that predicted when the neutrals are at rest. It is proposed that this rotational rate is due to new charged species being created outside the discharge proper by high-energy electrons in the vicinity of the leading edge of the rotating discharge. (Diss. Abstr. Int., B)

5090 AMPLIFICATION OF VACUUM-ULTRAVIOLET RADIATION IN DECAYING DENSE HELIUM PLASMA. Gudzenko, L. I.; Zemtsov, Yu. K.; Yakovlenko, S. I. (Moscow State Univ.). JETP Lett. (USSR) (Engl. Transl.): 12: 167-9(5 Sep 1970).

Translated from Zh. Eksp. Teor. Fiz., Pis'ma Red.; 12: 244-8(5 Sep 1970).

A study was made of the energy level populations of helium for the purpose of possible laser applications. Diagrams are given showing the time dependence of the population of He^+ levels n = 2 and n = 3 for decaying plasma. Amplification coefficients for the 1641 Å line for different plasma parameters are given. (M.O.W.)

5091 NONADIABATIC PARTICLE MOTION IN LINEAR AND TOROIDAL MULTIPOLE FIELDS. Howard, James Edward. Madison, Wis.; Univ. of Wisconsin (1969). 131p. University Microfilms Order No. 70-3561.

Thesis.

Nonadiabatic particle motion in static multipole magnetic fields was studied both theoretically and by means of numerical experiment. As a mirroring particle passes through a low field region where the field gradient is large, its magnetic moment μ, normally constant, may undergo sharp variations. Such changes are called nonadiabatic, and the object of this thesis is to predict them. (Diss. Abstr. Int., B) (TSS)

Kinetics (Experimental)

5092 (SC-T-70-4044) RADIATION LOSSES OF A HIGH-DENSITY Z-PINCH. Kaufmann, M. (Institut fuer Plasmaphysik, G.m.b.H., Garching (West Germany)). Translated for Sandia Labs., Albuquerque, N. Mex., from report IPP-1/86. 58p. Dep. NTIS.

An abstract of this paper, prepared from the original language, appeared as NSA 23: 6970. (M.O.W.)

5093 PROPERTIES OF HIGH CURRENT FREE-BURNING ARCS IN AIR. Nicolai, Leland M. (Air Force Academy, Colorado Springs, Colo.). Phys. Fluids; 13: 2983-6(Dec 1970).

The measured characteristic curves for free-burning arcs in air at pressures from 0.019 to 1.0 atm and high currents from 190 to 400 A are presented. The experimental results show that the characteristic curves are flat (E = const) at these high currents. Characteristic arc dimensions were determined from arc photographs. The results show the arc diameter to be proportional to $I^{\frac{1}{2}}$. Heated solid cylinder heat transfer ideas are applied to the free-burning arc data, and the functional form for the Nusselt number in terms of the Grashof and Prandtl number is determined. (auth)

Kinetics (Theoretical)

5094 (CEA-CONF-1629) CRITERIA FOR LOCAL THERMODYNAMIC EQUILIBRIUM. Drawin, H. W. (Commissariat a l'Energie Atomique, Fontenay-aux-Roses (France). Centre d'Etudes Nucleaires). 1970. 85p. (CONF-700706-3). Dep. NTIS (U. S. Sales Only).

From 5th Plasma Physics Symposium, Herceg-Novi, Yugoslavia.

The criteria of validity for local thermodynamic equilibrium (LTE) were established by considering the different terms in the zero-order Boltzmann collision equation. The conditions applicable to the establishment of a Maxwellian distribution for the free electrons were studied. It was shown that, in the most unfavorable case of an optically thin plasma, the Maxwellian distribution occurs when the degree of ionization is greater than 1%. Conditions become more favorable when elastic electron–atom collisions and resonance absorption are considered, and a Maxwellian distribution may be expected when the degree of ionization exceeds 0.1%. In the special case of heavy particles a Maxwellian distribution can generally be reached, since the particles are much less affected by inelastic collisions than the ions. The method of calculating the LTE criteria of validity in neutral and ionic systems was successfully applied to the cases of optically thin homogeneous plasmas, which were independent of time in partial LTE and then complete LTE. The influence of resonance absorption in the establishment of partial or complete equilibria in a stationary homogeneous plasma, and the influence of heavy particle collisions on the equilibrium population of strongly excited levels, were studied. The study of the criteria of validity was extended to the cases of quasi-stationary and quasi-homogeneous plasmas (optically thin and optically thick). The relaxation time necessary to establish a partial or complete LTE in a transient inhomogeneous plasma and the relaxation length in stationary nonuniform plasmas were determined. The validity of the Kirchoff law is discussed. (France)

5095 (CEA-R-4057) PROBLEMS IN RADIATION HYDRODYNAMICS. Bobin, Jean-Louis (Commissariat a l'Energie Atomique, Limeil-Brevannes (France). Centre d'Etudes). Sep 1970. 117p. (In French). Dep. NTIS (U. S. Sales Only).

Basic equations describing radiation hydrodynamics are given. Methods to integrate the radiation-transfer equation over angles and frequencies are presented in some detail. Examples deal with thermal waves and radiative shock front structure. (tr-auth) (France)

5096 (COO-2059-5) DIFFERENCE SCHEME FOR VLASOV'S EQUATION. Nuehrenberg, Juergen (Iowa Univ., Iowa City. Dept. of Physics and Astronomy). Jul 1970. Contract AT(11-1)-2059. 59p. Dep. NTIS.

A difference scheme is developed for the solution of the initial-value problem for the one-dimensional Vlasov equation for a collisionless electron plasma with a homogeneous ion background. Instead of the distribution function itself, its Fourier transform with respect to velocity is used. Case studies of nonlinear Landau damping, a stationary equilibrium, and a two-stream instability are presented as preliminary applications. (auth)

5097 (COO-2059-6) NUMERICAL INTEGRATION METHODS OF THE VLASOV EQUATION. Joyce, Glenn; Knorr, Georg; Meier, Homer K. (Iowa Univ., Iowa City. Dept. of Physics and Astronomy). [1970]. Contract AT(11-1)-2059. 17p. Dep. NTIS.

The methods of integrating the nonlinear Vlasov equation are reviewed and compared, and interrelations are investigated. Another method is given that allows a truncation of the resulting infinite matrix without causing numerical instabilities. Its application to the linear and nonlinear Vlasov equation is discussed. It is shown that the cause for numerical instability is based on approximating a continuous eigenvalue spectrum by a discrete spectrum. (auth)

5098 ION DISTRIBUTION FUNCTIONS IN COLLISIONLESS SURFACE IONIZED PLASMAS. Buzzi, J. M.; Doucet, H. J.; Gresillon, D. (Ecole Polytechnique, Paris). Phys. Fluids; 13: 3041-9(Dec 1970).

For a low-density surface-ionized plasma (e.g., in a Q machine) where Coulomb or binary collisions are negligible, a simple steady-state model of the plasma is obtained through the Vlasov and Poisson equations. Among the main predictions of this model, the electron-rich regime involves a truncated Maxwellian distribution function for the ion velocities parallel to the magnetic field. Experiments were carried out in a short single-ended Q machine for a cesium plasma. Curves of density versus neutral flux are plotted. With the help of a heated probe and an electrostatic ana-

XUM

lyzer, whose work functions are carefully taken into account, the ion distribution functions are deduced. In the observations they correspond to beams of 1 to 1.5 km/sec mean velocity and velocity spread that can be characterized by a parallel temperature of 150 to 300°K. These experiments and the theoretical model are in good agreement. (auth)

5099 DOWNSTREAM STATE OF COLLISIONLESS SHOCK WAVES. Goldberg, P.; Schindler, K. (European Space Research Inst., Frascati, Italy). Phys. Fluids; 13: 3056-8(Dec 1970).

The downstream state of collisionless shock waves may not, in general, be determined independently of the shock structure and of the dissipation mechanism. Several attempts to determine this state are discussed and shown to be either incorrect or unconvincing. (auth)

5100 TEACHING EXPERIENCE IN THERMONUCLEAR THEORY. Ma, Benjamin M. (Iowa State Univ., Ames). Trans. Amer. Nucl. Soc.; 13: 459-60(Nov 1970).

From Meeting of the American Nuclear Society, Washington, D. C. See CONF-701102.

5101 DIELECTRIC PERMEABILITY OF AN INHOMOGENEOUS RELATIVISTIC STREAM OF COLD PLASMA. El-Naggar, I. A.; Pakhomov, V. I.; Zayed, K. E. (Atomic Energy Establishment, Cairo). Plasma Phys.; 12: 459-60(Jun 1970).

Expressions are obtained for the components of the dielectric permeability tensor operator of a cold plasma stream with an inhomogeneous velocity profile and inhomogeneous particle density. (auth) (UK)

5102 FINITE-LARMOR-RADIUS ANALYSIS OF LAMINAR COLLISIONLESS SHOCKS. Coroniti, Ferdinand Vincent. Berkeley, Calif.; Univ. of California (1969). 206p. University Microfilms Order No. 70-13,032.

Thesis.

The structure of finite-β laminar collisionless fast and slow shock waves is investigated from the finite-Larmor-radius Chew-Goldberger-Low (FLR–CGL) hydromagnetic fluid equations. As a motivation for the shock study the linear dispersion relation for the three hydromagnetic waves is derived, including ion FLR dispersion. (TSS) (Diss. Abstr. Int., B)

Production

5103 PRODUCTION OF A QUASI-ELECTRON-FREE PLASMA USING ELECTRONIC ATTACHMENT. Doucet, H. J. (CNRS, Paris, France). Phys. Lett.; 33A: 283-4(16 Nov 1970).

A negative ion density of 10^{10} cm^{-3} is obtained by introducing iodine in a gas discharge where electrons are trapped in a potential well. The proportion of electrons is found to be only a few parts per thousand. (auth)

5104 LASER-PRODUCED PLASMAS FOR POWER GENERATION AND SPACE PROPULSION. Lubin, Moshe J. (Univ. of Rochester, N. Y.). Astronaut. Aeronaut.; 8: No. 11, 42-8(Nov 1970).

The review-type article discusses the two major uses of laser-induced fusion; space propulsion and electrical power generation from a fixed plant. A general discussion of laser systems and operations for possible use is given. (M.O.W.)

5105 INVESTIGATION OF A LOW-POWER MPD ARC. Boling, Norman Lee. Columbus, Ohio; Ohio State Univ. (1969). 150p. University Microfilms Order No. 70-13,983.

Thesis.

A general investigation is made of the ignition of the arc of and the plasma produced by an MPD engine operating at less than 3 kW and designed to function as a plasma wind tunnel for the testing of models and development of diagnostic techniques in flowing plasmas. A necessary condition for stable ignition of an arc is developed and experimentally tested. A Langmuir probe and a microwave interferometer are used to measure the electron density and temperature in a plane 30 cm from the anode exit of the engine. The electron temperature varies between 20,000 and 40,000°K, the higher values being found at low values of the externally applied magnetic field. The electron density at the measurement plane varies between 10^9 and 10^{11} electrons cm^{-3}, and is found to depend strongly upon the ambient pressure in the test tunnel. This dependence is explained in terms of diffusion to the wall of the plasma tunnel and in terms of the decrease in directed ion speed as the ambient tunnel pressure increases. The dependence of electron density upon gas (argon) input rate, arc current, and magnetic field is investigated. The electron density is found to exhibit peaks when the cyclotron frequency, due to the externally applied magnetic field, is approximately equal to the plasma frequency. The use of a Planar Guard Ring Langmuir probe to measure directed ion speed is described, and experiments indicate that this probe behaves like an ideal plane probe. An orifice probe is used to measure neutral-particle-directed speed. These neutral-particle speeds are shown to be negligible compared to the directed speed of the ions. (Diss. Abstr. Int., B)

Stability

Refer also to abstracts 5117, 5128, and 5129.

5106 (NYO-1480-161) COMPUTATION OF THE EQUILIBRIUM OF A PLASMA WITH HELICAL SYMMETRY. Friedman, Neal (New York Univ., N. Y. AEC Computing and Applied Mathematics Center). Sep 1970. Contract AT(30-1)-1480. 148p. Dep. NTIS.

The equilibrium configuration of a plasma confined by a helically symmetric magnetic field under magnetohydrodynamic assumptions was calculated. This entails solving an elliptic partial differential equation on a domain with a free boundary. To do so, the problem of solving the partial differential equation was separated from that of computing the location of the free boundary. A rectangle with fixed boundary is introduced as an auxiliary domain and the differential equation is solved there. To calculate the location of the free boundary, two variational problems are considered. One is the minimization of the Dirichlet–Douglas integral for conformal mapping; the other is the minimization of an integral connected with the energy of the free-boundary problem. The method of steepest descent is used to develop an iterative procedure suggested by the problem of minimizing these two functionals. Convergence of this algorithm yields a conformal mapping of the rectangle onto the original domain, allowing one to express the solution of the partial differential equation there. The conformal mapping has the additional property that, not only is the solution of the differential equation defined on the original domain, but it also satisfies the free-boundary condition there. (auth)

5107 DYNAMIC INSTABILITY IN STREAMING RELATIVISTIC PLASMAS. Buti, B. (Indian Inst. of Tech., New Delhi). Phys. Lett.; 33A: 237-8(2 Nov 1970).

The subluminous waves propagating transverse to the direction of the relative streaming, u (relativistic or nonrelativistic) of the relativistic plasmas are found to be dynamically unstable for $u \geq 0.09c$. (auth)

5108 LYAPUNOV STABILITY OF AN INHOMOGENEOUS TWO-STREAM PLASMA. Chervin, Robert M.; Sen, Amiya K. (Columbia Univ., New York). Phys. Fluids; 13: 3012-19(Dec 1970).

Lyapunov's direct method was adapted to the study of an electrostatic instability of a plasma by using Zubov's extension of the method to distributed parameter systems. Specifically, the linear stability of two inhomogeneous interpenetrating electron streams in a finite one-dimensional system is considered. Proper Lyapunov functionals are constructed for both stability and instability. It is seen that, as in the homogeneous case, the stability or instability depends on whether or not the thermal speed is greater or less than the streaming speed. In contrast to the methods of energy principle, the complete generality of Lyapunov's direct method is discussed. (auth)

5109 EXPLOSIVE PLASMA INSTABILITIES. Fukai, J. (Univ. of Tennessee, Knoxville); Krishan, S.; Harris, E. G. Phys. Fluids; 13: 3031-7(Dec 1970).

The interaction of three monochromatic waves (two positive-energy longitudinal waves and one negative-energy wave) is investigated. When only the first-order nonlinear interactions are considered, an explosive instability occurs. However, this instability is stabilized by the higher-order nonlinear interactions. The matrix elements of the three-wave and the four-wave interactions in a magnetized plasma are calculated. (auth)

5110 HIGH-FREQUENCY FLUTELIKE INSTABILITIES IN MULTICOMPONENT PLASMAS. Guest, G. E.; Farr, W. M.; Dory, R. A. (Oak Ridge National Lab., Tenn.). Phys. Fluids; 13: 3038-40(Dec 1970).

Plasma in a magnetic field B is subject to unstable electrostatic gyroharmonic waves propagating across B, if the distribution of f_0 of particle velocities $v_\perp$ ($\perp$ to B) has a region where $\partial f_0/\partial v_\perp > 0$. Stability limits are found for f_0 representative of mirror-confined plasmas having a "warm" Maxwellian species, an otherwise identical "hot" species with a region of positive $\partial f_0/\partial v_\perp$, and a neutralizing background. The waves are stable if the ratio of mean energies of the warm to hot species exceeds 0.1, or if the

ratio of densities does not fall in an unstable interval roughly characterized by $0.01 \lesssim N_W/N_H \lesssim 1$. It is important for fusion experiments that the conditions necessary for stability are less restrictive than the sufficient condition: $\partial f_0/\partial v_\perp < 0$ for all the species. (auth)

5111 SUPPRESSION OF A KELVIN–HELMHOLTZ INSTABILITY IN A CESIUM PLASMA BY PASSIVE FEEDBACK. Carlyle, D. C.; Lindman, E. L.; Oakes, M. E. (Univ. of Texas, Austin). Phys. Lett.; 33A: 297-8(16 Nov 1970).

An experiment resulting in the suppression of a Kelvin–Helmholtz instability by a passive feedback network is described. Stabilization results in a reduction in ion fluctuation amplitude and an increase in total plasma density. (auth)

5112 DRIFT INSTABILITY IN COLLISIONLESS ALKALI METAL PLASMAS. Politzer, Peter Alexander. Princeton, N. J.; Princeton Univ. (1969). 100p. University Microfilms Order No. 70-14,235.

Thesis.

Measurements of low-frequency ($\omega \ll \Omega_i$) oscillations in collisionless, low-β, alkali metal Q-device plasmas are reported. These oscillations are conclusively identified as density-gradient-driven drift waves by the agreement between experiment and the predictions of the linear theory with regard to frequency, wave number, and stabilization by ion Landau damping. The linear theory of collisionless drift waves is modified to take into account effects of cylindrical geometry. Also considered are radial gradients in the zero order diamagnetic drift and plasma rotation frequencies. The enhancement of resonant particle effects by the finite length of the plasma column is computed. The occurrence of discrete radial eigenfunctions is found to depend on the radial variation of the equilibrium plasma potential. The observed dependence of amplitude on r agrees with that predicted by the theory. The experimental results demonstrate the importance of centrifugal and Coriolis force effects in determining the oscillation frequency. Finally, the transition between collisionless and collision-dominated drift waves is explored, and the relationship between the observed amplitudes and the predictions of several nonlinear theories is examined. (Diss. Abstr. Int., B)

Thermonuclear Processes

Refer also to abstract 5100.

5113 (AD–710606) INFLUENCE OF AN AXIAL MAGNETIC FIELD ON NEUTRON PRODUCTION IN A PLASMA FOCUS DISCHARGE. Bernstein, Melvin J.; Hai, Francis (Aerospace Corp., El Segundo, Calif.). 15 Jul 1970. Contract F04701-70-C-0059. 30p. (TR–59(6220-50)-2; SAMSO-TR–70-284). NTIS.

An axial magnetic field of up to 1,200 Gauss was applied to a plasma focus discharge, and the effects on neutron production were investigated. Trapped fluxes of 34,000 and 57,000 Maxwells reduced the neutron yields by factors of 5 and 10, respectively. The applied field reduced the average energy shift of the axially emitted neutrons, decreased the ratio of the axial neutron flux to radial flux, and extended the length of the neutron source. An increase in the field from 720 to 1,200 Gauss did not further reduce the flux anistropy. Streak photography revealed that the minimum plasma radius became larger with increased distance from the anode and that the visible plasma boundary became indistinct at the time of most intense neutron emission. The trapped flux delayed the onset of this intense emission. These results are consistent with an acceleration mode of neutron emission. (auth) (USGRDR)

5114 (CLM-R-103) RADIATION DAMAGE EFFECTS IN THE CONTAINMENT VESSEL OF A THERMONUCLEAR REACTOR. Martin, D. G. (United Kingdom Atomic Energy Authority, Abingdon (England). Culham Lab.). Mar 1970. 69p. Dep. NTIS (U. S. Sales Only). UK 8s. 0d.

During the lifetime of a thermonuclear reactor the containment vessel, assumed here to be fabricated from niobium, will be irradiated by about 2×10^{23} of 14.1-MeV neutrons cm^{-2}. This will result in high concentrations of transmutation products (e.g., 10 at. % Zr) and an appreciable number of displacements of the atoms. A detailed discussion is given of the physical property changes due to this radiation damage for irradiation temperatures in the range 600 to 1200°C. Helium is expected to be the most serious transmutation product since it can aggregate into comparatively immobile bubbles and so produce swelling of the containment vessel. Assuming bubbles are maintained in equilibrium, it is shown that swelling under conditions anticipated in the reactor should not be too excessive (~ a few percent) for irradiation temperatures up to about 1000°C; also, that below this temperature, fracture under tensile stress due to the growth of bubbles is not expected in practice. Displacement damage may harden the material, enhance its creep rate, and result in swelling due to void formation. An attempt is made to predict the importance of these effects from the point of view of a reactor designer. Swelling due to voids could well be important, since void formation is predicted within the temperature range 600 to 1100°C. Erosion of the vessel and contamination of the plasma due to the evaporation of niobium atoms from thermal spikes located near the surface are shown to be unimportant. A number of experiments using currently available irradiation sources, which could shed further light on this subject, are suggested and discussed. (auth)

5115 (JINR–P4-5019) REACTIONS IN COMPLETE FUSION OF NUCLEI. Kalinkin, B. N.; Petkov, I. Z. (Joint Inst. for Nuclear Research, Dubna (USSR)). 1970. 18p. (In Russian). Dep. NTIS (U. S. Sales Only).

The process of complete fusion is discussed, taking into account the recent experimental data. The consequences ensuing from the model suggested by the authors earlier are considered. It is shown that investigation of the process of production of the compound nuclei can, in principle, give some information on their "macroscopic" characteristics, as well as on the value of the fission barrier in the conditions of strong "heating up." (auth)

5116 (SC-T-70-4046) RESEARCH ON STUDYING AND INCREASING THE PLASMA PARAMETERS ON "NON-CYLINDRICAL Z-PINCH" EQUIPMENT. Agafonov, V. I.; Belyaeva, I. F.; Vikhrev, V. V.; Ivanov, V. D.; Moiseeva, M. P.; Svirskii, E. B.; Filippov, N. V.; Filippova, T. I. (Akademiya Nauk SSSR, Moscow. Institut Atomnoi Energii). Translated by Fredric D. Killebrew (Sandia Labs., Albuquerque, N. Mex.), from report IAE-2017. 32p. Dep. NTIS.

Experimental research on plasma focus used with equipment having an increased energy storage in the capacitor bank (up to 140 kJ) is described. The dependence of the plasma focus parameters on the energy stored in the capacitor bank is discussed. The dependence of neutron yield K on energy stored in the bank is on the order of 2.5. As a result of the experiments, a neutron emission intensity of 19^{18} neutrons/sec is obtained, with an absolute yield on the order of 1.1×10^{11} n/shot. (M.O.W.)

5117 THERMAL EQUILIBRIUM AND STABILITY OF TOKAMAK DISCHARGES. Furth, H. P.; Rosenbluth, M. N.; Rutherford, P. H.; Stodiek, W. (Princeton Univ., N. J.). Phys. Fluids; 13: 3020-30(Dec 1970).

Steady-state temperature and magnetic field profiles are derived in cylindrical geometry, including classical electron–ion equilibration, Ohmic heating, and the classical ion thermal transport appropriate to tokamak geometry. To fit the experimental data, a direct electron heat loss must accompany any appreciable resistivity anomaly. The classical equilibrium can be thermally stable only if $T_i/T_e \gtrsim 2/3$. Direct electron heat loss by radiation is further destabilizing; but for typical parameters, stability can be achieved by a moderate amount of anomalous electron thermal conduction. The growth time of thermal instabilities is generally limited by the resistive skin time. The presence of a runaway component of the current allows shorter growth times, and this may be related to the present high-density limit in tokamaks. (auth)

5118 PRODUCTION OF NUCLEAR REACTIONS BY HIGHLY CONCENTRATED ELECTRON BEAMS. Bennett, Willard H. U. S. Patent 3,516,906. 23 Jun 1970. Filed 28 Nov 1966.

A method is described for producing fragments of a nuclear reaction process in which a metal, whose number on the Periodic Table of Elements is at least as high as 73, is bombarded with a beam of electrons. The beam is concentrated by first directing it into the self-magnetic field of a pinched discharge, and has an intensity so great that it raises the temperature of the metal so rapidly, and to such a high degree, as to produce nuclear reaction products. (Offic. Gaz.)

5119 BIFURCATION PROBLEM IN E-LAYER EQUILIBRIA. Marder, B.; Weitzner, H. (New York Univ., N. Y.). Plasma Phys.; 12: 435-45(Jun 1970).

Two methods are developed to solve the equation that describes the equilibrium magnetic field associated with an E-layer in an Astron device. Because of problems related to bifurcation, all solutions are not obtainable by standard numerical means. Two methods are developed that enable one to find all solutions. The appearance of bifurcations and the difficulties in computing solutions past points of bifurcation are typical of finite-beta plasma-equilibrium problems, and the methods proposed should have some general usefulness. (auth) (UK)

XU

5120 DENSE PLASMA FOCUS FORMATION BY DISK SYMMETRY. Buckwald, Robert Allen. Columbus, Ohio; Ohio State Univ. (1969). 89p. University Microfilms Order No. 70-13,090.

Thesis.

Using a disk-shaped discharge chamber, 25-cm in radius, a plasma focus was produced at times ranging from 15 to 3.5 μsec after the beginning of the discharge. The exact time depends on pressure. The focus had a density of greater than 10^{18} ions/cm^3 and a temperature of approximately 10^6°K. Contrary to indications from the dense plasma focus device, no difficulty was observed in focusing the device. Focus durations as long as 2.0 μsec were obtained. This time is an increase by a factor of 20 over the containment times observed in the dense plasma focus device at Los Alamos. Two simple models explain the discharge phenomena. First, the snow-plow model was seen to explain the compression and gave an order-of-magnitude estimate for collapse speeds observed in the disk focus device. Second, a simple ionization and avalanche model explained the time-dependent delays in starting the discharge. Voltage traces indicate the current column pulsates at low pressures. (Diss. Abstr. Int., B)

Wave Phenomena

Refer also to abstract 5109.

5121 (AD-709878) VISCOUS TAILS IN MHD. Fan, D. N.; Ludford, G. S. S. (Cornell Univ., Ithaca, N. Y.). 9 Jul 1968. Contract DA-31-124-ARO(D)-325. 16p. (AROD-5329:16-M). NTIS.

Electrostatic low-frequency waves, propagating with a $k_\perp \gg k_\parallel$ and with frequencies $\omega < \omega_c$ (ω_c = ion cyclotron frequency) in the radial edge of a thermalized, low-temperature and low-beta Cs plasma column, can be switched on and off by a fast change of dc voltage applied to a column aperture ring. From the oscillation growth and decay connected with the aperture voltage switch, growth and damping rates of this instability were derived. The method and the results of wave growth and damping rate measurements are given as a function of the wave frequency, plasma density, and the potential drop through the plasma column edge. (auth) (USGRDR)

5122 (COO-2059-4) EXCITATION OF ION BURSTS FROM GRIDS. Knorr, Georg (Iowa Univ., Iowa City. Dept. of Physics and Astronomy). Apr 1970. Contract AT(11-1)-2059. 28p. Dep. NTIS.

Experiments on ion bursts with a step function excitation of a grid are investigated theoretically. After the description of particle distributions and potentials in the sheath region, the ideal response of a probe located at a distance from the grid is calculated. It is shown how the declining part of the response function depends on the sheath characteristics. It is estimated that it should not be impossible to measure directly the far field of test particles in the initial part of the response function. (auth)

5123 (SU-IPR-366) LOW FREQUENCY AXISYMMETRIC WAVES IN A WEAKLY IONIZED MAGNETOPLASMA COLUMN. Duncan, A. J.; Forrest, J. R. (Stanford Univ., Calif. Inst. for Plasma Research). Aug 1970. Contract AT(04-3)-799. 62p. Dep. NTIS.

A simplified theory is developed for wave propagation in a homogeneous weakly ionized plasma in a uniform magnetic field, taking into account perturbations in the electron temperature and ionization rate. Ionization waves are predicted, and good qualitative and quantitative agreement with experiment is found. With increasing magnetic field or neutral gas pressure, these waves become unstable and grow to the nonlinear limit known as striations. Also, by including T_e as a variable, the ion-acoustic wave solutions are modified slightly, exhibiting cutoffs in frequency and wavenumber, as found experimentally. Experimental wave propagation measurements on a helium discharge for pressures in the range 38 to 600 mtorr, and for magnetic fields up to 300 G, are described. The dispersion characteristics of the dominant mode agree well with the predicted plane ionization wave. (auth)

5124 (SU-IPR-381) LAGRANGIAN APPROACH TO NONLINEAR WAVE INTERACTIONS IN A WARM PLASMA. Galloway, J. J.; Kim, H. (Stanford Univ., Calif. Inst. for Plasma Research). Aug 1970. Contract AT(04-3)-799. 36p. Dep. NTIS.

The coupled-mode equations and coupling coefficients for three-wave interaction are derived by a Lagrangian approach for a general medium. A derivation of the Low Lagrangian for a warm plasma is then given that avoids certain problems associated with the original analysis. An application of the Lagrangian method is made to the interaction between collinearly propagating electrostatic waves, and a coupling coefficient is derived that agrees with a previous result obtained by direct expansion of the nonlinear equations. The paper is primarily tutorial, and serves to demonstrate the efficacy of the Lagrangian approach to nonlinear wave interactions. (auth)

5125 (SU-IPR-389) STUDIES OF PLASMA OSCILLATIONS, 1 FEBRUARY 1970-31 JULY 1970. Status Report No. 36. (Stanford Univ., Calif. Inst. for Plasma Research). Aug 1970. Contract AT(04-3)-799. 43p. Dep. NTIS.

Continuing research during this six-month period is reported on the following: (1) low-frequency wave propagation and positive column instabilities, (2) electron cyclotron echoes and collision measurements, (3) wave-wave interaction phenomena, and (4) beam-plasma interactions. (M.O.W.)

5126 INTERACTION OF A QUASI-TRANSVERSE EXTRAORDINARY WAVE WITH DENSITY FLUCTUATIONS IN AN INHOMOGENEOUS MAGNETIZED PLASMA. Weyl, Guy M. (Avco Everett Research Lab., Everett, Mass.). Phys. Rev. Lett.; 25: 1417-19(16 Nov 1970).

Propagation of a quasi-transverse extraordinary wave through an inhomogeneous magnetized plasma is studied. Modulation of the reflection coefficient of the plasma due to density fluctuations in the region of evanescence of the wave is predicted. A measurement of the modulation is proposed as a diagnostic of certain plasma instabilities. (auth)

5127 KORTEWEG-DE VRIES EQUATION FOR DRIFT WAVES IN A COLLISIONLESS PLASMA. Orefice, A.; Pozzoli, R. (Univ., Milan). Phys. Lett.; 33A: 228-9(2 Nov 1970).

A generalized Korteweg-De Vries equation is derived for nonlinear drift waves propagating along the external uniform magnetic field. A relation is presented between amplitude and propagation velocity of solitary drift waves. (auth)

5128 ION CYCLOTRON INSTABILITY. Weibel, Erich S. (Univ. of California, Los Angeles). Phys. Fluids; 13: 3003-6 (Dec 1970).

Electrostatic ion cyclotron waves are investigated for a plasma consisting of two groups of counterstreaming ions in a background of stationary electrons. Under certain conditions such waves are weakly amplified. Analytic and numerical conditions for instability are presented. (auth)

5129 ORDINARY-MODE ELECTROMAGNETIC INSTABILITY IN COUNTERSTREAMING PLASMAS WITH ANISOTROPIC TEMPERATURES. Bornatici, M. (Goddard Space Flight Center, Greenbelt, Md.); Lee, Kai Fong. Phys. Fluids; 13: 3007-11 (Dec 1970).

The instability of the electromagnetic linearly polarized mode propagating perpendicular to a uniform magnetic field is studied by using the Vlasov equation for a counterstreaming electron plasma with anisotropic temperatures. An instability occurs if the streaming velocity exceeds a certain threshold value, which can be below that required to excite the electrostatic two-stream instability. It is found that temperature perpendicular to the field has a stabilizing effect, while parallel temperature enhances the electromagnetic instability. Typical growth rates are of the order of the electron cyclotron frequency. (auth)

5130 PROPAGATION OF ION WAVES IN A RADIO FREQUENCY ELECTRIC FIELD. Takamura, S.; Aihara, S.; Takayama, K. (Nagoya Univ., Japan). Phys. Fluids; 13: 3052-4(Dec 1970).

The wavelength of an ion wave decreases in an rf electric field. This phenomenon is explained by the additional pressure produced by the spatial modulation of the rf field by the ion wave. (auth)

5131 INVESTIGATION OF THE WAVE TRANSFORMATION CONDITIONS IN A PLASMA IN THE RANGE BETWEEN ELECTRON CYCLOTRON AND LOW HYBRID FREQUENCIES. Arkhipenko, V. I.; Budnikov, V. N.; Obukhov, A. A. (Ioffe Inst. of Physics and Tech., Leningrad). Phys. Lett.; 33A: 303-4(16 Nov 1970).

The location of the wave transformation region in a plasma was determined by the magnetic field perturbation method and shown to be in agreement with the two-dimensional transformation theory. (auth)

5132 SPREADING OF HIGH-FREQUENCY PLASMA ALONG A MAGNETIC FIELD NEAR THE ELECTRON CYCLOTRON HARMONICS. Budnikov, V. N.; Novik, K. M.; Obukhov, A. A. (Ioffe Inst. of Physics and Tech., Leningrad). Phys. Lett.; 33A: 304-5 (16 Nov 1970).

The effect of high-frequency plasma spreading along the magnetic lines of force at the magnetic field values corresponding to

electron cyclotron harmonics is described. The effect is associated with the formation of energetic electrons. (auth)

5133 STUDY OF DISPERSION RELATIONS FOR PLANE WAVES IN MULTICOMPONENT PLASMAS. Verheest, Frank George. Ghent; State Univ. of Ghent (1966). (In Dutch).
Thesis.

Linear wave phenomena in plasmas of arbitrary composition were studied. A collection of N different kinds of charged particles is considered, without placing any restriction upon the number N nor upon the values of charge and mass. A macroscopic point of view is used to describe each component of the plasma by the adequate moment equations derived from a Boltzmann equation per species. The collision model is for simplicity approximated by a relaxation term. The behavior of each constituent is assumed adiabatic, as far as pressure is concerned. The set of fluid equations can then be closed if they are supplemented by the equations of Maxwell. The equations are linearized in the usual fashion around an equilibrium state, taking the waves as small-amplitude perturbations. The dispersion relation in its most general form is arrived at by requiring the set of equations to have a nontrivial solution. The dispersion relation is then applied in some specialized cases, in order to recover known results from the literature and to classify them in a systematic way. (Diss. Abstr. Int., B) (TSS)

5134 ION–ELECTRON RESONANCES IN BOUNDED, HOT PLASMAS WITH AND WITHOUT STEADY MAGNETIC FIELD. Vandenplas, P. E.; Messiaen, A. M.; Monfort, J.-L.; Papier, J. J. (Ecole Royale Militaire, Brussels). Plasma Phys.; 12: 391-422(Jun 1970).

Recent results on the generation of plasma densities well above critical density in the electron wave domain have again shown the importance of considering the boundedness of actual plasmas to obtain the optimum coupling between a plasma and the rf power of an external source. This investigation of a hot (T_e and $T_i \neq 0$) bounded electron–ion plasma is conducted sequentially. It is shown that the resonances existing in the magnetoionic domain of a hot bounded plasma are only indirectly connected to the hybrid frequencies of an infinite cold plasma and emphasizes the need to consider a hot bounded plasma when investigating the coupling between an external rf field and a laboratory plasma. (auth) (UK)

Shielding

Refer also to abstracts 4218, 4246, 4256, 4374, 4938, 5166, 5242, 5243, 5489, 5490, and 6128–6130.

5135 (AAEC/TM-554) APPLICATION OF VARIATIONAL METHODS TO NEUTRON TRANSPORT IN SLABS. Donnelly, I. J. (Australian Atomic Energy Commission Research Establishment, Lucas Heights). Aug 1970. 21p. Dep. NTIS (U. S. Sales Only).

Monoenergetic neutron transport in a homogeneous slab is investigated, using two different formulations of the variational method and a simple trial function. One form leads to results that are correct for thick slabs, while the other is in error. An improved trial function is then developed to overcome a difficulty encountered in the simple one when the variational method is applied to slab materials that conserve neutrons. (auth) (Australia)

5136 MEASUREMENT OF DOSE BUILDUP FACTORS FOR LOW-ENERGY POINT ISOTROPIC GAMMA SOURCES IN WATER. Osanov, D. P.; Panova, V. P.; Radzievskii, G. B. This paper was summarized in At. Energ. (USSR); 24: 370(Apr 1968) as paper No. 189. (In Russian).

Dose buildup factors for a point isotropic source emitting photons in an infinite homogeneous medium may be found from the dose rate distribution. A flat disk-shaped ionization chamber was used to measure the dose rate distribution in water. Dose buildup factors were determined for 661-, 145-, 80-, and 30-keV photon energies. The results are given. (M.H.R.)

5137 OPTIMIZATION OF SHIELDS FOR PROTECTION OF UNMANNED SPACECRAFT SCIENTIFIC EXPERIMENTS. Steyn, J. J. (Nuclear Utility Services, Inc., Rockville, Md.); Harris, D. W. Trans. Amer. Nucl. Soc.; 13: 538-9(Nov 1970).
From Meeting of the American Nuclear Society, Washington, D. C. See CONF-701102.

5138 STREAMING OF GAMMA RADIATION IN TWO-LEGGED DUCTS. Chae, Yong S.; Snyder, James L. (Rutgers–The State Univ., New Brunswick, N. J.). Trans. Amer. Nucl. Soc.; 13: 631(Nov 1970).
From Meeting of the American Nuclear Society, Washington, D. C. See CONF-701102.

5139 PHASE SPACE TIME EVOLUTION METHOD, OR, HOW TO SOLVE TIME-DEPENDENT TRANSPORT PROBLEMS IN SPITE OF THE TRANSPORT EQUATION. Tavel, M. A. (Vassar Coll., Poughkeepsie, N. Y.); Zucker, Martin. Trans. Amer. Nucl. Soc.; 13: 695(Nov 1970).
From Meeting of the American Nuclear Society, Washington, D. C. See CONF-701102.

5140 ORTHOGONALITY IN FINITE SLAB GEOMETRY. Gibbs, Alan G. (Battelle-Northwest, Richland, Wash.). Trans. Amer. Nucl. Soc.; 13: 695-6(Nov 1970).
From Meeting of the American Nuclear Society, Washington, D. C. See CONF-701102.

5141 ENERGY REPRESENTATIONS IN NEUTRON TRANSPORT CALCULATIONS. Duderstadt, James J. (Univ. of Michigan, Ann Arbor). Trans. Amer. Nucl. Soc.; 13: 696-7(Nov 1970).
From Meeting of the American Nuclear Society, Washington, D. C. See CONF-701102.

5142 THERMAL X-RAY TRANSPORT PROBLEM. Pomraning, G. C. (Science Applications, Inc., La Jolla, Calif.). Trans. Amer. Nucl. Soc.; 13: 697(Nov 1970).
From Meeting of the American Nuclear Society, Washington, D. C. See CONF-701102.

5143 NEUTRON TRANSPORT IN TWO-DIMENSIONAL SLABS BY INVARIANT IMBEDDING. Zink, John C.; Lucey, J. W. (Univ. of Notre Dame, Ind.). Trans. Amer. Nucl. Soc.; 13: 855(Nov 1970).
From Meeting of the American Nuclear Society, Washington, D. C. See CONF-701102.

5144 MULTIGROUP DISCRETE ORDINATES RADIATION TRANSFER OPERATORS. Boulette, E. T. (Battelle-Northwest, Richland, Wash.). Trans. Amer. Nucl. Soc.; 13: 855-6(Nov 1970).
From Meeting of the American Nuclear Society, Washington, D. C. See CONF-701102.

5145 SCATTERING ANGLE BIASING FOR DEEP-PENETRATION X-RAY TRANSPORT. Stevens, C. A.; Coleman, W. A. (Science Applications, Inc., La Jolla, Calif.). Trans. Amer. Nucl. Soc.; 13: 859-60(Nov 1970).
From Meeting of the American Nuclear Society, Washington, D. C. See CONF-701102.

5146 GAMMA PHOTON ALBEDO DISTRIBUTIONS FOR FINITE MEDIA. Steyn, J. J. (Nuclear Utilities Services, Inc., Rockville, Md.); Huang, R.; Harris, D. W. Trans. Amer. Nucl. Soc.; 13: 860-1(Nov 1970).
From Meeting of the American Nuclear Society, Washington, D. C. See CONF-701102.

5147 TIME-DEPENDENT COUPLED NEUTRON-GAMMA CALCULATIONS IN POLYETHYLENE. Burgart, C. E. (Oak Ridge National Lab., Tenn.); Engle, W. W. Jr. Trans. Amer. Nucl. Soc.; 13: 861-2(Nov 1970).
From Meeting of the American Nuclear Society, Washington, D. C. See CONF-701102.

5148 LOW-ENERGY PHOTON TRANSPORT IN LIQUID NITROGEN. Harris, R. J. Jr.; Nowak, M. J. (Gulf Energy and Environmental Systems, Inc., San Diego, Calif.). Trans. Amer. Nucl. Soc.; 13: 875-6(Nov 1970).
From Meeting of the American Nuclear Society, Washington, D. C. See CONF-701102.

5149 BACKSCATTERING OF GAMMA RAYS FROM BARRIERS OF FINITE THICKNESS. Elias, E.; Segal, Y. (Technion-Israel Inst. of Tech., Haifa). Trans. Amer. Nucl. Soc.; 13: 878-9(Nov 1970).
From Meeting of the American Nuclear Society, Washington, D. C. See CONF-701102.

Solid-State Physics

5150 (UCB-34-P-20-PR-16) DYNAMIC NUCLEAR POLARIZATION AND SOLID STATE PHYSICS. Progress Report, July 15, 1969–August 1, 1970. Jeffries, C. D. (California Univ., Berkeley. Dept. of Physics). 1 Aug 1970. Contract AT(04-3)-36. 122p. Dep. NTIS.

Four papers, previously published and/or to be presented at conferences, are included. Their titles are: Polarization of Nuclei

in Solids by Optical Pumping; Polarized Solid Targets; Paramagnetic Resonance and Spin Lattice Relaxation in Ytterbium, Yttrium Ethyl Sulfate; and Measurement of Pair Interactions in Neodymium Ethyl Sulfate. Work in progress is discussed briefly. (D.L.C.)

Radiation Effects

Refer also to abstracts 4408, 4890, 4937, and 4939.

5151 (N-70-35737) PIEZORESISTIVE EFFECT IN ELECTRON IRRADIATED SILICON AND ITS APPLICATION TO THE IMPROVEMENT OF SEMICONDUCTOR STRAIN GAGES. Final Report. Loggins, C. D. Jr.; Littlejohn, M. A. (North Carolina State Univ., Raleigh. Semiconductor Device Lab.). 1 Jun 1970. 172p. (NASA-CR-66981; SDL-15). NTIS.

Research aimed at a better understanding of the influence that defect states and relaxation times have on the piezoresistivity of semiconductors is reported. The study includes an experimental phase in which data are obtained on n-type irradiated silicon as well as a theoretical phase in which a mathematical model is developed that fits the experimental results. (auth) (STAR)

5152 (ORO-3508-6) DIFFUSION OF GASES IN SOLIDS. Annual Progress Report, November 1, 1969-October 1, 1970. Elleman, Thomas S.; Ong, Andres Sy; Austin, John H. (North Carolina Univ., Raleigh. Dept. of Nuclear Engineering). 13 Oct 1970. Contract AT(40-1)-3508. 71p. Dep NTIS.

Progress on two separate programs is summarized: a study of the factors that affect rare-gas diffusion in ionic solids; and the measurement of tritium diffusion in fuel element claddings. I. Xenon-133 diffusion in CaF_2 single crystals was studied using fission-recoil doping to inject the xenon. Measurements on diffusion at 3×10^{11} fission fragments cm^{-2} were consistent with classical diffusion solutions with $D_0 = 9.5 \times 10^6$ cm^2sec^{-1} and $\Delta H = 4.42$ eV. An increase of one to two orders of magnitude in fission-recoil concentration resulted in a decrease in the apparent diffusion coefficient, an effect ascribed to the trapping of the gas atoms. A trapping model was developed and the values of trap concentration and trap retention time that best fit the experimental results were determined. These values were found to be inconsistent with a model of the trapping process based on clustering of the gas atoms, but consistent with one based on the assumption of radiation damage-induced defects as the trapping sites. II. The diffusion of tritium in Type 304 stainless steel was studied by injecting tritium into specimen surface layers through the $^6Li(n,\alpha)^3H$ reaction, heating to establish a diffusion gradient, and then analyzing the tritium in sections removed by electropolishing. Three characteristics of the tritium distribution were noted: a high surface tritium concentration, a classical diffusion component, and a long diffusion "tail" that corresponded to rapid diffusion. The classical diffusion component was consistent with solutions to Fick's diffusion equations over the temperature range 20 to 222°C with $D_0 = {}^{+0.94}_{-0.60}$ cm^2sec^{-1} and $\Delta H = 0.61 \pm 0.01$ eV. The high surface concentration apparently resulted from tritium adsorption in oxide surface films, while the rapid diffusion component was tentatively attributed to grain-boundary diffusion. (auth)

5153 COULOMB FRAGMENTATION OF InCl AND InI. Schumacher, M.; Weiss, J.; Langhoff, H. (Univ., Goettingen, Ger.). Phys. Lett.; 31B: 61-2(19 Jan 1970).

The molecules of InCl and InI break up by electron capture in ^{114m}In. The energy distributions of the Cd fragments were investigated by resonance scattering of the 558-keV γ quanta emitted after the electron capture. (auth)

5154 THEORETICAL INVESTIGATION OF THE POSSIBILITY OF CHEMICAL BINDING OF NEUTRONS IN F CENTERS. Schlitt, D. W. (Univ. of Nebraska, Lincoln). Phys. Rev., B; 2: 3437-9(15 Oct 1970).

A recent paper [Phys. Rev. Letters 23: 741(1969)] reported experimental evidence that neutrons can be chemically bound to trapped electrons. The spin-independent electron-neutron interaction due to the electromagnetic structure of the neutron is found to be inadequate to produce such a bound state. (auth)

5155 LOW-ENERGY IRRADIATION OF Ge MONOCRYSTALS BY INERT-GAS IONS He^+, Ne^+, Ar^+, Kr^+, AND Xe^+. Tishchenko, V. D. (Kiev State Univ.). Fiz. Tekh. Poluprov.; 2: 1825-30 (Dec 1968). (In Russian).

Absolute values of the coefficients of cathode sputtering for germanium single crystals were measured for different ion energies. The linear behavior of the energy relations obtained in near-threshold ranges permitted an evaluation of the minimum energies of ions for which noticeable cathode sputtering of the surfaces begins, parallel to the (100), (110), and (111) crystallographic planes. The values obtained are compared with the threshold for radiation displacement of atoms of germanium. (tr-auth)

5156 V_3 BAND IN LiF. Mayhugh, M. R.; Christy, R. W. (Dartmouth Coll., Hanover, N. H.). Phys. Rev., B; 2: 3330-2 (15 Oct 1970).

An optical absorption band is produced at 113 nm (11.0 eV) in both pure and Mg-doped LiF by irradiation with x rays at room temperature. This band, which appears to be intrinsic like the F band, is identified as the V_3 band. Its peak-wavelength position follows the same dependence on anion radius as has been found previously for alkali metal chlorides, bromides, and iodides. (auth)

5157 FORMATION OF COLOR CENTERS IN KCL:Tl BY GAMMA IRRADIATION AT 21°C. Butterworth, J. S. (Frankford Arsenal, Philadelphia); Esser, P. D.; Levy, P. W. Phys. Rev., B; 2: 3340-53(15 Oct 1970).

The formation of color centers in KCl, both "pure" and with thallium impurity, by ^{60}Co γ irradiation at 21°C, was studied. The samples were grown from zone-refined material that had been chemically purified. The pure crystals did not contain detectable amounts of thallium, while the doped crystals were adjusted to contain from 4 to 145 ppm of Tl impurity. Presumably, Tl^+ enters the KCl lattice substitutionally and, except possibly at the highest Tl concentrations, is incorporated as an isolated ion. As the irradiation dose increases, the Tl^+ A, B, and C bands decrease; however, the F band, a broad "V-region" absorption, and, except at lowest doses, the M band all concomitantly increase. The V-region absorption is a function of the Tl content. Below ~10^6 rad, the F-center formation rate increases and then decreases as the Tl content increases. Above 10^6 rad, the level of the F-center absorption decreases as the Tl^+ content increases. Also, the M-center concentration is proportional to the square of the corrected F-center concentration, and the M- to-F-center ratio increases as the Tl content increases. These and other observations indicate that, with few exceptions, if any, the effects on the coloring curves produced by substituting monovalent Tl^+ ions in the KCl lattice are very similar to those produced by substituting divalent impurities such as Ca^{2+} ions. Consequently, it must be concluded that the role of monovalent and divalent metallic impurities in the coloring process is similar and is not related to the initial valence state of the impurity. In particular, it would appear that those positive-ion vacancies that are almost certainly introduced when divalent ions are substituted in the KCl lattice, to provide charge neutrality, are not essential to the impurity-related coloring mechanisms. (auth)

5158 THERMALLY STIMULATED CONDUCTIVITY AND LUMINESCENCE IN KBr DUE TO γ IRRADIATION AT 10°K. Fuchs, W.; Taylor, A. (Cornell Univ., Ithaca, N.Y.). Phys. Rev., B; 2: 3393-3403(15 Oct 1970).

The annealing behavior of KBr, γ-irradiated at 10°K, was studied by means of simultaneous measurements of the thermally stimulated conductivity and luminescence and of the optical absorption. Over the investigated temperature range between 10 and 35°K, the conductivity and luminescence behaved very similarly, and the latter did not change its spectral distribution. All observed peaks have been ascribed to the annealing of the radioinduced imperfections of the lattice structure. Four peaks, appearing at 14, 17, 20, and 24°K with characteristic activation energies between 0.025 and 0.058 eV, which saturate in intensity after a moderate irradiation dose, are believed to be due to the generation of conduction electrons. A smaller peak at 22°K, which was observed only in the conductivity data, may be due to ionic motion. The most prominent peak appeared at 27°K, and it was shown by "thermal cleaning" experiments that this peak is caused by processes with activation energies of 0.062 and 0.100 eV. Here, too, the signals are believed to be caused by conduction electrons and their consecutive recombination with traps. The 0.062-eV process has "mixed-order" kinetics, i.e., there is an excess of recombination centers. At higher irradiation doses, the 0.100-eV process becomes dominant. This process seems to be associated with the first annealing stage of the H band, which had an activation energy of 0.097 eV. A tentative model of the H-center decay involves the dissociation of the H center followed by an interstitial-vacancy recombination. (auth)

5159 INFLUENCE OF IMPURITIES ON THE ROOM-TEMPERATURE COLORATION PROCESSES IN ALKALI HALIDES. Sastry, E. V. R.; Srinivasan, T. M. (Indian Inst. of Tech., Kanpur). Phys. Rev., B; 2: 3415-21(15 Oct 1970).

The F-center growth curves for undoped KCl and KCl crystals doped with Ba, Co, and Cd were obtained by x irradiation at room temperature. These growth curves are fitted to an equation with two exponential terms and a linear term, and the parameters occurring in the equation are evaluated. Two exponential terms are found to be adequate to describe the first-stage coloration. The analysis shows that the slower exponential component is strongly influenced by the presence of impurities; specifically, the rate

of coloration during the process responsible for this component decreases, and the saturation level for the process increases, on account of the impurities. The faster exponential component appears to be relatively insensitive to the presence of impurities. These results are discussed with reference to certain mechanisms that have been put forward to account for the first stage. (auth)

5160 RECOVERY OF LATTICE PARAMETER AND ELECTRICAL RESISTIVITY IN LOW-TEMPERATURE NEUTRON-IRRADIATED COPPER. Gruber, E. E.; Tesk, J. A.; Blewitt, T. H.; Black, R. E. (Argonne National Lab., Ill.). Phys. Rev., B; 2: 2849-58(15 Oct 1970).

The fast-neutron-irradiation-induced change and subsequent isochronal annealing recovery of the lattice parameter and electrical resistivity of copper were studied. A wire resistivity specimen and single crystal were irradiated together in liquid helium and transferred to a cryostat without warm up. The simultaneous recovery of both properties was measured at 4.2°K following isochronal anneals to temperatures as high as 675°K. The results of the three successful experimental runs were in good agreement. An analysis, based on linear superposition of the effects of the individual defects, is presented as the simplest and most direct approach to determine the migration mechanism as a function of temperature. The most significant and unambiguous conclusion of this analysis is that stage-III recovery in copper (220 to 280°K) is due to vacancy migration. Alternative explanations in terms of more complex phenomena appear less probable, but cannot be excluded with certainty. (auth)

5161 PHOTOCONDUCTIVITY SPECTRA OF IRRADIATED AND PLASTICALLY DEFORMED CRYSTALS OF GERMANIUM. Vasil'ev, A. V.; Rybakova, L. A.; Smirnov, L. S. (Novosibirsk Inst. of Physics of Semiconductors, USSR). Fiz. Tekh. Poluprov.; 2: 1720-3(Dec 1968). (In Russian).

For proof of the premise expressed earlier (Fiz. Tekh. Poluprov., 2: 904(1968)) that the majority of levels observed in the photoconductivity spectra of irradiated germanium is caused by residual impurities, the spectra were recorded of p-type (both initial and that transferred from n-type by alloying with Cu and Au) after irradiation with 3.5-MeV electrons; also, irradiated forms of initial n- and p-type with density of dislocations of 0, 10^3 and 10^5 cm^{-2} were investigated. Irradiation doses were changed from 10^{14} to 10^{17} el./cm^2. The experimental data obtained confirm the earlier expressed premise. (tr-auth)

5162 EPR OF A NEW BORON CENTER IN NEUTRON-IRRADIATED BeO. Herve, Alain; Maffeo, Bruno (CEA, Grenoble, France). J. Phys. (Paris); 31: 673-9(Jul 1970). (In French).

A synthetic single crystal of BeO was irradiated with fast neutrons (energy $\geq$ 1.0 MeV; integrated flux: 10^{18} n/cm^2) at 77°K and investigated by ESR without warmup. The spectrum was identified as being due to a boron impurity at an octahedral interstitial site of the lattice. The hyperfine interaction tensor is cylindrically symmetric; its principal axis lies in the $(1\bar{2}10)$ plane and makes an angle of 49° with the c axis. The constants of the spin Hamiltonian are: $g_{\parallel} = 2.0023 \pm 0.0010$; $g_{\perp} = 2.0028 \pm 0.0010$; $A_{\parallel} = 293 \pm 6$ G; $A_{\perp} = 255 \pm 5$ G. Calculations carried out for different charge states of the boron impurity indicate a strong localization of the unpaired electron on the boron. (tr-auth) (France)

5163 TEMPERATURE RISE OF SPECIMEN DUE TO ELECTRON IRRADIATION. Watanabe, M.; Someya, T.; Nagahama, Y. (Japan Electron Optics Lab. Co. Ltd., Tokyo). J. Phys., D (London); 3: 1461-8(Oct 1970).

A rise in specimen temperature due to electron irradiation was directly measured by using a microthermocouple composed of evaporated gold and palladium films. The temperature rise with an increase in electron current density was explained referring to the thermal conduction and thermal radiation effects. The experimental results obtained by varying irradiated areas and film thicknesses were compared with Leisegang's theory (1956). The thermal conductivity and thermal emissivity values for metallic films as well as the energy loss value that contributes to the temperature rise were estimated. (auth) (UK)

5164 NONEQUILIBRIUM CHARGE STATES OF 60-MeV IODINE IONS CHANNELED IN Au SINGLE CRYSTALS. Lutz, H. O.; Datz, S.; Moak, C. D.; Noggle, T. S. (Oak Ridge National Lab., Tenn.). Phys. Lett.; 33A: 309-10(16 Nov 1970).

Iodine ions (60 MeV) penetrating Au crystals in (100) planar channeling directions require ~1200 Å to reach equilibrium, implying a reduction of the charge-changing cross sections. Differences in most probable charge of up to 3.6 units in 20 are observed. (auth)

5165 SIMPLE ION SOURCE FOR IMPLANTATION DOPING OF SEMICONDUCTORS. Gwozdz, P. S.; Koehler, J. S. (Univ. of Illinois, Urbana). Rev. Sci. Instrum.; 41: 1677-8(Nov 1970).

A Lavite cylinder ion source for ion implantation of semiconductors is described. The heat from the hot tungsten filament vaporizes the solid source in the hollow anode, and the thermionic electron current from the filament ionizes the atoms by impact. Typical operating parameters for a CuCl source are given. (W.H.K.)

5166 FURTHER DATA ON GAMMA-INDUCED ELECTRICAL CHARGE AND COLORATION OF SHIELDING GLASSES. Eckels, T. W.; Mingesz, D. P. (Argonne National Lab., Ill.). Trans. Amer. Nucl. Soc.; 13: 847-8(Nov 1970).

From Meeting of the American Nuclear Society, Washington, D. C. See CONF-701102.

5167 PHOTON–ELECTRON TRANSPORT. I. THE K–N CROSS SECTION FOR SCATTERED ELECTRONS. Mingle, J. O. (Kansas State Univ., Manhattan). Trans. Amer. Nucl. Soc.; 13: 863(Nov 1970).

From Meeting of the American Nuclear Society, Washington, D. C. See CONF-701102.

Physical Properties

Refer also to abstracts 4766, 4795, 4817, and 4935.

5168 (COO–623-156) SOLID STATE PHYSICS PROGRAM ANNUAL PROGRESS REPORT. (Case-Western Reserve Univ., Cleveland, Ohio). Nov 1970. Contract AT(11-1)-623. 36p. Dep. NTIS.

CADMIUM FLUORIDES — elastic constants of, pressure derivatives of
FILMS — magnetization measurement on thin, apparatus design for
— temperature distribution in thin, determination using liquid crystals
LEAD — sound velocity measurements in superconducting
LITHIUM FLUORIDES — dielectric constants of, pressure and temperature dependences of static
NICKEL — deposition on substrates
POTASSIUM BROMIDES — dielectric constants of, pressure and temperature dependences of static
POTASSIUM CHLORIDES — dielectric constants of, pressure and temperature dependences of static
SODIUM BROMIDES — dielectric constants of, pressure and temperature dependences of static
SODIUM CHLORIDES — dielectric constants of, pressure and temperature dependences of static
SODIUM FLUORIDES — dielectric constants of, pressure and temperature dependences of static
SOLID STATE PHYSICS — research in (D.L.C.)

5169 (IS-T-379) TRANSPORT PROPERTIES OF Gd–Th, Gd–Mg, AND Y–Th ALLOYS. Mellon, Donald Williams (Ames Lab., Iowa). Oct 1970. Contract W-7405-eng-82. 110p. Dep. NTIS.

Thesis.

The electrical resistivity, thermal conductivity, and thermoelectric power were measured as functions of temperature from 5 to 300°K to look for a periodic magnetic structure in Gd alloyed with Th and Mg. A total of eight samples were measured: $Gd_{0.95}$ $Th_{0.05}$ b-axis and c-axis, $Gd_{0.90}$ $Th_{0.10}$ a-axis and c-axis, $Y_{0.95}$ $Th_{0.05}$ and $Y_{0.90}$ $Th_{0.10}$ basal plane, and polycrystalline $Gd_{0.94}$ $Mg_{0.06}$ and $Gd_{0.88}$ $Mg_{0.12}$ samples. The electrical resistivity of the $Gd_{0.88}$ $Mg_{0.12}$ sample indicates the existence of a periodic magnetic ordering, whereas the other alloys which were more Gd-rich order ferromagnetically. This result is interpreted as being further evidence that large "nesting" areas are the features of the Fermi surface which are necessary for the existence of a periodic magnetic state. The Gortner–Nordheim relation and Ziman's "R parameter" are used to discuss rigid-band model behavior for these alloys. Also, large magnon-drag peaks in the thermoelectric power of the Gd–Th alloys, which are not observed in either gadolinium or any of the other alloys, are explained by considering only the d-nature of the conduction band of the alloys. (auth)

5170 (JINR–P14-5358) DEBYE–WALLER FACTOR FOR TUNGSTEN. Alexandrov, Yu. A.; Balagurov, A. M.; Samosvat, G. S.; Fykin, L. E. (Joint Inst. for Nuclear Research, Dubna (USSR). Lab. of Neutron Physics). 1970. 9p. (In Russian). Dep. NTIS (U. S. Sales Only).

The Debye–Waller factor for tungsten is calculated according to the data on heat capacity. The diffraction Debye temperature for T = 293°K turned out to be 343°K. The obtained result is com-

pared with the calculation of the Debye–Waller factor on the phonon spectrum of tungsten and with the neutron-diffraction experiment. (auth)

5171 (ORO-3087-44) CONDUCTIVITY TENSORS IN METALS AND SEMICONDUCTORS. Progress Report No. 8, October 15, 1969–October 15, 1970. Reynolds, J. M. (Louisiana State Univ., Baton Rouge. Dept. of Physics and Astronomy). Contract AT(40-1)-3087. 14p. Dep. NTIS.

Research on transport phenomena in metals and semiconductors is reported. Electron–phonon scattering, Fermi surfaces, Knight shifts, and carrier effective masses were among the things studied. Virtually no data are given; a bibliography of eleven papers is included. (D.L.C.)

5172 DIFFUSION AND ISOTOPE EFFECT OF LITHIUM-ION DIFFUSION IN CRYSTALLINE SILVER CHLORIDE. Ptashnik, V. B.; Naumov, A. N. (Ioffe Inst. of Physics and Tech., Leningrad). Sov. Phys.-Solid State (Engl. Transl.); 12: 1174-6(Nov 1970).

Translated from Fiz. Tverd. Tela; 12: 1496-8(May 1970).

The diffusion coefficients of lithium in crystalline AgCl were measured by the method of layer removal over the temperature range 200 to 400°C. The lithium concentration in the layers was determined by means of isotope dilution. The results are in good agreement with the Arrhenius equation $D = D_0 \exp(-(\epsilon/kT))$, in which $D_0 = 10 \pm 6$ cm²/sec and $\epsilon = 1.035 \pm 0.004$ eV. In the same temperature range, the values of the diffusion isotope effect were measured: $E = [(D^6/D^7) - 1/(m^7/m^6)^{\frac{1}{2}} - 1]$, where D^6, D^7, m^6, and m^7, are the diffusion coefficients and the masses of the lithium isotopes ^{6}Li and ^{7}Li, respectively. Within experimental error, E turned out to be independent of temperature, having an average value of 0.75. It is concluded that diffusion of lithium occurs by a vacancy mechanism, on the basis of these results and on the basis of data from the literature on the rate of self-diffusion of silver and cation vacancies in the lattice. (auth)

5173 ELECTRON CONDUCTION THROUGH OXIDE FILMS ON ZIRCALOY-2. Shirvington, P. J. (Atomic Energy of Canada Ltd., Chalk River, Ont.). J. Nucl. Mater.; 37: 177-202 (Nov 1970).

Electronic characteristics extracted from I–V curves obtained in a molten salt were determined at 175 to 350°C for oxidation films on zirconium alloys. An aqueous electrochemical method determined the nature of the oxide layers over the intermetallic precipitates (the sites of electronic conduction through the oxides). For oxides formed on Zircaloy-2 in low-oxygen environments, electronic conduction occurred by Schottky emission or Poole–Frenkel excitation through a thin ZrO_2 layer over the intermetallic precipitates. For oxides formed in oxygenated environments, the ZrO_2 layer was doped with iron (and chromium or nickel) contributing an additional ohmic component of conduction. Under some conditions in molten salt and in 300°C water containing ferrous hydroxide, a layer of magnetite about 50 Å thick formed over the doped ZrO_2 and the resistance of the oxide dropped by ~ two orders of magnitude, with conduction occurring by a double-injection mechanism. These results are discussed in relation to the in-reactor enhancement of the oxidation rate of Zircaloy-2 in aqueous environments containing oxygen. (auth)

5174 CHOICE OF OPTIMAL CONDITIONS FOR EXPERIMENTAL OBSERVATION OF COHERENT SCATTERING OF γ QUANTA BY NUCLEI. Kudryavtsev, V. G.; Ryazanov, M. I. (Moscow Engineering Physics Inst.). JETP Lett. (USSR) (Engl. Transl.); 12: 109-11(5 Aug 1970).

Translated from Zh. Eksp. Teor. Fix., Pis'ma Red.; 12: 157-8(5 Aug 1970).

The ratio of the cross sections for coherent γ scattering by nuclei and Compton scattering is greatly increased if these processes are considered in a single crystal as opposed to an amorphous substance. This results from the fact that the effective length for scattering by nuclei is larger than that for Compton scattering. For the elements of the end of the periodic system, for example, the ratio of the cross sections of scattering by a nucleus and of Compton scattering by an individual atom may be ~5, but the ratio of the same cross sections in a single crystal may increase to 10^4. Thermal vibrations, however, can decrease the above ratios: the conditions under which this occurs are discussed. (R.W.R.)

5175 MAGNETORESISTANCE OF Er–Y ALLOYS AT LOW TEMPERATURES. Nikol'skii, G. S.; Zvyagina, N. M. (Physical-Technical Inst. of Low Temperatures, Kharkov). Sov. Phys.-Solid State (Engl. Transl.); 12: 1196-7(Nov 1970).

Translated from Fiz. Tverd. Tela; 12: 1525-7(May 1970).

Magnetoresistance isotherms from 4.2 to 25.5°K were measured for Er–14.5 at.% Y alloy and compared with those for pure Er. The isotherm curves were found to be different for the two materials: while for Er the magnetoresistance becomes increasingly more negative with temperature, it becomes more positive for the alloy. The spin-wave spectrum and antiferromagnetic ordering are discussed. (D.L.C.)

5176 TEMPERATURE DEPENDENCE OF ELECTRIC CONDUCTIVITY AND THERMAL ELECTROMOTIVE FORCES IN THE HOMOGENEOUS CARBIDE ALLOY REGIONS OF TITANIUM AND NIOBIUM. Samsonov, G. V.; Upadkhaya, G. Sh.; Nemchenko, V. F. (Inst. of Problems in Material Studies, Kiev. Kherson Pedagogical Inst., USSR). Teplofiz. Vys. Temp.; 7: 449-52 (May-Jun 1969). (In Russian).

Specific electric conductivity and absolute thermal emf of carbide alloys of niobium and titanium were measured at 50 to 1000°C in their regions of homogeneity. Experimental data revealed the relationship between physical properties of carbide compressed powders and formation of stable electron configurations of component atoms. (tr-auth)

5177 HALL EFFECT IN TERBIUM SINGLE CRYSTALS. Fedorov, G. V.; Volkenshtein, N. V. (Inst. of Metal Physics, Sverdlovsk, USSR). Sov. Phys.-Solid State (Engl. Transl.); 12: 1079-83(Nov 1970).

Translated from Fiz. Tverd. Tela; 12: 1374-9(May 1970).

The Hall effect was measured in two samples cut from a Tb single crystal (purity 99.9%, $\rho_{293°K}/\rho_{4.2°K} \approx 20$) between 4.2 and 350°K in magnetic fields up to 34 kG. The specific Hall emf for samples with H parallel to the [0001] direction depends linearly on the induction in the sample for all temperatures. For a sample with H parallel to $[1\bar{2}10]$, the relation $e_H(B)$ takes the form characteristic of ferromagnets in the ferromagnetic region. In the paramagnetic region, the spontaneous R_S and ordinary R_0 Hall coefficients were separated for both samples and found to be anisotropic. In the ferromagnetic region, R_S and R_0 could be separated only for samples with H parallel to $[1\bar{2}10]$. R_S and R_0 change sign twice with decreasing temperature. (auth)

5178 ELECTRICAL AND MAGNETIC PROPERTIES OF Pd–Mo SOLID SOLUTIONS CONTAINING SMALL ADDITIONS OF COBALT. Volkenshtein, N. V.; Ugodnikova, L. A.; Tsiovkin, Yu. N. (Inst. of Metal Physics, Sverdlovsk, USSR). Sov. Phys.-Solid State (Engl. Transl.); 12: 1160-6(Nov 1970).

Translated from Fiz. Tverd. Tela; 12: 1479-86(May 1970).

A study has been made of the temperature dependence of the electrical resistivity of solid solutions in the system palladium–molybdenum and of these alloys containing small additions of cobalt. There is a considerable decrease in the temperature dependence of the magnetic susceptibility of dilute solutions of cobalt in molybdenum on addition of palladium. The existence of a magnetic moment at the addition atoms can be inferred only from the presence of the characteristic low-temperature minimum in the temperature dependence of the resistivity. The magnetic component of the resistivity of alloys containing cobalt is satisfactorily described by the relation A ln T. On the basis of existing theories, a negative sign obtains for the exchange interaction between the conduction electrons and the magnetic moments of the addition in molybdenum-base alloys, while a positive sign obtains for this exchange in the case of palladium-base alloys containing 10 and 20 at.% molybdenum. (auth)

5179 VARIATIONS IN THE ELECTRICAL CONDUCTIVITY AND THE DETERMINATION OF THE STABLE DOMAINS AT HIGH TEMPERATURES FOR TERBIUM OXIDES AS A FUNCTION OF OXYGEN EQUILIBRIUM PRESSURE. Wilbert, Yves; Marion, Fernand (Univ., Amiens, France). Compt. Rend., Ser. C; 271: 736-9(28 Sep 1970). (In French).

The study of the isothermal and isobaric variations in the electrical conductivity of terbium oxides, together with x-ray crystallographic studies at high temperatures, allows the stable domains of the nonstoichiometric cubic oxide $TbO_{1.5+\gamma}$ and rhombohedric oxide $TbO_{1.714-z}$ to be determined. (tr-auth) (France)

5180 METAMAGNETIC PROPERTIES OF A SINGLE CRYSTAL OF $ErCrO_3$. Veyret, C.; Ayasse, J. B.; Chaussy, J.; Mareschal, J.; Sivardiere, J. (CNRS, Grenoble, France). J. Phys. (Paris); 31: 607-11(Jul 1970). (In French).

The metamagnetic properties of a single crystal $ErCrO_3$ were studied by magnetic measurements and neutron diffraction. The results show the strong anisotropy of erbium and a non-negligible coupling between the two sublattices. A low-temperature specific heat measurement shows that the C_z ordering of erbium moments is not cooperative. (auth)

5181 POSITION OF THE K-ABSORPTION EDGES OF IRON IN IRON–ALUMINUM AND IRON–MOLYBDENUM ALLOYS.

Kolobova, K. M.; Nemnonov, S. A.; Trapeznikov, V. A. (Inst. of Metal Physics, Moscow). Phys. Metals Metallogr. (USSR) (Engl. Transl.); 26: No. 6, 51-5(1968).

Translated from Fiz. Metal. Metalloved.; 26: No. 6, 1010-14 (1968).

The K-absorption edges of iron in solid solutions of Al in Fe (0.5 to 17 at. % Al) and Mo in Fe (0.5 to 10 wt % Mo) were studied. Two inflections were found in the initial range of absorption. The boundary between the occupied states (determined as the middle of the energy gap between the beginning of the rise in the absorption curve and the first long-wave inflection point) remains unchanged for all the Fe–Al alloys studied. The K, L_{III}, and M_{III} absorption edges of iron in the metal are compared. (auth)

5182 HALL EFFECT IN CERTAIN RARE-EARTH METALS AND ALLOYS. Volkov, D. I.; Kozlova, T. M.; Shafigullina, G. A. (Moscow State Univ.). Phys. Metals Metallogr. (USSR) (Engl. Transl.); 26: No. 6, 143-9(1968).

Translated from Fiz. Metal. Metalloved.; 26: No. 6, 1101-7 (1968).

The Hall effect and magnetic susceptibility were studied in Tb–Y and Dy–Y alloys, and also in pure Tb, Dy, and Y at 90 to 400°K in magnetic fields of up to 15 kOe. The field and temperature dependence of the Hall emf were found for the ferromagnetic, helicoidal antiferromagnetic, and paramagnetic states. Reversal of the Hall field was found on passing from the ferromagnetic to paramagnetic state. (auth)

5183 CALCULATION OF THE VIBRATION SPECTRUM OF TANTALUM. Almazov, A. B.; Zorina, E. L. (Moscow Mining Inst.). Phys. Metals Metallogr. (USSR) (Engl. Transl.); 26: No. 6, 156-7(1968).

Translated from Fiz. Metal. Metalloved.; 26: No. 6, 1112-13 (1968).

The lattice vibration spectra of Ta were calculated using expansion of the dynamic matrix in elliptical functions. The resulting dispersion curves of longitudinal and transverse branches for directions ⟨100⟩, ⟨111⟩, and ⟨110⟩ show good agreement with experiment. (D.L.C.)

5184 ELECTRICAL RESISTIVITY AND DEVIATIONS FROM MATTHIESSEN'S RULE IN DILUTE ALLOYS OF ALUMINUM, CADMIUM, SILVER, AND MAGNESIUM. Seth, R. S.; Woods, S. B. (Univ. of Alberta, Edmonton). Phys. Rev., B; 2: 2961-72 (15 Oct 1970).

Absolute values of the electrical resistivity of polycrystalline silver, aluminum, cadmium, and magnesium and over 20 dilute binary alloys of these metals with different solute concentrations were measured from 1.5 to 300°K. From the resistivity data, deviations Δ from Matthiessen's rule were evaluated for the alloys. Deviations with positive as well as negative sign have been observed at temperatures above 50°K. These deviations, for all except the hcp alloys of cadmium containing magnesium as a solute (Cd–Mg alloys), can be explained in terms of a two-band contribution, which can only be positive, and an interference term between the scattering of electrons by lattice vibrations of the host atoms and the excess potential due to the vibrating impurities, which can have either sign. The deviations for Ag–Cd, Ag–Mg, Ag–Al, and Al–Mg alloys increase linearly with temperature and those for Al–Ag, Cd–Ag, and Mg–Al decrease linearly with temperature in this range. Combined with published data for Mg–Ag alloys, these results are in excellent qualitative agreement with the predictions of Bhatia and Gupta, who showed that the interference term should be important at high temperatures and should change sign when the ions on the host and impurity sites are interchanged. This agreement is further strengthened by comparison of the slope $d\Delta/dT$ of the experimental results for the alloys of magnesium and aluminum with a semiquantitative calculation by Gupta. Near 250°K, Δ is negative and $d\Delta/dT$ is temperature dependent for Cd–Mg alloys, and further work is required to clarify this result. Below about 50°K deviations for all alloys are positive, and the various contributions are discussed. The precise resistivity results obtained over a wide temperature range extend the knowledge of deviations from Matthiessen's rule, but the complexity of the scattering processes makes a detailed comparison with theory difficult, particularly at low temperatures. (auth)

5185 BRILLOUIN-ZONE–FERMI-SURFACE INTERACTIONS IN PURE AND LEAD-DOPED INDIUM. Carriker, R. C.; Reynolds, C. A. (Univ. of Connecticut, Storrs). Phys. Rev., B; 2: 3146-57(15 Oct 1970).

Electrical resistivity anisotropies ($a \equiv \rho_\perp / \rho_\parallel$, direction referred to the c axis) of pure indium containing 0 to 9-at. % lead were measured at 4.2, 77, and 273°K. For pure indium it was found that $a(77) = 0.988 \pm 0.003$, while $a(273) = 1.037 \pm 0.003$; thus the direction of maximum resistivity changes from the c to the a direction as the temperature goes from 77 to 273°K. This behavior is interpreted in terms of the resistivity anisotropy model of Klemens, Van Baarle, and Gorter, which is also used to qualitatively explain the observed anisotropies of the indium–lead alloys studied. Anomalies in the resistivity anisotropy were observed at 3.5- and 7.0-at. % lead, which were traced to anomalous behavior in the resistivity perpendicular to the c axis. The behavior at 7.0-at. % lead is interpreted as the Fermi surface popping through the (200) zone boundary. The temperature-dependent resistivity anisotropies of indium–lead alloys at 77 and 273°K were determined, and at 273°K, the direction of maximum temperature-dependent resistivity was found to change from the a to the c direction between 6- and 7-at. % lead. This behavior is attributed to an increasing perturbation of the indium lattice periodic potential by the lead ions at the relatively high temperature of 273°K, and it is interpreted in terms of a breakdown in the δ-function potential approximation in the model of Klemens et al. (auth)

5186 SOUND PROPAGATION NEAR MAGNETIC PHASE TRANSITIONS. Luethi, B.; Moran, T. J.; Pollina, R. J. (Rutgers–The State Univ., New Brunswick, N. J.). J. Phys. Chem. Solids; 31: 1741-58(Aug 1970).

Experimental results on critical velocity and critical attenuation changes are presented and discussed. Whereas the critical velocity changes show a uniform behavior for all substances studied, namely a frequency-independent and a weak temperature-dependent effect, the critical attenuation changes show a wide variety of behavior for different materials. A given substance can be characterized by the following physical parameters: spin structure (ferro- or antiferromagnet), magnetic anisotropy, and range of spin interaction. In this way, the rare earth metals Gd, Tb, Dy, and Ho can be nicely accounted for by present theories. In insulators, the coupling of the sound to the energy density of the spin system seems to be very important as shown in EuO, and also in $RbMnF_3$ and MnF_2. These latter antiferromagnets are not fully understood yet however. In addition, other results (CoO, FeF_2) are discussed and results for Cr presented. (auth) (UK)

5187 ELECTRONIC DENSITY OF STATES AND CRYSTAL STRUCTURE IN IVA TRANSITION METALS. Merz, H. (Univ., Karlsruhe, Ger.). Phys. Lett.; 33A: 53-4(21 Sep 1970).

Bremsstrahlung isochromats of the hcp and bcc phases of Ti, Zr, and Hf are presented. They show directly that the density of states in the mid-part of the d-band decreases, when the phase transformation hcp → bcc occurs. (auth)

5188 REFLECTANCE STUDIES OF Ba, Sr, Eu, AND Yb. Endriz, J. G.; Spicer, W. E. (Stanford Univ., Calif.). Phys. Rev., B; 2: 1466-92(15 Sep 1970).

In situ reflectance measurements were made on films of the alkaline-earth metals barium (bcc) and strontium (fcc), and rare-earth metals europium (bcc) and ytterbium (fcc) from 1.0 to 11.6 eV. Extreme care was taken in all aspects of the work so that a Kramers–Krönig analysis of the reflectance data yielded optical constants ϵ_1, ϵ_2, σ, and α, which were accurate to better than ±20%. The volume-loss functions calculated from these optical constants yielded an agreement with loss-function peak positions obtained in Kunz's high-energy electron-loss experiments which was not seen in previous optical studies, and served as verification of the improved accuracy of the present study. A comparison of the interband optical conductivities for the alkaline-earth and rare-earth metals failed to indicate strong structure or increased oscillator strength in the rare-earth metals that could be unambiguously attributed to transitions from 4f electrons found in europium and ytterbium. The filled 4f-electron states in these two metals are known to be accessible to the spectral range of the present study, and an explanation, based on matrix elements, is proposed for this inability to excite such electrons. The structure observed in the interband conductivity of all four of these metals was correlated to crystal structure and showed much better agreement with the predictions of strong d-electron effects implied in recent band calculations than it did with the simple predictions of the nearly-free-electron theory. (auth)

5189 TRANSIENT FIELDS IN FERROMAGNETIC IRON AND GADOLINIUM. Heestand, G. M. (Univ. of Aarhus, Denmark); Hvelplund, P.; Skaali, B.; Herskind, B. Phys. Rev., B; 2: 3698-3702(1 Nov 1970).

Experiments studying the velocity dependence of the transient field for ^{196}Pt in Fe and the transient field for ^{194,196,198}Pt in Gd were carried out in order to make comparisons with the recent Lindhard–Winther theory. Agreement between theory and experiment is good concerning the shape of the velocity dependence, but the experimental value is a factor of 2 larger than theoretically predicted. A large precession due to the transient field (ϕ =

XUM

–51 ± 7 mRad) was found for Pt in Gd. A transient field precession for Pd and Cd in Gd was computed on the basis of recent radioactivity results. The internal field for Pt in Gd was measured to be –780 ± 120 kG, while former internal field values for Mo, Ru, and Hf in Gd were corrected for transient field effects. (auth)

5190 CRYSTAL STRUCTURE OF THE LOW-TEMPERATURE ANTIFERROMAGNETIC PHASE OF V_2O_3. Dernier, P. D.; Marezio, M. (Bell Telephone Labs., Murray Hill, N. J.). Phys. Rev., B; 2: 3771-6(1 Nov 1970).

At ~155°K, the metallic corundum structure of V_2O_3 distorts to an insulating monoclinic one. Structural refinements of this low-temperature phase by x-ray diffraction techniques show an increase in the nearest-neighbor vanadium–vanadium distances at the transition. This is in direct contrast to previously reported distortion models. In the a–c plane of the monoclinic structure, the vanadium–vanadium distance across the shared octahedral face increases from 2.697 to 2.745 Å, while the vanadium–vanadium distance across the shared octahedral edge increases from 2.882 to 2.987 Å when proceeding from the corundum structure to the monoclinic one. The oxygen octahedra become skewed about the central vanadium atom, while the average vanadium–oxygen distance remains essentially constant. The expansion of the vanadium–vanadium distances associated with this transition is similar to the Mott transition observed in the Cr_2O_3–V_2O_3 system in which the conduction electrons localize on their ionic sites when proceeding from the metal phase, α–V_2O_3, to the insulating one, α – $(V_{0.962}Cr_{0.038})_2O_3$. (auth)

5191 OBSERVATION OF NUCLEAR SPECIFIC HEAT IN V_2O_3. Andres, K. (Bell Telephone Labs., Murray Hill, N. J.). Phys. Rev., B; 2: 3768-71(1 Nov 1970).

In an attempt to determine the magnetic moment of vanadium in the proposed antiferromagnetic state in insulating V_2O_3, the nuclear specific heat was measured in the temperature range below 0.5°K. A nuclear Schottky anomaly varying with T^{-2} is observed that indicates an overall hyperfine splitting of 74 m °K and a hyperfine field of 168 kOe. Using a hyperfine coupling constant deduced by Jones from Knight-shift measurements in the metallic state of V_2O_3, this hyperfine field is consistent with an ordered moment of 1.2 μ_B per vanadium ion. (auth)

5192 GALVANOMAGNETIC PROPERTIES OF A SINGLE-CRYSTAL SPHERE BY THE INDUCED-TORQUE METHOD. II. MAGNETIC BREAKDOWN IN CADMIUM AND ZINC. Visscher, P. B.; Falicov, L. M. (Univ. of California, Berkeley). Phys. Rev., B; 2: 1522-5(15 Sep 1970).

Experimental data from induced-torque measurements on cadmium and zinc for magnetic field directions perpendicular to the hexagonal axis are analyzed theoretically. In both Cd and Zn, magnetic breakdown between the first- and second-zone Fermi surfaces (the "caps" and the "monster") found by Datars and Cook is discussed. The change in topology, from open to closed orbits, makes the torque method an accurate tool for measuring the magnetic-breakdown parameters B_0; these are 8.8 kG (for Cd, $\vec{B}$ parallel to $[10\bar{1}0]$), 18.7 kG (Cd; $\vec{B}$ in $[11\bar{2}0]$ direction), and 5.1 kG (Zn for $\vec{B}$ along a direction in the basal plane 7° from $[10\bar{1}0]$). For Zn, a second magnetic-breakdown phenomenon was found. This is between the first-zone "caps" and the third-zone "needles," and produces a transition between closed orbits and a different kind of open orbits. The breakdown parameter for this second effect is 38.5 kG. (auth)

5193 LES ELEMENTS DES TERRES RARES. TOME II. (Rare Earth Elements. Volume II). International Symposium on Rare Earth Elements, Held at Paris, Grenoble, France, 5–10 May 1969. Paris; Centre National de la Recherche Scientifique (1970). 602p. (In French and English). (CONF-690517).

The fifty-three papers of this second part illustrate experimental and theoretical studies made on rare earth compounds in solid-state physics: magnetism, neutron-diffraction study of magnetic ordering, neutron diffusion, specific heat, magneto-electricity and Kondo effect, magneto-optics, hyperfine field, resistivity, Fermi surfaces. Thirty-four of them were selected for NSA, one of which had been already abstracted (NSA 23: 32578). (France)

For abstracts of individual papers see: 4771, 4803, 5194–5219, 5225–5228, 5232, and 5233.

5194 MAGNETOCRYSTALLINE PROPERTIES OF SINGLE CRYSTALS OF RARE EARTHS OF THE SECOND SERIES. Feron, Jacques-Louis; Hug, Gerard; Pauthenet, Rene (LEPM-CNRS, Grenoble, France). pp 19-30 of Les Elements des Terres Rares. Tome II. Paris; Centre National de la Recherche Scientifique (1970). (In French).

From International Symposium on Rare Earths, Paris, Grenoble, France. See CONF-690517.

The magnetic properties of rare earth single crystals (Gd, Tb, Dy, Ho, and Er) were investigated in high magnetic fields up to 80 kOe at low temperatures. The anisotropy constants of these elements were deduced from the analysis of the magnetization curves. The anisotropy energy is quite small in gadolinium (10^6erg/cm^3); however, it is very large in the other elements (5×10^8 erg/cm^3). The thermal variation of the anisotropy constants is in good agreement with that given by the one-ion model. The experimental variation of the critical fields with temperature are explained with a model taking into account the elastic, magnetocrystalline, and magnetostrictive energies. The magnetostrictive energy is the largest term in terbium; the magnetocrystalline energy is the largest one in holmium; dysprosium shows an intermediate behavior. (tr-auth) (France)

5195 EFFECTS OF AN HYDROSTATIC PRESSURE AND OF AN UNIAXIAL STRESS ON THE MAGNETIC TRANSITION TEMPERATURES OF THE RARE EARTH SINGLE CRYSTALS: Gd, Tb, AND Dy. Bartholin, H.; Bloch, D. (LEPM-CNRS, Grenoble, France). pp 31-46 of Les Elements des Terres Rares. Tome II. Paris; Centre National de la Recherche Scientifique (1970). (In French).

From International Symposium on Rare Earths, Paris, Grenoble, France. See CONF-690517.

The magnetic ordering temperatures of Gd, Tb, and Dy single crystals were determined experimentally by hydrostatic pressure up to 6 kbar. The Curie temperature of gadolinium decreases with pressure. At high temperatures, terbium and dysprosium undergo an antiferromagnetic–paramagnetic transition at the Neel temperature. At lower temperatures a ferromagnetic–antiferromagnetic transition occurs at the Curie temperature. The rates of temperature decreases with pressure were determined. These variations result from the modifications of the exchange and anisotropy energies with the interatomic distance. In order to interpret the experimental results, a one-dimensional model was used, considering only the variation of the exchange energy with the parameter c of the crystal. Consequently, it was necessary to determine the variation of the Curie temperature of a gadolinium single crystal as a function of a uniaxial stress. Two different values were obtained for the rates of the temperature decrease with pressure, the stress being applied along the c-axis and along the a- or b-axis, respectively. The variation of the exchange interaction with the crystallographic parameters a, b, and c was deduced. The variation of the Curie temperature with hydrostatic pressure was deduced from these results together with the magnetic length anomalies and anisotropic forced magnetostriction. The calculated values are in good agreement with the experimental values. (tr-auth) (France)

5196 MAGNETIC DOMAIN STRUCTURES IN GADOLINIUM. Al-Bassam, T. S.; Corner, W. D. (Univ. of Durham, Eng.). pp 47-54 of Les Elements des Terres Rares. Tome II. Paris; Centre National de la Recherche Scientifique (1970).

From International Symposium on Rare Earths, Paris, Grenoble, France. See CONF-690517.

Single crystals of gadolinium with an oxide content considerably reduced by a solid-state electrolysis technique were obtained. After suitable polishing, domain patterns were observed on a basal plane surface and on surfaces containing the c-axis. The Bitter technique was used with a modified colloid for most of the observations, but a dry colloid technique was used at temperatures below 240°K. At 274°K, patterns on planes containing the c-axis show parallel 180° walls with a development of partial closure structures at the free surface and at oxide inclusions. Basal plane patterns indicate that the 180° walls are not plane and give more detailed information about the nature of the closure structures. The change in domain structure was studied for a temperature reduced to 130°K and under the influence of magnetic fields up to 1400 Oe. An interpretation of the patterns is suggested taking into account the relative magnitudes of the spontaneous magnetization and the magnetocrystalline anisotropy. (tr-auth) (France)

5197 MAGNETIC PROPERTIES OF RARE EARTH–NOBLE METAL EQUIATOMIC COMPOUNDS: DEPENDENCE ON THE STRUCTURE OF THE CONDUCTION BAND. Pierre, J. (LEPM-CNRS, Grenoble, France). pp 55-64 of Les Elements des Terres Rares. Tome II. Paris; Centre National de la Recherche Scientifique (1970). (In French).

From International Symposium on Rare Earths, Paris, Grenoble, France. See CONF-690517.

The antiferromagnetic ordering observed in RCu and RAg compounds is explained, using the theory of indirect exchange

through conduction electrons, taking into account the band structure of these compounds. (tr-auth) (France)

5198 MAGNETIZATION AND ^{59}Co HYPERFINE FIELD MEASUREMENTS IN $Gd(CoNi)_2$. Christopher, J. T.; Taylor, K. N. R. (Univ. of Durham, Eng.). pp 65-73 of Les Elements des Terres Rares. Tome II. Paris; Centre National de la Recherche Scientifique (1970).

From International Symposium on Rare Earths, Paris, Grenoble, France. See CONF-690517.

Measurements of the magnetization and hyperfine field strength in the system $Gd(CoNi)_2$ were made as a function of composition. The variation in transition metal moment is interpreted in terms of an itinerant electron model while the changes in the hyperfine field at the Co nucleus are taken to arise from the moment variation and a change in conduction electron concentration. (tr-auth) (France)

5199 MAGNETIC PROPERTIES OF R_3M COMPOUNDS OF THE RARE EARTH METALS AND OF THE TRANSITION METALS OF THE FIRST SERIES. Feron, Jacques-Louis; Gignoux, Damien; Lemaire, Remy; Paccard, Dominique (LEPM-CNRS, Grenoble, France). pp 75-80 of Les Elements des Terres Rares. Tome II. Paris; Centre National de la Recherche Scientifique (1970). (In French).

From International Symposium on Rare Earths, Paris, Grenoble, France. See CONF-690517.

The magnetic properties of the R_3M intermetallic compounds, where R is a rare earth element and M a transition metal of the first series, are described. The yttrium and samarium compounds show a weak paramagnetism which varies smoothly with the temperature. Tm_3Ni, Tm_3Co, and Er_3Co have a ferromagnetic behavior, the other compounds exhibit metamagnetism. The magnetization process of Gd_3Co at low temperature results from a compromise between applied field energy, exchange interactions, and magnetocrystalline anisotropy. In the other compounds, crystal field effects are too strong to explain the magnetic properties by similar model. (tr-auth) (France)

5200 MAGNETIC RESONANCE OF RARE EARTH–COBALT INTERMETALLIC COMPOUNDS AT 9.2 GHz. Marchand, Andre; Lancia, Roland (LEPM-CNRS, Grenoble, France). pp 81-6 of Les Elements des Terres Rares. Tome II. Paris; Centre National de la Recherche Scientifique (1970). (In French).

From International Symposium on Rare Earths, Paris, Grenoble, France. See CONF-690517.

Microwave resonance measurements were made on powdered specimens of rare earth–cobalt intermetallic compounds. Y_2Co_{17}, Er_2Co_{17}, YCo_3, $PrCo_3$, $NdCo_3$, $TbCo_3$, $HoCo_3$, $ErCo_3$, and Tb_3Co were studied. The values of the resonance field above and under the Curie temperature were compared and the shape of the resonance curve was briefly studied. (tr-auth) (France)

5201 FERRIMAGNETISM OF THE INTERMETALLIC COMPOUND Co_2Gd. Burzo, Emil; Pop, Iuliu; Tchetchernikov, V. I. (Univ. Babes-Bolyai, Cluj). pp 87-92 of Les Elements des Terres Rares. Tome II. Paris; Centre National de la Recherche Scientifique (1970). (In French).

From International Symposium on Rare Earths, Paris, Grenoble, France. See CONF-690517.

The variation with respect to temperature (94–1250°K) of the intensity of magnetization and the magnetic susceptibility of the intermetallic compound Co_2Gd was studied; the applied fields used varied between 640 and 9,800 Oe. This compound has a cubic crystal structure of the bêta-Cu_2Mg type (Laves phase). It exhibits ferrimagnetic behavior as well as a hyperbolic variation in its paramagnetic susceptibility consistent with the Néel Law. The ESR absorption line width shows a rapid decrease at the Curie point. The slow decrease in the thermal factor g with increasing temperatures is graphically presented. (tr-auth) (France)

5202 MAGNETIC PROPERTIES OF THE RARE EARTH HYDROXIDES. Wolf, W. P.; Meissner, H. E.; Catanese, C. A.; Scott, P. D. (Yale Univ., New Haven). pp 93-7 of Les Elements des Terres Rares. Tome II. Paris; Centre National de la Recherche Scientifique (1970).

From International Symposium on Rare Earths, Paris, Grenoble, France. See CONF-690517.

A brief summary is given of recent experiments on the preparation and properties of the rare earth hydroxides $R(OH)_3$, where R = La, Nd, Gd, Tb, Dy, Ho, Er, and Y. Magnetic, thermal, and optical measurements all indicate that $Tb(OH)_3$ is a particularly simple system, approximating closely to an Ising model of weakly coupled linear chains with a ferromagnetic Curie point of 3.71°K. The hydroxides of Dy and Ho are also ferromagnetic (T_c = 3.48° and 2.54°K) but their behavior is complicated by low-lying crystal field levels. $Gd(OH)_3$, $Nd(OH)_3$, and $Er(OH)_3$ appear to be antiferromagnets with relatively low Néel temperatures (0.94°, <0.6°K, and <1.2°K) caused by competing nearest- and next-nearest-neighbor, non-dipolar interactions. (tr-auth) (France)

5203 FIRST-ORDER TRANSITION IN EUROPIUM METAL. Cohen, R. L.; Hufner, S.; West, K. W. (Bell Telephone Labs., Murray Hill, N. J.). pp 101-8 of Les Elements des Terres Rares. Tome II. Paris; Centre National de la Recherche Scientifique (1970).

From International Symposium on Rare Earths, Paris, Grenoble, France. See CONF-690517.

The Moessbauer effect was used to study in detail the behavior of the hyperfine (hf) interaction in clean Eu metal near the magnetic ordering temperature. Since the size of the magnetic hf interaction is essentially proportional to the sublattice magnetization, the temperature dependence of the sublattice magnetization (the magnetic structure is "flat spiral"), at zero applied field was accurately measured. The experiments showed that at 88.6°K, the magnetization falls discontinuously from 0.4 of the saturation value to zero. Isomer shift measurements established unequivocally that the Eu ions are in the $2^+(^8S_{\frac{7}{2}})$ valence state at all temperatures. The disappearance of the hf field was attributed to a previously unrecognized first-order phase transition coincident with the magnetic ordering. Recent specific heat measurements supported this conclusion. The transition appears to involve a small crystallographic distortion (from the bcc structure existing above the ordering temperature) due to magnetostriction. Thermal expansion measurements were also performed on a bulk polycrystalline sample. Results of those measurements can be related to previously published specific heat and high-pressure experiments. This leads to an explanation for the reported anomalous behavior of the ordering temperature with pressure. Finally, the temperature dependence of the sublattice magnetization just below the transition is analyzed in terms of critical point theory. (tr-auth) (France)

5204 FLUCTUATIONS AND CRITICAL INDICES NEAR THE NEEL TEMPERATURE OF EUROPIUM. Meaden, G. T.; Sze, N. H. (Dalhousie Univ., Halifax, Nova Scotia). pp 109-17 of Les Elements des Terres Rares. Tome II. Paris; Centre National de la Recherche Scientifique (1970).

From International Symposium on Rare Earths, Paris, Grenoble, France. See CONF-690517.

The effect of magnetic phase transitions on the electrical resistivity of the rare earths is discussed, and the results obtained for antiferromagnetic Eu are compared with the recent theory of Suezaki and Mori. These authors predict that, above T_N, $(d\rho/dT)_{anom} = -C\epsilon^{-(\alpha+\gamma-1)} \equiv -C\epsilon^{-\frac{1}{3}}$, if $\alpha + \gamma = \frac{4}{3}$, where $\epsilon = |T - T_N|/T_N$, while below T_N, $(d\rho/dT)_{anom} = -D_\epsilon^{-(\alpha+\gamma)/2} + E_\epsilon^{-(\alpha+\gamma-1)}$. The first term ($\equiv -D_{\epsilon^{-\frac{2}{3}}}$), due to band gaps of magnetic origin, dominates $d\rho/dT$ in typical antiferromagnetic metals, but for Eu between $10^{-3} < \epsilon < 70 \times 10^{-3}$ (T_N – 0.1 to T_N – 6°K with T_N = 88.2°K) the resultant anomaly goes as $\epsilon^{-\frac{1}{3}}$ with a positive divergence and not a negative one. This strongly suggests that in Eu the resistive effect from such band gaps is absent (D = 0), and the possible origin of such behavior is discussed. Above T_N for $0.3 < \epsilon < 2.5$, there is an important exponential contribution to the resistivity which indicates that short-range-order persists in Eu up to ~250°K. (tr-auth) (France)

5205 MAGNETIC ORDERING AND THERMODYNAMIC PROPERTIES OF INDUCED MOMENT SYSTEMS. Cooper, Bernard R. (General Electric Co., Schenectady, N. Y.). pp 187-95 of Les Elements des Terres Rares. Tome II. Paris; Centre National de la Recherche Scientifique (1970).

From International Symposium on Rare Earths, Paris, Grenoble, France. See CONF-690517.

The magnetic behavior of rare earth systems is discussed when the crystal-field-only ground state of the rare earth ion is a singlet. A molecular field treatment is used to discuss the magnetization process and to point out the existence of a threshold value for the ratio of exchange to crystal-field interaction necessary for magnetic ordering. The theory of the collective excitations and the relationship of their behavior to the magnetic ordering process are then treated. Also, a discussion is given of the present experimental situation with regard to the variety of experimental techniques that can be used to increase understanding to induced-moment systems. Recent experiments on $Tb_xY_{1-x}Sb$, which directly show the transition from Van Vleck paramagnetism to antiferromagnetism at low temperature as the fraction of terbium increases, are discussed. (tr-auth) (France)

5206 PARAMAGNETIC ANISOTROPY: APPLICATION TO RARE EARTHS. Boutron, P. (LEPM-CNRS, Grenoble, France).

XUM

pp 197-209 of Les Elements des Terres Rares. Tome II. Paris; Centre National de la Recherche Scientifique (1970). (In French).

From International Symposium on Rare Earths, Paris, Grenoble, France. See CONF-690517.

The susceptibility of a single crystal of the most general symmetry was calculated above the ordering temperature. When the crystal contains only one magnetic sublattice, the anisotropy of the susceptibility varies as the square of the direction cosines of the applied magnetic field referred to the symmetry axes of a tensor defined by the single crystal. When J or S is a good quantum number, the anisotropy of the susceptibility depends only on two crystal field parameters. In the case of rare earth metals, the theoretical variations of the susceptibility with temperature and direction of the field are in agreement with the experimental variations. The thermal variation of the u_2^0 parameter was calculated using the theoretical expression for the anisotropy of the susceptibility. This variation is in agreement with the variation in the screened point-charge model calculated from the thermal expansion of the single crystals. (tr-auth) (France)

5207 MAGNETIC PROPERTIES OF Er-BASED BINARY RARE EARTH ALLOYS. Millhouse, A. H.; Koehler, W. C. (Oak Ridge National Lab., Tenn.). pp 213-22 of Les Elements des Terres Rares. Tome II. Paris; Centre National de la Recherche Scientifique (1970).

From International Symposium on Rare Earths, Paris, Grenoble, France. See CONF-690517.

Neutron-diffraction studies of single crystals of Er–Ho and Er–Dy alloys were carried out. In addition two single crystals of Er containing 10 and 25 at. % Tb were studied by this technique. In all three alloy systems, a change in the initial ordering direction, from the c-axis direction to the basal-plane direction occurs at ~10% Ho, Dy, or Tb. At 10% Tb a helically ordered basal plane moment appears at 97°K and then follows the usual saturation curve to 4.2°K where its magnitude is 4.6 μ_B/atom. The c-axis component first appears at 72°K and is sinusoidally modulated down to 50°K, then becomes squared in the region from 50 to 25°K, and ferromagnetically aligned from 25 to 4.2°K. A considerable thermal hysteresis occurs for the transition from the ferromagnetic to the squared c-axis structure, this transition occurring at 40°K on warming. The turn angles for the cone and squared structures are 41 and 45°/layer, respectively. At 4.2°K the c-axis component of the moment is 7.9 μ_B/atom. At 25% Tb only the helix and cone structures are observed. The basal-plane component of the moment appears at 128°K, increases to 7.0 μ_B/atom at 45°K, and then decreases to 5.9 μ_B/atom at 4.2°K. The c-axis component, which is ferromagnetically aligned throughout its ordered range, first appears at 45°K and is 6.7 μ_B/atom at 4.2°K. In all three alloy systems, the best agreement with the measured moment values is obtained by assuming that the Ho, Dy, or Tb moments are parallel to the Er moments within hexagonal layers at 4.2°K. This implies that the "multimoment" anisotropies dominate in these systems and that anisotropic exchange is probably an important source of the anisotropy. One alloy in the Gd–Er system exhibits the same magnetic structures as those found in pure Er. (tr-auth) (France)

5208 MAGNETIC PROPERTIES AND MAGNETIC STRUCTURES OF THE DyAl-TYPE EQUIATOMIC COMPOUNDS OF ALUMINUM AND RARE EARTH METALS. Becle, Christian; Lemaire, Remy (CNRS, Grenoble, France. CEA, Grenoble, France). pp 223-30 of Les Elements des Terres Rares. Tome II. Paris; Centre National de la Recherche Scientifique (1970). (In French).

From International Symposium on Rare Earths, Paris, Grenoble, France. See CONF-690517.

The rare earth–aluminum compounds of the DyAl type have magnetic properties that differ according to the alloyed rare earth metal. NdAl and TbAl are antiferromagnetic, HoAl has a ferromagnetic behavior, the others are metamagnetic. The noncolinear magnetic structure of NdAl, TbAl, HoAl, ErAl, and TmAl was by neutron diffraction. They are stabilized by strongly anisotropic magnetic interactions between rare earth atoms. (tr-auth) (France)

5209 MAGNETIC PROPERTIES AND MAGNETIC STRUCTURES OF RARE EARTH–Ni EQUIATOMIC COMPOUNDS. Lemaire, Remy; Paccard, Dominique (CNRS, Grenoble, France. CEA, Grenoble, France). pp 231-8 of Les Elements des Terres Rares. Tome II. Paris; Centre National de la Recherche Scientifique (1970). (In French).

From International Symposium on Rare Earths, Paris, Grenoble, France. See CONF-690517.

Rare earth–Ni equiatomic compounds exhibit a spontaneous magnetization at low temperature; however at 4.2°K, a field of 70 kOe is not sufficient to saturate them. Their magnetic properties differ according to the crystalline structure. HoNi and ErNi of FeB type have a noncolinear magnetic structure; in NdNi of CrB type the magnetic moments are parallel. In all those compounds, Ni is not magnetic. (tr-auth) (France)

5210 MAGNETIC STRUCTURE OF INTERMETALLIC COMPOUNDS RCo_3. Schweizer, J.; Yakinthos, J. (CEA, Grenoble, France). pp 239-50 of Les Elements des Terres Rares. Tome II. Paris; Centre National de la Recherche Scientifique (1970). (In French).

From International Symposium on Rare Earths, Paris, Grenoble, France. See CONF-690517.

A neutron-diffraction study of the intermetallic compounds RCo_3 (R = Pr, Nd, Tb, Ho, Er) was made. $PrCo_3$ and $NdCo_3$ are ferromagnetic. In $TbCo_3$, $HoCo_3$, and $ErCo_3$ the cobalt moments are aligned and anti-parallel to the rare earth moments. The easy magnetization axis is parallel to c for $PrCo_3$ and $ErCo_3$. At 4.2°K it is perpendicular to c for the other compounds but in $NdCo_3$ and $HoCo_3$ it rotates and becomes parallel to c at room temperature. The cobalt magnetic moments depend on the atomic number of the alloyed rare earth metal and on the crystallographic site. (tr-auth) (France)

5211 MAGNETIC PROPERTIES OF Ho_6Fe_{23} AND $HoFe_2$. Roe, G. J.; O'Keefe, T. J.; Moreau, J. M.; Michel, C.; James, W. J. (Univ. of Missouri, Rolla). pp 251-9 of Les Elements des Terres Rares. Tome II. Paris; Centre National de la Recherche Scientifique (1970).

From International Symposium on Rare Earths, Paris, Grenoble, France. See CONF-690517.

Powder samples of Ho_6Fe_{23} and $HoFe_2$ were examined by neutron diffraction. Ho_6Fe_{23} was found to have a ferrimagnetic structure with a saturation moment for holmium of 9.3μ_B and a mean moment for iron of 2.25μ_B. The magnetic and nuclear cells of Ho_6Fe_{23} are coincidental. The Curie points for Ho_6Fe_{23} and $HoFe_2$ are approximately 500 and 600°K respectively. It is believed that the magnetic cell of $HoFe_2$ is not coincidental with the nuclear cell. (tr-auth) (France)

5212 MAGNETIC STRUCTURE OF ErSi. Nguyen Van Nhung; Sivardiere, J.; Apostolov, A. (CEA, Grenoble, France. CNRS, Grenoble, France). pp 261-74 of Les Elements des Terres Rares. Tome II. Paris; Centre National de la Recherche Scientifique (1970). (In French).

From International Symposium on Rare Earths, Paris, Grenoble, France. See CONF-690517.

The compound ErSi of type CrB (space group Cmcm), was studied by magnetostatic measurements and neutron diffraction. It becomes antiferromagnetic below T_N = 10°K, it is then metamagnetic and the critical field is about 16 kOe at 2°K. The magnetic peaks observed at 1.5°K can be indexed in a unit cell doubled along the a and c directions. A complex colinear magnetic structure, which transforms according to the only four-dimensional representation of space group Cmcm associated with the wave vector $\vec{K} = \left[\frac{1}{2}\ 0\ \frac{1}{2}\right]$, is proposed. It is necessary to introduce pseudo-dipolar exchange forces to explain this structure. (tr-auth) (France)

5213 EXCHANGE INTERACTIONS IN RARE EARTH METALS. Moeller, H. Bjerrum (Danish Atomic Energy Commission, Risoe); Nielsen, M.; Mackintosh, A. R. pp 277-81 of Les Elements des Terres Rares. Tome II. Paris; Centre National de la Recherche Scientifique (1970).

From International Symposium on Rare Earths, Paris, Grenoble, France. See CONF-690517.

The temperature dependence of the magnon energies in Tb and alloys with Ho was measured by inelastic neutron scattering in both the helical and ferromagnetic phases. The results show that the exchange forces may change rapidly with temperature in the helical phase and abruptly at the ferromagnetic transition. The maximum in $\mathcal{J}(q)$ in the c-direction becomes more pronounced as the Ho concentration is increased, in agreement with the observed stability of periodic magnetic ordering in Ho. (tr-auth) (France)

5214 EXCHANGE AND CRYSTAL-FIELD INTERACTIONS IN ERBIUM AND HOLMIUM FROM INELASTIC NEUTRON SCATTERING MEASUREMENTS. Woods, A. D. B.; Stringfellow, M. W.; Holden, T. M.; Powell, B. M. (Atomic Energy of Canada Ltd., Chalk River, Ont.). pp 283-9 of Les Elements des Terres Rares. Tome II. Paris; Centre National de la Recherche Scientifique (1970).

From International Symposium on Rare Earths, Paris, Grenoble, France. See CONF-690517.

Inelastic scattering of thermal neutrons was used to study the

XUM

magnetic properties of erbium and holmium in both the magnetically ordered and the paramagnetic phases. In the conical phase, which occurs in both metals below about 20°K, the spin-wave dispersion relations were determined for both the c and the a axes at 4.6°K. The c-axis dispersion curve for holmium in its flat spiral phase was determined at 25°K. The measurements in the paramagnetic phase were mostly done at 296°K. The temperature dependence of selected modes was also determined. These observations support the hypothesis that the cone-to-spiral transition in holmium arises from an instability in the spin-wave mode for which $\vec{q} = \vec{k}_0$, where $\vec{k}_0$ is the spiral wave vector. This, in turn, arises from a change in sign in the second-order crystal field parameter as the temperature is raised. The temperature dependence of the same mode in erbium reflects a similar temperature dependence of the crystal-field parameters. Analysis of the spin-wave dispersion curves gives information about the exchange and crystal-field parameters, which are then used to calculate the neutron scattering from paramagnetic holmium and erbium. Comparison of the calculated and measured neutron energy distributions reveal minor discrepancies, but the overall agreement is reasonably satisfying. (tr-auth) (France)

5215 MAGNETIC STRUCTURE OF CUBIC RARE EARTH OXIDES. Quezel, S.; Bertaut, E. F.; Quezel, G. (CNRS, Grenoble, France. CEA, Grenoble, France). pp 293-311 of Les Elements des Terres Rares. Tome II. Paris; Centre National de la Recherche Scientifique (1970). (In French).

From International Symposium on Rare Earths, Paris, Grenoble, France. See CONF-690517.

A representation analysis is given for the magnetic modes allowed for the rare earth spins on the 24 sites of binary symmetry C_2 and on the 8 sites of ternary symmetry $C_{\bar{3}}$. These modes are compared with the already-known magnetic structures of Er_2O_3 and Yb_2O_3 and with the new structure of Tb_2O_3 in which, at temperatures as low as 1.5°C, only the spins on the 24 sites C_2 are ordered. Their noncolinear configuration is described by $A_{\overline{xxy}}\ C_{\overline{yzx}}$. The components $A_{\overline{xxy}}$ and $C_{\overline{yzx}}$ belong to the same representation. The values of the moment associated with the A-mode and the C-mode are $2.01\mu_B$ and $3.7\mu_B$, respectively. The total moment of Tb at 1.5°K is $4.2\mu_B$, which is much less than the free-ion value. (tr-auth) (France)

5216 MAGNETIC STRUCTURE OF Er_6WO_{12}. Montmory, M. C.; Bertaut, E. F.; Lovold, K. (CNRS, Grenoble, France. CEA, Grenoble, France). pp 349-61 of Les Elements des Terres Rares. Tome II. Paris; Centre National de la Recherche Scientifique (1970). (In French).

From International Symposium on Rare Earths, Paris, Grenoble, France. See CONF-690517.

Er_6WO_{12}, belongs to the group $R\bar{3}-C_{3i}^3$; the parameters of the unit cell are a = 6.404 Å, α = 98.715°. W, in the special position (000) has six neighbors; O and Er in the general position 6f have a sevenfold coordination. The neutron diffraction diagram recorded at 1.5°K shows a magnetic ordering that requires a doubling of the chemical cell in three dimensions and thus is characterized by a wave vector $\vec{k} = [\frac{1}{2}\frac{1}{2}\frac{1}{2}]$. The magnetic structure is discussed in connection with the space group $G_{\vec{k}}$ of the wave vector $\vec{k}$. $G_{\vec{k}}$ has six irreducible one-dimensional representations (two real and four complex ones). The structure belongs to a real one-dimensional representation, which allows its description in the Shubnikov group $R_i\bar{3}$. The spin direction is approximately [u, −u, −u] and the value of the moment is 6.0 + 0.4μ_B. (tr-auth) (France)

5217 MAGNETIC PROPERTIES OF GADOLINIUM ORTHOVANADATE. Cashion, J. D.; Cooke, A. H.; Hoel, L. A.; Martin, D. M.; Wells, M. R. (Oxford Univ.). pp 417-26 of Les Elements des Terres Rares. Tome II. Paris; Centre National de la Recherche Scientifique (1970).

From International Symposium on Rare Earths, Paris, Grenoble, France. See CONF-690517.

Magnetic measurements showed that $GdVO_4$ and $DyVO_4$ become antiferromagnetic below T_N = 2.5 and 3.0°K, respectively. The specific heat of $GdVO_4$ was measured from 0.5 to 12°K, and in detail near the λ point at 2.495°K. Measurements of the susceptibility in low fields over a range of temperature, and of the magnetic moment at 0.5°K in fields up to 70 kOe, show that the antiferromagnetic ordering is of the simplest two-sublattice type, produced by antiferromagnetic exchange interaction between each Gd^{3+} ion and its four nearest-neighbor Gd^{3+} ions in the zircon lattice of $GdVO_4$. The alignment axis is the crystalline c-axis; an important part of the anisotropy arises from magnetic dipole interaction. (tr-auth) (France)

5218 HEAT CAPACITY STUDIES OF INTERMETALLIC COMPOUNDS CONTAINING RARE EARTH ELEMENTS. Wallace, W. E.; Craig, R. S.; Thompson, A.; (and others) (Univ. of Pittsburgh). pp 427-41 of Les Elements des Terres Rares. Tome II. Paris; Centre National de la Recherche Scientifique (1970).

From International Symposium on Rare Earths, Paris, Grenoble, France. See CONF-690517.

Heat capacity results are presented for LaSb; PrSb; LaBi; PrBi; $REAl_2$ with RE = La, Ce, Pr, and Gd; $RENi_2$ with Re = Ce, Pr, and Nd; and $GdNi_5$. The temperature range covered is 7 to 300°K; in a few cases measurements were made below 4°K. Results for LaSb, LaBi, and $LaAl_2$ give no clear evidence for anything except vibrational and electronic contributions. PrSb, PrBi, and $PrNi_2$ exhibit Schottky-type thermal anomalies, which are attributed to excitation within the crystal field states. These are confirmed as Van Vleck paramagnets, with overall splittings of 280, 280 and 138°K, respectively. $PrAl_2$ exhibits a λ-type thermal anomaly around its Curie temperature, 31°K. The magnetic heat capacity anomaly for $GdAl_2$ extends from 4 to 180°K, suggesting that in this material the disordering process is weakly cooperative. $NdNi_2$ exhibits a λ-type thermal anomaly at 9°K and a Schottky-type anomaly. The latter is regarded as a crystal-field effect and an overall splitting of 431°K is indicated. (tr-auth) (France)

5219 MAGNETIZATION-DEPENDENT HALL EFFECT IN RARE EARTH METALS. Rhyne, James J. (Naval Ordnance Lab., Silver Spring, Md.). pp 521-9 of Les Elements des Terres Rares. Tome II. Paris; Centre National de la Recherche Scientifique (1970).

From International Symposium on Rare Earths, Paris, Grenoble, France. See CONF-690517.

The anomalous or magnetization-dependent contribution to the Hall effect was recently studied in single crystals of Tb, Dy, Ho, and Er. The basal-plane anomalous Hall coefficients for Tb and Dy are found to exhibit a unique change in sign below the magnetic ordering temperature, an effect that was not observed in the neighboring element Gd which behaves as expected theoretically for a localized ferromagnet. Possible mechanisms for this difference are discussed. Paramiagnetic data were taken with the field applied in two independent symmetry directions ((0001) and basal plane) and reflect the extreme anisotropy of the Fermi surface in these metals. The values of the anomalous coefficients R_s for all the elements studied are found to be temperature-independent over much of the paramagnetic range. The strong observed temperature variation of the Hall resistivity in this region is entirely due to that of the magnetic susceptibility. This result is a consequence of the dominance of spin-disorder scattering in the Hall effect. A second feature is the linear dependence of low-temperature R_s data on the magnetic spin disorder resistivity in Dy and Tb. The normal contribution to the Hall effect, that part of the Hall resistivity linearly dependent on H above saturation, was determined only in Tb below the ordering temperature. (tr-auth) (France)

5220 HEAT CAPACITY OF GADOLINIUM NEAR THE CURIE POINT. Lewis, Edwin Augustus Stevens. Urbana, Ill.; Univ. of Illinois (1969). 46p. University Microfilms Order No. 70-13,391.

Thesis.

The dependence of the heat capacity of gadolinium on temperature was observed close to the ferromagnetic Curie point at about 18°C. An "ac" or temperature modulation method allowed the use of very small single-crystal samples. The heat capacity peak for the best sample is rounded in a range of ½° at the Curie point (T_c). Outside this region, good power law fits are obtained for a range of values of the critical exponents α (above T_c) and α' (below T_c), the choice of which depends on the choice of T_c. The entire set of data, including that in the rounded region, fits an expression derived from a simple macroscopic model of rounding. The T_c specified by this fit makes $\alpha = -.09 \pm .05$ and $\alpha' = -.32 \pm .05$. The results on Curie point and rounding are in disagreement with recent conjectures of Cadieu and Douglass for gadolinium. (Diss. Abstr. Int., B)

Moessbauer Effects and NMR

Refer also to abstracts 4396 and 5467.

5221 (AD-710293) NUCLEAR QUADRUPOLE INTERACTION IN CRYSTALS BY THE MOESSBAUER EFFECT. Final Report, February 1969–June 1970. Schroeer, Dietrich (North Carolina Univ., Chapel Hill. Dept. of Physics). 30 Jun 1970. 9p. (AFOSR-70-1828-TR). NTIS.

The Moessbauer effect following Coulomb excitation by 3.3-MeV alpha particles was observed in ^{161}Dy and ^{151}Eu. Both the 43.8-keV state in ^{161}Dy and the 21.7-keV state in ^{151}Eu are promising candi-

dates for studying the radiation damage produced by the charged-particle bombardment. No time dependence was detected of the iron 1+ to 4+ charge states, resulting from the K-capture decay of ^{57}Co in sources of Cu_2O, MgO, and Al_2O_3. It was shown that CoO samples, produced by drying cobalt nitrate solutions at low temperatures, are made up of microcrystals. The Moessbauer isomer shift of ^{197}Au was measured in samples of gold microcrystals supported in gelatin, and can be correlated with the lattice contractions observed in these microcrystals. Both in bulk and microcrystal hematite, no evidence was found for a gradual Morin spin-flip transition. (auth) (USGRDR)

5222 ASYMMETRIC NUCLEAR MAGNETIC RESONANCE LINE SHAPES DUE TO NUCLEAR QUADRUPOLE AND ANISOTROPIC SHIFT INTERACTIONS. France, P. W.; Hooper, H. O. (Wayne State Univ., Detroit). J. Phys. Chem. Solids; 31: 2223-8(Oct 1970).

The symmetry of the central component of a polycrystalline NMR line shape caused by nuclear quadrupole and anisotropic magnetic interactions is examined theoretically. The asymmetry of the line shape is measured as the difference in the distances from the peaks of the first derivative to the center of the line. This asymmetry is found to vary as the square of the quadrupole coupling constant and inversely as the NMR frequency for the quadrupole interaction. For the anisotropic magnetic interaction, the asymmetry varies as the cube of the frequency. The results of the calculations are discussed with respect to conditions and applications. (auth) (UK)

5223 NUCLEAR ACOUSTIC RESONANCE IN NIOBIUM METAL. Buttet, J.; Gregory, E. H. (California Inst. of Tech., Pasadena). Phys. Lett.; 33A: 265-6(16 Nov 1970).

A nuclear acoustic resonance signal was observed in niobium. The $\Delta m = 2$ transition is due to a pure dynamic electric quadrupole interaction. The $\Delta m = 1$ transition is due to the electric quadrupole interaction and the coupling via the dipole magnetic moment. (auth)

5224 HIGH-PRESSURE NUCLEAR RESONANCE STUDY OF THE METAL–INSULATOR TRANSITION OF V_2O_3. Gossard, A. C.; McWhan, D. B.; Remeika, J. P. (Bell Telephone Labs., Murray Hill, N. J.). Phys. Rev., B; 2: 3762-8(1 Nov 1970).

^{51}V nuclear magnetic resonance (NMR) was observed in metallic V_2O_3 at pressures up to 65 kbar at 4.2°K. Pressures greater than 26 kbar suppress the metal-to-antiferromagnetic insulator transition, leaving V_2O_3 a metal at 4.2°K. ^{51}V NMR shows that the metallic phase, unlike the insulating phase, does not order magnetically down to 4.2°K. The measurements are the highest-pressure resonance measurements which have been reported in the He temperature range. Knight shifts and relaxation times were measured, the Knight shift having an anomalously strong dependence on volume. The relaxation time allows an upper limit of 10^{-13} sec to be placed on the spin fluctuation lifetime of the d electrons. (auth)

5225 HYPERFINE INTERACTIONS IN Er_2O_3 AND Yb_2O_3 BETWEEN 20 AND 1.5°K. Kalvius, G. M.; Shenoy, G. K.; Dunlap, B. D. (Argonne National Lab., Ill.). pp 477-84 of Les Elements des Terres Rares. Tome II. Paris; Centre National de la Recherche Scientifique (1970).

From International Symposium on Rare Earths, Paris, Grenoble, France. See CONF-690517.

Hyperfine interactions were measured in Er_2O_3 and Yb_2O_3 using the nuclear gamma ray resonance (Moessbauer effect) in ^{166}Er, ^{170}Yb, and ^{171}Yb. Measurements were made both above and below their Neel temperatures (T_N) of 3.4 and 2.3°K, respectively. For each of the oxides, the spectra obtained above T_N show pure quadrupole interactions, with two electric field gradients which are characteristic of the rare earth ions occupying the C_{3i} and C_2 sites. Below T_N, two magnetic hyperfine couplings are present in addition to the quadrupole interactions. The strengths of the hyperfine fields are lower than the free-ion values and are proportional to the magnetic moments of the rare earth ions. The hyperfine interactions are discussed in light of the magnetic structure and the electronic ground state for the rare earth ions in these oxides. (tr-auth) (France)

5226 ^{141}Pr AND ^{169}Tm NUCLEAR MAGNETIC RESONANCES IN VAN VLECK INTERMETALLIC PARAMAGNETS. Jones, E. D. (Sandia Labs., Albuquerque, N. Mex.). pp 495-501 of Les Elements des Terres Rares. Tome II. Paris; Centre National de la Recherche Scientifique (1970).

From International Symposium on Rare Earths, Paris, Grenoble, France. See CONF-690517.

The observations of the ^{141}Pr and ^{169}Tm nuclear magnetic resonances (NMR) in the NaCl-type Van Vleck intermetallic paramagnets PrP, PrAs, TmP, TmAs, and TmSb are discussed. The ^{141}Pr and ^{169}Tm NMR are observable for $T \leq 76°$ and $T \leq 27°K$, respectively. The NMR field shifts $(\Delta H/H)$ are very large $((\Delta H/H)^{141} \sim 6$ and $(\Delta H/H)^{169} \sim 80$ for $T = 4°K)$ and are in agreement with theoretical expectations based upon a six-fold cubic crystal field interaction giving rise to a singlet ground state (Γ_1) for both the Pr^{3+} ($^3H_4$) and Tm^{3+} ($^3H_6$) ions. Previous ^{31}P and ^{75}As Knight shift measurements, in these intermetallic compounds, have shown that these Knight shifts are proportional to the paramagnetic susceptibility of the rare-earth ion. Thus, using the results of the ^{31}P and ^{75}As Knight shift data and $(r^{-3}) = 11.7 \pm 0.1$ au for the Tm^{3+} ion, an analysis of the ^{169}Tm NMR data shows that the effective number of Bohr magnetons μ_{eff} of the Tm^{3+} ion in these intermetallic compounds is the same as the free-ion value. Assuming that μ_{eff} for the Pr^{3+} ion is also given by its free-ion value, the NMR data are used to evaluate (r^{-3}) for the Pr^{3+} ion with the results: $(r^{-3}) = 4.8 \pm 0.1$ au. In addition to the above mentioned intermetallic compounds, ^{141}Pr and ^{169}Tm, NMR data for praseodymium metal, PrSe, TmSe, and $TmAl_3$ are given. (tr-auth) (France)

5227 VIRTUAL BOUND STATES IN PLUTONIUM: KONDO EFFECT IN LaPu AND PrPu ALLOYS. Hill, H. H.; Elliott, R. O.; Miner, W. N. (Los Alamos Scientific Lab., N. Mex.). pp 541-50 of Les Elements des Terres Rares. Tome II. Paris; Centre National de la Recherche Scientifique (1970).

From International Symposium on Rare Earths, Paris, Grenoble, France. See CONF-690517.

Resistive minima indicative of a spin-compensated state (Kondo effect) are reported in fcc La–Pu alloys containing 1 to 17.5 at.% Pu and in double-hexagonal Pr–Pu alloys containing 2 to 20 at.% Pu. The results are discussed in relation to previous observations of Kondo effects in LaCe and PrCe alloys. Such effects are observed in La(R.E.) and Pr(R.E.) alloys only when the rare-earth (R.E.) solute is Ce. The explanation is that the effective sf exchange interaction must be antiferromagnetic in sign (as it is with Ce) in order to yield a Kondo effect. Cerium is unique among the rare earths in that its 4f electron occupies a virtual bound state. The resonant scattering of conduction electrons by this virtual level leads to an effective antiferromagnetic sf exchange interaction which dominates the usual ferromagnetic exchange characteristic of rare earths with truly bound 4f levels. Rocher and Friedel have suggested that the 5f electrons in the transuranic metal Pu also occupy virtual bound states. The observation of a Kondo effect in LaPu and PrPu alloys supports this hypothesis. (tr-auth) (France)

5228 INVESTIGATIONS ON THE PRESENCE OF THE KONDO EFFECT IN THE COMPOUND $CeAl_2$. van Daal, H. J.; Buschow, K. H. J. (Philips Gloeilampenfabrieken, Eindhoven, Netherlands). pp 551-7 of Les Elements des Terres Rares. Tome II. Paris; Centre National de la Recherche Scientifique (1970).

From International Symposium on Rare Earths, Paris, Grenoble, France. See CONF-690517.

The anomalous behavior in electrical resistivity of $CeAl_2$ was suppressed by appreciably lowering the density-of-states of the conduction electrons at the Fermi level. This decrease was effected by the partial substitution of Ce by Th in $CeAl_2$. This result further verifies the occurrence of the Kondo effect in $CeAl_2$. (tr-auth) (France)

5229 NUCLEAR MAGNETIC RESONANCE IN TRANSITION METAL BORIDES. Creel, Roger Bryan. Ames, Iowa; Iowa State Univ. (1969). 202p. University Microfilms Order No. 70-13,577.

Thesis.

NMR experiments were conducted to study the environment of the boron nucleus in the transition metal borides. The electric field gradient (EFG) parameters at the boron site were measured in several monoborides by analysis of the ^{11}B NMR spectra. This analysis was facilitated by comparison of the experimental traces with synthetic derivative line shapes generated by a computer. The experimental values of both η and ν_Q are an order of magnitude smaller than predicted on the basis of strong covalent bonding between neighboring boron atoms. The temperature dependence of the ^{11}B NMR signal was used to determine the Néel temperature of CrB_2. The NMR signal vanishes without shifting or broadening as the Néel temperature is approached, which indicates the antiferromagnetic ordering is without local moment, as in pure Cr. The analysis yields a Néel temperature of $T_N = 88.0 \pm 2.0°K$. The temperature dependence of the ^{11}B linewidth was used to determine the paramagnetic Curie temperature in MnB_2. The observation of the ^{11}B signal above the Curie temperature, but below the Néel temperature, is the first example of the observation of conventional NMR in an anti-

XUM

ferromagnet. The ^{11}B nuclear spin–lattice relaxation rates were measured in several of the transition metal diborides. The spin-$\frac{1}{2}$ tone-burst theory was extended to apply to the spin-$\frac{3}{2}$ case in the presence of a quadrupole interaction. It was found that the measured relaxation rates could be explained on the basis of a dominant core polarization relaxation mechanism. (Diss. Abstr. Int., B)

Theory

Refer also to abstracts 5483 and 5494.

5230 NOTE ON THE DETERMINATION OF THE DENSITY OF PHONON EIGENSTATES FROM THE INELASTIC INCOHERENT NEUTRON SCATTERING. Keating, D. T. (Brookhaven National Lab., Upton, N. Y.). J. Phys. Chem. Solids; 31: 1317-23(Jun 1970).

A method for determining the density of phonon eigenstates of a harmonic crystal from the inelastic incoherent neutron scattering is described. The neutron scattering contains, in addition to the one-phonon process, multiphonon processes. This scattering, including multiphonon processes, can always be expressed as a Fourier integral transform of a function of the phonon eigenstates; and, if the scattering is measured while keeping the magnitude of the scattering vector constant, the phonon eigenstates can be obtained by appropriate Fourier inversions. The method is illustrated using the phonon eigenstates recently determined for vanadium at 300°K from the measurement of the thermal diffuse x-ray scattering. Under the assumption that the only effect of temperature is the change in the occupation number of the eigenstates, the influence of temperature on the scattering, and the frequency distribution in the one-phonon approximation, are discussed. The integrated multiphonon processes are 16.6, 63.5, and 165% of the one-phonon process at 300, 1000, and 2000°K. (auth) (UK)

5231 COMPARISON OF STANDARD AND MODIFIED ORTHOGONALIZED PLANE-WAVE METHODS. Gray, D. M.; Karpien, R. J. (Watervliet Arsenal, N. Y.). Phys. Rev., B; 2: 1526-31(15 Sep 1970).

Electron energy levels are calculated for some selected irreducible representations of two crystals, Cu and $LaSn_3$, using both the standard orthogonalized plane-wave method (OPW) and a modified form of this method (MOPW). It is shown that (for a nonrelativistic non-self-consistent treatment, at least) the convergence, in the sense of the number of symmetrized plane waves required, is both more rapid and more reliable for MOPW than for OPW. For the two crystals chosen, standard OPW was found to be reasonably good for $LaSn_3$ but inadequate for Cu, whereas MOPW was quite adequate for both. (auth)

5232 EXCHANGE INTERACTION IN RARE EARTH METALS AND ALLOYS. Blandin, A. (Faculte des Sciences, Orsay, France). pp 505-19 of Les Elements des Terres Rares. Tome II. Paris; Centre National de la Recherche Scientifique (1970). (In French).

From International Symposium on Rare Earths, Paris, Grenoble, France. See CONF-690517.

The properties of metals and ordered or dilute alloys (La,Y) that are linked to the exchange interaction J between conduction and f electrons are reviewed. The origin, sign, order of magnitude of the interaction, and the K and K′ variation of the matrix elements of J are discussed in relation to various experimental properties: magnetism, nuclear resonance in metals and ordered alloys, superconductivity, and Kondo effect in dilute alloys. (tr-auth) (France)

5233 THEORETICAL COMMENTS ON THE VALENCE CHANGE OF RARE EARTH METALS. Coqblin, B. (Faculte des Sciences, Orsay, France). pp 579-92 of Les Elements des Terres Rares. Tome II. Paris; Centre National de la Recherche Scientifique (1970). (In French).

From International Symposium on Rare Earths, Paris, Grenoble, France. See CONF-690517.

A theoretical model is presented that can explain the anomalous behavior of the rare-earth metals having a change of valency with pressure or temperature. The theoretical model explains the anomalous phase diagram of cerium, the $\alpha \rightleftharpoons \gamma$ transition, the properties of the α phase, and the existence of the superconducting high-pressure phase. It can also give an explanation of the variation of the superconducting temperature for lanthanum and the properties of ytterbium under pressure. (France)

Theoretical Physics

Refer also to abstracts 5095, 5167, 5307, and 5497.

5234 (CEA-R-4007) APPROXIMATIONS DEDUCED FROM THE MILNE EQUATION ASSOCIATED TO THAT OF SCHROEDINGER. Dagens, Luc (Commissariat a l'Energie Atomique, Limeil-Brevannes (France). Centre d'Etudes). Nov 1970. 30p. (In French). Dep. NTIS (U. S. Sales Only).

New approximations for energy levels and corresponding wave functions in one dimension are derived. They are generalizations of WKB formulas and are valid about the turning points. The starting point is the Milne equation associated with the Schroedinger equation through the substitution $\psi = y \sin Y + \gamma$, $dY/dx = y^{-2}$. An outline of a rigorous proof is given, based upon the comparison equation method used by Erdélyi in a similar problem and using a new variational identity. A new proof of the WKB level formula is given as an application. The Milne transformation of these approximations is shown to give uniform asymptotic (for $\hbar \rightarrow 0$) approximations to the true wave functions, within a certain domain. The approximate density (in the functional meaning) associated to the new energy level formulas is derived and shown to verify the virial relation. (tr-auth) (France)

5235 (JINR-P2-5266) EQUIVALENCE THEOREM AND OBSERVABLES IN THE FIELD THEORY. Polubarinov, I. V. (Joint Inst. for Nuclear Research, Dubna (USSR). Lab. of Theoretical Physics). 1970. 10p. (In Russian). Dep. NTIS (U. S. Sales Only).

It is shown that the field theory remains invariant with respect to any substitutions of the field variables and unitary representations (equivalence theorem). From the point of view of quantum mechanics principles it is unnecessary to exploit the asymptotic conditions (which is usually done) in proving the equivalence theorem. This is an emergency method since in realistic theories, as a rule, one is able to construct a complete set of observables only at the included interaction. (auth)

5236 (JINR-P2-5283) MULTIPOLE CURRENT DISINTEGRATION IN CLASSICAL ELECTRODYNAMICS. Dubovik, V. M.; Cheshkov, A. A. (Joint Inst. for Nuclear Research, Dubna (USSR). Lab. of Theoretical Physics). 1970. 26p. (In Russian). Dep. NTIS (U. S. Sales Only).

A correct solution of the multipole expansion of the electromagnetic current density in classical electrodynamics is given. (tr-auth)

5237 (ORNL-TM-3203) SAMBO, A COLLISION ANALYSIS PACKAGE FOR MONTE CARLO CODES. Cain, V. R. (Oak Ridge National Lab., Tenn.). 1 Sep 1970. 68p. Dep. NTIS.

SAMBO is a package of computer routines which handles most of the drudgery associated with analysis of collisions in a Monte Carlo code. It was written for use with the MORSE multigroup Monte Carlo code but should be readily adaptable to incorporation into other random-walk-generating codes. An arbitrary number of detectors, energy-dependent response functions, energy bins, time bins, and angle bins are allowed, with virtually no numerical limitations other than the available core storage. Analysis is divided into: uncollided and total response (fluence integrated over each response function at each detector); fluence versus energy and detector; time-dependent response (time-dependent fluence integrated over each response at each detector); fluence versus time, energy, and detector; and fluence versus angle, energy, and detector. Each quantity in the above arrays is output along with an associated fractional standard deviation. (auth)

5238 MODIFIED WKB APPROXIMATION FOR PHASE SHIFTS. Lu, P. (Arizona State Univ., Tempe). Phys. Lett.; 33A: 223-4(2 Nov 1970).

Using the method suggested by Bertocchi et al., one can avoid the divergence and obtain the phase shift of the relativistic point Coulomb scattering to the order of $\hbar^2$ by using the WKB energy integral formula developed earlier by the author. (auth)

5239 CONTRIBUTIONS TO THE PHYSICS OF HIGH-ENERGY DENSITY. Gylden, Nils (Research Inst. of National Defence, Stockholm). FOA (Forsvarets Forsk.) Rep.; 4: No. 1, 1-8(Feb 1970).

Some theoretical investigations on the physics of extreme pressure and temperature are reviewed. The results presented concern the thermodynamic properties of matter. The Mie–Grueneisen equation of state, which is appropriate for high pressure and moderate temperature, is briefly discussed. A study of the properties under astrophysical conditions by means of the statistical (Thomas–Fermi–Kirzhnits) model of the atom is done. These results are used to calculate cross sections for absorption of electromagnetic radiation. The process studied is the "inverse bremsstrahlung." Some similarity properties of high pressure time-dependent flow are treated. High-pressure motion involved in the first stage of the expansion of a fission charge is treated in an approximate way. The effects of a high-altitude nuclear explo-

XUM

sion on a ballistic missile are discussed. The thermal and mechanical damages are considered, and the destruction radius is estimated. (Sweden)

5240 DENSITY OF STATES OF AN ELECTRON IN A FLUCTUATING POTENTIAL. Fowler, G. N. (Univ. of Exeter, Eng.). Phys. Lett.; 33A: 274-5(16 Nov 1970).

It is shown that a recent simple model calculation corresponds to a strong potential limit of the potential distribution whereas localized state effects refer to the weak potential limit. The weak potential limit for an r^{-6} potential is discussed. (auth)

5241 INVARIANT RELATIVE TO TRANSPOSITIONS OF IDENTICAL PARTICLES DESCRIPTION OF THE SPECTRUM OF ENERGY OPERATOR OF QUANTUM-MECHANICAL SYSTEMS. Sigalov, A. G.; Sigal, I. M. (Gorky State Univ., USSR). Teor. Mat. Fiz.; 5: No. 1, 73-93(Oct 1970). (In Russian).

The methods of investigating the spectrum of energy operators of many-particle quantum systems are developed, which are invariant relative to transpositions of identical particles. The configuration space of the system is decomposed into the sum of the sub-spaces corresponding to the motion of the system with respect to the mass center and the motion of the mass center itself. The corresponding decomposition of the energy operator of the system is obtained. The component of the energy operator which corresponds to the motion relative to the mass center is considered on hyperplane of the motion relative to the mass center. This ensures the invariance of the methods developed. (auth)

5242 METHOD FOR SOLVING TIME-DEPENDENT ELECTRON TRANSPORT PROBLEMS. Cordaro, M. (Long Island Lighting Co., Hicksville, N. Y.); Zucker, M. Trans. Amer. Nucl. Soc.; 13: 630-1(Nov 1970).

From Meeting of the American Nuclear Society, Washington, D. C. See CONF-701102.

5243 RADIATION QUANTITIES FROM A MOVING SOURCE OF RADIATION. Neuendorf, W. P. (Bechtel Corp., San Francisco). Trans. Amer. Nucl. Soc.; 13: 870(Nov 1970).

From Meeting of the American Nuclear Society, Washington, D. C. See CONF-701102.

XUM

PHYSICS (HIGH ENERGY)

Particle Interactions and Properties (Experimental)

5244 (CONF-700314) CONFERENCE ON EXPECTATIONS FOR PARTICLE REACTIONS AT THE NEW ACCELERATORS, MARCH 30–APRIL 1, 1970, MADISON, WISCONSIN. (Wisconsin Univ., Madison. Dept. of Physics). 603p. Dep. NTIS.

The conference included 18 papers, one of which was abstracted previously in NSA. For an abstract of this paper see abstract number 24: 37678. Separate abstracts were prepared for 17 papers. (J.F.P.)

For abstracts of individual papers see: 5245, 5256, 5265, 5280, 5281, 5302–5304, 5319, 5320, 5339, 5346, 5347, 5386, and 5443–5445.

5245 (CONF-700314–, Paper 5) COSMIC RAY EXPERIMENTS AND PROSPECTS. Jones, Lawrence W. (Michigan Univ., Ann Arbor). 23p.

From Conference on expectations for particle reactions at the new accelerators, March 30–April 1, 1970, Madison, Wisconsin.

A review is given of very high energy elementary particle interaction information determined from cosmic rays. The evidence for physical quarks, high-energy muons produced in cosmic rays, total inelastic cross section data, and the character of inelastic proton–proton interactions from cosmic ray experimental evidence are discussed. (J.F.P.)

Electromagnetic

Refer also to abstract 4375.

5246 (AD–709922) ELASTIC ELECTRON SCATTERING MEASUREMENTS OF THE NEUTRON CHARGE FORM FACTOR AT VERY-LOW MOMENTUM TRANSFERS. Stewart, Jake W. Jr. (Naval Postgraduate School, Monterey, Calif.). Jun 1970. 134p. NTIS.

Thesis.

Measurements of the ratio of the neutron–proton electric form factors, $G(E_n)/G(E_p)$, were made from elastic electron–deuteron scattering to a precision of approximately 1 to 2% for the range of momentum transfers, q^2 of 0.10 < or = q^2 < or = 0.8 F^{-2}, and for electron scattering angles of 45 to 120°. It was found that within experimental errors the slope as determined from the ratio, $G(E_n)/G(E_p)$, agrees with the thermal neutron–electron interaction slope when relativistic corrections and proper deuteron wave functions are applied to the electron–deuteron scattering results. (auth)

5247 (AD–710385) FORM FACTOR RATIO GE_NGE_p AT LOW-MOMENTUM TRANSFERS. Dally, E. B.; Bumiller, F. A.; Buskirk, F. R.; Stewart, J. W. (Stanford Univ., Calif. High-Energy Physics Lab. Naval Postgraduate School, Monterey, Calif.). Jul 1970. Contract Nonr-225(67). 18p. (HEPL–637). NTIS.

Measurements of the ratio of the deuteron-to-proton electric form factors, $G(E)_d/G(E)_p$, were made from elastic electron–deuteron scattering to a precision of approximately 1% for the range of momentum transfers, 0.10 < or = q squared < or = 0.8 f^{-2}, and for electron scattering angles of 45 degrees and 120 degrees. It was found that within experimental errors the slope as obtained from the ratio $G(E)_n/G(E)_p$ agrees with the extrapolated thermal neutron–electron interaction slope when relativistic corrections and Feshbach–Lomon deuteron wave functions are applied to the electron–deuteron scattering results. The deuteron radius was found to be 1.95 ± 0.02 f, which agrees with the radius predicted by the Feshbach–Lomon calculation. (auth)

5248 (DNPL/R–7, pp 71–85) RECENT RESULTS IN OMEGA MESON PHOTOPRODUCTION. Thorndike, E. H. (Rochester Univ., N. Y.).

From Vector meson production and omega–rho interference.

A review was given of experimental work on ρ^0 and ω photoproduction performed by the Rochester–Cornell Group, and the ω results were compared with those of the Bonn–Pisa Group (ω photoproduction from complex nuclei), the SLAC Bubble Chamber Group (ω photoproduction from H), the DESY–MIT and Daresbury Groups (interference of photoproduced ρ^0 and ω in the leptonic decay mode), and the Orsay colliding beam experiment. The Rochester Group has studied photoproduction of 8 GeV ρ^0 mesons from Be, C, Al, Cu, Sn, W and Pb, and 7 GeV ω mesons from H, D, Be, C, Al, Cu, and Pb. Results on complex nuclei have been published (Phys. Rev. Lett. 24: 336, 1246(1970)), but the final analysis of the H and D data is not yet completed. Headings were as follows: experimental procedure; ρ^0 results and interpretation; ω analysis and results; ω interpretation comparisons with other experimental work. (13 references) (UK)

5249 (DNPL/R–7, pp 87–94) OMEGA PHOTOPRODUCTION ON COMPLEX NUCLEI. Schmitz, W. (Bonn Univ. (West Germany). Physikalisches Institut).

From Vector meson production and omega–rho interference.

Omega photoproduction on C, Al, Zn, Ag, Ta and Pb at a mean photon energy of 5.5 GeV and for production angles between 0° and 6° was studied at DESY by the Pisa–Bonn Group. A description was given of the method adopted and the results obtained. (2 references) (UK)

5250 (DNPL/R–7, pp 139–72) PRODUCTION OF VECTOR MESONS BY e^+e^- ANNIHILATION. Perez-Y-Jorba, J. (Paris Univ., Orsay (France). Laboratoire de l'Accelerateur Lineaire).

From Vector meson production and omega–rho interference.

The e^+e^- annihilation in storage rings allows a study of the production of vector mesons under very favourable conditions. The production reaction is interesting in that production of the vector meson does not involve any strong interaction and only hadrons are found in the final state. The parameters of vector meson mass and width and its leptonic decay width can be deduced unambiguously, and hadronic branching ratios can be determined. The leptonic width is important since it enters into various tests of the vector meson dominance hypothesis. The experimental work also provides measurements of the $\omega-\phi$ mixing angles, and the various models of symmetry breakings can be tested. A list was given of the reactions studied to date. Headings were as follows: description of experimental devices (Novosibirsk experiment on ρ^0; Orsay experiment on ρ^0, ω, $\phi \rightarrow K_S^0K_L^0$ and $\phi \rightarrow 3\pi$; Novosibirsk experiment on $\phi \rightarrow K^+K^-$; Orsay experiment on K^+K^-); data processing (luminosity measurement; beam polarisation; radiative corrections); results (general description; Novosibirsk ρ^0 experiment; Orsay ρ^0 experiment and $\omega-\rho$ interference; ω results; Novosibirsk ϕ results; Orsay ϕ results); tests of VMD-sum rules, coupling constants and mixing angles. (37 references) (UK)

5251 (UCRL–19897) PHOTOPRODUCTION OF π^+ MESONS FROM A POLARIZED PROTON TARGET AT 5 AND 16 GeV. Morehouse, Charles Conover (California Univ., Berkeley. Lawrence Radiation Lab.). Aug 1970. Contract W-7405-eng-48. 107p. Dep. NTIS.

Thesis.

The measurement of the asymmetry in the cross section for the reaction $\gamma p \rightarrow \pi^+ n$ between the two states of polarization of the initial proton normal to the plane of scattering is described. The laboratory photon energies, k, were 5 GeV and 16 GeV, and the regions of momentum transfer, t, covered were $0.14 \leq \sqrt{-t} \leq 1.01$ GeV/c and $0.14 \leq \sqrt{-t} \leq 0.78$ GeV/c respectively. A butanol polarized target was used with the SLAC 20 GeV/c magnetic spectrometer. The data show a sizeable asymmetry at both 5 GeV and 16 GeV. The 16 GeV data peak at $\sqrt{-t} \sim 0.30$ GeV/c with an asymmetry of about −0.70, and 5 GeV data peak at $\sqrt{-t} \sim 0.80$ GeV/c with an asymmetry of about −0.70. (The direction of the normal to the scattering plane is along (photon in) × (pion out).) (auth)

5252 (UCRL–20093) SEARCH FOR POLARIZATION IN ELASTIC e^-p SCATTERING AT 15 AND 18 GeV. Powell, Thomas Mabrey (California Univ., Berkeley. Lawrence Radiation Lab.). Aug 1970. Contract W-7405-eng-48. 102p. Dep. NTIS.

Thesis.

The asymmetry in the elastic scattering of electrons from a polarized proton target was measured. An interference between the imaginary part of the two-photon-exchange amplitude and the one-photon-exchange amplitude could produce a polarization effect. The results indicate no asymmetry within the experimental accuracy of 1 to 2% at four-momentum transfer squared values of 0.38, 0.59, and 0.98 $(GeV/c)^2$. (auth)

5253 PHOTOPRODUCTION OF $K^+\Lambda$ AND $K^+\Sigma^0$ FROM HYDROGEN BETWEEN 1.3 AND 1.45 GeV. Bleckmann, A.; Herda, S.; Opara, U.; (and others) (Univ., Bonn). Z. Phys.; 239: 1-15(1970).

The differential cross section was measured for the reaction $\gamma + p \rightarrow K^+ + \Lambda$ at k = 1.3 GeV and CM angles between 6 and 90° and for the reaction $\gamma + p \rightarrow K^+ + \Sigma^0$ at k = 1.45 GeV and CM angles between 10 and 85°. In addition 10 differential cross sections of the two reactions in the energy region between k = 1.327 and 1.416 GeV and angles between θ_{CM} = 11.2 and 62° were obtained. The results are compared with Regge-cut-model fits by Meyer zu Hörste and

XUM

Pfeil taking into account all available K^+ photoproduction data. (auth)

5254 MEASUREMENT OF THE K^- CASCADE TIME IN LIQUID HELIUM. Fetkovich, J. G. (Carnegie-Mellon Univ., Pittsburgh); McKenzie, J.; Riley, B. R.; (and others). Phys. Rev., D; 2: 1803-7(1 Nov 1970).

The average cascade time of K^- mesons was measured in a helium bubble chamber. In a sample of about 36,000 stopped K^-, 44 τ decays at rest were found, corresponding to a cascade time of $(3.2 \pm 0.5) \times 10^{-10}$ sec. This result agrees with a previous measurement. (auth)

5255 PHOTONUCLEON AND PHOTOPION PRODUCTION FROM 400 MeV ELECTRONS IN THICK COPPER TARGETS. Gabriel, T. A.; Alsmiller, R. G. Jr. (Oak Ridge National Lab., Tenn.). Nucl. Phys.; B14: 303-15(1969).

Electron-photon cascade calculations were carried out for 400 MeV electrons incident on a thick (infinite) copper target. The photon track length per unit energy from these calculations was used in conjunction with a recently developed model of photonucleon and photopion production from photo-nucleus collisions to calculate the energy and angular distributions of high-energy photonucleons and photopions produced by 400 MeV electrons in a thick copper target. (auth)

Weak

5256 (CONF-700314–, Paper 6) EXPERIMENTAL NEUTRINO PHYSICS. Derrick, M. (Argonne National Lab., Ill.). 48p.

From Conference on expectations for particle reactions at the new accelerators, March 30–April 1, 1970, Madison, Wisconsin.

The experimental neutrino physics is summarized. The topics covered include the intermediate boson, the four-fermion and semileptonic interactions, enhancements in μp mass system, total cross section for $\nu + N$ interactions, and inelastic scattering. (J.F.P.)

5257 (UCI–10-P-19-40) RESEARCH PROGRAM IN NEUTRINO PHYSICS, COSMIC RAYS, AND ELEMENTARY PARTICLES. Progress Report, 1 October 1969–30 September 1970. Reines, F. (California Univ., Irvine). Aug 1970. Contract AT(11-1)-Gen-10. 51p. Dep. NTIS.

Research is reported on neutrino interactions, cosmic-ray muons, and neutrinos, and a search for quarks in the cosmic radiation. A list of publications is included. (J.F.P.)

5258 ANGULAR CORRELATION BETWEEN THE NEUTRON SPIN AND THE ANTINEUTRINO MOMENTUM IN THE NEUTRON DECAY. Erozolimskii, B. G.; Bondarenko, L. N.; Mostovoi, Yu. A.; (and others) (Kurchatov Inst. of Atomic Energy, Moscow). Phys. Lett.; 33B: 351-2(9 Nov 1970).

The angular correlation between the neutron spin and antineutrino momentum in the beta decay of polarized neutrons has been measured accurately. The resulting coefficient B of the correlation is 0.995 ± 0.034. (auth)

5259 MEASUREMENT OF THE DECAY PROBABILITY $K_L \to 2\pi^0$. Barmin, V. V. (Inst. for Theoretical and Experimental Physics, Moscow); Barylov, V. G.; Borisov, V. S.; (and others). Phys. Lett.; 33B: 377-80(9 Nov 1970).

Using the 180-liter ITEP liquid xenon bubble chamber the branching ratio $\Gamma(K_L \to 2\pi^0)/\Gamma(K_L \to 3\pi^0)$ was measured to be $(3.7 \pm 0.8) \times 10^{-3}$. $|\eta_{00}|$ was found to be $(2.02 \pm 0.23) \times 10^{-3}$. (auth)

5260 NONLEPTONIC DECAY OF SIGMA HYPERONS. Bangerter, Roger Odell. Berkeley, Calif.; Univ. of California (1969). 100p. University Microfilms Order No. 70-13,012. Thesis.

In this dissertation measurements of the decay parameters α_-, α_0 and α_+ for $\Sigma^- \to n\pi^-$, $\Sigma^+ \to p\pi^0$, and $\Sigma^+ \to n\pi^+$ are presented. Also the decay parameters Φ_- and Φ_+ were measured for $\Sigma^- \to n\pi^-$ and $\Sigma^+ \to n\pi^+$. The usual decay parameters α, β, and γ are related to Φ by the equations $\beta = (1 - \alpha^2)^{1/2} \sin\Phi$ and $\gamma = (1 - \alpha^2)^{1/2} \cos\Phi$. Polarized $\Sigma^\pm$ are produced by the reaction $K^-p \to \Sigma^\pm\pi^\mp$ in the Lawrence Radiation Laboratory's 25-inch hydrogen bubble chamber. The average momentum of the incident K^- beam is 385 MeV/c. The measurements of α are performed by observing the up-down asymmetry in the Σ decay distributions and the measurements of Φ are made by observing the left-right asymmetry in the np interactions of those decay neutrons that subsequently scattered on the hydrogen in the bubble chamber. The results $\alpha_- = -0.071 \pm 0.012$, $\alpha_0 = -0.999 \pm 0.022$, $\alpha_+/\alpha_0 = -0.062 \pm 0.016$, $\Phi_- = 14 \pm 19°$, and $\Phi_+ = 143 \pm 29°$ are obtained. These results are in agreement with the $|\Delta I| = 1/2$ rule. (Diss. Abstr. Int., B)

5261 COMPARISON OF THE POSITIVE AND NEGATIVE TAU PRIME PARTIAL DECAY RATES FOR KAONS. Herzo, Dennis Paul. Urbana, Ill.; Univ. of Illinois (1969). 118p. University Microfilms Order No. 70-13,350. Thesis.

A scintillation counter-optical spark chamber arrangement was used with incident positive and negative 3.5 GeV/c beams at the Argonne National Laboratory Zero Gradient Synchrotron to study τ' ($K^\pm \to \pi^\pm\pi^0\pi^0$) decays. A difference between the τ'^- and τ'^+ partial decay rates $\Gamma(\tau'^-)/\Gamma(\tau'^+) \neq 1$ would indicate the presence of a CP-violating $\Delta I \geq 5/2$ weak amplitude for these decays. Furthermore, a difference between the sum of the τ^- and τ'^- decay rates and the sum of the τ^+ and τ'^+ decay rates $[\Gamma(\tau^-) + \Gamma(\tau'^-)]/[\Gamma(\tau^+) + \Gamma(\tau'^+)] \neq 1$ where $\tau^\pm$ represents $K^\pm \to \pi^\pm\pi^+\pi^-$ decays would indicate the presence of a CPT violation in these decays provided the electromagnetic interaction could be neglected. The τ' decay is characterized by a charged pion and four π^0 decay photons. Aluminum plate spark chambers exhibited the track of the charged pion and the development of the showers from the photons. Scintillation counter arrays restricted the triggering of the spark chambers to those times when it was likely that a three- or four-shower τ' decay that originated within a four foot long vacuum tank was present in the chambers. Two independent scans of the spark chamber film plus a collation of their results determined the number of τ'^+ and τ'^- decays characterized by three or four showers. The measurement of ~20% of the events and a comparison of the resulting vertex distributions with the predictions of a Monte Carlo program served as a check on the scanning results. The number of τ' decays of each sign was normalized to the associated number of incident K mesons determined by the use of momentum-analyzing magnets, Cherenkov counters, and scintillators. Extreme care was taken to minimize possible differences between the detection efficiencies for positive and negative τ' decays. After small corrections for unavoidable asymmetries in the efficiencies were calculated and applied to the scanning results, it was found that $\Gamma(K^- \to \pi^-\pi^0\pi^0)/\Gamma(K^+ \to \pi^+\pi^0\pi^0) = 1.009 \pm 0.018$. Thus no indication of a CP violation in τ' decays was found. After combining the result with known results for the ratio of the τ^- to τ^+ partial decay rates and the τ and τ' partial decay rates themselves, it is found that $\Gamma(\tau^-) + \Gamma(\tau'^-)/\Gamma(\tau^+) + \Gamma(\tau'^+) - 1 = 0.0024 + 0.0045$. Therefore, also no evidence is found for a CPT violation in these decays. (Diss. Abstr. Int., B)

5262 TEST OF THE $\Delta S = \Delta Q$ RULE IN LEPTONIC DECAYS OF NEUTRAL K MESONS. Webber, Bryan Ronald. Berkeley, Calif.; Univ. of California (1969). 84p. University Microfilms Order No. 70-13,193. Thesis.

In 1.3 million hydrogen bubble chamber pictures, taken during an exposure of the 25-inch Lawrence Radiation Laboratory chamber to a 400-MeV/c K^- beam, about 18,000 reactions of the type $K^-p \to \bar{K}^0n$ followed by a visible decay of the neutral K meson were found. After applying many selection criteria, 252 events were found in which the decay is leptonic or radiative: neutral $K \to \pi^\pm e^\mp \nu$, $\pi^\pm \mu^\mp \nu$, or $\pi^+\pi^-\gamma$. An electron was identified in 81 of these events, and a muon in 38 of them. The remaining 133 events are treated as completely ambiguous between the leptonic and radiative decay hypotheses. By studying the time distributions of the identified and the ambiguous events, the $\Delta S = \Delta Q$ selection rule is tested and also the Sachs model of CP violation, which predicts a large CP-violating $\Delta S = -\Delta Q$ term in the leptonic decay amplitudes. Parameters are defined, x for the electronic decay distributions and x' for the muonic, that are real if CP is conserved in the leptonic decays and are zero if $\Delta S = \Delta Q$. From the identified events, it is found that $\mathrm{Re}(x) = 0.30^{+0.9}_{-1.2}$, $\mathrm{Im}(x) = 0.07^{+1.1}_{-0.8}$ and $\mathrm{Re}(x') = 0.19^{+2.2}_{-1.3}$, $\mathrm{Im}(x') = -0.12^{+2.7}_{-1.7}$. Since these results are consistent with the hypothesis $x = x'$, this assumption is made in order to parametrize the distribution of ambiguous events in terms of x, and combine the results for all 252 events, to obtain $\mathrm{Re}(x) = 0.25^{+0.8}_{-0.9}$ $\mathrm{Im}(x) = 0.00 \pm 0.08$. The relative likelihood of the value $x = 0$ is $e^{-3.2}$, so this value lies about 2.5 standard deviations from the most likely value, and to this extent the experiment indicates a violation of the $\Delta S = \Delta Q$ rule. No significant imaginary part of x is found, which makes the Sachs mechanism of CP violation appear unlikely, although this model may not be ruled out with certainty, since it makes only an order-of-magnitude prediction of Im(x). In order to correct the distribution of the ambiguous events for the background of $\pi^+\pi^-\gamma$ decays, one has to assume that radiative decay occurs only through inner bremsstrahlung in the process $K_S \to \pi^+\pi^-$. A study of 10 kinematically unambiguous $\pi^+\pi^-\gamma$ decays gives experimental support to this assumption. As consistency checks on the data, the leptonic decay rate of the K_L, $\Gamma_L(l)$, and the absolute value of the K_S-K_L mass difference, $|\delta|$ are measured. Assuming the most likely value of x, we find $\Gamma_L(l) = (11.5 \pm 1.1) \times 10^6$ sec^{-1} and $|\delta| = (0.56^{+0.06}_{-0.09}) \times 10^{10}$ sec^{-1} are found in good agreement with the established values of these quantities. (Diss. Abstr. Int., B)

5263 14307 TAU PLUS DECAYS ANALYZED TO OBSERVE POSSIBLE $\Delta T = 1/2$ VIOLATION, AND CP NONCONSERVATION. Mainkar, Vasant V. Bethlehem, Pa.; Lehigh Univ. (1969). 80p. University Microfilms Order No. 70-10,610.

Thesis.

There were 23263 tau decays of the K meson observed in photographs made of the Columbia Brookhaven 30-inch propane bubble chamber placed at the A.G.S. The magnetic field at the center of the chamber was about 14 kilo-gauss. The study is part of the collaborative investigation by Stevens Institute of Technology and Lehigh University of K^+ meson decay. A typical photograph includes about 100 meson tracks, of which 20 on the average are K mesons which stop in the chamber; most of the pion tracks do not end in the chamber, and on the average there is about one recognizable tau decay per frame. Systematic frame by frame scanning was therefore plausible. Track coordinates in three different views of the chamber were digitized and the tracks reconstructed in space by a computer program. The momentum of each track was obtained from its range. Various procedures were then used to confirm that the event was a tau decay within a given fiducial volume. About one third of the measured events did not pass these requirements and a total of 14307 events were used for analysis. About 2000 of these were obtained from the Lehigh University reading facility and 12000 from the Stevens Institute facility. The energy distribution of the final state pions in the selected events is compared to the existing theoretical models. Pion energy spectra are given in terms of Dalitz variables and fits are made to a matrix element expressed as a power series of the Dalitz coordinates X and Y. Another fit is made to two resonance models which treat the resonant interaction between outgoing pions. Separate dependence of the decay matrix element on each X,Y was first examined and the dependence was found to be linear on Y and none on X. Then investigation was made into the combined dependence on X and Y and a significant nonlinear contribution was observed. The various models are based on the assumption of isotopic spin change of $1/2$ from the initial to the final state. From the present investigation, it appears that this rule is only approximate and higher corrections are necessary. Parameters of τ^+ spectra are compared to those of τ^- spectra to detect possible violation of CP invariance in weak interactions. No evidence was seen to infer a large CP violation. (Diss. Abstr. Int., B)

5264 STUDY OF K^+ DECAYS INTO THREE PIONS. Zinchenko, Anatol. New Brunswick, N. J.; Rutgers-The State Univ. (1969). 118p. University Microfilms Order No. 70-10,111.

Thesis.

Samples of 144 τ' events and 5428 τ events were obtained from an exposure of 150,000 pictures to a stopping K^+ beam in the 30" propane bubble chamber at Brookhaven National Laboratory. Since each τ' event included at least one π^0 reconstructed from electron-pairs in addition to a stopping π^+, a fitting procedure, completely determines the kinematics of the τ' decay; to one's knowledge, this is the first sample of completely determined τ' events. The τ events constitute a sizeable contribution to the world data. It is found that the $K_{3\pi}$ decay amplitude for either mode is linear in the energy of any one of the three pions and that the experimental linear slopes are consistent in magnitude with theoretical linear slopes predicted by soft-pion limits in current algebra; no distinction can be made between $\Delta I = 1/2$ and $\Delta I = 3/2$ predictions with our statistics. However, the combined world data does not agree well with the $\Delta I = 1/2$ predictions and indicates that the current algebra predictions must be carefully refined including $\Delta I = 3/2$ and possible final state interactions. Phenomenological I-spin analysis predicts the ratio of the τ' and τ slopes for a pure I = 1 three pion state. The slope values averaged over all major experiments indicate that the $K_{3\pi}$ final state is not pure I = 1. That the experimental τ'^+ and τ'^0 slopes are equal is consistent with $\Delta I = 1/2$ and $3/2$. Since the τ^+ and τ^- slopes are equal within one standard deviation, no CP violation is apparent at this level of statistics. (Diss. Abstr. Int., B)

Strong (Baryon-Induced)

Refer also to abstracts 4373 and 5444.

5265 (CONF-700314-, Paper 4) IHEP (SERPUKHOV). CERN EXPERIMENTS. Allaby, J. V. (European Organization for Nuclear Research, Geneva (Switzerland)). 43p.

From Conference on expectations for particle reactions at the new accelerators, March 30-April 1, 1970, Madison, Wisconsin.

Experiments described using the Serpukhov synchotron include a survey of the fluxes of particles produced by the interactions of protons with suitable targets, the study of techniques for identifying the π^-, K^-, and $\bar{p}$ particles, and also some measurements of total cross sections at momenta from 20 to 65 GeV/c. The total cross sections for hadron-hadron interactions and the absorption cross sections for π^-, K^-, and $\bar{p}$ on various nuclei are tabulated, and curves are drawn for these cross sections as functions of the momenta. (J.F.P.)

5266 (IFVE-SEF-69-81) RELATIVE VALUE OF THE CROSS SECTIONS OF NN → W + (HADRONS) AND NN → (HADRONS) $\gamma,\gamma \rightarrow \mu + \mu$ REACTIONS. Folomeshkin, V. N. (Gosudarstvennyi Komitet po Ispol'zovaniyu Atomnoi Energii SSSR, Serpukhov. Institut Fiziki Vysokikh Energii). 1969. 13p. (In Russian). Dep. NTIS (U. S. Sales Only).

The muon background of electromagnetic origin in the experiments on the search for W-boson in NN-collisions is estimated. (auth)

5267 (IFVE-SEF/STF-69-46) POSSIBILITIES OF CARRYING OUT AN EXPERIMENT ON THE SEARCH FOR W-BOSON IN NN-COLLISIONS AT THE IHEP ACCELERATOR. Makeev, V. V.; Folomeshkin, V. N. (Gosudarstvennyi Komitet po Ispol'zovaniyu Atomnoi Energii SSSR, Serpukhov. Institut Fiziki Vysokikh Energii). 1969. 30p. (In Russian). Dep. NTIS (U. S. Sales Only).

The possibilities of carrying out an experiment on the search for W-boson in NN-collision at the IHEP accelerator are presented. The problems of pion-shielding, minimization of the muon background from the pions, the problem of the muon background from the γ-quantums etc., are investigated. (auth)

5268 (JINR-P1-5293) POLARIZATION OF SECONDARY PROTONS IN $pp \rightarrow \pi^+pn$ AND $pp \rightarrow \pi^0pp$ REACTIONS AT 669 MeV. Azhgirei, L. S.; Vzorov, I. K.; Zhmyrov, V. N.; Kuznetsov, A. S.; Meshcheryakov, M. G.; Stoletov, G. D.; Filozov, A. F.; Chizhikov, V. I. (Joint Inst. for Nuclear Research, Dubna (USSR). Lab. of Computing Techniques and Automation). 1970. 18p. (In Russian). Dep. NTIS (U. S. Sales Only).

At 8.3, 14.5 and 18.0° angles the polarization was measured for secondary protons emitted with energy of about 370 MeV in the $pp \rightarrow \pi^+pn$ and $pp \rightarrow \pi^0pp$ reactions at incident proton energy of 669 MeV. In the direction of the normal to the plane, containing the momentum vectors of incident and detected protons, the polarization values are found to be: P (8.3°) = 0.20 ± 0.05; P (14.5°) = 0.21 ± 0.05 and P (18.0°) = 0.15 ± 0.05. The obtained results can be described by the one-pion exchange model, in which the pion form factor of nucleons and the peculiarity in the behavior of the S_{11}-state amplitude of πN-system outside the mass surface are taken into account. (auth)

5269 EXPERIMENTAL STUDY OF THE MUONIC DECAYS OF SIGMA HYPERONS. Baggett, Neil Vance. College Park, Md.; Univ. of Maryland (1969). 121p. University Microfilms Order No. 70-13,706.

Thesis.

This experiment is based on observations of 540,000 3-view photographs from the Brookhaven AGS 30-inch hydrogen bubble chamber, exposed to a beam of stopping K^- mesons. The film, containing a total of 2.1×10^6 Σ^- and 10^6 Σ^+ from stopping K^-, was scanned for the decays $\Sigma^\pm \rightarrow n\mu^\pm\nu$, in which the μ stops and decays to an electron or positron. Based on 56 $\Sigma^- \rightarrow n\mu^-\nu$ events, the branching ratio $\Gamma(\Sigma^- \rightarrow n\mu^-\nu)/\Gamma(\Sigma^- \rightarrow \text{all}) = (0.43 \pm 0.09) \times 10^{-3}$ is found. This value is in good agreement with the V-A theory of weak interactions and the hypothesis of μ-e universality. No examples of $\Sigma^+ \rightarrow n\mu^+\nu$ were found, giving the upper limit $\Gamma(\Sigma^+ \rightarrow n\mu^+\nu)/\Gamma(\Sigma^- \rightarrow n\mu^-\nu) < 0.16$ with 90% confidence for these $\Delta S = \Delta Q$ transitions. (Diss. Abstr. Int., B)

5270 HYPERON-ANTIHYPERON PRODUCTION IN $\bar{p}p$ INTERACTIONS AT 2.4 AND 2.9 GeV/c. Schaik, Terry LeRoy. Ames, Iowa; Iowa State Univ. (1969). 67p. University Microfilms Order No. 70-13,628.

Thesis.

The results of a study of hyperon-antihyperon production in 2.4- and 2.9-GeV/c antiproton-proton interactions are presented. The experiment had a sensitivity of 2.2 events/μ barn. Three examples of $\Xi^-\bar{\Xi}^-$ production at 2.9 GeV/c were observed. The $\Lambda\bar{\Lambda}$ and $\Lambda\bar{\Sigma}^0$ + cc final states were observed to be highly peripheral, indicating a t-channel exchange dominance. However, a prediction for the differential cross section from a one meson exchange model with absorption, done for a slightly higher momenta (3.0 GeV/c), is not as sharply peaked as the data. The 3-body final states are produced peripherally only when the reaction is consistent with t-channel exchange of a known particle, and then only weakly. There is evidence for some $\Sigma(1385)$, $\Lambda(1404)$ and $\Lambda(1520)$ production in these 3-body final states, however, the statistics are very limited. (Diss. Abstr. Int., B)

5271 ANTIPROTON-NEUTRON ANNIHILATION AT REST INTO FINAL STATES OF 3 AND 4 PIONS. Gray, Lee John.

XUM

Syracuse, N. Y.; Syracuse Univ. (1969). 109p. University Microfilms Order No. 70-10,346.

Thesis.

The study of antiproton annihilations at rest with bound neutrons in deuterium leading to three visible pions is discussed. The antiprotons were produced by the 30-GeV proton alternating gradient synchrocyclotron (AGS) of the Brookhaven National Laboratory (BNL). The antiprotons then were separated from undesired particles and brought to rest in the BNL-Columbia 30-inch hydrogen bubble chamber filled with deuterium. The analysis of the 3-pronged events and 4-pronged events with a proton yielded examples of the reactions $\bar{p}d \rightarrow 2\pi^-\pi^+p$ and $\bar{p}d \rightarrow 2\pi^-\pi^+\pi^0 p$. The branching ratios for these final states with respect to all antiproton-neutron annihilations at rest have been found to be $(2.3 \pm .3)X10^{-2}$ and $(13.7 \pm 2.0)X10^{-2}$ respectively. The $2\pi^-\pi^+$ Dalitz plot is highly anisotropic and no satisfactory solution has been found in terms of the known $\pi\pi$ interactions. Introduction of additional new but reasonable $\pi\pi$ interactions — T = 0 $\pi\pi$ resonance and a T = 2 scattering length — improved the fit to the data but it still is far from being satisfactory. The $2\pi^-\pi^+\pi^0 p$ final state proceeds essentially through intermediate states of $2\pi p$. The branching ratios with respect to the $2\pi^-\pi^+\pi^0 p$ final state were determined to be $0.16 \pm .01$, $0.45 \pm .01$, $.39 \pm .01$ for $\rho^+\pi^-\pi^-$, $\rho^0\pi^-\pi^0$, and $\rho^-\pi^-\pi^+$ respectively and they strongly disagree with the predictions of $\widetilde{SU}(12)$. In addition, the reaction $\bar{p}d \rightarrow \pi^-\omega^0 p$ was identified with a branching ratio with respect to the $2\pi^-\pi^+\pi^0 p$ events of $.02 \pm .002$. The quantum numbers of the ω^0 have been confirmed not only from the study of its decay but also from the study of its production. Strong evidence is presented for an as yet unreported J = 0 $\pi\pi$ resonance with a mass of 1115 MeV. Since all the analysis will assume S-capture of antiprotons and that the nonannihilating nucleon behaves as a spectator, these two assumptions were tested and further evidence for their validity and limits are presented. Of particular interest is that 80% of the annihilations occur with a spectator nucleon while the remaining 20% involve the entire deuteron. This observation is consistent with a primary annihilation radius of 1.4F. (Diss. Abstr. Int., B)

5272 HIGH-ENERGY INTERACTIONS AT ACCELERATOR ENERGIES. Czyzewski, O. (Inst. of Nuclear Research, Krakow). pp 177-230 of Proceedings of the 11th International Conference on Cosmic Rays, Budapest, 25 August–4 September, 1969. /Bozoki, G. (ed.). Budapest; Central Research Inst. for Physics (1969).

See CONF-690814.

A review of particle interactions between 5 and 70 GeV/c is given. Elastic scattering, two-body reactions, and many-body processes are covered. (J.F.P.)

5273 HIGH ENERGY INTERACTIONS BELOW 1 TeV. Friedlaender, E. M. (Inst. of Atomic Physics, Bucharest). pp 445-60 of Proceedings of the 11th International Conference on Cosmic Rays, Budapest, 25 August–4 September, 1969. /Bozoki, G. (ed.). Budapest; Central Research Inst. for Physics (1969).

See CONF-690814.

A review of multiparticle production at 50 to 1000 GeV is given. This review covers cross sections, multiplicity, and angular and momentum distributions. Proton and pion reactions are considered. (J.F.P.)

5274 HIGH ENERGY INTERACTIONS ABOVE 1 TeV. Koshiba, M. (Tokyo Univ.). pp 461-95 of Proceedings of the 11th International Conference on Cosmic Rays, Budapest, 25 August–4 September, 1969. /Bozoki, G. (ed.). Budapest; Central Research Inst. for Physics (1969).

See CONF-690814.

A review is given of interactions above 1 TeV. Production of the aleph, pionization, cross sections and energy spectra, quarks and the monopole, and the future outlook are considered. (J.F.P.)

5275 HIGH ENERGY NUCLEAR ACTIVE PARTICLES IN EXTENSIVE AIR SHOWERS. Murty, G. T. Bombay; Bombay Univ. (1967).

Thesis.

A calorimetric measurement of the nuclear particles in extensive air showers was made and compared with theoretical Monte-Carlo estimates based on different models of high energy nuclear interactions. It is not possible to distinguish between different models. The broadening of their lateral distribution with shower size can be understood if the transverse momentum of the created particles and the inelasticity of the nuclear collisions increases above 10^{14} eV. (Indian Sci. Abstr.)

5276 STUDY OF PARTICLE PRODUCTION AT HIGH ENERGIES. Rangarajan, T. N. Bombay; Bombay Univ. (1967).

Thesis.

An emulsion and hydrogen bubble chamber study of several features of particle production in 24-GeV proton-nucleon collisions is described. The studied aspects include the energy-spectra and transverse-momentum distributions of pions and protons and the production of N*3/2 (1236) and other baryon resonances and their decay modes. The experimental data on charge ratio and transverse momenta of secondaries are found to be consistent with an isobar model in which proton-proton collisions lead to the creation of two bodies only. (Indian Sci. Abstr.)

5277 STUDY OF THE NON-MESONIC DECAY OF HYPER-NUCLEI PRODUCED BY K-MESONS OF 3.0 GeV/c MOMENTUM. Kasim, M. M.; Husain, A.; Basak, A. K.; Islam, A. K. M. A.; Mondal, A. S.; Ali, P. Nucleus (Karachi); 6: 138-45(Jul-Sep 1969).

From an examination of 2,670 beam stars collected by area scanning in a stack of Ilford K-5 emulsion exposed at CERN to K-mesons of 3.0 GeV/c, a total of 81 hyperfragments were found of which 63 decayed nonmesonically. The energy distribution of charged particles from the hyperfragment disintegrations shows a peak value at low energy and a group of fast protons are seen with a relatively wide energy spread. The relative strength of stimulation, R and the stimulation ratio, r for the heavy hyperfragments are found to be 2.8 and 0.82 respectively and the corresponding values for the light hyperfragments are 5.7 and 0.85 respectively. From this work it is concluded that the neutron stimulation process is the dominant process in the nonmesonic decay of heavy hyperfragments. (auth)

5278 REGGEIZED PION EXCHANGE AND THE 1425 MeV $\Delta^{++}(1238)\pi^-$ ENHANCEMENT IN $pp \rightarrow pp\,\pi^+\pi$ AT 7.9 GeV/c. Grether, D. F.; Sard, R. D. (Univ. of Illinois, Urbana). Nucl. Phys.; B14: 381-8(1969).

A Reggeized pion exchange model is shown to give a generally adequate description of the decay mode and decay angular distributions of any substantial resonance contribution to the 1425 MeV enhancement. They do not appear to be consistent with those expected of the N*(1400), the P_{11} resonance of π^-p phase-shift analysis. (auth)

Strong (Meson-Induced)

Refer also to abstracts 5369, 5371, and 5384.

5279 (CEA-R-4037) MEASUREMENT AND ANALYSIS OF THE DIFFERENTIAL CROSS SECTIONS FOR THE REACTION $\pi^-p \rightarrow \eta n$ AT SIX ENERGIES BETWEEN 2.9 AND 18.2 GeV/c. Borgeaud, Pierre A. (Commissariat a l'Energie Atomique, Saclay (France). Centre d'Etudes Nucleaires). Oct 1970. 119p. (In French). Dep. NTIS (U. S. Sales Only).

Thesis. Submitted to Univ. of Paris, Orsay, France.

A heavy plate spark chamber was used to detect the two gamma radiations of the neutral decay mode of the η meson produced in the reaction $\pi^-p \rightarrow \eta n$. The events were shown to be free of any contamination due to inelastic reactions. The differential cross sections showed a prominent forward peak. The results obtained were discussed in the framework of a single pole Regge model. Information on the A_2 trajectory was obtained and compared to that available by other methods, namely sum rules. (France)

5280 (CONF-700314–, Paper 10) MULTIPARTICLE PRODUCTION: EXPERIMENTAL. Erwin, A. R. (Wisconsin Univ., Madison. Dept. of Physics). 45p.

From Conference on expectations for particle reactions at the new accelerators, March 30–April 1, 1970, Madison, Wisconsin.

Several aspects of a 25-GeV/c π^- + p experiment are presented. These aspects are thought to relate to expectations for multiparticle production experiments at the higher energy accelerators. It is found that many things can be studied in multiparticle production, which might be accounted for more simply at higher energies such as 500 GeV/c. (J.F.P.)

5281 (CONF-700314–, Paper 15) SOME REACTIONS AT HIGH MOMENTUM TRANSFER AT NAL. Orear, Jay (Cornell Univ., Ithaca, N. Y. Lab. of Nuclear Studies). 23p.

From Conference on expectations for particle reactions at the new accelerators, March 30–April 1, 1970, Madison, Wisconsin.

The following reactions are considered: large-angle $\pi - p$, backward $\pi - p$, large-angle $p - p$, and secondary production at high momentum. An attempt is made to estimate what these cross sections will be at NAL energies and what will be the lower limits of detection capability at NAL. Some speculations are given concerning quark production and the physics which might be done with quark beams. (auth)

5282 (COO-1195-200) SPIN PARITY STUDIES OF THE ETA PI DECAY OF THE A2 MESON AND INVESTIGATION OF THE A2 PRODUCTION MECHANISM IN THE REACTION PI-MINUS PROTON GOES TO A2-MINUS PROTON. Lacy, Jeffrey

XUM

Linn (Illinois Univ., Urbana). Feb 1971. Contract AT(11-1)-1195. 109p. Dep. NTIS.

Thesis.

The results of a spin parity analysis of the $\eta\pi^-$ decay mode of the A_2^- meson produced in the reaction $\pi^-p \rightarrow A_2^-p$ are presented. Data for the analysis are drawn from bubble chamber experiments between 3.9 and 16 GeV/c. The analysis favors $J^P = 2^+$ for both the upper and lower regions of the A_2. Possible evidence for a weakly produced $J^P = 1^-$ daughter state is also presented. The evidence comes largely from an interference effect observed in the lower A_2 region. Using the $A_2^- \rightarrow \eta\pi^-$ data along with data on the decay channel $A_2^- \rightarrow \rho^0\pi^-$ at 5.0, 7.5, and 11.2 GeV/c, the production mechanism of the A_2^- in the reaction $\pi^-p \rightarrow A_2^-p$ is investigated. Assuming that this reaction is dominated by a t channel exchange mechanism the isospin and J parity of the exchange are investigated. The s and t cross section dependence of the data are compared with a simple Regge model. (auth)

5283 (COO-1428-238) $\pi^+p \rightarrow f^0\Delta^{++}$ AT 13.1 GeV/c. Gaidos, J. A.; Ezell, C. R.; Lamsa, J. W.; Willmann, R. B. (Purdue Univ., Lafayette, Ind. Dept. of Physics). [1970]. Contract AT (11-1)-1428. 12p. Dep. NTIS.

Data for the reaction $\pi^+p \rightarrow f^0\Delta^{2+}$ at 13.1 GeV/c are presented and discussed within a Reggeized pion exchange model with absorption. (auth)

5284 (JINR-E1-5085) STUDY OF THE DI-PION IN THE MASS VALUES REGION $M(\pi^0\pi^0) \leq 1.3$ GeV. Strugalski, Z. S.; Chuvilo, I. V.; Fenyves, E.; (and others). (Joint Inst. for Nuclear Research, Dubna (USSR)). 1970. 16p. Dep. NTIS (U. S. Sales Only).

The results of investigation of the $\pi^0 - \pi^0$ effective mass spectrum in the mass value region $M(\pi^0\pi^0) \leq 1.3$ GeV are presented. A peak is observed at $M(\pi^0\pi^0) = 730$ MeV. (auth)

5285 (RLO-2041-40) SCATTERING OF REAL PIONS ON EACH OTHER. Csonka, Paul L. (Oregon Univ., Eugene). [1970]. 23p. Dep. NTIS.

The feasibility of scattering real pions on each other is discussed. Estimates (based on machine parameters now realized or planned) are given for scattering in minirings, when the pion energies are low; for self-clashing and head-on colliding of pion beams when their laboratory energy is high. (auth)

5286 PUZZLE OF THE A2 MESON. Schuebelin, Peter (Brookhaven National Lab., Upton, N. Y.). Phys. Today; 23: No. 11, 32-8(Nov 1970).

Experimental research on the A2 meson is reviewed, and the properties of the A2 are described. The two-peaked structure of the A2 is found not to be due to two independent resonances. The double-peaked structure implies that the A2 meson is two particles with nearly the same mass or a single object of an entirely new type such as a double resonance or a dipole. There is as yet no satisfactory explanation for the double peaked structure. (J.F.P.)

5287 SEARCH FOR EXOTIC RESONANCES IN K^-d INTERACTIONS AT 3 GeV/c. Giacomelli, G. (Istituto Nazionale di Fisica Nucleare, Bologna); Lugaresi-Serra, P.; Minguzzi-Ranzi, A.; (and others). Phys. Lett.; 33B: 373-6(9 Nov 1970).

A systematic search for exotic states produced in K^-d interactions at 3 GeV/c is reported. From the analysis of the mass spectra of strange mesons, non-strange mesons, hyperons with $S = -1$ and $S = -2$, upper limits for the production cross sections of exotic resonances may be placed at one or two orders of magnitude smaller than for the production of normal resonances of same strangeness and baryon number. (auth)

5288 MEASUREMENTS OF PIONIC X-RAYS FROM HYDROGEN. Bailey, J. (CERN, Geneva); Placci, A.; Polacco, E.; (and others). Phys. Lett.; 33B: 369-72(9 Nov 1970).

Pionic X-rays were observed when negative pions are stopped in a hydrogen gas target. The intensity of the K lines was found to be about 0.12 X-ray/pion stopped; moreover $K_\alpha/K = 0.53 \pm 0.04$. (auth)

5289 STRANGE PARTICLE PRODUCTION IN π^+d INTERACTIONS FROM 1.1 TO 2.4 GeV/c. Davies, Donald Wayne. Berkeley, Calif.; Univ. of California (1969). 75p. University Microfilms Order No. 70-13,034.

Thesis.

Properties of strange-particle final states arising from reactions of 1.1 to 2.4 GeV/c π^+ mesons on deuterium were studied. Total cross sections on deuterium are presented and three reactions are analyzed in terms of the impulse model. $Y^*(1385)$ production dominates the $n\Lambda K^+\pi^+$ final state, and the reaction is described near threshold adequately by a K^* exchange model. The $n\Sigma^+K^0\pi^+$ final state is found to be primarily $n\Sigma^+K^{*+}$. The $\phi(1020)$ and $\Lambda(1520)$ are seen in the ppK^+K^- final state. (Diss. Abstr. Int., B)

5290 DIFFERENTIAL CROSS SECTION MEASUREMENTS OF THE REACTION $\pi^+ + p \rightarrow K^+ + Y_1^{*+}(1385)$ AT 4 AND 5.05 GeV/c. Ying, Shuh-pan. Ann Arbor, Mich.; Univ. of Michigan (1969). 54p. University Microfilms Order No. 70-14,690.

Thesis.

Approximately 1900 events were obtained in a counter and spark chamber experiment for the production of the baryon resonance $Y_1^{*+}(1385)$ in positive pion and proton collisions. Forward peaks of the differential cross section curves were found with slopes of 2.3 ± 0.3 and 2.6 ± 0.4 $(GeV/c)^{-2}$ for 4 and 5.05 GeV/c respectively. These data together with that on other decuplet production reactions allow one to test SU(3) symmetry. The results indicate a large amount of SU(3) breaking which can be corrected by assuming a mass difference between the strange and nonstrange exchange particles. (Diss. Abstr. Int., B)

5291 PROPERTIES OF THE η' MESON. Rittenberg, Alan. Berkeley, Calif.; Univ. of California (1969). 131p. University Microfilms Order No. 70-13,150.

Thesis.

The $\eta'(958)$ meson was studied in the reaction $K^-p \rightarrow \Lambda\eta'$, with K^- beam momenta ranging from 1.70 to 2.65 GeV/c. The Dalitz plots of η' decay into $\pi^+\pi^-\eta$ and $\pi^+\pi^-\gamma$ were examined, and from them it was determined that the most likely quantum numbers of the η' are $I^GJ^P = 0^+0^-$, although $J^P = 2^-$ cannot be completely ruled out. We have also shown that the decay into $\pi^+\pi^-\gamma$ is mediated by the decay $\eta' \rightarrow \rho^0\gamma$. An examination of the production process has yielded further evidence for the $J^P = 0^-$ assignment and suggested that the process takes place via $K^*(891)$ exchange in the t channel. Branching fractions and cross sections were determined, and finally a search for a negatively charged η' in the deuterium reaction $K^-d \rightarrow p\Lambda\eta'^-$ has confirmed the I = 0 assignment for the η'. (Diss. Abstr. Int., B)

5292 ANALYSIS OF THE REACTION $\pi^+p \rightarrow \pi^+p\pi^+\pi^-$ AT 11.0 GeV/c. Harms, Benjamin Carleton. Tallahassee; Florida State Univ. (1969). 206p. University Microfilms Order No. 70-11,122.

Thesis.

The reaction $\pi^+p \rightarrow \pi^+p\pi^+\pi^-$ is found to be dominated by ρ^0 and Δ^{++} (1236). There appears to be very little coproduction of these resonances. The events are analyzed by making a cut on the Peyrou distribution of the proton's laboratory momentum. The ρ^0 is found to be created in very peripheral (in a geometric sense) collisions, while the Δ^{++} (1236) is found in the less peripheral events. The A-mesons are also found in the peripheral region and have strong ρ^0, π^+ decay modes. The 3-π spectrum can be divided into two sets of four resonances by making certain cuts on the Δ^2 to the proton. These Δ^2 cuts apparently split the A_2 meson into the A_2^L and A_2^H. The $\Delta^2_{p\rightarrow p}$ distribution appears to have a periodic structure. The structure occurs for those events in the peripheral region and is completely absent in the events outside this region. The structure is well fit by an inelastic strong absorption model, but the model requires the proton to have a radius of 7 fm. Some evidence is presented to corroborate this value. A technique for removing unwanted background is discussed. The technique is used to select events which proceed via one-pion-exchange and plots obtained from these events are compared to the predictions of the one-pion-exchange model. (Diss. Abstr. Int., B)

5293 ESTIMATE OF CROSS SECTIONS OF REACTIONS $\pi^- + {}^{12}C \rightarrow {}^{12}B + m\pi^0(m = 1,2...)$ AND $\pi^- + {}^{12}C \rightarrow {}^{12}N + \pi^- + \pi^-$ AT 4 GeV/c. Abdullaeva, K. N.; Azimov, S. A.; Grishin, V. G.; (and others) (Inst. of Nuclear Physics, Tashkent). Yadern. Fiz.; 12: 535-7(Sep 1970). (In Russian).

Upper limits for cross sections of the reactions were estimated using the 24-liter propane bubble chamber of the High Energy Laboratory of the Joint Institute for Nuclear Research. The values obtained are 120 and 4 μbarn, respectively. (auth)

5294 SOME CONSEQUENCES FROM THE CONSTANT BEHAVIOR OF THE TOTAL CROSS SECTIONS AT ENERGIES MORE THAN 30 GeV. Aznauryan, I. G.; Solov'ev, L. D. (Inst. of High-Energy Physics, Moscow). Yadern. Fiz.; 12: 638-48 (Sep 1970). (In Russian).

The data on the total cross sections at energies up to 65 GeV obtained on the Serpukhov accelerator show that the differences of the total cross sections $\sigma(\pi^-) - \sigma(\pi^+)$ and $\sigma(K^-) - \sigma(K^+)$ may remain constant at energies more than 25 to 30 GeV. Some consequences from such behavior are considered. The differential cross section of the pion charge exchange and kaon-hydrogen regeneration amplitude at zero angle are calculated. (auth)

XUM

5295 TOTAL AND ABSORPTION CROSS SECTIONS OF π^-, K^-, AND $\bar{p}$ IN THE MOMENTUM RANGE 20 TO 65 GeV/c. Allabi, Ya. V.; Bushnin, Yu. B.; Gorin, Yu. P.; (and others) (Inst. of High Energy Physics, Moscow). Yadern. Fiz.; 12: 538-56(Sep. 1970). (In Russian).

Total cross section data are presented for negative pions, kaons, and antiprotons on protons and deuterons in the momentum range 20 GeV/c to 65 GeV/c in 5 GeV/c steps. Absorption cross sections are given for the same particles on nine nuclei (He, Li, Be, C, Al, Cu, Sn, Pb, and U) in the same momentum range. (auth)

5296 K^+p ELASTIC SCATTERING AT 4.6 GeV/c. MacNaughton, J. N.; Feinstein, L.; Marcelja, F.; Trilling, G. H. (Univ. of California, Berkeley). Nucl. Phys.; B14: 237-45 (1969).

The elastic scattering of K^+ mesons by protons at 4.6 GeV/c was studied in a hydrogen bubble chamber experiment. The elastic cross section was measured and found to be 3.85 ± 0.25 mb. The forward diffraction peak can be adequately fitted by a differential cross section of the form $d\sigma/dt = (d\sigma/dt)_0 e^{-B|t|}$, where $(d\sigma/dt)_0 = 16.0 \pm 1.3$ mb/(GeV/c)^2 and $B = 4.2 \pm 0.2$ (GeV/c)$^{-2}$. From this fit the magnitude of the ratio of real forward amplitude to imaginary forward amplitude is estimated to be $0.25^{+0.14}_{-0.25}$. Comparison with results of other experiments indicates that B has a momentum dependence extremely similar to that observed in proton–proton elastic scattering. (auth)

5297 PRODUCTION OF PROTON–ANTIPROTON AND KAON–ANTIKAON PAIRS IN FOUR-BODY REACTIONS OF 8 GeV/c π^+ AND 10 GeV/c K^- ON PROTONS. Aderholz, M. (Technische Hochschule, Aachen); Deutschmann, M.; Rumpf, K.; (and others). Nucl. Phys.; B14: 255-68(1969).

The production of $(p\bar{p})$, (K^+K^-) and $(\pi^+\pi^-)$ pairs in four-body reactions of 8 GeV/c π^+ and 10 GeV/c K^- on protons was studied. The cross sections for these processes are smaller in K^-p interactions than in π^+p interactions. For both π^+ and K^- induced reactions, the production of a K^+K^- pair is about 30 times less probable than that of a $\pi^+\pi^-$ pair. In K^-p interactions frequent production of ϕ but not of f^0 is observed, whereas in π^+p interactions f^0 production is observed but not ϕ production. The production of the N^* (3755) isobar decaying into $(p\bar{p})$, reported by other authors, is not confirmed. The results are discussed in terms of a simple additive quark model. (auth)

5298 SOME REMARKS ON THE Σ^- HYPERON CONVERSION RATE. Csejthey-Barth, M.; Schorochoff, G.; Van Binst, P. (Univ. Libre, Brussels). Nucl. Phys.; B14: 316-18(1969).

The reabsorption probability for Σ^- hyperons produced by K^- meson interactions at rest in freon CF_3Br was found to be 0.50 ± 0.05, in agreement with previous results obtained in various light or heavy elements. The implications of this result on some aspects of the K^- meson capture process are discussed. (auth)

5299 STUDY OF THE TRAPPING OF THE Λ^0 HYPERONS PRODUCED BY K^- MESON ABSORPTION IN A HEAVY LIQUID BUBBLE CHAMBER. Csejthey-Barth, M.; Schorochoff, G.; Van Binst, P. (Univ. Libre, Brussels). Nucl. Phys.; B14: 330-6 (1969).

The study of 4527 K^- meson interaction at rest in a bubble chamber filled with freon CF_3Br has led to a determination of the Λ-hyperon trapping probability: (19.6 ± 1.8) %. Combining this value with the results of similar studies in nuclear emulsion, the trapping probabilities in light and heavy nuclei are found to be (11 ± 5) % and (52 ± 15) %, respectively. (auth)

5300 INTERACTION OF K_2^0 MESONS IN COPPER AND WITH C, Cl, AND F NUCLEI. Aleksanyan, A. S. (Physical Inst., Erevan). Izv. Akad. Nauk Arm. SSR, Ser. Fiz.; 5: 83-7(1970). (In Russian).

The results of measurements of the total cross section of K_2^0-meson interaction with an average energy of 120 MeV in copper as well as of $\Lambda^0(\Sigma^0)$-hyperon production in C, Cl, F-nuclei are presented. The total cross section of K_2^0-meson interaction in copper, σ (K_2^0 Cu) = (1.28 ± 0.12) barn, and the hyperon production cross section, σ (Λ^0,Σ^0) = (29 ± 7) mbarn. (auth)

Particle Interactions and Properties (Theoretical)

5301 (DNPL/R-7, pp 29-70) PHOTOPRODUCTION OF VECTOR MESONS. Marshall, Robin (Massachusetts Inst. of Tech., Cambridge. Lab. for Nuclear Science. Deutsches Elektronen-Synchrotron, Hamburg (West Germany)).

From Vector meson production and omega–rho interference.

A review was presented, with emphasis on what is new or relatively new in this field, and what has changed. It was stated that there is still some uncertainty concerning the applicability of the vector dominance model, although this uncertainty appears to be diminishing. Headings were as follows: photoproduction of ρ on protons; photoproduction of ρ on complex nuclei; the real part of the ρ scattering amplitude $\beta\rho$; nuclear radii; photoproduction of ω; photoproduction of ϕ; total hadronic cross sections; are there any further vector mesons? (71 references) (UK)

General

Refer also to abstracts 5244 and 5417.

5302 (CONF-700314–, Paper 11) MULTIPERIPHERAL DYNAMICS. Frazer, W. R. (California Univ., La Jolla, San Diego. Dept. of Physics). 12p.

From Conference on expectations for particle reactions at the new accelerators, March 30–April 1, 1970, Madison, Wisconsin.

A dynamical multiperipheral model is described which follows almost inevitably from well-established singly peripheral model. This model makes some very direct predictions independent of model details, provides a credible dynamical model for j-plane singularities, and has possibilities for bootstrap theories. (J.F.P.)

5303 (CONF-700314–, Paper 16) THEOREMS ON HIGH ENERGY COLLISIONS. Eden, R. J. (Cambridge Univ. (England). Cavendish Lab.). 41p.

From Conference on expectations for particle reactions at the new accelerators, March 30–April 1, 1970, Madison, Wisconsin.

The review of high-energy collision theorems covers analyticity, unitarity, and polynomial bounds, bounds and inequalities based on axiomatic quantum field theory, bounds requiring special assumptions, relations between cross sections requiring special assumptions, experimental results and high-energy theorems, models and examples, and a summary of axiomatic bounds. (J.F.P.)

5304 (CONF-700314–, Paper 18) IMPORTANT PROBLEMS AND QUESTIONS FOR THE NEW ACCELERATORS. Drell, S. D. (Stanford Linear Accelerator Center, Calif.). 34p.

From Conference on expectations for particle reactions at the new accelerators, March 30–April 1, 1970, Madison, Wisconsin.

The topics discussed include the asymptotic limit, inelastic processes, deep inelastic electron scattering, hadronic processes, the parton model, massive lepton systems, and elastic scattering. (J.F.P.)

5305 (JINR–P2-4931) COVARIANT DENSITY MATRIX FOR ARBITRARY SPIN PARTICLES. Kopeliovich, B. Z. (Joint Inst. for Nuclear Research, Dubna (USSR)). 1970. 23p. (In Russian). Dep. NTIS (U. S. Sales Only).

The covariant expression of the polarization density matrix, or the projection operator, for the arbitrary integer or half-integer spin is derived in an explicit form. The covariant formalisms of Pauli–Firz and Rarita–Schwinger are used for describing higher fields. (J.F.P.)

5306 (NYO-4204-1) DIMENSIONS OF CURRENT OPERATORS. Beg, M. A. B. (Rockefeller Univ., New York); Bernstein, J. (Stevens Inst. of Tech., Hoboken, N. J.); Sirlin, A. (New York Univ., N. Y.). [1969]. Contract AT(30-1)-4204. 9p. Dep. NTIS.

Necessary and sufficient conditions for the spatial and temporal components of hadronic currents to have the same dimension are stated and proven. Some theoretical and experimental implications are discussed. (auth)

5307 (RLO-2041-49) THREE PARADOXES RELATED TO FULL CAUSALITY. Csonka, P. L. (Oregon Univ., Eugene). 17 Feb 1970. 21p. Dep. NTIS.

In a fully causal theory, certain problems can apparently have self contradictory solutions. This fact does not mean that full causality must be wrong. Three basic types of apparent contradictions are discussed, and it is shown that they can be resolved. (auth)

5308 CONSTRAINTS ON EQUAL-TIME COMMUTATORS FROM LORENTZ COVARIANCE. Sartori, G. (Univ., Padua. Istituto Nazionale di Fisica Nucleare, Padua). Lett. Nuovo Cim.; 4: 583-8(26 Sep 1970).

An equation in a previous work on Schwinger terms in the equal-time commutators between local operators required by covariance constraints is proven. For this proof the equation is rederived by means only of group-theoretical techniques implemented by the use of some formal properties of Σ_n commutators. The equation is proven in the case of two tensor operators. (J.F.P.)

XUM

5309 PARTICLE NUMBER FLUCTUATIONS IN HYDRODYNAMICAL THEORY OF MULTIPLE PRODUCTION. Daibog, E. I. (Moscow State Univ.). Yadern. Fiz.; 12: 655-9(Sep 1970). (In Russian).

It is shown that fluctuations of the particle number in the hydrodynamical theory result in a two-bump structure of the distribution. (auth)

5310 DOUBLE PARTIAL WAVE EXPANSION OF SCATTERING AMPLITUDES: THE GENERAL MASS CASE FOR SPINLESS PARTICLES WITH APPLICATIONS TO ELASTIC PROCESSES AND A SYSTEMATIC ANALYSIS OF THE SEMI-LEPTONIC DECAY MODE OF THE K-MESON. Ramond, Pierre Michel. Syracuse, N. Y.; Syracuse Univ. (1969). 101p. University Microfilms Order No. 70-10,383.

Thesis.

A double partial-wave expansion of the scattering amplitude of spinless particles of arbitrary masses is derived. The expansion has the merits of being diagonal in angular momentum, displaying the correct threshold and pseudothreshold behavior of the partial wave amplitudes, and of leading to an infinite array of finite-dimensional crossing relations for the partial waves. In particular elastic scattering is considered and an explicit construction of the polynomials relevant to this case is shown. The extension to the inclusion of spin is considered in its most elementary form in π-N scattering. "Partial wave crossing relations" are shown to be the direct consequence of crossing symmetry. Sum rules are derived for π-N scattering. A simple minded model for the partial wave amplitudes is introduced and is shown to lead to inconsistencies in the sum rules. An attempt is made to explain the existing data on the semi-leptonic modes of the K-meson by assuming strict conservation of the strangeness violating vector current. In particular a specific model of K^* dominance and magnetic type $K^*K\pi$ coupling is introduced. It is shown that such a model can reconcile the interpretation of the branching ratio and polarization data, although it does not give the correct shape for the π° spectrum. A more phenomenological model is shown to lead to the breaking of the μ-e universality hypothesis. (Diss. Abstr. Int., B)

5311 AEC AUTHORIZING LEGISLATION, FISCAL YEAR 1971. PART 2. HEARINGS BEFORE THE JOINT COMMITTEE ON ATOMIC ENERGY, CONGRESS OF THE UNITED STATES, NINETY-FIRST CONGRESS, SECOND SESSION ON PHYSICAL RESEARCH, BIOLOGY AND MEDICINE, AND PLOWSHARE, MARCH 3 AND 5, 1970. Washington, D. C.; Joint Committee on Atomic Energy (1970). 660p. GPO $2.75.

5312 HIGH ENERGY PHYSICS INDEX. VOLUME 8, NO. 18, 1970. Frankfurt am Main; Zentralstelle fuer Atomkernenergie-Dokumentation (1970). 69p.

5313 HIGH ENERGY PHYSICS INDEX. VOLUME 8, NO. 20, 1970. Frankfurt am Main; Zentralstelle fuer Atomkernenergie-Dokumentation (1970). 73p.

5314 HIGH ENERGY PHYSICS INDEX. VOLUME 8, NO. 19, 1970. Frankfurt am Main; Zentralstelle fuer Atomkernenergie-Dokumentation (1970). 69p.

5315 LOWER BOUNDS ON THE TRESHOLD CHARGE-EXCHANGE AMPLITUDE FROM DI-PION MASS DISTRIBUTIONS IN FINAL STATES. Tiktopoulos, George (Princeton Univ., N. J.). Phys. Rev. Lett.; 25: 1463-6(16 Nov 1970).

It is argued that the differential rates of production of neutral di-pions in a reaction of the type $X \rightarrow Y + (\pi\pi)$ have the form $d\sigma_{+-}/k^2dk = A + Bk + O(k^2)$, $d\sigma_{00}/k^2dk = C - Bk + O(k^2)$ for small values of k, the pion relative momentum in the di-pion rest frame. Determination of the coefficients A, B, and C would yield the bound $|\alpha_2 - \alpha_0| \geq 3|B|/2(AC)^{1/2}$, where α_1 is the $\pi\pi$ scattering length for isospin I. (auth)

5316 IMPLICATIONS OF ADLER ZEROS ON CURRENT-DIVERGENCE COMMUTATORS. Renner, B. (Cambridge Univ., Eng.); Wray, Dennis A. Nucl. Phys.; B14: 389-99(1969).

Matrix elements of current-divergences vanish or take simple forms between states of equal energy and momentum. This fact is exploited to test the consistency of certain soft-pion theorems. The most important result obtained is a new estimate of a parameter in $SU_3 \times SU_3$ symmetry breaking: earlier results on the relative magnitude of $SU_2 \times SU_2$ and SU_3 symmetry violations are confirmed. (auth)

5317 CONSTRUCTION OF COVARIANT AND GAUGE INVARIANT T* PRODUCTS. Gross, D. J. (CERN, Geneva); Jackiw, R. Nucl. Phys.; B14: 269-84(1969).

The problem of constructing sea-gull terms, which render time-ordered products of arbitrary operators Lorentz covariant, is investigated. The necessary and sufficient conditions that the commutators of operators must satisfy in order that it be possible to covariantize their time-ordered product are determined. An explicit formula for the sea-gull is given in terms of the relevant Schwinger term. It is shown that these considerations, which use formal equal time commutators, are equally valid for commutators defined by use of the Bjorken–Johnson–Low theorem. The question of whether sea-gulls and Schwinger terms cancel in the Ward–Takahashi identities which these covariant T* products satisfy is then considered. Necessary and sufficient conditions for this cancellation to take place are given. Specific examples of the general theory are given. (auth)

5318 KINEMATIC SEPARATION OF THREE-PARTICLE CHANNELS IN COUNTER EXPERIMENTS. Byckling, Eero; Kajantie, K. (Univ. of Helsinki). Nucl. Phys.; B14: 355-65 (1969).

Counter experiments for measuring three-particle final states are considered. The natural variables arising in connection with these experiments are momentum transfers to the detected particles and missing masses. The lab values of the particle momenta corresponding to fixed values of these variables, the conditions needed for the separation of unique three-particle channels, and the values of these variables accessible in counter experiments are determined. The required resolutions in momenta and angles are given. (auth)

Electromagnetic

Refer also to abstract 5830.

5319 (CONF-700314–, Paper 8) ELECTROMAGNETIC INTERACTIONS AT VERY HIGH ENERGY. Bjorken, J. D. (Stanford Linear Accelerator Center, Calif.). 21p.

From Conference on expectations for particle reactions at the new accelerators, March 30–April 1, 1970, Madison, Wisconsin.

Scaling laws having some experimental basis and which suggest how to extrapolate to higher energies are discussed. This includes two-body photoproduction and deep inelastic electroproduction. Also scaling behavior based on theoretical conjecture is considered. These scaling laws include predictions for the Feynman and Yang single-particle spectra and conjectures regarding hadron yields in colliding-beam experiments. The topics new particles, high transverse momenta, coherent phenomena in nuclei, and timelike electromagnetic form factors are briefly mentioned. (J.F.P.)

5320 (CONF-700314–, Paper 17) FIELD THEORETIC MODELS FOR HIGH ENERGY PROCESSES. Gasiorowicz, S. (Minnesota Univ., Minneapolis). 26p.

From Conference on expectations for particle reactions at the new accelerators, March 30–April 1, 1970, Madison, Wisconsin.

Diffraction scattering and diffraction dissociation and deep inelastic electron scattering at high energies in quantum field theoretic models are reviewed. (J.F.P.)

5321 (DEMO-70/1) REMARKS ON π^+-PHOTOPRODUCTION WITH LINEARLY POLARIZED PHOTONS. Papaioannou, G. M.; Verganelakis, A. (Democritus Nuclear Research Center, Athens (Greece)). [1969]. 12p. Dep. NTIS (U. S. Sales Only).

It is shown that the statement that polarized photons parallel to the production plane, to leading order in s select out only unnatural parity contributions in π^+ photoproduction, is not correct. It is found that natural spin parity contributions also enter to $(d\sigma/dt)_{||}$ which may well account for the observed behavior of Σ. (auth)

5322 (DNPL/R-7) VECTOR MESON PRODUCTION AND OMEGA–RHO INTERFERENCE. Proceedings of the Daresbury Study Weekend No. 1, 12–14 June 1970. Donnachie, A.; Gabathuler, E. (eds.) (Daresbury Nuclear Physics Lab. (England)). 1970. 249p. (CONF-700629).

Separate abstracts are provided for the ten presented papers in this field of high energy physics. (UK)

For abstracts of individual papers see: 5248–5250, 5301, 5323–5325, 5373, 5374, and 5446.

5323 (DNPL/R-7, pp 3-28) RECENT THEORETICAL WORK IN PHOTOPRODUCTION OF VECTOR MESONS. Kramer, G. (Hamburg Univ. (West Germany). Institut fuer Theoretische Physik (II)).

From Vector meson production and omega–rho interference.

Experimental work on the photoproduction of vector mesons, and in particular ρ^0 mesons, has reached a stage where the detailed mass dependences of the production process can be studied. Models were discussed that have been developed to describe these mass dependences and the background contributions to the effective two-body process which mass dependence outside the

XUM

resonance peak involves. The discussion was concentrated on ρ meson photoproduction, although most of the ideas could also be applied to ϕ photoproduction. After a general discussion about background in resonance production and the problem of "double counting," the following models to account for the mass dependence in $\pi^+\pi^-$ photoproduction on protons were considered: (a) a conventional resonance model for diffraction–dissociation, (b) the Soeding interference model, and (c) a dual resonance model of diffraction–dissociation. (12 references) (UK)

5324 (DNPL/R–7, pp 95–114) THEORETICAL INVESTIGATIONS ABOUT THE $\omega-\rho$ MIXING. Gourdin, M. (Paris Univ., Orsay (France). Laboratoire de Physique Theorique et Hautes Energies).

From Vector meson production and $\omega-\rho$ interference.

The $\omega-\rho$ mixing is due to a violation of isospin invariance in electromagnetic interaction, and has recently received considerable attention both theoretically and experimentally. It has been measured in (a) electron–positron annihilation into $\pi^+\pi^-$, (b) strong production of ρ^0 and π mesons followed by decay into the $\pi^+\pi^-$ mode, and (c) photoproduction of $\pi^+\pi^-$ and e^+e^- pairs on nuclei. The subject is discussed under the following headings: mixing formalism (propagator physical states, transition amplitude, conservation of probabilities, time reversal invariance); mixing parameters, and other processes for $\pi^+\pi^-$ photoproduction and for e^+e^- photoproduction. (28 references) (UK)

5325 (DNPL/R–7, pp 115–38) INTERFERENCE EFFECTS IN HIGH ENERGY VECTOR MESON PHOTOPRODUCTION. Gabathuler, Erwin (Daresbury Nuclear Physics Lab. (England)).

From Vector meson production and omega–rho interference.

The study of vector mesons, having the same quantum numbers as the photon, has proved to be an extensive field of research at electron accelerators. In vector meson photoproduction the real photon can be coupled to the vector meson by the simple vector dominance model and the cross sections for short-lived vector meson-nuclear interactions can be measured. In the decay of vector mesons into lepton pairs, where the vector meson is coupled to the lepton pairs through an intermediate time-like photon, the strength of the photon–vector meson coupling can be determined with certain assumptions about the physics of the production amplitudes. The advent of the storage ring, which enables the photon–vector meson coupling to be measured directly, provides a useful method of testing the assumptions about the production amplitudes, and the introduction of sizeable real parts in the forward vector meson photoproduction amplitudes using complex nuclei to determine the total vector meson cross sections is an obvious example of comparison. The results of vector meson production in storage rings and those from lepton pair decay of vector mesons in photoproduction have also produced some interesting comparisons. Headings of the paper were as follows: photoproduction of lepton pairs; the $\omega-\rho$ interference in lepton pairs; the $\omega-\rho$ interference in pion pairs. (29 references) (UK)

5326 ISOVECTOR ASYMMETRY IN rho-PRODUCTION, PION PHOTO- AND ELECTROPRODUCTION. Manweiler, R. (Cornell Univ., Ithaca, N. Y.); Schmidt, W. Phys. Lett.; 33B: 366–8(9 Nov 1970).

The asymmetry ratio ρ_{1-1}/ρ_{11} of the density matrix elements measured in ρ-production, pion photo- and electroproduction is discussed in the limit $s \to \infty$. The sensitivity of this asymmetry to the ratio $R = F_1(k^2)/F_\pi(k^2)$ of the nucleon to pion form factor is stressed, which may be different in the three reaction. The breakdown of vector meson dominance found in ρ_{1-1}/ρ_{11} is very likely also due to a change of R in going from $k^2 = 0$ to $k^2 = m_\rho^2$ and it will therefore persist even in the limit $s \to \infty$. (auth)

5327 ρ,ω PHOTOPRODUCTION PHASE: A POSSIBLE BREAKDOWN IN VECTOR DOMINANCE. Greenhut, G.; Weinstein, R. (Northeastern Univ., Boston). Phys. Lett.; 33B: 363–5(9 Nov 1970).

Using vector meson dominance with real (γ,V) coupling constants the relative (ρ,ω) photoproduction phase in nuclei is calculated as a function of assumed nucleon phases. Recent measurements of this phase are too large to be accommodated by these assumptions. (auth)

5328 SCALE-INVARIANT LIGHT-CONE COMMUTATORS AND UNIVERSAL STRUCTURE FUNCTIONS. Lu, E. Y. C. (Washington Univ., St. Louis). Lett. Nuovo Cim.; 4: 621–4(26 Sep 1970).

Previous considerations are generalized and broken scale invariance is exploited to deduce an attractive scheme for the commutators of SU(3) × SU(3) currents on the light cone. The assumptions lead to the strong conclusions that there are only two universal structure functions for asymptotic electroproduction on arbitrary targets and that the neutron and proton structure functions must be the same. Universality also holds for the sum of neutrino and antineutrino structure functions. (J.F.P.)

5329 SPIN-$\frac{3}{2}$ COMPTON SCATTERING. Dormuth, K.; Teshima, R. (Univ. of Alberta, Edmonton). Lett. Nuovo Cim.; 4: 796–8(24 Oct 1970).

It was recently demonstrated to second order that the system of a spin-$\frac{3}{2}$ field in interaction with the electromagnetic field can be consistently quantized using the technique of hyperquantization. The S-matrix obtained is used to calculate the differential cross section for scattering between a spin-$\frac{3}{2}$ particle and a photon. The total cross section is also calculated. (L.B.S.)

5330 DEEP INELASTIC SCATTERING AND THE NATURE OF PARTONS. Cabibbo, N. (Univ., Rome. Istituto Nazionale di Fisica Nucleare, Rome); Parisi, G.; Testa, M.; Verganelakis, A. Lett. Nuovo Cim.; 4: 569–74(26 Sep 1970).

In the parton model, from deep inelastic electron scattering, in which partons are associated with some of the usual hadrons, it is shown that one can obtain a simple description of the behavior of the two structure functions W_1 and νW_2 in the limit of very large $\omega = -2M\nu/q^2$, where ν is the energy loss of the electron and q^2 is the invariant momentum transfer. In particular νW_2 reaches a constant for large values of ω in agreement with the experimental results. Also the ratio of longitudinal to the transverse cross sections approaches a constant value. The hypothesis of considering the octet of $\frac{1}{2}^+$ baryons and the pseudoscalar octet as partons leads to $\sigma_{long}/\sigma_{trans} \approx 0.15$ to 0.2. If the scalar octet is also included the ratio increases to 0.3 to 0.4. The cases in which a parton is a spinless boson or a spin-$\frac{1}{2}$ fermion are considered. (J.F.P.)

5331 DENSITY-MATRIX FORMALISM FOR LEPTON–HADRON SCATTERING. Muzinich, I. J. (Brookhaven National Lab., Upton, N. Y.); Wang, Ling-lie; Wang, Jiunn-ming. Phys. Rev., D; 2: 1985–98(1 Nov 1970).

A density-matrix approach is presented for lepton-hadron reactions. A unified treatment is given of electroproduction, neutrino-induced production, decay, and colliding-beam-type processes. In this formulation, the lepton reactions are treated in a manner completely analogous to the hadronic reactions involving decaying resonances. The general content of the result for the differential cross section can be stated as a product of finite-dimensional representations of the SO(2,1) group or SO(3) group for the lepton pair and a hadronic density matrix. The group changes from noncompact SO(2,1) to compact SO(3), depending upon whether the momentum of the lepton pair involved in the interaction is spacelike or timelike. Formulas are given for general lepton-induced reactions. Specific reactions (total inelastic lepton scattering and leptonic pion, ρ, and N* production) are discussed in detail. In this formulation, the implications of Reggepole theory, low-energy theory, partial conservation of axial-vector current, and current algebra can be easily studied. (auth)

5332 VECTOR-DOMINANCE MODEL AND THE BACKGROUND PHOTOPRODUCTION OF PIONS. Bajpai, R. P. (Univ. of Manchester, Eng.). Lett. Nuovo Cim.; 4: 950–4(21 Nov 1970).

In the Regge-pole description of backward photoproduction using the N_α, N_γ, and Δ_δ trajectories, a larger Δ_δ contribution is required than is allowed by the vector dominance model. The role of the Δ_δ contribution is studied, and a search is made for a solution that involves little or no Δ_δ contribution. (L.B.S.)

5333 LOW-ENERGY THEOREMS FOR AMPLITUDES OF μ CAPTURE AND PION ELECTROMAGNETIC PRODUCTION. Vainshtein, A. I.; Zakharov, V. I. (Inst. of Nuclear Physics, Moscow). Yadern. Fiz.; 12: 610–19(Sep 1970). (In Russian).

On basis of the hypothesis of partial axial current conservation and assuming that the amplitude may be expanded in a series on the momenta, predictions are obtained for the effective pseudoscalar coupling in the proton μ capture and for the threshold cross sections of pion electro- and photoproduction on nucleons. (auth)

5334 SCATTERING OF CHARGED PARTICLES AT HIGH ENERGIES AND THE BETHE FORMULA. Kafiev, Yu. N. (Inst. of Mathematics, Novosibirsk, USSR). Yadern. Fiz.; 12: 562–9 (Sep 1970). (In Russian).

Electromagnetic corrections to strong interaction amplitude are considered. Violation of the Bethe formula, due to contribution from rescatterings or from scatterings on potentials with different radii, is studied. Assuming the Regge-type high-energy behavior of the amplitude a general form for the phase-shift is obtained. The experimental situation is discussed. (auth)

5335 POLARIZED γ QUANTA SCATTERING IN NUCLEAR FIELD WITH PRODUCTION OF e^+e^- PAIR AND SEVERAL PHO-

TONS. Nadzhafov, I. M. (Moscow State Univ.). Yadern. Fiz.; 12: 557-61(Sep 1970). (In Russian).

The differential cross section of the photoproduction of the e^-e^+ pair is calculated in a nuclear Coulomb field with the emission of one, two, and three photons for any energies but small scattering angles of particles taking into account longitudinal polarizations of electron, positron, and circular polarizations of photons. Deviations of the scattering angles of particles from 0° and π may amount up to several degrees. It is shown in particular that in the γ-quanta scattering in the nuclear Coulomb field with the production of the e^-e^+ pair and several photons under small angles, the odd number of hard photons would be mainly emitted. (auth)

5336 PHOTO- AND ELECTROPRODUCTION OF NEUTRAL RHO MESONS FROM NUCLEI. Julius, David Irwin. Ithaca, N. Y.; Cornell Univ. (1969). 161p. University Microfilms Order No. 70-8671.

Thesis.

A comprehensive account of methods involving nuclear targets is provided for the determination of basic parameters describing the coupling of rho mesons to photons and nucleons. A detailed investigation is made of the validity of the closure approximation in ρ^0 photoproduction from deuterium using a separable potential model of the n-p system for which all the amplitudes can be calculated analytically. It is found that the closure approximation underestimates the cross section by about five to ten percent, depending on the kinematics; the error always is largest for production in or near the forward direction. The calculation makes no special assumptions concerning the photoproduction amplitude from a single nucleon, so that the results are equally applicable to other hadronic processes involving a deuterium target. A model is constructed for coherent photoproduction of neutral ρ's from light nuclei which parallels the Glauber multiple diffraction theory for elastic processes, but which incorporates the substantial modifications required by the presence of the minimum momentum transfer accompanying the conversion of a photon to a massive rho. The additive phase shift assumption becomes inapplicable, and phenomenological potentials representing rho photoproduction and rho elastic scattering from an individual nucleon, rather than the corresponding production and scattering amplitudes, are required as input to the eikonal theory. Assumptions are made which reproduce the essential features of the Glauber model; however the shapes of the diffraction minima are severely altered by the incorporation into the theory of the mass change of the beam particle. Vector dominance enters the calculation in a rather more profound way than in the optical model treatment of heavy nuclei, and it is concluded that light nuclear targets can provide a rather incisive test of this hypothesis. A description is obtained of coherent ρ photoproduction which takes the rather substantial width of the ρ into account. The optical model analysis of Drell and Trefil is extended to include ρ-decay inside the nucleus, as well as the subsequent absorption of the decay pions. The eikonal method is used throughout, and is found to yield compact analytic expressions for the production amplitude. The decay effects produce an appreciable shift of the ρ peak toward lower mass for production in heavy nuclei and at the lower photon energies of current interest (2.7 to 4.5 GeV). On the whole the differential cross sections are not significantly affected in either shape or magnitude by the effects arising from ρ decay. In particular, the decay corrections do not appreciably influence the determination via vector dominance of the ρ-photon coupling constant. The dependence of the differential cross section on nuclear shape, target nucleon correlations and refractive components in the optical potentials is examined, and it is found that the results are moderately sensitive to these refinements. The problem of coherent electroproduction of rhos from heavy nuclei is treated by a simple extension of the Drell–Trefil theory. It is shown how the nucleon helicity nonflip amplitudes for rho-nucleon elastic scattering can be obtained in the usual way from the A-dependence of the forward cross section, and how the corresponding two amplitudes for rho photoproduction can be extracted from measurements of the decay pion angular distribution. (Diss. Abstr. Int., B)

5337 TWO-γ DECAYS OF PSEUDOSCALAR MESONS AND THE CONSTITUTION OF THE CURRENTS. Lai, C. S. (Univ. of Prince Edward Island, Charlottetown). Nucl. Phys.; B14: 348-54 (1969).

By studying the $\pi^0 \to 2\gamma$, $\eta \to 2\gamma$ and $X \to 2\gamma$ decays, an attempt to determine the possible model for the constitution of the currents is made. The $P\gamma\gamma$ couplings $g_{P\gamma\gamma}$ ($k^2 = -m_P^2$) are shown to contain two terms: one dependent on the charge of the fundamental triplet and the other linear in the square of the meson masses. The model of the integrally charged quarks, favored from the analysis of the radiative correction to the β decay, is also found to be favorable in the present consideration. (auth)

5338 K_{l3} FORM FACTORS OF THE VENEZIANO TYPE. Oyanagi, Yoshio (Tokyo Univ.). Nucl. Phys.; B14: 375-80(1969).

A model for K_{l3} as well as pion and kaon electric form factors is constructed in terms of the Veneziano-type scattering amplitudes combined with the field-current identity, PCAC and current algebra. No parameters remain to be determined from experiments. (auth)

Weak

Refer also to abstracts 5338 and 5536.

5339 (CONF-700314–, Paper 7) WEAK INTERACTIONS AT HIGH ENERGIES. Pais, A. (Rockefeller Univ., New York). 52p.

From Conference on expectations for particle reactions at the new accelerators, March 30–April 1, 1970, Madison, Wisconsin.

A survey of semi-leptonic phenomena induced by high-energy neutrino beams is given. Elastic form factor determinations from differential cross sections and polarization effects, total cross sections in the quasielastic approximation including sum rules and scaling, and qualitative questions from beyond the quasi-elastic approximation are considered. (J.F.P.)

5340 TESTS OF MODELS OF SCALE INVARIANCE WITH COSMIC-RAY NEUTRINO DATA. Castagnoli, C. (CNR, Turin); Etim, E.; Picchi, P. Lett. Nuovo Cim.; 4: 564-8(26 Sep 1970).

In the combined parton and diffractive scheme an interpretation was previously made of the prediction of the field-theoretical model according to which the values of neutrino and antineutrino total and differential cross sections with respect to the Bjorken variable $\omega = q^2/2M\nu$ are in the ratio 3 to 1. As a test of this model it is predicted that neutrino- and antineutrino-derived cosmic-ray muons underground should fall into two distinct groups of mean energies in the ratio 2 to 3 and production cross sections in the ratio 3 to 1. The results predicted by various models for the experimental total fluxes of neutrinos and antineutrinos are compared with experimental data for muon fluxes. It is found that the results are not in conflict with experiment. (J.F.P.)

5341 RADIATIVE CORRECTIONS TO WEAK SEMILEPTONIC DECAYS AND COMMUTATOR AMBIGUITIES. Orzalesi, C. A. (New York Univ., N. Y.). Lett. Nuovo Cim.; 4: 811-15(24 Oct 1970).

The question of whether or not commutator ambiquities might be a universal cure for the divergence difficulties leading from current algebra methods for radiative corrections to semileptonic weak decays is investigated. It is found that a negative answer follows from current algebra constraints alone. (L.B.S.)

5342 ON-SHELL CURRENT ALGEBRA AND RADIATIVE LEPTONIC DECAYS OF PIONS AND KAONS. Carron, Neal Jay. Urbana, Ill.; Univ. of Illinois (1969). 117p. University Microfilms Order No. 70-13,266.

Thesis.

The hard-meson method of Schnitzer and Weinberg is used to study the radiative leptonic decays of π and K. The original formalism for SU(2) is generalized to include the case of strangeness-changing axial-vector currents and the isoscalar part of the electromagnetic current. This method and dispersion relations are used to determine the form factors for the decays. It is shown that in the pole dominance approximation the relevant form factor in the axial-vector amplitude cannot be unsubtracted. Possible alterations of the results arising from relaxing a smoothness approximation are estimated to be small. Several symmetry breaking schemes for the evaluation of necessary coupling constants are discussed. The branching ratio for $K^+ \to \gamma e \nu$ is calculated to be $\sim 2 \times 10^{-5}$ for interesting structure dependent decays. Finally possible effects of electromagnetic violations of time reversal invariance in the decay are investigated. (Diss. Abstr. Int., B)

5343 CURRENT ALGEBRAS AND UNIVERSAL DIVERGENT RADIATIVE CORRECTIONS. Gaffney, George William. Stanford, Calif.; Stanford Univ. (1969). 82p. University Microfilms Order No. 70-10,454.

Thesis.

Using current algebras, the ultraviolet divergences occurring in the calculation of electromagnetic radiative corrections to any lowest-order weak process at arbitrary momentum transfer are examined. All orders in perturbation theory in the fine structure constant α are considered. The divergent parts of the radiative corrections are expressed in terms of matrix elements of equal-time current commutators by using the Bjorken expansion of time-ordered products of currents at large momenta. The validity of this expansion and of the use of "naive" current commutation relations in discussing various current algebra models are as-

XUM

sumed. The condition is imposed that the divergences contribute only to an unobservable, universal weak coupling constant renormalization. It is shown that, in models with operator Schwinger terms in the current commutators, this condition cannot be satisfied for nonzero momentum transfer. Also, it is not satisfied for a weak interaction theory mediated by a vector boson. Two current algebra models are exhibited which are satisfactory if the weak Hamiltonian has a local current-current form. For these models, the weak and electromagnetic currents of both the hadrons and the leptons obey the same commutation relations, and the Schwinger terms are c-numbers. One, a quark model of hadrons with integrally charged quarks together with the conventional lepton currents, gives finite radiative corrections. The second, the algebra of fields model for the total electromagnetic and weak currents, including leptons, contains only a universal divergent factor. These two results are shown to hold to all orders in α. In obtaining these results, divergent contributions to electromagnetic mass shifts and to electromagnetic renormalization effects in strong interaction processes are isolated and removed by adding a counter term to the interaction Hamiltonian. These divergences may thus be treated as a separate problem, which is not discussed in detail. (Diss. Abstr. Int., B)

5344 POSSIBLE PROPERTIES OF WEAK SIX-FERMION INTERACTION. Vanzha, A.; Isaev, A.; Lapidus, L. (Joint Inst. for Nuclear Research, Dubna, USSR). Yadern. Fiz.; 12: 595-604(Sep 1970). (In Russian).

Charged and neutral pion and K-meson decays into four leptons and muon decays into five leptons are considered from the point of view of studying properties of a possible six-fermion weak interaction. Expressions for particle spectra and estimates for decay widths are obtained. Of the most interest is the search for four-fermion decays of pions and kaons as well as the high energy neutrino experiments. (auth)

5345 HIGH-ENERGY NEUTRINO–NUCLEON SCATTERING CURRENT ALGEBRA AND PARTONS. Gross, David J.; Smith, C. H. Llewellyn (CERN, Geneva). Nucl. Phys.; B14: 337-47 (1969).

The structure functions F_i which describe high-energy neutrino–nucleon scattering are discussed. The analog of the Callan–Gross result for electroproduction is derived, viz. $q^2 \xrightarrow{\lim} -\infty$ $F_1 = q^2 \xrightarrow{\lim} -\infty$ $F_3 = 0$ with the algebra of field commutators and $q^2 \xrightarrow{\lim} -\infty$ $(F_2 - \omega F_1) = 0$ with the quark model commutators. A sum rule for F_3 is derived assuming that F_3 satisfies an unsubtracted dispersion relation, as suggested by Regge theory. The breakdown of these current algebra results in perturbation theory is discussed. The F_i are also discussed in the "parton" model, in which it is shown that F_3 is a measure of the average baryon number of the partons. In the "quark-parton" model of Bjorken and Paschos F_3 is small and the sum rule valid. In the "field theory parton" model of Drell, Levy and Yan F_3 is large, in contradiction to Regge theory, and the sum rule invalid. This model predicts that anti-neutrino scattering vanishes in the backward direction. (auth)

Strong (General)

Refer also to abstracts 5405 and 5409.

5346 (CONF-700314–, Paper 12) MULTIPERIPHERAL MODELS: PHENOMENOLOGY. Bali, Naren F. (Washington Univ., Seattle. Dept. of Physics). 55p. (RLO-1388-581).

From Conference on expectations for particle reactions at the new accelerators, March 30–April 1, 1970, Madison, Wisconsin.

Some multiperipheral models are discussed which may be useful to describe high-energy production processes in the new accelerators. The multi-Regge model, the five-point Veneziano function, the Caneschi–Pignotti model, and multiplicities are considered. (J.F.P.)

5347 (CONF-700314–, Paper 13) REGGE-TYPE MODELS FOR HIGH ENERGY SCATTERING. Durand III, Loyal (Wisconsin Univ., Madison. Dept. of Physics). 40p.

From Conference on expectations for particle reactions at the new accelerators, March 30–April 1, 1970, Madison, Wisconsin.

This review of Regge phenomenology covers very high energy hadron strong interactions, Regge cuts, and complex Regge trajectories. Also diffraction models for high energy p + p scattering are briefly considered. (J.F.P.)

5348 (COO-264-562) IS THE POMERANCHUK DECOUPLED FROM THE ORDINARY REGGE TRAJECTORIES. Barry, George W. (Chicago Univ., Ill.). Oct 1970. Contract AT(11-1)-264. 10p. (EFI-70-63). Dep. NTIS.

If the amplitude for diffraction scattering is independent of the universal slope of the ordinary Regge trajectories, there results a helicity selection rule, which corresponds to s-channel helicity conservation for the diffractive part of $\pi p \to \pi p$ and $\gamma p \to \rho^0 p$, in accordance with experiment. A crucial test of the selection rule is that electroproduced ρ^0's should be transversely polarized at high energy. (auth)

5349 (IFVE-STF-69-74) FORWARD SCATTERING AMPLITUDE BEHAVIOR AT HIGH ENERGIES. Khrustalev, O. A.; Savrin, V. I.; Tyurin, N. E. (Gosudarstvennyi Komitet po Ispol'zovaniyu Atomnoi Energii SSSR, Serpukhov. Institut Fiziki Vysokikh Energii). 1969. 10p. (In Russian). Dep. NTIS (U. S. Sales Only).

On the basis of the unitarity condition the behavior of the forward scattering amplitude at moderately large energies is investigated. Besides the way in which the total cross section of hadron scattering reaches the asymptotical limit is studied. (auth)

5350 (JINR-P1-5315) INTERFERENCE OF IDENTICAL PARTICLES IN THE PROCESSES INVOLVING THE RESONANCES. Grishin, V. G.; Kopylov, G. I.; Podgoretsky, M. I. (Joint Inst. for Nuclear Research, Dubna (USSR). Lab. of High Energy). 1970. 19p. (In Russian). Dep. NTIS (U. S. Sales Only).

The interference of identical particles in the processes involving the resonances is considered; the possibility of measuring, on this basis, the widths of resonance states is discussed. (auth)

5351 (NYO-2262-TA-225) SCALING BEHAVIOR IN MULTIPERIPHERAL DYNAMICS. Silverman, Dennis (Princeton Univ., N. J. Joseph Henry Labs. California Univ., La Jolla, San Diego. Dept. of Physics); Tan, Chung-I (Princeton Univ., N. J. Joseph Henry Labs. Brown Univ., Providence, R. I. Dept. of Physics). [1970]. Contract AF(638)-1545. 15p. Dep. NTIS.

The scaling of the single particle momentum distribution is demonstrated as a general property of all multiperipheral models which have been proposed. It is also shown that in these models pionization is approached as a smooth limit from scaling. The proof is based only on the most general multiperipheral assumption and on Pomeranchuk dominance at high energies which necessitates the experimental observation of scaling for the validity of any multiperipheral model. (auth)

5352 (SU-1206-235) IMPLICATIONS OF LOCAL DUALITY IN A SET OF COUPLED REACTIONS. King, M. J.; Wali, Kameshwar C. (Syracuse Univ., N. Y. Dept. of Physics). [1970]. 30p. (NYO-3399-235). Dep. NTIS.

This is an extension of an earlier study on PD → PD to two sets of coupled reactions (1) PD → PD, PD → PB, PB → PB, and (2) PV → PV, PV → PP, PP → PP. Some consequences of local duality are examined and compared to experiment in limited energy regions for the above reactions. The assumption that the imaginary parts of the direct channel helicity amplitudes vanish in the forward (backward) scattering if the crossed t-channel (u-channel) is exotic leads to systems of equations relating resonance contributions in the direct channel. The solutions predict certain patterns of particles degenerate in mass but with different SU(3), spin, and parity assignments. In particular, the inclusion of spin considerations yields the result that the particles on leading trajectories must be accompanied by daughters with prescribed ratios of coupling constants between the parent and daughter states. The link between these results and those which follow from a complementary description in terms of Regge residues is discussed. (auth)

5353 ELECTROSTATIC ANALOGUE FOR THE VIRASORO MODEL. Shapiro, J. A. (Univ. of Maryland, College Park). Phys. Lett.; 33B: 361-2(9 Nov 1970).

An alternative is proposed to the usual dual resonance model by considering charges and electrostatics on a sphere. The four point Born term is shown to give the Virasoro model with a particular value of the intercept (a = 2). (auth)

5354 QUARK WAY TO ASYMPTOPIA. Kim, Y. S. (Ohio State Univ., Columbus); Kwak, N. Lett. Nuovo Cim.; 4: 604-8 (26 Sep 1970).

A phenomenological model of the behavior of the hadron–hadron interaction cross sections at high energies is discussed relative to the quark model. Three energy phases of this behavior are considered. (J.F.P.)

5355 SOLUTION OF UNITARITY CONDITION FOR TWO-PARTICLE PROCESS AMPLITUDE AT HIGH ENERGIES. Savrin, V. I.; Tyurin, N. E.; Khrustalev, O. A. (Inst. of High-Energy Physics, Moscow). Yadern. Fiz.; 12: 630-3(Sep 1970). (In Russian).

The unitarity condition is solved for the amplitude of any two-particle channel in collision of high energy hadrons. The amplitude is determined by the sum of contributions of all inelastic processes in which the initial or final state contains more than two particles. (auth)

5356 RENORMALIZATION OF COUPLING CONSTANT FOR THE STRANGE VECTOR CURRENT. Belavin, A. A. (Inst. of Theoretical and Experimental Physics, Moscow). Yadern. Fiz.; 12: 605-9(Sep 1970). (In Russian).

The relation of the Adler–Weisberger type for $G_V^{\Delta S=1}$ and the Ademollo–Gatto theorem are obtained in terms of the model in which the SU_3 invariance is conserved due to the introduction of massless scalar kaons realizing nonlinear representation. (auth)

5357 FAST VARIATION OF HADRONIC AMPLITUDE AND BREHMSSTRAHLUNG OF γ QUANTUM. Ponomarev, L. A. (Inst. of Theoretical and Experimental Physics, Moscow). Yadern. Fiz.; 12: 570-9(Sep 1970). (In Russian).

Radiation of a γ quantum in hadronic processes in the domain of fast variation of the amplitude, is considered. The radiation is found from the interaction region, due to the sharp s dependence near a resonance and due to the sharp t dependence in high energy scattering at small t. Dependence of the amplitude, describing this radiation, on the virtual mass is shown. Possible measurements of the effects, due to the off-shell hadronic amplitude, in the radiative scattering at high energies are discussed. (auth)

5358 TREATMENT OF SPINS IN THE QUARK MODEL. Krzywicki, A.; Le Yaouanc, A. (Laboratoire de Physique Theorique et Hautes Energies, Orsay, France). Nucl. Phys.; B14: 246-54(1969).

It is demonstrated that the commonly used treatment of quark spins is inconsistent even at very small momentum transfers because of the internal motion of quarks within hadrons and the related Wigner rotations. A consistent formulation, valid for high-energy small angle scattering is proposed. (auth)

5359 DYNAMICAL SCHEME FOR LEADING TRAJECTORY AND THEORY OF FIREBALLS. Akimov, V. N.; Chernavskii, D. S.; Dremin, I. M.; Royzen, I. I. (Lebedev Inst. of Physics, Moscow). Nucl. Phys.; B14: 285-302(1969).

The quantum-field theory based on the Bethe–Salpeter equation is applied to investigate properties of the leading vacuum trajectory for the elastic amplitude and to describe high-energy inelastic processes. It is shown that it naturally explains the production of fireballs at very high energies. Parameters of the leading trajectory are related to characteristics of inelastic processes. (auth)

Strong (Baryon No. = 0)

5360 (RLO–2041-51) ENERGY AND ANGULAR RESOLUTION IN PION–PION SCATTERING AND OTHER COLLIDING BEAM EXPERIMENTS. Csonka, Paul L. (Oregon Univ., Eugene). [1970]. 15p. Dep. NTIS.

In certain types of colliding beam experiments, the interaction region may contain particles within a wide momentum range. It is described how the energy and angle dependance of the cross section can be measured under these circumstances. Pion–pion scattering in a miniring is given as an example. (auth)

5361 (TPJU–14/70) DETERMINATION OF THE $X^0(960)$ MESON SPIN-PARITY IN THE POLARIZATION EXPERIMENT. Klosinski, J.; Rembielinski, J.; Tybor, W. (Jagellonian Univ., Krakow (Poland). Dept. of Theoretical Physics). May 1970. 5p. Dep. NTIS (U. S. Sales Only).

To establish the $X^0(960)$ meson spin-parity it is suggested to study the forward production of the X^0 in the reaction $K^-p \rightarrow X^0\Lambda$ on the polarized target. (auth)

5362 NORMALIZATION OF $\bar{p}p \rightarrow 4\pi$ USING A DUAL SIX-POINT FUNCTION. Chaichian, M. (Durham Univ., Eng.); Hopkinson, J. F. L. Lett. Nuovo Cim.; 4: 616-20(26 Sep 1970).

The generalized Veneziano model is used for the normalization of the $\bar{p} + p \rightarrow 4\pi$ interaction at rest, a dual six-point function is used as the starting point. (J.F.P.)

5363 DUALITY AND SCATTERING LENGTHS. Mezincescu, L. A. (Inst. of Physics, Bucharest); Uretsky, J. L. Lett. Nuovo Cim.; 4: 579-82(26 Sep 1970).

Duality and scattering lengths as applied to pion–pion scattering are discussed. Also a sum rule for the correction Δ a to the scattering-length predictions of current algebra is given. (J.F.P.)

5364 LIGHT-CONE SINGULARITIES OF CURRENT COMMUTATORS AND MODIFIED WEINBERG SUM RULES. Morita, K. (Nagoya Univ., Japan). Lett. Nuovo Cim.; 4: 977-81(21 Nov 1970).

The idea of the asymptotic chiral symmetry is reformulated in terms of the structure of singularities of current commutators on the entire light cone. In particular, the Weinberg-type sum rules are derived in a simple way appealing neither to any specific model of equal-time commutators nor to the infinite-momentum method. In contrast with previous derivations, the second sum rule is modified in such a way that the Weinberg mass relation $m_{A_1}^2 = 2m_\rho^2$ is replaced with the Veneziano one $m_{A_1}^2 = 2m_\rho^2 - m_\pi^2$. It is argued that this minor change is amplified in the case of strangeness-changeness currents. The relation of this approach with the momentum-space consideration is also discussed. (L.B.S.)

5365 TEST FOR EXOTIC EXCHANGE IN $p\bar{p}$ INTERACTIONS. Thews, R. L. (Univ. of Arizona, Tucson). Lett. Nuovo Cim.; 4: 969-72(21 Nov 1970).

The standard properties of factorization are used to test for an I = 2 trajectory exchange in the following interaction: $pn \rightarrow \Delta^-\Delta^{++}$, $pn \rightarrow \Delta^{++}\Delta^-$, $p\bar{p} \rightarrow \Delta^{++}\bar{\Delta}^{--}$, and $p\bar{p} \rightarrow \Delta^0\bar{\Delta}^0$. (L.B.S.)

5366 INVESTIGATION OF AZIMUTHAL CORRELATIONS IN DECAYS OF HEAVY RESONANCES. Rechitskii, I. V.; Til, E. A. (Moscow State Univ.). Yadern. Fiz.; 12: 531-4(Sep 1970). (In Russian).

Arguments are given in the favor of existence of the azimuthal correlations in decays of ~1.5 to 2.5 GeV mesonic resonances. The expected correlations are observed in the region of masses of narrow resonances when analyzing the 17-GeV/c π^--meson interaction. (auth)

5367 PCAC, UNITARITY, AND THE σ-MODEL. Evanco, William Martin. Ithaca, N. Y.; Cornell Univ. (1969). 68p. University Microfilms Order No. 70-8667.

Thesis.

The renormalization of the σ-model is set up in order to show that PCAC is consistent with unitarity in the framework of this model. A formalism for taking derivatives of renormalized amplitudes in terms of renormalized field theoretic parameters is also established to enable a study of the dependence of amplitudes on the pion mass. (Diss. Abstr. Int., B)

5368 LOW BOUNDARIES FOR THE $\pi^0\pi^0$-MESON SCATTERING LENGTHS. Stroganov, Yu. G. (Inst. of High-Energy Physics, Moscow). Yadern. Fiz.; 12: 660-3(Sep 1970). (In Russian).

Low boundaries for the scattering length are obtained assuming the analyticity, unitarity, crossing symmetry and polynomial limit of the $\pi^0\pi^0$-scattering amplitude in the complex energy plane. In case of the negative s-wave scattering length a_0 the rest scattering lengths cannot be arbitrarily small. (auth)

5369 Kπ ELASTIC SCATTERING STUDIED BY THE CHEW–LOW EXTRAPOLATION METHOD. De Baere, W. (Laboratoire des Hautes Energies, Brussels); Debaisieux, J.; De Wolf, E.; (and others). Nucl. Phys.; B14: 425-36(1969).

The cross sections for elastic $K^+\pi^- \rightarrow K^+\pi^-$, and charge exchange, $K^+\pi^- \rightarrow K^0\pi^0$, scattering were determined using the Chew–Low extrapolation method, for Kπ masses up to 1.35 GeV. This was achieved by using 3026 events of the type $K^+p \rightarrow K^+\pi^-N^*(1236)$ and 1246 events of the type $K^+p \rightarrow K^0\pi^0N^*(1236)$ obtained in bubble chamber exposures at CERN. The cross section exhibits the known $K^*(892)$ resonance shape. A similar study for the $K^+\pi^+ \rightarrow K^+\pi^+$ elastic scattering was attempted. The partial wave expansion coefficients up to (Y_2^0) (without off-shell correction) were studied as a function of the Kπ masses. (auth)

5370 INTERNAL SYMMETRY IMPLICATIONS OF THE VENEZIANO MODEL IN PSEUDOSCALAR–PSEUDOSCALAR SCATTERING. Canning, G. P. (Oxford Univ.). Nucl. Phys.; B14: 437-57(1969).

The leading order Veneziano model amplitudes for (J^P) $0^- \times 0^-$ $0^- \times 0^-$ scattering constrained by the absence of "exotic" resonances is shown to predict the coupling constant relation of SU(3) coupled with the quark-model/SU(6) ideal singlet–octet mixing in the 1^-, 2^+, nonets. The Adler self-consistency condition is found to hold (for the most part) both for pions and kaons fulfilling Lovelace's conjecture. (auth)

Strong (Baryon No. = 1)

Refer also to abstracts 5294 and 5359.

5371 (CEA-N-1373) REGGE MODELS INCLUDING 4 POLES ρ,ρ', A2 AND A2', IN THE π-NUCLEON AND K-NUCLEON CHARGE EXCHANGE REACTIONS FROM 2 TO 20 GeV/c. De Brion, Jean-Pierre; Derem, Andre (Commissariat a l'Energie Atomique, Saclay (France). Centre d'Etudes Nucleaires). Nov 1970. 49p. (In French). Dep. NTIS (U. S. Sales Only).

All the available experimental data on the reactions $\pi^-p \rightarrow \pi^0n$, $\pi^-p \rightarrow \eta n$, $\bar{K}^-p \rightarrow K^0n$ and $K^+n \rightarrow K^0p$ are analyzed in the framework of an exchange model with four Regge poles ρ, ρ', A2 and A2'. The model is extrapolated towards low energies and gives a good description of the differential cross sections down to about 2 GeV.

XUM

The dominance of the SU(3) octet exchange, with spin and parity 1^- and 2^+, is not satisfied below 4 GeV, owing to difficulties which arise mainly from K^+ nucleon scattering. (France)

5372 (CNRS-CPT-70-P-331) APPROACH TO FORM FACTOR IN A COMPOSITE MODEL. Andriambololona, Raoelina; Bourrely, C. (Centre National de la Recherche Scientifique, Marseilles (France). Centre de Physique Theorique). Jun 1970. 23p. Dep. NTIS (U. S. Sales Only).

The electromagnetic form factor of the nucleon was derived from a composite model; the relation between the form factor and structure function of the composite nucleon was studied in detail, and the problem of the form factor in nucleon-antinucleon elastic scattering was investigated. (France)

5373 (DNPL/R-7, pp 173-205) OMEGA-RHO INTERFERENCE IN STRONG INTERACTIONS. Roos, Matts (European Organization for Nuclear Research, Geneva (Switzerland)).

From Vector meson production and omega-rho interference.

The phenomenological evaluation of $\rho-\omega$ interference effects is essentially the same whether concerned with photoproduction, colliding electron beams, or strong production. Matters of particular concern to strong interactions, and in particular a review of the experimental situation are presented. Headings are as follows: phenomenological formalism (general case; case of incoherent G-states); reaction $K^-p \to A\pi^+\pi^-$; reaction $\pi^-p \to n\pi^+\pi^-$; reaction $\pi^+p \to \pi^+\pi^-\Delta^{++}$; reaction $\pi^-p \to \pi^+\pi^-\pi^-p$; reaction $\bar{p}p \to \pi^+\pi^-\pi^+\pi^-$; reactions $\bar{p}n\pi^+\pi^-\pi^-$, $\pi^+\pi^-\pi^-\pi^0$, $2\pi^+3\pi^-$. (22 references) (UK)

5374 (DNPL/R-7, pp 207-13) RELATIVE PHASE OF ρ^- AND ω^- PRODUCTION AMPLITUDES IN REGGE PHENOMENOLOGY. Dass, G. V. (Rutherford High Energy Lab., Chilton (England)).

From Vector meson production and $\omega-\rho$ interference.

The nature of the $\rho-\omega$ interference pattern depends, among other things, on two relative phases— the phase for production and the phase for decay of these vector mesons, and experimental data represent the sum of these two phases. If the decay phase is known, this implies a determination of the production phase. The best means to investigate the decay phase is where the theory for production is thought to be well understood, for example in colliding beam experiments or perhaps in photoproduction experiments. The present study is concerned only with the production phases for reactions induced by pseudoscalar mesons. Because of its dependence on phases $\rho-\omega$ interference can provide a rather sensitive means for distinguishing between the different types of strong interaction models and application to a Regge pole model for $\pi^\pm$ induced reactions is considered; results for kaon induced reactions can be obtained as simple extensions. The effect of absorptive cuts is mentioned along with the $\pi-B$ exchange degeneracy argument of Goldhaber et al. (Phys. Letts. 30B: 249(1969)). (5 references) (UK)

5375 (TPJU-15/70) PREDICTIONS FOR THE DECAY DISTRIBUTIONS OF RESONANCES PRODUCED IN THE REACTIONS $0^-1/2^+ \to 0^+3/2^+, 0^-1/2^+ \to 1^+3/2^+$, AND $0^-1/2^+ \to 2^+3/2^+$. Muryn, B. (Jagellonian Univ., Krakow (Poland). Dept. of Theoretical Physics). May 1970. 11p. Dep. NTIS (U. S. Sales Only).

Using the additive quark model, the relations between statistical tensors for single and joint decay angular distributions in reactions $0^-1/2^+ \to 0^+3/2^+$, $0^-1/2^+ \to 1^+3/2^+$, and $0^-1/2^+ \to 2^+3/2^+$ are derived. (auth)

5376 π^--p INTERACTIONS IN THE PERIPHERAL MODEL. Seth, V. P.; Singh, C. P.; Agarwal, B. K.; Gupta, Y. M. (Univ. of Allahabad, India). Indian J. Pure Appl. Phys.; 7: 220-3(Apr 1969).

The pion production in π^--p interaction near 1 GeV was studied according to the peripheral model. Exchange of a nucleon and a pion gives good agreement with the experimental observation on the momentum distributions and angular distributions of outgoing pions. (auth)

5377 EFFECTIVE REGGE TRAJECTORIES FOR SOME TWO-BODY REACTIONS. Spiro, M.; Derem, A. (CEN de Saclay, Gif-sur-Yvette, France). Lett. Nuovo Cim.; 4: 593-603(26 Sep 1970).

Reactions of the type M + B → M′ + B′, where M, M′ are mesons of spin-parity 0^- and B, B′ are baryons of spin-parity $1/2^+$ or $3/2^+$ are considered. Restriction is made to those reactions where ρ, A_2, K*(890), or K**(1420) mesons are exchanged in the t-channel (forward scattering). A systematic study is made of effective Regge trajectories in reactions which experimentally are measured with sufficient accuracy. A list of the analyzed reactions with the particles exchanged in the t channel is given. (J.F.P.)

5378 TOTAL CROSS-SECTIONS AT INFINITE MOMENTUM AND THE LOW-ENERGY BACKGROUND. Lasinski, T. A. (Univ. of Chicago). Lett. Nuovo Cim.; 4: 609-15(26 Sep 1970).

It is found that the total cross sections at infinite momentum for π^+ p interactions are 24.1 ± 6.2 mb, using an evaluation of the Lehmann sum rule and the available real parts of the elastic scattering amplitude. The sum rule is evaluated removing the low-energy P_{33} contribution which is generally believed to be due to the Δ(1236). The resulting negative value for the total cross sections leads one to conclude that either all the higher-energy resonances interfere strongly with the background or that there is background present under the Δ(1236). In the latter case an estimate of such a background shows that the sum rule could give the above result for the total cross section upon removal of only the resonance contribution. It is shown that resonance-background interferences can lead to important corrections to finite-energy sum rule estimates of the π^+p total cross sections at infinite momentum. (J.F.P.)

5379 UNIT-SPACING STRUCTURE OF TRAJECTORIES FOR πN RESONANCES. Kanki, T. (Osaka Univ.). Lett. Nuovo Cim.; 4: 803-7(24 Oct 1970).

The duality model realized by the Veneziano representation suggests that there should exist multiplets with the same masses and angular momenta, and that these multiplets are fitted to recurrences of linear parallel trajectories with unit spacing in angular momentum. A new classification of 20 known πN resonances is proposed, and remarkable evidence for this structure of baryon trajectories is shown. The resonances are fitted into four recurrences, N^I and N^{II} for $I = 1/2$, Δ^I and Δ^{II} for $I = 3/2$. It is then discussed how the four recurrences of the trajectories become degenerate with each other in the limit that the nucleon and the (P_{33}; 1236) resonance have the same mass. (L.B.S.)

5380 REGGE-POLE ANALYSIS OF ρ^0 PRODUCTION. Butera, P.; Enriotti, M. (Univ., Milan. Istituto Nazionale di Fisica Nucleare, Milan). Lett. Nuovo Cim.; 4: 787-95(24 Oct 1970).

Some Regge models for the reaction $\pi^-p \to \rho^0n$ are compared with the experimental data at various energies for the t dependence of both the cross sections and the ρ spin density matrices. The analysis is made in order to take into account recent experimental data, to test the effectiveness of the conspiracy concept and the validity of the simple Regge-pole exchange approximation, and to investigate the relevance of A_1 exchange and a possible phenomenological description of the A_2 splitting. Strong indications are found that no simple evasive Regge model either with pole or with pole and cut exchange is able to reproduce satisfactorily the data, while some simple conspiracy models are clearly preferred by the fits. (L.B.S.)

5381 HOW GOOD WAS THE ABSORPTION MODEL? Fincham, D. G. (Univ. of Aberdeen, Scotland). Lett. Nuovo Cim.; 4: 767-70(24 Oct 1970).

It is shown that more absorption is needed in the "old-fashioned" absorption model to fit the high-energy inelastic scattering data. The $\pi^-p \to \rho p$ reaction is considered as an example, and comparisons are made of cross sections from other models. (L.B.S.)

5382 PHENOMENOLOGICAL REGGE TRAJECTORIES IN DIRECT-CHANNEL PION-PROTON ELASTIC SCATTERING. Stoessel, Edward Thomas. Ames, Iowa; Iowa State Univ. (1969). 79p. University Microfilms Order No. 70-13,637.

Thesis.

An investigation of the possibility of using a direct-channel Regge pole theory to describe low-energy scattering data is described. The model amplitude which is derived is similar to the modified Regge representation proposed by Mukherjee but is different in two important respects: The Mukherjee representation does not apply to a process in which the particles may have spin whereas the one presented applies to the helicity amplitudes of the general Jacob-Wick expansion. The Reggeization of a signatured helicity amplitude does not lead to a signatured model except in the spinless case. It is shown how to ensure the preservation of signature by including an appropriate part of the background integral. A preliminary numerical investigation of the pion-proton elastic scattering process is discussed and it is found that there is some likelihood of the success of a more extensive numerical study. (Diss. Abstr. Int., B)

5383 RELATIVISTIC GREEN'S FUNCTION APPROACH TO NUCLEONIC PROPERTIES. Brown, Warren David. Seattle; Univ. of Washington (1969). 264p. University Microfilms Order No. 70-14,738.

Thesis.

Single nucleon properties are obtained by solving a nonlinear integral equation for the nucleon Green's function and an integral equation for the vertex function. The field equations for nucleons interacting via the exchange of π, ω, and ρ mesons are written down and discussed. An integral equation for the one-nucleon

Green's function in Hartree–Fock approximation is then derived and solved. All divergences encountered in the case of pions and ω-mesons are removed by renormalizations, whereas nonremovable divergences in the case of the ρ-meson necessitate the introduction of a cut-off. The electromagnetic field is introduced into the problem. An integral equation is derived, in the Hartree–Fock approximation, for the vertex function describing the nucleon-photon interaction assuming only pions mediate the nucleon force. The equation is subtracted, renormalized and solved in first order to obtain the magnetic moment of the nucleon. The symmetry properties of the vertex function are also investigated. The integral equation derived is manipulated and a spectral representation performed leading to three coupled integral equations for the spectral functions. These integral equations are solved numerically to obtain a prediction for the magnetic moment of the nucleon which is exact in the Hartree–Fock approximation. The prediction for the isovector component of the magnetic moment (1.86) is very close to the experimental value (1.85), and although the prediction for the isoscalar component (−1.40) is far from the experimental value (−0.06), it is closer than the perturbation theory result (−1.64). The coupled integral equations are then extended to include ω-mesons and resolved, although the presence of the ω-mesons changes the values of the magnetic moments only slightly. The form factors and entire vertex function are considered. A first order expression for the vertex function for any values of the momentum variables is derived and reduced to simple quadratures. The quadratures are performed numerically on the mass shell yielding first order values for the form factors. The gamma algebra is eliminated from the integral equation for the vertex function and a Mandelstam-type spectral representation performed, leading to eight coupled integral equations for the Mandelstam spectral functions. These equations are discussed but not solved. Also, the analyticity properties of the vertex function in the Hartree–Fock approximation are investigated, and it is demonstrated that for both external momenta squared, a branch cut lies along the negative real axis from $-(M + m_\pi)^2$ to $-\infty$, where M is the nucleon mass and m_π is the pion mass. (Diss. Abstr. Int., B)

5384 STUDY OF THE REACTION $K^-N \rightarrow \Xi K$ FROM THRESHOLD TO 2.7 GeV/c. Muller, Richard A. Berkeley, Calif.; Univ. of California (1969). 62p. University Microfilms Order No. 70-13,127.

Thesis.

A partial wave analysis of the reactions $K^-p \rightarrow \Xi^-K^+$, $K^-p \rightarrow \Xi^0K^0$, and $K^-n \rightarrow \Xi^-K^0$ was performed. About 3000 events with beam momenta ranging from 1.2 to 2.7 GeV/c, obtained in the Berkeley 72 in. bubble chamber were used. New data are presented for the reaction $K^-n \rightarrow \Xi^-K^0$ at 2.1 and 2.64 GeV/c. The total cross sections at these momenta are 69^{+14}_{-13} μb and 36^{+10}_{-8} μb respectively. The polarization was measured from the sequential weak decays $\Xi \rightarrow \Lambda\pi$, $\Lambda \rightarrow p\pi^-$. By assuming that the parts of the invariant amplitudes that are due to baryon exchange factorize into functions that depend only on s = (total center of mass energy)^2 and u = (4-momentum of exchanged baryon)^2, powerful constraints on the partial wave amplitudes are generated. Using these constraints an energy dependent fit to the data was done. It is concluded from the fit that the data can be explained in terms of isotopic spin-0 baryon exchange, with small but important contributions from isotopic spin-1 baryon exchange and direct channel resonance production. Only known Y* resonances were included in the direct channel. The baryon exchange partial waves move in counter-clockwise circles in the Argand diagram, suggesting that they may have a "dual" interpretation as resonant partial waves. (Diss. Abstr. Int., B)

5385 ON THE Y(1327) HYPERON. Kopeliovich, V. B.; Nikolaev, N. N.; Okun, L. B. (Inst. of Theoretical and Experimental Physics, Moscow). Yadern. Fiz.; 12: 649-54(Sep 1970). (In Russian).

Possible decay channels and quantum numbers are discussed of the hyperon with mass 1327 MeV, that were recently suggested, in an experiment. It is shown that in case $J^P = 1/2^-$ one would expect comparable probabilities for the decays $Y \rightarrow \Lambda\pi^0\gamma$ and $Y \rightarrow \Lambda\gamma$. The decays $Y \rightarrow \Lambda\pi^0$ and $Y \rightarrow \Sigma\gamma$ would have somewhat smaller partial widths. If $J^P_Y = 1/2^+$, then the decays $Y \rightarrow \Lambda\gamma$ and $Y \rightarrow \Sigma\gamma$ would have comparable widths and the decays $Y \rightarrow \Lambda\pi^0\gamma$ and $Y \rightarrow \Lambda\pi^0$ would be essentially suppressed. Presence of the Y pole with $J^P = 1/2^+$ would lead to a considerable (about 10%) branching ratio for the decay $\Xi^0 \rightarrow \Lambda(\Sigma)\gamma$ and to the 10% breaking of the $\Delta T = 1/2$ rule in the decay $\Xi^0 \rightarrow \Lambda\pi^0$. It is noted that measurements of the branching ratio of the decays $Y \rightarrow \Lambda\pi^0\gamma$ and $Y \rightarrow \Lambda\pi^0$ in case $J^P_Y = 1/2^+$ may be used for determination of the life time of the Σ^0 hyperon. (auth)

Strong (Baryon No. ≥ 2)

Refer also to abstracts 5359, 5430, and 5433.

5386 (CONF-700314–, Paper 14) DIFFRACTION DISSOCIATION. Good, Myron L. (State Univ. of New York, Stony Brook). 20p.

From Conference on expectations for particle reactions at the new accelerators, March 30–April 1, 1970, Madison, Wisconsin.

Diffraction dissociation is defined to be those processes which combine the features of small-angle elastic scattering in the target particle with those of a transition of the beam particle that could but for energy occur in isolation. This combination allows orbital angular momentum to be transferred. The $\pi\rho$ final state in π reactions with nuclei and the data on a nucleon target are considered. It is pointed out that the basic mechanism is not yet understood and that possibly experiments at very high energy will help to explain this. (J.F.P.)

5387 (JINR–E2-5365) PROBLEM OF QUASIPOTENTIAL SMOOTHNESS IN QUANTUM FIELD THEORY MODELS. Barbashov, B. M.; Kuleshov, S. P.; Matveev, V. A.; Sissakian, A. N.; Tavkheliidze, A. N. (Joint Inst. for Nuclear Research, Dubna (USSR). Lab. of Theoretical Physics). 1970. 9p. Dep. NTIS (U. S. Sales Only).

An interpretation of the smooth complex quasipotential is given in the framework of the eikonal consideration of quantum field theory models. (auth)

5388 (JINR–P2-5058) NONSTRANGE BARYON–BARYON RESONANCES. Zulkarneev, R. Ya.; Rozanova, A. M. (Joint Inst. for Nuclear Research, Dubna (USSR)). 1970. 10p. (In Russian). Dep. NTIS (U. S. Sales Only).

Two peculiarities of the pp interaction mechanism in the region of 300 to 640 MeV are underlined. On the basis of the results of phenomenological analysis of pp scattering, performed under the assumption that in $^1D_2$ and $^3P_2$ states in pp-system there exists a strong absorption, it was established that this hypothesis is compatible with all the analyzed data on pp scattering and total cross sections at 640 MeV and does not contradict them. From consideration of energy dependence of the partial scattering amplitude by use of Argond diagrams, constructed on the basis of phase analysis, the possible existence of a resonance in the pp system (i.e. Y = B = 2) with mass 2050 ± 90 MeV and $J^P = 2^+$ is found. Attention is paid to the fact that the suggested hypothesis agrees with experimental data on energy dependence of the singlet pp scattering cross section at an angle of 90° (cms) which has a peak in the energy region of 300 to 550 MeV. However, for clearing up the nature of this peak both experimental and theoretical investigations are necessary. (auth)

5389 APPLICATIONS OF T-MATRIX PERTURBATION THEORY. Lu, An-hua. Troy, N. Y.; Rensselaer Polytechnic Inst. (1969). 120p. University Microfilms Order No. 70-11,326.

Thesis.

Three separable approximations for the off-energy shell t-matrix element t(p,k;s) are compared with those for a local central square well potential for negative energy s. One of them was treated by Reiner and the calculation is in agreement. It is found that the unitary pole approximation is in general the best of the three one-term separable approximations used. In the calculation of triton binding energy for a central local Hulthén potential, the rate of convergence of the Weinberg–Rotenberg series expansion is examined. It is found that the single term misses the four term result by 40%, two terms have an error of less than 6%; and three terms are good to within 2% of the value for 4 terms. A numerical procedure to evaluate multi-dimensional integrals is studied and it is found that the accuracy is moderately good. Fuda's first order t-matrix perturbation theory is applied to calculate the triton binding energy for a variety of two-body potentials. A 0.2 MeV difference is found between exact and perturbation results for a local Hulthén potential (developed into 4-term Weinberg series). Perturbation theory gives an error of 0.13 MeV for Mongan's two term separable potential which uses a tensor interaction. Finally, by using t-matrix perturbation theory, one can calculate the energy correction to the trinucleon (with a central potential) due to higher partial waves in the two-body interaction. It is found that waves beyond the $^1S_0$ and $^3S_1 + {}^3D_1$ contribute less than 0.01 MeV. (Diss. Abstr. Int., B)

5390 APPLICATIONS OF CLUSTER EXPANSION METHODS TO EXTENDED NUCLEAR MIXTURES. Mueller, George Paul. St. Louis; Washington Univ. (1969). 160p. University Microfilms Order No. 70-10,964.

Thesis.

In the last ten years the cluster expansion approach to many-body calculations was applied to a number of systems of strongly interacting particles; e.g., nuclear matter, the neutron gas, and liquid helium. These methods are generalized to allow mixtures of two strongly interacting components. Examples of these are

XUM

the alpha particle-nuclear matter mixture, the ^{3}He-^{4}He mixture, and the impurity problem, wherein one foreign particle is imbedded in a background of host particles. The formal analysis leading to an expression for the ground state energy of such a mixture was based on the Iwamoto and Yamada (IY) and factorized IY (FIY) cluster expansion techniques. These expressions for the energy are complete through second order in the cluster expansion. The definition of order is based, essentially, on the number of independent short-range functions that appear in the integrands of the energy expression. Cluster calculations are variational in nature. One chooses a trial correlation factor of suitable functional form which is dependent on several variational parameters. All of the new calculations reported on were performed by minimizing the appropriate energy expression, which were complete through second order. Many earlier cluster calculations involved only minimizing the first-order expression and then estimating the second order contribution. This latter method has proved inadequate in some cases. This formalism is applied to three particular cases: the calculation of the ground state energy of pure alpha matter and of the alpha-nucleon mixture, and the calculation of the binding energy of a lambda particle in nuclear matter. In the lambda case we found a large discrepancy between the calculated value of the binding energy and the value obtained by extrapolating from the binding energies of the light hypernuclei. This discrepancy was not relieved by introducing phenomenological Λ-N tensor or Λ-N-N three-body forces into the calculation. For a pure boson system we investigated the contributions to the energy of higher orders, particularly the third. A new, seemingly unexploited, technique for the numerical evaluation of many-dimensional integrals is discussed and then used to estimate the third order contributions to the ground state energy of alpha matter. Finally, there is a discussion of the problems arising when conducting cluster calculations. Usually one is faced with the task of limiting the effective range of the trial correlation factors, which serve as a basis of the trial wave functions. A number of conditions and restrictions were used to accomplish this purpose, but there exists no single rule that can be imposed for every system for which calculations are made. The argument is advanced that the next stage in the utilization of the cluster expansion approach ought to be the search for a physically motivated and generally applicable rule of this sort. (Diss. Abstr. Int., B)

5391 DISPERSION SUM RULES πd SCATTERING. Queen, N. M. (Joint Inst. for Nuclear Research, Moscow). Yadern, Fiz.; 12: 620-3(Sep 1970). (In Russian).

It is shown that the two-Regge pole model P, P′ satisfies the dispersion sum rules for the forward πd scattering with the values of trajectories $\alpha_{P,P'}(0)$ which are compatible with the values determined from the analysis of πN scattering. (auth)

5392 DYNAMICS OF SINGLE PION PRODUCTION IN HIGH-ENERGY HADRONIC INTERACTIONS. Satz, H. (CERN, Geneva). Nucl. Phys.; B14: 366-74(1969).

A one-pion exchange model with empirical momentum transfer damping is employed to predict the energy behavior of $\sigma(pp \to pn\pi^+)$ and of the branching ratio $\sigma(pp \to pn\pi^+)/\sigma(pp \to pp\pi^0)$. The results are found to agree well with experimental data and allow an investigation of and predictions for the asymptotic behavior of single-meson production in nucleon–nucleon and pion–nucleon interactions. (auth)

Particle Invariance Principles and Symmetries

General

5393 (IFVE-STF-69-85) UNITARY REPRESENTATIONS OF THE CONFORMAL GROUP. Leznov, A. N.; Fedoseev, I. A. (Gosudarstvennyi Komitet po Ispol'zovaniyu Atomnoi Energii SSSR, Serpukhov. Institut Fiziki Vysokikh Energii). 1969. 17p. (In Russian). Dep. NTIS (U. S. Sales Only).

Explicit expression of the invariant Hermitian form for all representations of the conformal group is found for which it exists. Unitary representations are selected by the condition of positive definiteness of the form. (auth)

5394 INVESTIGATION OF SYMMETRY BREAKING IN ELEMENTARY PARTICLE PHYSICS. Copley, Leslie Alexander. Toronto; Univ. of Toronto (1968).

Thesis.

The study of approximate symmetries in strong interaction physics has recently been the subject of immense theoretical interest. The group theoretical treatment of their breaking mechanisms and effects has already received exhaustive analysis. A step beyond this treatment is taken in the hope of obtaining a clearer understanding of the underlying dynamics. This is done by considering three distinct approaches to the problem of calculating, within a broken symmetry scheme, the dynamical parameters of a given hadronic system. For the purposes of identification the three approaches are referred to as the "external dynamics," algebraic and "internal dynamics" methods. The first of these involves explicit field theoretical calculations of hadronic scattering parameters based on the assumption of a well defined Lagrangian. In this approach the dynamical and group theoretical properties of the system enter as mutually complimentary components of the theory. In particular, one finds that predictions based on group theory alone serve as ideal tests of the "reality" of the assumed Lagrangian as well as of the approximation methods that may be used to sum the perturbation expansion. To illustrate this approach pseudoscalar meson-meson scattering is studied using the SU(3) extension of the $\lambda\phi^4$ interaction and kinematic breaking. The resulting perturbation series is summed with the assistance of Padé approximants. The most prominent discovery is that this model possesses a still higher approximate symmetry, O(8), which makes a number of new and interesting predictions for meson physics. These are studied in conjunction with the Padé approximant calculations of the effect symmetry breaking has on the p-wave resonances in the π-π, π-K and K-$\bar{K}$ scattering channels. The second approach is based on exact Lie algebras (current algebras) which may be thought of as the sources of the approximate group symmetries observed in nature. The operators in the algebras are physically observable (usually in weak and electromagnetic interactions) or, at least, physically identifiable. This method is conveniently equipped to make use of dispersion theory techniques and the most general of field theoretical concepts and thus avoids use of perturbation theory. A particular study of current algebra methods of deriving broken SU(3) sum rules for three-point coupling constants is made. It is found that current algebra does not intrinsically provide more information than is present in conventional group theoretical derivations. But, it is found that it exhibits much greater flexibility in absorbing subsidiary dynamical assumptions and exhibiting their effects. In so doing, a wide range of broken SU(3) sum rules for both strong- and weak-interaction coupling constants are rederived. The internal dynamics approach is an alternative title for the quark model which also serves as a possible explanation of the hierarchy of approximate physical symmetries. To study the implications of the quark model for symmetry breaking on parity-violating non-leptonic decays are considered. It is found that, correcting for spin-dependent effects, one obtains broken SU(6) sum rules for the decay amplitudes that are in excellent agreement with experiment. Further, one can extend their derivation to obtain a very successful relation between baryon and kaon decays. Finally, the three approaches are compared with each other as well as with the usual group theoretical techniques. However, rather than using this comparison to pass critical value judgements it is argued that the totality should be considered as a single, if nebulous, theory of elementary particles. (Diss. Abstr. Int., B)

5395 BROKEN SU(3) SUM RULES DERIVED FROM THE ASYMPTOTIC SU(3) SYMMETRY. Fourez, Gerard M. College Park, Md.; Univ. of Maryland (1969). 110p. University Microfilms Order No. 70-12,920.

Thesis.

Several results are derived from the broken SU(3) × SU(3) chiral algebra with the technique developed by Matsuda and Oneda called the "SU(3) approximation." The coupling constants for the decay of $J^P = 1^+$ mesons are calculated and the width of the K particles belonging to these multiplets are predicted; the results are in agreement with the present (but still unreliable) experimental data. The mixing angle between K_A and K_C (belonging respectively to the $J^{PC} = 1^{+-}$ and 1^{2+} multiplets) is found to be around 12°. Mass sum rules are derived from $[\dot{V}_{K^*}, A_{\pi^-}] = 0$ and $[V_{K^*}, A_{K^*}] = 0$ and the results from these different assumptions are compared. The influence of the mixing angle of the I = 0 particles is studied. Sum rules for some of the decay coupling constants of $J = 3/2, 1/2$ baryons are derived. The F wave decay of the $J = 1/2$ baryon is shown to be negligible compared with the P wave decay. The mass of the Ξ particle ($1/2^+$) is predicted, through an intermultiplet mass sum rule, to be 2.030 MeV, which is consistent with the most recent data. Finally the $\alpha = F/D + F$ ratio for the weak coupling constants of the Roper octet is calculated. (Diss. Abstr. Int., B)

5396 SYMMETRIES AND REFLECTIONS. SCIENTIFIC ESSAYS. Wigner, Eugene P. Cambridge, Mass.; Massachusetts Institute of Technology Press (1970). 286p. $3.95.

The discussion of symmetry and reflections covers invariance in physical theory, symmetry and conservation laws, invariance principles in natural philosophy, events, laws of nature and invariance principles, relativistic invariance and quantum phenomena struc-

ture of solid bodies, and the development of the compound nucleus model. The topics theoretical physics, radiation effects on solids, atomic energy, the measurement problem, the mind–body question, two kinds of reality, and the probability of the existence of a self-reproducing unit are considered. Lastly, the limits of science, mathematical effectiveness in natural sciences, the atomic age, and some historical discussions are included. (J.F.P.)

5397 APPLICATION OF THE COMMUTATION RELATIONS TO DETERMINATION OF EIGENVALUES OF OPERATORS. Zaitsev, A. A. Teor. Mat. Fiz.; 5: No. 1, 66-72(Oct 1970). (In Russian).

A method is developed for constructing the operators which change the eigenvalues of generators of a fixed representation of Lie algebra. The action of these operators on eigenfunctions of a chosen generator F_i gives other eigenfunctions of the same generator. The equations are deduced which determine the changes of eigenvalues of generators. The results obtained are applied to operators in the second quantization representation. (auth)

5398 PARTICLE–ANTIPARTICLE DOUBLETS AND THE FULL POINCARE GROUP. Ascoli, R. (Univ., Palermo, Italy); Termini, S.; Teppati, G. Nucl. Phys.; B14: 400-12(1969).

The representations of the full Poincaré group whose restriction to the proper group reduces into two irreducible representations are listed. Seven types of such representations are found. The possibility of interpreting them in the usual way as describing particle–antiparticle doublets is discussed. Only two of them do not exclude such an interpretation: the irreducible representation U_+ of Wigner and the reducible representation introduced by Ekstein. In some cases only this latter turns out to allow a physical interpretation. Some considerations are added concerning the existence of particles which are not transformed into themselves by time reversal and the physical equivalence of the two before mentioned representations, when describing one particle–antiparticle doublet with a superselection rule. (auth)

Applications (Electromagnetic and Weak)

Refer also to abstract 5715.

5399 (JINR–P2-5290) ON THE K_{l3} DECAYS IN CHIRAL DYNAMICS. Eliashvili, M. A. (Joint Inst. for Nuclear Research, Dubna (USSR). Lab. of Theoretical Physics). 1970. 19p. (In Russian). Dep. NTIS (U. S. Sales Only).

Effective Lagrangian calculation of K_{l3} form factors is performed using the additional assumption about the smoothness of $K^*-K\pi$ vertex. The relation between Glashow–Weinberg bounds on the κ–meson mass and SU (3) × SU (3) symmetry breaking parameter is established. The new values of decay constants F_K and F_κ are obtained. (auth)

5400 (UCRL–20041) SEARCH FOR T-VIOLATION IN THE INELASTIC SCATTERING OF ELECTRONS FROM A POLARIZED PROTON TARGET. Rock, Stephen (California Univ., Berkeley. Lawrence Radiation Lab.). Aug 1970. Contract W-7405-eng-48. 140p. Dep. NTIS.

Thesis.

The recent discovery of a violation of CP invariance has led to speculation on the origins and nature of the symmetry violating forces. This experiment is a search for this violation in the electromagnetic interactions of hadrons. A violation of time-reversal invariance in inelastic electron scattering from a polarized proton target was sought. A difference in cross sections (asymmetry) when the target was polarized in opposite directions along the normal to the scattering plane would mean either a time-reversal-invariance violation or a contribution from high order (α^3) effects. Data were taken using electron and positron beams to distinguish between the two possible causes of an asymmetry. Scattered electrons were detected in a magnetic spectrometer and the mass of the inferred outgoing hadronic state was calculated. The target polarization was reversed frequently in order to facilitate comparison of cross sections and to cancel random errors. The background from heavy unpolarized nuclei only contributed to an overall normalization factor. This was determined by supplementary measurements with carbon and CH_2 targets. Data were taken at SLAC energies in the region of resonance excitation of the outgoing hadron and at values of four-momentum transfer squared of 0.4, 0.6, and 1.0 $(GeV/c)^2$. The experimental errors were as small as 1.5% in asymmetry at certain kinematic conditions. No sizable violation of time-reversal invariance was found. (auth)

Applications (Strong)

5401 (DEMO–70/6) NUCLEON AXIAL VECTOR FORM FACTOR AND SO(4,2) GROUP. Kyriakopoulos, E. (Democritus Nuclear Research Center, Athens (Greece)). Apr 1970. 7p. Dep. NTIS (U. S. Sales Only).

Starting from the dynamical group SO(4,2) the nucleon axial vector form factor $G_A(t)$ is calculated. The expression $G_A(t) = G_A(0)/[1-(t/M_A^2)]^2$ is found in agreement with the recent accurate determination of $G_A(t)$ from threshold electropion production. (auth)

5402 RADIATIVE DECAYS OF MESONS IN BROKEN SU(3) SYMMETRY AND ELECTROMAGNETIC MASS SPLITTINGS IN THE 0^- OCTET. Esaibegyan, S. V.; Chkareuli, Dzh. L. (Inst. of Physics, Tbilisi, USSR). Yadern. Fiz.; 12: 580-94(Sep 1970). (In Russian).

Radiative decays of 0^- and 1^- mesons are considered in broken SU(3)-symmetry and using the vector dominance, the Veneziano model, and sum rules resulting from the finite radiative corrections to the pion and kaon β decay. Phenomenology of the SU(3)-symmetry breaking is completely elucidated, and predictions are presented for the decays $\rho \to \eta\gamma$, $\omega \to \eta\gamma$, $\varphi \to \eta\gamma$, $K^* \to K\gamma$. The obtained solutions for the symmetry breaking parameters result in an essential negative contribution to the $K^+ - K^0$ mass difference. Contributions from intermediate K and K_A mesons electromagnetic mass splitting are calculated also. Necessary account of the tadpole contribution is also noted. The total Δm value is in reasonable agreement with the experiment. Experiments in colliding beams, $e^+e^- \to \pi^0\gamma$ and $e^+e^- \to \eta\gamma$ are discussed. (auth)

Field Theories

General

5403 DUALITY INVARIANT ACTION PRINCIPLE IN VACUUM ELECTRODYNAMICS. Levman, G. M. (Univ. of British Columbia, Vancouver). Can. J. Phys.; 48: 2423-6(15 Oct 1970).

Although Maxwell's vacuum field equations are invariant under the so-called duality rotation, the usual Lagrangian density for the electromagnetic field, which is bilinear in the first derivatives of the electromagnetic potentials, does not exhibit that invariance. It is shown that if one takes the components of the electromagnetic field tensor as field variables then the most general Lorentz invariant Lagrangian density bilinear in the electromagnetic fields and their first derivatives is determined uniquely by the requirements of duality invariance. The ensuing field equations are identical with the iterated Maxwell equations. (auth) (Canada)

5404 BORN–INFELD PARTICLE; SMALL-SCALE PHENOMENA. Boillat, G. (Univ., Clermont-Ferrand, France). Lett. Nuovo Cim.; 4: 773-8(24 Oct 1970).

Small-scale phenomena associated with the Born-Infeld particle are studied. The propagation of disturbances in the field of the particle, the time variable, and the speed of propagation are examined. (L.B.S.)

Quantum Field Theory

Refer also to abstracts 5359, 5387, 5431, and 5436.

5405 (JINR–E2-5339) QUASI-POTENTIAL EQUATION FOR THE RELATIVISTIC HARMONIC OSCILLATOR. Donkov, A. D.; Kadyshevsky, V. G.; Mateev, M. D.; Mir-Kasimov, R. M. (Joint Inst. for Nuclear Research, Dubna (USSR). Lab. of Theoretical Physics). 1970. 29p. Dep. NTIS (U. S. Sales Only).

In the framework of the quasi-potential approach the relativistic generalization of the exactly soluble problem of the harmonic oscillator is studied. The quasi-potential wave functions are constructed as the expansions in terms of the wave functions of the corresponding nonrelativistic problem. The relativistic corrections to the energy levels are obtained. (auth)

5406 (JINR–P2-5305) EXAMPLE OF THE INFINITE-COMPONENT LOCAL FIELD WITH THE MASS SPECTRUM. Zaikov, R. P.; Palev, Ch. D. (Joint Inst. for Nuclear Research, Dubna (USSR). Lab. of Theoretical Physics). 1970. 7p. (In Russian). Dep. NTIS (U. S. Sales Only).

An example of the local infinite-component field with a mass spectrum, which is transformed over the nonunitary irreducible representation of Sp(4) group, is considered. (auth)

5407 (JINR–P2-5330) ON THE EQUALITY OF LOCAL ALGEBRAS OF RELATIVISTIC QUANTUM FIELD THEORY. Smondyrev, M. A. (Joint Inst. for Nuclear Research, Dubna (USSR). Lab. of Theoretical Physics). 1970. 13p. (In Russian). Dep. NTIS (U. S. Sales Only).

In the framework of the algebraic approach of Haag–Araki type to the axiomatic quantum field theory a necessary and sufficient

XUM

condition for the equality of two local W*-algebras $R(O_1)$ and $R(O_2)$ is proved. (auth)

5408 (NYO–3829-61) LOCALLY GENERATED DILATATION CHARGE IN THE THIRRING MODEL. Lowenstein, J. H.; Schroer, B. (Pittsburgh Univ., Pa. Dept. of Physics). Oct 1970. Contract AT(30-1)-3829. 26p. Dep. NTIS.

By applying a "normal product quantization" the energy–momentum tensor of the Thirring model is constructed as a local function of the Thirring fields. It is shown that the commutation relation of the dilatation current with the field is anomalous and that the space integrals converge on a dense set of states to the group generators. The appearance of anomalous dimensions for local products of Thirring fields is discussed in the special case of a bilinear mass interaction. (auth)

5409 DIVERGENCES AND RENORMALIZATION IN MULTILOOP DUAL DIAGRAMS. Cremmer, E. (Univ. de Paris, Orsay, France); Neveu, A. Phys. Lett.; 33B: 356-60(9 Nov 1970).

The new divergences which have recently been discovered in multiloop planar dual diagrams are analyzed. It is shown that they can be removed by defining a counterterm for each order in the coupling constant g^2. The physical interpretation of the counterterms as a mass renormalization is maintained at all orders in g^2. (auth)

5410 REMARKS ON THE YANG–MILLS GAUGE TRANSFORMATION. Bose, S. K. (Manchester Univ., Eng.). Lett. Nuovo Cim.; 4: 985-7(21 Nov 1970).

It is shown that in the usual vector gauge field formulation of Yang–Mills type the space-time-dependent transformation parameter is not completely arbitrary and depends on the vector gauge fields. (L.B.S.)

5411 COMPOSITE BOSONS IN NONLOCAL QUANTUM FIELD THEORY WITH $Z_3 \approx 1$. II. La Camera, M.; Wataghin, A. (Univ., Genoa. Istituto Nazionale di Fisica Nucleare, Genoa). Lett. Nuovo Cim.; 4: 955-8(21 Nov 1970).

A self-interacting Dirac field with four-fermion coupling is considered, assuming that the interaction is strong enough to produce a stable pseudoscalar boson bound state from a fermion-antifermion pair. It is shown that the four-fermion interaction can be replaced by an equivalent Yukawa coupling. It is also shown in the nonlocal quantum field theory and using a different renormalization procedure, that the compositeness condition leads to the value $Z_3 \approx 1$ for the boson wave function renormalization constant. (L.B.S.)

5412 DETERMINATION OF 2e/h BASED ON THE ac JOSEPHSON EFFECT. Harvey, I. K.; Macfarlane, J. C.; Frenkel, R. B. (National Standards Lab., Sydney). Phys. Rev. Lett.; 25: 853-6(28 Sep 1970).

A value for 2e/h was determined by the ac Josephson effect using niobium point-contact junctions. The value with respect to the international voltage standard as maintained at the Bureau International des Poids et Mesures, Sèvres ($V_{BIP\ Mes}$), is $2e/h = 483.59384 \pm 0.00010$ MHz/μV. (auth)

5413 FIELD THEORY OF THE CHARGED VECTOR BOSON. Sheinblatt, Marshall Jay. Boston; Northeastern Univ. (1968). 91p. University Microfilms Order No. 69-18,565.

Thesis.

A semi-quantized vector quantum electrodynamics is constructed by the investigation of the interaction of a quantized charged vector boson field with an external electromagnetic field. A nonsingular electromagnetic current operator is obtained by a method which is a generalization of that used to construct the analogous nonsingular electromagnetic current operator of spinor quantum electrodynamics. It is shown that the matrix element of the current operator is gauge invariant, divergenceless, and no more than logarithmically singular, to all orders of the external electromagnetic field. Consequently the theory is seen to be gauge invariant and renormalizable. A discussion is given of the possible extension of these results to the construction of a fully quantized theory. (Diss. Abstr. Int., B)

5414 FIELDS AND LOCAL OBSERVABLES IN THE AXIOMATIC ALGEBRAIC THEORY WITH SUPERSELECTION RULES. Khoruzhii, S. S. (Inst. of Mathematics, Moscow). Teor. Mat. Fiz.; 5: No. 1, 10-24(Oct 1970). (In Russian).

The problem of constructing fields from local observables is considered in the framework of a concrete algebraic theory with superselection rules proposed recently. The possibility of using methods developed previously is discussed. A number of results is obtained which concern the solution of the problem states and rest on the general postulates of local quantum theory only: the set of cyclic and separating vectors of local observable algebras of coherent superselection sectors is described in detail; the physical equivalence of the coherent sectors is proved, and a considerable amount of criteria is deduced for the local unitary equivalence of the sectors; a certain necessary condition of the duality theorem is found and the relation between the duality and local unitary equivalence is essentially clarified. (auth)

5415 CRITERION FOR A CERTAIN CANONICAL FERMI TRANSFORMATION TO BE PROPER. Kiperman, V. A. (Moscow State Univ.). Teor. Mat. Fiz.; 5: No. 1, 3-9(Oct 1970). (In Russian).

The canonical Fermi transformation analogous to the linear nonhomogeneous canonical Bose transformation is introduced and investigated. The necessary and sufficient condition for this transformation to be proper is obtained. (auth)

5416 CHARGES AND GENERATORS OF SYMMETRY TRANSFORMATIONS IN QUANTUM FIELD THEORY. Orzalesi, Claudio A. (Columbia Univ., New York). Rev. Mod. Phys.; 42: 381-408 (Oct 1970).

Within the Wightman approach to quantum field theory, the properties of formal charges, defined as space integrals for the fourth component of a local current are reviewed and clarified. The conditions for a formal charge to determine an operator (generator) are discussed, in connection with the well-known theorems of Goldstone and of Coleman. The symmetry transformations generated by this operator—given its existence—are also studied in some detail. For generators in a scattering theory, their additivity is proved and thus a simple way to characterize them from their matrix elements between one-particle states is provided. This characterization allows an immediate construction of the unitary operators implementing the symmetry transformations, and implies that all internal symmetry groups are necessarily compact. It is also indicated how to construct interacting fields having definite internal quantum numbers. The present status of the proof of Noether's theorem and of its converse is discussed in the light of the rather delicate properties of formal charges. (auth)

5417 APPLICATION OF Z = 0 APPROACH TO ρ-MESON AND $N^*(1240)$ RESONANCE. Braun, M. A. (Univ. of Delhi). Nucl. Phys.; B14: 413-24(1969).

The Z = 0 approach with a nonlocal interaction between the composite particle and elementary particles is generalized to spin 1 and $\frac{3}{2}$ particles. Applications are made to the ρ-meson and N^* (1240) resonance. The dispersion-technique is used to obtain solutions of the non-linear bootstrap equation that follows from the theory. The numerical results for the mass and width are (i) for ρ: $m_\rho = 390$ MeV, $\Gamma_\rho = 141$ MeV (ii) for N^*: $M = 1157$ MeV, $\Gamma_{N^*} = 61$ MeV. (auth)

Gravitation and General Relativity

5418 SCALE INVARIANCE AND THE ENERGY–MOMENTUM TENSOR. Bendix, Peter (Univ. of British Columbia, Vancouver). Can. J. Phys.; 48: 2371-5(15 Oct 1970).

A method is described by which an energy-momentum tensor can be constructed such that in addition to the usual properties of this tensor it acquires the property of scale invariance in the absence of masses and charges. (The new energy-momentum tensor constructed here is not the source of the gravitational field however.) It is shown that the usual construction for the massless Klein–Gordon field yields an energy-momentum tensor which is not scale invariant, whereas using the construction described here, one finds a scale invariant energy-momentum tensor for this case. (auth) (Canada)

5419 SEARCH FOR GRAVITATIONAL RADIATION. Clemens, Reginald Willis. College Park, Md.; Univ. of Maryland (1969). 159p. University Microfilms Order No. 70-11,617.

Thesis.

A search made for astronomical sources of gravitational radiation is described. The weakness of the coupling constant in general relativity makes it impossible to attempt a wave-zone transmitter-receiver experiment at present, although a previous induction zone experiment was successful. Thus, the only sources of gravitational radiation with a large enough power output to be detectable in the wave zone are astronomical sources. Work is reported on a search made for continuous sources of gravitational radiation and for gravitational radiation from pulsars. The first of these gave a null result, and the second determined that the earth can not be instrumented as a detector for gravitational radiation from pulsars due to a large noise background from microseisms. Theoretical work is reported concerning the "events" that have excited

two spatially separated gravity wave detectors in time coincidence. These calculations show that although some of the events may be statistical in origin, the premise that they are all statistical fluctuations can be discarded. Calculations are also made of the range at which the source of these events can be located and still be detectable with the gravity wave detectors considering first the bare detector bar, and then the bar and its associated electronics. (Diss. Abstr. Int., B)

5420 EXISTENCE THEOREM FOR THE INTEGRAL DIFFERENTIAL EQUATION SYSTEM OF EINSTEIN–LIOUVILLE. Choquet-Bruhat, Yvonne (Univ., Paris). Compt. Rend., Ser. A; 271: 625–8(28 Sep 1970). (In French).

The general energy inequalities of Leray–Gaarding–Dionne and a fixed point theorem are used to establish the existence of a solution of the Cauchy problem for the Einstein–Liouville coupled system in Sobolev spaces. The local problem is solved using the relevant coordinates to describe the system and the result is extended about a given initial variety. (France)

5421 RELATIVITY REEXAMINED. Brillouin, Leon. New York; Academic Press Inc. (1970). 119p. $6.75.

The topics discussed are quantum theory and relativity, some problems of restricted relativity, gravitation and relativity quantized atomic clocks, and distinction between mathematical sets of coordinates and physical frames of reference. Also considered are the special relativity Doppler effect, relativity and gravitation, and a gravistatic problem with spherical symmetry. (J.F.P.)

5422 NEW SUPERFLUID RELATIVITY GYROSCOPE. Ensley, D. L. (Univ. of California, Livermore). J. Appl. Phys.; 41: 4840–50(Nov 1970).

Experiments were performed in which mechanical radiation pressure, generated by a megahertz sound field in helium II, successfully supported a metal sphere three dimensionally. Because the field's forces are spherically symmetrical and stable, and because the isothermal environment provided by the quantum coherence properties of helium II eliminates convection currents, only extremely small stray torques act on the suspended mass. It is demonstrated that stray torques less than 10^{-7} dyn cm were present on the early test model, consistent with the theoretical predictions. Also presented is the predicted performance, based upon these results, of a more refined superfluid gyroscope which demonstrates the feasibility of observing general relativistic gyroscopic motion with a gyroscope rigidly connected to the earth. A proposed experiment to discriminate between Einstein's theory and competing theories of gravitation by measuring the spin–spin interaction between a gyroscope and the spinning earth is also discussed. (auth)

Scattering Theory

5423 (IFVE-STF-69-65) SOLUTION OF THE UNITARITY EQUATION FOR THE ELASTIC SCATTERING AMPLITUDE AT HIGH ENERGY. Khrustalev, O. A.; Savrin, V. I.; Tyurin, N. E. (Gosudarstvennyi Komitet po Ispol'zovaniyu Atomnoi Energii SSSR, Serpukhov. Institut Fiziki Vysokikh Energii). 1969. 21p. (In Russian). Dep. NTIS (U. S. Sales Only).

The unitarity equation is solved for the elastic scattering amplitude at high energy and at $-t \ll S$, when the contribution of the inelastic processes and the phase of a purely elastic scattering are given. (auth)

5424 (IFVE-STF-69-83) ON BEHAVIOR OF THE DIFFRACTION PEAK WIDTH AT HIGH ENERGIES IN THE CASE OF GAUSSIAN POTENTIAL . Volkov, G. G.; Mestvirishvily, M. A.; Rcheulishvili, G. L. (Gosudarstvennyi Komitet po Ispol'zovaniyu Atomnoi Energii SSSR, Serpukhov. Institut Fiziki Vysokikh Energii). 1969. 6p. (In Russian). Dep. NTIS (U. S. Sales Only).

The estimation of the diffractional peak width for scattering on the Gaussian type potentials is presented. (auth)

5425 (JINR–P4-5332) LOWER BOUNDS FOR THE SCATTERING PARAMETERS. Zakhariev, B. N.; Permyakov, V. P.; Fenin, Yu. I. (Joint Inst. for Nuclear Research, Dubna (USSR). Lab. of Theoretical Physics). 1970. 14p. (In Russian). Dep. NTIS (U. S. Sales Only).

The theorem about the variational bounds for definite combinations of K-matrix elements in the reactions with rearrangement of particles is proved. (auth)

5426 (NYO–2263-TA-226) CROSSED CHANNEL PARTIAL WAVE EXPANSIONS AND THE BETHE–SALPETER EQUATION. Saunders, L. M.; Saxton, O. H. N. (Princeton Univ., N. J. Joseph Henry Labs.); Tan, Chung-I (Princeton Univ., N. J. Joseph Henry Labs. Brown Univ., Providence, R. I. Dept. of Physics). Sep 1970. Contract AF49(638)-1545. 24p. Dep. NTIS.

The Bethe–Salpeter equation for the direct channel absorptive part of the scattering amplitude is analyzed in the ladder approximation to investigate the relation between SO(1,3) and SO(1,2) crossed channel partial wave analyses. The SO(1,2) expansion, used when the momentum transfer Q is space-like, is studied in detail in the limit $Q_\mu \to 0$. The connection between the SO(1,3) and SO(1,2) partial wave amplitudes at $Q_\mu = 0$ is obtained explicitly, as is the familiar result that a Toller pole is equivalent to an infinite sequence of integrally spaced Regge poles at $Q_\mu = 0$. (auth)

5427 OMNES EQUATION AND SUPERCONVERGENCE RELATIONS. Alberi, G. (Univ., Trieste, Italy); Mosconi, B.; Soper, P. J. Lett. Nuovo Cim.; 4: 761–6(24 Oct 1970).

Solutions to singular integral equations containing n bound-state poles are examined. It is shown that certain n superconvergence relations must be satisfied in order to admit a solution of the Omnes equation for the case of n bound states. (L.B.S.)

5428 ALLOWED SPECTRUM IN DUAL-RESONANCE MODELS. Gliozzi, G. (Istituto Nazionale di Fisica Nucleare, Turin); Galzenati, E.; Musto, R.; Nicodemi, F. Lett. Nuovo Cim.; 4: 991–6(21 Nov 1970).

The existence of Ward-like identities in dual-resonance models implies that there are intermediate states not coupled to the external particles (spurious states), leading to the problem of identifying the states actually contributing to the amplitude. The total amplitude in the dual-resonance model is given by the sum of the contributions corresponding to all noncyclic permutation of the external lines. Exploiting only the invariance of the full amplitude under twisting, it is found that it is possible to characterize the allowed states on the mass shell $|x,r\rangle$ as the solution of the equation $L_-|x,r\rangle = 0$ for even values of r. The solutions of this equation are given in closed form, and the method is generalized to give the solutions of each of the equations appearing in the Virasoro case. (L.B.S.)

5429 EIGENFUNCTION EXPANSIONS FOR SCATTERING IN TWO- AND THREE-PARTICLE SYSTEMS: AN APPROACH TOWARD OBTAINING EXACT SOLUTIONS OF THE FADDEEV EQUATIONS. Marcoux, Michael Oran. Bloomington, Ind.; Indiana Univ. (1969). 84p. University Microfilms Order No. 70-10,269.

Thesis.

The Lippman-Schwinger integral equation describing three-particle scattering by pair interaction has a noncompact kernel which prevents the application of present techniques for solving such an equation. The equation is transformed by L. D. Faddeev into coupled integral equations, the kernels of which are compact. This reformulation is achieved by introducing three scattering operators for the various single pair interactions defined on three-particle hilbert space. The Faddeev equations are transformed once more by using two scattering operators where only a single interaction is absent. The new equations are precisely of the same form as the Faddeev equations although more concise: $T_i(e) = T_i^1(e) + T_i^1(e)G_0(e)T_j(e)$, $T_i(e) = T_j^1(e) + T_j^1(e)G_0(e)T_i(e)$, where $T_i^1(e) = T_i(e)$ for $V_j = 0$, etc. A method of solving this last set of equations is proposed wherein sufficiency conditions on the interactions are stated to achieve an exact separable decomposition of the kernels. As is well known, this converts the integral equations to matrix equations which can then be routinely solved. The separable decomposition is equivalent to Weinberg's "quasi-particle" method for a three-particle system in which a single pair interaction is absent. Finally, an attempt is made to formulate the quasi-particle problem in a manner that can be practically solved. There are numerous directions in which one can go and it remains to be seen which is best. An infinite set of coupled ordinary differential equations in two variables is proposed along with integral boundary conditions on the amplitudes. Alternately, a single integro-differential equation is stated which can be viewed as a perturbation on the Schrödinger equation. In both approaches, more work has to be done before calculation is practical. (Diss. Abstr. Int. B)

5430 TOPICS IN SCATTERING THEORY. McCartor, Gary Don. College Station, Tex.; Texas A and M Univ. (1969). 96p. University Microfilms Order No. 70-11,559.

Thesis.

It is shown, in a certain rather general sense of convergence, and with appropriate restrictions on the potential and expansion functions, that the Kohn variational principle converges to the

XUM

correct answer in the case of two-particle S-wave scattering. The two-particle Bethe-Salpeter equation is studied and a contour is given which makes the kernel for the equation describing the scattering of two baryons in the ladder approximation nonsingular in the energy range between the first and second inelastic thresholds. (Diss. Abstr. Int., B)

5431 SECOND QUANTIZED NONRELATIVISTIC TIME-DEPENDENT SCATTERING THEORY, AND A GENERALIZATION OF THE IN–OUT FORMALISM TO INCLUDE COULOMB POTENTIALS. Klein, James Robert. New York; Fordham Univ. (1969). 311p. University Microfilms Order No. 70-11,437.

Thesis.

A mathematically rigorous field-theoretic (second-quantized) version of nonrelativistic time-dependent scattering theory is discussed. The structure of a model second quantized scattering theory describing identical bosons interacting via two-body forces is examined in detail. The only restriction on the two-body potentials involved enters through the requirement that the Möller operators in the first quantized theory exist and have certain properties which are expected to hold in a physically reasonable scattering theory. These properties are shown to exist for a large class of potentials. Coulomb potentials are included explicitly in this class. Thus, given the first quantized theory, one can pass immediately to the second quantized theory. The model theory studied is general enough to describe the scattering of both simple (or "elementary") and composite particles. Heuristic considerations as found in textbook treatments of the formal theory of scattering, ill-defined limit procedures, and such unproved things as eigenfunction expansions are avoided by extensive use of Hilbert space theory. In view of the difficulties encountered in any relativistic quantum field theory of interacting fields with respect to both existence and particle interpretation, methods analogous to those used in the relativistic case are used wherever possible. The in-out formalism is shown to exist in the sense that in-out scattering states are well-defined, free in-out fields exist (one for each "stable" particle in the theory), and the S-matrix is well-defined and unitary. These properties are shown to be a consequence of the general properties of the Möller operators in the first quantized theory (orthogonality of ranges, intertwining property, asymptotic completeness). The role of the asymptotic condition and the type of convergence involved is stressed. The in-out fields are shown to be strong limits of interpolating fields in a precisely defined sense. These interpolating fields are constructed explicitly and are shown to reduce to the usual Heisenberg field operators when Coulomb forces are absent. Difficulties with Coulomb potentials are discussed. As a preface to the work on second quantized scattering theory, a review of the formalism of second quantization and of some mathematical problems involved is given. The work of Jauch, Dollard, et al. on the first quantized nonrelativistic time-dependent scattering theory is also reviewed. Finally, the nonrelativistic analogue of the results of Lehman, Symanzik, and Zimmermann for the relativistic case is given. Reduction formulas are derived and nonrelativistic "Yang-Feldman" equations are established. It is also shown how one can express certain operators in terms of the in-out fields. In particular, the S-matrix is expressed as an expansion in terms of normal-ordered polynomials in the in-out fields, and S-matrix elements for any scattering process are related to vacuum expectation values of time-ordered products of interpolating fields. (Diss. Abstr. Int., B)

5432 SEPARABLE EXPANSIONS OF THE TWO-BODY T-MATRIX AND THE THREE-BODY PROBLEM. Harms, Edward Albert. Troy, N. Y.; Rensselaer Polytechnic Inst. (1969). 204p. University Microfilms Order No. 70-11,319.

Thesis.

The theory of a one-term separable approximation called the unitary pole approximation (UPA) is developed in a manner suitable for bound or antibound states. Methods for handling the antibound state are discussed and a few examples are given. A new separable expansion of the two-body potential is derived. The expansion, called the unitary pole expansion (UPE), has as its first term the UPA, satisfies unitarity in all orders, and gives the correct bound state pole for the two-body T-matrix. The convergence of the UPE is examined by comparing the T-matrices arising from different orders in the expansion with actual T-matrices obtained by solving the Lippmann-Schwinger equation. Both purely attractive local potentials and realistic two-nucleon potentials with soft core repulsion are used. Convergence is found to be very rapid especially in the case of potentials with repulsion. The expansion is investigated further by performing three-body bound state calculations. The convergence of the UPE is more rapid than other series expansions and is especially good for potentials with repulsion. In this case one term gives a binding energy accurate to within 0.1 MeV. The results indicate that for the type of problem investigated separable potentials are valid for studying three-nucleon systems. Also a general derivation of three-body scattering and bound state equations is given assuming separable two-body potentials. The approach is based upon the Lovelace version of the Faddeev equations and allows for the full complexity of the two-nucleon potential including an arbitrary number of partial waves and an arbitrary number of separable terms in each partial wave. (Diss. Abstr. Int., B)

5433 REGGEIZED-ABSORPTION MODEL AND RELATED MATTERS. Moore, Robert John. Madison, Wis.; Univ. of Wisconsin (1969). 102p. University Microfilms Order No. 69-22,444.

Thesis.

An absorption formula of the Sopkovich type is first derived by summing an iterated set of two-body scattering amplitudes in the framework of a coupled-channel system of Bethe-Salpeter equations (in the ladder approximation) in the approximation of retaining the contribution which comes from having physical intermediate-state particles only. Use of Reggeized-exchange-amplitudes for the "Born" exchanges in such a scheme gives the Reggeized-absorption model. The correction terms, which correspond to the multiple-exchange of Regge poles, are shown to have forms which are reminiscent of Regge cuts. Using a purely imaginary elastic scattering amplitude, the correction term corresponding to double-exchange (input Regge pole plus the Pomeranchuk) is found to interfere destructively with the single-exchange term (input Regge pole), leading to the possibility of a diffraction zero in the differential scattering cross section. For the case of spin-1/2, spin-0 scattering the helicity nonflip and helicity flip amplitudes are found to have absorptive corrections which differ in form, and the relevance of this to the polarization of the final-state baryon in these scatterings is discussed for the exchange of both t- and u-channel Regge poles. The question of the importance of off-shell contributions to iterated scattering amplitudes is investigated from two points of view—nonrelativistic potential scattering theory and relativistic theory. The example of scattering by an attractive Yukawa potential is considered, and examination of the scattering amplitude correct through the second Born approximation (double-scattering) shows that off-energy-shell contributions are not expected to be important at high energy in a potential model, but may be important at low energy. On the other hand, examination of the scattering amplitude through double-exchange (box diagram) for the scattering of scalar mesons in a ϕ^3 theory suggests that off-mass-shell contributions may be important at high energy in a field-theoretic model. The eikonal approximation of Glauber for these model calculations is compared to the "exact" solutions (through double-exchange terms), and it is found to correctly reproduce the single-exchange terms exactly but to give only the high-energy limits of the on-shell parts of the double-exchange terms. Finally, the relevance of these considerations to the more general problem of high-energy particle-nucleus scattering is discussed. (Diss. Abstr. Int., B)

5434 RELATIVISTIC EIKONAL APPROXIMATION FOR SUPERPOSITION OF TWO INTERACTIONS AND COULOMB INTERFERENCE. Andreev, I. V. (Lebedev Inst. of Physics, Moscow). Yadern. Fiz.; 12: 634-7(Sep 1970). (In Russian).

The scattering amplitude is constructed for two interactions in relativistic eikonal approximation. The cancellation of contributions from different diagrams in this approximation as well as the application to the calculation of the Coulomb-nuclear interference, are considered. (auth)

5435 FACTORIZATIONS OF AMPLITUDES AND MOVING BRANCH POINTS. Kaidalov, A. B.; Karnakov, B. M. (Inst. of Theoretical and Experimental Physics, Moscow). Yadern. Fiz.; 12: 624-9(Sep 1970). (In Russian).

Factorization relations are obtained for amplitudes of various processes at $t = 0$ on the basis of general properties of moving two-reggeon cuts. A possible experimental test of these relations is discussed. (auth)

5436 CONNECTION OF THE FIELD MATRIX ELEMENT WITH THE PHASES OF TWO-CHANNEL S-WAVE SCATTERING. Kharakhan, M. L.; Shirokov, Yu. M. (Moscow Mining Inst.). Teor. Mat. Fiz.; 5: No. 1, 39-46(Oct 1970). (In Russian).

An explicit formula is obtained which connects the physical S-matrix of the two-channel scattering with the discontinuity on the kinematical cut of the scalar field matrix element $\langle 2|A(x)|0\rangle$. The result is the direct generalization of that obtained for the one-channel case. (auth)

5437 ANALYTICAL PROPERTIES OF THE RELATIVISTIC SCATTERING AMPLITUDE IN QUASI-POTENTIAL APPROACH.

Skachkov, N. B. (Joint Inst. for Nuclear Research, Dubna, USSR). Teor. Mat. Fiz.; 5: No. 1, 57-65(Oct 1970). (In Russian).

The analytical properties of the relativistic scattering amplitude with respect to the momentum transfer and energy are studied in the quasipotential approach. The spectral representation in momentum transfer is obtained, which takes into account the relativistic kinematics, as does the analogous dispersion relation in quantum field theory. (auth)

5438 FAST-PARTICLE SCATTERING ON COULOMB AND SHORT-RANGE POTENTIALS. Savrin, V. I.; Tyurin, N. E.; Khrustalev, O. A. (Inst. of High-Energy Physics, Serpukhov, USSR). Teor. Mat. Fiz.; 5: No. 1, 47-56(Oct 1970). (In Russian).

Fast particle scattering on the potential, which is the sum of the Coulomb and short-range potentials, is considered. The representations of scattering amplitude for large and small scattering angles as well as the Bethe's interferention formula are obtained. (auth)

5439 SIGNATURE IN THE BARDAKCI AND RUEGG MODEL. Zakrzewski, W. J. (Cambridge Univ., Eng.). Nucl. Phys.; B14: 458-72(1969).

It is shown how signature can be incorporated into the Bardakçi–Ruegg model of the $2 \rightarrow 3$ processes. This is essentially done by summing the contributions of all the diagrams obtained by permitting external lines. In the calculations a slightly different form of the Bardakçi–Ruegg amplitude is used. Difficulties in removing odd daughters are discussed. The higher production processes are also mentioned and it is argued that the series of Hopkinson and Plahte should be regarded as coming from integral expressions with a wider range of convergence. (auth)

5440 VENEZIANO AMPLITUDES FOR REGGEONS AND SPINNING PARTICLES. Campbell, D. K.; Olive, D. I.; Zakrzewski, W. J. (Cambridge Univ., Eng.). Nucl. Phys.; B14: 319-29(1969).

The factorization of the residue associated with the spin-J particle lying on the leading trajectory in the multi-particle Veneziano model is exhibited and amplitudes for any number of such particles are derived. (auth)

Particle Accelerators

Refer also to abstracts 4366, 5285, 5360, 5506, 5507, 5550, and 5680.

5441 (AAEC/TM-544) BOPTIC: A BEAM TRANSPORT PROGRAM IN FORTRAN IV. Dangerfield, G. R.; Walsh, R. L. (Australian Atomic Energy Commission Research Establishment, Lucas Heights). Jul 1970. 44p. Dep. NTIS (U. S. Sales Only).

The FORTRAN IV program BOPTIC is designed to analyze the behavior of a beam of monoenergetic charged particles in a postacceleration beam transport system. This system may comprise any number of bending magnets, quadrupole magnets or flight tubes, arranged in any desired order. Matrix methods are employed to calculate the displacement and divergence of the beam as it traverses the system. Various optimization features are included. (auth) (Australia)

5442 (CEA-N-1232, pp 161-212) SACLAY ELECTRON LINEAR ACCELERATOR. (Commissariat a l'Energie Atomique, Saclay (France). Centre d'Etudes Nucleaires). (In French).

Topics covered are: first operation of the 300 MeV Saclay electron linear accelerator (ALS); ALS facilities under construction or study; and associated experimental techniques (electronic devices, computers, magnetic measurements, wire chambers). (France)

5443 (CONF-700314–, Paper 1) SERPUKHOV PROGRAM. Fields, T. (Argonne National Lab., Ill.). 13p.

From Conference on expectations for particle reactions at the new accelerators, March 30–April 1, 1970, Madison, Wisconsin.

Experiments nearing completion and those which are about to begin are listed. A description of the Serpukhov experimental facilities is also given. (J.F.P.)

5444 (CONF-700314–, Paper 2) EXPERIMENTAL PROGRAMME AT THE CERN INTERSECTING STORAGE RINGS. Winter, K. (European Organization for Nuclear Research, Geneva (Switzerland)). 34p.

From Conference on expectations for particle reactions at the new accelerators, March 30–April 1, 1970, Madison, Wisconsin.

The expected performance and limitations of the CERN intersecting storage rings are discussed. The experiments to be performed using the ISR include total cross section measurements, differential cross sections of elastic proton–proton scattering, diffraction dissociation and exchange processes, and particle production. (J.F.P.)

5445 (CONF-700314–, Paper 3) POSSIBILITIES FOR THE N.A.L. PROGRAM. Walker, James K. (National Accelerator Lab., Batavia, Ill.). 12p.

From Conference on expectations for particle reactions at the new accelerators, March 30–April 1, 1970, Madison, Wisconsin.

The main features of the National Accelerator Laboratory synchrotron are reviewed. The design and development are discussed. (J.F.P.)

5446 (DNPL/R-7, pp 215-43) PRELIMINARY RESULTS WITH ADONE. Grilli, M. (Comitato Nazionale per l'Energia Nucleare, Frascati (Italy). Laboratori Nazionali di Frascati).

From Vector meson production and omega–rho interference.

A brief account was given of the experiment set-ups and the analytical criteria, including luminosity measurements. Theoretical predictions were also discussed. Future experimental programmes were indicated. (18 references) (UK)

5447 (IFVE-OP-69-68) ISOCHRONOUS MAGNETIC OPTICAL SYSTEMS. Kotov, V. I.; Rzaev, R. A. (Gosudarstvennyi Komitet po Ispol'zovaniyu Atomnoi Energii SSSR, Serpukhov. Institut Fiziki Vysolikh Energii). 1969. 18p. (In Russian). Dep. NTIS (U. S. Sales Only).

On the basis of the formalism of four-dimensional matrices, symmetrical isochronal optical systems are considered. The properties of these systems are investigated on two examples in detail. (auth)

5448 (JINR-P9-5299) CHARGED RELATIVISTIC ELECTRON RING IN THE HELICAL MAGNETIC FIELD. Bonch-Osmolovsky, A. G. (Joint Inst. for Nuclear Research, Dubna (USSR). Lab. of High Energy). 1970. 21p. (In Russian). Dep. NTIS (U. S. Sales Only).

The conditions necessary for the ring equilibrium in the homogeneous and weakly focusing magnetic fields in the presence of the azimuthal component of the magnetic field are given. (auth)

5449 (JINR-P9-5311) DEUTERON ACCELERATION IN THE LHE SYNCHROPHASOTRON. Kazansky, G. S.; Mikhailov, A. I.; Pychkov, G. P. (Joint Inst. for Nuclear Research, Dubna (USSR). Lab. of High Energy). 1970. 9p. (In Russian). Dep. NTIS (U. S. Sales Only).

The basic principles are presented of the deuteron and α-particle acceleration in the synchrophasotron in two stages (the first stage up to 300 MeV, and the second one up to the maximum energy). The choice of the cycle of the synchrophasotron accelerating system and the peculiarities of the transition from one stage to another are described. The experimental results are given. (auth)

5450 (LA-4465, pp 4.1-2) CHARACTERISTICS OF AlK AND Al(NH_4) ALUM AS NEW MATERIALS FOR POLARIZED PROTON TARGETS. Bendt, Philip J. (Los Alamos Scientific Lab., N. Mex.).

From LASL contributions to the 3rd international symposium on polarization phenomena in nuclear reactions, Madison, Wisconsin, August 31–September 4, 1970.

5451 (LA-4465, pp 8.1-2) PROPOSED ULTRA-LOW TEMPERATURE POLARIZED TARGET FOR USE WITH SINGLE-BURST NEUTRON SOURCES. Lemley, J. R.; Keyworth, G. A. (Los Alamos Scientific Lab., N. Mex.).

From LASL contributions to the 3rd international symposium on polarization phenomena in nuclear reactions, Madison, Wisconsin, August 31–September 4, 1970.

5452 (LA-4465, pp 9.1-2) PERFORMANCE OF THE LASL POLARIZED SOURCE. McKibben, J. L.; Lawrence, G. P.; Ohlsen, Gerald G. (Los Alamos Scientifc Lab., N. Mex.).

From LASL contributions to the 3rd international symposium on polarization phenomena in nuclear reactions, Madison, Wisconsin, August 31–September 4, 1970.

5453 (LA-4465, pp 10.1-2) ABSOLUTE BEAM POLARIZATION DETERMINATION FOR THE LASL LAMB-SHIFT SOURCE BY THE QUENCH RATIO METHOD. Ohlsen, Gerald G.; Lawrence, G. P.; Keaton, P. W. Jr.; McKibben, J. L.; Armstrong, D. D. (Los Alamos Scientific Lab., N. Mex.).

From LASL contributions to the 3rd international symposium on polarization phenomena in nuclear reactions, Madison, Wisconsin, August 31–September 4, 1970.

5454 (LA-4465, pp 18.1-16) TRANSFER MATRIX METHOD FOR CALCULATING SPIN ABERRATIONS IN THE TRANSPORT OF POLARIZED BEAMS. Stevens, Ralph R. Jr.; Ohlsen, Gerald G. (Los Alamos Scientific Lab., N. Mex.).

From LASL contributions to the 3rd international symposium on polarization phenomena in nuclear reactions, Madison, Wisconsin, August 31–September 4, 1970.

5455 (LA–4465, pp 23,1-2) FIGURES OF MERIT FOR POLARIZED DEUTERON BEAMS. Keaton, P. W. Jr.; Ohlsen, Gerald G. (Los Alamos Scientific Lab., N. Mex.).

From LASL contributions to the 3rd international symposium on polarization phenomena in nuclear reactions, Madison, Wisconsin, August 31–September 4, 1970.

5456 (LA–4465, pp 33,1-2) PROPOSED 0.4 K POLARIZED PROTON TARGET CRYOSTAT FOR LAMPF. Edeskuty, F. J.; Hwang, C. F.; Williamson, K. D. Jr. (Los Alamos Scientific Lab., N. Mex.).

From LASL contributions to the 3rd international symposium on polarization phenomena in nuclear reactions, Madison, Wisconsin, August 31–September 4, 1970.

5457 (NP–18507) TECHNIQUE FOR MEASURING PHASE CHARACTERISTICS OF AN ION BEAM. Abroyan, M. A.; Golubev, V. P.; Solnyshkov, A. I.; Tarvid, G. V. (Scientific Research Inst. of Electro-Physical Apparatus, Leningrad (USSR)). 1970. 7p. (In Russian). Dep. NTIS (U. S. Sales Only).

Devices are described which permit the measurement of phase characteristics of a beam by 4-slit and 2-slit methods. Four-dimensional volume is measured by the device, which photorecords the diaphragming beam with subsequent photometering. Emittance is measured by the device with electrical modulation of the diaphragming beam. (auth)

5458 (NP–18510) STUDY OF THE PROCESSES OF REDISTRIBUTION OF PHASE DENSITY IN INTENSE PROTON BEAMS EXTRACTED FROM A DUO-PLASMATRON TYPE ION SOURCE. Kuznetsov, V. S.; Abroyan, M. A.; Fidel'skaya, R. P. (Scientific Research Inst. of Electro-Physical Apparatus, Leningrad (USSR)). 1970. 12p. (In Russian). Dep. NTIS (U. S. Sales Only).

Measurement results of the phase density redistribution in intense proton beams, extracted from a duoplasmatron type ion source are given and analyzed. It is found that the distribution in real beams differs considerably from that of microcanonical. With the help of numerical solutions of the system describing the beams with an arbitrary distribution, it is shown that the phase density redistribution takes place, and as a consequence, the current density redistribution and considerable distortion of the phase volume configuration occur. (auth)

5459 (NP–18516) CALCULATION OF LOSSES IN SUPERCONDUCTING COILS SUPPLIED BY PULSED CURRENT. Lefrancois, C. (Commissariat a l'Energie Atomique, Saclay (France). Centre d'Etudes Nucleaires). 3 Aug 1970. 43p. (In French). Dep. NTIS (U. S. Sales Only).

A method to calculate the loss energy produced in a pulsed superconducting magnet of any shape wound with solid core wires is described. The formulae are based on the BEAN's critical state model, and are derived from the simple case of a plane slab in a uniform external magnetic field, carrying a transport current perpendicular to the direction of this field and proportional to it. The computer program takes account of the magnetic field distribution inside the winding, and the total losses in the magnet are obtained by a numerical integration of the elementary losses in small volumes of superconductor which can be assumed to be in a uniform magnetic field. The results are in good agreement with experimental results obtained in our laboratory. (auth)

5460 (NP-18517) INFLUENCE OF COUPLING RESONANCES $2\nu_z \pm \nu_x =$ INTEGER ON MECHANISM OF THIRD RESONANCE EJECTION. Leleux, G. (Commissariat a l'Energie Atomique, Saclay (France). Centre d'Etudes Nucleaires). Feb 1970. 23p. (In French). Dep. NTIS (U. S. Sales Only).

Since in the process of ejection there can be considerable increase in the vertical emittance, a study of the coupling resonances $2\nu_z \pm \nu_x =$ integer taking into account with greater precision the energy dispersion of the beam. For simplification, the variation of hexapolar forces as a function of particle energy is not considered. The cumulative mechanism leading to an increase of the vertical emittance is discussed. (J.F.P.)

5461 (NP–18519) ANALYSIS OF THE EFFECTS OF DISPLACEMENT AND OF POSITIONING OF THE MEASURING PROBE OF A MAGNETIC FIELD ON THE PROPERTIES OF AN OPTICAL SYSTEM. Ribes, M.; Turck, B. (Commissariat a l'Energie Atomique, Saclay (France). Centre d'Etudes Nucleaires). [1970]. 44p. (In French). Dep. NTIS (U. S. Sales Only).

It is usual to ask the magnetic measurement systems to give accuracies better than the accuracy needed for the experiment. It is shown that this requirement is often not necessary. Using a trajectory program for a beam issued from a point object, the image displacements and aberrations created by positional errors of the measuring probe are analyzed. It is pointed out that the effect of these errors depends on the direction in which the probe is moved. Also, it is shown that if the errors at each point of measurement are not independent, the overall effect may be, in some cases, practically negligible. (auth)

5462 (PPAD–676-E) NASA BRIEFING ON HIGH ENERGY, HEAVY ION CAPABILITIES OF THE PRINCETON-PENNSYLVANIA ACCELERATOR. White, M. G. (Princeton-Pennsylvania Accelerator, Princeton, N. J.). 8 Oct 1970. Contract AT(30-1)-2137. 20p. Dep. NTIS.

The energy distribution and relative abundance of high-energy heavy ions in cosmic rays are discussed, and hazards of heavy cosmic particles to man and equipment are briefly considered. The capabilities of the Princeton–Pennsylvania Accelerator for acceleration of heavy ions are described. A proposal for a ceramic vacuum chamber for the accelerator is outlined, and expected parameters for heavy-ion acceleration are tabulated. (W.H.K.)

5463 (RHEL/R–199) NEW TARGET MATERIAL FOR THE RUTHERFORD FROZEN TARGET. Russell, F. M. (Rutherford High Energy Lab., Chilton (England)). Sep 1970. 11p. Dep. NTIS (U. S. Sales Only). UK 2s. 6d.

Measurements were made of the nuclear-spin relaxation times for various organic target materials in the temperature region below 2K and at magnetic field strengths greater than 25 kG. A mixture of glycerol : water with porphyrexide gives long relaxation times and high polarizations and was selected for use in the Rutherford frozen polarized target. (auth) (UK)

5464 (RHEL/R–203) EQUATIONS AND FORMULAE FOR MAGNETS WITH AIR CORED WINDINGS OF SADDLE COIL TYPE. Coupland, J. H. (Rutherford High Energy Lab., Chilton (England)). Aug 1970. 27p. Dep. NTIS (U. S. Sales Only). UK 4s. 6d.

As most of the formulae and the integral rule which are derived and developed in this report are not widely known, it is hoped that this treatment will be useful in accelerator and other laboratories where there is a growing interest in high magnets of the "saddle-coil" type using superconducting windings. (auth) (UK)

5465 (RHEL/R–206) NIMROD OPERATION AND DEVELOPMENT. Quarterly Report, April 1–June 30, 1970. Gray, D. E. (ed.) (Rutherford High Energy Lab., Chilton (England)). Sep 1970. 14p. Dep. NTIS (U. S. Sales Only). UK 2s. 6d.

The Nimrod beam was on for high energy physics research for 89% of HEP scheduled operating time. Four experiments were completed and seven continued through this quarter. A "heat-pipe" transport system which increases the operational effectiveness of liquid hydrogen targets is described. The development of wire grid electrodes in electrostatic separators, resulting in very large reductions in conditioning times coupled with lack of sensitivity to contamination, is reviewed. Some preliminary notes are given on resonant extraction system tests on X3, Nimrod's third extracted proton beam. (auth) (UK)

5466 (RPP/A–81) FROZEN POLARIZED TARGET. Banks, P. H. T.; Cragg, D. A.; Madden, D. R.; Nicholas, D. J.; Pickles, D. C.; Read, S. F. J.; Russell, F. M.; Warner, G. P.; Williams, W. G. (Rutherford High Energy Lab., Chilton (England)). 27 Aug 1970. 16p. (CONF-700811–2). Dep. NTIS (U. S. Sales Only).

From 3rd International Symposium on Polarization Phenomena in Nuclear Reactions, Madison, Wis.

A polarized proton target currently under development at the Rutherford Laboratory is described. The target has the twin objectives of high polarization and large angular access. In this new polarized target the material is first polarized by the solid-effect and when a high degree of polarization has been established the temperature of the target is lowered until the process of depolarization through spin relaxation becomes very slow. In this state the polarization is "frozen-in" and the target transferred to a holding magnetic field of low homogeneity but giving large angular access. Details are given of the design of the target together with the results obtained from work carried out to find a suitable material for this type of target. Porphyrexide-doped aqueous solutions of glycerol and porphyrexide-doped aqueous solutions of 1-butanol were studied. (auth)

5467 VERSATILE SYSTEM FOR IN-BEAM MOESSBAUER SPECTROSCOPY. Hardy, K. A.; Hicks, J. A.; Russell, D. C.; Wilenzick, R. M. (Tulane Univ., New Orleans). Rev. Sci. Instrum.; 41: 1652-4(Nov 1970).

An experimental system for Moessbauer studies following Coulomb excitation or nuclear reactions is described. A drift-free high velocity Doppler spectrometer is incorporated in

the apparatus, and a closed cycle helium refrigerator is used for cooling the target and absorber to low temperatures. The system also operates successfully as a conventional Moessbauer spectrometer with radioactive sources. (auth)

5468 CURRENT PROFILE MONITOR FOR USE IN SCANNING ELECTRON BEAM IRRADIATIONS. Okabe, Shigeru; Tsumori, Kunihiko; Tabata, Tatsuo (Radiation Center, Sakai, Japan). Rev. Sci. Instrum.; 41: 1537-9(Nov 1970).

A current profile monitor for the scanning electron beam from the accelerator is described. It utilizes the fact that the electrons scattered through large angles by the exit window of the scanner show a profile similar to that of the main beam at the irradiation site. The scattered electrons are collected by small probes arranged in a linear array parallel to the scanning direction, and the beam profile in this direction is displayed by a storage oscilloscope or an X–Y recorder. This device has been used for electrons of energies 4 to 16 MeV from a linear accelerator and proved to be useful for continual monitoring with negligible disturbance to the irradiation in progress. (auth)

5469 STUDIES OF HIGH-CURRENT RELATIVISTIC ELECTRON BEAM PROPAGATION. Hammer, David Andrew. Ithaca, N. Y.; Cornell Univ. (1969). 142p. University Microfilms Order No. 70-5796.

Thesis.

The propagation of high current relativistic electron beams is treated theoretically and experimentally. It was predicted that the amount of current that a neutralized uniform current density electron beam can carry is limited because of the pinch forces of the beam's self-magnetic field. Three models are developed involving distinct physical mechanisms which allow the propagation of arbitrarily large currents by an electron beam confined to a finite radius, and then some experimental observations made on high current electron beams are presented. (Diss. Abstr. Int., B) (TSS)

5470 TARGET HANDLING SYSTEM FOR THE 200-GeV PROTON ACCELERATOR. Grimson, J. H.; Lindberg, J. F.; Maschke, A. W.; Simanton, J. R.; Simon, J. P. (National Accelerator Lab., Batavia, Ill.). Trans. Amer. Nucl. Soc.; 13: 847(Nov 1970).

From Meeting of the American Nuclear Society, Washington, D. C. See CONF-701102.

5471 BIG EUROPEAN ACCELERATOR. Adams, John Bertram (European Organization for Nuclear Research, Geneva). Recherche (Paris); 1: 319-26(Sep 1970). (In French).

It has been more than ten years since the possibility of constructing a 300 GeV proton synchrotron was first considered. A comparison of the relative costs of the different types of machines has led to the study of a system constructed in sections without a magnet. It was shown that economies could be made on two points: the magnet gaps and the experimental building locations. Today, two projects present themselves to the CERN community. Project A has the intention of considering the total resources which the intending participating member states are able to supply. Project B considers the recommendations of the ECFA and the possibility of using the existing CERN synchrotron as an injector to attain the 300 GeV. (France)

5472 PHOTON ACTIVATION ANALYSIS WITH THE LIVERMORE ELECTRON LINEAR ACCELERATOR. Marsh, K. V. (Univ. of California, Livermore). Lab. Pract.; 19: 1017-24 (Oct 1970).

A description of the Livermore 30-MeV photon activation analysis facility is presented along with some results of the analysis of high-purity Be and Li. Construction details of the pneumatic transfer, irradiation, and counting equipment are given, and a bibliography of recent work in the field is included. (auth) (UK)

5473 OPERATIONAL CHARACTERISTICS AND ENTRANCE CONDITIONS OF A HIGH-CURRENT RELATIVISTIC ELECTRON BEAM ACCELERATOR. Clark, John Joseph. Ithaca, N. Y.; Cornell Univ. (1969). 146p. University Microfilms Order No. 70-5762.

Thesis.

The design and construction of a 500-kV, 100-kA, 50-nsec-pulse-duration electron beam accelerator used as a basic plasma-physics research tool are discussed. The operational characteristics of a high-field-emission diode, which is used to launch the electron beam in such an accelerator system, are discussed in detail. The diode is shown empirically to have two separate and distinct modes of operation, which depend on the diode aspect ratio, pressure, and total diode voltage and current. The first mode gives evidence of laminar electron flow, and the diode impedance is shown to be less than that predicted by the Child–Langmuir space-charge-limited flow equation by a factor of two, for diode pressures ranging from 5×10^{-3} to 10^{-5} torr. The second mode indicates a pressure-dependent diode "pinching" phenomenon in the gap region, wherein the electrons are radially compressed and for which the diode impedance is equal to or greater than Child–Langmuir impedance predictions. The electrons which form the beam are emitted from a metal–dielectric "plasma" cathode. The dielectric sections of this "plasma" cathode are shown to make an important contribution to the spatial uniformity of cathode emission by means of a surface multipactor or surface flashover effect that vaporizes enough of the dielectric to allow a plasma sheath to form in front of the cathode. There is evidence that the electrons, upon release from this sheath under space-charge-limited conditions, then determine the overall diode impedance. Simple theoretical models for estimating the conditions under which diode pinching should occur are extended and verified. Data on these pinch conditions are of extreme interest because they predetermine the propagation characteristics of the electron beam as it propagates in a drift space. Diode pinching has been observed to occur (by radiographs and distributed calorimetry) for values of $\nu/\gamma|_{\text{measured}}$ above 80% of $\nu/\gamma|_{\text{critical}}$. The time history of diode pinching was studied by means of a fast-streak/framing camera and indicates the following: since diode-pinching build-up times are generally about 30 nsec and are pressure independent, the electrons but not the ions are radially compressed; the degree of pinching in the diode (and therefore the electron spatial distribution) is pressure dependent whereas the overall diode impedance is pressure independent—at least over the available range of 5×10^{-3} to 10^{-5} torr; the electron trajectory angles at the anode plane increase up to what may be a saturation value as ν/γ increases from .66 to 1.05. Recommendations for the elimination of such diode pinching, when and if desirable, are made. (TSS) (Diss. Abstr. Int., B)

XUM

PHYSICS (NUCLEAR)

Neutron Interactions with Matter

Refer also to abstracts 4374, 4821, 4822, 5141, 5143, 5154, 5230, and 5237.

5474 (KFK–1197) NUCLEAR SPECTROSCOPY USING RADIATIVE NEUTRON CAPTURE AND NEUTRON-INDUCED FISSION. Michaelis, W. (Kernforschungszentrum, Karlsruhe (West Germany). Institut fuer Angewandte Kernphysik). Feb 1970. 30p. (CONF-700204–2). Dep. NTIS (U. S. Sales Only).

From IAEA Meeting on Research Reaction Utilization, Rome, Italy.

Experiments at research reactors in the field of nuclear spectroscopy are sketched. This research is performed using the radiative neutron capture reaction or neutron-induced fission. Current techniques are described very briefly. The following topics are discussed: studies of configuration mixing and two-quasiparticle states in nuclei with deformed equilibrium shape, investigations of shell-model configurations in even spherical nuclei, and the search for new regions of stable deformation or shape-isomers. Future trends are discussed, and some recommendations for future activities are given. (auth)

5475 (LA–4465, pp 7.1-2) UNDERGROUND NUCLEAR EXPLOSION AS A POLARIZED NEUTRON SOURCE. Keyworth, G. A.; Lemley, J. R. (Los Alamos Scientific Lab., N. Mex.).

From LASL contributions to the 3rd international symposium on polarization phenomena in nuclear reactions, Madison, Wisconsin, August 31–September 4, 1970.

5476 (ORNL-TM–2903) LEGCK, A SUBROUTINE TO ANALYZE LEGENDRE COEFFICIENTS FOR NEGATIVITY IN THE ANGULAR DISTRIBUTION. Irving, D. C. (Oak Ridge National Lab., Tenn.). 10 Sep 1970. 37p. Dep. CFSTI.

LEGCK is a subroutine package designed to analyze Legendre expansions of angular distributions for negative regions. The analysis is divided into two portions. The first check determines if the Legendre coefficients are "possible," that is, if any negativity is due only to the truncation of the Legendre expansion. The second test determines if there are regions of negativity in the truncated expansion and where such negative regions are. The report describes the subroutines in the package and discusses the operations performed by each subroutine. (auth)

5477 (UCRL–50857) COLLIMATION OF FAST NEUTRONS. Lent, Edward M. (California Univ., Livermore. Lawrence Radiation Lab.). 20 Apr 1970. 20p. Dep. NTIS.

The purpose of the work was to design collimator systems to enable measurement of the neutron spectra from nuclear devices. Various aspects of shielding and wall scattering are discussed, and relationships are presented to define collimator response to extended sources. A collimator system designed on the basis of the principles set forth has been used successfully in a field test. (auth)

5478 METHOD FOR SOLVING THE TIME-DEPENDENT NONHOMOGENEOUS THERMALIZATION EQUATION BY REDUCING IT TO A SYSTEM OF CAUCHY SINGULAR EQUATIONS. Caprini, I.; Corciovei, A.; Protopopescu, V. (Inst. of Atomic Physics, Bucharest). Rev. Roum. Phys.; 15: 533-48(1970).

The solution of the time-dependent nonhomogeneous thermalization equation is found by solving directly the Green's function problem, corresponding experimentally to a monoenergetic neutron pulse source. An analytical method developed by Leonard and Mullikin in radiative transfer problems is applied. Performing a finite Laguerre polynomial expansion of the scattering kernel, one employs a type of duality which yields a singular integral equation for the total source operator of the problem. In a particular case, the Cauchy equation is regularized and completely solved by quadratures. (auth)

5479 GALERKIN METHOD SOLUTION OF THE NEUTRON SLOWING DOWN EQUATIONS. Chiarella, C. (Wollongong University Coll., New South Wales). J. Nucl. Energy; 24: 133-42(Jun 1970).

An approximate formula for the calculation of the resonance escape probability in an isolated resonance is obtained from a Galerkin method solution of the slowing down equations with the narrow resonance approximation applied to the external moderator. For certain U/D_2O and U/C lattices comparison of the exact resonance escape probability with the Galerkin method and λ method approximations to the resonance escape probability indicates that the Galerkin method yields a quite good approximation which is often superior to the λ method. (auth) (UK)

5480 PRECISION OF WIGNER'S APPROXIMATION. Pashkin, Yu. G. At. Energ. (USSR); 28: 147-8(Feb 1970). (In Russian).

Wigner's approximation of the rational asymptotic neutron escape probability makes the simplifying assumption that the formula for the effective resonance integral is assumed to be the same for the heterogeneous and homogeneous cases. The resultant error is indicated by tabulating the pertinent values calculated by the approximation method and exactly by computer. In view of the fact that Wigner's approximation was found to result in a large (about 10%) error in the effective resonance integral, it was considered desirable to determine the asymptotic collision probability with a higher precision, as well as to derive an analytic expression for the effective resonance integral. This requires an examination of the mathematical meaning of Wigner's approximation. Comparison of the values revealed that use of the improved formula helps to reduce the error to less than 2%. (TTT)

5481 MEASUREMENT OF INTERACTION CROSS SECTIONS OF 0.3 TO 5.0 MeV NEUTRONS WITH AIR. Terekhin, V. A.; Kryzhanovskii, V. A.; Poretskii, L. B. This paper was summarized in At. Energ. (USSR); 26: 454-5(May 1969) as paper No. 296. (In Russian).

Spectra of 0.3–5.0 MeV neutrons which have penetrated air layers 40, 167, and 370 m thick were measured and used to calculate average cross sections. These are compared with average cross sections calculated by formula. The agreement between calculation and experiment indicates that the calculated values of the average cross sections are good to about 2%. (R.W.R.)

5482 APPROXIMATE SCATTERING KERNEL FOR NEUTRON SLOWING DOWN. Yamamura, Yasunori; Sekiya, Tamotsu (Osaka Univ.). J. Nucl. Sci. Technol. (Tokyo); 7: 478-81(Sep 1970).

One of the principal difficulties in analytic approaches to the neutron slowing down problem arises from the complicated form possessed by the scattering kernels. By taking into account the higher terms of the Taylor expansion of the collision term, a more nearly exact synthetic kernel than that obtainable by the G.G. method is derived. This approximate kernel possesses the following merits: It is improved to the extent that the Placzek oscillation appears in the collision density following the occurrence of a sharp scattering or absorption resonance; the P_4 expansion of the elastic scattering angular distribution can be meaningfully taken into account; and the method can be easily extended to approximate treatment of the degradation term in the integro-differential equation of the P_1 approximation. (R.W.R.)

5483 THEORY OF NEUTRON SCATTERING FROM LATTICE VIBRATIONS. Tani, Kensuke (Kyoto Univ.). J. Phys. Soc. Jap.; 29: 594-605(Sep 1970).

The theory of neutron scattering from lattice vibrations is redeveloped from the first principles. The expression for the scattering cross section contains factors depending on the anharmonicity explicitly, in addition to the conventional results and recent results based on the phonon Green function. Near the Curie temperature T_c of displacive-type ferroelectrics a certain term in the factors depends anomalously on temperature because of softening of frequencies and becomes comparable to or even greater than the conventional term. A similar deviation near the magnetic critical point is discussed briefly. A general theory of phonons at arbitrary temperature is also developed by using the correlation function method which includes the ordinary phonon theory as the limiting case of the absolute zero, and the dispersion of the Cochran mode is determined. A self-consistent method of determining the frequency of a phonon is proposed. (auth)

5484 SLOWING DOWN OF NEUTRONS IN MIXTURES BY THE METHOD OF GREEN'S FUNCTIONS. Tang, Ing M.; Kastenberg, William E. (Univ. of California, Los Angeles). J. Nucl. Energy; 24: 207-16(Jul 1970).

The formulation and approximate solution to the slowing down problem in homogeneous media by the method of Green's functions for a binary mixture of nuclei is presented. Some numerical examples are included. As a first step, solutions to the purely scattering problem for a binary mixture are obtained in closed form. These elementary solutions are then used as Green's functions for the absorption case. This transformation yields a Volterra in integral equation having the correct asymptotic limits for the flux when properly normalized. In general, the resulting integral equation cannot be solved in closed form, thus several approximate results were obtained. (auth) (UK)

5485 NEUTRON DIFFUSION PARAMETER DETERMINATION USING THE PULSED NEUTRON SOURCE TECHNIQUES WITH SPHERES OF HEAVY WATER. McGhee, B. W.; Haroon, M. R.; Graham, W. W. (Georgia Inst. of Tech., Atlanta). Nucleus (Karachi); 6: 126-37(Jul-Sep 1969).

The neutron diffusion parameters of heavy water were determined by the pulsed neutron source technique using D_2O in spherical aluminum shells. The decay of the neutron population as a function of time was monitored using a ^3He ionization chamber and a ^6Li-loaded plastic scintillator, with a multichannel analyzer. The time-asymptotic decay constant for each sphere was calculated from the experimental data by the channel-dropping method. Values of the geometric buckling were calculated using the average radius, with a wall-thickness correction and two methods of calculating the extrapolation length. Temperature and purity corrections were made to the decay constants, and the diffusion parameters were obtained by fitting to both three and four parameter expansions for the decay constant in the buckling. The infinite medium decay constant was both calculated and evaluated by fitting. The theory, analysis, and equipment of the pulsed source experiment and this investigation are discussed. The results of the investigation are presented and discussed. (auth)

5486 ENTRAINMENT OF NEUTRONS BY A MOVING MEDIUM. Vasil'ev, G. Ya.; Kaminker, D. M.; Konoplev, K. A.; Kostritsa, A. A. At. Energ. (USSR); 28: 356-7(Apr 1970). (In Russian).

There is a possibility of observing neutron entrainment by a moving medium experimentally from the change in diffusion length at velocities of the moving medium a good deal less than the average velocity of the thermal motion of the neutrons. A collimated neutron beam (54 × 11 mm) fell perpendicularly on a water-filled tube having an internal diameter of 96 mm and a wall thickness of 4 mm. In order to decrease the background of scattered neutrons, the water tube was covered with sheet cadmium 0.5 mm thick having holes to admit the neutron beam. The neutron flux was determined from the activation of gold foil placed along the tube axis at distances of 4.15, 5.65, 7.15 and 8.65 cm on both sides from the beam center. The measurements were carried out at a flow velocity of 15.4 m/sec in the water tube. The water temperature was held constant at 8°C. The results of the measurements showed the existence of neutron entrainment by the moving medium because of an observed change in thermal neutron flux with a change in the direction of water flow. The value of the diffusion coefficient was found to be 3.67×10^4 cm^2/sec. The value found by this new method is in good agreement with other reported values of the diffusion coefficient. (TTT)

5487 ASYMPTOTIC BEHAVIOR OF A GENERALIZED CADILHAC THERMALIZATION MODEL. Caprini-Gologan, I. (Inst. of Atomic Physics, Bucharest). Rev. Roum. Phys.; 15: 669-80(1970).

The convergence of the generalized Cadilhac thermalization model in the epithermal region is investigated by comparing its predictions with the exact asymptotic solution of Corngold. Some numerical calculations for the first iteration of the model are performed and the experimental implications of the results are discussed. (auth)

5488 CORRECTIONS TO GREEN-TYPE SCATTERING KERNEL FOR THE STUDY OF NEUTRON THERMALIZATION. Caprini, I.; Protopopescu, V.; Purica, I. (Inst. of Atomic Physics, Bucharest). Rev. Roum. Phys.; 15: 141-50(1970).

The validity of the general model for the study of neutron thermalization proposed by Purica is analyzed from a mathematical standpoint. In this model one considers that the thermalization kernel can be suitably approximated by a Green function and a remainder, whose contribution becomes more and more unimportant, by using an iterative procedure. The convergence of this method is established by proposing a suitable form, experimentally justified, for the corrections to the Green-type part of the scattering kernel. (auth)

5489 TIME-DEPENDENT NEUTRON SPECTRA MEASUREMENTS IN WATER. Menzel, J. H.; Slovacek, R. E.; Gaerttner, E. R. (Rensselaer Polytechnic Inst., Troy, N. Y.). Nucl. Sci. Eng.; 42: 119-36(Nov 1970).

Time-dependent neutron spectra in the center of an externally pulsed finite ($7.16 \times 25.02 \times 25.4$ cm^3) H_2O medium at 37.8°C were measured over an energy range $0.01 \text{ eV} < E < 0.25$ eV and for times extending from approximately zero to 100 μsec after the pulse. The phased mechanical chopper time-of-flight technique using the Rensselaer LINAC was combined with an on-line computer to obtain these measurements. Experimental results are presented in the form of the time behavior of neutrons at various energies (neutron life histories), time moments, neutron spectra at various times, and the steady-state spectrum, as well as the energy velocity moments. Time-dependent diffusion theory calculations using a 70-group Haywood-II hydrogen kernel and a mass-16 free gas oxygen kernel were performed with and without spatial harmonics. The results of the theoretical calculations employing time-dependent diffusion theory indicate that the average velocity is within 2% of the asymptotic value after 16 μsec, less than the measured value. The agreement between experiment and calculation is, however, considerably better than had been obtained in the only previously published study; in that investigation, time-dependent spectra measurements made on a large water medium indicated that the thermalization time was greater than 100 μsec. (M.H.R.)

5490 PARTIAL SEPARATION OF THE VARIABLES FOR CALCULATING THE EFFICIENCY OF A PLATE LATTICE. Gurin, V. N. This paper was summarized in At. Energ. (USSR); 24: 258(Mar 1968) as paper No. 186. (In Russian).

Analytic expressions were derived for the capture rate of epithermal neutrons in a plate of cell with constant boundary conditions. These expressions are used to formulate the method of partial separation of the space and energy variables as when the boundary conditions vary slightly with energy. The first concept of this method, though in a somewhat different form, was suggested by V. V. Orlov in 1958. The space–energy distribution of the neutrons can be found by solving the age–diffusion equation with constant boundary conditions and constant source of the epithermal neutrons. The solution is found by a Laplace transformation. For boron-containing absorbants in a heavy moderator, the error of the method is –10%. (M.H.R.)

5491 THEORY OF NEUTRON SCATTERING IN DIATOMIC CRYSTALS CONTAINING IMPURITIES. Augst, G. R. (Inst. of Physics, Tbilisi, USSR). Sov. Phys.-Solid State (Engl. Transl.); 12: 1031-5(Nov 1970).

Translated from Fiz. Tverd. Tela; 12: 1311-16(May 1970).

By use of retarded Green's functions, expressions are obtained for the coherent and incoherent differential cross sections for the inelastic scattering of neutrons on diatomic cubic crystals containing small impurity concentrations. The problem is solved in a general form without including the changes in the force constants. The possibility of removing the degeneracy where the phonon branches cross because of the impurities introduced is analyzed. The changes in the force constants are included for an NaCl type crystal within the nearest-neighbor interaction model. (auth)

5492 NEUTRON VELOCITY SPECTRUM IN HEAVY NUCLEI. Kostritsa, A. A.; Neimotin, E. I. This paper was summarized in At. Energ. (USSR); 24: 61(Jan 1968) as paper No. 176. (In Russian).

The spectral characteristics of neutrons placed in a medium of heavy nuclei moving with velocity are considered. It is shown how the energy lost by the neutrons during deceleration goes into heating the neutron gas as a function of two variables, the absorption cross section and the nuclear speed. (R.W.R.)

5493 CALCULATION BY THE MONTE-CARLO METHOD OF NEUTRON DISTRIBUTION IN MEDIA CONTAINING HYDROGEN. Starikov, V. N.; Enikeeva, F. Kh. This paper was summarized in At. Energ. (USSR); 26: 282-3(Mar 1969) as paper No. 267. (In Russian).

The Monte-Carlo method is used to calculate the spatial distribution of neutrons with an energy $E \leq 0.1$ eV in a borehole-seam system. The method of correlated sampling is used, and a new algorithm for drawing the direction of the neutrons and the symmetry of the individual parts of the neutron trajectories is devised. Certain approximations are made because of the presence of hydrogen in the rocks and drilling fluid. The spatial distribution of neutrons for boreholes of 30-cm diameter filled with salt water (250 g/l NaCl) is given. A seam of limestone with different hydrogen contents was investigated. The density of neutrons is a maximum at the borehole–seam boundary. (R.W.R.)

5494 SLOW-NEUTRON SCATTERING CROSS-SECTIONS OF DEBYE-SPECTRUM SPACE LATTICES. Weil, J. W. (International Atomic Energy Agency, Vienna). Czech. J. Phys.; 20: 950-2(1970).

The expression for the classical high-temperature limit of the self-correlation function in energy–momentum space in the case of a system of harmonic oscillators is already known. This result is extended to a vibrating lattice with a Debye spectrum. The self-correlation function is related to the slow-neutron double-differential scattering cross section. (R.W.R.)

XUM

5495 STUDY OF NEUTRON TRANSPORT IN IRON WITH AN ASSESSMENT OF DATA FILES. Malaviya, B. K.; Kaushal, N. N.; Becker, M.; Burns, E. T.; (and others) (Rensselaer Polytechnic Inst., Troy, N. Y.). Trans. Amer. Nucl. Soc.; 13: 757-8(Nov 1970).

From Meeting of the American Nuclear Society, Washington, D. C. See CONF-701102.

5496 AGE AND FAST EFFECT FOR FISSION AND 14-MeV NEUTRON SOURCES IN Be AND BeO: SENSITIVITY TO CROSS-SECTION DATA. Weisbin, C. R.; Goldstein, H.; Lidofsky, L. J. (Columbia Univ., New York). Trans. Amer. Nucl. Soc.; 13: 758-9(Nov 1970).

From Meeting of the American Nuclear Society, Washington, D. C. See CONF-701102.

5497 EVALUATION OF THE COMPTON CURRENTS FROM A 14-MeV NEUTRON SOURCE IN THE INTERMEDIATE ALTITUDE RANGE. Brooks, Joan (Mathematical Applications Group, Inc., White Plains, N. Y.; Celnik, Jacob; Schamberger, R. D. Trans. Amer. Nucl. Soc.; 13: 856-7(Nov 1970).

From Meeting of the American Nuclear Society, Washington, D. C. See CONF-701102.

5498 TIME DEPENDENT MONOENERGETIC NEUTRON TRANSPORT IN A FINITE SLAB WITH INFINITE REFLECTORS. Newman, Perry Allan. Blacksburg, Va.; Virginia Polytechnic Inst. (1970). 145p. University Microfilms Order No. 70-13,693.

Thesis.

The initial-value transport problem of monoenergetic neutrons migrating in a thin slab surrounded by infinitely thick reflectors is solved by using the normal-mode expansion technique of Case. The results obtained indicate that the reflector may give rise to a branch-cut integral term typical of a semi-infinite medium while the central slab may contribute a summation over discrete residue terms. Exact expressions are obtained for these discrete time eigenvalues, and numerical results are presented showing the behavior of real time eigenvalues as a function of the material properties of the slab and reflector. These eigenvalues are finite in number and all of them may disappear into the branch cut or continuum as the material properties are varied; such disappearing eigenvalues correspond to exponentially time-decaying modes. The two largest eigenvalues can be compared with critical dimensions of slabs and spheres, and it is shown that the numerical values agree with criticality results of others. In the limit of purely absorbing reflectors or a bare slab, the present solution has the properties which have been previously reported by others who used the Lehner–Wing technique to solve corresponding problems. (auth) (Diss. Abstr. Int., B)

5499 COHERENT NEUTRON SCATTERING IN POLYCRYSTALLINE ZIRCONIUM HYDRIDE. Mariani, Leo Paul. University Park, Pa.; Pennsylvania State Univ. (1969). 51p. University Microfilms Order No. 70-7229.

Thesis.

A computational scheme for the numerical evaluation of the various types of slow-neutron coherent-scattering cross sections of any given sample of polycrystalline zirconium hydride is devised. At some prespecified temperature and sample composition, one can numerically generate any of a group of slow-neutron coherent-scattering cross sections. This group includes the doubly differential, the angular differential, and the total one-phonon inelastic—as well as the angular differential and the total elastic—coherent-scattering cross sections. In order to represent the cross sections of interest mathematically, theoretical expressions resulting from the exploitation of the first Born approximation and the Fermi pseudopotential are suitably modified to accommodate a perfect polycrystal, which is dynamically represented in the harmonic approximation. The lattice-dynamical parameters, which are implicit in these mathematical expressions, are determined via the application of a central-force lattice-dynamical model. An innovation is introduced into the Born and von Kármán method of lattice-dynamical calculation by applying the Monte Carlo technique of random sampling to the selection of wave-propagation vectors from the reduced Brillouin zone. Numerical calculations are carried out with the aid of the code system COSCAT. Various calculated results are presented and discussed. Comparisons with experimental data and previously calculated results are also presented. (auth) (Diss. Abstr. Int., B)

5500 COLD NEUTRON SCATTERING AT CH_3-, CH_2-, AND OH-PROTONS IN METHANOL AND ETHANOL. Fischer, C. O. (Hahn-Meitner-Institut fuer Kernforschung, Berlin). Ber. Bunsenges. Phys. Chem.; 74: 696-9(Jul 1970).

Total cross sections of CH_3OH, CH_3OD, CH_2DOH, CHD_2OH, CD_3OH, CH_3CH_2OH, CH_3CH_2OD, CH_3CD_2OH, and CD_3CH_2OH were measured with cold neutrons between 5 Å and 15 Å. The slopes S of the scattering cross section per proton vs the neutron wavelength indicate the different microdynamic behavior of the individual protons inside the molecule. In methanol $S = 3.4 \pm 0.8$ barn/Å for an OH-proton and $S = 12.1 \pm 0.5$ barn/Å for a CH_3-proton; this difference is explained by a relatively free internal CH_3 rotation and a hindered motion of the OH-proton. In ethanol the OH-proton with 1.3 ± 0.8 barn/Å seems to be much more hindered than in methanol, whereas a CH_3-proton with $S = 9.8 \pm 0.4$ barn/Å behaves quite similarly to a CH_2-proton with 9.1 ± 0.5 barn/Å. (auth)

5501 SOLUTION OF THE INITIAL-VALUE NEUTRON-TRANSPORT PROBLEM FOR A SLAB WITH INFINITE REFLECTORS. Newman, Perry A. (Langley Research Center, Hampton, Va.); Bowden, Robert L. J. Math. Phys. (N. Y.); 11: 2445-58(Aug 1970).

The initial-value transport problem of monoenergetic neutrons migrating in a thin slab surrounded by infinitely thick reflectors is solved for isotropic scattering by using the normal-mode expansion technique. The results obtained indicate that the reflectors may give rise to a branch-cut integral term typical of a semi-infinite medium while the central slab may contribute a summation over discrete residue terms. Exact expressions are obtained for these discrete time eigenvalues, and sample numerical results are presented showing the behavior of real-time eigenvalues as a function of the material properties of the slab and reflector. In the limit of purely absorbing reflectors or a bare slab, the present solution has the properties which have been previously reported. (auth)

5502 DEPENDENCE OF SCATTERING TRANSPORT LENGTH ON NEUTRON ENERGY IN H_2O, D_2O, AND GRAPHITE. Goshchitskii, B. N.; Gusev, V. V.; Konstantinov, L. V.; Korotovskikh, P. M.; Sidorov, S. K.; Chernobrovkin, V. V.; Chudinov, V. G. At. Energ. (USSR); 29: 91-5(Aug 1970). (In Russian).

Both the intensity and the energy spectrum of neutrons extracted from a through tangential reactor channel by means of various scatterers placed inside were studied. It has been shown that such experiments utilizing the "reciprocal" scattering geometry may be used for determining the scattering transport neutron length in scatterer material. Measurements were made in H_2O, D_2O, and graphite with the water-cooled and water-moderated reactor UBB-2 tangential channel in the neutron energy region 0.12 eV to 0.004 eV. The results of the measurements are compared with those of other authors. For D_2O a decrease of scattering transport length was found within a neutron energy region 0.011 eV to 0.015 eV (wave lengths of about 2.8 to 2.3 Å). This result has not been found in other works. In all other cases the results are in good agreement with data available in the literature. (auth)

5503 IMPROVEMENTS IN AND RELATING TO A NEUTRON-EMITTING TRITIATED TARGET. Detaint, Jacques (to Commissariat a l'Energie Atomique). British Patent 1,205,359. 16 Sep 1970. Priority date 8 Aug 1968, France.

A tritiated target is described for the production of neutrons by the $T(d,n)^4He$ reaction. The tritiated layer is separated from its passive support by a thin barrier formed of a metal in which hydrogen isotopes diffuse slowly: deuterons pass easily through this barrier into the support, but the barrier retards diffusion of tritium out of the tritiated layer into the support. Deuterium may be removed from the downstream side of the support by evacuating the cavity formed there or by filling the cavity with a solution which forms an electrolyte or a chemical reagent. Thus, a neutron-emitting target is obtained in which elimination of the deuterium or diffusion of the deuterium into the support substantially restricts the speed at which the tritiated layer is enriched with deuterium at the expense of tritium, so greatly lengthening the total life of the target. (R.W.R.)

5504 CORRECTION OF THE FINITE VOLUME OF SCATTERER EFFECT ON THE MEASUREMENT OF DIFFERENTIAL ELASTIC AND INELASTIC NEUTRON CROSS SECTIONS. PART I. CORRECTION OF SINGLE-SCATTERING PROCESSES. Hermsdorf, D.; Hoehn, J.; Seelinger, D. (Technische Univ., Dresden). Kernenergie; 13: 263-4(Aug 1970). (In German).

A method is shown which estimates the effect on the measured values of the finite geometry of the scatterer used for measuring differential cross sections. In part I, the effects of flux attenuation and angular spread are discussed, and a way is found to take them into account. Parts II and III deal with estimating the fraction of multiply scattered neutrons and their influence on the measured values. Correction of these effects was done by Blok and Jonker's method. With this, the method hitherto used only for calculating elastic multiple scattering is extended to the correction of multiple scattering effect in inelastic scattering processes. A condition is given for applicability of Blok and Jonker's correction method. All partial computations described in this paper and necessary for de-

termining the corrections were programmed for the small-size computer "Cellatron SER 2c." The programs are available by order, or there is a possibility of the authors' undertaking such computations. (auth)

5505 NONASYMPTOTIC STRUCTURE OF THE SPECTRUM OF RETARDED NEUTRONS IN THE NEIGHBORHOOD OF "INTERMEDIATE" RESONANCES. Luk'yanov, A. A.; Yusef, M. Yu. A. This paper was summarized in At. Energy. (USSR); 26: 540(Jun 1969) as paper No. 308. (In Russian).

The structure of the spectrum of neutrons in a two-component retarding medium, observed close to the resonance of the heavy component, is connected with the nonasymptotic part of the retardation equation. This equation is solved numerically for a hydrogen–iron medium for the resonance $E_0 = 28$ keV in ^{56}Fe for various values of the cross section of the retarding medium. Values of the effective resonance integral J_{eff} are tabulated. At certain concentrations, the values of J_{eff} differ substantially from the results of the NR approximation because of the nonasymptotic part of the spectrum at resonance; indeed, the effective integral may exceed the value for the case of "infinite dilution." (R.W.R.)

Nuclear Properties and Reactions, A≤5

Refer also to abstracts 5389, 5549, 5600, 5716, 5735, 5812, 5870, and 6160.

5506 (CEA-N-1232, pp 81-159) INVESTIGATIONS WITH THE CYCLOTRONS. (Commissariat a l'Energie Atomique, Saclay (France). Centre d'Etudes Nucleaires). (In French).

Topics covered are: spectroscopic study of ^{209}Bi by inelastic proton scattering; interpretation of 24.5 MeV proton elastic and inelastic scattering experiments on Sn even isotopes; measurement of spin correlation coefficients in proton–proton scattering at 37 MeV; inelastic scattering of polarized protons by ^{24}Mg, ^{28}Si and ^{40}Ca; pick-up reactions with polarized protons on ^{57}Fe, ^{53}Cr, ^{64}Ni, ^{90}Zr, ^{91}Zr, ^{118}Sn, ^{119}Sn; inelastic scattering of polarized protons on ^{208}Pb, near the $g_{\frac{9}{2}}$ analog resonance; deuteron break-up with 10.5 and 24.5 MeV polarized protons; elastic scattering of 18 MeV polarized protons from ^{27}Al; study of $^{56}Fe(^3He,t)^{56}Co$ at 30.2 MeV; one-hole states in ^{138}Ba, ^{140}Ce, ^{142}Nd, ^{144}Sm; energy levels of ^{49}Sc from $^{48}Ca(^3He,d)$ and (α,t); scattering of polarized deuterons on ^{12}C and ^{90}Zn; experimental techniques (scattering chamber, semiconductor particle detectors, electronics, on-line computers, high energy magnetic spectrometry with high resolution). (France)

5507 (LA-4465) LASL CONTRIBUTIONS TO THE 3rd INTERNATIONAL SYMPOSIUM ON POLARIZATION PHENOMENA IN NUCLEAR REACTIONS, MADISON, WISCONSIN, AUGUST 31–SEPTEMBER 4, 1970. (Los Alamos Scientific Lab., N. Mex.). Jul 1970. Contract W-7405-eng-36. 98p. (CONF-700811). Dep. CFSTI.

The 35 papers included are listed by title only in NSA. (J.W.R.)

For abstracts of individual papers see: 4321, 4391, 5450–5456, 5475, 5508–5525, 5553, and 5802–5807.

5508 (LA-4465, pp 1.1-2) PHASE SHIFTS FROM n-^{4}He ELASTIC SCATTERING EXPERIMENTS NEAR 20 MeV. Niiler, A.; Drosg, M.; Hopkins, J. C.; Seagrave, J. D. (Los Alamos Scientific Lab., N. Mex.).

From LASL contributions to the 3rd international symposium on polarization phenomena in nuclear reactions, Madison, Wisconsin, August 31–September 4, 1970.

5509 (LA-4465, pp 2.1-2) REACTANCE MATRIX ANALYSIS OF THE d-^{3}He, p-^{4}He SYSTEM AT 10-MeV DEUTERON LABORATORY ENERGY. Hale, G. M.; Dodder, D. C.; Witte, K. (Los Alamos Scientific Lab., N. Mex.).

From LASL contributions to the 3rd international symposium on polarization phenomena in nuclear reactions, Madison, Wisconsin, August 31–September 4, 1970.

5510 (LA-4465, pp 3.1-3) COMPARISON OF DOUBLE SCATTERING AND POLARIZED ION SOURCE MEASUREMENTS OF ^{4}He(d,d)^{4}He POLARIZATION AT 11.5 MeV. Starkovich, V. S.; Ohlsen, G. G. (Los Alamos Scientific Lab., N. Mex.).

From LASL contributions to the 3rd international symposium on polarization phenomena in nuclear reactions, Madison, Wisconsin, August 31–September 4, 1970.

5511 (LA-4465, pp 5.1-2) ELASTIC SCATTERING OF POLARIZED TRITONS. Armstrong, D. D.; Keaton, P. W. Jr.; Veeser, L. R. (Los Alamos Scientific Lab., N. Mex.).

From LASL contributions to the 3rd international symposium on polarization phenomena in nuclear reactions, Madison, Wisconsin, August 31–September 4, 1970.

5512 (LA-4465, pp 6.1-2) STUDY OF THE ^{3}He(d,p)^{4}He REACTION. Keaton, P. W. Jr.; Armstrong, D. D.; Dodder, D. C.; Lawrence, G. P.; McKibben, J. L.; Ohlsen, Gerald G. (Los Alamos Scientific Lab., N. Mex.).

From LASL contributions to the 3rd international symposium on polarization phenomena in nuclear reactions, Madison, Wisconsin, August 31–September 4, 1970.

5513 (LA-4465, pp 12.1-2) NEUTRON POLARIZATION IN THE T(d,n)^{4}He REACTION USING A POLARIZED INCIDENT BEAM. Broste, W. B.; Lawrence, G. P.; McKibben, J. L.; Ohlsen, G. G.; Simmons, J. E. (Los Alamos Scientific Lab., N. Mex.).

From LASL contributions to the 3rd international symposium on polarization phenomena in nuclear reactions, Madison, Wisconsin, August 31–September 4, 1970.

5514 (LA-4465, pp 13.1-2) PRELIMINARY MEASUREMENTS OF NEUTRON POLARIZATION FROM THE D(d,n)^{3}He REACTION USING A POLARIZED INCIDENT BEAM. Simmons, J. E.; Broste, W. B.; Lawrence, George P.; Ohlsen, Gerald G. (Los Alamos Scientific Lab., N. Mex.).

From LASL contributions to the 3rd international symposium on polarization phenomena in nuclear reactions, Madison, Wisconsin, August 31–September 4, 1970.

5515 (LA-4465, pp 14.1-2) ASYMMETRIES IN DEUTERON SCATTERING FROM A POLARIZED ^{3}He TARGET. Watt, Bob E.; Leland, W. T. (Los Alamos Scientific Lab., N. Mex.).

From LASL contributions to the 3rd international symposium on polarization phenomena in nuclear reactions, Madison, Wisconsin, August 31–September 4, 1970.

5516 (LA-4465, pp 15.1-2) POLARIZATION OF 22-MeV NEUTRONS ELASTICALLY SCATTERED FROM LIQUID TRITIUM AND DEUTERIUM. Seagrave, J. D.; Hopkins, J. C.; Kerr, E. C.; Sherman, R. H.; Niiler, A.; Walter, R. K. (Los Alamos Scientific Lab., N. Mex.).

From LASL contributions to the 3rd international symposium on polarization phenomena in nuclear reactions, Madison, Wisconsin, August 31–September 4, 1970.

5517 (LA-4465, pp 16.1-2) POLARIZATION IN NUCLEON–DEUTERON SCATTERING AT MEDIUM ENERGIES. Franco, Victor (Brooklyn Coll., N. Y. Los Alamos Scientific Lab., N. Mex.).

From LASL contributions to the 3rd international symposium on polarization phenomena in nuclear reactions, Madison, Wisconsin, August 31–September 4, 1970.

5518 (LA-4465, pp 19.1-2) ABSOLUTE POLARIZATION DETERMINATION OF MASS-3 NUCLEI. Keaton, P. W. Jr.; Armstrong, D. D.; Veeser, L. R. (Los Alamos Scientific Lab., N. Mex.).

From LASL contributions to the 3rd international symposium on polarization phenomena in nuclear reactions, Madison, Wisconsin, August 31–September 4, 1970.

5519 (LA-4465, pp 22.1-2) QUADRATIC RELATIONS BETWEEN THE T(d,n)^{4}He OBSERVABLES. Ohlsen, Gerald G.; Gammel, J. L.; Keaton, P. W. Jr. (Los Alamos Scientific Lab., N. Mex.).

From LASL contributions to the 3rd international symposium on polarization phenomena in nuclear reactions, Madison, Wisconsin, August 31–September 4, 1970.

5520 (LA-4465, pp 24.1-2) STUDY OF ^{3}He(d,d)^{3}He SCATTERING AT 10 AND 12 MeV. Dodder, D. C.; Armstrong, D. D.; Keaton, P. W. Jr.; Lawrence, G. P.; McKibben, J. L.; Ohlsen, Gerald G. (Los Alamos Scientific Lab., N. Mex.).

From LASL contributions to the 3rd international symposium on polarization phenomena in nuclear reactions, Madison, Wisconsin, August 31–September 4, 1970.

5521 (LA-4465, pp 28.1-2) SCATTERING OF POLARIZED PROTONS BY TRITONS AT 13.6 MeV. Detch, J. L. Jr.; Jett, J. H.; Jarmie, Nelson (Los Alamos Scientific Lab., N. Mex.).

From LASL contributions to the 3rd international symposium on polarization phenomena in nuclear reactions, Madison, Wisconsin, August 31–September 4, 1970.

5522 (LA-4465, pp 29.1-2) POLARIZATION ANGULAR DISTRIBUTION FROM THE T(d,n)^{4}He REACTION AT 7.0 AND 11.4 MeV. Broste, W. B.; Simmons, J. E. (Los Alamos Scientific Lab., N. Mex.).

XUM

From LASL contributions to the 3rd international symposium on polarization phenomena in nuclear reactions, Madison, Wisconsin, August 31–September 4, 1970.

5523 (LA–4465, pp 30,1-2) NEUTRON–HELIUM POLARIZATION AT 27.3 AND 30.3 MeV. Broste, W. B.; Simmons, J. E. (Los Alamos Scientific Lab., N. Mex.).

From LASL contributions to the 3rd international symposium on polarization phenomena in nuclear reactions, Madison, Wisconsin, August 31–September 4, 1970.

5524 (LA–4465, pp 32,1-2) ASYMMETRIES IN PROTONS FROM THE REACTION OF DEUTERONS WITH A POLARIZED ^{3}He TARGET. Watt, Bob E.; Leland, W. T. (Los Alamos Scientific Lab., N. Mex.).

From LASL contributions to the 3rd international symposium on polarization phenomena in nuclear reactions, Madison, Wisconsin, August 31–September 4, 1970.

5525 (LA–4465, pp 34,1-2) ANALYZING POWER OF THE T($\vec{d}$,α)n REACTION AT LOW ENERGIES. Ohlsen, Gerald G.; McKibben, J. L.; Lawrence, G. P. (Los Alamos Scientific Lab., N. Mex.).

From LASL contributions to the 3rd international symposium on polarization phenomena in nuclear reactions, Madison, Wisconsin, August 31–September 4, 1970.

5526 (UCRL–19943) POLARIZATION AND CROSS-SECTION MEASUREMENTS IN p-^{4}He SCATTERING FROM 20 TO 40 MeV. Bacher, A. D.; Plattner, G. R.; Conzett, H. E.; Clark, D. J.; Grunder, H.; Tivol, W. F. (California Univ., Berkeley. Lawrence Radiation Lab.). Jul 1970. Contract W-7405-eng-48. 2p. (CONF-700811–1). Dep. NTIS.

From 3rd International Symposium on Polarization Phenomena in Nuclear Reactions, Madison, Wis.

An axially injected polarized proton beam was used to measure p–^{4}He elastic scattering between 20 and 40 MeV. The beam polarization was approximately 0.75. Angular distributions of cross sections and polarizations were measured at 2 MeV intervals at 20 laboratory angles between 17.5 and 150°. Results are shown for 24 and 26 MeV, as well as a contour plot of the complete polarization data. The effect of the 16.65-MeV $\frac{3}{2}^+$ state of ^{5}Li is clearly seen near 23 MeV. (R.W.R.)

5527 STRONG PION–ALPHA SCATTERING WITH ELECTROMAGNETIC CORRECTIONS. Christensen, Ronald Arlie. Berkeley, Calif.; Univ. of California (1969). 98p. University Microfilms Order No. 70-6076.

Thesis.

Electromagnetic corrections to pion–alpha scattering for spacelike q^2 are calculated to see if they can be used to determine r_π. The low-momentum t-dependence of the off-shell strong amplitude used in this calculation is determined with the help of crossing symmetry, current algebra, and PCAC. The relativistic corrections are found to be just as important as those which are also included in nonrelativistic treatments. When only the nonrelativistic terms are used, the large value of r_π (2 to 3 fermis) obtained recently from $\pi^+\alpha$ scattering is reproduced. Including the relativistic terms brings the resulting value of r_π down to approximately 1 fermi. This is consistent with the values obtained by using inelastic electron–proton scattering. The $\pi^+\alpha$ results are quite sensitive to the details of the $\pi\alpha$ nuclear interaction, which is only roughly approximated. (auth) (Diss. Abstr. Int., B)

5528 INELASTIC ELECTRON SCATTERING FROM ^{4}He AT LOW MOMENTUM TRANSFER. Walcher, Th. (Technische Hochschule, Darmstadt, Ger.). Z. Phys.; 237: 368-80(1970). (In German).

By using a liquid helium target, inelastic electron scattering from ^{4}He was investigated at momentum transfers below 0.5 fm^{-1} with improved resolution. The assignment 0^+ for the state at (20.10 ± 0.05) MeV (measured excitation energy) has been confirmed, and new values for the monopole matrix element (1.10 ± 0.16) fm^2 and the total width (270 ± 50) keV were derived. The giant resonance region shows evidence for the M2 resonance at 24 MeV. (auth)

5529 CHARGE FORM FACTOR OF ^{4}He WITH A TENSOR VELOCITY-DEPENDENT POTENTIAL. Jain, S. C. (Univ. of Allahabad, India). Indian J. Pure Appl. Phys.; 7: 645-6(Sep 1969).

The charge form factor of the alpha particle was calculated assuming its ground state wavefunction to be a mixture of the principal $^1S_0$ and $^5D_0^{(1)}$ states. The parameters of the wavefunction are obtained from a variational calculation of the binding energy of ^{4}He with a mixture of central velocity-dependent and tensor interactions. The charge form factor thus calculated was found to be somewhat greater than the experimental value. (auth)

5530 CALCULATION OF THE ELECTRODISINTEGRATION CROSS SECTION OF ^{4}He. Mueller-Arnke, A. (Technische Hochschule, Darmstadt, Ger.). Z. Phys.; 239: 223-34(1970).

In the framework of a previously discussed translationally invariant particle-hole model the T = 1 part of the differential electrodisintegration cross section of ^{4}He is calculated. A comparison with a recent measurement of this reaction gives fairly quantitative agreement, but it is suggested that in the region below 26 MeV excitation energy besides the 2^-T = 1 state, the 2^-T = 0 state presumably gives an appreciable contribution to the cross section thus indicating that the usually observed isospin selection rule does not work in this case. (auth)

5531 NEUTRON–DEUTERON BREAKUP MODELS. Cahill, R. T.; Sloan, I. H. (Univ. of New South Wales, Kensington). Phys. Lett.; 33B: 195-6(12 Oct 1970).

Numerical calculations on three separable-potential models for the three-body breakup reaction n + d → n + n + p at a neutron laboratory energy of 14.4 MeV are reported. Proton spectra in the n–n final-state interaction region are shown. (auth)

5532 POLARIZATION TRANSFER AT 0° IN THE D(d,n)^{3}He AND H(d,n)pp REACTIONS. Blyth, C. O.; Dunscombe, P. B.; McKee, J. S. C.; Pope, C. (Univ. of Birmingham, Eng.). Phys. Lett.; 33B: 211-12(12 Oct 1970).

The polarization transfer to the 0°-neutrons in the D(d,n)^{3}He reaction was measured, and arguments are given to show that simple stripping and rearrangement processes are sufficient to predict the result. Results for the H(d,n)pp reaction are included. (auth)

5533 KINEMATICALLY INCOMPLETE AND COMPLETE STUDIES OF THE BREAKUP OF ^{4}He BY 47-MeV PROTONS. Rogers, Joel Guild. Los Angeles; Univ. of California (1969). 128p. University Microfilms Order No. 70-8248.

Thesis.

The reactions induced by 47 MeV protons on ^{4}He were investigated in a kinematically incomplete experiment, by observing trion and deuteron spectra, and in a kinematically complete experiment, by observing correlated trion–proton spectra. The reactions studied included ^{4}He(p,d)^{3}He, ^{4}He(p,^{3}He)pn, and ^{4}He(p,t)pp. Natural helium gas targets were employed. The single-counter (kinematically incomplete) observations were performed with a dE/dx–E counter telescope. Spectra and angular distributions were analyzed using the Watson–Migdal Theory and direct reaction theory of Dar, respectively. The kinematically complete experiment was performed using two counter telescopes, one to observe ^{3}He's and tritons from the reactions ^{4}He(p,^{3}Hep)n and ^{4}He(p,tp)p and one to observe the correlated protons. Proton spectra showed strong enhancements from the nucleon–nucleon final state interactions, either pp or np, which were found to be in good agreement with the predictions of the Watson–Migdal Theory. A Chew–Low type extrapolation procedure was used to extract the np singlet scattering length giving the best fit to the proton spectrum from ^{4}He(p,^{3}Hep)n; this scattering length was in agreement with the value from np free scattering. The triton spectra showed peaks due to a sequential reaction process via the continuum resonance states of the ^{4}He system. These enhancements could be identified with previously observed ^{4}He levels of known spin and parity assignments. (TSS) (Diss. Abstr. Int., B)

5534 PROTON–PROTON QUASI-FREE SCATTERING IN THE p + d → p + p + n REACTION FOR E_p = 4.5 TO 13.0 MeV. Valkovic, V.; Von Witsch, W.; Rendic, D.; Phillips, G. C. (Rice Univ., Houston, Tex.). Phys. Lett.; 33B: 208-10 (12 Oct 1970).

Low-energy proton–proton quasi-free scattering was studied by coincidence detection of the two outgoing protons at $\theta_1 = -\theta_2 = 30°$ in the p + d → p + p + n reaction. The impulse approximation gives a good description of the measured spectral shapes and when normalized with a factor N = 0.2, describes the energy dependence of the peak cross section surprisingly well. (auth)

5535 ELECTROMAGNETIC STRUCTURE OF THE ^{3}He NUCLEUS. McCarthy, J. S.; Sick, I.; Whitney, R. R.; Yearian, M. R. (Stanford Univ., Calif.). Phys. Rev. Lett.; 25: 884-8 (28 Sep 1970).

The electromagnetic structure of the ^{3}He nucleus has been investigated by means of high-energy electron scattering. A separation of the charge and magnetic form factors has been accomplished. The charge form-factor data extend to q^2 = 20 fm^{-2} and exhibit a diffraction minimum at q^2 = 11.6 fm^{-2}; the magnetic scattering is measured to q^2 = 12.5 fm^{-2}. The results are discussed in terms of models for the charge and magnetic distributions of the nucleus. (auth)

5536 RADIOACTIVITY OF FREE NEUTRONS. Byrne, J. (Univ. of Sussex, Brighton, Eng.). Contemp. Phys.; 11: 359-86 (Jul 1970).

The theory of nuclear β-decay has developed in two stages. The presentation of Pauli's neutrino hypothesis at the 1933 Solvay Conference initiated the first stage, and a period of renewed activity followed the discovery in 1957 that parity was not conserved in the process. Two distinct interactions, of polar vector and axial vector form respectively, are responsible for β-decay, and the neutron is itself the most suitable β-active nucleus with which to study the basic properties of these interactions. For this reason a continuing effort has been made to refine and improve the precision of measurements of the β-decay of the neutron. In this article the most important features of the phenomenon of β-radioactivity are summarized, the techniques employed to study the radioactivity and related properties of free neutrons are discussed in some detail, and the experimental results interpreted in terms of established theory in the field of weak interactions. (auth) (UK)

5537 NUCLEAR FORCES IN o-s SHELL NUCLEI. Bruels, Mark Charles. Lawrence, Kan.; Univ. of Kansas (1969). 105p. University Microfilms Order No. 70-11,004.

Thesis.

The Bolsterli–Feenberg perturbation technique is applied to the recent potentials of Nestor, Davies, Krieger, and Baranger. Binding energies, RMS radii, and percentage D states are calculated for the o-s shell nuclei ^{2}H, ^{3}H, and ^{4}He. The Coulomb energies of ^{3}He and ^{4}He are also calculated. The Goldhammer potential is used to check programming accuracy. A novel approach to the separation method for solving the Bethe–Goldstone equation with reference spectrum techniques is presented. The separation method is found to be much less accurate than the Bolsterli–Feenberg perturbation method due to the explicit momentum dependence of the Baranger potentials. Agreement of the Baranger potentials with experiment is satisfactory. (Diss. Abstr. Int., B)

5538 EXPERIMENTAL OBSERVATION OF A PREDICTED EXCHANGE RESONANCE IN ^{3}He + ^{4}He ELASTIC SCATTERING. Brown, Ronald E. (Univ. of Minnesota, Minneapolis); Gross, E. E.; van der Woude, A. Phys. Rev. Lett.; 25: 1346-8(9 Nov 1970). (COO-1265-100).

Resonating-group calculations predict a backward-peaked, exchange resonance in the ^{3}He + ^{4}He elastic-scattering cross section. The energy dependence of the elastic-scattering differential cross section at 173.2° (c.m.) was measured and a resonance structure which has many of the predicted characteristics was observed. (auth)

5539 ANGULAR DISTRIBUTION OF THE PHOTONUCLEAR REACTION ^{3}He(γ,p)^{2}H. Bock, H.; Walenta, H. (Univ., Heidelberg). Z. Phys.; 238: 56-68(1970). (In German).

The angular distribution of the photonuclear reaction ^{3}He(γ,p)^{2}H was measured with an excitation energy E_x = 16 to 27 MeV by using a 3.25 MeV betatron. In agreement with a theoretical calculation of Bösch et al., the coefficients of the distribution $f(\theta) = b(a/b + \sin^2\theta(1 + \beta \cdot \cos\theta + \gamma \cdot \cos^2\theta))$ were found to be $a/b \leq 0.14$; $\beta = 0.77$ (+0.14; −0.07); $\gamma \leq 0.30$. This was the first attempt to use spark chambers as a detection device for photonuclear reactions in the low-energy range. It appears to be a promising new facility. (auth)

5540 ANGULAR DISTRIBUTION OF 24 MeV NEUTRONS SCATTERED BY PROTONS. Rothenberg, Lawrence Neil. Madison, Wis.; Univ. of Wisconsin (1970). 74p. University Microfilms Order No. 70-8328.

Thesis.

Recoil-proton spectra from n–p elastic scattering were measured for an incident neutron energy of 24.0 MeV. The neutron source was the T(d,n)^{4}He reaction at 0°. A counter telescope consisting of two silicon surface-barrier transmission detectors and a CsI crystal E detector was used to detect recoil protons from a polyethylene foil mounted on a platinum backing. The telescope was set at angles of 0, 15, 30, and 45°. A triple coincidence pulse produced by recoiling protons simultaneously satisfying E and ΔE requirements in the three detectors gated linear pulses from each of the detectors. The pulse-height spectrum from each detector was stored in a separate 64-channel section of computer memory. Backgrounds were determined by taking runs with a carbon target, a blank platinum target, and with the polyethylene target in place without tritium in the target. Chance coincidence contributions were found by placing delay in one of the arms of the coincidence circuit. Corrections for the finite solid angles subtended by the polyethylene target and the E detector aperture were made to determine a mean proton recoil angle for each telescope setting. These mean angles were 7.9, 16.8, 30.8, and 45.3°. Conversion of angles and angular distributions to the CM system used relativistic kinematics. The CM neutron scattering angles were 164.1, 146.1, 118.2, and 89.0°. The ratio $\sigma(164°)/\sigma(89°)$ was 1.134 ± 0.016 where the error quoted is based on counting statistics. In order to obtain the differential cross section the CM relative angular distribution was normalized to a total cross section of 397.2 mb. Since no experimental data for the forward hemisphere were available, the normalization was based on a $A(1 + B\cos^2\theta)$ angular distribution. It gave A = 30.1 ± 0.3 mb/sr and B = 0.146 ± 0.017, in good agreement with Gammel's prediction B = 0.143. Other two-parameter fits were also made. A $(Y-IV)_{pp+np}$ nucleon–nucleon phase-shift-analysis fit to the data by Breit et al. is presented, as well as recent Livermore phase shifts derived from a fit to nucleon–nucleon scattering data which was constrained to fit exactly a preliminary value of $\sigma(165°)/\sigma(89°)$ obtained in the present experiment. (auth) (Diss. Abstr. Int., B)

5541 CLASSIFICATION OF THE SPIN–ISOSPIN FUNCTIONS OF THE IDENTICAL-NUCLEON SYSTEM. Grama, N. (Inst. for Atomic Physics, Bucharest). Lett. Nuovo Cim.; 4: 869-72 (7 Nov 1970).

A system of n identical nucleons obeying the generalized exclusion principle is considered. A method based on the plethysm is used for the classification of the spin–isospin functions of the identical-nucleon system. The method proposed for the calculation of the classification is illustrated for the case where n = 11. (R.W.R.)

5542 TENSOR FORCE AND EXCHANGE CURRENTS IN THE TRITON BETA DECAY. Riska, D. O. (NORDITA, Copenhagen); Brown, G. E. Contract AT(30-11)-4032. Phys. Lett.; 32B: 662-4(14 Sep 1970).

The correction due to exchange currents to the one-body ^{3}H → ^{3}He β-decay amplitude is estimated by treating the D-state part of the wave function in a simple, approximative way. The main effect comes from the S–D cross terms. (auth)

5543 REACTION ^{4}He(γ,d)d AND THE 2^+ EXCITED STATE OF ^{4}He AT 30 MeV. Erdas, F.; Mosconi, B.; Pompei, A.; Quarati, P. (Univ., Cagliari, Italy). Phys. Lett.; 32B: 659-61 (14 Sep 1970).

The existence of the 2^+ excited state at 30 MeV in ^{4}He is strongly favored by calculations that include the interaction between the outgoing deuterons in the reaction ^{4}He(γ,d)d. (auth)

5544 STUDY OF THE PHOTODISINTEGRATION OF ^{4}He. Wait, G. D.; Kundu, S. K.; Shin, Y. M.; Stubbins, W. F. (Saskatchewan Accelerator Lab., Saskatoon). Phys. Lett.; 33B: 163-5 (28 Sep 1970).

Results on measurements of differential and total photodisintegration cross sections for ^{4}He below 85 MeV are presented. The asymmetry in the angular distribution suggests possible dynamic correlations in the ground state. (auth)

5545 RADIATIVE np CAPTURE AND MESON EXCHANGE CURRENTS. Adler, Ronald J. (Virginia Polytechnic Inst., Blacksburg); Chertok, Benson T.; Miller, Henry C. Phys. Rev., C; 2: 69-84(Jul 1970).

The experimental cross section for radiative np capture is 334.2 ± 0.5 mb. Theoretical calculations to date yield a result about 10% lower. In this work a number of mesonic exchange currents are calculated by using a simple phenomenological method and nonrelativistic wave functions. An increase of about 2–3% in the cross section is obtained, almost entirely due to π exchange. Since this is numerically too small to resolve the discrepancy, other possible contributions to the cross sections are discussed. Previous work on the impulse approximation and the meson exchange effect are reviewed; no discrepancies remain between the numerically accurate theoretical treatments, and the errors in the remaining treatments are discussed. (auth)

5546 PHASE SHIFT ANALYSIS OF P–D ELASTIC SCATTERING. Clews, C. J.; Berovic, N. (Univ. of Birmingham, Eng.). Phys. Lett.; 33B: 347-8(9 Nov 1970).

An energy-dependent phase-shift analysis of p–D elastic scattering data is performed in the energy region from E_p = 3 to E_p = 6 MeV. All S, P, and D wave "split" phases are treated as free parameters. (auth)

5547 EXPERIMENTAL INVESTIGATION OF MESON EFFECTS IN HIGH-ENERGY PHOTODISINTEGRATION OF LIGHT NUCLEI. Picozza, P. (CNEN, Frascati, Italy); Schaerf, C.; Scrimaglio, R.; (and others). Nucl. Phys.; A157: 190-208 (1970).

The ^{3}He(γ,p)d and ^{4}He(γ,p)t differential cross sections at 90° in the c.m.s. were measured in the γ-ray energy region 200–500 MeV using a liquid helium target and spark chamber technique. The ^{4}He photodisintegration shows a resonant behavior in the energy interval 240–330 MeV, not observed in the ^{3}He process. Such different behavior can be tentatively interpreted, in analogy with deuteron

XUM

photodisintegration, on the basis of a pion photoproduction and the re-absorption model. (auth)

5548 ANGULAR DISTRIBUTION OF FINAL STATE INTERACTING n–p PAIRS IN THE REACTION p + d → p + p + n. Brueckmann, H.; Kluge, W.; Matthaey, H.; Schaenzler, L.; Wick, K. (Kernforschungszentrum, Karlsruhe, Ger. Univ., Karlsruhe, Ger.). Nucl. Phys.; A157: 209-30(1970).

The three-particle reaction p + d → p + p + n was investigated systematically at a deuteron bombarding energy of 52.3 MeV. Kinematically complete experiments were carried out by detecting the two protons in coincidence. The kinematical conditions were chosen predominantly to observe the effect of the n–p final state interaction. All the data are analyzed in terms of the Watson–Migdal model of final state interactions. At specific kinematical conditions the impulse approximation turns out to be a more general and better description. An angular distribution was obtained for the production of singlet and triplet final state interacting n–p pairs with zero relative energy in the n–p subsystem. A relation is derived which connects the measured angular distribution for triplet final state interaction in the three-nucleon reaction quantitatively with the angular distribution of elastic p–d scattering. The systematic study proves that values of the nucleon–nucleon scattering lengths can be extracted with a high degree of reliability from three-particle reactions under properly chosen kinematical conditions. (auth)

Nuclear Properties and Reactions, 6≤A≤19

Refer also to abstracts 5327, 5506, 5573, 5602, 5635, 5640, 5666, 5680, 5685, 5716, 5735, 5792, 5809, 5841, 5865, 5866, and 6106.

5549 (BNL-400(3rd Ed.)(Vol.1)) ANGULAR DISTRIBUTIONS IN NEUTRON-INDUCED REACTIONS. VOLUME I. Z = 1 TO 20. Garber, Donald I.; Stroemberg, Lars G.; Goldberg, Murrey D.; Cullen, Dermott E.; May, Victoria M. (Brookhaven National Lab., Upton, N. Y.). Jan 1970. 452p. (EANDC(US)-138(U)). Dep. CFSTI.

The significant experimental observations on the angular distributions of scattered neutrons and of the products of the reactions of fast neutrons with nuclei are compiled. This tabulation gives in considerable detail the results of angular distribution experiments and indicates where they are published. Data are presented in graphical or tabular form. If sufficient differential elastic scattering data are available, a three-dimensional orthographic display of fitted curves vs neutron energy is constructed. Where a body of data exists in the form of coefficients of Legendre polynomials, these are presented in tabular form and the differential cross sections synthesized from these coefficients are presented in an orthographic display. (R.W.R.)

5550 (CEA-N-1232) ANNUAL PROGRESS REPORT OF THE NUCLEAR PHYSICS DEPARTMENT, OCTOBER 1968–SEPTEMBER 1969. (Commissariat a l'Energie Atomique, Saclay (France). Centre d'Etudes Nucleaires). 229p. (In French). Dep. CFSTI (U. S. Sales Only).

Progress is reported on nuclear physics experiments carried out with the Saclay accelerators (Tandem Van de Graaff, cyclotrons, 300 MeV electron linear accelerator). Separate abstracts were prepared for each of the three sections. (France)

For abstracts of individual sections see: 5442, 5506, and 5680.

5551 (CEA-R-4047) GAMMA-RAY PRODUCTION CROSS SECTIONS FOR 5-, 6.6- AND 8.7-MeV NEUTRONS WITH NITROGEN, OXYGEN, SCANDIUM, AND GOLD. Bertin, Andre; Bertrand, Francoise; Clayeux, Genevieve (Commissariat a l'Energie Atomique, Limeil-Brevannes (France). Centre d'Etudes). Aug 1970. 39p. (In French). Dep. NTIS (U. S. Sales Only).

An investigation into the inelastic scattering of fast neutrons by nitrogen, oxygen, scandium and gold was made in order to determine, when possible, cross sections for gamma ray production. A single-crystal NaI(Tl) spectrometer was used to detect the gamma rays emitted by the samples for neutron energies of 5 MeV, 6.6 MeV and 8.7 MeV. Cross sections for the production of 1.63-MeV, 2.31-MeV and 4.46-MeV gamma rays by ^{14}N, 6.13-MeV gamma rays by ^{16}O and 0.718-MeV and 1.238-MeV gamma rays by ^{45}Sc were measured at the different angles: 30°, 45°, 60°, 90°, and 120°. An integrated gamma ray production cross section for gold is given for energy groups from 0.5 MeV to 7 MeV. Cross sections are given in mb/sr with an accuracy of ±14% for the E_γ = 2 MeV energy range and of ±20% in the upper range. (auth) (France)

5552 (ITF-70-50) ALLOWANCE FOR THE WAVE FUNCTION DISTORTION UNDER MULTIPOLE ANALYSIS OF FAST NUCLEON SCATTERING BY NUCLEI. Sitenko, A. G.; Fursa, A. D.; Dotsenko, I. S. (Akademiya Nauk Ukrainskoi SSR, Kiev. Institut Teoreticheskoi Fiziki). 1970. 20p. (In Russian). Dep. NTIS (U. S. Sales Only).

Allowance is made for wave-function distortion in the initial and final states within the framework of the multipole formalism in describing high-energy nucleon scattering by nuclei. The distorted optical potential is calculated on the basis of the two-nucleon interaction in accordance with the multiple scattering theory. The numerical calculations of the angular distributions are carried out for elastic scattering of protons by ^{12}C and also for inelastic scattering of protons by ^{12}C with excitation of the 0^+, 1^+, 2^+, and 3^- levels when T = 0 and 1^+ and 2^+ levels when T = 1. A comparison with the experimental data for a proton energy of 185 MeV is carried out. The character of the angular dependence and the absolute magnitudes of the cross sections agree well in many cases with the experimental values. (auth)

5553 (LA-4465, pp 25,1-2) MEASUREMENT OF THE VECTOR AND TENSOR ANALYZING POWER OF d–^{4}He ELASTIC SCATTERING AT 12 MeV. Lawrence, G. P.; Dodder, D. C.; Keaton, P. W. Jr.; Armstrong, D. D.; McKibben, J. L.; Ohlsen, Gerald G. (Los Alamos Scientific Lab., N. Mex.).

From LASL contributions to the 3rd international symposium on polarization phenomena in nuclear reactions, Madison, Wisconsin, August 31–September 4, 1970.

5554 COMMENTS ON ISOSPIN OF THE ^{11}B GIANT RESONANCE. Hayward, Evans (National Bureau of Standards, Washington, D. C.); Schwartz, Robert B.; Murray, Kenneth M. Phys. Rev., C; 2: 761-2(Aug 1970).

It was recently shown that in the photodisintegration of ^{11}B certain expected γ rays were missing. A partial explanation is offered here for the failure to observe these transitions. It is also pointed out that no conclusions about the strength of the T = $\frac{3}{2}$ giant resonance can be drawn from this experiment. (auth)

5555 BETA DECAY OF ^{19}O TO THE $\frac{1}{2}^-$ STATE OF ^{19}F. Cooper, John C.; Crasemann, Bernd (Univ. of Oregon, Eugene). Phys. Rev., C; 2: 451-7(Aug 1970).

The intensity of the unique first-forbidden 4.708-MeV outer branch of the ^{19}O β spectrum, leading to the 110-keV $\frac{1}{2}^-$ hole state in ^{19}F, has been determined as $(4.8^{+1.3}_{-0.9}) \times 10^{-4}$ per ^{19}O decay. Consequently, the comparative half-life is $f_1t = (1.5^{+0.5}_{-0.3}) \times 10^{10}$ sec, and the strength of the transition is $\langle C_1 \rangle^2 = 0.13^{+0.05}_{-0.03}$ F^2. This result was found from the analysis of β-γ coincidence spectra obtained from reactor-irradiated water samples that had been enriched in ^{18}O. An upper limit of 6×10^{-4} is set on the branching of the 197-keV level decay in ^{19}F through the 110-keV state. The results can be used to infer the extent of wave-function admixture (core excitation) in the ground state of ^{19}O. (auth)

5556 EVEN-PARITY STATES OF ^{17}O. Bobker, J. (Polytechnic Inst. of Brooklyn). Phys. Rev., C; 2: 322-3(Jul 1970).

An exact shell-model framework, used in an earlier paper to interpret the odd-parity (T = $\frac{1}{2}$) states of ^{17}O below 8-MeV excitation, is extended to the even-parity (T = $\frac{1}{2}$) states in this range. Good agreement between experimental and theoretical energies is achieved. A negative result is that the lowest $\frac{3}{2}^+$ state is calculated to have essentially zero single-particle strength. (auth)

5557 FAST-NEUTRON SPECTROSCOPY OF THE REACTION $^9Be(p,n)^9B$ AT 20 MeV. Anderson, J. D.; Wong, C.; Pohl, B. A.; McClure, J. W. (Univ. of California, Livermore). Phys. Rev., C; 2: 319-21(Jul 1970).

Recently a high-resolution proton recoil spectrometer was used to measure the neutron spectrum from 20-MeV proton bombardment of ^9Be. Evidence for levels in ^9B at 1.4- and 3.2-MeV excitation was presented. Using time-of-flight techniques, the neutron spectrum was remeasured, and no evidence was found for these levels. (auth)

5558 INELASTIC ELECTRON SCATTERING FROM THE REGION OF THE ^{16}O GIANT RESONANCE WITH PRIMARY ENERGIES BELOW 60 MeV. Goldmann, A.; Stroetzel, M. (Technische Hochschule, Darmstadt, Ger.). Z. Phys.; 239: 235-48(1970). (In German).

The ^{16}O giant resonance was investigated between 21 and 26 MeV excitation energy for inelastic momentum transfers <0.5 fm^{-1}. Integrated longitudinal and transverse E1 matrix elements are obtained separately. The possibility of E2 contributions is discussed. (auth)

5559 (d,α) REACTION ON ^{13}C. Klabes, R.; Baldeweg, F.; Bredel, V.; Guratzsch, H.; Stiller, G.; Tesch, S. (Zentralinstitut

fuer Kernforschung, Rossendorf, Ger.). Nucl. Phys.; A152: 232-40(1970).

Angular distributions of α-particles leading to the ground state and the first three excited states of ^{11}B have been measured at bombarding energies 12.1, 13.3 and 14.1 MeV. DWBA calculations have been carried out on the basis of the two-nucleon transfer theory of Glendenning. Differential and relative integrated cross sections are in tolerable agreement with the experiment. (auth)

5560 MANY-PARTICLE MANY-HOLE STATES IN ^{16}O. de Takacsy, N.; Das Gupta, S. (McGill Univ., Montreal). Nucl. Phys.; A152: 657-72(1970).

A method is proposed for the study of the energy spectra of collective many-particle many-hole states in nuclei near closed shells. In particular the 4p–4h and 3p–3h states of ^{16}O are investigated. In the latter case, the mixing with the 1p–1h states is also calculated. The results are compared with the available experimental energy spectra. (auth)

5561 INELASTIC SCATTERING OF α-PARTICLES FROM ^{12}C BELOW 18.0 MeV. Morgan, J. F.; Weisser, D. C. (California Inst. of Tech., Pasadena). Contract Nonr-220(47). Nucl. Phys.; A151: 561-8(1970).

The inelastic scattering of α-particles leading to the 7.65 MeV and the 9.65 MeV states of ^{12}C was studied from lab energy of 18.0 MeV down to 2 MeV above the threshold for each reaction. Angular distributions were obtained at energies where significant structure appeared in the excitation functions. The measured total cross sections were used to evaluate the effect of inelastic scattering processes on the rate of the $3\alpha \rightarrow {}^{12}C$ reaction in stellar interiors. (auth)

5562 THE $^{12}C(d,^6Li)^8Be$ α-CLUSTER PICKUP REACTION WITH 52 MeV DEUTERONS. Eichelberger, W.; Plieninger, R. D.; Velten, E. (Univ., Karlsruhe, Ger. Kernforschungszentrum, Karlsruhe, Ger.). Nucl. Phys.; A149: 441-8(1970).

A $^{12}C(d,^6Li)^8Be$ α-cluster pickup experiment with deuterons of 51.8 ± 0.3 MeV was performed at the Karlsruhe isochronous cyclotron to get information about the α-cluster structure of the ^{12}C nucleus. The absolute differential cross section was measured for angles between 12° and 128° c.m. Several ^6Li groups were found in the spectra due to the residual ^8Be nucleus in the ground state and the excited states. The angular distribution of the $^{12}C(d,^6Li)$ differential cross section corresponding to the ^8Be ground state shows a sharp diffraction structure. The cross sections corresponding to the first excited state (2.9 MeV) of the ^8Be residual nucleus is higher by a factor of about 5 with little structure in the distribution. In the two-cluster approximation of Phillips and Tombrello the [^8Be(2.9 MeV)+α] parent state of the ^{12}C nucleus seems to be dominant with respect to α-clustering. (auth)

5563 REACTIONS $^{14}N(p,^3He)^{12}C$, $^{14}N(d,\alpha)^{12}C$, $^{13}C(p,d)^{12}C$ AND THE 4^+ LEVEL OF ^{12}C. Scott, D. K. (Oxford Univ.); Portner, P. M.; Nelson, J. M.; Shotter, A. C.; Mitchell, A. J.; Chant, N. S.; Montague, D. G.; Ramavataram, K. Nucl. Phys.; A141: 497-531 (1970).

In a study of the two-nucleon transfer reaction $^{14}N(p,^3He)^{12}C$ at 50 MeV, strong transitions are observed to the ground state, 4.43, 12.71, 14.08, 15.11 and 16.11 MeV levels of ^{12}C. The first four of these levels are also strongly excited in the $^{14}N(d,\alpha)^{12}C$ reaction, which is investigated at incident energies of 15 and 20 MeV. A detailed comparison of the data is made with the theory of direct reactions, using intermediate coupling, shell-model wave functions for ^{12}C, and a finite-range non-local formulation of the DWBA. Good agreement between theory and experiment is obtained with realistic optical-model potentials for all reaction channels. The analysis identifies the 14.08 MeV level as the lowest 4^+ state of ^{12}C. This assignment is supported by a study of the single-nucleon transfer reaction $^{13}C(p,d)^{12}C$ at 50 MeV in which a 4^+ state cannot be reached by 1p shell neutron pick-up. In this reaction the 14.08 MeV level is not observed. The angular distributions for the observed levels at 0.0, 4.43, 12.71, 15.11 and 16.11 MeV are satisfactorily explained with a finite-range non-local DWBA theory and with spectroscopic factors derived from intermediate coupling shell-model wave functions. (auth)

5564 CORRELATION STRUCTURE OF ^6Li. Lodhi, M. A. K.; Mires, R. W. (Texas Tech. Univ., Lubbock). Nucl. Phys.; A149: 625-40(1970).

A simplified scheme of incorporating the residual potentials and nucleon–nucleon correlation effects in the independent particle shell-model (IPSM) wave functions of nuclei is used. This method is particularly convenient for nuclei with two valence nucleons (or holes). This scheme is applied to calculate the energy spacings and electron scattering form factor of ^6Li. Using the variational principle, the correct energy spacings and the values of the parameters for several potential functions are reported. The ^6Li form factors are also calculated as obtained from the electron scattering using the simple harmonic oscillator wave functions with and without the correlation term. The correlated form factors show considerable improvement over the uncorrelated resul both qualitatively and quantitatively when compared with the experimental data. This work also concludes the clustering effect of the valence nucleons. (auth)

5565 LIFETIME MEASUREMENTS IN ^{16}O. Bertin, M. C.; Pixley, R. E. (Stanford Univ., Calif.). Nucl. Phys.; A150: 247-56(1970).

The lifetimes of three excited states in ^{16}O have been measured by the Doppler shift attenuation method. The states studied were 8.87 MeV (2^-), 240 ± 40 fs, 10.95 MeV (0^-), 8 ± 5 fs, and 11.08 MeV MeV (3^+), 57 ± 19 fs. The gamma decay modes of the latter two states were also studied and branching ratios were extracted. (auth)

5566 CLOSE SIMILARITIES IN THE EXCITATION FUNCTIONS FROM THE ELASTIC ^{16}O SCATTERING FROM NUCLEI WITH A ≈ 16. Siemssen, R. H. (Argonne National Lab., Ill.); Fortune, H. T.; Malmin, R.; Richter, A.; Tippie, J. W.; Singh, P. P. Phys. Rev. Lett.; 25: 536-9(24 Aug 1970).

Close similarities are found in the gross structures of the excitation functions from the elastic scattering of ^{16}O from ^{14}N, ^{15}N, and ^{18}O. The picture emerging from the optical-model analysis of these data is that of an interaction potential which is totally absorbing for the low-l partial waves and which is very transparent for the surface partial waves. (auth)

5567 ENERGY LEVELS OF LIGHT NUCLEI A = 13-15. Ajzenberg-Selove, F. (Univ. of Pennsylvania, Philadelphia). Nucl. Phys., A152: 1-221(1970).

Compilation of energy levels for nuclei with A = 13, 14, and 15, with emphasis on material leading to information about the structure of the A = 13 to 15 systems. (75 pages of references) (auth)

5568 MEASUREMENT OF $T_Z = -3/2$ MASSES AND THE ISOBARIC MULTIPLET MASS EQUATION. Trentelman, G. F.; Preedom, B. M.; Kashy, E. (Michigan State Univ., East Lansing). Phys. Rev. Lett.; 25: 530-2(24 Aug 1970).

Precise measurements of the masses of ^9C, ^{13}O, and ^{21}Mg have been made using a magnetic spectrograph. The results are used to test the isobaric-multiplet mass equation. (auth)

5569 REMARKS ON THE MEASUREMENT OF POLARIZATION OF ^6Li IONS. Fick, D. (Univ., Erlangen-Nuernberg, Ger.). Z. Phys.; 237: 131-6(1970).

The determination of the polarization of ^6Li ions is discussed. It is shown that, independent of the reaction mechanism, the following relations between the analyzing powers for polarized deuterons and polarized ^6Li ions hold for the $^6Li(d,\alpha)^4He$-reaction: for all scattering angles ϑ: $A_{yy}^{(d)}(E,\vartheta) = A_{yy}^{(Li)}(E,\vartheta)$; for the scattering angle $\vartheta = \pi/2$ only: $A_{zz}^{(d)}(E,\vartheta=\pi/2) = A_{zz}^{(Li)}(E,\vartheta=\pi/2)$ and $A_{xx-yy}^{(d)}(E,\vartheta=\pi/2) = A_{xx-yy}^{(Li)}(E,\vartheta=\pi/2)$. By use of these identities the determination of the polarization of ^6Li-beams is reduced to the experimentally well-established determination of the polarization of deuterons. (auth)

5570 CALCULATION OF THE ODD-PARITY SPECTRUM OF ^{16}O AND ^{40}Ca FROM THE INTERACTION BETWEEN NUCLEONS: METHOD AND FIRST RESULTS. Haug, Peter K. (Univ., Munich). Z. Phys.; 238: 289-311(1970).

In the framework of an exact many-body theory based on the formalism of Green's functions, an eigenvalue equation capable of describing single-particle excitations of a Fermi system is rederived. The effective two-particle interaction entering this equation is extracted free of all adjustable parameters from a very simple nucleon–nucleon interaction by solving the corresponding integral equation for nuclear matter and using a local-density approximation. The method is used to describe those states of the doubly magic nuclei ^{16}O and ^{40}Ca which probably can be understood as one-particle–one-hole excitations from the ground state, i.e., low-lying negative parity levels; and — in view of the simplicity of the interaction assumed — reasonably good agreement with experimental evidence is obtained. (auth)

5571 (^3He, α) REACTION ON ^7Li FROM 5.0 TO 8.0 MeV. Orihara, Hikonojo; Baba, Mamour; Akiyama, Masatsugu; Iwasaki, Shin; Nakagawa, Takemi; Ueno, Hiroaki; Watanabe, Masayuki (Tohoku Univ., Sendai). J. Phys. Soc. Jap.; 29: 533-9(Sep 1970).

Angular distributions were measured for α_0, α_1, and α_2 groups from the $^7Li(^3He,\alpha)^6Li$ reaction at the bombarding energies of 6.0 and 7.5 MeV. Pronounced backward peakings were observed for the α_0 and α_2 groups. The excitation curves were also measured over the range from 5.0 to 8.0 MeV at the laboratory angles of 20° and 160°. These curves show no resonant behavior in the whole studied bombarding energy range. A dominant backward

XUM

maximum and a forward peak were well described by the plane-wave Born approximations with and without exchange, respectively. The triton-plus-^{3}He cluster structure for the ground and second excited states in ^{6}Li is discussed. The neutron reduced widths Θ_n^2 were deduced. (auth)

5572 EXCITATION OF THE GIANT RESONANCE IN ^{12}C BY INELASTIC ELECTRON SCATTERING. Torizuka, Y.; Yamaguchi, A.; Terasawa, T.; Kojima, Y.; Nakahara, K.; Oyamada, M.; Itoh, K.; Nakada, A.; Mitunobu, S.; Kimura, M. (Tohoku Univ., Sendai). Phys. Rev. Lett.; 25: 874-7(28 Sep 1970).

The longitudinal and transverse form-factor spectra for electroexcitation of the ^{12}C giant resonance were determined separately. Results are presented for an excitation energy range of from 15 to 30 MeV and for a momentum-transfer range of 0.84–1.56 F^{-1}. We have found levels with the following excitation energies (MeV), spins, and parities: 18.6 (3$^-$), 19.6 (4$^-$), 20.0 (2$^+$), 20.6 (3$^+$), 21.6 (3$^-$), 22.0 (1$^-$), 22.7 (1$^-$), and 23.8 (1$^-$). We have also found new evidence of the spin–isospin mode for the 22.7-MeV (1$^-$) excitation. (auth)

5573 SYSTEMATIC SEARCH FOR THE LOWEST T = 2 STATE OF ^{12}C USING DEUTERON- AND ^{3}He-INDUCED REACTIONS. Black, J. L.; Caelli, W. J.; Watson, R. B. (Australian National Univ., Canberra). Phys. Rev. Lett.; 25: 877-81(28 Sep 1970).

The reactions ^{9}Be(^{3}He,$\gamma\gamma$), ^{10}B(d,p), ^{10}B(d,α), and ^{10}B(d,$\gamma\gamma$) have been used to search for the lowest T = 2 state of ^{12}C. A possible candidate for the state has been observed in ^{9}Be(^{3}He,$\gamma\gamma$) at E_x = 27.585 ± 0.005 MeV. For the other three reactions, no resonances were observed and upper limits have been set on partial widths. (auth)

5574 POLARIZATION OF NEUTRONS FROM THE ^{13}C(^{3}He,n_0)^{15}O AND ^{24}Mg(^{3}He,n_0)^{26}Si REACTIONS BETWEEN 4 AND 6 MeV. DeMartini, David Charles. Columbus, Ohio; Ohio State Univ. (1969). 179p. University Microfilms Order No. 70-6762.

Thesis.

The polarization of the neutrons from the ^{13}C(^{3}He,n_0)^{15}O reaction was measured with targets between 270 and 530 keV thick at four bombarding energies between 4.2 and 5.7 MeV for eight reaction angles back to 130° in the laboratory system. Two polarization angular distributions of the neutrons from the ^{24}Mg(^{3}He,n_0)^{26}Si reaction were also measured at incident beam energies of 5.0 and 5.8 MeV. These measurements were made with 400 keV thick targets at a minimum of nine angles back to a maximum laboratory reaction angle of 135°. In both reactions the observed polarizations were large and slowly varying with energy. The maximum observed polarizations were +0.68 ± 0.10 at 5.2 MeV and 70° (lab) for the ^{13}C(^{3}He,n_0)^{15}O reaction and +0.71 ± 0.16 at 5.0 MeV and 135° (lab) for the ^{24}Mg(^{3}He,n_0)^{26}Si reaction. Zero-range DWBA calculations gave reasonable agreement with the angular dependence of the previous cross section and present polarization data throughout the energy range investigated for the ^{13}C(^{3}He,n_0)^{15}O reaction. It was necessary to include spin-dependent distortions in the exit channel to account for the observed polarizations. The best fits were obtained with optical model parameter sets having a real potential well depth approximately three times the value appropriate to describe single nucleon elastic scattering from carbon. A discrepancy between the predicted and observed values for the magnitude of the cross section remains to be satisfactorily resolved. No satisfactory fits to the angular dependence of the cross section and polarization data in this energy region were achieved with calculations based on the assumption of three overlapping compound resonances. Although reasonable fits to the angular dependence of the cross section were obtained with both DWBA calculations and calculations assuming two broad overlapping compound nucleus states, neither type of calculation was successful in reproducing the observed angular dependence of the polarization in the ^{24}Mg(^{3}He,n_0)^{26}Si reaction. The DWBA calculated polarization angular distributions were particularly insensitive to variations in the calculation parameters indicating the value of polarization measurements in testing the applicability of the DWBA theory to any particular reaction. (Diss. Abstr. Int., B)

5575 THREE-ALPHA MODEL OF ^{12}C. Becker, Stephen F. New Brunswick, N. J.; Rutgers–The State Univ. (1969). 84p. University Microfilms Order No. 70-10,045.

Thesis.

A model for ^{12}C is considered in which the nucleus is treated as being composed of three rigid alpha-particles. The O$^+$ bound states of the system are studied using the Faddeev equations. As input into these equations, a separable alpha-alpha interaction is used to simulate the strong part of the alpha-alpha "effective potential." A method is also discussed in which the input into the Faddeev equations is still separable but contains a "large" part of the Coulomb effects. In addition to the S-wave term, a D-wave term was included in the alpha-alpha interaction. This term is found to give a negligible contribution to the three-alpha binding energies. A repulsive term in the S-wave was also included. Solving the Faddeev equations without repulsion in the alpha-alpha interaction, a ground state (–12.8 MeV) and one excited state (–3.1 MeV) are found. With the repulsive term included, the ground state binding energy is reduced to 6.24 MeV and no excited state is found. The ground state wave function (without the repulsion) is then used to calculate the ^{12}C electromagnetic form factor, which is slightly larger than the experimental form factor. Finally, a T-matrix perturbation theory for the Faddeev equations is developed and some applications of this theory to the three-alpha system are suggested. (Diss. Abstr. Int., B)

5576 DEPOLARIZATION OF NEGATIVE MUONS IN LOW-Z MUONIC ATOMS WITH NONZERO NUCLEAR SPIN. Favart, D.; Brouillard, F.; Grenacs, L.; (and others) (Univ., Louvain, Belgium). Phys. Rev. Lett.; 25: 1348-50(9 Nov 1970).

The decay asymmetries resulting from the residual polarization of negative muons were measured in the components of the ground-state hyperfine doublet of ^{6}Li, ^{7}Li, ^{9}Be, ^{10}B, and ^{11}B muonic atoms. The results show a characteristic consequence of the muon–nucleus magnetic dipole coupling during the muonic cascade. (auth)

5577 ONE-NEUTRON TRANSFER REACTIONS ^{9}Be(^{16}O,^{17}O[0.871])^{8}Be AND ^{12}C(^{16}O,^{17}O[0.871])^{12}C. Barker, P. H.; Cockburn, P. M.; Seiler, H. P.; Marmier, P. (Technische Hochschule, Zurich). Phys. Rev. Lett.; 25: 1350-2(9 Nov 1970).

The total cross sections for the reactions ^{9}Be(^{16}O,^{17}O [0.871])^{8}Be and ^{13}C(^{16}O,^{17}O[0.871])^{12}C were measured at energies well below the Coulomb barrier. The data were fitted with the Buttle and Goldfarb formulation of distorted-wave Born-approximation theory and spectroscopic factors extracted. (auth)

5578 INVESTIGATION OF THE PHOTONUCLEAR REACTIONS ^{12}C(γ,n), ^{12}C(γ,2n), ^{39}K(λ,n), AND ^{40}Ca(γ,np) UP TO THE MESON THRESHOLD. Kayser, K.; Collin, W.; Filss, P.; (and others) (Physikalisch-Technische Bundesanstalt, Brunswick). Z. Phys.; 239: 447-60(1970). (In German).

In order to obtain data on the photon absorption process between the giant resonance and the meson threshold the cross sections of the reactions ^{12}C(γ,n)^{11}C, ^{12}C(γ,2n)^{10}C, ^{39}K(γ,n)^{38}K^g, and ^{40}Ca(γ,np)^{38}K^g have been determined by the analysis of yield curves. Though the (γ,n) cross sections grow small with increasing photon energy they are different from zero up to energies of 60 MeV and above. The cross section of the reaction ^{12}C(γ,2n) is extremely small; its highest value amounts to 0.15% of the highest value of the ^{12}C(γ,n) reaction. The measured ^{40}Ca(γ,np) cross section is of the order predicted by the naive quasi-deuteron model. The integrated cross sections of the above reactions up to 140 MeV are 85 ± 7, 0.90 ± 0.10, 139 ± 16, and 76 ± 7 MeV mb respectively. (auth)

5579 OPTICAL MODEL ANALYSIS FOR ELASTIC DEUTERON SCATTERING ON LIGHT NUCLEI. El-Nadi, M.; Zohni, O.; Hussein, H. M. (Cairo Univ.). Ann. Phys. (Leipzig); 25: 1-9(1970).

An optical model analysis for the elastic deuteron scattering on light nuclei (^{7}Li, ^{9}Be, ^{11}B, ^{12}B and ^{16}O) is studied at energies about 28 MeV. Satisfactory fits to the experimental data are found using the volume and the surface absorption nuclear potentials. The effect of varying the resulting parameters on the differential cross section is discussed. (auth)

5580 ANALOGS OF GIANT RESONANCE STATES AND THEIR EXPERIMENTAL DISCOVERY. Ueberall, H. (Catholic Univ. of America, Washington, D. C. Naval Research Lab., Washington, D. C.). Acta Phys. Austr.; 30: 89-107(1969).

The T = 1 giant resonances in closed-shell nuclei such as ^{12}C, ^{16}O, or ^{40}Ca may be excited by photon absorption or inelastic electron scattering. Their T_3 = ±1 analogs in the neighboring nuclei should play a role in weak interactions; and a search for these states using muon capture or, alternatively, radiative pion capture was suggested. Recent experiments using such methods have been able to furnish a direct experimental proof for the existence of these analog states. (auth)

5581 APPLICATION OF EXTENDED R-MATRIX THEORY TO ELASTIC SCATTERING OF NEUTRONS BY ^{12}C. Yost, K. J.; Pitkanen, P. H. (Oak Ridge National Lab., Tenn.). Trans. Amer. Nucl. Soc.; 13: 728-9(Nov 1970).

From Meeting of the American Nuclear Society, Washington, D. C. See CONF-701102.

XUM

5582 INTEGRAL GAMMA-RAY PRODUCTION CROSS-SECTION MEASUREMENTS WITH A Pu-Be NEUTRON SOURCE. Rogers, V. C. (Brigham Young Univ., Provo, Utah); Hedengren, D. C.; Perkins, M. W.; Rasmussen, N. C.; Hui, B. H. Trans. Amer. Nucl. Soc.; 13: 864-5(Nov 1970).

From Meeting of the American Nuclear Society, Washington, D. C. See CONF-701102.

5583 EXCITATION ENERGIES AND DECAY PROPERTIES OF T = 3/2 STATES IN ^{17}O, ^{17}F, AND ^{21}Na. McDonald, Arthur Bruce. Pasadena, Calif.; California Inst. of Tech. (1970). 170p. University Microfilms Order No. 70-12,446.

Thesis.

The two lowest T = 3/2 levels in ^{21}Na were studied in the ^{19}F(^{3}He,n), ^{20}Ne(p,p), and ^{20}Ne(p,p') reactions; and their excitation energies, spins, parities, and widths were determined. In a separate investigation, branching ratios were measured for the isospin-nonconserving particle decays of the lowest T = 3/2 levels in ^{17}O and ^{17}F to the ground state and first two excited states of ^{16}O, by studying the ^{15}N(^{3}He,n)^{17}F*(p)^{16}O and ^{18}O(^{3}He,α)^{17}O*(n)^{16}O reactions. The ^{19}F(^{3}He,n)^{21}Na reaction was studied at incident energies between 4.2 and 5.9 MeV using a pulsed-beam neutron-time-of-flight spectrometer. Two T = 3/2 levels were identified at excitation energies of 8.99 ± 0.05 MeV (J > 1/2) and 9.22 ± 0.015 MeV ($J^\pi = 1/2^+$, Γ < 40 keV). The spins and parities were determined by a comparison of the measured angular distributions with the results of DWBA calculations. These two levels were also observed as isospin-forbidden resonances in the ^{20}Ne (p,p) and ^{20}Ne(p,p') reactions. Excitation energies were measured and spins, parities, and widths were determined from single-level dispersion-theory analysis. Isospin assignments were made on the basis of excitation energies, spins, parities, and widths. Branching ratios for the isospin-nonconserving proton decays of the 11.20-MeV, T = 3/2 level in ^{17}F were measured by the ^{15}N(^{3}He,n)^{17}F*(p)^{16}O reaction to be 0.088 ± 0.016 to the ground state of ^{16}O and 0.22 ± 0.04 to the unresolved 6.05- and 6.13-MeV levels of ^{16}O. Branching ratios for the neutron decays of the analogous T = 3/2 level, at 11.08 MeV in ^{17}O, were measured by the ^{16}O(^{3}He,α)^{17}O*(n)^{16}O reaction to be 0.91 ± 0.15 to the ground state of ^{16}O and 0.05 ± 0.02 to the unresolved 6.05- and 6.13-MeV states. By comparing the ratios of reduced widths for the mirror decays, the form of the isospin impurity in the T = 3/2 levels is shown to depend on T_z. (auth) (Diss. Abstr. Int., B)

5584 SCATTERING AND REACTIONS OF POLARIZED PROTONS AND DEUTERONS FROM BERYLLIUM. Loyd, David Heron Jr. Madison, Wis.; Univ. of Wisconsin (1970). 181p. University Microfilms Order No. 70-8307.

Thesis.

A polarized beam from a tanden Van de Graaff accelerator was used to measure the azimuthal asymmetry of the reaction products produced by polarized protons and deuterons incident on a ^{9}Be target. The analyzing power (the azimuthal asymmetry when a reaction is initiated by a completely polarized beam) was deduced from the measured asymmetry and the known beam polarization. Angular distributions of the analyzing power of ^{9}Be(p,p)^{9}Be were measured at twelve energies between 3.0 and 12.0 MeV. Angular distributions of the analyzing powers of the reactions ^{9}Be(p,p')^{9}Be*(E_x = 2.43 MeV) and ^{9}Be(p,d)^{8}Be(E_x = 0.0 MeV) were measured at eight energies between 5.0 and 12.0 MeV. An optical-model analysis was performed of the polarization in elastic scattering and of previously measured elastic scattering cross sections. The optical model was found to reproduce the data only for incident proton energies of 9.0 MeV or greater. Angular distributions of the analyzing powers were also measured for the reactions ^{9}Be(d,d)^{9}Be, ^{9}Be(d,p)^{10}Be (E_x = 0.0 MeV), ^{9}Be(d,p)^{10}Be (E_x = 3.37 MeV), and ^{9}Be(d,t)^{8}Be(E_x = 0.0 MeV) initiated by 9.0-MeV vector-polarized deuterons. An optical-model analysis was performed of the deuteron vector polarization data at 9.0 MeV. Using these parameters and the proton parameters from the analysis mentioned above, Distorted Wave Born Approximation (DWBA) calculations were made for comparison with the (d,p), (d,t), and some of the (p,d) data. Only the (d,p) ground state reaction was well reproduced by DWBA. (auth) (Diss. Abstr. Int.,B)

5585 BACKWARD ANGLE SCATTERING OF 50-MeV PROTONS FROM C, O, N, AND Be. Clarke, N. M. (King's Coll., London); Burge, E. J.; Smith, D. A.; Dore, J. C. Nucl. Phys.: A157: 145-65(1970).

Measurement of the angular distributions for the differential cross section and polarization was made for the scattering of 50-MeV protons from several light nuclei. These data supplement earlier work and extend the angular range to the extreme backward angles. The data were analyzed using an optical model with the usual Saxon–Woods form factors to represent the potential shapes. It was found that the use of an "unconventional" geometry for the absorption potential gave rise to a systematic variation in the optimum parameter values for all potentials whereas there was considerable variation if a conventional geometry was used. The quality of the fits however is still unsatisfactory and suggests that the present treatment of the absorption potential is probably responsible for the difficulties encountered in an optical-model analysis of proton scattering from light nuclei. (auth)

5586 ALPHA CLUSTERS IN HARTREE–FOCK CALCULATIONS. Eichler, Joerg (Hahn-Meitner-Institut fuer Kernforschung, Berlin); Faessler, Amand. Nucl. Phys.; A157: 166-76(1970).

Hartree–Fock calculations were performed for ^{12}C, ^{16}O and ^{20}Ne without requiring axial symmetry. Instead, the less restrictive condition is imposed that all single-particle wave functions be invariant under rotations of 120° about the z-axis. The calculation thus allows for possible triangular structures expected in certain light alpha nuclei. Using a Yale–Shakin potential for the two-body interaction no deviation from axial symmetry is obtained. For a Volkov force with a sufficiently strong Majorana exchange contribution (M = 0.75) the Hartree–Fock solution does show trigonal symmetry, although the cluster-like mass concentrations are much less pronounced than in nuclear models which contain the cluster structure from the very outset. (auth)

5587 ENERGY LEVELS OF ^{18}Ne FROM THE ^{20}Ne(p,t)^{18}Ne REACTION. Falk, W. R.; Kidney, R. J.; Kulisic, P.; Tandon, G. K. (Univ. of Manitoba, Winnipeg, Can.). Nucl. Phys.; A157: 241-62(1970).

Angular distributions of tritons from the ^{20}Ne(p,t)^{18}Ne reaction were measured at a proton bombarding energy of 42.6 MeV. In addition to the excitation of the established states at 1.887, 3.376, 3.576 and 3.616 MeV, strong groups were also seen at 4.53, 5.10, 6.28 and 9.17 MeV. The 4.53-MeV state is found to have a spin-parity of 1^-. The 5.10 MeV group is probably a doublet comprised of a 2^+ and a 3^- state. A tentative 4^+ assignment is given to the 6.28 MeV state. DWBA calculations were made using the finite-range two-nucleon transfer code of Nelson and Macefield. Various wave functions describing ^{18}Ne and ^{20}Ne, taken from the work of Arima et al., Wildenthal et al., Kuo and Zuker, were used in calculating the spectroscopic amplitudes for transitions to the various final states in ^{18}Ne. The sensitivity of the DWBA results to the binding energy of the single-particle states is discussed. (auth)

5588 FOUR-NUCLEON TRANSFER REACTION INDUCED BY ^{10}B ON ^{12}C. Hildenbrand, K. D.; Gutbrod, H. H.; von Oertzen, W.; Bock, R. (Max-Planck-Institut fuer Kernphysik, Heidelberg. Univ., Marburg, Ger.). Nucl. Phys.; A157: 297-304(1970).

The four-nucleon transfer reaction induced by ^{10}B on ^{12}C was studied above the Coulomb barrier. The population of final states of ^{16}O is less selective than in other four-nucleon transfer reactions induced by ^{6}Li, ^{7}Li, or ^{16}O. This fact as well as the structureless angular distributions can be explained by the complexity of the structure of the ground state of ^{10}B, which has large components with a lower degree of symmetry than the α-particle. (auth)

5589 DIRECT REACTIONS ON ^{10}Be. Auton, D. L. (Univ. of Chicago, Argonne National Lab., Ill.). Nucl. Phys.; A157: 305-22(1970).

A ^{10}Be target was prepared from neutron-irradiated beryllium by the AREMIS isotope separator. Angular distributions from the (d,p), (d,t), (p,p') and (d,d) reactions on ^{10}Be were obtained with this target. Protons leading to the ground state and first excited state of ^{11}Be at 12.0 MeV incident deuteron energy indicate spin and parity assignments of $1/2^+$ and $1/2^-$, respectively. At an incident deuteron energy of 15.0 MeV, tritons could be detected up to an excitation of 5.5 MeV in ^{9}Be. No evidence was seen for an l = 1 transition to known states at less than 3.0 MeV excitation in ^{9}Be other than that to the ground state. Spectroscopic factors for observed states in the (d,p) and (d,t) reactions were obtained in DWBA analyses with reasonable parameters. Elastic and inelastic scattering of protons on ^{10}Be were observed at several incident energies from 12.0 MeV to 16.0 MeV. The elastic scattering was compared with optical-model calculations, and a B(E2) value for the 3.37 MeV ($2^+ \rightarrow 0^+$) transition was obtained by comparison of measured inelastic angular distributions with DWBA predictions. Spectroscopic information concerning transitions within the 1p shell is in good agreement with the values obtained in the shell-model calculations of Cohen and Kurath. (auth)

5590 ANGULAR DISTRIBUTION OF NEUTRONS FROM DEUTERON-BOMBARDED LITHIUM. Saxena, M. K. (Lucknow Univ., India). Indian J. Pure Appl. Phys.; 8: 108(Feb 1970).

XUM

The angular distribution of neutrons from the $^{7}Li(d,n)^{8}Be$ nuclear reaction was experimentally obtained for the first excited state (2.2 MeV) of ^{8}Be. The observed yield agrees closely with the predicted value of yield for $l_p = 1$, and suggests that the stripping process predominates in the present case where the deuteron bombarding energy is away from the resonance. The target nucleus directly accepts a proton of $l_p = 1$, and the spin of this level is either 0 or 2 with even parity. (auth)

5591 EXPERIMENTAL EVIDENCE FOR THE NONSTATISTICAL SHAPE OF THE BETA SPECTRUM OF ^{14}C. Sonntag, Ch.; Rebel, H.; Ribbat, B.; Thio, S. K.; Gramm, W. R. (Univ., Heidelberg). Lett. Nuovo Cim.; 4: 717-19(10 Oct 1970).

Studies of the shape of the ^{14}C beta spectrum obtained with three different spectrometers are reported. The ^{14}C was in the form of a small CO_2 admixture to the counter gas (Ar/methane). After the different correction procedures for the counters are made, the energy spectra agree for all three spectrometers. The spectra converge to a form which in all cases deviates from the statistical shape. The shape factor S(W) is strongly energy dependent and indicates the influence of higher-order beta matrix elements. (R.W.R.)

5592 EVIDENCE FOR A $J^{\pi} = 8^{+}$ STATE IN ^{16}O. Comfort, J. R. (Argonne National Lab., Ill.); Morrison, G. C.; Zeidman, B.; Fortune, H. T. Phys. Lett.; 32B: 685-8(14 Sep 1970).

A 4p−4h state near 20.8 MeV in ^{16}O, populated by the $^{12}C(^{6}Li,d)^{16}O$ and $^{12}C(^{7}Li,t)^{16}O$ reactions, is found to have a high spin value. It is suggested to be the $J^{\pi} = 8^{+}$ member of the first even-parity rotational band. (auth)

5593 CALCULATION OF THE HEAVY-PARTICLE STRIPPING PROCESS IN THE REACTION $^{11}B(d,n)^{12}C$. Yamaji, Shuhei (Inst. of Physical and Chemical Research, Saitama, Japan); Yoshida, Shiro. Progr. Theor. Phys. (Kyoto); 44: 125-52(Jul 1970).

A method for microscopic calculation of the cross section in the distorted-wave Born approximation (DWBA) is developed. The form factor in the transition amplitude is expanded with harmonic-oscillator wave functions. This method is convenient for study of the center-of-mass effect of the target nucleus and for evaluation of the heavy-particle stripping term without assuming the interaction as a one-body potential. Numerical calculations are performed for a heavy-particle stripping term on the reaction $^{11}B(d,n)^{12}C$. The result obtained using a sum of two-body interactions with reasonable strength is similar to that obtained using a one-body potential, and it cannot explain the backward peak of experimental results. (auth)

5594 FORM FACTOR OF HEAVY-ION TRANSFER REACTION AT LOW-ENERGY REGION. Kaneko, Tsuneo (Niigata Univ., Japan). Progr. Theor. Phys. (Kyoto); 44: 292-4(Jul 1970).

The reaction $^{14}N(^{14}N,^{13}N)^{15}N$ is considered in the DWBA formalism. The form factor in the transition amplitude is examined in the form $(\beta r)^{n}e^{-\beta r}$ with n = 0, 1, 2, and 3, as well as the usual −1. Comparison with data at 8 MeV cms indicates better agreement for n = 2 than n = −1 for $\beta = 0.73$ F^{-1}. This indicates that the transfer process is a long-range one, at least for this reaction. (R.W.R.)

5595 PHOTODISINTEGRATION OF ^{15}N. Hsieh, S. T. (National Tsing Hua Univ., Hsinchu, Taiwan). Phys. Lett.; 32B: 647-8(14 Sep 1970).

The photodisintegration of ^{15}N is examined within the framework of shell-model calculations. The result is in qualitative agreement with experimental data. (auth)

5596 STUDY OF DETAILED BALANCE FOR $^{16}O(d,\alpha)^{14}N$ AND $^{14}N(\alpha,d)^{16}O$ AS A TEST OF TIME REVERSAL INVARIANCE. Pledger, Douglas Bruce. Madison, Wis.; Univ. of Wisconsin (1970). 91p. University Microfilms Order No. 70-8325.

Thesis.

Measurements were made of differential cross-sections for $^{16}O(d,\alpha)^{14}N$ and $^{14}N(\alpha,d)^{16}O$; and the results were compared as a test of detailed balance and, hence, time reversal invariance. The angle of observation (178.2° center-of-mass) was chosen to increase the sensitivity of the measurements to T violations. The reactions occurred in a differentially pumped gas scattering chamber previously employed for p−p measurements, and reaction products were observed in an annular solid-state detector. Considerable effort was exerted throughout to minimize systematic errors. $^{16}O(d,\alpha)^{14}N$ cross sections were measured at 21 energies between 6.875 and 7.415 MeV center-of-mass. The $^{14}N(\alpha,d)^{16}O$ cross section was measured at 18 different energies in this range. This region includes a sharp maximum in cross section, over which cross-section measurements can be made most precisely, and a minimum, at which measurements should be most sensitive to T violations. The effects of target thickness and straggling were unfolded from the $^{16}O(d,\alpha)^{14}N$ data, and an analytic expression was obtained for cross section as a function of energy. This expression was used to predict the $^{14}N(\alpha,d)^{16}O$ cross sections which would be measured if detailed balance held. Comparison was made between these values and those which were actually observed. Detailed balance was found to hold within an average total uncertainty of ±0.56% over the energy region. (auth)

5597 PHOTONUCLEAR REACTIONS IN OXYGEN AND THEIR USE FOR THE CONTROL OF ENERGY AND PHOTON SPECTRUM AT ELECTRON ACCELERATORS. Filss, P.; Collin, W.; Guldbakke, S.; (and others) (Physikalisch-Technische Bundesanstalt, Brunswick). Z. Phys.; 239: 461-70(1970). (In German).

The yields of the photonuclear reactions $^{16}O(\gamma,n)$ and $^{16}O(\gamma,2n)$ were measured with a newly constructed device for fluid samples. The well-known structures of the (γ,n) cross section were used for the energy calibration of the accelerator. Though the yield should be strongly dependent on small changes of the bremsstrahlung spectrum, no difference was found between a thin or a thick target. The conclusion is that the thick target is, in effect, also a thin target under the accelerator conditions. The $(\gamma,2n)$ cross section was measured for the first time between threshold and 120 MeV. It is unusually small compared to the (γ,n) cross section. (auth)

5598 FAST-NEUTRON ENERGY DETERMINATIONS. Davis, Jay Clarence. Madison, Wis.; Univ. of Wisconsin (1969). 84p.

Thesis.

The techniques necessary for accurate determination of the energy of fast neutrons produced by particle beams from the Wisconsin Tandem Accelerator were investigated. The analyzing magnet of the accelerator was recalibrated to an accuracy of ±0.05% by observing the thresholds of the ^{7}Li, ^{13}C, ^{19}F, ^{27}Al, ^{54}Fe, and $^{58}Ni(p,n)$ reactions and that of the $^{2}H(^{16}O,n)$ reaction for oxygen charge states +3 and +4. The magnet calibration was found to be field dependent, changing by 1% over the proton energy range from 2 to 25 MeV. Energy loss and straggling were studied for Ni foils used as entrance windows on gas targets. The accuracy with which neutron energies could be calculated was determined by locating narrow resonance peaks in the C and O neutron total cross sections between 1 and 7 MeV. The neutron sources used were the $^{7}Li(p,n)$, $T(p,n)$, and $D(d,n)$ reactions. Variations between determinations with different sources were consistent with the quoted uncertainty of about 0.1% in neutron energy. The positions of resonance peaks in the interaction of neutrons with light nuclei previously used as energy reference points for measurements of the n−p total cross section for fast neutrons were determined. The effects of energy shifts upon values of the n−p singlet effective range deduced from the cross section measurements were examined. Although the energy changes suggested by this work reduce differences among values of r_s obtained at different laboratories, further measurements to determine the parameters of the n−p interaction will be required to resolve inconsistencies in both the slow- and fast-neutron results. (auth) (Diss. Abstr. Int., B)

5599 β-DECAY RATES AND THE ROLE OF THE $d_{\frac{5}{2}}$-ORBIT IN LIGHT s−d-SHELL NUCLEI. McGrory, J. B. (Oak Ridge National Lab., Tenn. Michigan State Univ., East Lansing). Phys. Lett.; 33B: 327-30(9 Nov 1970).

The effects of the $d_{\frac{5}{2}}$ single-particle orbit in shell-model calculations of light s−d-shell nuclei are discussed. It is shown that these effects are significant in the calculation of log-ft values for allowed Gamow−Teller β decays. (auth)

5600 SEARCH FOR GIANT-RESONANCE EXCITATION BY RADIATIVE CAPTURE OF π^{-} IN ^{16}O. Alder, J. C. (Univ., Lausanne, Switzerland); Jenefsky, R.; Joseph, C.; Vaucher, B.; Bressani, T.; Chiavassa, E.; Favier, J.; Schinzel, D.; Zupancic, C. Lett. Nuovo Cim.; 4: 256-60(8 Aug 1970).

A π^{-} beam with momentum 250 MeV/c was used to measure simultaneously the neutron time of flight and the γ-ray energy following radiative pion capture by ^{16}O. The γ-ray energy was measured with a NaI crystal, and the neutrons were detected by an array of seven liquid scintillators. No structure which could result from giant-resonance excitation appears in the total neutron time-of-flight spectrum or the total γ-ray energy spectrum. By plotting each of these spectra with respect to narrow windows in the other, however, one finds considerable evidence for the presence of events corresponding to $E_n \simeq 4.5$ MeV and E_γ around 110 MeV, which can be associated with excitation of the 2^{-} dipole giant-resonance state in ^{16}N. There is, on the other hand, no evidence for the predicted 8 MeV neutrons resulting

from the decay of quadrupole states. The radiative-capture rate to the 2^- level is of the order of 2×10^{-3} per stopped pion, i.e., about 10% of the total radiative-capture rate. (R.W.R.)

5601 ON THE THEORY OF (^{6}Li,d) AND (^{7}Li,t) REACTIONS. Dolinskii, E. I.; Turovtsev, V. V.; Yarmukhamedov, R. (Moscow State Univ.). Phys. Lett.; 33B: 147-9(28 Sep 1970).

Arguments showing that the mechanisms of the (^{6}Li,d) and (^{7}Li,t) reactions can be more complicated than the conventional α-particle stripping are presented. (auth)

Nuclear Properties and Reactions, $20 \leq A \leq 89$

Refer also to abstracts 5118, 5506, 5550, 5551, 5568, 5570, 5574, 5578, 5580, 5582, 5586, 5587, 5599, 5680, 5681, 5685, 5687, 5716, 5735, 5791–5793, 5834, and 5866.

5602 (ANU-P-501) STUDY OF THE ENERGY LEVELS OF ^{27}Si. Barker, F. C.; Carter, K. W.; Kean, D. C.; Piluso, C. J.; Spear, R. H. (Australian National Univ., Canberra. Research School of Physical Sciences). 1970. 7p. Dep. CFSTI (U. S. Sales Only).

The energy levels of ^{27}Si between 3.5 and 5.5 MeV excitation were studied by magnetic analysis of the reaction ^{28}Si(^{3}He,α)^{27}Si. The level scheme was compared with that of ^{27}Al in the light of an apparent regularity in the parity dependence of energy differences of corresponding levels in mirror nuclei of the 2s–1d shell. It was concluded that levels in ^{27}Si at 4.459 and 4.487 MeV probably have spins of $^7/_2$ and $^{11}/_2$, not necessarily respectively, and positive parity. (auth) (Australia)

5603 (FOA-4-4440) NEUTRON CAPTURE CROSS SECTIONS IN F, Mg, Al, Si, P, AND S FROM 20 TO 80 keV. Nystroem, G.; Lundberg, B.; Bergqvist, I. (Forsvarets Forskningsanstalt, Stockholm (Sweden)). Sep 1970. 26p. Dep. NTIS (U. S. Sales Only).

Neutron radiative-capture cross sections have been measured in the energy region 20 to 80 keV using time-of-flight techniques with a 12.7 cm × 10.2 cm NaI(Tl) scintillator. The samples studied were natural samples of F, Mg, Al, Si, P and S. Radiative widths were determined for the resonances in ^{19}F at 27 keV (1.4 ± 0.3 eV) and 50 keV (1.5 ± 0.3 eV), in ^{24}Mg at 84 keV (4.0 ± 0.9 eV) and in ^{27}Al at 35 keV (1.9 ± 0.3 eV). Resonances were also observed in Mg at 45 keV, in Si at 38 keV and 68 keV, in P at 27 keV and in S at 30 keV and 42 keV. (auth) (Sweden)

5604 (N-70-25281) STUDY OF THE ODD STRONTIUM ISOTOPES WITH STRIPPING AND PICKUP REACTIONS. Bercaw, Robert W.; Warner, Robert E. (National Aeronautics and Space Administration, Cleveland, Ohio. Lewis Research Center). Apr 1970. 54p. (NASA-TN-D-5765; E-5233). NTIS.

The (d,t) and (d,p) reactions induced by 20.65-MeV deuterons were used to study the levels of ^{87}Sr and ^{85}Sr up to an excitation of 3 MeV. The mass defect of ^{83}Sr was determined by the (d,t) reaction, and its level structure below 3 MeV was investigated. The cross sections were analyzed with the distorted-wave Born approximation to determine the orbital of momenta, the neutron transfers, and the spectroscopic factors. Tentative spin assignments were made on the basis of sum values and the j-dependence of the cross section. (auth) (STAR)

5605 (UCRL-72624) β-γ (CP) CORRELATION MEASUREMENTS IN ALLOWED TRANSITIONS. Bloom, S. D. (California Univ., Livermore. Lawrence Radiation Lab.). 31 Jul 1970. 39p. (CONF-700807-4). Dep. CFSTI.

From Conference on Angular Correlations in Nuclear Disintegration, Delft, The Netherlands.

The results which have been achieved by applying the technique of $\beta-\gamma$ (CP) correlation to allowed β decays are reviewed. It is assumed that all questions regarding the nature of the β interaction are well understood. The $\beta-\gamma$ (CP) technique has been reasonably useful in spin assignment and the measurement of electromagnetic multipole mixing: a table of nuclides for which such information has been obtained is given, as well as a list of some additional candidates. The technique has also been a major factor in advancing empirical knowledge of isospin in bound nuclear states by leading to a determination of the absolute value of the Fermi matrix element, which can be interpreted as denoting an isospin impurity. A relatively moderate extension of both theoretical and experimental work might yield a much more quantitative understanding, not only of isospin mixing, but also of the charge-dependent nuclear force, as well as of some of the more esoteric consequences of the CVC theory of β decay. (R.W.R.)

5606 (UCSB-34-P-144-7) NUCLEAR STRUCTURE RESEARCH. Progress Report, Task A. Eisberg, Robert M. (California Univ., Santa Barbara). Sep 1970. Contract AT(04-3)-34. 30p. Dep. NTIS.

The completion of a set of measurements of the binding energies of proton hole states in $1f_{\frac{7}{2}}$ nuclei is reported. These measurements used a modification of equipment developed for earlier ^{89}Y(p,2p) angular correlation experiments at the UCLA cyclotron. This equipment will be used for additional (p,2p) experiments if the energy resolution in the new beam area of the cyclotron proves to be as good as predicted. Also reported are measurements of the effect of nuclear reactions in the response of solid state detectors, and of the development of a very successful new technique to overcome the serious experimental difficulties due to nuclear reactions in such detectors. The first use of the new technique will be to make measurements of inelastic proton scattering at very small angles. A description of the reasons for doing this, and of the equipment that has been constructed for the purpose, is contained in the final section of this report. (auth)

5607 LEVELS OF ^{70}Zn FROM THE INELASTIC SCATTERING OF 42 MeV ALPHA-PARTICLES. Cooper, L. R.; Easterday, H. T.; Zafiratos, C. D. (Oregon State Univ., Corvallis). Nuovo Cim.; 69A: 545-50(21 Oct 1970).

Energy levels of ^{70}Zn were excited by inelastic scattering of 42-MeV α particles. Spin and parity assignments to several levels are made on the basis of the diffraction model and by comparison of level systematics of the even-mass zinc isotopes. The structure of ^{70}Zn is discussed in the framework of the vibrational model. (auth)

5608 INTERNAL CONVERSION OF M3 ISOMERIC TRANSITIONS IN ^{58}Co AND ^{60}Co. Campbell, J. L. (Univ. of Guelph, Ont.); Goble, R. J.; Smith, H. J.; Dragoun, O. Nucl. Phys.; A152: 631-40 (1970).

A high-resolution Ge(Li) x-ray spectrometer was used to measure the K conversion coefficients of the 24.87 keV M3 transition in ^{58}Co and the 58.57 keV M3 transition in ^{60}Co. The values found, 2030 ± 90 and 43.1 ± 1.8 respectively, are approximately 10% greater than theoretical predictions for pure M3 transitions. Predictions of various atomic models agree closely among themselves. (auth)

5609 T = $^3/_2$ ANALOGUE STATE IN ^{63}Ni. Devins, D. W. (Indiana Univ., Bloomington); Rickey, M. E.; Hayakawa, S.; Rost, E. Nucl. Phys.; A150: 187-92(1970).

The T = $^3/_2$ analog of the ground state of ^{63}Co has been observed in ^{63}Ni by the ^{64}Ni(p,d)^{63}Ni reaction with 27.5-MeV incident protons. The observed excitation energy of this state, 11.85 ± 0.08 MeV, yields a Coulomb displacement energy ΔE_c = 8.97 ± 0.08 MeV in excellent agreement with known values in this mass region. The angular distribution for this state is consistent with assignments of $J^\pi = ^7/_2^-$, and, when compared with coupled-channel calculations, yields a spectroscopic factor of 0.21, indicating considerable fragmentation of the strength of the transition. (auth)

5610 MASS OF ^{39}Ca. Kemper, K. W.; McKenna, C. M.; Nelson, J. W. (Florida State Univ., Tallahassee). Phys. Rev., C; 2: 213-14(Jul 1970).

The ground-state threshold for the reaction ^{39}K(p,n)^{39}Ca has been measured to be 7.492 ± 0.006 MeV. The absolute value of the total reaction cross section has been determined from threshold to 10.5-MeV bombarding energy. From the threshold energy, the mass excess of ^{39}Ca is calculated to be –27281 ± 6 keV, which agrees within the error limits with positron end-point results but not with an earlier measurement of this threshold. (auth)

5611 SHELL-MODEL STRUCTURE OF ^{42}Ca THROUGH ^{50}Ca. McGrory, J. B.; Wildenthal, B. H.; Halbert, E. C. (Oak Ridge National Lab., Tenn.). Phys. Rev., C; 2: 186-212(Jul 1970).

The low-lying states of the calcium isotopes ^{43}Ca through ^{50}Ca are discussed within the framework of the conventional shell model. An inert ^{40}Ca core is assumed. Calculations are made in several basis-vector spaces involving active $0f_{\frac{7}{2}}$, $1p_{\frac{3}{2}}$, $0f_{\frac{5}{2}}$, $1p_{\frac{1}{2}}$, and $0g_{\frac{9}{2}}$ neutron orbits. In one set of calculations, we use a "realistic" effective interaction derived for this mass region by Kuo and Brown. The shell-model results suggest that, in this effective interaction, the interactions of $f_{\frac{7}{2}}$ neutrons with $p_{\frac{3}{2}}$, $p_{\frac{1}{2}}$, and $f_{\frac{5}{2}}$ neutrons are too strong. In other calculations, with a modified Kuo-Brown interaction, we find the calculated spectra for the low-lying states of the calcium isotopes are in agreement with observed spectra, with several significant exceptions. The exceptions are that the second 0^+ and 2^+ states observed in ^{42}Ca, ^{44}Ca, and ^{46}Ca are not accounted for in the calculation. Calculated spectroscopic factors for $f_{\frac{7}{2}}$ transfers are in good agreement with experimental spectroscopic factors, and the observed centroids of the $p_{\frac{3}{2}}$ single-particle strengths are reasonably well reproduced. The results also indicate that "core-excitation" effects are significant above about 2.5 MeV in ^{42}Ca through ^{48}Ca. (auth)

XUM

5612 LEVELS IN ^{53}Mn, ^{58}Co, ^{63}Zn, AND ^{70}Ga FROM THE (p,n) REACTION. Tanaka, S.; Stelson, P. H.; Bass, W. T.; Lin, J. (Oak Ridge National Lab., Tenn.). Phys. Rev., C; 2: 160-6(Jul 1970).

Energy levels in ^{53}Mn, ^{58}Co, ^{63}Zn, and ^{70}Ga were located by means of the (p,n) reaction. Neutron spectra were measured with approximately 10-keV energy resolution by the time-of-flight method with flight paths of 7.9 and 9.2 m. Several sets of close-lying levels were resolved, and many new levels were found in ^{53}Mn up to an excitation energy of 4 MeV. In ^{58}Co, a total of 36 levels was observed in the first 2.5 MeV of excitation, and in ^{63}Zn, a total of 11 levels up to 1.5-MeV excitation energy. In ^{70}Ga, 66 levels were observed in the first 2.7 MeV of excitation energy; 16 new levels were found in the region between 2.26 and 2.73 MeV. (auth)

5613 ENERGY LEVELS OF ^{27}Al FROM THE REACTION ^{26}Mg(p,n)^{26m}Al. Mo, T.; Delaune, C. I.; Nelson, J. W. (Florida State Univ., Tallahassee). Phys. Rev., C; 2: 1006-11(Sep 1970).

The excitation function for all neutron groups leading to the formation of the 6.38-sec first excited state of ^{26}Al was measured for incident proton energies from 5.2 to 8.0 MeV by detecting the residual radioactivity. Resonances were observed corresponding to 19 levels in ^{27}Al ranging in excitation energy from 13.43 to 16.10 MeV. For the first four resonances, which are due to the n_1 group alone, neutron angular distributions were measured. R-matrix calculations produced fits to the excitation curve and angular distributions which permit spin and parity assignments of $\frac{1}{2}^+$, $\frac{3}{2}^+$, $\frac{3}{2}^-$, and $\frac{5}{2}^+$ to the levels of excitation energies 13.433, 13.703, 13.867, and 13.998 ± 0.015 MeV, respectively. Possible correspondence to isobaric analog states in ^{27}Mg is discussed. (auth)

5614 BETA DECAY OF ^{40}Cl AND LEVELS OF ^{40}Ar. Kern, B. D.; Winters, R. W.; Jerrell, M. E. (Univ. of Kentucky, Lexington). Phys. Rev., C; 2: 948-57(Sep 1970).

Radioactive ^{40}Cl was produced by the reaction ^{40}Ar(n,p)^{40}Cl through bombardment of a liquid-argon target with 14.9-MeV neutrons. γ rays were observed with 6-, 15-, and 35-cc Ge(Li) crystal detectors, and with two NaI(Tl) crystal detectors in coincidence. Twenty-three γ rays with energies from 262 to 6334 keV were assigned to transitions in ^{40}Ar. The β-ray relative intensities were deduced from the relative intensities of the γ rays, and log ft values were calculated. It was concluded that all levels in ^{40}Ar up to and including the 3518-keV level have even parity. Seven levels from 3681 to 6335 keV in ^{40}Ar have odd parity and spin of 1, 2, or 3. The ground energy level of ^{40}Cl has spin-parity 2^-, if in fact the 3681-keV level of ^{40}Ar has spin-parity 3^-. (auth)

5615 LEVELS OF ^{88}Sr FROM THE ^{86}Sr(t,p)^{88}Sr REACTION. Ragaini, R. C.; Knight, J. D.; Leland, W. T. (Los Alamos Scientific Lab., N. Mex.). Phys. Rev., C; 2: 1020-36(Sep 1970).

The levels of ^{88}Sr up to an excitation energy of 7 MeV have been investigated by the ^{86}Sr(t,p) reaction with 15-MeV tritons. Proton spectra were measured by a ΔE-E counter telescope system with an overall resolution of 35 keV, and close-lying peaks were resolved by additional measurements with a magnetic spectrograph. Angular distributions were measured from 12.5 to 90°, and comparisons with zero-range distorted-wave Born-approximation calculations permitted spin assignments of 32 of the 45 levels observed. Four excited 0^+ states were observed. From a comparison of their cross sections with the ^{88}Sr(t,p)^{90}Sr ground-state cross section, no one of them could be identified as the pairing vibration state; the strength of the latter appears to be fragmented. The data are compared with previous information on the ^{88}Sr level structure. (auth)

5616 PROPERTIES OF THE LOW-LYING STATES OF ^{48}Ca. Benczer-Koller, N. (Rutgers–The State Univ., New Brunswick, N. J.); Seaman, G. G.; Bertin, M. C.; Tape, J. W.; MacDonald, Jack R. Phys. Rev., C; 2: 1037-40(Sep 1970).

The energies, spins, decay modes, and lifetimes of the first three excited states of ^{48}Ca have been determined. The results are: 3.832 MeV (2^+), 0.053 ± 0.024 psec; 4.284 MeV (0^+), 322 ± 16 psec; and 4.507 MeV (3^-), $8.8^{+3.5}_{-2.5}$ psec. (auth)

5617 ANALYSIS OF STRIPPING TO QUASIBOUND LEVELS IN ^{41}Sc. Youngblood, D. H.; Kozub, R. L.; Kenefick, R. A.; Hiebert, J. C. (Texas A and M Univ., College Station). Phys. Rev., C; 2: 477-88(Aug 1970).

Angular distributions have been measured for 15 levels observed in the ^{40}Ca(^{3}He,d)^{41}Sc reaction at 40-MeV bombarding energy. Distorted-wave Born approximation calculations for the proton unstable excited states quasibound by the Coulomb and centrifugal barrier were performed using a form factor corresponding to an unbound (resonance) level in a Woods-Saxon well. The resulting spectroscopic factors are found to be insensitive to the scattering phase shifts, and in agreement with those obtained by elastic scattering. Most of the available $1f_{\frac{7}{2}}$, $2p_{\frac{3}{2}}$, and $2p_{\frac{1}{2}}$ strength and a large portion of the $1f_{\frac{5}{2}}$ strength is observed below 6-MeV excitation. Little $1g_{\frac{9}{2}}$ or $2d_{\frac{5}{2}}$ strength is observed. (auth)

5618 STUDIES ON ^{21}Ne AND ^{23}Ne VIA THE ^{20}Ne(d,p)^{21}Ne AND ^{22}Ne(d,p)^{23}Ne REACTIONS. Howard, A. J.; Pronko, J. G.; Whitten, C. A. Jr. (Yale Univ., New Haven). Contract AT(30-1)-3223. Nucl. Phys.; A152: 317-36(1970).

Angular distribution measurements have been performed on the ^{20}Ne(d,p)^{21}Ne and ^{22}Ne(d,p)^{23}Ne reactions at E_d = 16.4 and 12.1 MeV, respectively. The results for ^{21}Ne indicate that l_n = 2 transfer is involved in the formation of the 350, 3735, 4526, 5338, 5550, 5822 and 6606 keV states, whereas l_n = 1 transfer is associated with the 4730 and 5694 keV levels. The only l_n = 0 transfer detected in the present ^{20}Ne(d,p)^{21}Ne studies involved formation of the 2790, 2796 keV composite of states. In the case of the ^{22}Ne(d,p)^{23}Ne reaction, l_n = 2 transfer was discerned for the angular distributions associated with the ground, 2314, 3433, 3988 keV and probably the 5186 keV ^{23}Ne states. The 3218 and 3836 keV ^{23}Ne levels were formed by l_n = 1 transfers, and the 1018 keV state displayed l_n = 0 transfer characteristics in its formation. No l_n = 3 stripping strength is observed in the formation of the bound states for either the ^{21}Ne or ^{23}Ne systems. Distorted-wave Born approximation fits were applied to the data and the associated spectroscopic factors were extracted. A synthesis of existing information concerning the formation of ^{21}Ne and ^{23}Ne states via the (d,p) reaction is presented, and a discussion concerning the observed spectroscopic strengths and those predicted within the framework of the strong-coupling collective model representation is given. (auth)

5619 RESEARCH ON NUCLIDES FAR FROM THE STABILITY LINE. Verheul, H. (Free Univ., Amsterdam). Ned. Tijdschr. Natuurk.; 35: 197-217(Jul 1969). (In Dutch).

Experimental work on far-unstable nuclides is rendered difficult by their short half-life and the difficulties of the chemical and isotopic separation. Such studies yield mass formulas allowing to calculate constants with high precision; delayed neutron or proton decay could provide information on the atomic number A and the excitation energy of the neutron-active level of daughter nuclides. The potential methods for preparing such "remote" nuclides are reviewed; they include nuclear, photonuclear, fission and heavy-ion reactions. The generated nuclides may be separated from the target material by chemical methods or by mass separation techniques. Isotope separation on-line (ISOL) methods are reviewed in greater detail. Short-lived isotopes studied at the Free University are listed; shell models of Co, Ni and Cu isotopes have been published. The 34-MeV cyclotron of the University has been used to produce many isotopes with $T_{\frac{1}{2}}$ > 20 sec. A pneumatic transport system is used to transport the material from the target area to the separator 75 m away. (Review article, 36 references) (TTT)

5620 NUCLEAR DATA SHEETS: A = 50 to 54. Nucl. Data, Sect. B; 3: B3.5,6.i-vii; B3.5,6.1-217(Apr 1970).

Experimental data on the decay and level schemes for A = 50 through 54 nuclei are tabulated. Inconsistencies and discrepancies in the data are discussed. (J.W.R.)

5621 DECAY OF ^{69}As. Boswell, G. G. J.; McGee, T. (Univ. of Salford, Eng.). J. Inorg. Nucl. Chem.; 32: 2805-8(Aug 1970).

The decay of ^{69}As was investigated as part of a study of the neutron deficient isotopes produced by bombarding medium mass nuclides with heavy ions. Natural Co foils were bombarded for 30 min. with a 15 to 25 μa beam of 120-MeV carbon ions in a heavy ion linear accelerator, the desired reaction being ^{59}Co (^{12}C, 2n)^{69}As, the compound nucleus ^{71}As decaying by neutron emission to give ^{69}As, ^{69}As and ^{70}As. The target was allowed to cool for 60 min. to enable ^{69}As to decay to ^{69}Ge, and in order to determine whether ^{69}As had been produced in the reaction the Ge daughters which had grown from an initially pure As fraction were milked and their gamma spectrum examined. The observed gamma transitions corresponded to those attributed to ^{69}Ge; hence ^{69}As must have been present in the original As fraction. The decay of the gross activity of an isolated As sample was followed on a GM counter, and analysis of the decay curve indicated components with half-lives of 40 hr., 50 min., and 15 min. The 40 hr. component was assigned to the decay of ^{69}Ge, the 50 min. component to the decay of ^{70}As, and the 15 min. activity to the decay of ^{69}As. A more accurate determination of the half-life of ^{69}As was made by comparing the activities of consecutive Ge fractions milked at 15 min. intervals from an initially pure As sample, the half-life found being 14.9 min. The investigation showed that ^{69}As decays with a half-life of 14.9 ± 0.9 min. by the emission of electromagnetic radiations of 0.087, 0.145 and 0.233 MeV and positions of maximum energy 2.95 MeV. (UK)

5622 QUADRUPOLE MOMENTS OF THE FIRST EXCITED STATES IN ^{20}Ne AND ^{22}Ne. Nakai, K.; Stephens, F. S.; Diamond, R. M. (Univ. of California, Berkeley). Nucl. Phys.; A150: 114-28(1970).

Static quadrupole moments of the first excited states of ^{20}Ne and ^{22}Ne have been measured using the reorientation effect in projectile excitation. The Ne nuclei, accelerated by the Berkeley Hilac, were Coulomb excited by thin targets of ^{120}Sn, ^{130}Te or ^{148}Sm and the gamma-ray yields in coincidence with particles scattered at angles of 90° and 160° were evaluated using the de Boer-Winther Coulomb excitation program. The results obtained are $Q(^{20}Ne,2^+) = -0.24 \pm 0.03$ b, $B(E2,^{20}Ne,0^+ \rightarrow 2^+) = 0.048 \pm 0.007$ $e^2 \cdot b^2$, $Q(^{22}Ne,2^+) = -0.21 \pm 0.04$ b, and $B(E2,^{22}Ne,0^+ \rightarrow 2^+) = 0.033 \pm 0.006$ $e^2 \cdot b^2$. (auth)

5623 NUCLEAR INTERACTIONS OF ^{45}Sc AND ^{68}Zn WITH PROTONS OF MEDIUM ENERGY. McGee, T.; Rao, C. L.; Saha, G. B.; Yaffe, L. (McGill Univ., Montreal). Nucl. Phys.; A150: 11-29(1970).

Cross sections for the following reactions with ^{45}Sc (p,n), (p,2n), (p,pn), (p,3p), and (p,3pn), and ^{68}Zn (p,n), (p,2n), (p,3n), (p,2p) and (p,p3n) + (p,4n) produced by protons of energy up to 85 MeV have been measured using radiochemical methods. Comparisons have been made with calculations based on the statistical and cascade-evaporation theories. It is shown that the nuclear reactions proceed via a compound nucleus mechanism at lower energies and by a combination of the compound nucleus and direct interaction mechanisms at higher energies. (auth)

5624 ELECTRON AND GAMMA TRANSITIONS IN ^{45}Sc. Eastham, D. A.; Phillips, W. R. (Univ. of Manchester, Eng.). Nucl. Phys.; A146: 112-28(1970).

Energy levels below 1.5 MeV excitation energy in ^{45}Sc have been studied via Coulomb excitation with ^{4}He particles and via the inelastic proton scattering process. Cross-section measurements for E2 excitation of the 377, 720, and 1237 keV levels provided values for the B(E2)↑, of the upward transitions. Angular distribution measurements on the de-excitation gamma rays limited spin assignments to the levels and mixing ratios in the gamma transitions. The gamma rays observed after inelastic proton scattering clarified the decay schemes of most of the low levels: observation of conversion electrons that occurred in the decays of the 377, 543 and 720 keV states enabled spin and parity values of $(^3/_2,^5/_2)^-$, $^5/_2(+)$ and $^5/_2^-$ to be assigned to those levels. The scheme obtained for ^{45}Sc is compared to model predictions and the similarity to the structures of the other scandium isotopes suggests the usefulness of the mixing of two-hole configurations in the description of the natural parity levels. (auth)

5625 THERMAL NEUTRON CAPTURE GAMMA RAYS FROM THE ^{26}Mg(n,γ)^{27}Mg REACTION. Selin, E.; Wallander, E. (Chalmers Univ. of Tech., Goteborg). Nucl. Phys.; A150: 305-10(1970).

Thermal-neutron capture γ rays from ^{26}Mg were measured with a Ge(Li) detector in pair and anticoincidence spectrometer arrangements. An internal target of enriched ^{26}Mg was used. The reaction Q-value was determined. Energies and intensities of the γ rays are reported, and a decay scheme is presented. Absolute thermal-neutron capture cross sections for ^{24}Mg(n,γ)^{25}Mg and ^{25}Mg(n,γ)^{26}Mg were determined from neutron capture in natural magnesium. (auth)

5626 EXCITED STATES OF ^{44}Ca. Lawley, N.; Dawson, N.; Jones, G. D.; Main, I. G.; Mulhern, P. J.; Symes, R. D.; Thomas, M. F. (Univ. of Liverpool). Nucl. Phys.; A149: 95-112(1970).

Excited states of ^{44}Ca have been studied using p−γ coincidence measurements with a Ge(Li) detector and p−γ angular correlations. Precise excitation energies have been obtained for 12 levels. Electromagnetic decay modes have been established for 10 levels, and branching ratios measured in 6 cases. The angular correlations yield a spin 1 assignment to the state at 3.661 MeV and spin 2 assignments to the states at 3.303 MeV, 3.775 MeV and 4.20 MeV, and also confirm a number of previous spin assignments. From the observed modes of decay we tentatively assign spin 4 or 5 to the state at 3.359 MeV. Multipole mixing ratios have been measured for 5 transitions from levels at 2.285 MeV, 2.657 MeV, 3.049 MeV and 3.775 MeV. A number of the levels may be classified fairly successfully in terms of seniority; possible deformed admixtures are suggested in some other states. (auth)

5627 LEVELS OF ^{34}Cl BELOW 3 MeV. Sykes, D. H. (Rijksuniversiteit, Groningen, Netherlands). Nucl. Phys.; A149: 418-25(1970).

Gamma-ray decay properties of levels of ^{34}Cl have been investigated in a study of the ^{32}S(He-3,pγ)^{34}Cl reaction. The 0.460 and 0.667 MeV levels have both been assigned spin J = 1. Possible spin values are given for the levels at 1.231, 1.891, 2.587 and 2.720 MeV. Branching ratios were determined and evidence was found that the 2.162 MeV level is a doublet. (auth)

5628 LIFETIME MEASUREMENTS IN s-d SHELL NUCLEI. IV. MEAN LIVES OF ^{31}Si LEVELS. Graber, H. D.; Glaudemans, P. W. M.; Endt, P. M. (Rijksuniversiteit, Utrecht). Nucl. Phys.; A149: 1-10(1970).

Mean lives, branching ratios, and excitation energies of the lowest six levels in ^{31}Si were measured with the reaction ^{30}Si(d,pγ)^{31}Si. The γ-rays were detected in coincidence with protons. From Doppler-shift attenuation measurements mean lives were determined of 790 ± 170, 890 ± 210, 55 ± 25, 20 ± 20, 550 ± 120 and <15 fs for the levels at E_x = 0.75, 1.69, 2.32, 2.79, 3.13 and 3.53 MeV, respectively. The electromagnetic transition rates between the positive parity states agree very well with values following from many-particle shell-model calculations. (auth)

5629 LEVEL STRUCTURE OF ^{47}Ti. Rao, M. N. (Oak Ridge National Lab., Tenn.); Rapaport, J.; Belote, T. A.; Dorenbusch, W. E. Contract AT(30-1)-2098. Nucl. Phys.; A151: 351-68(1970).

The ^{48}Ti(^{3}He,α)^{47}Ti, ^{47}Ti(p,p′γ)^{47}Ti, and ^{45}Sc(^{3}He,p)^{47}Ti reactions were studied at 13.0, 6.5, and 12.0 MeV bombarding energies, respectively, with the MIT multiple-gap spectrograph. Transitions from the (^{3}He,α) reaction were observed up to an excitation energy of 8.757 MeV, including the isobaric analogs of three states in ^{47}Sc. Data for the (p,p′γ) reaction were taken for states up to 1.545-MeV excitation energy. Five transitions from the ^{45}Sc(^{3}He,p)^{47}Ti reaction were studied in the first 3.5 MeV of excitation. The results for the transfer reactions were analyzed in the distorted-wave Born approximation. (auth)

5630 SCHEMATIC MODEL CALCULATIONS FOR ^{40}K(β⁻)^{40}Ca. Towner, I. S. (Nuclear Physics Lab., Oxford). Nucl. Phys.; A151: 97-106(1970).

The experimental lifetime of the unique third-forbidden beta-decay branch ^{40}K(β⁻)^{40}Ca is five times longer than single-particle estimates for the transition. Using an extended version of the schematic model, this hindrance can be traced to the repulsive nature of the T = 1 particle-hole force. (auth)

5631 GAMMA DECAY OF ^{39}K LEVELS MEASURED WITH THE ^{38}Ar(p,γ)^{39}K REACTION. Maripuu, S. (Rijksuniversiteit, Utrecht). Nucl. Phys.; A151: 465-78(1970).

The ^{38}Ar(p,γ)^{39}K reaction has been studied in the E_p = 1.25 to 2.35 MeV range. The strengths of 41 resonances have been determined relative to the strength of a ^{36}Ar(p,γ)^{37}K resonance. The branching ratios of ten resonances and of ten bound states have been measured with a 50 cm^3 Ge(Li) detector; the reaction Q-value is Q = 6380.6 ± 1.2 keV. A spin J = $^3/_2$ has been assigned to the 3.02, 4.08 and 7.74 MeV levels on the basis of angular distribution measurements. Doppler shift attenuation measurements have been performed on γ-rays deexciting the 2.52, 3.02 and 4.08 MeV levels. The 7.74 MeV state is interpreted as the analog of the first excited state (E_x = 1.27 MeV, $J^\pi = ^3/_2^-$) in ^{39}Ar. The experimental properties of ^{39}K levels are compared with recent shell-model calculations. The analog to anti-analog M1 strength is compared with the strengths of other similar transitions and with theoretical calculations. (auth)

5632 POLARIZATION OF PROTONS INELASTICALLY SCATTERED ON ^{24}Mg, ^{52}Cr, AND ^{58}Ni. Ruh, A.; Marmier, P. (Eidgenoessische Technische Hochschule, Zurich). Nucl. Phys.; A151: 479-503(1970).

The polarization of protons elastically and inelastically scattered on ^{24}Mg, ^{52}Cr and ^{58}Ni leaving the residual nucleus in its first excited state was measured with a carbon polarimeter. The energy of the incident protons was varied between 5.38 and 5.95 MeV and the lab scattering angle between 45° and 120°. In addition, the excitation functions were measured for ^{24}Mg (p,p$_1$)^{24}Mg* between 5 and 6 MeV and for ^{52}Cr(p,p$_0$)^{52}Cr and ^{52}Cr(p,p$_1$)^{52}Cr* between 5 and 6.5 MeV. Large values of the polarization were determined for the protons scattered on ^{24}Mg and in agreement with the predictions of the statistical CN model, no polarization was observed for the protons inelastically scattered on ^{58}Ni. Relatively large polarizations were found in the inelastic scattering on ^{52}Cr which seems to indicate a violation of the statistical assumptions. The latter had been believed to be fulfilled, since (p,p′γ) angular correlation measurements on ^{52}Cr had given excellent agreement with the statistical CN theory. On the other hand, the angular cross-correlation function of the cross-section fluctuations also does not agree with the statistical theory. The correlated intermediate structure of the excitation functions can probably be interpreted as an excitation of doorway states which in turn would also explain the measured polarizations. (auth)

XUM

5633 GAMMA-RAY TRANSITIONS IN ^{29}P. Williams, R. P.; Buccino, S. G.; Wellborn, C. C. (Tulane Univ., New Orleans). Nucl. Phys.; A151: 504-12(1970).

A study was made at the 1.381-MeV resonance of the ^{28}Si(p,γ)^{29}P reaction. Lifetimes of the resonance level and of the first and second excited states in ^{29}P were determined with the Doppler shift attenuation method, to be $0.013^{+0.008}_{-0.005}$, $0.24^{+0.11}_{-0.06}$ and $0.39^{+0.19}_{-0.10}$ ps, respectively. Accurate energies were determined for the four γ-rays seen at this resonance and for the three energy levels involved. Angular distribution measurements yielded an unambiguous spin assignment of $^1/_2$ for the resonance level, and the γ-ray branching ratio of this level was obtained. (auth)

5634 DECAY OF ^{85m}Kr. Wohn, F. K.; Talbert, W. L., Jr.; Halbig, J. K. (Ames Lab., Iowa). Nucl. Phys.; A152: 561-9(1970).

The allowed beta spectrum and internal conversion electron spectrum in the decay of ^{85m}Kr were measured with the high resolution $\pi\sqrt{2}$ magnetic spectrometer of the TRISTAN on-line isotope separator system, and the ^{85m}Kr gamma-ray spectrum was measured with a high resolution Ge(Li) detector. The half-life of ^{85m}Kr was found to be 4.480 ± 0.008 h. The allowed beta decay of ^{85m}Kr was found to have an end-point energy of 840 ± 2 keV, an intensity of 78.8% and a log ft of 5.15. Using the PBS method for calculating internal conversion coefficients, the 150.99 ± 0.05 keV transition in ^{85}Rb was found to be of pure M1 multipolarity with a K-shell internal conversion coefficient α_K of 0.0400 ± 0.0008 and a K/L/M ratio of 89/10/2.2. The 304.47 ± 0.05 keV isomeric transition in ^{85}Kr was found to be a pure M4 multipole with α_K = 0.432 ± 0.020 and a K/L/M ratio of 67/10/2.0. The gamma-ray energies were determined by both Ge(Li) and spectrometer measurements. (auth)

5635 NUMERICAL CONSTRUCTION OF DECAY SCHEMES. Johnson, L. V.; Kennett, T. J. (McMaster Univ., Hamilton, Ont.). Nucl. Instrum. Methods; 87: 109-14(1970).

A method is outlined for constructing a decay scheme from the energies of gamma ray transitions observed in the (n,γ) reaction and from the energies of the associated levels obtained in measurements of the (d,p) reaction. This method is also capable of accommodating any $\gamma-\gamma$ coincidence information or any foreknowledge of the decay structure. Discussed are the statistical uncertainties involved in the decay scheme analysis process and how these uncertainties can be minimized in the construction procedure. The method has been successfully applied to the ^{40}K decay scheme and the results are provided. (auth)

5636 INVESTIGATION OF A POSSIBLE VIOLATION OF THE INDEPENDENCE OF THE DECAY OF A COMPOUND NUCLEUS OF THE SPIN OF THE INPUT CHANNEL. Karadzhev, K. V.; Man'ko, V. I.; Nersesyan, A. N.; Chukreev, F. E. JETP Lett. (USSR) (Engl. Transl.); 12: 104-5(5 Aug 1970).

Translated from Zh. Eksp. Teor. Fiz., Pis'ma Red.; 12: 149-51(5 Aug 1970).

The excitation function for the reaction ^{31}P(p,γ_0)^{32}S was measured as well as the ratio of the gamma yields at 90 and 0°. The ratio N(90°)/N(0°) = 5.54 ± 0.5; this value implies that the spin-mixing coefficient $t = 0.98^{+0.02}_{-0.06}$. These measurements confirm that, within experimental error, the coefficient of spin mixing is the same for the reactions ^{31}P(p,α)^{28}Si, ^{31}P(p,p)^{31}P, and ^{31}P(p,γ_0)^{32}S. (R.W.R.)

5637 STUDY OF NUCLEAR STATES OF SEVERAL ODD-A NUCLEI 68 ≤ Z ≤ 79 THROUGH ELECTROMAGNETIC EXCITATION FROM 2.3 TO 3.6 MeV. Johnson, W. T. K. (American Univ., Washington, D. C.); Chertok, B. T.; Dick, C. E. Phys. Rev. Lett.; 25: 599-602(31 Aug 1970).

Thirty-four excited states have been studied between 2.3 and 3.5 MeV in ^{167}Er, ^{179}Hf, ^{191}Ir, and ^{197}Au by observing the decay of the isomeric levels in these nuclei following electron and photon activation. Twenty-eight of these states are observed for the first time. Of the 34 observed transitions, M1 + E2 multipolarity assignment is made to 20, two are identified as E0 transitions, and one is assigned E1 multipolarity. Accurate values for the isomeric half lives are also presented. (auth)

5638 ANALYSIS OF THE ^{58}Ni(n,p)^{58}Co REACTIONS LEADING TO PARENT ANALOGUES OF COLLECTIVE STATES. Obu, Mitsuaki; Terasawa, Tokuo (Tokyo Univ.). Progr. Theor. Phys. (Kyoto); 43: 1231-43(May 1970).

The proton energy spectra for the reaction ^{58}Ni(n,p)^{58}Co at E_n = 14.8 MeV show two strong peaks at E_p = 11.5 and 14.5 MeV at forward angles. The experimental data on these peaks are analyzed by assuming that they correspond to the direct (n,p) reactions leading to the parent analog states P of the E1 and M1 giant resonance states C of ^{58}Ni. The parent analog states P are obtained by using the relation $|P\rangle \propto T_+|C\rangle$ from the E1 and M1 giant resonance states C, which are treated in the particle–hole framework. Calculations are performed for the Q values and for the differential cross sections for the (n,p) reactions leading to these parent analog states. The theoretical results are in good agreement with the experimental data on the peaks in the proton spectra. The strengths of the isospin- and spin–isospin-dependent parts of the effective two-body interaction between the incident and target nucleons are adjusted to yield the observed cross sections, and their values determined are consistent with those deduced from other experimental data. (auth)

5639 SPECTRA AND DIFFERENTIAL CROSS SECTIONS OF 14 MeV NEUTRON INELASTIC SCATTERING FROM IRON. Haussen, W.; Schweitzer, Th.; Seeliger, D.; Seidel, K. (Technische Univ., Dresden). Kernenergie; 13: 226-8(Jul 1970). (In German).

Spectra and angular distributions of 14-MeV neutrons inelastically scattered from iron have been measured by using time-of-flight techniques in the energy range from 2 to 11 MeV. From the results of the measurements, differential inelastic scattering cross sections for 1-MeV energy ranges have been obtained. From the shape of the spectra in the energy range from 3 to 4 MeV the mean nuclear temperature was found to be (1.49 ± 0.7) MeV. The fraction of direct inelastic scattering processes in the energy range from 5 to 11 MeV is at least 20 per cent. (auth)

5640 MASS OF ^{13}O AND THE ISOBARIC MULTIPLET MASS EQUATION. Mendelson, Robert; Wozniak, G. J.; Bacher, A. D.; Loiseaux, J. M.; Cerny, Joseph (Univ. of California, Berkeley). Phys. Rev. Lett.; 25: 533-6(24 Aug 1970).

The mass excess of ^{13}O has been determined to be 23.107 ± 0.015 MeV. This yields a value for d, the coefficient of T_3^2 in the isobaric-multiplet mass equation, of −0.8 ± 3.4 keV for the A = 13 quartet. Additional values for d, obtained from new measurements of the masses of ^{17}Ne, ^{21}Mg, and ^{25}Si, are also consistent with zero. (auth)

5641 PRECISION-MEASUREMENT OF ^{27}Al(n,α) CROSS SECTION FOR 14.43-MeV NEUTRONS. Hille, M.; Vonach, H. (Technische Hochschule, Munich); Stengl, G.; Bruenlich, W.; Werner, E. Z. Phys.; 237: 155-79(1970). (In German).

A precision measurement of the ^{27}Al(n,α)^{24}Na cross section at 14.43 MeV was performed. Aluminum samples were irradiated in an accurately known neutron flux determined by the associated particle method. The induced ^{24}Na activity was measured with a scintillation detector accurately calibrated by means of ^{24}Na standards by the $\beta-\gamma$ coincidence method. By carefully minimizing all sources of systematic errors an overall accuracy of 0.7% on a 99.5-(3σ) confidence level was obtained. The measurements result in a cross section of 117.0 mb for ^{27}Al(n,α)^{24}Na for neutrons of an average energy of 14.43 MeV and an energy width of approximately 0.2 MeV. (auth)

5642 SUPPLEMENTARY DATA CONCERNING THE ^{58}Ni(p,p'γ) REACTION. Alberts, W. G.; Bondenmiller, K. H.; Buhl, S. (Univ., Heidelberg). Z. Phys.; 238: 360-71(1970).

Angular correlation measurements for the ^{58}Ni(p,p'γ) reaction were performed at E_p = 8.1 MeV. Method II of Litherland and Ferguson was used to determine multipole mixing ratios of the γ radiation and spins of most of the excited levels up to 4.11 MeV The results confirm for the most part recent measurements of van Patter et al.; the 2775-keV state was verified to have a spin of J = 2. Several discrepancies and additional information concerning the 3531-, 3774-, 3898-, and 4108-keV levels are discussed. A spin value of J = 1 is assigned to the 3531-keV level, clearly ruling out former assignments of 4^+ and 0^+. A J = 4 assignment is proposed for the 3774-keV state, contrary to the generally assumed value of J = 3, which these measurements do not support. (auth)

5643 BACKWARD-ANGLE ANOMALIES IN INELASTIC ALPHA-PARTICLE SCATTERING ON ^{40}Ca. Schmeing, H.; Santo, R. (Max-Planck-Institut fuer Kernphysik, Heidelberg). Phys. Lett.; 33B: 219-21(12 Oct 1970).

Angular distributions for the ^{40}Ca(α,α') reaction were measured at 29 MeV up to 176° with 60 keV resolution. The 0^+ and 1^- states show a backward rise similar to that previously observed for the elastic channel; others do not. (auth)

5644 ISOBARIC ANALOG RESONANCE WIDTHS AND THE DISTRIBUTION OF COULOMB MIXING STRENGTH IN NUCLEI. Mekjian, A. Z. (Rutgers–The State Univ., New Brunswick, N. J.). Phys. Rev. Lett.; 25: 888-92(28 Sep 1970).

Experimental data on the microgiant spreading widths of analog resonances indicate that these widths decrease slightly with increasing mass number A for A = 37 to 50 and then increase again

XUM

for A > 60. A calculation is presented in which this remarkable property can be understood in terms of a model in which the distribution of Coulomb mixing strength in a nucleus has two peaks with the analog state lying between these two peaks and moving with respect to them with changes in A and T_ζ. (auth)

5645 STUDIES OF WEAK β BRANCHING IN ^{55}Cr AND ^{206}Tl DECAY. Zoller, W. H.; Walters, W. B. (Massachusetts Inst. of Tech., Cambridge). Contract AT(30-1)-905. J. Inorg. Nucl. Chem.; 32: 2465-71(Aug 1970).

Weak β branches in the decay of 3.5 min ^{55}Cr of 0.038 percent and 0.0033 percent were measured to levels in ^{55}Mn at 1528.2 and 2251.8 keV, respectively. Upper limits were also set for the β branching to other well-known levels in ^{55}Mn. A weak β branch of 0.0056 percent was measured for decay of 4.2 min ^{206}Tl to the 803.3 keV level in ^{206}Pb. (auth) (UK)

5646 E2 EFFECTIVE CHARGES OF THE $f_{\frac{7}{2}}$ PROTON AND NEUTRON DEDUCED FROM THE LIFETIMES OF THE 6^+ STATES IN ^{50}Ti, ^{54}Fe, AND ^{42}Ca. Nomura, T.; Gil, C.; Saito, H.; Yamazaki, T.; Ishihara, M. (Tokyo Univ.). Phys. Rev. Lett.; 25: 1342-5 (9 Nov 1970).

The half-lives of the lowest 6^+ states in ^{50}Ti, ^{54}Fe, and ^{42}Ca were measured to be 0.41 ± 0.02, 1.24 ± 0.04, and 5.52 ± 0.15 nsec, respectively. The deduced polarization charges δe_{eff} are around 0.65e both for the $f_{\frac{7}{2}}$ proton and neutron. (auth)

5647 SOME RADIOACTIVE CHARACTERISTICS OF CALCIUM. Sitar, B.; Chrapan, J.; Oravec, J.; Durcek, K. (Komenskys Univ., Bratislava. Research Inst. of Hygiene, Bratislava). Jad. Energ.; 16: 303-4(Sep 1970). (In Czech).

The energy spectra of ^{41}Ca and ^{45}Ca were measured with a proportional counter. The half-life of ^{45}Ca was determined. (auth)

5648 PHOTONEUTRON SPECTRA OF ^{31}P AND ^{27}Al. Mutsuro, Naoshi; Kawamura, Nobuaki (Tohoku Univ., Sendai). Kakuriken Kenkyu Hokoku; 2: No. 2, 47-56(Dec 1969). (In Japanese).

The basic preliminary experiment concerning the energy dependence of detector efficiency and the calibration of a time analyzer, etc. was similar to that reported previously. The photoneutron spectra of ^{31}P and ^{27}Al were measured. The energy of the incident electron beam was E_e = 26 MeV. The photoneutrons from the reaction ^{31}P(γ,n) were detected. The linearity of the time analyzer was confirmed. The width of the time analyzer was 9 ns/channel. The T−O− F resolution was ≲0.1 ns/m. The measured energy spectrum is shown and analyzed. The experiment for ^{27}Al failed due to the bad beam condition. (NSA of Japan)

5649 MAGNETIC-DIPOLE TRANSITIONS IN THE $(\pi d_{\frac{5}{2}})(\nu f_{\frac{7}{2}})$ QUARTET. Segel, R. E. (Argonne National Lab., Ill. Northwestern Univ., Evanston, Ill.). Phys. Rev. Lett.; 25: 1352-5 (9 Nov 1970).

The mean lives of the second and third excited states in ^{40}K are $(0.65 \pm 0.15) \times 10^{-12}$ and $(1.6 \pm 0.3) \times 10^{-12}$ sec, respectively. The relative speeds of the three M1 transitions between the four lowest states are incompatible with these states being pure $(\pi d_{\frac{5}{2}})^{-1} \times (\nu f_{\frac{7}{2}})$ — even if effective moments are used; neither small components of the most likely shell-model impurities nor any possible E2 admixture improves the fit. A similar situation appears to hold in ^{38}Cl. (auth)

5650 ACCURATE DETERMINATION OF THE $P_K\omega_K$ VALUE AND THE FLUORESCENCE YIELD ω_K OF Rb AFTER ELECTRON-CAPTURE DECAY OF ^{85}Sr. Bambynek, W.; Reher, D. (EURATOM, Geel, Belgium). Z. Phys.; 238: 49-55(1970).

The $P_K\omega_K$ value of Rb following ^{85}Sr decay is determined to be $P_K\omega_K = 0.586 \pm 0.003$ by using two independent methods for the measurements of the K-X-ray emission rate. With this result and $P_K = 0.877 \pm 0.003$ deduced from literature, the fluorescence yield of Rb is found to be $\omega_K = 0.668 \pm 0.006$. (auth)

5651 $p_{\frac{3}{2}}$ ANALOG STATE IN ^{51}V. Klapdor, H. V. (Max-Planck Institut fuer Kernphysik, Heidelberg); Buchholz, K.; Kaestner, F. Z. Phys.; 238: 11-22(1970). (In German).

In an investigation of $T = \frac{1}{2}$ analog states in ^{51}V the ^{50}Ti(p,γ) excitation curve was measured for proton bombarding energies 1280−1480 keV and 2340−2660 keV. From the (p,γ) resonances 29 new virtual levels in the region of 9316−9510 keV excitation energy in ^{51}V were determined. The strong resonance at E_p = 1371 keV was identified as the isobaric analog state of the ^{51}Ti ground state by determining spin and parity of this resonance to be $\frac{3}{2}^-$. There is no evidence for a strong analog resonance in ^{51}V corresponding to the 1.16-MeV $p_{\frac{3}{2}}$ state in ^{51}Ti. The γ decay of the $p_{\frac{3}{2}}$ analog state was studied by measuring branching ratios and angular distributions of primary γ transitions with a Ge(Li) detector. M1−E2 mixing ratios were determined for these transitions. The total width of the resonance for γ decay is found to be $\Gamma_\gamma = 1.6 \pm 0.4$ eV. New bound levels in ^{51}V are introduced at 3576, 4651 and 4661 keV excitation energy. The J^π values of the 3085-, 4770-, and 4863-keV states are determined to be $\frac{3}{2}^-$, $\frac{5}{2}^-$, $\frac{3}{2}^-$, respectively. The analog−antianalog M1 transition strength is found to be considerably reduced compared to the situation in s−d shell nuclei. (auth)

5652 REEVALUATION OF THE CONVERSION COEFFICIENT OF THE 14.4-keV TRANSITION IN ^{57}Fe. Freund, H. U.; McGeorge, J. C. (Georgia Inst. of Tech., Atlanta). Z. Phys.; 238: 6-10(1970).

Existing values of the conversion coefficient of the 14.4-keV transition in ^{57}Fe are reevaluated using new K-shell fluorescence yields and recent decay scheme information. Previous disagreements are removed and the mean values found are $\alpha_T = 8.26 \pm 0.19$, $\alpha_K = 7.37 \pm 0.17$. (auth)

5653 TEST OF THE COLLECTIVE CORRELATIONS CALCULATION OF THE DIPOLE STATES OF ^{28}Si. Drechsel, Dieter (Univ. of Virginia, Charlottesville. Univ., Frankfurt am Main); Spicer, B. M. Z. Phys.; 238: 1-5(1970).

The relative populations of final states in ^{27}Al following the ^{28}Si(γ,p)^{27}Al reaction are calculated in the framework of the collective-correlations model of the giant resonance. Satisfactory agreement is found for all final states up to 2.7 MeV; however, the population of the 2.98-MeV $(\frac{3}{2}^+)$ final state, which is the only one based on the two-phonon states of ^{28}Si, disagrees with experiment by a factor of 20. (auth)

5654 ANOMALOUS L = 1 SHAPES OF ANGULAR DISTRIBUTIONS FOR (^{3}He,t) TRANSITIONS TO 0^+ ANTIANALOG STATES IN ^{64,66}Ga and ^{40}K. Hinrichs, R. A.; Sherr, R.; Crawley, G. M.; Proctor, I. (Michigan State Univ., East Lansing). Phys. Rev. Lett.; 25: 829-31(21 Sep 1970).

The (^{3}He,t) reaction on ^{64,66}Zn and ^{40}Ar to the 0^+ analog and antianalog states was studied at 35 MeV. The angular distributions for the $T < 0^+$ states show an L = 1 shape; this implies a need for modifications in the conventional description of (^{3}He,t) reactions. (auth)

5655 L/K- AND M/L-ELECTRON CAPTURE RATIO IN THE DECAY OF ^{65}Zn. Krafft, O. (Univ., Muenster, Ger.). Z. Phys.; 238: 78-89(1970). (In German).

The L/K- and the L/M-capture ratio of ^{65}Zn was investigated. For the transitions to the first excited state of ^{65}Cu $(N_L/N_K)_A = 0.120 \pm 3\%$ and $(N_M/N_L)_A = 0.153 \pm 13\%$, and for both transitions to the ground state and the first excited state simultaneously $(N_L/N_K)_C = 0.118 \pm 3\%$. The values for N_L/N_K agree well with the results of Santos Ocampo and Conway but are higher than the results of Totzek and Hoffmann. All values are discussed in view of the different theoretical values obtainable. (auth)

5656 MEASUREMENTS OF FAST-NEUTRON CAPTURE INTEGRALS IN THE CFRMF. Scoville, J. J.; Nisle, R. G.; Howes, B. W.; Harker, Y. D. (Idaho Nuclear Corp., Idaho Falls). Trans. Amer. Nucl. Soc.; 13: 755-7(Nov 1970).

From Meeting of the American Nuclear Society, Washington, D. C. See CONF-701102.

5657 HIGH-RESOLUTION (n,xγ) CROSS-SECTION MEASUREMENTS USING A LINAC. Orphan, V. J.; Hoot, C. G.; John, Joseph (Gulf Energy and Environmental Systems, Inc., San Diego, Calif.). Trans. Amer. Nucl. Soc.; 13: 863-4(Nov 1970).

From Meeting of the American Nuclear Society, Washington, D. C. See CONF-701102.

5658 HINDRANCE OF THE M1 TRANSITION FROM THE ANALOG STATE TO THE ANTIANALOG STATE AND CHARGE-EXCHANGE SPIN-FLIP COLLECTIVE MODE. Hirata, M. (Tokyo Univ.). Phys. Lett.; 32B: 656-8(14 Sep 1970).

It is shown that the hindrance of M1 transition from the analog state to the antianalog state in ^{49}Sc or ^{51}V can be explained by introducing the charge-exchange spin-flip collective mode. Existence of a collective state is predicted. (auth)

5659 INTERNAL CONVERSION COEFFICIENTS FOR ELECTRON-SPIN-POLARIZED ^{57}Fe. Yokoo, Yoshimatsu (Osaka Univ.); Kodama, Takeshi; Morita, Masato. Progr. Theor. Phys. (Kyoto); 44: 294-5(Jul 1970).

The decay of the 14.4-keV level of ^{57}Fe by internal conversion is studied. The difference D in the relative intensities W of the

XUM

conversion electrons which are initially bound with spin up or down (case I or II) is given by $D = (W_I - W_{II})/W_I$. The numerical values of the difference D and the conversion coefficients for K_I, L_I, M_I, and N_I are reported. (R.W.R.)

5660 A $g_{\frac{9}{2}}$ ANALOG RESONANCE IN THE $^{58}Ni(p,\gamma)^{59}Cu$ REACTION. Fodor, Ilona; Szentpetery, I.; Szuecs, Judit (Central Research Inst. for Physics, Budapest). Phys. Lett.; 32B: 689-90(14 Sep 1970).

A $g_{\frac{9}{2}}$ analog resonance was found in the $^{58}Ni(p,\gamma)^{59}Cu$ reaction, with a strong M1 transition to the corresponding anti-analog state. (auth)

5661 NUCLEAR CHARGE DISTRIBUTION AND BORN APPROXIMATION FOR HIGH-ENERGY ELECTRON SCATTERING. Hwang, Jenn-lin; Wang, Jeng-chuen (National Taiwan Univ., Taipei). Chin. J. Phys. (Taiwan); 8: 8-15(Apr 1970).

The charge distribution $D(\rho)$ of ^{40}Ca is determined from the rule of nuclear radii proposed earlier. Since $D(\rho)$ is a superposition of the charge distributions of individual nucleons having the analytic form of Fourier transforms, the direct connection between $D(\rho)$ and the structure of the electron elastic scattering cross section is easily observed. The scattering cross sections of 183 MeV and 250 MeV electrons by the ^{40}Ca nucleus are calculated in the Born approximation with the Gaussian and exponential types of distribution for the proton charge. The results are compared with the experimental data of Hahn et. al. and those of Croissiaux et. al., as well as with the calculation of Kulkarni and Swamy; these comparisons reveal that the proposed forms of charge distribution $D(\rho)$ can yield a close approximation to the exact cross section of the rms radius of the proton within the nucleus if appropriately chosen. (auth)

5662 STUDY OF $^{27}Al(n,d)^{26}Mg$ REACTION BY 14.1-MeV NEUTRONS. Wang, Wei-noon; Wang, Ming-chien (National Tsing Hua Univ., Hsinchu, Taiwan). Chin. J. Phys. (Taiwan); 8: 1-5(Apr 1970).

The $^{27}Al(n, d)^{26}Mg$ reaction was studied at neutron energy of 14.1 MeV by using a counter telescope. Angular distributions corresponding to ^{26}Mg levels at 0, 1.81, and 2.97 MeV were measured and compared with the distorted wave Born approximation theory. The cross sections, l values, and spectroscopic factors were obtained. The experimental results seem to agree with the predictions of the rotational model. (auth)

5663 PRODUCTION OF ^{18}F FRAGMENTS RESULTING FROM Si UNDER THE ACTION OF 660 MeV PROTONS. Fedoseev, G. A.; Moskaleva, L. P. (Inst. of Geochemistry and Analytical Chemistry, Moscow). Yadern. Fiz.; 11: 1146-51 (Jun 1970). (In Russian).

Differential energy distributions of ^{18}F fragments resulting from Si under the action of 660-MeV protons are measured. The experimental data obtained are compared with the results of calculations of phase space for supposed reactions of ^{18}F production. Based on the analysis, the conclusion is reached that an essential contribution to the mechanism of the reaction of the ^{18}F production from ^{28}Si is given by the process of inelastic interaction of the initial proton with a heavy fragment of the type ^{19}F. (auth)

5664 LIFETIME OF THE 5^- 4585 keV ^{38}Ar LEVEL. Engelbertink, G. A. P.; Jones, K. W.; Olness, J. W.; Warburton, E. K. (Brookhaven National Lab., Upton, N. Y.). Phys. Lett.; 33B: 353-5(9 Nov 1970).

The mean lifetime of the $J^\pi = 5^-$ ^{38}Ar level at an excitation energy of 4585 keV was measured by the gas-target variant of the recoil-distance technique. The result of 181 ± 13 ps is 1.6 times as long as recent shell-model predictions. (auth)

5665 AN EXPLANATION OF THE ANOMALOUS BACKWARD ENHANCEMENT OF ELASTIC α-SCATTERING CROSS SECTIONS NEAR A = 40 IN TERMS OF AN EXTENDED OPTICAL MODEL. Eberhard, K. A. (Florida State Univ., Tallahassee). Phys. Lett.; 33B: 343-6(9 Nov 1970).

Elastic α-scattering cross sections for the target nuclei ^{36}Ar, ^{40}Ar, ^{39}K, ^{41}K, ^{40}Ca, ^{42}Ca, and ^{44}Ca are calculated and compared with the data at 24.2 MeV by using an extended optical model with an l-dependent absorption. It is shown that the large differences in the experimental cross sections at backward angles for the above nuclei result from different angular momentum mismatches between the elastic and the reaction channels, which in turn are due to the different (α,n) Q values. (auth)

5666 METHOD OF PSEUDO-BOUND STATES FOR STRIPPING TO UNBOUND LEVELS. Cole, B. J.; Huby, R.; Mines, J. R. (Univ. of Liverpool). Phys. Lett.; 33B: 320-2(9 Nov 1970).

A simple approximate method of performing DWBA calculations for stripping to unbound levels is presented together with some applications. (auth)

5667 ANGULAR CORRELATION AND GAMMA-RAY BRANCHING RATIO STUDIES OF ^{40}Ar. Place, Ralph L. Lexington, Ky.; Univ. of Kentucky (1969). 187p. University Microfilms Order No. 70-12,367.

Thesis.

Properties of the 2.53-MeV and 3.21-MeV levels of ^{40}Ar were studied by means of angular correlation measurements of the $p-p'-\gamma$ and $\gamma-\gamma$ types. In addition, the gamma-ray branching characteristics of the second through seventh excited levels of ^{40}Ar were measured by means of $p'-\gamma$ coincidence techniques. The correlation studies of the 2.53-MeV level show that, at an incident proton energy of 5.21 MeV, the reaction proceeds mainly via $J^\pi = 2^{(+)}_1$ level in the intermediate compound nucleus ^{41}Ar. The channel-spin mixing ratio for the inelastically scattered proton leading to the 2.53-MeV level is −0.88. The gamma-ray amplitude mixing ratio for the de-excitation 2.53-MeV → 1.46-MeV was determined as 0.24. The spin of the 2.53-MeV level is assigned J = 2. Results of $\gamma-\gamma$ angular correlation measurements for the cascade (3.21 → 1.46 → 0.0) MeV, coupled with the observation of a ground state crossover transition from the 3.21-MeV level, limit the spin of the 3.21-MeV level to J = 1,2. Results of the experiment are discussed in light of several nuclear models. (TSS) (Diss. Abstr. Int., B)

5668 MOESSBAUER MEASUREMENTS OF QUADRUPOLE-MOMENT RATIOS OF THE FIRST EXCITED 2^+ STATES OF $^{176,178,180}Hf$. Chow, Y. W.; Howes, R. H.; Swerdlow, P. H.; Yen, C. S.; Wu, C. S. (Columbia Univ., New York). Phys. Lett.; 32B: 682-4(14 Sep 1970).

The quadrupole-moment ratios of the first excited 2^+ states of ^{176}Hf, ^{178}Hf, and ^{180}Hf were measured with the Mössbauer effect following Coulomb excitation. The target was a single crystal of metallic hafnium with its c axis making an angle of 45° with the surface of the crystal. Three absorbers of cubic crystals of HfC were prepared with separated $^{176,178,180}Hf$ isotopes. The determined ratios are $Q_{22}(180)$: $Q_{22}(178)$: $Q_{22}(176) = 1 : (1.03 \pm 0.02) : (1.05 \pm 0.02)$. These results are compared with the predictions from the rotational model. (auth)

5669 CORE-EXCITED STATES IN ^{54}Fe. Pittel, S. (Franklin Inst., Swarthmore, Pa.). Phys. Lett.; 33B: 158-60(28 Sep 1970).

The influence of 3h−1p and 4h−2p states on the $J = 0^+$ spectrum of ^{54}Fe is studied. The results are consistent with the ^{56}Ni calculation of Wong and Davies. The 2.56-MeV 0^+ level is found to be predominantly $4h(J_h = 0, T_h = 0) - 2p(J_p = 0, T_p = 1)$. (auth)

5670 CORE EXCITATION IN ^{30}P. Greene, M. Wayne; Green, L. L.; Jones, G. D. (Univ. of Liverpool). Phys. Lett.; 32B: 680-1(14 Sep 1970).

A study of ^{30}P by the $^{29}Si(^3He,d)$ reaction indicates that the level at 2.84 MeV excitation has $J^\pi = 1^+$, in conflict with a previous $J^\pi = 3^+$ assignment. Spectroscopic factors obtained for levels below 3.5 MeV excitation are compared with predictions from collective and shell-model calculations. (auth)

5671 EVIDENCE FOR ISOSPIN SPLITTING OF THE GIANT DIPOLE STATE IN ^{26}Mg. Wu, C. (Yale Univ., New Haven); Firk, F. W. K.; Berman, B. L. Contract AT(30-1)-2726. Phys. Lett.; 32B: 675-7(14 Sep 1970).

Direct evidence for T splitting of the dipole state in ^{26}Mg is obtained by studying the energy spectra of photoneutrons from the two components. The states centered around 17 MeV decay strongly to the ground or low-lying states of ^{25}Mg ($T = \frac{1}{2}$), whereas those around 22 MeV decay only to the known $T = \frac{3}{2}$ states in ^{25}Mg. (auth)

5672 PROTON–GAMMA ANGULAR CORRELATIONS IN THE REACTIONS $^{26}Mg(d,p)^{27}Mg$ and $^{28}Si(d,p)^{29}Si$. Adams, A.; Calvert, J. M. (Univ. of Manchester, Eng.). Nucl. Phys.; A157: 273-96(1970).

Angular correlations were measured for the p_1 and p_2 groups in the reaction $^{26}Mg(d,p)^{27}Mg$ leading to the 0.984 MeV and 1.69 MeV excited states. Deuteron energies of 4.37 MeV and 5.34 MeV were used. Similar measurements were made for the p_1, p_2, p_3, p_8 and p_{10} groups in the $^{28}Si(d,p)^{29}Si$ reaction leading to levels at 1.27, 2.03, 2.43, 4.08 and 4.93 MeV at similar deuteron energies. Analysis in terms of DWBA and PWBA was carried out and statistical tensors obtained for the excited states. Theory does not give a satisfactory description of all of the observations.

Branching ratios were also measured for the gamma-transitions from several of the excited states of ^{29}Si. (auth)

5673 IN-BEAM PROTON–GAMMA RAY COINCIDENCE STUDIES USING A LARGE COAXIAL Ge(Li) DETECTOR. Moss, Joel Marshall. Berkeley, Calif.; Univ. of California (1969). 194p. University Microfilms Order No. 70-6173.

Thesis.

Two different applications were made of particle-gamma ray coincidence techniques: first, in the ^{54}Fe(p,p')^{54}Fe reaction at 10 MeV and then, in the reactions ^{54,56}Fe(p,p')^{54,56}Fe at 19.6 MeV. In both experiments a large coaxial Ge(Li) counter was used to detect the gamma rays. In the ^{54}Fe(p,p')^{54}Fe reaction at 10 MeV, the angular correlation of gamma rays coincident with protons detected near 180° was measured. On the basis of this information, unambiguous spin assignments were made to the 3.345(3), 4.074(3), 4.579(2), 4.781(3), and 4.950(4) MeV states. Model dependent assignments and spin limitations were made for several other states. The angular correlation analysis also yielded multipole mixing ratios for several transitions and branching ratios for the decay of all states of ^{54}Fe below 5 MeV. From an analysis of the observed Doppler shifts of the coincident gamma rays, mean lifetimes were derived for the 1.409, 2.959, 3.164, 3.836, 4.048, 4.074, 4.265, 4.287, 4.781, and 4.950 MeV states. Coincident gamma rays perpendicular to the reaction plane, as a function of proton scattering angle, were observed in the reactions ^{54,56}Fe (p,p')^{54,56}Fe at 19.6 MeV. Analysis of these data yielded angular distributions of the spin-flip probability in the inelastic excitation of the first 2^+ states in both nuclei. The spin-flip probabilities were compared to the predictions of both the collective and microscopic models of inelastic proton scattering. Also included in the theoretical analysis were high precision differential cross section measurements made here, and inelastic asymmetry data from Saclay. (Diss. Abstr. Int., B)

5674 MIXING OF HARTREE–FOCK STATES IN ^{28}Si. Dang, G. Do (Laboratoire de Physique Theorique et Hautes Energies, Orsay, France). Nucl. Phys.: A157: 231-40(1970).

It is well known that the Hartree–Fock equations in the sd shell for ^{28}Si possess an oblate, a prolate and a spherical solution. From the deformed solutions, rotational bands are obtained by projection. The states with the same spin are non-orthogonal and form an oblique basis. The mixing of these states was calculated by requiring that linear combinations of them are eigenstates of the Hamiltonian. It is found that the oblate and spherical J = 0 states are strongly mixed while J ≠ 0 states are practically pure deformed states. The three lowest 0^+ states are assigned to the oblate, spherical and prolate components. Their transition probabilities to the first 2^+ states are calculated and are found to agree with experimental results, while their relative positions may be accounted for by second-order perturbations. (auth)

5675 ^{54}Fe(d,n)^{55}Co REACTION AND THE LEVEL SCHEME OF ^{55}Co. Hagen, M.; Janetzki, U.; Maier, K. H. (Hahn-Meitner-Institut fuer Kernforschung, Berlin). Nucl. Phys.: A157: 177-89(1970).

The ^{54}Fe(d,n)^{55}Co reaction was studied at E_d = 5.8 MeV with a time-of-flight spectrometer. The excitation energies of 42 levels including 15 so far unknown were determined. Absolute differential cross sections for 13 levels are analyzed by DWBA calculations including finite-range and nonlocality corrections. The level scheme of ^{55}Co, especially spin assignments, is critically reviewed and the spectroscopic factors are discussed with respect to the completeness of the shell closure in ^{56}Ni. (auth)

5676 M1 GAMMA TRANSITIONS FROM ISOBARIC ANALOGUE STATES INDUCED BY THE ^{55}Mn(p,γ)^{56}Fe REACTION AND GAMOW–TELLER BETA TRANSITIONS OF ^{56}Mn. Sakai, M. (Tokyo Univ.); Bertini, R.; Gehringer, C. Nucl. Phys.; A157: 113-29(1970).

The isobaric analog states corresponding to the low-lying excited states in ^{56}Mn were induced by the ^{55}Mn(p,γ)^{56}Fe reaction. High-energy γ-rays from the isobaric analog states were measured with a 84 cm^3 coaxial Ge(Li) detector. The M1 matrix elements of the γ-transitions were discussed in connection with the Gamow–Teller matrix elements of the β-decays of ^{56}Mn. (auth)

5677 (p,t) REACTION ON ^{42}Ca, ^{44}Ca, AND ^{48}Ca. Hefele, H.: Lynen, U.; Santo, R. (Max-Planck-Institut fuer Kernphysik, Heidelberg). Nucl. Phys.: A157: 93-105(1970).

The (p,t) reaction on ^{42}Ca, ^{44}Ca and ^{48}Ca was investigated at E_p = 20 MeV. The angular distributions were analyzed by DWBA using pure shell-model configurations as well as wave functions from different shell-model calculations. The analyses show that particle-hole admixtures in the states involved can explain the weak excitation of the first excited 0^+ states. The results are discussed with respect to other (p,t) data and (t,p) data on Ca isotopes. (auth)

5678 PHOTONUCLEAR TRITIUM YIELDS AT 90 MeV. Currie, L. A.; Rodriguez-Pasques, R. H. (National Bureau of Standards, Washington, D. C.). Nucl. Phys.: A157: 49-60 (1970).

Photonuclear (γ,t) yields were determined for Al, Zn, Sn and Bi using 90 MeV bremsstrahlung from the NBS electron synchrotron. The National Bureau of Standards P2 ionization chamber was used for primary monitoring of the bremsstrahlung beam; supplementary C and Cu activation foils, whose absolute yields are reported, were employed for relative intensity measurements. Tritium yields were determined by quantitative extraction from the molten samples with hydrogen carrier followed by activity measurement by means of low-level gas counters. The observed yields were generally consistent with those of other workers at lower energies. Comparison of the tritium yields with the results of statistical model calculations suggests the predominance of non-evaporative processes in the higher mass region (A ≳ 100). (auth)

5679 PHOTONUCLEAR REACTIONS ABOVE THE GIANT RESONANCE: RATIOS OF (γ,2n) TO (γ,pn) YIELDS IN ^{50}Cr, ^{54}Fe, ^{89}Y, AND ^{92}Mo. Walters, W. B.; Van Hise, J. R.; Switzer, W. L.; Hummel, J. P. (Univ. of Illinois, Urbana). Nucl. Phys.; A157: 73-80(1970).

Yield ratios for the (γ,2n) and (γ,pn) reactions in ^{50}Cr, ^{54}Fe, ^{89}Y and ^{92}Mo were studied to obtain information about the mechanism of photonuclear reactions occurring at energies just above the giant resonance region. The yield ratios were obtained by measuring the radioactivities of the product nuclei in samples that had been irradiated with bremsstrahlung in the 150 to 305 MeV energy range. In the case of the reactions in natural chromium and iron targets, corrections were made for the contributions from higher-order reactions involving heavier target isotopes using data from irradiations involving highly enriched ^{52}Cr and ^{56}Fe targets. The resulting (γ,2n) to (γ,pn) yield ratios were 0.095 ± 0.025 for ^{50}Cr with 250 MeV bremsstrahlung, 0.10 ± 0.03 for ^{54}Fe at 250 MeV, 7.4 ± 1.0 for ^{89}Y at 150 MeV, and 0.41 ± 0.05 and 0.49 ± 0.05 for ^{92}Mo at 150 and 280 MeV, respectively. In the case of the ^{54}Fe(γ,pn)^{52}Mn reaction, an isomer ratio of 0.11 ± 0.06 for the fraction of the yield populating the ground state at 250 MeV was obtained. The isomeric yield ratio and the isobaric yield ratios were compared with ratios calculated on the basis of a compound nucleus mechanism using the statistical theory. The results of the comparison indicate that a compound nucleus mechanism can account for these reactions that are important in the energy range just above the giant resonance region. (auth)

Nuclear Properties and Reactions, A ≥ 90

Refer also to abstracts 4333, 5118, 5153, 5474, 5506, 5550, 5551, 5582, 5605, 5635, 5644, 5645, 5656, 5668, 5678, 5679, 5772, 5810, 5835, 5864, 5866, and 6204.

5680 (CEA-N-1232, pp 1-80) INVESTIGATIONS WITH THE TANDEM VAN DE GRAAFF. (Commissariat a l'Energie Atomique, Saclay (France). Centre d'Etudes Nucleaires). (In French).

Topics covered are: Saclay Tandem Van de Graaff operation and transformation; negative ion source with charge exchange in lithium vapors; ^{11}B + p resonance at 2.65 MeV with α–α coincidences; ^{13}C(^{6}Li,t)^{16}O reaction at 20 MeV; ^{17}O levels by ^{15}N(^{3}He,p)^{17}O reaction; research of the 2p-1h component in ^{29}Si by the ^{27}Al(^{3}He,p) ^{29}Si reaction; ^{40}Ca levels; excited states of ^{42}Ca; spectroscopy of ^{58}Ni by (p,p'γ) reaction; spectroscopy of ^{63}Ni and ^{65}Ni; ^{114}Cd(^{3}He,d) ^{115}In reaction; analog states in ^{140}Ce; analog resonances in deformed nuclei; transfer reactions induced by a lithium beam; experimental techniques. (France)

5681 (CNEA–274) RESONANCE INTEGRALS OF NEUTRON ACTIVATION OF ^{74}Se, ^{78}Se, ^{80}Se, ^{81}Br, ^{127}I, ^{130}Te, ^{138}Ba, ^{140}Ce, AND ^{142}Ce. Ricabarra, M. D.; Turjanski, R.; Ricabarra, G. H.; Bigham, C. B. (Comision Nacional de Energia Atomica, Buenos Aires (Argentina)). 1970. 26p. (In Spanish). Dep. NTIS (U. S. Sales Only).

A lithium-drifted germanium gamma-ray spectrometer was used to make accurate intercomparisons of the ratio of resonance-integral to thermal-activation cross section by measuring cadmium ratios or relative activation rates in two different neutron spectra. The standard, gold, or secondary standard, indium, was mixed uniformly in the samples and the activities resolved with the spec-

XUM

trometer. Expressed as Westcott S values, the results relative to $S_0 = 17.7$ for gold were as follows: ^{74}Se: 10.3 ± 0.1; ^{78}Se: 12.3 ± 0.3; ^{80}Se: 2.65 ± 0.02; ^{81}Br: 24.3 ± 0.5; ^{127}I: 27.8 ± 0.5; ^{130}Te: 2.10 ± 0.07; ^{136}Ba: 0.649 ± 0.004; ^{140}Ce: 0.476 ± 0.003; and ^{142}Ce: 0.865 ± 0.005. (auth)

5682 (IS-T-389) CONSTRUCTION OF A THREE CRYSTAL SPECTROMETER AND A STUDY OF THE DECAY OF ^{90}Nb. Simmons, S. Oliver (Ames Lab., Iowa). Oct 1970. Contract W-7405-eng-82. 72p. Dep. NTIS.

Thesis.

A gamma ray spectrometer consisting of a Ge(Li) detector partially surrounded by two NaI(Tl) scintillators has been constructed. The instrument has two modes of operation, the pair spectrometer mode for analyzing high energy gamma rays (above 1.022 MeV) and the Compton suppression mode for studying weak gamma rays in the presence of intense higher energy background radiation. The decay of ^{90}Nb to levels in ^{90}Zr was investigated using the three crystal spectrometer in the Compton suppression mode to reduce background from the intense 2186 and 2319 keV transitions. Energies and absolute intensities of thirteen gamma ray transitions were determined. Using the K-conversion electron intensities from the work of other investigators and the gamma ray intensities from this work, conversion coefficients for the transitions were calculated. Comparison with theoretical values enabled deduction of the multipolarities of most of the transitions. The conventional shell model description of the levels of ^{90}Zr in terms of two protons in ($p_{1/2}$) and ($g_{9/2}$) orbitals is inconsistent with the observation of a strong E1 transition between the first 6^+ and 5^- levels. A calculation is presented which shows that this can be explained by mixing a 10^{-2}% component of ($g_{9/2}$) ($h_{11/2}$) into the wave function for the 5^- state. (auth)

5683 (IS-T-391) DECAY OF ^{95}Ru AND ^{103}Tc. Hein, Warren Walter (Ames Lab., Iowa). Nov 1970. Contract W-7405-eng-82. 89p. Dep. NTIS.

Thesis.

The decay of ^{95}Ru to levels in ^{95}Tc was investigated with Ge(Li) detectors used singly and in coincidence. A NaI(Tl) anticoincidence shield was used to suppress the Compton background in the singles spectrum, increasing sensitivity to low intensity gamma rays. Energies and intensities were determined for 36 transitions. Gamma-ray cascades are identified by Ge(Li)–Ge(Li) coincidence measurements. From these data, a decay scheme which accommodates 33 transitions was constructed. Branching ratios and log(ft) values for the decay to levels of ^{95}Tc were calculated. Spins and parities were deduced from the beta- and gamma-ray branching ratios. The proposed decay scheme accommodates 33 of these transitions. The experimental levels of ^{95}Tc are compared with the predictions of the effective interaction calculations. A search for ^{93}Ru activity was performed with targets irradiated in a bremsstrahlung beam. Investigations with isotopically separated samples showed the 50 second gamma-ray activity observed in a natural ruthenium target to be from the decay of ^{103}Tc produced by the ^{104}Ru(γ,p) reaction. This decay was studied using Ge(Li) gamma-ray singles and Ge(Li)–Ge(Li) coincidence measurements. Energies and intensities were determined for 28 transitions. Twenty-six of these transitions were placed in a decay scheme based on recent reaction studies. An explanation for the observed 1.7 millisecond isomeric state is given in terms of this decay scheme. Possible spin and parity assignments for the ground state of ^{103}Tc are discussed. (auth)

5684 (JINR-P4-5221) A SINGLE-PARTICLE STATE OF DEFORMED NUCLEI IN TRANSURANIUM REGION OF SAXON–WOODS POTENTIAL. Gareev, F. A.; Ivanova, S. P. (Joint Inst. for Nuclear Research, Dubna (USSR). Lab. of Theoretical Physics). 1970. 23p. (In Russian). Dep. CFSTI (U. S. Sales Only).

Use of the anisotropic oscillator potential by S. G. Nilsson as the mean nuclear field is not fully satisfactory, although for some rare earths the results agree with experimental data. In the transuranium region Nilsson's scheme presents additional difficulties. An earlier approximation method of the author for solving Schrödinger's equation by means of the Saxon–Woods potential for spherical and deformed nuclei has been successfully applied to describe the properties of nuclei in the rare-earth region. The method is precise and retains the advantages of Nilsson's approximation while overcoming its shortcomings. This one-particle level scheme is presented for nuclei in the transuranium region by calculating the levels of the A = 239 nucleus. The order of filling of the ground states was not sufficiently well indicated by the scheme; however, introduction of a hexagonal deformation resulted in a satisfactory one-particle scheme for odd transuranium nuclei. (TTT)

5685 (KFKI-70-18-NAC) TWO-DIMENSIONAL (T_γ,E_γ) MAPPING OF SHORT-LIVED NUCLIDES. Nagy, A. Z.; Csoke, A.; Szabo, E. (Magyar Tudomanyos Akademia Kozponti Fizikai Kutato Intezete, Budapest). 1970. 23p. Dep. CFSTI (U. S. Sales Only).

A (T_γ,E_γ) map of 117 reported gamma emitters with half-lives less than 1 minute and gamma energies from 0.01 to 10 MeV produced by (n,α), (n,p), (n,2n), (n,γ), or (n,n'γ) reactions with fast or thermal neutrons is presented. Various reactions, including cross sections and threshold energies, which can be used to produce these nuclides are tabulated. The publication can be used to select activities for activation analysis with different types of neutron sources. (R.W.R.)

5686 (TID-25566) TEMPERATURE-DEPENDENT AND MULTI-LEVEL EFFECTS ON NEUTRON RESONANCE CROSS SECTIONS. Shea, Thomas E. (Rensselaer Polytechnic Inst., Troy, N. Y.). Sep 1970. 252p. Dep. NTIS.

Thesis.

The effects of temperature dependence and multilevel interference on neutron resonance cross sections and their manifestations on cross section-dependent quantities are examined through the application of the Quasi-Resonance Multilevel cross section formalism. Cross section expressions in this formalism are derived from the level matrix form of the R-Matrix formalism, and are given in terms of Lorentzian shape functions. The effects of nuclear thermal motion on the cross-section expressions are given in terms of the standard Doppler-broadening functions. The Quasi-Resonance Triplet Approximation is introduced to facilitate the application of the formalism to the fissile nuclides. The Triplet-Approximation fission parameters are studied in detail. For ^{235}U, they are determined to be negligibly intercorrelated and, in all cases studied, well represented by the chi-square frequency functions. The average symmetric fission parameter and its corresponding chi-square number of degrees of freedom are seen to be energy-dependent. The Triplet Approximation is applied to the calculation of the ^{235}U fission cross section in the range from 18 to 66 eV. The approximation gives an improved representation of the cross-section line shape over the single-level type calculations. A weak-interference correction is introduced. When used with the Triplet Approximation, the comparisons with R-Matrix calculations are further enhanced. Fission integrals as well as pointwise cross sections are compared with experiment, with quite good agreement. The average capture and fission cross sections and the average alpha for ^{235}U are computed in the energy range below 2.5 keV. Again, agreement between theory and experiment is quite good. The Triplet Approximation is applied to the Bramblett–Czirr experiment on shielded fission integrals for ^{235}U in the resolved and unresolved resonance regions. The results indicate a need for additional cross-section measurements. Comparison calculations are in reasonable agreement with the data. (auth)

5687 (UCRL-19949) EXCITED STATE IN EVEN–EVEN FISSION PRODUCTS. Cheifetz, E.; Jared, R. C.; Thompson, S. G.; Wilhelmy, J. B. (California Univ., Berkeley. Lawrence Radiation Lab.). Aug 1970. Contract W-7405-eng-48. 22p. (CONF-700815-2). Dep. NTIS.

From Conference on the Properties of Nuclei Far from the Region of Beta Stability, Leysin, Switzerland.

Experimental results are presented on the ground state bands of 31 even–even nuclei produced in the primary fission of ^{252}Cf. Systematics of the energies and life-times of the transitions are given. From these data there is evidence indicating that a region of deformation in the A ≈ 100 region may exist. (auth)

5688 (UCRL-19961) HEAVY-ION IN-BEAM SPECTROSCOPY. Diamond, R. M. (California Univ., Berkeley. Lawrence Radiation Lab.). Aug 1970. Contract W-7405-eng-48. 48p. (CONF-700815-4). Dep. NTIS.

From Conference on the Properties of Nuclei Far from the Region of Beta Stability, Leysin, Switzerland.

The advantages of using heavy-ion beams for in-beam gamma-ray and conversion-electron spectroscopy are pointed out. A number of examples of heavy-ion in-beam studies are given to illustrate typical work. These include measurements of B(E2)'s, g factors, and energy-level transitions. (83 references) (R.W.R.)

5689 DELAYED NEUTRON GROUPS FROM ^{235}U AND ^{233}U AND SHORT-LIVED DELAYED PHOTONEUTRON GROUPS FROM ^{235}U AND ^{233}U IN D_2O. Rambo, George Earle. Blacksburg, Va.; Virginia Polytechnic Inst. (1969). 137p.

Thesis.

A study of the delayed neutron groups from ^{235}U and ^{233}U was made by using the rotating chopper method. The uranium targets

were irradiated by a pulsed beam from a reactor, and the neutron activity of the targets during the closed portion of the chopper rotation cycle was measured as a function of time. The chopper and a multi-channel analyzer were coordinated to allow rapid data accumulation by superimposing data from successive chopper rotations. Several chopper rotation speeds were used to enhance the various half-life delayed neutron groups. The decay curves were fit to a sum of exponentials by a least-squares computer program which determined the half-lives and abundances of the groups. The abundances were corrected for non-saturation and build-up. The half-lives, $T_{\frac{1}{2}}$, and relative abundances, β_i/β, of the groups found are given. No delayed neutron groups with $T_{\frac{1}{2}}$ less than 0.326 sec were found, even though the experiment was capable of resolving half-lives as short as a few milliseconds. A search for short-lived delayed photoneutron groups from ^{235}U and ^{233}U in D_2O was made. The same experimental technique was used except that the uranium targets were mounted at the center of a sphere filled with D_2O. No delayed photoneutron groups with significant abundance were found with half-lives between 0.002 seconds and 10 seconds. (TSS) (Diss. Abstr. Int., B)

5690 NUCLEAR PHOTOACTIVATION OF ^{179}Hf. Boivin, Michel; Zecevic, Vasco (Paris Univ.). Compt. Rend., Ser. B; 270: 1627-9(22 Jun 1970). (In French).

The photoactivation of hafnium-179 was studied using a natural hafnium sample, and the existence of six nuclear levels at 650, 880, 1030, 1160, 1400, and 1605 keV was demonstrated; the cross sections for these levels were determined and likely characteristics suggested. (auth) (France)

5691 FISSION OF EXCITED NUCLEI AND POSSIBILITIES OF NEW ISOTOPE SYNTHESIS. Oganesyan, Yu. Ts.; Penionzhkevitch, Yu. E. (Joint Inst. for Nuclear Research, Dubna, USSR). J. Phys. (Paris); 31: 259-68(Apr 1970). (In French).

Experimental data on the measurement of mass and charge distributions of fission fragments of excited heavy nuclei up to Z = 110 are given. Fission of heavy nuclei is considered with relation to producing neutron-enriched isotopes as fission fragments and the comparison with other methods of synthesis of these nuclei is made. (auth) (France)

5692 COMPETITION BETWEEN NEUTRON EMISSION AND FISSION AT MODERATE EXCITATION ENERGIES IN THE URANIUM REGION. Bishop, Charles Joseph. Seattle; Univ. of Washington (1969). 113p. University Microfilms Order No. 70-8438.

Thesis.

The ratio of the probability of neutron emission to the probability of fission Γ_n/Γ_f has been studied to determine its dependence on excitation energy of the compound nucleus. Neutrons were detected in coincidence with fission fragments at 0 and 90° with respect to the fragments. Pre-fission neutrons (related to Γ_n) are isotropic while post-fission neutrons (related to Γ_f) are highly correlated with the fragment direction. ^{233}U and ^{238}U were bombarded with 11.5–22 MeV protons and post-fission/pre-fission neutron ratios determined. ^{252}Cf, a spontaneous fissioning nuclide, was also studied. Results for ^{238}U + p indicate that Γ_n/Γ_f decreases an average of 1.25–1.50 per excitation energy step increase of ~6.5 MeV. By using conventional statistical-model calculations with a Fermi-gas level-density expression, the results can be accounted for by assuming $a_f/a_n \sim 1.1$ and $a_f = A/9$. An alternative explanation involving the dimensionality (degrees of freedom) needed to describe the fission process adequately is briefly discussed — many additional degrees of freedom would be necessary to explain the experimental results. Within the limits of the experiment $\nu_{scission}$, the number of scission neutrons per fission, is 0.3 for ^{252}Cf and <0.1 for ^{235}U. ^{238}U requires a $\nu_{scission}$ of ~0.2. Results indicate that ν as a function of A shows the sawtooth curve structure. An increase in excitation energy results in a washing-out of the structure of the curve, with most of the additional neutrons coming from the heavier fragment. (TSS) (Diss. Abstr. Int., B)

5693 DECAY OF ^{126m}Sb AND THE ENERGY LEVELS OF ^{126}Te. Murty, K. S. N.; Pathak, B. P.; Gujrathi, S. C. (Saha Inst. of Nuclear Physics, Calcutta). Z. Phys.; 237: 313-19 (1970).

The decay characteristics of 19-min ^{126m}Sb have been studied using Ge(Li) and scintillation spectrometers. The sources of ^{126m}Sb were obtained by the (n,p) reaction on enriched ^{126}Te. The gamma rays of energies 414.4 ± 0.3, 666.7 ± 0.5, and 696.1 ± 0.5 keV were found decaying with a half-life of 19 min. The study of beta spectra employing an anthracene crystal yielded two beta groups with end-point energies of 1.9 ± 0.15 and 2.5 ± 0.15 MeV. The results of singles and coincidence measurements have been incorporated into a decay scheme with excited states of ^{126}Te at 666.7, 1,362.8, and 1,777.2 keV. (auth)

5694 HIGH-RESOLUTION STUDIES OF TRANSITIONS IN THE DECAY CHAIN ^{146}Gd TO ^{146}Eu TO ^{146}Sm. Antman, S.; Pettersson, H.; Zehlev, Z.; Adam, I. (Univ. of Uppsala). Z. Phys.; 237: 292-312(1970).

Transitions in ^{146}Eu and ^{146}Sm were studied using a double-focusing beta-ray spectrometer and a Ge(Li) detector. Internal conversion and gamma-ray intensities were determined. The internal-conversion spectrum of the three 155-, 115-, and 116-keV cascading transitions in ^{146}Eu was studied for all subshells, K-, L-, and M-subshell ratios were determined and E2/M1 mixing ratios were deduced for these three transitions. Intensities from the N- and (O + P)-shells were determined and compared to theoretical calculations. All internal conversion intensities were found to be in agreement with theoretical data for pure M1 character with small E2 admixtures for all the three transitions. Selected parts of the internal-conversion spectrum of the transitions in ^{146}Sm were restudied at 0.06% momentum resolution. This study was mainly concentrated on four transition doublets feeding and de-exciting the close-lying levels at 1,380 and 1,381 keV. A new transition with 702.20 keV energy was detected in the 702–703 keV-transition group. Internal conversion coefficients were deduced using reported gamma-ray intensities. Multipole characters of the transitions were deduced and used as a basis for a discussion of the spins and parities of the lower-lying excited states of ^{146}Sm. (auth)

5695 HIGH-RESOLUTION L- AND M-SUBSHELL INTERNAL-CONVERSION STUDIES OF LOW-ENERGY TRANSITIONS IN ^{149}Sm AND ^{151}Eu. Antman, S.; Pettersson, H.; Zehlev, Z.; Adam, I. (Univ. of Uppsala). Z. Phys.; 237: 285-91(1970).

The internal-conversion subshell intensities of the (21.529 ± 0.014)-keV transition in ^{151}Eu and the (22.494 ± 0.011)-keV transition in ^{149}Sm have been determined in a high resolution investigation using a double-focusing iron-core spectrometer. The subshell ratios yielded unambiguous M1 + E2 multipole mixtures for both transitions. $\delta^2(E2/M1)$ for the 21.53-keV transition was determined to be $(8.8 \pm 0.7) \cdot 10^{-4}$; and for the 22.49-keV transition, to be $(5.5 \pm 1.2) \cdot 10^{-3}$. (auth)

5696 NEUTRON-DEFICIENT ISOTOPES OF POLONIUM. Jones, A. G.; Aten, A. H. W. Jr. (Instituut voor Kernphysisch Onderzoek, Amsterdam). Radiochim. Acta; 13: 176-81(Jun 1970).

The isotopes $^{200,201,202,203,204,205}Po$ were produced by (^3He,xn) reactions on natural and enriched lead targets and studied with lithium-drifted germanium detectors and alpha detectors. Sixty-one transitions were seen following the decay of the polonium isotopes; and eight new transitions, in the decay of $^{201,202}Bi$ daughters. Estimates are made of the α/EC ratio for $^{201,202,203,204,205}Po$. (auth)

5697 DECAY OF ^{143}Sm TO LEVELS IN ^{143}Pm. De Frenne, D.; Jacobs, E.; Demuynck, J. (Rijksuniversiteit, Ghent). Z. Phys. 237: 327-34(1970).

The beta decay of ^{143}Sm was reinvestigated with the aid of a Ge(Li) detector. Levels of ^{143}Pm at 271.8, 1,056.5, 1,173.4, 1,342.1, 1,403.2, 1,514.9, 1,752.8, 1,816.3, 1,853.6, (2,000), 2,009.0, 2,080.5, 2,344, 2,443, 2,463, 2,906 and (3,054) keV were established. Log-ft values for all observed beta transitions have been calculated. Spin and parity assignments have been made from electron capture and position disintegration considerations and gamma branches. The experimental level scheme of ^{143}Pm is compared with the results of 1 and 3 q.p. calculations for N = 82 nuclei. (auth)

5698 RADIOACTIVE DECAY OF ^{199}Au. Murty, V. Radhakrishna (Panjab Univ., Chandigarh, India); Jnanananda, Swami. Indian J. Pure Appl. Phys.; 6: 223-5(1968).

The fractional intensities of cross-over and cascade are obtained in the decay of ^{199}Au with the help of 4π sum-peak coincidence spectrometer. The ratio of the transition probabilities $T(E_2)_{208}/T(M_1)_{50}$ obtained from the properties of core excitation model is found to be in good agreement with the experimental value than the same value computed from the single particle estimate. The relative gamma intensities are computed assuming the beta intensities. (auth)

5699 ROTATIONAL BANDS OF ^{171}Lu OBTAINED BY ^{171}Hf DECAY. Gizon, J.; Barneoud, D.; Valentin, J. (Institut des Sciences Nucleaires, Grenoble, France). Nucl. Phys.; A148: 561-82(1970).

The energy levels of ^{171}Lu, populated from the electron capture of ^{171}Hf(12.4h), have been examined with high-resolution 180° spectrographs, two iron-free double focussing spectrometers, silicon detectors and Ge(Li) detectors. Gamma-gamma coincidence techniques have also been used. Properties of the rotational levels are established in terms of the Bohr and Mottelson unified model a

the single-particle Nilsson model. The following intrinsic states are identified: $1/2^+[404]$, ground; $1/2^-[541]$, 71.1 keV; $1/2^+[411]$, 208.1 keV; $5/2^+[402]$, 295.8 keV; $9/2^-[514]$, 469.5 keV; $7/2^-[523]$, 662.0 keV. Some E1 relative transition probabilities are discussed, taking into account the Coriolis coupling. (auth)

5700 VALIDITY OF ξ APPROXIMATION OF THE 1400 keV BETA DECAY IN ^{143}Ce. Narasimha Raju, M. L.; Sastry, D. L. (Andhra Univ., Waltair, India). Indian J. Pure Appl. Phys.; 8: 365-6(Jun 1970).

The energy dependence of the 1400 keV β-57 keV γ directional correlation in the decay of ^{143}Ce was measured with a conventional fast-slow scintillation coincidence spectrometer. The results indicate that the angular correlation is isotropic and the 1400 keV beta transition fits into the ξ approximation. (auth)

5701 E2 AND M1 TRANSITION PROBABILITIES IN ^{193}Au AND ^{195}Au. Fogelberg, B. (Uppsala Univ. Swedish Research Council's Lab., Studsvik); Baecklin, A.; Berg, V.; Malmskog, S. G. Nucl. Phys.; A153: 301-15(1970).

High-resolution conversion electron- and γ-ray spectroscopy has been made on the transitions depopulating the three lowest excited states in ^{193}Au and ^{195}Au. The half-lives of these levels have been measured with the delayed coincidence method. The multipole assignments are for the transitions in ^{193}Au: 38.22 keV M1 + (17.7 ± 1.0)% E2, 219.75 keV E2, 257.97 keV M1 + (21 ± 7)% E2 and for ^{195}Au: 61.44 keV M1 + (16.6 ± 1.0)% E2, 180.32 keV M1 + <3% E2, 200.38 keV E2, 261.74 keV M1 + (21.5 < 4.0)% E2. The obtained half-lives are for ^{193}Au: 38.22 keV level (3.81 ± 0.18) ns, 224.84 keV level < 0.03 ns, 257.97 keV level (45 ± 20) ps and for ^{195}Au: 61.44 keV level (3.0 ± 0.2) ns, 241.72 keV level <0.03 ns, 261.79 keV level (54 ± 10) ps. A systematic compilation of absolute E2 and M1 transition rates in odd-mass Au nuclei is given and compared to the predictions of the pairing-plus-quadrupole force model and the core-excitation model. (auth)

5702 NEUTRON FISSION AND CAPTURE CROSS-SECTION MEASUREMENTS FOR ^{233}U IN THE ENERGY REGION 0.02 TO 1 eV. Weston, L. W. (Oak Ridge National Lab., Tenn.); Gwin, R.; de Saussure, G.; (and others). Nucl. Sci. Eng.; 42: 143-9(Nov 1970).

The relative neutron capture and fission cross section in the neutron energy range 0.02 to 1.0 eV were simultaneously measured. The data are normalized by means of the previously reported total cross section. The technique used consisted of passing a pulsed neutron beam through a ^{233}U fission chamber placed at the center of a large liquid scintillator. The prompt-neutron capture gamma rays were detected only in the liquid scintillator whereas a fission event was characterized by coincident signals from the liquid scintillator and fission chamber. This technique provides a new method of obtaining eta in this neutron energy range which is not subject to the same type of errors as are associated with a direct measurement. Comparisons with previously published data are given. (auth)

5703 STATIC ELECTRIC QUADRUPOLE MOMENT OF THE FIRST EXCITED STATE OF ^{148}Sm. Gertzman, H. S.; Cline, D.; Gove, H. E.; Lesser, P. M. S.; Schwartz, J. J. (Univ. of Rochester, N. Y.). Nucl. Phys.; A151: 273-81(1970).

From measurements of Coulomb excitation of the 551 keV first excited state of ^{148}Sm using helium and oxygen ions, it has been possible to obtain a value for the static quadrupole moment of this state. The data yield two solutions corresponding to the choice of sign for the interference term due to virtual excitation of the second 2^+ excited state at 1454 keV. These results are: $B(E2; 0^+ \rightarrow 2^+) = 0.706 \pm 0.024 (e\cdot b)^2$ and $Q(2^+) = +0.28 \pm 0.28$ e·b assuming a negative interference term, and $B(E2) = 0.705 \pm 0.025$ $(e\cdot b)^2$ and $Q(2^+) = -0.24 \pm 0.28$ e·b assuming a positive interference term. A comparison with previously published results for this isotope and for neighboring nuclei suggests that the positive interference term is the more likely choice. (auth)

5704 ALPHA DECAY OF ^{255}No AND ^{257}No. Eskola, Pirkko; Eskola, Kari; Nurmia, Matti; Ghiorso, Albert (Univ. of California, Berkeley). Phys. Rev., C; 2: 1058-62(Sep 1970).

The α decay of ^{255}No and ^{257}No produced by ^{248}Cf(^{12}C,α2n)^{255}No and ^{248}Cm(^{13}C,4n)^{257}No reactions, respectively, has been studied. Five α-particle groups with energies and intensities 8.30(3%), 8.25(6%), 8.11(57%), 7.92(19%), and 7.76 MeV (15%) were assigned to ^{255}No; and three α-particle groups with energies 8.32, 8.27, and 8.22 MeV to ^{257}No. The half-lives of ^{255}No and ^{257}No were measured to be 200 ± 10 and 26 ± 2 sec, respectively. The decay schemes of ^{255}No and ^{257}No are discussed. (auth)

5705 ENERGY LEVELS OF ^{156}Gd AS POPULATED BY ELECTRON CAPTURE FROM ^{156}Tb. Peek, N. F. (Univ. of California, Davis). Phys. Rev., C; 2: 587-91(Aug 1970).

Thirty-six transitions from the excited levels of ^{156}Gd as fed by electron capture in ^{156}Tb have been studied. Level spins and parities, along with transition multipolarities, have been determined utilizing germanium solid-state detectors for the γ rays and the Davis precision solenoidal β-ray spectrometer for the conversion electrons. The energies as measured by the spectrometer are determined to well within one part in 7000. A decay scheme is presented and the energy levels are discussed. (auth)

5706 M1/E2 MULTIPOLE MIXING OF THE 563 AND 569 keV TRANSITIONS IN ^{134}Ba. Singh, B.; Taylor, H. W. (Univ. of Toronto). Nucl. Phys.; A145: 561-8(1970).

Using directional correlation techniques, the multipole mixing of the 563 and 569 keV transitions in ^{134}Ba has been determined. The former is essentially pure E2, whereas the latter contains only a 6% E2 admixture. The results are compared with conversion electron measurements. (auth)

5707 POSSIBLE OBLATE SHAPE OF $9/2^-$ ISOMER IN ^{190}Tl. Newton, J. O.; Cirilov, S. D.; Stephens, F. S.; Diamond, R. M. (Univ. of California, Berkeley). Nucl. Phys.; A148: 593-614(1970).

Low-lying $9/2^-$ isomeric states have been previously observed in the neutron-deficient odd-mass thallium nuclei from mass 201 to 193. But there has as yet been no satisfactory explanation for the existence of such states, as the closest single-particle state is the $h_{9/2}$ orbital some 4 MeV higher in energy. We have studied the transitions and states leading to this isomeric level in ^{190}Tl by in-beam spectroscopic techniques. Among the most prominent states observed above the isomeric level are an $1^1/2^-$, $1^3/2^-$, and possibly a $1^5/2^-$ state. Very similar levels have been found in the other light odd-mass thallium nuclei. Combining a pairing-energy correction suggested by Blomqvist with the idea that the observed negative parity levels form a rotational band based on the $9/2^-[505]$ Nilsson state in a nucleus with oblate deformation seems to explain all the information presently available on these levels. (auth)

5708 NUCLEAR-ORIENTATION STUDY OF THE FIRST-FORBIDDEN β DECAYS OF ^{198}Au. Pratt, W. P. Jr.; Schermer, R. I.; Steyert, W. A. (Los Alamos Scientific Lab., N. Mex.). Phys. Rev., C; 2: 608-14(Aug 1970).

Using a ^{3}He–^{4}He dilution refrigerator coupled with adiabatic demagnetization, ^{198}Au has been polarized in a magnetized Fe foil at 5 mK. By measuring the directional distribution of the γ rays emitted following the $2^- \rightarrow 2^+$ first-forbidden β decays to ^{198}Hg, the β dealignment parameters U_2 and U_4 have been determined. For the 0.96-MeV transition, it is found that $U_2 = 0.795 \pm 0.007$ and $U_4 = 0.347 \pm 0.03$. This implies that about 60% of the total decays carry off no angular momentum, about 39% carry off one unit of angular momentum, while 1% ± 1% carry off two units of angular momentum. For the 0.29-MeV transition, it is found that $U_2 = 1.047 \pm 0.054$, implying that less than 1% of the decays carry off one or two units of angular momentum. (auth)

5709 E2 STRENGTH OF THE 191 keV TRANSITION IN ^{197}Au. Sharma, R. P.; Nielsen, H. L. (Univ. of Aarhus, Denmark). Nucl. Phys.; A152: 401-3(1970).

The $(L_1 + L_2)/L_3$ internal conversion ratio of the 191-keV gamma ray in ^{197}Au was remeasured using a ^{197}Hg source, and found to be 66 ± 5 corresponding to (1.9 ± 0.3)% E2. Similarly, the 268 keV transition was found to be >92% E2. From these data and the known Coulomb excitation cross section of the 268 keV state a B(E2) value of 21 s.p.u. is deduced for the 191-keV transition. (auth)

5710 DETERMINATION OF THE LIFETIME AND MAGNETIC MOMENT OF THE $p_{\frac{1}{2}}^{-1}$ NEUTRON HOLE STATE IN ^{207}Pb FROM COULOMB EXCITATION. Klapdor, H. V.; von Brentano, P.; Grosse, E.; Haberkant, K. (Max-Planck-Institut fuer Kernphysik, Heidelberg). Nucl. Phys.; A152: 263-72(1970).

The dipole-quadrupole mixing ratio δ(M1E2) in the γ-decay of the 0.897 MeV $p_{\frac{1}{2}}^{-1}$ neutron hole state in ^{207}Pb has been determined by measuring the angular distribution of the deexcitation γ-rays following Coulomb excitation with 14.4 MeV α-particles. From the measured value $\delta = 0.096 \pm 0.011$ the reduced M1 transition probability has been found to be $B(M1) = (0.37 \pm 0.09)(e\hbar/2Mc)^2$, implying a mean lifetime for the $p_{\frac{1}{2}}^{-1}$ state of $\tau = 0.21 \pm 0.04$ psec. The effective gyromagnetic ratio of the neutron hole has been calculated to be $g_{\frac{1}{2}}^{eff} = (0.57 \pm 0.06) \times g_{\frac{1}{2}}^{free}$. (auth)

5711 GROUND-STATE QUASIROTATIONAL BANDS AND OTHER STATES IN $^{130\ 132\ 134\ 136\ 138\ 140}$Ce. Smith, G. L.; Draper, J. E. (Univ. of California, Davis). Phys. Rev., C; 1: 1548-63 (Apr 1970).

The even cerium isotopes 130 through 140 are investigated by Ba(α,xnγ)Ce. The energies, relative intensities, angular distributions, and time distributions of the γ rays relative to the cyclotron beam bunch are measured. The results show transitions from

states up to 8^+ in ^{130}Ce (253.2, 456.4, 613.9, and 729.0 keV ± 1 keV), up to 10^+ in ^{132}Ce (325.6, 533.5, 684.5, 789.0, and 875 keV), and up to 8^+ in ^{134}Ce (409.4, 639.9, 814.8, and 947 keV). Several transitions from states not in the ground-state band are assigned in the three heaviest isotopes. The most prominent transitions (ground-state band; others) are for ^{136}Ce: 551.7, 761.7, 898.8; 328.6, 623.6, 664.3, and 1051.9 keV; for ^{138}Ce: 787.9, 1037.4; 302.1, 390.7, 402.8, 417.5, 430.1, and 815.0 keV; and for ^{140}Ce: 1596.7, 486.7, 202.0, 222.0, 1317.5, and 1404.1 keV. A 22-nsec level is found in ^{140}Ce. Significant long-lived (≳200 nsec) feeding of the ground-state band is observed in each Ce isotope. (auth)

5712 EVIDENCE FOR THE MISSING 2- STATE IN ^{110}Ag. Kane, W. R.; Scharff-Goldhaber, G. (Brookhaven National Lab., Upton, N. Y.). Phys. Rev., C; 2: 314-19(Jul 1970).

In spite of ingenious investigations of the isomeric decay of 253-day ^{110m}Ag by several groups of authors, the missing low-energy first excited (2–) state in ^{110}Ag has so far escaped detection. High-precision studies of the γ rays from the ^{109}Ag(n,γ)^{110}Ag reaction, as well as coincidence studies, now provide conclusive evidence for this level at an energy of 1.28 ± 0.10 keV. (auth)

5713 STUDY OF THE ENERGY LEVELS OF ^{203}Tl USING (γ,γ′) REACTION. Moreh, R.; Nof, A.; Wolf, A. (Nuclear Research Centre-Negev, Beer Sheva, Israel). Phys. Rev., C; 2: 249-55(Jul 1970).

Elastic and inelastic nuclear resonant scattering of monochromatic photons from ^{203}Tl has been studied using a 20-cc Ge(Li) detector. The γ source was obtained from thermal-neutron capture in titanium. The scattering isotope was identified by using an isotopically enriched thallium target. The energy of the resonance level in ^{203}Tl was found to be 6.418 MeV. Assuming the high-energy lines to be primary transitions deexciting the resonance level, some 14 energy levels were found from the ground state up to 2.9 MeV, 4 of which may be identified with recently reported levels. By measuring the angular distribution of the scattered radiation, the spin of the 6.418-MeV level was determined to be $\frac{1}{2}$, and thus, based on the assumption of dipole transitions, the spins of several low-lying levels were found to be either $\frac{1}{2}$ or $\frac{3}{2}$. The total radiative width of the resonance level was determined and found to be $\Gamma_\gamma = 0.32 \pm 0.06$ eV and $\Gamma_0/\Gamma_\gamma = 0.026$. The spectral shape of scattered radiation was found to have a strong intensity bump at about 5 MeV; this is discussed in the light of similar bumps obtained in (n,γ) and (d,pγ) reactions on nuclei in the same mass region. (auth)

5714 DECAY SCHEMES OF ^{161}Tb AND ^{103}Ru. Murty, V. Radhakrishna (Panjab Univ., Chandigarh, India); Jnanananda, Swami. Indian J. Pure Appl. Phys.; 6: 605-8(1968).

The sum coincidence spectra with gates at 132, 103 and 75 keV are recorded in the decay of terbium-161 and the observed cascades support the level scheme given by Koehler et al. [Koehler, P.F.M., Slack, L. & Gove, N. B., Phys. Rev., 130 (1963), 1503]. In addition, indications of a level at 375 keV and a weak gamma transition of 300 keV proposed are present in the adder and zero bias 4Π sum-peak coincidence spectra. From both the sum and 4Π sum-peak coincidence spectra in the decay of ruthenium-103, the levels at 363 and 298 keV, fed by very small percentage of beta components, are well established. The possibility of explaining this level scheme on the basis of the core excitation model is suggested. (auth)

5715 TEST OF TIME-REVERSAL INVARIANCE OF THE ELECTROMAGNETIC INTERACTION ON THE 73 keV γ-TRANSITION IN ^{193}Ir. Zech, E. (Technische Hochschule, Munich). Z. Phys.; 239: 197-210(1970). (In German).

In order to test the time-reversal invariance of the electromagnetic interaction of nucleons the phase angle η between the E2- and M1-matrix-elements of the mixed $\frac{1}{2}^+ - \frac{3}{2}^+$-transition in ^{193}Ir was measured in a Moessbauer experiment. In a measurement which avoids possible systematic errors the sine of the phase angle which is proportional to the time-reversal odd part of the transition matrix element was deduced. The value is $\sin\eta = M_{odd}/M_{even} = (1.6 \pm 2.4) \cdot 10^{-3}$. In accordance with the results of other experiments there is no evidence for a strong violation of time-reversal invariance in the electromagnetic interaction as postulated by Bernstein, Feinberg, and Lee. (auth)

5716 RADIOACTIVE ATOMS. AUGER-ELECTRON, α-, β-, γ-, AND X-RAY DATA. Martin, M. J.; Blichert-Toft, P. H. (Oak Ridge National Lab., Tenn.). Nucl. Data, Sect. A; 8: 1-198(Oct 1970).

Decay schemes and decay characteristics are presented for 105 radioactive atoms of special importance in nuclear medicine, health physics, and industrial applications. Listed in tabular form are "best" values for half-lives, energies, intensities, equilibrium absorbed-dose constants, and 90% absorbed-dose ranges (in water) for each of the atomic and nuclear radiations emitted by these radioactive atoms. Data basic to the adopted values are also given with appropriate literature references. (auth)

5717 ANGULAR DISTRIBUTION OF NEUTRON CAPTURE γ-RAYS FROM POLARIZED ^{159}Tb NUCLEI. Bosch, D. (Technische Hochschule, Munich). Z. Phys.; 239: 57-72(1970). (In German).

The anisotropy of high-energy capture γ-rays from polarized ^{159}Tb nuclei was measured. Polarization of ^{159}Tb was achieved by cooling single crystals of Terbium-Ethylsulfate to T = 0.35°K in an external field of 4 kOe. With the results of this measurement, it was possible to deduce the spins of 11 levels in ^{160}Tb between 64 keV and 767 keV. Furthermore the Q-value of the reaction ^{159}Tb(n,γ)^{160}Tb was determined to be Q = (6,374.0 ± 1.5) keV. (auth)

5718 HIGH-RESOLUTION SPECTROSCOPIC STUDY OF THE GAMMA RADIATION FROM THE DECAY OF ^{96}Nb. Taylor, H. W.; Singh, B.; Cox, R. J.; Kukoc, A. H. (Univ. of Toronto). Z. Phys.; 239: 42-56(1970).

The decay of 24h ^{96}Nb was studied with a Ge(Li) spectrometer and with a Ge(Li)–NaI(Tl) coincidence spectrometer. A total of 27 gamma-ray transitions were observed, their energies and intensities measured. All but one of these were incorporated into the level scheme of ^{96}Mo. The level at 1,625.9 keV reported recently in (n_{th},γ) work on ^{95}Nb was also observed through the decay of ^{96}Nb. No experimental evidence was found for previously proposed levels at 2,657 and 2,791 keV in ^{96}Mo. (auth)

5719 SYNTHESIS AND SEARCH OF HEAVY TRANSURANIC ELEMENTS. Flerov, G. N. At. Energ. (USSR); 28: 302-9 (Apr 1970). (In Russian).

The lifetime of the transuranic elements decreases with increasing value of the atomic number Z. The short half-lives of elements 102, 103, and 104 make it difficult to identify these elements. The data for the discovery of these elements originated mainly from Berkeley, California and from Dubna, USSR. The author reviews the data and feels that the Dubna group should be given priority for the discovery of the three heaviest elements, 102, 103, and 104. The search for superheavy elements in the region of atomic numbers Z = 110 to 126 is continuing, for it is felt that in this region is an island of stability surrounded by a sea of relatively unstable elements. Evidence is presented for the existence of eka-lead (Z = 114) in nature with a half-life of about 10^8 years. An important experiment in proving the possible existence of eka-lead will be measuring the number of neutrons given off by a fission event (this number may be as high as 10 for superheavy elements). The discovery of one long-lived superheavy element in nature can lead to the discovery of other shorter-lived elements by the use of irradiation with various particles with subsequent study of the elements formed by means of chemical methods. (TTT)

5720 DETERMINATION OF MAGNETIC MOMENT STIMULATED BY ^{121}Sb STATE. Irkaev, S. M.; Valiev, Kh. Kh.; Golovnin, V. A.; Kuz'min, R. N. (Moscow State Univ.). Dokl. Akad. Nauk Tadzh. SSR; 13: No. 6, 16-18(1970). (In Russian).

The Moessbauer effect was used for determination of the magnetic moment of the 712 excited state of ^{121}Sb. A value of $\mu = 2.45 \pm 0.02$ R. M. was found based on a value of $\mu = 3.359 \pm 0.001$ R. M. for the ground state. (R.V.J.)

5721 MEASUREMENT OF THE ^{171}Tm ISOMERIC LIFETIME AS A TEACHING LABORATORY EXPERIMENT. Knoll, G. F.; Vagelatos, N. (Univ. of Michigan, Ann Arbor). J. Nucl. Energy; 24: 227-35(Sep 1970).

A teaching experiment is described in which two methods are applied to determine the lifetime of an isomeric state in ^{171m}Tm. One method, a single channel measurement, utilizes a delayed coincidence technique while the second, a multichannel measurement, employs time-to-pulse height conversion. Both serve to illustrate several principles of coincidence and timing measurements and can give results of good accuracy. (auth) (UK)

5722 OSNOVNYE KHARAKTERISTIKI IZOTOPOV TYAZHELYKH ELEMENTOV. (Principal Characteristics of Isotopes of Heavy Elements). Gorbachev, V. M.; Zamyatnin, Yu. S.; Lbov, A. A. Moscow; Atomizdat (1970). 128p.

The handbook contains data on physical characteristics of heavy elements from thorium to Kurchatovium and on nuclear properties of these elements. The physical constants of the element's isotopes properties and data on radioactive decay are included. Methods for accumulating transuranium elements are described. (635 references are included) (R.V.J.)

5723 NEUTRON EMISSION IN ALPHA-PARTICLE-ACCOMPANIED FISSION. Nardi, Eran (Soreq Research Center, Yavne,

XUM

Israel. Weizmann Inst. of Science, Rehovoth, Israel); Fraenkel, Zeev. Phys. Rev., C; 2: 1156-66(Sep 1970).

A four-parameter correlation experiment, which measured neutron emission in "long-range alpha" (LRA) fission is described. The energies of both the fission fragments and of the α particle as well as the time of flight of the neutron were recorded. The experimental data were analyzed with the aid of a computer, and the method of analysis is described. The pre-neutron-emission mass distribution of LRA fission as well as some properties of the neutrons as a function of α-particle energy are discussed. In addition, the neutron kinetic energy as a function of fragment mass is given. The probability of α-particle emission as a function of the fission-fragment mass ratio is also discussed. (auth)

5724 GAMMA RAYS FROM THERMAL AND RESONANCE NEUTRON CAPTURE IN ^{121}Sb AND ^{123}Sb. Bhat, M. R.; Chrien, R. E.; Garber, D. I.; Wasson, O. A. (Brookhaven National Lab., Upton, N. Y.). Phys. Rev., C; 2: 1115-25(Sep 1970).

Prompt high-energy γ rays resulting from neutron capture at thermal energies and in the resonances of ^{121}Sb and ^{123}Sb were studied with the high flux beam reactor fast chopper using high-resolution Ge(Li) detectors. The binding energy B_n of the last neutron in ^{122}Sb and ^{124}Sb was determined to be 6807 ± 2 and 6468 ± 2 keV, respectively. Based on prompt capture γ data, a spin of 4 was assigned to the 21.6-eV resonance of ^{123}Sb. Energy levels populated by the neutron-capture γ rays are given up to an excitation energy of 2475 keV in ^{122}Sb and up to 2221 keV in ^{124}Sb. These data are compared with the existing (d,p) data on ^{121}Sb and ^{123}Sb. The low-energy (<511 keV) γ rays originating in neutron capture in the different resonances were also studied. For ^{121}Sb, the observed spectra fell into two classes, each having its own characteristic intensity distribution depending on the spin of the capturing state. By comparing these spectra with those originating from the 6.24-eV resonance (3^+) and the 15.4-eV resonance (2^+), the following spins were assigned to the resonances in ^{121}Sb: 29.7 eV (3), 53.5 eV (2), 64.5 eV (3), 73.8 eV (2), 111.4 eV (2), and 126.8 eV (3). Similar, but more tentative, spin assignments were made for resonances in ^{123}Sb. The low-energy spectra were also used to measure the half-life of the 61.6-keV isomeric state in ^{122}Sb by a new method. This experimental procedure is described. The half-life of the isomeric state is 2.3 ± 0.6 μsec. (auth)

5725 NUCLEAR LEVEL STRUCTURE OF ^{169}Er. Mulligan, T. J. (Florida State Univ., Tallahassee); Sheline, R. K.; Bunker, M. E.; Jurney, E. T. Phys. Rev., C; 2: 655-72(Aug 1970).

Levels in ^{169}Er were studied through the reactions ^{168}Er(d,p)^{169}Er and ^{170}Er(d,t)^{169}Er, using 12-MeV deuterons, and via thermal-neutron capture in ^{168}Er. Over 40 states below 1.5 MeV are populated in the charged-particle reactions. These data, coupled with the ≈150 capture γ rays observed, lead to a level scheme that includes the following spectroscopic assignments (rotational band-head energy in keV, followed by the Nilsson single-particle state believed to be dominant): 0.0, $1/2^-$ [521], with associated rotational band to spin $11/2^-$; 92.2, $5/2^-$[512], with band to $11/2^-$; 243.7, $1/2^+$[633], with band to $13/2^+$; 562.1, $1/2^-$[510], with band to $7/2^-$; 714.5, $3/2^-$[521], with band to $11/2^-$; 823, $7/2^-$[514], with band to $9/2^-$; 850, $5/2^-$[523], with band to $11/2^-$; and 1081.8, $3/2^-$[512], with band to $1/2^-$. In addition, a level at 860.2 keV is assigned as the head of a $K^\pi = 3/2^+$ band that is mainly the (K−2) γ-vibrational state associated with $7/2^+$[633]. The data suggest that the 562.1-, 714.5-, and 1081.8-keV bands also have significant vibrational admixtures. Several features of the level scheme, including certain γ-ray branching ratios, are interpreted in terms of Coriolis mixing. The neutron separation energy for ^{169}Er is determined as 6003.1 ± 0.3 keV, and the Q value for the ^{170}Er(d,t)^{169}Er reaction is found to be −950 ± 30 keV. (auth)

5726 LEVELS IN ^{167}Tm EXCITED IN THE REACTION ^{165}Ho(α,2nγ)^{167}Tm. Winter, G.; Funke, L.; Hohmuth, K.; Kaun, K. H.; Kemnitz, P.; Sodan, H. (Zentralinstitut fuer Kernforschung, Rossendorf, Ger.). Nucl. Phys.; A151: 337-50(1970).

Using in-beam techniques the γ-radiation following the reaction ^{165}Ho(α,2nγ)^{167}Tm was studied with germanium detectors. Measurements of energies and intensities, angular distributions, and $\gamma\gamma$ coincidences were performed at a bombarding energy of 27 MeV. Furthermore, the relative intensities of the γ-transitions were measured at α-particle energies of 21, 23, and 25 MeV. A level scheme of ^{167}Tm was established containing rotational levels of the single-particle states $1/2$[411], $1/2$[404] and $1/2$[523] up to spin values $23/2$, $21/2$ and $23/2$, respectively. An additional rotational band with the members $9/2^-$, $13/2^-$, $17/2^-$, $21/2^-$ and $25/2^-$ was found and interpreted as due to the $1/2$[541] Nilsson orbital. In order to describe the rotational energies we used in the energy formula one or two terms with alternating sign for the $1/2$ and $1/2$ bands, respectively. The quantities $(g_K - g_R)^2/Q^2$ and $[(g_K - g_R)/Q]^2$ $(1 \pm b_0)^2$ were evaluated. (auth)

5727 TRANSITION PROBABILITIES BETWEEN THE FIRST TWO EXCITED STATES OF ^{159}Tb. Armbruster, R.; Dar, Y.; Gerber, J.; Macher, A.; Vivien, J. P. (Centre de Recherches Nucleaires, Strasbourg). Nucl. Phys.; A153: 460-4(1970). (In French).

The mean life of the second excited state in ^{159}Tb was measured with the microwave method. The result obtained is $\tau(5/2^+$, 137 keV, ^{159}Tb) = 51.4 ± 6.2 ps. The deduced value of $|g_K - g_R|$ is found to be in agreement with branching ratio measurements. Magnetic parameters are calculated from available data. A discrepancy is observed between measured values of parameters connecting the first excited state to the ground state. (auth)

5728 DECAY OF ^{194}Au TO THE LEVELS OF ^{194}Pt. Benson, G. D. (Vanderbilt Univ., Nashville); Ramayya, A. V.; Albridge, R. G.; O'Kelley, G. D. Nucl. Phys.; A150: 311-45(1970).

The γ rays emitted in the decay of ^{194}Au have been investigated by means of Ge(Li) detectors. The energies and intensities of 93 γ-rays have been determined from the γ-ray singles spectrum. Two-parameter γ-γ coincidence experiments, with two Ge(Li) detectors, have been performed. The coincidence relations were used by the authors to construct a level scheme for ^{194}Pt, consisting of 36 excited states. The ambiguities previously reported in the locations of several transitions have been removed, and several transitions have been placed in new positions. New levels at 1229.3, 1373.6, 2134.2, 2158.0, 2184.8 and 2287.3 keV have been postulated and five previously reported levels have been removed from the scheme. K-conversion coefficients, calculated from the γ-ray intensities of this work and the K-conversion electron intensities of Bergman and Bäckström, were used to determine the multipolarities of the transitions and the spin and parity assignments of the levels. Four levels are proposed as possible members of the quintet of three-phonon states. (auth)

5729 ELASTIC AND INELASTIC DEUTERON SCATTERING FROM ^{124}Te AND ^{146}Nd. Christensen, P. R.; Loevhoeiden, G.; Rasmussen, J. (Univ. of Copenhagen). Nucl. Phys.; A149: 302-22(1970).

Excitation energies and differential cross sections for inelastic scattering of 12.0 MeV deuterons leading to collective states in ^{124}Te and ^{146}Nd have been measured. A possible candidate for a 0^+ two-phonon state is found in ^{124}Te. For the one-phonon 2^+ and 3^- states, the experimentally observed angular distributions have been compared to predictions from DWBA theory, and vibrational amplitudes $\beta_\lambda R$ have been extracted. The B(E2) and B(E3) values were determined by Coulomb excitation by means of α-particles of 12.0 and 14.0 MeV. The electromagnetic vibrational amplitudes $\beta_\lambda R_c$ are compared to those deduced from the (d,d') cross sections and to results from inelastic α-particle scattering. Second-order DWBA theory is used to interpret the excitation of two-phonon 2^+ and 4^+ states. An appreciably better fit to the observed cross sections for the excitation of the second 2^+ state is obtained if a small admixture of the one-phonon 2^+ is assumed for this state. Similarly, a hexadecapole component has to be included in the wave function for the 4^+ state. (auth)

5730 NUCLEAR MATRIX ELEMENTS OF THE 437-keV BETA TRANSITION IN THE DECAY OF ^{125}Sb. Narasimha Raju, M. L.; Seshagiri Rao, V.; Sastry, D. L. (Andhra Univ., Waltair, India). Phys. Rev., C; 2: 566-71(Aug 1970).

The energy dependence of the 437-keV β−176-keV γ directional correlation is measured with a conventional slow-fast scintillation assembly. The results are in good agreement with those of Dubard et al. The matrix-element parameters of this β transition are determined using the present results and the allowed shape of the β spectrum. The matrix-element parameters indicate that an algebraic cancellation among rank-1 matrix elements is responsible for the retardation of the 437-keV β transition. The ratio of the matrix elements $\int\vec{\alpha}$ and $\int i\vec{r}$ is not in agreement with the value predicted on the basis of conserved-vector-current theory. (auth)

5731 NUCLEAR STRUCTURE EFFECT IN INTERNAL CONVERSION OF THE 57.54 keV E1 TRANSITION IN ^{180}Hf. Dragoun, O.; Plajner, Z.; Martin, B. (Max-Planck-Institut fuer Kernphysik, Heidelberg). Nucl. Phys.; A150: 291-9(1970).

Measurements have been performed on relative conversion line intensities of the highly K-forbidden E1 transition ($8^- \rightarrow 8^+$) of 57.54 keV in ^{180}Hf. Anomalies observed for the L, M, N subshell and O total intensity ratios were explained with the nuclear current parameter $\eta = -7.0 \pm 0.3$ and nuclear charge parameter $\xi = 10 \pm 50$. (auth)

5732 BETA-GAMMA CIRCULAR POLARIZATION CORRELATION IN ^{97}Nb. Behrens, H.; Brodt, F. (Univ., Karlsruhe, Ger. Kernforschungszentrum Karlsruhe, Ger.). Nucl. Phys.; A150: 269-72(1970). (In German).

The β-γ circular polarization asymmetry of the β 1296 keV γ 658 keV transition in ^{97}Nb has been measured. The result is A = −0.492 ± 0.031. From this value the spin and parity of the 658 keV level in ^{97}Mo is determined as $^7/_2^+$. (auth)

5733 DECAY OF ^{178}Re(13.2 min), ^{177}Re(14.0 min), AND ^{176}Re(5.7 min). Goudsmit, P. F. A.; Konijn, J.; de Boer, F. W. N. (Instituut voor Kernphysisch Onderzoek, Amsterdam). Nucl. Phys.; A151: 513-31(1970).

The decay of ^{178}Re(13.2 ± 0.2 min), ^{177}Re(14.0 ± 1.0 min) and ^{176}Re(5.7 ± 0.8 min) is studied with several techniques. In the ^{178}Re decay 112 transitions are observed in the energy region between 100 and 3600 keV. Gamma-gamma coincidences are measured. The lowest three members of the ground state band of ^{178}W (105.9 ± 0.3 (2^+), 343.2 ± 0.4 (4^+), 695.1 ± 0.7 keV (6^+)) are excited. The decay of three members of a K = 2^- band (1045.0 ± 0.6 (2^-), 1121.1 ± 0.6 (3^-), 1225.8 ± 0.6 keV (4^-)) and of two members of a K = 0^+ band [1082.8 ± 0.6 (2^+), 1275.7 ± 0.6 keV (4^+)] are observed. The existence of 20 further levels at the following energies is deduced: 1110.7 ± 0.4 (2^+), 1380.9 ± 0.8 (4^+), 1449.9 ± 0.5 (2^+), 1598.3 ± 0.4, 1864.4 ± 0.6, 3301.4 ± 0.6, 3369.0 ± 0.5 (2^+), 3383.3 ± 0.5, 3499.4 ± 0.7, 3506.0 ± 0.8, 3511.9 ± 0.7 (2^+), 3515.2 ± 0.7, 3551.4 ± 0.5, 3580.4 ± 0.7, 3585.7 ± 0.8, 3595.2 ± 0.8, 3634.7 ± 0.8, 3706.8 ± 0.7, 3807.7 ± 0.7 and 3811.2 ± 0.7 keV. The end-point of a positron branch populating the 343.2 keV level is measured as 3.30 ± 0.18 MeV. An I = 3, K < 3 assignment is made for the ground state of ^{178}Re. In the decay of ^{177}Re 19 transitions are observed. The $2^+ \rightarrow 0^+$ and $4^+ \rightarrow 2^+$ transitions in the ground state band of ^{176}W are observed in the decay of ^{176}Re; an upper limit is given for the intensity of the $6^+ \rightarrow 4^+$ transition. (auth)

5734 DECAY SCHEMES OF 109 d ^{127m}Te and 9.4 h ^{127g}Te. Apt, K. E.; Walters, W. B.; Gordon, G. E. (Massachusetts Inst. of Tech., Cambridge). Contract AT(30-1)-905. Nucl. Phys.; A152: 344-53(1970).

Gamma rays emitted in the decay of a secular equilibrium mixture of 109 d ^{127m}Te and 9.4 h ^{127g}Te and in the decay of ^{127g}Te alone have been investigated using high-resolution Ge(Li) detectors. In the decay of the equilibrium mixture, five new γ-rays have been observed with energies: 172.1, 375.0, 618.6, 628.6 and 651.0 keV. New β-transitions observed in the decay of ^{127g}Te are to levels at 375.0 keV and 618.6 keV, and a new transition to a 628.6 keV level is observed in ^{127m}Te decay. Comparative β- and γ-ray counting of equilibrium ^{127}Te sources with a low-background, proportional counter and Ge(Li) detectors, respectively, established absolute values for β-group intensities to levels of ^{127}I. The I.T. branching of ^{127m}Te was found to be 97.6%, and the β-group intensity from ^{127g}Te to the ^{127}I ground state is 98.8%. The log ft values of 8.7, 9.7 and 8.7 for allowed β-transitions to the levels at 619, 375 and 203 keV, respectively, disclose severe hindrances that reflect dissimilarities in parent and daughter state wave functions. Hindered first-forbidden β-transitions were also observed. (auth)

5735 FORTRAN NUCLIDIC-MASS TABLE WITH SELF-MODIFICATION FEATURE. Lewis, S. A. (Univ. of California, Davis); May, E. C.; Moorhead, J. B. Nucl. Instrum. Methods; 87: 133-4(1970).

A computer program is described which is a FORTRAN subroutine to provide nuclidic masses in amu for any Z and A by a table look-up method. A companion program modifies the internal tables of the subroutine when changes or additions to the known masses become available. (auth)

5736 PRECISION GAMMA RAY ENERGIES IN THE ENERGY INTERVAL BETWEEN 45 AND 1275 keV. Raeside, D. E. (Univ. of Michigan, Ann Arbor). Nucl. Instrum. Methods; 87: 7-11 (1970).

Curved-crystal spectrometers have been utilized to obtain measurements of more than forty gamma ray energies in the energy interval between 45 and 1275 keV for nuclei with 109 ≤ A ≤ 193 including ^{109}Cd, ^{152}Eu, ^{153}Sm, ^{154}Eu, ^{155}Eu, ^{156}Eu, ^{170}Tm, ^{191}Os, and ^{193}Os. Many of these energy measurements have sufficiently small uncertainties associated with them to make them useful for the calibration of Ge(Li) spectra. (auth)

5737 FOUR-PARTICLE–TWO-HOLE CORE EXCITATION IN HEAVY NUCLEI. Goetz, U.; Hadermann, J.; Alder, K. (Univ., Basel). Helv. Phys. Acta; 43: 514-35(Aug 1970).

Four-particle–two-hole core excitation in heavy nuclei with two nucleons outside the closed shells is investigated by including the highest core orbits into the configuration space of a shell-model calculation. The core excitation is supposed to be effected by an interaction between core nucleons and valence nucleons that is essentially the same as the well-known residual interaction between the valence nucleons. The nucleons in the core are assumed to be excited only in pairs coming from the same core orbit. The angular momentum of the core, therefore, is always even. For the description of core-excited configurations in second-quantization formalism an orthogonal system of four-fermion operators is constructed by using a phenomenological interaction potential with appropriate spin–spin and tensor parts and restricting to excitations with core-spin 0, energy levels and transition probabilities of the nuclei ^{206}Pb, ^{210}Po, and ^{206}Hg are calculated. (auth)

5738 STUDY OF SOME ASPECTS OF FISSION INDUCED BY RESONANCE NEUTRONS IN ^{235}U. Wagemans, Cyriel. Ghent; State Univ. of Ghent (1969). (In Dutch).

Thesis.

In order to study some properties of fission induced by resonance neutrons, an experimental device based on the time-of-flight technique was developed. The pulsed neutrons were obtained by bombarding a uranium target with a very energetic pulsed electron-beam. In the first part of this work the relative fission cross-section was measured for neutron energies from 0.009 eV to 24 eV and normalized at thermal energy to the value σ_f^0 = 581.2 barns. This normalization enables calculation of the absolute fission integral $\int_{1.8\,eV}^{11\,eV} \sigma_F(E)dE$ = 237.5 ± 2.1 barn–eV, a very convenient integral for the normalization of fission cross sections that are not measured down to thermal energy. Furthermore, an extensive analysis of the other available measurements is made. The very important differences (≈20%) between the different measurements are considerably reduced by normalizing these data to the reference integral. In the second part, the cross sections for binary fission (2 heavy fragments) and ternary fission (2 heavy fragments and an energetic light particle) were measured. The ratio of binary-to-ternary fission events is compared for several well-isolated resonance peaks (below 21 eV), and a variation is found outside the statistical errors. (auth) (Diss. Abstr. Int., B)

5739 LEVELS OF ^{144}Pr FROM THE DECAY OF ^{144}Ce. Anttila, A.; Piiparinen, M. (Univ. of Helsinki). Z. Phys.; 237: 126-30(1970).

The level scheme of ^{144}Pr has been studied from the decay of ^{144}Ce. The intensities and energies of gamma rays have been determined with an X-ray Ge(Li) detector. The K-shell internal conversion coefficients for γ rays have been measured with the K X-ray/γ-ray ratio method using NaI(Tl)–X-ray Ge(Li) coincidence techniques. (auth)

5740 NEW ISOTOPE OF PALLADIUM ^{116}Pd. Aronsson, P. O.; Ehn, E.; Rydberg, J. (Chalmers Univ. of Tech., Goteborg). Phys. Rev. Lett.; 25: 590-3(31 Aug 1970).

A new continuous solvent-extraction technique has been developed for fast chemical isolation and identification of short-lived radioisotopes. It was applied to a search for ^{116}Pd as a product of 14-MeV neutron-induced fission of ^{238}U. The ^{116}Pd was identified through its daughter ^{116}Ag and found to have a half-life of 13.6 ± 1.2 sec. At the same time the half-lives of ^{113}Pd and ^{115}Pd were confirmed to be 91 ± 12 sec and 30 ± 2 sec, respectively. (auth)

5741 EXCITED LEVELS IN THE DECAY ^{185}Os → ^{185}Re. Plajner, Z.; Brabec, V.; Maly, L.; Rizek, J.; Vejs, M. (Nuclear Research Inst., Rez, Czech.). Z. Phys.; 237: 180-8(1970).

The energies and intensities of the transitions in the ^{185}Os decay have been determined using Ge(Li) detectors and an iron-yoke double-focusing beta-ray spectrometer. Internal conversion measurements performed at a resolution of 0.15% made it possible to determine the multipole character of the nine strongest transitions. The proposed decay scheme has been tested by a two-parameter coincidence experiment. It has been found that the experimental data agree roughly with the theoretical predictions of Nilsson model description if the Coriolis interaction is taken into account. (auth)

5742 ANOMALOUS ORBITAL MAGNETISM OF PROTON DEDUCED FROM THE MAGNETIC MOMENT OF THE 11^- STATE OF ^{210}Po. Yamazaki, T. (Tokyo Univ.); Nomura, T.; Nagamiya, S.; Katou, T. Phys. Rev. Lett.; 25: 547-50(24 Aug 1970).

The g factor of the 24-nsec ($h_{9/2}i_{13/2}$) 11^- state of ^{210}Po has been determined to be 1.090 ± 0.016 by the spin-rotation method in the reaction ^{208}Pb(α,2n). The anomalous g_l^{eff} factor of 1.09 ± 0.02 has been deduced from this value and the known g factor of $h_{9/2}$ under the assumption of the renormalized single particle operator $\vec{\mu} = g_l^{eff}\vec{l} + g_s^{eff}\vec{s}$. (auth)

5743 BETA-RAY ASYMMETRY FROM ORIENTED ^{110m}Ag. Knott, T. F. (Harvard Univ., Cambridge, Mass.); Andrews, H. R.; Cohen, E. J.; Pipkin, F. M.; Santry, D. C. Phys. Rev. Lett.; 25: 543-6(24 Aug 1970).

XUM

A new technique for the study of the beta rays emitted by polarized nuclei is presented. This technique uses two silicon detectors arranged in coincidence so as to discriminate against gamma rays and back scattering from the detectors. This technique has been used to study the asymmetry of the beta rays in the decay of ^{110m}Ag. (auth)

5744 EXCITED $K^{\pi} = 0^+$ BANDS IN ^{172}Yb. Greenwood, R. C. (Idaho Nuclear Corp., Idaho Falls); Reich, C. W.; Vegors, S. H. Jr. Phys. Lett.; 33B: 213-15(12 Oct 1970).

Four excited $K^{\pi} = 0^+$ bands, with band-heads at 1042, 1404, 1794, and 1894 keV, have been observed in ^{172}Yb from study of the ^{171}Yb(n,γ) reaction with both thermal and 2-keV neutrons. (auth)

5745 WEAK COUPLING IN THE ^{209}Bi $5^- \otimes h_{\frac{9}{2}}$ DECUPLET. Francillon, G.; Terrien, Y.; Vallois, G. (CEN, Saclay, France). Phys. Lett.; 33B: 216-18(12 Oct 1970).

The ^{209}Bi(p,p′) reaction was investigated in order to observe the excitation of the $(5^- \otimes h_{\frac{9}{2}})$ decuplet; the overall resolution was better than 10 keV. The results are consistent with weak-coupling model predictions. Pairing and blocking effects are shown to be important by means of a schematic calculation. (auth)

5746 INFLUENCE OF THE MAGNETIC-DIPOLE AND ELECTRIC-QUADRUPOLE INTERACTION ON THE $\gamma-\gamma$ ANGULAR CORRELATION. Pandey, R. C. (Technische Univ., Berlin). Exp. Tech. Phys.; 17: 377-90(1969). (In German).

The influence of the combined magnetic-dipole and electric-quadrupole interaction with an applied static magnetic field on the excited state of nuclei (source with polycrystalline form) is described. Measurements were performed for the $\frac{5}{2}$ excited state of ^{181}Hf. This method enables one to measure the magnetic and electric precession frequencies simultaneously, but there are certain reasons that limit its application which are discussed here. (auth)

5747 STUDY OF THE EXCITED STATES OF ^{175}Yb FROM THE DECAY OF ^{175}Tm. Jacobs, E.; De Frenne, D.; Uyttenhove, J. (Rijksuniversiteit, Ghent). Z. Phys.; 238: 335-42(1970).

The decay of ^{175}Tm was investigated by means of Ge(Li) spectrometers. Excited states of ^{175}Yb at 104.5, 514.8, 555.8, 601.9, 638.9, 697.7, 811.5, 871.4, 919.8, 991.8, 1,009.4, (1,066.7), 1,308.9, 1,468.0, 1,497.0, (1,620), 1,682.4, 1,690.7, 1,793.3, 1,864.5, 1,891.5, (2,081.0), 2,093.0, 2,114.5 and 2,138.2 keV are observed in the beta decay of ^{175}Tm. Spin and parity assignments for all observed levels have been made from beta disintegration considerations and gamma branches. The experimental level scheme is described in terms of the Nilsson model, and possible three-quasiparticle excitations are discussed. (auth)

5748 STUDIES OF SELECTED NEUTRON-DEFICIENT ISOTOPES. Hopke, Philip Karl. Princeton, N. J.; Princeton Univ. (1969). 96p. University Microfilms Order No. 70-8369.

Thesis.

The theory of electron-capture beta decay is briefly reviewed, and a description of the method of calculating atomic electron wave functions at the nuclear surface is given. The advantages and disadvantages of a gas-filled proportional counter for low-energy electrons are discussed. A useful correlation between neutron and proton numbers of stable isotopes for even–even nuclei is extended to the cases of odd-N and odd-Z nuclei. Samples of ^{157}Tb were prepared by irradiating enriched ^{156}Dy in the Materials Testing Reactor. The L_1 to K electron-capture ratio was determined as 2.65 ± 0.20 by using a beryllium-windowed sodium-iodide spectrometer. This value implies a Q value for electron capture to the ground state of ^{157}Gd of 66 ± 6 keV, which also permits electron capture to the first excited state at 54 keV. A search was made for photons of this energy using a germanium semi-conductor detector having an energy resolution of 0.75 keV FWHM. Photons having an energy of 54.35 ± 0.05 keV were observed in ^{157}Tb sources. By using the measured photon intensity and the intensity of the K x rays, a branching ratio of (0.34 ± 0.2)% is calculated for electron capture to the first excited state. A sample of ^{163}Ho was prepared by the neutron irradiation of ^{162}Er followed by chemical purification and isotopic separation. This nuclide ^{163}Ho appears to decay by electron capture from the M and higher shells. A half-life of 33 ± 23 years has previously been reported. A search for L x rays was made. The M to L capture ratio was found to be greater than 229. From this datum an upper limit for the Q value for electron capture can be deduced to be 9.3 ± 1.5 keV. The Q value for the electron capture decay of ^{193}Pt was determined to be 60.8 ± 3.0 keV from a measurement of the endpoints of the L and M shell electron capture internal bremsstrahlung. The partial half-life for the L capture decay is 620 ± 250 years. The decay of the odd-mass isotopes of polonium to levels in ^{203}Bi, ^{205}Bi, and ^{207}Bi was studied. Isotopically separated sources were produced. Gamma-ray and conversion-electron spectra were observed. With the aid of Ge(Li)–Ge(Li) gamma–gamma coincidences, level schemes are constructed for these three bismuth isotopes. (TSS) (Diss. Abstr.)

5749 DECAY OF ^{144}Ce. Potnis, V. R.; Agin, G. P.; Mandeville, C. E. (Michigan Tech. Univ., Houghton). J. Phys. Soc. Jap.; 29: 559-62(Sep 1970).

The energies and relative intensities of the gamma rays of ^{144}Ce have been determined with use of a Ge(Li) detector. The quantum energies are 33.7, 40.8, 53.4, 80.1, 99.8, and 133.5 keV, the associated relative intensities being 2.3 ± 0.2, 5 ± 4, 1.1 ± 0.1, 16 ± 1, 0.39 ± 0.04, and 100 ± 6. These data have been interpreted to indicate excited nuclear energy states in ^{144}Pr at 59.03, 80.1, 99.8 and 133.5 keV. (auth)

5750 LOW-LYING STATES OF ^{152}Gd. Gono, Yasuyuki (Tokyo Univ.). J. Phys. Soc. Jap.; 29: 563-8(Sep 1970).

The gamma rays and the internal conversion electrons following the ^{153}Eu(p,2n)^{152}Gd and ^{150}Sm(α,2n)^{152}Gd reactions were measured. The energies and the spins and parities of excited levels of ^{152}Gd were determined to be 344 (2+), 616 (0+), 755 (4+), 931 (2+), 1227 (6+), 1282 (4+), 1668 (6+), 1747 (8+) and 2301 keV (10+) from the relative gamma-ray yields and the conversion coefficients. E0 components were observed in the 616-keV, 587-keV 527-keV, and 441-keV transitions. The dimensionless ratio X of the E0–E2 mixture of $4_2^+ \rightarrow 4_1^+$ transition was determined to be 0.14 ± 0.07. (auth)

5751 NUCLEAR ENERGY LEVELS OF ^{133}Cs AND ^{141}Pr FROM THE (n,n′γ) REACTION. Dave, Vibhakar Ratilal. New Orleans; Tulane Univ. (1969). 81p.

Thesis.

The nuclear energy levels of ^{133}Cs and ^{141}Pr were investigated by high-resolution measurements of γ-rays following neutron inelastic scattering. Data were taken at twenty neutron energies between 0.2 and 2.2 MeV for ^{133}Cs and at eleven neutron energies between 1.2 and 2.2 MeV for ^{141}Pr. A 30 cc Ge(Li) detector was used to detect the γ-rays. The scatterers consist of 493 gm of cesium carbonate powder and 318 gm of praseodymium oxide powder in lucite rings. The energies of photopeaks of γ-rays attributed to neutron inelastic scattering were accurately determined and the areas of the peaks were used to obtain the γ-ray production cross sections. An iron ring scatterer was used to observe the 845-keV γ-ray from the ^{56}Fe(n,n′γ) reaction for use as a cross section standard. A total of 41 γ-rays from inelastic scattering were observed in ^{133}Cs. The decay scheme below 437 keV has been established from earlier investigations but no information on levels above this energy has been reported. The present work is consistent with the earlier results and in addition new levels at 633, 706, 728, 768, 819, 872, 917, 942, 1090 and 1175 keV were assigned from threshold measurements, excitation functions and energy sum considerations. Additional high energy γ-rays are presented from which level assignments were not made. A total of 34 γ-rays was observed in ^{141}Pr of which five were assigned to decays from new levels at 1856, 1974, 2017 and 2104 keV and from a tentative level at 1900 keV. A decay scheme for ^{141}Pr is presented and compared with the measurements from other (n,n′γ) and radioactive decay investigations. The spins of the levels below 1650 keV are discussed and compared with other experimental and theoretical results. (Diss. Abstr. Int., B)

5752 ISOBARIC ANALOG RESONANCES IN PROTON ELASTIC SCATTERING FROM ^{110}Cd, ^{112}Cd, AND ^{114}Cd. Mistry, Vitthalbhai Dahyabhai. Austin, Tex.; Univ. of Texas (1969). 132p. University Microfilms Order No. 70-10,839.

Thesis.

Excitation functions were measured for elastic and inelastic scattering of protons from ^{110}Cd, ^{112}Cd and ^{114}Cd at proton energies from 6.0 MeV to 11.0 MeV. The isobaric analog resonances observed in ^{111}In, ^{113}In and ^{115}In nuclei were analyzed by fitting the elastic excitation functions using a shell model approach to reaction theory to extract quantitative nuclear structure information for the parent analog states in ^{111}Cd, ^{113}Cd and ^{115}Cd. Spectroscopic factors were evaluated, and their dependence on the choice of optical and bound state potentials has been studied. Coulomb displacement energies were also obtained from these data. Comparisons have been made with existing (d,p) work on ^{110}Cd, ^{112}Cd and ^{114}Cd. For most states there is reasonable agreement between the (p,p$_0$) and (d,p) results. (Diss. Abstr. Int., B)

5753 ELECTRON CAPTURE DECAY OF ^{181}W: L SUBSHELL FLUORESCENCE AND COSTER–KRONIG YIELDS IN Ta. Mohan, S. (Georgia Inst. of Tech., Atlanta); Fink, R. W.; Wood, R. E.; Palms, J. M.; Rao, P. Venugopala. Z. Phys.; 239: 423-8(1970).

The Ta L x-ray spectrum from the 140 d electron capture decay of ^{181}W was studied with high resolution semiconductor detectors and fast coincidence techniques. Measurement of L x-ray–K x-ray and L x-ray–γ-ray coincidence rates yielded the following L shell fluorescence and Coster–Kronig yields and radiative decay branching ratios: $\omega_2 = 0.250 \pm 0.013$, $\omega_3 = 0.228 \pm 0.013$ (corrected for angular correlation effects), $f_{23} = 0.180 \pm 0.007$, $\nu_1 = 0.218 \pm 0.016$, $s_3 = 0.205 \pm 0.010$, $s_2 = 0.215 \pm 0.010$, $f_{13} + f_{12}f_{23} = 0.36 \pm 0.02$, and $\omega_1 + f_{12}\omega_2 = 0.14 \pm 0.02$, from which upper limits were obtained of $f_{13} < 0.36$ and $\omega_1 < 0.14$. (auth)

5754 DECAY SCHEME OF 5.3 h ^{113}Ag AND 1.2 MIN ^{113m}Ag. Matumoto, Zyun-itiro; Tamura, Tsutomu (Japan Atomic Energy Research Inst., Tokai). J. Phys. Soc. Jap.; 29: 1116-28(Nov 1970).

The β- and γ-radiations of ^{113g,m}Ag were studied by using Ge(Li), NaI(Tl) and anthracene detectors. The activities were produced by the ^{114}Cd(γ,p) reaction. By various coincidences, including Ge(Li)–Ge(Li) configuration, most of the 30 γ-rays of the 5.3 h ^{113}Ag observed were fitted to a level scheme of ^{113}Cd consisting of the following 16 levels; 263.7, 298.4, 316.1, 583.9, 603.0, 681.0, 708.5, 821.0, 883.6, 936.3, 988.7, 1050.1, 1126.7, 1194.9, 1479.4 and 1665.5 keV. In the ^{113m}Ag decay a total of 7 γ-rays were observed to populate the five levels at 298.4, 316.1, 441.9, 583.9 and 708.5 keV. The spins and parities were tentatively assigned from the transition intensities, and were compared with the results of (d,p) experiments. (auth)

5755 ENERGY DEPENDENCE OF $\bar{\nu}_p$ FOR NEUTRON INDUCED FISSION OF ^{235}U BELOW 2.0 MeV. Boldeman, J. W.; Walsh, R. L. (Australian Atomic Energy Research Establishment, Sutherland). J. Nucl. Energy; 24: 191-205(Jul 1970).

Accurate measurements were made of the energy dependence of $\bar{\nu}_p$ for neutron induced fission of ^{235}U in the energy range 0–2 MeV. The $\bar{\nu}_p(E_n)$ dependence was found to be linear, and the data are best represented by the straight line $(2.412 \pm 0.005) + (0.114 \pm 0.008)E_n$. No effects related to the discrete nature of the low lying fission channels were observed. (auth)

5756 POSSIBILITIES OF ISOTOPE SYNTHESIS IN FISSION REACTION. Oganesyan, Yu. Ts.; Penionzhkevich, Yu. E.; Shamsutdinov, A. O.; (and others). At. Energ. (USSR); 29: 264-71(Oct 1970). (In Russian).

Production cross sections of different isotopes with Z from 42 up to 79 obtained as fragments of the uranium fission by ^{12}C, ^{20}Ne, ^{22}Ne and ^{40}Ar ions are determined. Identification and determination of isotope yields are performed by the spectrometric method using a Ge(Li) detector. The cross sections measured are compared with production cross sections of the same isotopes in reactions with fast protons. The data obtained are discussed from the point of view of the possibility of synthesis of isotopes located far from the stability region. (auth)

5757 SYNTHESIS OF ELEMENT 105. Flerov, G. N.; OGANESYAN, Yu. Ts.; Lobanov, Yu. V.; (and others). At. Energ. (USSR); 29: 243-50(Oct 1970). (In Russian).

When bombarding ^{243}Am with the ^{22}Ne ions an emitter of the spontaneous fission fragments with $\tau_{\frac{1}{2}} = (1.8 \pm 0.6)$ sec was recorded; its yield corresponds to the cross section $(5.0 \pm 1.5) \times 10^{-34}$ cm^2 for the branch of spontaneous fission. An integral angular distribution of ^{243}Am + ^{22}Ne reaction products and a dependence of the production cross section of a new isotope on the ^{22}Ne energy were measured. It follows from these data and the analysis of the check experiment results that the atomic number of the isotope, being spontaneously fissionable with $\tau_{\frac{1}{2}} = (1.8 \pm 0.6)$ sec, is 105. The spontaneous fission of ^{256,257}103 isotopes was studied. It is shown that for these nuclei the half-life is more than 10^5 sec with respect to the spontaneous fission. The properties of the ^{258}103 isotope are discussed on the basis of experimental data. (auth)

5758 INVESTIGATION OF STATISTICALLY PERTURBED ANGULAR CORRELATIONS OF ^{154}Gd AND ^{156}Gd in DIFFERENT LIQUID SOURCES. Wagner, H. F.; Forker, M.; Weigand, U. (Univ., Bonn). Z. Phys.; 238: 69-77(1970).

The statistical perturbations of γ–γ angular correlations involving the first 2^+ rotational state of ^{154}Gd and ^{156}Gd were time-differentially investigated. Liquid sources of 3^+ ions of Gadolinium in 1N perchloric acid, 0.5N and 1N hydrochloric acid, and 1.3N and 2.6N sulfuric acid were used. Influences of the various chemical surroundings on the ratio λ_4/λ_2 of the attenuation parameters were studied. A simultaneous measurement of the angular correlation of the 874-keV–123-keV cascade and the 2,098-keV–89-keV cascade of ^{154}Gd and ^{156}Gd, respectively, was performed in perchloric solution. From the ratio of the attenuation parameters λ_2, obtained by this experiment, the ratio of the magnetic g factors of the first 2^+ levels of these isotopes is calculated to be $g^{154}/g^{156} = 1.11 \pm 0.08$. (auth)

5759 SEARCH FOR A LONG-LIVED SPONTANEOUS-FISSION ISOMER OF ^{241}Pu. Bemis, C. E.; Silva, R. J.; Bigelow, J. E. (Oak Ridge National Lab., Tenn.). Inorg. Nucl. Chem. Lett.; 6: 747-52(Sep 1970).

The existence of a (0.34 ± 0.11)-yr isomeric state in ^{241}Pu was recently postulated, and is thought to be associated with a new type of fission isomeric state. The occurrence of an exceptionally long-lived isomeric state in ^{241}Pu was attributed to the presence of the $[505]11/2^-$ neutron orbital at the Fermi surface and the large distortions characteristic of the fission isomers. This odd neutron orbital would increase the height of the second potential barrier owing to the unusually large specialisation energy, and the spontaneous fission half-life for an isomer of ^{241}Pu with this configuration was estimated to be of the order of months. The possible existence of a (~0.3)-yr spontaneous-fission isomer in ^{241}Pu, and the opportunities it would afford for detailed studies of shape isomerism in nuclei, prompted an exhaustive search for this isomer by means of a variety of production methods. An attempt is described to produce the isomer in the ^{240}Pu(n,γ), the ^{242}Pu(n,2n), and the ^{238}U(α,n) reactions. The experimental procedure is described in detail, and upper limits for the production of (~0.3)-yr ^{241}Pu in various reactions are tabulated. Results are discussed; attempts to observe this isomer directly in the above reactions were unsuccessful. (UK)

5760 DETERMINATION OF THE QUADRUPOLE RATIO Q^{3+}/Q^{2+} IN ^{172}Yb. Wagner, H. F.; Lange, J. (Univ., Bonn). Z. Phys.; 238: 35-42(1970).

Statistically perturbed angular correlations of ^{160}Dy and ^{172}Yb were time-differentially investigated in liquid sources. Ethyl alcohol and concentrated hydrochloric acid at various temperatures were used as solvents. The ratio of the spectroscopic quadrupole moments of the 2^+ rotational and the 3^+ isomeric level in ^{172}Yb is evaluated as $Q^{3+}/Q^{2+} = 1.33 \pm 0.14$. (auth)

5761 EXPERIMENTAL STUDY OF THE ISOMERIC STATES ^{101m}Ru, ^{103m}Ru, and ^{101m}Tc. Uyttenhove, J.; Demuynck, J.; Dorikens, M.; Dorikens-Vanpraet, L. (Rijksuniversiteit, Ghent). Z. Phys.; 238: 90-8(1970).

In natural ruthenium isomeric states were produced by photonuclear reactions with LINAC Bremsstrahlung of 26 MeV. They were identified as 526.6 ± 0.7 keV; $T_{\frac{1}{2}} = 22.5 \pm 0.5$ μsec in ^{101}Ru, 192.0 ± 0.2 keV; $T_{\frac{1}{2}} = 760 \pm 50$ μsec in ^{101}Tc, and 210.9 ± 0.2 keV; $T_{\frac{1}{2}} = 1560 \pm 50$ μsec in ^{103}Ru. The experimental techniques are described. (auth)

5762 SCATTERING OF 4-MeV NEUTRONS AT ANGLES CLOSE TO 180°. Morozov, V. M.; Gorlov, G. V.; Zubov, Yu. G.; Lebedeva, N. S. JETP Lett. (USSR) (Engl. Transl.) 12: 125-7(20 Aug 1970).

Translated from Zh. Eksp. Teor. Fiz., Pis'ma Red.; 12: 181-3(20 Aug 1970).

Differential elastic scattering cross sections for a polarized beam of 4-MeV neutrons on Bi, In, Pb, Sn, and U were measured over the angular range 146-177°. Despite considerable shielding efforts the background in the measurements with In, Sn, and U reached 80-90% of the total detector count at $\theta = 177°$. From these results the differential cross sections for the elastic scattering of unpolarized neutrons and the polarizing abilities of the nuclei in neutron elastic scattering were determined. The estimated error of the cross section measurements was 10-15%. For all targets except U the differential cross section increases with scattering angle. (R.W.R.)

5763 ISOMERIC CROSS-SECTION RATIOS AND TOTAL CROSS-SECTIONS FOR THE ^{113}In(n,2n) ^{112gm}In AND ^{115}In(n,2n) ^{114gm}In REACTIONS. Grochulski, W.; Karolyi, J.; Marcinkowski, A.; Piotrowski, J.; Saad, E.; Siwek, K.; Wilhelmi, Z. (Univ. of Warsaw. Inst. of Nuclear Research, Warsaw). Acta Phys. Pol.; B1: 271-4(Jul-Sep 1970).

The isomeric ratios and excitation functions were measured for the ^{113}In(n,2n)^{112gm}In and ^{115}In(n,2n)^{114gm}In reactions in the neutron energy range from 13.1 MeV to 18.2 MeV. The results are compared with the statistical-model predictions. Use was made of modified nuclear level-density formulas, based on superconductivity theory, which account for the pairing and shell effects. (auth)

5764 DIRECTIONAL CORRELATIONS OF GAMMA RAYS IN ^{125}I. Ludziejewski, J.; Klamra, W.; Kownacki, J. (Inst. of Nuclear Research, Swierk, Poland). Acta Phys. Pol.; B1: 189-200(Jul-Sep 1970).

Angular correlations of γ rays in the decay of ^{125}Xe were measured. The source was obtained by implanting Xe ions in

XUM

aluminium foil. The results, together with the log-ft values of electron-capture transitions and the transition multipolarities, allow the assignment of spins and parities to the following levels: $^{7}/_{2}^{+}$ to 113.6 keV, $^{5}/_{2}^{+}$ to 372.1 keV and $^{3}/_{2}^{+}$ to 453.8 keV. They also suggest $^{3}/_{2}$ spin values for the 1090-, 1180.5-, and 1383-keV levels. The perturbation of the 74.9–113.6-keV correlation is discussed. The spin value for the 113.6-keV level and negative sign for the mixing amplitude of the 113.6-keV transition emerge from the analysis, irrespective of perturbation of the angular correlation. Several new transitions in coincidence with 453.8-keV γ quanta were observed. (auth)

5765 FISSION YIELDS OF OVER 40 STABLE AND LONG-LIVED FISSION PRODUCTS FOR THERMAL NEUTRON FISSIONED ^{233}U, ^{235}U, ^{239}Pu, AND ^{241}Pu AND FAST REACTOR FISSIONED ^{235}U AND ^{239}Pu. Lisman, F. L.; Abernathey, R. M.; Maeck, W. J.; Rein, J. E. (Idaho Nuclear Corp., Idaho Falls). Nucl. Sci. Eng.; 42: 191-214(Nov 1970).

The thermal fission yields of 43 mass chains for ^{233}U, ^{235}U, ^{239}Pu, and ^{241}Pu and the fast reactor fission yields of 45 mass chains for ^{235}U and ^{239}Pu have been measured with a relative standard deviation of 1 to 2%. The data were obtained mainly by measuring long-lived and stable fission products by the technique of isotope dilution mass spectrometry. This paper has two sections: the first reports the fission yields, the second describes the chemical analysis techniques for the fission products. (auth)

5766 (n,2n) EXCITATION FUNCTIONS FOR ^{93}Nb AND ^{103}Rh WITH SPECIAL RESPECT TO THE ISOMERIC STATES IN ^{92}Nb AND ^{102}Rh. Paulsen, A.; Widera, R. (EURATOM, Geel, Belgium). Z. Phys.; 238: 23-34(1970).

By means of the activation technique the excitation functions for the reactions ^{93}Nb(n,2n)^{92m}Nb(10.15d), ^{103}Rh(n,2n)^{102m}Rh(2.9y), and ^{103}Rh(n,2n)^{102g}Rh(206d) were measured with an average total uncertainty of about ±8% between 10 and 20 MeV neutron energy. In addition, the total ^{93}Nb(n,2n) cross-section was compared with the ^{59}Co(n,2n) cross-section at 16.8 MeV by direct neutron detection using the time-of-flight technique. The results are compared with statistical theory, especially with theoretical expectations for the isomeric cross-section ratios; these are only in reasonable agreement with the experiment if one assumes a ground state spin $I_g = 5$ for ^{92}Nb and $I_g = 2$ for ^{102}Rh. (auth)

5767 REDETERMINATION OF THE ^{238}U(sp.f.) DECAY CONSTANT BY FISSION TRACKS IN A U-STAINED BOHEMIAN GLASS OF KNOWN AGE. Thiel, K.; Herr, W. (Univ., Cologne). Trans. Amer. Nucl. Soc.; 13: 527(Nov 1970).

From Meeting of the American Nuclear Society, Washington, D. C. See CONF-701102.

5768 LOW-ENERGY PHOTOFISSION OF HEAVY ELEMENTS: EXPERIMENTAL RESULTS. Bramblett, R. L.; Gozani, T.; Ginaven, R. O.; Rundquist, D. E. (Gulf Energy and Environmental Systems, Inc., San Diego, Calif.). Trans. Amer. Nucl. Soc.; 13: 707(Nov 1970).

From Meeting of the American Nuclear Society, Washington, D. C. See CONF-701102.

5769 PHYSICS OF DELAYED NEUTRONS: EXPERIMENTAL. Keepin, G. Robert (Los Alamos Scientific Lab., N. Mex.). Trans. Amer. Nucl. Soc.; 13: 709(Nov 1970).

From Meeting of the American Nuclear Society, Washington, D. C. See CONF-701102.

5770 DELAYED-NEUTRON YIELD VS ENERGY MEASUREMENTS. Krick, M. S.; Evans, A. E. (Los Alamos Scientific Lab., N. Mex.). Trans. Amer. Nucl. Soc.; 13: 746(Nov 1970).

From Meeting of the American Nuclear Society, Washington, D. C. See CONF-701102.

5771 MEASUREMENT OF THE CAPTURE CROSS SECTION OF ^{238}U UP TO 100 keV. Perez, R. B.; de Saussure, G.; Silver, E. G.; Ingle, R. W. (Oak Ridge National Lab., Tenn.). Trans. Amer. Nucl. Soc.; 13: 753(Nov 1970).

From Meeting of the American Nuclear Society, Washington, D. C. See CONF-701102.

5772 INTEGRAL MEASUREMENT OF THE CAPTURE-TO-FISSION RATIO IN ^{239}Pu AT INTERMEDIATE ENERGIES. Takahashi, H.; Weinstock, E. V. (Brookhaven National Lab., Upton, N. Y.). Trans. Amer. Nucl. Soc.; 13: 754-5(Nov 1970).

From Meeting of the American Nuclear Society, Washington, D. C. See CONF-701102.

5773 ENERGY INTEGRAL TESTS OF DIFFERENTIAL FISSION CROSS-SECTION DATA. Chromik, Joseph J.; Draper, E. Linn Jr. (Univ. of Texas, Austin). Trans. Amer. Nucl. Soc.; 13: 755(Nov 1970).

From Meeting of the American Nuclear Society, Washington, D. C. See CONF-701102.

5774 MULTIPLICATION EFFECTS IN MEASUREMENTS OF DELAYED-NEUTRON ENERGY SPECTRA. Sloan, W. Robert; Woodruff, Gene L.; Arthur, J. B.; Parker, Richard C. (Univ. of Washington, Seattle). Trans. Amer. Nucl. Soc.; 13: 759-60(Nov 1970).

From Meeting of the American Nuclear Society, Washington, D. C. See CONF-701102.

5775 DELAYED-NEUTRON ABUNDANCES AND HALF-LIVES FROM 14.7-MeV FISSION. East, L. V.; Augustson, R. H.; Menlove, H. O.; Masters, C. F. (Los Alamos Scientific Lab., N. Mex.). Trans. Amer. Nucl. Soc.; 13: 760-1(Nov 1970).

From Meeting of the American Nuclear Society, Washington, D. C. See CONF-701102.

5776 EPITHERMAL-NEUTRON CAPTURE GAMMA RAYS FROM SHIELD MATERIALS: DEPLETED URANIUM. John, Joseph; Orphan, V. J.; Hoot, C. G. (Gulf Energy and Environmental Systems, Inc., San Diego, Calif.). Trans. Amer. Nucl. Soc.; 13: 865-6(Nov 1970).

From Meeting of the American Nuclear Society, Washington, D. C. See CONF-701102.

5777 NEUTRON ENERGY-DEPENDENT CAPTURE GAMMA-RAY YIELDS FOR ^{238}U AND ^{181}Ta. Yost, K. J.; White, J. E.; Fu, C. Y. (Oak Ridge National Lab., Tenn.). Trans. Amer. Nucl. Soc.; 13: 866-8(Nov 1970).

From Meeting of the American Nuclear Society, Washington, D. C. See CONF-701102.

5778 GROSS STRUCTURE OF GIANT DIPOLE RESONANCE ON NUCLEI OF THE TRANSITION REGION $N \simeq 90$. Vasil'ev, O. V.; Semenov, V. I. (Saratov State Univ., USSR). JETP Lett. (USSR) (Engl. Transl.); 11: 356-8(5 Jun 1970).

Translated from Zh. Eksp. Teor. Fiz., Pis'ma Red.; 11: 520-3 (5 Jun 1970).

Nuclei with $N \simeq 90$ are noted for the instability of their form. In order to ascertain how such an instability can affect the properties of the dipole spectrum of a nucleus, photoneutron and photoabsorption cross sections were measured for ^{152,154,156,158}Gd and ^{151,153}Eu in the photon energy range of 8 to 22 MeV. A clear-cut splitting of the giant resonance (the Okamoto–Danos effect) is noticed for ^{152}Gd; this indicates that this is not simply a spherical nucleus executing harmonic quadrupole oscillations. Since ^{152}Gd has a relatively small mean-square deformation, the surprising similarity of the form of its giant resonance to the curve of photoabsorption by ^{154}Gd can be regarded as an indication of its having both small and large (positive) equilibrium deformations. ^{153}Eu also exhibits the Okamoto–Danos effect. As the deformation potential of odd nuclei is expected to be steeper than that of even–even nuclei, dipole transitions to states with a deformation different from β should be forbidden in the case of odd nuclei in accordance with the Franck–Condon principle. (R.W.R.)

5779 GAMMA-VIBRATION OF NUCLEI AT EQUILIBRIUM AND SADDLE POINT. Zielinska-Pfabe, M. (Inst. for Nuclear Research, Warsaw). Phys. Lett.; 33B: 153-4(28 Sep 1970).

The gamma-vibrational parameters B_γ and C_γ and the energy E_γ of the gamma-vibrational state of deformed nuclei are calculated as functions of the ϵ-deformation in the whole region between the equilibrium and the saddle point. Both the microscopic and macroscopic descriptions are used. The following result is obtained: when ϵ increases from its equilibrium value to the saddle-point value, the nucleus begins to be stiffer with respect to the gamma-vibration. (auth)

5780 PROTON SCATTERING TO THE $3/2^-$ STATE OF ^{207}Pb. Geramb, H. V.; Amos, K. (Univ. of Georgia, Athens). Phys. Lett.; 32B: 665-7(14 Sep 1970).

The inelastic scattering of 20.2-MeV protons to the $^{3}/_{2}^{-}$ state of ^{207}Pb(Q = 0.97 MeV) is analyzed by using an antisymmetrized distorted-wave approximation using central, tensor, and core-polarization interactions. (auth)

5781 QUANTUM MECHANICAL CORRECTIONS FOR DOUBLE COULOMB EXCITATION IN ^{152}Sm AND THE DETERMINATION OF THE E4 TRANSITION PROBABILITY. Alder, K.; Morf, R.; Roesel, F. (Univ. of Basel). Phys. Lett.; 32B: 645-6(14 Sep 1970).

Quantal corrections are computed for double Coulomb excitation. These corrections are significant for the determination of the E4 matrix element in ^{152}Sm. (auth)

5782 PHENOMENOLOGICAL DESCRIPTION OF ANHARMONIC QUADRUPOLE VIBRATIONS. Sips, L.; Lopac, V. (Inst. Rudjer Boskovic, Zagreb). Phys. Lett.; 32B: 649-51 (14 Sep 1970).

The phenomenological description of anharmonic quadrupole vibrations including third-order terms is reexamined. It is demonstrated that the smallness of cross-over ($\Delta N = 2$) transitions can be maintained in the presence of large $\Delta N = 0$ transitions that incorporate the quadrupole moment. (auth)

5783 NON-ADIABATIC EFFECTS IN ROTATIONAL BANDS OF THE ODD PROTON NUCLEUS ^{155}Tb. Winter, G.; Funke, L.; Kaun, K. H.; Kemnitz, P.; Sodan, H. (Zentralinstitut fuer Kernforschung, Rossendorf, Ger.). Phys. Lett.; 33B: 161-2(28 Sep 1970).

An anomalous rotational band found in ^{155}Tb by in-beam γ-ray spectroscopy is interpreted in terms of the Coriolis coupling between the Nilsson orbitals based on the $h_{11/2}$ proton shell-model state. (auth)

5784 SOME YIELDS AND ISOMERIC YIELD RATIOS OF INDIUM ISOTOPES PRODUCED BY HIGH-ENERGY FISSION. Hageboe, E. (CERN, Geneva). J. Inorg. Nucl. Chem.; 32: 2489-2500(Aug 1970).

Cross sections of some indium isotopes from fission of uranium with 570 MeV and 18.2 GeV protons were determined. Charge dispersion curves were obtained for A = 117 at the two energies. The first has $N/Z_p = 1.414$ and a full width at half-maximum of 2.93 Z units; the second is double-humped with a neutron-rich part equal in form and position to the curve at 570 MeV. The excitation function for ^{111}In is constructed and peaks above 10 GeV. A thick-target recoil study of ^{111}In at 570 MeV, 7.1 GeV, and 18.2 GeV shows a decrease in kinetic energy by a factor of 2, and also a considerable decrease in the cascade deposition energy in this energy range. The independent high-spin to low-spin isomeric yield ratios of the ^{117}In isomers were determined by irradiation of uranium and bismuth with protons of energies ranging from 159 MeV to 18.2 GeV. These ratios seem to be constant (23 ± 5) above 250 MeV proton energy, independent of target. (auth) (UK)

5785 ANOMALOUS TRANSMISSION OF NEUTRONS IN A PERFECT CdS CRYSTAL. Shil'shtein, S. Sh.; Marukhin, V. L.; Kalanov, M.; Somenkov, V. A.; Sysoev, L. A. JETP Lett. (USSR) (Engl. Transl.); 12: 56-8(20 Jul 1970).

Translated from Zh. Eksp. Teor. Fiz., Pis'ma Red.; 12: 80-3 (20 Jul 1970).

Reflection and transmission of neutrons by a perfect α-CdS crystal of intermediate thickness were investigated in a range of energies comparable with the resonance-excitation energy of ^{113}Cd (0.178 eV). The widths of the reflection curves agree with the calculated ones and are determined by the dispersion of the two-crystal spectrometer. The Laue reflections are weaker than the Bragg ones by only one order of magnitude, whereas in the case of ordinary reflection the difference would amount to two or three orders. The results confirm the conservation of coherence in resonant scattering, as manifest by the existence of anomalous transmission of neutrons near the resonance (the effect of suppression of the inelastic channels). (R.W.R.)

5786 NUCLEAR ORIENTATION OF ^{113m}Cd, ^{115}Cd, AND ^{115m}Cd. Chaney, Robert Lee. Seattle; Univ. of Washington (1969). 180p. University Microfilms Order No. 70-8412.

Thesis.

Nuclear orientation of ^{113m}Cd, ^{115}Cd, and ^{115m}Cd was achieved in gas samples by optical pumping using the cadmium 3261-Å ($5\ ^1S_0 - 5\ ^3P_1$) intercombination line. Precise measurements were obtained for the ratios of the nuclear resonance frequencies for these isotopes relative to ^{111}Cd, and the differential hyperfine-structure anomalies were calculated from these ratios. By means of a previous measurement of the ^{111}Cd-to-proton nuclear-resonance-frequency ratio and the proton nuclear magnetic moment, the nuclear magnetic moments of the cadmium isotopes were calculated. The results for the measurements of the nuclear-magnetic-resonance-frequency ratios, the differential hyperfine-structure anomalies, and the nuclear magnetic moments are given. The measurements obtained for ^{113m}Cd and ^{115m}Cd represent an extension of the optical-pumping technique to large nuclear spins ($I = 11/2$). A number of new effects are explained by using the density-matrix formalism to extend the theory of optical pumping to isotopes with large nuclear spin. Considered in the treatment are the effects of an rf magnetic field that produces the nuclear-magnetic-resonance transitions, the light beam that provides the optical pumping, and interactions with the container walls that produce nuclear-spin relaxation. Pumping parameters are included which can be used to specify the case of non-uniform power spectral densities in the pumping light. Finally, the relaxation term includes both magnetic-dipole and electric-quadrupole relaxation processes. A method for obtaining solutions to the density-matrix equations that describe the equilibrium conditions of the system is developed. The technique, which includes a very useful approximation procedure, is adapted for implementation on a digital computer. (auth) (Diss. Abstr. Int., B)

5787 OBSERVATION OF INTERFERENCE OF THE PHOTOEFFECT AND INTERNAL CONVERSION IN RESONANT ABSORPTION OF M1 GAMMA QUANTA BY ^{119}Sn. Mitrofanov, K. P.; Plotnikova, M. V.; Rokhlov, N. I.; Shpinel, V. S. (Moscow State Univ.). JETP Lett. (USSR) (Engl. Transl.); 12: 60-2(20 Jul 1970).

Translated from Zh. Eksp. Teor. Fiz., Pis'ma Red.; 12: 85-8 (20 Jul 1970).

The possibility of interference between the photoelectric effect and internal conversion in resonant absorption of gamma quanta was investigated for the M1 gamma transition of ^{119}Sn. By detecting the electrons emitted from a thin layer of absorber atoms in a plane perpendicular to the γ-ray direction it is possible to observe the interference asymmetry of the spectrum. The value determined for the interference coefficient averaged over forward electron emission directions was $+(3 \pm 1) \times 10^{-3}$. This work establishes that interference of internal conversion and the photoelectric effect takes place in the case of M1 gamma transitions, and that the properties of this phenomenon agree with predictions. (R.W.R.)

5788 Γ PARTICLE-HOLE STATES IN ^{208}Pb. Perez, S. M. (Nuclear Physics Lab., Oxford). (Phys. Lett.; 33B: 317-19(9 Nov 1970).

The dipole states of ^{208}Pb are calculated using single-particle wavefunctions generated in a Saxon–Woods well and an effective particle–hole interaction. It is found that the experimental energy and concentration of dipole strength of the giant dipole resonance are reproduced with radius parameters yielding similar proton and neutron rms radii. (auth)

5789 CAPTURE CROSS SECTIONS IN THE keV REGION. Campbell, Wayne Wesley. Blacksburg, Va.; Virginia Polytechnic Inst. (1970). 81p. University Microfilms Order No. 70-11,504.

Thesis.

Natural silver and the isotopes ^{107}Ag, ^{109}Ag, ^{115}In, and ^{127}I were irradiated by the monoenergetic neutrons emitted at 90° to a proton beam striking a ^{7}Li target. These samples were then counted for their β and γ activity, and their absolute cross sections relative to the cross section of ^{127}I at 24 keV were calculated over the energy range of from 3 to 155 keV. These measured cross-section versus energy curves were used to determine the γ-ray strength functions, $\langle\Gamma_\gamma\rangle/\langle D_0\rangle$, the s-wave neutron strength functions, $\langle\Gamma_n^0\rangle/\langle D\rangle$, and the p-wave neutron strength functions, $\langle\Gamma_n^1\rangle/\langle D\rangle$. Because of data limitations it has been assumed that the γ-ray strength function is the same for both s- and p-wave neutrons. The cross sections determined are in general good agreement with the values previously reported but differ somewhat in shape. This shape variance results in values for the average resonance parameters which are somewhat higher than values reported by other workers. (TSS) (Diss. Abstr. Int., B)

5790 COMPUTER ANALYSIS OF FISSION DATA. Alexander, P. (Teledyne Isotopes, Westwood, N. J.); Lightbody, D.; Patton, W. A. Contract DASA-01-69-C-0057. Nucl. Instrum. Methods; 86: 99-107(1970).

A two-part computer program was written to aid in the analysis and interpretation of experimental fission data. The first part of the program calculates the population of all members of any radioactive decay chain at any point in time using as input the initial population distribution and the structure of the decay chain. The program may also be used to perform a time integration of the population for any member to give the number of decays during a specified time interval. The second part of the program uses as input the experimentally measured yield values derived from extractions at various times after fission of one or more members of a particular fission-product decay chain. The independent fission yield to any given mass chain is assumed to be distributed according to a Gaussian function. The parameters Z_p and w characterizing this distribution are varied so as to minimize the quantity χ^2 which is based on the difference between the calculated and experimentally determined fission yield values. The application of the first part of the program is discussed in connection with several fission-chain population problems. The use of a novel technique for deducing the values of the independent fission-yield distribution parameters is described for neutron-induced fission of ^{235}U and ^{239}Pu. This technique utilizes the second part of the computer program and is employed to extract the independent xenon yields for the fission chains with mass number 133 and 135. (auth)

XUN

5791 ROLE OF THE STATIC CHARGE OF THE NUCLEUS IN DETERMINING THE PROBABILITY OF THE E0 PAIR CONVERSION. Pazoiski, S. V. (Viteb Pedagogical Inst., USSR). Vestsi Akad. Navuk BSSR, Ser. Fiz.-Mat. Navuk; No. 2, 118-19(1970). (In Belrussian).

The effect of the distribution of the static charge of the nucleus on the corrected probability of the E0 conversion under pair formation is investigated. The calculations, carried out for Z = 20, 64, 68, and 92, reveal that this effect is quite large and must also be taken into account in the case of the E0 conversion of shells. It is found that the ratio of the E0 conversion probability at the shells due to the E0 pair formation probability depends only slightly on the charge distribution. (TTT)

5792 MAGNETIC QUADRUPOLE γ TRANSITIONS IN ATOMIC NUCLEI. Letessier, Jocelyne; Foucher, Roger (Institut de Physique Nucleaire, Orsay, France). Ann. Phys. (Paris); 4: 55-84 (Jan-Feb 1969). (In French).

After a brief review of the calculation of transition probabilities, the probabilities for pure M2 transitions are calculated for nuclei with Z and N near the magic numbers, deformed nuclei, intermediate nuclei, and odd–odd nuclei. E1 + M2 transitions are considered briefly. The results are tabulated and illustrated graphically. (261 references.) (J.S.R.)

5793 RADIATIVE PION ABSORPTION IN MEDIUM AND HEAVY NUCLEI. Guy, R.; Eisenberg, J. M. (Univ. of Virginia, Charlottesville). Phys. Lett.; 33B: 137-9(28 Sep 1970).

The distribution of spin–isospin strength is studied for radiative pion absorption in medium and heavy nuclei, including corrections to the leading (Kroll–Ruderman) term in the transition operator. Results are presented for absorption in ^{40}Ca, ^{90}Zr, and ^{208}Pb. (auth)

5794 ISOMERIC SHIFT AND MAGNETIC HYPERFINE SPLITTING OF MUONIC ATOMS IN THE LEAD REGION. Klemt, V. (Univ., Munich); Speth, J.; Goeke, K. Phys. Lett.; 33B: 331-3(9 Nov 1970).

Using the method of quasi-particles in interacting Fermi systems the isomeric shift and magnetic hyperfine splitting are calculated for the nuclei ^{207}Tl, ^{207}Pb, ^{209}Bi, and ^{209}Pb. The values obtained are compared with experiment. (auth)

5795 M1 GIANT RESONANCE IN ^{208}Pb FROM THRESHOLD PHOTONEUTRON MEASUREMENTS. Bowman, C. D.; Baglan, R. J.; Berman, B. L.; Phillips, T. W. (Univ. of California, Livermore). Phys. Rev. Lett.; 25: 1302-5(2 Nov 1970).

From threshold photoneutron cross-section and angular-distribution measurements on ^{208}Pb, seven 1^+ states were detected, which have a total M1 strength of 51 eV. This M1 strength, centered at an excitation energy of 7.9 MeV and spread over a range of 700 keV, constitutes at least half and perhaps all of the total M1 strength obtained from shell-model calculations. (auth)

5796 DECAY OF ^{104}Tc (18-MIN). Pinston, J. A.; Blachot, J.; Schussler, F. (CEN, Grenoble, France). Nucl. Phys.; A157: 323-36(1970). (In French).

The study of the β- and γ-activity of ^{104}Tc (18 min) produced by ^{104}Ru(n,p) and the fission of ^{235}U was performed to determine the Q_β (4250 ± 100 keV) of the ^{104}Tc disintegration as well as a tentative level scheme (25 levels) of ^{104}Ru. (auth)

5797 STUDY OF THE ^{232}Th(d,t)^{231}Th AND ^{238}U(d,t)^{237}U REACTIONS. Boyno, J. S.; Elze, Th. W.; Huizenga, J. R. (Univ. of Rochester, N. Y.). Nucl. Phys.; A157: 263-72(1970).

The ^{232}Th(d,t)^{231}Th and ^{238}U(d,t)^{237}U reactions were studied with a 17-MeV deuteron beam. The experimental spectroscopic factors for the emitted tritons were compared with the theoretical spectroscopic factors, calculated including Coriolis band mixing. From this comparison, the following Nilsson bands are assigned in ^{231}Th: [633↓], [631↑], [752↑], [501↓]; in ^{237}U: [631↓], [622↑], [743↑], [631↑], [501↓], [633↓]. Additional tentative assignments in both nuclei are discussed. (auth)

5798 ENERGY LEVELS OF ^{203}Tl AND ^{205}Tl FROM THE (n,n'γ) REACTION. Barnard, E.; Coetzee, N.; De Villiers, J. A. M.; Reitmann, D.; Van der Merwe, P. (Atomic Energy Board, Pelindaba, S. Afr.). Nucl. Phys.; A157: 130-6(1970).

The energy levels of ^{203}Tl and ^{205}Tl were studied by means of the (n,n'γ) reaction. The de-excitation γ-rays were observed in a time-of-flight gated Ge(Li) detector. Based on these γ-rays, energy level schemes were proposed up to an excitation of 1280 keV in ^{203}Tl and 1342 keV in ^{205}Tl. The level schemes are compared with those deduced from other types of reaction studies and with the predictions of the single-hole collective model. (auth)

5799 (p,t) REACTIONS ON THE EVEN TIN ISOTOPES. Fleming, Donald G. (Univ. of Copenhagen); Blann, Marshall; Fulbright, H. W.; Robbins, John A. Nucl. Phys.; A157: 1-31(1970).

The reactions ^{A}Sn(p,t)$^{A-2}$Sn were studied with even-A targets and 20 MeV protons. Experimental cross sections are compared with the results of distorted-wave Born approximation calculations, the two-nucleon structure factors being constructed from the BCS wave functions of both Arvieu and of Clement and Baranger. The basic two-quasiparticle model works well. Comparing the observed cross sections with the results of calculations based on the Clement and Baranger wave functions suggests the need for including the $3p_{\frac{1}{2}}$, $3p_{\frac{3}{2}}$ and $2f_{\frac{5}{2}}$ shells in the quasiparticle ground state. (auth)

Nuclear Theory

Refer also to abstracts 5389, 5390, 5405, 5507, 5531, 5570, 5601, 5669, 5684, and 5737.

5800 (AD–706717) RADIATIVE CORRECTIONS TO ELECTRON SCATTERING FROM COMPLEX NUCLEI. Uberall, H. (Naval Research Lab., Washington, D. C.). 1 May 1970. 82p. (NRL–7080). NTIS.

A review of the present status of radiative corrections to electron scattering from complex nuclei is given, both from the theoretical standpoint and with a view to practical applications. The first section presents a description of the general features of radiative corrections. The following four sections discuss the individual processes entering into radiative and line shape corrections and their synthesis, while the rest of the report is concerned with individual processes contributing to the radiation tail and their synthesis (or "unfolding procedure"). (auth) (USGRDR)

5801 (AD–706835) NUCLEAR ROTATIONAL BANDS AND SL (3,R) SYMMETRY. Weaver, L.; Biedenharn, L. C. (Duke Univ., Durham, N. C. Dept. of Physics). 1970. 13p. NTIS.

An expression is derived that involves no adjustable parameters for the ratios of interband E(2) transition probabilities in deformed even–even nuclei. The derivation is based on the idea, due to Gell-Mann, that the relevant operators generate the algebra of SL(3,R). (auth) (USGRDR)

5802 (LA–4465, pp 11,1-2) RAPID METHOD FOR THE MEASUREMENT OF ANALYZING TENSORS IN REACTIONS INDUCED BY POLARIZED DEUTERONS. Lawrence, G. P.; Ohlsen, Gerald G.; McKibben, J. L.; Keaton, P. W. Jr.; Armstrong, D. D. (Los Alamos Scientific Lab., N. Mex.).

From LASL contributions to the 3rd international symposium on polarization phenomena in nuclear reactions, Madison, Wisconsin, August 31–September 4, 1970.

5803 (LA–4465, pp 20,1-2) FORMALISM FOR A(d,n)B OR A(d,p)B POLARIZATION TRANSFER REACTIONS. Gammel, J. L.; Keaton, P. W. Jr.; Ohlsen, Gerald G. (Los Alamos Scientific Lab., N. Mex.).

From LASL contributions to the 3rd international symposium on polarization phenomena in nuclear reactions, Madison, Wisconsin, August 31–September 4, 1970.

5804 (LA–4465, pp 21,1-2) FORMALISM FOR A(p,p)A AND A(d,d)A POLARIZATION TRANSFER. Ohlsen, Gerald G.; Keaton, P. W. Jr. (Los Alamos Scientific Lab., N. Mex.).

From LASL contributions to the 3rd international symposium on polarization phenomena in nuclear reactions, Madison, Wisconsin, August 31–September 4, 1970.

5805 (LA–4465, pp 26,1-2) CONSIDERATIONS ON POLARIZED NEUTRON PRODUCTION BY (d,n) POLARIZATION TRANSFER REACTIONS AT 0°. Ohlsen, Gerald G.; Keaton, P. W. Jr.; Simmons, J. E. (Los Alamos Scientific Lab., N. Mex.).

From LASL contributions to the 3rd international symposium on polarization phenomena in nuclear reactions, Madison, Wisconsin, August 31–September 4, 1970.

5806 (LA–4465, pp 27,1-6) PRECISE METHOD FOR THE DETERMINATION OF SECONDARY STANDARDS FOR DEUTERON ANALYZING TENSORS. Keaton, P. W. Jr.; Armstrong, D. D.; Lawrence, G. P.; McKibben, J. L.; Ohlsen, Gerald G. (Los Alamos Scientific Lab., N. Mex.).

From LASL contributions to the 3rd international symposium on polarization phenomena in nuclear reactions, Madison, Wisconsin, August 31–September 4, 1970.

5807 (LA–4465, pp 35,1-2) FORMALISM FOR SPIN-3/2 BEAMS. Keaton, P. W. Jr. (Los Alamos Scientific Lab., N. Mex.).

From LASL contributions to the 3rd international symposium on polarization phenomena in nuclear reactions, Madison, Wisconsin, August 31–September 4, 1970.

5808 (N-70-32786) SYSTEMATIC METHOD OF CALCULATING REDUCED MATRIX ELEMENTS OF SINGLE-PARTICLE OPERATORS. Ford, William F.; Braley, Richard C. (National Aeronautics and Space Administration, Cleveland, Ohio. Lewis Research Center). Jul 1970. 34p. (NASA-TN-D-5879; E-5366). NTIS.

Many nuclear properties involve the evaluation of reduced matrix elements of single-particle operators between the initial and final nuclear states. A systematic means of calculating such matrix elements was developed in terms of inelastic transition densities, which essentially give the probability for absorption of angular momentum J = L + S by the last nucleon as a function of its distance from the nuclear origin. These densities may be expanded in terms of Gauss–Laguerre functions, permitting substantial simplification in the matrix element calculation. Examples and useful formulas are presented. (auth) (STAR)

5809 ON THE QUADRUPOLE FORCE IN NUCLEAR SPECTROSCOPY. Olivieri, E. (Univ., Rome); Salusti, E. Nuovo Cim.; 69A: 551-63(21 Oct 1970).

Deformed nuclei are studied by using an iterative technique which has been successfully used in the spherical-nuclei region: once the data of a nucleus with A particles is known, those of a nucleus with A + 1 particles can be calculated. The nuclear forces are critically discussed, and the validity of the classical P_2 interaction is justified. The results are compared with those of the Elliott model. Reasonable agreement is obtained with the experimental levels of ^{19}F. (auth)

5810 NUCLEUS AT THE FISSION SADDLE POINT AS ACTIVATED COMPLEX. Rollier, Mario A.; Moretto, Luciano G. (Univ., Pavia, Italy). Gazz. Chim. Ital.; 100: 381-90(Apr 1970). (In Italian).

The properties of the fission saddle point are described and compared with those of the "activated complex" in the kinetics of chemical reactions. The analogies between the collective Hamiltonian of a molecule and the collective Hamiltonian of a nucleus are stressed. The formalism for the evaluation of the fission decay width and the fission probability is deduced on the basis of the transition state at the fission saddle point. The fission-fragment angular distribution theory, furthermore, is discussed on the basis of the wave functions associated with the transition-state levels. The way to obtain information regarding the transition-state properties through the analysis of experimental fission cross sections and fission-fragment angular distributions is also considered. (auth)

5811 GENERAL METHOD FOR FORMULATING A MICROSCOPIC THEORY OF NUCLEAR COLLECTIVE MOTION. Nadjakov, E.; Mikhailov, I. N. (Inst. of Physics, Sofia. Joint Inst. for Nuclear Research, Dubna, USSR). Compt. Rend. Acad. Bulg. Sci.; 23: 495-8(1970).

A method for treating nuclear rotation in three dimensions, which is very similar to the random phase approximation for vibrations, has been developed. By treating different modes in a unified way, the theory is extended to solve the problem of a microscopic description of their coupling. The Hamiltonian of an even–even nucleus is written in second-quantized form in its Hartree–Fock basis. The procedure is illustrated by considering harmonic vibrations in deformed nuclei and rotations in deformed nuclei uncoupled to other modes. (R.W.R.)

5812 CHARGE ASYMMETRY IN TWO NUCLEON INTERACTION. Yalcin, C.; Birsen, N. (Middle East Technical Univ., Ankara). Phys. Lett.; 33B: 203-4(12 Oct 1970).

By using the charge-symmetry-breaking contribution to the one-boson exchange potential models and including both pseudoscalar and vector mesons, the charge asymmetric energy in $^3H-^3He$ nuclei is calculated. The result is $\Delta n = 0.04$ MeV. (auth)

5813 GROUP-THEORETICAL ANALYSIS OF β-DECAYS OF SOME $j = 3/2$ LIGHT NUCLEI. D'Andrea, A.; Scalia, M. (Univ., Rome). Nuovo Cim.; 69A: 702-11(21 Oct 1970).

A test of the generalized pairing-force model is performed by the analysis of β transitions between nuclear states classified through the I,R.'s of Sp_4 in the j-j scheme. The log ft theoretical values obtained in this way are compared with the experimental data: satisfactory results are found which seem to support the use of symplectic symmetry in the model. (auth)

5814 QUARTET STRUCTURE IN LIGHT NUCLEI. Danos, M.; Spicer, B. M. (Univ. of Melbourne). Z. Phys.; 237: 320-6(1970).

The nature of the low-lying even-parity, even-spin states of 4n nuclei is discussed in terms of the quartet scheme, and many of their properties can be given by it. These states are also the low-lying states important in the collective correlations model of the giant dipole resonance, and the quartet scheme thus provides a description of them. (auth)

5815 ANGULAR-MOMENTUM-PROJECTED HARTREE–FOCK THEORY. Faessler, Amand; Plastino, A. (Univ., Muenster, Ger.). Z. Phys.; 239: 73-82(1970).

The Euler Lagrange equations corresponding to the Hartree-Fock variational problem after angular momentum projection (PHF) are derived. The exact equations are simplified employing the Gaussian overlap approximation. The solution of the PHF equations in this approximation is seen to be not much more complicated than the solution of the normal HF problem. (auth)

5816 TRANSITION PROBABILITIES AND STATIC MOMENTS OF EXCITED STATES IN EVEN–EVEN NUCLEI. Speth, J. (Technische Univ., Munich). Z. Phys.; 239: 249-65(1970).

A new approach is made to calculate the generalized single-particle density matrix $p^{\mu\nu}$ in even-even nuclei. It is shown that this quantity is included in the three particle response function, for which a renormalized equation is derived. Taking into account in a consequent way the effective particle-hole interaction a formula is obtained for the static moment of excited states and the transition probability between such states which is essentially different from the usual RPA theory. (auth)

5817 HEAVY ION NUCLEAR PHYSICS. Hooton, B. W. (Atomic Energy Research Establishment, Harwell, Eng.). Phys. Bull. (London); 21: 389-92(Sep 1970).

The characteristics of heavy ion reactions are described. The associated Coulomb effects and their application to the measurement of static nuclear quadrupole moments are considered. The compound system formed by the fusion of two heavy ions is discussed and graphs given of cross section against energy in center of mass of elastic scattering of ^{16}O on ^{16}O for scattering angles from 49° to 90°. Momentum effects and their applications are considered and the production of the theoretically predicted stable superheavy elements discussed. Heavy ion accelerators, in particular the tandem accelerator and the cyclotron, are described. (UK)

5818 ANALYSIS OF THE LANE EQUATIONS FOR ISOBARIC ANALOG RESONANCES. Huefner, Joerg; Shakin, C. M. (Massachusetts Inst. of Tech., Cambridge). Contract AT(30-1)-2098. Ann. Phys. (N. Y.); 52: 486-506(May 1969). (MIT-2098-497; DSR-7796).

Lane's coupled equations are solved explicitly to give an exact S-matrix in the form of a one-level formula with a renormalized interaction. The renormalization is usually negligible or easily treated in perturbation theory. The unrenormalized one-level formula is shown to provide a very accurate representation of the exact S-matrix. The extraction of the resonance parameters from the one-level formula is studied in detail. The energy dependence of the open-channel propagator is important in the calculation of these parameters, and also leads to a difference between the background phase and the potential scattering phase. The role of the imaginary potential in the Lane equations is investigated and it is found that the absorptive potential may be treated in first-order perturbation theory. A relation between the S-matrix of the Lane equations and that of the microscopic theory is developed. (auth)

5819 KRUTOV MODEL FOR DEFORMED EVEN–EVEN NUCLEI. Varshni, Y. P.; Bose, S. (Univ. of Ottawa). J. Phys., A (London); 3: 524-32(Sep 1970).

Rotational energy levels of the ground state band of a number of deformed even–even nuclei have been calculated using the models proposed by Krutov in 1968 and by Davydov and Filippov in 1958. The parameters, occurring in these models, have been evaluated by two different methods. The results are compared with the experimental values and the relative merits of the models discussed. (auth) (UK)

5820 POLARIZATION EFFECTS IN BREMSSTRAHLUNG RADIATION OF ELECTRONS ON NUCLEI WITH A MAGNETIC DIPOLE MOMENT. Ablakulov, Kh. A. (Moscow State Univ.). Izv. Akad. Nauk Uzb. SSR, Ser. Fiz.-Mat. Nauk; No. 1, 69-74 (1970). (In Russian)

A study of the effect of the magnetic dipole of a nucleus with spin I on the bremsstrahlung radiation of unpolarized and longitudinally polarized electrons shows that the effect of the nuclear magnetic moment increases substantially at high energies and large transmitted momenta. Magnetic bremsstrahlung radiation as a result of magnetic scattering predominates with backward emission of photons at an angle of 180°. The process of bremsstrahlung radiation of arbitrarily polarized electrons is investigated in the field of an unpolarized nucleus having a magnetic dipole moment. Formulas are given for the degree of circularly

polarized bremsstrahlung radiation as a function of the state of polarization of the electron (longitudinally polarized electron, or transversely polarized electron). The degree of circularly polarized bremsstrahlung radiation is increased on taking into account the magnetic dipole moment of the nucleus. (TTT)

5821 APPROXIMATION OF GREEN'S FUNCTIONS. Beck, F.; Fuchssteiner, B. (Technische Hochschule, Darmstadt, Ger.). Z. Phys.; 239: 276-88(1970).

Special symmetries of the Green's functions of a non-relativistic many fermion-system and conservation laws, expressible by hermitian generators, are formulated as relations for a Green's function operator. Approximations for the Green's functions, defined as partial summations of the perturbation expansion, and consistent with the symmetries and conservation laws are presented. (auth)

5822 n-PARTICLE FRACTIONAL PARENTAGE COEFFICIENTS FOR ANTICOMMUTING CREATION OPERATORS. Quesne, C. (Univ. Nacional de Mexico, Mexico City). Rev. Mex. Fis.; 19: No. 1, 109-15(1970).

The general relation between the n-particle fractional parentage coefficients for anticommuting creation operators and the well-known fractional parentage coefficients for antisymmetric states is derived. (auth)

5823 DIRECT NUCLEAR REACTION THEORIES. Austern, Norman. Interscience Monographs and Texts in Physics and Astronomy. Volume XXV. New York: John Wiley and Sons, Inc. (1970). 399p. $19.95.

Chapters are included on wave packets, direct reactions, useful formulas, basic DI theories, applications of the DW method, coupled channels, high-energy wavefunction models, spectroscopic applications of stripping, polarizations and angular correlations, DW exchange and recoil effects, and unified and dispersion theories. (J.W.R.)

5824 CALCULATION OF BROAD THREE-NUCLEON RESONANCES FOR A SOFT-CORE TWO-NUCLEON POTENTIAL. Benoehr, H. C. (Univ. of Surrey, Guildford, Eng.). Nucl. Phys.; A149: 426-40(1970).

A model is constructed in order to investigate the resonance behavior of the three-nucleon system. For a simple soft-core two-nucleon potential it is found that broad resonances for the quantum numbers L, S, T = 1, $\frac{1}{2}$, $\frac{3}{2}$ and 1, $\frac{3}{2}$, $\frac{1}{2}$. The results for the T = $\frac{1}{2}$ states are in agreement with the phase shifts for the elastic nucleon–deuteron scattering. The predictions for the T = $\frac{3}{2}$ states support the experiments (and the interpretation put forward by the authors) of Ohlsen et al., and of Williams et al. (auth)

5825 HOW REALISTIC IS THE TABAKIN NUCLEON–NUCLEON POTENTIAL? Signell, Peter (Michigan State Univ., East Lansing). Phys. Rev., C; 2: 1171-3(Sep 1970).

It is shown that the Tabakin potential apparently predicts a deuteron quadrupole moment smaller than that previously assumed by a factor of 3. This discrepancy arises from the original use of an inaccurate formula relating the quadrupole moment of the deuteron to the threshold slope of the $^3S_1-^3D_1$ coupling parameter ϵ_1. The new value indicates a corresponding Tabakin tensor force that is considerably weaker than is required. Also, the small D-wave spin-orbit splitting given by the Tabakin potential at 142 MeV is different from the small experimental value. (auth)

5826 HIGHER-ORDER CORRECTIONS TO INTERNAL CONVERSION. Hager, R.; Seltzer, E. (California Inst. of Tech., Pasadena). Contract AT(04-3)-63. Phys. Rev., C; 2: 902-4 (Sep 1970).

Higher-order corrections to internal conversion and γ emission involving atomic electrons were calculated. Experimental anomalies in low-energy E2 L-subshell ratios are substantially explained by these calculations. (auth)

5827 NON-LOCAL POTENTIAL APPROACH IN THE RELATIVISTIC NUCLEON–NUCLEON SCATTERING. Eriksson, John R. (Aktiebolaget Atomenergi, Studsvik, Sweden). Nucl. Phys.; A149: 501-12(1970).

The momentum space factor m/E represents to a considerable extent the momentum dependence of the relativistic single-particle exchange amplitudes in the elastic N-N scattering. Starting from the non-locality derived from m/E, as proposed by Wong, a computationally feasible method of integrating the Schrödinger equation is given. A closed form of the nonlocality for the s-wave is discussed. (auth)

5828 THE j-DEPENDENCE OF POLARIZATION EFFECTS IN (d,p) STRIPPING PROCESSES. Goldfarb, L. J. B. (Univ. of Manchester, Eng.); Seyler, R. G. Nucl. Phys.; A149: 545-61 (1970).

An attempt is made to unravel the separate contributions from the spin-dependent deuteron and proton waves in deuteron stripping reactions as they are revealed by sets of polarization measurements. These polarization measurements involve in one case asymmetries owing to vector-polarized deuterons and, in the other case, proton polarizations associated with unpolarized deuterons. For a given l-value of the transferred neutron, the results differ according to the two j-values. Examination is restricted to small angles in the neighbourhood of the stripping peak where the j-dependence is most striking. Numerical calculations are made for the ^{40}Ca (d,p) and ^{90}Zr (d,p) reactions covering a range of deuteron energies from 5 to 15 MeV for s, p and d-wave neutron transfers. (auth)

5829 MULTIPLICITY OF STATES IN A SINGLE SHELL. Nomura, Masao (Tokyo Univ.). Nucl. Phys.; A150: 193-215 (1970).

Two methods are proposed to get the multiplicity of states with the total angular momentum J (L) in a j^n (l^n) configuration. One gives the multiplicity by means of a set of numbers specified by special algebraic relations. It is especially powerful for small values of J. The other method makes use of a special kind of sum rule about c.f.p. Some relations between multiplicities and Racah coefficients are derived. These two methods do not require any discussion of the z-component of angular momentum. (auth)

5830 TRINUCLEON CALCULATIONS WITH RANK-TWO SEPARABLE POTENTIALS. Brady, Thomas Joseph. Troy, N. Y.; Rensselaer Polytechnic Inst. (1969). 181p. University Microfilms Order No. 70-11,313.

Thesis.

The three-body Faddeev equations for the trinucleon binding energy, BE_3, and doublet scattering length, ^2a, are solved for a number of rank-two separable potentials. These potentials, some of which are due to Mongan, contain both attraction and repulsion and fit the phase parameters with varying degrees of accuracy. The phase shifts given by the Mongan potentials are in good agreement with experiment; however the percentage of D state, P_D, in the deuteron wave function, given by these potentials is quite small ($P_D \approx 1\%$). The potentials, which use forms first proposed by Tabakin, give higher P_D (2%,4%) but poorer fits to the phase shifts. The results span a range of BE_3 = 8.76 MeV, ^2a = 0.416 f to BE_3 = 10.16 MeV, ^2a = –0.377 f, these extremes being obtained with the Mongan potentials. Calculations indicate that the inclusion of repulsion in the singlet state lowers BE_3 by 0.5 to 1.5 MeV depending on the potential used, while repulsion in the triplet state subtracts a few tenths of a MeV from the binding energy. In an attempt to decide the validity of potentials such as Mongan's, which have small P_D, the sensitivity of the deuteron form factors to this parameter is investigated. These form factors are obtained from e-d elastic scattering. Using Yamaguchi-type one-term separable potentials with P_D = 1, 4 and 7%, it is found that the e-d scattering cross section is relatively insensitive to this parameter. In calculations with Mongan's potential it is found that, due to ignorance concerning the magnitude of meson exchange contributions, no definite decision can be made about Mongan's fits. Finally a method due to Hall and Post for obtaining lower bounds on the triton energy is examined. The bound is compared to the exact binding energy obtained from solution of the Faddeev equations for a wide variety of potentials, including purely central, central with hard core, spin-dependent central and noncentral potentials. The results indicate that the bound is of use in the cases where the potential is central but contains no hard core. For a hard core or noncentral potential, the bound lies so far from the exact answer as to be relatively valueless. (Diss. Abstr. Int., B)

5831 RECONSTRUCTION OF NN POTENTIALS FROM NUCLEAR DATA. Baz, A. I.; Gorbatov, A. M.; Demin, V. F.; Pasynkov, I. G. JETP Lett. (USSR) (Engl. Transl.): 12: 105-6(5 Aug 1970).

Translated from Zh. Eksp. Teor. Fiz., Pis'ma Red.; 12: 151-3(5 Aug 1970).

The parameters of the central NN potentials were determined from the binding energies and the radii of the nuclei ^{4}He, ^{16}O, ^{40}Ca, ^{92}Zr, ^{176}Yb, and ^{244}Pu. The calculation was made in the fundamental approximation of the K-harmonics method. The NN potentials in states with specified spin and isospin of the two nucleons were chosen in the form of a superposition of two Gaussian potentials. The problem of saturation of the nuclear force was considered by investigating the dependence of the binding energy and the nuclear radii of the potential $V_{3,3}$. This potential from the region of saturation of nuclear matter leads to a "disintegration" of the nuclei. (R.W.R.)

5832 CORRELATION BETWEEN THE INTENSITY OF THE SPECIFIC X RADIATION AND THE CHARGE OF THE NUCLEUS.

Trusov, V. F. (Latvian State Univ., Riga). Izv. Vyssh. Ucheb. Zaved., Fiz.; 13: 148-50(1970). (In Russian).

In the study of radiative electric-multipole transitions in the x-radiation range of the spectrum, especially in the case of heavy elements, the theory of relativity and the retardation effect must be taken into consideration. The electric-multipole transition probability is derived by calculating the oscillator forces corresponding to the $K \rightarrow L_{II}$ and $K \rightarrow L_{III}$ transitions of the K series. As the charge is increased, the Z effect of screening of the internal electrons decreases, becoming very small for heavy atoms. An analytical method is used for calculating the intensity relations of the x-radiation lines. By solving the Dirac equation under consideration of the finite dimensions of the nucleus, matrix elements and oscillator forces are derived; this determines the dependence of the relative intensity I_{α_2} on Z. Differences between theory and experimental results are probably due to spin–spin and spin–extraneous-orbit type interactions between electrons, and to radiative corrections. These complex effects can be evaluated only on a semiempirical basis. (TTT)

5833 TRINUCLEON FORM FACTORS CALCULATED FROM REALISTIC LOCAL POTENTIALS. Tjon, J. A. (State Univ. of New York, Stony Brook); Gibson, B. F.; O'Connell, J. S. Phys. Rev. Lett.; 25: 540-2(24 Aug 1970).

Charge and magnetic form factors are calculated using solutions of the three-nucleon Faddeev equations with the local two-nucleon potentials of Reid and of Malfliet and Tjon. The results give reasonable agreement with the data up to 9-fm^{-2} transfer, but do not reproduce the minimum at 11.8 fm^{-2} in the ^3He charge form factor. (auth)

5834 USE OF THE EIKONAL APPROXIMATION IN THE OPTICAL-MODEL CALCULATION. Simbel, M. H.; Abul-Magd, A. Y. (Cairo Univ., Giza, Egypt). Z. Phys.; 238: 321-8(1970).

Numerical calculations show that the eikonal approximation reproduces well the optical-model phase shifts for alpha-particle scattering by medium nuclei. The results are not so good for the differential cross sections; however, they are considerably improved by including the Coulomb effects. (auth)

5835 NUCLEAR-DENSITY DISTRIBUTION FOR NUCLEUS–NUCLEUS SCATTERING. Fliessbach, Torsten (Technische Hochschule, Munich). Z. Phys.; 238: 329-34(1970).

It is suggested that for nucleus–nucleus scattering there is no pronounced density compression in the overlap region, even at very high energies. (auth)

5836 ON THE THREE-ALPHA MODEL FOR ^{12}C. Zickendraht, W. (Univ., Marburg, Ger.). Z. Phys.; 238: 343-51(1970).

For the 3α model of ^{12}C two simple cases are discussed. In the first case a potential is introduced which has a strong minimum when the three α particles are at the corners of an equilateral triangle. Only small vibrations around this equilibrium position are allowed. This model does not give the desired level sequence. In the second case this potential is dropped and one finds surprisingly good agreement with the experimental level sequence. (auth)

5837 BAHCALL CORRECTIONS TO ELECTRON CAPTURE AND THE HARTREE–FOCK REARRANGEMENT. Faessler, Amand; Huster, E.; Krafft, O.; Krahn, F. (Univ., Muenster, Ger.). Z. Phys.; 238: 352-9(1970).

The Bahcall correction factors $X^{L/K}$ and $X^{M/L}$ for L/K and M/L electron capture ratio respectively are calculated including the Hartree–Fock (HF) rearrangement. The rearrangement takes into account that the atom after the electron capture is not in the HF ground state. The selfconsistent single-electron orbits for the excited states with a hole in the K, L, or M shell are calculated using the Herman-Skillman and the Froese HF codes. The rearrangement changes the correction factor in the right direction, but the reduction is too small. Only for very light atoms is the alteration larger than 1%, and, therefore, it is in general smaller than the present experimental errors. (auth)

5838 CONSTRUCTION OF TRIAL FUNCTIONS FOR NUCLEAR GROUND-STATE PROBLEMS. Mueller, Dieter (Technische Univ., Hanover). Z. Phys.; 238: 379-88(1970).

Variational calculations yield upper bounds on the ground-state energy which often become approximately stationary when the flexibility of the trial function is increased. It is shown that this apparent convergence is no safe criterion for a good approximation of the ground-state energy E_0. To avoid this uncertainty it is proposed to expand the trial function with respect to the function basis $\{H^{\nu} \cdot \varphi_0\}$ where φ_0 is a suitable zeroth order approximation of the wave function. The application of this method to a three-particle system with the central potential of Baker et al., yields an upper bound $\bar{E}_0 = -12.3$ MeV, which is lower than the upper bounds published so far except that obtained by Appel. The computational effort is very small. (auth)

5839 EFFECTIVE CHARGE FACTOR FOR THE RADIATIVE CAPTURE OF FAST NUCLEONS. Zimanyi, J.; Halpern, I.; Madsen, V. A. (Univ. of Copenhagen). Phys. Lett.; 33B: 205-7(12 Oct 1970).

The effective charge factor for E1 capture of fast nucleons is found to depend significantly on the single-particle state into which the nucleon is captured. This fact helps explain discrepancies between theory and experiment which were found using the customary state-independent form for the effective charge factor. (auth)

5840 T_2^3 TERM IN THE ISOBARIC MULTIPLET EQUATION. Bertsch, G.; Kahana, S. (Brookhaven National Lab., Upton, N. Y.). Phys. Lett.; 33B: 193-4(12 Oct 1970).

A perturbation theory estimate of a three-body term involving either the Coulomb or a mixture of Coulomb and charge-dependent forces is made in the j-coupled shell model. An effect of the order of 1 keV is found for the T_2^3 coefficient, consistent with all experimentally known multiplets except possibly that for mass 9. (auth)

5841 POTENTIALS FOR FAST AND SLOW HEAVY-ION-COLLISIONS WITHIN THE TWO CENTER SHELL MODEL. Pruess, K. (Univ., Frankfurt am Main); Greiner, W. Phys. Lett.; 33B: 197-202(12 Oct 1970).

Fast and slow collisions are the two limiting cases for ion–ion interactions. They are formulated and discussed within the two-center shell model. Calculations of the real part of the potential are performed for some typical cases. The imaginary part of the potential is also formulated in this framework. (auth)

5842 NUCLEAR REACTIONS. Jackson, D. F. London, Methuen and Company, Ltd, (1970). 270p. 65s.

Subjects discussed are: nuclear models, basic scattering theory, electromagnetic interactions, the compound nucleus, the optical model, direct inelastic scattering, strong absorption, transfer and knock-out reactions, and high energy nuclear reactions. (UK)

5843 HARMONIC OSCILLATOR IN PROLATE SPHEROIDAL COORDINATES. I. COULOMB INTERACTION OF AN OSCILLATOR PROTON WITH AN EXTERIOR CHARGE. Demeur, M. (Univ. Libre, Brussels); Reidemeister, G. Bull. Cl. Sci., Acad. Roy. Belg.; 56: 190-213(1970).

The three dimensional harmonic oscillator was quantized in prolate spheroidal coordinates using the properties of the constants of the motion. The Coulomb interaction of an oscillator proton with an exterior charge was investigated by means of both a first-order perturbation calculation and the variational method. The same problem modified by the presence of a spin-orbit interaction was emphasized. Comparison with other works related to the subject was made. (auth)

5844 HIGHER APPROXIMATION EFFECTS IN INTERNAL CONVERSION PROCESSES. Krutov, V. A.; Knyazkov, O. M. Ann. Phys. (Leipzig); 25: 10-23(1970).

A theoretical study of the higher approximation effects in the processes of one-conversion de-excitation of the excited nuclear state was carried out for the system: nucleus plus electronic shell. The processes of de-excitation over intermediate electron-nucleus states (the so-called "electron-nucleus bridge", being referred to as ENB in what follows) are considered in detail. The optimal conditions for ENB effect manifestation are discussed, numerical estimates being carried out in some cases. One-conversion nuclear de-excitation associated with MO-transition, strictly forbidden in the usual approximation, is a striking example of ENB. Such de-excitation probability proves to be rather large (for example, it equals $2 \cdot 10^4$ sec^{-1} for Z = 50 and for the transition energy 1 MeV, when the single-particle model is used). (auth)

5845 APPROXIMATE NUCLEAR WAVE FUNCTION. Lee, Kiuck (Marquette Univ., Milwaukee); Kim, Chunghum. J. Korean Phys. Soc.; 3: 21-5(Mar 1970).

An approximation to the pair correlation amplitude $f_{\alpha\beta}(ij)$ is obtained by using the Lennard-Jones method of approximation. It is employed in the A-nucleon wave function, and the expectation value of the total Hamiltonian is calculated. It is then found that $2 < \sum_{i<j} f_{\alpha i \alpha j}(ij) > \simeq \lambda$, which is an adjustable constant. (auth)

5846 AVERAGE PARTICLE ENERGY IN BETA DECAY. Dillman, L. T. (Oak Ridge National Lab., Tenn.). Health Phys.; 19: 385-9(Sep 1970).

Theoretical methods which may be employed to compute as accurately as possible the ratio of the average kinetic energy

XUM

to the end-point kinetic energy for β^+ or β^- spectra of varying classifications of forbiddenness are discussed. Graphs of this ratio as a function of end-point kinetic energy for 11 different atomic numbers and for allowed, unique first-forbidden and unique second-forbidden β^+ and β^- transitions are presented. Results for any energy and any atomic number may be obtained by interpolation. (auth) (UK)

5847 NATURE OF NUCLEAR WAVE FUNCTIONS. Gillet, Vincent (CEN de Saclay, Gif-sur-Yvette, France). Ann. Phys. (Paris); 4: 561-78(Sep-Oct 1969). (In French).

A few current problems of the microscopic theory of nuclear structure are presented to illustrate the main mechanisms (average field, pairing, and alignment) which govern interacting nucleon systems. The material concerns the deviation of nuclear ground states from the Hartree–Fock approximation; the inverse-gap-equation method for the analysis of the spectra of odd-even superconducting nuclei; the effects of core polarization on vibrational transitions; and, finally, the description of rotational spectra in the stretch scheme. (auth)

5848 TIME-DEPENDENT BEHAVIOR OF A CLASSICAL MODEL FOR REACTIONS INVOLVING ISOBARIC ANALOG STATES. Mello, P. A.; Moshinsky, M. (Univ. Nacional de Mexico, Mexico City). Rev. Mex. Fis.; 19: 157-77(1970).

The time-dependent behavior of a classical model for two-channel reactions involving isobaric analog states is studied. It is first shown that the poles of the S-matrix for the classical system are excluded from the upper half of the first Riemann sheet of the wave-number plane. The influence of the S-matrix poles in a time-dependent description of the problems is investigated. It is found that the poles in the first Riemann sheet give the usual exponentially decaying response in time (resonance effect), plus a "diffraction in time" effect, consisting of terms that also go to zero as $t \to \infty$, but as an inverse power of t. On the other hand, the poles in the second Riemann sheet give rise only to "diffraction in time" effects. It is made plausible, although it is not proved, that in the corresponding quantum-mechanical problem, only the poles in the lower half of the first sheet that are in the fourth quadrant above the bisector at $7\pi/4$ behave as resonance states. (auth)

5849 VARIATIONAL ANALYSIS WITH HARMONIC-OSCILLATOR STATES FOR SQUARE POTENTIALS. Aguilera-Navarro, V. C.; Mendez V., R. M. (Univ. Nacional de Mexico, Mexico City). Rev. Mex. Fis.; 19: 119-32(1970).

A variational analysis for the square-well potential problem with a repulsive soft core using harmonic-oscillator trial wave functions is discussed. The core has a relatively small effect on the approximation except when its radius compares with that of the well. The dependence of the approximation on the number of quanta and the frequency of the oscillator is also discussed. (auth)

5850 NEAR-BARRIER FISSION INDUCED WITH PHOTONS AND NEUTRONS. Huizenga, John R. (Univ. of Rochester, N. Y.). Trans. Amer. Nucl. Soc.; 13: 707(Nov 1970).

From Meeting of the American Nuclear Society, Washington, D. C. See CONF-701102.

5851 THEORY OF DELAYED-NEUTRON PHYSICS. Tomlinson, L. (Atomic Energy Research Establishment, Harwell, Eng.). Trans. Amer. Nucl. Soc.; 13: 707-9(Nov 1970).

From Meeting of the American Nuclear Society, Washington, D. C. See CONF-701102.

5852 OFF-SHELL BEHAVIOUR OF PHASE-SHIFT EQUIVALENT MOMENTUM-DEPENDENT POTENTIALS. Srivastava, M. K. (McMaster Univ., Hamilton, Ont.). Nucl. Phys.; A157: 61-72(1970).

Families of momentum-dependent potentials, phase-shift equivalent to the Hamada–Johnston potential and to the separable potential of Mongan, are obtained. Their off-shell behavior is investigated. It is found that wide variations in the off-shell matrix elements can be produced, though, qualitatively, the general trend remains similar to that of a local potential. It is pointed out that an additional contribution of ≈1 MeV in the binding energy per particle in nuclear matter can be obtained without any decrease in the "wound" integral. (auth)

5853 PROTON–NEUTRON CORRELATIONS IN MEDIUM AND HEAVY NUCLEI. Akhiezer, I. A.; Barts, B. I.; Bolotin, Yu. L. (Kharkov State Univ.). JETP Lett. (USSR) (Engl. Transl.); 11: 385-7(5 Jun 1970).

Translated from Zh. Eksp. Teor. Fiz., Pis'ma Red.; 11: 557-9 (5 Jun 1970).

It has been proposed that the densities and, hence, the chemical potentials of the proton and neutron distributions in nuclei are equal; whether or not this is true should strongly influence certain conclusions of the superconducting model of the nucleus. A possible proton–neutron (pn) pairing is considered, in which the interaction encompasses pairs of nucleons in the state with S = 1 and T = 0 (quasideuteron). It is shown that such a pairing alters appreciably (contrasted with the usual pp and nn pairing) the isotropic structure of the correlation functions of the nucleons in the nucleus, and that the scattering cross section has an essentially different character from that predicted by the two-fluid pairing model. (R.W.R.)

5854 OPTICAL MODEL POTENTIAL FOR DEUTERONS. Bauer, M.; Bloch, C. (Univ. de Mexico, Mexico City). Phys. Lett.; 33B: 155-7(28 Sep 1970).

It is shown that, in deuteron scattering, the interactions of the neutron and the proton with the nucleus are given by the corresponding optical potentials evaluated at an energy depending on the scattering angle and ranging between half and twice the deuteron energy. (auth)

5855 INVESTIGATION OF THE ALPHA-PARTICLE MODEL FOR LIGHT NUCLEI. Brink, D. M. (Oxford Univ.); Friedrich, H.; Weiguny, A.; Wong, C. W. Phys. Lett.; 33B: 143-6(28 Sep 1970).

The alpha-particle model of Margenau and Bloch and Brink is used to study the ground-state properties, the relative energies of different alpha configurations, and configuration mixing of light 4N nuclei from ^{12}C to ^{28}Si. (auth)

5856 ODD-EVEN STAGGERING OF NUCLEAR RADII. Reehal, Balbir Singh. Pittsburgh; Carnegie-Mellon Univ. (1970). 114p. University Microfilms Order No. 70-9995.

Thesis.

The odd–even staggering of nuclear radii, as observed in the isotope shifts of atomic and mu-atomic spectra, is calculated using the pairing-plus-quadrupole model. The effect is explained on the basis that the mean square deformation β^2 associated with zero-point motion of quadrupole vibrations is greater for even than for odd nuclei. The radius change is related to a change in β^2 by using the incompressible fluid model. The theoretical value of $\Delta\beta^2$ is obtained by computing $\langle Q^2 \rangle$ for even and for odd nuclei. For the even wave functions the BCS vacuum of the pairing force is used, with ground-state correlations admixed in perturbation theory by the qudrupole force with the Tamm–Dancoff phonons; and for the odd wave function a one quasi-particle state is used as intermediate states with ground state correlation admixtures properly blocked by the odd quasi-particle plus one quasi-particle coupled to one phonon. Near the end of the shell, instead of BCS, a one- and two-particle calculation is done. In addition, B(E2) transitions for odd mass nuclei are calculated by using the Kisslinger–Sorensen model for odd nuclei and including contributions up to two phonons. Odd–even mass differences are also calculated, with the effects of the quadrupole force taken into account. The model seems to explain the staggering effect in most cases. The agreement with experiment for B(E2) transitions and odd–even mass differences is good except for nuclei which may be considered nearly deformed. (auth) (Diss. Abstr. Int., B)

5857 SHELLS IN A SIMPLE ANISOTROPIC HARMONIC OSCILLATOR. Wong, C. Y. (Oak Ridge National Lab., Tenn.). Phys. Lett.; 32B: 668-71(14 Sep 1970).

In a simple anisotropic harmonic-oscillator model, shells are located at those deformations for which the axes of the equipotential surfaces are reciprocally commensurate. (auth)

5858 FADDEEV EQUATIONS AND CLUSTER MODEL APPROXIMATIONS. Osman, A. (Cairo Univ.). Lett. Nuovo Cim.; 4: 817-18(31 Oct 1970).

A cluster expansion is developed that uses the generalized Faddeev equations for the multiparticle scattering problem. An expression for the function M(D(S)) is derived, and it is demonstrated how approximating M(D(S)) by its poles presents a solvable model for interacting several-particle systems by cluster deformation. (R.W.R.)

5859 APPLICATION OF THE HARTREE–FOCK METHOD IN NUCLEAR THEORY. Zofka, J. (Nuclear Research Inst., Rez, Czech.). Czech. J. Phys.; 20: 926-38(1970).

A review of the Hartree–Fock (HF) self-consistent method as used in nuclear theory is presented. After deriving the fundamental HF equations the two-particle potentials for HF calculations are shown, and the particular HF methods are described. In addition, the results of some papers on HF methods are reproduced and discussed. (auth)

5860 INVESTIGATION OF EQUILIBRIUM β_{20} AND β_{40} DEFORMATIONS OF RARE-EARTH AND TRANSURANIUM NUCLEI AND DEPENDENCES OF ONE-PARTICLE PROPERTIES ON THE DEFORMATION PARAMETERS. Gareev, F. A.; Ivanova, S. P.; Pashkevich, V. V. (Joint Inst. for Nuclear Research, Dubna, USSR). Yadern. Fiz.; 11: 1200-12(Jun 1970). (In Russian).

Equilibrium values of the deformation parameters β_{20} and β_{40} are calculated for nuclei in rare-earth and transuranium regions using the level scheme for the Saxon–Woods potential. The values are shown to be nonzero. Effect of β_{40} on properties of one-particle states in deformed nuclei is studied. (auth)

5861 OPTICAL POTENTIAL FOR HIGH-ENERGY SCATTERING. Petkov, I. Zh. (Joint Inst. for Nuclear Research, Dubna, USSR). Teor. Mat. Fiz.; 4: 216-21(Aug 1970). (In Russian).

In the high-energy approximation the formula for the optical potential is derived in terms of the effective coupling potentials between elastic and inelastic channels. The coupling potentials define approximately the two-particle nuclear correlation function. It is shown that taking account of the effective nuclear excitation energy can lead to the partial filling of diffraction minima of electron elastic scattering by nuclei. (auth)

5862 DEPENDENCE OF NUCLEAR MATTER BINDING ENERGY ON THE HIGH ENERGY PHASE SHIFTS. Srivastava, M. K. (Univ. of Roorkee, India). Phys. Lett.; 33B: 341-2(9 Nov 1970).

The dependence of the binding energy per particle in nuclear matter on the phase shifts beyond 350 MeV lab is investigated. Second-rank separable potentials are used. It is found that the results are rather insensitive to the form of the phase shifts in the high-energy region. (auth)

5863 NON-CENTRAL FORCES IN LOW ENERGY NUCLEAR PHYSICS. Pask, C. (Univ. of New South Wales, Kensington, Australia). Phys. Lett.; 33B: 325-6(9 Nov 1970).

The importance of noncentral forces in low-energy nuclear physics is discussed with particular reference to calculations of the properties of three-nucleon systems. (auth)

5864 $K\alpha_1$ X-RAY ISOTOPIC SHIFT FOR $^{140}Ce-^{142}Ce$ AND THE DIFFERENCES IN NUCLEAR CHARGE RADII OF Ce ISOTOPES. Van Eijk, C. W. E.; Visscher, M. J. C. (University of Tech., Delft, Netherlands). Phys. Lett.; 33B: 349-50(9 Nov 1970).

The volume isotopic shift of the $K\alpha_1$ X rays was measured for $^{140}Ce-^{142}Ce$. From the result, $\Delta E_V = 51.4 \pm 1.9$ MeV, the difference in the mean square nuclear charge radii was derived: $\Delta\langle r^2\rangle = 0.274 \pm 0.010$ fm^2. By using this value to normalize optical isotopic shift data, the differences in the charge radii of all stable Ce isotopes are obtained. (auth)

5865 ALPHA-CLUSTER MODEL CALCULATION OF ^{12}C. Yukawa, T.; Yoshida, S. (Rutgers–The State Univ., New Brunswick, N. J.). Phys. Lett.; 33B: 334-6(9 Nov 1970).

Energy expectation values of ^{12}C are calculated using Brink's formalism of the α-cluster model. The results suggest that a molecular-like structure is favorable for the low-lying states of ^{12}C. (auth)

5866 DYNAMIC NUCLEAR EFFECTS IN PIONIC AND KAONIC ATOMS. Haff, P. K.; Eisenberg, J. M. (Univ. of Virginia, Charlottesville). Phys. Lett.; 33B: 133-6(28 Sep 1970).

Corrections are calculated to absorption widths in pionic and kaonic atoms due to the admixture of excited nuclear states. Effects as large as 12% and 27% are indicated for pionic and kaonic atoms, respectively. (auth)

5867 ON THE RELATION BETWEEN HARD-CORE AND VELOCITY-DEPENDENT POTENTIALS. AN APPLICATION TO THE PHOTONUCLEAR SUM RULES. Finkler, P. (Univ. of Nebraska, Lincoln); Valk, H. S. Z. Phys.; 236: 144-52(1970).

A canonical transformation relating hard-core and velocity-dependent nucleon–nucleon potentials is applied to the Srivastava potential, and an equivalent hard-core potential is found. It is shown that the deuteron photonuclear electric-dipole integrated and bremsstrahlung-weighted cross sections resulting from the two equivalent potentials are essentially the same. The reasons for this agreement suggest that differences between the two sets of cross sections may remain small in other nuclei employing this type of potential. (auth)

5868 ACCURATE GRAPHICAL METHODS FOR THE ANALYSIS OF ASYMMETRIC BREIT–WIGNER RESONANCES IN NUCLEAR REACTIONS. Seitz, H. (Univ. of Texas, Austin). Nucl. Instrum. Methods; 86: 157-61(1970).

A formula for Breit–Wigner resonances in excitation functions of nuclear reactions is derived for the general case that the scattering amplitudes contain nonresonant parts. This formula is used to develop graphical methods, which lead to accurate resonance parameters. The importance of these methods lies in their simplicity and generality. (auth)

5869 FAITHFUL AND PSEUDO-BOUND THEORIES FOR STRIPPING TO UNBOUND LEVELS. Huby, R. (Univ. of Liverpool). Phys. Lett.; 33B: 323-4(9 Nov 1970).

A well-founded, or faithful, theory of stripping to unbound levels, based on Weinberg quasiparticles, is described; and it is shown to lend to a simpler, pseudo-bound, approximation. (auth)

5870 EXAMPLES OF A UNIFIED NUCLEAR REACTION THEORY. Federsel, H.; Kanellopoulos, E.-J.; Suenkel, W.; Wildermuth, K. (Univ., Tuebingen, Ger.). Phys. Lett.; 33B: 140-2 (28 Sep 1970).

As examples for a new treatment of nuclear reactions in the frame of a unified theory, elastic $\alpha-n$ and $\alpha-\alpha$ scattering is calculated by a method in which one splits the wave function of the nucleus into an internal and external part. The results are compared with the corresponding resonating-group calculations. (auth)

5871 YAMAGUCHI'S DEUTERON WAVE FUNCTION. Burnap, C.; Levinger, J. S.; Siebert, B. (Rensselaer Polytechnic Inst., Troy, N. Y.). Phys. Lett.; 33B: 337-40(9 Nov 1970).

Yamaguchi's separable tensor potential generates a deuteron wave function, which substituted in the Schrödinger equation gives an equivalent local potential. This potential disagrees badly with OPEP for low percentage D-state (less than 2%), but not so seriously for higher percentage. (auth)

5872 THREE-BODY MODEL FOR THE ISOBARIC ANALOG RESONANCE ON EVEN–ODD TARGET. Beregi, P.; Lovas, I. (Central Research Inst. for Physics, Budapest). Phys. Lett.; 33B: 150-2(28 Sep 1970).

A generalization of the Lane model is proposed for the description of reactions involving the excitation of the isobaric analog state. The model, formulated in the framework of Faddeev's theory, takes into account explicitly the degrees of freedom of the last odd neutron of the target. (auth)

5873 COMPARISON BETWEEN HARTREE–FOCK AND THOMAS–FERMI CALCULATIONS USING EFFECTIVE INTERACTIONS. Lombard, R. J. (Institut de Physique Nucleaire, Orsay, France). Phys. Lett.; 32B: 652-5(14 Sep 1970).

Comparisons are made between Hartree–Fock theory and the energy-density formalism in the case of finite nuclei, using two simple interactions. As far as the bulk properties of nuclei are concerned, the two approaches yield similar results. The energy-density formalism has a tendency to yield densities with tails shorter than the Hartree–Fock, a feature which seems bound to the Thomas–Fermi approximation. (auth)

5874 GAMMA–GAMMA ANGULAR CORRELATIONS: A MODEL FOR STATISTICAL PERTURBATION WITH ANY CORRELATION TIME. Scherer, C. (Univ. Federal do Rio Grande do Sul, Porto Alegre, Brazil). Nucl. Phys.; A157: 81-92(1970).

The differential form of the perturbed angular correlation is studied for a gas model. An expression for $W(\theta,t)$ is obtained, which is also valid for the case where the correlation time τ_c is of the order of the time interval t between the two radiations. In the limits $\tau_c \to \infty$ and $\tau_c \ll t$ the known results are recovered. Some numerical results are given. (auth)

5875 PARITY AND TIME REVERSAL INVARIANCE AND THE M-MATRIX. Berovic, N. (Univ. of Birmingham, Eng.). Nucl. Phys.; A157: 106-12(1970).

Parity and time reversal conditions are derived for M-matrix elements in a manner applicable to any choice of coordinate axes. (auth)

5876 OCCUPANCY OF SPHERICAL SHELLS IN THE GROUND STATE OF EVEN 2s-1d SHELL NUCLEI. Castel, B. (Queen's Univ., Kingston, Can.); Johnstone, I. P.; Singh, B. P.; Parikh, J. C. Nucl. Phys.; A157: 137-44(1970).

A projected Hartree–Fock calculation is carried out to estimate the occupation probabilities in ground states of even sd shell nuclei. A direct comparison with experimental occupation numbers is made possible by using French's sum rules. The calculated occupation numbers are also used to calculate the matrix element $\langle g.s.|\vec{l}\cdot\vec{s}|g.s.\rangle$ and the results compared with other models as well as with experimental estimates. (auth)

5877 COULOMB MIXING OF ISOSPIN STATES. II. NUCLEON–NUCLEON POTENTIALS AND THE CENTROID ENERGY FOR COULOMB MIXING. Mekjian, Z. (Rutgers–The State Univ., New Brunswick, N. J.). Nucl. Phys.; A157: 32-48(1970).

The average or centroid energy of the states into which an analog

state mixes via the charge dependent Coulomb force is calculated. The calculation is based on the minimal assumption of the constancy of the density of nuclear matter inside a sphere. With this assumption, the kinetic and potential energy contributions to this average energy are given. The kinetic contribution is a multiple of the uncertainty energy of a nucleon confined to this sphere. The average potential energy term is shown to involve the fluctuations, propagated by the nuclear force, in the Coulomb field at a point. The potential energy is then calculated for the phenomenological Hamada–Johnston force for both central and tensor components. The contribution to this energy from a one-pion-exchange potential and from one-boson-exchange potentials are also discussed. The average potential energy of the states coupled to the analog is found to be much smaller than the average kinetic energy in these states. The reasons for the small potential contribution are discussed in detail. (auth)

REACTOR TECHNOLOGY

Commercial Power Reactors

Refer also to abstracts 4088, 4201, 4775, and 4779.

5878 (UCRL-Trans-10495) ATOMIC POWER PLANTS. A Survey Based on Papers Presented at the 7th World Energy Conference in 1968. Feynberg, S. M. Translated for Univ. of California, Lawrence Radiation Lab., Livermore, from Izv. Akad. Nauk SSSR, Energ. Transp.; No. 1, 3-31(Jan-Feb 1969). 89p. Dep. NTIS.

Reviewed briefly are the basic achievements in the technology and economics of atomic power plants with "traditional" thermal-neutron reactors. Development rates of the atomic-power industry are analyzed in connection with the problem of ensuring adequate supplies of uranium raw material. Geological estimates of cheap uranium–ore reserves are measured against atomic-power requirements, it being assumed that the latter will rapidly increase. It is shown that difficulties in obtaining cheap uranium will not be encountered before the start of the next century. Discussed, too, is the problem of building advanced thermal reactors, i.e., convertors running on thorium. It is pointed out that the demand for natural uranium can be sharply reduced without loss of economic efficiency. An analysis is made of the theoretical bases of the process of expanded conversion of nuclear fuel in fast- and thermal-neutron breeder reactors. The prospective competitiveness of "fast" breeders is compared with that of "thermal" breeders. It is suggested that "thermal" breeders and convertors may prove an efficient alternative to "fast" breeders, and over the next fifty years may reduce the demand for natural uranium even more than the latter. Also discussed in the problem of finding the best combination of reactors of different types, and new methods of producing nuclear fuel are cited: the electronuclear method, thermonuclear-blast method, and thermonuclear fusion in hot plasma. (24 references) (auth)

5879 PROSPECTS OF AUTOMATION IN THE CONTROL OF NUCLEAR POWER PLANTS. Costantin, P.; Parthier, S.; Schuster, W. (AEG-Telefunken, Frankfurt am Main). Neue Tech., B; 12: 12-16(1970). (In German).

Starting in 1975, automation of a nuclear power station will consist of the following: a free programmed double computer system that automatically handles total information flux and controls processes and subordinate small computers belonging to special functioning groups; a deficiency-free, solidly wired, control of functional groups connecting computer and control console which automatically locates and indicates malfunctions; a small control panel with TV screens, printout machines, and emergency control console; and a time sharing terminal of a computer center for off-line problems. With independent priority, reactor safety will be retained as a solidly wired redundant system. (tr-auth)

5880 STATE OF SUPPLY OF THE COMMUNITY WITH NUCLEAR FUELS. Oboussier, F. Neue Tech., B; 10: 232-6 (1968). (In German).

The commission of the European atomic community conservatively estimates nuclear stations with a total power of 40,000 MW(e) on January 1, 1980; the probable total power may be closer to 60,000 MW(e). Nuclear installations will require 90,000 tons of U between 1970 and 1980. Proven reserves in the European community cover only one third of the total amount; therefore, the community depends on international supply, especially from the USA and Canada. With respect to enrichment, France serves only military projects, Britain is very limited, and the community depends almost entirely on the USA. Since the future and availability of the American gaseous diffusion plants are uncertain, the development of separation installations is under consideration. Presently existing supply agreements and their legal aspects between the USA and the European community are discussed in detail. (H.B.G.)

5881 OCEAN NUCLEAR INDUSTRIAL COMPLEX. Yoda, Yoichi (Nippon Steel Corp., Tokyo). Genshiryoku Kogyo; 16: No. 6, 4-9(Jun 1970). (In Japanese).

The proposed plan for a nuclear power station located at sea with an industrial complex formed around it is described. With the tremendous advance in GNP in Japan, the sites of industries, including nuclear power generation, must be sought in the coastal ocean. The advance in industries and problems related to the rapid growth, including the problem of sites, in Japan, are reviewed. The conceptions of an ocean-based nuclear energy industrial complex are presented. (Japan)

5882 RADWASTE DESIGN FOR NO PLANT-ORIGINATED RADIOACTIVE LIQUID DISCHARGE. Wilson, Robert L.; (Sacramento Municipal Utility District, Calif.); Lee, Jay Y.; Stiens, Robert. Trans. Amer. Nucl. Soc.; 13: 485-6(Nov 1970).
From Meeting of the American Nuclear Society, Washington, D. C. See CONF-701102.

5883 MATERIALS SELECTED FOR THE FORT ST. VRAIN PRESTRESSED CONCRETE REACTOR VESSEL. Hildebrand, J. F.; Hedgecock, P. D.; Watson, J. F.; Hull, L. J. (Gulf General Atomic, Inc., San Diego, Calif.). Trans. Amer. Nucl. Soc.; 13: 588(Nov 1970).
From Meeting of the American Nuclear Society, Washington, D. C. See CONF-701102.

5884 COMMERCIAL POWER GENERATION FROM HTGR NUCLEAR STEAM SYSTEMS. Bernier, R. G.; Goodjohn, A. J. (Gulf General Atomic, Inc., San Diego, Calif.). Trans. Amer. Nucl. Soc.; 13: 772(Nov 1970).
From Meeting of the American Nuclear Society, Washington, D. C. See CONF-701102.

5885 EVOLUTIONARY TRENDS IN BWR PRIMARY SYSTEM AND CONTAINMENT DESIGNS. Roy, G. M.; Jones, C. R. (General Electric Co., Sunnyvale, Calif.). Trans. Amer. Nucl. Soc.; 13: 772-3(Nov 1970).
From Meeting of the American Nuclear Society, Washington, D. C. See CONF-701102.

5886 WASTE HEAT AND FOG CONTROL. Conn, Robert (Brookhaven National Lab., Upton, N. Y.); Papay, Lawrence. Trans. Amer. Nucl. Soc.; 13: 782-3(Nov 1970).
From Meeting of the American Nuclear Society, Washington, D. C. See CONF-701102.

5887 TRAINING OF PERSONNEL TO OPERATE THE MILLSTONE POINT COMPANY NUCLEAR BOILING WATER REACTOR POWER PLANT. Council, W. (Northeast Utilities, Wethersfield, Conn.). Trans. Amer. Nucl. Soc.; 13: 803(Nov 1970).
From Meeting of the American Nuclear Society, Washington, D. C. See CONF-701102.

5888 SHIELDING THE FORT ST. VRAIN HTGR. Finch, William C. (Gulf General Atomic, Inc., San Diego, Calif.). Trans. Amer. Nucl. Soc.; 13: 871(Nov 1970).
From Meeting of the American Nuclear Society, Washington, D. C. See CONF-701102.

5889 INTEGRATING SHIELD DESIGN AND THE NUCLEAR REACTOR PLANT. Reed, H. F. (Sargent and Lundy Engineers, Chicago). Trans. Amer. Nucl. Soc.; 13: 871-2(Nov 1970).
From Meeting of the American Nuclear Society, Washington, D. C. See CONF-701102.

Operation and Economics

Refer also to abstract 6143.

5890 (DOCKET-50010-71) DRESDEN NUCLEAR POWER STATION, UNIT 1. Failure of North Emergency Condenser Condensate Valve. (Commonwealth Edison Co., Chicago, Ill.). 4 Dec 1970. 1p. Dep. NTIS.

5891 (DOCKET-50133-43) HUMBOLDT BAY POWER PLANT, UNIT NO. 3. Operation with Less Than Normal Off Site Power for More Than Twelve Hours. (Pacific Gas and Electric Co., San Francisco, Calif.). 28 Nov 1970. 2p. Dep. NTIS.

5892 (DOCKET-50155-53) BIG ROCK POINT NUCLEAR PLANT. Release of Noble Gases to Discharge Canal. (Consumers Power Co., Jackson, Mich.). 1 Dec 1970. 4p. Dep. NTIS.

5893 (DOCKET-50237-110) DRESDEN NUCLEAR POWER STATION, UNIT 2. Abnormal Occurrence Report: Turbine Trip and Reactor Scram. (Commonwealth Edison Co., Chicago, Ill.). 15 Jun 1970. 2p. Dep. NTIS.

5894 (DOCKET-50237-111) DRESDEN NUCLEAR POWER STATION, UNIT 2. Control Rod Drives in Excess of 7.00 Second Maximum Insertion Time. (Commonwealth Edison Co., Chicago, Ill.). 27 Nov 1970. 2p. Dep. NTIS.

5895 TRAINING OF PERSONNEL TO OPERATE THE MILLSTONE POINT COMPANY NUCLEAR BOILING WATER REACTOR POWER PLANT. Anderson, James L. (General Electric Co.,

XUM

Morris, Ill.); Counsil, William G. Trans. Amer. Nucl. Soc.; 13: 456(Nov 1970).
From Meeting of the American Nuclear Society, Washington, D. C. See CONF-701102.

5896 SCHEDULING GENERATION ON SYSTEMS WITH FOSSIL AND NUCLEAR UNITS. Kiefer, W. M.; Koncel, E. F. (Commonwealth Edison Co., Chicago). Trans. Amer. Nucl. Soc.; 13: 768(Nov 1970).
From Meeting of the American Nuclear Society, Washington, D. C. See CONF-701102.

5897 POWER SYSTEMS OPTIMIZATION APPROACH TO NUCLEAR FUEL MANAGEMENT. Hoskins, R. E. (Tennessee Valley Authority, Chattanooga); Rees, F. J. Trans. Amer. Nucl. Soc.; 13: 768-70(Nov 1970).
From Meeting of the American Nuclear Society, Washington, D. C. See CONF-701102.

5898 COMPUTERIZED MODEL OF THE NUCLEAR SECTOR OF AN ELECTRICITY GENERATING SYSTEM. Iliffe, C. E. (United Kingdom Atomic Energy Authority, Risley, Eng.). Trans. Amer. Nucl. Soc.; 13: 770(Nov 1970).
From Meeting of the American Nuclear Society, Washington, D. C. See CONF-701102.

5899 FACTORS AFFECTING THE JUSTIFICATION OF NUCLEAR UNITS IN GENERATION EXPANSION. Day, J. T. (Westinghouse Electric Corp., Pittsburgh). Trans. Amer. Nucl. Soc.; 13: 770-1(Nov 1970).
From Meeting of the American Nuclear Society, Washington, D. C. See CONF-701102.

5900 LOWER COSTS THROUGH HIGHER POWER DENSITY AND IMPROVED FUEL MANAGEMENT. Webb, R. A. (Babcock and Wilcox Co., Lynchburg, Va.). Trans. Amer. Nucl. Soc.; 13: 773-4(Nov 1970).
From Meeting of the American Nuclear Society, Washington, D. C. See CONF-701102.

5901 IMPROVING THE PERFORMANCE OF LARGE REACTORS. Wilhelm, W. K. (Combustion Engineering, Inc., Windsor, Conn.). Trans. Amer. Nucl. Soc.; 13: 774(Nov 1970).
From Meeting of the American Nuclear Society, Washington, D. C. See CONF-701102.

5902 EFFECTS OF FUEL THERMAL LIMITS ON GAS-COOLED FAST BREEDER ECONOMICS. Bennett, L. L.; Thomas, W. E.; Sanders, J. P. (Oak Ridge National Lab., Tenn.). Trans. Amer. Nucl. Soc.; 13: 775(Nov 1970).
From Meeting of the American Nuclear Society, Washington, D. C. See CONF-701102.

5903 REACTOR OPERATING AND MAINTENANCE COSTS. Susskind, H.; Raseman, C. J. (Brookhaven National Lab., Upton, N. Y.). Trans. Amer. Nucl. Soc.; 13: 783-4(Nov 1970).
From Meeting of the American Nuclear Society, Washington, D. C. See CONF-701102.

5904 MID-RANGE OPTIMIZATION OF A NUCLEAR POWER PLANT. Widmer, Hans; Mason, Edward A.; MacAvoy, Paul W. (Massachusetts Inst. of Tech., Cambridge). Trans. Amer. Nucl. Soc.; 13: 784-5(Nov 1970).
From Meeting of the American Nuclear Society, Washington, D. C. See CONF-701102.

5905 SHORT-RANGE OPTIMIZATION OF USE OF A NUCLEAR POWER PLANT. Widmer, Hans; Mason, Edward A.; MacAvoy, Paul W. (Massachusetts Inst. of Tech., Cambridge). Trans. Amer. Nucl. Soc.; 13: 785-6(Nov 1970).
From Meeting of the American Nuclear Society, Washington, D. C. See CONF-701102.

5906 PEACH BOTTOM REFUELING AND MAINTENANCE EXPERIENCE. Ullrich, W. T. (Philadelphia Electric Co.). Trans. Amer. Nucl. Soc.; 13: 787-8(Nov 1970).
From Meeting of the American Nuclear Society, Washington, D. C. See CONF-701102.

5907 REMOTE MAINTENANCE DURING THE RECOVERY FROM THE ENRICO FERMI FUEL MELTING INCIDENT. Branyan, Charles E. (Power Reactor Development Co., Monroe, Mich.); Johnson, Kenneth P.; Matte III, Joseph. Trans. Amer. Nucl. Soc.; 13: 788-9(Nov 1970).
From Meeting of the American Nuclear Society, Washington, D. C. See CONF-701102.

5908 RADIOACTIVE MAINTENANCE ON DFR. Kirk, J. (United Kingdom Atomic Energy Authority, Risley, Eng.). Trans. Amer. Nucl. Soc.; 13: 789(Nov 1970).
From Meeting of the American Nuclear Society, Washington, D. C. See CONF-701102.

5909 PLANNING FOR FLEXIBILITY IN THE OPERATION, MAINTENANCE, AND REFUELING OF A PWR. Arthur, J. E.; Platt, C. E.; McCoy, W. L. (Rochester Gas and Electric Co., N. Y.). Trans. Amer. Nucl. Soc.; 13: 822(Nov 1970).
From Meeting of the American Nuclear Society, Washington, D. C. See CONF-701102.

5910 SUMMARY OF CONNECTICUT YANKEE CORE I OPERATIONAL PROBLEMS. Hartley, F. W. (Connecticut Yankee Atomic Power Co., East Hampton). Trans. Amer. Nucl. Soc.; 13: 822-3(Nov 1970).
From Meeting of the American Nuclear Society, Washington, D. C. See CONF-701102.

5911 OPERATING EXPERIENCES DURING THE STARTUP OF DRESDEN UNIT II. Worden, W. P. (Commonwealth Edison Co., Chicago). Trans. Amer. Nucl. Soc.; 13: 823-4(Nov 1970).
From Meeting of the American Nuclear Society, Washington, D. C. See CONF-701102.

Safety and Siting

5912 (DOCKET-1155-85) LA CROSSE BOILING WATER REACTOR. Nuclear Instrumentation Automatic Gain Control System, Addendum. (Allis-Chalmers Mfg. Co., Bethesda, Md. Atomic Energy Div.). Dec 1970. 10p. (ACNP-70503.1). Dep. NTIS.

5913 (DOCKET-50003-60) INDIAN POINT STATION, UNIT NO. 1. Investigation of Spent Fuel Shipping Cask External Neutron Radiation Levels. (Consolidated Edison Co. of New York, Inc., New York). 28 Aug 1970. 1p. Dep. NTIS.

5914 (DOCKET-50010-72) DRESDEN NUCLEAR POWER STATION, UNIT 1. Minimizing Radioactive Off-Gas Release Rate. (Commonwealth Edison Co., Chicago, Ill.). 3 Dec 1970. 1p. Dep. NTIS.

5915 (DOCKET-50010-73) DRESDEN NUCLEAR POWER STATION, UNIT 1. Comments on Uniform Recording and Reporting Guide, Minor Corrections. (Commonwealth Edison Co., Chicago, Ill.). 4 Dec 1970. 1p. Dep. NTIS.

5916 (DOCKET-50016-87) ENRICO FERMI ATOMIC POWER PLANT, UNIT 1. Request for Additional Information on Sodium Service Piping. (Division of Reactor Licensing (AEC), Washington, D. C.). 3 Dec 1970. 2p. Dep. NTIS.

5917 (DOCKET-50133-44) HUMBOLDT BAY POWER PLANT, UNIT NO. 3. License No. DPR-7: Technical Specifications Change No. 29. (Division of Reactor Licensing (AEC), Washington, D. C.). 3 Dec 1970. 1p. Dep. NTIS.

Revised control rod withdrawal time limit is authorized. Permission for testing maximum control rod withdrawal rates is granted. (D.C.C.)

5918 (DOCKET-50219-116) OYSTER CREEK NUCLEAR POWER PLANT, UNIT NO. 1. Provisional Operating License No. DPR-16, Amendment 2. (Division of Reactor Licensing (AEC), Washington, D. C.). 2 Dec 1970. 20p. Dep. NTIS.

Revised operating safety limits for reactor components and systems are presented. Protective instrumentation requirements are listed. Authorization for 1690MW(t) operation is included. Safety evaluation for 1690MW(t) operation is presented. (D.C.C.)

5919 (DOCKET-50220-53) NINE MILE POINT NUCLEAR STATION. Electrical Output Oscillations When Approaching 510 MW(e) Gross Output. (Niagara Mohawk Power Corp., Syracuse, N. Y.). 5 Dec 1970. 5p. Dep. NTIS.

5920 (DOCKET-50220-54) NINE MILE POINT NUCLEAR STATION. Petition Requesting Amendment of License, Amendment 3. Technical Supplement to Petition to Increase Power Level, Third Addendum. (Niagara Mohawk Power Corp., Syracuse, N. Y.). 4 Dec 1970. 50p. Dep. NTIS.

Information on the emergency core cooling system requirements for coolant loss accident conditions at increased power level is presented. (D.C.C.)

5921 (DOCKET-50237-88) DRESDEN NUCLEAR POWER STATION, UNIT 2. Financial Qualifications and Certificate of Service. (Commonwealth Edison Co., Chicago, Ill.). 4 Oct 1965. 12p. Dep. NTIS.

5922 (DOCKET-50237-98) DRESDEN NUCLEAR POWER STATION, UNIT 2. Modification of Standby Gas Treatment Sys-

tem and Automatic Pressure Relief Subsystem. (Commonwealth Edison Co., Chicago, Ill.). 7 Oct 1969. 2p. (DOCKET-50249-50). Dep. NTIS.

5923 (DOCKET-50237-101) DRESDEN NUCLEAR POWER STATION, UNIT 2. Operator Retraining Program. (Commonwealth Edison Co., Chicago, Ill.). 10 Apr 1970. 3p. Dep. NTIS.

5924 (DOCKET-50237-103) DRESDEN NUCLEAR POWER STATION, UNIT 2. License Application. (Commonwealth Edison Co., Chicago, Ill.). 15 Apr 1965. 4p. Dep. NTIS.

5925 (DOCKET-50237-108) DRESDEN NUCLEAR POWER STATION, UNIT 2. Approval of Test Program Involving Irradiation of Cobalt-59. (Division of Reactor Licensing (AEC), Washington, D. C.). 14 Jan 1970. 1p. Dep. NTIS.

5926 (DOCKET-50237-109) DRESDEN NUCLEAR POWER STATION, UNIT 2. Crud Deposition Test Does Not Require a Change to Technical Specifications. (Division of Reactor Licensing (AEC), Washington, D. C.). 23 Jan 1970. 1p. Dep. NTIS.

5927 (DOCKET-50280-28) SURRY POWER STATION, UNITS 1 AND 2. Lateral Load Pile Test. Preliminary Safety Analysis Report, Amendment 16, Pt. B. (Virginia Electric and Power Co., Richmond). Jul 1968. 29p. (DOCKET-50281-28). Dep. NTIS.

Lateral load tests for prototype steel piles of the fuel building support foundation are described. Computer analyses are made of the amount of lateral deflections of the piles supporting the fuel building, relative to the soil in which they are to be embedded, under earthquake loadings. Results are listed. (D.C.C.)

5928 (DOCKET-50280-29) SURRY POWER STATION, UNITS 1 AND 2. Preoperational Environmental Radiation Surveillance Program, May 1, 1968-June 30, 1970. Preliminary Safety Analysis Report, Amendment 16, Pt. C. (Virginia Electric and Power Co., Richmond). 68p. (DOCKET-50281-29). Dep. NTIS.

5929 (DOCKET-50280-30) SURRY POWER STATION, UNITS 1 AND 2. Preliminary Safety Analysis Report, Amendment 16, Pt. A-1 (Includes Final Safety Analysis Report, Suppl. Vol. 1). (Virginia Electric and Power Co., Richmond). 1 Dec 1970. 400p. (DOCKET-50281-30). Dep. NTIS.

Information on Surry Power Reactor Units 1 and 2 is presented under the following broad topics: general; site; reactor; reactor coolant system; containment systems; and engineered safeguard features. (D.C.C.)

5930 (DOCKET-50280-31) SURRY POWER STATION, UNITS 1 AND 2. Preliminary Safety Analysis Report, Amendment 16, Pt. A-2 (Includes Final Safety Analysis Report, Suppl. Vol. 2). (Virginia Electric and Power Co., Richmond). 1 Dec 1970. 242p. (DOCKET-50281-31). Dep. NTIS.

Information on Surry Power Reactor Units 1 and 2 is presented under the following broad topics: instrumentation and control; electrical systems; auxiliary and emergency systems; steam and power conversion systems; radioactive wastes and radiation protection; conduct of operations; initial tests and operation; and safety analysis. (D.C.C.)

5931 (DOCKET-50295-15) ZION STATION, UNITS 1 AND 2. Technical Specifications; Appendix A to Operating License. (Commonwealth Edison Co., Chicago, Ill.). 25 Nov 1970. 117p. (DOCKET-50304-15). Dep. NTIS.

5932 (DOCKET-50295-16) ZION STATION, UNITS 1 AND 2. Preliminary Safety Analysis Report, Amendment 12 (Includes Final Safety Analysis Report, Vol. 1). (Commonwealth Edison Co., Chicago, Ill.). 1 Dec 1970. 456p. (DOCKET-50304-16). Dep. NTIS.

Information on Zion Power Reactor Units 1 and 2 is presented under the following broad topics: introduction and summary; site and environment; and reactor. (D.C.C.)

5933 (DOCKET-50295-17) ZION STATION, UNITS 1 AND 2. Preliminary Safety Analysis Report, Amendment 12 (Includes Final Safety Analysis Report, Vol. 2). (Commonwealth Edison Co., Chicago, Ill.). 1 Dec 1970. 340p. (DOCKET-50304-17). Dep. NTIS.

Information on Zion Power Reactor Units 1 and 2 is presented under the following broad topics: reactor coolant system, and containment. (D.C.C.)

5934 (DOCKET-50295-18) ZION STATION, UNITS 1 AND 2. Preliminary Safety Analysis Report, Amendment 12 (Includes Final Safety Analysis Report, Vol. 3). (Commonwealth Edison Co., Chicago, Ill.). 1 Dec 1970. 414p. (DOCKET-50304-18). Dep. NTIS.

Information on Zion Power Reactor Units 1 and 2 is presented under the following broad topics: engineered safety features, and instrumentation and control. (D.C.C.)

5935 (DOCKET-50295-19) ZION STATION, UNITS 1 AND 2. Preliminary Safety Analysis Report, Amendment 12 (Includes Final Safety Analysis Report, Vol. 4). (Commonwealth Edison Co., Chicago, Ill.). 1 Dec 1970. 300p. (DOCKET-50304-19). Dep. NTIS.

Information on Zion Power Reactor Units 1 and 2 is presented under the following broad topics: electrical systems, and auxiliary systems. (D.C.C.)

5936 (RISO-214, pp 127-69) ONTARIO HYDRO NUCLEAR GENERATING STATION SAFETY AND PRODUCTION RELIABILITY. Kelly, R. J. (Hydro-Electric Power Commission of Ontario, Toronto).

From Proceedings of the meeting of specialists on the reliability of mechanical components and systems for nuclear reactor safety, Risoe, September 24-26, 1969.

The development of the safety and production reliability standards is traced. Experience with various units of equipment at the operating stations is reviewed in terms of these standards. The application of this experience to the stations now under construction is described. 9 references. (auth) (Denmark)

5937 (RISO-214, pp 457-79) RELIABILITY ASPECTS OF SAFETY EVALUATION OF NUCLEAR POWER PLANTS. Takemura, K. (Tokyo Univ. of Mercantile Marine (Japan)); Hattori, S. (Chubu Electric Power Co. [Nagoya (Japan)]).

From Proceedings of the meeting of specialists on the reliability of mechanical components and systems for nuclear reactor safety, Risoe, September 24-26, 1969.

In Japan reliability analysis is explored as a tool for safety assessment. The risks in Japan from natural hazards, diseases, industrial hazards, and accidents are given as a basis for establishment of a risk level for nuclear power plants. Reliability data for 132 diesel emergency power systems are given together with reliability data for the Japan Power Demonstration Reactor (12.5 MW). (Denmark)

5938 LEAKAGE TESTS ON REACTOR CONTAINMENT VESSELS. Tsutsui, Mitsuo (Ministry of International Trade and Industry, Tokyo). Karyoku Hatsuden; 20: 1231-6(Dec 1969). (In Japanese).

The Japan Electric Association is preparing the criteria for containment leakage tests according to the U.S. AEC Technical Safety Guide. The Guide "Reactor Containment Leakage Testing and Surveillance Requirements," and the leakage test performed on the Tsuruga atomic power station before its completion (drywell and suppression chamber) are described. The U.S. AEC Guide includes the following: Test A—leakage test by pressurizing the whole containment vessel; Test B—leakage test at the vessel penetrations etc.; Test C—performance and leakage tests for separation (for an accident) valves; and Test D—performance test for the safety systems under Test A conditions. (Japan)

5939 ASEISMATIC DESIGN FOR A NUCLEAR POWER PLANT. Akino, Kinji; Tamura, Masaya (Japan Atomic Power Co., Tokyo). Karyoku Hatsuden; 21: 372-85(Apr 1970). (In Japanese).

The principle of the aseismatic design for a nuclear power plant is to protect the residents in the neighboring area and the operators of the plant from radiation during and after an earthquake, and to provide adequate strength to every installation of the station and components. At Tsuruga nuclear power station, all buildings, structures, equipments, piping and their supports are classified into four classes, As, A, B and C, according to their degree of importance for plant safety. The values of horizontal seismic coefficient used for determining design load on the class As and A buildings and structures are determined as the result of dynamic analysis. As to the class C and class B, the values 1.2 and 1.5 times as much as those specified by the Building Standard Law of Japan are employed respectively. The input disturbance used for dynamic analysis is the seismic waves of El Centro and San Francisco Golden Gate Park earthquakes and 0.25 g acceleration. All equipment, piping and their supports are designed to be as rigid as possible, although spring anchors and hydraulic snubbers are employed where thermal requirements prohibit the use of a rigid support to resist earthquake vibration while allowing sufficient flexibility for thermal expansion. (Japan)

XUM

5940 PUBLIC RESISTANCE TO NUCLEAR REACTOR SITING. Jopling, David G.; Gage, Stephen J. (Univ. of Texas, Austin). Trans. Amer. Nucl. Soc.; 13: 460-1(Nov 1970).
From Meeting of the American Nuclear Society, Washington, D. C. See CONF-701102.

5941 TRITIUM SOURCES AND RELEASE TO THE ENVIRONMENT. Oestmann, M. J. (Argonne National Lab., Ill.). Trans. Amer. Nucl. Soc.; 13: 486-7(Nov 1970).
From Meeting of the American Nuclear Society, Washington, D. C. See CONF-701102.

Power Reactor Development

Refer also to abstracts 4183, 4185, 4203, 4210, 4262, 4294, 4388, 4389, 4736, 4738, 4748, 4770, 4835, and 4863.

5942 (DP-Report-490) ELEVENTH SEMI-ANNUAL REPORT FOR THE PERIOD JULY 1, 1965–DECEMBER 31, 1965. Project DRAGON. Ashworth, F. P. O. (ed.) (Atomic Energy Establishment, Winfrith (England)). Jun 1966. 180p. Dep. NTIS.
GRAPHITE—properties in gas cooled reactor core components, chemical and physical
HIGH-TEMPERATURE GAS-COOLED REACTOR EXPERIMENT—physics parameters of
—core components in, corrosion and properties of graphite
—coolant for, heat transfer and gas flow properties of helium
—fuels for, preparation and properties of pyrolytic carbon coated ceramic particle
—fuels for, irradiation testing of
—instrument development for
—fuel cycle for, analysis of optimum economic
—fuel reprocessing for, equipment and procedures for
URANIUM CARBIDES—ThC_2-UC_2, preparation and properties of coated particle fuels (D.C.C.)

5943 (GEAP-13595) FABRICATION OF NON-FUEL CORE COMPONENTS FOR SEFOR. Ikeuye, D. T.; Young, F. E. (General Electric Co., Sunnyvale, Calif. Breeder Reactor Development Operation). Feb 1970. Contract AT(04-3)-540. 152p. Dep. NTIS.

The fabrication data and processes for the production of the extension rods, tightener rods, tightener sleeves, and special rods for the SEFOR reactor are documented. The extension rods provide the neutron and γ shielding above the core. The functions of the tightener rods are to lock the surrounding "fuel rod-extension rod" assembly in position in the fuel channel, to provide additional shielding above the core, and to increase the Doppler effect. The tightener sleeve is the basic internal structural member of the fuel assembly and serves to provide spacing between the fuel rods. The major tooling, techniques of fabrication, fabrication processes, and quality control efforts used in the fabrication of the non-fuel core components are described. (auth)

5944 HIGH-TEMPERATURE REACTORS. Schulten, R. Neue Tech., B; 10: 242-7(1968). (In German).

The present status as well as research and development are discussed for gas-cooled high-temperature reactors with special emphasis on projects in West Germany. Considered are economics, safety, breeding, closed-cycle He turbines, and use of the high-temperature gas for chemical syntheses based on coal and steel. The total German project is subdivided into three major phases: operation of the research reactor AVR; construction and operation of both the Geesthacht II reactor and the pebble-bed prototype reactor with high-temperature He turbine; and design and construction of a 600 MW(e) demonstration power station with He turbine. (H.B.G.)

5945 VARIOUS PROBLEMS ASSOCIATED WITH THE DESIGN OF NUCLEAR REACTORS. Egusa, Tatsuo (Tohoku Univ., Sendai). Karyoku Hatsuden; 20: 1237-8(Dec 1969). (In Japanese).

The advance in development and manufacture of nuclear reactors in Japan, with regard to the future, may be compared to the case of thermal power stations some 15 years ago. In the construction of reactor plants in Japan, unexpected failures or successes have been experienced; at all events, however, the technology in nuclear power generation is advancing steadily. Now that safety aspects of nuclear power generation have been established, the next problem in the design of reactor plants concerns the plant integrity, which is the reflection of an economy of nuclear power generation. This may be achieved by review-survey studies on the installed components of nuclear power plants. (Japan)

5946 OECD HALDEN REACTOR PROJECT. Doederlein, J. M.; Knudsen, K. D.; Lunde, J. E. (Institutt for Atomenergi, Halden, Norway). Trans. Amer. Nucl. Soc.; 13: 463-4(Nov 1970).
From Meeting of the American Nuclear Society, Washington, D. C. See CONF-701102.

5947 HIGH-TEMPERATURE REACTOR DEVELOPMENT IN THE DRAGON PROJECT. Shepherd, L. R.; Saunders, A. R. (OECD Dragon Reactor Project, Winfrith, Eng.). Trans. Amer. Nucl. Soc.; 13: 464-5(Nov 1970).
From Meeting of the American Nuclear Society, Washington, D. C. See CONF-701102.

5948 EBR-II IRRADIATION EFFECTS OF RUPTURE OF TYPE 316 STAINLESS STEEL. Barker, R. W.; Holmes, J. J. (Hanford Engineering Development Lab., Richland, Wash.). Trans. Amer. Nucl. Soc.; 13: 591-2(Nov 1970).
From Meeting of the American Nuclear Society, Washington, D. C. See CONF-701102.

5949 MECHANICAL PROPERTIES OF EBR-II IRRADIATED 20 PERCENT COLD-WORKED TYPE 316 STAINLESS STEEL. Ward, A. L.; Blackburn, L. D.; Lovell, A. J. (Hanford Engineering Development Lab., Richland, Wash.). Trans. Amer. Nucl. Soc.; 13: 593(Nov 1970).
From Meeting of the American Nuclear Society, Washington, D. C. See CONF-701102.

5950 BURST TESTS OF EBR-II IRRADIATED FUEL PIN SECTIONS. Fish, R. L.; Holmes, J. J.; Leggett, R. D. (Hanford Engineering Development Lab., Richland, Wash.). Trans. Amer. Nucl. Soc.; 13: 593-4(Nov 1970).
From Meeting of the American Nuclear Society, Washington, D. C. See CONF-701102.

Kinetics and Dynamics

Refer also to abstracts 6114, 6159, 6165, 6172, and 6178.

5951 (DOCKET-50231-58) SOUTHWEST EXPERIMENTAL FAST OXIDE REACTOR. Reactivity Coefficients, as Determined from Tests Through 10 MW. (General Electric Co., Sunnyvale, Calif. Breeder Reactor Development Operation). 2 Dec 1970. 44p. Dep. NTIS.

5952 (DP-Report-442) RELATIVE POWER DISTRIBUTION AND INTEGRAL SPECTRUM MEASUREMENTS ON THE FIRST DRAGON CORE. Project DRAGON. Reed, D. L.; Bartlett, A. C. (Atomic Energy Establishment, Winfrith (England)). Jul 1966. 50p. Dep. NTIS.

The experimental methods used for determining the radial and axial ^{235}U reaction rate distributions and the integral spectrum in the first core of Dragon are described. Small ^{235}U foils were used for the reaction rate measurements and similar sized composite foils of Au and Mn were used for the spectrum measurements. The results obtained are compared with the theoretical power distributions and integral spectrum so that estimates of the veracity of the models used for the theoretical calculations can be made. 7 references. (auth)

5953 (DP-Report-445) TRANSFER FUNCTION INVESTIGATIONS ON THE FIRST DRAGON CORE. Project DRAGON. Blake, J. P. H.; Davis, E. H.; Hammond, A. D.; Reber, J.; Woloch, F. (Atomic Energy Establishment, Winfrith (England)). Jul 1966. 94p. Dep. NTIS.

The Dragon Transfer Function Analyzer was commissioned and successfully used for reactor measurements at zero power and power levels of 2.5 and 10 MW during the reactor operation program on the first core. Theoretical and experimental investigations connected with the use of transfer function analysis for the determination of control rod reactivities, temperature feed-back effects, and neutron lifetime are described. The analysis of high frequency measurements in connection with neutron lifetime investigations was complicated by the presence of undesired control mechanism characteristics, which were therefore measured separately on a test rig. The experimental results obtained for control rod reactivity measurements and temperature feed-back effects agree with theory to within the experimental errors. The measurements of neutron lifetime are also in agreement, but also indicate the presence of spatial effects at very high frequencies. 50 references. (auth)

5954 ANALYTIC STUDIES OF FAST REACTOR FLUX AND IMPORTANCE SPECTRA. Dunn, Floyd Eugene. Troy, N. Y.; Rensselaer Polytechnic Inst. (1969). 286p. University Microfilms Order No. 70-11,315.
Thesis.

A model has been developed that leads to analytic expressions for fast reactor fundamental mode flux and importance spectra. In the process of developing the model it was necessary to make improvements in slowing down theory. When these improvements are incorporated into the model, both the gross shape and the detailed fluctuations of the flux spectrum are given accurately. The importance spectrum also gives fairly good agreement with multigroup spectra. The model uses the Greuling–Goertzel form of the slowing down equations. The model provides a rapid and accurate means for calculating broad group multi-group constants from basic cross section data. In cases where one broad group microscopic cross section set might be used for many different compositions because the cost of calculating new cross section sets by conventional multi-group methods is considered to be too expensive, the faster model procedure might make it feasible to calculate an appropriate cross section set for each different composition, thus providing more accurate results. (Diss. Abstr.)

5955 FAST-NEUTRON SPECTRUM MODELS AND THEIR APPLICATION TO SPECIFIC MATERIALS. Burns, Edward T.; Becker, Martin (Rensselaer Polytechnic Inst., Troy, N. Y.). Trans. Amer. Nucl. Soc.; 13: 687-9(Nov 1970).
From Meeting of the American Nuclear Society, Washington, D. C. See CONF-701102.

5956 MULTIGROUP POINT KINETICS WITH FEEDBACK. Dunn, Stephen A.; Cunningham, James P. (Westinghouse Electric Corp., Pittsburgh). Trans. Amer. Nucl. Soc.; 13: 702-3 (Nov 1970).
From Meeting of the American Nuclear Society, Washington, D. C. See CONF-701102.

5957 DOPPLER CONSIDERATIONS FOR HIGH-TEMPERATURE GAS-FUELED CAVITY REACTORS. Bettenhausen, L. H.; Meem, J. L. (Univ. of Virginia, Charlottesville). Trans. Amer. Nucl. Soc.; 13: 712-13(Nov 1970).
From Meeting of the American Nuclear Society, Washington, D. C. See CONF-701102.

5958 INTERFERENCE EFFECTS OF ^{232}Th–^{233}Pa ABSORPTION RESONANCES IN HOMOGENEOUS SYSTEMS. Ballariny, M. V. (Brazilian Nuclear Energy Commission, Rio de Janeiro); Marable, J. H. Trans. Amer. Nucl. Soc.; 13: 714-15(Nov 1970).
From Meeting of the American Nuclear Society, Washington, D. C. See CONF-701102.

5959 INTEGRAL-TRANSPORT-THEORY ANALYSIS OF RESONANCE ABSORPTION MEASUREMENTS IN NEUTRON BEAMS. Bohl, W. R.; Foell, W. K. (Univ. of Wisconsin, Madison). Trans. Amer. Nucl. Soc.; 13: 715-16(Nov 1970).
From Meeting of the American Nuclear Society, Washington, D. C. See CONF-701102.

5960 FBR BLANKET DEPLETION STUDIES: EFFECT OF NUMBER OF ENERGY GROUPS. Brewer, S. T.; Driscoll, M. J.; Mason, E. A. (Massachusetts Inst. of Tech., Cambridge). Trans. Amer. Nucl. Soc.; 13: 723-4(Nov 1970).
From Meeting of the American Nuclear Society, Washington, D. C. See CONF-701102.

5961 SYNTHESIS OF FAST REACTOR SPECTRA. Ombrellaro, P. A.; Snider, M. A. (Argonne National Lab., Ill.). Trans. Amer. Nucl. Soc.; 13: 724-5(Nov 1970).
From Meeting of the American Nuclear Society, Washington, D. C. See CONF-701102.

5962 SUCCESSIVE SPACE-ENERGY SYNTHESIS FOR FAST REACTORS. Cockayne, J. E.; Ott, K. O. (Purdue Univ., Lafayette, Ind.). Trans. Amer. Nucl. Soc.; 13: 725-6(Nov 1970).
From Meeting of the American Nuclear Society, Washington, D. C. See CONF-701102.

5963 DEPLETED-URANIUM, NICKEL, AND STEEL-REFLECTED EBR-II CRITICAL ASSEMBLIES ON ZPR-3: EXPERIMENTS AND CALCULATIONS. Meneghetti, D. (Argonne National Lab., Ill.); Keeney, W. P.; Vosburgh, R. O.; (and others). Trans. Amer. Nucl. Soc.; 13: 733-4(Nov 1970).
From Meeting of the American Nuclear Society, Washington, D. C. See CONF-701102.

5964 REACTIVITY WORTH OF TANTALUM IN A FAST REACTOR SPECTRUM. Tuttie, R. J.; Springer, T. H. (Atomics International, Canoga Park, Calif.). Trans. Amer. Nucl. Soc.; 13: 735-6(Nov 1970).
From Meeting of the American Nuclear Society, Washington, D. C. See CONF-701102.

5965 ACCURACY OF SPACE-COLLAPSE FOR FAST BREEDER FUEL CYCLE ANALYSIS. Alcouffe, Raymond E.; Hirons, Thomas J. (Los Alamos Scientific Lab., N. Mex.). Trans. Amer. Nucl. Soc.; 13: 740-1(Nov 1970).
From Meeting of the American Nuclear Society, Washington, D. C. See CONF-701102.

5966 MULTIPLE REACTION RATE WEIGHTING IN FAST REACTOR SPACE-ENERGY SYNTHESIS. Neuhold, R. J. (Babcock and Wilcox Co., Lynchburg, Va.). Trans. Amer. Nucl. Soc.; 13: 741-2(Nov 1970).
From Meeting of the American Nuclear Society, Washington, D. C. See CONF-701102.

5967 NONLINEAR CONTAMINATION IN FREQUENCY RESPONSE TESTS. Buckner, M. R. (Savannah River Lab., Aiken, S. C.); Kerlin, T. W. Trans. Amer. Nucl. Soc.; 13: 765-6(Nov 1970).
From Meeting of the American Nuclear Society, Washington, D. C. See CONF-701102.

5968 OPTIMAL DISCRETE LEVEL SIGNALS FOR REACTOR FREQUENCY RESPONSE TESTS. Buckner, M. R. (Savannah River Lab., Aiken, S. C.); Kerlin, T. W. Trans. Amer. Nucl. Soc.; 13: 766-7(Nov 1970).
From Meeting of the American Nuclear Society, Washington, D. C. See CONF-701102.

5969 THEORETICAL PREDICTION OF LOCAL BOILING VOID DISTRIBUTION IN A WATER REACTOR CHANNEL. Sha, W. T. (Argonne National Lab., Ill.). Trans. Amer. Nucl. Soc.; 13: 815-16(Nov 1970).
From Meeting of the American Nuclear Society, Washington, D. C. See Conf-701102.

5970 DISTRIBUTION OF GAMMA ENERGY DEPOSITION IN A FAST REACTOR. Miller, L. B.; Jarka, R. E. (Argonne National Lab., Ill.). Trans. Amer. Nucl. Soc.; 13: 831-2(Nov 1970).
From Meeting of the American Nuclear Society, Washington, D. C. See CONF-701102.

5971 EXPLORATORY CALCULATIONS FOR A GASEOUS CORE FAST BREEDER REACTOR. Kallfelz, J. M.; Williams, J. R. (Georgia Inst. of Tech., Atlanta). Trans. Amer. Nucl. Soc.; 13: 832-4(Nov 1970).
From Meeting of the American Nuclear Society, Washington, D. C. See CONF-701102.

5972 SOME PHYSICS ASPECTS OF A SMALL ONCE-THROUGH PEBBLE-BED REACTOR. Hansen, U.; Schulten, R.; Teuchert, E. (Kernforschungsanlage, Juelich, Ger.). Trans. Amer. Nucl. Soc.; 13: 834(Nov 1970).
From Meeting of the American Nuclear Society, Washington, D. C. See CONF-701102.

5973 SELECTION OF FISSION YIELDS. McElroy, W. N. (Hanford Engineering Development Lab., Richland, Wash.); Kellogg, L. S.; Armani, R. J.; Tochilin, E.; Zimmer, W. H. Trans. Amer. Nucl. Soc.; 13: 868-9(Nov 1970).
From Meeting of the American Nuclear Society, Washington, D. C. See CONF-701102.

Control Systems

5974 COMPUTER CONTROL DEVELOPMENTS AT THE OECD HALDEN REACTOR PROJECT. Lunde, J. E. (Institutt for Atomenergi, Halden, Norway). Trans. Amer. Nucl. Soc.; 13: 463(Nov 1970).
From Meeting of the American Nuclear Society, Washington, D. C. See CONF-701102.

5975 AVAILABILITY AND COST OF ^{10}B FOR REACTOR CONTROL. Fersch, K. E.; Hoynacki, J. J.; Pepkowitz, L. P. (Nuclear Materials and Equipment Corp., Lewiston, N. Y.). Trans. Amer. Nucl. Soc.; 13: 796(Nov 1970).
From Meeting of the American Nuclear Society, Washington, D. C. See CONF-701102.

Shielding

Refer also to abstract 6125.

5976 SOME TYPICAL RADIATION STREAMING PROBLEMS IN SODIUM-COOLED FAST REACTORS. Gerstl, Siegfried A. W. (Westinghouse Advanced Reactors Div., Madison, Pa.). Trans. Amer. Nucl. Soc.; 13: 857-8(Nov 1970).
From Meeting of the American Nuclear Society, Washington, D. C. See CONF-701102.

XUM

5977 ANALYSIS AND DESIGN METHODS FOR LIGHT-WATER POWER REACTOR SHIELDS. Cygelman, A. I. (Burns and Roe, Inc., Hempstead, N. Y.). Trans. Amer. Nucl. Soc.; 13: 870-1(Nov 1970).

From Meeting of the American Nuclear Society, Washington, D. C. See CONF-701102.

5978 WNES SHIELDING APPLICATION: PREDICTIONS AND MEASUREMENTS. Locante, John; Sejvar, James; Schoen, Gerald (Westinghouse Electric Corp., Pittsburgh). Trans. Amer. Nucl. Soc.; 13: 872(Nov 1970).

From Meeting of the American Nuclear Society, Washington, D. C. See CONF-701102.

Cooling Systems

5979 (DP-Report-435) HEAT TRANSFER AND PRESSURE DROP IN HIGH TEMPERATURE HELIUM COOLED POWER REACTORS. PARAMETRIC SURVEY ON INTERNALLY COOLED ANNULAR FUEL. Project DRAGON. Marien, P. (Atomic Energy Establishment, Winfrith (England)). May 1966. 28p. Dep. NTIS.

The results of a parametric survey are presented as a tool allowing the study of the interactions between the various design and operating parameters of HTGC power reactors. A considerable number of problems can be solved with this tool concerning the design and operating conditions of HTGC power reactors using internally cooled annular fuel. (auth)

5980 (KFK-1183) SUPERHEATED STEAM FILTER. PART I. John, H. (Kernforschungszentrum, Karlsruhe (West Germany). Institut fuer Reaktorbauelemente). May 1970. 59p. (In German). Dep. NTIS (U. S. Sales Only).

The filtration of superheated steam is very important in a steam cooled nuclear reactor because any solids carried along from the reactor constitute a great contamination hazard to the entire steam circuit. Since practically no such filters have been known before, a number of materials which appeared to be suitable were experimentally investigated for their applicability. The results of these experiments are presented. 5 references. (auth)

5981 (RISO-214, pp 289-300) REVIEW OF THE SAFETY ASPECTS OF THE DESIGN OF PRESTRESSED CONCRETE PRESSURE VESSELS WITH REFERENCE TO LIMIT STATE DESIGN. Yu, C. W.; Gill, S. (Imperial Coll. of Science and Tech., London (England)).

From Proceedings of the meeting of specialists on the reliability of mechanical components and systems for nuclear reactor safety, Risoe, September 24-26, 1969.

The shortcomings of the three existing design criteria for concrete pressure vessels are described: the elastic response of the structure must be below permissible code values under design load and test pressure; the mode of failure under overload conditions must be gradually recognizable before ultimate structural collapse; and there must be an adequate margin (2.5 to 3 times) against ultimate failure. Limit state design considers variations in loading and material strength from a probabilistic viewpoint and should be seriously considered in design. This will require more data about statistical distributions and the effect on design parameters of construction, commissioning and operation. It is advocated that these data should be collected from existing vessels. 5 references. (Denmark)

5982 (RISO-214, pp 301-22) ANALYSIS OF A GERMAN PRESSURE VESSEL AND BOILER DRUM STATISTICS. Mieze, G. (Technischer Ueberwachungs-Verein e. V., Cologne (West Germany). Institut fuer Reaktorsicherheit).

From Proceedings of the meeting of specialists on the reliability of mechanical components and systems for nuclear reactor safety, Risoe, September 24-26, 1969.

A description of the pressure vessel characteristics is given. Failure reports are explained. Analysis of the primary data and the determination of failure rates are shown. The observed failure modes are reviewed. The analysis of the primary data, the determination of failure rates and the relevance of the data to nuclear pressure vessels are discussed. 8 references. (auth) (Denmark)

5983 (RISO-214, pp 323-34) SURVEY OF PRESSURE VESSELS BUILT TO A HIGH STANDARD OF CONSTRUCTION. Phillips, C. A. G. (United Kingdom Atomic Energy Authority, Risley (England). Authority Health and Safety Branch); Warwick, R. G. (Associated Offices Technical Committee (UK)).

From Proceedings of the meeting of specialists on the reliability of mechanical components and systems for nuclear reactor safety, Risoe, September 24-26, 1969.

Statistics of failures are given for conventional pressure vessels of high-standard construction. A selection of vessels is made in order to make the results comparable to nuclear vessels. For these vessels in operation in the United Kingdom a probability of potentially dangerous faults is found to be 1.3×10^{-3} per vessel year and of catastrophic failures 0.7×10^{-4} per vessel year. The failures are broken down into different causes and, for those revealed in service, the kind of inspection leading to discovery. 4 references. (Denmark)

5984 (RISO-214, pp 335-43) ASPECTS OF DESIGN RELIABILITY OF PRESSURE TUBES FOR HEAVY WATER MODERATED REACTORS. Montagnani, M.; Putzeys, J. (European Atomic Energy Community, Ispra (Italy). Joint Nuclear Research Center).

From Proceedings of the meeting of specialists on the reliability of mechanical components and systems for nuclear reactor safety, Risoe, September 24-26, 1969.

For a heavy-water moderated and organic-liquid cooled reactor, it is proposed to use SAP (Sintered Aluminium Powder) to fabricate the pressure tubes. A test program was performed to study the consequences of a pressure tube burst, i.e., strains introduced in the neighboring channels, in the vessel and in the safety systems. The long-term mechanical resistance of SAP is determined by its creep behaviour. A statistical analysis of experimental creep rupture test results allows determination of the thickness of the pressure tubes for a certain rupture probability under normal operating conditions. On the basis of the results of both studies a reliability concept can be introduced for determination of design criteria for the pressure tubes. 7 references. (auth) (Denmark)

5985 GASIFICATION OF GRAPHITE UNDER HTGR OPERATING AND POTENTIAL ACCIDENT CONDITIONS. Tingey, G. L.; Clark, D. E.; Giberson, R. C. (Battelle-Northwest, Richland, Wash.). Trans. Amer. Nucl. Soc.; 13: 587-8(Nov 1970).

From Meeting of the American Nuclear Society, Washington, D. C. See CONF-701102.

5986 CORROSION PRODUCT RADIOACTIVITY IN THE FFTF AND OTHER REACTOR SYSTEMS. Kabele, T. J.; Brehm, W. F. Jr. (Battelle-Northwest, Richland, Wash.). Trans. Amer. Nucl. Soc.; 13: 673-4(Nov 1970).

From Meeting of the American Nuclear Society, Washington, D. C. See CONF-701102.

5987 MAINTENANCE OF RADIOACTIVE SODIUM SYSTEMS AT EBR-II. Leman, J. D.; Waldo, J. B. (Argonne National Lab., Idaho Falls, Idaho). Trans. Amer. Nucl. Soc.; 13: 787(Nov 1970).

From Meeting of the American Nuclear Society, Washington, D. C. See CONF-701102.

5988 EFFECTS OF INERT CELL IMPURITIES ON METAL-COOLED SYSTEMS. Myers, R. V. (General Electric Co., Fayetteville, Ark.). Trans. Amer. Nucl. Soc.; 13: 823(Nov 1970).

From Meeting of the American Nuclear Society, Washington, D. C. See CONF-701102.

Fuels

Refer also to abstracts 4138 and 4889.

5989 (GA-10264) HIGH-TEMPERATURE FAST-FLUX IRRADIATION EXPERIMENT FOR MIXED-OXIDE FUEL RODS. Flynn, P. W.; Hinz, R. F.; Langer, S.; Lindgren, J. R.; Price, R. J.; Washburn, T. N.; Weinberg, A. F. (Gulf General Atomic, Inc., San Diego, Calif.). 15 Oct 1970. Contract AT(04-3)-167. 80p. Dep. NTIS.

The GGA fast-flux experiment in EBR-II will study fuel-rod specimens with cladding temperatures in the range of 650°C to 800°C and at linear power-generation rates of 14 to 16 kW/ft. The mixed oxide fuel is contained in 20% cold-worked 316 stainless steel and will achieve burnups ranging from 2.7 to 10.7% FIMA. The capsules are generally of the B-7B type with a stainless steel annular thermal barrier Na bonded to the fuel rod and to the capsule tube. SiC temperature monitors are placed in various positions along the thermal barrier to allow postirradiation determination of capsule temperatures utilizing dimensional changes during isochronal annealing of the SiC. Activated charcoal has been placed in all of the fuel rods to determine the effects of fast neutron irradiation on the sorption characteristics of the charcoal for fission products. All eight fuel rods contain sealed charcoal capsules for postirradiation sorption experiments. Three of the fuel rods also contain charcoal traps connected to the fueled region to study the fission-product distribution in the trap under reactor operating conditions. 16 references. (auth)

5990 (ORNL-4589) GAS-COOLED REACTOR PROGRAM SEMIANNUAL PROGRESS REPORT FOR PERIOD ENDING MARCH 31, 1970. (Oak Ridge National Lab., Tenn.). Nov 1970. Contract W-7405-eng-26. 158p. Dep. NTIS.

BOILERS—welds in high temperature gas cooled reactor, corrosion resistance of nickel alloy
CESIUM ISOTOPES Cs-137—release from Triso coated uranium oxide (UO_2) fuel particles
CONCRETES—creep under prestressed concrete reactor vessel operating conditions
—moisture migration in reactor grade
FISSION PRODUCTS—release from high burnup coated particle fuels
NEUTRONS, FAST—effects on thorium oxide (ThO_2)–uranium oxide (UO_2) coated particle fuels
—effects on Type 316 stainless steel clad plutonium oxide (PuO_2)–uranium oxide (UO_2) and uranium oxide (UO_2) fuel elements
NICKEL ALLOYS AND SYSTEMS—corrosion resistance in steam generator welds
PLUTONIUM OXIDES PuO_2—PuO_2–UO_2, radiation testing of Type 316 stainless steel clad fuel pellets of
PRESSURE VESSELS—structural characteristics of prestressed concrete, methods for analysis of
—failure of prestressed concrete, model tests on
REACTOR FUEL ELEMENTS—radiation effects on thorium oxide (ThO_2)–uranium oxide (UO_2) coated particle, fast neutron
—fabrication of coated particle
—fission product release from uranium oxide (UO_2) coated particle
—radiation effects on Type 316 stainless steel clad plutonium oxide (PuO_2)–uranium oxide (UO_2) and uranium oxide (UO_2), fast neutron
REACTOR FUELS—fission product release from high burnup coated particle
REACTORS, BREEDER—fuel elements for gas cooled fast, irradiation testing of
REACTORS, FAST—fuel elements for gas cooled breeder, irradiation testing of
REACTORS, GAS-COOLED—development during October 1969 to March 1970
—fuel elements for high temperature, development and irradiation testing of
—fuels for high temperature, irradiation testing of coated particle
—steam generators for high temperature, corrosion resistance of nickel alloy welds in
—pressure vessels for, development of prestressed concrete
REACTORS, POWER—development of gas cooled, during October 1969 to March 1970
THORIUM OXIDES ThO_2—ThO_2–UO_2, radiation testing of coated particle fuels of
URANIUM OXIDES UO_2—ThO_2–UO_2, radiation testing of coated particle fuels of
—PuO_2–UO_2, radiation testing of Type 316 stainless steel clad fuel pellets of
—radiation testing of Type 316 stainless steel clad fuel pellets of (D.C.C.)

5991 BASIC PROBLEMS IN THE DETERMINATION OF NUCLEAR FUEL PERFORMANCE. Walke, Gerald J. (Consumers Power Co., Jackson, Mich.). Trans. Amer. Nucl. Soc.: 13: 472-3(Nov 1970).
From Meeting of the American Nuclear Society, Washington, D. C. See CONF-701102.

5992 THERMAL PERFORMANCE AND RESTRUCTURING OF PELLET AND SPHERE-PAC FUELS. Fitts, R. B.; DeCarlo, V. A.; Long, E. L. Jr.; Olsen, A. R. (Oak Ridge National Lab., Tenn.). Trans. Amer. Nucl. Soc.: 13: 549-51(Nov 1970).
From Meeting of the American Nuclear Society, Washington, D. C. See CONF-701102.

5993 MICROSTRUCTURE OF MIXED-OXIDE FUEL IRRADIATED IN A THERMAL-NEUTRON FLUX. Lannin, T. E. (General Electric Co., Pleasanton, Calif.); Melde, G. F.; Perry, K. J.; Rosenbaum, H. S.. Trans. Amer. Nucl. Soc.: 13: 551-2 (Nov 1970).
From Meeting of the American Nuclear Society, Washington, D. C. See CONF-701102.

5994 BEHAVIOR OF DISCRETE PuO_2 PARTICLES IN THERMAL RECYCLE FUEL DURING RAPID POWER TRANSIENTS. Freshley, M. D. (Battelle-Northwest, Richland, Wash.); Aitken, E. A.; Wadekamper, D. C.; Johnson, R. L.; Lussie, W. G. Trans. Amer. Nucl. Soc.: 13: 552(Nov 1970).
From Meeting of the American Nuclear Society, Washington, D. C. See CONF-701102.

5995 BEHAVIOR OF LARGE PuO_2 PARTICLES IN A RAPID POWER TRANSIENT. Evans, S. K.; Aitken, E. A. (General Electric Co., Pleasanton, Calif.). Trans. Amer. Nucl. Soc.: 13: 553(Nov 1970).
From Meeting of the American Nuclear Society, Washington, D. C. See CONF-701102.

5996 BEHAVIOR OF Pu RECYCLE FUEL IN A SPERT POWER TRANSIENT. Evans, S. K. (General Electric Co., Pleasanton, Calif.); O'Neill, G. L.; Aitken, E. A.; Johnson, R. T. Trans. Amer. Nucl. Soc.: 13: 554(Nov 1970).
From Meeting of the American Nuclear Society, Washington, D. C. See CONF-701102.

5997 EFFECT OF TEMPERATURE ON FISSION GAS RELEASE FROM COATED FUEL PARTICLES. Langer, S.; Baldwin, N. L. (Gulf General Atomic Inc., San Diego, Calif.). Trans. Amer. Nucl. Soc.: 13: 561-2(Nov 1970).
From Meeting of the American Nuclear Society, Washington, D. C. See CONF-701102.

5998 GCFR FUEL ROD DESIGN CONSIDERATIONS. Thompson, W. I. (Gulf General Atomic, Inc., San Diego, Calif.). Trans. Amer. Nucl. Soc.: 13: 570-1(Nov 1970).
From Meeting of the American Nuclear Society, Washington, D. C. See CONF-701102.

5999 FUEL-CLAD GAP CONDUCTANCE IN FAST REACTOR OXIDE FUELS. Lawrence, L. A.; Horn, G. R.; Christensen, J. A. (Hanford Engineering Development Lab., Richland, Wash.). Trans. Amer. Nucl. Soc.: 13: 572-3(Nov 1970).
From Meeting of the American Nuclear Society, Washington, D. C. See CONF-701102.

6000 MECHANICAL MODEL OF THERMAL DIFFERENTIAL EXPANSION AT FIRST STARTUP OF A MIXED-OXIDE FUEL PIN. Oldberg, S. Jr.; Hines, D. P. (General Electric Co., Sunnyvale, Calif.). Trans. Amer. Nucl. Soc.: 13: 573-4(Nov 1970).
From Meeting of the American Nuclear Society, Washington, D. C. See CONF-701102.

6001 CORRELATION OF PREDICTIONS AND OBSERVATIONS IN MIXED-OXIDE FUEL. Leggett, R. D.; Ballard, E. O.; Bard, F. E.; Weber, J. W.; Pember, L. A.; Jackson, R. J. (Hanford Engineering Development Lab., Richaland, Wash.). Trans. Amer. Nucl. Soc.: 13: 574-6(Nov 1970).
From Meeting of the American Nuclear Society, Washington, D. C. See CONF-701102.

6002 FUEL-CLADDING MECHANICAL INTERACTION DURING STARTUP. Homan, F. J. (Oak Ridge National Lab., Tenn.). Trans. Amer. Nucl. Soc.: 13: 576-7(Nov 1970).
From Meeting of the American Nuclear Society, Washington, D. C. See CONF-701102.

6003 HTGR FUEL DESIGN AND IRRADIATION PERFORMANCE. Luby, C. S.; Harmon, D. P.; Aikins, R. J.; Goeddel, W. V. (Gulf General Atomic, Inc., San Diego, Calif.). Trans. Amer. Nucl. Soc.: 13: 580(Nov 1970).
From Meeting of the American Nuclear Society, Washington, D. C. See CONF-701102.

6004 IRRADIATION PERFORMANCE OF LOOSE AND BONDED BEDS OF COATED FUEL PARTICLES. Scott, J. L.; Coobs, J. H.; Robbins, J. M.; Conlin, J. A. (Oak Ridge National Lab., Tenn.). Trans. Amer. Nucl. Soc.: 13: 580-1(Nov 1970).
From Meeting of the American Nuclear Society, Washington, D. C. See CONF-701102.

6005 SOME ASPECTS OF THE FUEL FABRICATION DEVELOPMENT FOR THE U. K. GAS-COOLED MARK III REACTOR. D'Eye, R. W. M. (United Kingdom Atomic Energy Authority, Springfields, Eng.). Trans. Amer. Nucl. Soc.: 13: 581-2(Nov 1970).
From Meeting of the American Nuclear Society, Washington, D. C. See CONF-701102.

6006 PREPARATION AND PERFORMANCE OF HTGR FUEL IN GERMANY. Liebmann, B. G. (Institut fuer Reaktorentwicklung, Juelich, Ger.); Hackstein, K. G. Trans. Amer. Nucl. Soc.: 13: 582(Nov 1970).
From Meeting of the American Nuclear Society, Washington, D. C. See CONF-701102.

XUM

6007 FUEL DEVELOPMENT FOR A LOW-ENRICHED HTR. Bairiot, H. (Belgonucleaire, Brussels); Vangeel, J.; Aerts, L. Trans. Amer. Nucl. Soc.: 13: 582-3(Nov 1970).
From Meeting of the American Nuclear Society, Washington, D. C. See CONF-701102.

6008 EVALUATION WORK ON COATED FUEL PARTICLES. Bildstein, H. (Reactor Center, Seibersdorf, Austria). Trans. Amer. Nucl. Soc.: 13: 584(Nov 1970).
From Meeting of the American Nuclear Society, Washington, D. C. See CONF-701102.

6009 FISSION GAS RELEASE FROM AN HTGR-TYPE FUEL ROD. Adams, C. C.; Anderson, E. E.; Bell, W. E.; Besenbruch, G. E.; Graves, J. N. (Gulf General Atomic, Inc., San Diego, Calif.). Trans. Amer. Nucl. Soc.: 13: 584-5(Nov 1970).
From Meeting of the American Nuclear Society, Washington, D. C. See CONF-701102.

6010 SOME OBSERVATIONS ON FISSION PRODUCT RELEASE FROM OVERHEATED HTGR FUEL ELEMENTS. de Nordwall, J. H. (Oak Ridge National Lab., Tenn.). Trans. Amer. Nucl. Soc.: 13: 585-6(Nov 1970).
From Meeting of the American Nuclear Society, Washington, D. C. See CONF-701102.

6011 EFFECTS OF TRANSVERSE FLOW ON FISSION PRODUCT TRANSPORT THROUGH GRAPHITE TUBES. Oezisik, M. N. (North Carolina State Univ., Raleigh); Silverman, M. D. Trans. Amer. Nucl. Soc.: 13: 586-7(Nov 1970).
From Meeting of the American Nuclear Society, Washington, D. C. See CONF-701102.

6012 PLUTONIUM AND FISSION PRODUCT MIGRATION IN MIXED-OXIDE FUELS DURING IRRADIATION. Bahl, J. K. (Bhabha Atomic Research Center, Bombay); Freshley, M. D. Trans. Amer. Nucl. Soc.: 13: 599-600(Nov 1970).
From Meeting of the American Nuclear Society, Washington, D. C. See CONF-701102.

6013 ESTIMATION OF FISSION GAS DISTRIBUTION IN LMFBR MIXED-OXIDE FUEL ELEMENTS. Bump, T. R. (Argonne National Lab., Ill.). Trans. Amer. Nucl. Soc.: 13: 600-1(Nov 1970).
From Meeting of the American Nuclear Society, Washington, D. C. See CONF-701102.

6014 MOVEMENT OF FISSION GAS BUBBLES AND INCLUSIONS IN MIXED-OXIDE FUEL. Michels, L. C.; Poeppel, R. B.; Neimark, L. A. (Argonne National Lab., Ill.). Trans. Amer. Nucl. Soc.: 13: 601-2(Nov 1970).
From Meeting of the American Nuclear Society, Washington, D. C. See CONF-701102.

6015 FISSION GAS RELEASE MEASUREMENTS FROM FAST BREEDER $(U,Pu)O_2$ FUEL. Longest, A. W. (Oak Ridge National Lab., Tenn.); Baldwin, N.; Conlin, J. A.; Fitts, R. B.; Lindgren, J. R. Trans. Amer. Nucl. Soc.: 13: 604(Nov 1970).
From Meeting of the American Nuclear Society, Washington, D. C. See CONF-701102.

6016 TRANSIENT PERFORMANCE OF SOL-GEL $(U,Pu)O_2$ SPHERE-PAC AND PELLET FUELS. Cox, C. M.; Manthos, E. J.; Cuneo, D. R. (Oak Ridge National Lab., Tenn.). Trans. Amer. Nucl. Soc.: 13: 653-4(Nov 1970).
From Meeting of the American Nuclear Society, Washington, D. C. See CONF-701102.

6017 EFFECT ON ADJACENT PINS OF SWELLING OF A FAILED PIN. Gee, William R. Jr. (General Electric Co., Sunnyvale, Calif.). Trans. Amer. Nucl. Soc.: 13: 660-1(Nov 1970).
From Meeting of the American Nuclear Society, Washington, D. C. See CONF-701102.

6018 FAST REACTOR FUEL FAILURE THRESHOLDS AND MECHANISMS. Field, John H.; Thomas, Garry R. (General Electric Co., Sunnyvale, Calif.). Trans. Amer. Nucl. Soc.; 13: 719(Nov 1970).
From Meeting of the American Nuclear Society, Washington, D. C. See CONF-701102.

6019 PRESSURE EQUALIZATION SYSTEM FOR GCFR FUEL ELEMENTS. Campana, Robert J. (Gulf General Atomic, Inc., San Diego, Calif.). Trans. Amer. Nucl. Soc.; 13: 775-6 (Nov 1970).
From Meeting of the American Nuclear Society, Washington, D. C. See CONF-701102.

6020 ACCOMMODATION OF RADIATION SWELLING IN THE GCFR. Hopkins, H.; Buttemer, D.; Dee, J. (Gulf General Atomic, Inc., San Diego, Calif.). Trans. Amer. Nucl. Soc.; 13: 776-7(Nov 1970).
From Meeting of the American Nuclear Society, Washington, D. C. See CONF-701102.

6021 EFFECT OF SUBASSEMBLY CLEARANCE ON FAST REACTOR PERFORMANCE CHARACTERISTICS. Madell, J. T. (Argonne National Lab., Ill.). Trans. Amer. Nucl. Soc.; 13: 777 (Nov 1970).
From Meeting of the American Nuclear Society, Washington, D. C. See CONF-701102.

6022 COLD-WRAPPER TUBE APPROACH FOR ACCOMMODATING STEEL SWELLING IN LMFBR'S. Huebotter, P. R.; Bump, T. R. (Argonne National Lab., Ill.). Trans. Amer. Nucl. Soc.; 13: 778-9(Nov 1970).
From Meeting of the American Nuclear Society, Washington, D. C. See CONF-701102.

6023 (U,Pu)C AS AN ALTERNATE RELOAD FUEL FOR LMFBR'S INITIALLY FUELED WITH $(U,Pu)O_2$. Tomonto, James R.; Fiscella, John M. (United Nuclear Corp., Elmsford, N. Y.). Trans. Amer. Nucl. Soc.; 13: 779-80(Nov 1970).
From Meeting of the American Nuclear Society, Washington, D. C. See CONF-701102.

6024 FUEL CYCLE DEVELOPMENT: DECISION ANALYSIS UNDER UNCERTAINTY. Scarborough, J. C. (Nuclear Utilities Services, Inc., Rockville, Md.). Trans. Amer. Nucl. Soc.; 13: 786(Nov 1970).
From Meeting of the American Nuclear Society, Washington, D. C. See CONF-701102.

6025 PROGRESS IN XENON TAGGING. Henault, P. B.; Larson, W. J.; Rice, R. E.; Wilkes, C. W. (Argonne National Lab., Idaho Falls, Idaho). Trans. Amer. Nucl. Soc.; 13: 797-8 (Nov 1970).
From Meeting of the American Nuclear Society, Washington, D. C. See CONF-701102.

6026 XENON TAG PROOF TEST. Henault, P. B. (Argonne National Lab., Idaho Falls, Idaho); Ebersole, E. R.; Laug, M. T.; Villarreal, R.; Walker, D. E. Trans. Amer. Nucl. Soc.; 13: 798(Nov 1970).
From Meeting of the American Nuclear Society, Washington, D. C. See CONF-701102.

6027 SUBCHANNEL COOLANT TEMPERATURES OF EBR-II INSTRUMENTED SUBASSEMBLY PNL-17(XX02). Millhollen, M. K.; Sutey, A. M. (Battelle-Northwest, Richland, Wash.). Trans. Amer. Nucl. Soc.; 13: 806-7(Nov 1970).
From Meeting of the American Nuclear Society, Washington, D. C. See CONF-701102.

6028 TRANSFER OF COOLANT BETWEEN ADJACENT SUBCHANNELS IN WIRE WRAP AND GRID SPACER ROD BUNDLES. Marian, V. R.; Hines, D. P. (General Electric Co., Sunnyvale, Calif.). Trans. Amer. Nucl. Soc.; 13: 807-8(Nov 1970).
From Meeting of the American Nuclear Society, Washington, D. C. See CONF-701102.

6029 ADAPTING COMMERCIAL HEATERS TO SIMULATE LMFBR FUEL RODS IN SODIUM. Clark, David L. (Oak Ridge National Lab., Tenn.). Trans. Amer. Nucl. Soc.; 13: 817-18 (Nov 1970).
From Meeting of the American Nuclear Society, Washington, D. C. See CONF-701102.

6030 PARALLEL-FLOW-INDUCED VIBRATION OF AN EBR-II SUBASSEMBLY. Chang, L. K. (Argonne National Lab., Ill.). Trans. Amer. Nucl. Soc.; 13: 829(Nov 1970).
From Meeting of the American Nuclear Society, Washington, D. C. See CONF-701102.

6031 NEUTRONIC AND THERMAL HYDRAULIC ANALYSES OF MIXED CORES FOR EBR-II. Gillette, J. L.; Golden, G. H. (Argonne National Lab., Ill.). Trans. Amer. Nucl. Soc.; 13: 830(Nov 1970).
From Meeting of the American Nuclear Society, Washington, D. C. See CONF-701102.

6032 LIFE-I, A HISTORY-DEPENDENT ANALYSIS OF FAST REACTOR FUEL ELEMENT BEHAVIOR. Jankus, V. Z.; Weeks, R. W. (Argonne National Lab., Ill.). Trans. Amer. Nucl. Soc.; 13: 830-1(Nov 1970).
From Meeting of the American Nuclear Society, Washington, D. C. See CONF-701102.

6033 PROFILOMETER FOR THE DIMENSIONAL INSPECTION OF IRRADIATED LMFBR FUEL ELEMENTS. Koprowski, B. J.; Donahue, D. A.; Neimark, L. A. (Argonne National Lab., Ill.). Trans. Amer. Nucl. Soc.; 13: 851(Nov 1970).

From Meeting of the American Nuclear Society, Washington, D. C. See CONF-701102.

Auxiliary and Emergency Systems

6034 (ORNL-TM-2412(Pt.5)) DESIGN CONSIDERATIONS OF REACTOR CONTAINMENT SPRAY SYSTEMS. PART V. PROTECTIVE COATINGS TESTS. Griess, J. C.; Row, T. H.; Watson, C. D.; West, G. A. (Oak Ridge National Lab., Tenn.). Oct 1970. Contract W-7405-eng-26. 50p. Dep. NTIS.

Protective coatings to be used in reactor containment structures were subjected to the high temperature and radiation conditions possible in such containment structures following a design basis accident. It is necessary to assure that the coatings are not removed in large quantities that might inhibit or negate proper operation of emergency cooling equipment. Thirty-five different protective coatings were tested in a recirculating loop facility, while 106 different coatings were placed in the Carolinas-Virginia Test Reactor containment building and subjected to four steam system blowdown tests. In the loop tests the coatings were examined for resistance to two proposed containment spray system solutions, 0.15 m NaOH + 0.28 m $Na_2S_2O_3$, at several temperatures. The blowdown tests at CVTR also included some spraying with process water for pressure reduction. 12 references. (auth)

6035 (ORNL-TM-2412(Pt.8)) DESIGN CONSIDERATIONS OF REACTOR CONTAINMENT SPRAY SYSTEMS. PART VIII. BOILING WATER REACTOR ACCIDENT RADIOLYSIS STUDIES. Zittel, H. E. (Oak Ridge National Lab., Tenn.). Oct 1970. Contract W-7405-eng-26. 18p. Dep. NTIS.

Boiling water reactors (BWR) currently under construction are designed so that in case of a loss-of-coolant accident, water from the pressure suppression pool can be recirculated through the reactor core. The primary function of this recirculating water is pressure suppression during the system blowdown sequence and core cooling. During this post-accident function the water may be expected to be exposed to a radiation dose of $>10^8$ rads in a relatively short time. Because of the relatively small containment volume of a typical BWR the rate of evolution as well as the "steady-state" concentration of radiolytic gas is extremely important. The effects of various parameters on these points are considered. The parameters covered are flow rate (100 to 10,000 gpm), temperature (65 to 125°C), gas-liquid ratio (1.0 to 5.0), and composition of cover gas (air, 95% N_2 – 5% O_2). The variation of these parameters within the limits specified indicates that the lower limit for "steady-state" radiolytic hydrogen concentration is between ~3 to 4 vol %. (auth)

6036 (RISO-214, pp 41-55) RELIABILITY AND AVAILABILITY OF TWO BWR SHUT-DOWN SYSTEMS. Daublebsky, P. K.; Koch, E. H. (Allgemeine Elektricitaets-Gesellschaft, Frankfurt am Main (West Germany)).

From Proceedings of the meeting of specialists on the reliability of mechanical components and systems for nuclear reactor safety, Risoe, September 24–26, 1969.

Two scram systems were used to show that a system that has to perform the same job on request simultaneously for many independent components (control rods), can be built more reliably and more economically if an oversize network of components is used instead of a system composed of many independent blocks. This holds true even if some of the components need not be supplied. The analysis shows that commonly used failure rates are too poor for the carefully fabricated and thoroughly controlled components of reactor stand-by systems. It is described in detail to what extent system availability may be maintained by reduction of control time in case one component of an oversize system needs repair and the others are not available during test. (auth) (Denmark)

6037 (RISO-214, pp 57-70) RELIABILITY ASSESSMENT OF A NOVEL LIQUID ROD SHUT-DOWN SYSTEM. Galli de Paratesi, S.; Ghiurghi, L.; Musik, H. (European Atomic Energy Community, Ispra (Italy). Joint Nuclear Research Center).

From Proceedings of the meeting of specialists on the reliability of mechanical components and systems for nuclear reactor safety, Risoe, September 24–26, 1969.

Special systems of liquid shutdown rods have been developed for the installation of safety rods and related mechanisms, and a prototype system is now under completion. The full-scale prototype, which follows a feasibility mock-up, has been deemed necessary mainly for long-term operation and reliability tests before the system is put in actual service in a reactor. An attempt is made to predict the system reliability before any practical result can be drawn from the prototype testing. The prediction is based on published failure rate data for electro-mechanical devices, and the exponential distribution is used throughout. Calculations will include fractional dead time for unrevealed and revealed faults and the relevant probabilities and spurious trip probabilities. The numerical results of the prediction are intended as a preliminary evaluation, to be confirmed and/or completed with data gathered during the prototype operation and bench tests on components. 5 references. (auth) (Denmark)

6038 (RISO-214, pp 91-126) RELIABILITY OF EMERGENCY CORE COOLING SYSTEMS OF LIGHT WATER NUCLEAR POWER PLANTS. Bastl, W.; Gieseler, H. (Technische Hochschule, Munich (West Germany). Institut fuer Mess- und Regelungstechnik); Maurer, H. A. (European Communities, Brussels (Belgium). Commission).

From Proceedings of the meeting of specialists on the reliability of mechanical components and systems for nuclear reactor safety, Risoe, September 24–26, 1969.

Two emergency core cooling systems installed in German light-water power plants were compared. On the basis of detailed flow schemes and reliability diagrams the functions of the different subsystems are discussed with respect to two examples of loss-of-coolant accidents. The reliability of these systems is analysed and compared. The study was performed by means of a digital computer program. (auth) (Denmark)

6039 (RISO-214, pp 213-46) SYSTEM DESIGN OF REACTOR CHARGING EQUIPMENT BASED ON RELIABILITY CONSIDERATIONS. Hennings, U. (Brown Boveri/Krupp Reaktorbau G.m.b.H., Mannheim (West Germany)). (In German).

From Proceedings of the meeting of specialists on the reliability of mechanical components and systems for nuclear reactor safety, Risoe, September 24–26, 1969.

The charging equipment for fuel elements in a 300 MW(e) pebble bed reactor is described. Estimates are made of the reliability of different redundant configurations of the inspection system. Based on generic failure rates for all mechanical components, system unavailability is predicted to be 19 days in 30 years and 0.9 days in 30 years respectively. (Denmark)

6040 (RISO-214, pp 247-53) DEMONSTRATION OF THE PERFORMANCE AND RELIABILITY OF THE GENERAL ELECTRIC CO. BOILING WATER REACTOR MAIN STEAMLINE ISOLATION VALVES. Jacobs, I. M. (General Electric Co., San Jose, Calif. Atomic Power Equipment Dept.).

From Proceedings of the meeting of specialists on the reliability of mechanical components and systems for nuclear reactor safety, Risoe, September 24–26, 1969.

A demonstration programme is described in which tests are performed on valves in the main steam line isolating the inner containment in case of steam line rupture. The valves were tested close to the severe conditions of high steam flow and high velocity steam-water mixtures in the event of steam line break. 7 references. (Denmark)

6041 CORE THERMAL PERFORMANCE MARGINS FOR BOTTOM FLOODING ECC SYSTEMS. Shumway, R. W.; Zane, J. O. (Idaho Nuclear Corp., Idaho Falls). Trans. Amer. Nucl. Soc.; 13: 678-9(Nov 1970).

From Meeting of the American Nuclear Society, Washington, D. C. See CONF-701102.

6042 EFFECT OF 75 TO 100 PERCENT FLOW BLOCKAGE ON BOTTOM COOLING HEAT TRANSFER EFFECTIVENESS. Dominicis, D. P.; Cadek, F. F.; Leyse, R. H.; Cermak, J. O. (Westinghouse Electric Corp., Pittsburgh). Trans. Amer. Nucl. Soc.; 13: 681-2(Nov 1970).

From Meeting of the American Nuclear Society, Washington, D. C. See CONF-701102.

6043 ECC VARIABLE FLOODING RATE SIMULATION PWR FLECHT TEST RESULTS. Cadek, F. F.; Dominicis, D. P.; Leyse, R. H.; Cermak, J. O. (Westinghouse Electric Corp., Pittsburgh). Trans. Amer. Nucl. Soc.; 13: 682-3(Nov 1970).

From Meeting of the American Nuclear Society, Washington, D. C. See CONF-701102.

6044 IN-CORE DETECTOR FOR MEASURING POWER AND BREEDING DISTRIBUTIONS IN POWER BREEDERS. Goldstein, N. P.; Sun, K. H.; Gonzalez, J. L. (Westinghouse Electric Corp., Pittsburgh). Trans. Amer. Nucl. Soc.; 13: 791(Nov 1970).

XUM

From Meeting of the American Nuclear Society, Washington, D. C. See CONF-701102.

6045 INTEGRATED REACTOR PROTECTIVE SYSTEM. Ball, R. M.; Kubik, R. N.; Lewis, R. H. (Babcock and Wilcox Co., Lynchburg, Va.). Trans. Amer. Nucl. Soc.; 13: 791-2(Nov 1970).
From Meeting of the American Nuclear Society, Washington, D. C. See CONF-701102.

6046 SODIUM-VAPOR MONITOR. Meyer, J. F. (Argonne National Lab., Ill.); Johnson, T. W.; Sustman, J. E. Trans. Amer. Nucl. Soc.; 13: 794(Nov 1970).
From Meeting of the American Nuclear Society, Washington, D. C. See CONF-701102.

6047 GAS DETECTION WITH A CHOKED CONVERGING-DIVERGING NOZZLE. Henry, Robert E. (Argonne National Lab., Ill.). Trans. Amer. Nucl. Soc.; 13: 794-5(Nov 1970).
From Meeting of the American Nuclear Society, Washington, D. C. See CONF-701102.

6048 PRODUCTION OF BOILING IN THE HIGH FLUX ISOTOPE REACTOR FOR THE PURPOSE OF INVESTIGATING BOILING DETECTION METHODS. Binford, F. T.; Haack, L. A. (Oak Ridge National Lab., Tenn.). Trans. Amer. Nucl. Soc.; 13: 798-9(Nov 1970).
From Meeting of the American Nuclear Society, Washington, D. C. See CONF-701102.

6049 CONTAMINATION CONTROL OF SODIUM FIRES FROM LIQUID-METAL-COOLED REACTORS. First, Melvin W. (Harvard School of Public Health, Boston). Trans. Amer. Nucl. Soc.; 13: 842(Nov 1970).
From Meeting of the American Nuclear Society, Washington, D. C. See CONF-701102.

Operation and Economics

6050 (DOCKET-50231-59) SOUTHWEST EXPERIMENTAL FAST OXIDE REACTOR. Malfunction of the Emergency Electrical System Tie Breakers. (General Electric Co., Sunnyvale, Calif. Breeder Reactor Development Operation). 5 Aug 1970. 4p. Dep. NTIS.

6051 (DP-Report-434) FUEL CYCLES IN HIGH TEMPERATURE REACTORS: THE APPROACH TOWARDS THERMAL BREEDING ON THE THORIUM FUEL CYCLE. Project DRAGON. Graziani, G. (Atomic Energy Establishment, Winfrith (England)). May 1966. 27p. Dep. NTIS.

The high conversion High Temperature Reactor systems were studied on a continuous charge/discharge basis. The total fuel cycle costs was calculated for different cost assumptions. The role of high conversion systems in an expanding economy was investigated with regards to the conservation of the nuclear resources. (auth)

6052 (DP-Report-440) HELTOT: A PROGRAMME SYSTEM FOR ANALYSIS OF FUEL CYCLES ASSUMING OFF-LOAD REFUELLING (SUITABLE FOR URANIUM SYSTEMS: BURN-UP, COSTING, DATA PROCESSING). Project DRAGON. Bruneder, H. (Atomic Energy Establishment, Winfrith (England)). Jun 1966. 131p. Dep. NTIS.

A program system is described which enables evaluation of a fuel cycle survey, consisting of a zero-dimensional off-load burn-up program (HELIOS), a cost program and a data evaluation part. Auxiliary programs for input preparation and plotting automatically results on graphs are incorporated as well. It is mainly intended for Th/^{235}U systems. (auth)

6053 POWER REACTOR STRATEGIES AND THEIR EFFECTS ON FUEL CYCLE REQUIREMENTS. Boxer, L. W. (European Nuclear Energy Agency, Paris). Trans. Amer. Nucl. Soc.; 13: 467-8(Nov 1970).
From Meeting of the American Nuclear Society, Washington, D. C. See CONF-701102.

6054 CONSIDERATIONS ON THE IN-CORE FUEL MANAGEMENT DURING STARTUP OF A FAST BREEDER REACTOR. Billaux, M.: (Belgonucleaire, Brussels): Goldschmidt, P.: Vandenberg, C.: Spenke, H.: Wehmann, U. Trans. Amer. Nucl. Soc.: 13: 469(Nov 1970).
From Meeting of the American Nuclear Society, Washington, D. C. See CONF-701102.

6055 NUCLEAR AND ECONOMIC PERFORMANCE OF NIOBIUM AND MOLYBDENUM IN LMFBR CORES. Bennett, L. L.; Thomas, W. E.; Homan, F. J. (Oak Ridge National Lab., Tenn.). Trans. Amer. Nucl. Soc.; 13: 469-70(Nov 1970).
From Meeting of the American Nuclear Society, Washington, D. C. See CONF-701102.

6056 COMPARISON OF RECYCLE IN LWR'S AND HTGR'S. Macnabb, W. V.; Scarborough, J. C. (NUS Corp., Rockville, Md.). Trans. Amer. Nucl. Soc.; 13: 470-1(Nov 1970).
From Meeting of the American Nuclear Society, Washington, D. C. See CONF-701102.

6057 INDIFFERENCE VALUE OF ^{232}U IN AN HTGR. Macnabb, W. V.; Born, U. (NUS Corp., Rockville, Md.). Trans. Amer. Nucl. Soc.; 13: 471-2(Nov 1970).
From Meeting of the American Nuclear Society, Washington, D. C. See CONF-701102.

6058 SEFOR EXPERIMENTS. Pflasterer, G. R.; Skavdahl, R. E.; Noble, L. D. (General Electric Co., Sunnyvale, Calif.). Trans. Amer. Nucl. Soc.; 13: 719-20(Nov 1970).
From Meeting of the American Nuclear Society, Washington, D. C. See CONF-701102.

6059 MAINTENANCE OF THE MOLTEN SALT REACTOR EXPERIMENT. Haubenreich, Paul N. (Oak Ridge National Lab., Tenn.). Trans. Amer. Nucl. Soc.; 13: 789-90(Nov 1970).
From Meeting of the American Nuclear Society, Washington, D. C. See CONF-701102.

6060 GAP CONDUCTANCE OF OXIDE FUEL ELEMENTS IRRADIATED IN EBR-II. Cushman, R. A. (Argonne National Lab., Idaho Falls, Idaho). Trans. Amer. Nucl. Soc.; 13: 806 (Nov 1970).
From Meeting of the American Nuclear Society, Washington, D. C. See CONF-701102.

Safety and Siting

Refer also to abstract 6104.

6061 (IN-1431) WHAM PREDICTION OF SEMISCALE TEST RESULTS. Gruen, G. E. (Idaho Nuclear Corp., Idaho Falls). Oct 1970. Contract AT(10-1)-1230. 49p. Dep. NTIS.

The WHAM computer code was used extensively for prediction of subcooled pressure histories in the semiscale system. The various semiscale configurations included a vessel with internals simulating those of a large pressurized water reactor, and a vessel with a coolant loop having a double-ended-break capability. Comparisons of the analytical results with the experimental data showed that WHAM accurately predicts the pressure histories for blowdowns produced by small breaks. Less accurate, but more conservative, predictive results were obtained from analyses of large breaks. The conclusion was reached that calculated pressure histories from WHAM are sufficiently reliable for use as forcing function input to structural dynamics codes employed in predictive analyses of postulated large PWR decompressions. (auth)

6062 (RISO-214) PROCEEDINGS OF THE MEETING OF SPECIALISTS ON THE RELIABILITY OF MECHANICAL COMPONENTS AND SYSTEMS FOR NUCLEAR REACTOR SAFETY, RISOE, 24-26 SEPTEMBER 1969. (Danish Atomic Energy Commission, Risoe, Research Establishment). Feb 1970. 646p. (In several languages). (CONF-690951). NTIS (U. S. Sales Only).

Information on reactor systems is presented under the following headings: light mechanical systems and equipment; heavy dynamic mechanical systems and equipment; structures; and relevant experience from various fields. Separate abstracts are included for 16 of the 26 papers presented. (Denmark)

For abstracts of individual papers see: 4187, 5936, 5937, 5981-5984, 6036-6040, 6094, and 6189-6191.

6063 FAST REACTOR SAFETY IN THE NUCLEAR SCIENCE AND ENGINEERING CURRICULUM AT UCLA. Kastenberg, William E.; Erdmann, R. C. (Univ. of California, Los Angeles). Trans. Amer. Nucl. Soc.; 13: 458-9(Nov 1970).
From Meeting of the American Nuclear Society, Washington, D. C. See CONF-701102.

6064 IMPROVED METHOD FOR ASSESSING DAMAGE TO THE REACTOR VESSEL IN A FAST REACTOR ACCIDENT. Ma, P. Y.; Shum, R. H. (Argonne National Lab., Ill.). Trans. Amer. Nucl. Soc.; 13: 643-4(Nov 1970).
From Meeting of the American Nuclear Society, Washington, D. C. See CONF-701102.

XUM

6065 APPROACH FOR DETERMINING THE EFFECTIVE ENERGY RELEASE OF A FAST REACTOR ACCIDENT. Shum, R. H.; Ma, P. Y. (Argonne National Lab., Ill.). Trans. Amer. Nucl. Soc.; 13: 644-5(Nov 1970).
From Meeting of the American Nuclear Society, Washington, D. C. See CONF-701102.

6066 FAST REACTOR IMPLOSION STUDIES. Erdmann, R. C.; Boudreau, Jay E. (Univ. of California, Los Angeles). Trans. Amer. Nucl. Soc.; 13: 645-6(Nov 1970).
From Meeting of the American Nuclear Society, Washington, D. C. See CONF-701102.

6067 LIQUID FILM THICKNESS FOR SLUG EXPULSION. Fauske, Hans K.; Ford, W. D.; Grolmes, Michael A. (Argonne National Lab., Ill.). Trans. Amer. Nucl. Soc.; 13: 646-7(Nov 1970).
From Meeting of the American Nuclear Society, Washington, D. C. See CONF-701102.

6068 DELINEATION OF LMFBR SINGLE SUBASSEMBLY ACCIDENTS. Baker, L. Jr.; MacFarlane, D. R.; Marchaterre, J. F. (Argonne National Lab., Ill.). Trans. Amer. Nucl. Soc.; 13: 647-8(Nov 1970).
From Meeting of the American Nuclear Society, Washington, D. C. See CONF-701102.

6069 EFFECTS OF FUEL CHILLING ON DOPPLER-CONTROLLED FAST REACTOR ACCIDENTS. Davis, Richard; Kastenberg, William E.; Erdmann, Robert C. (Univ. of California, Los Angeles). Trans. Amer. Nucl. Soc.; 13: 648-9(Nov 1970).
From Meeting of the American Nuclear Society, Washington, D. C. See CONF-701102.

6070 COMPREHENSIVE ANALYSIS OF FLOW-INDUCED ACCIDENT INITIATING CONDITIONS IN AN LMFBR. Scott, J. H.; Williams, R. L. (Babcock and Wilcox Co., Lynchburg, Va.). Trans. Amer. Nucl. Soc.; 13: 649-50(Nov 1970).
From Meeting of the American Nuclear Society, Washington, D. C. See CONF-701102.

6071 QUASI THREE-DIMENSIONAL APPROACH FOR ESTIMATING SODIUM VOIDING INCOHERENCY. Waltar, Alan E.; Padilla, Andrew Jr. (Hanford Engineering Development Lab., Richland, Wash.). Trans. Amer. Nucl. Soc.; 13: 650(Nov 1970).
From Meeting of the American Nuclear Society, Washington, D. C. See CONF-701102.

6072 FURTHER STUDIES OF NON-COHERENT EFFECTS IN FAST REACTOR SODIUM VOIDING ACCIDENTS. Scott, J. H. (Babcock and Wilcox Co., Lynchburg, Va.); Reynolds, A. B. Trans. Amer. Nucl. Soc.; 13: 650-1(Nov 1970).
From Meeting of the American Nuclear Society, Washington, D. C. See CONF-701102.

6073 COOLANT VOIDING AND PRESSURE GENERATION DUE TO BOILING, FISSION GAS RELEASE, AND MOLTEN FUEL-COOLANT INTERACTION. Fauske, H. K. (Argonne National Lab., Ill.); Chawla, T. C.; Cronenberg, A. W.; Marchaterre, J. F. Trans. Amer. Nucl. Soc.; 13: 656-7(Nov 1970).
From Meeting of the American Nuclear Society, Washington, D. C. See CONF-701102.

6074 Na CRITICAL POINT DATA UNCERTAINTY IN Na-FUEL INTERACTION. Weatherwax, H. D.; Koehler, W. H. (Texas A and M Univ., College Station). Trans. Amer. Nucl. Soc.; 13: 657-8(Nov 1970).
From Meeting of the American Nuclear Society, Washington, D. C. See CONF-701102.

6075 RATE-LIMITED MODEL OF MOLTEN FUEL-COOLANT INTERACTIONS. Cho, D. H.; Wright, R. W. (Argonne National Lab., Ill.). Trans. Amer. Nucl. Soc.; 13: 659-60(Nov 1970).
From Meeting of the American Nuclear Society, Washington, D. C. See CONF-701102.

6076 MOLTEN UO_2-SODIUM DROPPING EXPERIMENTS. Armstrong, D. R.; Testa, F. J.; Raridon, D. Jr. (Argonne National Lab., Ill.). Trans. Amer. Nucl. Soc.; 13: 660(Nov 1970).
From Meeting of the American Nuclear Society, Washington, D. C. See CONF-701102.

6077 LOCAL CORE ACCIDENTS: A COMPARISON BETWEEN LMFBR'S AND LWR'S. van Erp, J. B.; Judd, A. M. (Argonne National Lab., Ill.). Trans. Amer. Nucl. Soc.; 13: 670(Nov 1970).
From Meeting of the American Nuclear Society, Washington, D. C. See CONF-701102.

6078 ANALYSIS BY STATIC SIMULATION FOR SHOCK PULSE LOADING OF CORE COMPONENTS. Cole, J. M. (General Electric Co., Sunnyvale, Calif.). Trans. Amer. Nucl. Soc.; 13: 671-2(Nov 1970).
From Meeting of the American Nuclear Society, Washington, D. C. See CONF-701102.

6079 PREDICTION AND MEASUREMENT OF ACOUSTIC WAVE PROPAGATION IN TWO-PHASE MEDIA. Mecredy, R. C.; Wigdortz, J. M.; Hamilton, L. J. (Univ. of Michigan, Ann Arbor). Trans. Amer. Nucl. Soc.; 13: 672-3(Nov 1970).
From Meeting of the American Nuclear Society, Washington, D. C. See CONF-701102.

6080 RADIONUCLIDES IN EFFLUENTS FROM BOILING WATER REACTOR. Brinck, W. L.; Krieger, H. L.; Gold, S.; Kolde, H. E.; Kahn, B. (Public Health Service, Cincinnati). Trans. Amer. Nucl. Soc.; 13: 674-5(Nov 1970).
From Meeting of the American Nuclear Society, Washington, D. C. See CONF-701102.

6081 SPACE-TIME KINETICS STUDIES FOR COMMERCIAL POWER REACTORS. Denning, R. S. (Battelle Memorial Inst., Columbus, Ohio). Trans. Amer. Nucl. Soc.; 13: 676(Nov 1970).
From Meeting of the American Nuclear Society, Washington, D. C. See CONF-701102.

6082 CONSEQUENCES OF EXTENSIVE FUEL MELTDOWN IN VARIOUS EBR-II CORE CONFIGURATIONS. Golden, G. H.; Shum, R. H. (Argonne National Lab., Ill.). Trans. Amer. Nucl. Soc.; 13: 677(Nov 1970).
From Meeting of the American Nuclear Society, Washington, D. C. See CONF-701102.

6083 FRACTURE OF SOLIDIFYING PARTICLES. Hsiao, K. H.; Cox, J. E.; Witte, L. C. (Univ. of Houston, Tex.). Trans. Amer. Nucl. Soc.; 13: 678(Nov 1970).
From Meeting of the American Nuclear Society, Washington, D. C. See CONF-701102.

6084 COOLANT FLOW DISTRIBUTION DURING DECOMPRESSION OF A SINGLE-LOOP SIMULATED PWR SYSTEM. Olson, D. J.; Whitbeck, J. F. (Idaho Nuclear Corp., Idaho Falls). Trans. Amer. Nucl. Soc.; 13: 679-80(Nov 1970).
From Meeting of the American Nuclear Society, Washington, D. C. See CONF-701102.

6085 SYSTEM THERMODYNAMICS AND EMERGENCY CORE COOLING SYSTEMS. Redfield, J. A.; Murphy, J. H. (Westinghouse Electric Corp., West Mifflin, Pa.). Trans. Amer. Nucl. Soc.; 13: 680-1(Nov 1970).
From Meeting of the American Nuclear Society, Washington, D. C. See CONF-701102.

6086 PROBLEMS IN FAST REACTOR CORE SAFETY. Wolfe, B. (Hanford Engineering and Development Lab., Richland, Wash.). Trans. Amer. Nucl. Soc.; 13: 717(Nov 1970).
From Meeting of the American Nuclear Society, Washington, D. C. See CONF-701102.

6087 AEC PROGRAMS IN FAST REACTOR CORE SAFETY. Pressesky, A. J.; Sinclair, E. E. (Atomic Energy Commission, Washington, D. C.). Trans. Amer. Nucl. Soc.; 13: 717-18(Nov 1970).
From Meeting of the American Nuclear Society, Washington, D. C. See CONF-701102.

6088 CORE MELT-THROUGH IN LMFBR'S. Fontana, M. H. (Oak Ridge National Lab., Tenn.). Trans. Amer. Nucl. Soc.; 13: 720-1(Nov 1970).
From Meeting of the American Nuclear Society, Washington, D. C. See CONF-701102.

6089 LARGE ACCIDENTS. Stratton, W. R.; Engle, L. B.; Peterson, D. M. (Los Alamos Scientific Lab., N. Mex.). Trans. Amer. Nucl. Soc.; 13: 721-2(Nov 1970).
From Meeting of the American Nuclear Society, Washington, D. C. See CONF-701102.

6090 ELRAFT: A COMPUTER PROGRAM FOR THE EFFICIENT LOGIC REDUCTION ANALYSIS OF FAULT TREES. Semanderes, Stavros N. (Westinghouse Electric Corp., Pittsburgh). Trans. Amer. Nucl. Soc.; 13: 781-2(Nov 1970).
From Meeting of the American Nuclear Society, Washington, D. C. See CONF-701102.

6091 CLASSIFICATION OF CRITICAL CHARACTERISTICS IN NUCLEAR PLANT DESIGN. Wilson, Robert L.; Jackson, John P. (Sacramento Municipal Utility District, Calif.). Trans. Amer. Nucl. Soc.; 13: 783(Nov 1970).

XUM

From Meeting of the American Nuclear Society, Washington, D. C. See CONF-701102.

6092 PRESSURE GENERATION AND POTENTIAL WORK ENERGY DURING FUEL-SODIUM THERMAL INTERACTION. Temme, M. I.; Goldstein, M. B.; Tschamper, P. M. (General Electric Co., Sunnyvale, Calif.). Trans. Amer. Nucl. Soc.; 13: 818(Nov 1970).
From Meeting of the American Nuclear Society, Washington, D. C. See CONF-701102.

Research and Test Reactors

Refer also to abstracts 4320, 4814, 5963, 5986, 5996, 6016, 6126, 6140, 6162, and 6185.

6093 (RCN–118) MEASUREMENTS AND CALCULATIONS ON THERMAL, ARGONAUT TYPE, CORES IN THE STEK-FACILITY AT PETTEN. Coehoorn, J.; Klippel, H. Th.; de Meulemeester, F. M.; (and others). (Reactor Centrum Nederland, Petten). Feb 1970. 69p. Dep. NTIS (U. S. Sales Only).

In November 1967, it was decided to convert the existing, heavily shielded, light water critical experiment KRITO at the Petten site of RCN, into a coupled fast-thermal system, in the fast zone of which by oscillator methods integral cross-sections of actual fission product-mixtures, -elements and -nuclides are to be measured. After completion of the construction in early May 1969, the new facility STEK (Fast-Thermal Experiment in KRITO) and its instrumentation have been thoroughly tested until a license was obtained for the loading of fuel in the thermal zone of the core. The possibility to build up the thermal Argonaut type cores in STEK was included in the design and it was decided to start the experimental program with the build-up of these cores to obtain experience with the installation and to have a starting point in the approach of the first coupled fast-thermal core. Thus the inner zone of the core was completely filled with graphite elements and then fuel plates were loaded in steps as symmetrically as possible in the 4 × 10 elements in the 4 slabs I, II, III and IV. On May 22nd, first criticality was obtained with a loading of 740 fuel plates, i.e., 15.34 kg ^{235}U (min. critical loading 725 fuel plates, 15.05 kg). In this 4-slab core a series of standard experiments have been performed such as the calibration of the control plates and stop rods, the measurement of the thermal neutron flux distribution and the reactor power, kinetic experiments to determine the neutron lifetime and coupling between the separate slabs and finally oscillator experiments to test the oscillator system and inverse kinetic program with the on-line computer. Afterwards a 3-slab core, a 2-slab core (adjacent slabs), a 2-slab core (opposite slabs) and a 1-slab core have been built up to determine the critical masses and neutron lifetimes and the neutron coupling coefficients between the slabs. The results of all these measurements are presented and are in some cases compared with calculations. (auth) (Netherlands)

6094 (RISO–214, pp 597-625) GENERAL PRINCIPLES OF A SAFETY ASSESSMENT THROUGH RELIABILITY ANALYSIS OF THE ESSOR PLANT. Cuoco, A.; Galvagni, R. (Comitato Nazionale per l'Energia Nucleare, Rome (Italy)); Leonelli, F. (European Atomic Energy Community, Ispra (Italy). Joint Nuclear Research Center).

From Proceedings of the meeting of specialists on the reliability of mechanical components and systems for nuclear reactor safety, Risoe, September 24–26, 1969.

For the purpose of a safety analysis of the ESSOR plant as comprehensive as possible, a probabilistic classification of both accident causes and engineered safeguards of the reactor plant has been prepared. This approach makes a homogeneous solution to the problem of the credibility of multiple faults possible. (auth) (Denmark)

6095 SUBCRITICAL FAST REACTOR AS A UNIVERSITY RESEARCH FACILITY. Ott, K. O. (Purdue Univ., Lafayette, Ind.); Terrell, C. W. Trans. Amer. Nucl. Soc.: 13: 456-7(Nov 1970).
From Meeting of the American Nuclear Society, Washington, D. C. See CONF-701102.

6096 FAILURE THRESHOLD TREAT EXPERIMENT WITH AN UNIRRADIATED PROTOTYPICAL FFTF FUEL ELEMENT. Rothman, A. B. (Argonne National Lab., Ill.); Agrawal, A. K.; Purviance, R. T.; (and others). Trans. Amer. Nucl. Soc.: 13: 652(Nov 1970).
From Meeting of the American Nuclear Society, Washington, D. C. See CONF-701102.

6097 HIGH-ENERGY TRANSIENT MELTDOWN OF IRRADIATED UO_2 IN A TREAT MARK-II LOOP. Deitrich, L. W. (Argonne National Lab., Ill.); Willis, F. L.; Purviance, R. T.; (and others). Trans. Amer. Nucl. Soc.; 13: 652-3(Nov 1970).
From Meeting of the American Nuclear Society, Washington, D. C. See CONF-701102.

6098 EFFECTS OF FISSION GAS ON TRANSIENT OVERPOWER FUEL ROD FAILURE. Stuart, Robin G.; Thomas, Garry R. (General Electric Co., Sunnyvale, Calif.). Trans. Amer. Nucl. Soc.; 13: 654-6(Nov 1970).
From Meeting of the American Nuclear Society, Washington, D. C. See CONF-701102.

6099 ACOUSTIC AND INERTIAL CONSTRAINTS IN MOLTEN FUEL-COOLANT INTERACTIONS. Wright, R. W.; Cho, D. H. (Argonne National Lab., Ill.). Trans. Amer. Nucl. Soc.: 13: 658-9(Nov 1970).
From Meeting of the American Nuclear Society, Washington, D. C. See CONF-701102.

6100 CRITICALITY CALCULATIONS AND MEASUREMENTS ON ENRICHED URANIUM METAL-SOLUTION COMBINATIONS. Hunt, D. C.; Rothe, R. E. (Dow Chemical Co., Golden, Colo.). Trans. Amer. Nucl. Soc.; 13: 662-3(Nov 1970).
From Meeting of the American Nuclear Society, Washington, D. C. See CONF-701102.

6101 NEW SMALL MASS CRITICAL CONFIGURATION. Olson, R. S.; Robkin, M. A. (Univ. of Washington, Seattle). Trans. Amer. Nucl. Soc.; 13: 669(Nov 1970).
From Meeting of the American Nuclear Society, Washington, D. C. See CONF-701102.

6102 CAPABILITIES OF THE PBF FOR LMFBR SAFETY TESTING. Johnson, R. T.; Crocker, J. G. (Idaho Nuclear Corp., Idaho Falls). Trans. Amer. Nucl. Soc.; 13: 670-1(Nov 1970).
From Meeting of the American Nuclear Society, Washington, D. C. See CONF-701102.

6103 RISK ESTIMATE FOR AN URBAN-SITED RESEARCH REACTOR. Otway, Harry J.; Lohrding, Ronald K.; Battat, Morris E. (Los Alamos Scientific Lab., N. Mex.). Trans. Amer. nucl. Soc.; 13: 675-6(Nov 1970).
From Meeting of the American Nuclear Society, Washington, D. C. See CONF-701102.

6104 DESIGN BASIS FOR THE LOSS-OF-FLUID TEST (LOFT) FACILITY. Davis, P. R.; Larson, J. R.; Curet, H. D. (Idaho Nuclear Corp., Idaho Falls). Trans. Amer. Nucl. Soc.: 13: 681(Nov 1970).
From Meeting of the American Nuclear Society, Washington, D. C. See CONF-701102.

6105 MEASURED NEUTRON SPECTRUM IN FTR-3, A PLUTONIUM-FUELED FAST SPECTRUM REACTOR. Yule, T. J.; Bennett, E. F. (Argonne National Lab., Ill.). Trans. Amer. Nucl. Soc.; 13: 687(Nov 1970).
From Meeting of the American Nuclear Society, Washington, D. C. See CONF-701102.

6106 FAST-NEUTRON SPECTRUM AND TIME MOMENTS OF PULSE DECAY IN A BULK ALUMINUM ASSEMBLY. Golay, M. W.; Kaushal, N. N.; Malaviya, B. K. (Rensselaer Polytechnic Inst., Troy, N. Y.). Trans. Amer. Nucl. Soc.: 13: 689(Nov 1970).
From Meeting of the American Nuclear Society, Washington, D. C. See CONF-701102.

6107 SPACE-DEPENDENT STEADY-STATE THERMAL-NEUTRON SPECTRA IN BERYLLIUM ABOVE THE CRITICAL BUCKLING. Lake, J. A.; Kallfelz, J. M. (Georgia Inst. of Tech., Atlanta). Trans. Amer. Nucl. Soc.; 13: 690-1(Nov 1970).
From Meeting of the American Nuclear Society, Washington, D. C. See CONF-701102.

6108 SPATIAL AND FEEDBACK EFFECTS IN THE GEORGIA TECH RESEARCH REACTOR. Bridges, D. N.; Reynolds, M. J.; Clement, J. D. (Georgia Inst. of Tech., Atlanta). Trans. Amer. Nucl. Soc.; 13: 699(Nov 1970).
From Meeting of the American Nuclear Society, Washington, D. C. See CONF-701102.

6109 PLUTONIUM AND ^{238}U DOPPLER MEASUREMENTS IN A PLUTONIUM-FUELED FAST CRITICAL ASSEMBLY. Pond, R. B.; Daughtry, J. W.; Till, C. E.; Groh, E. F.; Swanson, C. D. (Argonne National Lab., Ill.). Trans. Amer. Nucl. Soc.; 13: 710 (Nov 1970).
From Meeting of the American Nuclear Society, Washington, D. C. See CONF-701102.

6110 MEASUREMENT AND ANALYSIS OF REACTIVITY DOPPLER EFFECTS IN ZPR-3 ASSEMBLY 53. Kaiser, R. E.;

XUM

Gasidlo, J. M. (Argonne National Lab., Idaho Falls, Idaho). Trans. Amer. Nucl. Soc.; 13: 710-11(Nov 1970).
From Meeting of the American Nuclear Society, Washington, D. C. See CONF-701102.

6111 INTERCOMPARISON OF DOPPLER MEASUREMENTS MADE IN FAST CRITICAL ASSEMBLIES. Royden, Herbert N. (Atomics International, Canoga Park, Calif.). Trans. Amer. Nucl. Soc.; 13: 711-12(Nov 1970).
From Meeting of the American Nuclear Society, Washington, D. C. See CONF-701102.

6112 INVESTIGATION OF SODIUM-VOIDING REACTIVITIES AND OTHER SAFETY PARAMETERS IN FAST CRITICAL ASSEMBLIES. Till, C. E.; Davey, W. G. (Argonne National Lab., Ill.). Trans. Amer. Nucl. Soc.; 13: 718-19(Nov 1970).
From Meeting of the American Nuclear Society, Washington, D. C. See CONF-701102.

6113 PREDICTED CHARACTERISTICS WITH ACTUAL OBSERVATION FOR THE DEMONSTRATION REACTOR BENCHMARK ASSEMBLY ZPPR-2. Kaiser, R. E.; Norris, R. J.; Olson, A. P.; Paik, N. C. (Argonne National Lab., Idaho Falls, Idaho). Trans. Amer. Nucl. Soc.; 13: 732(Nov 1970).
From Meeting of the American Nuclear Society, Washington, D. C. See CONF-701102.

6114 CRITICAL EXPERIMENT NORMALIZATION FOR LMFBR'S. Specht, Eugene R. (Atomics International, Canoga Park, Calif.). Trans. Amer. Nucl. Soc.; 13: 732-3(Nov 1970).
From Meeting of the American Nuclear Society, Washington, D. C. See CONF-701102.

6115 MATERIAL WORTH MEASUREMENTS IN THE BENCHMARK CRITICAL ASSEMBLY ON ZPPR. Kaiser, R. E.; Norris, R. J.; Paik, N. C. (Argonne National Lab., Idaho Falls, Idaho). Trans. Amer. Nucl. Soc.; 13: 734-5(Nov 1970).
From Meeting of the American Nuclear Society, Washington, D. C. See CONF-701102.

6116 EXPERIMENTAL DETERMINATION OF THE PERTURBATION DENOMINATOR IN FAST CRITICAL ASSEMBLIES. Redman, W. C.; Bretscher, M. M. (Argonne National Lab., Ill.). Trans. Amer. Nucl. Soc.; 13: 736(Nov 1970).
From Meeting of the American Nuclear Society, Washington, D. C. See CONF-701102.

6117 CALCULATION OF THE REACTIVITY WORTH OF SMALL SAMPLES. Oosterkamp, W. J. (Kernforschungszentrum, Karlsruhe, Ger.). Trans. Amer. Nucl. Soc.; 13: 736-7(Nov 1970).
From Meeting of the American Nuclear Society, Washington, D. C. See CONF-701102.

6118 CALCULATION OF NEUTRON DETECTOR RESPONSE IN A SUBCRITICAL REACTOR. Waltz, W. R.; Walter, J. F. (Westinghouse Electric Corp., West Mifflin, Pa.). Trans. Amer. Nucl. Soc.; 13: 767(Nov 1970).
From Meeting of the American Nuclear Society, Washington, D. C. See CONF-701102.

6119 NRTS–ATR 1.4-MW FLOW-REVERSAL TEST: PRELIMINARY HEAT TRANSFER RATES AND COEFFICIENTS. Hanson, G. H.; Griebenow, M. L.; Richert, K. D. (Idaho Nuclear Corp., Idaho Falls). Trans. Amer. Nucl. Soc.; 13: 811-13(Nov 1970).
From Meeting of the American Nuclear Society, Washington, D. C. See CONF-701102.

6120 PULSE REACTOR RESEARCH AND SOME OPERATIONAL CONSIDERATIONS. Leonard, B. E. (Armed Forces Radiobiology Research Inst., Bethesda, Md.). Trans. Amer. Nucl. Soc.; 13: 825-6(Nov 1970).
From Meeting of the American Nuclear Society, Washington, D. C. See CONF-701102.

6121 ESTABLISHING SAFETY LIMITS AND LIMITING SAFETY SYSTEM SETTINGS FOR RESEARCH (PULSE) REACTORS. Lobbin, Fred (Hittman Nuclear and Development Corp., Columbia, Md.). Trans. Amer. Nucl. Soc.; 13: 826(Nov 1970).
From Meeting of the American Nuclear Society, Washington, D. C. See CONF-701102.

6122 PULSTAR: SIX YEARS OF OPERATION AND UTILIZATION. Burnett, P. T. (Western New York Nuclear Research Center, Inc., Buffalo). Trans. Amer. Nucl. Soc.; 13: 826-7(Nov 1970).
From Meeting of the American Nuclear Society, Washington, D. C. See CONF-701102.

6123 VISCOUS DAMPING OF PULSED REACTOR FUEL ELEMENTS. Grossman, R. J.; Hamilton, L. J. (Univ. of Michigan, Ann Arbor). Trans. Amer. Nucl. Soc.; 13: 828(Nov 1970).
From Meeting of the American Nuclear Society, Washington, D. C. See CONF-701102.

6124 ANALYSIS OF NEUTRON DISTRIBUTIONS IN THE ZPPR/FTR-2 SHIELD EXPERIMENTS. Martin, J. K.; Paquette, R. C. (Westinghouse Advanced Reactors Div., Madison, Pa.). Trans. Amer. Nucl. Soc.; 13: 876-7(Nov 1970).
From Meeting of the American Nuclear Society, Washington, D. C. See CONF-701102.

6125 GAMMA-RAY DOSE EVALUATIONS FOR THE ZPR-3/EBR-II CRITICAL ASSEMBLIES. Simons, G. G. (Argonne National Lab., Idaho Falls, Idaho); Stenstrom, D. G.; Meneghetti, D.; Keeney, W. P. Trans. Amer. Nucl. Soc.; 13: 880-1(Nov 1970).
From Meeting of the American Nuclear Society, Washington, D. C. See CONF-701102.

Rocket and Space Reactors

Refer also to abstract 4252.

6126 COMPARISON OF EXPERIMENTALLY MEASURED AND CALCULATED HEATING RATES INTERNAL TO THE PAX R-1 REACTOR. Hill, D. J. (Westinghouse Electric Corp., Pittsburgh). Trans. Amer. Nucl. Soc.: 13: 437-8(Nov 1970).
From Meeting of the American Nuclear Society, Washington, D. C. See CONF-701102.

6127 HEAT TRANSFER OPTIMIZATION AND REACTIVITY OF NUCLEAR ROCKET REACTORS. Simpson, Terry R.; Mason, Edward A. (Massachusetts Inst. of Tech., Cambridge). Trans. Amer. Nucl. Soc.; 13: 438(Nov 1970).
From Meeting of the American Nuclear Society, Washington, D. C. See CONF-701102.

6128 RADIATION TRANSPORT ANALYSES OF NUCLEAR ROCKET ENGINE COMPONENTS. Normand, E.; Lindstrom, D. G.; Wilcox, A. D. (Aerojet Nuclear Systems Co., Sacramento, Calif.). Trans. Amer. Nucl. Soc.; 13: 438-9(Nov 1970).
From Meeting of the American Nuclear Society, Washington, D. C. See CONF-701102.

6129 MONTE CARLO RADIATION TRANSPORT ANALYSES OF THE NERVA NOZZLE ASSEMBLY. Warkentin, J. K. (Radiation Research Associates, Inc., Fort Worth, Tex.); Courtney, J. C. Trans. Amer. Nucl. Soc.; 13: 439-40(Nov 1970).
From Meeting of the American Nuclear Society, Washington, D. C. See CONF-701102.

6130 COMPARISON OF EXPERIMENTALLY MEASURED AND CALCULATED NEUTRON AND PHOTON RADIATION LEVELS INTERNAL AND EXTERNAL TO MOCKUPS OF NUCLEAR ROCKET SHIELDS. Anderson, S. L.; Magaw, J. R. (Westinghouse Electric Corp., Pittsburgh). Trans. Amer. Nucl. Soc.; 13: 440-1(Nov 1970).
From Meeting of the American Nuclear Society, Washington, D. C. See CONF-701102.

6131 SHIELDING REQUIREMENTS FOR MANNED AND UNMANNED NERVA MISSIONS. Warman, E. A.; Rogers, D. R. (Aerojet Nuclear Systems Co., Sacramento, Calif.). Trans. Amer. Nucl. Soc.; 13: 441-2(Nov 1970).
From Meeting of the American Nuclear Society, Washington, D. C. See CONF-701102.

6132 IN-FLIGHT COOLANT MANAGEMENT CONSIDERATIONS FOR THE NERVA REACTOR COOLDOWN. Misra, Balabhadra; Altseimer, John H.; Hart, Gene D. (Aerojet Nuclear Systems Co., Sacramento, Calif.). Trans. Amer. Nucl. Soc.; 13: 442(Nov 1970).
From Meeting of the American Nuclear Society, Washington, D. C. See CONF-701102.

6133 SPHERICAL GAS CORE REACTOR PHYSICS MEASUREMENTS. Lofthouse, J. H.; Kunze, J. F. (Idaho Nuclear Corp., Idaho Falls). Trans. Amer. Nucl. Soc.; 13: 443(Nov 1970).
From Meeting of the American Nuclear Society, Washington, D. C. See CONF-701102.

6134 ANGULAR AND WAVELENGTH DEPENDENCE OF THERMAL RADIATION TRANSMITTED THROUGH REFRACTORY AEROSOLS. Williams, J. R.; Jacobs, W. R.; Byrn, N. R. (Geor-

XUM

gia Inst. of Tech., Atlanta). Trans. Amer. Nucl. Soc.; 13: 443-4(Nov 1970).
From Meeting of the American Nuclear Society, Washington, D. C. See CONF-701102.

6135 RADIANT HEAT TRANSFER IN HEATED AEROSOLS AT 100 ATMOSPHERES PRESSURE. Partain, W. L.; Williams, J. R.; Clement, J. D. (Georgia Inst. of Tech., Atlanta). Trans. Amer. Nucl. Soc.; 13: 444-5(Nov 1970).
From Meeting of the American Nuclear Society, Washington, D. C. See CONF-701102.

6136 ROVER: AN INTERMEDIATE STEP TO GAS. Mills, Carroll B. (Los Alamos Scientific Lab., N. Mex.). Trans. Amer. Nucl. Soc.; 13: 445-6(Nov 1970).
From Meeting of the American Nuclear Society, Washington, D. C. See CONF-701102.

6137 STUDY OF A GAS CORE REACTOR: MHD POWER PLANT CONCEPT. Williams, J. R. (Georgia Inst. of Tech., Atlanta). Trans. Amer. Nucl. Soc.; 13: 446-7(Nov 1970).
From Meeting of the American Nuclear Society, Washington, D. C. See CONF-701102.

6138 SPACECRAFT CONFIGURATION AND OPERATIONAL TRADEOFFS FOR NUCLEAR POWER SOURCES. Haffner, J. W.; Liley, B. (North American Rockwell Corp., Downey, Calif.). Trans. Amer. Nucl. Soc.; 13: 447(Nov 1970).
From Meeting of the American Nuclear Society, Washington, D. C. See CONF-701102.

6139 OPERATING REACTIVITY FEEDBACK EFFECTS IN THE NERVA REACTOR. Call, D. W. (Westinghouse Electric Corp., Pittsburgh). Trans. Amer. Nucl. Soc.; 13: 699-700(Nov 1970).
From Meeting of the American Nuclear Society, Washington, D. C. See CONF-701102.

6140 PRELIMINARY ANALYSIS OF A MOLYBDENUM-REFLECTED, FAST SPECTRUM CRITICAL ASSEMBLY. Klann, Paul G. (Lewis Research Center, Cleveland); Mayo, Wendell; Springer, T. H. Trans. Amer. Nucl. Soc.; 13: 731(Nov 1970).
From Meeting of the American Nuclear Society, Washington, D. C. See CONF-701102.

6141 EVALUATION OF ELECTRICALLY TESTED NERVA REACTOR FUEL ELEMENTS. Guzek, J. C.; Davidson, S. L.; Khan, M. P. (Westinghouse Electric Corp., Pittsburgh). Trans. Amer. Nucl. Soc.; 13: 816-17(Nov 1970).
From Meeting of the American Nuclear Society, Washington, D. C. See CONF-701102.

6142 HIGH REYNOLDS NUMBER, LOW TEMPERATURE, NOBLE GAS ADSORPTION BED DESIGN. Fenstermacher, Charles A. (Los Alamos Scientific Lab., N. Mex.). Trans. Amer. Nucl. Soc.; 13: 834-5(Nov 1970).
From Meeting of the American Nuclear Society, Washington, D. C. See CONF-701102.

Process Heat and Desalination Reactors

Refer also to abstract 5881.

6143 PRELIMINARY DESIGN AND FEASIBILITY STUDY OF A NUCLEAR-POWERED AGRO-INDUSTRIAL COMPLEX IN IRAN. Jalali-Mossallam, Ebrahim. Ames, Iowa; Iowa State Univ. (1969). 94p. University Microfilms Order No. 70-13,593.
Thesis.
The technical and economic feasibility of a relatively large nuclear-powered agro-industrial complex along the south desert coastal region of Iran for the production of basic industrial and agricultural products using desalted water is analyzed. It was found that for power requirements larger than 300 MW(e) a nuclear-fueled power plant is the only choice which is economically feasible. Considering the advantages and disadvantages of different reactor types and the conditions of the South coast of Iran, the boiling water reactor was found to be the most suitable for the production of steam for power and water production. Then a preliminary design of a boiling water reactor with 2800 MW thermal capacity was performed. An economic analysis was made to find which industrial and agricultural products are profitable on the basis of estimated costs of electricity and water of 3.4 mills/kwhr and 20¢/1000 gal respectively. A second economic analysis was made to find the internal rate of return of the entire complex with a capacity of 500 Mgd water and 1200 MW(e) power. Since the power and water required for production uses would be produced within the complex, the costs of power and water were not estimated directly, but rather all the capital and operation costs for producing these inputs were included in arriving at the total costs for operating the overall complex. (Diss. Abstr.)

6144 DESIGN EVALUATION OF SMALL NUCLEAR POWER-DESALTING PLANTS. Anderson, R. T.; Bell, J. H. (Hittman Nuclear and Development Corp., Columbia, Md.). Trans. Amer. Nucl. Soc.; 13: 827-8(Nov 1970).
From Meeting of the American Nuclear Society, Washington, D. C. See CONF-701102.

Marine and Portable Power Reactors

Refer also to abstract 5990.

6145 (AD-709898) ANALYSIS OF NEUTRON-EMBRITTLEMENT AND FLUX-DENSITY CONSIDERATIONS OF THE ARMY SM-1 REACTOR PRESSURE VESSEL. Serpan, Charles Z. Jr. (Naval Research Lab., Washington, D. C.). 22 Jun 1970. 24p. (NRL-7101). NTIS.
The Army SM-1 reactor was evaluated with respect to the increase in transition temperature of the A212-B steel pressure vessel. Although steel from the heat forming the vessel is not available for irradiation-response behavior testing, the initial transition temperature of 40°F (4°C) was determined from vessel steel. A relationship between increasing embrittlement for a 4-in.-thick plate of A212-B steel, representing the ASTM reference heat for this composition, and increasing neutron fluence was established for the irradiation temperature conditions of the SM-1 reactor. Combining with this the Army-imposed transition temperature limit for the SM-1 reactor vessel of 295°F (146°C) results in a fluence value of 2.65 × 10 to the 19th power n/sq.cm. > 0.5 MeV for a lifetime vessel exposure. The neutron flux level for the vessel was established by extrapolating a core-region flux measurement using the results of a calculated neutron spectrum at the reactor vessel. (auth) (USGRDR)

6146 THROUGH- THICKNESS DUCTILITY IN AN IRRADIATED REACTOR PRESSURE VESSEL WALL. Serpan, Charles Z. Jr. (Naval Research Lab., Washington, D. C.). Trans. Amer. Nucl. Soc.; 13: 611-13(Nov 1970).
From Meeting of the American Nuclear Society, Washington, D. C. See CONF-701102.

Production Reactors

Kinetics

Refer also to abstracts 5954, 5956, 5959, 5962, and 5965–5968.

6147 BOUNDS FOR THE SOLUTIONS OF NONLINEAR PARABOLIC EQUATIONS. Reister, David Bryan. Berkeley, Calif.; Univ. of California (1969). 237p. University Microfilms Order No. 70-13,147.
Thesis.
A comparison theorem of the Nagumo-Westphal type is used to find upper and lower bounds for the solutions of the nonlinear parabolic equations that determine the space-time behavior of a nuclear reactor with temperature feedback. Pontryagin's Maximum Principle is used to determine optimal bounds. Previous comparison theorems are not valid for problems with negative temperature feedback. To find bounds for these problems, a new general comparison theorem has been proven. This theorem permits the coupling of the upper and lower bounds which negative feedback requires. Furthermore, the theorem is applicable to multiregion problems. The comparison theorem is used to derive an ordinary differential equation that determines the amplitude function for each choice of the control function. Using optimal control theory, the control function is chosen to minimize the upper bound and maximize the lower bound. Bounds have been determined for reactors with prompt, adiabatic, and Newtonian feedback. The bounds satisfy ordinary differential equations which closely resemble the point kinetics equations. Using the bounds, simple expressions for the maximum values of the neutron flux and temperature in a reactor have been developed. (Diss. Abstr.)

6148 RESPONSE OF A COUPLED-CORE REACTOR TO A LOCALIZED OSCILLATION OF THE ABSORPTION CROSS SECTION. Nodean, Walter Charles. Ames, Iowa; Iowa State Univ. (1969). 100p. University Microfilms Order No. 70-13,616.
Thesis.

A method is proposed for determining the spatially dependent frequency response of a coupled-core reactor. This method gives an essentially exact solution to the diffusion equations by a technique based on the classical Green's function solution of a differential equation. The frequency response of a model of the Iowa State University UTR-10 reactor, which is a coupled-core Argonaut type reactor, is determined. The results obtained are consistent with expected behavior. A parametric analysis is performed for the UTR-10 model. The reactor parameters which are varied include: (1) neutron energy group, (2) neutron group speed, (3) the delayed neutron fraction β, and (4) the coupling region width. In addition, the effect of neglecting delayed neutrons and considering the inverse of the fast neutron group speed to be approximately zero is investigated. The spatial dependence of the frequency response is determined by varying the position of the neutron absorber oscillator and detector. The results of this study are compared to those obtained by independent studies of this same reactor model using the modal analysis technique. (Diss. Abstr.)

6149 IBM INTERACTIVE REACTOR COMPUTATION SYSTEM. Blaine, R. A.; Rago, A.; Petersen, E.; (and others) (IBM Palo Alto Scientific Center, Calif.). Trans. Amer. Nucl. Soc.; 13: 616-7(Nov 1970).
From Meeting of the American Nuclear Society, Washington, D. C. See CONF-701102.

6150 NEW SOLUTION OF THE POINT KINETICS EQUATIONS. da Nobrega, J. A. W.; Henry, A. F. (Massachusetts Inst. of Tech., Cambridge). Trans. Amer. Nucl. Soc.; 13: 620 (Nov 1970).
From Meeting of the American Nuclear Society, Washington, D. C. See CONF-701102.

6151 TWO-STAGE MONTE CARLO CALCULATIONS OF DELAYED-NEUTRON RESPONSE. Carter, L. L.; Smith, D. B. (Los Alamos Scientific Lab., N. Mex.). Trans. Amer. Nucl. Soc.; 13: 621(Nov 1970).
From Meeting of the American Nuclear Society, Washington, D. C. See CONF-701102.

6152 NONLINEAR PROGRAMMING APPROACH TO OPTIMAL CONTROL OF NUCLEAR REACTORS. Malan, G. F.; Koen, B. V. (Univ. of Texas, Austin). Trans. Amer. Nucl. Soc.; 13: 621-2(Nov 1970).
From Meeting of the American Nuclear Society, Washington, D. C. See CONF-701102.

6153 COMPARISON THEOREMS FOR NONLINEAR POINT REACTOR DYNAMICS EQUATIONS. Ziskind, Richard; Kastenberg, Willaim E. (Univ. of California, Los Angeles). Trans. Amer. Nucl. Soc.; 13: 622-3(Nov 1970).
From Meeting of the American Nuclear Society, Washington, D. C. See CONF-701102.

6154 COARSE MESH ACCELERATION OF S_N ITERATIONS. Nakamura, S. (Ohio State Univ., Columbus). Trans. Amer. Nucl. Soc.; 13: 625(Nov 1970).
From Meeting of the American Nuclear Society, Washington, D. C. See CONF-701102.

6155 NEW FORM OF THE P_3 APPROXIMATION. Selengut, D. S. (Knolls Atomic Power Lab., Schenectady, N. Y.). Trans. Amer. Nucl. Soc.; 13: 625-6(Nov 1970).
From Meeting of the American Nuclear Society, Washington, D. C. See CONF-701102.

6156 COLLISION PROBABILITY METHOD FOR REACTOR CELLS WITH ANISOTROPIC SCATTERING. Waelti, P. (Gulf General Atomic, Inc., San Diego, Calif.). Trans. Amer. Nucl. Soc.; 13: 626-7(Nov 1970).
From Meeting of the American Nuclear Society, Washington, D. C. See CONF-701102.

6157 TWO-GROUP TRANSPORT CRITICALITY SOLUTIONS AND ASSOCIATED CONTINUUM EXPANSION COEFFICIENT RESONANCE BEHAVIOR. Forster, R. A.; Metcalf, D. R. (Univ. of Virginia, Charlottesville). Trans. Amer. Nucl. Soc.; 13: 627-8 (Nov 1970).
From Meeting of the American Nuclear Society, Washington, D. C. See CONF-701102.

6158 SPHERICAL HARMONICS SOLUTION OF THE TWO-GROUP LINEAR TRANSPORT EQUATION. Shieh, P. S. (Mississippi State Univ., State College). Trans. Amer. Nucl. Soc.; 13: 628-9(Nov 1970).
From Meeting of the American Nuclear Society, Washington, D. C. See CONF-701102.

6159 IMPORTANCE OF DISCRETE-ORDINATE RAY EFFECTS IN FAST REACTOR DESIGN STUDIES. Miller, L. B.; Jarka, R. E. (Argonne National Lab., Upton, N. Y.). Trans. Amer. Nucl. Soc.; 13: 629-30(Nov 1970).
From Meeting of the American Nuclear Society, Washington, D. C. See CONF-701102.

6160 NEUTRON SLOWING DOWN TIME KERNEL FOR GRAPHITE. Rooney, V. L.; Sackett, J. I.; Hastings, R. M.; Brehm, R. L.; Seale, R. L. (Univ. of Arizona, Tucson). Trans. Amer. Nucl. Soc.; 13: 691-2(Nov 1970).
From Meeting of the American Nuclear Society, Washington, D. C. See CONF-701102.

6161 FEEDBACK-INDUCED SPATIAL EFFECTS IN A SIMPLE PROMPT CRITICAL REACTOR EXCURSION. Christensen, John M. (Univ. of Cincinnati); Maynard, C. W. Trans. Amer. Nucl. Soc.; 13: 700-1(Nov 1970).
From Meeting of the American Nuclear Society, Washington, D. C. See CONF-701102.

6162 EXAMINATION OF ERRORS INTRODUCED BY THE FEW-GROUP DIFFUSION THEORY APPROXIMATION IN SPACE-DEPENDENT KINETICS CALCULATIONS. Foulke, L. R. (Westinghouse Electric Corp., West Mifflin, Pa.). Trans. Amer. Nucl. Soc.; 13: 701-2(Nov 1970).
From Meeting of the American Nuclear Society, Washington, D. C. See CONF-701102.

6163 MULTIVARIABLE FEEDBACK SYNTHESIS WITH CROSS-COUPLING FOR A THERMIONIC REACTOR MODEL. Ferg, D. A.; Brehm, R. L. (Univ. of Arizona, Tucson). Trans. Amer. Nucl. Soc.; 13: 703-4(Nov 1970).
From Meeting of the American Nuclear Society, Washington, D. C. See CONF-701102.

6164 PARAMETRIC STABILITY ANALYSIS OF SYSTEMS WITH TIME DELAY. Kearns, Kenneth D.; Brehm, R. L. (Univ. of Arizona, Tucson). Trans. Amer. Nucl. Soc.; 13: 704-5(Nov 1970).
From Meeting of the American Nuclear Society, Washington, D. C. See CONF-701102.

6165 ANISOTROPIC ELASTIC MODERATION OF NEUTRONS. Stacey, Weston M. Jr. (Argonne National Lab., Ill.). Trans. Amer. Nucl. Soc.; 13: 726-7(Nov 1970).
From Meeting of the American Nuclear Society, Washington, D. C. See CONF-701102.

6166 DEGENERATE THERMALIZATION KERNEL FOR UNIT CELL CALCULATIONS. Versluis, R. M.; Mockel, A. J. (Univ. of Florida, Gainesville). Trans. Amer. Nucl. Soc.; 13: 727-8(Nov 1970).
From Meeting of the American Nuclear Society, Washington, D. C. See CONF-701102.

6167 QUANTUM CORRECTION OF THE NEUTRON TRANSPORT EQUATION. Takahashi, Hiroshi (Brookhaven National Lab., Upton, N. Y.). Trans. Amer. Nucl. Soc.; 13: 729-30(Nov 1970).
From Meeting of the American Nuclear Society, Washington, D. C. See CONF-701102.

6168 INACCURACY IN THE CALCULATION OF MATERIAL REACTIVITY WORTHS. Almenas, K.; Laperches, C. (Univ. of Maryland, College Park). Trans. Amer. Nucl. Soc.; 13: 737-8 (Nov 1970).
From Meeting of the American Nuclear Society, Washington, D. C. See CONF-701102.

6169 SOLUTION OF THE NEUTRON DIFFUSION EQUATION BY SPACE-ENERGY FACTORIZATION. Stacey, Weston M. Jr. (Argonne National Lab., Ill.). Trans. Amer. Nucl. Soc.; 13: 739(Nov 1970).
From Meeting of the American Nuclear Society, Washington, D. C. See CONF-701102.

6170 ANOTHER ANOMALY IN VARIATIONAL FLUX SYNTHESIS METHODS. Luco, V.; Woodruff, W. L. (Argonne National Lab., Ill.). Trans. Amer. Nucl. Soc.; 13: 739-40(Nov 1970).
From Meeting of the American Nuclear Society, Washington, D. C. See CONF-701102.

XUM

6171 COLLIDED FLUX DIFFUSION THEORY. Harris, D. R. (Los Alamos Scientific Lab., N. Mex.). Trans. Amer. Nucl. Soc.; 13: 742-3(Nov 1970).
From Meeting of the American Nuclear Society, Washington, D. C. See CONF-701102.

6172 OPTIMAL CONTROL OF NUCLEAR REACTOR DEPLETION. Wade, David C.; Terney, William B. (Knolls Atomic Power Lab., Schenectady, N. Y.). Trans. Amer. Nucl. Soc.; 13: 743-4(Nov 1970).
From Meeting of the American Nuclear Society, Washington, D. C. See CONF-701102.

6173 SIMPLIFIED EIGENVALUE PROBLEM SOLUTIONS IN DIFFUSION CALCULATION. Choong, Philip T.; Soodak, Harry (United Nuclear Corp., Elmsford, N. Y.). Trans. Amer. Nucl. Soc.; 13: 744-5(Nov 1970).
From Meeting of the American Nuclear Society, Washington, D. C. See CONF-701102.

6174 NOISE TECHNIQUE FOR MEASURING REACTIVITY INDEPENDENT OF β/Λ. Ackermann, N. J. Jr. (Oak Ridge National Lab., Tenn.); Robinson, J. C. Trans. Amer. Nucl. Soc.; 13: 764-5 (Nov 1970).
From Meeting of the American Nuclear Society, Washington, D. C. See CONF-701102.

6175 HYDRODYNAMIC AND NEUTRONIC COUPLING IN A CIRCULATING CRITICAL GAS. Deresh, B. A.; Erdmann, R. C. (Univ. of California, Los Angeles). Trans. Amer. Nucl. Soc.; 13: 813-14(Nov 1970).
From Meeting of the American Nuclear Society, Washington, D. C. See CONF-701102.

6176 GREEN'S FUNCTION FORMULATION OF LAPLACE-TRANSFORMED MULTIGROUP DIFFUSION EQUATIONS. Ringham, Michael Richard. Ames, Iowa; Iowa State Univ. (1969). 64p. University Microfilms Order No. 70-13,625.
Thesis.

The space- and time-dependent multigroup diffusion equations are Laplace-transformed with respect to time. The resultant coupled set of ordinary differential equations are solved for values of the Laplace transform variable s consistent with the numerical inversion scheme to be utilized in returning to the time domain. A Green's function formulation is utilized, and the resultant set of integral equations is approximated by conventional numerical weighting techniques to obtain an explicit relationship for the energy group and space dependent s domain flux vector. The model considered is that of a two-group reflected slab reactor which is symmetric in its unperturbed state. Both symmetric and non-symmetric perturbations are considered. The quality of the time-domain solutions is found to depend on two parameters which arise in the development. The solutions obtained are compared to those obtained from a version of the WIGLE codes. The technique shows promise and with modification might compare favorably with the WIGLE in accuracy and computer speed. (auth) (Diss. Abstr. Int., B)

Dynamics

6177 IMPROVED SPATIAL DIFFERENCING FOR SPACE-TIME AND STATIC MOVABLE MATERIAL DIFFUSION PROBLEMS. Yasinsky, J. B.; Foulke, L. R. (Westinghouse Electric Corp., West Mifflin, Pa.). Trans. Amer. Nucl. Soc.; 13: 618 (Nov 1970).
From Meeting of the American Nuclear Society, Washington, D. C. See CONF-701102.

6178 STUDIES OF SPECTRAL SYNTHESIS IN SPATIALLY DEPENDENT FAST REACTOR DYNAMICS. Stacey, Weston M. Jr. (Argonne National Lab., Ill.). Trans. Amer. Nucl. Soc.; 13: 619-20(Nov 1970).
From Meeting of the American Nuclear Society, Washington, D. C. See CONF-701102.

6179 HYBRID METHOD FOR SPATIAL DYNAMIC ANALYSIS. Saphier, D. (Soreq Nuclear Research Center, Yavne, Israel); Yiftah, S.; Merle, J. P. Trans. Amer. Nucl. Soc.; 13: 623-4(Nov 1970).
From Meeting of the American Nuclear Society, Washington, D. C. See CONF-701102.

6180 ASYMPTOTIC BEHAVIOR OF THE SOLUTION TO A NONLINEAR SYSTEM OF INTEGRODIFFERENTIAL EQUATIONS OCCURRING IN REACTOR DYNAMICS. Helliwell, William Stanley. Providence; Brown Univ. (1969). 74p. University Microfilms Order No. 70-8733.
Thesis.

The asymptotic behavior of solutions to nonlinear Volterra integral equations is obtained by using functional analytic techniques. The theory is then applied to a system of equations describing the temperature and power output of a nuclear reactor. (auth) (Diss. Abstr. Int., B)

Experimental Applications

6181 (AEEW-R-549) ANALYSIS OF HEAVY WATER MODERATED CLUSTER LATTICES USING THE WIMS CODE. Kemshell, P. B. (Atomic Energy Establishment, Winfrith (England)). May 1969. 29p. Dep. NTIS (U. S. Sales Only). UK 4s. 6d.

A survey of a comprehensive series of measurements in the Canadian ZED-2 reactor has been used to study the ability of the lattice cell code WIMS to predict the neutron physics of heavy water moderated rod clusters. The calculational methods and data options used were identical with those used in a previous study of the extensive series of simulated SGHW lattices at AEE, Winfrith, and the comparisons between theory and experiments for the two systems are generally consistent. Certain discrepancies between calculated and measured cluster averaged reaction rates are noted but the spatial distribution of reaction rates is well predicted by WIMS. The Canadian lattices cover a wide range of cluster geometry, coolant type and lattice pitch, and when allowance is made for end-fittings the predicted eigenvalues are encouragingly consistent. (auth) (UK)

6182 EFFECT OF SOURCE GEOMETRY PATTERN UPON FOIL ACTIVATION FOR DIFFUSION LENGTH MEASUREMENT. Eckley, Wayne (Naval Academy, Annapolis). Trans. Amer. Nucl. Soc.; 13: 461-2(Nov 1970).
From Meeting of the American Nuclear Society, Washington, D. C. See CONF-701102.

6183 MEASUREMENT OF NEUTRON DIFFUSION LENGTHS IN HIGHLY ABSORBING SOLUTIONS. Nguyen, Dong H.; Slayton, Marshall T. (Naval Postgraduate School, Monterey, Calif.). Trans. Amer. Nucl. Soc.; 13: 690(Nov 1970).
From Meeting of the American Nuclear Society, Washington, D. C. See CONF-701102.

6184 SPACE-DEPENDENT THERMAL-NEUTRON FLUX IN SYSTEMS WITH STRONG ANISOTROPIES. Turski, Ronald B.; Bull, Stanley R. (Univ. of Missouri, Columbia). Trans. Amer. Nucl. Soc.; 13: 693-4(Nov 1970).
From Meeting of the American Nuclear Society, Washington, D. C. See CONF-701102.

6185 SPACE-TIME KINETICS EXPERIMENTS AND CALCULATIONS FOR A LOOSELY COUPLED CORE. Rydin, R. A.; Burke, J. A.; Moore, W. E.; Seemann, K. W. (Knolls Atomic Power Lab., Schenectady, N. Y.). Trans. Amer. Nucl. Soc.; 13: 698(Nov 1970).
From Meeting of the American Nuclear Society, Washington, D. C. See CONF-701102.

6186 PULSED MODERATOR STUDIES USING A TIME-FOCUSED CRYSTAL SPECTROMETER. Graham, Kingsley F.; Carpenter, John M. (Univ. of Michigan, Ann Arbor). Trans. Amer. Nucl. Soc.; 13: 762(Nov 1970).
From Meeting of the American Nuclear Society, Washington, D. C. See CONF-701102.

6187 INTEGRAL TRANSPORT THEORY ANALYSIS OF SMALL-SAMPLE REACTIVITY MEASUREMENTS. McGrath, Peter Edwin. Madison, Wis.; Univ. of Wisconsin (1969). 244p. University Microfilms Order No. 70-3613.
Thesis.

Integral transport theory, within the collision probability formulation, was applied to calculations of small-sample reactivity worths. Since the collision probability formulation is extremely cumbersome for an entire reactor calculation, some trade-off with a lower order theory was necessary. This was accomplished by adopting a procedure in which one attempts a blending of diffusion theory, used to represent the unperturbed reactor, and integral transport theory, used to represent the sample and that portion of the reactor significantly perturbed by the sample. Perturbation theory, with the integral transport theory flux and adjoint equations, is used to derive the equation for the calculation of the small-sample reactivity effect. Through the use of the relationship between the diffusion theory adjoint (importance function) and the integral transport theory adjoint, the perturbation equation is reduced. The result is that the denominator of the perturbation equation (representing the entire reactor) can be calculated with

XUM

diffusion theory, and the numerator (representing the sample and environment perturbed by the sample) with integral transport theory. This theory forms the basis for a computer code COPERT, written in 3600 FORTRAN for the CDC-3600 computer and used in conjunction with the one-dimensional diffusion theory code MACH 1. The code permits a maximum of 30 energy groups, with 15 groups of downscattering, and 15 regions. Utilizing the code COPERT some of the material substitution experiments performed in the fast critical assemblies ZPR-3 Assembly 48 and ZPR-6 Assembly 6 were analyzed. (Diss. Abstr.)

Reactor Components, Fuels, and Accessories

Refer also to abstracts 4182, 4188, 4254, 4270–4274, 4309, 4739, 4841, 4886, and 4888.

6188 (AE-404) REDUCTION OF NOISE IN CLOSED LOOP SERVO SYSTEMS. Nygaard, K. (Aktiebolaget Atomenergi, Studsvik (Sweden)). 1970. 24p. Dep. NTIS (U. S. Sales Only).

A noise power reduction of more than three powers of ten was obtained in a loop simulated on an analog computer. The noise reduction was achieved under the condition that the dynamic behaviour of the loop should remain unchanged. It is characteristic of the method shown that it can be used without particular knowledge of the noise power frequency spectrum and that noise power measurements are not demanded. 11 references. (auth) (Sweden)

6189 (RISO-214, pp 11-20) RELIABILITY PREDICTION OF MECHANICAL INSTRUMENTATION EQUIPMENT FOR PROCESS CONTROL. Hensley, G. (United Kingdom Atomic Energy Authority, Risley (England). Authority Health and Safety Branch).

From Proceedings of the meeting of specialists on the reliability of mechanical components and systems for nuclear reactor safety, Risoe, September 24–26, 1969.

The reliability of mechanical instrumentation is dependent, among other things, on the failure rates of the individual equipments which can be calculated by means of a prediction technique. By considering the effects of each component failure, and allocating the relevant failure rate for the component fault mode considered, a prediction can be made of the failure rate of a complete equipment of components. As an example, the effects of failure of some of the more important components of a simple pressure switch are analyzed. Typical failure rates are given for components and equipments, and the effects of some common faults on achievable system reliability are discussed. 6 references. (auth) (Denmark)

6190 (RISO-214, pp 71-90) RELIABILITY OF A CONTAINMENT ISOLATION SYSTEM. Mieze, G. (Technischer Ueberwachungs-Verein e. V., Cologne (West Germany). Institut fuer Reaktorsicherheit).

From Proceedings of the meeting of specialists on the reliability of mechanical components and systems for nuclear reactor safety, Risoe, September 24–26, 1969.

The reliability of a containment isolation is analysed, and the results are compared with a reliability standard. A short description is given of the analysed containment isolation system and related systems. The function of the systems is explained. The procedure of the reliability analysis is explained including failure effect analysis, development of the fault tree, selection of appropriate input data, and the calculation of the overall system reliability. The fault tree is calculated by means of a Monte Carlo method computer programme. The results obtained from the computer are given and interpreted. The overall reliability of the system is compared with a reliability standard. The derivation of that standard is explained and discussed. 4 references. (auth) (Denmark)

6191 (RISO-214, pp 255-87) FRACTURE MECHANICS APPROACH TO THE ASSESSMENT OF RELIABILITY OF REACTOR PRESSURE TUBES. Basile, D.; Volta, G. (European Atomic Energy Community, Ispra (Italy). Joint Nuclear Research Center).

From Proceedings of the meeting of specialists on the reliability of mechanical components and systems for nuclear reactor safety, Risoe, September 24–26, 1969.

A quantitative evaluation is attempted of the reliability of zirconium pressure tubes taking into account embrittlement, distribution of cracks, load distribution and inspection limiting the maximum defect size. An example of how different factors can be statistically considered together in an actual structure or of tubes experimentally installed in the ESSR reactor is presented. 6 references. (Denmark)

6192 TRANSACTIONS OF THE AMERICAN NUCLEAR SOCIETY 1970 WINTER MEETING, NOVEMBER 15–19, 1970, WASHINGTON, D. C. Farmakes, Ruth (ed.). Trans. Amer. Nucl. Soc.; 13: 437-888(Nov 1970). (CONF-701102).

The transactions include summaries of 501 papers. Each paper is title listed in NSA. (D.C.C.)

For abstracts of individual papers see: 4035–4038, 4050, 4106–4109, 4129, 4148, 4149, 4170–4181, 4193–4200, 4206–4212, 4219–4248, 4251–4254, 4256, 4268–4314, 4336–4357, 4364–4367, 4381, 4382, 4385, 4386, 4400–4403, 4409, 4415, 4432–4436, 4479, 4500–4502, 4517, 4518, 4532, 4682, 4683, 4713, 4772–4777, 4804, 4819–4833, 4838, 4859–4862, 4874–4876, 4894, 4928, 4990, 5100, 5137–5149, 5166, 5167, 5242, 5243, 5470, 5495–5497, 5581, 5582, 5656, 5657, 5767–5777, 5850, 5851, 5882–5889, 5895–5911, 5940, 5941, 5946–5950, 5955–5978, 5985–5988, 5991–6033, 6041–6049, 6053–6060, 6063–6092, 6095–6142, 6144, 6146, 6149–6175, 6177–6179, 6182–6186, and 6193–6214.

6193 FOR WEST POINT'S NUCLEAR ENGINEERS: [REACTOR = COMPUTER]. Miller, James R. C.; Wheeler, David E. (Military Academy, West Point, N. Y.). Trans. Amer. Nucl. Soc.; 13: 457(Nov 1970).

From Meeting of the American Nuclear Society, Washington, D. C. See CONF-701102.

6194 USE OF ARGONNE NATIONAL LABORATORY COMPUTERS IN NUCLEAR ENGINEERING EDUCATION. Kalifelz, John M. (Georgia Inst. of Tech., Atlanta); Meyer, Lois E.; Dinni, Louis W. Trans. Amer. Nucl. Soc.; 13: 457-8(Nov 1970).

From Meeting of the American Nuclear Society, Washington, D. C. See CONF-701102.

6195 NEW COURSE IN FINANCIAL MANAGEMENT AND ECONOMICS OF NUCLEAR POWER. Clement, Joseph D.; Tarpley, Fred A. Jr. (Georgia Inst. of Tech., Atlanta). Trans. Amer. Nucl. Soc.; 13: 460(Nov 1970).

From Meeting of the American Nuclear Society, Washington, D. C. See CONF-701102.

6196 FUEL ASSEMBLY TRANSITION JOINT DEVELOPMENT. Rogers, G. D. (Combustion Engineering, Inc., Windsor, Conn.). Trans. Amer. Nucl. Soc.; 13: 562(Nov 1970).

From Meeting of the American Nuclear Society, Washington, D. C. See CONF-701102.

6197 IN-PILE DIMENSIONAL CHANGES OF ThO_2–UO_2 FUEL RODS WITH NON-FREE-STANDING CLADDING. Giovengo, J. F. (Westinghouse Electric Corp., West Mifflin, Pa.). Trans. Amer. Nucl. Soc.; 13: 563-4(Nov 1970).

From Meeting of the American Nuclear Society, Washington, D. C. See CONF-701102.

6198 IRRADIATION OF Mo–UO_2 FUEL PIN AT 2700°F TO 8.5 PERCENT BURNUP. McDonald, Glen E. (Lewis Research Center, Cleveland). Trans. Amer. Nucl. Soc.; 13: 564-5(Nov 1970).

From Meeting of the American Nuclear Society, Washington, D. C. See CONF-701102.

6199 GRAPHIC DISPLAY OF THE HYDRODYNAMICS OF COLLAPSING FLUID SLABS. Wantland, J. L. (Oak Ridge National Lab., Tenn.). Trans. Amer. Nucl. Soc.; 13: 615(Nov 1970).

From Meeting of the American Nuclear Society, Washington, D. C. See CONF-701102.

6200 TELECOMMUNICATIONS AND INFORMATION SYSTEMS AT CTC. Kidd, E. M.; Price, C. E. (Union Carbide Corp., Oak Ridge, Tenn.). Trans. Amer. Nucl. Soc.; 13: 615 (Nov 1970).

From Meeting of the American Nuclear Society, Washington, D. C. See CONF-701102.

6201 GRAPHIC DISPLAY INTERACTION IN NUCLEAR PHYSICS. Colonias, John C. (Univ. of California, Berkeley). Trans. Amer. Nucl. Soc.; 13: 616(Nov 1970).

From Meeting of the American Nuclear Society, Washington, D. C. See CONF-701102.

6202 ALPHAMERIC DISPLAYS IN NUCLEAR REACTOR COMPUTATIONS. Jensen, J. C.; Suich, J. E.; Knight, F. D.; Honeck, H. C. (Savannah River Lab., Aiken, S. C.). Trans. Amer. Nucl. Soc.; 13: 617(Nov 1970).

From Meeting of the American Nuclear Society, Washington, D. C. See CONF-701102.

6203 SLOW-NEUTRON LEAKAGE TIME DISTRIBUTIONS OF SOME SMALL HYDROGENOUS MODERATORS. Graham, Kingsley F.; Carpenter, John M. (Univ. of Michigan, Ann Arbor). Trans. Amer. Nucl. Soc.; 13: 692-3(Nov 1970).

From Meeting of the American Nuclear Society, Washington, D. C. See CONF-701102.

6204 APPLICATION OF NEUTRON TRANSIENT PHENOMENA IN HEAVY MODERATORS TO NONDESTRUCTIVE TECHNIQUES. Stegemann, D. H. (Technische Univ., Hanover). Trans. Amer. Nucl. Soc.; 13: 709(Nov 1970).
From Meeting of the American Nuclear Society, Washington, D. C. See CONF-701102.

6205 ANALYSIS OF RESONANCE INTEGRALS OF ThO_2 RODS. Steen, N. M. (Westinghouse Electric Corp., West Mifflin, Pa.). Trans. Amer. Nucl. Soc.; 13: 713-14(Nov 1970).
From Meeting of the American Nuclear Society, Washington, D. C. See CONF-701102.

6206 OPTIMUM DIAMETER OF WIRES FOR NEUTRON FLUX MEASUREMENTS. Segal, Y.; Velner, S. (Technion-Israel Inst. of Tech., Haifa). Trans. Amer. Nucl. Soc.; 13: 763-4(Nov 1970).
From Meeting of the American Nuclear Society, Washington, D. C. See CONF-701102.

6207 NEW WIDE-RANGE LINEAR CHANNEL FOR ACCURATE REACTOR POWER MEASUREMENTS. Corte, Ernesto (Gulf Electronic Systems, San Diego, Calif.). Trans. Amer. Nucl. Soc.; 13: 793-4(Nov 1970).
From Meeting of the American Nuclear Society, Washington, D. C. See CONF-701102.

6208 OPERATING EXPERIENCE WITH THE CARDINAL PLANT TRAINING SIMULATOR. Grimes, Sterling (American Electric Power Service Corp., New York). Trans. Amer. Nucl. Soc.; 13: 802(Nov 1970).
From Meeting of the American Nuclear Society, Washington, D. C. See CONF-701102.

6209 TRAINING PERSPECTIVE ON THE USE OF THE BWR SIMULATOR. Knoble, Ronald C. (General Electric Co., Morris, Ill.). Trans. Amer. Nucl. Soc.; 13: 802-3(Nov 1970).
From Meeting of the American Nuclear Society, Washington, D. C. See CONF-701102.

6210 STARTUP OF BABCOCK AND WILCOX PWR SIMULATOR. Beach, R. R. (Babcock and Wilcox Co., Lynchburg, Va.). Trans. Amer. Nucl. Soc.; 13: 803-4(Nov 1970).
From Meeting of the American Nuclear Society, Washington, D. C. See CONF-701102.

6211 MODULAR CONCEPTS APPROACH FOR INDIVIDUAL TRAINING NEEDS OF REACTOR PLANT PERSONNEL. Hanlen, D. F. (Westinghouse Electric Corp., Pittsburgh). Trans. Amer. Nucl. Soc.; 13: 804(Nov 1970).
From Meeting of the American Nuclear Society, Washington, D. C. See CONF-701102.

6212 OPERATOR LICENSE EXAMINATIONS USING NUCLEAR POWER PLANT SIMULATORS. Collins, Paul F. (Atomic Energy Commission, Washington, D. C.). Trans. Amer. Nucl. Soc.; 13: 804-5(Nov 1970).
From Meeting of the American Nuclear Society, Washington, D. C. See CONF-701102.

6213 COMPARISON OF MEASURED AND CALCULATED INTEGRAL FLUXES AND SPECTRA IN A PRESSURE VESSEL MOCKUP. Simons, R. L. (Hanford Engineering Development Lab., Richland, Wash.); Kellogg, L. S.; Barry, K. M.; Serpan, C. Z. Jr. Trans. Amer. Nucl. Soc.; 13: 884(Nov 1970).
From Meeting of the American Nuclear Society, Washington, D. C. See CONF-701102.

6214 NEUTRON FLUENCE-TO-KERMA FACTORS AND MASS ENERGY TRANSFER COEFFICIENTS FOR VARIOUS MATERIALS IN REACTOR NEUTRON FIELDS. Leonard, B. E. (Armed Forces Radiobiology Research Inst., Bethesda, Md.). Trans. Amer. Nucl. Soc.; 13: 885-7(Nov 1970).
From Meeting of the American Nuclear Society, Washington, D. C. See CONF-701102.

XUM

GENERAL

6215 (AEC-tr-7202) DETERMINATION OF THE AVERAGE EFFECTIVE RADIUS OF VAPORIZATION CENTERS IN THE NUCLEATE BOILING OF LIQUIDS. Ratiani, G. V.; Shekriladze, I. G.; Magrakvelidze, T. Sh. Translated from Soobshch. Akad. Nauk Gruz. SSR; 57: 137-40(1970). 7p. Dep. NTIS.

6216 (AEC-tr-7203) TEMPERATURE DEPENDENCE OF THE SURFACE TENSION OF WATER. Volyak, L. Translated from Dokl. Akad. Nauk SSSR; 74: 307-10(1950). 9p. Dep. NTIS

6217 (ANL-ES-2) PHYSICAL (HYDRAULIC) MODELING OF HEAT DISPERSION IN LARGE LAKES: A REVIEW OF THE STATE OF THE ART. Silberman, Edward; Stefan, Heinz (Minnesota Univ., Minneapolis. St. Anthony Falls Hydraulic Lab.). 17 Aug 1970. Contract W-31-109-eng-38; Subcontract 31-109-38-2404. 112p. Dep. NTIS.
For Argonne National Lab., Ill.

6218 (BDX-613-142) DESIGN OF JOINTS FOR FILAMENT-WOUND CYLINDERS. Forman, George W. (Bendix Corp., Kansas City, Mo.). May 1966. Contract AT(29-1)-613. 52p. Dep. NTIS.

6219 (BDX-613-143) DESIGN AND DEVELOPMENT OF A THREE-DIMENSIONAL INTERLOCKED, FILAMENT-WOUND COMPOSITE. Forman, George W. (Bendix Corp., Kansas City, Mo.). Jan 1967. 20p. Dep. NTIS.

6220 (BDX-613-180) DETERMINATION OF FOAM DENSITY. Pettie, C. B. (Bendix Aerospace-Electronics Co., Kansas City, Mo.). Oct 1970. Contract AT(29-1)-613. 42p. Dep. NTIS.

6221 (BNL-tr-383) CONTRIBUTION TO THE STUDY OF MOLECULAR REFLECTION. Daury, Gerard. Translated for Brookhaven National Lab., Upton, N. Y., from Ann. Physics. (Paris); 4: 327-70(1969). 76p. Dep. NTIS.

6222 (BNWL-SA-3335) REMOTE POSITION MEASUREMENT USING LASER OPTICS. Jensen, J. D. (Battelle-Northwest, Richland, Wash. Pacific Northwest Lab.). 28 May 1970. 14p. (CONF-700542-1). Dep. NTIS.
From Conference on Electronic Instrumentation, Moscow, Idaho.

6223 (CALT-767-P-4-66) LINEAR $H + H_2$: EXACT AND APPROXIMATE REACTION PROBABILITIES. Kuppermann, Aron (California Inst. of Tech., Pasadena. Arthur A. Noyes Lab. of Chemical Physics). [1970]. 18p. Dep. NTIS.

6224 (CALT-822-16) A SIMPLE MODEL FOR AMORPHOUS ANTIFERROMAGNETS. Hasegawa, Ryusuke (California Inst. of Tech., Pasadena. W. M. Keck Lab. of Engineering Materials). Dec 1970. Contract AT(04-3)-822. 7p. Dep. NTIS.

6225 (COO-623-150) SOLID STATE PHYSICS PROGRAM. ACCURATE DETERMINATION OF THE DIELECTRIC CONSTANT BY THE METHOD OF SUBSTITUTION. Technical Report No. 63. Andeen, Carl; Fontanella, John; Schuele, Donald (Case-Western Reserve Univ., Cleveland, Ohio). Mar 1970. Contract AT(11-1)-623. 21p. Dep. NTIS.

6226 (COO-623-151) SOLID STATE PHYSICS PROGRAM. STRUCTURE AND INTRINSIC STRESS OF PLATINUM THIN FILMS. Technical Report No. 64. Rottmayer, Robert E. (Case-Western Reserve Univ., Cleveland, Ohio. Dept. of Physics). Jun 1970. Contract AT(11-1)-623. 83p. Dep. NTIS.

6227 (COO-623-152) SOLID STATE PHYSICS PROGRAM. THEORY OF THERMOELECTRIC POWER IN METALS AND ALLOYS. Technical Report No. 65. Nielsen, P. E.; Taylor, P. L. (Case-Western Reserve Univ., Cleveland, Ohio). Jun 1970. Contract AT(11-1)-623. 85p. Dep. NTIS.

6228 (COO-623-153) SOLID STATE PHYSICS PROGRAM. LOW FREQUENCY DIELECTRIC CONSTANTS OF LiF, NaF, NaCl, NaBr, KCl, KBr BY THE METHOD OF SUBSTITUTION. Technical Report No. 66. Andeen, Carl; Fontanella, John; Schuele, Donald (Case-Western Reserve Univ., Cleveland, Ohio). Oct 1970. Contract AT(11-1)-623. 28p. Dep. NTIS.

6229 (COO-623-154) SOLID STATE PHYSICS PROGRAM. LOW FREQUENCY DIELECTRIC CONSTANTS OF THE ALKALINE EARTH FLUORIDES BY THE METHOD OF SUBSTITUTION. Technical Report No. 67. Andeen, Carl; Fontanella, John; Schuele, Donald (Case-Western Reserve Univ., Cleveland, Ohio). Oct 1970. Contract AT(11-1)-623. 22p. Dep. NTIS.

6230 (COO-623-155) SOLID STATE PHYSICS PROGRAM. CAPACITIVE GAGE FOR THE ACCURATE MEASUREMENT OF HIGH PRESSURES. Technical Report No. 68. Andeen, Carl; Fontanella, John; Schuele, Donald (Case-Western Reserve Univ., Cleveland, Ohio). Oct 1970. Contract AT(11-1)-623. 23p. Dep. NTIS.

6231 (COO-623-164) UHV MOESSBAUER EMISSION SPECTRA OF THIN IRON FILMS. Varma, M. N.; Hoffman, R. W. (Case-Western Reserve Univ., Cleveland, Ohio. Dept. of Physics). [1969]. 7p. Dep. NTIS.

6232 (COO-1140-192) PROGRESS REPORT, NOVEMBER 1, 1969-OCTOBER 31, 1970. (Kansas Univ., Lawrence). Contract AT(11-1)-1140. 29p. Dep. NTIS.

6233 (IJS-575) SPIN-LATTICE RELAXATION BY QUASI-SPIN WAVES IN ORDER-DISORDER TYPE FERROELECTRICS: POLARIZATION FLUCTUATIONS IN $Ca_2Sr(C_2H_5CO_2)_6$. Blinc, R.; Zumer, S.; Lahajnar, G. (Institut Jozef Stefan, Ljubljana (Yugoslavia)). Jan 1970. 17p. Dep. NTIS.

6234 (LA-4440-TR) NUMERICAL EXPERIMENTS WITH A NONLINEAR CHAIN. Izrailev, F. M.; Khisamutdinov, A. I.; Chirikov, B. V. (Akademiya Nauk SSSR, Novosibirsk. Institut Yadernoi Fiziki). Translated by Helen J. Dahlby (Los Alamos Scientific Lab., N. Mex.), from Preprint 252. 21p. Dep. NTIS.

6235 (LA-4442-TR) THIRD REPORT ON THE ACTIVITY OF THE RESPIRATORY PROTECTION WORKING GROUP. Ohl, Rolf. Translated for Los Alamos Scientific Lab., N. Mex., from Atemschutz-Inform.; 8: No. 1, 3-6(1969). 5p. Dep. NTIS.

6236 (LA-4518) SONIC LIMITATIONS AND STARTUP PROBLEMS OF HEAT PIPES. Deverall, J. E.; Kemme, J. E.; Florschuetz, L. W. (Los Alamos Scientific Lab., N. Mex.). Sep 1970. Contract W-7405-eng-36. 25p. Dep. NTIS.

6237 (LA-4525) ENERGY INEQUALITIES IN SOME NONLINEAR INITIAL-VALUE PROBLEMS. Wendroff, Burton (Los Alamos Scientific Lab., N. Mex.). Aug 1970. Contract W-7405-eng-36. 14p. Dep. NTIS.

6238 (LA-4531) COMPREHENSIVE APPROACH TO COMPUTER ARITHMETIC. Gardiner, V.; Metropolis, N. (Los Alamos Scientific Lab., N. Mex.). Oct 1970. Contract W-7405-eng-36. 10p. Dep. NTIS.

6239 (MLM-1766(TR)) TITANOUS CHLORIDE IN THE QUANTITATIVE DETERMINATION OF ARSENIC, ANTIMONY, AND BISMUTH. Oliverior, A. Translated for Mound Lab., Miamisburg, Ohio, from Ann. Chim. Appl.; 21: 211-16(1931). 10p. Dep. NTIS.

6240 (NLCO-1066) "GIRLS": GENERAL INDEXING IN RECIPROCAL LATTICE SPACE. Hill. R. W. (National Lead Co. of Ohio, Cincinnati). Nov 1970. Contract AT(30-1)-1156. 25p. Dep. NTIS.

6241 (NYO-1371-63) GENETIC TRANSFORMATION IN HEMOPHILUS INFLUENZAE. Three Year Comprehensive Report, September 15, 1967-September 14, 1970. Herriott, Roger M. (Johns Hopkins Univ., Baltimore, Md. Dept. of Biochemistry). Contract AT(30-1)-1371. 41p. Dep. NTIS.

6242 (NYO-1480-160) EXACT BOUNDS ON TRANSPORT COEFFICIENTS. Krinsky, Sam; Percus, Jerome K. (New York Univ., N. Y. AEC Computing and Applied Mathematics Center). Jul 1970. Contract AT(30-1)-1480. 109p. Dep. NTIS.

6243 (NYO-2394-40) PRECIPITATION AND DISLOCATIONS IN AN ALUMINUM-SILICON ALLOY. Prince, K. D.; Richman, M. H. (Brown Univ., Providence, R. I. Div. of Engineering). Aug 1970. Contract AT(30-1)-2394. 140p. Dep. NTIS.

6244 (NYO-2802-70) MECHANISM OF BIOLUMINESCENCE, CHEMILUMINESCENCE, AND ENERGY TRANSFER. Progress Report, 1968-1970. Seliger, H. H. (Johns Hopkins Univ., Baltimore, Md. McCollum-Pratt Inst.). Oct 1970. Contract AT(30-1)-2802. 19p. Dep. NTIS.

6245 (NYO-4100-3) TRANSMISSION SECONDARY EMISSION (TSE) MULTIPLIERS USING HIGH GAIN SECONDARY EMITTERS. Final Report, June 23, 1969-June 26, 1970. Martinelli, R. U. (David Sarnoff Research Center, Princeton, N. J. Electro-Optics Lab.). 25 Aug 1970. Contract AT(30-1)-4100. 52p. Dep. NTIS.

XUM

6246 (ORNL-TM-1950(Rev.1)) PROGRAM WEIGHT: A FORTRAN IV PROGRAM FOR EVALUATION OF WEIGHTING FUNCTIONS USED IN SMALL-ANGLE X-RAY SCATTERING. Buchanan, Mary G.; Hendricks, Robert W. (Oak Ridge National Lab., Tenn.). Nov 1970. Contract W-7405-eng-26. 65p. Dep. NTIS.

6247 (ORNL-tr-2395) SIsignificance OF EXCHANGEABLE IONS IN THE FORMATION OF STRUCTURE IN THIXOTROPIC GELS. Weiss, Armin; Frank, R. Translated by R. Gregg Mansfield (Oak Ridge National Lab., Tenn.), from Kolloid-Z.; 177: 47-56(1961). 17p. Dep. NTIS.

6248 (RLO-2221-T-4-3) WATER EXCHANGE KINETICS IN LABILE AQUO AND SUBSTITUTED AQUO TRANSITION METAL IONS BY MEANS OF ^{17}O NMR STUDIES. Hunt, John P. (Washington State Univ., Pullman. Dept. of Chemistry). [1970]. 20p. Dep. NTIS.

6249 (SC-RR-69-369) SLADE: A COMPUTER PROGRAM FOR THE STATIC ANALYSIS OF THIN SHELLS. Key, Samuel W.; Beisinger, Zelma E. (Sandia Labs., Albuquerque, N. Mex.). Nov 1970. 191p. Dep. NTIS.

6250 (SC-RR-70-615) EFFICIENT RUNGE-KUTTA CODES. Shampine, L. F.; Watts, H. A. (Sandia Labs., Albuquerque, N. Mex.). Sep 1970. 63p. Dep. NTIS.

6251 (SC-T-70-4042) EQUATION FOR ROD OSCILLATIONS AT HIGH TEMPERATURES. Kalynyak, N. I. Translated by Fredric D. Killebrew (Sandia Labs., Albuquerque, N. Mex.), from Izv. Akad. Nauk SSSR, Mekh. Tverd. Tela; No. 2, 121-7(1970). 9p. Dep. NTIS.

6252 (SC-T-70-4045) MECHANISM OF THERMAL DISSOCIATION OF DIATOMIC MOLECULES. Losev, S. A.; Shatalov, O. P. Translated by Fredric D. Killebrew (Sandia Labs., Albuquerque, N. Mex.), from Fiz. Goreniya Vzryva; No. 6, 30-4 (Mar 1970). 10p. Dep. NTIS.

6253 (UCRL-50890) FREE-RADICAL MICROWAVE ROTATIONAL SPECTROSCOPY WITH A RESONANT CAVITY. Hrubesh, Lawrence W. (California Univ., Livermore. Lawrence Radiation Lab.). 16 Jul 1970. 63p. Dep. NTIS.
Thesis. Submitted to Univ. of Wyoming, Laramie.

6254 (UCRL-72099) OBSERVATIONS ON TRANSFORMATION TEMPERATURES, MICROSTRUCTURE, HARDNESS, AND DIMENSIONAL ANISOTROPY ON THERMAL CYCLING OF A 300-GRADE MARAGING STEEL. Goldberg, Alfred; Snell, Earle O. Jr. (California Univ., Livermore. Lawrence Radiation Lab.). 6 Feb 1970. 59p. (CONF-700812-2). Dep. NTIS.
From 2nd Inter-American Conference on Materials Technology, Mexico City, Mex.

6255 (UCSD-34-P-143-27) COMPRESSIONAL COOLING OF ^3He TO MILLIDEGREE TEMPERATURES. Johnson, R. T.; Wheatley, J. C. (California Univ., La Jolla, San Diego. Dept. of Physics). [1970]. 50p. Dep. NTIS.

6256 (UCSD-34-P-143-33) MAGNETIZATION OF DILUTE Cu-Mn ALLOYS AT VERY LOW TEMPERATURES. Hirschkoff, E. C.; Symko, O. G.; Wheatley, J. C. (California Univ., La Jolla, San Diego. Dept. of Physics). [1970]. Contract AT(04-3)-34. 6p. Dep. NTIS.

6257 (WHAN-IR-38) BPLOT, A MULTIPURPOSE PLOTTING ROUTINE FOR USE WITH THE CALCOMP PLOTTER. Graves, N. J.; Bourquin, R. D. (WADCO Corp., Richland, Wash.). Oct 1970. Contract AT(45-1)-2170. 36p. Dep. NTIS.

XUM

CORPORATE AUTHOR INDEX

In the Corporate Author Index, technical report literature is indexed by the organization or institution responsible for issuing the report. Entries are given for all report literature and for published literature for which a corporate author approach is especially desirable, e.g., symposium and conference proceedings.

Each entry under a corporate author gives the publication title and the *NSA* volume and abstract numbers. Report numbers, where applicable, are given in parentheses at the end of the entry.

A

AEROSPACE CORP., EL SEGUNDO, CALIF.
Influence of an axial magnetic field on neutron production in a plasma focus discharge, 25:5113 (AD-710606)
Radial diffusion of outer-zone electrons, 25:5002 (AD-710604)
AEROSPACE RESEARCH LABS., WRIGHT-PATTERSON AFB, OHIO.
Time-resolved energy distributions in a striating discharge, 25:5077 (AD-710597)
AKADEMIYA NAUK SSSR, MOSCOW. INSTITUT ATOMNOI ENERGII.
Research on studying and increasing the plasma parameters on ''non-cylindrical Z-pinch'' equipment, 25:5116 (SC-T-70-4046)
AKADEMIYA NAUK SSSR, NOVOSIBIRSK. INSTITUT YADERNOI FIZIKI.
Numerical experiments with a nonlinear chain, 25:6234 (LA-4440-TR)
AKADEMIYA NAUK UKRAINSKOI SSR, KIEV. INSTITUT TEORETICHESKOI FIZIKI.
Allowance for the wave function distortion under multipole analysis of fast nucleon scattering by nuclei, 25:5552 (ITF-70-50)
AKTIEBOLAGET ATOMENERGI, STUDSVIK (SWEDEN).
Reduction of noise in closed loop servo systems, 25:6188 (AE-404)
ALLGEMEINE ELEKTRICITAETS-GESELLSCHAFT, FRANKFURT AM MAIN (WEST GERMANY).
Reliability and availability of two BWR shut-down systems, 25:6036 (RISO-214, pp 41-55)
ALLIS-CHALMERS MFG. CO., BETHESDA, MD. ATOMIC ENERGY DIV.
La Crosse Boiling Water Reactor. Nuclear instrumentation automatic gain control system, Addendum, 25:5912 (DOCKET-1155-85)
AMES LAB., IOWA.
Anion exchange separations of metal ions in thiocyanate media, 25:4137 (IS-T-377)
Construction of a three crystal spectrometer and study of the decay of ^{90}Nb, 25:5662 (IS-T-389)
Decay of ^{95}Ru and ^{103}Tc, 25:5683 (IS-T-391)
Electron energy loss to surface excitations in thin films, 25:4937 (IS-T-380)
Transport properties of Gd--Th, Gd--Mg, and Y--Th alloys, 25:5169 (IS-T-379)
ARGONNE CANCER RESEARCH HOSPITAL, CHICAGO, ILL.
Additional system for bone densitometry studies, 25:4634 (CONF-700515-, pp 33-47)
ARGONNE NATIONAL LAB., ILL.
Curium-244 and ^{145}Sm--^{145}Pm x-ray sources, 25:4647 (CONF-700515-, pp 274-9)
Experimental neutrino physics, 25:5256 (CONF-700314-, Paper 6)
In vivo measurement of the mineral content of a section of the radius, 25:4621 (CONF-680211-, pp 204-15)
Measurement of bone mineral using computer analysis of microradiographs, 25:4638 (CONF-700515-, pp 195-8)
Multiple-source urban atmospheric dispersion model, 25:4161 (ANL/ES-CC-7)
Physical modeling of heat dispersion in large lakes, 25:6217 (ANL-ES-2)
Prog. rpt. on sodium technology, 4--6/70, 25:4736 (ANL/ST-3)
Serpukhov program, 25:5443 (CONF-700314-, Paper 1)
ASSOCIATED OFFICES TECHNICAL COMMITTEE (UK).
Survey of pressure vessels built to a high standard of construction, 25:5983 (RISO-214, pp 323-34)
ATOMIC ENERGY ESTABLISHMENT, WINFRITH (ENGLAND).
Analysis of heavy water moderated cluster lattices using WIMS code, 25:6181 (AEEW-R-549)
Computer interface methods and standards, 25:4387 (AEEW-M-986)
Corrosion experiments on coated fuel particles using xenon release technique, 25:4882 (DP-Report-436)
Differential concentration gas chromatograph for the analysis of low levels of impurities in He, 25:4012 (DP-Report-443)
Dimensional changes in graphite during high-temperature irradiation, 25:4883 (DP-Report-473)
Dimensional changes of graphite specimens irradiated in Dragon fuel element. II, 25:4885 (DP-Report-556(Pt.2))
Dimensional changes of graphite specimens irradiated in dragon fuel element 700. project dragon, 25:4884 (DP-Report-556(Pt.1))
Facilities at Risoe for post-irradiation examination of Dragon Project experiments, 25:4262 (DP-Report-446)
Fuel cycles in High Temperature Reactors: approach towards thermal breeding on Th fuel cycle, 25:6051 (DP-Report-434)
Fuel particle coatings at very high magnification, 25:4863 (DP-Report-574)
Graphite oxidation under irradiation by tracer of CO_2 in high pressure He carrier gas, 25:4881 (DP-Report-352)
HELTOT: program system for analysis of fuel cycles assuming off-load refueling, 25:6052 (DP-Report-440)
High temperature corrosion of Nimonic-75 and various steels in gases at low partial pressures, 25:4738 (DP-Report-527)
Laboratory experiments carried out on clam seals. project dragon, 25:4183 (DP-Report-484)
Materials for boiler tubes of a HTGC power reactor, 25:4748 (DP-Report-537)
Parametric survey on internally cooled annular fuel, 25:5979 (DP-Report-435)
Prog. rpt. on Dragon Project, semiannual, 7-12/65, 25:5942 (DP-Report-490)
Pulsed ultrasonic thermometer. project dragon, 25:4388 (DP-Report-498)
Recent results from the in-pile carbon transport loop. project dragon, 25:4835 (DP-Report-448)
Relative power distribution and integral spectrum measurements on first Dragon core, 25:5952 (DP-Report-442)
Resonant probe ultrasonic thermometer, 25:4389 (DP-Report-590)
Thermal conductivity of a hollow right cylinder of solid material, 25:4203 (DP-Report-578)
Transfer function investigations on first Dragon core, 25:5953 (DP-Report-445)
ATOMIC ENERGY OF CANADA LTD., CHALK RIVER (ONTARIO).
Cosmic ray NM-64 neutron monitor data. XVI, 25:4575 (AECL-3736)
ATOMIC ENERGY OF CANADA LTD., CHALK RIVER (ONTARIO). CHALK RIVER NUCLEAR LABS.
Radium-226 content of water and plankton from the Chalk River area, 25:4473 (AECL-3687)
ATOMIC ENERGY RESEARCH ESTABLISHMENT, HARWELL (ENGLAND).
Assessment of medical requirements for workers in nuclear installations, 25:4529 (AERE-R-6523)
Nuclear accident dosimetry systems, 25:4377 (AERE-R-6498)
ATOMIC INDUSTRIAL FORUM, INC., NEW YORK.
Health physics practices and experiences of isotope producers and distributors, 25:4515
ATOMIC WEAPONS RESEARCH ESTABLISHMENT, ALDERMASTON (ENGLAND).
Influence of impurities on the properties of uranium, 25:4747 (AWRE-O-63/70)
ATOMICS INTERNATIONAL, CANOGA PARK, CALIF.
Prog. rpt. on unclassified programs, 1970, 25:4051 (AI-AEC-12972)
AUBURN UNIV., ALA. DEPT. OF CHEMICAL ENGINEERING.
Prog. rpt. on synthesis, identification, and purification of C_4 and C_5 fluorocarbons from radiolysis, 11/70, 25:4111 (ORO-3909-2)
AUSTRALIAN ATOMIC ENERGY COMMISSION RESEARCH ESTABLISHMENT, LUCAS HEIGHTS.
Application of variational methods to neutron transport

in slabs, 25:5135 (AAEC/TM-554)
BOPTIC: beam transport program in FORTRAN IV, 25:5441 (AAEC/TM-544)
Flow of spheres in cylindrical vessels. II, 25:4182 (AAEC/E-207)
AUSTRALIAN NATIONAL UNIV., CANBERRA. RESEARCH SCHOOL OF PHYSICAL SCIENCES.
Energy levels of ^{27}Si, 25:5602 (ANU-P-501)

B

BALLISTIC RESEARCH LABS., ABERDEEN PROVING GROUND, MD.
Electron spin resonance studies on γ-irradiated $KMnO_4$, 25:4110 (AD-710231)
BATTELLE MEMORIAL INST., COLUMBUS, OHIO.
Survey report on structural design of piping systems and components, 25:4188 (TID-25553)
BATTELLE-NORTHWEST, RICHLAND, WASH. PACIFIC NORTHWEST LAB.
^{235}U depletion as a potential independent cross-check of the plutonium content of spent power reactor fuels, 25:4257 (BNWL-SA-3304)
Amount and characteristics of plutonium made airborne under thermal stress, 25:4258 (BNWL-SA-3379)
Automation in analytic chemistry: methods and motivation, 25:4008 (BNWL-SA-3341)
Evaluation of Hanford Basic Thermoluminescence Dosimeter, 25:4378 (BNWL-CC-2633)
Fall chinook salmon spawning in the Columbia River near Hanford, 1947--1969, 25:4474 (BNWL-1515)
Fundamental materials problems in nuclear reactors, 25:4812 (BNWL-SA-3495)
In vivo neutron activation analysis of total body bone mass, 25:4042 (CONF-680211-, pp 496-516)
Irradiation induced swelling and creep in fast reactor materials, 25:4810 (BNWL-SA-3283)
Modifications of a triode sputtering unit to provide maximum flexibility for use in a radioactive glove box environment, 25:4259 (BNWL-SA-3609)
Observations on the nucleation and growth of voids in nickel, 25:4811 (BNWL-SA-3300)
Pulsed current electroplating, 25:4741 (BNWL-CC-491)
Remote position measurement using laser optics, 25:6222 (BNWL-SA-3335)
Scavenging in perspective, 25:4162 (BNWL-SA-3450)
Temperature, timing, and seaward migration of juvenile chinook salmon from the central Columbia River, 25:4504 (BNWL-1472)
Uniaxial and biaxial creep-rupture of Type 316 stainless steel after fast reactor irradiation, 25:4816 (WHAN-FR-19)
BENDIX AEROSPACE-ELECTRONICS CO., KANSAS CITY, MO.
Determination of foam density, 25:6220 (BDX-613-180)
BENDIX CORP., KANSAS CITY, MO.
Design and development of three-dimension interlocked, filament-wound composite, 25:6219 (BDX-613-143)
Design of joints for filament-wound cylinders, 25:6218 (BDX-613-142)
BONN UNIV. (WEST GERMANY). PHYSIKALISCHES INSTITUT.
Omega photoproduction on complex nuclei, 25:5249 (DNPL/R-7, pp 87-94)
BROOKHAVEN NATIONAL LAB., UPTON, N. Y.
Angular distributions in neutron-induced reactions. I, 25:5549 (BNL-400(3rd Ed.)(Vol.1))
Environmental monitoring radiation levels at BNL, 25:4503 (BNL-50196)
BROOKLYN COLL., N. Y.
Polarization in nucleon--deuteron scattering at medium energies, 25:5517 (LA-4465, pp 16.1-2)
BROWN BOVERI/KRUPP REAKTORBAU G.M.B.H., MANNHEIM (WEST GERMANY).
System design of reactor charging equipment based on reliability considerations, 25:6039 (RISO-214, pp 213-46)
BROWN UNIV., PROVIDENCE, R. I. DEPT. OF PHYSICS.
Crossed channel partial wave expansions and the Bethe--Salpeter equation, 25:5426 (NYO-2263-TA-226)
Scaling behavior in multiperipheral dynamics, 25:5351 (NYO-2262-TA-225)
BROWN UNIV., PROVIDENCE, R. I. DIV. OF ENGINEERING.
Precipitation and dislocations in an aluminum--silicon alloy, 25:6243 (NYO-2394-40)
BUREAU OF COMMERCIAL FISHERIES, ANN ARBOR, MICH.
Application of ionizing radiations tc extension of refrigerated storage of freshwater perch, 25:4734 (TID-25467)
BUREAU OF MINES, RENO, NEV. RENO METALLURGY RESEARCH CENTER.
Characteristics of electrowon and of hydrogen-reduced molybdenum powder and sheet, 25:4740 (BM-RI-7455)
BUREAU OF RADIOLOGICAL HEALTH, ROCKVILLE, MD. DIV. OF ELECTRONIC PRODUCTS.
In-plant survey of television receivers for x-radiation emission capability, 25:4522 (BRH/DEP-70-24)

C

CALIFORNIA INST. OF TECH., PASADENA. ARTHUR A. NOYES LAB. OF CHEMICAL PHYSICS.
Linear $H + H_2$: exact and approximate reaction probabilities, 25:6223 (CALT-767-P-4-66)
CALIFORNIA INST. OF TECH., PASADENA. W. M. KECK LAB. OF ENGINEERING MATERIALS.
Model for amorphous antiferromagnets, 25:6224 (CALT-822-16)
CALIFORNIA UNIV., BERKELEY.
Prog. rpt. on effects of radiation on brain activity and development, 8/69--7/70, 25:4457 (UCB-34-P-82-9)
CALIFORNIA UNIV., BERKELEY. DEPT. OF PHYSICS.
Prog. rpt. on dynamic nuclear polarization and solid state physics, annual, 7/15/69--8/1/70, 25:5150 (UCB-34-P-20-PR-16)
CALIFORNIA UNIV., BERKELEY. LAWRENCE RADIATION LAB.
Excited state in even--even fission products, 25:5687 (UCRL-19949)
Heavy-ion in-beam spectroscopy, 25:5688 (UCRL-19961)
Photoproduction of π^+ mesons from a polarized proton target at 5 and 16 GeV, 25:5251 (UCRL-19897)
Polarization and cross-section measurements in p-^{4}He scattering from 20 to 40 MeV, 25:5526 (UCRL-19943)
Search for polarization in elastic e-p scattering at 15 and 18 GeV, 25:5252 (UCRL-20093)
Search for T-violation in inelastic scattering of electrons from polarized proton target, 25:5400 (UCRL-20041)
Simplified helium cryostats for superconducting dipoles and quadrupole magnets, 25:4189 (UCRL-19764)
Vaporization mechanism of gallium arsenide single crystals, 25:4074 (UCRL-19685)
CALIFORNIA UNIV., IRVINE.
Research program in neutrino physics, cosmic rays, and elementary particles. Progress report, 1 October 1969--30 September 1970, 25:5257 (UCI-10-P-19-40)
CALIFORNIA UNIV., LA JOLLA, SAN DIEGO. DEPT. OF PHYSICS.
Compressional cooling of ^3He to millidegree temperatures, 25:6255 (UCSD-34-P-143-27)
Continuously operating ^4He evaporation refrigerator, 25:5061 (UCSD-34-P-143-31)
Experiments of the future at ultra-low temperatures (< 0.3°K), 25:5035 (UCSD-34-P-143-30)
Magnetization of dilute Cu--Mn alloys at very low temperatures, 25:6256 (UCSD-34-P-143-33)
Multiperipheral dynamics, 25:5302 (CONF-700314-, Paper 11)
Principles and methods of dilution refrigeration. II, 25:5062 (UCSD-34-P-143-32)
Scaling behavior in multiperipheral dynamics, 25:5351 (NYO-2262-TA-225)
CALIFORNIA UNIV., LIVERMORE. LAWRENCE RADIATION LAB.
Beta--γ (CP) correlation measurements in allowed transitions, 25:5605 (UCRL-72624)
Collimation of fast neutrons, 25:5477 (UCRL-50857)
Free-radical microwave rotational spectroscopy with a resonant cavity, 25:6253 (UCRL-50890)
Plugging of high efficiency filters by water spray, 25:4190 (UCRL-50923)
Thermal cycling of maraging steel, 25:6254 (UCRL-72059)
CALIFORNIA UNIV., LOS ANGELES. LAB. OF NUCLEAR MEDICINE AND RADIATION BIOLOGY.
Appearance of brain-specific antigen in developing rat brain, 25:4694 (UCLA-12-791)
Biochemistry, 25:4458 (UCLA-12-782, pp 1-21)
Biophysics, 25:4016 (UCLA-12-782, pp 83-8)
Environmental radiation, 25:4477 (UCLA-12-782, pp 49-81)
Nuclear medicine, 25:4657 (UCLA-12-782, pp 85-125)
Prog. rpt. on nuclear medicine and radiation biology, annual, 6/30/70, 25:4425 (UCLA-12-782)
Radiobiology, 25:4459 (UCLA-12-782, pp 23-47)
CALIFORNIA UNIV., SANTA BARBARA.
Nuclear structure research. Progress report, Task A, 25:5606 (UCSB-34-P-144-7)
CAMBRIDGE UNIV. (ENGLAND). CAVENDISH LAB.
Theorems on high energy collisions, 25:5303 (CONF-700314-, Paper 16)
CASE INST. OF TECH., CLEVELAND, OHIO.
Theory of thermoelectric power in metals and alloys, 25:6227 (COO-623-152)
CASE-WESTERN RESERVE UNIV., CLEVELAND, OHIO.
Accurate determination of dielectric constant by method of substitution, 25:6225 (COO-623-150)
Capacitive gage for accurate measurement of high pressures, 25:6230 (COO-623-155)
Low frequency dielectric constants of alkaline earth fluorides by method of substitution, 25:6229 (COO-623-154)
Low frequency dielectric constants of LiF, NaF, NaCl, NaBr, KCl, KBr by method of substitution, 25:6228 (COO-623-153)
Prog. rpt. on dislocation-solute atom interactions in alloys, 10/70, 25:4786 (COO-1676-13)
Prog. rpt. on solid state physics program, annual, 11/69--10/70, 25:5168 (COO-623-156)
CASE-WESTERN RESERVE UNIV., CLEVELAND, OHIO. DEPT. OF PHYSICS.
Structure and intrinsic stress of Pt thin films, 25:6226 (COO-623-151)
UHV Moessbauer emission of thin iron films, 25:6231 (COO-623-164)

XUM

CATHOLIC UNIV. OF AMERICA, WASHINGTON, D.C. DEPT. OF PHYSICS.
Production of low-energy muons by neutral components of cosmic radiation at sea level, 25:4974 (AD-710278)
CENTRAL ELECTRICITY GENERATING BOARD, BERKELEY (ENGLAND). BERKELEY NUCLEAR LABS.
Predicting the heavy element composition of irradiated reactor fuels, 25:4815 (RD/B/N-1722)
CENTRE NATIONAL DE LA RECHERCHE SCIENTIFIQUE, MARSEILLES (FRANCE). CENTRE DE PHYSIQUE THEORIQUE.
Approach to form factor in a composite model, 25:5372 (CNRS-CPT-70-P-331)
CENTRE NATIONAL DE LA RECHERCHE SCIENTIFIQUE, PARIS (FRANCE).
Conference on rare earth elements, Paris, Grenoble, France, 5/69. II, 25:5193
CENTRO INFORMAZIONI STUDI ESPERIENZE, MILAN (ITALY).
Beta detection efficiency curves for ^{40}K, ^{90}Y, ^{90}Sr--^{90}Y, ^{137}Cs, ^{144}Pr, ^{147}Pm, ^{155}Eu, and ^{204}Tl in sources of definite chemical form as function of their thickness, 25:4029 (CISE-N-119)
Corrosion rate of Zircaloy-2 in steam--water mixture under reactor radiations, 25:4737 (CISE-R-290)
CESKOSLOVENSKA AKADEMIE VED, REZ. USTAV JADERNEHO VYZKUMU.
Production of carrier-free radiostrontium ^{85}Sr, 25:4126 (UJV-2431-Ch)
CHICAGO DEPT. OF ENVIRONMENTAL CONTROL, ILL.
Multiple-source urban atmospheric dispersion model, 25:4161 (ANL/ES-CC-7)
CHICAGO UNIV., ILL.
Pomeranchuk decoupled from the ordinary Regge trajectories, 25:5348 (COO-264-562)
CHICAGO UNIV., ILL. DEPT. OF RADIOLOGY.
Additional system for bone densitometry studies, 25:4634 (CONF-700515-, pp 33-47)
Bone densitometry: clinical applications, 25:4626 (CONF-680211-, pp 308-19)
CHUBU ELECTRIC POWER CO., NAGOYA (JAPAN).
Reliability aspects of safety evaluation of nuclear power plants, 25:5937 (RISO-214, pp 457-79)
COLORADO UNIV., DENVER. MEDICAL CENTER.
Growth of uterine, placental and fetal vasculature, 25:4655 (COO-1762-6)
COMISION NACIONAL DE ENERGIA ATOMICA, BUENOS AIRES (ARGENTINA).
Resonance integrals of neutron activation of ^{74}Se, ^{78}Se, ^{80}Se, ^{81}Br, ^{127}I, ^{130}Te, ^{138}Ba, ^{140}Ce, and ^{142}Ce, 25:5681 (CNEA-274)
COMITATO NAZIONALE PER L'ENERGIA NUCLEARE, FRASCATI (ITALY). LABORATORI NAZIONALI DI FRASCATI.
Preliminary results with Adone, 25:5446 (DNPL/R-7, pp 215-43)
COMITATO NAZIONALE PER L'ENERGIA NUCLEARE, ROME (ITALY).
General principles of a safety assessment through reliability analysis of ESSOR plant, 25:6094 (RISO-214, pp 597-625)
Theoretical reliability assessment of a fire protection system, 25:4187 (RISO-214, pp 21-40)
COMMISSARIAT A L'ENERGIE ATOMIQUE, CADARACHE (FRANCE). CENTRE D'ETUDES NUCLEAIRES.
Analog computer for calculating the ratio of amplitude of two pulses, 25:4362 (CEA-N-1314)
Mathematical processing of scintigraphic images, 25:4611 (CEA-R-3920)
COMMISSARIAT A L'ENERGIE ATOMIQUE, FONTENAY-AUX-ROSES (FRANCE). CENTRE D'ETUDES NUCLEAIRES.
Counter current extraction of neptunium by tributylphosphate solutions from aqueous nitric--nitrous acid solutions, 25:4135 (CEA-R-4097)
Criteria for local thermodynamic equilibrium, 25:5094 (CEA-CONF-1629)
Partial melting of low density mixed oxide $(U,Pu)O_2$ at beginning of irradiation, 25:4879 (CEA-CONF-1659)
Physiological data on swine for use in radiobiology: plasma and blood volumes, 25:4411 (CEA-R-4031)
Processing of irradiated mixed plutonium and uranium oxides, 25:4134 (AEC-tr-7198)
Remote handling in operation of the installation ATTILA, 25:4261 (CEA-R-4067)
Study of α and epsilon phases of Pu by high-hydrostatic pressures, 25:4785 (CEA-R-4092)
COMMISSARIAT A L'ENERGIE ATOMIQUE, GRENOBLE (FRANCE). CENTRE D'ETUDES NUCLEAIRES.
Characterization of compounds and materials by neutron diffraction, 25:4151 (CEA-CONF-1500)
COMMISSARIAT A L'ENERGIE ATOMIQUE, LIMEIL-BREVANNES (FRANCE). CENTRE D'ETUDES.
Approximations deduced from Milne equation associated to that of Schroedinger, 25:5234 (CEA-R-4007)
Gamma-ray production cross sections for 5-, 6.6- and 8.7-MeV neutrons with nitrogen, oxygen, scandium, and gold, 25:5551 (CEA-R-4047)
Problems in radiation hydrodynamics, 25:5095 (CEA-R-4057)
Thomson scattering and Rayleigh scattering in argon plasma jet, 25:5078 (CEA-R-3998)
COMMISSARIAT A L'ENERGIE ATOMIQUE, SACLAY (FRANCE). CENTRE D'ETUDES NUCLEAIRES.
Analysis of the effects of displacement and of positioning of the measuring probe of a magnetic field on the properties of an optical system, 25:5461 (NP-18519)
Calculation of losses in superconducting coils supplied by pulsed current, 25:5459 (NP-18516)
Differential cross sections for reaction $\pi^- p \to \eta n$ between 2.9 and 18.2 GeV/c, 25:5279 (CEA-R-4037)
Electron probe microanalysis of highly radioactive materials, 25:4011 (CEA-N-1340)
Elementary model of the macroscopic effects of neutron irradiation in graphite, 25:4880 (CEA-N-1374)
Influence of coupling resonances $2\nu_z = \nu_x$ = integer on mechanism of third resonance ejection, 25:5460 (NP-18517)
Investigations with the cyclotrons, 25:5506 (CEA-N-1232, pp 81-159)
Investigations with the tandem Van de Graaff, 25:5680 (CEA-N-1232, pp 1-80)
Prog. rpt. on nuclear physics, annual, 10/68--9/69, 25:5550 (CEA-N-1232)
Regge models including 4 poles rho, rho', A2 and A2', in π-nucleon and K-nucleon charge exchange reactions from 2 to 20 GeV/c, 25:5371 (CEA-N-1373)
Saclay electron linear accelerator, 25:5442 (CEA-N-1232, pp 161-212)
Separation methods of noble fission gases from gaseous effluents, 25:4260 (CEA-Bib-184)
COMMONWEALTH EDISON CO., CHICAGO, ILL.
Dresden Nuclear Power Station, Unit 1. Comments on uniform recording and reporting guide, minor corrections, 25:5915 (DOCKET-50010-73)
Dresden Nuclear Power Station, Unit 1. Failure of north emergency condenser condensate valve, 25:5890 (DOCKET-50010-71)
Dresden Nuclear Power Station, Unit 1. Minimizing radioactive off-gas release rate, 25:5914 (DOCKET-50010-72)
Dresden Nuclear Power Station, Unit 2. Abnormal occurrence report: turbine trip and reactor scram, 25:5893 (DOCKET-50237-110)
Dresden Nuclear Power Station, Unit 2. Control rod drives in excess of 7.00 second maximum insertion time, 25:5894 (DOCKET-50237-111)
Dresden Nuclear Power Station, Unit 2. Financial qualifications and certificate of service, 25:5921 (DOCKET-50237-88)
Dresden Nuclear Power Station, Unit 2. License application, 25:5924 (DOCKET-50237-103)
Dresden Nuclear Power Station, Unit 2. Modification of standby gas treatment system and automatic pressure relief subsystem, 25:5922 (DOCKET-50237-98)
Dresden Nuclear Power Station, Unit 2. Operator retraining program, 25:5923 (DOCKET-50237-101)
Zion Station, Units 1 and 2. Preliminary safety analysis report, Amendment 12 (includes final safety analysis report, Vol. 1), 25:5932 (DOCKET-50295-16)
Zion Station, Units 1 and 2. Preliminary safety analysis report, Amendment 12 (includes final safety analysis report, Vol. 2), 25:5933 (DOCKET-50295-17)
Zion Station, Units 1 and 2. Preliminary safety analysis report, Amendment 12 (includes final safety analysis report, Vol. 3), 25:5934 (DOCKET-50295-18)
Zion Station, Units 1 and 2. Preliminary safety analysis report, Amendment 12 (includes final safety analysis report, Vol. 4), 25:5935 (DOCKET-50295-19)
Zion Station, Units 1 and 2. Technical specifications; Appendix A to operating license, 25:5931 (DOCKET-50295-15)
CONSOLIDATED EDISON CO. OF NEW YORK, INC., NEW YORK.
Indian Point Station, Unit No. 1. Investigation of spent fuel shipping cask external neutron radiation levels, 25:5913 (DOCKET-50003-60)
CONSUMERS POWER CO., JACKSON, MICH.
Big Rock Point Nuclear Plant. Release of noble gases to discharge canal, 25:5892 (DOCKET-50155-53)
CORNELL UNIV., ITHACA, N. Y.
Viscous tails in MHD, 25:5121 (AD-709878)
CORNELL UNIV., ITHACA, N. Y. DEPT. OF MATERIALS SCIENCE AND ENGINEERING.
Effects produced by adding Re to alloys of W and C, 25:4746 (AD-710275)
Prog. rpt. on study of interaction between magnetic fluxoids and crystal defects in type II superconductors, 10/70, 25:5036 (NYO-4060-5)
CORNELL UNIV., ITHACA, N. Y. LAB. OF NUCLEAR STUDIES.
Some reactions at high momentum transfer at NAL, 25:5281 (CONF-700314-, Paper 15)

D

DAMES AND MOORE, NEW YORK.
West Valley Reprocessing Plant. Foundation investigation: proposed plutonium fuel plant, West Valley, New York, 25:4154 (DOCKET-50201-52)
West Valley Reprocessing Plant. Soils and foundation investigation: proposed Iodine Recovery Building, West Valley, New York, 25:4155 (DOCKET-50201-53)
DAMES AND MOORE, SAN FRANCISCO, CALIF.
West Valley Reprocessing Plant. Site investigation: proposed Spent Nuclear Fuel Processing Plant, near Springville, New York, 25:4153 (DOCKET-50201-51)

XUM

DANISH ATOMIC ENERGY COMMISSION, RISOE. RESEARCH ESTABLISHMENT.
Environmental radioactivity in the Faroes in 1969, 25:4476 (RISO-221)
Meeting on the reliability of mechanical components and systems for nuclear reactor safety, Risoe, Denmark, 9/69, 25:6062 (RISO-214)
DARESBURY NUCLEAR PHYSICS LAB. (ENGLAND).
Interference effects in high energy vector meson photoproduction, 25:5325 (DNPL/R-7, pp 115-38)
Vector meson production and omega--rho interference. Proceedings of the Daresbury Study Weekend No. 1, 12--14 June 1970, 25:5322 (DNPL/R-7)
DATA DYNAMICS, INC., LOS ANGELES, CALIF.
Fallout computational techniques, 25:4506 (AD-703266)
DAVID SARNOFF RESEARCH CENTER, PRINCETON, N.J. ELECTRO-OPTICS LAB.
Prog. rpt. on transmission secondary emission multipliers using high gain secondary emitters, final, 6/23/69--6/26/70, 25:6245 (NYO-4100-3)
DEMOCRITUS NUCLEAR RESEARCH CENTER, ATHENS (GREECE).
Nucleon axial vector form factor and SO(4,2) group, 25:5401 (DEMO-70/6)
Remarks on π^+-photoproduction with linearly polarized photons, 25:5321 (DEMO-70/1)
DEUTSCHES ELEKTRONEN-SYNCHROTRON, HAMBURG (WEST GERMANY).
Photoproduction of vector mesons, 25:5301 (DNPL/R-7, pp 29-70)
DIVISION OF REACTOR LICENSING (AEC), WASHINGTON, D. C.
Dresden Nuclear Power Station, Unit 2. Approval of test program involving irradiation of cobalt-59, 25:5925 (DOCKET-50237-108)
Dresden Nuclear Power Station, Unit 2. Crud deposition test does not require a change to technical specifications, 25:5926 (DOCKET-50237-109)
Enrico Fermi Atomic Power Plant, Unit 1. Request for additional information on sodium service piping, 25:5916 (DOCKET-50016-87)
Humboldt Bay Power Plant, Unit No. 3. License No. DPR-7: technical specifications Change No. 29, 25:5917 (DOCKET-50133-44)
Oyster Creek Nuclear Power Plant, Unit No. 1. Provisional Operating License No. DPR-16, Amendment 2, 25:5918 (DOCKET-50219-116)
DUKE UNIV., DURHAM, N.C. DEPT. OF PHYSICS.
Nuclear rotational bands and SL (3,R) symmetry, 25:5801 (AD-706835)
DUKE UNIV., DURHAM, N. C. DEPT. OF PHYSIOLOGY AND PHARMACOLOGY.
Prog. rpt. on the effect of radiation on mucosal phospholipase activity, 1967--70, 25:4455 (ORO-3329-7)

E

EDSEL B. FORD INST. FOR MEDICAL RESEARCH, DETROIT, MICH. DIV. OF NUCLEAR SPECTROSCOPY AND RADIATION PHYSICS.
Two photon absorptiometric analysis using ^{109}Cd, 25:4646 (CONF-700515-, pp 272-3)
EUROPEAN ATOMIC ENERGY COMMUNITY, ISPRA (ITALY). JOINT NUCLEAR RESEARCH CENTER.
Aspects of design reliability of pressure tubes for heavy water moderated reactors, 25:5984 (RISO-214, pp 335-43)
Fracture mechanics approach to the assessment of reliability of reactor pressure tubes, 25:6191 (RISO-214, pp 255-87)
General principles of a safety assessment through reliability analysis of ESSOR plant, 25:6094 (RISO-214, pp 597-625)
Reliability assessment of a novel liquid rod shut-down system, 25:6037 (RISO-214, pp 57-70)
EUROPEAN COMMUNITIES, BRUSSELS (BELGIUM). COMMISSION.
Reliability of emergency core cooling systems of light water nuclear power plants, 25:6038 (RISO-214, pp 91-126)
EUROPEAN ORGANIZATION FOR NUCLEAR RESEARCH, GENEVA (SWITZERLAND).
Experimental program at CERN intersecting storage rings, 25:5444 (CONF-700314-, Paper 2)
IHEP (Serpukhov). CERN experiments, 25:5265 (CONF-700314-, Paper 4)
Omega--rho interference in strong interactions, 25:5373 (DNPL/R-7, pp 173-205)

F

FELS RESEARCH INST., YELLOW SPRINGS, OHIO.
Bone mineral measurements from x-ray images, 25:4614 (CONF-680211-, pp 80-95)
Phalangeal Atlas: an application of radiographic photodensitometry, 25:4641 (CONF-700515-, pp 224-36)
FLORIDA UNIV., GAINESVILLE. ENGINEERING AND INDUSTRIAL EXPERIMENT STATION.
Quantitative determination of the structure--property relationships in nuclear fuel element materials. Quarterly progress report, June 15--September 15, 1970, 25:4841 (SRO-552-5)
FLORIDA UNIV., GAINESVILLE. RADIATION BIOLOGY LAB.
Prog. rpt. on radiation biology, 8/69--6/70, 25:4456 (ORO-3596-15)
FORSVARETS FORSKNINGSANSTALT, STOCKHOLM (SWEDEN).
Neutron capture cross sections in F, Mg, Al, Si, P, and S from 20 to 80 keV, 25:5603 (FOA-4-4440)

G

GENERAL ELECTRIC CO., PHILADELPHIA, PA. MISSILE AND SPACE DIV.
Prog. rpt. on MHD power system for nuclear electric propelled unmanned spacecraft, 5/69--5/70, 25:4992 (N-70-34006)
GENERAL ELECTRIC CO., PHILADELPHIA, PA. SPACE DIV.
Applications of avalanche type semiconductor radiation detectors. Final Report, October 1968--November 1969, 25:4323 (NYO-4028-TA-1)
GENERAL ELECTRIC CO., SAN JOSE, CALIF. ATOMIC POWER EQUIPMENT DEPT.
Demonstration of performance and reliability of General Electric Co. Boiling Water Reactor main steamline isolation valves, 25:6040 (RISO-214, pp 247-53)
GENERAL ELECTRIC CO., SAN JOSE, CALIF. REACTOR FUELS AND REPROCESSING DEPT.
Prog. rpt. on Zircaloy-clad UO_2 fuel rod evaluation program, 2--4/70, 25:4886 (GEAP-10204)
GENERAL ELECTRIC CO., SUNNYVALE, CALIF. BREEDER REACTOR DEVELOPMENT OPERATION.
Fabrication of non-fuel core components for SEFOR, 25:5943 (GEAP-13595)
Southwest Experimental Fast Oxide Reactor. Malfunction of the emergency electrical system tie breakers, 25:6050 (DOCKET-50231-59)
Southwest Experimental Fast Oxide Reactor. Reactivity coefficients, as determined from tests through 10MW, 25:5951 (DOCKET-50231-58)
GESELLSCHAFT FUER STRAHLENFORSCHUNG M.B.H., MUNICH (WEST GERMANY).
Dosimetry in microbiology, 25:4507 (EUR-4506)
GILBERT AND PILCHER, INC., BATON ROUGE, LA.
Establishment of high-level radioactive materials management centers in salt dome structures, 25:4264 (NP-18527)
GOSUDARSTVENNYI KOMITET PO ISPOL'ZOVANIYU ATOMNOI ENERGII SSSR, SERPUKHOV. INSTITUT FIZIKI VYSOKIKH ENERGII.
Behavior of diffractional peak width at high energies in case of Gaussian potential, 25:5424 (IFVE-STF-69-83)
Forward scattering amplitude behavior at high energies, 25:5349 (IFVE-STF-69-74)
Isochronous magnetic optical systems, 25:5447 (IFVE-CP-69-68)
Program of connection of measuring microscopes PUOS with computer Minsk-2, 25:4369 (IFVE-SPK-69-53)
Relative value of cross sections of NN → W + (Hadrons) and NN → (Hadrons) γ, $\gamma \rightarrow \mu + \mu$ reactions, 25:5266 (IFVE-SEF-69-81)
Search for W-boson in NN-collisions at IHEP accelerator, 25:5267 (IFVE-SEF/STF-69-46)
Solution of the unitarity equation for the elastic scattering amplitude at high energy, 25:5423 (IFVE-STF-69-65)
Unitary representations of the conformal group, 25:5393 (IFVE-STF-69-85)
GOSUDARSTVENNYI KOMITET PO ISPOL'ZOVANIYU ATOMNOI ENERGII SSSR, SUKHUMI. FIZIKO-TEKHNICHESKII INSTITUT.
Conference on diagnosis of high-temperature plasma, Sukhumi, USSR, 5/70, 25:5080 (LA-4520-TR)
GULF GENERAL ATOMIC, INC., SAN DIEGO, CALIF.
High-temperature fast-flux irradiation experiment for mixed-oxide fuel rods, 25:5989 (GA-10264)
HTGR fuel reprocessing: head-end treatment of experimental small-scale HTGR fuel elements, 25:4136 (GAMD-9260(Pt.2))
Microdetermination of fluorine in high-purity tungsten metal by photoactivation analysis, 25:4043 (GA-10125)

H

HAHN-MEITNER-INSTITUT FUER KERNFORSCHUNG, BERLIN (WEST GERMANY).
Graphic display terminal for nuclear experiments with on-line computer. I, 25:4390 (HMI-B-100)
HAMBURG UNIV. (WEST GERMANY). INSTITUT FUER THEORETISCHE PHYSIK (II).
Recent theoretical work in photoproduction of vector mesons, 25:5323 (DNPL/R-7, pp 3-28)
HAMMERSMITH HOSPITAL, LONDON (ENGLAND).
Age-related bone changes in women, 25:4616 (CONF-680211-, pp 115-35)
HOSPITAL FOR SPECIAL SURGERY, NEW YORK.
Chemical and physical nature of bone mineral, 25:4412 (CONF-680211-, pp 5-24)
HYDRO-ELECTRIC POWER COMMISSION OF ONTARIO, TORONTO.
Ontario Hydro nuclear generating station safety and production reliability, 25:5936 (RISO-214, pp 127-69)

I

IDAHO NUCLEAR CORP., IDAHO FALLS.
Effect of fast neutron irradiation on the mechanical properties of hafnium, 25:4813 (IN-1440)
WHAM prediction of semiscale test results, 25:6061 (IN-1431)
ILLINOIS UNIV., CHICAGO. MEDICAL CENTER.
Mobilization of radioactive emitters from bone, final report, 4/66--8/70, 25:4423 (COO-1601-23)
ILLINOIS UNIV., URBANA.
Spin parity studies of eta pi decay of A2 meson, 25:5282 (COO-1195-200)
IMPERIAL COLL. OF SCIENCE AND TECH., LONDON (ENGLAND).
Review of the safety aspects of the design of prestressed concrete pressure vessels with reference to limit state design, 25:5981 (RISO-214, pp 285-300)
INDIANA UNIV., INDIANAPOLIS. MEDICAL CENTER.
Measurement of bone mass in the radius, 25:4624 (CONF-680211-, pp 283-96)
INNSBRUCK UNIV. (AUSTRIA). INSTITUT FUER THEORETISCHE PHYSIK.
Turbulent heating in plasmas, 25:5068 (AD-710318)
INSTITUT FUER PLASMAPHYSIK, G.M.B.H. GARCHING (WEST GERMANY).
Prog. rpt. on plasma physics, annual, 1968, 25:5066 (NP-18495)
Radiation losses of a high-density Z-pinch, 25:5092 (SC-T-70-4044)
INSTITUT JOZEF STEFAN, LJUBLJANA (YUGOSLAVIA).
Spin-lattice relaxation by quasi-spin waves in order-disorder type ferroelectrics, 25:6233 (IJS-575)
INSTITUTE OF NUCLEAR RESEARCH, WARSAW (POLAND).
Numerical calculations of the electrical parameters in a Faraday-type MHD generator with two-dimensional gas flow, 25:4991 (INR-1199)
INTER-AMERICAN INST. OF AGRICULTURAL SCIENCES, TURRIALBA (COSTA RICA).
Application of nuclear energy to agriculture. Annual report, 25:4732 (NYO-2043-216)
Entomology, 25:4733 (NYO-2043-216, pp 19-48)
Radiation botany and plant genetics, 25:4717 (NYO-2043-216, pp 1-18)
Soil chemistry, 25:4052 (NYO-2043-216, pp 48-73)
IOWA UNIV., IOWA CITY. DEPT. OF PHYSICS AND ASTRONOMY.
Difference scheme for Vlasov's equation, 25:5096 (COO-2059-5)
Excitation of ion bursts from grids, 25:5122 (COO-2059-4)
Numerical integration methods of Vlasov equation, 25:5097 (COO-2059-6)

J

JAGELLONIAN UNIV., KRAKOW (POLAND). DEPT. OF THEORETICAL PHYSICS.
Decay distributions of resonances, 25:5375 (TPJU-15/70)
Determination of $X^0(960)$ meson spin-parity in polarization experiment, 25:5361 (TPJU-14/70)
JAPAN ATOMIC ENERGY RESEARCH INST., TOKYO.
Process of carburization in austenite stainless steel, 25:4739 (JAERI-Memo-4132)
JET PROPULSION LAB., PASADENA, CALIF.
Prog. rpt. on MHD power system for nuclear electric propelled unmanned spacecraft, 5/65--5/70, 25:4992 (N-70-34006)
JOHNS HOPKINS UNIV., BALTIMORE, MD. DEPT. OF BIOCHEMISTRY.
Genetic transformation in hemophilus influenzae, comprehensive report, 9/15/67--9/14/70, 25:6241 (NYC-1371-63)
JOHNS HOPKINS UNIV., BALTIMORE, MD. MC COLLUM-PRATT INST.
Prog. rpt. on mechanism of bioluminescence and energy transfer, 1968--70, 25:6244 (NYO-2802-70)
JOINT COMMITTEE ON ATOMIC ENERGY (U. S. CONGRESS).
AEC authorizing legislation, fiscal year 1971. Part 2. Hearings before the Joint Committee on Atomic Energy, Congress of the United States, Ninety-First Congress, second session on physical research, biology and medicine, and plowshare, March 3 and 5, 1970, 25:5311
JOINT INST. FOR NUCLEAR RESEARCH, DUBNA (USSR).
Covariant density matrix for arbitrary spin particles, 25:5305 (JINR-P2-4931)
Di-pion in mass values region $M(\pi^0\pi^0)$ less than or equal to 1.3 GeV, 25:5284 (JINR-E1-5085)
Mesic atom processes in hydrogen, 25:4952 (JINR-P4-5039)
Nonstrange baryon--baryon resonances, 25:5388 (JINR-P2-5058)
Reactions in complete fusion of nuclei, 25:5115 (JINR-P4-5019)
Time-of-flight and coordinate measurements in a 130 cm scintillation counter, 25:4316 (JINR-E1-5098)
JOINT INST. FOR NUCLEAR RESEARCH, DUBNA (USSR). LAB. OF COMPUTING TECHNIQUES AND AUTOMATION.
Polarization of secondary protons in pp + π^+pn and pp + π^0pp reactions at 669 MeV, 25:5268 (JINR-P1-5293)
JOINT INST. FOR NUCLEAR RESEARCH, DUBNA (USSR). LAB. OF HIGH ENERGY.
Charged relativistic electron ring in the helical magnetic field, 25:5448 (JINR-P9-5299)
Deuteron acceleration in LHE synchrophasotron, 25:5449 (JINR-P9-5311)
Interference of identical particles in the processes involving the resonances, 25:5350 (JINR-P1-5315)
Ionization counter dE/dx filled with liquid Xe, 25:4319 (JINR-P13-5403)
JOINT INST. FOR NUCLEAR RESEARCH, DUBNA (USSR). LAB. OF NEUTRON PHYSICS.
Debye--Waller factor for W, 25:5170 (JINR-P14-5358)
JOINT INST. FOR NUCLEAR RESEARCH, DUBNA (USSR). LAB. OF NUCLEAR PROBLEMS.
Dynamics of vapor bubbles in liquid hydrogen and ultrasonic bubble chambers, 25:4371 (JINR-P13-5327)
JOINT INST. FOR NUCLEAR RESEARCH, DUBNA (USSR). LAB. OF THEORETICAL PHYSICS.
Equality of local algebras of relativistic quantum field theory, 25:5407 (JINR-P2-5330)
Equivalence theorem and observables in the field theory, 25:5235 (JINR-P2-5266)
Example of the infinite-component local field with the mass spectrum, 25:5406 (JINR-P2-5305)
K/sub 13/ decays in chiral dynamics, 25:5359 (JINR-P2-5290)
Lower bounds for the scattering parameters, 25:5425 (JINR-P4-5332)
Multipole current disintegration in classical electrodynamics, 25:5236 (JINR-P2-5283)
Problem of quasipotential smoothness in quantum field theory models, 25:5387 (JINR-E2-5365)
Quasi-potential equation for the relativistic harmonic oscillator, 25:5405 (JINR-E2-5339)
Single-particle state of deformed nuclei in transuranium region of Saxon--Woods potential, 25:5684 (JINR-P4-5221)

K

KAISER FOUNDATION RESEARCH INST., OAKLAND, CALIF.
Clinical trial of the ^{125}I isotope scanning device as a screening method for the early detection of osteoporosis, 25:4651 (CONF-700515-, pp 340-50)
KANSAS STATE UNIV., MANHATTAN.
X-radiation effects on biology of Heterakis gallinarum and Histomonas meleagridis, 25:4692 (COO-1209-13)
KANSAS UNIV., LAWRENCE.
Prog. rpt. on high temperature chemistry, annual, 11/1/69--10/31/70, 25:6232 (COO-1140-192)
KAROLINSKA INSTITUTET, STOCKHOLM (SWEDEN).
Bone salt determination by x-ray spectrophotometry, 25:4642 (CONF-700515-, pp 237-42)
KATHARINENHOSPITAL DER STADT STUTTGART (WEST GERMANY). ZENTRALROENTGENINSTITUT.
Quantitative measurements of bone mineral content by densitometric methods, 25:4622 (CONF-680211-, pp 216-49)
KERNFORSCHUNGSANLAGE, JUELICH (WEST GERMANY). INSTITUT FUER REAKTORWERKSTOFFE.
Procedure for identification of fuel element spheres of high-temperature reactors with the help of emission spectral analysis at 40 atmospheres of helium, 25:4013 (JUL-671-RW)
KERNFORSCHUNGSZENTRUM, KARLSRUHE (WEST GERMANY). INSTITUT FUER ANGEWANDTE KERNPHYSIK.
Nuclear spectroscopy using radiative neutron capture and neutron-induced fission, 25:5474 (KFK-1197)
KERNFORSCHUNGSZENTRUM, KARLSRUHE (WEST GERMANY). INSTITUT FUER ANGEWANDTE REAKTORPHYSIK.
Development of safeguards procedures for a reprocessing plant similar to the WAK type, 25:4263 (KFK-1102)
KERNFORSCHUNGSZENTRUM, KARLSRUHE (WEST GERMANY). INSTITUT FUER MATERIAL UND FESTKOERPERFORSCHUNG.
Change in thermal conductivity of an oxide fuel element during burn up, 25:4839 (KFK-1245)
Production, detection, annealing of crystal lattice point defects by neutron irradiation of ceramic materials, 25:4887 (KFK-1215)
KERNFORSCHUNGSZENTRUM, KARLSRUHE (WEST GERMANY). INSTITUT FUER REAKTORBAUELEMENTE.
Superheated steam filter. I, 25:5580 (KFK-1183)
KYOTO UNIV. (JAPAN). RESEARCH REACTOR INST.
Radiation control program at Kyoto Univ., 1968, 25:4508 (KURRI-TR-63)
Second neutron measurements symposium, 25:4320 (KURRI-TR-59)

L

LOCKHEED-GEORGIA CO., MARIETTA.
Space radiation hazards to Project Skylab photographic film, 25:4405 (N-70-32671)
LOS ALAMOS SCIENTIFIC LAB., N. MEX.
Absolute beam polarization determination for the LASL Lamb-shift source by the quench ratio method, 25:5453 (LA-4465, pp 10.1-2)
Absolute polarization determination of mass-3 nuclei, 25:5518 (LA-4465, pp 19.1-2)
Analyzing power of the T(d,α)n reaction at low energies, 25:5525 (LA-4465, pp 34.1-2)
Asymmetries in deuteron scattering from a polarized ^3He target, 25:5515 (LA-4465, pp 14.1-2)
Asymmetries in protons from the reaction of deuterons with a polarized ^3He target, 25:5524 (LA-4465, pp 32.1-2)

Characteristics of AlK and $Al(NH_4)$ alum as new materials for polarized proton targets, 25:5450 (LA-4465, pp 4.1-2)
Comparison of double scattering and polarized ion source measurements of $^4He(d,d)^4He$ polarization at 11.5 MeV, 25:5510 (LA-4465, pp 3.1-3)
Comprehensive approach to computer arithmetic, 25:6238 (LA-4531)
Considerations on polarized neutron production by (d,n) polarization transfer reactions at 0°, 25:5805 (LA-4465, pp 26.1-2)
Elastic scattering of polarized tritons, 25:5511 (LA-4465, pp 5.1-2)
Energy inequalities in some nonlinear initial-value problems, 25:6237 (LA-4525)
Figures of merit for polarized deuteron beams, 25:5455 (LA-4465, pp 23.1-2)
Formalism for A(d,n)B or A(d,p)B polarization transfer reactions, 25:5803 (LA-4465, pp 20.1-2)
Formalism for A(p,p)A and A(d,d)A polarization transfer, 25:5804 (LA-4465, pp 21.1-2)
Formalism for spin-3/2 beams, 25:5807 (LA-4465, pp 35.1-2)
Improvements in performance of a liquid helium scintillation counter, 25:4321 (LA-4465, pp 31.1-2)
LASL contributions to the 3rd international symposium on polarization phenomena in nuclear reactions, Madison, Wisconsin, August 31--September 4, 1970, 25:5507 (LA-4465)
Measurement of the vector and tensor analyzing power of d--^{4}He elastic scattering at 12 MeV, 25:5553 (LA-4465, pp 25.1-2)
Neutron polarization in the $T(d,n)^4He$ reaction using a polarized incident beam, 25:5513 (LA-4465, pp 12.1-2)
Neutron--helium polarization at 27.3 and 30.3 MeV, 25:5523 (LA-4465, pp 30.1-2)
Performance of the LASL polarized source, 25:5452 (LA-4465, pp 9.1-2)
Phase shifts from n--^{4}He elastic scattering experiments near 20 MeV, 25:5508 (LA-4465, pp 1.1-2)
Polarization angular distribution from the $T(d,n)^4He$ reaction at 7.0 and 11.4 MeV, 25:5522 (LA-4465, pp 25.1-2)
Polarization in nucleon--deuteron scattering at medium energies, 25:5517 (LA-4465, pp 16.1-2)
Polarization of 22-MeV neutrons elastically scattered from liquid tritium and deuterium, 25:5516 (LA-4465, pp 15.1-2)
Precise method for the determination of secondary standards for deuteron analyzing tensors, 25:5806 (LA-4465, pp 27.1-6)
Preliminary measurements of neutron polarization from the $D(d,n)^3He$ reaction using a polarized incident beam, 25:5514 (LA-4465, pp 13.1-2)
Prog. rpt. on CMF-13 research on carbon and graphite, 5--7/70, 25:4840 (LA-4526)
Proposal for a Lamb-shift polarimeter, 25:4391 (LA-4465, pp 17.1-6)
Proposal for the detection of mother molecules in comets by their microwave lines, 25:4915 (LA-4542)
Proposed 0.4 K polarized proton target cryostat for LAMPF, 25:5456 (LA-4465, pp 33.1-2)
Proposed ultra-low temperature polarized target for use with single-burst neutron sources, 25:5451 (LA-4465, pp 8.1-2)
Quadratic relations between the $T(d,n)^4He$ observables, 25:5519 (LA-4465, pp 22.1-2)
Rapid method for the measurement of analyzing tensors in reactions induced by polarized deuterons, 25:5802 (LA-4465, pp 11.1-2)
Reactance matrix analysis of the d--^{3}He, p--^{4}He system at 10-MeV deuteron laboratory energy, 25:5509 (LA-4465, pp 2.1-2)
Scattering of polarized protons by tritons at 13.6 MeV, 25:5521 (LA-4465, pp 28.1-2)
Sonic limitations and startup problems of heat pipes, 25:6236 (LA-4518)
Study of $^3He(d,d)^3He$ scattering at 10 and 12 MeV, 25:5520 (LA-4465, pp 24.1-2)
Study of the $^3He(d,p)^4He$ reaction, 25:5512 (LA-4465, pp 6.1-2)
Transfer matrix method for calculating spin aberrations in the transport of polarized beams, 25:5454 (LA-4465, pp 18.1-16)
Underground nuclear explosion as a polarized neutron source, 25:5475 (LA-4465, pp 7.1-2)

LOUISIANA STATE UNIV., BATON ROUGE. DEPT. OF PHYSICS AND ASTRONOMY.
Prog. rpt. on conductivity tensors in metals and semiconductors, 10/15/69--10/15/70, 25:5171 (ORO-3087-44)

LOYOLA UNIV., MAYWOOD, ILL. STRITCH SCHOOL OF MEDICINE.
Prog. rpt. on metabolism and removal of ^{90}Sr and ^{226}Ra in man, annual, 1969--1970, 25:4424 (TID-25567)

LYON UNIV. (FRANCE).
Application of cross-correlation method in nuclear physics, 25:4392 (LYCEN-7032)

LYON UNIV. (FRANCE). INSTITUT DE PHYSIQUE NUCLEAIRE.
Application of cross-correlation method in nuclear physics, 25:4392 (LYCEN-7032)

M

MCDONNELL DOUGLAS ASTRONAUTICS CO.-WEST, HUNTINGTON BEACH, CALIF.
Statistical analysis of solar cosmic ray proton dose, 25:4509 (MDC G-363)

MAGYAR TUDOMANYOS AKADEMIA KOZPONTI FIZIKAI KUTATO INTEZETE, BUDAPEST.
Two-dimensional (T/sub 1/2/, E/sub γ/) mapping of short-lived nuclides, 25:5685 (KFKI-70-18-NAC)

MALMO GENERAL HOSPITAL (SWEDEN). DEPT. OF ORTHOPEDIC SURGERY.
Bone densitometry using a single beam from a radionuclide source, 25:4627 (CONF-680211-, pp 319-28)

MASSACHUSETTS GENERAL HOSPITAL, BOSTON.
Restraint device for scanning dogs, 25:4654 (CONF-700515-, pp 424-7)

MASSACHUSETTS INST. OF TECH., CAMBRIDGE. LAB. FOR NUCLEAR SCIENCE.
Photoproduction of vector mesons, 25:5301 (DNPL/R-7, pp 29-70)

MAYO CLINIC, ROCHESTER, MINN.
Mineral density in normal and osteoporotic bone, 25:4629 (CONF-680211-, pp 411-21)
New method of evaluating bone loss in osteoporosis, 25:4639 (CONF-700515-, pp 199-204)

MAYO FOUNDATION, ROCHESTER, MINN.
New method of evaluating bone loss in osteoporosis, 25:4639 (CONF-700515-, pp 199-204)

MECHANICAL TECHNOLOGY INC., LATHAM, N. Y.
Prog. rpt. on liquid metal bearings technology, 5--7/70, 25:4185 (NYO-3930-8)

MEDICAL RESEARCH COUNCIL, LEEDS (ENGLAND). MINERAL METABOLISM UNIT.
Bone patterns in aging and osteoporosis, 25:4618 (CONF-680211-, pp 159-77)
Internal relationships between skeletal parameters in twenty-three male skeletons, 25:4652 (CONF-700515-, pp 365-82)

MICHAEL REESE HOSPITAL, CHICAGO, ILL.
In vivo measurement of the mineral content of a section of the radius, 25:4621 (CONF-680211-, pp 204-15)
New method of evaluating bone loss in osteoporosis, 25:4639 (CONF-700515-, pp 199-204)

MICHIGAN UNIV., ANN ARBOR.
Cosmic ray experiments and prospects, 25:5245 (CONF-700314-, Paper 5)
Structure of electron bubbles in liquid helium from photo-ejection under pressure, 25:5034 (TID-25601)

MINNESOTA UNIV., MINNEAPOLIS.
Evaluation of the significance of the contribution of coherent scattering of an X ray beam to darkening of radiographic film, 25:4640 (CONF-700515-, pp 205-23)
Field theoretic models for high energy processes, 25:5320 (CONF-700314-, Paper 17)

MINNESOTA UNIV., MINNEAPOLIS. ST. ANTHONY FALLS HYDRAULIC LAB.
Physical modeling of heat dispersion in large lakes, 25:6217 (ANL-ES-2)

N

NATIONAL ACCELERATOR LAB., BATAVIA, ILL.
Possibilities for the N.A.L. program, 25:5445 (CONF-700314-, Paper 3)

NATIONAL AERONAUTICS AND SPACE ADMINISTRATION, CLEVELAND, OHIO. LEWIS RESEARCH CENTER.
Study of the cdd strontium isotopes with stripping and pickup reactions, 25:5604 (N-70-25281)
Systematic method of calculating reduced matrix elements of single-particle operators, 25:5808 (N-70-32786)
Thermal neutron absorber buildup in irradiated beryllium, 25:4814 (N-70-32313)

NATIONAL AERONAUTICS AND SPACE ADMINISTRATION, HOUSTON, TEX. MANNED SPACECRAFT CENTER.
Line broadening of the triplet diffuse series of helium in an arc-jet plasma, 25:5082 (N-70-33122)

NATIONAL AERONAUTICS AND SPACE ADMINISTRATION, HUNTSVILLE, ALA. GEORGE C. MARSHALL SPACE FLIGHT CENTER.
Analysis of effect of high-energy protons on ATM photographic film, 25:4407 (N-70-35923)
Radiation degradation of selected films, 25:4406 (N-70-35843)

NATIONAL AERONAUTICS AND SPACE ADMINISTRATION, LANGLEY STATION, VA. LANGLEY RESEARCH CENTER.
Dynamical evolution of disk galaxies, 25:4925 (N-70-33057)

NATIONAL AIR POLLUTION CONTROL ADMINISTRATION, WASHINGTON, D.C.
Multiple-source urban atmospheric dispersion model, 25:4161 (ANL/ES-CC-7)

NATIONAL BIOMEDICAL RESEARCH FOUNDATION, SILVER SPRING, MD.
Evaluation of the significance of the contribution of coherent scattering of an X ray beam to darkening of radiographic film, 25:4640 (CONF-700515-, pp 205-23)
High-speed area-measuring scanning densitometer, 25:4620 (CONF-680211-, pp 191-203)

NATIONAL HEART INST., BETHESDA, MD.
Clinical use of an in-vivo measurement of bone mineral content, 25:4625 (CONF-680211-, pp 296-308)

NATIONAL INST. OF ARTHRITIS AND METABOLIC DISEASES, BETHESDA, MD.
Progress in methods of bone mineral measurement. Conference held in Bethesda, Maryland, 2/68, 25:4612 (CONF-680211)

NATIONAL INSTITUTES OF HEALTH, BETHESDA, MD.
Clinical use of an in-vivo measurement of bone mineral content, 25:4625 (CONF-680211-, pp 296-308)

NATIONAL LEAD CO. OF OHIO, CINCINNATI.
Automatic determination of thorium in aqueous and organic solutions, 25:4014 (NLCO-1072)
GIRLS: general indexing in reciprocal lattice space, 25:6240 (NLCO-1066)

NAVAL POSTGRADUATE SCHOOL, MONTEREY, CALIF.
Elastic electron scattering measurements of the neutron charge form factor at very-low momentum transfers, 25:5246 (AD-709922)
Form factor ratio GE/sub n//GE/sub p/ at low-momentum transfers, 25:5247 (AD-710385)

NAVAL RESEARCH LAB., WASHINGTON, D. C.
Analysis of neutron-embrittlement and flux-density considerations of Army SM-1 reactor pressure vessel, 25:6145 (AD-709898)
Dislocation channeling in irradiated metals, 25:4809 (AD-710358)
Radiative corrections to electron scattering from complex nuclei, 25:5800 (AD-706717)
Survey on photon activation analysis using NRL Linac, 25:4041 (AD-709901)

NEW BRUNSWICK LAB. (AEC), N. J.
Analysis of elemental boron, 25:4009 (TID-25190)

NEW YORK OPERATIONS OFFICE (AEC), N. Y. HEALTH AND SAFETY LAB.
Mass transfer of aerosols with axial diffusion in circular tubes, 25:4204 (HASL-238)

NEW YORK UNIV., N. Y.
Dimensions of current operators, 25:5306 (NYO-4204-1)

NEW YORK UNIV., N. Y. AEC COMPUTING AND APPLIED MATHEMATICS CENTER.
Computation of the equilibrium of a plasma with helical symmetry, 25:5106 (NYO-1480-161)
Exact bounds on transport coefficients, 25:6242 (NYO-1480-160)

NIAGARA MOHAWK POWER CORP., SYRACUSE, N. Y.
Nine Mile Point Nuclear Station. Electrical output oscillations when approaching 510 MW(e) gross output, 25:5919 (DOCKET-50220-53)
Nine Mile Point Nuclear Station. Petition requesting amendment of license, Amendment 3. Technical supplement to petition to increase power level, Third Addendum, 25:5920 (DOCKET-50220-54)

NORLAND INSTRUMENTS, FORT ATKINSON, WIS.
Precision of the Norland Instruments bone mineral analyzer, 25:4633 (CONF-700515-, pp 28-32)

NORTH CAROLINA STATE UNIV., RALEIGH. DEPT. OF NUCLEAR ENGINEERING.
Prog. rpt. on diffusion in solids, annual, 11/69--10/70, 25:5152 (ORO-3508-6)

NORTH CAROLINA STATE UNIV., RALEIGH. SEMICONDUCTOR DEVICE LAB.
Piezoresistive effect in electron irradiated silicon and its application to improvement of semiconductor strain gages, 25:5151 (N-70-35737)

NORTH CAROLINA UNIV., CHAPEL HILL. DEPT. OF PHYSICS.
Nuclear quadrupole interaction in crystals by Moessbauer effect, 25:5221 (AD-710293)

NUCLEAR FUEL SERVICES, INC., WEST VALLEY, N.Y.
West Valley Reprocessing Plant. Foundation investigation: proposed plutonium fuel plant, West Valley, New York, 25:4154 (DOCKET-50201-52)
West Valley Reprocessing Plant. Site investigation: proposed Spent Nuclear Fuel Processing Plant, near Springville, New York, 25:4153 (DOCKET-50201-51)
West Valley Reprocessing Plant. Soils and foundation investigation: proposed Iodine Recovery Building, West Valley, New York, 25:4155 (DOCKET-50201-53)
West Valley Reprocessing Plant. Topographical map showing existing and proposed facilities, 25:4156 (DOCKET-50201-54)

NUCLEAR MATERIALS AND EQUIPMENT CORP., APOLLO, PA.
Safety and radiation report of radioisotope powered cardiac pacemaker program, 25:4215 (NUMEC-3731-23)
Spectrographic analysis response of a carrier to plutonium--uranium mixed oxides, 25:4015 (NUMEC-3524-76)

O

OAK RIDGE NATIONAL LAB., TENN.
Design considerations of reactor containment spray systems. Part V. Protective coatings tests, 25:6034 (ORNL-TM-2412(Pt.5))
Design considerations of reactor containment spray systems. Part VIII. Boiling water reactor accident radiolysis studies, 25:6035 (ORNL-TM-2412(Pt.8))
Dissolution of calcium--strontium carbonate and its subsequent movement in the ground, 25:4265 (ORNL-TM-3130)
Engineering development studies for Molten-Salt Breeder Reactor Processing No. 1, 25:4138 (ORNL-TM-3053)
Gas-Cooled Reactor Program semiannual progress report for period ending March 31, 1970, 25:5990 (ORNL-4589)
Hydraulic performance and cavitation characteristics of electromagnetic helical induction pump, 25:4186 (ORNL-TM-2995)
LEGCK, a subroutine to analyze Legendre coefficients for negativity in the angular distribution, 25:5476 (ORNL-TM-2903)
Prog. rpt. on Molecular Anatomy Program, 3--8/70, 25:4656 (ORNL-4615)
Prog. rpt. on transportation systems and dual purpose blast shelters, 7/70, 25:4255 (ORNL-TM-3016)
Program WEIGHT: FORTRAN IV program for evaluation of weighting functions used in small-angle x-ray scattering, 25:6246 (ORNL-TM-1956(Rev.1))
Radiological considerations in the use of natural gas from nuclearly stimulated wells, 25:4525 (ORNL-TM-3216)
Research on stimulated exoelectron emission from lunar materials, 25:4935 (ORNL-TM-3131)
SAMBO: collision analysis package for Monte Carlo codes, 25:5237 (ORNL-TM-3203)
Survey report on structural design of piping systems and components, 25:4188 (TID-25553)

OREGON UNIV., EUGENE.
Energy and angular resolution in pion--pion scattering and other colliding beam experiments, 25:5360 (RLO-2041-51)
Scattering of real pions on each other, 25:5285 (RLO-2041-40)
Three paradoxes related to full causality, 25:5307 (RLO-2041-49)

P

PACIFIC GAS AND ELECTRIC CO., SAN FRANCISCO, CALIF.
Humboldt Bay Power Plant, Unit No. 3. Operation with less than normal off site power for more than twelve hours, 25:5891 (DOCKET-50133-43)

PACKARD INSTRUMENT CO., DOWNERS GROVE, ILL.
Additional system for bone densitometry studies, 25:4634 (CONF-700515-, pp 33-47)
Features and performance characteristics of the Packard Osteodensitometer, 25:4635 (CONF-700515-, pp 48-57)

PARIS UNIV., ORSAY (FRANCE).
Differential cross sections for reaction $\pi^- p \to \eta n$ between 2.9 and 18.2 GeV/c, 25:5279 (CEA-R-4037)

PARIS UNIV., ORSAY (FRANCE). LABORATOIRE DE L'ACCELERATEUR LINEAIRE.
Production of vector mesons by e^+e^- annihilation, 25:5250 (DNPL/R-7, pp 139-72)

PARIS UNIV., ORSAY (FRANCE). LABORATOIRE DE PHYSIQUE THEORIQUE ET HAUTES ENERGIES.
Theoretical investigations about ω--rho mixing, 25:5324 (DNPL/R-7, pp 95-114)

PENNSYLVANIA STATE UNIV., UNIVERSITY PARK. ICNOSPHERE RESEARCH LAB.
Double Langmuir probe measurements in a magnetized positive column, 25:5081 (N-70-32453)
Experiment to obtain excess electron energy loss factor, 25:5001 (AD-710426)

PENNSYLVANIA UNIV., PHILADELPHIA. DEPT. OF RADIOLOGY.
Two wavelength technique for the measurement of bone mineral content in vivo, 25:4645 (CONF-700515-, pp 263-71)

PITTSBURGH UNIV., PA. DEPT. OF PHYSICS.
Locally generated dilatation charge in Thirring model, 25:5408 (NYO-3829-61)

PLASMA SCIENCES LABS., INC., VAN NUYS, CALIF.
Absorption corrections for optically thick plasmas, 25:5088 (AD-710218)

PRINCETON-PENNSYLVANIA ACCELERATOR, PRINCETON, N. J.
NASA briefing on high energy, heavy ion capabilities of Princeton-Pennsylvania accelerator, 25:5462 (PPAD-676-E)

PRINCETON UNIV., N.J. JOSEPH HENRY LABS.
Crossed channel partial wave expansions and the Bethe--Salpeter equation, 25:5426 (NYO-2263-TA-226)
Scaling behavior in multiperipheral dynamics, 25:5351 (NYO-2262-TA-225)

PUBLIC HEALTH SERVICE, SAN FRANCISCO, CALIF. HOSPITAL.
Mineral content changes in the os calcis, ulna, and radius induced by prolonged bed rest, 25:4653 (CONF-700515-, pp 408-22)

PURDUE UNIV., LAFAYETTE, IND. DEPT. OF PHYSICS.
$\pi^+ p \to f^0 \Delta^{++}$ at 13.1 GeV/c, 25:5283 (COO-1428-238)

R

REACTOR CENTRUM NEDERLAND, PETTEN.
Measurements and calculations on thermal, Argonaut type, cores in STEK-facility at Petten, 25:6093 (RCN-118)

RENSSELAER POLYTECHNIC INST., TROY, N. Y.
Temperature-dependent and multi-level effects on neutron resonance cross sections, 25:5686 (TID-25566)

ROCHESTER UNIV., N. Y.
Recent results in ω meson photoproduction, 25:5248 (DNPL/R-7, pp 71-85)

ROCHESTER UNIV., N. Y. DEPT. OF RADIATION BIOLOGY AND BIOPHYSICS.
Biological effects of microwave exposure: an overview, 25:4708 (UR-49-1256)
ROCKEFELLER UNIV., NEW YORK.
Dimensions of current operators, 25:5306 (NYO-4204-1)
Weak interactions at high energies, 25:5339 (CONF-700314-, Paper 7)
ROME UNIV. (ITALY). ISTITUTO DI FISICA.
Search for excess electron photo-ejection in liquid He, 25:5060 (NP-18484)
ROYAL POSTGRADUATE MEDICAL SCHOOL, LONDON (ENGLAND).
Age-related bone changes in women, 25:4616 (CONF-680211-, pp 115-35)
RUTHERFORD HIGH ENERGY LAB., CHILTON (ENGLAND).
Equations and formulae for magnets with air cored windings of saddle coil type, 25:5464 (RHEL/R-203)
Frozen polarized target, 25:5466 (RPP/A-81)
New target material for Rutherford frozen target, 25:5463 (RHEL/R-199)
Prog. rpt. on Nimrod operation and development, 4--6/70, 25:5465 (RHEL/R-206)
Relative phase of rho$^-$ and ω^- production amplitudes in Regge phenomenology, 25:5374 (DNPL/R-7, pp 207-13)

S

SAHLGREN HOSPITAL, GOTEBORG (SWEDEN).
Determination of bone mineral content in lumbar vertebrae by a double gamma-ray technique, 25:4643 (CONF-700515-, pp 243-54)
SAINT MARGARET'S HOSPITAL, BOSTON, MASS.
Effect of irradiation on biochemical changes of mammalian cells, 25:4454 (NYO-3240-55)
SANDIA LABS., ALBUQUERQUE, N. MEX.
Calorimeters for measuring high-energy, high-intensity, pulsed electron beams, 25:4379 (SC-TM-69-298)
Close-in airblast from the Buggy Event. Project Buggy I, 25:4168 (PNE-320)
Efficient Runge--Kutta codes, 25:6250 (SC-RR-70-615)
Prog. rpt. on aerospace nuclear safety, 7--9/70, 25:4216 (SC-PR-70-682)
SLADE: computer program for static analysis of thin shells, 25:6249 (SC-RR-69-369)
Survey of factors which influence stress corrosion crack initiation in several uranium base alloys, 25:4749 (SC-DR-70-718)
SCIENTIFIC RESEARCH INST. OF ELECTRO-PHYSICAL APPARATUS, LENINGRAD (USSR).
Study of the processes of redistribution of phase density in intense proton beams extracted from a duo-plasmatron type ion source, 25:5458 (NP-18510)
Technique for measuring phase characteristics of an ion beam, 25:5457 (NP-18507)
SLOAN-KETTERING INST. FOR CANCER RESEARCH, NEW YORK.
Specifications of photon absorptiometer for bone mineral measurements, 25:4648 (CONF-700515-, pp 291-302)
SOUTHERN INTERSTATE NUCLEAR BOARD, ATLANTA, GA.
Establishment of high-level radioactive materials management centers in salt dome structures, 25:4264 (NP-18527)
SOUTHWEST RESEARCH INST., SAN ANTONIO, TEX.
Survey report on structural design of piping systems and components, 25:4188 (TID-25553)
STANFORD LINEAR ACCELERATOR CENTER, CALIF.
Electromagnetic interactions at very high energy, 25:5319 (CONF-700314-, Paper 8)
Important problems and questions for the new accelerators, 25:5304 (CONF-700314-, Paper 18)
STANFORD UNIV., CALIF. HIGH-ENERGY PHYSICS LAB.
Form factor ratio GE/sub n//GE/sub p/ at low-momentum transfers, 25:5247 (AD-710385)
STANFORD UNIV., CALIF. INST. FOR PLASMA RESEARCH.
Lagrangian approach to nonlinear wave interactions in a warm plasma, 25:5124 (SU-IPR-381)
Low frequency axisymmetric waves in a weakly ionized magnetoplasma column, 25:5123 (SU-IPR-366)
Prog. rpt. on plasma oscillations, 2/1/70--7/31/70, 25:5125 (SU-IPR-389)
STATE UNIV. OF NEW YORK, STONY BROOK.
Diffraction dissociation, 25:5366 (CONF-700314-, Paper 14)
STEVENS INST. OF TECH., HOBOKEN, N. J.
Dimensions of current operators, 25:5306 (NYO-4204-1)
SYRACUSE UNIV., N. Y. DEPT. OF PHYSICS.
Implications of local duality in a set of coupled reactions, 25:5352 (SU-1206-235)

T

TECHNISCHE HOCHSCHULE, MUNICH (WEST GERMANY). INSTITUT FUER MESS- UND REGELUNGSTECHNIK.
Reliability of emergency core cooling systems of light water nuclear power plants, 25:6038 (RISO-214, pp 91-126)
TECHNISCHER UEBERWACHUNGS-VEREIN E. V., COLOGNE (WEST GERMANY). INSTITUT FUER REAKTORSICHERHEIT.
Analysis of a German pressure vessel and boiler drum statistics, 25:5982 (RISO-214, pp 301-22)
Reliability of a containment isolation system, 25:6150 (RISO-214, pp 71-90)
TEXAS UNIV., HOUSTON. GRADUATE SCHOOL OF BIOMEDICAL SCIENCES.
Assessment of bone mass by roentgenographic density techniques, 25:4613 (CONF-680211-, pp 27-80)
TEXAS UNIV., SAN ANTONIO. DEPT. OF RADIOLOGY.
Polychromatic x-ray beam to represent a monoenergetic photon sources. I. Limitations and correction factors for photon detectors, 25:4650 (CONF-700515-, pp 314-31)
TEXAS WOMAN'S UNIV., DENTON.
Assessment of bone mass by roentgenographic density techniques, 25:4613 (CONF-680211-, pp 27-80)
X-ray bone densitometry in short and long duration studies, 25:4615 (CONF-680211-, pp 95-115)
THERMO ELECTRON CORP., WALTHAM, MASS.
Development of a passive self-reading personnel dosimeter, 25:4376 (AD-710007)
Emitter temperature dependence of lower mode current, 25:4752 (TEE-4125-4)
Performance reproducibility of cylindrical diodes with CVD fluoride tungsten--niobium electrodes, 25:4751 (TEE-4125-3)
Sublimed emitter and collector coatings, 25:4750 (TEE-4125-2)
Thermionic performance of fluoride CVD W--Nb converter, 25:4993 (TEE-4125-1)
TOKYO UNIV. (JAPAN). INST. FOR NUCLEAR STUDY.
Control and read out system of scaler, 25:4370 (INS-TH-67)
Program for analysis of bubble-chamber photographs, 25:4372 (SJC-T-70-3)
TOKYO UNIV. OF MERCANTILE MARINE (JAPAN).
Reliability aspects of safety evaluation of nuclear power plants, 25:5937 (RISO-214, pp 457-79)
TORONTO WESTERN HOSPITAL (ONTARIO).
Interrelationships between cortical bone thickness, mineral mass, and mineral density in human radius: a roentgenologic-densitometric study, 25:4617 (CONF-680211-, pp 135-59)
TOULOUSE UNIV. (FRANCE). CENTRE DE PHYSIQUE ATOMIQUE ET NUCLEAIRE.
Spectra and flux of electrons and photons at any point in an irradiated system, 25:4322 (NP-18433)

U

UNITED KINGDOM ATOMIC ENERGY AUTHORITY, ABINGDON (ENGLAND). CULHAM LAB.
Measurement of plasma parameters in Tokamak T3-A by Thomson scattering, 25:5079 (CLM-R-107)
Radiation damage effects in the containment vessel of a thermonuclear reactor, 25:5114 (CLM-R-103)
UNITED KINGDOM ATOMIC ENERGY AUTHORITY, LONDON (ENGLAND).
Report and accounts of UKAEA for the year ended 31 Mar 1970 together with Comptroller and Auditor Generals report on accounts, 25:4088 (NP-18528)
UNITED KINGDOM ATOMIC ENERGY AUTHORITY, RISLEY (ENGLAND). AUTHORITY HEALTH AND SAFETY BRANCH.
Reliability prediction of mechanical instrumentation equipment for process control, 25:6189 (RISO-214, pp 11-20)
Survey of pressure vessels built to a high standard of construction, 25:5983 (RISO-214, pp 323-34)
UNITED KINGDOM ATOMIC ENERGY AUTHORITY, SPRINGFIELDS (ENGLAND). REACTOR GROUP.
Limiting aspects of UO_2 performance, 25:4888 (TRG-Report-1937)
UNITED NUCLEAR CORP., ELMSFORD, N. Y. RESEARCH AND ENGINEERING CENTER.
Prog. rpt. on fast reactor mixed-carbide fuel element development, 4-6/70, 25:4889 (UNC-5263)

V

VIRGINIA ELECTRIC AND POWER CO., RICHMOND.
Surry Power Station, Units 1 and 2. Lateral Load Pile Test. Preliminary safety analysis report, Amendment 16, Pt. B, 25:5927 (DOCKET-50280-28)
Surry Power Station, Units 1 and 2. Preliminary safety analysis report, Amendment 16, Pt. A-2 (includes final safety analysis report, Suppl. Vol. 2), 25:5930 (DOCKET-50280-31)
Surry Power Station, Units 1 and 2. Preliminary safety analysis report, Amendment 16, Pt. A-1 (includes final safety analysis report, Suppl. Vol. 1), 25:5929 (DOCKET-50280-30)
Surry Power Station, Units 1 and 2. Preoperational environmental radiation surveillance program, May 1, 1968--June 30, 1970. Preliminary safety analysis report, Amendment 16, Pt. C, 25:5928 (DOCKET-50280-29)

W

WADCO CORP., RICHLAND, WASH.
BPLOT, multipurpose plotting routine for use with CALCOMP plotter, 25:6257 (WHAN-IR-38)
Uniaxial and biaxial creep-rupture of Type 316 stainless

steel after fast reactor irradiation, 25:4816 (WHAN-FR-19)
WASHINGTON STATE UNIV., PULLMAN. DEPT. OF CHEMISTRY.
Water exchange kinetics in labile aquo and substituted aquo transition metal ions by means of ^{17}O NMR studies, 25:6248 (RLO-2221-T-4-3)
WASHINGTON UNIV., ST. LOUIS, MO. EDWARD MALLINCKRODT INST. OF RADIOLOGY.
Automatic scanner-computer analysis of radiographic bone trabecular activity, 25:4637 (CONF-700515-, pp 188-94)
WASHINGTON UNIV., SEATTLE. DEPT. OF PHYSICS.
Multiperipheral models: phenomenology, 25:5346 (CONF-700314-, Paper 12)
WASHINGTON UNIV., SEATTLE. SCHOOL OF MEDICINE.
In vivo neutron activation analysis of total body bone mass, 25:4042 (CONF-680211-, pp 456-516)
WELLESLEY COLL., MASS. DEPT. OF BIOLOGICAL SCIENCES.
Effects of radiation on migratory orientation of salamanders, 25:4475 (NYO-3654-8)
WESTERN INFIRMARY, GLASGOW (SCOTLAND).
Mineral and density changes in bone with age in normal and pathological states, 25:4615 (CONF-680211-, pp 177-91)
WESTINGHOUSE ELECTRIC CORP., PITTSBURGH, PA. ASTRONUCLEAR LAB.
Radiochemistry of mercury, 25:4133 (NAS-NS-3026(Rev.))
WISCONSIN UNIV., MADISON.
Effects of fat on bone mineral measurements, 25:4644 (CONF-700515-, pp 255-62)
Theoretical accuracy and precision in the photon attenuation measurement of bone mineral, 25:4631 (CONF-700515-, pp 1-21)
WISCONSIN UNIV., MADISON. BONE MINERAL LAB.
Conference on bone measurement, Chicago, Ill., 5/70, 25:4630 (CONF-700515)
WISCONSIN UNIV., MADISON. DEPT. OF PHYSICS.
Conference on expectations for particle reactions at new accelerators, 3--4/70, Madison, Wis, 25:5244 (CONF-700314)
Multiparticle production: experimental, 25:5280 (CONF-700314-, Paper 10)
Regge-type models for high energy scattering, 25:5347 (CONF-700314-, Paper 13)
WISCONSIN UNIV., MADISON. DEPT. OF RADIOLOGY.
Absorptiometric bone mineral determination using ^{153}Gd, 25:4649 (CONF-700515-, pp 308-12)
Measurement of bone mineral by the direct photon absorption method: principles and instrumentation, 25:4623 (CONF-680211-, pp 253-68)
Preliminary report on a direct digital readout system for absorptiometric determination of bone mineral content, 25:4632 (CONF-700515-, pp 22-7)
WISCONSIN UNIV., MADISON. INSTRUMENTATION CENTER.
Preliminary report on a direct digital readout system for absorptiometric determination of bone mineral content, 25:4632 (CONF-700515-, pp 22-7)
WUERZBURG UNIV. (WEST GERMANY). NUKLEARMEDIZINISCHE ABT.
Sensitive method for separate calculation of mineral content in cancellous and compact bone of the finger by a ^{125}I profile scanner. Effect of calcium and fluoride therapy on demineralized bone, 25:4636 (CONF-700515-, pp 169-87)

Y

YALE UNIV., NEW HAVEN, CONN. SCHOOL OF MEDICINE.
Radiographic trabecular quantitation of human lumbar vertebrae in situ: progress in development of method and digital computer analysis, 25:4628 (CONF-680211-, pp 331-51)

Z

ZENTRALSTELLE FUER ATOMKERNENERGIE-DOKUMENTATION, FRANKFURT AM MAIN (WEST GERMANY).
High energy physics index. Vol. 8, No. 20, 1970, 25:5313
High energy physics index, Vol. 8, No. 18, 1970, 25:5312
High energy physics index, Vol. 8, No. 19, 1970, 25:5314
Technology index for plasmaphysics research and fusion reactors, Vol. 4, No. 9, 1970, 25:5067

PERSONAL AUTHOR INDEX

Authors' names are indexed in the form appearing in the abstracted publication. Each entry under an author's name gives the publication title and the *NSA* volume and abstract numbers. Report numbers, where applicable, are given in parentheses at the end of the entry.

Because of problems involved in the mechanical preparation of this index, all accent marks are omitted. The following changes in spelling have been introduced to reduce some of the confusion which might result from omitting the accents:

Germanic	ä appears as	ae
Germanic	ö	oe
Germanic	ü	ue
Scandinavian	ø	oe

A

AARKROG, A., Environmental radioactivity in the Faroes in 1969, 25:4476 (RISO-221)

ABBOTT, L. G., Clinical trial of two sunscreening creams, 25:4608

ABDULLAEV, T., Influence of pollen radiation on crossing ability and variability in cotton, 25:4499

ABDULLAEVA, K. N., Estimate of cross sections of reactions $\pi^- + {}^{12}C \to {}^{12}B + m\pi^0$ (m = 1,2...) and $\pi^- + {}^{12}C \to {}^{12}N + \pi^- + \pi^-$ at 4 GeV/c, 25:5293

ABE, Mitsuyuki, Studies on restorative effect of taurine in radiation injury and its clinical application, 25:4603

ABEND, P., Graphic display terminal for nuclear experiments with on-line computer. I, 25:4390 (HMI-B-100)

ABERNATHEY, R. M., Fission yields of over 40 stable and long-lived fission, 25:5765

ABLAKULOV, Kh. A., Polarization effects in bremsstrahlung radiation of electrons on nuclei with a magnetic dipole moment, 25:5820

ABROL, Y. P., Reversal of inhibitory effects of γ-rays on seedling growth of wheat, 25:4718

ABROYAN, M. A., Study of the processes of redistribution of phase density in intense proton beams extracted from a duo-plasmatron type ion source, 25:5458 (NP-18510)

Technique for measuring phase characteristics of an ion beam, 25:5457 (NP-18507)

ABUL-MAGD, A. Y., Use of the eikonal approximation in the optical-model calculation, 25:5834

ACKERMANN, N. J. Jr., Noise technique for measuring reactivity independent of β/Λ, 25:6174

ADAM, I., Internal-conversion studies of low-energy transitions in ^{149}Sm and ^{151}Eu, 25:5695

Transitions in decay chain ^{146}Gd to ^{146}Eu to ^{146}Sm, 25:5694

ADAMS, A., Reactions ^{26}Mg(d,p)^{27}Mg and ^{28}Si(d,p)^{29}Si, 25:5672

ADAMS, C. C., Fission gas release from an HTGR-type fuel rod, 25:6009

ADAMS, G. E., Electron transfer studies of nucleic acid derivatives in solutions containing radiosensitizers, 25:4540

Molecular mechanisms of cellular radiosensitization and protection, 25:4535

ADAMS, John Bertram, Big European accelerator, 25:5471

ADAMS, M. W., Gamma irradiation studies on seeds seedlings Phaseolus, 25:4723

ADERHOLZ, M., Production of proton--antiproton and kaon--antikaon pairs, 25:5297

ADLER, Ronald J., Radiative np capture and meson exchange currents, 25:5545

AERTS, L., Fuel development for a low-enriched HTR, 25:6007

AGAFONOV, V. I., Research on studying and increasing the plasma parameters on ''non-cylindrical Z-pinch'' equipment, 25:5116 (SC-T-70-4046)

AGARWAL, B. K., Interactions (π^---p) in peripheral model, 25:5376

AGARWAL, R. P., Photochemical precipitation of Th and Ce and their separation from other ions in aqueous solution, 25:4026

AGEEV, P. Ya., Removal of volatile impurities from vacuum melts, 25:4744

AGIN, G. P., Decay of ^{144}Ce, 25:5749

AGOSTINI, Cesare, Prevention by cysteine of fatty liver induced by CCl_4 and ethionine, 25:4600

AGRAWAL, A. K., Failure threshold TREAT experiment with an unirradiated prototypical FFTF fuel element, 25:6056

AGUILERA-NAVARRO, V. C., Variational analysis with harmonic-oscillator states for square potentials, 25:5849

AIHARA, S., Propagation of ion waves in a radio frequency electric field, 25:5130

AIKINS, R. J., HTGR fuel design and irradiation performance, 25:6003

AILION, David C., Self-switching damping circuit for high power pulse NMR, 25:4396

AINSCOUGH, J. B., Limiting aspects of UO_2 performance, 25:4888 (TRG-Report-1937)

AINSWORTH, E. J., Survival-promoting effects of endotoxin in mice, dogs, and sheep, 25:4586

AITKEN, E. A., Behavior of discrete PuO_2 particles in thermal recycle fuel, 25:5994

Behavior of large PuO_2 particles in a rapid power transient, 25:5995

Behavior of Pu recycle fuel in a SPERT power transient, 25:5996

Measuring plutonium homogeneity in fast reactor fuels, 25:4875

Plutonium homogeneity in thermal recycle fuels, 25:4874

AJZENBERG-SELOVE, F., Energy levels of light nuclei A = 13-15, 25:5567

AKASOFU, S.-I., Diagnostics of the magnetosphere using geomagnetic, auroral, and airglow phenomena, 25:5023

AKHIEZER, I. A., Proton--neutron correlations in medium and heavy nuclei, 25:5853

AKIMOV, V. N., Dynamical scheme for leading trajectory and theory of fireballs, 25:5359

AKINO, Kinji, Aseismatic design for a nuclear power plant, 25:5939

AKISHIN, P. A., Mass spectrometric studies of thermodynamic properties of binary system NaF--MeF$_3$ (Me = Sc, Y, La). II, 25:4857

AKIYAMA, Masatsugu, Reaction (^{3}He,α) on ^{7}Li from 5.0 to 8.0 MeV, 25:5571

AKULICHEV, V. A., Dynamics of vapor bubbles in liquid hydrogen and ultrasonic bubble chambers, 25:4371 (JINR-P13-5327)

AL-BASSAM, T. S., Magnetic domain structures in gadolinium, 25:5196

ALBERI, G., Omnes equation and superconvergence relations, 25:5427

ALBERTS, W. G., Supplementary data concerning ^{58}Ni(p,p'γ) reaction, 25:5642

ALBRIDGE, R. G., Decay of ^{194}Au, 25:5728

ALCOUFFE, Raymond E., Accuracy of space-collapse for fast breeder fuel cycle analysis, 25:5965

ALDER, J. C., Giant-resonance excitation by radiative capture of π^- in ^{16}O, 25:5600

ALDER, K., Four-particle--two-hole core excitation in heavy nuclei, 25:5737

Quantum mechanical corrections for double Coulomb excitation in ^{152}Sm, 25:5781

ALEKSANYAN, A. S., Interaction of K_2^0 mesons in Cu and with C, Cl, and F nuclei, 25:5300

ALEKSEEV, V. N., Dynamics of vapor bubbles in liquid hydrogen and ultrasonic bubble chambers, 25:4371 (JINR-P13-5327)

ALEXANDER, P., Computer analysis of fission data, 25:5790

Repair of DNA and the mode of action of sensitizers and protectors in biological systems of different complexity, 25:4536

ALEXANDROV, Yu. A., Debye--Waller factor for W, 25:5170 (JINR-P14-5358)

ALEXEFF, I., Plasma confinement in a high magnetic field toroidal quadrupole, 25:5070

ALI, P., Non-mesonic decay of hypernuclei produced by K-mesons of 3.0 GeV/c momentum, 25:5277

ALIMOV, Sh. A., Local ordering and resistivity of Ni--W and Pd--Co alloys, 25:4766

ALLABI, Ya. V., Total and absorption cross sections of π^-, K$^-$ and antip in the momentum range 20 to 65 GeV/c, 25:5295

XUM

ALLABY, J. V., IHEP (Serpukhov). CERN experiments, 25:5265 (CONF-700314-, Paper 4)
ALLAN, H. R., EAS: radio pulses, 25:4987
ALLEN, J. A., Experiments on the uptake of radioactive phosphorus by bivalves and its subsequent distribution within the body, 25:4448
ALLIBERT, Colette, Phase equilibriums in Ni--Nb--W and Ni--W systems, 25:4788
ALMANOV, G. A., Free radicals in irradiated monocrystals of l-leucine hydrochloride, 25:4092
ALMAZOV, A. B., Calculation of the vibration spectrum of tantalum, 25:5163
ALMENAS, K., Inaccuracy in the calculation of material reactivity worths, 25:6168
ALSMILLER, R. G. Jr., Photonucleon and photopion production from 400 MeV electrons in thick copper targets, 25:5255
ALTIERI, F. D., Implantable electrical power source for an artificial heart system, 25:4235
ALTSCHULER, S. J., Surface density as a useful parameter in the storage and handling of fissile metal, 25:4284
ALTSEIMER, John H., In-flight coolant management considerations for NERVA reactor cooldown, 25:6132
AMARAL-MENDES, J. J., Histopathology of primary lung tumors in mouse, 25:4699
AMMOSOV, V. V., Program of connection of measuring microscopes PUOS with computer Minsk-2, 25:4369 (IFVE-SPK-69-53)
AMOS, K., Proton scattering to 3/2- state of ^{207}Pb, 25:5780
AMSTER, H. J., Design of intermediate-energy neutron spectrometers and their calibration with photoneutrons, 25:4364
ANANTHAKRISHNAN, S., Phase and amplitude changes of vlf signals associated with PCA events, 25:5020
ANDEEN, Carl, Accurate determination of dielectric constant by method of substitution, 25:6225 (COO-623-150)
Capacitive gage for accurate measurement of high pressures, 25:6230 (COO-623-155)
Low frequency dielectric constants of LiF, NaF, NaCl, NaBr, KCl, KBr by method of substitution, 25:6228 (COO-623-153)
Low frequency dielectric constants of alkaline earth fluorides by method of substitution, 25:6229 (COO-623-154)
ANDERSEN, Per H., Photoelectric observations of Nova Serpentis 1970, 25:4901
ANDERSON, E. E., Fission gas release from an HTGR-type fuel rod, 25:6009
ANDERSON, J. B., Mineral and density changes in bone with age in normal and pathological states, 25:4619 (CONF-680211-, pp 177-91)
ANDERSON, J. D., Fast-neutron spectroscopy of the reaction ^{9}Be(p,n)^{9}B at 20 MeV, 25:5557
ANDERSON, James L., Training of personnel to operate Millstone Point Company nuclear boiling water reactor power plant, 25:5895
ANDERSON, K. A., Solar particles and related solar phenomena, 25:4927
ANDERSON, Oscar Albin, Laser light-scattering measurement of plasma temperature, density, and correlation spectrum, 25:5086
ANDERSON, R. N., Application of nitride-forming reactions to reprocessing of spent nuclear fuels, 25:4149
ANDERSON, R. T., Design evaluation of small nuclear power-desalting plants, 25:6144
ANDERSON, S. L., Neutron and photon radiation levels internal and external to mockups of nuclear rocket shields, 25:6130
ANDO, Toshihiko, Electric polarizability of molecular hydrogen as calculated by use of the nonsymmetrical wave function, 25:4949
ANDREEV, I. V., Relativistic eikonal approximation for superposition of two interactions and Coulomb interference, 25:5434
ANDREEV, V. N., Phase transition and switching effect in V_2O_3, 25:4759
ANDRES, K., Observation of nuclear specific heat in V_2O_3, 25:5191
ANDREWS, H. R., Beta-ray asymmetry from oriented /sup 110m/Ag, 25:5743
ANDRIAMBOLOLONA, Raoelina, Approach to form factor in a composite model, 25:5372 (CNRS-CPT-70-P-331)
ANDRIANOV, M. A., System MoO_3--BaO, 25:4873
System MoO_3--CeO_2, 25:4872
ANGHILERI, Leopoldo J., /sup 99m/Tc labeling of erythrocytes, 25:4414
ANNO, G., Response of solid-state detectors to monoenergetic neutrons, 25:4351
ANNO, G. H., Response of miniature G--M tubes to monoenergetic gamma radiation, 25:4349
ANNO, George H., Response of a shielded 300-micron silicon detector to gamma rays, 25:4350
TOPS RTG nuclear radiation environment analysis, 25:4242
ANOROVA, G. A., Radiosensitizing properties of some barenes (ortho-1,1 dicarbaclovododecaborane), 25:4588
ANTMAN, S., Internal-conversion studies of low-energy transitions in ^{149}Sm and ^{151}Eu, 25:5695
Transitions in decay chain ^{149}Gd to ^{149}Eu to ^{149}Sm, 25:5694
ANTOCICCO, S., Theoretical reliability assessment of a fire protection system, 25:4187 (RISO-214, pp 21-40)
ANTTILA, A., Levels of ^{149}Pr from the decay of ^{149}Ce, 25:5739
APOSTOLOV, A., Magnetic structure of ErSi, 25:5212
APT, K. E., Decay schemes of /sup 127m/Te and /127g/Te, 25:5734
APTIKAEVA, G. F., Vicia faba seedling chromosome damages by split dose, 25:4497
ARAPOVA, L. P., Investigation of the alloy Ni--25 at. percent W after isothermal [high-temperature] annealing, 25:4794
Metastable phase of the type Ni_3Mo in Ni--25 at. percent W alloy, 25:4789
ARBORELIUS, Mans Jr., Four quandrant radiospirometry in normal and diseased states, 25:4671
ARBORELUS, Mans Jr., Technetium--indium double lung scanning, 25:4677
ARCHBOLD, T. F., Comments on phase transformations in beta isomorphous titanium alloys, 25:4805
ARIENT, M., Cardiovascular, biochemical, and haematological changes after the application of AET, 25:4599
ARIMA, Masashi, Hot spring therapy of radiation injury. XXVI, 25:4610
ARKHIPENKO, V. I., Wave transformation conditions in plasma, 25:5131
ARMANI, R. J., Selection of fission yields, 25:5973
ARMBRUSTER, R., First two excited states of ^{159}Tb, 25:5727
ARMSTRONG, D. D., Absolute beam polarization determination for the LASL Lamb-shift source by the quench ratio method, 25:5453 (LA-4465, pp 10.1-2)
Absolute polarization determination of mass-3 nuclei, 25:5518 (LA-4465, pp 19.1-2)
Elastic scattering of polarized tritons, 25:5511 (LA-4465, pp 5.1-2)
Measurement of the vector and tensor analyzing power of d--^{3}He elastic scattering at 12 MeV, 25:5553 (LA-4465, pp 25.1-2)
Precise method for the determination of secondary standards for deuteron analyzing tensors, 25:5806 (LA-4465, pp 27.1-6)
Rapid method for the measurement of analyzing tensors in reactions induced by polarized deuterons, 25:5802 (LA-4465, pp 11.1-2)
Study of ^{3}He(d,d)^{3}He scattering at 10 and 12 MeV, 25:5520 (LA-4465, pp 24.1-2)
Study of the ^{3}He(d,p)^{4}He reaction, 25:5512 (LA-4465, pp 6.1-2)
ARMSTRONG, D. R., Molten UO_2--Na dropping experiments, 25:6076
ARNABOLDI, A., Radiosensitizing effect of L-erythro-α,β-dihydroxybutyraldehyde on Ehrlich ascites tumour cells. Cytokinetic analysis of tumour growth, 25:4564
ARNIKAR, H. J., Aqueluminescence from gamma-irradiated halides, 25:4076
ARNOLD, E. D., Shielded neutron shipping cask, 25:4311
ARONOV, A. G., Phase transition and switching effect in V_2O_3, 25:4759
ARONSSON, P. O., New isotope of palladium ^{114}Pd, 25:5740
ARTHUR, J. B., Multiplication effects in measurements of delayed-neutron energy spectra, 25:5774
ARTHUR, J. E., Planning for flexibility in operation, maintenance, and refueling of PWR, 25:5909
ASCOLI, R., Particle--antiparticle doublets and the full Poincare group, 25:5398
ASHBURN, William, Clinical use of an in-vivo measurement of bone mineral content, 25:4625 (CONF-680211-, pp 296-308)
ASHKIN, A., Atomic-beam deflection by resonance-radiation pressure, 25:4941
ASHWOOD-SMITH, M. J., Radiosensitization of bacterial and mammalian cells with carbonyl compounds and ketoaldehydes with special reference to the properties of phenylglyoxal, 25:4557
ASHWORTH, F. P. O., Prog. rpt. on Dragon Project, semiannual, 7-12/65, 25:5942 (DP-Report-490)
ASKEW, W. C., Prog. rpt. on synthesis, identification, and purification of C_6 and C_7 fluorocarbons from radiolysis, 11/70, 25:4111 (ORO-3909-2)
ASTVATSATUROV, R. G., Time-of-flight and coordinate measurements in a 130 cm scintillation counter, 25:4318 (JINR-E1-5098)
ATEN, A. H. W. Jr., Neutron-deficient isotopes of polonium, 25:5696
AUBRY, M. P., Diagnostics of the magnetosphere from ground-based measurements of electromagnetic waves, 25:5030
AUDOLY, S., Resistometric investigation on SAP alloys neutron irradiated at 100°K, 25:4890
AUGST, G. R., Theory of neutron scattering in diatomic crystals containing impurities, 25:5491
AUGUSTSON, R. H., Delayed-neutron abundances and half-lives from 14.7-MeV fission, 25:5775
AUSTERN, Norman, Direct nuclear reaction theories, 25:5823
AUSTIN, John H., Prog. rpt. on diffusion in solids, annual, 11/69--10/70, 25:5152 (ORO-3508-6)
AUTON, D. L., Direct reactions of ^{10}Be, 25:5585
AVDONINA, E. N., Relation of concentration to yield of H in the γ radiolysis of mixtures of cyclohexane and benzene, 25:4121
AYASSE, J. B., Metamagnetic properties of a single crystal of $ErCrO_3$, 25:5180
AYYANGAR, K. M. M. S., Delayed coincidence spectrometer for lifetime studies, 25:4363

AZHGIREI, L. S., Polarization of secondary protons in pp → π^+pn and pp → π^0pp reactions at 665 MeV, 25:5268 (JINR-P1-5293)
AZIMOV, S. A., Estimate of cross sections of reactions π^- + ^{12}C → ^{12}B + mπ^0 (m = 1,2...) and π^- + ^{12}C → ^{12}N + π^- + π^- at 4 GeV/c, 25:5293
AZNAURYAN, I. G., Some consequences from constant behavior of total cross sections at energies more than 30 GeV, 25:5294

B

BABA, Mamour, Reaction (^{3}He,α) on ^{7}Li from 5.0 to 8.0 MeV, 25:5571
BABIC, E., Enhanced superconductivity in ultrarapidly quenched bulk Al--Cu alloy, 25:5056
BACCA, J. P., Interim examination of EBR-II experimental irradiations at Fuels and Examination Facility, 25:4301
BACCICHETTI, F., ^{60}Co gamma-ray effect on mouse Ehrlich ascites tumour cells in the presence of some coumarin derivatives, 25:4565
BACHER, A. D., Mass of ^{13}O and isobaric multiplet mass equation, 25:5640
Polarization and cross-section measurements in p-^{4}He scattering from 20 to 40 MeV, 25:5526 (UCRL-19943)
BACQ, Z. M., Radioprotectors and plasma enzymes, 25:4594
BADIELLO, Roberto, Pulse radiolysis of selenium-containing radioprotectors. I, 25:4115
Radiation chemistry of selenium-containing protective agents, 25:4546
Radioprotection by selenium-containing compounds, 25:4545
BADRA, Kh. M., Thermodynamics of rare earth metals at low temperatures. I, 25:4760
BAECKLIN, A., E2 and M1 transition probabilities in ^{193}Au and ^{195}Au, 25:5701
BAGGETT, Neil Vance, Experimental study of the muonic decays of sigma hyperons, 25:5269
BAGLAN, R. J., M1 giant resonance in ^{208}Pb from threshold photoneutron measurements, 25:5795
BAGNALL, C., Interstitial transfer in sodium systems, 25:4773
BAHL, J. K., Plutonium and fission product migration in mixed-oxide fuels during irradiation, 25:6012
Sintering of thoria powders. V, 25:4836
BAILEY, J., Measurements of pionic x-rays from hydrogen, 25:5288
BAINS, M. S., Carboxylates of metals. I. Uranium(IV) carboxylates, 25:4057
Carboxylates of metals. II. Thorium carboxylates, 25:4056
BAIRIOT, H., Fuel development for a low-enriched HTR, 25:6007
BAJAJ, Y. P. S., Gamma irradiation studies on seeds seedlings Phaseolus, 25:4723
BAJPAI, R. P., Vector-dominance model and the background photoproduction of pions, 25:5332
BAKER, Blair Coleman, Proton NMR studies of 8-quinolinol and several of its metal chelates and electrochemistry of U--EDTA complexes, 25:4081
BAKER, L. Jr., Delineation of LMFBR single subassembly accidents, 25:6068
BALAGUROV, A. M., Debye--Waller factor for W, 25:5170 (JINR-P14-5358)
BALANOV, E. I., Superconductor/normal metal/superconductor point contacts, 25:5037
BALDEWEG, F., Reaction (d,α) on ^{13}C, 25:5559
BALDWIN, D. H., Tensile behavior of polycrystalline zirconium at 4.2°K, 25:4768
BALDWIN, N., Fission gas release measurements from fast breeder (U,Pu)O_2 fuel, 25:6015
BALDWIN, N. L., Effect of temperature on fission gas release from coated fuel particles, 25:5997
BALI, Naren F., Multiperipheral models: phenomenology, 25:5346 (CONF-700314-, Paper 12)
BALL, R. M., Integrated reactor protective system, 25:6045
BALLARD, E. O., Correlation of predictions and observations in mixed-oxide fuel, 25:6001
BALLARINY, M. V., Interference effects of ^{232}Th--^{233}Pa absorption resonances in homogeneous systems, 25:5958
BALLARIO, M. C., Solar and geomagnetic events of the year 1968, 25:5022
BAMBYNEK, W., P/sub K/ω/sub K/ value and fluorescence yield ω/sub K/ of Rb, 25:5650
BANERJEE, Amitav, Complexes between U(VI) and dioxydiquinone, 25:4078
BANGERTER, Roger Odell, Nonleptonic decay of sigma hyperons, 25:5260
BANKS, P. H. T., Frozen polarized target, 25:5466 (RPP/A-81)
BANSAL, R. C., Ultra-clear carbon surfaces. IV, 25:4846
BANTYSH, A. N., Isotopic exchange laws. VII, 25:4072
BARANOV, V. F., Passage of electrons through matter, 25:4938
BARBASHOV, B. M., Problem of quasipotential smoothness in quantum field theory models, 25:5387 (JINR-E2-5365)
BARBIER, J., Contrast improvement of images obtained in cellulose nitrate film by track-etch methods, 25:4346
BARD, F. E., Correlation of predictions and observations in mixed-oxide fuel, 25:6001
BARELKO, E. V., Effect of additions of aromatic hydrocarbons on chemical radiation stability of TBP in dodecane solution, 25:4116
BARKALOV, I. M., Radiation cross-linkage of polyisobutylene in presence of monomer additions, 25:4101
BARKER, F. C., Energy levels of ^{27}Si, 25:5602 (ANU-P-501)
BARKER, P. H., One-neutron transfer reactions, 25:5577
BARKER, R. W., EBR-II irradiation effect of rupture of Type 316 stainless steel, 25:5948
Uniaxial and biaxial creep-rupture of Type 316 stainless steel after fast reactor irradiation, 25:4816 (WHAI-FR-19)
BARMIN, V. V., Decay probability K/sub L/ → 2ν^0, 25:5259
BARNABY, C. F., Gas centrifuge problem, 25:4213 (CONF-691051-, pp 145-53)
BARNARD, E., Energy levels of ^{203}Tl and ^{205}Tl, 25:5798
BARNEOUD, D., Rotational bands of ^{171}Lu, 25:5659
BARNES, J., Radiosensitization of bacterial and mammalian cells with carbonyl compounds and ketoaldehydes with special reference to the properties of phenylglyoxal, 25:4557
BARNES, John W., Small hot cell chemistry plant, 25:4308
BARNES, R., An unusual hazard in forgery detection, 25:4710
BARNETT, C. F., Channel electron multipliers in magnetic fields, 25:4331
Improvements in detection efficiency of Johnston multiplier, 25:4332
BARNETT, E., Mineral and density changes in bone with age in normal and pathological states, 25:4615 (CONF-680211-, pp 177-91)
BARONENKO, V. A., Certain mechanisms of change in vasomotor function in normal animals and in the initial stage of development of experimental hypertension under the effect of sunlight and ultraviolet rays, 25:4657
BARRY, George W., Pomeranchuk decoupled from the ordinary Regge trajectories, 25:5348 (COO-264-562)
BARRY, K. M., Comparison of measured and calculated integral fluxes and spectra in a pressure vessel mockup, 25:6213
BARSELL, A. W., Prompt and multiorbital reentry of small radioisotope heaters at superorbital velocities, 25:4221
BARTHOLIN, H., Effects of pressure and stress on magnetic transition temperatures of rare earth single crystals, 25:5195
BARTHOLOMAE, K. P., Charge determination of cosmic-ray tracks in polycarbonate plastic detectors, 25:4338
BARTLETT, A. C., Relative power distribution and integral spectrum measurements on first Dragon core, 25:5552 (DP-Report-442)
BARTON, C. J., Radiological considerations in the use of natural gas from nuclearly stimulated wells, 25:4525 (ORNL-TM-3216)
BARTON, John P., Radiographic inspection of a developmental ^{244}Cm--Be neutron source, 25:4253
BARTS, B. I., Proton--neutron correlations in medium and heavy nuclei, 25:5853
BARTTER, Frederic C., Clinical use of an in-vivo measurement of bone mineral content, 25:4625 (CONF-680211-, pp 296-308)
BARYLOV, V. G., Decay probability K/sub L/ → 2ν^0, 25:5259
BASAK, A. K., Non-mesonic decay of hypernuclei produced by K-mesons of 3.0 GeV/c momentum, 25:5277
BASHIR, Abdul Kabir Abdul, Ion cyclotron heating of hydrogen plasma by two-phase excitation, 25:5076
BASILE, D., Fracture mechanics approach to the assessment of reliability of reactor pressure tubes, 25:6191 (RISO-214, pp 255-87)
Reliability evaluation of brittle materials and of welded structures, 25:4753
BASKIN, Y., Enthalpy-of-formation data on compounds of uranium, 25:4843
BASS, W. T., Levels in ^{53}Mn, ^{58}Co, ^{63}Zn, and ^{70}Ga from the (p,n) reaction, 25:5612
BASSANI, C., Resistometric investigation on SAP alloys neutron irradiated at 100°K, 25:4890
BASTL, W., Reliability of emergency core cooling systems of light water nuclear power plants, 25:6038 (RISO-214, pp 91-126)
BATES, J. L., Insulation resistivity measurements at high temperatures, 25:4401
BATTAGLIA, A., Beta detection efficiency curves for ^{40}K, ^{90}Y, ^{90}Sr--^{90}Y, ^{137}Cs, ^{144}Pr, ^{147}Pm, ^{155}Eu, and ^{204}Tl in sources of definite chemical form as function of their thickness, 25:4029 (CISE-N-119)
BATTAT, Morris E., Risk estimate for an urban-sited research reactor, 25:6103
BAUER, M., Optical model potential for deuterons, 25:5854
BAUGNET-MAHIEU, L., Action of SH-containing radioprotectors on nucleic acid metabolism, 25:4596
BAZ, A. I., Reconstruction of NN potentials from nuclear data, 25:5831
BAZIN, Jean, Electron probe microanalysis of highly radioactive materials, 25:4011 (CEA-N-1340)
BEACH, R. R., Startup of Babcock and Wilcox PWR simulator, 25:6210
BEATTIE, R. J. D., L-shell fluorescence in ^{238}Pu, 25:4947
BEAUMARIAGE, M. L., Radioprotectors and plasma enzymes, 25:4594
BECK, F., Approximation of Green's functions, 25:5821

BECK, J. N., Radioactive strontium and barium fallout, 25:4163
BECKER, C. D., Temperature, timing, and seaward migration of juvenile chinook salmon from the central Columbia River, 25:4504 (BNWL-1472)
BECKER, Klaus, Research on stimulated excelectron emission from lunar materials, 25:4935 (ORNL-TM-3131)
Some applications of nuclear track etching in polymers, 25:4347
BECKER, M., Study of neutron transport in iron with an assessment of data files, 25:5455
BECKER, Martin, Fast-neutron spectrum models and their application to specific materials, 25:5955
BECKER, Stephen F., Three-alpha model of ^{12}C, 25:5575
BECKERS, R. M., In-cell crane, manipulator, and television systems for TURF, 25:4303
BECLE, Christian, Magnetic properties and structures of DyAl-type compounds of Al and rare earth metals, 25:5208
BEESON, J. J., Kinetics of gamma-induced polymerization of methyl methacrylate-clay composites, 25:4107
BEESTON, J. M., Effect of fast neutron irradiation on the mechanical properties of hafnium, 25:4813 (IN-1440)
BEG, M. A. B., Dimensions of current operators, 25:5306 (NYO-4204-1)
BEHRENS, H., Beta--gamma circular polarization correlation in ^{97}Nb, 25:5732
BEISINGER, Zelma E., SLADE: computer program for static analysis of thin shells, 25:6245 (SC-RR-69-369)
BELAVIN, A. A., Renormalization of coupling constant for the strange vector current, 25:5356
BELL, J. H., Design evaluation of small nuclear power-desalting plants, 25:6144
BELL, T. K., Measuring ^{51}Cr in presence of ^{59}Fe, 25:4513
BELL, W. E., Fission gas release from an HTGR-type fuel rod, 25:6009
BELLETTI, Sergio, Application of fast electrons to the treatment of diseases of the eye ball and eye socket, 25:4690
BELOBORODOVA, N. L., Changes in the peripheral blood following chronic and acute poisoning with U_3O_8, 25:4445
BELOTE, T. A., Level structure of ^{47}Ti, 25:5629
BELTER, W. G., Current status of US waste management programs, 25:4275
BELYAEV, Yu. N., Scattering of atoms of H in noble gases, 25:4957
BELYAEVA, I. F., Research on studying and increasing the plasma parameters on "non-cylindrical Z-pinch" equipment, 25:5116 (SC-T-70-4046)
BEMENT, A. L., Fundamental materials problems in nuclear reactors, 25:4812 (BNWL-SA-3495)
BEMIS, C. E., Search for long-lived spontaneous fission isomer of ^{241}Pu, 25:5759
BENCINI, M., Renal clearance of radiophosphate in thyroid disease, 25:4451
BENCZER-KOLLER, N., Properties of the low-lying states of ^{48}Ca, 25:5616
BENDA, S., L-shell fluorescence in ^{238}Pu, 25:4947
BENDEL, Warren L., Survey on photon activation analysis using NRL Linac, 25:4041 (AD-705901)
BENDIX, Peter, Scale invariance and the energy--momentum tensor, 25:5418
BENDT, Philip J., Characteristics of AlK and Al(NH_4) alum as new materials for polarized proton targets, 25:5450 (LA-4465, pp 4.1-2)
BENEDETTI, G. R., Computer programs for irradiation planning in high-energy therapy, 25:4514
BENNETT, E. F., Measured neutron spectrum in FTR-3, 25:6105
BENNETT, L. L., Effects of fuel thermal limits on gas-cooled fast breeder economics, 25:5902
Nuclear and economic performance of Nb and Mo in LMFBR cores, 25:6055
BENNETT, Willard H., Production of nuclear reactions by highly concentrated electron beams, 25:5118
BENOEHR, H. C., Broad three-nucleon resonances for a soft-core two-nucleon potential, 25:5824
BENSON, G. D., Decay of ^{196}Au, 25:5728
BENTLEY, H. B., Internal relationships between skeletal parameters in twenty-three male skeletons, 25:4652 (CONF-700515-, pp 365-82)
BEN-YOSEF, N., Optical investigations of electrostatic turbulence in plasma, 25:5083
BERCAW, Robert W., Study of the odd strontium isotopes with stripping and pickup reactions, 25:5604 (N-70-25281)
BEREGI, P., Three-body model for the isobaric analog resonance on even--odd target, 25:5872
BERENYI, Denes, Modern physical methods for analytical determination of Fe, 25:4010
BERG, V., E2 and M1 transition probabilities in ^{193}Au and ^{195}Au, 25:5701
BERGAMINI, P. G., Absorption and distribution of ^{137}Cs by Trifolium pratense, 25:4449
BERGER, Harold, Radiographic inspection of a developmental ^{244}Cm--Be neutron source, 25:4253
Use of sparking techniques to enhance track-etch radiographs, 25:4348
BERGQVIST, I., Neutron capture cross sections in F, Mg, Al, Si, P, and S from 20 to 80 keV, 25:5603 (FOA-4-4440)
BERMAN, B. L., Isospin splitting of giant dipole state in ^{26}Mg, 25:5671
M1 giant resonance in ^{208}Pb from threshold photoneutron measurements, 25:5795
BERNARD, P. J., Pulmonary hemosiderosis in a 5-year old child with a trisomy 18, 25:4685
BERNARDI, R., Comparative study of the changes in the elimination of 17-ketosteroids in male rats after surgical and radiation-induced castration and histologic study of the testes irradiated with scalar doses, 25:4707
BERNAT, Michel, Uranium, Th, K, and Ar in marine phillipsites, 25:4164
BERNHEIM, Frederick, Prog. rpt. on the effect of radiation on mucosal phospholipase activity, 1967--70, 25:4455 (ORO-3329-7)
BERNIER, R. G., Commercial power generation from HTGR nuclear steam systems, 25:5884
BERNS, Michael W., Enzyme inactivation with ultraviolet laser energy (2650 Angstroms), 25:4461
BERNSTEIN, B., Concrete-polymer building blocks, 25:4859
BERNSTEIN, J., Dimensions of current operators, 25:5306 (NYO-4204-1)
BERNSTEIN, Melvin J., Influence of an axial magnetic field on neutron production in a plasma focus discharge, 25:5113 (AD-710606)
BERTHIUS, P., Isotopic exchange reaction between ammonium bromide and butyl bromide, 25:4071
Radioelectrochemical determination of microgram iodide, 25:4027
BEROVIC, N., Parity and time reversal invariance and P-matrix, 25:5875
Phase shift analysis of P--P elastic scattering, 25:5546
BERTAUT, E. F., Characterization of compounds and materials by neutron diffraction, 25:4151 (CEA-CONF-1500)
Magnetic structure of cubic rare earth oxides, 25:5215
Magnetic structure of Er_6WO_{12}, 25:5216
BERTIN, Andre, Gamma-ray production cross sections for 5-, 6.6- and 8.7-MeV neutrons with nitrogen, oxygen, scandium, and gold, 25:5551 (CEA-R-4047)
BERTIN, M. C., Lifetime measurements in ^{14}O, 25:5565
Properties of the low-lying states of ^{48}Ca, 25:5616
BERTINI, R., M1 gamma transitions from isobaric analogue states, 25:5676
BERTRAM, Levin, In vivo measurement of the mineral content of a section of the radius, 25:4621 (CONF-680211-, pp 204-15)
BERTRAND, Francoise, Gamma-ray production cross sections for 5-, 6.6- and 8.7-MeV neutrons with nitrogen, oxygen, scandium, and gold, 25:5551 (CEA-R-4047)
BERTSCH, G., T/sub 2/^{3} term in isobaric multiplet equation, 25:5840
BERZIN, A. K., Calculation by Monte Carlo method of distribution of photoneutrons from a beam of γ radiation with initial energy of 4.1 MeV, 25:4152 (CSIRO-Trans-10083)
BESENBRUCH, G. E., Fission gas release from an HTGR-type fuel rod, 25:6009
BETTENHAUSEN, L. H., Doppler considerations for high-temperature gas-fueled cavity reactors, 25:5957
BETZ, E. H., Metabolic effects of sulphur-containing radioprotective drugs, 25:4595
BETZL, M., Automatically controlled neutron diffraction goniometer, 25:4394
BEULICH, H., Applicability of anion exchange with mixtures of nitric acid and methanol for the separation of rare earths, 25:4139
BEVILACQUA, R., ^{60}Co gamma-ray effect on mouse Ehrlich ascites tumour cells in the presence of some coumarin derivatives, 25:4565
BHANDARI, A. M., Mandelates of lanthanum, praseodymium, neodymium, and uranium, 25:4055
BHANDARKAR, M. K., Effect of deuterium oxide on gibberellic acid-induced a-amylase in germinating barley seeds, 25:4464
BHAT, M. R., Gamma rays from thermal and resonance neutron capture in ^{121}Sb and ^{123}Sb, 25:5724
BHAT, R., Sintering of beryllia. III, 25:4637
BHAT, T. R., Maleic acid complexes of rare earth and other metals. I, 25:4075
BHATTACHARJEE, S. B., Influence of DNA replication on x-ray sensitivity of bacteria, 25:4725
BHATTACHARYA, S., Effect of deuterium oxide on gibberellic acid-induced a-amylase in germinating barley seeds, 25:4464
BHAUMIK, Gayaram, Influence of DNA replication on x-ray sensitivity of bacteria, 25:4725
BIALKOWSKI, Jacek, Simple time-to-amplitude converter for fast coincidence measurements, 25:4334
BIANCHERIA, A., Postirradiation observations of sodium-bonded (U,Pu)C fuels, 25:4894
BIEDENHARN, L. C., Nuclear rotational bands and SL (3,R) symmetry, 25:5801 (AD-706835)
BIERI, Rudolf H., Uranium, Th, K, and Ar in marine phillipsites, 25:4164
BIGELOW, J. E., Search for long-lived spontaneous fission isomer of ^{241}Pu, 25:5759
BIGHAM, C. B., Resonance integrals of neutron activation of ^{74}Se, ^{76}Se, ^{80}Se, ^{81}Br, ^{127}I, ^{130}Te, ^{138}Ba, ^{140}Ce, and ^{142}Ce, 25:5681 (CNEA-274)
BILDSTEIN, H., Evaluation work on coated fuel particles, 25:6008
BILLAUX, M., Considerations on the in-core fuel management

XUM

during startup of a fast breeder reactor, 25:6054
BILLEN, D., Survival and repair of DNA after ultraviolet exposure, 25:4731
BINFORD, F. T., Production of boiling in the high flux isotope reactor for the purpose of investigating boiling detection methods, 25:6048
BINNEY, S. E., Design of intermediate-energy neutron spectrometers and their calibration with photoneutrons, 25:4364
BIRKENMAYER, Eline, Chemical protection of mice inflicted with irradiation and open skin wounds, 25:4576
BIRSEN, N., Charge asymmetry in two nucleon interaction, 25:5812
BISHOP, Charles Joseph, Competition between neutron emission and fission at moderate excitation energies in the uranium region, 25:5692
BISHOP, D. M., Testing of instruments and material balance methods for plutonium safeguard control, 25:4297
BIST, B. M. S., Study of oxidation of ytterbium and holmium thin films in the electron microscope, 25:4767
BJORKEN, J. D., Electromagnetic interactions at very high energy, 25:5319 (CONF-700314-, Paper 8)
BLACHOT, J., Decay of ^{104}Tc (18-min), 25:5796
BLACK, J. L., Search for lowest T = 2 state of ^{12}C, 25:5573
BLACK, R. E., Recovery of lattice parameter and electrical resistivity in low-temperature neutron-irradiated copper, 25:5160
BLACKBURN, L. D., Mechanical properties of EBR-II irradiated 20 percent cold-worked Type 316 stainless steel, 25:5949
Yield strength and creep strain estimates for irradiated stainless steel, 25:4820
BLACKSTONE, R., Dimensional changes in graphite during high-temperature irradiation, 25:4883 (DP-Report-473)
BLAGIN, V. B., Control of reinforced concrete construction by means of fast neutrons, 25:4249
BLAINE, R. A., IBM interactive reactor computation system, 25:6149
BLAKE, J. P. H., Transfer function investigations on first Dragon core, 25:5953 (DP-Report-445)
BLANC, D., Mobility of radioactive ions, 25:4395
BLANDIN, A., Exchange interaction in rare earth metals and alloys, 25:5232
BLANN, Marshall, Reactions (p,t) on even Sn isotopes, 25:5799
BLASEWITZ, Albert G., Status of Waste Solidification Demonstration Program, 25:4276
BLECKMANN, A., Photoproduction of K$^+\Lambda$ and K$^+\Sigma^0$ from H, 25:5253
BLEWITT, T. H., Recovery of lattice parameter and electrical resistivity in low-temperature neutron-irradiated copper, 25:5160
BLICHERT-TOFT, P. H., Radioactive atoms. Auger-electron, α-, β-, γ-, and x-ray data, 25:5716
BLINC, R., Spin-lattice relaxation by quasi-spin waves in order-disorder type ferroelectrics, 25:6233 (IJS-575)
BLOCH, C., Optical model potential for deuterons, 25:5854
BLOCH, D., Effects of pressure and stress on magnetic transition temperatures of rare earth single crystals, 25:5195
BLOCH, Peter, Two wavelength technique for the measurement of bone mineral content in vivo, 25:4645 (CONF-700515-, pp 263-71)
BLOCK, Seymour S., Chelation and radiation protection, 25:4553
BLOMEKE, J. O., Demonstrational repository for solid radioactive wastes, 25:4277
Design and safety considerations in the shipment of solidified wastes, 25:4278
BLOOM, Arthur D., Cytogenetic effects of low doses of ionizing radiations on human cells, 25:4500
BLOOM, Gerald, Isotope-powered, indwelling intracranial pressure sensor, 25:4241
Radioisotope-induced, negative surface charge for thrombus resistance, 25:4434
BLOOM, S. D., Beta--γ (CP) correlation measurements in allowed transitions, 25:5605 (UCRL-72624)
BLUE, Gary D., Electron impact cross sections for group-III metal atoms, 25:4956
BLUM, P. W., Impact ionization by neutral interplanetary particles, 25:5021
BLYTH, C. O., Polarization transfer at 0° in the D(d,n)^{3}He and H(d,n)pp reactions, 25:5532
BOBIN, Jean-Louis, Problems in radiation hydrodynamics, 25:5095 (CEA-R-4057)
BOBKER, J., Even-parity states of ^{17}O, 25:5556
BOCK, H., Angular distribution of photonuclear reaction ^{3}He(γ,p)^{2}H, 25:5539
BOCK, R., Four-nucleon transfer reaction induced by ^{10}B on ^{12}C, 25:5588
BOCKSTAHLER, Larry E., Ultraviolet light enhanced reactivation of a mammalian virus, 25:4727
BOECKER, B. B., Retention in beagle dog of ^{140}LaCl$_3$, 25:4426
BOEDER, H., Effect of hot-pressing on the structure of carbon artifacts, 25:4867
BOER, M. H., Gametogenesis and oviposition in Lymnaea stagnalis as influenced by γ-irradiation and hunger, 25:4693
BOERNER, W., Sensitive method for separate calculation of mineral content in cancellous and compact bone of the finger by a ^{125}I profile scanner. Effect of calcium and fluoride therapy on demineralized bone, 25:4636 (CONF-700515-, pp 169-87)
BOGGS, J. Vincent, Portable low-energy photon calibration source, 25:4248
BOHABOY, P. E., Thermal conductivity of physically mixed $(U_{0.8}Pu_{0.2})O_{2-x}$, 25:4862
BOHL, W. R., Integral-transport-theory analysis of resonance absorption measurements in neutron beams, 25:5959
BOHN, E. M., Non-perturbing fission counter for use in plate-type critical assemblies, 25:4353
BOILLAT, G., Born--Infeld particle; small-scale phenomena, 25:5404
BOIVIN, Michel, Nuclear photoactivation of ^{179}Hf, 25:5690
BOLDEMAN, J. W., Energy dependence of anti ν_p for neutron fission of ^{235}U, 25:5755
BOLING, Norman Lee, Low-power MPD arc, 25:5105
BOLOTIN, Yu. L., Proton--neutron correlations in medium and heavy nuclei, 25:5853
BONCH-OSMOLOVSKY, A. G., Charged relativistic electron ring in the helical magnetic field, 25:5448 (JINR-PS-5259)
BOND, Howard E., Three eclipsing binaries found spectroscopically, 25:4900
BOND, V. P., Radiation standards, 25:4532
BONDARENKO, L. N., Neutron spin and antineutrino momentum in neutron decay, 25:5258
BONDARENKO, S. I., Superconductor/normal metal/superconductor point contacts, 25:5037
BONDENMILLER, K. H., Supplementary data concerning ^{58}Ni(p,p'γ) reaction, 25:5642
BONFANTI, G., Beta detection efficiency curves for ^{40}K, ^{90}Y, ^{90}Sr--^{90}Y, ^{137}Cs, ^{144}Pr, ^{147}Pm, ^{155}Eu, and ^{204}Tl in sources of definite chemical form as function of their thickness, 25:4029 (CISE-N-119)
BONNIER, Etienne, Phase equilibriums in Ni--Nb--W and Ni--W systems, 25:4788
BOOMAN, Glenn L., Input accountability by remote weighing of processing plant tanks, 25:4296
BOOT, S. J., Nuclear accident dosimetry systems, 25:4377 (AERE-R-6498)
BORDIN, F., ^{60}Co gamma-ray effect on mouse Ehrlich ascites tumour cells in the presence of some coumarin derivatives, 25:4565
BORG, I. Y., Microfracturing in postshot Gasbuggy rocks, 25:4178
BORGEAUD, Pierre A., Differential cross sections for reaction $\pi^-p \to \eta n$ between 2.9 and 18.2 GeV/c, 25:5279 (CEA-R-4037)
BORISOV, V. S., Decay probability $K/\mu L \to 2\pi^0$, 25:5259
BORN, U., Indifference value of ^{233}U in an HTGR, 25:6057
BORNATICI, M., Ordinary-mode electromagnetic instability in counterstreaming plasmas with anisotropic temperatures, 25:5129
BORNHORST, W. J., Radioisotope-fueled vapor cycle power supply for an artificial heart, 25:4234
BORRA, Ermanno F., Photoelectric observations of Nova Serpentis 1970, 25:4901
BORRELLO, G., Renal clearance of radiophosphate in thyrcid disease, 25:4451
BOSCH, D., Angular distribution of neutron capture γ-rays from polarized ^{159}Tb nuclei, 25:5717
BOSE, S., Krutov model for deformed even--even nuclei, 25:5819
BOSE, S. K., Yang--Mills gauge transformation, 25:5410
BOSWELL, G. G. J., Decay of ^{69}As, 25:5621
BOTTS, William V., Radioisotope heat source, 25:4217
BOUDREAU, Jay E., Fast reactor implosion studies, 25:6066
BOULETTE, E. T., Multigroup discrete ordinates radiation transfer operators, 25:5144
BOURGEOIS, M., Remote handling in operation of the installation ATTILA, 25:4261 (CEA-R-4067)
BOURQUIN, R. D., BPLOT, multipurpose plotting routine for use with CALCOMP plotter, 25:6257 (WHAN-IR-38)
BOURRELY, C., Approach to form factor in a composite model, 25:5372 (CNRS-CPT-70-P-331)
BOUTRON, P., Paramagnetic anisotropy, 25:5206
BOWDEN, Robert L., Neutron-transport problem for slab with infinite reflectors, 25:5501
BOWEN, H. J. M., Removal of ^{24}Na from neutron-activated samples, 25:4044
BOWMAN, C. D., M1 giant resonance in ^{208}Pb from threshold photoneutron measurements, 25:5795
BOXER, L. W., Power reactor strategies and their effects on fuel cycle requirements, 25:6053
BOYNO, J. S., Reactions ^{232}Th(d,t)^{231}Th and ^{238}U(d,t)^{237}U, 25:5797
BOZOKI, G., Conference on cosmic rays, Budapest, 8--9/69, 25:4976
BRABEC, V., Excited levels in the decay ^{185}Cs $\to$ ^{185}Re, 25:5741
BRACE, K., Effects of irradiation of the parotid gland and pancreas on human isoamylases, 25:4452
BRADY, Thomas Joseph, Trinucleon calculations with rank-two separable potentials, 25:5830
BRAGER, H. R., Heavy-ion-bombarded 20 percent cold-worked Type 316 stainless steel, 25:4829
BRALEY, Richard C., Systematic method of calculating reduced matrix elements of single-particle operators, 25:5808 (N-70-32786)
BRAMBLETT, R. L., Low-energy photofission of heavy

elements: experimental results, 25:5768
Use of fission product gamma rays following photofission for nondestructive assays of nuclear materials, 25:4291
BRANCH, David, Search for ^{26}AlH in spectra of technetium stars, 25:4899
BRANSFORD, C. L., TLD 700 (^{7}LiF) response to reactor neutrons, 25:4382
BRANSCME, Edwin D. Jr., Conference on current status of liquid scintillation counting, Cambridge, Mass., 3--4/69, 25:4358
BRANYAN, Charles E., Remote maintenance during recovery from Enrico Fermi fuel melting incident, 25:5907
BRAUN, Hildegard, Influence of chemical radiosensitizing agents on organs and cell structures, 25:4587
BRAUN, Lorne David, Radio-astronomy observations as a frequency of 35 GHz, 25:4918
BRAUN, M. A., Application of Z = 0 approach to rho-meson and N*(1240) resonance, 25:5417
BRAUN, Walter, Collisional deactivation of H(2^2P)* fluorescence, 25:4964
BRECCIA, Alberto, Radioprotection by selenium-containing compounds, 25:4545
BREDEL, V., Reaction (d,α) on ^{13}C, 25:5559
BREEDIS, J. F., Reply to comments on phase transformations in beta isomorphous titanium alloys, 25:4806
BREGADZE, I. F., Vicia faba seedling chromosome damages by split dose, 25:4497
BREHM, R. L., Multivariable feedback synthesis with cross-coupling for a thermionic reactor model, 25:6163
Neutron slowing down time kernel for graphite, 25:6160
Parametric stability analysis of systems with time delay, 25:6164
BREHM, W. F. Jr., Corrosion product radioactivity in FFTF and other reactor systems, 25:5586
BREINING, H., Bile duct carcinomas after thorotrast, 25:4716
BRENDEL, M., Repair of alkylation and radiation damage in yeast, 25:4480
BRENT, Robert L., Biological effects of low-level radiation on the embryo, 25:4713
BRESSANI, T., Giant-resonance excitation by radiative capture of π^- in ^{16}O, 25:5600
BRETONNIERE, Serge, Method and apparatus for measuring apparent density by gamma radiation, 25:4764
BRETSCHER, M. M., Experimental determination of the perturbation denominator in fast critical assemblies, 25:6116
BRETT, J., Porosity and anomalous recrystallization behavior in doped tungsten wire, 25:4799
BREUNLICH, W., Precision-measurement of ^{27}Al(n,α) cross section for 14.43-MeV neutrons, 25:5641
BREWER, S. T., FBR blanket depletion studies: effect of number of energy groups, 25:5560
BRIDGES, Bryn A., Radiosensitization of bacterial and mammalian cells with carbonyl compounds and ketoaldehydes with special reference to the properties of phenylglyoxal, 25:4557
BRIDGES, D. N., Spatial and feedback effects in Georgia Tech Research Reactor, 25:6108
BRILLOUIN, Leon, Relativity reexamined, 25:5421
BRINHALL, J. L., Observations on the nucleation and growth of voids in nickel, 25:4811 (BNWL-SA-3300)
Void formation in nickel during irradiation, 25:4819
BRINCK, W. L., Radionuclides in effluents from boiling water reactor, 25:6080
BRINK, D. M., Alpha-particle model for light nuclei, 25:5855
BRINKMAN, C. R., Effect of fast neutron irradiation on the mechanical properties of hafnium, 25:4813 (IN-1440)
BROADBENT, James C., Disappearance of iodoalbumin from pericardial sac in a patient with myxedema, 25:4658
BRODT, F., Beta--gamma circular polarization correlation in ^{97}Nb, 25:5732
BROLLEY, J. E., Proposal for a Lamb-shift polarimeter, 25:4391 (LA-4465, pp 17.1-6)
BROMBERG, Bertram E., The effect of total-body irradiation on wound healing and the hematopoietic system in mice, 25:4705
BROOKS, Joan, Evaluation of Compton currents from 14-MeV neutron source in intermediate altitude range, 25:5497
BROOKS, L. H., HTGR fuel reprocessing: head-end treatment of experimental small-scale HTGR fuel elements, 25:4136 (GAMD-9260(Pt.2))
BROSTE, W. B., Improvements in performance of a liquid helium scintillation counter, 25:4321 (LA-4465, pp 31.1-2)
Neutron polarization in the T(d,n)^{4}He reaction using a polarized incident beam, 25:5513 (LA-4465, pp 12.1-2)
Neutron--helium polarization at 27.3 and 30.3 MeV, 25:5523 (LA-4465, pp 30.1-2)
Polarization angular distribution from the T(d,n)^{4}He reaction at 7.0 and 11.4 MeV, 25:5522 (LA-4465, pp 29.1-2)
Preliminary measurements of neutron polarization from the D(d,n)^{3}He reaction using a polarized incident beam, 25:5514 (LA-4465, pp 13.1-2)
BROUILLARD, F., Depolarization of negative muons in low-Z muonic atoms, 25:5576
BROWN, C. L., Critical approach and exponential experiments with prototype FFTF driver fuel pins in water, 25:4280
BROWN, Donald P., Gas-flow method for detection of fast neutrons in reactors, 25:4355
BROWN, G. E., Tensor force and exchange currents in the triton beta decay, 25:5542
BROWN, H. L., Pneumatic tube transfer system for radioactive samples, 25:4306
BROWN, J. B. Jr., Bubble migration in UO_2, 25:4853
BROWN, M. H., Miniature nuclear batteries, 25:4240
BROWN, Ronald E., Exchange resonance in ^{3}He + ^{4}He elastic scattering, 25:5538
BROWN, Warren David, Relativistic Green's function approach to nucleonic properties, 25:5383
BROWNELL, Gordon L., Survey of recent instrumentation advances, 25:4337
BRUCKLACHER, D., Creep of UO_2 under irradiation, 25:4853
BRUECKMANN, H., Final state interacting n-p pairs in the reaction p + d + p + p + n, 25:5548
BRUELS, Mark Charles, Nuclear forces in o-s shell nuclei, 25:5537
BRUNDAGE, Robert S., On-line monitor of natural gas lines for ^{3}H and ^{85}Kr, 25:4352
BRUNEDER, H., HELTOT: program system for analysis of fuel cycles assuming off-load refueling, 25:6052 (DP-Report-440)
BRUNNE, M., Ion oscillations in EGD flow in channels, 25:4996
BRUNO, Fred P., Technetium--indium double lung scanning, 25:4677
BRUNS, L., Survival and repair of DNA after ultraviolet exposure, 25:4731
BRUSQUET, Y., Pulmonary hemosiderosis in a 9-year old child with a trisomy 18, 25:4685
BRUSTAD, T., Radioprotective effect of cysteine on lysozyme in dilute aqueous solution, 25:4544
BUBLITZ, R., Graphic display terminal for nuclear experiments with on-line computer. I, 25:4390 (HPI-B-100)
BUCCINO, S. G., Gamma-ray transitions in ^{29}P, 25:5633
BUCHANAN, Mary G., Program WEIGHT: FORTRAN IV program for evaluation of weighting functions used in small-angle x-ray scattering, 25:6246 (ORNL-TM-1950(Rev.1))
BUCHHOLZ, K., p/sub 3/2/ analogue state in ^{51}V, 25:5651
BUCKNER, M. R., Nonlinear contamination in frequency response tests, 25:5967
Optimal discrete level signals for reactor frequency response tests, 25:5968
BUCKWALD, Robert Allen, Dense plasma focus formation by disk symmetry, 25:5120
BUDKE, L., Radiation protection by disulphides in tissue culture, 25:4560
BUDNIKOV, V. N., Spreading of high-frequency plasma along magnetic field, 25:5132
Wave transformation conditions in plasma, 25:5131
BUFFALOE, Thomas S., Measurement of in vivo radioactivity, 25:4324
BUHL, S., Supplementary data concerning ^{58}Ni(p,p'γ) reaction, 25:5642
BUKOWIECKI, Jerzy, Fisher apparatus measurement of average particle diameter in powder metallurgy, 25:4184 (LA-4404-TR)
BULL, Stanley R., Space-dependent thermal-neutron flux in systems with strong anisotropies, 25:6184
BULUSU, L., Internal relationships between skeletal parameters in twenty-three male skeletons, 25:4652 (CONF-700515-, pp 365-82)
BUMILLER, F. A., Form factor ratio GE/sub n//GE/sub p/ at low-momentum transfers, 25:5247 (AD-710385)
BUMP, T. R., Cold-wrapper tube approach for accommodating steel swelling in LMFBR's, 25:6022
Estimation of fission gas distribution in LMFBR mixed-oxide fuel elements, 25:6013
BUNKER, M. E., Level structure of ^{169}Er, 25:5725
BURBIDGE, E. Margaret, Absorption lines of quasi-stellar objects, 25:4919
BURCH, W. D., Design and installation of TURF californium facility, 25:4304
Transfer of californium sources by pneumatic rabbit, 25:4305
BURCH, William, Two wavelength technique for the measurement of bone mineral content in vivo, 25:4645 (CONF-700515-, pp 263-71)
BURCHSTED, C. A., Fire prevention and control in nuclear air cleaning systems, 25:4196
BURESCH, F. E., Influence of single irradiation and heat treatment on the properties of BeO, 25:4852
BURGART, C. E., Simultaneous fast-neutron spectral measurements by time-of-flight and pulse-height unfolding techniques, 25:4366
Time-dependent coupled neutron--gamma calculations in polyethylene, 25:5147
BURGE, E. J., Backward angle scattering of 50-MeV protons from C, O, N, and Be, 25:5585
BURKE, Edward W. Jr., UBV photometric study of IQ Persei, 25:4902
BURKE, J. A., Space--time kinetics experiments and calculations for a loosely coupled core, 25:6185
BURKHEAD, Martin S., UBV observations of 3C 273. III, 25:4916
BURLANT, William J., Radiation-curable-vinyl resin paints and coated article, 25:4095
BURNAP, C., Yamaguchi's deuteron wave function, 25:5871
BURNETT, P. T., PULSTAR: six years of operation, 25:6122

BURNS, E. T., Study of neutron transport in iron with an assessment of data files, 25:5455
BURNS, Edward T., Fast-neutron spectrum models and their application to specific materials, 25:5955
BURZO, Emil, Ferrimagnetism of the intermetallic compound Co_2Gd, 25:5201
BUSCH, G., Distortions of lattice of some trivalent compounds of rare earths, 25:4803
BUSCHOW, K. H. J., Kondo effect in compound $CeAl_2$, 25:5228
BUSHNIN, Yu. B., Total and absorption cross sections of π^-, K^- and antip in the momentum range 20 to 65 GeV/c, 25:5295
BUSHONG, Stewart C., Radiation control in roentgenology, 25:4531
BUSKIRK, F. R., Form factor ratio GE/sub n//GE/sub p/ at low-momentum transfers, 25:5247 (AD-710385)
BUSLAEV, Yu. A., Thermal stability of ammonium uranyl fluorides, 25:4082
BUSTARD, Thomas S., Design of radioisotope heat source subsystems for heart devices, 25:4230
Results of bench model testing of radioisotope heat source subsystems for heart devices, 25:4231
BUSULINI, L., ^{60}Co gamma-ray effect on mouse Ehrlich ascites tumour cells in the presence of some coumarin derivatives, 25:4565
BUTERA, P., Regge-Pole analysis of rho^0 production, 25:5380
BUTI, B., Dynamic instability in streaming relativistic plasmas, 25:5107
BUTKOVICH, Theodore R., Influence of water in rocks on underground nuclear explosion effects, 25:4179
BUTTEMER, D., Accommodation of radiation swelling in GCFR, 25:6020
BUTTERWORTH, J. S., Formation of color centers in KCL:Tl by gamma irradiation at 21°C, 25:5157
BUTTET, J., Nuclear acoustic resonance in niobium metal, 25:5223
BUZZELL, John, Radiographic inspection of a developmental ^{244}Cm--Be neutron source, 25:4253
BUZZELLI, G., Microdetermination of fluorine in high-purity tungsten metal by photoactivation analysis, 25:4043 (GA-10125)
BUZZI, J. M., Ion distribution functions in collisionless surface ionized plasmas, 25:5096
BUZZI, Silvano, Aluminum and Si abundances of some Italian meteorites as determined by instrumental activation analysis, 25:4048
BYAKOV, V. M., Mechanism of formation of products of radiolysis of H_2O, 25:4120
BYCKLING, Eero, Kinematic separation of three-particle channels in counter experiments, 25:5318
BYRN, N. R., Angular and wavelength dependence of thermal radiation transmitted through refractory aerosols, 25:6134
BYRNE, J., L-shell fluorescence in ^{239}Pu, 25:4947
Radioactivity of free neutrons, 25:5536

C

CABELA, E., Influence of cycloheximide on the radiosensitivity of Saccharomyces cerevisiae, 25:4556
CABIBBO, N., Deep inelastic scattering and the nature of partons, 25:5330
CADEK, F. F., ECC variable flcoding rate simulation PWR FLECHT test results, 25:6043
Effect of 75 to 100 percent flow blockage on bottom cooling heat transfer effectiveness, 25:6042
CAELLI, W. J., Search for lowest T = 2 state of ^{12}C, 25:5573
CAHILL, R. T., Neutron--deuteron breakup models, 25:5531
CAIN, V. R., SAMBO: collision analysis package for Monte Carlo codes, 25:5237 (ORNL-TM-3263)
CALAIS, D., Influence of the allotropic transformation β reversible α and of oxygen on the distribution of plutonium in dilute ZrPu and TiPu alloys, 25:4790
CALDER, V., Matrix-isolation spectra of H_2S and D_2S, 25:4066
CALL, D. W., Operating reactivity feedback effects in NERVA reactor, 25:6139
CALLEBAUT, M., Disorientation response of chicks which survived 2-β-aminoethylisothiouronium-Br-HBr (AET) administration during early embryogenesis, 25:4601
CALVERT, J. M., Reactions $^{26}Mg(d,p)^{27}Mg$ and $^{28}Si(d,p)^{29}Si$, 25:5672
CALZAVARA, F., Comparative study of the changes in the elimination of 17-ketosteroids in male rats after surgical and radiation-induced castration and histologic study of the testes irradiated with scalar doses, 25:4707
CAMERON, J. R., Conference on bone measurement, Chicago, Ill., 5/70, 25:4630 (CONF-700515)
Preliminary report on a direct digital readout system for absorptiometric determination of bone mineral content, 25:4632 (CONF-700515-, pp 22-7)
CAMERON, John, Measurement of bone mineral by the direct photon absorption method: principles and instrumentation, 25:4623 (CONF-680211-, pp 253-68)
CAMERON, John R., In vivo diagnostic applications of external radioactive sources, 25:4682
CAMPANA, Robert J., Pressure equalization system for GCFR fuel elements, 25:6019
CAMPANACCI, L., Nephropathy secondary to irradiation, 25:4714
CAMPBELL, D. K., Veneziano amplitudes for Reggeons and spinning particles, 25:5440
CAMPBELL, J. L., M3 isomeric transitions in ^{58}Co and ^{60}Co, 25:5608
CAMPBELL, R. W., Response of miniature G--M tubes to monoenergetic gamma radiation, 25:4349
CAMPBELL, Wayne Wesley, Capture cross sections in the keV region, 25:5789
CAMPE, Kazimieras M., Interplanetary spacecraft: RTG radiation analysis, 25:4247
CANCELLIERE, G., In vitro radiosensitization of Ehrlich ascites tumour cells and pure enzymes by iodine compounds, 25:4569
CANNING, G. P., Internal symmetry implications of the Veneziano model in pseudoscalar--pseudoscalar scattering, 25:5370
CAPRINI, I., Corrections to scattering kernel for study of neutron thermalization, 25:5488
Solving time-dependent nonhomogeneous thermalization equation, 25:5478
CAPRINI-GOLOGAN, I., Asymptotic behavior of a generalized cadilhac thermalization model, 25:5487
CAPUTI, R. W., Track-etch research and development, 25:4345
CARAFOLI, E., Subcellular distribution of ^{45}Ca and ^{89}Sr in rat liver, 25:4431
CARBOTTE, J. P., Temperature dependence of superconducting energy gap of amorphous Bi, 25:5042
CARDINALE, Antonio, Separation methods of noble fission gases from gaseous effluents, 25:4260 (CEA-Blb-184)
CAREY, G. W., Prog. rpt. on synthesis, identification, and purification of C_6 and C_7 fluorocarbons from radiolysis, 11/70, 25:4111 (ORO-3909-2)
CARLONE, Cosmo, Collisional deactivation of H(2^{2}P)* fluorescence, 25:4964
CARLSON, R. E., Longitudinal modes in hydrogen and deuterium halide crystals, 25:4065
CARLTON, Terry S., Correlated wave functions for the ground state of H-, He, and Li+, 25:4548
CARLYLE, D. C., Suppression of Kelvin--Helmholtz instability in Cs plasma, 25:5111
CARNES, M. D., Hot cell stereomacroscope and positioning stage for viewing objects in either a horizontal or vertical plane, 25:4309
CARPENTER, D. L., Ground-based whistler method of studying magnetospheric plasma, 25:5029
CARPENTER, John M., Pulsed moderator studies using a time-focused crystal spectrometer, 25:6186
Slow-neutron leakage time distributions of some small hydrogenous moderators, 25:6203
CARR, K. R., New methods for measuring compaction of ceramic insulators in sheathed thermocouples, 25:4402
CARRIER, G. F., Electrostatic probe in a reacting gas, 25:5084
CARRIKER, R. C., Brillouin-zone--Fermi-surface interactions in pure and lead-doped indium, 25:5185
CARRINGTON, Tucker, Collisional deactivation of H(2^{2}P)* fluorescence, 25:4964
CARRON, Neal Jay, On-shell current algebra and radiative leptonic decays of pions and kaons, 25:5342
CARTER, K. W., Energy levels of ^{27}Si, 25:5602 (ANU-P-501)
CARTER, L. L., Two-stage Monte Carlo calculations of delayed-neutron response, 25:6151
CARTER, R. D., Safe fissile material spacing in water, 25:4285
CASARA, S., Nephropathy secondary to irradiation, 25:4714
CASARETT, A. P., Radiobiological effects of simulated nuclear power sources for artificial hearts, 25:4433
CASHION, J. D., Magnetic properties of gadolinium orthovanadate, 25:5217
CASTAGNOLI, C., Tests of models of scale invariance with cosmic-ray neutrino data, 25:5340
CASTEL, B., Occupancy of spherical shells in the ground state of even 2s-1d shell nuclei, 25:5876
CASTELLANI, A., Radiosensitizing effect of L-erythro-α,β-dihydroxybutyraldehyde on Ehrlich ascites tumour cells. Cytokinetic analysis of tumour growth, 25:4564
CATANESE, C. A., Magnetic properties of the rare earth hydroxides, 25:5202
CELINSKI, Z., Numerical calculations of the electrical parameters in a Faraday-type MHD generator with two-dimensional gas flow, 25:4991 (INR-1199)
CELNIK, Jacob, Evaluation of Compton currents from 14-MeV neutron source in intermediate altitude range, 25:5497
CERMAK, J. O., ECC variable flcoding rate simulation PWR FLECHT test results, 25:6043
Effect of 75 to 100 percent flow blockage on bottom cooling heat transfer effectiveness, 25:6042
CERNY, Joseph, Mass of ^{13}O and isobaric multiplet mass equation, 25:5640
CERRAI, E., Corrosion rate of Zircaloy-2 in steam--water mixture under reactor radiations, 25:4737 (CISE-R-290)
CHADWICK, K. H., Fading of radiation-induced optical density in polymethylmethacrylate on oxygen diffusion, 25:4384
CHAE, Yong S., Streaming of gamma radiation in two-legged ducts, 25:5138
CHAICHIAN, M., Normalization of anti pp → 4π using dual six-point function, 25:5362

CHAMBAREL, Andre, Forced vortex in electroconducting viscous liquid in magnetic field, 25:5000
CHANDA, R. N., Plutonium waste counter, 25:4292
CHANDLER, J. M., Transfer of californium sources by pneumatic rabbit, 25:4305
CHANEY, Robert Lee, Nuclear orientation of /sup 113m/Cd, ^{115}Cd, and /sup 115m/Cd, 25:5786
CHANG, Ko Chang, Preparation of /sup 113m/In colloid as scanning agent and its organ distribution in rats, 25:4437
CHANG, Kochang, Liver scan using /sup 113m/ In colloid, 25:4687
CHANG, L. K., Parallel-flow-induced vibration of EBR-II subassembly, 25:6030
CHANG, Seung Haann, LDH of rats exposed to gamma-irradiation, 25:4605
CHANT, N. S., Reactions ^{14}N(p,^{3}He)^{12}C, ^{14}N(d,α)^{12}C, ^{13}C(p,d)^{12}C, 25:5563
CHAO, Tao-nan, Adsorption of monovalent astatine cation by cesium phosphotungstate and hydrated tungsten oxide from nitric acid solutions, 25:4053 (ANL-Trans-861)
CHASE, Jay Benton, Electron energy loss to surface excitations in thin films, 25:4537 (IS-T-380)
CHASSANY, J., Twelve years of health physics in a plutonium production plant, 25:4526
CHAUDHURI, Jyoti P., 5-hydroxytryptamine protection of rat bone-marrow chromosomes against x-irradiation in vivo, 25:4585
CHAURE, B. D., Aquoluminescence from gamma-irradiated halides, 25:4076
CHAUSSY, J., Metamagnetic properties of a single crystal of $ErCrO_3$, 25:5180
CHAWLA, T. C., Coolant voiding and pressure generation due to boiling, fission gas release, and molten fuel-coolant interaction, 25:6073
CHEBOTAREV, N. T., System MoO_3--BaO, 25:4873
System MoO_3--CeO_2, 25:4872
CHEIFETZ, E., Excited state in even--even fission products, 25:5687 (UCRL-19949)
CHEN, Ke Wei, Asymmetry effects on heat transfer and fluid flow in rod bundles, 25:4206
CHEN, T. S., Radioactive strontium and barium fallout, 25:4163
CHERKASHINA, T. N., Photometric determination of low amounts of thorium in biological materials, 25:4443
CHERNAVSKII, D. S., Dynamical scheme for leading trajectory and theory of fireballs, 25:5359
CHERNOBROVKIN, V. V., Dependence of scattering transport length on neutron energy in H_2O, D_2O, and graphite, 25:5502
CHERNOV, B. G., Removal of volatile impurities from vacuum melts, 25:4744
CHERTOK, B. T., Study of nuclear states of several odd-A nuclei 68 less than or equal to Z less than or equal to 75 through electromagnetic excitation from 2.3 to 3.6 MeV, 25:5637
CHERTOK, Benson T., Radiative np capture and meson exchange currents, 25:5545
CHERTOK, Robert J., Body distribution and biological availability of radionuclides produced by Project Schooner, 25:4435
CHERVIN, Robert M., Lyapunov stability of an inhomogeneous two-stream plasma, 25:5108
CHESHKOV, A. A., Multipole current disintegration in classical electrodynamics, 25:5236 (JINR-P2-5283)
CHESWORTH, R. H., Design of a ^{238}Pu-powered implantable thermal engine for heart assist devices, 25:4232
CHEVRIER, Jean-Pierre, Method and apparatus for measuring apparent density by gamma radiation, 25:4764
CHIANG, Hai Hung, Count-rate range of GM counter, 25:4361
CHIARELLA, C., Galerkin method solution of the neutron slowing down equations, 25:5479
CHIAVASSA, E., Giant-resonance excitation by radiative capture of π^- in ^{16}O, 25:5600
CHIRIKOV, B. V., Numerical experiments with a nonlinear chain, 25:6234 (LA-4440-TR)
CHIZHIKOV, V. I., Polarization of secondary protons in pp + π^+pn and pp + π^0pp reactions at 669 MeV, 25:5268 (JINR-P1-5293)
CHKAREULI, Dzh. L., Radiative decays of mesons in broken SU(3) symmetry and electromagnetic mass splittings in the 0$^-$ octet, 25:5402
CHO, D. H., Acoustic and inertial constraints in molten fuel-coolant interactions, 25:6099
Rate-limited model of molten fuel-coolant interactions, 25:6075
CHO, S. M., Critical and Leidenfrost point heat fluxes in sodium-heated steam generator, 25:4211
CHOI, Byung-ho., Angular distribution of fast electrons emitted from inner atomic shells by proton impact, 25:4968
CHOONG, Philip T., Passive nuclear attitude control system for solar probes, 25:4222
Simplified eigenvalue problem solutions in diffusion calculation, 25:6173
CHOPOROV, D. Ya., Saturated vapor pressure of solid UF_4, 25:4079
CHOQUET-BRUHAT, Yvonne, Existence theorem for integral differential equation system of Einstein--Liouville, 25:5420
CHOU, Y. W., Moessbauer measurements of quadrupole-moment ratios of first excited 2$^+$ states of ^{176} ^{178} ^{180}Hf, 25:5668
CHRAPAN, J., Some radioactive characteristics of calcium, 25:5647
CHRIEN, R. E., Gamma rays from thermal and resonance neutron capture in ^{121}Sb and ^{123}Sb, 25:5724
CHRISTENSEN, D. E., ^{235}U depletion as a potential independent cross-check of the plutonium content of spent power reactor fuels, 25:4257 (BNWL-SA-3304)
CHRISTENSEN, J. A., Fuel-clad gap conductance in fast reactor oxide fuels, 25:5999
Molybdenum distribution in irradiated oxide fuels, 25:4891
Molybdenum distribution in irradiated oxide fuels, 25:4804
CHRISTENSEN, John M., Feedback-induced spatial effects in a simple prompt critical reactor excursion, 25:6161
CHRISTENSEN, P. R., Deuteron scattering from ^{124}Te and ^{144}Nd, 25:5729
CHRISTENSEN, Ronald Arlie, Strong pion--alpha scattering with electromagnetic corrections, 25:5527
CHRISTIAN, J. W., Slip in single crystals of niobium--molybdenum alloys deformed in compression, 25:4800
CHRISTOPHER, J. T., Magnetization and ^{59}Cc hyperfine field measurements in Gd($CoNi)_2$, 25:5158
CHRISTY, R. W., V_3 band in LiF, 25:5156
CHROMIK, Joseph J., Energy integral tests of differential fission cross-section data, 25:5773
CHUBB, W., Role of grain boundaries in swelling of UN at 1600 to 1700°C, 25:4826
CHUDINOV, E. G., Saturated vapor pressure of solid UF_4, 25:4079
CHUDINOV, V. G., Dependence of scattering transport length on neutron energy in H_2O, D_2O, and graphite, 25:5502
CHUDNOVSKII, F. A., Phase transition and switching effect in V_2O_3, 25:4759
CHUKREEV, F. E., Violation of independence of decay of compound nucleus, 25:5636
CHUNG, Kyu Hoi, Insect pest control using sterile-male technique. I, 25:4735
CHUVILO, I. V., Di-pion in mass values region M($\pi^0\pi^0$) less than or equal to 1.3 GeV, 25:5284 (JINR-E1-5085)
CIARANFI, E., Radiosensitizing effect of L-erythro-α,β-dihydroxybutyraldehyde on Ehrlich ascites tumour cells. Cytokinetic analysis of tumour growth, 25:4564
CICCARONE, P., Radioprotection and modification of glycolysis in Ehrlich ascites tumour cells, 25:4566
CIRILOV, S. D., Oblate shape of $^9/_2^-$ isomer in ^{199}Tl, 25:5707
CITTADINI, G., Radioprotective action of haematoporphyrin on endogenous spleen colony-forming units, 25:4572
CLARK, D. E., Gasification of graphite under HTGR operating and potential accident conditions, 25:5585
CLARK, D. J., Polarization and cross-section measurements in p-^{4}He scattering from 20 to 40 MeV, 25:5526 (UCRL-19943)
CLARK, D. L., Hydraulic performance and cavitation characteristics of electromagnetic helical induction pump, 25:4186 (ORNL-TM-2995)
CLARK, David L., Adapting commercial heaters to simulate LMFBR fuel rods in sodium, 25:6029
CLARK, John Joseph, Operational characteristics of high-current relativistic electron beam accelerator, 25:5473
CLARKE, N. M., Backward angle scattering of 50-MeV protons from C, O, N, and Be, 25:5585
CLARKE, R. H., Predicting the heavy element composition of irradiated reactor fuels, 25:4815 (RD/B/N-1722)
CLAUDSON, T. T., Irradiation induced swelling and creep in fast reactor materials, 25:4810 (BNWL-SA-3283)
CLAYEUX, Genevieve, Gamma-ray production cross sections for 5-, 6.6- and 8.7-MeV neutrons with nitrogen, oxygen, scandium, and gold, 25:5551 (CEA-R-4047)
CLAYTON, Donald D., Nucleosynthesis in stars, 25:4914
CLAYTON, E. D., Criticality of Pu nitrate solutions containing Raschig rings, 25:4281
CLEARY, Robert M., Healing length of the superconducting order parameter, 25:5049
CLEMENS, Reginald Willis, Search for gravitational radiation, 25:5419
CLEMENT, J. D., Radiant heat transfer in heated aerosols at 100 atmospheres pressure, 25:6135
Spatial and feedback effects in Georgia Tech Research Reactor, 25:6108
CLEMENT, Joseph D., New course in financial management and economics of nuclear power, 25:6195
CLEWS, C. J., Phase shift analysis of P--D elastic scattering, 25:5546
CLINE, D., First excited state of ^{148}Sm, 25:5703
COCKAYNE, J. E., Successive space-energy synthesis for fast reactors, 25:5962
COCKBURN, P. M., One-neutron transfer reactions, 25:5577
COEHOORN, J., Measurements and calculations on thermal, Argonaut type, cores in STEK-facility at Petten, 25:6093 (RCN-118)
COETZEE, N., Energy levels of ^{203}Tl and ^{205}Tl, 25:5798
COHEN, E. J., Beta-ray asymmetry from oriented /sup 110m/Ag, 25:5743
COHEN, Judith G., Nature of BD + 17° 4708, 25:4906
COHEN, R. L., First-order transition in europium metal, 25:5203
COHEN, R. W., Effect of microwave phonons on

superconductive tunneling, 25:5043
COLBERT, C., Phalangeal Atlas: an application of radiographic photodensitometry, 25:4641 (CONF-700515-, pp 224-36)
COLBERT, Charles, Bone mineral measurements from x-ray images, 25:4614 (CONF-680211-, pp 80-95)
COLE, B. J., Method of pseudo-bound states for stripping to unbound levels, 25:5666
COLE, Donald W., Design of radioisotope heat sources for human implantation, 25:4229
COLE, J. M., Analysis by static simulation for shock pulse loading of core components, 25:6078
COLEMAN, James R., Population safety considerations of an implantable isotopic power source, 25:4236
COLEMAN, W. A., Scattering angle biasing for deep-penetration x-ray transport, 25:5145
COLEMAN, W. J., Modifications of a triode sputtering unit to provide maximum flexibility for use in a radioactive glove box environment, 25:4259 (BNWL-SA-3609)
COLLIN, W., Photonuclear reactions in oxygen and their use for the control of energy and photon spectrum at electron accelerators, 25:5597
Reactions $^{12}C(\gamma,n)$, $^{12}C(\gamma,2n)$, $^{39}K(\gamma,n)$, and $^{40}Ca(\gamma,np)$ up to the meson threshold, 25:5578
COLLINGWOOD, I., L-shell fluorescence in ^{238}Pu, 25:4947
COLLINS, G. B., Computer interface methods and standards, 25:4387 (AEEW-M-986)
COLLINS, Paul F., Operator license examinations using nuclear power plant simulators, 25:6212
COLOMBO, P., Development of concrete-polymer materials and composites, 25:4838
COLONIAS, John C., Graphic display interaction in nuclear physics, 25:6201
COMAR, C. L., Radiobiological effects of simulated nuclear power sources for artificial hearts, 25:4433
COMFORT, J. R., Evidence for J/sup π/ = 8$^+$ state in ^{16}O, 25:5592
COMI, Paola, Prevention by cysteine of fatty liver induced by CCl_4 and ethionine, 25:4600
CONDE, J. F. G., High temperature corrosion of Nimonic-75 and various steels in gases at low partial pressures, 25:4738 (DP-Report-527)
Materials for boiler tubes of a HTGC power reactor, 25:4748 (DP-Report-537)
CONGEL, F., Use of sparking techniques to enhance track-etch radiographs, 25:4348
CONGEL, F. J., Automatic system for counting etched holes in thin dielectric plastics, 25:4340
CONLEY, L. A., Multiple-source urban atmospheric dispersion model, 25:4161 (ANL/ES-CC-7)
CONLIN, J. A., Fission gas release measurements from fast breeder $(U,Pu)O_2$ fuel, 25:6015
Irradiation performance of loose and bonded beds of coated fuel particles, 25:6004
CONN, Robert, Waste heat and fog control, 25:5886
CONTE, Madeleine, Partial melting of low density mixed oxide $(U,Pu)O_2$ at beginning of irradiation, 25:4879 (CEA-CONF-1659)
CONTY, Claude, Electron probe microanalysis of highly radioactive materials, 25:4011 (CEA-N-1340)
CONZETT, H. E., Polarization and cross-section measurements in p-^{4}He scattering from 20 to 40 MeV, 25:5526 (UCRL-15943)
COOBS, J. H., Irradiation performance of loose and bonded beds of coated fuel particles, 25:6004
COOK, J. A., Removal of ^{24}Na from neutron-activated samples, 25:4044
COOKE, A. H., Magnetic properties of gadolinium orthovanadate, 25:5217
COOPER, Bernard R., Magnetic ordering and thermodynamic properties of induced moment systems, 25:5205
COOPER, John C., Beta decay of ^{19}O, 25:5555
COOPER, L. R., Levels of ^{70}Zn, 25:5667
COOPER, M. H., Radiochemical measurement of mass transfer coefficients in forced-convection sodium, 25:4774
COOPER, W. W., Radioactive strontium and barium fallout, 25:4163
COOPS, M. S., Shielded neutron shipping cask, 25:4311
Trigger-actuated motion locks for master-slave manipulators, 25:4312
COPELAND, E. S., Structure-function studies of the aminothiol radioprotectants, 25:4548
COPLEY, Leslie Alexander, Symmetry breaking in elementary particle physics, 25:5394
COQBLIN, B., Theoretical comments on the valence change of rare earth metals, 25:5233
CORCIOVEI, A., Solving time-dependent nonhomogeneous thermalization equation, 25:5478
CORDARO, M., Method for solving time-dependent electron transport problems, 25:5242
CORNELISSE, C. J., Gametogenesis and oviposition in Lymnaea stagnalis as influenced by γ-irradiation and hunger, 25:4693
CORNER, W. D., Magnetic domain structures in gadolinium, 25:5196
CORNET, Jean-Andre, Study of α and epsilon phases of Pu by high-hydrostatic pressures, 25:4785 (CEA-R-4092)
CORONITI, Ferdinand Vincent, Finite-Larmor-radius analysis of laminar collisionless shocks, 25:5102
CORRIN, B., Phagocytic potential of pulmonary alveolar epithelium, 25:4410
CORTE, Ernesto, New wide-range linear channel for accurate reactor power measurements, 25:6207
COSGROVE, G. E., Induction of carcinoma of the glandular stomach by whole-body irradiation, 25:4703
COSTANTIN, P., Prospects of automation in the control of nuclear power plants, 25:5875
COSTELLO, D. G., Isotopic source assay system for nuclear materials, 25:4038
COUNCIL, W., Training of personnel to operate Millstone Point Company nuclear boiling water reactor power plant, 25:5887
COUNSIL, William G., Training of personnel to operate Millstone Point Company nuclear boiling water reactor power plant, 25:5895
COUPLAND, J. H., Equations and formulae for magnets with air cored windings of saddle coil type, 25:5464 (RHEL/R-203)
COURTNEY, J. C., Monte Carlo radiation transport analyses of the NERVA nozzle assembly, 25:6129
COWAN, Clyde L., Production of low-energy muons by neutral components of cosmic radiation at sea level, 25:4974 (AD-710278)
COX, A., Additional system for bone densitometry studies, 25:4634 (CONF-700515-, pp 33-47)
COX, Anna, Bone densitometry: clinical applications, 25:4626 (CONF-680211-, pp 308-19)
COX, C. M., Transient performance of sol-gel $(U,Pu)O_2$ Sphere-Pac and pellet fuels, 25:6016
COX, J. E., Fracture of solidifying particles, 25:6083
COX, R. J., Gamma radiation from the decay of ^{99}Nb, 25:5718
COX, Thomas, Isotope-powered, indwelling intracranial pressure sensor, 25:4241
CRAGG, D. A., Frozen polarized target, 25:5466 (RPP/A-81)
CRAIG, P. H., Radiobiological effects of simulated nuclear power sources for artificial hearts, 25:4433
CRAIG, R. S., Heat capacity studies of intermetallic compounds containing rare earth elements, 25:5218
CRAMP, W. A., Modification of post-irradiation DNA degradation in E. coli B/r, 25:4551
CRASEMANN, Bernd, Beta decay of ^{19}O, 25:5555
CRAWLEY, G. M., Anomalous L = 1 shapes of angular distributions for (^{3}He,t) transitions to 0$^+$ antianalog states in ^{64},^{66}Ga and ^{40}K, 25:5654
CREEL, Roger Bryan, Nuclear magnetic resonance in transition metal borides, 25:5229
CREMMER, E., Divergences and renormalization in multiloop dual diagrams, 25:5409
CRISTEA, Al., Kinetic investigations on the influence of radiosensitizing vitamin K_3 on the haemoglobin-methaemoglobin equilibrium, 25:4598
CRISTY, G. A., Prog. rpt. on transportation systems and dual purpose blast shelters, 7/70, 25:4255 (ORNL-TM-3016)
CROCKER, J. G., Capabilities of PBF for LMFBR safety testing, 25:6102
CROKE, E. J., Multiple-source urban atmospheric dispersion model, 25:4161 (ANL/ES-CC-7)
CRONENBERG, A. W., Coolant voiding and pressure generation due to boiling, fission gas release, and molten fuel-coolant interaction, 25:6073
CROSS, F. T., In-phantom dosimetry of ^{238}Pu heat sources, 25:4517
CROW, J. E., Superconductivity and normal-state conduction mechanism in oxidized thin aluminum films, 25:5039
CROWLEY, B. K., MARVEL experiment, 25:4177
CROWSON, D. L., Safeguards in the USA: an updating, 25:4270
CSEJTHEY-BARTH, M., Remarks on Σ^- hyperon conversion rate, 25:5298
Trapping of Λ^0 hyperons produced by K^- meson absorption, 25:5299
CSOKE, A., Two-dimensional (T/sub 1/2/, E/sub γ/) mapping of short-lived nuclides, 25:5685 (KFKI-70-18-NAC)
CSONKA, P. L., Three paradoxes related to full causality, 25:5307 (RLO-2041-49)
CSONKA, Paul L., Energy and angular resolution in pion--pion scattering and other colliding beam experiments, 25:5360 (RLO-2041-51)
Scattering of real pions on each other, 25:5285 (RLO-2041-40)
CUDDIHY, R. G., Retention in beagle dog of $^{140}LaCl_3$, 25:4426
CULLEN, Dermott E., Angular distributions in neutron-induced reactions. I, 25:5549 (BNL-400(3rd Ed.)(Vol.1))
CUNEO, D. R., Transient performance of sol-gel $(U,Pu)O_2$ Sphere-Pac and pellet fuels, 25:6016
CUNNINGHAM, James P., Multigroup point kinetics with feedback, 25:5956
CUOCO, A., General principles of a safety assessment through reliability analysis of ESSOR plant, 25:6054 (RISO-214, pp 597-625)
CURET, H. D., Design basis for LOFT facility, 25:6104
CURRIE, L. A., Photonuclear tritium yields at 90 MeV, 25:5678
CUSHMAN, R. A., Gap conductance of oxide fuel elements irradiated in EBR-II, 25:6060
CYGELMAN, A. I., Analysis and design methods for light-water power reactor shields, 25:5977
CZYZEWSKI, O., High-energy interactions at accelerator energies, 25:5272

XUM

D

DAGENS, Luc, Approximations deduced from Milne equation associated to that of Schrcedinger, 25:5234 (CEA-R-4007)

DAHLKE, L. W., Neutron radiography of mixed-oxide fuels, 25:4254

DAIBOG, E. I., Particle number fluctuations in hydrodynamical theory of multiple production, 25:5309

DALE, I. M., Neutron activation analysis for transition elements in rocks, 25:4047

DALGARNO, A., Metastable species in the ionosphere, 25:5011

DALLY, E. B., Form factor ratio GE/sub n//GE/sub p/ at low-momentum transfers, 25:5247 (AD-710385)

DAMINOV, G., Determination of O in Si by photonuclear reaction, 25:4046

DAMLE, P. S., Aquoluminescence from gamma-irradiated halides, 25:4076

D'ANDREA, A., Group-theoretical analysis of β-decays of some j = 3/2 light nuclei, 25:5813

DANG, G. Do, Mixing of Hartree--Fock states in ^{28}Si, 25:5674

DANGERFIELD, G. R., BOPTIC: beam transport program in FORTRAN IV, 25:5441 (AAEC/TM-644)

DA NOBREGA, J. A. W., New solution of the point kinetics equations, 25:6150

DANOS, M., Quartet structure in light nuclei, 25:5814

DAR, Y., First two excited states of ^{159}Tb, 25:5727

DAS, M., Photochemical precipitation of Th and Ce and their separation from other ions in aqueous solution, 25:4026

DAS GUPTA, S., Many-particle many-hole states in ^{16}O, 25:5560

DASS, G. V., Relative phase of rho- and ω- production amplitudes in Regge phenomenology, 25:5374 (DNPL/R-7, pp 207-13)

DATZ, S., Charge states of 60-MeV iodine ions channeled in Au, 25:5164

DAUBLEBSKY, P. K., Reliability and availability of two BWR shut-down systems, 25:6036 (RISO-214, pp 41-55)

DAUGHTREY, S. P., MAPLE IB: ^{60}Co-fueled thermoelectric generator, 25:4226

DAUGHTRY, J. W., Plutonium and ^{238}U Doppler measurements in plutonium-fueled fast critical assembly, 25:6109

DAUMAS, M. T., Crystalline parameter of delta-phase Pu--Ga alloys, 25:4801

DAURY, Gerard, Contribution to the study of molecular reflection, 25:6221 (BNL-tr-383)

DAVE, Vibhakar Ratilal, Nuclear energy levels of ^{133}Cs and ^{141}Pr from the (n,n'γ) reaction, 25:5751

DAVERHOEG, N., Anomalous helium production in nickel, 25:4821

Helium accumulating dosimeters for high neutron fluences and long irradiation periods, 25:4381

Helium production in Fe, Cr, Ni, Ti, and Cu due to fission neutron part of reactor spectra, 25:4822

New boron analysis method, 25:4037

DAVEY, W. G., Investigation of sodium-voiding reactivities and other safety parameters in fast critical assemblies, 25:6112

DAVIDOVA, E., Protective effect of para-aminopropiophenone and propylene glycol on the haematopoietic stem cells of mice, 25:4571

DAVIDOVICH, R. L., Thermal stability of ammonium uranyl fluorides, 25:4082

DAVIDSON, Jack D., Spinal cord dosimetry in ^{131}I-IHSA cisternography, 25:4510

DAVIDSON, S. L., Evaluation of electrically tested NERVA reactor fuel elements, 25:6141

DAVIES, Donald Wayne, Strange particle production in π⁺d interactions from 1.1 to 2.4 GeV/c, 25:5289

DAVIES, J. V., Fast intermediate reactions sensitizing alcohol dehydrogenase to radiation, 25:4543

DAVIES, W., Coulometric determination of uranium with a platinum working electrode, 25:4025

DAVIS, D. N., Space radiation hazards to Project Skylab photographic film, 25:4405 (N-70-32671)

DAVIS, E. H., Transfer function investigations on first Dragon core, 25:5953 (DP-Report-445)

DAVIS, J. H., Space radiation hazards to Project Skylab photographic film, 25:4405 (N-70-32671)

DAVIS, Jay Clarence, Fast-neutron energy determinations, 25:5598

DAVIS, P. R., Design basis for LOFT facility, 25:6104

DAVIS, Rachel P., Effect of capsule content variations on thyroid uptake results, 25:4661

DAVIS, Richard, Effects of fuel chilling on Doppler-controlled fast reactor accidents, 25:6069

DAWSON, N., Excited states of ^{44}Ca, 25:5626

DAY, J. T., Factors affecting the justification of nuclear units in generation expansion, 25:5899

DAZHAEV, P. Sh., Local ordering and resistivity of Ni--W and Pd--Co alloys, 25:4766

DEAKIN, M. J., Clinical trial of two sunscreening creams, 25:4608

DEAN, C. J., Repair of DNA and the mode of action of sensitizers and protectors in biological systems of different complexity, 25:4536

DE BAERE, W., Kw elastic scattering studies by the Chew--Low extrapolation method, 25:5369

DEBAISIEUX, J., Kw elastic scattering studies by the Chew--Low extrapolation method, 25:5369

DE BOER, F. W. N., Decay of ^{179}Re, ^{177}Re, and ^{176}Re, 25:5733

DE BRION, Jean-Pierre, Regge models including 4 poles rho, rho', A2 and A2', in π-nucleon and K-nucleon charge exchange reactions from 2 to 20 GeV/c, 25:5371 (CEA-N-1373)

DECARLO, V. A., Thermal performance and restructuring of pellet and sphere-pac fuels, 25:5992

DECROISETTE, Michel, Thomson scattering and Rayleigh scattering in argon plasma jet, 25:5078 (CEA-R-3998)

DEE, J., Accomodation of radiation swelling in GCFR, 25:6020

DE FRENNE, D., Decay of ^{153}Sm to levels in ^{153}Pm, 25:5697

Excited states of ^{175}Yb from decay of ^{175}Tm, 25:5747

DEHOFF, R. T., Quantitative determination of the structure--property relationships in nuclear fuel element materials. Quarterly progress report, June 15--September 15, 1970, 25:4841 (SRO-552-5)

DEI-CAS, R., Ion heating in a Penning discharge, 25:5075

DEITRICH, L. W., High-energy transient meltdown of irradiated UO_2 in a TREAT Mark-II loop, 25:6097

DELAFIELD, H. J., Nuclear accident dosimetry systems, 25:4377 (AERE-R-6498)

DELAPALME, A., Characterization of compounds and materials by neutron diffraction, 25:4151 (CEA-CONF-1500)

DELAUNE, C. I., Energy levels of ^{27}Al, 25:5613

DELONG, L. E., Continuously operating ^{3}He evaporation refrigerator, 25:5061 (UCSD-34-P-143-31)

DEMARTINI, David Charles, Polarization of neutrons from ^{13}C(^{3}He,n_0)^{15}O and ^{24}Mg(^{3}He,n_0)^{26}Si reactions, 25:5574

DE MEULEMEESTER, F. M., Measurements and calculations on thermal, Argonaut type, cores in STEK-facility at Petten, 25:6093 (RCN-118)

DEMEUR, M., Harmonic oscillator in prolate spheroidal coordinates. I, 25:5843

DEMIN, V. F., Reconstruction of NN potentials from nuclear data, 25:5831

DEMUYNCK, J., Decay of ^{153}Sm to levels in ^{153}Pm, 25:5697

Isomeric states /sup 101m/Ru, /sup 103m/Ru, and /sup 101m/Tc, 25:5761

DENISIK, S. A., Calculation by Monte Carlo method of distribution of photoneutrons from a beam of γ radiation with initial energy of 4.1 MeV, 25:4152 (CSIRO-Trans-10083)

DENNING, R. S., Space--time kinetics studies for commercial power reactors, 25:6081

DENNIS, J. A., Nuclear accident dosimetry systems, 25:4377 (AERE-R-6498)

DE NORDWALL, J. H., Fission product release from overheated HTGR fuel elements, 25:6010

DEREM, A., Effective Regge trajectories for some two-body reactions, 25:5377

DEREM, Andre, Regge models including 4 poles rho, rho', A2 and A2', in π-nucleon and K-nucleon charge exchange reactions from 2 to 20 GeV/c, 25:5371 (CEA-N-1373)

DERESH, B. A., Hydrodynamic and neutronic coupling in a circulating critical gas, 25:6175

DERNIER, P. D., Crystal structure of antiferromagnetic phase of V_2O_3, 25:5190

DERRICK, M., Experimental neutrino physics, 25:5256 (CONF-700314-, Paper 6)

DE SAUSSURE, G., Measurement of capture cross section of ^{238}U, 25:5771

Neutron fission and capture cross section measurements for ^{233}U, 25:5702

DETAINT, Jacques, Improvements in neutron-emitting target, 25:5503

DE TAKACSY, N., Many-particle many-hole states in ^{16}O, 25:5560

DETCH, J. L. Jr., Scattering of polarized protons by tritons at 13.6 MeV, 25:5521 (LA-4465, pp 28.1-2)

DETILLEUX, E., Versatility in reprocessing irradiated fuels, 25:4148

DEUTSCHMANN, M., Production of proton--antiproton and kaon--antikaon pairs, 25:5297

DE VELLIS, Jean, Appearance of brain-specific antigen in developing rat brain, 25:4694 (UCLA-12-791)

DEVERALL, J. E., Sonic limitations and startup problems of heat pipes, 25:6236 (LA-4518)

DE VILLIERS, J. A. M., Energy levels of ^{203}Tl and ^{205}Tl, 25:5798

DEVINS, D. W., T = 9/2 analogue state in ^{63}Ni, 25:5609

DEWEY, D. L., Influence of sulphur-containing protective agents on bacteriophage survival curve shapes, 25:4549

DEW-HUGHES, D., Measurement of energy dissipated in superconductors during flux jumps, 25:5044

DE WOLF, E., Kw elastic scattering studies by the Chew--Low extrapolation method, 25:5369

DEY, Arun K., Complexes between U(VI) and dioxydiquinone, 25:4078

D'EYE, R. W. M., Fuel fabrication development for the UK gas-cooled Mark III reactor, 25:6005

DIAMOND, R. M., Heavy-ion in-beam spectroscopy, 25:5688 (UCRL-19961)

Oblate shape of $^9/_2^-$ isomer in ^{199}Tl, 25:5707

Quadrupole moments excited states in ^{20}Ne and ^{22}Ne, 25:5622

DIAMOND, Stephen Alan, Behavior of an ionized gas in a

homopolar device, 25:5089
DIAZ, N. J., Novel, high counting rate neutron detection system, 25:4354
DICK, C. E., Study of nuclear states of several odd-A nuclei 68 less than or equal to Z less than or equal to 75 through electromagnetic excitation from 2.3 to 3.6 MeV, 25:5637
DICKEY, J. M., Superconductivity and normal-state conduction mechanism in oxidized thin aluminum films, 25:5039
DIENST, W., Creep of UO_2 under irradiation, 25:4893
Production, detection, annealing of crystal lattice point defects by neutron irradiation of ceramic materials, 25:4887 (KFK-1215)
DIENSTBIER, Z., Cardiovascular, biochemical, and haematological changes after the application of AET, 25:4599
DIETZ, G., Economics of radiation versus heat-catalyst curing for wood-plastic flooring plant, 25:4109
DILLMAN, L. T., Average particle energy in beta decay, 25:5846
DILLON, R. S., Design and safety considerations in the shipment of solidified wastes, 25:4278
DINNI, Louis W., Use of Argonne National Laboratory computers in nuclear engineering education, 25:6194
DI VITA, G., Indanetrione, menadione, Synkavit, and N-ethylmaleimide tested as radiosensitizers on murine ascitic tumour irradiated in vitro and grown in vivo, 25:4562
DMITRENKO, I. M., Superconductor/normal metal/superconductor point contacts, 25:5037
DMITRIEVA, L. A., Interrelation between solar wind and geomagnetic field, 25:5026
DOBBEN, G., Additional system for bone densitometry studies, 25:4634 (CONF-700515-, pp 33-47)
DOBO, Janos, Structural and kinetic factors in radiation graft-copolymerization, 25:4105
DOBRY, H., Computer programs for irradiation planning in high-energy therapy, 25:4514
DODDER, D. C., Measurement of the vector and tensor analyzing power of d--^{4}He elastic scattering at 12 MeV, 25:5553 (LA-4465, pp 25.1-2)
Reactance matrix analysis of the d--^{3}He, p--^{4}He system at 10-MeV deuteron laboratory energy, 25:5509 (LA-4465, pp 2.1-2)
Study of ^{3}He(d,d)^{3}He scattering at 10 and 12 MeV, 25:5520 (LA-4465, pp 24.1-2)
Study of the ^{3}He(d,p)^{4}He reaction, 25:5512 (LA-4465, pp 6.1-2)
DODSON, M. H., Simplified equations for double-spiked isotopic analyses, 25:4028
DOEDERLEIN, J. M., OECD Halden Reactor Project, 25:5946
DOGUCHI, Masao, Effects of gamma irradiation on wheat gluten, 25:4465
DOHERTY, David G., Chelation and radiation protection, 25:4553
DOLCATER, David Lee, Cation exchange selectivity and mineralogy of soil clay materials, 25:4160
DOLINSKII, E. I., Theory of (^{6}Li,d) and (^{7}Li,t) reactions, 25:5601
DOMINICIS, D. P., ECC variable flooding rate simulation PWR FLECHT test results, 25:6043
Effect of 75 to 100 percent flow blockage on bottom cooling heat transfer effectiveness, 25:6042
DONAHUE, D. A., Profilometer for dimensional inspection of irradiated LMFBR fuel elements, 25:6033
DONKOV, A. D., Quasi-potential equation for the relativistic harmonic oscillator, 25:5405 (JINR-E2-5339)
DONNACHIE, A., Vector meson production and omega--rho interference. Proceedings of the Daresbury Study Weekend No. 1, 12--14 June 1970, 25:5322 (DNPL/R-7)
DONNELLY, I. J., Application of variational methods to neutron transport in slabs, 25:5135 (AAEC/TM-554)
DOOLEY III, George J., Auger electron spectroscopy: metallurgical applications, 25:4798
DORE, Earl K., Radioaerosol inhalation scanning, 25:4678
DORE, J. C., Backward angle scattering of 50-MeV protons from C, O, N, and Be, 25:5585
DORE, J. E., Considerations in the evaluation of aluminum master alloys, 25:4780
DORE, Michael A., Gamma-ray source characteristics of PuO_2, 25:4245
RTG/radioisotope heater shielding for sensitive science instruments on spacecraft, 25:4246
DORENBUSCH, W. E., Level structure of ^{47}Ti, 25:5629
DORIKENS, M., Isomeric states /sup 101m/Ru, /sup 103m/Ru, and /sup 101m/Tc, 25:5761
DORIKENS-VANPRAET, L., Isomeric states /sup 101m/Ru, /sup 103m/Ru, and /sup 101m/Tc, 25:5761
DORLHAC, Francois, Forced vortex in electroconducting viscous liquid in magnetic field, 25:5000
DORMAN, L. I., Geophysical effects and properties of the various components of the cosmic radiation in the atmosphere, 25:4984
DORMUTH, K., Spin-$^3/_2$ Compton scattering, 25:5329
DORY, R. A., High-frequency flutelike instabilities in multicomponent plasmas, 25:5110
DOSTAL, M., Protective effect of cystamine, AET, serotonin, and mexamine against fractionated lethal gamma-irradiation, 25:4581
DOTSENKO, I. S., Allowance for the wave function distortion under multipole analysis of fast nucleon scattering by nuclei, 25:5552 (ITF-70-50)
DOUCET, H. J., Ion distribution functions in collisionless surface ionized plasmas, 25:5098
Production of a quasi-electron-free plasma using electronic attachment, 25:5103
DOYLE, Frank H., Age-related bone changes in women, 25:4616 (CONF-680211-, pp 115-35)
DRAGOUN, O., Internal conversion of the 57.54 keV E1 transition in ^{180}Hf, 25:5731
M3 isomeric transitions in ^{58}Co and ^{60}Co, 25:5608
DRAPER, E. Linn Jr., Energy integral tests of differential fission cross-section data, 25:5772
DRAPER, J. E., Ground-state quasirotational bands and other states in ^{130} ^{132} ^{134},^{136} ^{138} ^{140}Ce, 25:5711
DRAWIN, H. W., Criteria for local thermodynamic equilibrium, 25:5094 (CEA-CONF-1625)
DRECHSEL, Dieter, Collective correlations calculation of dipole states of ^{28}Si, 25:5653
DRELL, S. D., Important problems and questions for the new accelerators, 25:5304 (CONF-700314-, Paper 18)
DREMIN, I. M., Dynamical scheme for leading trajectory and theory of fireballs, 25:5359
DREYER, R., Separation of nuclear isomers of ^{80}Br on metal surfaces, 25:4127
DRIOLE, Jean, Phase equilibriums in Ni--Nb--W and Ni--W systems, 25:4788
DRISCOLL, M. J., FBR blanket depletion studies: effect of number of energy groups, 25:5960
DROSG, M., Phase shifts from n--^{4}He elastic scattering experiments near 20 MeV, 25:5508 (LA-4465, pp 1.1-2)
DUBEY, S., Mandelates of lanthanum, praseodymium, neodymium, and uranium, 25:4055
DUBOVIK, V. M., Multipole current disintegration in classical electrodynamics, 25:5236 (JINR-P2-5283)
DUBROVINA, A. N., Investigation of the alloy Ni--25 at. percent W after isothermal [high-temperature] annealing, 25:4794
Metastable phase of the type Ni_3Mo in Ni--25 at. percent W alloy, 25:4789
DUDERSTADT, James J., Energy representations in neutron transport calculations, 25:5141
DUFF, R., Economics of radiation versus heat-catalyst curing for wood-plastic flooring plant, 25:4109
DUFFEY, D., Construction materials for neutron capture gamma-ray spectroscopy with ^{252}Cf sources, 25:4772
DUFFEY, Dick, Detection and analysis of titanium ore using ^{252}Cf, 25:4036
DUKAT, Alexander J., Nondestructive gamma assay of plutonium-contaminated solid waste in drums, 25:4253
DUMONTEIL, G., Manufacture of metallic uranium nuclear fuels: some industrial and economic aspects, 25:4743
DUNCAN, A. J., Low frequency axisymmetric waves in a weakly ionized magnetoplasma column, 25:5123 (SU-IPR-366)
DUNHAM, V. C., Double Langmuir probe measurements in a magnetized positive column, 25:5081 (N-70-32493)
DUNLAP, B. D., Hyperfine interactions in Er_2O_3 and Yb_2O_3 between 20 and 1.5°K, 25:5225
DUNN, Floyd Eugene, Analytic studies of fast reactor flux and importance spectra, 25:5954
DUNN, Stephen A., Multigroup point kinetics with feedback, 25:5956
DUNSCOMBE, P. B., Polarization transfer at 0° in the D(d,n)^{3}He and H(d,n)pp reactions, 25:5532
DUPLAN, J. F., Radiosensitizing effect of Mitomycin C on haematopoietic colony forming cells, 25:4570
DUQUETTE, D. J., Fractographic study of stage I fatigue cracking in a nickel-base superalloy single crystal, 25:4765
DURAND III, Loyal, Regge-type models for high energy scattering, 25:5347 (CONF-700314-, Paper 13)
DURCEK, K., Some radioactive characteristics of calcium, 25:5647
DUTT, N. K., Spectrophotometric determinations of Ti and Nb, 25:4020
DUTT, Yag, Potentiometric investigation of metal complexes with phenanthrenequinone monoxime, 25:4080
DUYCKAERTS, Claire, Blood redox potentials of rats and mice injected with cystamine, 25:4593
DZHEMILEV, Z. A., Association of chromosomes of Macaca mulatta in irradiated leucocytes, 25:4493
DZHIBGASHVILI, G. G., Spectroscopic investigation of the low-temperature radiolysis of some polyolefins, 25:4118

E

EAST, L. V., Delayed-neutron abundances and half-lives from 14.7-MeV fission, 25:5775
EASTERDAY, H. T., Levels of ^{70}Zn, 25:5607
EASTHAM, D. A., Electron and gamma transitions in ^{45}Sc, 25:5624
EATHER, R. H., Ionization produced by auroral proton precipitation, 25:5010
EBERHARD, K. A., Anomalous backward enhancement of elastic α-scattering cross sections near A = 40, 25:5665
EBERSOLE, E. R., Xenon tag proof test, 25:6026
EBERT, M., Damaging radiation chemical events, 25:4705
Fast intermediate reactions sensitizing alcohol dehydrogenase to radiation, 25:4543

XUM

ECKELS, T. W., Further data on gamma-induced electrical charge and coloration of shielding glasses, 25:5166
ECKERMAN, Keith, Curium-244 and ^{145}Sm--^{145}Pm x-ray sources, 25:4647 (CONF-700515-, pp 274-9)
ECKLEY, Wayne, Effect of source geometry pattern upon foil activation for diffusion length measurement, 25:6182
ECONOMOU, Thanasis E., Alpha-scattering technique of chemical analysis, 25:4034
EDELEN, Dominic G. B., Relativity and the question of discretization in astronomy, 25:4533
EDEN, R. J., Theorems on high energy collisions, 25:5303 (CONF-700314-, Paper 16)
EDESKUTY, F. J., Proposed 0.4 K polarized proton target cryostat for LAMPF, 25:5456 (LA-4465, pp 33.1-2)
EGAMBERDIEV, A., Influence of pollen radiation on crossing ability and variability in cotton, 25:4495
EGOROV, Yu. V., Clarification and deactivation of waste waters by frothing flotation, 25:4141
EGUCHI, Hiroshi, Radiation chemistry of foods. IV, 25:4117
EGUSA, Tatsuo, Various problems associated with the design of nuclear reactors, 25:5945
EHN, E., New isotope of palladium ^{116}Pd, 25:5740
EICHELBERGER, W., Reaction $^{12}C(d,^6Li)^8Be$ α-cluster pickup, 25:5562
EICHLER, Joerg, Alpha clusters in Hartree--Fock calculations, 25:5586
EIDUS, L. Kh., Vicia faba seedling chromosome damages by split dose, 25:4497
EISBERG, Robert M., Nuclear structure research. Progress report, Task A, 25:5606 (UCSB-34-P-144-7)
EISENBERG, J. M., Dynamic nuclear effects in pionic and kaonic atoms, 25:5866
Radiative pion absorption in medium and heavy nuclei, 25:5793
ELIAS, E., Backscattering of gamma rays from barriers of finite thickness, 25:5145
ELIASHVILI, M. A., K/sub l3/ decays in chiral dynamics, 25:5399 (JINR-P2-5290)
ELICH, J. J. Ph., Anisotropy in ejection patterns due to generation of focusing collisions by channeled particles, 25:4939
ELINSON, S. V., Photometric determination of Nb with reagent PAR in complex Cu-base alloys, 25:4018
ELKIND, M. M., Drug-radiation damage interaction and its relevance to radiosensitization in mammalian cells, 25:4558
ELLEMAN, Thomas S., Prog. rpt. on diffusion in solids, annual, 11/69--10/70, 25:5152 (GRO-3508-6)
ELLER, E. L., High-energy calibration using ^{252}Cf neutron source, 25:4223
ELLERT, G. V., Uranium sulfide transport, 25:4059
ELLIOTT, R. O., Kondo effect in LaPu and PrPu alloys, 25:5227
ELLIS, C. F., Fallout computational techniques, 25:4506 (AD-703266)
EL-NADI, M., Optical model analysis for elastic deuteron scattering on light nuclei, 25:5579
EL-NAGGAR, I. A., Dielectric permeability of an inhomogeneous relativistic stream of cold plasma, 25:5101
ELYUSHIN, V. P., Mechanism of the interaction of V_2O_5 with C. II, 25:4842
ELZE, Th. W., Reactions $^{232}Th(d,t)^{231}Th$ and $^{238}U(d,t)^{237}U$, 25:5797
EMELYANOV, V. S., Offensive weapons and means of protection, 25:4167 (CONF-691051-, pp 192-8)
EMEL'YANOVA, L. I., Visualizing dislocation structure of Mo by etching in Ar flow, 25:4796
EMMERSON, Peter T., Modification of DNA in Escherichia coli exposed to x-rays by triacetoneamine N-oxyl and oxygen, 25:4550
Reaction of triacetoneamine-N-oxyl with radiation-induced radicals from DNA and from deoxyribonucleotides in aqueous solution, 25:4541
ENDRES, G. W. R., Response of selected totally depleted and lithium-drifted silicon detectors to monoenergetic gamma and neutron radiation, 25:4356
ENDRIZ, J. G., Reflectance studies of Ba, Sr, Eu, and Yb, 25:5188
ENDT, P. M., Lifetime measurements in s-d shell nuclei. IV, 25:5628
ENGE, W., Charge distribution of cosmic-ray tracks in polycarbonate plastic detectors, 25:4338
ENGELBERTINK, G. A. P., Lifetime of 5- 4585 keV ^{38}Ar level, 25:5664
ENGLE, G. B., Density and structural distributions in artificial graphites, 25:4866
ENGLE, L. B., Large accidents, 25:6089
ENGLE, W. W. Jr., Time-dependent coupled neutron--gamma calculations in polyethylene, 25:5147
ENIKEEVA, F. Kh., Calculation of neutron distribution in hydrogen, 25:5493
ENRIOTTI, M., Regge-Pole analysis of rho^0 production, 25:5380
ENSLEY, D. L., New superfluid relativity gyroscope, 25:5422
EPOV, D. G. Thermal stability of ammonium uranyl fluorides, 25:4062
ERDAS, F., Reaction $^4He(\gamma,d)d$ and 2^+ excited state of ^4He at 30 MeV, 25:5543
ERDMANN, R. C., Fast reactor implosion studies, 25:6066
Fast reactor safety in nuclear science and engineering curriculum, 25:6063
Hydrodynamic and neutronic coupling in a circulating critical gas, 25:6175
ERDMANN, Robert C., Effects of fuel chilling on Doppler-controlled fast reactor accidents, 25:6069
ERIKSSON, John R., Relativistic nucleon--nucleon scattering, 25:5827
ERNST, D., Sublimed emitter and collector coatings, 25:4750 (TEE-4125-2)
EROZOLIMSKII, B. G., Neutron spin and antineutrino momentum in neutron decay, 25:5258
ERRERA, Maurice, Excision repair of non-replicated uv-damaged E. coli DNA, 25:4463
ERTEL, G., Production of isotopes, labeled compounds, and sealed radiation sources, 25:4128
ERWIN, A. R., Multiparticle production: experimental, 25:5280 (CONF-700314-, Paper 10)
ESAIBEGYAN, S. V., Radiative decays of mesons in broken SU(3) symmetry and electromagnetic mass splittings in the 0- octet, 25:5402
ESKOLA, Kari, Alpha decay of ^{255}No and ^{257}No, 25:5704
ESKOLA, Pirkko, Alpha decay of ^{255}No and ^{257}No, 25:5704
ESSER, P. D., Formation of color centers in KCL:Tl by gamma irradiation at 21°C, 25:5157
ESTOURNEL, R., Twelve years of health physics in a plutonium production plant, 25:4526
ETIM, E., Tests of models of scale invariance with cosmic-ray neutrino data, 25:5340
EVANCO, William Martin, PCAC, unitarity, and the sigma-model, 25:5367
EVANS, A. E., Delayed-neutron yield vs energy measurements, 25:5770
EVANS, A. G., Construction materials for neutron capture gamma-ray spectroscopy with ^{252}Cf sources, 25:4772
EVANS, S. K., Behavior of large PuO_2 particles in a rapid power transient, 25:5995
Behavior of Pu recycle fuel in a SPERT power transient, 25:5996
Measuring plutonium homogeneity in fast reactor fuels, 25:4875
Plutonium homogeneity in thermal recycle fuels, 25:4874
Thermal conductivity of physically mixed $(U_{0.8}Pu_{0.2})O/sub 2-x/$, 25:4862
EVENS, Ronald G., Clinical use of an in-vivo measurement of bone mineral content, 25:4625 (CONF-680211-, pp 296-308)
EVERETT, M. R., Dimensional changes of graphite specimens irradiated in dragon fuel element 700. project dragon, 25:4884 (DP-Report-556(Pt.1))
Dimensional changes of graphite specimens irradiated in Dragon fuel element. II, 25:4885 (DP-Report-556(Pt.2))
EZELL, C. R., $\pi^+p \to f^0 \Delta^{++}$ at 13.1 GeV/c, 25:5283 (COO-1428-238)
EZERSKA, K., Gas phase radiolysis of hydrogen sulfide and propane under the influence of the particles formed in the reaction $^{10}B(n,\alpha)^7Li$, 25:4115

F

FAESSLER, Amand, Alpha clusters in Hartree--Fock calculations, 25:5586
Angular-momentum-projected Hartree--Fock theory, 25:5815
Bahcall corrections to electron capture and the Hartree--Fock rearrangement, 25:5837
FAHR, H. J., Impact ionization by neutral interplanetary particles, 25:5021
FALICOV, L. M., Galvanomagnetic properties of a single-crystal sphere by the induced-torque method. II. Magnetic breakdown in cadmium and zinc, 25:5192
FALK, W. R., Energy levels of ^{19}Ne, 25:5587
FAL'KO, Igor I., Energy spectrum of superconductors with overlapping bands, 25:5041
FALKSON, Geoffrey, Radiosensitization by procarbazine in the treatment of malignant mesothelioma, 25:4685
FALKSON, H. C., Radiosensitization by procarbazine in the treatment of malignant mesothelioma, 25:4685
FALL, Daniel J., Ashing technique as a more precise method for the radioassay of ^{51}Cr in feces, 25:4032
FAN, D. N., Viscous tails in MHD, 25:5121 (AD-709878)
FARMAKES, Ruth, Conference of the American Nuclear Society, Washington, D. C., 11/70, 25:6192
FARR, W. M., High-frequency flutelike instabilities in multicomponent plasmas, 25:5110
FARVOLDEN, S., Anomalous helium production in nickel, 25:4821
Helium accumulating dosimeters for high neutron fluences and long irradiation periods, 25:4381
Helium production in Fe, Cr, Ni, Ti, and Cu due to fission neutron part of reactor spectra, 25:4822
New boron analysis method, 25:4037
FAUGERAS, P., Processing of irradiated mixed plutonium and uranium oxides, 25:4134 (AEC-tr-7198)
FAUSKE, H. K., Coolant voiding and pressure generation due to boiling, fission gas release, and molten fuel-coolant interaction, 25:6073
FAUSKE, Hans K., Liquid film thickness for slug expulsion, 25:6067
FAVART, D., Depolarization of negative muons in low-Z

muonic atoms, 25:5576
FAVIER, J., Giant-resonance excitation by radiative capture of π^- in ^{16}O, 25:5600
FEDERSEL, H., Unified nuclear reaction theory, 25:5870
FEDIN, E. I., Effect of substituents on hydrogen exchange reaction of some ferrocene derivatives, 25:4069
FEDOROV, G. V., Hall effect in terbium single crystals, 25:5177
FEDOSEEV, G. A., Production of ^{18}F fragments from Si, 25:5663
FEDOSEEV, I. A., Unitary representations of the conformal group, 25:5393 (IFVE-STF-69-85)
FEINBERG, E. L., Extensive air showers (theory), 25:4986
FEINSTEIN, L., K+p elastic scattering at 4.6 GeV/c, 25:5296
FEL'DMAN, I. I., Space--energy and time distribution of neutrons in boron-containing media, 25:4159
FELDMAN, M. J., Interim examination of EBR-II experimental irradiations at Fuels and Examination Facility, 25:4301
FELDSCHREIBER, P., Repair of DNA and the mode of action of sensitizers and protectors in biological systems of different complexity, 25:4536
FENDELL, F. E., Electrostatic probe in a reacting gas, 25:5084
FENIN, Yu. I., Lower bounds for the scattering parameters, 25:5425 (JINR-P4-5332)
FENSTERMACHER, Charles A., High Reynolds number, low temperature, noble gas adsorption bed design, 25:6142
FENYVES, E., Di-pion in mass values region M($\pi^0\pi^0$) less than or equal to 1.3 GeV, 25:5284 (JINR-E1-5085)
FERG, D. A., Multivariable feedback synthesis with cross-coupling for a thermionic reactor model, 25:6163
FERGUSON, E. E., Ion chemistry of D region, 25:5013
FERON, Jacques-Louis, Magnetic properties of R_3M compounds of rare earth and transition metals, 25:5199
Magnetocrystalline properties of single crystals of rare earths of the second series, 25:5194
FERRARO, John R., Metal isotope and high pressure effects on the infrared active skeletal vibrations in metal sandwich compounds, 25:4067
FERRELL, E. F., Characteristics of electrowon and of hydrogen-reduced molybdenum powder and sheet, 25:4740 (EM-RI-7455)
FERRI, G. G., Comparative study of the changes in the elimination of 17-ketosteroids in male rats after surgical and radiation-induced castration and histologic study of the testes irradiated with scalar doses, 25:4707
FERSCH, K. E., Availability and cost of ^{10}B for reactor control, 25:5975
FETKOVICH, J. G., Measurement of K^- cascade time in liquid He, 25:5254
FEYGUIN, F. Z., Magnetosphere parameters based on Pc-1 type micropulsations, 25:5027
FEYNBERG, S. M., Atomic power plants, 25:5878 (UCRL-Trans-10495)
FICHARDT, T., Radiosensitization by procarbazine in the treatment of malignant mesothelioma, 25:4689
FICK, D., Measurement of polarization of ^6Li ions, 25:5569
FICKEN, V., /sup 99m/Tc brain scanning in Herpes virus type I encephalitis, 25:4660
FIDEL'SKAYA, R. P., Study of the processes of redistribution of phase density in intense proton beams extracted from a duo-plasmatron type ion source, 25:5458 (NP-18510)
FIELD, John H., Fast reactor fuel failure thresholds and mechanisms, 25:6018
FIELDEN, E. M., Effect of 5-bromouracil incorporation on energy transfer in irradiated DNA, 25:4542
FIELDEN, E. Martin, Pulse radiolysis of selenium-containing radioprotectors. I, 25:4115
Radiation chemistry of selenium-containing protective agents, 25:4546
FIELDS, T., Serpukhov program, 25:5443 (CONF-700314-, Paper 1)
FILIPPOV, B. V., Evolution of charged particles from the point source in the field of magnetic dipole, 25:5004
FILIPPOV, N. V., Research on studying and increasing the plasma parameters on ''non-cylindrical Z-pinch'' equipment, 25:5116 (SC-T-70-4046)
FILIPPOVA, T. I., Research on studying and increasing the plasma parameters on ''non-cylindrical Z-pinch'' equipment, 25:5116 (SC-T-70-4046)
FILIPPOVICH, I. V., Biochemical mechanism of radioprotective action of aminothiols, 25:4592
FILOZOV, A. F., Polarization of secondary protons in pp + π^+pn and pp + π^0pp reactions at 665 MeV, 25:5268 (JINR-P1-5293)
FILSS, P., Photonuclear reactions in oxygen and their use for the control of energy and photon spectrum at electron accelerators, 25:5597
Reactions $^{12}C(\gamma,n)$, $^{12}C(\gamma,2n)$, $^{39}K(\gamma,n)$, and $^{40}Ca(\gamma,np)$ up to the meson threshold, 25:5578
FINCH, William C., Shielding Fort St. Vrain HTGR, 25:5888
FINCHAM, D. G., How good was the absorption model, 25:5381
FINE, Ben S., Burn injury after carbon dioxide laser irradiation, 25:4704
FINE, I. Y., High-energy calibration using ^{252}Cf neutron source, 25:4223
FINE, Samuel, Burn injury after carbon dioxide laser irradiation, 25:4704
FINK, Charles R., Radioisotope-fueled organic Rankine power system, 25:4225
FINK, R. W., Electron capture decay of ^{181}W, 25:5753
FINKEL, V. A., Crystal structure of Be at 77 to 300° K, 25:4795
FINKLER, P., Relation between hard-core and velocity-dependent potentials, 25:5867
FIRK, F. W. K., Isospin splitting of giant dipole state in ^{26}Mg, 25:5671
FIRST, Melvin W., Contamination control of sodium fires from liquid-metal-cooled reactors, 25:6045
FISCELLA, John M., (U,Pu)C as alternate reload fuel for LMFBR's, 25:6023
FISCHER, C. O., Cold neutron scattering at CH_2-, CH_3-, and OH-protons in methanol and ethanol, 25:5500
FISH, R. L., Burst tests of EBR-II irradiated fuel pin sections, 25:5950
FISHMAN, S. G., Diffusivity and isotope-effect measurements in equiatomic Fe--Co, 25:4761
FITTS, R. B., Fission gas release measurements from fast breeder $(U,Pu)O_2$ fuel, 25:6015
Thermal performance and restructuring of pellet and sphere-pac fuels, 25:5992
FITZER, E., Effect of hot-pressing on the structure of carbon artifacts, 25:4867
FLATAU, Carl R., Can mankind benefit from man extension systems, 25:4200
FLEMING, Donald G., Reactions (p,t) on even Sn isotopes, 25:5799
FLEROV, G. N., Synthesis and search of heavy transuranic elements, 25:5719
Synthesis of element 105, 25:5757
FLIESSBACH, Torsten, Nuclear-density distribution for nucleus--nucleus scattering, 25:5835
FLORSCHUETZ, L. W., Sonic limitations and startup problems of heat pipes, 25:6236 (LA-4518)
FLYNN, P. W., High-temperature fast-flux irradiation experiment for mixed-oxide fuel rods, 25:5589 (GA-10264)
FODOR, Ilona, Analog resonance in $^{58}Ni(p,\gamma)^{59}Cu$ reaction, 25:5660
FOELL, W. K., Integral-transport-theory analysis of resonance absorption measurements in neutron beams, 25:5959
FOGELBERG, B., E2 and M1 transition probabilities in ^{193}Au and ^{195}Au, 25:5701
FOGLIZZO, R., Infrared and Raman spectra of pyrazinium halides, 25:4068
FOLOMESHKIN, V. N., Relative value of cross sections of NN + W + (Hadrons) and NN + (Hadrons) γ, γ + μ + μ reactions, 25:5266 (IFVE-SEF-69-81)
Search for W-boson in NN-collisions at IHEP accelerator, 25:5267 (IFVE-SEF/STF-69-46)
FOLTZ, J. V., Comparison of the substructures and properties of nickel, TD--Ni, Chromel-A, Inconel 600, and TD--NiCr following explosive-shock deformation, 25:4802
FONTAN, J., Mobility of radioactive ions, 25:4355
FONTANA, M. H., Core melt-through in LMFBR's, 25:6088
FONTANELLA, John, Accurate determination of dielectric constant by method of substitution, 25:6225 (COO-623-150)
Capacitive gage for accurate measurement of high pressures, 25:6230 (COO-623-155)
Low frequency dielectric constants of LiF, NaF, NaCl, NaBr, KCl, KBr by method of substitution, 25:6228 (COO-623-153)
Low frequency dielectric constants of alkaline earth fluorides by method of substitution, 25:6229 (COO-623-154)
FORD, W. D., Liquid film thickness for slug expulsion, 25:6067
FORD, William F., Systematic method of calculating reduced matrix elements of single-particle operators, 25:5808 (N-70-32786)
FORKER, M., Statistically perturbed angular correlations of ^{154}Gd and ^{156}Gd in different liquid sources, 25:5758
FORLAND, Marvin, Bone densitometry: clinical applications, 25:4626 (CONF-680211-, pp 308-19)
FORMAN, George W., Design and development of three-dimension interlocked, filament-wound composite, 25:6219 (BDX-613-143)
Design of joints for filament-wound cylinders, 25:6218 (BDX-613-142)
FORREST, J. R., Low frequency axisymmetric waves in a weakly ionized magnetoplasma column, 25:5123 (SU-IPR-366)
FORREST, M. J., Measurement of plasma parameters in Tokamak T3-A by Thomson scattering, 25:5079 (CLM-R-107)
FORSTER, R. A., Two-group transport criticality solutions and associated continuum expansion coefficient resonance behavior, 25:6157
FORTUNE, H. T., Evidence for J/sup π/ = 8^+ state in ^{16}O, 25:5592
Excitation functions from elastic ^{16}O scattering from nuclei with A approximately 16, 25:5566
FORYS, M., Gas phase radiolysis of hydrogen sulfide and propane under the influence of the particles formed in the reaction $^{10}B(n,\alpha)^7Li$, 25:4119
FOSTER, J. L., Sensitization of anoxic fern spores to x-rays by chemicals known to be effective in bacteria,

25:4573
FOUCHER, Roger, Magnetic quadrupolar γ transitions in atomic nuclei, 25:5792
FOULKE, L. R., Examination of errors introduced by the few-group diffusion theory approximation in space-dependent kinetics calculations, 25:6162
Improved spatial differencing for space--time and static movable material diffusion problems, 25:6177
FOUREZ, Gerard M., Broken SU(3) sum rules derived from the asymptotic SU(3) symmetry, 25:5355
FOWLER, G. N., Density of states of an electron in a fluctuating potential, 25:5240
FRAENKEL, Zeev, Neutron emission in alpha-particle-accompanied fission, 25:5723
FRANCE, P. W., Asymmetric NMR line shapes due to nuclear quadrupole and anisotropic shift interactions, 25:5222
FRANCILLON, G., Weak coupling in the ^{209}Bi 5⁻ x h/sub 9/2/ decuplet, 25:5745
FRANCO, Victor, Polarization in nucleon--deuteron scattering at medium energies, 25:5517 (LA-4465, pp 16.1-2)
FRANK, R., Significance of exchangeable ions in the formation of structure in thixotropic gels, 25:6247 (ORNL-tr-2395)
FRANKLIN, R. E., Importance of pulse-height analysis in the gamma-ray attenuation technique for measurement of soil moisture, 25:4158
FRANZGROTE, Ernest J., Alpha-scattering technique of chemical analysis, 25:4034
FRAZER, W. R., Multiperipheral dynamics, 25:5302 (CONF-700314-, Paper 11)
FREDERICK, S. F., Hydrogen induced sustained load crack growth in Ti--6Al--4V, 25:4762
FREEMAN, G. R., Kinetics of electron and ion reactions during the γ radiolysis of liquid neopentane, 25:4113
FREESTONE, R. M. Jr., Simultaneous fast-neutron spectral measurements by time-of-flight and pulse-height unfolding techniques, 25:4366
FRENKEL, R. B., Determination of 2e/h based on the ac Josephson effect, 25:5412
FRENZEL, W., Fissionable material balance and safeguards, 25:4266
FRESHLEY, M. D., Behavior of discrete PuO_2 particles in thermal recycle fuel, 25:5994
Plutonium and fission product migration in mixed-oxide fuels during irradiation, 25:6012
FREUND, H. U., Conversion coefficient of 14.4-keV transition in ^{57}Fe, 25:5652
FREY, Kenneth J., Induced variability in diploid and polyploid Avena, 25:4484
FRIEDLAENDER, E. M., High energy interactions below 1 TeV, 25:5273
FRIEDMAN, A. M., Curium-244 and ^{145}Sm--^{145}Pm x-ray sources, 25:4647 (CONF-700515-, pp 274-5)
FRIEDMAN, Neal, Computation of the equilibrium of a plasma with helical symmetry, 25:5106 (NYO-1480-161)
FRIEDMAN, Ronald J., Mineral content changes in the os calcis, ulna, and radius induced by prolonged bed rest, 25:4653 (CONF-700515-, pp 408-22)
FRIEDMAN, S., Porosity and anomalous recrystallization behavior in doped tungsten wire, 25:4799
FRIEDMAN, W., Plasma confinement in a high magnetic field toroidal quadrupole, 25:5070
FRIEDRICH, H., Alpha-particle model for light nuclei, 25:5855
FRIEDRICH, H. B., Longitudinal modes in hydrogen and deuterium halide crystals, 25:4065
FRIEDRICH, K., Determination of O, water, and N in refractory metals. V, 25:4022
FRITZ-NIGGLI, Hedi, Chemical sensitization of the damaging effects on embryos produced by low radiation doses: the role of energy metabolism and immediate repair, 25:4575
FROMMER, Peter L., Animal-implanted nuclear powered pacemakers, 25:4238
FU, C. Y., Neutron energy-dependent capture gamma-ray yields for ^{238}U and ^{181}Ta, 25:5777
FUCHS, W., Thermally stimulated conductivity and luminescence in KBr due to γ irradiation at 10°K, 25:5158
FUCHSSTEINER, B., Approximation of Green's functions, 25:5821
FUHRER, J., Radiosensitizing effect of Mitomycin C on haematopoietic colony forming cells, 25:4570
FUJIMAKI, Masao, Radiation chemistry of foods. IV, 25:4117
FUKAI, J., Explosive plasma instabilities, 25:5109
FUKUDA, Masasi, Studies on restorative effect of taurine in radiation injury and its clinical application, 25:4603
FUKUI, K., Charge determination of cosmic-ray tracks in polycarbonate plastic detectors, 25:4338
FUKUSHIMA, Naoshi, Spatial extent of the return current of the auroral-zone electrojet. II, 25:5003
FULBRIGHT, H. W., Reactions (p,t) on even Sn isotopes, 25:5799
FULFORD, P. J., Asymmetry effects on heat transfer and fluid flow in rod bundles, 25:4206
Periodic in situ annealing to reduce stainless-steel swelling in LMFBR, 25:4823
FUMELLI, M., Ion heating in a Penning discharge, 25:5075
FUNKE, L., Levels in ^{157}Tm, 25:5726
Non-adiabatic effects in rotational bands of odd proton nucleus ^{155}Tb, 25:5783
FUQUAY, J. J., Scavenging in perspective, 25:4162 (BNWL-SA-3450)
FURLAN, M., Effect of polycation on tumour cells in vivo, 25:4563
Methyl hydrazine radiosensitized Ehrlich ascites tumour cells, 25:4567
FURSA, A. D., Allowance for the wave function distortion under multipole analysis of fast nucleon scattering by nuclei, 25:5552 (ITF-70-50)
FURTH, H. P., Thermal equilibrium and stability of Tokamak discharges, 25:5117
FUTSUHARA, Yuzo, Breeding of a new rice variety Reimei by gamma-ray irradiation, 25:4487
FYKIN, L. E., Debye--Waller factor for W, 25:5170 (JINR-P14-5358)

G

GABATHULER, E., Vector meson production and omega--rho interference. Proceedings of the Daresbury Study Weekend No. 1, 12--14 June 1970, 25:5322 (DNPL/R-7)
GABATHULER, Erwin, Interference effects in high energy vector meson photoproduction, 25:5325 (DNPL/R-7, pp 115-38)
GABILLY, Yves, Method and apparatus for measuring apparent density by gamma radiation, 25:4764
GABRIEL, T. A., Photonucleon and photopion production from 400 MeV electrons in thick copper targets, 25:5255
GADDA, F., Corrosion rate of Zircaloy-2 in steam--water mixture under reactor radiations, 25:4737 (CISE-R-290)
GADDIS, H. R., Transmission electron microscopy of polycrystalline graphite, 25:4868
GAERTNER, R., Determination of the activity coefficients of uranyl perchlorate in aqueous solutions, 25:4086
GAERTTNER, E. R., Time-dependent neutron spectra measurements in water, 25:5489
GAFFNEY, George William, Current algebras and universal divergent radiative corrections, 25:5343
GAGE, Stephen J., Public resistance to nuclear reactor siting, 25:5940
GAIDOS, J. A., $\pi^+p \to f^0 \Delta^{++}$ at 13.1 GeV/c, 25:5283 (CCC-1428-238)
GAIDOVA, E. S., Morphological changes in the lungs and other organs in rats on intratracheal administration of thorium dioxide, 25:4702
GALIKINE, V., Influence of single irradiation and heat treatment on the properties of BeO, 25:4852
GALLAGHER, Francis X., Uranium--O system at high pressure, 25:4793
GALLI DE PARATESI, S., Reliability assessment of a novel liquid rod shut-down system, 25:6037 (RISO-214, pp 57-70)
GALLOWAY, J. J., Lagrangian approach to nonlinear wave interactions in a warm plasma, 25:5124 (SU-IPR-381)
GALVAGNI, R., General principles of a safety assessment through reliability analysis of ESSOR plant, 25:6054 (RISO-214, pp 597-625)
GALZENATI, E., Allowed spectrum in dual-resonance models, 25:5428
GAMBINO, R. J., Correlation of superconducting transition temperature with empirical pseudopotential, 25:5048
GAMMAGE, R. B., Research on stimulated exoelectron emission from lunar materials, 25:4935 (ORNL-TM-3131)
GAMMEL, J. L., Formalism for A(d,n)B or A(d,p)B polarization transfer reactions, 25:5603 (LA-4465, pp 20.1-2)
Quadratic relations between the T(d,n)^{4}He observables, 25:5519 (LA-4465, pp 22.1-2)
GANASSI, E. E., Vicia faba seedling chromosome damages by split dose, 25:4497
GANGULI, D., Reconnaissance of the system BeO--Al_2O_3--SiO_2--H_2O, 25:4871
GANT, Preston, On-line monitor of natural gas lines for ^{3}H and ^{85}Kr, 25:4352
GARBER, D. I., Gamma rays from thermal and resonance neutron capture in ^{121}Sb and ^{123}Sb, 25:5724
GARBER, Donald I., Angular distributions in neutron-induced reactions. I, 25:5549 (BNL-400(3rd Ed.)(Vol.1))
GARDINER, V., Comprehensive approach to computer arithmetic, 25:6238 (LA-4531)
GARDNER, C. O., Mutation studies involving quantitative traits, 25:4485
GAREEV, F. A., Equilibrium deformations of rare-earth and transuranium nuclei, 25:5860
Single-particle state of deformed nuclei in transuranium region of Saxon--Woods potential, 25:5684 (JINR-P4-5221)
GARNER, Francis Albert, Dependence of neutron radiation damage in metals on crystal lattice geometry, 25:4834
GARRARD, L. A., Effect of uranyl nitrate on sucrose production and storage in corn scutellum slices, 25:4720
GARSCADDEN, A., Time-resolved energy distributions in a striating discharge, 25:5077 (AD-710597)
GARSIDE, B. K., Analytical model of the recording process in neutron radiography, 25:4251
GARY, S. P., Electron heating by ion-wave turbulence, 25:5072
GASIDLO, J. M., Measurement and analysis of reactivity

Doppler effects in ZPR-3 Assembly 53, 25:6110
GASIOROWICZ, S., Field theoretic models for high energy processes, 25:5320 (CONF-700314-, Paper 17)
GATT, F. C., Flow of spheres in cylindrical vessels. II, 25:4182 (AAEC/E-207)
GAUR, B. K., Effect of deuterium oxide on gibberellic acid-induced α-amylase in germinating barley seeds, 25:4464
GAWLOWSKI, J., Radiolysis of ethylene in presence of hydrogen sulfide, 25:4122
GAZDA, I. William, Variations in coefficient of thermal expansion as a function of prestressing, 25:4852
GEE, William R. Jr., Effect on adjacent pins of swelling of a failed pin, 25:6017
GEGUZIN, Ya. E., Study of diffusion by tracks left by nuclear reaction products in a solid detector, 25:4845
GEHRINGER, C., M1 gamma transitions from isobaric analogue states, 25:5676
GEIGER, W. S., Criticality safety specialist's views [on implications of ANSI Criticality Safety Standard N16.1], 25:4286
GELL, M., Fractographic study of stage I fatigue cracking in a nickel-base superalloy single crystal, 25:4765
GENERALOVA, M. V., Translocations in Crepis capillaris after x irradiation, 25:4496
GENERALOVA, V. V., New method of determining absorbed doses of gamma radiation, 25:4520
GENNARI, C., Renal clearance of radiophosphate in thyroid disease, 25:4451
GENTHON, J. P., Elementary model of the macroscopic effects of neutron irradiation in graphite, 25:4880 (CEA-N-1374)
GERAME, H. V., Proton scattering to 3/2⁻ state of ^{207}Pb, 25:5780
GERBER, J., First two excited states of ^{159}Tb, 25:5727
GERSTL, Siegfried A. W., Some typical radiation streaming problems in sodium-cooled fast reactors, 25:5976
GERTKEN, Richard H., UBV photometric study of IQ Persei, 25:4902
GERTZMAN, H. S., First excited state of ^{148}Sm, 25:5703
GHIORSO, Albert, Alpha decay of ^{258}No and ^{257}No, 25:5704
GHIURGHI, L., Reliability assessment of a novel liquid rod shut-down system, 25:6037 (RISO-214, pp 57-70)
GHOTRA, J. S., Carboxylates of metals. I. Uranium(IV) carboxylates, 25:4057
GIACOMELLI, G., Exotic resonances in K⁻d interactions at 3 GeV/c, 25:5287
GIBALA, R., Prog. rpt. on dislocation-solute atom interactions in alloys, 10/70, 25:4786 (COO-1676-13)
GIBBS, Alan G., Orthogonality in finite slab geometry, 25:5140
GIBERSON, R. C., Gasification of graphite under HTGR operating and potential accident conditions, 25:5985
GIBSON, B. F., Trinucleon form factors calculated from realistic local potentials, 25:5833
GIEDD, Ronald E., Thermal conductivity of normal and superconducting indium--lead alloys, 25:5055
GIESELER, H., Reliability of emergency core cooling systems of light water nuclear power plants, 25:6038 (RISO-214, pp 91-126)
GIGNOUX, Damien, Magnetic properties of R_2M compounds of rare earth and transition metals, 25:5199
GIL, C., E2 effective charges of the f/sub 7/2/ proton and neutron, 25:5646
GILBERT, E. R., Irradiation creep by loop unfaulting, 25:4830
GILL, S., Review of the safety aspects of the design of prestressed concrete pressure vessels with reference to limit state design, 25:5981 (RISO-214, pp 289-300)
GILLESPIE, F. E., Fast fission chamber amplifier--discriminator system, 25:4333
GILLET, Vincent, Nature of nuclear wave functions, 25:5847
GILLETTE, J. L., Neutronic and thermal hydraulic analyses of mixed cores for EBR-II, 25:6031
GILLIAM, D. M., Counting of heavily etched fission fragment tracks in polycarbonate, 25:4342
GILLON, J.-J., Medical supervision of workers exposed to ionizing radiations, 25:4523
GILMARTIN, J. T., Environmental monitoring radiation levels at BNL, 25:4503 (BNL-50196)
GILSON, Albert J., Conference on pulmonary investigation with radionuclides, Miami, Fla., 3/69, 25:4662
Determination of ventilation, 25:4668
GINAVEN, R. O., Low-energy photofission of heavy elements: experimental results, 25:5768
Use of fission product gamma rays following photofission for nondestructive assays of nuclear materials, 25:4291
GINGERICH, Karl A., Electron impact cross sections for group-III metal atoms, 25:4956
GIOVENGO, J. F., In-pile dimensional changes of ThO_2--UO_2 fuel rods with non-free-standing cladding, 25:6197
GIRARD, J. P., Ion heating in a Penning discharge, 25:5075
GIRAUD, F., Pulmonary hemosiderosis in a 9-year old child with a trisomy 18, 25:4685
GIZON, J., Rotational bands of ^{171}Lu, 25:5699
GLAUDEMANS, P. W. M., Lifetime measurements in s-d shell nuclei. IV, 25:5628
GLENN, H. D., MARVEL experiment, 25:4177
GLIOZZI, G., Allowed spectrum in dual-resonance models, 25:5428
GLOTOV, V. I., Evaluation of energy spectra of neutrons generated in the earth, 25:4374
GOBIN, P., Application of internal friction to the study of graphitization, 25:4870
GOBLE, R. J., M3 isomeric transitions in ^{58}Co and ^{60}Co, 25:5608
GOEDDEL, W. V., HTGR fuel design and irradiation performance, 25:6003
GOEKE, K., Isomeric shift and magnetic hyperfine splitting of muonic atoms in the lead region, 25:5794
GOETZ, U., Four-particle--two-hole core excitation in heavy nuclei, 25:5737
GOKHBERG, M. B., Magnetosphere parameters based on Pc-1 type micropulsations, 25:5027
GOLAY, M. W., Fast-neutron spectrum and time moments of pulse decay in a bulk aluminum assembly, 25:6106
GOLD, S., Radionuclides in effluents from boiling water reactor, 25:6080
GOLD, Thomas, Pulsars and the origin of high energy particles, 25:4978
GOL'DANSKII, V. I., Radiation cross-linkage of polyisobutylene in presence of monomer additions, 25:4101
GOLDBERG, Alfred, Thermal cycling of maraging steel, 25:6254 (UCRL-72099)
GOLDBERG, Murray D., Angular distributions in neutron-induced reactions. I, 25:5549 (BNL-400(3rd Ed.)(Vol.1))
GOLDBERG, P., Downstream state of collisionless shock waves, 25:5099
GOLDEN, G. H., Consequences of extensive fuel meltdown in various EBR-II core configurations, 25:6082
Neutronic and thermal hydraulic analyses of mixed cores for EBR-II, 25:6031
GOLDFARB, L. J. B., Polarization effects in (d,p) stripping processes, 25:5828
GOLDMANN, A., Inelastic electron scattering from the region of the ^{16}O giant resonance, 25:5558
GOLDSCHMIDT, P., Considerations on the in-core fuel management during startup of a fast breeder reactor, 25:6054
Stochastic model for safeguards inspections, 25:4273
GOLDSMITH, Naomi F., Clinical trial of the ^{123}I isotope scanning device as a screening method for the early detection of osteoporosis, 25:4651 (CONF-700515-, pp 340-50)
GOLDSTEIN, H., Age and fast effect for fission and 14-MeV neutron sources in Be and BeO, 25:5496
GOLDSTEIN, M. B., Pressure generation and potential work energy during fuel-sodium thermal interaction, 25:6052
GOLDSTEIN, N. P., In-core detector for measuring power and breeding distributions in power breeders, 25:6044
GOLDSTEIN, Rubin, Analysis of accountability data in safeguards, 25:4274
GOLLAN, F., /sup 99m/Tc--technetium dioxide for liver scanning, 25:4413
GOLLIHER, K. G., Neutron radiography development progras for SNAP-8 fuel elements, 25:4252
GOLOVNIN, V. A., Determination of magnetic moment stimulated by ^{121}Sb state, 25:5720
GOLUBEV, V. P., Technique for measuring phase characteristics of an ion beam, 25:5457 (NP-18507)
GOMBAS, P., Relation of equation of statistical atomic models and Schroedinger equation, 25:4970
GOMBERG, Henry J., Possibilities of recovering copper from chalcopyrite by nuclear underground leaching in situ, 25:4176
GOMBOSI, E., Conference on cosmic rays, Budapest, 8--9/69, 25:4976
GONO, Yasuyuki, Low-lying states of ^{152}Gd, 25:5750
GONSER, John, Nondestructive gamma assay of plutonium-contaminated solid waste in drums, 25:4293
GONZALEZ, J. L., In-core detector for measuring power and breeding distributions in power breeders, 25:6044
GOOD, Myron L., Diffraction dissociation, 25:5386 (CONF-700314-, Paper 14)
GOODJOHN, A. J., Commercial power generation from HTGR nuclear steam systems, 25:5884
GOODMAN, Leonard S., In vivo measurement of the mineral content of a section of the radius, 25:4621 (CONF-680211-, pp 204-15)
GOODRICH, David George, Low-temperature deformation characteristics of high-purity zirconium single crystals, 25:4784
GOODRICH, Jack K., Imaging devices, 25:4325
Imaging devices: clinical attributes, 25:4326
Importance of reproducible lung scanning, 25:4674
Measurement of in vivo radioactivity, 25:4324
GOPAL-AYENGAR, A. R., Mechanism of radiosensitization by some sulphydryl poisons, 25:4552
GORBACHEV, V. M., Principal characteristics of isotopes of heavy elements, 25:5722
GORBATOV, A. M., Reconstruction of NN potentials from nuclear data, 25:5831
GORBENKO-GERMANOV, D. S., Effect of the participation of the acid in forming the hydrogen bond during electrophilic deuterio-exchange, 25:4073
GORBUNOV, V. I., Control of reinforced concrete construction by means of fast neutrons, 25:4249
GORDON, G. E., Decay schemes of /sup 127m/Te and /127g/Te, 25:5734
GORDON, R. L., Insulation resistivity measurements at high temperatures, 25:4401

XUM

Polarization effects in oxide insulators, 25:4400
GORICHEV, P. A., Program of connection of measuring microscopes PUOS with computer Minsk-2, 25:4369 (IFVE-SFK-68-53)
GORIN, Yu. P., Total and absorption cross sections of π^-, K^- and antip in the momentum range 20 to 65 GeV/c, 25:5295
GORLOV, G. V., Scattering of 4-MeV neutrons at angles close to 180°, 25:5762
GORTEN, Ralph J., Effect of capsule content variations on thyroid uptake results, 25:4661
GOSCHCHITSKII, B. N., Dependence of scattering transport length on neutron energy in H_2O, D_2O, and graphite, 25:5502
GOSSARD, A. C., High-pressure NMR study of metal--insulator transition of V_2O_3, 25:5224
GOTSIRIDZE, G. A., Effect of the bone marrow breakdown products on hemopoiesis, 25:4533
GOTTSCHALK, Bernard, Low pass filter, 25:4399
GOUDSMIT, P. F. A., Decay of ^{176}Re, ^{177}Re, and ^{176}Re, 25:5733
GOURDIN, M., Theoretical investigations about ω--rho mixing, 25:5324 (DNPL/R-7, pp 95-114)
GOURISSE, Daniel, Counter current extraction of neptunium by tributylphosphate solutions from aqueous nitric--nitrous acid solutions, 25:4135 (CEA-R-4097)
GOUTIER, R., Action of SH-containing radioprotectors on nucleic acid metabolism, 25:4596
GOVE, H. E., First excited state of ^{148}Sm, 25:5703
GOZANI, T., Isotopic source assay system for nuclear materials, 25:4038
Low-energy photofission of heavy elements: experimental results, 25:5768
Physics and nuclear material safeguards, 25:4290
GRABER, H. D., Lifetime measurements in s-d shell nuclei. IV, 25:5628
GRAHAM, Kingsley F., Pulsed moderator studies using a time-focused crystal spectrometer, 25:6186
Slow-neutron leakage time distributions of some small hydrogenous moderators, 25:6203
GRAHAM, L. W., Dimensional changes in graphite during high-temperature irradiation, 25:4683 (DP-Report-473)
Dimensional changes of graphite specimens irradiated in Dragon fuel element. II, 25:4685 (DP-Report-556(Pt.2))
GRAHAM, W. W., Neutron diffusion parameter determination using the pulsed neutron source techniques with spheres of heavy water, 25:5485
GRAIKOSKI, John T., Application of ionizing radiations to extension of refrigerated storage of freshwater perch, 25:4734 (TID-25467)
GRAMA, N., Classification of the spin--isospin functions of the identical-nucleon system, 25:5541
GRAMM, W. R., Nonstatistical shape of beta spectrum of ^{14}C, 25:5591
GRANQUIST, D. P., ^{235}U depletion as a potential independent cross-check of the plutonium content of spent power reactor fuels, 25:4257 (BNWL-SA-3304)
GRANT, G. A., Radiation protection by disulphides in tissue culture, 25:4560
GRAUL, E. H., Neutron microdosimetry for rabbit eye, 25:4521
GRAVES, J. N., Fission gas release from an HTGR-type fuel rod, 25:6009
GRAVES, N. J., BPLOT, multipurpose plotting routine for use with CALCOMP plotter, 25:6257 (WHAN-IR-38)
GRAY, D. E., Prog. rpt. on Nimrod operation and development, 4--6/70, 25:5465 (RHEL/R-206)
GRAY, D. M., Comparison of standard and modified orthogonalized plane-wave methods, 25:5231
GRAY, Lee John, Antiproton--neutron annihilation at rest into final states of 3 and 4 pions, 25:5271
GRAY, P. S., Differential concentration gas chromatograph for the analysis of low levels of impurities in He, 25:4012 (DP-Report-443)
GRAY, W., Coulometric determination of uranium with a platinum working electrode, 25:4025
GRAZIANI, G., Fuel cycles in High Temperature Reactors: approach towards thermal breeding on Th fuel cycle, 25:6051 (DP-Report-434)
GREEN, Joseph B. Jr., Plowshare explosive shielding, 25:4175
GREEN, L. L., Core excitation in ^{30}P, 25:5670
GREEN, L. O., Differential concentration gas chromatograph for the analysis of low levels of impurities in He, 25:4012 (DP-Report-443)
GREEN, Michael A., Simplified helium cryostats for superconducting dipoles and quadrupole magnets, 25:4189 (UCRL-19764)
GREEN, T. S., Spectrograph for the simultaneous measurement of velocity spectra and charge-to-mass ratios of ions, 25:4397
GREENBERG, A., Radioaerosol inhalation scanning, 25:4678
GREENE, M. Wayne, Core excitation in ^{30}P, 25:5670
GREENHUT, G., rho,ω photoproduction phase: possible breakdown in vector dominance, 25:5327
GREENSTEIN, Jesse L., Nature of BD + 17° 4708, 25:4906
GREENSTOCK, C. L., Electron transfer studies of nucleic acid derivatives in solutions containing radiosensitizers, 25:4540
GREENWOOD, R. C., Excited K/sup π/ = 0$^+$ bands in ^{172}Yb, 25:5744
GREGORY, E. H., Nuclear acoustic resonance in niobium metal, 25:5223
GREINER, W., Potentials for fast and slow heavy-ion-collisions within the two center shell model, 25:5641
GRENACS, L., Depolarization of negative muons in low-Z muonic atoms, 25:5576
GRESILLON, D., Ion distribution functions in collisionless surface ionized plasmas, 25:5098
GRETHER, D. F., Reggeized pion exchange, 25:5278
GRIEBENOW, M. L., NRTS--ATR 1.4-MW flow reversal test, 25:6119
GRIESS, J. C., Design considerations of reactor containment spray systems. Part V. Protective coatings tests, 25:6034 (ORNL-TM-2412(Pt.5))
GRILLI, M., Preliminary results with Adone, 25:5446 (DNPL/R-7, pp 215-43)
GRIMES, Sterling, Operating experience with Cardinal Plant Training Simulator, 25:6208
GRIMSON, J. H., Target handling system for 200-GeV proton accelerator, 25:5470
GRISHIN, V. G., Estimate of cross sections of reactions π^- + ^{12}C + ^{12}B + $m\pi^0$ (m = 1,2...) and π^- + ^{12}C + ^{12}N + π^- + π^- at 4 GeV/c, 25:5293
Interference of identical particles in the processes involving the resonances, 25:5350 (JINR-P1-5315)
GROCHULSKI, W., Isomeric cross-section ratios and total cross-sections for the ^{113}In(n,2n)/sup 112gm/In and ^{115}In(n,2n)/sup 114gm/In reactions, 25:5763
GROH, E. F., Plutonium and ^{238}U Doppler measurements in plutonium-fueled fast critical assembly, 25:6109
GROLMES, Michael A., Liquid film thickness for slug expulsion, 25:6067
GROSS, D. J., Construction of covariant and gauge invariant T* products, 25:5317
GROSS, David J., High-energy neutrino--nucleon scattering current algebra and partons, 25:5345
GROSS, E. E., Exchange resonance in ^{3}He + ^{3}He elastic scattering, 25:5536
GROSSE, E., Lifetime and magnetic moment of neutron hole state in ^{207}Pb, 25:5710
GROSSMAN, R. J., Viscous damping of pulsed reactor fuel elements, 25:6123
GRUBER, E. E., Recovery of lattice parameter and electrical resistivity in low-temperature neutron-irradiated copper, 25:5160
GRUEN, G. E., WHAM prediction of semiscale test results, 25:6061 (IN-1431)
GRUNDER, H., Polarization and cross-section measurements in p-^{3}He scattering from 20 to 40 MeV, 25:5526 (UCRL-19943)
GUARISE, G. B., Polymerization induced by gamma radiation of styrene under pressure, 25:4104
GUDZENKO, L. I., Amplification of vacuum-ultraviolet radiation in decaying dense helium plasma, 25:5090
GUERNET, Jacques, Electron probe microanalysis of highly radioactive materials, 25:4011 (CEA-N-1340)
GUEST, G. E., High-frequency flutelike instabilities in multicomponent plasmas, 25:5110
GUINN, Vincent P., Role and half-life in activation analysis, 25:4050
GUJRATHI, S. C., Decay of /sup 126m/Sb and the energy levels of ^{126}Te, 25:5693
GULDBAKKE, S., Photonuclear reactions in oxygen and their use for the control of energy and photon spectrum at electron accelerators, 25:5597
GUNDIAH, S., Studies on polyvinyl acetate solutions by means of radiation-induced crosslinking, 25:4094
GUNTHER, B., Emitter temperature dependence of lower mode current, 25:4752 (TEE-4125-4)
Performance reproducibility of cylindrical diodes with CVD fluoride tungsten--niobium electrodes, 25:4751 (TEE-4125-3)
GUPTA, D., Development of safeguards procedures for a reprocessing plant similar to the WAK type, 25:4263 (KFK-1102)
Diffusivity and isotope-effect measurements in equiatomic Fe--Co, 25:4761
GUPTA, P. C., Model for cell survival after irradiation, 25:4691
GUPTA, Y. M., Interactions (π^---p) in peripheral model, 25:5376
GURATZSCH, H., Reaction (d,α) on ^{13}C, 25:5559
GURIN, V. N., Partial separation of the variables for calculating the efficiency of a plate lattice, 25:5490
GUSEV, V. V., Dependence of scattering transport length on neutron energy in H_2O, D_2O, and graphite, 25:5502
GUSTAFSON, Lars, Regional cerebral blood flow in organic dementia with early onset, 25:4681
GUTBROD, H. H., Four-nucleon transfer reaction induced by ^{10}B on ^{12}C, 25:5588
GUY, R., Radiative pion absorption in medium and heavy nuclei, 25:5793
GUZEK, J. C., Evaluation of electrically tested NERVA reactor fuel elements, 25:6141
GWIN, R., Neutron fission and capture cross section measurements for ^{233}U, 25:5702
GWOZDZ, P. S., Simple ion source for implantation doping of semiconductors, 25:5165
GYLDEN, Nils, Contributions to the physics of high-energy density, 25:5239

H

HAACK, L. A., Production of boiling in the high flux isotope reactor for the purpose of investigating boiling detection methods, 25:6048
HAAS, T. W., Auger electron spectroscopy: metallurgical applications, 25:4798
HAASE, D. W., Xenon-128 production process development, 25:4129
HABERKANT, K., Lifetime and magnetic moment of neutron hole state in ^{207}Pb, 25:5710
HACKSTEIN, K. G., Preparation and performance of HTGR fuel in Germany, 25:6006
HADERMANN, J., Four-particle--two-hole core excitation in heavy nuclei, 25:5737
HAEFELE, W., Development of safeguards procedures for a reprocessing plant similar to the WAK type, 25:4263 (KFK-1102)
HAFF, P. K., Dynamic nuclear effects in pionic and kaonic atoms, 25:5866
HAFFNER, J. W., Spacecraft configuration and operational tradeoffs for nuclear power sources, 25:6138
HAGEBOE, E., Indium isotopes produced by high-energy fission, 25:5784
HAGEN, A., Development of safeguards procedures for a reprocessing plant similar to the WAK type, 25:4263 (KFK-1102)
HAGEN, M., Reaction ^{54}Fe(d,n)^{55}Co and level scheme of ^{55}Co, 25:5675
HAGER, R., Higher-order corrections to internal conversion, 25:5826
HAGIE, Laird T., Operating computerized safeguard and criticality system for plutonia and urania, 25:4295
HAGIWARA, Miyuki, Radiation induced chain reaction and its application to polymer chemistry, 25:4097
HAGMANN, D. B., Interim examination of EBR-II experimental irradiations at Fuels and Examination Facility, 25:4301
HAHN, Yukap, Single-particle formulation of electron--atom scatterings, 25:4966
HAI, Francis, Influence of an axial magnetic field on neutron production in a plasma focus discharge, 25:5113 (AD-710606)
HALBERT, E. C., Shell-model structure of ^{42}Ca through ^{50}Ca, 25:5611
HALBIG, J. K., Decay of /sup 85m/Kr, 25:5634
HALBRITTER, J., Change of eigenstate in a superconducting rf cavity due to a nonlinear response, 25:5063
HALE, G. M., Reactance matrix analysis of the d--^{3}He, p--^{3}He system at 10-MeV deuteron laboratory energy, 25:5509 (LA-4465, pp 2.1-2)
HALL, Douglas S., UBV photometric study of IQ Persei, 25:4902
HALLMAN, D., Concrete-polymer building blocks, 25:4859
HALPERN, I., Effective charge factor for the radiative capture of fast nucleons, 25:5839
HALPERN, S. E., /sup 99m/Tc brain scanning in Herpes virus type I encephalitis, 25:4660
HAMBLEN, David Gordon, Critical magnetic field curves of superconducting Mo and Cd above 0.03°K, 25:5057
HAMILTON, L. J., Prediction and measurement of acoustic wave propagation in two-phase media, 25:6079
Viscous damping of pulsed reactor fuel elements, 25:6123
HAMMER, David Andrew, High-current relativistic electron beam propagation, 25:5469
HAMMITT, F. G., Time-dependent nucleate boiling requirements for liquid sodium, 25:4210
HAMMOND, A. D., Transfer function investigations on first Dragon core, 25:5953 (DP-Report-445)
HANDLEY, G. R., Effect of water sprinklers on array criticality safety analyses, 25:4282
HANLEN, D. F., Modular concepts approach for individual training needs of reactor plant personnel, 25:6211
HANLEY, P. E., Sorption pumped ^{4}He II cryostat for sustaining temperatures below 1°K for long periods, 25:5065
HANSEN, U., Some physics aspects of a small once-through pebble-bed reactor, 25:5972
HANSON, C. L., Shielded neutron shipping cask, 25:4311
Trigger-actuated motion locks for master-slave manipulators, 25:4312
HANSON, G. H., NRTS--ATR 1.4-MW flow reversal test, 25:6119
HARBERT, John C., Spinal cord dosimetry in ^{131}I-IHSA cisternography, 25:4510
HARBOURNE, B. L., Postirradiation observations of sodium-bonded (U,Pu)C fuels, 25:4894
HARDY, K. A., In-beam Moessbauer spectroscopy, 25:5467
HARE, G. E., MAPLE IB: ^{60}Co-fueled thermoelectric generator, 25:4226
HARKER, Y. D., Measurements of fast-neutron capture integrals in CFRMF, 25:5656
HARMISON, L. T., Design of a ^{238}Pu-powered implantable thermal engine for heart assist devices, 25:4232
Radioisotope-fueled Stirling engine artificial heart power system, 25:4233
Radioisotope-fueled vapor cycle power supply for an artificial heart, 25:4234
HARMON, D. P., HTGR fuel design and irradiation performance, 25:6003
HARMS, A. A., Analytical model of the recording process in neutron radiography, 25:4251
HARMS, Benjamin Carleton, Analysis of the reaction $\pi^+p \to \pi^+p\pi^+\pi^-$ at 11.0 GeV/c, 25:5292
HARMS, Edward Albert, Separable expansions of the two-body T-matrix and the three-body problem, 25:5432
HAROON, M. R., Neutron diffusion parameter determination using the pulsed neutron source techniques with spheres of heavy water, 25:5485
HARRIS, C. Craig, Imaging devices, 25:4325
Imaging devices: clinical attributes, 25:4326
Importance of reproducible lung scanning, 25:4674
Measurement of in vivo radioactivity, 25:4324
HARRIS, D. R., Collided flux diffusion theory, 25:6171
HARRIS, D. W., Gamma photon albedo distributions for finite media, 25:5146
Optimization of shields for protection of unmanned spacecraft scientific experiments, 25:5137
HARRIS, Dale W., Interplanetary spacecraft: RTG radiation analysis, 25:4247
HARRIS, E. G., Explosive plasma instabilities, 25:5109
HARRIS, L. Jr., Experimental test of pulse-height spectrum unfolding, 25:4365
HARRIS, R. J. Jr., Low-energy photon transport in liquid nitrogen, 25:5148
HARRIS, Richard Elgin, Transmission of far-infrared radiation through films of superconducting amorphous Bi and Ga, 25:5059
HARRIS, William H., Restraint device for scanning dogs, 25:4654 (CONF-700515-, pp 424-7)
HARRISON, Florence L., Some effects of nuclear detonations on aquatic ecosystems, 25:4479
HART, Gene D., In-flight coolant management considerations for NERVA reactor cooldown, 25:6132
HARTLEY, F. W., Summary of Connecticut Yankee Core I operational problems, 25:5910
HARVEY, I. K., Determination of 2e/h based on the ac Josephson effect, 25:5412
HASEGAWA, Akira, Chemical and hygienic studies on natural radioactive spa. IV, 25:4711
HASEGAWA, Masayoshi, Development of steels for nuclear power plant, 25:4770
HASEGAWA, Ryusuke, Model for amorphous antiferromagnets, 25:6224 (CALT-822-16)
HASTINGS, R. M., Neutron slowing down time kernel for graphite, 25:6160
HATTA, Osamu, Hot spring therapy of radiation injury. XXVI, 25:4610
HATTORI, S., Reliability aspects of safety evaluation of nuclear power plants, 25:5937 (RISC-214, pp 457-79)
HAUBENREICH, Paul N., Maintenance of Molten Salt Reactor Experiment, 25:6059
HAUG, Peter K., Odd-parity spectrum of ^{16}O and ^{40}Ca, 25:5570
HAUSSEN, W., Spectra and differential cross sections of 14 MeV neutron inelastic scattering from Fe, 25:5635
HAVERFIELD, A. J., Response of selected totally depleted and lithium-drifted silicon detectors to monoenergetic gamma and neutron radiation, 25:4356
HAVLIK, B., Radium-226 content of water and plankton from the Chalk River area, 25:4473 (AECL-3687)
HAVLIK, Borivoj, Radioactive pollution of rivers in Czechoslovakia, 25:4157
HAWTHORNE, J. Russell, Neutron irradiation embrittlement characteristics of A533-B electroslag weldments, 25:4833
HAYAKAWA, Hironobu, Silica gel as support for inorganic ion-exchangers for determination of ^{137}Cs in natural waters, 25:4033
HAYAKAWA, S., T = 9/2 analogue state in ^{63}Ni, 25:5605
HAYNES, R. H., Repair of alkylation and radiation damage in yeast, 25:4480
HAYWARD, Evans, Isospin of the ^{11}B giant resonance, 25:5554
HAZAMA, Kazuo, Adaptability of mutant in mulberry tree, 25:4486
HEACOCK, R. R., Micropulsation Pc-1 phase and polarization comparisons between College and Kotzebue, Alaska, 25:5005
HEDENGREN, D. C., Integral gamma-ray production cross-section measurements with Pu--Be neutron source, 25:5582
HEDGECOCK, P. D., Materials selected for Fort St. Vrain prestressed concrete reactor vessel, 25:5883
HEESTAND, G. M., Transient fields in ferromagnetic iron and gadolinium, 25:5189
HEFELE, H., Reaction (p,t) on ^{42}Ca, ^{44}Ca, and ^{48}Ca, 25:5677
HEFT, Robert E., Radionuclide distribution in particles produced by the Schooner Event, 25:4180
HEIDMANN, Jean, Diameter--luminosity relation and distance of the Virgo galaxy cluster, 25:4921
HEIN, Warren Walter, Decay of ^{95}Ru and ^{103}Tc, 25:5683 (IS-T-391)
HEINZ, W., Fissionable material balance and safeguards, 25:4266
HELLIWELL, William Stanley, Asymptotic behavior of the solution to a nonlinear system of integrodifferential equations occurring in reactor dynamics, 25:6180
HELPAP, B., Bile duct carcinomas after thorotrast, 25:4716
HENAULT, P. B., Progress in xenon tagging, 25:6025

XUM

Xenon tag proof test, 25:6026
HENDERSON, P., Neutron activation analysis for transition elements in rocks, 25:4047
HENDRICKS, Robert W., Program WEIGHT: FORTRAN IV program for evaluation of weighting functions used in small-angle x-ray scattering, 25:6246 (ORNL-TM-1950(Rev.1))
HENNINGER, R. J., Design of intermediate-energy neutron spectrometers and their calibration with photoneutrons, 25:4364
HENNINGS, U., System design of reactor charging equipment based on reliability considerations, 25:6039 (RISO-214, pp 213-46)
HENRY, A. F., New solution of the point kinetics equations, 25:6150
HENRY, Robert E., Gas detection with a choked converging-diverging nozzle, 25:6047
HENRY III, Leonard Francis, Studies of plastic deformation in the zinc--cadmium and copper--aluminum alloy systems, 25:4783
HENSLEY, G., Reliability prediction of mechanical instrumentation equipment for process control, 25:6189 (RISO-214, pp 11-20)
HERBIG, G. H., Spectroscopic astrophysics, 25:4913
HERDA, S., Photoproduction of $K^+\Lambda$ and $K^+\Sigma^0$ from H, 25:5253
HERMSDORF, D., Correction of the finite volume of scatterer effect on the measurement of differential elastic and inelastic neutron cross sections. I, 25:5504
HERNADI, F., Analysis of the radioprotective effect of cysteine on Escherichia coli strains, 25:4554
HERR, W., Redetermination of the ^{238}U decay constant by fission tracks in a U-stained Bohemian glass, 25:5767
HERRIOTT, Roger M., Genetic transformation in hemophilus influenzae, comprehensive report, 5/15/67--9/14/70, 25:6241 (NYO-1371-63)
HERRMANN, G., Safety and radiation protection, 25:4140
HERSCHMAN, Harvey R., Appearance of brain-specific antigen in developing rat brain, 25:4694 (UCLA-12-791)
HERSKIND, B., Transient fields in ferromagnetic iron and gadolinium, 25:5189
HERVE, Alain, EPR of a new boron center in neutron-irradiated BeO, 25:5162
HERZO, Dennis Paul, Comparison of the positive and negative tau prime partial decay rates for kaons, 25:5261
HEUCK, Friedrich, Quantitative measurements of bone mineral content by densitometric methods, 25:4622 (CONF-680211-, pp 216-49)
HEUSER, J., Autoradiography of labeled amino acids in giant squid synpase, 25:4418
HEUSGHEM, C., Radioprotectors and plasma enzymes, 25:4594
HEYN, Arno H. A., Photochemical precipitation of Th and Ce and their separation from other ions in aqueous solution, 25:4026
HICKS, J. A., In-beam Moessbauer spectroscopy, 25:5467
HIDALGO, John U., Computer techniques, 25:4393
Lung scans in spatial perspective, 25:4670
HIEBERT, J. C., Stripping to quasibound levels in ^{41}Sc, 25:5617
HILBERT, R. F., Role of grain boundaries in swelling of UN at 1600 to 1700°C, 25:4826
HILDEBRAND, J. F., Materials selected for Fort St. Vrain prestressed concrete reactor vessel, 25:5883
HILDENBRAND, K. D., Four-nucleon transfer reaction induced by ^{10}B on ^{12}C, 25:5588
HILL, A. J. Jr., Fire prevention and protection in hot cells, 25:4193
HILL, C. W., Space radiation hazards to Project Skylab photographic film, 25:4405 (N-70-32671)
HILL, D. J., Comparison of experimentally measured and calculated heating rates internal to PAX R-1 reactor, 25:6126
HILL, H. H., Kondo effect in LaPu and PrPu alloys, 25:5227
HILL, R. W., GIRLS: general indexing in reciprocal lattice space, 25:6240 (NLCO-1066)
HILLE, M., Precision-measurement of $^{27}Al(n,\alpha)$ cross section for 14.43-MeV neutrons, 25:5641
HILLIG, D. R., Neutron radiography development program for SNAP-8 fuel elements, 25:4252
HILLS, Jack Gilbert, Origin and dynamical evolution of the solar system, 25:4921
HINES, D. P., Mechanical model of thermal differential expansion at first startup of a mixed-oxide fuel pin, 25:6000
Transfer of coolant between adjacent subchannels in wire wrap and grid spacer rod bundles, 25:6028
HINKLEY, D. E., Study of the components of the exposure in cylindrical structures, 25:4256
HINRICHS, R. A., Anomalous L = 1 shapes of angular distributions for (^3He,t) transitions to 0^+ antianalog states in ^{64} ^{66}Ga and ^{40}K, 25:5654
HINTEREGGER, H. E., Extreme ultraviolet solar spectrum and its variation during a solar cycle, 25:4925
HINZ, R. F., High-temperature fast-flux irradiation experiment for mixed-oxide fuel rods, 25:5985 (GA-10264)
HIRATA, M., Hindrance of M1 transition from analog state to antianalog state and charge exchange spin-flip collective mode, 25:5658
HIRONS, Thomas J., Accuracy of space-collapse for fast breeder fuel cycle analysis, 25:5965
HIRSCH, P. R., Argon atmosphere filter system in HFEF hot cell, 25:4197
HIRSCHKOFF, E. C., Magnetization of dilute Cu--Mn alloys at very low temperatures, 25:6256 (UCSD-34-P-143-33)
HOCHREITER, L. E., Velocity profile and pressure drop measurements in fully developed mercury pipe flow, 25:4207
HOEHN, J., Correction of the finite volume of scatterer effect on the measurement of differential elastic and inelastic neutron cross sections. I, 25:5504
HOEKSTRA, Henry R., Uranium--O system at high pressure, 25:4793
HOEL, L. A., Magnetic properties of gadolinium ortho-vanadate, 25:5217
HOFFMAN, Morton Z., Photochemical precipitation of Th and Ce and their separation from other ions in aqueous solution, 25:4026
HOFFMAN, R. W., UHV Moessbauer emission of thin iron films, 25:6231 (COO-623-164)
HOFFMANN, G., Problems of radiation dosimetry in endolymphatic therapy, 25:4512
HOHL, Frank, Dynamical evolution of disk galaxies, 25:4929 (N-70-33057)
HOHMUTH, K., Levels in ^{167}Tm, 25:5726
HOLDEN, T. M., Exchange and crystal-field interactions in Er and Ho, 25:5214
HOLMES, J. J., Burst tests of EBR-II irradiated fuel pin sections, 25:5950
EBR-II irradiation effect of rupture of Type 316 stainless steel, 25:5948
Effect of cold work on irradiation-induced swelling, 25:4824
Irradiation creep by loop unfaulting, 25:4830
System for predicting postirradiation tensile properties, 25:4831
HOLMGREN, A., Isotopic exchange reaction between ammonium bromide and butyl bromide, 25:4071
Radioelectrochemical determination of microgram iodide, 25:4027
HOLT, P. D., Nuclear accident dosimetry systems, 25:4377 (AERE-R-6498)
HOLTZ, Robert E., Further study of the pressure-temperature history model of liquid-metal boiling inception, 25:4212
HOLZER, Fred, Plowshare and the environment, 25:4171
HOMAN, F. J., Fuel-cladding mechanical interaction during startup, 25:6002
Nuclear and economic performance of Nb and Mo in LMFBR cores, 25:6055
HOMMA, S., Present status of postirradiation examination facility, 25:4298
HONECK, H. C., Alphameric displays in nuclear reactor computations, 25:6202
HONG, Chang Gi D., Liver scan using /sup 113m/ In colloid, 25:4687
Preparation of /sup 113m/In colloid as scanning agent and its organ distribution in rats, 25:4437
HONG, William Jong-jau, Studies of recrystallization in dilute alloys of magnesium, 25:4808
HOOPER, H. O., Asymmetric NMR line shapes due to nuclear quadrupole and anisotropic shift interactions, 25:5222
HOOT, C. G., Epithermal-neutron capture gamma rays from shield materials: depleted uranium, 25:5776
High-resolution $(n,x\gamma)$ cross-section measurements using Linac, 25:5657
HOOTON, B. W., Heavy ion nuclear physics, 25:5817
HOPKE, Philip Karl, Studies of selected neutron-deficient isotopes, 25:5748
HOPKINS, H., Accommodation of radiation swelling in GCFR, 25:6020
HOPKINS, J. C., Phase shifts from n--^{4}He elastic scattering experiments near 20 MeV, 25:5508 (LA-4465, pp 1.1-2)
Polarization of 22-MeV neutrons elastically scattered from liquid tritium and deuterium, 25:5516 (LA-4465, pp 15.1-2)
HOPKINSON, J. F. L., Normalization of anti pp + 4π using dual six-point function, 25:5362
HORACEK, K., Kinetics of electron and ion reactions during the γ radiolysis of liquid neopentane, 25:4113
HORN, G. R., Fuel-clad gap conductance in fast reactor oxide fuels, 25:5999
HORSMAN, A., Internal relationships between skeletal parameters in twenty-three male skeletons, 25:4652 (CONF-700515-, pp 365-82)
HOSEA, J. C., Mapping a toroidal magnetic field, 25:5074
HOSHINO, Takao, Bromouridine (BUdR) as a radiosensitizing agent of malignant brain tumours, 25:4688
HOSKINS, R. E., Power systems optimization approach to nuclear fuel management, 25:5897
HOUSTON, M. D., Compressive creep of UO_2--22 percent PuC_2, 25:4861
HOWARD, A. J., Reactions $^{20}Ne(d,p)^{21}Ne$ and $^{22}Ne(d,p)^{23}Ne$, 25:5618
HOWARD, Alma, Dose-modifying factors and inhibitors of repair, 25:4574
HOWARD, Edgar, Radioisotope-induced, negative surface charge for thrombus resistance, 25:4434
HOWARD, James Edward, Nonadiabatic particle motion in linear and toroidal multipole fields, 25:5091
HOWES, B. W., Measurements of fast-neutron capture integrals in CFRMF, 25:5656
HOWES, R. H., Moessbauer measurements of quadrupole-moment ratios of first excited 2^+ states of ^{176} ^{178} ^{180}Hf, 25:5668

HOYNACKI, J. J., Availability and cost of ^{10}B for reactor control, 25:5975
HOYOS, Jorge Meneses, Biological effects of ionizing radiation and means of protection against it, 25:4524
HRUBESH, Lawrence W., Free-radical microwave rotational spectroscopy with a resonant cavity, 25:6253 (UCRL-50890)
HRUBY, J., Production of carrier-free radiostrontium ^{85}Sr, 25:4126 (UJV-2431-Ch)
HSIAO, K. H., Fracture of solidifying particles, 25:6083
HSIEH, S. T., Photodisintegration of ^{15}N, 25:5595
HUANG, R., Gamma photon albedo distributions for finite media, 25:5146
HUBY, R., Faithful and pseudo-bound theories for stripping to unbound levels, 25:5869
Method of pseudo-bound states for stripping to unbound levels, 25:5666
HUCKINS, Claire, Technique for radioautography of germ cells, 25:4421
HUCKLE, J., Radiosensitization of bacterial and mammalian cells with carbonyl compounds and ketoaldehydes with special reference to the properties of phenylglyoxal, 25:4557
HUEBENER, R. P., Current-pulse effect in the intermediate state of superconducting lead films, 25:5053
HUEBNER, Walter F., Proposal for the detection of mother molecules in comets by their microwave lines, 25:4915 (LA-4542)
HUEBOTTER, P. R., Cold-wrapper tube approach for accommodating steel swelling in LMFBR's, 25:6022
Periodic in situ annealing to reduce stainless-steel swelling in LMFBR, 25:4823
HUEFNER, Joerg, Lane equations for isobaric resonances, 25:5818
HUELLER, J., Applicability of anion exchange with mixtures of nitric acid and methanol for the separation of rare earths, 25:4139
HUERTAS, M. L., Mobility of radioactive ions, 25:4395
HUETTERMANN, Juergen, Electron spin resonance studies of free radicals formed from crotic acid, 25:4093
HUFFMAN, F. N., Radioisotope-fueled vapor cycle power supply for an artificial heart, 25:4234
Studies on dogs with implanted ^{238}Pu sources, 25:4432
HUFNER, S., First-order transition in europium metal, 25:5203
HUG, Gerard, Magnetocrystalline properties of single crystals of rare earths of the second series, 25:5194
HUGHES, T. G., Reprocessing of oxide fuel at Windscale, 25:4146
HUI, E. H., Integral gamma-ray production cross-section measurements with Pu--Be neutron source, 25:5582
HUIZENGA, J. R., Reactions $^{232}Th(d,t)^{231}Th$ and $^{238}U(d,t)^{237}U$, 25:5797
HUIZENGA, John R., Near-barrier fission induced with photons and neutrons, 25:5850
HULL, A. P., Environmental monitoring radiation levels at BNL, 25:4503 (BNL-50196)
HULL, L. J., Materials selected for Fort St. Vrain prestressed concrete reactor vessel, 25:5883
HUMMEL, J. P., Photonuclear reactions above the giant resonance, 25:5679
HUMPHREYS, Roberta M., Near-infrared spectrum of VY Canis Majoris, 25:4908
Recent spectrogram of AG Carinae, 25:4909
HUMPHREYS, T. E., Effect of uranyl nitrate on sucrose production and storage in corn scutellum slices, 25:4720
HUNDHAUSEN, A. J., Solar wind properties and the state of the magnetosphere, 25:5024
HUNT, D. C., Criticality calculations and measurements on enriched uranium metal-solution combinations, 25:6100
HUNT, John P., Water exchange kinetics in labile aquo and substituted aquo transition metal ions by means of ^{17}O NMR studies, 25:6248 (RLO-2221-T-4-3)
HUNZINGER, W., Safety and radiation protection, 25:4140
HURSEN, Thomas F., Animal-implanted nuclear powered pacemakers, 25:4238
HUSAIN, A., Non-mesonic decay of hypernuclei produced by K-mesons of 3.0 GeV/c momentum, 25:5277
HUSSEIN, H. M., Optical model analysis for elastic deuteron scattering on light nuclei, 25:5579
HUSTER, E., Bahcall corrections to electron capture and the Hartree--Fock rearrangement, 25:5837
HVELPLUND, P., Transient fields in ferromagnetic iron and gadolinium, 25:5189
HWANG, C. F., Proposed 0.4 K polarized proton target cryostat for LAMPF, 25:5456 (LA-4465, pp 33.1-2)
HWANG, Jenn-lin, Nuclear charge distribution and Born approximation for high-energy electron scattering, 25:5651

I

ICHIKAWA, Ryushi, Problems of marine disposal of radioactive waste, 25:4316
IINUMA, T. A., Optimal data processing radioisotope imaging, 25:4359
IKEBUCHI, Hidaharu, Chemical and hygienic studies on natural radioactive spa. IV, 25:4711
IKEUYE, D. T., Fabrication of non-fuel core components for SEFOR, 25:5943 (GEAP-13595)
ILIFFE, C. E., Computerized model of the nuclear sector of an electricity generating system, 25:5858
ILLING, R. G., Prog. rpt. on aerospace nuclear safety, 7--9/70, 25:4216 (SC-PR-70-682)
INGLE, R. W., Fast fission chamber amplifier--discriminator system, 25:4333
Measurement of capture cross section of ^{238}U, 25:5771
INGVAR, David H., Regional cerebral blood flow in organic dementia with early onset, 25:4681
INOUE, Yoriteru, Disposal of radioactive waste into ground, 25:4315
IONKINA, E. M., Properties of the chromium--nickel alloys containing niobium and molybdenum, 25:4782
IRIZARRY, H., Effect of gamma radiation dosages on rooting of pineapple crown sections, shoot emergence, and growth, 25:4719
IRKAEV, S. M., Determination of magnetic moment stimulated by ^{121}Sb state, 25:5720
IRVING, D. C., LEGCK, a subroutine to analyze Legendre coefficients for negativity in the angular distribution, 25:5476 (ORNL-TM-2503)
ISAEV, A., Possible properties of weak six-fermion interaction, 25:5344
ISAWA, T., Radioaerosol inhalation scanning, 25:4678
ISHIGURE, Kenkichi, Nuclear magnetic resonance of tetrafluoroethylene--isobutylene copolymers obtained by γ-ray irradiation, 25:4102
ISHIHARA, M., E2 effective charges of the f/sub 7/2/ proton and neutron, 25:5646
ISHIHARA, Takehiko, Recent trend in radioactive waste management in Japan, 25:4317
ISHIKAWA, Masashi, Construction and operation of (ATR) component test loop, 25:4192
ISLAM, A. K. M. A., Non-mesonic decay of hypernuclei produced by K-mesons of 3.0 GeV/c momentum, 25:5277
ITO, H., Present status of postirradiation examination facility, 25:4298
ITO, Yoshio, Mechanical sodium pump for liquid metal cooled fast breeder reactor, 25:4201
ITOH, K., Excitation of the giant resonance in ^{12}C by inelastic electron scattering, 25:5572
ITZCHAK, Y., Double contrast examination of small intestine, 25:4686
IVANENKO, I. P., Extensive air showers (theory), 25:4986
IVANOV, V. D., Research on studying and increasing the plasma parameters on ''non-cylindrical Z-pinch'' equipment, 25:5116 (SC-T-70-4046)
IVANOVA, S. P., Equilibrium deformations of rare-earth and transuranium nuclei, 25:5860
Single-particle state of deformed nuclei in transuranium region of Saxon--Woods potential, 25:5684 (JINR-P4-5221)
IVANOV-KHOLODNYI, G. S., Upper atmospheric ionization due to photoionization and collision of charged particles, 25:5015
IVERSON, H. G., Characteristics of electrowon and of hydrogen-reduced molybdenum powder and sheet, 25:4740 (BM-RI-7455)
IVLEV, A. A., Isotopic exchange laws. VII, 25:4072
IWAI, Tadashi, Production of polyacetal resin by radiation polymerization, 25:4098
IWASAKI, Shin, Reaction (^3He,α) on ^7Li from 5.0 to 8.0 MeV, 25:5571
IZRAILEV, F. M., Numerical experiments with a nonlinear chain, 25:6234 (LA-4440-TR)

J

JACKEL, D., Graphic display terminal for nuclear experiments with on-line computer. I, 25:4390 (HMI-B-100)
JACKIW, R., Construction of covariant and gauge invariant T* products, 25:5317
JACKSON, D. F., Nuclear reactions, 25:5842
JACKSON, John P., Classification of critical characteristics in nuclear plant design, 25:6051
JACKSON, R. J., Correlation of predictions and observations in mixed-oxide fuel, 25:6001
JACOBI, K. W., Neutron microdosimetry for rabbit eye, 25:4521
JACOBS, A. E., Theory of isolated vortex in pure superconductor near T = T/sub c/, 25:5051
JACOBS, D. G., Dissolution of calcium--strontium carbonate and its subsequent movement in the ground, 25:4265 (ORNL-TM-3130)
Radiological considerations in the use of natural gas from nuclearly stimulated wells, 25:4525 (ORNL-TM-3216)
JACOBS, E., Decay of ^{143}Sm to levels in ^{143}Pm, 25:5657
Excited states of ^{175}Yb from decay of ^{175}Tm, 25:5747
JACOBS, I. M., Demonstration of performance and reliability of General Electric Co. Boiling Water Reactor main steamline isolation valves, 25:6040 (RISO-214, pp 247-53)
JACOBS, W. R., Angular and wavelength dependence of thermal radiation transmitted through refractory aerosols, 25:6134
JACOBSON, Bertil, Bone salt determination by x-ray spectrophotometry, 25:4642 (CONF-700515-, pp 237-42)
JACQUINOT, J., Determination of the pressure anisotropy in

XUM

a mirror-confined plasma, 25:5085
JAIN, S. C., Charge form factor of ^{4}He with a tensor velocity-dependent potential, 25:5529
JALALI-MOSSALLAM, Ebrahim, Design study of nuclear-powered agro-industrial complex in Iran, 25:6143
JAMES, Dean B., Nondestructive gamma assay of plutonium-contaminated solid waste in drums, 25:4293
JAMES, W. J., Magnetic properties of Ho_6Fe_{23} and $HoFe_2$, 25:5211
JANDACEK, R. J., Structure-function studies of the aminothiol radioprotectants, 25:4548
JANETZKI, U., Reaction $^{54}Fe(d,n)^{55}Co$ and level scheme of ^{55}Co, 25:5675
JANKUS, V. Z., LIFE-I, history-dependent analysis of fast reactor fuel element behavior, 25:6032
JARED, R. C., Excited state in even--even fission products, 25:5687 (UCRL-19949)
JARKA, R. E., Distribution of gamma energy deposition in a fast reactor, 25:5970
Importance of discrete-ordinate ray effects in fast reactor design studies, 25:6159
JARMIE, Nelson, Scattering of polarized protons by tritons at 13.6 MeV, 25:5521 (LA-4465, pp 28.1-2)
JAROSCH, J. F., Mockup of remotely operated, high-purity, inert-atmosphere sodium analysis facility, 25:4310
JARVIS, J. P., Design and installation of TURF californium facility, 25:4304
Transfer of californium sources by pneumatic rabbit, 25:4305
JEANPIERRE, G., Manufacture of metallic uranium nuclear fuels: some industrial and economic aspects, 25:4743
JEANTET, E., Remote handling in operation of the installation ATTILA, 25:4261 (CEA-R-4067)
JEFFRIES, C. D., Prog. rpt. on dynamic nuclear polarization and solid state physics, annual, 7/15/69--6/1/70, 25:5150 (UCB-34-P-20-PR-16)
JELATIS, D. G., Where do we go from here with master-slave manipulators, 25:4313
JENEFSKY, R., Giant-resonance excitation by radiative capture of π^- in ^{16}O, 25:5600
JENKINS, D. A., Electric quadrupole transitions in muonic ^{208}Pb, 25:4953
JENKINS, V. K., Effects of estradiol on splenic repopulation in irradiated mice, 25:4471
JENSEN, J. C., Alphameric displays in nuclear reactor computations, 25:6202
JENSEN, J. D., Remote position measurement using laser optics, 25:6222 (BNWL-SA-3335)
JERRELL, M. E., Beta decay of ^{40}Cl and levels of ^{40}Ar, 25:5614
JESSEPH, J. E., Radiosensitivity of immune responses, 25:4470
JETT, J. H., Scattering of polarized protons by tritons at 13.6 MeV, 25:5521 (LA-4465, pp 28.1-2)
JNANANANDA, Swami, Decay schemes of ^{161}Tb and ^{103}Ru, 25:5714
Delayed coincidence spectrometer for lifetime studies, 25:4363
Radioactive decay of ^{199}Au, 25:5698
JOHN, H., Superheated steam filter. I, 25:5980 (KFK-1183)
JOHN, Joseph, Epithermal-neutron capture gamma rays from shield materials: depleted uranium, 25:5776
High-resolution (n,xγ) cross-section measurements using Linac, 25:5657
JOHNSEN, Edwin G., Low-cost teleoperators: a new industrial concept, 25:4198
JOHNSON, A. E., /sup 99m/Tc--technetium dioxide for liver scanning, 25:4413
JOHNSON, C. E., Radiative lifetime of metastable 2^1S_0 state of He, 25:4944
JOHNSON, Everett R., Energy transfer in alkali halide matrices, 25:4096
JOHNSON, Kenneth P., Remote maintenance during recovery from Enrico Fermi fuel melting incident, 25:5907
JOHNSON, L. V., Numerical construction of decay schemes, 25:5635
JOHNSON, R. L., Behavior of discrete PuO_2 particles in thermal recycle fuel, 25:5994
JOHNSON, R. T., Behavior of Pu recycle fuel in a SPERT power transient, 25:5996
Capabilities of PBF for LMFBR safety testing, 25:6102
Compressional cooling of ^3He to millidegree temperatures, 25:6255 (UCSD-34-P-143-27)
Principles and methods of dilution refrigeration. II, 25:5062 (UCSD-34-P-143-32)
JOHNSON, Raleigh F. Jr., Effect of capsule content variations on thyroid uptake results, 25:4661
JOHNSON, T. W., Sodium-vapor monitor, 25:6046
JOHNSON, W. T. K., Study of nuclear states of several odd-A nuclei 68 less than or equal to Z less than or equal to 75 through electromagnetic excitation from 2.3 to 3.6 MeV, 25:5637
JOHNSTON, A. R., Measuring ^{51}Cr in presence of ^{59}Fe, 25:4513
JOHNSTON, C. Conrad Jr., Measurement of bone mass in the radius, 25:4624 (CONF-680211-, pp 283-96)
JOHNSTON, James O., Clinical trial of the ^{125}I isotope scanning device as a screening method for the early detection of osteoporosis, 25:4651 (CONF-700515-, pp 340-50)
JOHNSTON, Kenneth, Light variation of EM Cephei, 25:4903
JOHNSTON, Phillip A., Applications of avalanche type semiconductor radiation detectors. Final Report, October 1968--November 1969, 25:4323 (NYO-4028-TA-1)
JOHNSTONE, I. P., Occupancy of spherical shells in the ground state of even 2s-1d shell nuclei, 25:5876
JONECKO, A., Regeneration of peripheral blood in thymectomized mice after sublethal whole-body irradiation, 25:4469
JONES, A. G., Neutron-deficient isotopes of polonium, 25:5696
JONES, C. R., Evolutionary trends in BWR primary system and containment designs, 25:5885
JONES, E. D., Praseodymium-141 and ^{169}Tm NMR in Van Vleck intermetallic paramagnets, 25:5226
JONES, G. D., Core excitation in ^{30}P, 25:5670
Excited states of ^{44}Ca, 25:5626
JONES, K. W., Lifetime of 5- 4585 keV ^{38}Ar level, 25:5664
JONES, Lawrence W., Cosmic ray experiments and prospects, 25:5245 (CONF-700314-, Paper 5)
JONES, T. D., Response of selected totally depleted and lithium-drifted silicon detectors to monoenergetic gamma and neutron radiation, 25:4356
JONES, W. B. G., Radioprotective effect of cysteine on lysozyme in dilute aqueous solution, 25:4544
JOOSSE, J., Gametogenesis and oviposition in Lymnaea stagnalis as influenced by γ-irradiation and hunger, 25:4693
JOPLING, David G., Public resistance to nuclear reactor siting, 25:5940
JOSEPH, C., Giant-resonance excitation by radiative capture of π^- in ^{16}O, 25:5600
JOSHI, B. D., Chemical separation and spectrographic determination of trace amounts of rare earths in uranium using LiF--AgCl carrier, 25:4021
JOUQUET, G., Application of internal friction to the study of graphitization, 25:4870
JOWSEY, Jenifer, Mineral density in normal and osteoporotic bone, 25:4629 (CONF-680211-, pp 411-21)
New method of evaluating bone loss in osteoporosis, 25:4639 (CONF-700515-, pp 199-204)
JOYCE, Glenn, Numerical integration methods of Vlasov equation, 25:5097 (COO-2059-6)
JUDD, A. M., Local core accidents: comparison between LMFBR's and LWR's, 25:6077
JUDY, P., Absorptiometric bone mineral determination using ^{153}Gd, 25:4649 (CONF-700515-, pp 308-12)
JUDY, Philip F., Theoretical accuracy and precision in the photon attenuation measurement of bone mineral, 25:4631 (CONF-700515-, pp 1-21)
JULIUS, David Irwin, Photo- and electroproduction of neutral rho mesons from nuclei, 25:5336
JURNEY, E. T., Level structure of ^{169}Er, 25:5725

K

KABELE, T. J., Corrosion product radioactivity in FFTF and other reactor systems, 25:5986
KADERAVEK, F., Physiologic reactions following large dose infrared radiation, 25:4715
KADYSHEVSKY, V. G., Quasi-potential equation for the relativistic harmonic oscillator, 25:5405 (JINR-E2-5339)
KAESTNER, F., p/sub 3/2/ analogue state in ^{51}V, 25:5651
KAFIEV, Yu. N., Scattering of charged particles at high energies and Bethe formula, 25:5334
KAGANOVSKII, Yu. S., Study of diffusion by tracks left by nuclear reaction products in a solid detector, 25:4845
KAGIYA, Tsutomu, Radiation induced chain reaction and its application to polymer chemistry, 25:4097
KAHANA, S., T/sub 2/^{3} term in isobaric multiplet equation, 25:5840
KAHN, B., Radionuclides in effluents from boiling water reactor, 25:6080
KAIDALOV, A. B., Factorizations of amplitudes and moving branch points, 25:5435
KAISER, R. E., Material worth measurements in benchmark critical assembly on ZPPR, 25:6115
Measurement and analysis of reactivity Doppler effects in ZPR-3 Assembly 53, 25:6110
Predicted characteristics with actual observation for ZPPR-2, 25:6113
KAISER, W. C., Non-perturbing fission counter for use in plate-type critical assemblies, 25:4363
KAJANTIE, K., Kinematic separation of three-particle channels in counter experiments, 25:5318
KAJIMURA, K., Nonlinear excess conductivity in superconducting aluminum films above the transition temperature, 25:5040
KALANOV, M., Anomalous transmission of neutron in a perfect CdS crystal, 25:5785
KALINKIN, B. N., Reactions in complete fusion of nuclei, 25:5115 (JINR-P4-5019)
KALISHINA, L. N., Express-method for determining ^{90}Sr in plants, 25:4039
KALLFELZ, F. A., Radiobiological effects of simulated nuclear power sources for artificial hearts, 25:4423
KALLFELZ, J. M., Exploratory calculations for a gaseous core fast breeder reactor, 25:5971
Space-dependent steady-state thermal-neutron spectra in beryllium above the critical buckling, 25:6107
KALLFELZ, John M., Use of Argonne National Laboratory

computers in nuclear engineering educatien, 25:6194
KALVIUS, G. M., Hyperfine interactions in Er_2O_3 and Yb_2O_3 between 20 and 1.5°K, 25:5225
KALYAZIN, E. P., Mechanism of formatien of products of radiolysis of H_2O, 25:4120
KALYNYAK, N. I., Equatien for rod cscillations at high temperatures, 25:6251 (SC-T-70-4042)
KAMETANI, Katsuaki, Chemical and hygienic studies on natural radioactive spa. IV, 25:4711
KAMIDE, Yohsuke, Spatial extent of the return current of the auroral-zone electrojet. II, 25:5003
KAMINKER, D. M., Entrainment of neutrons by a moving medium, 25:5486
KAMINSKI, Edward Eugene Jr., Anion exchange separations of metal ions in thiocyanate media, 25:4137 (IS-T-377)
KAMIYA, Kunio, Removal efficiency of charcoal filter for removing radioactive iodine, 25:4142
KAMIYAMA, Hiroshi, Ionizing effect of bremsstrahlung associated with precipitating electrons, 25:5007
KAMYSHOV, N. V., Scattering of atoms of H in noble gases, 25:4957
KANDA, Keiji, Second neutron measurements symposium, 25:4320 (KURRI-TR-59)
KANE, W. R., Evidence for the missing 2- state in ^{110}Ag, 25:5712
KANEKO, Tsuneo, Form factor of heavy-ion transfer reaction at low-energy region, 25:5594
KANELLOPOULOS, E.-J., Unified nuclear reaction theory, 25:5870
KANKI, T., Unit-spacing structure of trajectories for πN resonances, 25:5379
KANO, E., Drug-radiation damage interaction and its relevance to radiosensitization in mammalian cells, 25:4558
KAPLAN, A. M., Radiation cross-linkage of polyisobutylene in presence of monomer additions, 25:4101
KAPLAN, Henry S., Radiosensitization by the halogenated pyrimidine analogues: laboratory and clinical investigations, 25:4537
KAPOOR, R. N., Mandelates of lanthanum, praseodymium, neodymium, and uranium, 25:4055
KARADZHEV, K. V., Violation of independence of decay of compound nucleus, 25:5636
KARAZIYA, R. I., Effect of second-order relativistic corrections in the cases of complex electronic configurations, 25:4971
KARI, Cs., Analysis of the radioprotective effect of cysteine on Escherichia coli strains, 25:4554
KARNAKOV, B. M., Factorizations of amplitudes and moving branch points, 25:5435
KAROLYI, J., Isomeric cross-section ratios and total cross-sections for the ^{113}In(n,2n)/sup 112gm/In and ^{115}In(n,2n)/sup 114gm/In reactions, 25:5763
KARPIEN, R. J., Comparison of standard and modified orthogonalized plane-wave methods, 25:5231
KARPOV, V. L., Spectroscopic investigation of the low-temperature radiolysis of some polyolefins, 25:4118
KASHY, E., T/sub Z/ = -$^3/_2$ masses and isobaric multiplet mass equation, 25:5568
KASIM, M. M., Non-mesonic decay of hypernuclei produced by K-mesons of 3.0 GeV/c momentum, 25:5277
KASSNER, T. F., Thermodynamic and kinetic aspects of carbon transport in sodium--steel systems, 25:4755
KASTENBERG, William E., Comparison theorems for nonlinear point reactor dynamics equations, 25:6153
Effects of fuel chilling on Doppler-controlled fast reactor accidents, 25:6069
Fast reactor safety in nuclear science and engineering curriculum, 25:6063
Slowing down of neutrons in mixtures, 25:5484
KASTNER, J., Curium-244 and ^{145}Sm--^{145}Pm x-ray sources, 25:4647 (CONF-700515-, pp 274-9)
KASTNER, Sidney O., Average energies of ground, singly, and doubly excited configurations in highly ionized atoms, 25:4945
KASYMOV, A. K., Determination of O in Si by photonuclear reaction, 25:4046
KATHREN, R. L., Evaluation of Hanford Basic Thermoluminescence Dosimeter, 25:4378 (BNWL-CC-2633)
KATOU, T., Anomalous orbital magnetism of proton deduced from magnetic moment of 11⁻ state of ^{210}Po, 25:5742
KATSNEL'SON, A. A., Local ordering and resistivity of Ni--W and Pd--Co alloys, 25:4766
KATSURAYA, Yukimari, Radiation control program at Kyoto Univ., 1968, 25:4508 (KURRI-TR-63)
KAUFMANN, M., Radiation losses of a high-density Z-pinch, 25:5092 (SC-T-70-4044)
KAUN, K. H., Levels in ^{167}Tm, 25:5726
Non-adiabatic effects in rotational bands of odd proton nucleus ^{155}Tb, 25:5783
KAUSHAL, N. N., Fast-neutron spectrum and time moments of pulse decay in a bulk aluminum assembly, 25:6106
Study of neutron transport in iron with an assessment of data files, 25:5495
KAWAI, T., Studies on polyvinyl acetate solutions by means of radiation-induced crosslinking, 25:4094
KAWAMURA, Nobuaki, Photoneutron spectra of ^{31}P and ^{27}Al, 25:5648
KAYSER, K., Reactions ^{12}C(γ,n), ^{12}C(γ,2n), ^{39}K(γ,n), and ^{40}Ca(γ,np) up to the meson threshold, 25:5578
KAYUSHIN, L. P., Photochemical conversions of paramagnetic centres in γ-irradiated monocrystal of l-cystine dihydrochloride, 25:4091
KAZANSKY, G. S., Deuteron acceleration in LHE synchrophasotron, 25:5445 (JINR-P9-5311)
KEAN, D. C., Energy levels of ^{27}Si, 25:5602 (ANU-P-501)
KEARNS, Kenneth D., Parametric stability analysis of systems with time delay, 25:6164
KEATING, D. T., Density of phonon eigenstates from inelastic incoherent neutron scattering, 25:5230
KEATON, P. W. Jr., Absolute beam polarization determination for the LASL Lamb-shift source by the quench ratio method, 25:5453 (LA-4465, pp 10.1-2)
Absolute polarization determination of mass-3 nuclei, 25:5518 (LA-4465, pp 19.1-2)
Considerations on polarized neutron production by (d,n) polarization transfer reactions at 0°, 25:5805 (LA-4465, pp 26.1-2)
Elastic scattering of polarized tritons, 25:5511 (LA-4465, pp 5.1-2)
Figures of merit for polarized deuteron beams, 25:5455 (LA-4465, pp 23.1-2)
Formalism for A(d,n)B or A(d,p)B polarization transfer reactions, 25:5803 (LA-4465, pp 20.1-2)
Formalism for A(p,p)A and A(d,d)A polarization transfer, 25:5804 (LA-4465, pp 21.1-2)
Formalism for spin-3/2 beams, 25:5807 (LA-4465, pp 35.1-2)
Measurement of the vector and tensor analyzing power of d--^{4}He elastic scattering at 12 MeV, 25:5553 (LA-4465, pp 25.1-2)
Precise method for the determination of secondary standards for deuteron analyzing tensors, 25:5806 (LA-4465, pp 27.1-6)
Quadratic relations between the T(d,n)^{4}He observables, 25:5519 (LA-4465, pp 22.1-2)
Rapid method for the measurement of analyzing tensors in reactions induced by polarized deuterons, 25:5802 (LA-4465, pp 11.1-2)
Study of ^{3}He(d,d)^{3}He scattering at 10 and 12 MeV, 25:5520 (LA-4465, pp 24.1-2)
Study of the ^{3}He(d,p)^{4}He reaction, 25:5512 (LA-4465, pp 6.1-2)
KEDROVSKII, O. L., Prospective applications of underground nuclear explosions in national economy of USSR, 25:4169 (UCRL-Trans-10477)
KEENEY, W. P., Depleted-uranium, nickel, and steel-reflected EBR-II critical assemblies on ZPR-3: experiments and calculations, 25:5963
Gamma-ray dose evaluations for ZPR-3/EBR-II critical assemblies, 25:6125
KEEPIN, G. Robert, Physics of delayed neutrons: experimental, 25:5769
KEGLEY, T. M. Jr., Use of cellulose nitrate for alpha autoradiography in metallography, 25:4344
KEIL, R., Strontium-90 in biological materials, 25:4427
KELBER, Charles, Dual spectrum concept for LMFBR fuel assay, 25:4294
KELLOGG, L. S., Comparison of measured and calculated integral fluxes and spectra in a pressure vessel mockup, 25:6213
Selection of fission yields, 25:5973
KELLY, M. J., Radiological considerations in the use of natural gas from nuclearly stimulated wells, 25:4525 (ORNL-TM-3216)
KELLY, R. J., Ontario Hydro nuclear generating station safety and production reliability, 25:5536 (RISO-214, pp 127-69)
KEMME, J. E., Sonic limitations and startup problems of heat pipes, 25:6236 (LA-4518)
KEMMLER-SACK, Sibylle, Spectroscopic investigations in system MeUO$_4$--ThO$_2$ with Me = Nd, Dy, Ho, Yb, and Y, 25:4084
KEMNITZ, P., Levels in ^{167}Tm, 25:5726
Non-adiabatic effects in rotational bands of odd proton nucleus ^{155}Tb, 25:5783
KEMP, E. F., Reprocessing of oxide fuel at Windscale, 25:4146
KEMPER, K. W., Mass of ^{39}Ca, 25:5610
KEMPPEL, Roger Raymond, Diagnostic studies of H plasmas heated by two-phase excitation at cyclotron frequency, 25:5087
KEMSHELL, P. B., Analysis of heavy water moderated cluster lattices using WIMS code, 25:6181 (AEEW-R-545)
KENDRICK, H., Experimental test of pulse-height spectrum unfolding, 25:4365
KENEFICK, R. A., Stripping to quasibound levels in ^{41}Sc, 25:5617
KENNEDY, A. S., Multiple-source urban atmospheric dispersion model, 25:4161 (ANL/ES-CC-7)
KENNETT, T. J., Numerical construction of decay schemes, 25:5635
KENNEY, J. F., Micropulsations: a diagnostic tool, 25:5028
KERLIN, T. W., Nonlinear contamination in frequency response tests, 25:5967
Optimal discrete level signals for reactor frequency response tests, 25:5968
KERN, B. D., Beta decay of ^{40}Cl and levels of ^{40}Ar, 25:5614
KERR, E. C., Polarization of 22-MeV neutrons elastically scattered from liquid tritium and deuterium, 25:5516 (LA-4465, pp 15.1-2)

XUM

KESSEL'MAN, V. S., Path lengths of light ions in solid bodies, 25:4940
KESSER, G. M., Prog. rpt. on sodium technology, 4--6/70, 25:4736 (ANL/ST-3)
KESSLER, Ernest George Jr., High-resolution study of the He II 6560- and 10124-A transitions, 25:4950
KEVLISHVILI, G. E., Effect of the bone marrow breakdown products on hemopoiesis, 25:4533
KEY, Samuel W., SLADE: computer program for static analysis of thin shells, 25:6245 (SC-RR-69-369)
KEYWORTH, G. A., Proposed ultra-low temperature polarized target for use with single-burst neutron sources, 25:5451 (LA-4465, pp 8.1-2)
  Underground nuclear explosion as a polarized neutron source, 25:5475 (LA-4465, pp 7.1-2)
KHACHATURYAN, M. N., Time-of-flight and coordinate measurements in a 130 cm scintillation counter, 25:4318 (JINR-E1-5098)
KHALIKOV, P. Kh., Chromosome damages induced by γ-ray doses in Crepis capillaris, 25:4498
KHALKIN, V. A., Adsorption of monovalent astatine cation by cesium phosphotungstate and hydrated tungsten oxide from nitric acid solutions, 25:4053 (ANL-Trans-861)
KHAN, M. P., Evaluation of electrically tested NERVA reactor fuel elements, 25:6141
KHAN, N. A., Repair of alkylation and radiation damage in yeast, 25:4480
KHARAKHAN, M. L., Connection of field matrix element with phases of two-channel S-wave scattering, 25:5436
KHARE, Mohan, Energy transfer in alkali halide matrices, 25:4096
KHATAMI, A. I., Effect of substituents on hydrogen exchange reaction of some ferrocene derivatives, 25:4069
KHISAMUTDINOV, A. I., Numerical experiments with a nonlinear chain, 25:6234 (LA-444C-TR)
KHORUZHII, S. S., Fields and local observables in the axiomatic algebraic theory with superselection rules, 25:5414
KHRUSTALEV, B. M., Clarification and deactivation of waste waters by frothing flotation, 25:4141
KHRUSTALEV, O. A., Fast-particle scattering on Coulomb and short-range potentials, 25:5438
  Forward scattering amplitude behavior at high energies, 25:5349 (IFVE-STF-69-74)
  Solution of the unitarity equation for the elastic scattering amplitude at high energy, 25:5423 (IFVE-STF-69-65)
  Solution of unitarity condition for two-particle process amplitude at high energies, 25:5355
KHVOSTOVA, V. V., Present state of mutation breeding in USSR, 25:4489
KIBA, Toshiyasu, Silica gel as support for inorganic ion-exchangers for determination of ^{137}Cs in natural waters, 25:4033
KIDD, E. M., Telecommunications and information systems at CTC, 25:6200
KIDNEY, R. J., Energy levels of ^{18}Ne, 25:5587
KIDO, Yasumasa, Chemical and hygienic studies on natural radioactive spa. IV, 25:4711
KIEFER, J., Effects of caffeine on sensitivity to ultraviolet light of HeLa cells, 25:4607
KIEFER, W. M., Scheduling generation on systems with fossil and nuclear units, 25:5896
KIM, C. M., Radiation breeding of perennial plants. I, 25:4724
KIM, Chung-hum, Approximate nuclear wave function, 25:5845
KIM, H., Lagrangian approach to nonlinear wave interactions in a warm plasma, 25:5124 (SU-IPR-381)
KIM, I. P., Radiation cross-linkage of polyisobutylene in presence of monomer additions, 25:4101
KIM, Y. S., Quark way to asymptopia, 25:5354
KIMURA, Itsuo, Second neutron measurements symposium, 25:4320 (KURRI-TR-59)
KIMURA, M., Excitation of the giant resonance in ^{12}C by inelastic electron scattering, 25:5572
KING, Charles R., Development of an experimental technique to thermally shock graphites, 25:4851
KING, Harry F., Gaussian geminals for electron pair correlation, 25:4973
KING, K. J., High-energy calibration using ^{252}Cf neutron source, 25:4223
KING, M. J., Implications of local duality in a set of coupled reactions, 25:5352 (SU-1206-235)
KING, W. T., Infrared dispersion in liquid benzene and benzene-d_6, 25:4064
KINKADE, K. H., Contact maintenance and equipment evaluation after six years of continuous remote operation inside a hot cell, 25:4300
  Entering a hot cell after six years of remote spent-fuel processing, 25:4299
KIPERMAN, V. A., Criterion for certain canonical Fermi transformation to be proper, 25:5415
KIRK, J., Radioactive maintenance on DFR, 25:5908
KISHINEVSKAYA, M. B., New method of determining absorbed doses of gamma radiation, 25:4520
KISSICK, W. A., Experiment to obtain excess electron energy loss factor, 25:5001 (AD-710426)
KISSINGER, H. E., Observations on the nucleation and growth of voids in nickel, 25:4811 (BNWL-SA-3300)
  Void formation in nickel during irradiation, 25:4819
KLABES, R., Reaction (d,α) on ^{13}C, 25:5559
KLAMRA, W., Directional correlations of gamma rays in ^{125}I, 25:5764
KLANN, Paul G., Preliminary analysis of molybdenum-reflected, fast spectrum critical assembly, 25:6140
KLAPDOR, H. V., Lifetime and magnetic moment of neutron hole state in ^{207}Pb, 25:5710
  p/sub 3/2/ analogue state in ^{51}V, 25:5651
KLAVINS, Andrew, Interpretation error in molecular beam experiments, 25:4942
KLEIN, Edmund, Burn injury after carbon dioxide laser irradiation, 25:4704
KLEIN, James Robert, Second quantized nonrelativistic time-dependent scattering theory, and a generalization of the in--out formalism to include Coulomb potentials, 25:5431
KLEIN, Nathan, Gated photomultiplier technique for use in pulse radiolysis, 25:4398
KLEMPARSKAYA, N. N., Dynamics of autoimmune processes, 25:4472
KLEMS, G. J., Prog. rpt. on dislocation-solute atom interactions in alloys, 10/70, 25:4786 (COO-1676-13)
KLEMT, V., Isomeric shift and magnetic hyperfine splitting of muonic atoms in the lead region, 25:5794
KLESSMANN, H., Graphic display terminal for nuclear experiments with on-line computer. I, 25:4390 (HPI-B-100)
KLEYKAMP, H., Change in thermal conductivity of an oxide fuel element during burn up, 25:4839 (KFK-1245)
KLIMA, R., Drift of untrapped particles in a Tokamak, 25:5071
KLIMASHIN, G. M., Superconductivity of titanium carbide, 25:5038
KLIPPEL, H. Th., Measurements and calculations on thermal, Argonaut type, cores in STEK-facility at Petten, 25:6093 (RCN-118)
KLOPOVA, Zh. G., Use of sodium butyldithiocarbaminate in the spectrophotometric determination of niobium, 25:4017
KLOSINSKI, J., Determination of $X^0(960)$ meson spin-parity in polarization experiment, 25:5361 (TPJU-14/70)
KLUGE, W., Final state interacting n-p pairs in the reaction p + d → p + p + n, 25:5548
KNAFLICH, H. B., Micropulsations: a diagnostic tool, 25:5028
KNAPP, D. E., Thermionic and betavoltaic nuclear power sources for pacemaking, 25:4237
KNIGHT, F. D., Alphameric displays in nuclear reactor computations, 25:6202
KNIGHT, J. D., Levels of ^{88}Sr from the $^{86}Sr(t,p)^{88}Sr$ reaction, 25:5615
KNOBLE, Ronald C., Training perspective on use of BWR simulator, 25:6209
KNOBLOCH, V., Production of carrier-free radiostrontium ^{85}Sr, 25:4126 (UJV-2431-Ch)
KNOLL, G. F., Counting of heavily etched fission fragment tracks in polycarbonate, 25:4342
  Thulium-171 isomeric lifetime, 25:5721
KNORR, Georg, Excitation of ion bursts from grids, 25:5122 (COO-2059-4)
  Numerical integration methods of Vlasov equation, 25:5097 (COO-2059-6)
KNOTT, T. F., Beta-ray asymmetry from oriented /sup 110m/Ag, 25:5743
KNUDSEN, K. D., OECD Halden Reactor Project, 25:5946
KNUTSEN, A. B., High temperature corrosion of Nimonic-75 and various steels in gases at low partial pressures, 25:4736 (DP-Report-527)
KNYAZEV, D. A., Isotopic exchange laws. VII, 25:4072
KNYAZKOV, C. M., Higher approximation effects in internal conversion processes, 25:5844
KOBAYASHI, Keiji, Second neutron measurements symposium, 25:4320 (KURRI-TR-59)
KOBAYASHI, Shigeaki, Mechanical sodium pump for liquid metal cooled fast breeder reactor, 25:4201
KOCH, E. F., Influence of grain boundaries on the fracture mode of zirconium and Zircaloy-2, 25:4765
KOCH, E. M., Reliability and availability of two BWR shut-down systems, 25:6036 (RISO-214, pp 41-55)
KOCH, Paul, Turbulent heating in plasmas, 25:5068 (AD-710318)
KOCIK, J., Use of the potentiostat in the microstructural examination of uranium, 25:4792
KODAMA, Takeshi, Internal conversion coefficients for electron-spin-polarized ^{57}Fe, 25:5659
KOEHLER, J. S., Simple ion source for implantation doping of semiconductors, 25:5165
KOEHLER, W. C., Magnetic properties of Er-based binary rare earth alloys, 25:5207
KOEHLER, W. H., Na critical point data uncertainty in Na-fuel interaction, 25:6074
KOEN, B. V., Nonlinear programming approach to optimal control of nuclear reactors, 25:6152
KOH, Chang Soon, Liver scan using /sup 113m/ In colloid, 25:4687
  Preparation of /sup 113m/In colloid as scanning agent and its organ distribution in rats, 25:4437
KOIDE, Minoru, Uranium, Th, K, and Ar in marine phillipsites, 25:4164
KOJIMA, Y., Excitation of the giant resonance in ^{12}C by inelastic electron scattering, 25:5572
KOLDE, H. E., Radionuclides in effluents from boiling water reactor, 25:6080

XUM

KOLESNIKOV, E. E., Formation of ATP in nuclei and mitochondria and the influence of β-mercaptoethylamine, 25:4597
KOLESNIKOV, E. K., Evolution of charged particles from the point source in the field of magnetic dipole, 25:5004
KOLKER, H. J., Variational formulation of the Harris expansion technique, 25:4955
KOLLJACH, A., Graphic display terminal for nuclear experiments with on-line computer. I, 25:4390 (HMI-B-100)
KOLOBOVA, K. M., Position of K-absorption edges of Fe in Fe--Al and Fe--Mo alloys, 25:5181
KOLPAKOV, I. F., Time-of-flight and coordinate measurements in a 130 cm scintillation counter, 25:4318 (JINR-E1-5098)
KONCEL, E. F., Scheduling generation on systems with fossil and nuclear units, 25:5896
KONDRAT'EV, Yu. A., Influence of neutron flux on dispersion-hardening steels, 25:4817
KONERMANN, Gerhard, Role of the CNS on the radioprotective effect of 5-hydroxytryptamine, 25:4584
KONIJN, J., Decay of ^{178}Re, ^{177}Re, and ^{176}Re, 25:5733
KONISHI, Takeharu, Program for analysis of bubble-chamber photographs, 25:4372 (SJC-T-70-3)
KONOPLEV, K. A., Entrainment of neutrons by a moving medium, 25:5486
KONSTANTINOV, L. V., Dependence of scattering transport length on neutron energy in H_2O, D_2O, and graphite, 25:5502
KOPELIOVICH, B. Z., Covariant density matrix for arbitrary spin particles, 25:5305 (JINR-P2-4931)
KOPELIOVICH, V. B., Y(1327) hyperon, 25:5365
KOPRIWA, Beatrix Markus, Technique for radioautography of germ cells, 25:4421
KOPROWSKI, B. J., Profilometer for dimensional inspection of irradiated LMFBR fuel elements, 25:6033
KOPYLOV, G. I., Interference of identical particles in the processes involving the resonances, 25:5350 (JINR-P1-5315)
KORANDA, J. J., Tritium distribution, residence time, and inventory in Sedan crater ejecta, 25:4181
KORBEL, K., Applicability of the radiogauges for measuring the density of the flowing solid--liquid mixtures, 25:4896
KOROTOVSKIKH, P. M., Dependence of scattering transport length on neutron energy in H_2O, D_2O, and graphite, 25:5502
KORTH, G. E., Effect of fast neutron irradiation on the mechanical properties of hafnium, 25:4813 (IN-1440)
KOSANKE, H. D., Flux monitor utilizing track-etch film for unattended safeguards application, 25:4341
KOSHCHEENKO, N. N., Biochemical mechanism of radioprotective action of aminothiols, 25:4592
KOSHIBA, M., High energy interactions above 1 TeV, 25:5274
KOSTER, Curtis P., Packaging assembly for radioactive materials, 25:4267
KOSTRITSA, A. A., Entrainment of neutrons by a moving medium, 25:5486
Neutron velocity spectrum in heavy nuclei, 25:5492
KOTAS, P., Activation analysis of trace impurities in SiO_2 and Si_3N_4, 25:4045
KOTOV, V. I., Isochronous magnetic optical systems, 25:5447 (IFVE-OP-69-68)
KOUL, M. K., Reply to comments on phase transformations in beta isomorphous titanium alloys, 25:4806
KOURILEK, K., Cardiovascular, biochemical, and haematological changes after the application of AET, 25:4599
KOUTS, Herbert, Technical progress in nuclear materials safeguards, 25:4272
KOVACS, Ps., Analysis of the radioprotective effect of cysteine on Escherichia coli strains, 25:4554
KOVBA, L. M., Reaction of ZrO_2 with U_3O_8, 25:4864
KOVNER, D. S., Modeling channel characteristics of dc MHD machine, 25:4995
KOWNACKI, J., Directional correlations of gamma rays in ^{128}I, 25:5764
KOZLOVA, T. M., Hall effect in certain rare-earth metals and alloys, 25:5182
KOZUB, R. L., Stripping to quasibound levels in ^{41}Sc, 25:5617
KOZYREVA, E. V., Formation of ATP in nuclei and mitochondria and the influence of β-mercaptoethylamine, 25:4597
Radiosensitizing properties of some barenes (ortho-1,1 dicarbaclovododecaborane), 25:4588
KOZYRSKII, O. I., Changes in work-hardened surface layers of W, Nb, and Mo as result of annealing, 25:4797
KRAEMER, R., Development of safeguards procedures for a reprocessing plant similar to the WAK type, 25:4263 (KFK-1102)
KRAEVOI, S. Ya., Chromosome damages induced by γ-ray doses in Crepis capillaris, 25:4498
KRAFFT, O., Bahcall corrections to electron capture and the Hartree--Fock rearrangement, 25:5837
L/K- and M/L-electron capture ratio in decay of ^{65}Zn, 25:5655
KRAHN, F., Bahcall corrections to electron capture and the Hartree--Fock rearrangement, 25:5637
KRAMER, Edward J., Prog. rpt. on study of interaction between magnetic fluxoids and crystal defects in type II superconductors, 10/70, 25:5036 (NYO-4060-5)
KRAMER, G., Recent theoretical work in photoproduction of vector mesons, 25:5323 (DNPL/R-7, pp 3-28)
KRATZER, Myron B., New era for international safeguards, 25:4269
KREPLIN, Robert W., Solar cycle variation of soft x-ray emission, 25:4923
KRETSCHMAR, R., Determination of the activity coefficients of uranyl perchlorate in aqueous solutions, 25:4086
KRICK, M. S., Delayed-neutron yield vs energy measurements, 25:5770
KRIEGER, H. L., Radionuclides in effluents from boiling water reactor, 25:6080
KRIKS, H.-J., Use of excelectron emission from BeO in dosimetry, 25:4380
KRINSKY, Sam, Exact bounds on transport coefficients, 25:6242 (NYO-1480-160)
KRISHAN, S., Explosive plasma instabilities, 25:5109
KRIVENKO, V. G., Photochemical conversions of paramagnetic centres in γ-irradiated monocrystal of l-cystine dihydrochloride, 25:4091
KRSNIK, R., Enhanced superconductivity in ultrarapidly quenched bulk Al--Cu alloy, 25:5056
KRUEGER, Earl C., Radioisotope-fueled organic Rankine power system, 25:4225
KRUEGER, H., Neutron microdosimetry for rabbit eye, 25:4521
KRUGER, O. L., Compressive creep of UO_2--22 percent PuO_2, 25:4861
KRUGER, Paul, Recovery of high-viscosity petroleum by steam from geothermal heat, 25:4174
KRUPNOVA, G. F., Effect of fractionated x irradiation on the root-tip cells, 25:4492
KRUTOV, V. A., Higher approximation effects in internal conversion processes, 25:5844
KRYZHANOVSKII, V. A., Measurement of interaction cross sections of 0.3 to 5.0 MeV neutron with air, 25:5481
KRZYWICKI, A., Treatment of spins in the quark model, 25:5358
KUBIK, R. N., Integrated reactor protective system, 25:6045
KUDRICK, J. A., Implantable electrical power source for an artificial heart system, 25:4235
KUDRYAVTSEV, A. S., Effects of radiation on catalytic properties of complexes of azomethanes and ions of transition metals, 25:4103
KUDRYAVTSEV, V. G., Coherent scattering of γ quants by nuclei, 25:5174
KUHL, David E., Computer processing of images in nuclear medicine, 25:4336
KUIPER, Donald H., Ashing technique as a more precise method for the radicassay of ^{51}Cr in feces, 25:4032
KUKACKA, L. E., Development of concrete-polymer materials and composites, 25:4838
KUKOC, A. H., Gamma radiation from the decay of ^{99}Nb, 25:5718
KUKULA, F., Activation analysis of trace impurities in SiO_2 and Si_3N_4, 25:4045
KULCINSKI, G. L., Void formation in nickel during irradiation, 25:4819
KULESHOV, S. P., Problem of quasipotential smoothness in quantum field theory models, 25:5387 (JINR-E2-5365)
KULIKOV, Yu. V., Ionization counter dE/dx filled with liquid Xe, 25:4319 (JINR-P13-5403)
KULISIC, P., Energy levels of ^{18}Ne, 25:5587
KUMAR, Jitendra, Study of oxidation of ytterbium and holmium thin films in the electron microscope, 25:4767
KUMAR, Sudhir, Effect of gibberellic acid on gamma irradiated barley seeds, 25:4490
KUNTA, U. S., Radiation sensitivity of plant pigments. I, 25:4467
KUNDU, S. K., Photodisintegration of ^{4}He, 25:5544
KUNZE, J. F., Spherical gas core reactor physics measurements, 25:6133
KUPPERMANN, Aron, Linear H + H_2: exact and approximate reaction probabilities, 25:6223 (CALT-767-P-4-66)
KURKA, Gerard, Thermal gradients produced in UO_2 heated by the Joule effect, 25:4847
KURLYANDSKAYA, E. B., Certain aspects of the toxicology of insoluble compounds of ^{232}Th and ^{238}U, 25:4439
Effect of U_3O_8 on the body of the pregnant female and the foetus, 25:4446
Toxicology of radioactive substances. IV, 25:4438
KURODA, P. K., Radioactive strontium and barium fallout, 25:4163
KURSANOV, D. N., Effect of substituents on hydrogen exchange reaction of some ferrocene derivatives, 25:4069
KURTZ, Edward F., Testing of instruments and material balance methods for plutonium safeguard control, 25:4297
KUS, J. E., Features and performance characteristics of the Packard Osteodensitometer, 25:4635 (CONF-700515-, pp 48-57)
KUSY, R. P., Radiation-curing of composites of metals and polymers, 25:4108
KUTSEV, V. S., Mass spectrometric investigation of thermal dissociation of Sm and Eu carbides, 25:4855
KUZ'MIN, R. N., Determination of magnetic moment stimulated by ^{121}Sb state, 25:5720
KUZNETSOV, A. S., Polarization of secondary protons in pp + π^+pn and pp + π^0pp reactions at 669 MeV, 25:5268

XUM

(JINR-P1-5293)
KUZNETSOV, V. S., Study of the processes of redistribution of phase density in intense proton beams extracted from a duo-plasmatron type ion source, 25:5458 (NP-18510)
KWAK, N., Quark way to asymptopia, 25:5354
KYRIAKOPOULOS, E., Nucleon axial vector form factor and SC(4,2) group, 25:5401 (DEMO-70/6)
KYSHTOBAEVA, G. M., Mass spectrometric investigation of thermal dissociation of Sm and Eu carbides, 25:4855

L

LABAHN, R. W., Anomalies in scattering of electrons from He, 25:4961
LA CAMERA, M., Composite bosons in nonlocal quantum field theory with Z_3 approximately 1. II, 25:5411
LACY, Jeffrey Linn, Spin parity studies of eta pi decay of A2 meson, 25:5282 (COO-1195-200)
LAGERLOEF, B., DNA replication in radiation-induced thymomas of mice, 25:4460
LAHAJNAR, G., Spin-lattice relaxation by quasi-spin waves in order-disorder type ferroelectrics, 25:6233 (IJS-575)
LAI, C. S., Two-γ decays of pseudoscalar mesons and the constitution of the currents, 25:5337
LAIDLER, J. J., New candidate LMFBR cladding alloy, 25:4775
LAKE, J. A., Space-dependent steady-state thermal-neutron spectra in beryllium above the critical buckling, 25:6107
LAKE, Suzanne, Body distribution and biological availability of radionuclides produced by Project Schooner, 25:4435
LAMB, D., Dimensional changes of graphite specimens irradiated in dragon fuel element 700. project dragon, 25:4884 (DP-Report-556(Pt.1))
LAMBIET-COLLIER, M., Reduction of short- and long-term radiation effects by mixtures of chemical protectors, 25:4582
LAMSA, J. W., $\pi^+p \to f^0 \Delta^{++}$ at 13.1 GeV/c, 25:5283 (COO-1428-238)
LANCIA, Roland, Magnetic resonance of rare earth--Co intermetallic compounds at 9.2 GHz, 25:5200
LANE, D., Irradiation gastritis simulating carcinoma, 25:4712
LANEGRASSE, L., Mobility of radioactive ions, 25:4395
LANFREDINI, L., Radioprotective action of haematoporphyrin on endogenous spleen colony-forming units, 25:4572
LANGE, J., Quadrupole ratio Q^{3+}/Q^{2+} in ^{172}Yb, 25:5760
LANGENDORFF, Hanns, 5-hydroxytryptamine protection of rat bone-marrow chromosomes against x-irradiation in vivo, 25:4585
LANGER, S., Effect of temperature on fission gas release from coated fuel particles, 25:5557
High-temperature fast-flux irradiation experiment for mixed-oxide fuel rods, 25:5585 (GA-10264)
LANGFORD, W. J., Metallurgical properties of irradiated cold-worked Zr--2.5 wt. percent Nb pressure tubes, 25:4825
LANGFORD, W. R., Photometry of visual binaries, 25:4898
LANGHOFF, H., Coulomb fragmentation of InCl and InI, 25:5153
LANGHOFF, P. W., Bounds for oscillator-strength sums from approximate quadratures, 25:4546
LANGLEY, R. A., Clinical trial of two sunscreening creams, 25:4608
LANGUILLE, A., Influence of the allotropic transformation β reversible α and of oxygen on the distribution of plutonium in dilute ZrPu and TiPu alloys, 25:4790
LANNIN, T. E., Microstructure of mixed-oxide fuel irradiated in a thermal-neutron flux, 25:5993
LANZEROTTI, L. J., Radial diffusion of outer-zone electrons, 25:5002 (AD-710604)
LANZL, L. H., Additional system for bone densitometry studies, 25:4634 (CONF-700515-, pp 33-47)
LANZL, Lawrence, Bone densitometry: clinical applications, 25:4626 (CONF-680211-, pp 308-19)
LAPERCHES, C., Inaccuracy in the calculation of material reactivity worths, 25:6168
LAPIDUS, L., Possible properties of weak six-fermion interaction, 25:5344
LAPINSKI, N. P., Use of sparking techniques to enhance track-etch radiographs, 25:4348
LARREA, Pablo A., Idealized data handling system, 25:4328
LARSEN, F. Bundgaard, Facilities at Risoe for post-irradiation examination of Dragon Project experiments, 25:4262 (DP-Report-446)
LARSEN, R. M., Survival-promoting effects of endotoxin in mice, dogs, and sheep, 25:4586
LARSON, J. R., Design basis for LOFT facility, 25:6104
LARSON, K. H., Plutonium in soil, plants, and small mammals, 25:4478
LARSON, W. J., Progress in xenon tagging, 25:6025
LASINSKI, T. A., Total cross-sections at infinite momentum and the low-energy background, 25:5378
LASKIEWICZ, R. A., Sputtering of uranium by fission, 25:4827
LASSNER, E., Determination of O, water, and N in refractory metals. V, 25:4022
LAST, G. A., Evaluation of PuO_2 homogeneity in PuO_2--UO_2 fast reactor fuel, 25:4676
LATIMER, T. W., Postirradiation observations of sodium-bonded (U,Pu)C fuels, 25:4894
LAUG, M. T., Xenon tag proof test, 25:6026
LAUGER-HACHE, Michel, Electron probe microanalysis of highly radioactive materials, 25:4011 (CEA-N-1340)
LAUGHLIN, John S., Role of the cyclotron in nuclear medicine, 25:4683
LAURENS, Paul, French nuclear-powered pacemaker program, 25:4239
LAUTER, E. A., Anomalies of lower ionosphere ionization in medium latitudes, 25:5006
LAVROVSKII, K. P., Chemical action of laser radiation on acetylene, 25:4070
LAWLESS, J. L., Plutonium waste counter, 25:4292
LAWLEY, N., Excited states of ^{44}Ca, 25:5626
LAWRENCE, Cynthia A., Effect of capsule content variations on thyroid uptake results, 25:4661
LAWRENCE, G. P., Absolute beam polarization determination for the LASL Lamb-shift source by the quench ratio method, 25:5453 (LA-4465, pp 10.1-2)
Analyzing power of the T(d,α)n reaction at low energies, 25:5525 (LA-4465, pp 34.1-2)
Measurement of the vector and tensor analyzing power of d--^{4}He elastic scattering at 12 MeV, 25:5553 (LA-4465, pp 25.1-2)
Neutron polarization in the T(d,n)^{4}He reaction using a polarized incident beam, 25:5513 (LA-4465, pp 12.1-2)
Performance of the LASL polarized source, 25:5452 (LA-4465, pp 9.1-2)
Precise method for the determination of secondary standards for deuteron analyzing tensors, 25:5806 (LA-4465, pp 27.1-6)
Proposal for a Lamb-shift polarimeter, 25:4351 (LA-4465, pp 17.1-6)
Rapid method for the measurement of analyzing tensors in reactions induced by polarized deuterons, 25:5802 (LA-4465, pp 11.1-2)
Study of ^{3}He(d,d)^{3}He scattering at 10 and 12 MeV, 25:5520 (LA-4465, pp 24.1-2)
Study of the ^{3}He(d,p)^{4}He reaction, 25:5512 (LA-4465, pp 6.1-2)
LAWRENCE, George P., Preliminary measurements of neutron polarization from the D(d,n)^{3}He reaction using a polarized incident beam, 25:5514 (LA-4465, pp 13.1-2)
LAWRENCE, L. A., Fuel-clad gap conductance in fast reactor oxide fuels, 25:5959
Molybdenum distribution in irradiated oxide fuels, 25:4891
Molybdenum distribution in irradiated oxide fuels, 25:4804
LBOV, A. A., Principal characteristics of isotopes of heavy elements, 25:5722
LEARY, J. A., Purification, encapsulation, and characterization of ^{238}Pu for implantation purposes, 25:4228
LEBEDEV, V. E., Space--energy and time distribution of neutrons in boron-containing media, 25:4155
LEBEDEVA, N. S., Scattering of 4-MeV neutrons at angles close to 180°, 25:5762
LEBLANC, P., Airway closure, 25:4428
LECLERCQ-AUBRETON, M. Y., Versatility in reprocessing irradiated fuels, 25:4148
LECLERE, Jacques, Partial melting of low density mixed oxide $(U,Pu)O_2$ at beginning of irradiation, 25:4875 (CEA-CONF-1659)
LEDBETTER, H. M., Cubic to orthorhombic transformation in Au--47.5 Cd, 25:4807
LEDLEY, Robert S., Evaluation of the significance of the contribution of coherent scattering of an X ray beam to darkening of radiographic film, 25:4640 (CONF-700515-, pp 205-23)
High-speed area-measuring scanning densitometer, 25:4620 (CONF-680211-, pp 191-203)
LE DUIGOU, A., Manufacture of metallic uranium nuclear fuels: some industrial and economic aspects, 25:4743
LEE, Chung Choo, Insect pest control using sterile-male technique. I, 25:4735
LEE, D., Influence of grain boundaries on the fracture mode of zirconium and Zircaloy-2, 25:4769
Recrystallization and mechanical behavior of Zircaloy-2 tubing, 25:4757
LEE, Jay Y., Radwaste design for no plant-originated radioactive liquid discharge, 25:5882
LEE, Jong I., /sup 99m/Tc labeling of erythrocytes, 25:4414
LEE, Kai Fong, Ordinary-mode electromagnetic instability in counterstreaming plasmas with anisotropic temperatures, 25:5129
LEE, Kiuck, Approximate nuclear wave function, 25:5845
LEE, Philip H., Restraint device for scanning dogs, 25:4654 (CONF-700515-, pp 424-7)
LEE, Vincent J., UBV observations of 3C 273. III, 25:4916
LEENHOUTS, H. P., Fading of radiation-induced optical density in polymethylmethacrylate on oxygen diffusion, 25:4384
LEFRANCOIS, C., Calculation of losses in superconducting coils supplied by pulsed current, 25:5459 (NP-18516)
LEGGETT, R. D., Burst tests of EBR-II irradiated fuel pin sections, 25:5950
Correlation of predictions and observations in mixed-

oxide fuel, 25:6001
LEHMANN, A. R., Repair of DNA and the mode of action of sensitizers and protectors in biological systems of different complexity, 25:4536
LELAND, W. T., Asymmetries in deuteron scattering from a polarized ^{3}He target, 25:5515 (LA-4465, pp 14.1-2)
Asymmetries in protons from the reaction of deuterons with a polarized ^{3}He target, 25:5524 (LA-4465, pp 32.1-2)
Levels of ^{88}Sr from the ^{88}Sr(t,p)^{88}Sr reaction, 25:5615
LELEUX, Achille, Electron probe microanalysis of highly radioactive materials, 25:4011 (CEA-N-1340)
LELEUX, G., Influence of coupling resonances 2v/sub z/+-v/sub x/ = integer on mechanism of third resonance ejection, 25:5460 (NP-18517)
LELIEVRE, P., Metabolic effects of sulphur-containing radioprotective drugs, 25:4595
LEMAIRE, Remy, Magnetic properties and magnetic structures of rare earth--Ni equiatomic compounds, 25:5209
Magnetic properties and structures of DyAl-type compounds of Al and rare earth metals, 25:5208
Magnetic properties of R_3M compounds of rare earth and transition metals, 25:5199
LEMAN, J. D., Maintenance of radioactive sodium systems at EBR-II, 25:5987
LEMLEY, J. R., Proposed ultra-low temperature polarized target for use with single-burst neutron sources, 25:5451 (LA-4465, pp 8.1-2)
Underground nuclear explosion as a polarized neutron source, 25:5475 (LA-4465, pp 7.1-2)
LEMSTRA, W., Radioprotection by hypoxia and some chemical protectors, 25:4578
LE NADAN, A., Generalized oscillator strengths for $1^1S \rightarrow 2^1S$ transition in He, 25:4959
LENGEMANN, F. W., Cesium-134 retention by rats, 25:4450
LENT, Edward M., Collimation of fast neutrons, 25:5477 (UCRL-50857)
LEONARD, B. E., Neutron fluence-to-kerma factors and mass energy transfer coefficients for various materials in reactor neutron fields, 25:6214
Pulse reactor research and some operational considerations, 25:6120
TLD 700 (^{7}LiF) response to reactor neutrons, 25:4382
LEONAS, V. B., Scattering of atoms of H in noble gases, 25:4957
LEONELLI, F., General principles of a safety assessment through reliability analysis of ESSOR plant, 25:6094 (RISO-214, pp 597-625)
LEONTIC, B., Enhanced superconductivity in ultrarapidly quenched bulk Al--Cu alloy, 25:5056
LEPLAE, L., Boson method in superconductivity: application to the study of vortex lines, 25:5052
LERCH, I. A., Bioluminescence and radiation response of Photobacterium fischeri H-2, 25:4730
LERNER, Morris W., Analysis of elemental boron, 25:4009 (TID-25190)
LESHCHENKO, S. S., Spectroscopic investigation of the low-temperature radiolysis of some polyolefins, 25:4116
LESSER, P. M. S., First excited state of ^{148}Sm, 25:5703
LESSLER, Richard M., Plowshare explosive shielding, 25:4175
LETAVET, A. A., Toxicology of radioactive substances. IV, 25:4438
LETESSIER, Jocelyne, Magnetic quadrupolar γ transitions in atomic nuclei, 25:5792
LEVINE, Lawrence, Appearance of brain-specific antigen in developing rat brain, 25:4694 (UCLA-12-791)
LEVINE, P. J., Postirradiation observations of sodium-bonded (U,Pu)C fuels, 25:4894
LEVINGER, J. S., Yamaguchi's deuteron wave function, 25:5871
LEVMAN, G. M., Duality invariant action principle in vacuum electrodynamics, 25:5403
LEVY, F., Distortions of lattice of some trivalent compounds of rare earths, 25:4803
LEVY, Francoise, Taking samples of radioactive substances, 25:4516
LEVY, P. W., Formation of color centers in KCL:Tl by gamma irradiation at 21°C, 25:5157
LEWIS, Edwin Augustus Stevens, Heat capacity of Gd near the Curie point, 25:5220
LEWIS, R. H., Integrated reactor protective system, 25:6045
LEWIS, S. A., FORTRAN nuclidic-mass table with self-modification feature, 25:5735
LE YAOUANC, A., Treatment of spins in the quark model, 25:5358
LEYSE, R. H., ECC variable flooding rate simulation PWR FLECHT test results, 25:6043
Effect of 75 to 100 percent flow blockage on bottom cooling heat transfer effectiveness, 25:6042
LEZNOV, A. N., Unitary representations of the conformal group, 25:5393 (IFVE-STF-69-85)
LHERMENIER, Andre, Partial melting of low density mixed oxide $(U,Pu)O_2$ at beginning of irradiation, 25:4879 (CEA-CONF-1659)
LIDOFSKY, L. J., Age and fast effect for fission and 14-MeV neutron sources in Be and BeO, 25:5496
LIEB, D., Thermionic performance of fluoride CVD W--Nb converter, 25:4993 (TEE-4125-1)
LIEBECQ, Claude, Blood redox potentials of rats and mice injected with cystamine, 25:4593
LIEBERMAN, D. S., Diffusivity and isotope-effect measurements in equiatomic Fe--Co, 25:4761
LIEBMANN, B. G., Preparation and performance of HTGR fuel in Germany, 25:6006
LIGHTBODY, D., Computer analysis of fission data, 25:5790
LILEY, B., Nuclear particle detection system response analysis, 25:4928
Spacecraft configuration and operational tradeoffs for nuclear power sources, 25:6138
LILLICRAP, S. C., Effect of 5-bromouracil incorporation on energy transfer in irradiated DNA, 25:4542
LIN, J., Levels in ^{53}Mn, ^{58}Co, ^{63}Zn, and ^{70}Ga from the (p,n) reaction, 25:5612
LIN, Jeong-long, Vibrational excitation in Morse oscillator, 25:4954
LINDBERG, J. F., Target handling system for 200-GeV proton accelerator, 25:5470
LINDELL, S. E., Four quandrant radiospirometry in normal and diseased states, 25:4671
LINDGREN, J. R., Fission gas release measurements from fast breeder $(U,Pu)O_2$ fuel, 25:6015
High-temperature fast-flux irradiation experiment for mixed-oxide fuel rods, 25:5989 (GA-10264)
LINDMAN, E. L., Suppression of Kelvin--Helmholtz instability in Cs plasma, 25:5111
LINDOP, Patricia J., Strontium-90 and infant mortality, 25:4505 (CONF-691051-, pp 324-35)
LINDSEY, W. J., Production of ^{238}Pu, 25:4227
LINDSTROM, D. G., Radiation transport analyses of nuclear rocket engine components, 25:6128
LINGEN, Peter Ralf, Procedure for identification of fuel element spheres of high-temperature reactors with the help of emission spectral analysis at 40 atmospheres of helium, 25:4013 (JUL-671-RW)
LIPPERT, J., Environmental radioactivity in the Faroes in 1969, 25:4476 (RISO-221)
LISMAN, F. L., Fission yields of over 40 stable and long-lived fission, 25:5765
LITTBRAND, B., Composite radioprotective and radiosensitizing effect of an organic free radical, 25:4561
LITTLEJOHN, M. A., Piezoresistive effect in electron irradiated silicon and its application to improvement of semiconductor strain gages, 25:5151 (N-70-35737)
LITWIN, Martin S., Burn injury after carbon dioxide laser irradiation, 25:4704
LLOYD, David J., Possible contribution of diffusive grain-boundary pore growth to creep deformation of ceramic materials, 25:4848
LLOYD, Elizabeth, Measurement of bone mineral using computer analysis of microradiographs, 25:4638 (CONF-700515-, pp 195-8)
LLOYD, R. C., Criticality of Pu nitrate solutions containing Raschig rings, 25:4281
LOBANOV, Yu. V., Synthesis of element 105, 25:5757
LOBBIN, Fred, Establishing Safety Limits and Limiting Safety System settings for research (pulse) reactors, 25:6121
LOCANTE, John, WNSE shielding application, 25:5578
LOCKER, David J., Delta-function scattering, 25:4962
LODGE, F. M. K., Electrical conductivity of dysprosium thin films, 25:4771
LODHI, M. A. K., Correlation structure of ^{6}Li, 25:5564
LOEVHOEIDEN, G., Deuteron scattering from ^{126}Te and ^{144}Nd, 25:5729
LOFBERG, R. T., Structure-function studies of the aminothiol radioprotectants, 25:4548
LOFTHOUSE, J. H., Spherical gas core reactor physics measurements, 25:6133
LOFTON, D. B., Fallout computational techniques, 25:4506 (AD-703266)
LOGGINS, C. D. Jr., Piezoresistive effect in electron irradiated silicon and its application to improvement of semiconductor strain gages, 25:5151 (N-70-35737)
LOH, P. C., Uv inactivated virion preparations and cell death, 25:4729
LOHMANN, Wolfgang, Charge transfer complexes and the mechanism of action of cysteamine and penicillamine, 25:4547
LOHRDING, Ronald K., Method for estimating risk from Plowshare detonation, 25:4172
Risk estimate for an urban-sited research reactor, 25:6103
LOISEAUX, J. M., Mass of ^{13}O and isobaric multiplet mass equation, 25:5640
LOKEN, Merle, Evaluation of pulmonary disease using ^{133}Xe, 25:4676
LOMBARD, David B., Disposal of radioactive wastes in nuclear chimneys, 25:4279
LOMBARD, R. J., Comparison between Hartree--Fock and Thomas--Fermi calculations using effective interactions, 25:5873
LONG, A. B., Non-perturbing fission counter for use in plate-type critical assemblies, 25:4353
LONG, E. L. Jr., Thermal performance and restructuring of pellet and sphere-pac fuels, 25:5992
LONGEST, A. W., Fission gas release measurements from fast breeder $(U,Pu)O_2$ fuel, 25:6015
LOPAC, V., Phenomenological description of anharmonic quadrupole vibrations, 25:5782
LOPER, David E., General solution for the linearized Ekman-

XUM

-Hartmann layer on a spherical boundary, 25:4998
Steady hydromagnetic boundary layer near a rotating, electrically conducting plate, 25:4999
LORENZ, R., Preparation of Th--Pa alloys, 25:4791
LOSEV, N. F., Quantitative x-ray spectrofluorescence analysis, 25:4024
LOSEV, S. A., Mechanism of thermal dissociation of diatomic molecules, 25:6252 (SC-T-70-4045)
LOU, Catherine Yuen-Chien, Vaporization mechanism of gallium arsenide single crystals, 25:4074 (UCRL-19685)
LOVAS, I., Three-body model for the isobaric analog resonance on even--odd target, 25:5872
LOVE, T. A., Simultaneous fast-neutron spectral measurements by time-of-flight and pulse-height unfolding techniques, 25:4366
LOVELL, A. J., Mechanical properties of EBR-II irradiated 20 percent cold-worked Type 316 stainless steel, 25:5949
Uniaxial and biaxial creep-rupture of Type 316 stainless steel after fast reactor irradiation, 25:4816 (WHAN-FR-19)
LOVETT, D. B., Flux monitor utilizing track-etch film for unattended safeguards application, 25:4341
Track-etch research and development, 25:4345
LOVOLI, K., Magnetic structure of Er_2WO_{12}, 25:5216
LOWENSTEIN, J. H., Locally generated dilatation charge in Thirring model, 25:5408 (NYO-3829-61)
LOYD, David Heron Jr., Scattering and reactions of polarized protons and deuterons from beryllium, 25:5584
LU, An-hua, Applications of T-matrix perturbation theory, 25:5389
LU, E. Y. C., Scale-invariant light-cone commutators and universal structure functions, 25:5328
LU, P., Modified WKB approximation for phase shifts, 25:5238
LUBIN, M. J., Plasma confinement in a high magnetic field toroidal quadrupole, 25:5070
LUBIN, Moshe J., Laser-produced plasmas for power generation and space propulsion, 25:5104
LUBY, C. S., HTGR fuel design and irradiation performance, 25:6003
LUCEY, J. W., Neutron transport in two-dimensional slabs by invariant imbedding, 25:5143
LUCO, V., Another anomaly in variational flux synthesis methods, 25:6170
LUDFORD, G. S. S., Viscous tails in MHD, 25:5121 (AD-709878)
LUDLOW, J. O., Pneumatic tube transfer system for radioactive samples, 25:4306
LUDZIEJEWSKI, J., Directional correlations of gamma rays in ^{128}I, 25:5764
LUETHI, B., Sound propagation near magnetic phase transitions, 25:5186
LUGARESI-SERRA, P., Exotic resonances in K-d interactions at 3 GeV/c, 25:5287
LUKHMINSKII, B. E., Calculation by Monte Carlo method of distribution of photoneutrons from a beam of γ radiation with initial energy of 4.1 MeV, 25:4152 (CSIRO-Trans-10083)
LUK'YANOV, A. A., Spectrum of retarded neutrons, 25:5505
LUNDBERG, B., Neutron capture cross sections in F, Mg, Al, Si, P, and S from 20 to 80 keV, 25:5603 (FOA-4-4440)
LUNDE, J. E., Computer control developments, 25:5974
OECD Halden Reactor Project, 25:5946
LUNDGREN, P. R., Incorporation of ^{14}C in cerebral glycogen of normal and x-irradiated rats, 25:4453
LUNDQUIST, J. R., Pulsed current electroplating, 25:4741 (ENWL-CC-491)
LUSHBAUGH, C. C., Induction of carcinoma of the glandular stomach by whole-body irradiation, 25:4703
LUSSIE, W. G., Behavior of discrete PuO_2 particles in thermal recycle fuel, 25:5994
LUST, L. F., Mockup of remotely operated, high-purity, inert-atmosphere sodium analysis facility, 25:4310
LUTZ, H. O., Charge states of 60-MeV iodine ions channeled in Au, 25:5164
LUTZ, Thomas Edward, Intercomparison of three spectroscopic luminosity criteria, 25:4910
LUZ, Z., ESR of SO_2^-, 25:4124
LYNDS, C. Roger, Absorption lines of quasi-stellar objects, 25:4919
LYNEN, U., Reaction (p,t) on ^{42}Ca, ^{44}Ca, and ^{48}Ce, 25:5677
LYNN, K. R., X- and γ-radiolysis of some tryptophan dipeptides, 25:4114
LYTLE, C. David, Ultraviolet light enhanced reactivation of a mammalian virus, 25:4727
LYTTKENS, L., Spectrometry for determination of isotopic mixtures, 25:4031

M

MA, Benjamin M., Teaching experience in thermonuclear theory, 25:5100
MA, P. Y., Approach for determining the effective energy release of a fast reactor accident, 25:6065
Improved method for assessing damage to the reactor vessel in a fast reactor accident, 25:6064
MACAVOY, Paul W., Mid-range optimization of use of a nuclear power plant, 25:5904
Short-range optimization of use of a nuclear power plant, 25:5905
MACDONALD, Jack R., Properties of the low-lying states of ^{48}Ca, 25:5616
MACFARLANE, D. R., Delineation of LMFBR single subassembly accidents, 25:6068
MACFARLANE, J. C., Determination of 2e/h based on the ac Josephson effect, 25:5412
MACHER, A., First two excited states of ^{159}Tb, 25:5727
MACK, Pauline Beery, Assessment of bone mass by roentgenographic density techniques, 25:4613 (CONF-680211-, pp 27-80)
MACKINTOSH, A. R., Exchange interactions in rare earth metals, 25:5213
MACKWORTH, A. J., Binding between gas bubbles and grain boundaries, 25:4850
MACLENNAN, C. G., Radial diffusion of outer-zone electrons, 25:5002 (AD-710604)
MACNABB, W. V., Comparison of recycle in LWR's and HTGR's, 25:6056
Indifference value of ^{233}U in an HTGR, 25:6057
MACNAUGHTON, J. N., K$^+$p elastic scattering at 4.6 GeV/c, 25:5296
MADDEN, D. R., Frozen polarized target, 25:5466 (RPP/A-81)
MADELL, J. T., Effect of subassembly clearance on fast reactor performance characteristics, 25:6021
MADSEN, V. A., Effective charge factor for the radiative capture of fast nucleons, 25:5839
MAECK, W. J., Fission yields of over 40 stable and long-lived fission, 25:5765
MAFFEO, Bruno, EPR of a new boron center in neutron-irradiated BeO, 25:5162
MAGAW, J. R., Neutron and photon radiation levels internal and external to mockups of nuclear rocket shields, 25:6130
MAGDON, E., Effect of 6-azauridine on irradiated tumours, 25:4590
MAGRAKVELIDZE, T. Sh., Determination of the average effective radius of vaporization centers in the nucleate boiling of liquids, 25:6215 (AEC-tr-7202)
MAH, S. Q., Current-induced ion heating in a toroidal plasma, 25:5069
MAHAN, R. E., Automation in analytic chemistry: methods and motivation, 25:4008 (BNWL-SA-3341)
MAIER, K. H., Reaction $^{56}Fe(d,n)^{57}Co$ and level scheme of ^{57}Co, 25:5675
MAIN, I. G., Excited states of ^{44}Ca, 25:5626
MAINKAR, Vasant V., 14307 tau plus decays analyzed, 25:5263
MAISIN, J. R., Disorientation response of chicks which survived 2-β-aminoethylisothiouronium-Br-HBr (AET) administration during early embryogenesis, 25:4601
Reduction of short- and long-term radiation effects by mixtures of chemical protectors, 25:4582
MAKEEV, V. V., Search for W-boson in NN-collisions at IHEP accelerator, 25:5267 (IFVE-SEF/STF-69-46)
MAKOWSKI, Edgar L., Growth of uterine, placental and fetal vasculature, 25:4655 (COO-1762-6)
MAKSIMOV, Yu. V., Chemical action of laser radiation on acetylene, 25:4070
MALACZYNSKI, G., Ion oscillations in EGD flow in channels, 25:4996
MALAN, G. F., Nonlinear programming approach to optimal control of nuclear reactors, 25:6152
MALASHKEVICH, N. I., Ionization counter dE/dx filled with liquid Xe, 25:4319 (JINR-P13-5403)
MALAVIYA, B. K., Fast-neutron spectrum and time moments of pulse decay in a bulk aluminum assembly, 25:6106
Study of neutron transport in iron with an assessment of data files, 25:5495
MALEK, G. J., Hydrodynamic stability in curved steam generator tubes, 25:4208
MALLARD, John R., Physical aspects of scintiscanning, 25:4684
MALLIARIS, A., Radiation-curing of composites of metals and polymers, 25:4108
MALMIN, R., Excitation functions from elastic ^{16}O scattering from nuclei with A approximately 16, 25:5566
MALMSKOG, S. G., E2 and M1 transition probabilities in ^{193}Au and ^{195}Au, 25:5701
MALY, L., Excited levels in the decay $^{185}Os \rightarrow {}^{185}Re$, 25:5741
MAMELLE, J., The development of safety measures in reprocessing plants, 25:4527
MANCE, A., Use of the potentiostat in the microstructural examination of uranium, 25:4792
MANCINI, F., Boson method in superconductivity: application to the study of vortex lines, 25:5052
MANCINI, G., Radioprotective action of haematoporphyrin on endogenous spleen colony-forming units, 25:4572
MANDAL, Sukumar, Complexes between U(VI) and dioxydiquinone, 25:4078
MANDEVILLE, C. E., Decay of ^{144}Ce, 25:5749
MAN'KO, V. I., Violation of independence of decay of compound nucleus, 25:5636
MANOWITZ, B., Development of concrete-polymer materials and composites, 25:4838
MANTHOS, E. J., Transient performance of sol-gel $(U,Pu)C_2$ Sphere-Pac and pellet fuels, 25:6016
MANWEILER, R., Isovector asymmetry in rho-production, pion photo- and electroproduction, 25:5326

MARABLE, J. H., Interference effects of ^{232}Th--^{233}Pa absorption resonances in homogeneous systems, 25:5958
MARCELJA, F., K+p elastic scattering at 4.6 GeV/c, 25:5296
MARCHAND, Andre, Magnetic resonance of rare earth--Co intermetallic compounds at 9.2 GHz, 25:5200
MARCHATERRE, J. F., Coolant voiding and pressure generation due to boiling, fission gas release, and molten fuel-coolant interaction, 25:6073
Delineation of LMFBR single subassembly accidents, 25:6068
MARCINKOWSKI, A., Isomeric cross-section ratios and total cross-sections for the $^{113}In(n,2n)$/sup 112gm/In and $^{115}In(n,2n)$/sup 114gm/In reactions, 25:5763
MARCOUX, Michael Oran, Eigenfunction expansions for scattering in two- and three-particle systems, 25:5429
MARDER, B., Bifurcation problem in E-layer equilibria, 25:5119
MARESCHAL, J., Metamagnetic properties of a single crystal of $ErCrO_3$, 25:5180
MAREZIO, M., Crystal structure of antiferromagnetic phase of V_2O_3, 25:5190
MARIAN, V. R., Transfer of coolant between adjacent subchannels in wire wrap and grid spacer rod bundles, 25:6028
MARIANI, Leo Paul, Coherent neutron scattering in polycrystalline zirconium hydride, 25:5499
MARIEN, P., Parametric survey on internally cooled annular fuel, 25:5979 (DP-Report-435)
MARININ, V. G., Investigation of ion heating during development of high-frequency cluster centrifugal instability, 25:5073
MARION, Fernand, Electrical conductivity and stable domains at high temperatures for terbium oxides, 25:5179
MARIPUU, S., Gamma decay of ^{39}K levels, 25:5631
MARK, H., Design of intermediate-energy neutron spectrometers and their calibration with photoneutrons, 25:4364
MARKS, Asher, Archaic methods of regional ventilation, 25:4665
MARLEY, J. L., Spectrographic analysis response of a carrier to plutonium--uranium mixed oxides, 25:4015 (NUMEC-3524-76)
MARMIER, P., One-neutron transfer reactions, 25:5577
Protons scattered on ^{24}Mg, ^{52}Cr, and ^{58}Ni, 25:5632
MARRIAN, D. H., Indanetrione, menadione, Synkavit, and N-ethylmaleimide tested as radiosensitizers on murine ascitic tumour irradiated in vitro and grown in vivo, 25:4562
MARSH, K. V., Photon activation analysis, 25:5472
MARSH, Ogden J., Method of restoring crystals damaged by irradiation, 25:4895
MARSHALL, J. D., X-ray spectra calculations for complex detector geometries, 25:4403
MARSHALL, Robin, Photoproduction of vector mesons, 25:5301 (INPL/R-7, pp 29-70)
MARTIN, B., Internal conversion of the 57.54 keV E1 transition in ^{180}Hf, 25:5731
MARTIN, C. G., Testing of instruments and material balance methods for plutonium safeguard control, 25:4297
MARTIN, D. G., Radiation damage effects in the containment vessel of a thermonuclear reactor, 25:5114 (CLM-R-103)
MARTIN, D. M., Magnetic properties of gadolinium orthovanadate, 25:5217
MARTIN, J. C., Improvements in performance of a liquid helium scintillation counter, 25:4321 (LA-4465, pp 31.1-2)
MARTIN, J. K., Analysis of neutron distributions in ZPPR/FTR-2 shield experiments, 25:6124
MARTIN, J. R., Tritium distribution, residence time, and inventory in Sedan crater ejecta, 25:4181
MARTIN, M. J., Radioactive atoms. Auger-electron, α-, β-, γ-, and x-ray data, 25:5716
MARTIN, P., Electric quadrupole transitions in muonic ^{208}Pb, 25:4953
MARTINELLI, R. U., Prog. rpt. on transmission secondary emission multipliers using high gain secondary emitters, final, 6/23/69--6/26/70, 25:6245 (NYO-4100-3)
MARTINI, W. R., Radioisotope-fueled Stirling engine artificial heart power system, 25:4233
MARTY, A. M., Mobility of radioactive ions, 25:4395
MARUKHIN, V. I., Anomalous transmission of neutron in a perfect CdS crystal, 25:5785
MARVANOVA, H., Effect of bursectomy and thymectomy on cellular immunological reactions in chickens, 25:4468
MARX, G., Natural neutrinos, 25:4589
MASAGUTOV, V. S., Determination of O in Si by photonuclear reaction, 25:4046
MASCHKE, A. W., Target handling system for 200-GeV proton accelerator, 25:5470
MASON, E. A., FBR blanket depletion studies: effect of number of energy groups, 25:5560
MASON, Edward A., Heat transfer optimization and reactivity of nuclear rocket reactors, 25:6127
Mid-range optimization of a nuclear power plant, 25:5904
Passive nuclear attitude control system for solar probes, 25:4222
Short-range optimization of use of a nuclear power plant, 25:5905
MASON, G. W., Two octyl phenyl phosphinic acids, (R)(C_6H_5)PO(OH), as extractants for selected M(III) and M(VI) metallic cations, 25:4147
MASTEL, B., Observations on the nucleation and growth of voids in nickel, 25:4811 (BNWL-SA-3300)
MASTERS, C. F., Delayed-neutron abundances and half-lives from 14.7-MeV fission, 25:5775
MASUDA, Koji, Media and surviving fraction of x-irradiated HeLa S3 cells, 25:4606
MATEEV, M. D., Quasi-potential equation for the relativistic harmonic oscillator, 25:5405 (JINR-E2-5339)
MATHER, W., Absorptiometric bone mineral determination using ^{153}Gd, 25:4649 (CONF-700515-, pp 308-12)
MATHUR, B. S., Maleic acid complexes of rare earth and other metals. I, 25:4075
MATHUR, P. K., Annealing of ^{60}Co recoil atoms in alpha and beta cobalt phthalocyanine, 25:4130
MATSUBARA, Sho, Chromosomal damages in circulating lymphocytes induced by therapeutic irradiation, 25:4491
MATSUDA, Masamichi, Sodium test facility, 25:4191
MATSUI, Sei-ichi, Enzyme inactivation with ultraviolet laser energy (2650 Angstroms), 25:4461
MATTE III, Joseph, Remote maintenance during recovery from Enrico Fermi fuel melting incident, 25:5507
MATTELIN, G., Disorientation response of chicks which survived 2-β-aminoethylisothiouronium-Br-HBr (AET) administration during early embryogenesis, 25:4601
Reduction of short- and long-term radiation effects by mixtures of chemical protectors, 25:4582
MATTERN, F. C. M., Relation between deposition of long lived fission products and dietary ingestion, 25:4519
MATTHAEY, H., Final state interacting n-p pairs in the reaction p + d + p + p + n, 25:5548
MATUMOTO, Zyun-itiro, Decay scheme of 5.3 h ^{113}Ag and 1.2 min /sup 113m/Ag, 25:5754
MATVEENKO, A. V., Mesic atom processes in hydrogen, 25:4952 (JINR-P4-5039)
MATVEEV, V. A., Problem of quasipotential smoothness in quantum field theory models, 25:5387 (JINR-E2-5365)
MAURER, A., Insurance of atomic risks, 25:4530
MAURER, H. A., Reliability of emergency core cooling systems of light water nuclear power plants, 25:6038 (RISO-214, pp 91-126)
MAXIA, Vera, Aluminum and Si abundances of some Italian meteorites as determined by instrumental activation analysis, 25:4048
MAY, E. C., FORTRAN nuclidic-mass table with self-modification feature, 25:5735
MAY, Victoria M., Angular distributions in neutron-induced reactions. I, 25:5549 (BNL-400(3rd Ed.)(Vol.1))
MAYER, James W., Method of restoring crystals damaged by irradiation, 25:4895
MAYHAN, K. G., Kinetics of gamma-induced polymerization of methyl methacrylate-clay composites, 25:4107
MAYHUGH, M. R., V_3 band in LiF, 25:5156
MAYNARD, C. W., Feedback-induced spatial effects in a simple prompt critical reactor excursion, 25:6161
MAYO, Wendell, Preliminary analysis of molybdenum-reflected, fast spectrum critical assembly, 25:6140
MAZESS, R. B., Absorptiometric bone mineral determination using ^{153}Gd, 25:4649 (CONF-700515-, pp 308-12)
Preliminary report on a direct digital readout system for absorptiometric determination of bone mineral content, 25:4632 (CONF-700515-, pp 22-7)
MAZESS, Richard B., Effects of fat on bone mineral measurements, 25:4644 (CONF-700515-, pp 255-62)
MAZZACURATI, V., Search for excess electron photo-ejection in liquid He, 25:5060 (NP-18484)
MCARDLE, K. T., Velocity dependence of relative total cross section for He + He from 2070 to 2750 m/sec, 25:4965
MCCARTHY, J. S., Electromagnetic structure of the ^3He nucleus, 25:5535
MCCARTOR, Gary Don, Topics in scattering theory, 25:5430
MCCLURE, J. W., Fast-neutron spectroscopy of the reaction $^9Be(p,n)^9B$ at 20 MeV, 25:5557
MCCOY, W. L., Planning for flexibility in operation, maintenance, and refueling of PWR, 25:5905
MCCRELESS, Thomas, G., Government regulator's views [on implications of ANSI Criticality Safety Standard N16.1], 25:4288
MCCULLOUGH, David C., Spinal cord dosimetry in ^{131}I-IHSA cisternography, 25:4510
MCDONALD, Arthur Bruce, Excitation energies and decay properties of $T = 3/2$ states in ^{17}O, ^{17}F, and ^{21}Ne, 25:5583
MCDONALD, Glen E., Irradiation of Mo--UC_2 fuel pin at 27000°F to 8.5 percent burnup, 25:6198
MCDONALD, K., Microdetermination of flucrine in high-purity tungsten metal by photoactivation analysis, 25:4043 (GA-10125)
MCELROY, Jack L., Status of Waste Solidification Demonstration Program, 25:4276
MCELROY, Michael B., Ionization processes in the atmospheres of Venus and Mars, 25:4936
MCELROY, W. N., Selection of fission yields, 25:5973
Yield strength and creep strain estimates for irradiated stainless steel, 25:4820
MCFARLANE, I. D., Measurement of energy dissipated in superconductors during flux jumps, 25:5044
MCGEE, T., Decay of ^{69}As, 25:5621
Interactions of ^{45}Sc and ^{68}Zn with protons, 25:5623
MCGEORGE, J. C., Conversion coefficient of 14.4-keV

XUM

transition in ^{57}Fe, 25:5652
MCGHEE, B. W., Neutron diffusion parameter determination using the pulsed neutron source techniques with spheres of heavy water, 25:5485
MCGRATH, Peter Edwin, Integral transport theory analysis of small-sample reactivity measurements, 25:6187
MCGRORY, J. B., Beta-decay rates and role of d/sub 3/2/-orbit in light s--d-shell nuclei, 25:5599
Shell-model structure of ^{42}Ca through ^{50}Ca, 25:5611
MCINTYRE, D. R., Fate of Schooner fallout radionuclides ingested by dairy cow, 25:4436
MCKEE, J. S. C., Polarization transfer at 0° in the D(d,n)^{3}He and H(d,n)pp reactions, 25:5532
MCKENNA, C. M., Mass of ^{39}Ca, 25:5610
MCKENZIE, J., Measurement of K- cascade time in liquid He, 25:5254
MCKIBBEN, J. L., Absolute beam polarization determination for the LASL Lamb-shift source by the quench ratio method, 25:5453 (LA-4465, pp 10.1-2)
Analyzing power of the T(d,α)n reaction at low energies, 25:5525 (LA-4465, pp 34.1-2)
Measurement of the vector and tensor analyzing power of d--^{4}He elastic scattering at 12 MeV, 25:5553 (LA-4465, pp 25.1-2)
Neutron polarization in the T(d,n)^{4}He reaction using a polarized incident beam, 25:5513 (LA-4465, pp 12.1-2)
Performance of the LASL polarized source, 25:5452 (LA-4465, pp 9.1-2)
Precise method for the determination of secondary standards for deuteron analyzing tensors, 25:5806 (LA-4465, pp 27.1-6)
Rapid method for the measurement of analyzing tensors in reactions induced by polarized deuterons, 25:5802 (LA-4465, pp 11.1-2)
Study of ^{3}He(d,d)^{3}He scattering at 10 and 12 MeV, 25:5520 (LA-4465, pp 24.1-2)
Study of the ^{3}He(d,p)^{4}He reaction, 25:5512 (LA-4465, pp 6.1-2)
MCLACHLAN, D. S., Quantum oscillations in low-kappa Type II superconducting microcylinder. II, 25:5046
Quantum oscillations in low-kappa Type II superconducting microcylinder. I, 25:5045
MCLEOD, K. C., Coulometric determination of uranium with a platinum working electrode, 25:4625
MCNAMARA, D. H., Photometry of visual binaries, 25:4898
MCNEAL, R. J., Production of positive ions and electrons in collisions of 1- to 25-keV protons and H atoms with CO, CO_2, CH_4, and NH_3, 25:4963
MCNEESE, L. E., Engineering development studies for Molten-Salt Breeder Reactor Processing No. 1, 25:4138 (ORNL-TM-3053)
MCWHAN, D. B., High-pressure NMR study of metal--insulator transition of V_2O_3, 25:5224
MEADEN, G. T., Fluctuations and critical indices near Neel temperature of Eu, 25:5204
MECREDY, R. C., Prediction and measurement of acoustic wave propagation in two-phase media, 25:6079
MEEM, J. L., Doppler considerations for high-temperature gas-fueled cavity reactors, 25:5557
MEEMA, H. E., Interrelationships between cortical bone thickness, mineral mass, and mineral density in human radius: a roentgenologic-densitometric study, 25:4617 (CONF-680211-, pp 135-59)
MEEMA, Silvia, Interrelationships between cortical bone thickness, mineral mass, and mineral density in human radius: a roentgenologic-densitometric study, 25:4617 (CONF-680211-, pp 135-59)
MEGERTH, F. H., Prog. rpt. on Zircaloy-clad UO_2 fuel rod evaluation program, 2--4/70, 25:4886 (GEAP-10204)
MEHRISHI, J. N., Cell membrane characteristics of Ehrlich ascites tumour cells irradiated with small doses of ionizing radiations in the presence of radioprotective and radiosensitizing drugs, 25:4568
MEIER, Homer K., Numerical integration methods of Vlasov equation, 25:5097 (COO-2059-6)
MEINHOLD, Charles B., Sources of exposure to the public, 25:4518
MEISSNER, H. E., Magnetic properties of the rare earth hydroxides, 25:5202
MEKJIAN, A. Z., Isobaric analog resonance widths and distribution of Coulomb mixing strength in nuclei, 25:5644
MEKJIAN, Z., Coulomb mixing of isospin states. II, 25:5677
MELDE, G. F., Microstructure of mixed-oxide fuel irradiated in a thermal-neutron flux, 25:5953
MELLO, P. A., Time-dependent behavior of a classical model for reactions involving isobaric analog states, 25:5848
MELLON, Donald Williams, Transport properties of Gd--Th, Gd--Mg, and Y--Th alloys, 25:5169 (IS-T-379)
MELONI, Sandro, Aluminum and Si abundances of some Italian meteorites as determined by instrumental activation analysis, 25:4048
MENCHEN, William R., Nuclear safety program on the SNAP-23A power system, 25:4220
MENDELSON, Robert, Mass of ^{13}C and isobaric multiplet mass equation, 25:5640
MENDES, A. M., Phase and amplitude changes of vlf signals associated with PCA events, 25:5020
MENDEZ V., R. M., Variational analysis with harmonic-oscillator states for square potentials, 25:5849
MENDOLA, R., Nephropathy secondary to irradiation, 25:4714
MENDOZA, A., Radiation safety, 25:4528
MENEGHETTI, D., Depleted-uranium, nickel, and steel-reflected EBR-II critical assemblies on ZPR-3: experiments and calculations, 25:5563
Gamma-ray dose evaluations for ZPR-3/EBR-II critical assemblies, 25:6125
MENLOVE, H. O., Delayed-neutron abundances and half-lives from 14.7-MeV fission, 25:5775
MENNIGMANN, Horst-Dieter, Photoreactivation of E. coli after inactivation, 25:4728
MENZEL, J. H., Time-dependent neutron spectra measurements in water, 25:5489
MERLE, J. P., Hybrid method for spatial dynamic analysis, 25:6179
MERLIN, J., Application of internal friction to the study of graphitization, 25:4870
MERZ, H., Electronic density of states and crystal structure in IVA transition metals, 25:5187
MESHCHERYAKOV, M. G., Polarization of secondary protons in pp → π^+pn and pp → π^0pp reactions at 665 MeV, 25:5268 (JINR-P1-5293)
MESSERSCHMIDT, Otfried, Chemical protection of mice inflicted with irradiation and open skin wounds, 25:4576
MESSIAEN, A. M., Ion--electron resonances in bounded, hot plasmas with and without steady magnetic field, 25:5134
MESTVIRISHVILY, M. A., Behavior of diffractional peak width at high energies in case of Gaussian potential, 25:5424 (IFVE-STF-69-83)
METCALF, D. R., Two-group transport criticality solutions and associated continuum expansion coefficient resonance behavior, 25:6157
METROPOLIS, N., Comprehensive approach to computer arithmetic, 25:6238 (LA-4531)
MEYER, J. F., Sodium-vapor monitor, 25:6046
MEYER, Lois E., Use of Argonne National Laboratory computers in nuclear engineering education, 25:6194
MEYERS, R., Sublimed emitter and collector coatings, 25:4750 (TEE-4125-2)
MEZINCESCU, L. A., Duality and scattering lengths, 25:5363
MICHAELIS, W., Nuclear spectroscopy using radiative neutron capture and neutron-induced fission, 25:5474 (KFK-1197)
MICHAELSON, Sol M., Biological effects of microwave exposure: an overview, 25:4708 (UR-49-1256)
MICHAELSON, Solomon M., Effects of thoracic irradiation upon cardiopulmonary function in the dog, 25:4706
MICHEL, C., Magnetic properties of Ho_4Fe_{23} and $HoFe_2$, 25:5211
MICHEL, Chr, Chemical sensitization of the damaging effects on embryos produced by low radiation doses: the role of energy metabolism and immediate repair, 25:4575
MICHELS, L. C., Movement of fission gas bubbles and inclusions in mixed-oxide fuel, 25:6014
MICHIYOSHI, Itaru, Measurement of flow rate using temperature fluctuation caused by vortex street, 25:4205
MIDDELBOE, Victor, Accuracy and sensitivity in optical ^{15}N-analysis, 25:4019
MIERS, Richard Ernest, Production and loss of fast metastable He atoms during charge changing collisions, 25:4969
MIEZE, G., Analysis of a German pressure vessel and boiler drum statistics, 25:5982 (RISO-214, pp 301-22)
Reliability of a containment isolation system, 25:6150 (RISO-214, pp 71-90)
MIHAJLOVIC, A., Use of the potentiostat in the microstructural examination of uranium, 25:4792
MIHALAS, Dimitri, Stellar atmospheres, 25:4512
MIKAELSEN, K., Modifying effects of water content, oxygen, and cysteine on genetic effects of gamma and fast neutron radiations in barley seeds, 25:4604
MIKAILOFF, Hubert, Partial melting of low density mixed oxide $(U,Pu)O_2$ at beginning of irradiation, 25:4875 (CEA-CONF-1659)
MIKHAILOV, A. I., Deuteron acceleration in LHE synchrophasotron, 25:5445 (JINR-P9-5311)
MIKHAILOV, I. N., Formulating microscopic theory of nuclear collective motion, 25:5811
MIKHAILOV, S. K., Visualizing dislocation structure of Fe by etching in Ar flow, 25:4796
MIKOSHIBA, N., Nonlinear excess conductivity in superconducting aluminum films above the transition temperature, 25:5040
MILEDI, R., Autoradiography of labeled amino acids in giant squid synpase, 25:4418
MILIC-EMILI, J., Airway closure, 25:4428
Radioactive gases, 25:4663
Use of radioactive gas in the investigation of pulmonary function, 25:4666
MILLER, Esther S., /sup 99m/Tc labeling of erythrocytes, 25:4414
MILLER, G. H., Electric quadrupole transitions in muonic ^{208}Pb, 25:4953
MILLER, H., Preliminary report on a direct digital readout system for absorptiometric determination of bone mineral content, 25:4632 (CONF-700515-, pp 22-7)
MILLER, Henry C., Radiative np capture and meson exchange currents, 25:5545

MILLER, James R. C., For West Point's nuclear engineers: [reactor = computer], 25:6193
MILLER, L. B., Distribution of gamma energy deposition in a fast reactor, 25:5970
Importance of discrete-ordinate ray effects in fast reactor design studies, 25:6159
MILLER, R., Interstitial transfer in sodium systems, 25:4773
MILLHOLLEN, M. K., Subchannel coolant temperatures of EBR-II instrumented subassembly PNL-17(XX02), 25:6027
MILLHOUSE, A. H., Magnetic properties of Er-based binary rare earth alloys, 25:5207
MILLS, Carroll B., Rover: an intermediate step to gas, 25:6136
MIMA, Genjiro, Constitutional investigations on the miscibility gap in iron--chromium and iron--chromium--vanadium systems, 25:4787
MINER, W. N., Kondo effect in LaPu and PrPu alloys, 25:5227
MINES, J. R., Method of pseudo-bound states for stripping to unbound levels, 25:5666
MINGESZ, D. P., Further data on gamma-induced electrical charge and coloration of shielding glasses, 25:5166
MINGLE, J. O., Photon--electron transport. I, 25:5167
MINGUZZI-RANZI, A., Exotic resonances in K-d interactions at 3 GeV/c, 25:5287
MIOERNER, G., Four quandrant radiospirometry in normal and diseased states, 25:4671
MIQUEL, J., Incorporation of ^{14}C in cerebral glycogen of normal and x-irradiated rats, 25:4453
MIRES, R. W., Correlation structure of ^{6}Li, 25:5564
MIR-KASIMOV, R. M., Quasi-potential equation for the relativistic harmonic oscillator, 25:5405 (JINR-E2-5339)
MIROUZE, J., Application of two radio-immunological methods to the assessment of growth hormone, 25:4422
MISHIMA, J., Amount and characteristics of plutonium made airborne under thermal stress, 25:4258 (BNWL-SA-3379)
MISITI-DORELLO, P., In vitro radiosensitization of Ehrlich ascites tumour cells and pure enzymes by iodine compounds, 25:4569
MISRA, Balabhadra, In-flight coolant management considerations for NERVA reactor cooldown, 25:6132
MISRA, S. N., Mandelates of lanthanum, praseodymium, neodymium, and uranium, 25:4055
MISTRY, Vitthalbhai Dahyabhai, Isobaric analog resonances in proton elastic scattering from ^{110}Cd, ^{112}Cd, and ^{114}Cd, 25:5752
MISUSTOVA, J., Importance of hypothermy in the mechanism of the protective action of sodium fluoroacetate, 25:4580
MITCHELL, A. J., Reactions $^{14}N(p,^{3}He)^{12}C$, $^{14}N(d,\alpha)^{12}C$, $^{13}C(p,d)^{12}C$, 25:5563
MITCHELL, F. A., Survival-promoting effects of endotoxin in mice, dogs, and sheep, 25:4586
MITROFANOV, K. P., Photoeffect and internal conversion in resonant absorption of M1 gamma quanta by ^{119}Sn, 25:5787
MITSUI, Hiroshi, Radiation induced chain reaction and its application to polymer chemistry, 25:4097
MITUNOBU, S., Excitation of the giant resonance in ^{12}C by inelastic electron scattering, 25:5572
MIZUNO, Masao, Liquidus curve of ZrO_2--Y_2O_3 system measured by solar furnace, 25:4869
MO, T., Energy levels of ^{27}Al, 25:5613
MOAK, C. D., Charge states of 60-MeV iodine ions channeled in Au, 25:5164
MOBSBY, E. G. H., Pulsed ultrasonic thermometer. project dragon, 25:4388 (DP-Report-498)
Resonant probe ultrasonic thermometer, 25:4389 (DP-Report-590)
MOCKEL, A. J., Degenerate thermalization kernel for unit cell calculations, 25:6166
MOEKEN, H., Fissionable material balance and safeguards, 25:4266
MOELLER, H. Bjerrum, Exchange interactions in rare earth metals, 25:5213
MOH, Carl C., Application of nuclear energy to agriculture. Annual report, 25:4732 (NYO-2043-216)
MOHAN, S., Electron capture decay of ^{181}W, 25:5753
MOISEEVA, M. P., Research on studying and increasing the plasma parameters on ''non-cylindrical Z-pinch'' equipment, 25:5116 (SC-T-70-4046)
MOLL, E., Sensitive method for separate calculation of mineral content in cancellous and compact bone of the finger by a ^{125}I profile scanner. Effect of calcium and fluoride therapy on demineralized bone, 25:4636 (CONF-700515-, pp 169-87)
MOLL, H., Absorption of ^{45}Ca from intestinal tract of rat, 25:4430
MOLOKHIA, Mohamed M., Neutron activation analysis of trace elements in skin. IV, 25:4049
MONDAL, A. S., Non-mesonic decay of hypernuclei produced by K-mesons of 3.0 GeV/c momentum, 25:5277
MONFORT, J.-L., Ion--electron resonances in bounded, hot plasmas with and without steady magnetic field, 25:5134
MONTAGNANI, M., Aspects of design reliability of pressure tubes for heavy water moderated reactors, 25:5984 (RISO-214, pp 335-43)
MONTAGUE, D. G., Reactions $^{14}N(p,^{3}He)^{12}C$, $^{14}N(d,\alpha)^{12}C$, $^{13}C(p,d)^{12}C$, 25:5563
MONTHORY, M. C., Magnetic structure of Er_4WO_{12}, 25:5216
MOODER, L. E. J., Metallurgical properties of irradiated cold-worked Zr--2.5 wt. percent Nb pressure tubes, 25:4825
MOORE, Philip F., Drill core processing facility, 25:4307
MOORE, Richard, Evaluation of the significance of the contribution of coherent scattering of an X ray beam to darkening of radiographic film, 25:4640 (CONF-700515-, pp 205-23)
MOORE, Robert John, Reggeized-absorption model and related matters, 25:5433
MOORE, W. E., Space--time kinetics experiments and calculations for a loosely coupled core, 25:6185
MOORE, W. H., Radiosensitivity of immune responses, 25:4470
MOORHEAD, J. B., FORTRAN nuclidic-mass table with self-modification feature, 25:5735
MOORTHY, V. K., Sintering of beryllia. III, 25:4837
Sintering of thoria powders. V, 25:4836
MORAN, T. J., Sound propagation near magnetic phase transitions, 25:5186
MOREAU, J. M., Magnetic properties of Ho_6Fe_{23} and $HoFe_2$, 25:5211
MOREH, R., Study of the energy levels of ^{203}Tl using (γ,γ') reaction, 25:5713
MOREHOUSE, Charles Conover, Photoproduction of π^+ mesons from a polarized proton target at 5 and 16 GeV, 25:5251 (UCRL-19897)
MORETTO, Luciano G., Nucleus at the fission saddle point as activated complex, 25:5810
MORF, R., Quantum mechanical corrections for double Coulomb excitation in ^{152}Sm, 25:5781
MORGAN, C. S., Transmission electron microscopy of polycrystalline graphite, 25:4868
MORGAN, J. F., Scattering of α-particles from ^{12}C, 25:5561
MORGAN, Walter, Disorientation response of chicks which survived 2-β-aminoethylisothiouronium-Br-HBr (AET) administration during early embryogenesis, 25:4601
MORITA, K., Light-cone singularities of current commutators and modified Weinberg sum rules, 25:5364
MORITA, Makio, Radiation chemistry of foods. IV, 25:4117
MORITA, Masato, Internal conversion coefficients for electron-spin-polarized ^{57}Fe, 25:5659
MORK, H. M., Plutonium in soil, plants, and small mammals, 25:4478
MORONI, Max, Analog computer for calculating the ratio of amplitude of two pulses, 25:4362 (CEA-N-1314)
MOROSON, H., Effect of polycation on tumour cells in vivo, 25:4563
Methyl hydrazine radiosensitized Ehrlich ascites tumour cells, 25:4567
MOROSON, Harold, Radiation protection and sensitization. Proceedings of the second international symposium on radiosensitizing and radioprotective drugs, Rome, 6--8 May 1969, 25:4534
MOROZOV, V. M., Scattering of 4-MeV neutrons at angles close to 180°, 25:5762
MORRISON, G. C., Evidence for J/sup π/ = 8+ state in ^{16}O, 25:5592
MORROW, Andrew G., Animal-implanted nuclear powered pacemakers, 25:4238
MOSCONI, B., Omnes equation and superconvergence relations, 25:5427
Reaction $^{4}He(\gamma,d)d$ and 2^+ excited state of ^{4}He at 30 MeV, 25:5543
MOSHINSKY, M., Time-dependent behavior of a classical model for reactions involving isobaric analog states, 25:5848
MOSKALEVA, L. P., Production of ^{18}F fragments from Si, 25:5663
MOSS, F. E., Search for excess electron photo-ejection in liquid He, 25:5060 (NP-18484)
MOSS, Joel Marshall, In-beam proton--gamma ray coincidence studies using a large coaxial Ge(Li) detector, 25:5673
MOSTOVOI, Yu. A., Neutron spin and antineutrino momentum in neutron decay, 25:5258
MOTES, Bill G., On-line monitor of natural gas lines for ^{3}H and ^{85}Kr, 25:4352
MOTT, William E., Design of radioisotope heat sources for human implantation, 25:4229
Slow-neutron transmission analysis, 25:4035
MOVCHAN, L. A., Effects of radiation on catalytic properties of complexes of azomethanes and ions of transition metals, 25:4103
MOVSESYAN, M. A., Change of sodium potassium and calcium content in the heart muscle, 25:4698
MOZLEY, James M., Absorbed dose considerations for radiopharmaceuticals, 25:4511
MUDROVA, B., Production of carrier-free radiostrontium ^{85}Sr, 25:4126 (UJV-2431-Ch)
MUELLER, Dieter, Construction of trial functions for nuclear ground-state problems, 25:5838
MUELLER, Eva-Maria, Oxide fuel element thermal conductivity dependence upon porosity, 25:4856
MUELLER, George Paul, Applications of cluster expansion methods to extended nuclear mixtures, 25:5390
MUELLER-ARNKE, A., Electrodisintegration cross section of ^{4}He, 25:5530
MUKHAMEDZHANOVA, D., Influence of pollen radiation on crossing ability and variability in cotton, 25:4455
MULHERN, P. J., Excited states of ^{44}Ca, 25:5626
MULIGAN, David D., Chelation and radiation protection,

25:4553
MULLER, Richard A., Study of the reaction K-N → ΞK from threshold to 2.7 GeV/c, 25:5384
MULLIGAN, T. J., Level structure of ^{169}Er, 25:5725
MULLINS, L. J., Purification, encapsulation, and characterization of ^{238}Pu for implantation purposes, 25:4228
MUNOZ RIBADENEIRA, F. J., Possibilities of recovering copper from chalcopyrite by nuclear underground leaching in situ, 25:4176
MUNTUS, R., Ionic radii for use in geochemistry, 25:4085
MURANO, R., In vivo neutron activation analysis of total body bone mass, 25:4042 (CONF-680211-, pp 496-516)
MURATA, Toshifumi, Removal efficiency of charcoal filter for removing radioactive iodine, 25:4142
MURPHY, J. H., System thermodynamics and emergency core cooling systems, 25:6085
MURPHY, Kenneth, Isotope-powered, indwelling intracranial pressure sensor, 25:4241
MURPHY, Preston V., Development of a passive self-reading personnel dosimeter, 25:4376 (AD-710007)
MURR, L. E., Comparison of the substructures and properties of nickel, TD--Ni, Chromel-A, Inconel 600, and TD--NiCr following explosive-shock deformation, 25:4802
MURRAY, A. J., Spectrographic analysis response of a carrier to plutonium--uranium mixed oxides, 25:4015 (NUMEC-3524-76)
MURRAY, Kenneth M., Isospin of the ^{118} giant resonance, 25:5554
MURROW, Jack, Plugging of high efficiency filters by water spray, 25:4190 (UCRL-50923)
MURTY, G. T., High energy nuclear active particles in extensive air showers, 25:5275
MURTY, K. S. N., Decay of /sup 126m/Sb and the energy levels of ^{126}Te, 25:5693
MURTY, V. Radhakrishna, Decay schemes of ^{161}Tb and ^{103}Ru, 25:5714
Radioactive decay of ^{199}Au, 25:5698
MURYN, B., Decay distributions of resonances, 25:5375 (TPJU-15/70)
MUSAJO, L., ^{60}Co gamma-ray effect on mouse Ehrlich ascites tumour cells in the presence of some coumarin derivatives, 25:4565
MUSHER, Jeremy I., Electric polarizability of molecular hydrogen as calculated by use of the nonsymmetrical wave function, 25:4949
MUSIK, H., Reliability assessment of a novel liquid rod shut-down system, 25:6037 (RISO-214, pp 57-70)
MUSSO, G., Reliability evaluation of brittle materials and of welded structures, 25:4753
MUSTO, R., Allowed spectrum in dual-resonance models, 25:5428
MUTSURO, Naoshi, Photoneutron spectra of ^{31}P and ^{27}Al, 25:5648
MUZINICH, I. J., Density-matrix formalism for lepton--hadron scattering, 25:5331
MYATT, J., Miniature nuclear batteries, 25:4240
MYERS, L. S. Jr., Electron spin resonance studies of free radicals formed from orotic acid, 25:4093
MYERS, R. V., Effects of inert cell impurities on metal-cooled systems, 25:5988

N

NADJAKOV, E., Formulating microscopic theory of nuclear collective motion, 25:5811
NADOR, K., Radioprotective effect of N-substituted AET-derivatives having amino acid structure, 25:4577
NADZHAFOV, I. M., Polarized γ quanta scattering in nuclear field with production of e^+e^- pair and several photons, 25:5335
NAGAHAMA, Y., Temperature rise of specimen due to electron irradiation, 25:5163
NAGAI, Masakatsu, Bromouridine (BUdR) as a radiosensitizing agent of malignant brain tumours, 25:4688
NAGAMIYA, S., Anomalous orbital magnetism of proton deduced from magnetic moment of 11^- state of ^{210}Po, 25:5742
NAGATA, H., Protection of mice against ionizing radiations by adrenochrome monoguanylhydrazone methansulphonate; a promising agent for clinical use, 25:4589
NAGY, A. Z., Two-dimensional (T/sub 1/2/, E/sub γ/) mapping of short-lived nuclides, 25:5685 (KFKI-70-18-NAC)
NAGY, Zs., Analysis of the radioprotective effect of cysteine on Escherichia coli strains, 25:4554
X-ray sensitivity of E. coli B cells as affected by cysteine, 25:4555
NAIR, K. Manikantan, Effect of oxygen activity on structure of ZrO_2, 25:4878
NAKADA, A., Excitation of the giant resonance in ^{12}C by inelastic electron scattering, 25:5572
NAKAGAWA, Takemi, Reaction (^{3}He,α) on ^{7}Li from 5.0 to 8.0 MeV, 25:5571
NAKAHARA, K., Excitation of the giant resonance in ^{12}C by inelastic electron scattering, 25:5572
NAKAI, K., Quadrupole moments excited states in ^{20}Ne and ^{22}Ne, 25:5622
NAKAMOTO, K., Metal isotope and high pressure effects on the infrared active skeletal vibrations in metal sandwich compounds, 25:4067
NAKAMURA, S., Coarse mesh acceleration of S/sub N/ iterations, 25:6154
NAM, Sang Yul, LDH of rats exposed to gamma-irradiation, 25:4605
NARASIMHA RAJU, M. L., 437-keV beta transition in the decay of ^{125}Sb, 25:5730
Validity of xi approximation of the 1400 keV beta decay in ^{143}Ce, 25:5700
NARAYANAN, G. Hari, Comments on phase transformations in beta isomorphous titanium alloys, 25:4805
NARDI, A. J., Westinghouse Plutonium Fuels Development Laboratory, design philosophy, and startup experience, 25:4302
NARDI, Eran, Neutron emission in alpha-particle-accompanied fission, 25:5723
NATESAN, K., Thermodynamic and kinetic aspects of carbon transport in sodium--steel systems, 25:4755
NAUGOLNYKH, K. A., Dynamics of vapor bubbles in liquid hydrogen and ultrasonic bubble chambers, 25:4371 (JINR-P13-5327)
NAUMOV, A. N., Diffusion and isotope effect of lithium-ion diffusion in crystalline silver chloride, 25:5172
NEEF, N., Influence of single irradiation and heat treatment on the properties of BeO, 25:4892
NEFEDOVA, M. N., Effect of substituents on hydrogen exchange reaction of some ferrocene derivatives, 25:4069
NEGRO, V., New cosmic-ray ionization measurements at balloon altitudes, 25:4950
NEIMARK, L. A., Movement of fission gas bubbles and inclusions in mixed-oxide fuel, 25:6014
Postirradiation observations of sodium-bonded (U,Pu)C fuels, 25:4894
Profilometer for dimensional inspection of irradiated LMFBR fuel elements, 25:6033
NEIMOTIN, E. I., Neutron velocity spectrum in heavy nuclei, 25:5492
NEKHENDZI, Yu. A., Properties of the chromium--nickel alloys containing niobium and molybdenum, 25:4782
NELP, W. B., In vivo neutron activation analysis of total body bone mass, 25:4042 (CONF-680211-, pp 496-516)
NELSON, J. M., Reactions ^{14}N(p,^{3}He)^{12}C, ^{14}N(d,α)^{12}C, ^{13}C(p,d)^{12}C, 25:5563
NELSON, J. W., Energy levels of ^{27}Al, 25:5613
Mass of ^{39}Ca, 25:5610
NEMCHENKO, V. F., Temperature dependence of electric conductivity and thermal electromotive forces in the homogeneous carbide alloy regions of titanium and niobium, 25:5176
NEMNONOV, S. A., Position of K-absorption edges of Fe in Fe--Al and Fe--Mo alloys, 25:5181
NEMTSEVA, L. S., Chromosome damages induced by γ-ray doses in Crepis capillaris, 25:4498
NENTWICH, D., Development of safeguards procedures for a reprocessing plant similar to the WAK type, 25:4263 (KFK-1102)
NERSESYAN, A. N., Violation of independence of decay of compound nucleus, 25:5636
NESHPOR, V. S., Superconductivity of titanium carbide, 25:5038
NESS, Norman F., Magnetic structure of interplanetary space, 25:4926
NEUBAUER, H., Neutron microdosimetry for rabbit eye, 25:4521
NEUENDORF, W. P., Radiation quantities from a moving source of radiation, 25:5243
NEUHOLD, R. J., Multiple reaction rate weighting in fast reactor space-energy synthesis, 25:5966
NEVEU, A., Divergences and renormalization in multiloop dual diagrams, 25:5409
NEWMAN, Perry A., Neutron-transport problem for slab with infinite reflectors, 25:5501
NEWMAN, Perry Allan, Time dependent monoenergetic neutron transport in a finite slab with infinite reflectors, 25:5498
NEWTON, J. O., Oblate shape of $^9/_2^-$ isomer in ^{199}Tl, 25:5707
NGUYEN, Dong H., Measurement of neutron diffusion lengths in highly absorbing solutions, 25:6183
NGUYEN VAN NHUNG, Magnetic structure of ErSi, 25:5212
NIAS, A. H. W., Effects of caffeine on sensitivity to ultraviolet light of HeLa cells, 25:4607
NICHOLAS, C. J., Frozen polarized target, 25:5466 (RPP/A-81)
NICHOLSON, Patrick S., Possible contribution of diffusive grain-boundary pore growth to creep deformation of ceramic materials, 25:4848
NICODEMI, F., Allowed spectrum in dual-resonance models, 25:5428
NICOLAI, Leland M., Properties of high current free-burning arcs in air, 25:5093
NICOLAU, Cl., Kinetic investigations on the influence of radiosensitizing vitamin K_3 on the haemoglobin-methaemoglobin equilibrium, 25:4598
NIEDZIELSKI, J., Radiolysis of ethylene in presence of hydrogen sulfide, 25:4122
NIEHAUS, R. J., Radial velocity observations of μ^1 Bootis, 25:4904
NIELSEN, H. L., E2 strength of 191 keV transition in ^{197}Au, 25:5709
NIELSEN, M., Exchange interactions in rare earth metals, 25:5213
NIELSEN, P. E., Theory of thermoelectric power in metals

and alloys, 25:6227 (COO-623-152)
NIILER, A., Phase shifts from n--^{4}He elastic scattering experiments near 20 MeV, 25:5508 (LA-4465, pp 1.1-2)
Polarization of 22-MeV neutrons elastically scattered from liquid tritium and deuterium, 25:5516 (LA-4465, pp 15.1-2)
NIKITIN, V. P., Superconductivity of titanium carbide, 25:5038
NIKOLAEV, N. N., Y(1327) hyperon, 25:5385
NIKOLAEV, V. A., Influence of neutron flux on dispersion-hardening steels, 25:4817
NIKOL'SKII, G. S., Magnetoresistance of Er--Y alloys at low temperatures, 25:5175
NILSSON, A.-M., Isotopic exchange reaction between ammonium bromide and butyl bromide, 25:4071
Radioelectrochemical determination of microgram iodide, 25:4027
NILSSON, Bo E., Bone densitometry using a single beam from a radionuclide source, 25:4627 (CONF-680211-, pp 319-28)
NISHIDA, Atsuhiro, Origin of geomagnetic variations, 25:5025
NISHIO, Gunji, Process of carburization in austenite stainless steel, 25:4739 (JAERI-Memo-4132)
NISLE, R. G., Measurements of fast-neutron capture integrals in CFRMF, 25:5656
NIZZA, Pierre, Physiological data on swine for use in radiobiology: plasma and blood volumes, 25:4411 (CEA-R-4031)
NOBLE, L. D., SEFOR experiments, 25:6658
NODEAN, Walter Charles, Response of a coupled-core reactor to a localized oscillation of the absorption cross section, 25:6148
NOF, A., Study of the energy levels of ^{203}Tl using (γ,γ') reaction, 25:5713
NOGGLE, T. S., Charge states of 60-MeV iodine ions channeled in Au, 25:5164
NOGUCHI, Tetsuo, Liquidus curve of ZrO_2--Y_2O_3 system measured by solar furnace, 25:4865
NOMURA, Masao, Multiplicity of states in a single shell, 25:5829
NOMURA, T., Anomalous orbital magnetism of proton deduced from magnetic moment of 11$^-$ state of ^{210}Po, 25:5742
E2 effective charges of the f/sub 7/2/ proton and neutron, 25:5646
NOON, Edward L., RTG/radioisotope heater shielding for sensitive science instruments on spacecraft, 25:4246
NOONAN, Thomas W., Cosmic density, 25:4932
NORCO, J. E., Multiple-source urban atmospheric dispersion model, 25:4161 (ANL/ES-CC-7)
NORDIN, B. E. C., Bone patterns in aging and osteoporosis, 25:4618 (CONF-680211-, pp 159-77)
Internal relationships between skeletal parameters in twenty-three male skeletons, 25:4652 (CONF-700515-, pp 365-82)
NORDYKE, Milo D., Use of multiple explosives for nuclear gas stimulation, 25:4173
NORMAN, J. C., Studies on dogs with implanted ^{238}Pu sources, 25:4432
NORMAND, E., Radiation transport analyses of nuclear rocket engine components, 25:6128
NORRIS, R. J., Material worth measurements in benchmark critical assembly on ZPPR, 25:6115
Predicted characteristics with actual observation for ZPPR-2, 25:6113
NORSEEV, Yu. V., Adsorption of monovalent astatine cation by cesium phosphotungstate and hydrated tungsten oxide from nitric acid solutions, 25:4053 (ANL-Trans-861)
NOTEA, A., Atomic nuclear resolution of beta backscattering gauges, 25:4386
NOVAK, A., Infrared and Raman spectra of pyrazinium halides, 25:4068
NOVAK, L., Importance of hypothermy in the mechanism of the protective action of sodium fluoroacetate, 25:4580
Radioprotective effects of sodium fluoroacetate and its probable mechanism of action, 25:4579
NOVIK, K. M., Spreading of high-frequency plasma along magnetic field, 25:5132
NOVIKOV, N. P., Chemical action of laser radiation on acetylene, 25:4070
NOVIKOV, V. I., Superconductivity of titanium carbide, 25:5038
NOVIKOVA, I. S., Photometric determination of Nb with reagent PAR in complex Cu-base alloys, 25:4018
NOVOSELOV, G. P., System MoO_3--BaO, 25:4873
System MoO_3--CeO_2, 25:4872
NOWAK, M. J., Low-energy photon transport in liquid nitrogen, 25:5148
NUEHRENBERG, Juergen, Difference scheme for Vlasov's equation, 25:5096 (COO-2059-5)
NUMRICH, Susan K., Survey on photon activation analysis using NRL Linac, 25:4041 (AD-709501)
NURMIA, Matti, Alpha decay of ^{255}No and ^{257}No, 25:5704
NYGAARD, K., Reduction of noise in closed loop servo systems, 25:6188 (AE-404)
NYSTROEM, G., Neutron capture cross sections in F, Mg, Al, Si, P, and S from 20 to 80 keV, 25:5603 (FOA-4-4440)
NYSTROM, R. E., Time-dependent nucleate boiling requirements for liquid sodium, 25:4210

O

OAKES, M. E., Suppression of Kelvin--Helmholtz instability in Cs plasma, 25:5111
OBOUSSIER, F., State of supply of the community with nuclear fuels, 25:5880
O'BRIEN, Keran, Monte Carlo unfolding of neutron spectra, 25:4367
OBU, Mitsuaki, Analysis of ^{58}Ni(n,p)^{58}Co reactions, 25:5638
OBUKHOV, A. A., Spreading of high-frequency plasma along magnetic field, 25:5132
Wave transformation conditions in plasma, 25:5131
OCHIAI, Fumio, Program for analysis of bubble-chamber photographs, 25:4372 (SJC-T-70-3)
OCKERS, S. T., Hydrogen supercharging during thermal cycling of zirconium, 25:4756
O'CONNELL, J. S., Trinucleon form factors calculated from realistic local potentials, 25:5833
ODELL, T. T. Jr., Effects of estradiol on splenic repopulation in irradiated mice, 25:4471
ODOR, D. L., Kodak type III film for photodosimetry, 25:4383
OEBERG, P. Aa., Spectrometry for determination of isotopic mixtures, 25:4031
OESTLING, S. G., Spectrometry for determination of isotopic mixtures, 25:4031
OESTMANN, M. J., Tritium sources and release to the environment, 25:5941
OEZISIK, M. N., Effects of transverse flow on fission product transport through graphite tubes, 25:6011
OGANESYAN, Yu. Ts., Fission of excited nuclei, 25:5651
Possibilities of isotope synthesis in fission reaction, 25:5756
Synthesis of element 105, 25:5757
OGURA, Nobukazu, Breaking at the welds, 25:4781
OHANIAN, M. J., Novel, high counting rate neutron detection system, 25:4354
OHL, Rolf, Activity of respiratory protection working group, 25:6235 (LA-4442-TR)
OHLSEN, G. G., Comparison of double scattering and polarized ion source measurements of ^{4}He(d,d)^{4}He polarization at 11.5 MeV, 25:5510 (LA-4465, pp 3.1-3)
Neutron polarization in the T(d,n)^{4}He reaction using a polarized incident beam, 25:5513 (LA-4465, pp 12.1-2)
OHLSEN, Gerald G., Absolute beam polarization determination for the LASL Lamb-shift source by the quench ratio method, 25:5453 (LA-4465, pp 10.1-2)
Analyzing power of the T(d,α)n reaction at low energies, 25:5525 (LA-4465, pp 34.1-2)
Considerations on polarized neutron production by (d,n) polarization transfer reactions at 0°, 25:5805 (LA-4465, pp 26.1-2)
Figures of merit for polarized deuteron beams, 25:5455 (LA-4465, pp 23.1-2)
Formalism for A(d,n)B or A(d,p)B polarization transfer reactions, 25:5803 (LA-4465, pp 20.1-2)
Formalism for A(p,p)A and A(d,d)A polarization transfer, 25:5804 (LA-4465, pp 21.1-2)
Measurement of the vector and tensor analyzing power of d--^{4}He elastic scattering at 12 MeV, 25:5553 (LA-4465, pp 25.1-2)
Performance of the LASL polarized source, 25:5452 (LA-4465, pp 9.1-2)
Precise method for the determination of secondary standards for deuteron analyzing tensors, 25:5806 (LA-4465, pp 27.1-6)
Preliminary measurements of neutron polarization from the D(d,n)^{3}He reaction using a polarized incident beam, 25:5514 (LA-4465, pp 13.1-2)
Proposal for a Lamb-shift polarimeter, 25:4351 (LA-4465, pp 17.1-6)
Quadratic relations between the T(d,n)^{4}He observables, 25:5519 (LA-4465, pp 22.1-2)
Rapid method for the measurement of analyzing tensors in reactions induced by polarized deuterons, 25:5802 (LA-4465, pp 11.1-2)
Study of ^{3}He(d,d)^{3}He scattering at 10 and 12 MeV, 25:5520 (LA-4465, pp 24.1-2)
Study of the ^{3}He(d,p)^{4}He reaction, 25:5512 (LA-4465, pp 6.1-2)
Transfer matrix method for calculating spin aberrations in the transport of polarized beams, 25:5454 (LA-4465, pp 18.1-16)
OHNEDA, Akira, Extraction of plasma insulin in radioimmunoassay, 25:4420
OHTSUBO, Akira, Measurement of flow rate using temperature fluctuation caused by vortex street, 25:42C5
OIE, H. K., Uv inactivated virion preparations and cell death, 25:4729
OKABE, Hisataka, Program for analysis of bubble-chamber photographs, 25:4372 (SJC-T-70-3)
OKABE, Shigeru, Current profile monitor for scanning electron beam, 25:5468
OKAJIMA, Kazuhisa, Thermodynamic study on the activities of both components in binary molten alloys, 25:4754
O'KEEFE, T. J., Magnetic properties of Ho_6Fe_{23} and $HoFe_2$, 25:5211
O'KELLEY, G. D., Decay of ^{196}Au, 25:5728
OKOLICSANYI, L., Nephropathy secondary to irradiation, 25:4714

XUM

OKUN, L. B., Y(1327) hyperon, 25:5385
OLDBERG, S. Jr., Mechanical model of thermal differential expansion at first startup of a mixed-oxide fuel pin, 25:6000
OLDFIELD, W., Bubble migration in UO_2, 25:4853
OLINESCU, R., Kinetic investigations on the influence of radiosensitizing vitamin K_3 on the haemoglobin-methaemoglobin equilibrium, 25:4558
OLIVE, D. I., Veneziano amplitudes for Reggeons and spinning particles, 25:5440
OLIVERIOR, A., Titanous chloride in the quantitative determination of As, Sb, and Bi, 25:6239 (MLM-1766(TR))
OLIVIERI, E., Quadrupole force in nuclear spectroscopy, 25:5809
OLNESS, J. W., Lifetime of 5- 4585 keV ^{38}Ar level, 25:5664
OLSEN, A. R., Thermal performance and restructuring of pellet and sphere-pac fuels, 25:5592
OLSEN, H. N., Absorption corrections for optically thick plasmas, 25:5088 (AD-710218)
OLSON, A. P., Predicted characteristics with actual observation for ZPPR-2, 25:6113
OLSON, D. J., Coolant flow distribution during decompression of a single-loop simulated PWR system, 25:6084
OLSON, R., Additional system for bone densitometry studies, 25:4634 (CONF-700515-, pp 33-47)
OLSON, R. E., Westinghouse Plutonium Fuels Development Laboratory, design philosophy, and startup experience, 25:4302
OLSON, R. S., New small mass critical configuration, 25:6101
OLSON, Robert S., Enzyme inactivation with ultraviolet laser energy (2650 Angstroms), 25:4461
OLSSON, R. G., Pore characteristics of carbons, 25:4856
OLTMAN, B. G., Curium-244 and ^{145}Sm--^{145}Pm x-ray sources, 25:4647 (CONF-700515-, pp 274-5)
Use of sparking techniques to enhance track-etch radiographs, 25:4348
OMBRELLARO, P. A., Synthesis of fast reactor spectra, 25:5961
OMHOLT, A., Ionization in auroras detected by atomic oxygen and nitrogen lines, 25:5009
ONDREJ, M., Brood pattern of crossovers in Drosophila males, 25:4481
O'NEILL, G. L., Behavior of Pu recycle fuel in a SPERT power transient, 25:5996
Plutonium homogeneity in thermal recycle fuels, 25:4874
ONG, Andrea Sy, Prog. rpt. on diffusion in solids, annual, 11/69--10/70, 25:5152 (ORO-3508-6)
OOSTERKAMP, W. J., Automatic counting of solid-state fission track recorders, 25:4343
Calculation of the reactivity worth of small samples, 25:6117
OPARA, U., Photoproduction of K+Λ and K+I° from H, 25:5253
ORAN, William, Radiation degradation of selected films, 25:4406 (N-70-35843)
ORAVEC, J., Some radioactive characteristics of calcium, 25:5647
OREAR, Jay, Some reactions at high momentum transfer at NAL, 25:5281 (CONF-700314-, Paper 15)
OREFICE, A., Korteweg--De Vries equation for drift waves, 25:5127
ORIHARA, Hikonojo, Reaction (^{3}He,α) on ^{7}Li from 5.0 to 8.0 MeV, 25:5571
ORMEROD, M. G., Repair of DNA and the mode of action of sensitizers and protectors in biological systems of different complexity, 25:4536
ORPHAN, V. J., Epithermal-neutron capture gamma rays from shield materials: depleted uranium, 25:5776
High-resolution (n,xγ) cross-section measurements using Linac, 25:5657
ORSETTI, A., Application of two radio-immunological methods to the assessment of growth hormone, 25:4422
ORSINI, A., Pulmonary hemosiderosis in a 9-year old child with a trisomy 18, 25:4685
ORT, M., Absorptiometric bone mineral determination using ^{153}Gd, 25:4649 (CONF-700515-, pp 308-12)
ORTH, D. A., Process engineer's views [on implications of ANSI Criticality Safety Standard N16.1], 25:4287
ORZALESI, C. A., Radiative corrections to weak semileptonic decays and commutator ambiguities, 25:5341
ORZALESI, Claudio A., Charges and generators of symmetry transformations in quantum field theory, 25:5416
OSANOV, D. P., Measurement of dose buildup factors for low-energy point isotropic gamma sources in water, 25:5136
OSMAN, A., Faddeev equations and cluster model approximations, 25:5858
OTT, K. O., Subcritical fast reactor as a university research facility, 25:6095
Successive space-energy synthesis for fast reactors, 25:5962
OTTAVI, Henri, Mathematical processing of scintigraphic images, 25:4611 (CEA-R-3920)
OTTOLENGHI, Athos, Prog. rpt. on the effect of radiation on mucosal phospholipase activity, 1967--70, 25:4455 (ORO-3329-7)
OTWAY, Harry J., Method for estimating risk from Plowshare detonation, 25:4172
Risk estimate for an urban-sited research reactor, 25:6103
OWEN, W. S., Effects produced by adding Re to alloys of W and C, 25:4746 (AD-710275)
OWENS, D. R., Differential concentration gas chromatograph for the analysis of low levels of impurities in He, 25:4012 (DP-Report-443)
OYAMADA, M., Excitation of the giant resonance in ^{12}C by inelastic electron scattering, 25:5572
OYANAGI, Yoshio, K/sub 13/ form factors of the Venezianc type, 25:5338

P

PACANSKY, Jacob, Matrix-isolation spectra of H_2S and D_2S, 25:4066
PACCARD, Dominique, Magnetic properties and magnetic structures of rare earth--Ni equiatomic compounds, 25:5209
Magnetic properties of R_2M compounds of rare earth and transition metals, 25:5199
PACKAN, N. H., Voids in re-irradiated aluminum, 25:4816
PADDEN, T. R., Type 316 stainless-steel tubing for LMFBR fuel element cladding, 25:4776
PADILLA, Andrew Jr., Quasi three-dimensional approach for estimating sodium voiding incoherency, 25:6071
PAES DE BARROS, M. H., Phase and amplitude changes of vlf signals associated with PCA events, 25:5020
PAESOLD, G., Determination of O, water, and N in refractory metals. V, 25:4022
PAIGE, D. M., Contact maintenance and equipment evaluation after six years of continuous remote operation inside a hot cell, 25:4300
Entering a hot cell after six years of remote spent-fuel processing, 25:4295
PAIK, N. C., Material worth measurements in benchmark critical assembly on ZPPR, 25:6115
Predicted characteristics with actual observation for ZPPR-2, 25:6113
PAILTHORP, K. G., In vivo neutron activation analysis of total body bone mass, 25:4042 (CONF-680211-, pp 496-516)
PAIS, A., Weak interactions at high energies, 25:5339 (CONF-700314-, Paper 7)
PAJEWSKI, M., Double contrast examination of small intestine, 25:4686
PAK, Charles Y. C., Clinical use of an in-vivo measurement of bone mineral content, 25:4625 (CONF-680211-, pp 296-308)
PAKHOMOV, V. I., Dielectric permeability of an inhomogeneous relativistic stream of cold plasma, 25:5101
PAL, Yash, Electron--photon component of cosmic rays, 25:4980
PALAZZUOLI, V., Renal clearance of radiophosphate in thyroid disease, 25:4451
PALEV, Ch. D., Example of the infinite-component local field with the mass spectrum, 25:5406 (JINR-P2-5305)
PALITTI, F., Radioprotection and modification of glycolysis in Ehrlich ascites tumour cells, 25:4566
PALMA, G., Polymerization induced by gamma radiation of styrene under pressure, 25:4104
PALMAS, G., Absorption and distribution of ^{137}Cs by Trifolium pratense, 25:4449
PALMER, H. E., In vivo neutron activation analysis of total body bone mass, 25:4042 (CONF-680211-, pp 496-516)
PALMS, J. M., Electron capture decay of ^{181}W, 25:5753
PAN, Kee-chuan, Gaussian geminals for electron pair correlation, 25:4973
PANDEY, R. C., Influence of magnetic-dipole and electric-quadrupole interaction of the γ--γ angular correlation, 25:5746
PANOVA, V. P., Measurement of dose buildup factors for low-energy point isotropic gamma sources in water, 25:5136
PAPAIOANNOU, G. M., Remarks on π+-photoproduction with linearly polarized photons, 25:5321 (DEMO-70/1)
PAPAY, Lawrence, Waste heat and fog control, 25:5886
PAPIER, J. J., Ion--electron resonances in bounded, hot plasmas with and without steady magnetic field, 25:5134
PAPIROV, I. I., Crystal structure of Be at 77 to 300° K, 25:4795
PAQUETTE, R. C., Analysis of neutron distributions in ZPPR/FTR-2 shield experiments, 25:6124
PARDUE, W. M., Compressive creep of UO_2--22 percent PuO_2, 25:4861
PARIBOK, V. P., Effect of fractionated x irradiation on the root-tip cells, 25:4492
PARIKH, J. C., Occupancy of spherical shells in the ground state of even 2s-1d shell nuclei, 25:5876
PARISI, G., Deep inelastic scattering and the nature of partons, 25:5330
PARK, Chang Kyu, Insect pest control using sterile-male technique. I, 25:4735
PARK, Seung Heui, Insect pest control using sterile-male technique. I, 25:4735
PARKER, E. N., Report on quasi-stationary modulation papers, 25:4982
PARKER, Richard C., Multiplication effects in measurements of delayed-neutron energy spectra, 25:5774
PARKER, W., Rapid simultaneous elution and electrodeposition of radioactive nuclides adsorbed on paper, 25:4030

PARKINSON, Ronald Y., Radioisotope heat source, 25:4217
PARLEE, N. A. D., Application of nitride-forming reactions to reprocessing of spent nuclear fuels, 25:4149
PARTAIN, W. L., Radiant heat transfer in heated aerosols at 100 atmospheres pressure, 25:6135
PARTHIER, S., Prospects of automation in the control of nuclear power plants, 25:5879
PASHKEVICH, V. V., Equilibrium deformations of rare-earth and transuranium nuclei, 25:5660
PASHKIN, Yu. G., Precision of Wigner's approximation, 25:5480
PASK, C., Non-central forces in low energy nuclear physics, 25:5863
PASYNKOV, I. G., Reconstruction of NN potentials from nuclear data, 25:5831
PATEL, B. M., Chemical separation and spectrographic determination of trace amounts of rare earths in uranium using LiF--AgCl carrier, 25:4021
PATEL, C. C., Antipyrine complexes of Ti(IV), Zr(IV), Th(IV), and U(VI) perchlorates, 25:4087
PATEL, K. C., Variation in ascorbic acid content and ascorbate-oxidase activity during germination in dark of γ-irradiated castor seeds, 25:4466
PATEL, R. D., Variation in ascorbic acid content and ascorbate-oxidase activity during germination in dark of γ-irradiated castor seeds, 25:4466
PATHAK, B. P., Decay of /sup 126m/Sb and the energy levels of ^{126}Te, 25:5693
PATHAK, K. M., Development of water Cherenkov counter, 25:4375
PATRESE, P., Nephropathy secondary to irradiation, 25:4714
PATRIKEEV, Yu. I., Influence of neutron flux on dispersion-hardening steels, 25:4817
PATTERSON, D. E., Fire protection criteria for nuclear facilities, 25:4194
PATTERSON, James H., Alpha-scattering technique of chemical analysis, 25:4034
PATTON, W. A., Computer analysis of fission data, 25:5790
PAUL, R. C., Carboxylates of metals. I. Uranium(IV) carboxylates, 25:4057
Carboxylates of metals. II. Thorium carboxylates, 25:4056
PAULSEN, A., Excitation functions (n,2n) for ^{93}Nb and ^{103}Rh, 25:5766
PAUTHENET, Rene, Magnetocrystalline properties of single crystals of rare earths of the second series, 25:5194
PAVLOV, Yu. A., Mechanism of the interaction of V_2O_5 with C. II, 25:4842
PAVLOVSKAYA, N. A., Photometric determination of low amounts of thorium in biological materials, 25:4443
PAVLOVSKII, O. A., Passage of electrons through matter, 25:4938
PAXTON, H. M., Dynamic strain aging in 304 stainless steel, 25:4777
PAZ-CASTILLO, Fernando, Recovery of high-viscosity petroleum by steam from geothermal heat, 25:4174
PAZOISKI, S. V., Role of static charge of nucleus in determining the probability of E0 pair conversion, 25:5791
PEACOCK, N. J., Measurement of plasma parameters in Tokamak T3-A by Thomson scattering, 25:5079 (CLM-R-107)
PEARSON, Dale A., Comparison of foil activation techniques and other methods in fast-neutron spectrum measurements, 25:4357
PEEK, N. F., Energy levels of ^{156}Gd, 25:5705
PEERY, Benjamin F., Search for ^{26}AlH in spectra of technetium stars, 25:4895
PEISHEL, F. L., Design and installation of TURF californium facility, 25:4304
PEKARSKII, G. Sh., Control of reinforced concrete construction by means of fast neutrons, 25:4249
PELLEGRINI, G., Lattice thermal expansion of pyrocarbons produced in a fluidized bed, 25:4854
PEMBER, L. A., Correlation of predictions and observations in mixed-oxide fuel, 25:6001
PENIONZHKEVICH, Yu. E., Possibilities of isotope synthesis in fission reaction, 25:5756
PENIONZHKEVITCH, Yu. E., Fission of excited nuclei, 25:5691
PENN, A. W., Miniature nuclear batteries, 25:4240
PENNER, H., Effect of electron rays on the strength of the exocarp of cherries, 25:4721
PENNINGTON, W. Herbert, Animal-implanted nuclear powered pace-makers, 25:4238
PEPKOWITZ, L. P., Availability and cost of ^{10}B for reactor control, 25:5975
PEPPARD, D. F., Two octyl phenyl phosphinic acids, (R)(C_6H_5)PC(OH), as extractants for selected M(III) and M(VI) metallic cations, 25:4147
PERCUS, Jerome K., Exact bounds on transport coefficients, 25:6242 (NYO-1480-160)
PERDEREAU, Bernard, Physiological data on swine for use in radiobiology: plasma and blood volumes, 25:4411 (CEA-R-4031)
PERESSE, J., Generalized oscillator strengths for $1^1S \rightarrow 2^1S$ transition in He, 25:4959
PEREVALOV, A. V., Space--energy and time distribution of neutrons in boron-containing media, 25:4159
PEREZ, Lawrence J. Jr., Population safety considerations of an implantable isotopic power source, 25:4236
PEREZ, R. B., Measurement of capture cross section of ^{238}U, 25:5771
PEREZ, S. M., GAMMA particle-hole states in ^{208}Pb, 25:5788
PEREZ-Y-JORBA, J., Production of vector mesons by e^+e^- annihilation, 25:5250 (DNPL/R-7, pp 135-72)
PERIN, A., Radiosensitizing effect of L-erythro-α,β-dihydroxybutyraldehyde on Ehrlich ascites tumour cells. Cytokinetic analysis of tumour growth, 25:4564
PERKINS, M. W., Integral gamma-ray production cross-section measurements with Pu--Be neutron source, 25:5582
PERMYAKOV, V. P., Lower bounds for the scattering parameters, 25:5425 (JINR-P4-5332)
PERONA, J. J., Design and safety considerations in the shipment of solidified wastes, 25:4278
PERRIMOND, H., Pulmonary hemosiderosis in a 9-year old child with a trisomy 18, 25:4685
PERROT, M., Remote handling in operation of the installation ATTILA, 25:4261 (CEA-R-4067)
PERRY, K. J., Microstructure of mixed-oxide fuel irradiated in a thermal-neutron flux, 25:5993
PETERS, Laurence E. Jr., Thermal neutron absorber buildup in irradiated beryllium, 25:4814 (N-70-32313)
PETERSEN, E., IBM interactive reactor computation system, 25:6149
PETERSON, D. M., Large accidents, 25:6089
PETERSON, David Dee, Study of low-energy, heavy cosmic rays using a plastic charged-particle detector, 25:4373
PETERSON, W. S., Considerations in the evaluation of aluminum master alloys, 25:4780
PETKOV, I. Z., Reactions in complete fusion of nuclei, 25:5115 (JINR-P4-5019)
PETKOV, I. Zh., Optical potential for high-energy scattering, 25:5861
PETTERSSON, H., Internal-conversion studies of low-energy transitions in ^{149}Sm and ^{151}Eu, 25:5695
Transitions in decay chain ^{144}Gd to ^{140}Eu to ^{140}Sm, 25:5694
PETTIE, C. B., Determination of foam density, 25:6220 (BDX-613-180)
PETUKHOV, B. S., Boiling of liquid alkali metals in tubes, 25:4202 (BNL-tr-365)
PEYRESBLANQUES, H., Twelve years of health physics in a plutonium production plant, 25:4526
PFANNENSTIEL, P., Problems of radiation dosimetry in endolymphatic therapy, 25:4512
PFLASTERER, G. R., SEFOR experiments, 25:6058
PHIL, D., Mineral density in normal and osteoporotic bone, 25:4629 (CONF-680211-, pp 411-21)
New method of evaluating bone loss in osteoporosis, 25:4639 (CONF-700515-, pp 199-204)
PHILLIPS, C. A. G., Survey of pressure vessels built to a high standard of construction, 25:5983 (RISO-214, pp 323-34)
PHILLIPS, G. C., Proton--proton quasi-free scattering in the p + d → p + p + n reaction for E/sub p/ = 4.5 to 13.0 MeV, 25:5534
PHILLIPS, T. W., M1 giant resonance in ^{208}Pb from threshold photoneutron measurements, 25:5795
PHILLIPS, W. R., Electron and gamma transitions in ^{48}Sc, 25:5624
PHILLIPS, William A., Radionuclide distribution in particles produced by the Schooner Event, 25:4186
PIANTELLI, F., Absorption and distribution of ^{137}Cs by Trifolium pratense, 25:4449
PIATTI, Giovanni, Fibre-reinforced alloy, 25:4742
PICCHI, P., Tests of models of scale invariance with cosmic-ray neutrino data, 25:5340
PICKETT, A. G., Survey report on structural design of piping systems and components, 25:4188 (TID-25553)
PICKLES, D. C., Frozen polarized target, 25:5466 (RPP/A-81)
PICOZZA, P., Meson effects in high-energy photodisintegration of light nuclei, 25:5547
PIENE, K., High temperature corrosion of Nimonic-75 and various steels in gases at low partial pressures, 25:4738 (DP-Report-527)
PIERRE, J., Magnetic properties of rare earth--noble metal equiatomic compounds, 25:5197
PIHL, A., Chemical protection against ionizing radiation by sulphur-containing agents, 25:4538
PIIPARINEN, M., Levels of ^{144}Pr from the decay of ^{144}Ce, 25:5739
PILUSO, C. J., Energy levels of ^{27}Si, 25:5602 (ANU-P-501)
PINSTON, J. A., Decay of ^{104}Tc (18-min), 25:5756
PIOTROWSKI, J., Isomeric cross-section ratios and total cross-sections for the ^{113}In(n,2n)/sup 112gm/In and ^{115}In(n,2n)/sup 114gm/In reactions, 25:5763
PIPKIN, F. M., Beta-ray asymmetry from oriented /sup 110m/Ag, 25:5743
PITEO, J. W., Fractographic study of stage I fatigue cracking in a nickel-base superalloy single crystal, 25:4765
PITKANEN, P. H., Application of extended R-matrix theory to elastic scattering of neutrons by ^{12}C, 25:5581
PITTEL, S., Core-excited states in ^{54}Fe, 25:5669
PITTINATO, G. F., Hydrogen induced sustained load crack growth in Ti--6Al--4V, 25:4762
PIXLEY, R. E., Lifetime measurements in ^{19}O, 25:5565
PLACCI, A., Measurements of pionic x-rays from hydrogen, 25:5288
PLACE, Ralph L., Angular correlation and gamma-ray branching ratio studies of ^{40}Ar, 25:5667
PLAJNER, Z., Excited levels in the decay ^{185}Os → ^{185}Re,

XUM

25:5741
Internal conversion of the 57.54 keV E1 transition in ^{180}Hf, 25:5731
PLASTINO, A., Angular-momentum-projected Hartree--Fock theory, 25:5815
PLATT, C. E., Planning for flexibility in operation, maintenance, and refueling of PWR, 25:5909
PLATTNER, G. R., Polarization and cross-section measurements in p-^{4}He scattering from 20 to 40 MeV, 25:5526 (UCRL-19943)
PLAVEC, Miroslav, Mass exchange in binary stars, 25:4897
PLEDGER, Douglas Bruce, Study of detailed balance for ^{16}O(d,α)^{14}N and ^{14}N(α,d)^{16}O as a test of time reversal invariance, 25:5596
PLIENINGER, R. D., Reaction ^{12}C(d,^{6}Li)^{8}Be α-cluster pickup, 25:5562
PLOMTEUX, G., Radioprotectors and plasma enzymes, 25:4594
PLOTNIKOVA, M. V., Photoeffect and internal conversion in resonant absorption of M1 gamma quanta by ^{119}Sn, 25:5787
POCHAT, A., Generalized oscillator strengths for $1^1S \rightarrow 2^1S$ transition in He, 25:4959
PODGORETSKY, M. I., Interference of identical particles in the processes involving the resonances, 25:5350 (JINR-P1-5315)
PODOSEK, Frank Anthony, Early solar system abundances of ^{129}I and ^{244}Pu, 25:4922
POE, Norman D., Radioaerosol inhalation scanning, 25:4678
POEPPEL, R. B., Movement of fission gas bubbles and inclusions in mixed-oxide fuel, 25:6014
POHL, B. A., Fast-neutron spectroscopy of the reaction ^{9}Be(p,n)^{9}B at 20 MeV, 25:5557
POIRIER, V., Sublimed emitter and collector coatings, 25:4750 (TEE-4125-2)
POLACCO, E., Measurements of pionic x-rays from hydrogen, 25:5288
POLITZER, Peter Alexander, Drift instability in collisionless alkali metal plasmas, 25:5112
POLLARD, H. Marvin, Ashing technique as a more precise method for the radioassay of ^{51}Cr in feces, 25:4032
POLLINA, R. J., Sound propagation near magnetic phase transitions, 25:5186
POLLITT, N., Corrosion experiments on coated fuel particles using xenon release technique, 25:4882 (DP-Report-436)
POLUBARINOV, I. V., Equivalence theorem and observables in the field theory, 25:5235 (JINR-P2-5266)
POLYAKOV, V. P., Mechanism of the interaction of V_2O_5 with C. II, 25:4842
POMPEI, A., Reaction ^{4}He(γ,d)d and 2^+ excited state of ^{4}He at 30 MeV, 25:5543
POMRANING, G. C., Thermal x-ray transport problem, 25:5142
POND, R. B., Plutonium and ^{238}U Doppler measurements in plutonium-fueled fast critical assembly, 25:6109
PONOMAREV, L. A., Fast variation of hadronic amplitude and Brehmsstrahlung of γ quantum, 25:5357
PONOMAREV, L. I., Mesic atom processes in hydrogen, 25:4952 (JINR-P4-5039)
POOLE, M. J., Miniature nuclear batteries, 25:4240
POP, Iuliu, Ferrimagnetism of the intermetallic compound Co_2Gd, 25:5201
POPE, C., Polarization transfer at 0° in the D(d,n)^{3}He and H(d,n)pp reactions, 25:5532
PORETSKII, L. B., Measurement of interaction cross sections of 0.3 to 5.0 MeV neutron with air, 25:5481
PORTEOUS, Donald D., The effect of total-body irradiation on wound healing and the hematopoietic system in mice, 25:4705
PORTNER, P. M., Reactions ^{14}N(p,^{3}He)^{12}C, ^{14}N(d,α)^{12}C, ^{13}C(p,d)^{12}C, 25:5563
PORTNOY, Benjamin, Neutron activation analysis of trace elements in skin. IV, 25:4049
POSNER, Aaron S., Chemical and physical nature of bone mineral, 25:4412 (CONF-680211-, pp 5-24)
POSPISIL, J., Cardiovascular, biochemical, and haematological changes after the application of AET, 25:4599
POSPISIL, M., Effect of adrenalectomy on acute changes in erythropoiesis in the spleen and bone marrow of mice irradiated with sublethal exposures, 25:4696
POTEET, Wade Martin, Effects of superconducting transition on quadrupole resonance in La, 25:5058
POTNIS, V. R., Decay of ^{144}Ce, 25:5749
POTTER, G. D., Fate of Schooner fallout radionuclides ingested by dairy cow, 25:4436
POUNDS, K. A., Solar x radiation below 25 A, 25:4924
POWELL, B. M., Exchange and crystal-field interactions in Er and Ho, 25:5214
POWELL, C. F., Nature of the primary cosmic radiation, 25:4977
POWELL, Thomas Mabrey, Search for polarization in elastic e-p scattering at 15 and 18 GeV, 25:5252 (UCRL-20093)
POWERS, H. G., Evaluation of PuO_2 homogeneity in PuO_2--UO_2 fast reactor fuel, 25:4876
POWERS, R. J., Electric quadrupole transitions in muonic ^{208}Pb, 25:4953
POZZOLI, R., Korteweg--De Vries equation for drift waves, 25:5127
PRALL, J. R., Automatic determination of thorium in aqueous and organic solutions, 25:4014 (NLCO-1072)
PRASAD, R. Y., Bremsstrahlung x-ray flux and its ionizing effect in the lower ionosphere, 25:5019
PRATT, W. P. Jr., First-forbidden β decays of ^{198}Au, 25:5708
PREEDOM, B. M., T/sub Z/ = $-^3/_2$ masses and isobaric multiplet mass equation, 25:5568
PRESSESKY, A. J., AEC programs in fast reactor core safety, 25:6087
PREUSS, Luther E., Two photon absorptiometric analysis using ^{109}Cd, 25:4646 (CONF-700515-, pp 272-3)
PRICE, C. E., Telecommunications and information systems at CTC, 25:6200
PRICE, R. J., High-temperature fast-flux irradiation experiment for mixed-oxide fuel rods, 25:5585 (GA-10264)
PRINCE, K. D., Precipitation and dislocations in an aluminum--silicon alloy, 25:6243 (NYO-2394-40)
PRINCE, Robert Harry, Interaction of low-energy atmospheric ions with controlled surfaces, 25:4943
PRINCIOTTA, Frank T., Design of radioisotope heat source subsystems for heart devices, 25:4230
Results of bench model testing of radioisotope heat source subsystems for heart devices, 25:4231
PROCTOR, I., Anomalous L = 1 shapes of angular distributions for (^{3}He,t) transitions to 0$^+$ antianalog states in ^{64}Ga and ^{40}K, 25:5654
PROFIS, A., Double contrast examination of small intestine, 25:4686
PRONKO, J. G., Reactions ^{20}Ne(d,p)^{21}Ne and ^{22}Ne(d,p)^{23}Ne, 25:5618
PROTOPOPESCU, V., Corrections to scattering kernel for study of neutron thermalization, 25:5488
Solving time-dependent nonhomogeneous thermalization equation, 25:5478
PRUESS, K., Potentials for fast and slow heavy-ion-collisions within the two center shell model, 25:5841
PSHENICHNOV, Yu. P., Method for producing microautoradiograms of the surface of irradiated aluminum, 25:4250
PSHEZHETSKII, S. Ya., Reactions of photoexcited radicals of the allyl type with the hydrocarbon molecules in the solid phase, 25:4125
PTACEK, V., Effect of adrenalectomy on acute changes in erythropoiesis in the spleen and bone marrow of mice irradiated with sublethal exposures, 25:4696
PTASHNIK, V. B., Diffusion and isotope effect of lithium-ion diffusion in crystalline silver chloride, 25:5172
PUDOVKIN, M. I., Interrelation between solar wind and geomagnetic field, 25:5026
PULATOVA, M. K., Photochemical conversions of paramagnetic centres in γ-irradiated monocrystal of l-cystine dihydrochloride, 25:4091
PURDY, C., Kodak type III film for photodosimetry, 25:4383
PURICA, I., Corrections to scattering kernel for study of neutron thermalization, 25:5488
PURVIANCE, R. T., Failure threshold TREAT experiment with an unirradiated prototypical FFTF fuel element, 25:6096
High-energy transient meltdown of irradiated UO_2 in a TREAT Mark-II loop, 25:6097
PUSHKAREV, V. V., Clarification and deactivation of waste waters by frothing flotation, 25:4141
PUTZEYS, J., Aspects of design reliability of pressure tubes for heavy water moderated reactors, 25:5584 (RISO-214, pp 335-42)
PYATILETOVA, N. M., Photometric determination of Nb with reagent PAR in complex Cu-base alloys, 25:4018
PYCHKOV, G. P., Deuteron acceleration in LHE synchrophasotron, 25:5449 (JINR-PS-5311)

Q

QUARATI, P., Reaction ^{4}He(γ,d)d and 2^+ excited state of ^{4}He at 30 MeV, 25:5543
QUATTROCHI, A., Metal isotope and high pressure effects on the infrared active skeletal vibrations in metal sandwich compounds, 25:4067
QUEEN, N. M., Dispersion sum rules for πd scattering, 25:5391
QUESNE, C., n-particle fractional parentage coefficients for anticommuting creation operators, 25:5822
QUEZEL, G., Magnetic structure of cubic rare earth oxides, 25:5215
QUEZEL, S., Magnetic structure of cubic rare earth oxides, 25:5215
QUINN III, James L., Pulmonary scanning in the diagnosis of pulmonary thromboembolism, 25:4680
QUINTILIANI, M., Fast intermediate reactions sensitizing alcohol dehydrogenase to radiation, 25:4543
X-ray sensitivity of E. coli B cells as affected by cysteine, 25:4555
QUINTILIANI, Marcello, Radiation protection and sensitization. Proceedings of the second international symposium on radiosensitizing and radioprotective drugs, Rome, 6--8 May 1969, 25:4534

R

RADMAN, Miroslav, Excision repair of non-replicated uv-damaged E. coli DNA, 25:4463
RADZIEVSKII, G. B., Measurement of dose buildup factors for low-energy point isotropic gamma sources in water,

25:5136
RAESIDE, D. E., Precision gamma ray energies, 25:5736
RAFF, R. A. V., Grafting of organic polymers onto inorganic substrates by gamma irradiation, 25:4106
RAFT, P. D., New cosmic-ray ionization measurements at balloon altitudes, 25:4990
RAGAINI, R. C., Levels of ^{88}Sr from the ^{86}Sr(t,p)^{88}Sr reaction, 25:5615
RAGO, A., IBM interactive reactor computation system, 25:6149
RAMACHANDRAN, V., Tensile behavior of polycrystalline zirconium at 4.2°K, 25:4768
RAMACHANDRA RAO, D., ^{2}PI--X ^{2}PI system of ^{14}N^{80}Se and ^{14}N^{78}Se, 25:4063
RAMAKRISHNAN, T. V., Radiation sensitivity of plant pigments. I, 25:4467
RAMAMURTHY, P., Antipyrine complexes of Ti(IV), Zr(IV), Th(IV), and U(VI) perchlorates, 25:4087
RAMAVATARAM, K., Reactions ^{14}N(p,^{3}He)^{12}C, ^{14}N(d,α)^{12}C, ^{13}C(p,d)^{12}C, 25:5563
RAMAYYA, A. V., Decay of ^{194}Au, 25:5728
RAMBO, George Earle, Delayed neutron groups from ^{235}U and ^{233}U and short-lived delayed photoneutron groups from ^{235}U and ^{233}U in D_2O, 25:5689
RAMOND, Pierre Michel, Double partial wave expansion of scattering amplitudes, 25:5310
RANGARAJAN, T. N., Study of particle production at high energies, 25:5276
RAO, E. S. M., Aquoluminescence from gamma-irradiated halides, 25:4076
RAO, E. V. Narasimha, Delayed coincidence spectrometer for lifetime studies, 25:4363
RAO, C. L., Interactions of ^{45}Sc and ^{68}Zn with protons, 25:5623
RAO, M. N., Level structure of ^{47}Ti, 25:5629
RAO, P. Venugopala, Electron capture decay of ^{181}W, 25:5753
RAO, Y. K., Discussion of kinetics of the graphite--uranium dioxide reaction from 1400° to 1756°C, 25:4849
RAPAPORT, J., Level structure of ^{47}Ti, 25:5629
RAPP, R. E., Principles and methods of dilution refrigeration. II, 25:5062 (UCSD-34-P-143-32)
RAPPENEAU, J., Application of internal friction to the study of graphitization, 25:4870
RARIDON, D. Jr., Molten UO_2--Na dropping experiments, 25:6076
RASEMAN, C. J., Reactor operating and maintenance costs, 25:5903
RASMUSSEN, J., Deuteron scattering from ^{124}Te and ^{146}Nd, 25:5729
RASMUSSEN, N. C., Integral gamma-ray production cross-section measurements with Pu--Be neutron source, 25:5582
RASPOPOV, O. M., Interrelation between solar wind and geomagnetic field, 25:5026
RATHI, S. K., Radiosensitizing action of androgen on the ovaries of Heteropneustes fossilis (Bloch), 25:4591
RATIANI, G. V., Determination of the average effective radius of vaporization centers in the nucleate boiling of liquids, 25:6215 (AEC-tr-7202)
RAUH, E., Sensitive method for separate calculation of mineral content in cancellous and compact bone of the finger by a ^{125}I profile scanner. Effect of calcium and fluoride therapy on demineralized bone, 25:4636 (CONF-700515-, pp 169-87)
RAY, J. A., Channel electron multipliers in magnetic fields, 25:4331
Improvements in detection efficiency of Johnston multiplier, 25:4332
RAY, W. E., Type 316 stainless-steel tubing for LMFBR fuel element cladding, 25:4776
RCHEULISHVILI, G. L., Behavior of diffractional peak width at high energies in case of Gaussian potential, 25:5424 (IFVE-STF-69-83)
READ, S. F. J., Frozen polarized target, 25:5466 (RPP/A-81)
REAM, Joseph T., Radioisotope-fueled thermoelectric milliwatt power supplies, 25:4215
REBEL, H., Nonstatistical shape of beta spectrum of ^{14}C, 25:5591
REBER, J., Transfer function investigations on first Dragon core, 25:5953 (DP-Report-445)
RECHITSKII, I. V., Investigation of azimuthal correlations in decays of heavy resonances, 25:5366
REDFIELD, J. A., System thermodynamics and emergency core cooling systems, 25:6085
REDLICH, J., Separation of nuclear isomers of ^{80}Br on metal surfaces, 25:4127
REDMAN, J. D., Three-dimensional x-ray pictures, 25:4404
REDMAN, W. C., Experimental determination of the perturbation denominator in fast critical assemblies, 25:6116
REED, D. L., Relative power distribution and integral spectrum measurements on first Dragon core, 25:5952 (DP-Report-442)
REED, H. F., Integrating shield design and the nuclear reactor plant, 25:5889
REED-HILL, R. E., Tensile behavior of polycrystalline zirconium at 4.2°K, 25:4768
REEHAL, Balbir Singh, Odd--even staggering of nuclear radii, 25:5856
REES, F. J., Power systems optimization approach to nuclear fuel management, 25:5897
REHER, D., P/sub K/w/sub K/ value and fluorescence yield w/sub K/ of Rb, 25:5650
REICH, C. W., Excited K/sup π/ = 0⁺ bands in ^{172}Yb, 25:5744
REICHEL, P., Automatically controlled neutron diffraction goniometer, 25:4394
REIDEMEISTER, G., Harmonic oscillator in prolate spheroidal coordinates. I, 25:5843
REIER, Melvin, Response of a shielded 300-micron silicon detector to gamma rays, 25:4350
REIN, J. E., Fission yields of over 40 stable and long-lived fission, 25:5765
REINERS, Chr, Sensitive method for separate calculation of mineral content in cancellous and compact bone of the finger by a ^{125}I profile scanner. Effect of calcium and fluoride therapy on demineralized bone, 25:4636 (CONF-700515-, pp 169-87)
REINES, F., Research program in neutrino physics, cosmic rays, and elementary particles. Progress report, 1 October 1969--30 September 1970, 25:5257 (LCI-10-P-19-40)
REISTER, David Bryan, Bounds for the solutions of nonlinear parabolic equations, 25:6147
REITER, S. E., In-plant survey of television receivers for x-radiation emission capability, 25:4522 (BRH/DEP-70-24)
REITMANN, D., Energy levels of ^{203}Tl and ^{205}Tl, 25:5758
REMBIELINSKI, J., Determination of X^0(960) meson spin-parity in polarization experiment, 25:5361 (TPJU-14/70)
REMEIKA, J. P., High-pressure NMR study of metal--insulator transition of V_2O_3, 25:5224
REMY, C., Influence of the allotropic transformation β reversible α and of oxygen on the distribution of plutonium in dilute ZrPu and TiPu alloys, 25:4790
REMY, Jacques, Physiological data on swine for use in radiobiology: plasma and blood volumes, 25:4411 (CEA-R-4031)
RENDIC, D., Proton--proton quasi-free scattering in the p + d → p + p + n reaction for E/sub p/ = 4.5 to 13.0 MeV, 25:5534
RENNER, B., Implications of Adler zeros on current-divergence commutators, 25:5316
REUVENI, A., ESR of SO_2^-, 25:4124
REVESZ, L., Composite radioprotective and radiosensitizing effect of an organic free radical, 25:4561
REYNOLDS, A. B., Further studies of non-coherent effects in fast reactor sodium voiding accidents, 25:6072
REYNOLDS, C. A., Brillouin-zone--Fermi-surface interactions in pure and lead-doped indium, 25:5185
Thermal conductivity of normal and superconducting indium--lead alloys, 25:5055
REYNOLDS, J. M., Prog. rpt. on conductivity tensors in metals and semiconductors, 10/15/69--10/15/70, 25:5171 (CRO-3087-44)
REYNOLDS, M. J., Spatial and feedback effects in Georgia Tech Research Reactor, 25:6108
REZVANOV, R. A., Space--energy and time distribution of neutrons in boron-containing media, 25:4155
RHEE, Chong Hoen, Liver scan using /sup 113m/ In colloid, 25:4687
Preparation of /sup 113m/In colloid as scanning agent and its organ distribution in rats, 25:4437
RHINES, F. N., Quantitative determination of the structure--property relationships in nuclear fuel element materials. Quarterly progress report, June 15--September 15, 1970, 25:4841 (SRO-552-5)
RHYNE, James J., Magnetization-dependent Hall effect in rare earth metals, 25:5219
RIBBAT, B., Nonstatistical shape of beta spectrum of ^{14}C, 25:5591
RIBES, M., Analysis of the effects of displacement and of positioning of the measuring probe of a magnetic field on the properties of an optical system, 25:5461 (NF-18519)
RICABARRA, G. H., Resonance integrals of neutron activation of ^{74}Se, ^{76}Se, ^{80}Se, ^{81}Br, ^{127}I, ^{130}Te, ^{138}Ba, ^{140}Ce, and ^{142}Ce, 25:5681 (CNEA-274)
RICABARRA, M. D., Resonance integrals of neutron activation of ^{74}Se, ^{76}Se, ^{80}Se, ^{81}Br, ^{127}I, ^{130}Te, ^{138}Ba, ^{140}Ce, and ^{142}Ce, 25:5681 (CNEA-274)
RICE, R. E., Progress in xenon tagging, 25:6025
RICH, C., In vivo neutron activation analysis of total body bone mass, 25:4042 (CONF-680211-, pp 496-516)
RICHARDSON, E. C., Structure-function studies of the aminothiol radioprotectants, 25:4548
RICHERT, K. D., NRTS--ATR 1.4-MW flow reversal test, 25:6119
RICHMAN, M. H., Precipitation and dislocations in an aluminum--silicon alloy, 25:6243 (NYO-2354-40)
RICHTER, A., Excitation functions from elastic ^{16}O scattering from nuclei with A approximately 16, 25:5566
RICKEY, M. E., T = 9/2 analogue state in ^{53}Ni, 25:5609
RIDGWAY, K. R., Calculated critical arrays of fissile materials, 25:4283
RIEDL, H., Rapid simultaneous elution and electrodeposition of radioactive nuclides adsorbed on paper, 25:4030
RIGATO, M., Absorption and distribution of ^{137}Cs by Trifolium pratense, 25:4449

RIGGLE, P., Radioisotope-fueled Stirling engine artificial heart power system, 25:4233
RIGGS, B. Lawrence, New method of evaluating bone loss in osteoporosis, 25:4639 (CONF-700515-, pp 199-204)
RILEY, B. R., Measurement of K- cascade time in liquid He, 25:5254
RINGENBERG, Richard Ray, Extragalactic radio sources in uniform model universes, 25:4934
RINGHAM, Michael Richard, Green's function formulation of Laplace-transformed multigroup diffusion equations, 25:6176
RISEBERG, L. A., Spin conservation in ionizing collisions between He(2^3S_1) metastable atoms, 25:4960
RISKA, D. O., Tensor force and exchange currents in the triton beta decay, 25:5542
RITTENBERG, Alan, Properties of the eta' meson, 25:5291
RIZEK, J., Excited levels in the decay ^{185}Os → ^{185}Re, 25:5741
ROBBINS, J. M., Irradiation performance of loose and bonded beds of coated fuel particles, 25:6004
ROBBINS, John A., Reactions (p,t) on even Sn isotopes, 25:5799
ROBERTS, J. H., Automatic system for counting etched holes in thin dielectric plastics, 25:4340
ROBERTS, J. J., Multiple-source urban atmospheric dispersion model, 25:4161 (ANL/ES-CC-7)
ROBERTS, M., Plasma confinement in a high magnetic field toroidal quadrupole, 25:5070
ROBIN, Eugene, Pathophysiologic aspects of pulmonary embolism, 25:4679
ROBINSON, D. C., Measurement of plasma parameters in Tokamak T3-A by Thomson scattering, 25:5079 (CLM-R-167)
ROBINSON, J. C., Noise technique for measuring reactivity independent of β/Λ, 25:6174
ROBKIN, M. A., Neutron radiography of mixed-oxide fuels, 25:4254
New small mass critical configuration, 25:6101
ROCHEDEREUX, Y., Remote handling in operation of the installation ATTILA, 25:4261 (CEA-R-4067)
ROCK, Stephen, Search for T-violation in inelastic scattering of electrons from polarized proton target, 25:5400 (UCRL-20041)
ROCK, Theodore J., Gated photomultiplier technique for use in pulse radiolysis, 25:4398
ROCKOFF, S. David, Automatic scanner-computer analysis of radiographic bone trabecular activity, 25:4637 (CONF-700515-, pp 188-94)
Radiographic trabecular quantitation of human lumbar vertebrae in situ: progress in development of method and digital computer analysis, 25:4628 (CONF-680211-, pp 331-51)
RODABAUGH, E. C., Survey report on structural design of piping systems and components, 25:4188 (TID-25553)
RODIER, J., Twelve years of health physics in a plutonium production plant, 25:4526
RODRIGUEZ-PASQUES, R. H., Photonuclear tritium yields at 90 MeV, 25:5678
ROE, G. J., Magnetic properties of Ho_4Fe_{23} and $HoFe_2$, 25:5211
ROENRIG, D., Influence of single irradiation and heat treatment on the properties of BeO, 25:4892
ROESEL, F., Quantum mechanical corrections for double Coulomb excitation in ^{152}Sm, 25:5781
ROESMER, Josef, Radiochemistry of mercury, 25:4133 (NAS-NS-3026(Rev.))
ROGERIEUX, Marcellin, Analog computer for calculating the ratio of amplitude of two pulses, 25:4362 (CEA-N-1314)
ROGERS, C. A., Critical approach and exponential experiments with prototype FFTF driver fuel pins in water, 25:4280
ROGERS, D. R., Shielding for NERVA missions, 25:6131
ROGERS, G. D., Fuel assembly transition joint development, 25:6196
ROGERS, H. C., Influence of grain boundaries on the fracture mode of zirconium and Zircaloy-2, 25:4769
ROGERS, Joel Guild, Kinematically incomplete and complete studies of the breakup of ^{4}He by 47-MeV protons, 25:5533
ROGERS, Lee F., Polychromatic x-ray beam to represent n monoenergetic photon sources. I. Limitations and correction factors for photon detectors, 25:4650 (CONF-700515-, pp 314-31)
ROGERS, V. C., Integral gamma-ray production cross-section measurements with Pu--Be neutron source, 25:5582
ROGGENKAMP, P. L., Production of ^{238}Pu, 25:4227
ROGINSKII, V. A., Reactions of photoexcited radicals of the allyl type with the hydrocarbon molecules in the solid phase, 25:4125
ROKHLOV, N. I., Photoeffect and internal conversion in resonant absorption of M1 gamma quanta by ^{119}Sn, 25:5787
ROLLIER, Mario A., Nucleus at the fission saddle point as activated complex, 25:5810
ROMAGNOLI, G. F., Nephropathy secondary to irradiation, 25:4714
ROMANOV, V. P., Chromosome damages induced by γ-ray doses in Crepis capillaris, 25:4498
ROMANOVA, E. A., Radiosensitizing properties of some barenes (ortho-1,1 dicarbaclovododecaborane), 25:4588
ROMANTZEV, E. F., Biochemical mechanism of radioprotective action of aminothiols, 25:4592
Formation of ATP in nuclei and mitochondria and the influence of β-mercaptoethylamine, 25:4557
Radiosensitizing properties of some barenes (ortho-1,1 dicarbaclovododecaborane), 25:4588
ROMETSCH, R., Adaptation of Agency's safeguards work to NPT, 25:4271
ROMNEY, E. M., Plutonium in soil, plants, and small mammals, 25:4478
ROONEY, V. L., Neutron slowing down time kernel for graphite, 25:6160
ROOS, Bengt, Determination of bone mineral content in lumbar vertebrae by a double gamma-ray technique, 25:4643 (CONF-700515-, pp 243-54)
ROOS, Matts, Omega--rho interference in strong interactions, 25:5373 (DNPL/R-7, pp 173-205)
ROOSENDAAL, H. E., Anisotropy in ejection patterns due to generation of focusing collisions by channeled particles, 25:4939
ROSE, F. A., Precision of the Norland Instruments bone mineral analyzer, 25:4633 (CONF-700515-, pp 28-32)
ROSEN, Charles A., Experimental mobile automation, 25:4159
ROSEN, S., Concrete-polymer building blocks, 25:4859
ROSENBAUM, H. S., Measuring plutonium homogeneity in fast reactor fuels, 25:4875
Microstructure of mixed-oxide fuel irradiated in a thermal-neutron flux, 25:5993
ROSENBLUTH, M. N., Thermal equilibrium and stability of Tokamak discharges, 25:5117
ROSENGREN, Bengt, Determination of bone mineral content in lumbar vertebrae by a double gamma-ray technique, 25:4643 (CONF-700515-, pp 243-54)
ROSS, C. P., AEC ^{60}Co heat source programs, 25:4224
ROSS, R., Applicability of anion exchange with mixtures of nitric acid and methanol for the separation of rare earths, 25:4139
ROST, E., T = 9/2 analogue state in ^{43}Ni, 25:5609
ROTBLAT, J., Strontium-90 and infant mortality, 25:4505 (CONF-691051-, pp 324-35)
ROTHE, R. E., Criticality calculations and measurements on enriched uranium metal-solution combinations, 25:6100
ROTHENBERG, Lawrence Neil, Angular distribution of 24 MeV neutrons scattered by protons, 25:5540
ROTHMAN, A. B., Failure threshold TREAT experiment with an unirradiated prototypical FFTF fuel element, 25:6056
ROTHWARF, Allen, Transition metals and Froehlich mechanism for superconductivity, 25:5047
ROTIVAL, Michel, Application of cross-correlation method in nuclear physics, 25:4392 (LYCEN-7032)
ROTTENBACH, R., Determination of the activity coefficients of uranyl perchlorate in aqueous solutions, 25:4086
ROTTMAYER, Robert E., Structure and intrinsic stress of Pt thin films, 25:6226 (CCO-623-151)
ROULET, Roger, Monitoring beta and gamma radiation, 25:4335
ROUND, K. J., MAPLE IB: ^{60}Co-fueled thermoelectric generator, 25:4226
ROUNDS, Donald E., Enzyme inactivation with ultraviolet laser energy (2650 Angstroms), 25:4461
ROUSSEL, Emile, Electron probe microanalysis of highly radioactive materials, 25:4011 (CEA-N-1340)
ROUX, A., Nonlinear mechanisms associated with wave particle interactions in the magnetosphere, 25:5031
ROW, T. H., Design considerations of reactor containment spray systems. Part V. Protective coatings tests, 25:6034 (ORNL-TM-2412(Pt.5))
ROWE, D. S., Sensitivity of radial-immunodiffusion assay, 25:4417
ROWLAND, F. S., Recoil tritium reactions with methyl isocyanide and methyl cyanide. Estimates of energy deposition for the T-for-H reaction, 25:4131
ROY, G. M., Evolutionary trends in BWR primary system and containment designs, 25:5885
ROYDEN, Herbert N., Intercomparison of Doppler measurements made in fast critical assemblies, 25:6111
ROYZEN, I. I., Dynamical scheme for leading trajectory and theory of fireballs, 25:5359
ROZANOVA, A. M., Nonstrange baryon--baryon resonances, 25:5388 (JINR-P2-5058)
RUBANOVSKAYA, A. A., Effect of U_3O_8 in experimental work, 25:4444
RUBIN, A. G., Optical investigations of electrostatic turbulence in plasma, 25:5083
RUDNICKI, M. I., Design of a ^{238}Pu-powered implantable thermal engine for heart assist devices, 25:4232
RUDZIKAS, Z. B., Effect of second-order relativistic corrections in the cases of complex electronic configurations, 25:4971
RUEDORFF, Walter, Spectroscopic investigations in system $MeUO_4$--ThO_2 with Me = Nd, Dy, Ho, Yb, and Y, 25:4084
RUETHER, W., Neutron microdosimetry for rabbit eye, 25:4521
RUFEH, F., Thermionic performance of fluoride CVD W--Nb converter, 25:4993 (TEE-4125-1)
RUFF, F., Airway closure, 25:4428
RUH, A., Protons scattered on ^{24}Mg, ^{52}Cr, and ^{58}Ni, 25:5632
RUMPF, K., Production of proton--antiproton and kaon--antikaon pairs, 25:5297
RUNDQUIST, D. E., Low-energy photofission of heavy elements: experimental results, 25:5768
Use of fission product gamma rays following photofission

XUM

for nondestructive assays of nuclear materials, 25:4291
RUSSELL, D. C., In-beam Moessbauer spectroscopy, 25:5467
RUSSELL, F. M., Frozen polarized target, 25:5466 (RPP/A-81)
New target material for Rutherford frozen target, 25:5463 (RHEL/R-199)
RUSSELL, Moses E., Effect of capsule content variations on thyroid uptake results, 25:4661
RUSSELL, W. L., Genetic effects of low-level radiation, 25:4501
RUTHERFORD, P. H., Thermal equilibrius and stability of Tokamak discharges, 25:5117
RYABTSOV, V. D., Ionization counter dE/dx filled with liquid Xe, 25:4319 (JINR-P13-5403)
RYAZANOV, M. I., Coherent scattering of γ quanta by nuclei, 25:5174
RYBAKOVA, L. A., Photoconductivity spectra of irradiated and plastically deformed crystals of germanium, 25:5161
RYDBERG, J., New isotope of palladium ^{116}Pd, 25:5740
RYDIN, R. A., Space--time kinetics experiments and calculations for a loosely coupled core, 25:6185
RZAEV, R. A., Isochronous magnetic optical systems, 25:5447 (IFVE-OP-65-68)

S

SAAD, E., Isomeric cross-section ratios and total cross-sections for the ^{113}In(n,2n)/sup 112gm/In and ^{115}In(n,2n)/sup 114gm/In reactions, 25:5763
SACKETT, J. I., Neutron slowing down time kernel for graphite, 25:6160
SAETTLER, A. W., Gamma irradiation studies on seeds seedlings Phaseolus, 25:4723
SAGAWA, Norihiko, Mechanical sodium pump for liquid metal cooled fast breeder reactor, 25:4201
SAGUES, A. A., Prog. rpt. on dislocation-solute atom interactions in alloys, 10/70, 25:4786 (COO-1676-13)
SAHA, G. B., Interactions of ^{45}Sc and ^{68}Zn with protons, 25:5623
SAHA, P., Reconniassance of the system BeO--Al_2O_3--SiO_2--H_2O, 25:4871
SAHOO, B., Preparation of some U(IV) fluoride complexes, 25:4058
SAIKA, A., Electric polarizability of molecular hydrogen as calculated by use of the nonsymmetrical wave function, 25:4949
SAITO, H., E2 effective charges of the f/sub 7/2/ proton and neutron, 25:5646
SAKAI, M., M1 gamma transitions from isobaric analogue states, 25:5676
SAKAMOTO, K., Drug-radiation damage interaction and its relevance to radiosensitization in mammalian cells, 25:4558
SAKAO, Hiroshi, Thermodynamic study on the activities of both components in binary molten alloys, 25:4754
SAKSONOV, P. P., Use of combined radiation protection compounds, 25:4609
SALIN, A., Calculations on high-energy charge transfer with the continuum distorted-wave method, 25:4558
SALUSTI, E., Quadrupole force in nuclear spectroscopy, 25:5809
SAMOSVAT, G. S., Debye--Waller factor for W, 25:5170 (JINR-P14-5358)
SAMPOLI, M., Search for excess electron photo-ejection in liquid He, 25:5060 (NP-18484)
SAMSONOV, G. V., Temperature dependence of electric conductivity and thermal electromotive forces in the homogeneous carbide alloy regions of titanium and niobium, 25:5176
SAMUELSON, Gary L., Self-switching damping circuit for high power pulse NMR, 25:4356
SAMUELSON, Reid Robert, Radiation damage in miniature avalanche diodes, 25:4408
SANDBERG, G. W., Studies on dogs with implanted ^{238}Pu sources, 25:4432
SANDERS, J. P., Effects of fuel thermal limits on gas-cooled fast breeder economics, 25:5902
SANDFORD, Brian P., Ionization processes in the polar cap, 25:5008
SANNA, Robert, Monte Carlo unfolding of neutron spectra, 25:4367
SANNER, T., Chemical protection against ionizing radiation by sulphur-containing agents, 25:4538
SANNIKOV, V. V., Measurement of plasma parameters in Tokamak T3-A by Thomson scattering, 25:5079 (CLM-R-107)
SANO, Keiji, Bromouridine (BUdR) as a radiosensitizing agent of malignant brain tumours, 25:4688
SANSOT, M., Pulmonary hemosiderosis in a 9-year old child with a trisomy 18, 25:4685
SANTO, R., Backward-angle anomalies in inelastic alpha-particle scattering on ^{40}Ca, 25:5643
Reaction (p,t) on ^{42}Ca, ^{44}Ca, and ^{48}Ca, 25:5677
SANTRY, D. C., Beta-ray asymmetry from oriented /sup 110m/Ag, 25:5743
SAPARLYEV, Ch., Express-method for determining ^{90}Sr in plants, 25:4039
SAPHIER, D., Hybrid method for spatial dynamic analysis, 25:6179
SARAN, Mohan Singh, Carboxylates of metals. I. Uranium(IV) carboxylates, 25:4057
Carboxylates of metals. II. Thorium carboxylates, 25:4056
SARD, R. D., Reggeized pion exchange, 25:5278
SARKAR, Satya Kinkar, Solubility of oxygen in zirconium carbide, 25:4877
SARTORI, G., Constraints on equal-time commutators from Lorentz covariance, 25:5308
SARUKHANOV, A. G., Change of sodium potassium and calcium content in the heart muscle, 25:4698
SASTRY, D. L., 437-keV beta transition in the decay of ^{125}Sb, 25:5730
Validity of xi approximation of the 1400 keV beta decay in ^{143}Ce, 25:5700
SASTRY, E. V. R., Influence of impurities on the room-temperature coloration processes in alkali halides, 25:5159
SASTRY, Gummuluru N., Faint blue objects in cD clusters of galaxies, 25:4930
SATO, Fumiaki, Bromouridine (BUdR) as a radiosensitizing agent of malignant brain tumours, 25:4688
SATO, Shinichiro, Extraction of plasma insulin in radioimmunoassay, 25:4420
SATPATHY, K. C., Preparation of some U(IV) fluoride complexes, 25:4058
SATZ, H., Dynamics of single pion production in high-energy hadronic interactions, 25:5392
SAUER, P., Absorption of ^{45}Ca from intestinal tract of rat, 25:4430
SAUNDERS, A. R., High-temperature reactor development in Dragon Project, 25:5947
SAUNDERS, L. M., Crossed channel partial wave expansions and the Bethe--Salpeter equation, 25:5426 (NYO-2263-TA-226)
SAVANT, V. V., Antipyrine complexes of Ti(IV), Zr(IV), Th(IV), and U(VI) perchlorates, 25:4057
SAVICH, I. A., Effects of radiation on catalytic properties of complexes of azomethanes and ions of transition metals, 25:4103
SAVILLE, D. A., Electrohydrodynamic stability: fluid cylinders in longitudinal electric fields, 25:4557
SAVRIN, V. I., Fast-particle scattering on Coulomb and short-range potentials, 25:5438
Forward scattering amplitude behavior at high energies, 25:5349 (IFVE-STF-69-74)
Solution of the unitarity equation for the elastic scattering amplitude at high energy, 25:5423 (IFVE-STF-69-65)
Solution of unitarity condition for two-particle process amplitude at high energies, 25:5355
SAWADA, Kiyoshi, Silica gel as support for inorganic ion-exchangers for determination of ^{137}Cs in natural waters, 25:4033
SAWANT, P. L., Radiation sensitivity of plant pigments. I, 25:4467
SAXENA, G. S., Importance of pulse-height analysis in the gamma-ray attenuation technique for measurement of soil moisture, 25:4158
SAXENA, M. K., Angular distribution of neutrons from deuteron-bombarded lithium, 25:5590
SAXTON, O. H. N., Crossed channel partial wave expansions and the Bethe--Salpeter equation, 25:5426 (NYO-2263-TA-226)
SCALABRINO, G., Radiosensitizing effect of L-erythro-α,β-dihydroxybutyraldehyde on Ehrlich ascites tumour cells. Cytokinetic analysis of tumour growth, 25:4564
SCALIA, M., Group-theoretical analysis of β-decays of some $j = 3/2$ light nuclei, 25:5813
SCANDRETT, John, Automatic scanner-computer analysis of radiographic bone trabecular activity, 25:4637 (CONF-700515-, pp 188-94)
SCARASCIA-MUGNOZZA, G. T., Mutation breeding of plants in Italy, 25:4488
SCARBOROUGH, J. C., Comparison of recycle in LWR's and HTGR's, 25:6056
Fuel cycle development: decision analysis under uncertainty, 25:6024
SCARFE, C. D., Mass functions of binaries with giant primaries, 25:4905
Radial velocity observations of μ¹ Bootis, 25:4504
SCARONI, A., Corrosion rate of Zircaloy-2 in steam--water mixture under reactor radiations, 25:4737 (CISE-R-290)
SCHAAR, J., Automatic counting of solid-state fission track recorders, 25:4343
SCHAENZLER, L., Final state interacting n-p pairs in the reaction p + d → p + p + n, 25:5548
SCHAERF, C., Meson effects in high-energy photodisintegration of light nuclei, 25:5547
SCHALK, Terry LeRoy, Hyperon--antihyperon production in anti PP interactions at 2.4 and 2.9 GeV/c, 25:5270
SCHAMBERGER, R. D., Evaluation of Compton currents from 14-MeV neutron source in intermediate altitude range, 25:5497
SCHARFF-GOLDHABER, G., Evidence for the missing 2- state in ^{110}Ag, 25:5712
SCHAVEY, R. E., Features and performance characteristics of the Packard Osteodensitometer, 25:4635 (CONF-700515-, pp 48-57)
SCHEARER, L. D., Spin conservation in ionizing collisions between He(2^3S_1) metastable atoms, 25:4960

SCHECTER, D. J., Grafting of organic polymers onto inorganic substrates by gamma irradiation, 25:4106
SCHEIL, W., Achromatic lesions induced by x-rays in chromosomes of Vicia faba, 25:4454
SCHEMMEL, R. R., Insulation resistivity measurements at high temperatures, 25:4401
Polarization effects in oxide insulators, 25:4400
SCHERER, C., Gamma--gamma angular correlations, 25:5874
SCHERFF, H. L., Preparation of Th--Pa alloys, 25:4791
SCHERMER, R. I., First-forbidden β decays of ^{198}Au, 25:5708
SCHINDLER, K., Downstream state of collisionless shock waves, 25:5099
SCHINZEL, D., Giant-resonance excitation by radiative capture of π^- in ^{16}O, 25:5600
SCHLAET, F., Cold-working maximum of internal friction, 25:4778
SCHLITT, D. W., Possibility of chemical binding of neutrons in F centers, 25:5154
SCHLUETER, G., Hydrodynamic stability in curved steam generator tubes, 25:4208
SCHMEING, H., Backward-angle anomalies in inelastic alpha-particle scattering on ^{40}Ca, 25:5643
SCHMIDT, W., Isovector asymmetry in rho-production, pion photo- and electroproduction, 25:5326
SCHMITZ, W., Omega photoproduction on complex nuclei, 25:5249 (DNPL/R-7, pp 87-94)
SCHMONSEES, W. G., Two photon absorptiometric analysis using ^{109}Cd, 25:4646 (CONF-700515-, pp 272-3)
SCHNEIBERG, K., Regeneration of peripheral blood in thymectomized mice after sublethal whole-body irradiation, 25:4469
SCHNEIDER, Kenneth J., Status of Waste Solidification Demonstration Program, 25:4276
SCHNEIDER, R. A., ^{235}U depletion as a potential independent cross-check of the plutonium content of spent power reactor fuels, 25:4257 (BNWL-SA-3304)
SCHOEN, Gerald, WNSE shielding application, 25:5978
SCHOFER, N. L., Two octyl phenyl phosphinic acids, (R)(C_6H_5)PO(OH), as extractants for selected M(III) and M(VI) metallic cations, 25:4147
SCHOROCHOFF, G., Remarks on Σ^- hyperon conversion rate, 25:5298
Trapping of Λ^0 hyperons produced by K^- meson absorption, 25:5299
SCHOWENGERDT, Franklin Dean, Energy-loss spectra by 25- to 125-keV protons on He, 25:4967
SCHREINER, Bernard F. Jr., Effects of thoracic irradiation upon cardiopulmonary function in the dog, 25:4706
SCHROCK, S., Interstitial transfer in sodium systems, 25:4773
SCHROIT, A., Additional system for bone densitometry studies, 25:4634 (CONF-700515-, pp 33-47)
SCHROIT, A. G., Features and performance characteristics of the Packard Osteodensitometer, 25:4635 (CONF-700515-, pp 48-57)
SCHROEER, Dietrich, Nuclear quadrupole interaction in crystals by Moessbauer effect, 25:5221 (AD-710293)
SCHROER, B., Locally generated dilatation charge in Thirring model, 25:5408 (NYO-3825-61)
SCHUEBELIN, Peter, Puzzle of the A2 meson, 25:5286
SCHUELE, Donald, Accurate determination of dielectric constant by method of substitution, 25:6225 (COO-623-150)
Capacitive gage for accurate measurement of high pressures, 25:6230 (COO-623-155)
Low frequency dielectric constants of LiF, NaF, NaCl, NaBr, KCl, KBr by method of substitution, 25:6228 (COO-623-153)
Low frequency dielectric constants of alkaline earth fluorides by method of substitution, 25:6229 (COO-623-154)
SCHULTEN, R., High-temperature reactors, 25:5944
Some physics aspects of a small once-through pebble-bed reactor, 25:5972
SCHULZ, Michael, Radial diffusion of outer-zone electrons, 25:5002 (AD-710604)
SCHULZE, J. F., Calorimeters for measuring high-energy, high-intensity, pulsed electron beams, 25:4379 (SC-TM-65-298)
SCHUMACHER, M., Coulomb fragmentation of InCl and InI, 25:5153
SCHUSKE, C. L., Surface density as a useful parameter in the storage and handling of fissile metal, 25:4284
SCHUSSLER, F., Decay of ^{104}Tc (18-min), 25:5796
SCHUSTER, W., Prospects of automation in the control of nuclear power plants, 25:5879
SCHUTT, Paul F., Thermionic converter, 25:4994
SCHWABE, K., Determination of the activity coefficients of uranyl perchlorate in aqueous solutions, 25:4086
SCHWARTZ, J. J., First excited state of ^{148}Sm, 25:5703
SCHWARTZ, Robert B., Isospin of the ^{11}B giant resonance, 25:5554
SCHWEITZER, Donald G., Super conductor magnetic energy storage system, 25:5064
SCHWEITZER, Th., Spectra and differential cross sections of 14 MeV neutron inelastic scattering from Fe, 25:5639
SCHWEIZER, J., Magnetic structure of intermetallic compounds RCo_3, 25:5210
SCHWENDIMAN, L. C., Amount and characteristics of plutonium made airborne under thermal stress, 25:4258 (BNWL-SA-3379)
SCOTT, Carl Douglas, Line broadening of the triplet diffuse series of helium in an arc-jet plasma, 25:5082 (N-70-33122)
SCOTT, D. K., Reactions ^{14}N(p,^{3}He)^{12}C, ^{14}N(d,α)^{12}C, ^{13}C(p,d)^{12}C, 25:5563
SCOTT, F. A., Mockup of remotely operated, high-purity, inert-atmosphere sodium analysis facility, 25:4310
SCOTT, J. E., Spectrographic analysis response of a carrier to plutonium--uranium mixed oxides, 25:4015 (NUMEC-3524-76)
SCOTT, J. H., Flow-induced accident initiating conditions in an LMFBR, 25:6070
Further studies of non-coherent effects in fast reactor sodium voiding accidents, 25:6072
SCOTT, J. L., Irradiation performance of loose and bonded beds of coated fuel particles, 25:6004
SCOTT, P. D., Magnetic properties of the rare earth hydroxides, 25:5202
SCOVILLE, J. J., Measurements of fast-neutron capture integrals in CFRMF, 25:5656
SCRIMAGLIO, R., Meson effects in high-energy photodisintegration of light nuclei, 25:5547
SEAGRAVE, J. D., Phase shifts from n--^{4}He elastic scattering experiments near 20 MeV, 25:5508 (LA-4465, pp 1.1-2)
Polarization of 22-MeV neutrons elastically scattered from liquid tritium and deuterium, 25:5516 (LA-4465, pp 15.1-2)
SEALE, R. L., Neutron slowing down time kernel for graphite, 25:6160
SEAMAN, G. G., Properties of the low-lying states of ^{58}Ce, 25:5616
SEBESTYEN, A., Conference on cosmic rays, Budapest, 8--9/69, 25:4976
SEDLIAKOVA, M., Survival and repair of DNA after ultraviolet exposure, 25:4731
SEELIGER, D., Spectra and differential cross sections of 14 MeV neutron inelastic scattering from Fe, 25:5639
SEELINGER, D., Correction of the finite volume of scatterer effect on the measurement of differential elastic and inelastic neutron cross sections. I, 25:5504
SEEMANN, K. W., Space--time kinetics experiments and calculations for a loosely coupled core, 25:6185
SEGAL, Y., Atomic nuclear resolution of beta backscattering gauges, 25:4386
Backscattering of gamma rays from barriers of finite thickness, 25:5149
Optimum diameter of wires for neutron flux measurements, 25:6206
SEGANTI, L., Radioprotection and modification of glycolysis in Ehrlich ascites tumour cells, 25:4566
SEGEL, R. E., Magnetic-dipole transitions in the (νd/sub 3/2)(νf/sub 7/2/) quartet, 25:5649
SEIDEL, K., Spectra and differential cross sections of 14 MeV neutron inelastic scattering from Fe, 25:5639
SEIDEN, P. E., Correlation of superconducting transition temperature with empirical pseudopotential, 25:5048
SEILER, H. P., One-neutron transfer reactions, 25:5577
SEITZ, H., Analysis of asymmetric Breit--Wigner resonances in nuclear reactions, 25:5868
SEJRSEN, P., Washout of ^{133}Xe after intramuscular injection and direct measurement of blood flow in skeletal muscle, 25:4429
SEJVAR, James, WNSE shielding application, 25:5978
SEKIGUCHI, Fumihiko, Radiation-induced internal disbudding as a tool for enlarging mutation sectors, 25:4483
SEKIYA, Tamotsu, Approximate scattering kernel for neutron slowing down, 25:5482
SELENGUT, D. S., New form of P_3 approximation, 25:6155
SELIGER, H. H., Prog. rpt. on mechanism of bioluminescence and energy transfer, 1968--70, 25:6244 (NYO-2802-70)
SELIN, E., Thermal neutron capture gamma rays from ^{26}Mg(n,γ)^{27}Mg, 25:5625
SELTZER, E., Higher-order corrections to internal conversion, 25:5826
SELZER, Robert, Radiographic trabecular quantitation of human lumbar vertebrae in situ: progress in development of method and digital computer analysis, 25:4628 (CONF-680211-, pp 331-51)
SEMANDERES, Stavros N., ELRAFT: computer program for Efficient Logic Reduction Analysis of Fault Trees, 25:6090
SEMENCHENKO, V. K., Thermodynamics of rare earth metals at low temperatures. I, 25:4760
SEMENOV, L. F., Radioprotective action of compounds not containing sulphur, 25:4539
SEMENOV, V. I., Gross structure of giant dipole resonance on nuclei of transition region N approximately equal to 90, 25:5778
SEN, Amiya K., Lyapunov stability of an inhomogeneous two-stream plasma, 25:5108
SENFTLE, F. E., Construction materials for neutron capture gamma-ray spectroscopy with ^{252}Cf sources, 25:4772
Detection and analysis of titanium ore using ^{252}Cf, 25:4036
SENTMAN, Lee H., Interpretation error in molecular beam experiments, 25:4942
SERIANNI, R. W., Repair of DNA and the mode of action of sensitizers and protectors in biological systems of different complexity, 25:4536
SERPAN, C. Z. Jr., Comparison of measured and calculated

XUM

integral fluxes and spectra in a pressure vessel mockup, 25:6213
SERPAN, Charles Z. Jr., Analysis of neutron-embrittlement and flux-density considerations of Army SM-1 reactor pressure vessel, 25:6145 (AD-709898)
Damage threshold for pressure vessel steel embrittlement lower than 1 MeV, 25:4832
Through- thickness ductility in an irradiated reactor pressure vessel wall, 25:6146
SERVAIS, F., Stochastic model for safeguards inspections, 25:4273
SESHADRI, T., Spectrophotometric determinations of Ti and Nb, 25:4020
Stabilities of divalent and trivalent metal complexes of hydroxamic acids, 25:4083
SESHAGIRI RAO, V., 437-keV beta transition in the decay of ^{125}Sb, 25:5730
SESONSKE, Alexander, Velocity profile and pressure drop measurements in fully developed mercury pipe flow, 25:4207
SESSA, A., Radiosensitizing effect of L-erythro-α,β-dihydroxybutyraldehyde on Ehrlich ascites tumour cells. Cytokinetic analysis of tumour growth, 25:4564
SETH, R. S., Electrical resistivity and deviations from Matthiessen's rule in dilute alloys of aluminum, cadmium, silver, and magnesium, 25:5184
SETH, V. P., Interactions (ν---p) in peripheral model, 25:5376
SETKINA, V. N., Effect of substituents on hydrogen exchange reaction of some ferrocene derivatives, 25:4069
SETLOW, Jane K., Macromolecular synthesis in irradiated bacteria, 25:4462
SETLOW, Richard B., Macromolecular synthesis in irradiated bacteria, 25:4462
SEVAST'YANOV, V. G., Uranium sulfide transport, 25:4059
SEVIER, P. E., Considerations in the evaluation of aluminum master alloys, 25:4780
SEYLER, R. G., Polarization effects in (d,p) stripping processes, 25:5828
SHA, W. T., Theoretical prediction of local boiling void distribution in a water reactor channel, 25:5969
SHADMI, Yehuda, Average energies of ground, singly, and doubly excited configurations in highly ionized atoms, 25:4945
SHAFIGULLINA, G. A., Hall effect in certain rare-earth metals and alloys, 25:5182
SHAKIN, C. M., Lane equations for isobaric resonances, 25:5818
SHALYT, S. S., Superconductivity of titanium carbide, 25:5038
SHAMPINE, L. F., Efficient Runge--Kutta codes, 25:6250 (SC-RR-70-615)
SHAMSUTDINOV, A. D., Possibilities of isotope synthesis in fission reaction, 25:5756
SHANK, Norman Eugene, Pulse radiolysis studies of aromatic radical cations in 1,2-dichloroethane, 25:4112
SHANKAR, J., Maleic acid complexes of rare earth and other metals. I, 25:4075
Radiation and catalysis, 25:4099
SHAPIRO, J. A., Electrostatic analogue for Virasoro model, 25:5353
SHARMA, R. P., E2 strength of 191 keV transition in ^{197}Au, 25:5709
SHASHKOV, V. S., Use of combined radiation protection compounds, 25:4609
SHATALOV, O. P., Mechanism of thermal dissociation of diatomic molecules, 25:6252 (SC-T-70-4045)
SHATENSHTEIN, A. I., Effect of the participation of the acid in forming the hydrogen bond during electrophilic deuterio-exchange, 25:4073
SHCHEREDIN, V. P., Mass spectrometric studies of thermodynamic properties of binary system NaF--MeF_3 (Me = Sc, Y, La). II, 25:4857
SHEA, Thomas E., Temperature-dependent and multi-level effects on neutron resonance cross sections, 25:5686 (TID-25566)
SHEBOLDAEV, S. B., Mechanism of the interaction of V_2O_5 with C. II, 25:4842
SHEFFIELD, G. V., Mapping a toroidal magnetic field, 25:5074
SHEINELATT, Marshall Jay, Field theory of the charged vector boson, 25:5413
SHEJBAL, J., In vitro radiosensitization of Ehrlich ascites tumour cells and pure enzymes by iodine compounds, 25:4569
SHEKRILADZE, I. G., Determination of the average effective radius of vaporization centers in the nucleate boiling of liquids, 25:6215 (AEC-tr-7202)
SHELINE, R. K., Level structure of ^{169}Er, 25:5725
SHELTON, Russell D., Analysis of effect of high-energy protons on ATM photographic film, 25:4407 (N-70-35923)
SHENOY, G. K., Hyperfine interactions in Er_2O_3 and Yb_2O_3 between 20 and 1.5°K, 25:5225
SHENOY, M. A., Mechanisms of radiosensitization by some sulphydryl poisons, 25:4552
SHEPELA, Adam, Diffusion of ^{14}C in W and W--Re alloys, 25:4763
SHEPETNOV, R. V., Interrelation between solar wind and geomagnetic field, 25:5026
SHEPHERD, D. M., In-cell crane, manipulator, and television systems for TURF, 25:4303
SHEPHERD, L. R., High-temperature reactor development in Dragon Project, 25:5947
SHEPPARD, J. C., In-phantom dosimetry of ^{238}Pu heat sources, 25:4517
SHERMAN, R. H., Polarization of 22-MeV neutrons elastically scattered from liquid tritium and deuterium, 25:5516 (LA-4465, pp 15.1-2)
SHERR, R., Anomalous L = 1 shapes of angular distributions for (^{3}He,t) transitions to 0$^+$ antianalog states in ^{64} ^{66}Ga and ^{40}K, 25:5654
SHIEH, P. S., Spherical harmonics solution of the two-group linear transport equation, 25:6158
SHIELS, S., Interstitial transfer in sodium systems, 25:4773
SHIL'SHTEIN, S. Sh., Anomalous transmission of neutron in a perfect CdS crystal, 25:5785
SHIMMINS, J., Mineral and density changes in bone with age in normal and pathological states, 25:4619 (CONF-680211-, pp 177-91)
SHIMOKAWA, Junichi, Process of carburization in austenite stainless steel, 25:4739 (JAERI-Memo-4132)
SHIN, Y. M., Photodisintegration of ^{4}He, 25:5544
SHIROKOV, Yu. M., Connection of field matrix element with phases of two-channel S-wave scattering, 25:5436
SHIRVINGTON, P. J., Electron conduction through oxide films on Zircaloy-2, 25:5173
SHMELEV, O. A., Program of connection of measuring microscopes PUOS with computer Minsk-2, 25:4369 (IFVE-SPK-69-53)
SHOOP, C. Robert, Effects of radiation on migratory orientation of salamanders, 25:4475 (NYO-3654-8)
SHOTTER, A. C., Reactions ^{14}N(p,^{3}He)^{12}C, ^{14}N(d,α)^{12}C, ^{13}C(p,d)^{12}C, 25:5563
SHPINEL, V. S., Photoeffect and internal conversion in resonant absorption of M1 gamma quanta by ^{119}Sn, 25:5787
SHUGART, H. A., Radiative lifetime of metastable 2^1S_0 state of He, 25:4944
SHUKLA, R. V., Excitation mechanism of sodium D lines in nightglow, 25:5018
SHUM, R. H., Approach for determining the effective energy release of a fast reactor accident, 25:6065
Consequences of extensive fuel meltdown in various EBR-II core configurations, 25:6082
Improved method for assessing damage to the reactor vessel in a fast reactor accident, 25:6064
SHUMWAY, R. W., Core thermal performance margins for bottom flooding ECC systems, 25:6041
SHYN, Tong Wha, Measurement of $2^2S/\text{sub } {}^1/_2$--$2^2P/\text{sub } {}^3/_2$ energy separation in H, 25:4951
SICK, I., Electromagnetic structure of the ^{3}He nucleus, 25:5535
SIDOROV, L. N., Mass spectrometric studies of thermodynamic properties of binary system NaF--MeF_3 (Me = Sc, Y, La). II, 25:4857
SIDOROV, S. K., Dependence of scattering transport length on neutron energy in H_2O, D_2O, and graphite, 25:5502
SIEBERT, B., Yamaguchi's deuteron wave function, 25:5871
SIEGEL, Stanley, Uranium--O system at high pressure, 25:4793
SIEMSSEN, R. H., Excitation functions from elastic ^{16}O scattering from nuclei with A approximately 16, 25:5566
SIGAL, I. M., Description of spectrum of energy operator of quantum-mechanical systems, 25:5241
SIGALOV, A. G., Description of spectrum of energy operator of quantum-mechanical systems, 25:5241
SIGNELL, Peter, How realistic is the Tabakin nucleon--nucleon potential, 25:5825
SILAEV, E. A., Ionization counter dE/dx filled with liquid Xe, 25:4319 (JINR-P13-5403)
SILBERMAN, Edward, Physical modeling of heat dispersion in large lakes, 25:6217 (ANL-ES-2)
SILONOV, V. M., Local ordering and resistivity of Ni--W and Pd--Co alloys, 25:4766
SILVA, R. J., Search for long-lived spontaneous fission isomer of ^{241}Pu, 25:5759
SILVER, Brian L., ESR of SO_2^-, 25:4124
SILVER, E. G., Measurement of capture cross section of ^{238}U, 25:5771
SILVERMAN, Dennis, Scaling behavior in multiperipheral dynamics, 25:5351 (NYO-2262-TA-225)
SILVERMAN, M. D., Effects of transverse flow on fission product transport through graphite tubes, 25:6011
SIMANTON, J. R., Target handling system for 200-GeV proton accelerator, 25:5470
SIMBEL, M. H., Use of the eikonal approximation in the optical-model calculation, 25:5834
SIMMONS, J. E., Considerations on polarized neutron production by (d,n) polarization transfer reactions at 0°, 25:5805 (LA-4465, pp 26.1-2)
Improvements in performance of a liquid helium scintillation counter, 25:4321 (LA-4465, pp 31.1-2)
Neutron polarization in the T(d,n)^{4}He reaction using a polarized incident beam, 25:5513 (LA-4465, pp 12.1-2)
Neutron--helium polarization at 27.3 and 30.3 MeV, 25:5523 (LA-4465, pp 30.1-2)
Polarization angular distribution from the T(d,n)^{4}He reaction at 7.0 and 11.4 MeV, 25:5522 (LA-4465, pp 29.1-2)
Preliminary measurements of neutron polarization from the D(d,n)^{3}He reaction using a polarized incident beam,

XUM

25:5514 (LA-4465, pp 13.1-2)
SIMMONS, S. Oliver, Construction of a three crystal spectrometer and study of the decay of ^{90}Nb, 25:5682 (IS-T-389)
SIMON, J. P., Target handling system for 200-GeV proton accelerator, 25:5470
SIMONS, G. G., Gamma-ray dose evaluations for ZPR-3/EBR-II critical assemblies, 25:6125
SIMONS, R. L., Comparison of measured and calculated integral fluxes and spectra in a pressure vessel mockup, 25:6213
Yield strength and creep strain estimates for irradiated stainless steel, 25:4820
SIMPSON, J. L., Testing of instruments and material balance methods for plutonium safeguard control, 25:4297
SIMPSON, Terry R., Heat transfer optimization and reactivity of nuclear rocket reactors, 25:6127
SIMS, C. S., Tissue equivalent ionization chamber, 25:4330
SINCLAIR, E. E., AEC programs in fast reactor core safety, 25:6087
SINCLAIR, R. M., Mapping a toroidal magnetic field, 25:5074
SINCLAIR, Warren K., Sensitization by hydroxyurea and protection by cysteamine of Chinese hamster cells during the cell cycle, 25:4659
SINGER, Ralph M., Further study of the pressure-temperature history model of liquid-metal boiling inception, 25:4212
SINGH, B., Gamma radiation from the decay of ^{96}Nb, 25:5718
M1/E2 multipole mixing of 563 and 569 keV transitions in ^{134}Ba, 25:5706
SINGH, B. B., Mechanisms of radiosensitization by some sulphydryl poisons, 25:4552
SINGH, B. P., Occupancy of spherical shells in the ground state of even 2s-1d shell nuclei, 25:5876
SINGH, C. P., Interactions (π^---p) in peripheral model, 25:5376
SINGH, Manmohan, New method of evaluating bone loss in osteoporosis, 25:4639 (CONF-700515-, pp 199-204)
SINGH, P. P., Excitation functions from elastic ^{16}O scattering from nuclei with A approximately 16, 25:5566
SINGH, R. N., Bremsstrahlung x-ray flux and its ionizing effect in the lower ionosphere, 25:5019
SINGH, R. P., Potentiometric investigation of metal complexes with phenanthrenequinone monoxime, 25:4080
SINGH, Tej, Complexes between U(VI) and dicxydiquinone, 25:4078
SINHA, S. K., Reversal of inhibitory effects of γ-rays on seedling growth of wheat, 25:4718
SIPS, L., Phenomenological description of anharmonic quadrupole vibrations, 25:5782
SIRLIN, A., Dimensions of current operators, 25:5306 (NYO-4204-1)
SIROHI, G. S., Reversal of inhibitory effects of γ-rays on seedling growth of wheat, 25:4718
SISSAKIAN, A. N., Problem of quasipotential smoothness in quantum field theory models, 25:5387 (JINR-E2-5365)
SITAR, B., Some radioactive characteristics of calcium, 25:5647
SITENKO, A. G., Allowance for the wave function distortion under multipole analysis of fast nucleon scattering by nuclei, 25:5552 (ITF-70-50)
SIVARDIERE, J., Magnetic structure of ErSi, 25:5212
Metamagnetic properties of a single crystal of $ErCrO_3$, 25:5180
SIVIERO, E., Polymerization induced by gamma radiation of styrene under pressure, 25:4104
SIWEK, K., Isomeric cross-section ratios and total cross-sections for the ^{113}In(n,2n)/sup 112gm/In and ^{115}In(n,2n)/sup 114gm/In reactions, 25:5763
SJOESTRAND, U., Spectrometry for determination of isotopic mixtures, 25:4031
SKAALI, B., Transient fields in ferromagnetic iron and gadolinium, 25:5189
SKACHKOV, N. B., Analytical properties of the relativistic scattering amplitude in quasi-potential approach, 25:5437
SKARSGARD, H. M., Current-induced ion heating in a toroidal plasma, 25:5069
SKAVDAHL, R. E., SEFOR experiments, 25:6058
SKOELDBORN, Holger, Determination of bone mineral content in lumbar vertebrae by a double gamma-ray technique, 25:4643 (CONF-700515-, pp 243-54)
SKOFRONICK, J. G., Velocity dependence of relative total cross section for He + He from 2070 to 2750 m/sec, 25:4965
SLAWECKI, M. A., Pneumatic tube transfer system for radioactive samples, 25:4306
SLAYTON, Marshall T., Measurement of neutron diffusion lengths in highly absorbing solutions, 25:6183
SLOAN, I. H., Neutron--deuteron breakup models, 25:5531
SLOAN, W. Robert, Multiplication effects in measurements of delayed-neutron energy spectra, 25:5774
SLOVACEK, R. E., Time-dependent neutron spectra measurements in water, 25:5485
SLOVOKHOTOVA, N. A., Spectroscopic investigation of the low-temperature radiolysis of some polyolefins, 25:4118
SLOVYANSKIKH, V. K., Uranium sulfide transport, 25:4059
SMAGINA, E. I., Mass spectrometric investigation of thermal dissociation of Sm and Eu carbides, 25:4855
SMIDT, F. A. Jr., Unusual interstitial aggregates in vanadium irradiated at 0.15 T/sub m/, 25:4828
SMIDT, Fred A. Jr., Dislocation channeling in irradiated metals, 25:4809 (AD-710358)
SMIRNOV, L. S., Photoconductivity spectra of irradiated and plastically deformed crystals of germanium, 25:5161
SMIRNOV, V. A., Time-of-flight and coordinate measurements in a 130 cm scintillation counter, 25:4318 (JINR-E1-5098)
SMITH, B. C., Thermochemical studies of Th(IV) and U(IV) chlorides, 25:4077
SMITH, C. H. Llewellyn, High-energy neutrino--nucleon scattering current algebra and partons, 25:5345
SMITH, C. W. Jr., /sup 99m/Tc brain scanning in Herpes virus type I encephalitis, 25:4660
SMITH, D. A., Backward angle scattering of 50-MeV protons from C, O, N, and Be, 25:5585
SMITH, D. B., Two-stage Monte Carlo calculations of delayed-neutron response, 25:6151
SMITH, D. R., In-plant survey of television receivers for x-radiation emission capability, 25:4522 (BRH/DEP-70-24)
SMITH, Deryk A., Mineral and density changes in bone with age in normal and pathological states, 25:4615 (CONF-680211-, pp 177-91)
SMITH, Edward M., Absorbed dose considerations for radiopharmaceuticals, 25:4511
Idealized data handling system, 25:4328
SMITH, G. L., Ground-state quasirotational bands and other states in ^{130} ^{132} ^{134} ^{136} ^{138} ^{140}Ce, 25:5711
SMITH, H. J., M3 isomeric transitions in ^{59}Co and ^{60}Co, 25:5608
SMITH, Morton C., Prog. rpt. on CMF-13 research on carbon and graphite, 5--7/70, 25:4840 (LA-4526)
SMITH, S. D., Enthalpy-of-formation data on compounds of uranium, 25:4843
SMITH, T. H., Prompt and multiorbital reentry of small radioisotope heaters at superorbital velocities, 25:4221
SMITH, T. M., In-plant survey of television receivers for x-radiation emission capability, 25:4522 (BRH/DEP-70-24)
SMOAK III, William M., Conference on pulmonary investigation with radionuclides, Miami, Fla., 3/69, 25:4662
Pathophysiology of perfusion in pulmonary disease, 25:4675
SMONDYREV, M. A., Equality of local algebras of relativistic quantum field theory, 25:5407 (JINR-P2-5330)
SNELL, Earle O. Jr., Thermal cycling of maraging steel, 25:6254 (UCRL-72099)
SNIDER, M. A., Synthesis of fast reactor spectra, 25:5961
SNYDER, H. J., Type 316 stainless-steel tubing for LMFBR fuel element cladding, 25:4776
SNYDER, James L., Streaming of gamma radiation in two-legged ducts, 25:5138
SNYDER, R. G., Bond polarizability interpretation of Raman intensities of cyclohexane and cyclohexane-d_{12}, 25:4061
Interpretation of the Raman spectrum of polyethylene and deuteropolyethylene, 25:4062
SODAN, H., Levels in ^{167}Tm, 25:5726
Non-adiabatic effects in rotational bands of odd proton nucleus ^{155}Tb, 25:5783
SOERENSEN, Arne, Facilities at Risoe for post-irradiation examination of Dragon Project experiments, 25:4262 (DP-Report-446)
SOHN, C. Y., Radiation breeding of perennial plants. I, 25:4724
SOLNYSHKOV, A. I., Technique for measuring phase characteristics of an ion beam, 25:5457 (NP-18507)
SOLOMON, J., Nonlinear mechanisms associated with wave particle interactions in the magnetosphere, 25:5031
SOLOV'EV, L. D., Some consequences from constant behavior of total cross sections at energies more than 30 GeV, 25:5294
SOLUNSKII, V. I., Study of diffusion by tracks left by nuclear reaction products in a solid detector, 25:4845
SOLUNSKII, Yu. S., Study of diffusion by tracks left by nuclear reaction products in a solid detector, 25:4845
SOLYANINA, I. P., Effect of additions of aromatic hydrocarbons on chemical radiation stability of TBP in dodecane solution, 25:4116
SOMENKOV, V. A., Anomalous transmission of neutron in a perfect CdS crystal, 25:5785
SOMEYA, T., Temperature rise of specimen due to electron irradiation, 25:5163
SOMOGYI, A., Conference on cosmic rays, Budapest, 8--9/69, 25:4976
Modulation dynamics, 25:4983
SONG, In Chul, The effect of total-body irradiation on wound healing and the hematopoietic system in mice, 25:4705
SONNTAG, Ch., Nonstatistical shape of beta spectrum of ^{14}C, 25:5591
SOODAK, Harry, Simplified eigenvalue problem solutions in diffusion calculation, 25:6173
SOPER, P. J., Cones equation and superconvergence relations, 25:5427
SORENSON, James A., Effects of fat on bone mineral

measurements, 25:4644 (CONF-700515-, pp 255-62)
Measurement of bone mineral by the direct photon absorption method: principles and instrumentation, 25:4623 (CONF-680211-, pp 253-68)
SOWINSKI, Kenneth P., Alpha-scattering technique of chemical analysis, 25:4034
SPEAR, R. H., Energy levels of ^{27}Si, 25:5602 (ANU-P-501)
SPEAR, Ward G., Gas-flow method for detection of fast neutrons in reactors, 25:4355
SPECHT, Eugene R., Critical experiment normalization for LMFBR's, 25:6114
SPEIRS, C. F., Mineral and density changes in bone with age in normal and pathological states, 25:4619 (CONF-680211-, pp 177-91)
SPENCER, Herta, Prog. rpt. on metabolism and removal of ^{90}Sr and ^{226}Ra in man, annual, 1969--1970, 25:4424 (TID-25567)
SPENKE, H., Considerations on the in-core fuel management during startup of a fast breeder reactor, 25:6054
SPETH, J., Isomeric shift and magnetic hyperfine splitting of muonic atoms in the lead region, 25:5794
Transition probabilities and static moments of excited states in even--even nuclei, 25:5816
SPICER, B. M., Collective correlations calculation of dipole states of ^{28}Si, 25:5653
Quartet structure in light nuclei, 25:5814
SPICER, W. E., Reflectance studies of Ba, Sr, Eu, and Yb, 25:5188
SPIERS, E. W., Measuring ^{51}Cr in presence of ^{59}Fe, 25:4513
SPIRO, M., Effective Regge trajectories for some two-body reactions, 25:5377
SPIVACK, M. A., Parylene thin films for radiation applications, 25:4329
SPLICHAL, W. F., Pocket radiation dose integrator and monitor, 25:4360
SPRINGER, T. H., Preliminary analysis of molybdenum-reflected, fast spectrum critical assembly, 25:6140
Reactivity worth of tantalum in a fast reactor spectrum, 25:5964
SPRUIT, J. J., Phalangeal Atlas: an application of radiographic photodensitometry, 25:4641 (CONF-700515-, pp 224-36)
SREE RAMULU, K., Induced systematic mutations in Sorghum, 25:4495
SRINIVASAN, T. M., Influence of impurities on the room-temperature coloration processes in alkali halides, 25:5159
SRIVASTAVA, A. N., Excitation mechanism of sodium D lines in nightglow, 25:5018
SRIVASTAVA, M. K., Dependence of nuclear matter binding energy on the high energy phase shifts, 25:5862
Off-shell behaviour of phase-shift equivalent momentum-dependent potentials, 25:5852
SRIVASTAVA, O. N., Study of oxidation of ytterbium and holmium thin films in the electron microscope, 25:4767
STACEY, Weston M. Jr., Anisotropic elastic moderation of neutrons, 25:6165
Solution of the neutron diffusion equation by space-energy factorization, 25:6169
Studies of spectral synthesis in spatially dependent fast reactor dynamics, 25:6178
STAHL, A., Pulmonary hemosiderosis in a 9-year old child with a trisomy 18, 25:4685
STANKO, V. I., Radiosensitizing properties of some barenes (ortho-1,1 dicarbaclovododecaborane), 25:4588
STARIKOV, V. N., Calculation of neutron distribution in hydrogen, 25:5493
STARKOVICH, V. S., Comparison of double scattering and polarized ion source measurements of ^{4}He(d,d)^{4}He polarization at 11.5 MeV, 25:5510 (LA-4465, pp 3.1-3)
STATHAM, C. D., Slip in single crystals of niobium--molybdenum alloys deformed in compression, 25:4800
STAUB, Roy T., Tumor thrombus of the right atrium displayed by rapid sequence scintiphotography, 25:4659
STEARNS, E. H., Trigger-actuated motion locks for master-slave manipulators, 25:4312
STEELE, William A., Radionuclide distribution in particles produced by the Schooner Event, 25:4180
STEEN, H. B., Effect of various dry electron scavengers on the radioluminescence of indole in polar solution, 25:4089
STEEN, N. M., Analysis of resonance integrals of ThO_2 rods, 25:6205
STEFAN, Heinz, Physical modeling of heat dispersion in large lakes, 25:6217 (ANL-ES-2)
STEGEMANN, D. H., Application of neutron transient phenomena in heavy moderators to nondestructive techniques, 25:6204
STEHLIK, G., Influence of cyclcheximide on the radiosensitivity of Saccharomyces cerevisiae, 25:4556
STEICHEN, J. M., Dynamic strain aging in 304 stainless steel, 25:4777
STEINBERG, M., Development of concrete-polymer materials and composites, 25:4838
STELJES, J. F., Cosmic ray NM-64 neutron monitor data. XVI, 25:4975 (AECL-3736)
STELSON, P. H., Levels in ^{53}Mn, ^{58}Co, ^{63}Zn, and ^{70}Ga from the (p,n) reaction, 25:5612
STENGL, G., Precision-measurement of ^{27}Al(n,α) cross section for 14.43-MeV neutrons, 25:5641
STENSTROM, D. G., Gamma-ray dose evaluations for ZPR-3/EBR-II critical assemblies, 25:6125
STEPHENS, F. S., Oblate shape of $^{9}/_{2}^{-}$ isomer in ^{199}Tl, 25:5707
Quadrupole moments excited states in ^{20}Ne and ^{22}Ne, 25:5622
STEPHENSON, L. L., Survey of factors which influence stress corrosion crack initiation in several uranium base alloys, 25:4749 (SC-DR-70-718)
STERNBERG, Joseph, Study of lung functions with radionuclides, 25:4673
STEVENS, C. A., Scattering angle biasing for deep-penetration x-ray transport, 25:5145
STEVENS, J. W., Film and transition boiling around spheres, 25:4209
STEVENS, Ralph R. Jr., Transfer matrix method for calculating spin aberrations in the transport of polarized beams, 25:5454 (LA-4468, pp 18.1-16)
STEWART, J. W., Form factor ratio GE/sub n//GE/sub p/ at low-momentum transfers, 25:5247 (AD-710385)
STEWART, Jake W. Jr., Elastic electron scattering measurements of the neutron charge form factor at very-low momentum transfers, 25:5246 (AD-709922)
STEYERT, W. A., First-forbidden β decays of ^{198}Au, 25:5708
STEYN, J. J., Gamma photon albedo distributions for finite media, 25:5146
Optimization of shields for protection of unmanned spacecraft scientific experiments, 25:5137
STIENS, Robert, Radwaste design for no plant-originated radioactive liquid discharge, 25:5882
STILLER, G., Reaction (d,α) on ^{13}C, 25:5559
STILLER-WINKLER, R., Regeneration of peripheral blood in thymectomized mice after sublethal whole-body irradiation, 25:4469
STODIEK, W., Thermal equilibrium and stability of Tokamak discharges, 25:5117
STOESSEL, Edward Thomas, Phenomenological regge trajectories in direct-channel pion--proton elastic scattering, 25:5382
STOLETOV, G. D., Polarization of secondary protons in pp + π^{+}pn and pp + π^{0}pp reactions at 669 MeV, 25:5268 (JINR-P1-5293)
STONER, R. D., Radiosensitivity of immune responses, 25:4470
STORA, Jean Pierre, Effect of porosity on thermal conductivity of uranium dioxide, 25:4844
STORHOK, V. W., Role of grain boundaries in swelling of UN at 1600 to 1700°C, 25:4826
STOTT, A. N. B., Assessment of medical requirements for workers in nuclear installations, 25:4529 (AERE-R-6523)
STRAALSUND, J. L., Effect of cold work on irradiation-induced swelling, 25:4824
STRACKEE, L., Relation between deposition of long lived fission products and dietary ingestion, 25:4519
STRAIT, E. N., Automatic system for counting etched holes in thin dielectric plastics, 25:4340
STRAKER, E. A., Simultaneous fast-neutron spectral measurements by time-of-flight and pulse-height unfolding techniques, 25:4366
STRANDJORD, Nels M., Bone densitometry: clinical applications, 25:4626 (CONF-680211-, pp 308-19)
STRANIK, D. A., Evaluation of PuO_2 homogeneity in PuO_2--UO_2 fast reactor fuel, 25:4876
STRATTON, W. R., Large accidents, 25:6085
STRAUB, R. F., Radiosensitivity of immune responses, 25:4470
STREFFER, Christian, Role of the CNS on the radioprotective effect of 5-hydroxytryptamine, 25:4584
STRILCHUK, A. R., Current-induced ion heating in a toroidal plasma, 25:5069
STRINGFELLOW, M. W., Exchange and crystal-field interactions in Er and Ho, 25:5214
STROEMBERG, Lars G., Angular distributions in neutron-induced reactions. I, 25:5549 (BNL-400(3rd Ed.)(Vol.1))
STROETZEL, M., Inelastic electron scattering from the region of the ^{16}O giant resonance, 25:5558
STROGANOV, Yu. G., Low boundaries for $\pi^{0}\pi^{0}$-meson scattering lengths, 25:5368
STROMATT, R. W., Pulsed current electroplating, 25:4741 (BNWL-CC-491)
STRONGIN, Myron, Superconductivity and normal-state conduction mechanism in oxidized thin aluminum films, 25:5039
STRONSKI, I., Radiochemical separation of microamounts of In--Cd, In--Sn--Te, and Sb--Sn by extraction chromatography, 25:4143
STRUGALSKI, Z. S., Di-pion in mass values region M($\pi^{0}\pi^{0}$) less than or equal to 1.3 GeV, 25:5284 (JINR-E1-5085)
STRUXNESS, E. G., Radiological considerations in the use of natural gas from nuclearly stimulated wells, 25:4525 (ORNL-TM-3216)
STUART, Robin G., Effects of fission gas on transient over-power fuel rod failure, 25:6098
STUBBINS, W. F., Photodisintegration of ^{4}He, 25:5544
STUPINA, N. N., Local ordering and resistivity of Ni--W and Pd--Co alloys, 25:4766
SUBBARAM, K. V., ^{2}PI--X ^{2}PI system of ^{14}N^{80}Se and ^{14}N^{78}Se, 25:4063
SUBRAMANIAN, R. B., Grafting of organic polymers onto inorganic substrates by gamma irradiation, 25:4106
SUBRAMANIAN, S., Oxides and oxyions of the non-metals.

XUM

XIV and XIX, 25:4090
SUENKEL, W., Unified nuclear reaction theory, 25:5870
SUGAHARA, T., Protection of mice against ionizing radiations by adrenochrome monoguanylhydrazone methansulphonate; a promising agent for clinical use, 25:4589
SUICH, J. E., Alphameric displays in nuclear reactor computations, 25:6202
SUIKOVA, L. A., Vicia faba seedling chromosome damages by split dose, 25:4497
SUN, K. H., In-core detector for measuring power and breeding distributions in power breeders, 25:6044
SUNDSFJORD, Johan A., Radioimmunoassay of angictensin II in plasma, 25:4419
SUSSKIND, H., Reactor operating and maintenance costs, 25:5903
SUSTMAN, J. E., Sodium-vapor monitor, 25:6046
SUTEY, A. M., Subchannel coolant temperatures of EBR-II instrumented subassembly PNL-17(XX02), 25:6027
SVANBERG, L., Four quandrant radiospirometry in normal and diseased states, 25:4671
SVIRSKII, E. B., Research on studying and increasing the plasma parameters on ''non-cylindrical Z-pinch'' equipment, 25:5116 (SC-T-70-4046)
SVOBODA, K., Production of carrier-free radiostrontium ^{85}Sr, 25:4126 (UJV-2431-Ch)
SWANSON, C. D., Plutonium and ^{238}U Doppler measurements in plutonium-fueled fast critical assembly, 25:6109
SWANSON, V. A., Neutron radiography development program for SNAP-8 fuel elements, 25:4252
SWANSTROM, R. H., Argon atmosphere filter system in HFEF hot cell, 25:4197
SWARTZ, H. M., Structure-function studies of the aminothiol radioprotectants, 25:4548
SWENSON, Edward W., Four quandrant radiospircmetry in normal and diseased states, 25:4671
Technetium--indium double lung scanning, 25:4677
SWERDLOW, P. H., Moessbauer measurements of quadrupole-moment ratios of first excited 2^+ states of ^{176} ^{178} ^{180}Hf, 25:5668
SWIDER, W., Ionic reactions for meteoric elements, 25:5012
SWIFT, Jerry J., Gamma spectra: density relaticnships in a gamma backscatter density gauge, 25:4385
SWITZER, W. L., Photonuclear reactions above the giant resonance, 25:5679
SYAO-SHAN, Comparative toxicity of soluble and insoluble compounds of ^{232}Th, 25:4440
SYKES, D. H., Levels of ^{36}Cl below 3 MeV, 25:5627
SYMES, R. D., Excited states of ^{44}Ca, 25:5626
SYMKO, O. G., Continuously operating ^{4}He evaporation refrigerator, 25:5061 (UCSD-34-P-143-31)
Magnetization of dilute Cu--Mn alloys at very low temperatures, 25:6256 (UCSD-34-P-143-33)
SYMONS, M. C. R., Oxides and cxyions of the non-metals. XIV and XIX, 25:4090
SYROVATSKII, S. I., Origin and acceleration mechanisms, 25:4979
SYSOEV, L. A., Anomalous transmission of neutron in a perfect CdS crystal, 25:5785
SZABO, E., Two-dimensional (T/sub 1/2/, E/sub γ/) mapping of short-lived nuclides, 25:5685 (KFKI-70-18-NAC)
SZE, N. H., Fluctuations and critical indices near Neel temperature of Eu, 25:5204
SZENTPETERY, I., Analog resonance in $^{58}Ni(p,\gamma)^{59}Cu$ reaction, 25:5660
SZTANYIK, B. L., Radioprotective effect of a mixture of AET and 5-methoxytryptamine in x-irradiated mice, 25:4583
Radioprotective effect of N-substituted AET-derivatives having amino acid structure, 25:4577
SZUECS, Judit, Analog resonance in $^{58}Ni(p,\gamma)^{59}Cu$ reaction, 25:5660

T

TABATA, Tatsuo, Current profile monitor for scanning electron beam, 25:5468
TABATA, Yoneho, Nuclear magnetic resonance of tetrafluoroethylene--isobutylene copolymers obtained by γ-ray irradiation, 25:4102
TAHERZADEH, M., Neutron emission characteristics of a PuO_2 source, 25:4244
Response of solid-state detectors to moncenergetic neutrons, 25:4351
TAJIMA, Makoto, Radiation chemistry of foods. IV, 25:4117
TAKAHASHI, H., DNA replication in radiation-induced thymomas of mice, 25:4460
Integral measurement of capture-to-fission ratio in ^{239}Pu, 25:5772
TAKAHASHI, Hiroshi, Quantum correction of the neutron transport equation, 25:6167
TAKAHASHI, Masaji, Clinical studies of intra-arterial infusion of 5-bromodeoxyuridine plus 5-fluorouracil and radiation, 25:4602
TAKAMURA, S., Propagation of icn waves in a radio frequency electric field, 25:5130
TAKAYAMA, K., Propagation of icn waves in a radio frequency electric field, 25:5130
TAKEMURA, K., Reliability aspects of safety evaluation of nuclear power plants, 25:5937 (RISO-214, pp 457-79)
TALAMINI, G., Polymerization induced by gamma radiation of styrene under pressure, 25:4104
TALBERT, W. L. Jr., Decay of /sup 85m/Kr, 25:5634
TALLENTIRE, A., Radiation resistance of spores, 25:4726
TAMURA, Masaya, Aseismatic design for a nuclear power plant, 25:5939
TAMURA, Tsutomu, Decay scheme of 5.3 h ^{113}Ag and 1.2 min /sup 113m/Ag, 25:5754
TAN, C. W., Mass transfer of aerosols with axial diffusion in circular tubes, 25:4204 (HASL-238)
TAN, Chung-I, Crossed channel partial wave expansions and the Bethe--Salpeter equation, 25:5426 (NYO-2263-TA-226)
Scaling behavior in multiperipheral dynamics, 25:5351 (NYO-2262-TA-225)
TANAKA, E., Optimal data processing radioisotope imaging, 25:4359
TANAKA, S., Levels in ^{53}Mn, ^{58}Co, ^{63}Zn, and ^{70}Ga from the (p,n) reaction, 25:5612
TANAKA, T., Protection of mice against ionizing radiations by adrenochrome monoguanylhydrazone methansulphonate; a promising agent for clinical use, 25:4589
TANAKA, Yoshimasa, Clinical studies of intra-arterial infusion of 5-bromodeoxyuridine plus 5-fluorouracil and radiation, 25:4602
TANDON, G. K., Energy levels of ^{19}Ne, 25:5587
TANG, I-ming, Motion of order parameter in type-II transition-element superconductors, 25:5050
TANG, Ing M., Slowing down of neutrons in mixtures, 25:5484
TANI, Kensuke, Theory of neutron scattering from lattice vibrations, 25:5483
TAPE, J. W., Properties of the low-lying states of ^{48}Ca, 25:5616
TAPLIN, George V., Radioaerosol inhalation scanning, 25:4678
TARAMASCO, H., Pulmonary hemosiderosis in a 5-year old child with a trisomy 18, 25:4685
TARPLEY, Fred A. Jr., New course in financial management and economics of nuclear power, 25:6195
TARVID, G. V., Technique for measuring phase characteristics of an icn beam, 25:5457 (NP-18507)
TAUBE, M., Gas phase radiolysis of hydrogen sulfide and propane under the influence of the particles formed in the reaction $^{10}B(n,\alpha)^{7}Li$, 25:4115
TAUBENHEIM, J., Anomalies of lower ionosphere ionization in medium latitudes, 25:5006
TAUXE, W. Newlon, Disappearance of iodoalbumin from pericardial sac in a patient with myxedema, 25:4658
TAVEL, M. A., Phase space time evolution method, or, how to solve time-dependent transport problems in spite of transport equation, 25:5139
TAVKHELIDZE, A. N., Problem of quasipotential smoothness in quantum field theory models, 25:5387 (JINR-E2-5365)
TAYLOR, A., Thermally stimulated conductivity and luminescence in KBr due to γ irradiation at 10°K, 25:5158
TAYLOR, Clement R., Radiation-curable-vinyl resin paints and coated article, 25:4095
TAYLOR, G., Economics of radiation versus heat-catalyst curing for wood-plastic flooring plant, 25:4109
TAYLOR, G. R., Radiochemical measurement of mass transfer coefficients in forced-convection sodium, 25:4774
TAYLOR, George S., Importance of pulse-height analysis in the gamma-ray attenuation technique for measurement of soil moisture, 25:4158
TAYLOR, H. W., Gamma radiation from the decay of ^{94}Nb, 25:5718
M1/E2 multipole mixing of 563 and 569 keV transitions in ^{134}Ba, 25:5706
TAYLOR, J. F., Survival-promoting effects of endotoxin in mice, dogs, and sheep, 25:4586
TAYLOR, K. N. R., Electrical conductivity of dysprosium thin films, 25:4771
Magnetization and ^{59}Cc hyperfine field measurements in $Gd(CoNi)_2$, 25:5198
TAYLOR, L. L., Effects of irradiation of the parotid gland and pancreas on human isoamylases, 25:4452
TAYLOR, P. L., Theory of thermoelectric power in metals and alloys, 25:6227 (COO-623-152)
TCHETCHERNIKOV, V. I., Ferrimagnetism of the intermetallic compound Cc_2Gd, 25:5201
TEAGAN, P., Performance reproducibility of cylindrical diodes with CVD fluoride tungsten--niobium electrodes, 25:4751 (TEE-4125-3)
TEMME, M. I., Pressure generation and potential work energy during fuel-sodium thermal interaction, 25:6092
TENAGLIA, G., Theoretical reliability assessment of a fire protection system, 25:4187 (RISO-214, pp 21-40)
TEPLOV, E. V., Program of connection of measuring microscopes PUOS with computer Minsk-2, 25:4365 (IFVE-SPK-69-53)
TEPPATI, G., Particle--antiparticle doublets and the full Poincare group, 25:5398
TERADA, Kikuo, Silica gel as support for inorganic ion-exchangers for determination of ^{137}Cs in natural waters, 25:4033
TERASAWA, T., Excitation of the giant resonance in ^{12}C by inelastic electron scattering, 25:5572
TERASAWA, Tokuo, Analysis of $^{58}Ni(n,p)^{58}Co$ reactions, 25:5638
TEREKHIN, V. A., Measurement of interaction cross sections

XUM

of 0.3 to 5.0 MeV neutron with air, 25:5481
TERMINI, S., Particle--antiparticle doublets and the full Poincare group, 25:5398
TERNEY, William B., Optimal control of nuclear reactor depletion, 25:6172
TER-POGOSSIAN, Michel M., Advanced and research imaging devices, 25:4327
Cyclotron products, 25:4664
New frontiers in pulmonary investigation, 25:4669
TERRELL, C. W., Subcritical fast reactor as a university research facility, 25:6095
TERRIEN, Y., Weak coupling in the ^{209}Bi 5- x h/sub 9/2/ decuplet, 25:5745
TESCH, S., Reaction (d,α) on ^{13}C, 25:5559
TESHIMA, R., Spin-$^3/_2$ Compton scattering, 25:5329
TESK, J. A., Recovery of lattice parameter and electrical resistivity in low-temperature neutron-irradiated copper, 25:5160
TESTA, F. J., Molten UO_2--Na dropping experiments, 25:6076
TESTA, M., Deep inelastic scattering and the nature of partons, 25:5330
TEUCHERT, E., Some physics aspects of a small once-through pebble-bed reactor, 25:5972
THAKUR, Lambodar, Thermochemical studies of Th(IV) and U(IV) chlorides, 25:4077
THANKI, R. J., Variation in ascorbic acid content and ascorbate-oxidase activity during germination in dark of γ-irradiated castor seeds, 25:4466
THEWS, R. L., Test for exotic exchange in p anti p interactions, 25:5365
THIEL, K., Redetermination of the ^{238}U decay constant by fission tracks in a U-stained Bohemian glass, 25:5767
THIO, S. K., Nonstatistical shape of beta spectrum of ^{14}C, 25:5591
THOMAS, E., Kinetic investigations on the influence of radiosensitizing vitamin K_3 on the haemoglobin-methaemoglobin equilibrium, 25:4598
THOMAS, Garry R., Effects of fission gas on transient overpower fuel rod failure, 25:6098
Fast reactor fuel failure thresholds and mechanisms, 25:6018
THOMAS, J. W., Modification of Tsivoglou method for Rn daughters in air, 25:4040
THOMAS, K. C., Type 316 stainless-steel tubing for LMFBR fuel element cladding, 25:4776
THOMAS, M. F., Excited states of ^{44}Ca, 25:5626
THOMAS, W. E., Effects of fuel thermal limits on gas-cooled fast breeder economics, 25:5902
Nuclear and economic performance of Nb and Mo in LMFBR cores, 25:6055
THOMPSON, A., Heat capacity studies of intermetallic compounds containing rare earth elements, 25:5218
THOMPSON, S. G., Excited state in even--even fission products, 25:5687 (UCRL-19949)
THOMPSON, W. I., GCFR fuel rod design considerations, 25:5998
THORNDIKE, E. H., Recent results in ω meson photoproduction, 25:5248 (DNPL/R-7, pp 71-85)
THORSEN, Helen C., Disappearance of iodoalbumin from pericardial sac in a patient with myxedema, 25:4658
TIKHONOV, L. V., Changes in work-hardened surface layers of W, Nb, and Mo as result of annealing, 25:4757
TIKTOPOULOS, George, Threshold charge-exchange amplitude from di-pion distributions in final states, 25:5315
TIL, E. A., Investigation of azimuthal correlations in decays of heavy resonances, 25:5366
TILL, C. E., Investigation of sodium-voiding reactivities and other safety parameters in fast critical assemblies, 25:6112
Plutonium and ^{238}U Doppler measurements in plutonium-fueled fast critical assembly, 25:6109
TIMIRAS, Paola S., Prog. rpt. on effects of radiation on brain activity and development, 8/69--7/70, 25:4457 (UCB-34-P-82-9)
TING, C. T., Recoil tritium reactions with methyl isocyanide and methyl cyanide. Estimates of energy deposition for the T-for-H reaction, 25:4131
TINGEY, G. L., Gasification of graphite under HTGR operating and potential accident conditions, 25:5985
TIPPETS, R., Light variation of gamma Coronae Borealis, 25:4907
TIPPIE, J. W., Excitation functions from elastic ^{16}O scattering from nuclei with A approximately 16, 25:5566
TIPPING, R. M., Clinical trial of two sunscreening creams, 25:4608
TISHCHENKO, V. D., Low-energy irradiation of Ge monocrystals by inert-gas ions, 25:5155
TIVOL, W. F., Polarization and cross-section measurements in p-^{4}He scattering from 20 to 40 MeV, 25:5526 (UCRL-19943)
TJON, J. A., Trinucleon form factors calculated from realistic local potentials, 25:5823
TOBISCH, J., Automatically controlled neutron diffraction goniometer, 25:4394
TOCHILIN, E., Selection of fission yields, 25:5973
TOENNESEN, K. H., Washout of ^{133}Xe after intramuscular injection and direct measurement of blood flow in skeletal muscle, 25:4429
TOKHRIYA, N., Influence of pollen radiation on crossing ability and variability in cotton, 25:4499
TOKIN, I. B., Absorption of lipids by cells of duodenal epithelium, 25:4695
TOLGSKAYA, M. S., Pathomorphological changes in animals following acute and chronic poisoning with L_3O_8, 25:4447
TOMAN, J., Additional system for bone densitometry studies, 25:4634 (CONF-700515-, pp 33-47)
TOMASKO, Martin George, Heliur core flash hydrodynamics, 25:4911
TOMAZIC, B., Extraction of traces of rare-earth elements from aqueous solutions of nitric acid, 25:4150
TOMLINSON, L., Theory of delayed-neutron physics, 25:5851
TOMONTO, James R., (U,Pu)C as alternate reload fuel for LMFBR's, 25:6023
Requirements for radiation protection during handling of plutonium recycle fuel rods and assemblies, 25:4314
TONNELIER, Claude, Taking samples of radioactive substances, 25:4516
TORIZUKA, Y., Excitation of the giant resonance in ^{12}C by inelastic electron scattering, 25:5572
TOUSSAINT, N., Preparation of Th--Pa alloys, 25:4751
TOWNER, I. S., Schematic model calculations for ^{40}K(β-)^{40}Ca, 25:5630
TOYOTA, Takayoshi, Extraction of plasma insulin in radioimmunoassay, 25:4420
TRAIKOVICH, Miodrag, Absorption, distribution, and excretion of certain soluble compounds of natural thorium, 25:4441
TRAPEZNIKOV, V. A., Position of K-absorption edges of Fe in Fe--Al and Fe--Mo alloys, 25:5181
TRAUT, H., Achromatic lesions induced by x-rays in chromosomes of Vicia faba, 25:4494
TRENTELMAN, G. F., T/sub Z/ = $-^3/_2$ masses and isobaric multiplet mass equation, 25:5568
TRIKHA, K. C., Potentiometric investigation of metal complexes with phenanthrenequinone monoxime, 25:4080
TRILLING, G. H., K+p elastic scattering at 4.6 GeV/c, 25:5296
TRIULZI, C., Beta detection efficiency curves for ^{40}K, ^{90}Y, ^{90}Sr--^{90}Y, ^{137}Cs, ^{144}Pr, ^{147}Pm, ^{155}Eu, and ^{204}Tl in sources of definite chemical form as function of their thickness, 25:4029 (CISE-N-119)
TROITSKAYA, V. A., Interrelation between solar wind and geomagnetic field, 25:5026
Magnetosphere parameters based on Pc-1 type micropulsations, 25:5027
TROMBKA, J. I., High-energy calibration using ^{252}Cf neutron source, 25:4223
TRUEMPER, J., Extensive air showers (experiment), 25:4585
TRUSCELLO, Vincent, Nuclear interaction of RTG's with scientific instruments for deep space probes, 25:4409
TRUSOV, V. F., Correlation between the intensity of the specific x radiation and the charge of the nucleus, 25:5832
TSCHAMPER, P. M., Pressure generation and potential work energy during fuel-sodium thermal interaction, 25:6092
TSIOVKIN, Yu. N., Electrical and magnetic properties of Pd--Mo solid solutions, 25:5178
TSUMORI, Kunihiko, Current profile monitor for scanning electron beam, 25:5468
TSUTSUI, Mitsuo, Leakage tests on reactor containment vessels, 25:5938
TSVETKOV, Yu. D., Free radicals in irradiated monocrystals of l-leucine hydrochloride, 25:4092
TSVETKOVA, Z. N., Effect of additions of aromatic hydrocarbons on chemical radiation stability of TBP in dodecane solution, 25:4116
TULENKO, James S., Requirements for radiation protection during handling of plutonium recycle fuel rods and assemblies, 25:4314
TUNESI, Giuseppe, Application of fast electrons to the treatment of diseases of the eye ball and eye socket, 25:4690
TURCK, B., Analysis of the effects of displacement and of positioning of the measuring probe of a magnetic field on the properties of an optical system, 25:5461 (NF-18519)
TURJANSKI, R., Resonance integrals of neutron activation of ^{74}Se, ^{78}Se, ^{80}Se, ^{81}Br, ^{127}I, ^{130}Te, ^{138}Ba, ^{140}Ce, and ^{142}Ce, 25:5681 (CNEA-274)
TURKDOGAN, E. T., Pore characteristics of carbons, 25:4856
TURKEVICH, Anthony L., Alpha-scattering technique of chemical analysis, 25:4034
TURNER, B. E., Masers in space, 25:4917
TURNER, D. T., Radiation-curing of composites of metals and polymers, 25:4108
TUROVTSEV, V. V., Theory of (^{6}Li,d) and (^{7}Li,t) reactions, 25:5601
TURSKI, Ronald B., Space-dependent thermal-neutron flux in systems with strong anisotropies, 25:6184
TUTTLE, R. J., Reactivity worth of tantalum in a fast reactor spectrum, 25:5964
TUYN, J. W. N., Fast-neutron-induced etch-pit distributions in Makrofol Polycarbonate foil, 25:4335
TYBOR, W., Determination of X^0(960) meson spin-parity in polarization experiment, 25:5361 (TPJU-14/70)
TYURIN, N. E., Fast-particle scattering on Coulomb and short-range potentials, 25:5438
Forward scattering amplitude behavior at high energies, 25:5349 (IFVE-STF-69-74)
Solution of the unitarity equation for the elastic scattering amplitude at high energy, 25:5423 (IFVE-

XUM

STF-69-65)
Solution of unitarity condition for two-particle process amplitude at high energies, 25:5355

U

UBERALL, H., Radiative corrections to electron scattering from complex nuclei, 25:5800 (AD-706717)
UDOVICH, Carl, Metal isotope and high pressure effects on the infrared active skeletal vibrations in metal sandwich compounds, 25:4067
UEBERALL, H., Analogs of giant resonance states and their experimental discovery, 25:5560
UENO, Hiroaki, Reaction (^{3}He,α) on ^{7}Li from 5.0 to 8.0 MeV, 25:5571
UGODNIKOVA, L. A., Electrical and magnetic properties of Pd--Mo solid solutions, 25:5178
ULITCHNY, M. G., Prog. rpt. on dislocation-solute atom interactions in alloys, 10/70, 25:4786 (COO-1676-13)
ULLRICH, W. T., Peach Bottom refueling and maintenance experience, 25:5906
UMANSKII, Ya. S., Investigation of the alloy Ni--25 at. percent W after isothermal [high-temperature] annealing, 25:4794
Metastable phase of the type Ni_3Mo in Ni--25 at. percent W alloy, 25:4789
UMEZAWA, H., Boson method in superconductivity: application to the study of vortex lines, 25:5052
UPADKHAYA, G. Sh., Temperature dependence of electric conductivity and thermal electromotive forces in the homogeneous carbide alloy regions of titanium and niobium, 25:5176
UPTON, A. C., Effects of estradiol on splenic repopulation in irradiated mice, 25:4471
Induction of carcinoma of the glandular stomach by whole-body irradiation, 25:4703
UPTON, Arthur C., Genetic and biological effects of low-level radiation, 25:4502
UPTON, Joseph W. Jr., Gas-flow method for detection of fast neutrons in reactors, 25:4355
URAKUBO, Goro, Chemical and hygienic studies on natural radioactive spa. IV, 25:4711
URETSKY, J. L., Duality and scattering lengths, 25:5363
USATENKO, Yu. I., Use of sodium butyldithiocarbaminate in the spectrophotometric determination of niobium, 25:4017
USTINOV, O. A., System MoO_3--BaO, 25:4873
System MoO_3--CeO_2, 25:4872
UVAROVA, K. A., Use of sodium butyldithiocarbaminate in the spectrophotometric determination of niobium, 25:4017
UYTTENHOVE, J., Excited states of ^{175}Yb from decay of ^{175}Tm, 25:5747
Isomeric states /sup 101m/Ru, /sup 103m/Ru, and /sup 101m/Tc, 25:5761

V

VACEK, A., Protective effect of para-aminopropiophenone and propylene glycol on the haematopoietic stem cells of mice, 25:4571
VACHON, Lawrence J., Nuclear safety program on the SNAP-23A power system, 25:4220
VAGELATOS, N., Thulium-171 isomeric lifetime, 25:5721
VAINSHTEIN, A. I., Low-energy theorems for amplitudes of μ capture and pion electromagnetic production, 25:5333
VALCKX, F. P. G., Ion heating in a Penning discharge, 25:5075
VALENTIN, J., Rotational bands of ^{171}Lu, 25:5699
VALERI, A., Theoretical reliability assessment of a fire protection system, 25:4187 (RISO-214, pp 21-40)
VALETTE, L., Graphite oxidation under irradiation by tracer of CO_2 in high pressure He carrier gas, 25:4881 (DP-Report-352)
VALIEV, Kh. Kh., Determination of magnetic moment stimulated by ^{121}Sb state, 25:5720
VALK, H. S., Relation between hard-core and velocity-dependent potentials, 25:5867
VALKOVIC, V., Proton--proton quasi-free scattering in the p + d + p + p + n reaction for E/sub p/ = 4.5 to 13.0 MeV, 25:5534
VALLOIS, G., Weak coupling in the ^{209}Bi S$^-$ x h/sub 9/2/ decuplet, 25:5745
VAN BINST, P., Remarks on Σ^- hyperon conversion rate, 25:5298
Trapping of Λ^0 hyperons produced by K$^-$ meson absorption, 25:5299
VAN CRAEYNEST, Jean Claude, Effect of porosity on thermal conductivity of uranium dioxide, 25:4844
VAN DAAL, H. J., Kondo effect in compound $CeAl_2$, 25:5228
VANDENBERG, C., Considerations on the in-core fuel management during startup of a fast breeder reactor, 25:6054
VANDENPLAS, P. E., Ion--electron resonances in bounded, hot plasmas with and without steady magnetic field, 25:5134
VAN DER BORGHT, O., Basic nuclear aspects of autohistoradiography, 25:4416
VAN DER MERWE, P., Energy levels of ^{203}Tl and ^{205}Tl, 25:5798
VAN DER WOUDE, A., Exchange resonance in ^{3}He + ^{4}He elastic scattering, 25:5538
VAN DYCK, R. S. Jr., Radiative lifetime of metastable 2^1S_0 state of He, 25:4944
VAN EIJK, C. W. E., Ka$_1$ x-ray isotopic shift for ^{140}Ce--^{142}Ce and differences in nuclear charge radii of Ce isotopes, 25:5864
VAN ERP, J. B., Local core accidents: comparison between LMFBR's and LWR's, 25:6077
VANGEEL, J., Fuel development for a low-enriched HTR, 25:6007
VAN HISE, J. R., Photonuclear reactions above the giant resonance, 25:5679
VAN HULST, H., Phalangeal Atlas: an application of radiographic photodensitometry, 25:4641 (CONF-700515-, pp 224-36)
VAN MASSENHOVE, G., Graphite oxidation under irradiation by tracer of CO_2 in high pressure He carrier gas, 25:4881 (DP-Report-352)
Recent results from the in-pile carbon transport loop. project dragon, 25:4835 (DP-Report-448)
VAN VELZE, P. L., Automatic counting of solid-state fission track recorders, 25:4343
VAN VOLKENBURGH, Gregg, Collisional deactivation of H(2^2P)* fluorescence, 25:4964
VANZHA, A., Possible properties of weak six-fermion interaction, 25:5344
VARGA, Judith A., Dissolution of calcium--strontium carbonate and its subsequent movement in the ground, 25:4265 (ORNL-TM-3130)
VARMA, M. N., UHV Moessbauer emission of thin iron films, 25:6231 (COO-623-164)
VARSHNI, Y. P., Krutov model for deformed even--even nuclei, 25:5819
VARTERESZ, V., Radioprotective effect of a mixture of AET and 5-methoxytryptamine in x-irradiated mice, 25:4583
Radioprotective effect of N-substituted AET-derivatives having amino acid structure, 25:4577
VASHISHTA, P., Temperature dependence of superconducting energy gap of amorphous Bi, 25:5042
VASIL'EV, A. V., Photoconductivity spectra of irradiated and plastically deformed crystals of germanium, 25:5161
VASIL'EV, G. Ya., Entrainment of neutrons by a moving medium, 25:5486
VASIL'EV, O. V., Gross structure of giant dipole resonance on nuclei of transition region N approximately equal to 90, 25:5778
VASIN, M. V., Use of combined radiation protection compounds, 25:4609
VASTOLA, F. J., Ultra-clear carbon surfaces. IV, 25:4646
VASUDEVAN, A. K., Prog. rpt. on dislocation-solute atom interactions in alloys, 10/70, 25:4786 (COO-1676-13)
VATTUONE, G. M., Fate of Schoener fallout radionuclides ingested by dairy cow, 25:4436
VAUCHER, B., Giant-resonance excitation by radiative capture of π^- in ^{16}O, 25:5600
VEESER, L. R., Absolute polarization determination of mass-3 nuclei, 25:5518 (LA-4465, pp 1S.1-2)
Elastic scattering of polarized tritons, 25:5511 (LA-4465, pp 5.1-2)
VEGORS, S. H. Jr., Excited K/sup π/ = 0$^+$ bands in ^{172}Yb, 25:5744
VEJS, K., Excited levels in the decay ^{185}Cs + ^{185}Re, 25:5741
VELEZ FORTUNO, J., Effect of gamma radiation dosages on rooting of pineapple crown sections, shoot emergence, and growth, 25:4719
VELNER, S., Optimum diameter of wires for neutron flux measurements, 25:6206
VELTEN, E., Reaction ^{12}C(d,^{6}Li)^{8}Be α-cluster pickup, 25:5562
VENINGA, T. S., Radioprotection by hypoxia and some chemical protectors, 25:4578
VENKATESWARLU, K. S., Radiation and catalysis, 25:4055
VERBETSKII, V. N., Reaction of ZrO_2 with U_3O_8, 25:4864
VERGANELAKIS, A., Deep inelastic scattering and the nature of partons, 25:5330
Remarks on π^+-photoproduction with linearly polarized photons, 25:5321 (DEMO-70/1)
VERGHESE, K., Sputtering of uranium by fission, 25:4827
VERHEEST, Frank George, Dispersion relations for plane waves in multicomponent plasmas, 25:5133
VERHEUL, H., Research on nuclides far from the stability line, 25:5619
VERMEIL, C., Hot H atoms in gas-phase photochemistry, 25:4132
VERNOV, S. N., Earth's radiation belts, 25:5033
VERSLUIS, R. M., Degenerate thermalization kernel for unit cell calculations, 25:6166
VESELY, D., Slip in single crystals of niobium--molybdenum alloys deformed in compression, 25:4800
VETKEVICH, V. V., Investigation of circumsolar plasma by pulsar translucing, 25:4920 (CSIRO-Trans-5897)
VEYRET, C., Metamagnetic properties of a single crystal of $ErCrO_3$, 25:5160
VIAMONTE, Manuel Jr., Pathophysiology of perfusion in pulmonary disease, 25:4675
VIDAL, F., Application of two radio-immunological methods to the assessment of growth hormone, 25:4422
VIGNESOULT, Nicole, Electron probe microanalysis of highly radioactive materials, 25:4011 (CEA-N-1340)

VIGROUX, E., Vertical distribution of atmospheric ozone from analysis of direct solar radiation, 25:5017
VIKHREV, V. V., Research on studying and increasing the plasma parameters on ''non-cylindrical Z-pinch'' equipment, 25:5116 (SC-T-70-4046)
VILLARREAL, R., Xenon tag proof test, 25:6026
VINTERS, J. V., Pore characteristics of carbons, 25:4856
VIRMANI, Y. P., Radiation and catalysis, 25:4099
VISSCHER, M. J. C., $K\alpha_1$ x-ray isotopic shift for ^{140}Ce--^{142}Ce and differences in nuclear charge radii of Ce isotopes, 25:5864
VISSCHER, P. B., Galvanomagnetic properties of a single-crystal sphere by the induced-torque method. II. Magnetic breakdown in cadmium and zinc, 25:5192
VIVIEN, J. P., First two excited states of ^{159}Tb, 25:5727
VOGEL, John M., Mineral content changes in the os calcis, ulna, and radius induced by prolonged bed rest, 25:4653 (CONF-700515-, pp 408-22)
VOGT, Fred B., Assessment of bone mass by roentgenographic density techniques, 25:4613 (CONF-680211-, pp 27-80)
VOICE, Eric, Fuel particle coatings at very high magnification, 25:4863 (DP-Report-574)
VOLKENSHTEIN, N. V., Electrical and magnetic properties of Pd--Mo solid solutions, 25:5178
Hall effect in terbium single crystals, 25:5177
VOLKOV, D. I., Hall effect in certain rare-earth metals and alloys, 25:5182
VOLKOV, G. G., Behavior of diffractional peak width at high energies in case of Gaussian potential, 25:5424 (IFVE-STF-69-83)
VOLLAND, H., Thermospheric density variations as an oscillator circuit system, 25:5016
VOLTA, G., Fracture mechanics approach to the assessment of reliability of reactor pressure tubes, 25:6191 (RISO-214, pp 255-87)
Reliability evaluation of brittle materials and of welded structures, 25:4753
VOLYAK, L., Temperature dependence of the surface tension of water, 25:6216 (AEC-tr-7203)
VONACH, H., Precision-measurement of $^{27}Al(n,\alpha)$ cross section for 14.43-MeV neutrons, 25:5641
VON BONSDORFF, H., Thermal conductivity of a hollow right cylinder of solid material, 25:4203 (DP-Report-578)
VON BRENTANO, P., Lifetime and magnetic moment of neutron hole state in ^{207}Pb, 25:5710
VON OERTZEN, W., Four-nucleon transfer reaction induced by ^{10}B on ^{12}C, 25:5588
VON SONNTAG, C., Radiation chemistry of alcohols. XII, 25:4123
VON WITSCH, W., Proton--proton quasi-free scattering in the p + d + p + p + n reaction for E/sub p/ = 4.5 to 13.0 MeV, 25:5534
VORTMAN, L. J., Close-in airblast from the Buggy Event. Project Buggy I, 25:4168 (PNE-320)
VOS, C., Radiation protection by disulphides in tissue culture, 25:4560
VOSBURGH, R. O., Depleted-uranium, nickel, and steel-reflected EBR-II critical assemblies on ZPR-3: experiments and calculations, 25:5963
VOSE, George P., X-ray bone densitometry in short and long duration studies, 25:4615 (CONF-680211-, pp 95-115)
VOSS, G., Preparation of Th--Pa alloys, 25:4791
VYDYANATH, H. R., Comparison of the substructures and properties of nickel, TD--Ni, Chromel-A, Inconel 600, and TD--NiCr following explosive-shock deformation, 25:4802
VZOROV, I. K., Polarization of secondary protons in pp + π^+pn and pp + π^0pp reactions at 665 MeV, 25:5268 (JINR-P1-5293)

W

WACKER, Adolf, Photoreactivation of E. coli after inactivation, 25:4728
WADE, David C., Optimal control of nuclear reactor depletion, 25:6172
WADEKAMPER, D. C., Behavior of discrete PuO_2 particles in thermal recycle fuel, 25:5994
Measuring plutonium homogeneity in fast reactor fuels, 25:4875
Plutonium homogeneity in thermal recycle fuels, 25:4874
WAELBROECK, F., Determination of the pressure anisotropy in a mirror-confined plasma, 25:5085
WAELTI, P., Collision probability method for reactor cells with anisotropic scattering, 25:6156
WAGEMANS, Cyriel, Study of some aspects of fission induced by resonance neutrons in ^{235}U, 25:5738
WAGGENER, Robert G., Polychromatic x-ray beam to represent n monoenergetic photon sources. I. Limitations and correction factors for photon detectors, 25:4650 (CONF-700515-, pp 314-31)
WAGNER, H. F., Quadrupole ratio Q^{3+}/Q^{2+} in ^{172}Yb, 25:5760
Statistically perturbed angular correlations of ^{154}Gd and ^{156}Gd in different liquid sources, 25:5758
WAGNER, Henry N. Jr., Research and biomedical applications, 25:4415
WAIT, G. D., Photodisintegration of ^4He, 25:5544
WAKELIN, R. J., Influence of impurities on the properties of uranium, 25:4747 (AWRE-O-63/70)
WALCHER, Th., Inelastic electron scattering from ^4He at low momentum transfer, 25:5528
WALDO, J. B., Maintenance of radioactive sodium systems at EBR-II, 25:5987
WALENTA, H., Angular distribution of photonuclear reaction $^3He(\gamma,p)^2H$, 25:5539
WALI, Kameshwar C., Implications of local duality in a set of coupled reactions, 25:5352 (SU-1206-235)
WALKE, Gerald J., Basic problems in the determination of nuclear fuel performance, 25:5991
WALKER, D. E., Xenon tag proof test, 25:6026
WALKER, Donald S., Radiation protection and sensitization. Proceedings of the second international symposium on radiosensitizing and radioprotective drugs, Rome, 6--8 May 1969, 25:4534
WALKER, G. K., Migration of helium bubbles in a 20 percent Cr/25 percent Ni/Nb stabilised steel, 25:4758
WALKER, James K., Possibilities for the N.A.L. program, 25:5445 (CONF-700314-, Paper 3)
WALKER, P. L. Jr., Ultra-clear carbon surfaces. IV, 25:4846
WALLACE, W. E., Heat capacity studies of intermetallic compounds containing rare earth elements, 25:5218
WALLANDER, E., Thermal neutron capture gamma rays from $^{26}Mg(n,\gamma)^{27}Mg$, 25:5625
WALSH, R. L., BOPTIC: beam transport program in FORTRAN IV, 25:5441 (AAEC/TM-544)
Energy dependence of anti ν/sub p/ for neutron fission of ^{235}U, 25:5755
WALTAR, Alan E., Quasi three-dimensional approach for estimating sodium voiding incoherency, 25:6071
WALTER, J. F., Calculation of neutron detector response in a subcritical reactor, 25:6118
WALTER, R. K., Polarization of 22-MeV neutrons elastically scattered from liquid tritium and deuterium, 25:5516 (LA-4465, pp 15.1-2)
WALTERS, W. B., Decay schemes of /sup 127m/Te and /127g/Te, 25:5734
Photonuclear reactions above the giant resonance, 25:5679
Weak β branching in ^{55}Cr, 25:5645
WALTON, A., Neutron activation analysis for transition elements in rocks, 25:4047
WALTZ, W. R., Calculation of neutron detector response in a subcritical reactor, 25:6118
WANG, Chung-shan, Role of an extraterrestrial ring current in dynamics of aurora, 25:5032
WANG, Jeng-chuen, Nuclear charge distribution and Born approximation for high-energy electron scattering, 25:5661
WANG, Jiunn-ming, Density-matrix formalism for lepton--hadron scattering, 25:5331
WANG, Ling-lie, Density-matrix formalism for lepton--hadron scattering, 25:5331
WANG, Ming-chien, Reaction $^{27}Al(n,d)^{26}Mg$ at 14.1 MeV, 25:5662
WANG, Wei-noon, Reaction $^{27}Al(n,d)^{26}Mg$ at 14.1 MeV, 25:5662
WANTLAND, J. L., Graphic display of the hydrodynamics of collapsing fluid slabs, 25:6199
WARBURTON, E. K., Lifetime of 5^- 4585 keV ^{38}Ar level, 25:5664
WARD, A. L., Dynamic strain aging in 304 stainless steel, 25:4777
Mechanical properties of EBR-II irradiated 20 percent cold-worked Type 316 stainless steel, 25:5545
System for predicting postirradiation tensile properties, 25:4831
WARD, C. H., Prog. rpt. on synthesis, identification, and purification of C_6 and C_7 fluorocarbons from radiolysis, 11/70, 25:4111 (ORO-3909-2)
WARD, John F., Electron spin resonance studies of free radicals formed from orotic acid, 25:4093
WARKENTIN, J. K., Monte Carlo radiation transport analyses of the NERVA nozzle assembly, 25:6129
WARMAN, E. A., Shielding for NERVA missions, 25:6131
WARNER, E. E., Prompt and multiorbital reentry of small radioisotope heaters at superorbital velocities, 25:4221
WARNER, G. P., Frozen polarized target, 25:5466 (RPP/A-81)
WARNER, Robert E., Study of the odd strontium isotopes with stripping and pickup reactions, 25:5604 (N-70-25281)
WARWICK, R. G., Survey of pressure vessels built to a high standard of construction, 25:5982 (RISO-214, pp 322-34)
WASHBURN, T. N., High-temperature fast-flux irradiation experiment for mixed-oxide fuel rods, 25:5585 (GA-10264)
WASSEF, Marguerite A., Thermochemical studies of Th(IV) and U(IV) chlorides, 25:4077
WASSON, O. A., Gamma rays from thermal and resonance neutron capture in ^{121}Sb and ^{123}Sb, 25:5724
WASSON, T. L., Fallout computational techniques, 25:4506 (AD-703266)
WATAGHIN, A., Composite bosons in nonlocal quantum field theory with Z_3 approximately 1. II, 25:5411
WATANABE, M., Temperature rise of specimen due to electron irradiation, 25:5163
WATANABE, Masayuki, Reaction $(^3He,\alpha)$ on ^7Li from 5.0 to 8.0 MeV, 25:5571
WATARI, Tsutomu, Bromouridine (BUdR) as a radiosensitizing agent of malignant brain tumours, 25:4666
WATSON, C. D., Design considerations of reactor containment

XUM

spray systems. Part V. Protective coatings tests, 25:6034 (ORNL-TM-2412(Pt.5))
WATSON, C. J. H., Centrifugal uranium isotope separation and nuclear weapon proliferation, 25:4214 (CONF-691051-, pp 354-61)
WATSON, D. G., Fall chinook salmon spawning in the Columbia River near Hanford, 1947--1969, 25:4474 (BNWL-1515)
WATSON, J. F., Materials selected for Fort St. Vrain prestressed concrete reactor vessel, 25:5883
WATSON, R. B., Search for lowest T = 2 state of ^{12}C, 25:5573
WATT, Bob E., Asymmetries in deuteron scattering from a polarized ^{3}He target, 25:5515 (LA-4465, pp 14.1-2)
Asymmetries in protons from the reaction of deuterons with a polarized ^{3}He target, 25:5524 (LA-4465, pp 32.1-2)
WATTS, H. A., Efficient Runge--Kutta codes, 25:6250 (SC-RR-70-615)
WEATHERWAX, H. D., Na critical point data uncertainty in Na-fuel interaction, 25:6074
WEAVER, L., Nuclear rotational bands and SL (3,R) symmetry, 25:5801 (AD-706835)
WEBB, R. A., Lower costs through higher power density and improved fuel management, 25:5900
WEBBER, Bryan Ronald, Test of the $\Delta S = \Delta Q$ rule in leptonic decays of neutral K mesons, 25:5262
WEBBER, W. R., Protons and nuclei in the galactic radiation, 25:4981
WEBER, J. W., Correlation of predictions and observations in mixed-oxide fuel, 25:6001
WEBER, R. F., Time-resolved energy distributions in a striating discharge, 25:5077 (AD-710557)
WEEKS, R. W., LIFE-I, history-dependent analysis of fast reactor fuel element behavior, 25:6032
WEGNER, K. E., Fallout computational techniques, 25:4506 (AD-703266)
WEHMANN, U., Considerations on the in-core fuel management during startup of a fast breeder reactor, 25:6054
WEI, L., Economics of radiation versus heat-catalyst curing for wood-plastic flooring plant, 25:4109
WEIBEL, Erich S., Ion cyclotron instability, 25:5128
WEIDENBAUM, B., Flux monitor utilizing track-etch film for unattended safeguards application, 25:4341
Track-etch research and development, 25:4345
WEIDNER, James P., Chelation and radiation protection, 25:4553
WEIGAND, U., Statistically perturbed angular correlations of ^{159}Gd and ^{156}Gd in different liquid sources, 25:5758
WEIGUNY, A., Alpha-particle model for light nuclei, 25:5855
WEIL, J. W., Slow-neutron scattering cross-sections of Debye-spectrum space lattices, 25:5494
WEINBERG, A. F., High-temperature fast-flux irradiation experiment for mixed-oxide fuel rods, 25:5989 (GA-10264)
WEINSTEIN, R., rho,w photoproduction phase: possible breakdown in vector dominance, 25:5327
WEINSTOCK, E. V., Integral measurement of capture-to-fission ratio in ^{239}Pu, 25:5772
WEISBIN, C. R., Age and fast effect for fission and 14-MeV neutron sources in Be and BeO, 25:5496
WEISS, Armin, Significance of exchangeable ions in the formation of structure in thixotropic gels, 25:6247 (CRNL-tr-2395)
WEISS, J., Coulomb fragmentation of InCl and InI, 25:5153
WEISSER, D. C., Scattering of α-particles from ^{12}C, 25:5561
WEISSLEDER, H., Problems of radiation dosimetry in endolymphatic therapy, 25:4512
WEITMAN, J., Anomalous helium production in nickel, 25:4821
Helium accumulating dosimeters for high neutron fluences and long irradiation periods, 25:4381
Helium production in Fe, Cr, Ni, Ti, and Cu due to fission neutron part of reactor spectra, 25:4822
New boron analysis method, 25:4037
WEITZNER, H., Bifurcation problem in E-layer equilibria, 25:5119
WELLBORN, C. C., Gamma-ray transitions in ^{29}P, 25:5633
WELLS, M. R., Magnetic properties of gadolinium orthovanadate, 25:5217
WELSH, R. E., Electric quadrupole transitions in muonic ^{208}Pb, 25:4953
WELT, M., Concrete-polymer building blocks, 25:4859
WENDLAND, D. E., Fallout computational techniques, 25:4506 (AD-703266)
WENDROFF, Burton, Energy inequalities in some nonlinear initial-value problems, 25:6237 (LA-4525)
WERNER, E., Precision-measurement of $^{27}Al(n,\alpha)$ cross section for 14.43-MeV neutrons, 25:5641
WERTH, Glenn C., Review of Soviet program on nuclear explosives for the national economy, 25:4170
WEST, G. A., Design considerations of reactor containment spray systems. Part V. Protective coatings tests, 25:6034 (ORNL-TM-2412(Pt.5))
WEST, John B., Distribution of blood flow and ventilation with ^{15}O, ^{13}N, and ^{11}C, 25:4667
Pulmonary investigation using ^{133}Xe, 25:4672
WEST, K. W., First-order transition in europium metal, 25:5203
WESTLAKE, D. G., Hydrogen supercharging during thermal cycling of zirconium, 25:4756
WESTON, L. W., Fast fission chamber amplifier--discriminator system, 25:4333
Neutron fission and capture cross section measurements for ^{233}U, 25:5702
WETHINGTON, John A. Jr., Disposal of radioactive wastes in nuclear chimneys, 25:4279
WEYL, Guy M., Interaction of extraordinary wave with density fluctuations in plasma, 25:5126
WHEATLEY, J. C., Compressional cooling of ^{3}He to millidegree temperatures, 25:6255 (UCSD-34-P-143-27)
Continuously operating ^{4}He evaporation refrigerator, 25:5061 (UCSD-34-P-143-31)
Experiments of the future at ultra-low temperatures (< 0.3°K), 25:5035 (UCSD-34-P-143-30)
Magnetization of dilute Cu--Mn alloys at very low temperatures, 25:6256 (UCSD-34-P-143-33)
WHEATLEY, John C., Principles and methods of dilution refrigeration. II, 25:5062 (UCSD-34-P-143-32)
WHEELER, David E., For West Point's nuclear engineers: [reactor = computer], 25:6193
WHITBECK, J. F., Coolant flow distribution during decompression of a single-loop simulated PWR system, 25:6084
WHITE, J. E., Neutron energy-dependent capture gamma-ray yields for ^{238}U and ^{181}Ta, 25:5777
WHITE, Kevin J., Electron spin resonance studies on γ-irradiated $KMnO_4$, 25:4110 (AD-710231)
WHITE, M. G., NASA briefing on high energy, heavy ion capabilities of Princeton-Pennsylvania accelerator, 25:5462 (PPAD-676-E)
WHITNEY, E. D., Quantitative determination of the structure--property relationships in nuclear fuel element materials. Quarterly progress report, June 15--September 15, 1970, 25:4841 (SRO-552-5)
WHITNEY, R. R., Electromagnetic structure of the ^{3}He nucleus, 25:5535
WHITTAKER, E. J. W., Ionic radii for use in geochemistry, 25:4085
WHITTEN, C. A. Jr., Reactions $^{20}Ne(d,p)^{21}Ne$ and $^{22}Ne(d,p)^{23}Ne$, 25:5618
WICK, K., Final state interacting n-p pairs in the reaction p + d → p + p + n, 25:5548
WICKER, Alain, Phase equilibriums in Ni--Nb--W and Ni--W systems, 25:4788
WIDERA, R., Excitation functions (n,2n) for ^{93}Nb and ^{103}Rh, 25:5766
WIDMER, Hans, Mid-range optimization of a nuclear power plant, 25:5904
Short-range optimization of use of a nuclear power plant, 25:5905
WIGDORTZ, J. M., Prediction and measurement of acoustic wave propagation in two-phase media, 25:6075
WIGGINS, P. F., Construction materials for neutron capture gamma-ray spectroscopy with ^{252}Cf sources, 25:4772
Detection and analysis of titanium ore using ^{252}Cf, 25:4036
WIGNER, Eugene P., Symmetries and reflections. Scientific essays, 25:5396
WIKANDER, G., Isotopic exchange reaction between ammonium bromide and butyl bromide, 25:4071
WILBERT, Yves, Electrical conductivity and stable domains at high temperatures for terbium oxides, 25:5175
WILCKEN, S. K., Light variation of gamma Coronae Borealis, 25:4907
WILCOCK, P. D., Measurement of plasma parameters in Tokamak T3-A by Thomson scattering, 25:5079 (CLM-R-107)
WILCOX, A. D., Radiation transport analyses of nuclear rocket engine components, 25:6128
WILDENTHAL, B. H., Shell-model structure of ^{42}Ca through ^{50}Ca, 25:5611
WILDERMUTH, K., Unified nuclear reaction theory, 25:5870
WILENZICK, R. M., In-beam Moessbauer spectroscopy, 25:5467
WILHELM, W. K., Improving the performance of large reactors, 25:5901
WILHELMI, Z., Isomeric cross-section ratios and total cross-sections for the $^{113}In(n,2n)$/sup 112gm/In and $^{115}In(n,2n)$/sup 114gm/In reactions, 25:5763
WILHELMY, J. B., Excited state in even--even fission products, 25:5687 (UCRL-19949)
WILKES, C. W., Progress in xenon tagging, 25:6025
WILKINSON, Ray, Effects of caffeine on sensitivity to ultraviolet light of HeLa cells, 25:4607
WILLIAMS, A. K., Recent improvements in fire suppression and control for glove-box operations at Rocky Flats, 25:4195
WILLIAMS, Clyde M., Technetium--indium double lung scanning, 25:4677
WILLIAMS, I. G. K., Problems of radioactive waste management, 25:4268
WILLIAMS, J. R., Angular and wavelength dependence of thermal radiation transmitted through refractory aerosols, 25:6134
Exploratory calculations for a gaseous core fast breeder reactor, 25:5971
Gas core reactor: MHD power plant concept, 25:6137
Radiant heat transfer in heated aerosols at 100 atmospheres pressure, 25:6135
WILLIAMS, John S., Radioisotope heat source, 25:4217
WILLIAMS, R. L., Flow-induced accident initiating conditions in an LMFBR, 25:6070

XUM

WILLIAMS, R. P., Gamma-ray transitions in ^{29}P, 25:5633
WILLIAMS, W. G., Frozen polarized target, 25:5466 (RPP/A-81)
WILLIAMSON, K. D. Jr., Proposed 0.4 K polarized proton target cryostat for LAMPF, 25:5456 (LA-4465, pp 33.1-2)
WILLIAMSON, S. J., Bulk upper critical field of clean type-II superconductors: V and Nb, 25:5054
WILLIS, F. L., High-energy transient meltdown of irradiated UC_2 in a TREAT Mark-II loop, 25:6097
WILLMANN, R. B., $\pi^+p \rightarrow f^0 \Delta^{++}$ at 13.1 GeV/c, 25:5283 (COO-1428-238)
WILLSON, R. L., Electron transfer studies of nucleic acid derivatives in solutions containing radiosensitizers, 25:4540
WILLSON, Robin L., Reaction of triacetoneamine-N-oxyl with radiation-induced radicals from DNA and from deoxyribonucleotides in aqueous solution, 25:4541
WILSON, Albert G., Relativity and the question of discretization in astronomy, 25:4533
WILSON, Robert L., Classification of critical characteristics in nuclear plant design, 25:6091
Radwaste design for no plant-originated radioactive liquid discharge, 25:5882
WINCHESTER, R. V., X- and γ-radiolysis of some tryptophan dipeptides, 25:4114
WINTER, G., Levels in ^{167}Tm, 25:5726
Non-adiabatic effects in rotational bands of odd proton nucleus ^{155}Tb, 25:5783
WINTER, K., Experimental program at CERN intersecting storage rings, 25:5444 (CONF-700314-, Paper 2)
WINTERS, R. W., Beta decay of ^{40}Cl and levels of ^{40}Ar, 25:5614
WITTE, K., Reactance matrix analysis of the d--^{3}He, p--^{4}He system at 10-MeV deuteron laboratory energy, 25:5509 (LA-4465, pp 2.1-2)
WITTE, L. C., Film and transition boiling around spheres, 25:4209
Fracture of solidifying particles, 25:6083
WOHN, F. K., Decay of /sup 85m/Kr, 25:5634
WOLF, A., Study of the energy levels of ^{203}Tl using (γ,γ') reaction, 25:5713
WOLF, Fred, TOPS RTG nuclear radiation environment analysis, 25:4242
WOLF, R. O., Effects of irradiation of the parotid gland and pancreas on human isoamylases, 25:4452
WOLF, W. P., Magnetic properties of the rare earth hydroxides, 25:5202
WOLFE, B., Problems in fast reactor core safety, 25:6086
WOLFENDALE, A. W., Muons, 25:4988
WOLOCH, F., Transfer function investigations on first Dragon core, 25:5953 (DP-Report-445)
WONG, C., Fast-neutron spectroscopy of the reaction $^9Be(p,n)^9B$ at 20 MeV, 25:5557
WONG, C. W., Alpha-particle model for light nuclei, 25:5855
WONG, C. Y., Shells in a simple anisotropic harmonic oscillator, 25:5857
WOOD, R. E., Electron capture decay of ^{181}W, 25:5753
WOODLEY, H. J., Laboratory experiments carried out on class seals. project dragon, 25:4183 (DP-Report-484)
WOODRUFF, Gene L., Multiplication effects in measurements of delayed-neutron energy spectra, 25:5774
WOODRUFF, W. L., Another anomaly in variational flux synthesis methods, 25:6170
WOODS, A. D. B., Exchange and crystal-field interactions in Er and Ho, 25:5214
WOODS, Hugh Wilroy, Graphite phase diagram and properties in liquid core nuclear rocket pressure--temperature range, 25:4865
WOODS, S. B., Electrical resistivity and deviations from Matthiessen's rule in dilute alloys of aluminum, cadmium, silver, and magnesium, 25:5184
WOODS, W. K., Production of ^{238}Pu, 25:4227
WORDEN, W. P., Operating experiences during startup of Dresden Unit II, 25:5911
WOZNIAK, G. J., Mass of ^{13}O and isobaric multiplet mass equation, 25:5640
WRAY, Dennis A., Implications of Adler zeros on current-divergence commutators, 25:5316
WRIGHT, R. W., Acoustic and inertial constraints in molten fuel-coolant interactions, 25:6055
Rate-limited model of molten fuel-coolant interactions, 25:6075
WU, C., Isospin splitting of giant dipole state in ^{26}Mg, 25:5671
WU, C. S., Moessbauer measurements of quadrupole-moment ratios of first excited 2^+ states of ^{176} ^{178} ^{180}Hf, 25:5668

Y

YAFFE, L., Interactions of ^{45}Sc and ^{68}Zn with protons, 25:5623
YAKINTHOS, J., Magnetic structure of intermetallic compounds RCo_3, 25:5210
YAKOVLENKO, S. I., Amplification of vacuum-ultraviolet radiation in decaying dense helium plasma, 25:5090
YALCIN, C., Charge asymmetry in two nucleon interaction, 25:5812
YAMADA, Toyoaki, Liquidus curve of ZrO_2--Y_2O_3 system measured by solar furnace, 25:4869
YAMAGATA, Shoichi, Extraction of plasma insulin in radioimmunoassay, 25:4420
YAMAGUCHI, A., Excitation of the giant resonance in ^{12}C by inelastic electron scattering, 25:5572
YAMAGUCHI, Masaharu, Constitutional investigations on the miscibility gap in iron--chromium and iron--chromium--vanadium systems, 25:4787
YAMAJI, Shuhei, Heavy-particle stripping process in reaction $^{11}B(d,n)^{12}C$, 25:5593
YAMAKAWA, Kunio, Radiation-induced internal disbudding as a tool for enlarging mutation sectors, 25:4483
YAMAMURA, Yasunori, Approximate scattering kernel for neutron slowing down, 25:5482
YAMAZAKI, T., Anomalous orbital magnetism of proton deduced from magnetic moment of 11- state of ^{210}Po, 25:5742
E2 effective charges of the f/sub 7/2/ proton and neutron, 25:5646
YAMPOLSKII, Yu. P., Chemical action of laser radiation on acetylene, 25:4070
YAN, Comparative toxicity of soluble and insoluble compounds of ^{232}Th, 25:4440
YAN, Shay-shan, Effect of thorium dioxide on the peripheral blood of rats, 25:4700
YAN, Syao-shan, Behaviour of thorium dioxide in rats after intratracheal and intraperitoneal administration, 25:4442
Effect of thorium dioxide on arterial pressure and threshold of stimulation of the nerve-muscle apparatus in rats, 25:4701
Morphological changes in the lungs and other organs in rats on intratracheal administration of thorium dioxide, 25:4702
YARMUKHAMEDOV, R., Theory of (^{6}Li,d) and (^{7}Li,t) reactions, 25:5601
YAROSLAVTSEV, V. D., Control of reinforced concrete construction by means of fast neutrons, 25:4249
YASINSKY, J. B., Improved spatial differencing for space--time and static movable material diffusion problems, 25:6177
YATES, A. C., Bounds for oscillator-strength sums from approximate quadratures, 25:4946
YAZDANBAKHSCH, I., Bile duct carcinomas after thorotrast, 25:4716
YEARIAN, M. R., Electromagnetic structure of the ^{3}He nucleus, 25:5535
YEN, C. S., Moessbauer measurements of quadrupole-moment ratios of first excited 2^+ states of ^{176} ^{178} ^{180}Hf, 25:5668
YIFTAH, S., Hybrid method for spatial dynamic analysis, 25:6179
YIM, K. B., Radiation breeding of perennial plants. I, 25:4724
YING, Shuh-pan, Differential cross section measurements of the reaction $\pi^+ + p \rightarrow K^+ + Y_1^{*+}(1385)$ at 4 and 5.65 GeV/c, 25:5290
YODA, Yoichi, Ocean nuclear industrial complex, 25:5881
YOKOO, Yoshimatsu, Internal conversion coefficients for electron-spin-polarized ^{57}Fe, 25:5659
YONEZAWA, T., Vertical distribution of ionization at the F2 peak, 25:5014
YONEZAWA, Toshio, Development of steels for nuclear power plant, 25:4770
YOSHIDA, H., Present status of postirradiation examination facility, 25:4298
YOSHIDA, Heitaro, Heat resisting steels and alloys for HTGR, 25:4779
YOSHIDA, S., Alpha-cluster model calculation of ^{12}C, 25:5865
YOSHIDA, Shiro, Heavy-particle stripping process in reaction $^{11}B(d,n)^{12}C$, 25:5593
YOST, K. J., Application of extended R-matrix theory to elastic scattering of neutrons by ^{12}C, 25:5581
Neutron energy-dependent capture gamma-ray yields for ^{238}U and ^{181}Ta, 25:5777
YOU, Y. S., Radiation breeding of perennial plants. I, 25:4724
YOUNG, F. E., Fabrication of non-fuel core components for SEFOR, 25:5943 (GEAP-13595)
YOUNG, H. C., Hydraulic performance and cavitation characteristics of electromagnetic helical induction pump, 25:4186 (ORNL-TM-2995)
YOUNG, Robert A., Collisional deactivation of $H(2^2P)^*$ fluorescence, 25:4964
YOUNGBLOOD, D. H., Stripping to quasibound levels in ^{41}Sc, 25:5617
YU, C. W., Review of the safety aspects of the design of prestressed concrete pressure vessels with reference to limit state design, 25:5981 (RISC-214, pp 285-300)
YUCKER, W. R., Statistical analysis of solar cosmic ray proton dose, 25:4509 (MDC G-363)
YUILE, Charles L., Effects of thoracic irradiation upon cardiopulmonary function in the dog, 25:4706
YUKAWA, T., Alpha-cluster model calculation of ^{12}C, 25:5865
YULE, T. J., Measured neutron spectrum in FTR-3, 25:6105
YURISH, M., Method for producing microautoradiograms of the surface of irradiated aluminum, 25:4250
YUSEF, M. Yu. A., Spectrum of retarded neutrons, 25:5505
YUST, C. S., Transmission electron microscopy of polycrystalline graphite, 25:4868

XUM

Z

ZACHER, Richard, Automatic scanner-computer analysis of radiographic bone trabecular activity, 25:4637 (CONF-700515-, pp 188-94)

ZAFIRATOS, C. D., Levels of ^{70}Zn, 25:5607

ZAHN, J., Graphic display terminal for nuclear experiments with on-line computer. I, 25:4350 (HMI-B-100)

ZAHN, Lyle L., Manager's views [on implications of ANSI Criticality Safety Standard N16.1], 25:4289

ZAIKOV, R. P., Example of the infinite-component local field with the mass spectrum, 25:5406 (JINR-P2-5305)

ZAITSEV, A. A., Application of the commutation relations to determination of eigenvalues of operators, 25:5397

ZAKHARIEV, B. N., Lower bounds for the scattering parameters, 25:5425 (JINR-P4-5332)

ZAKHAROV, V. I., Low-energy theorems for amplitudes of μ capture and pion electromagnetic production, 25:5333

ZAKRZEWSKI, W. J., Signature in the Bardakci and Ruegg model, 25:5439

Veneziano amplitudes for Reggeons and spinning particles, 25:5440

ZAMYATNIN, Yu. S., Principal characteristics of isotopes of heavy elements, 25:5722

ZANCA, Peter, Polychromatic x-ray beam to represent n monoenergetic photon sources. I. Limitations and correction factors for photon detectors, 25:4650 (CONF-700515-, pp 314-31)

ZANE, J. O., Core thermal performance margins for bottom flooding ECC systems, 25:6041

ZAREMBO, Yu. I., Thermodynamics of the reduction of thorium dioxide by calcium, 25:4054 (IS-Trans-83)

ZATSEPINA, L. N., Express-method for determining ^{90}Sr in plants, 25:4039

ZAVADIL, S., Evaluation of various methods for stimulation of sugarbeet seed, 25:4722

ZAVIANTSEFF, V. T., RTG effects of CCEM detectors in a plasma analyzer for Pioneer F/G, 25:4243

ZAYED, K. E., Dielectric permeability of an inhomogeneous relativistic stream of cold plasma, 25:5101

ZECEVIC, Vasco, Nuclear photoactivation of ^{179}Hf, 25:5690

ZECH, E., Time-reversal invariance of the electromagnetic interaction on the 73 keV γ-transition in ^{193}Ir, 25:5715

ZEHLEV, Z., Internal-conversion studies of low-energy transitions in ^{149}Sm and ^{151}Eu, 25:5695

Transitions in decay chain ^{160}Gd to ^{160}Eu to ^{160}Sm, 25:5694

ZEIDMAN, B., Evidence for J/sup π/ = 8$^+$ state in ^{16}O, 25:5592

ZEIGARNIK, Yu. A., Boiling of liquid alkali metals in tubes, 25:4202 (BNL-tr-365)

ZEIGER, Louis S., Spinal cord dosimetry in ^{131}I-IHSA cisternography, 25:4510

ZELANO, A. J., Infrared dispersion in liquid benzene and benzene-d_6, 25:4064

ZELMAN, Donald, The effect of total-body irradiation on wound healing and the hematopoietic system in mice, 25:4705

ZEMTSOV, Yu. K., Amplification of vacuum-ultraviolet radiation in decaying dense helium plasma, 25:5090

ZERBIB, Jean-Claude, Taking samples of radioactive substances, 25:4516

ZHMYROV, V. N., Polarization of secondary protons in pp + π^+pn and pp + π^0pp reactions at 669 MeV, 25:5268 (JINR-P1-5293)

ZHULANOVA, Z. I., Formation of ATP in nuclei and mitochondria and the influence of β-mercaptoethylamine, 25:4597

ZICKENDRAHT, W., Three-alpha model for ^{12}C, 25:5836

ZIELINSKA-PFABE, M., Gamma-vibration of nuclei at equilibrium and saddle point, 25:5779

ZIMANYI, J., Effective charge factor for the radiative capture of fast nucleons, 25:5839

ZIMMER, W. H., Selection of fission yields, 25:5573

ZINCHENKO, Anatol, Study of K$^+$ decays into three pions, 25:5264

ZINK, John C., Neutron transport in two-dimensional slabs by invariant imbedding, 25:5143

ZIPFEL, Christie Lewis, Structure of electron bubbles in liquid helium from photo-ejection under pressure, 25:5034 (TID-25601)

ZISKIND, Richard, Comparison theorems for nonlinear point reactor dynamics equations, 25:6153

ZITTEL, H. E., Design considerations of reactor containment spray systems. Part VIII. Boiling water reactor accident radiolysis studies, 25:6035 (ORNL-TM-2412(Pt.8))

ZOFKA, J., Application of Hartree--Fock method in nuclear theory, 25:5859

ZOHNI, O., Optical model analysis for elastic deuteron scattering on light nuclei, 25:5579

ZOLLER, W. H., Weak β branching in ^{55}Cr, 25:5645

ZORIC, I., Enhanced superconductivity in ultrarapidly quenched bulk Al--Cu alloy, 25:5056

ZORINA, E. L., Calculation of the vibration spectrum of tantalum, 25:5183

ZRELOV, V. P., Cherenkov radiation in high-energy physics, 25:4368 (AEC-tr-7059(Pt.1))

ZUBOV, Yu. G., Scattering of 4-MeV neutrons at angles close to 180°, 25:5762

ZUCKER, M., Method for solving time-dependent electron transport problems, 25:5242

ZUCKER, Martin, Phase space time evolution method, or, how to solve time-dependent transport problems in spite of transport equation, 25:5139

ZULKARNEEV, R. Ya., Nonstrange baryon--baryon resonances, 25:5388 (JINR-P2-5058)

ZUMER, S., Spin-lattice relaxation by quasi-spin waves in order-disorder type ferroelectrics, 25:6233 (IJS-575)

ZUMWALT, Lloyd R., Concentration dependence of the diffusion coefficient of volatile fission product metals in graphite, 25:4860

ZUPANCIC, C., Giant-resonance excitation by radiative capture of π^- in ^{16}O, 25:5600

ZVYAGINA, N. M., Magnetoresistance of Er--Y alloys at low temperatures, 25:5175

ZVYAGINTSEVA, E. N., Effect of the participation of the acid in forming the hydrogen bond during electrophilic deuterio-exchange, 25:4073

ZYGAN, H., Can macroscopic tests of Coulomb's law result in a revision of present atomic theory, 25:4972

XUM

SUBJECT INDEX

Cross references are included in cumulative subject indexes and in *Subject Headings Used by the USAEC Division of Technical Information* (USAEC report TID-5001).

The reader is also referred to *Guide to Abstracting and Indexing for Nuclear Science Abstracts* (USAEC report TID-4576).

Most headings in the subject index are specific materials, things, and processes. The headings are followed by modifiers that describe the properties of, or processes applied to, the headings.

All index entries cite *NSA* volume and abstract numbers; volume number precedes the colon and the abstract number follows it. The designation (R) following the abstract number indicates a progress report; (P) indicates a patent; and (T) indicates a translation. Abstracts for reports other than progress reports carry no letter designation. Report numbers, where applicable, are included in parentheses after the abstract number of the citation. Published literature (journal article or book) can be identified by the absence of a report number.

Ideas presented in the original literature, rather than key words, have been indexed. The indexers have selected what seemed the most probable and logical place to look for typical information. Since it is not always possible to anticipate where a user would look for information, the cumulative indexes include numerous cross references. Consideration of synonymous or closely related terms will prove valuable.

Information is indexed for the greatest use to the greatest number of users. This requires that a topic be indexed to headings that most specifically describe it and not ordinarily to the headings that describe its ultimate use or to the general class headings that include the specific headings. For example, information on boiler design for the Fermi Fast Breeder Reactor would be indexed under the headings BOILERS and FERMI FAST BREEDER REACTOR but not necessarily under the headings REACTORS, FAST or REACTORS, BREEDER.

General or broad headings are reserved for general summaries, reviews, comprehensive reports, and similar literature.

Subject Heading Styles

Generally, the direct form of subject entry is used rather than inverted headings; e.g., AMINO ACIDS rather than ACIDS, AMINO; HELIUM ISOTOPES He-4 rather than HELIUM—ISOTOPES He-4 or HELIUM—He-4 ISOTOPES. Note, however, that in some cases parenthetic modifying terms or inverted headings such as NEUTRONS, FAST, are used where the alphabetical arrangement of a direct entry would cause information to be scattered. In addition, organic compounds are usually entered in the index in the inverted form to facilitate grouping like or related compounds with the parent compounds; e.g., BENZENE, BROMO- rather than BROMOBENZENE. In general, the nomenclature used is that of the subject indexes to *Chemical Abstracts*.

Alphabetization

Subject headings are alphabetized word by word. Parenthetic qualifiers, numbers, and Greek letters within subject headings are disregarded in alphabetizing unless there are two or more headings that are otherwise identical, in which case the qualifier, numerical progression, or spelled names for the Greek letters determine the order.

Examples:

M-Capture
  see ELECTRON CAPTURE
MAGNESIUM
MAGNESIUM ALLOYS AND SYSTEMS
MANGANESE FLUORIDES
MANGANESE FLUORIDES MnF_2
MESONS
MESONS (π)
MESONS (ρ)
1-PENTANOL
2-PENTANOL

Modifying Phrases

The modifiers appearing under a subject heading are written specifically to show the relation between the item being indexed and the heading. The modifier therefore contains a maximum of useful information. Although the modifier begins with the word judged to be of greatest use to the greatest number of users, there is still need for the searcher to consider all modifiers under the heading(s) of interest.

Modifiers usually form meaningful phrases when combined with the subject heading. Some are intended to be read following the subject heading, e.g., the entry HYDROGEN—sorption by charcoal should be read "hydrogen sorption by charcoal." As a result of placing the important word first, however, many modifiers must be rearranged for smooth reading, e.g., FORMALDEHYDE—yields in radiolysis of ethyl ether, effects of deuterium on, should be read "effects of deuterium on formaldehyde yields in radiolysis of ethyl ether" and URANIUM—crystal structure of, effect of cooling rate on allotropic transformations in, should be read "effect of cooling rate on allotropic transformations in crystal structure of uranium."

Special characters are added to modifiers in the fields of physics and reactor technology; if the modifier does not establish the experimental or theoretical character of a reference, a symbol (E), (T), or (E/T) is placed immediately after the modifying phrase and before the abstract number.

XUM

Physical States and Configurations of Materials

The specific physical state, if other than normal, or the geometric configuration of the material is included in the modifying phrase; e.g., information on liquid metals is indexed under the specific metal with "liquid" in the modifier and carbon crucibles is indexed under CARBON with "crucibles" appropriately placed in the modifier. The information on carbon crucibles is also indexed under CRUCIBLES.

Nomenclature of Inorganic Compounds

Inorganic compounds are indexed to subject headings in the direct form. Cations are listed in the order of increasing valence for polycationic salts of varying valence and in alphabetic order for polycationic salts in which all cations have the same valence; e.g., SODIUM ALUMINUM SILICATES and POTASSIUM SODIUM SULFATES. If more than one anionic species is presented in a compound, the anions are arranged alphabetically, e.g., BERYLLIUM FLUORIDE HYDROXIDES.

Nomenclature of Organic Compounds

Organic compounds are indexed by subject headings based on the indexes to *Chemical Abstracts* except in the area of enzymes, in which specific enzymes, named according to the 1964 recommendations of the International Union of Biochemistry, are used. In many cases nonproprietary names for drugs are used as subject headings, and cross references are made from the systematic chemical names. Subject headings for hormones appear in the inverted style at HORMONES.

Nomenclature of Life Sciences

Subject headings for plants are names of phyla with one exception: members of the Phylum Tracheophyta are indexed under class or subclass names. Scientific names (genus and species) are used as the initial, or file, word in the modifying phrase. Scientific names are omitted only when the name is not available in the literature or cannot be found in available references.

Subject headings for animals are the names of phyla with the following exceptions: (1) members of Phylum Arthropoda and Phylum Chordata are indexed under appropriate class name, and (2) common names are used for members of Class Mammalia.

Subject headings are entered for various classes of commodities, and specific products are identified in the file-word position of the modifier. In the following examples, approved subject headings are capitalized and typical modifier file words are listed in lower case.

Example 1	Example 2
CEREALS	MEATS
bread	beef
flour	fish
oats	mutton
rice	pork
rye	poultry
wheat	seafood

Diseases, pathological conditions, and in vitro studies of atypical cells and tissues are indexed under subject headings for the organism affected, under the appropriate anatomical structure of physiological phenomenon affected, and under the appropriate disease heading. Subject headings for diseases (defined as any deviation from the norm) are DISEASES; DISEASES, INFECTIOUS; DISEASES, NEOPLASTIC; DISEASES, PHYSIOLOGICAL; DISEASES, PLANT; and DISEASES, TRAUMATIC.

Diseases of mixed etiology are treated in the following manner: neoplastic diseases that are also classified as infectious or physiological are indexed under DISEASES, NEOPLASTIC; diseases in which a microorganism is the etiologic agent are classified under DISEASES, INFECTIOUS; physiological anomalies that are neither neoplastic nor infectious are indexed under DISEASES, PHYSIOLOGICAL; the acute radiation syndrome, nonspecific radiation injuries, trauma, and wounds or incisions inflicted mechanically are indexed under DISEASES, TRAUMATIC.

Specific diseases or pathological conditions are named in the file-word position of the modifier, in the author's terminology, and are set off from the remainder of the modifier by commas. Neoplasms are designated as benign or malignant in the file-word position when more specific information is not available.

Multicomponent Alloys and Other Systems

Multicomponent alloys and systems, except well-known trade names, are indexed under a subject heading for each component in the form "element systems" for nonmetals or "element alloys and systems" for metals. The modifier begins with element symbols for each component arranged alphabetically. In addition, if significance is placed on the base metal of the alloy, this is indicated by adding "-base" to the element symbol.

Example: A 1.5C, 12Cr, 0.25V, 0.8Mo, bal Fe alloy is indexed as

```
CARBON SYSTEMS
  C--Cr--Fe-base--Mo--V, ...
CHROMIUM ALLOYS AND SYSTEMS
  C--Cr--Fe-base--Mo--V,...
IRON ALLOYS AND SYSTEMS
  C--Cr--Fe-base--Mo--V, ...
MOLYBDENUM ALLOYS AND SYSTEMS
  C--Cr--Fe-base--Mo--V, ...
VANADIUM ALLOYS AND SYSTEMS
  C--Cr--Fe-base--Mo--V, ...
```

Well-known alloys, such as ZIRCALOY-2, are indexed under the trade name; cross references from each component of the alloy to the trade name appear in cumulative indexes.

Multicomponent systems in which nonmetallic elements are present in large percentage and which are commonly referred to as systems or mixtures are indexed in a manner similar to alloys.

Example: A tungsten–silicon preparation is indexed as

```
TUNGSTEN ALLOYS AND SYSTEMS
  Si--W, ...
SILICON SYSTEMS
  Si--W, ...
```

Multicompound systems and mixtures of inorganic compounds are indexed under the subject heading for each component compound; the modifiers begin with an alphabetical listing of compound formulas.

Example: A lead titanate–lead zirconate mixture is indexed as

```
LEAD TITANATES
  PbTiO3--PbZrO3
LEAD ZIRCONATES
  PbTiO3--PbZrO3
```

XUM

A mixed system of compounds and elements is indexed by a combined form of the preceding conventions; e.g., a dispersion of copper and alumina would be indexed as

ALUMINUM OXIDES
  Al_2O_3--Cu, ...
COPPER ALLOYS AND SYSTEMS
  Al_2O_3--Cu, ...

Mixtures of organic compounds are indexed under subject headings for each component of the mixture; the modifiers begin with an alphabetical listing of compound names.

Example:

ACETIC ACID
  acetic acid--BF_3, ...
BORON FLUORIDES
  acetic acid--BF_3, ...

Example:

BENZENE, CHLORO-
  bromophenol--chlorobenzene, ...
PHENOL, BROMO-
  bromophenol--chlorobenzene, ...

If modifiers for alloys and systems are included with other modifiers under the same subject heading, they are filed last.

Example:

CARBON SYSTEMS
  deposition on nuclear fuel particles
  molecular structure of
  neutron total cross section for
  sorptive properties for xenon
  Young's modulus for
  Al--C--Cr, superconductivity in
  B--C, phase studies for
  C--U--Zr, fabrication and physical properties of

Nomenclature of High Energy Physics

Information on particle-particle events is indexed under subject headings for the specific particles involved. The modifier file word *interactions* is followed by the specific interaction written in symbolic form. Particle nomenclature and symbols follow that of Rosenfeld, et al. *Data on Particles and Resonant States,* UCRL-8030 (latest revision). For consistency the incident particle is always written first. The mass (in MeV) of a resonance state is included in parentheses after the symbol to avoid ambiguity. Hyperfragments are indicated in modifiers as in the following examples: Λ-He^5, Σ-H^3, $\Lambda\Lambda$-Be^{10}. The superscript on the right indicates the total number of baryons in the composite system.

Examples:

MESONS (π^-)
  interactions $\pi^- + p \rightarrow \Lambda + K^+ + \pi^-$ at 6 GeV/c in hydrogen bubble chamber, $\Lambda K(1700)$ enhancement in, (E)
BARYONS, RESONANCE (N^*)
  production of $\Delta^{++}(1236)$ and $\Delta^0(1236)$ from $K^- + p \rightarrow K^- + p + \pi^+ + \pi^-$ interactions at 2.63 and 2.70 GeV/c, (E)
HYPERFRAGMENTS
  binding energy of $\Lambda\Lambda$-He^6, three-body α--Λ--Λ model for

Subject headings are also provided for specific models and theories.

Examples:

ELEMENTARY PARTICLE MODELS (TRIPLET)
  hadron total cross sections in quark, numerical analysis of
CURRENT ALGEBRA
  PCAC hypothesis for A_1 and rho dominance in $\pi \rightarrow e + \nu + \gamma$ decay
REGGE POLE THEORY
  predictions for polarization in $K^- + p \rightarrow$ anti $K^0 + n$, $\pi^- + p \rightarrow \pi^0 + n$, and $\pi^- + p \rightarrow$ eta + n interactions at high energies
SYMMETRY GROUPS
  $SU(2) \times SU(4)$ intermediate-coupling model for nucleon and hyperon isobars

Nomenclature of Reactor Technology

Subject headings for reactors are of three types:

(1) Specific reactors, e.g., ARGONNE RESEARCH REACTOR, SAXTON POWER REACTOR

(2) Reactors having a common physics or engineering characteristic, e.g., REACTORS, FAST; REACTORS, ORGANIC-COOLED; REACTORS, PRESSURIZED-WATER

(3) Reactors having a common purpose, e.g., REACTORS, POWER; REACTORS, RESEARCH

Information on specific reactors, type (1), is indexed under the one specific subject heading. Information on classes or types of reactors, types (2) (characteristics) and (3) (purpose), is indexed under all applicable headings. For example, information on a heavy-water-moderated organic-cooled power reactor is indexed under REACTORS, HEAVY WATER-MODERATED; REACTORS, ORGANIC-COOLED; and REACTORS, POWER.

Subject headings exist for selected reactor components, e.g., REACTOR FUEL ELEMENTS. When applicable, headings for components are indexed even though they may have been included in a modifier under a type (1) or (2) heading. The materials in reactor components are indexed when the information is peculiar to the material.

Modifier file words under reactor headings are of two primary types: one type expresses reactor characteristics, e.g., reactivity; the other, components, e.g., control rod. If no subject heading appears for a reactor component, the heading REACTORS is used, and the component is used as the modifier file word.

XUM

A

ABDOMEN
retention of thorium dioxide in cavity of, of rats 15 months following intraperitoneal administration, 25:4442
ACCELERATORS
beam optical systems for, properties of isochronous magnetic, 25:5447 (IFVE-OP-69-68)
design and operational characteristics of 100-kA 500-kV electron, for plasma research, 25:5473
magnets for, calculation of energy losses in pulsed superconducting, 25:5459 (NP-18516)
operation of high-energy particle, development of remote systems for, 25:4200
ACCIDENTS
legal liabilities in, developments in, 25:4530
ACETAMIDE, 2-IODO-
effects on x-radiosensitivity of duodenum crypt cells in mice, 25:4587
ACETIC ACID
reactions with uranyl acetate,, uranyl chloride, and zinc amalgam, preparation of uranium(IV) acetates from, 25:4057
acetic acid--H_2CrO_4,, effects on electrochemical behavior of uranium, 25:4792
ACETIC ACID, [(CARBOXYMETHYLIMINO)BIS(ETHYLENENITRILO)]TETRA-
effects on plutonium-239 uptake by plants from soil, 25:4478
ACETIC ACID, CHLORO-
effects on phosphorescence produced by x radiation effects on indole in polar solution, 25:4089
ACETIC ACID, (ETHYLENEDINITRILO)TETRA-
complexes with uranium(VI), electrochemistry of, 25:4081
ACETIC ACID, FLUORO-
radioprotective effects of, on mice, reaction mechanisms for x, 25:4579
radioprotective effects of, on mice, reaction mechanisms for x, 25:4580
ACETIC ACID, IODO-
effects on γ-radiosensitivity of Escherichia coli, 25:4552
effects on x-radiosensitivity of duodenum crypt cells in mice, 25:4587
effects on x-radiosensitivity of Ehrlich ascites tumor cells in cultures, 25:4569
effects on x-radiosensitivity of enzymes in solutions, 25:4569
effects on x-radiosensitivity of rat embryos, 25:4575
ACETIC ACID, MERCAPTOPHENYL-
radioprotective effects of, on Escherichia coli, x, 25:4553
ACETIC ACID, TRICHLORO-
effects on phosphorescence produced by x radiation effects on indole in polar solution, 25:4089
ACETIC ACID, VINYL ESTER, POLYMERS
radioinduced crosslinking of, γ, 25:4094
ACETOACETIC ACID
effects on x-radiosensitivity of fern spores, 25:4573
ACETONE
effects as additive on reactions of hydrated radiolytic electrons with biological and food extracts, 25:4117
effects of colony forming ability of uv irradiated Escherichia coli, 25:4728
ACETONITRILE
reactions with recoil tritium atoms, kinetics of, 25:4131
ACETYLCHOLINESTERASE
radiation effects on activity of, in developing brain of rats, x, 25:4457(R) (UCB-34-P-82-S)
ACRYLONITRILE
radioinduced cross linking with poly(2-methylpropene), calorimetric studies on effects of dose on γ, 25:4101
radioinduced graft polymerization of, onto graphite, γ, 25:4106
ACTINIDES
energy levels of, calculation using Saxon--Woods potential, (T), 25:5684 (JINR-P4-5221)
fission fragments of, mass and charge distributions of, (E), 25:5691
nuclear deformation parameters and quadrupole and hexadecapole moments for, (T), 25:5860
properties of, handbook on physical and nuclear, 25:5722
ACTIVATION ANALYSIS
half-life in instrumental, calculation of role of, 25:4050
method for photon, using NRL Linac, 25:4041 (AD-709901)
methods for carbon, nitrogen, and oxygen in sodium using protons, 25:4736(R) (ANL/ST-3)
sodium-24 removal methods in, 25:4044
tables of gamma energies and half-lives for, 25:5685 (KFKI-70-18-NAC)
ADENOSINE MONOPHOSPHATES
polymers, complexes with poly U, effects of, on metabolism in polymorphonuclear leukocytes of x-irradiated guinea pigs, 25:4454 (NYO-3240-55)
ADENOSINE 5'-TRIPHOSPHATE
synthesis in mitochondria and nuclei in liver and thymus of rats, effects of cysteamine on, 25:4597
ADRENOCHROME
monoguanylhydrazone methanesulfonate, radioprotective effects of, on mice, internal β, and external γ and x, 25:4589
ADVANCED TEST REACTOR
coolant loss accident conditions in, heat transfer characteristics for 1.4 MW reverse flow, (E/T), 25:6119
AEROSOLS
use of radioisotope-labeled, for inhalation scanning of human lungs, review of equipment and procedures for, 25:4678
AET
effects on nervous system of chickens following administration to embryos, 25:4601
effects on synthesis of DNA and RNA in thymus gland of rats, tracer study of, 25:4592
effects on synthesis of DNA in spleen and thymus of rats, 25:4596
radioprotective effects of N-substituted derivatives of, on mice, x, 25:4577
radioprotective effects of, on mice, combined effects of cysteamine, cysteine, glutathione, and serotonin against x, 25:4582
radioprotective effects of, on mice, combined effects of 5-methoxytryptamine on x, 25:4582
radioprotective effects of, on mice, x, 25:4553
radioprotective effects of, on rats, γ, 25:4581
radioprotective effects of, reaction mechanisms for, in dogs and rats, x, 25:4599
AGE
effects on closure of airways in human lungs, 25:4428
effects on pulmonary ventilation in man, 25:4666
AGRICULTURE
nuclear energy uses in, 25:4732(R) (NYO-2043-216)
AIR
analysis for bismuth-214, lead-214, and polonium-218, alpha detection method for, 25:4040
neutron attenuation at 0.3 to 5.0 MeV, cross sections for, (E), 25:5481
AIRGLOW
characteristics of, for magnetospheric diagnostics, (E/T), 25:5023
sodium-D lines in nightglow, excitation mechanisms of, (E/T), 25:5018
ALANINE, PHENYL-N-TRYPTOPHYL-
radiolysis of aerated solutions of, yields from γ and x, 25:4114
ALANINE, N-TRYPTOPHYL-
radiolysis of aerated solutions of, yields from γ and x, 25:4114
ALBUMINS
labeling with iodine-131, 25:4411 (CEA-R-4031)
ALCOHOL DEHYDROGENASE
radiosensitivity of activity of, in solutions, effects of iodine compounds on x, 25:4569
radiosensitivity of, in aqueous solutions, effects of iodine compounds on ionizing, 25:4543
ALKALI METALS
boiling inspection in liquid, pressure--temperature model for, 25:4212
heat transfer to boiling, in tubes, comparison of calculated and measured values for, 25:4202(T) (BNL-tr-365)
plasma of, drift instabilities in Q devices, (E), 25:5112
ALKALINE EARTH FLUORIDES
dielectric constants of, low-frequency, 25:6229 (COO-623-154)
ALLOYS
activities of components of binary liquid, modified Gibbs--Duhem equation for calculation of, 25:4754
radioinduced creep in, loop unfaulting mechanism for neutron, 25:4830
thermoelectric power in, (T), 25:6227 (COO-623-152)
ALPHA PARTICLES
detection in lymphoid tissues of rats following intratracheal administration of thorium oxide, 25:4442
detection of solar, response analysis of system for, 25:4928
effects on gaseous hydrogen sulfide or propane, 25:4119
effects on helium release from molybdenum, 25:4216(R) (SC-PR-70-682)
interactions $\pi^+ + \alpha + \pi^+ + \alpha$, electromagnetic corrections including relativistic terms for, (T), 25:5527
reactions (α,2n) with holmium-165 at 21 to 27 MeV, gamma spectra and angular distributions, (E), 25:5726
reactions (α,2n) with samarium-150 at 30 MeV, gamma and conversion-electron spectra from, (E), 25:5750
reactions (α,d) with nitrogen-14 at 6.875 to 7.415 MeV cms, differential cross sections from, (E), 25:5596
reactions (α,t) with calcium-48 at 44 MeV, triton spectra from, (E), 25:5506 (CEA-N-1232, pp 81-155)
scattering by argon-36 and -40, calcium-40, -42, and -44, and potassium-39 and -41 at 24.1 MeV, optical-model analysis with l-dependent absorption of angular distributions from elastic, (T), 25:5665
scattering by calcium-40 at 29 MeV, differential cross sections and energy spectra for elastic and inelastic, (E), 25:5643

scattering by carbon-12 at 12.5 to 18.0 MeV, angular distributions and total cross sections for, (E), 25:5561
scattering by helium-4, unified nuclear reaction theory for elastic, (T), 25:5870
scattering by nickel-58 at 64 MeV, angular distributions and reflection coefficients from eikonal approximation for, (T), 25:5834
scattering by oxygen-16, nuclear density distributions in elastic, (T), 25:5835
scattering by samarium-148 at 10 to 13 MeV, angular ditributions for inelastic, (E), 25:5703
scattering by samarium-152 at 10.38 MeV, quantum-mechanical corrections to probability for double Coulomb excitation from inelastic, (T), 25:5781
scattering by zinc-70 at 42 MeV, angular distributions and energy spectra from inelastic, (E), 25:5607

ALUMINUM
antiproton absorption at 20 to 65 GeV/c, cross sectons for, (E), 25:5295
antiproton absorption cross sections at 20 tc 40 GeV/c, (E), 25:5265 (CONF-700314-, Paper 4)
complexes with 8-quinolinol, structure of, NMR spectral studies on, 25:4081
complexes with hydroxamic acids, stability studies on, 25:4083
determination in boron, 25:4009 (TID-25190)
determination in meteorites by instrumental pile neutron activation, 25:4048
determination in PuO_2--U_3O_8, effects of ratic of plutonium oxide to uranium oxide cn spectrographic, 25:4015 (NUMEC-3524-76)
determination in titanium ore by neutron capture gamma spectroscopy using californium-252 source, 25:4036
effects of alloying additions of, on purification of iron--nickel vacuum melts, relations with composition and reduced pressure, 25:4744
effects of impurities of, cn properties of uranium, 25:4747 (AWRE-O-63/70)
electric conductivity at 1.5 to 300°K, absolute, (E/T), 25:5184
electron reactions with, ionization cross sections for, (E), 25:4556
electron scattering by, angular and energy distributions for 0.4- to 2.0-MeV. (T), 25:4938
electron transport normal to slab of, modified PSTE method for, 25:5242
fabrication of precision tubes of, equipment and methods for, 25:4745
gamma scattering from, barriers of finite thickness, (E), 25:5149
meson (K-) absorption at 20 to 65 GeV/c, cross sections for, (E), 25:5295
meson (K-) absorption cross sections at 20 tc 40 GeV/c, (E), 25:5265 (CONF-700314-, Paper 4)
meson (π^-) absorption at 20 to 65 GeV/c, cross sections for, (E), 25:5295
meson (π^-) absorption cross sections at 20 tc 40 GeV/c, (E), 25:5265 (CONF-700314-, Paper 4)
neutron spectra in pulsed assembly, fast, (E/T), 25:6106
properties for use as encapsulating material for californium-252 sources for neutron capture gamma-ray spectroscopy, 25:4772
radiation effects on void formation in preirradiated high-purity, fast neutron, 25:4818
radioautograms of surfaces of thermal neutron-irradiated, method for production of micro-, 25:4250
separation from aqueous solutions by ion exchange using Alamine 336 or Amberlyst A-21 in thiocyanate solutions, 25:4137 (IS-T-377)
separation from gallium and iron by icn exchange in thiocyanate solutions using Alamine 336, 25:4137 (IS-T-377)
superconducting films above transition temperature, nonlinear excess conductivity in, (E/T), 25:5040
superconductivity and normal-state conduction mechanism in oxidized thin films of, (E/T), 25:5039

ALUMINUM ALLOYS AND SYSTEMS
electric conductivity at 1.5 to 300°K of dilute, deviations from Matthiessen's rule in, (E/T), 25:5184
Al--Ce, Kondo effect suppression in $CeAl_2$ by thorium addition, 25:5228
Al--Ce, preparation and properties cf Al_4Ce fiber-reinforced, 25:4742(P)
Al--Ce, thermal capacity of $CeAl_2$ at low temperatures, 25:5218
Al--Cu, superconductivity in ultrarapidly quenched bulk, enhanced, (E/T), 25:5056
Al--Cu-base, deformation of monocrystalline, effects of temperature on, 25:4783
Al--Er, magnetic structure of ErAl, neutron-diffraction study, 25:5208
Al--Fe-base, K-absorption spectrum edge in, 25:5181
Al--Gd, thermal capacity of $GdAl_2$ at low temperatures, 25:5218
Al--Ho, magnetic structure of HoAl, neutron-diffraction study, 25:5208
Al--La, thermal capacity of $LaAl_2$ at low temperatures, 25:5218
Al--Nd, magnetic structure of NdAl, neutron-diffraction study, 25:5208
Al--Pr, thermal capacity of $PrAl_2$ at low temperatures, 25:5218
Al--Tb, magnetic structure of TbAl, neutron-diffraction study, 25:5208
Al--Ti-base--V, crack growth in, at sustained loads, effects of hydrogen on, 25:4762
Al--Ti-base--V, fabrication of precision tubes of, equipment and methods for, 25:4745
Al--Tm, magnetic structure of TmAl, neutron-diffraction study, 25:5208
Al--Tm, thulium-169 NMR in $TmAl_2$, 25:5226
Al-base--B, microstructure of master alloys of, evaluation of, 25:4780
Al-base--B, properties of master alloys of, evaluation of chemical and physical, 25:4780
Al-base--B--Ti, microstructure of master alloys of, evaluation of, 25:4780
Al-base--B--Ti, properties of master alloys of, evaluation of chemical and physical, 25:4780
Al-base--Ti, microstructure of master alloys of, evaluation of, 25:4780
Al-base--Ti, properties of master alloys of, evaluation of chemical and physical, 25:4780

ALUMINUM ISOTOPES Al-26
abundance in R And and 19 TX Pis, (E), 25:4859

ALUMINUM ISOTOPES Al-27
abundance in R And and 19 TX Pis, (E), 25:4859
energy levels from magnesium-26(p,n) reactions, (E), 25:5613
energy levels from silicon-28 (γ,p) reactions, relative populations from collective-correlations model, (T), 25:5653
helium-3 reactions (He-3,p) at 18 MeV, proton spectra and angular distributions for, (E), 25:5680 (CEA-N-1232, pp 1-80)
neutron capture at 20 to 80 keV, cross sections for, (E), 25:5603 (FOA-4-4440)
neutron reactions (n,α) at 14.43 MeV, cross sections for, (E), 25:5641
neutron reactions (n,d) at 14.1 MeV, energy spectra and DWBA analysis of angular distributions from, (E/T), 25:5662
photon reactions (γ,t) at 90 MeV, triton yield in, (E), 25:5678
proton elastic scattering at 18 MeV using polarized beam, depolarization parameter for, (E), 25:5506 (CEA-N-1232, pp 81-159)

ALUMINUM ISOTOPES Al-28
energy levels from neutron resonances in aluminum-27, radiative widths for, (E), 25:5603 (FOA-4-4440)

ALUMINUM OXIDES
creep strain of, effects of grain-boundary porosity growth on high-temperature, 25:4848
iron-58 Moessbauer effect in, effects of iron valence in, 25:5221 (AD-710293)
radiation effects on crystal structure of, neutron, 25:4887 (KFK-1215)
Al_2O_3--BeO--H_2O--SiO_2, phase studies of subsolidus phase relations of, at 300 to 700°C, 25:4871

AMERICIUM
separation from aqueous chloride solutions by solvent extraction using cyclooctylphenylphosphinic acid or octylphenylphosphinic acid, 25:4147

AMERICIUM ISOTOPES Am-241
use as γ source for transmission scanning of bones for measurement of mineral content, 25:4645 (CONF-700515-, pp 263-71)
use as γ source for transmission scanning of human bones for measurement of mineral content, 25:4635 (CONF-700515-, pp 48-57)
use as γ source for transmission scanning of human bones for measurement of mineral content, 25:4634 (CONF-700515-, pp 33-47)
use as γ source for transmission scanning of human bones for measurement of mineral content, 25:4631 (CONF-700515-, pp 1-21)
use as γ source for transmission scanning of human bones for measurement of mineral content, 25:4643 (CONF-700515-, pp 243-54)
use as γ source for transmission scanning of human bones for measurement of mineral content, 25:4648 (CONF-700515-, pp 291-302)
use as γ source for transmission scanning of human bones for measurement of mineral content, 25:4627 (CONF-680211-, pp 319-28)
use as γ source for transmission scanning of soft tissues for measurement of lipid content, 25:4646 (CONF-700515-, pp 272-3)
use in implantable sensor for monitoring intracranial pressures, 25:4241

AMERICIUM OXIDES
fabrication of americium-241-enriched sources of, for dosimeter calibration, 25:4248

AMIDE POLYMERS
Ni--nylon, radicinduced curing of composites of, γ, 25:4108

AMINES
radioprotective effects of, on mammals, ionizing, 25:4539

AMINO ACIDS
content of uv-irradiated Escherichia, effects of, on repair synthesis of DNA, 25:4731

XUM

radiation effects on composition of, in wheat gluten, γ, 25:4465
radiation effects on content of, in developing brain of rats, 25:4457(R) (UCB-34-P-82-S)
radiation effects on, in aqueous solutions, protective effects of selenium compounds against ionizing, 25:4545
AMINO GROUP
radioprotective effects of, relation of molecular structure to, 25:4548
AMMONIA
effects of deuterated, on ion and molecule yields from γ radiolysis of 2,2-dimethylpropane, 25:4113
hydrogen-atom reactions at 1 to 25 keV with, cross sections for ionization in, (E), 25:4563
proton reactions at 1 to 25 keV with, cross sections for electron capture and total ionization in, (E), 25:4963
AMMONIUM ACID FLUORIDES
reactions with uranium formate, preparation of uranium ammonium fluoride from, 25:4058
AMMONIUM ALUMINUM SULFATES
properties of polarized proton targets of, 25:5450 (LA-4465, pp 4.1-2)
AMMONIUM COMPOUNDS, SUBSTITUTED
tetramethylammonium fluoride, complexes with uranium(IV) fluorides, preparation of, 25:4058
AMMONIUM HYDROXIDES
reactions with mandelic acid and uranyl nitrate, production of $(NH_4)_2UO_2(O_2C_8H_6)_2$ from, 25:4055
AMMONIUM URANIUM FLUORIDES
preparation by reactions of ammonium acid fluoride with uranium formate, 25:4058
AMMONIUM URANYL FLUORIDES
thermal decomposition of, mechanism of, 25:4082
AMPHIBIA
Ambystoma maculatum, radiation effects on breeding and migration of, x, 25:4475 (NYO-3554-8)
Bufo americanus, radiation effects on survival of, correlation with DNA content of liver cells, x, 25:4475 (NYO-3554-8)
Bufo woodhousei, radiation effects on survival of, correlation with DNA content of liver cells, x, 25:4475 (NYO-3554-8)
Plethodon cinereus, radiation effects on survival of, correlation with DNA content of liver cells, x, 25:4475 (NYO-3554-8)
Rana catesbeiana, radiation effects on survival of, correlation with DNA content of liver cells, x, 25:4475 (NYO-3554-8)
Rana clamitans, radiation effects on survival of, correlation with DNA content of liver cells, x, 25:4475 (NYO-3554-8)
Scaphiopus bombifrons, radiation effects on survival of, correlation with DNA content of liver cells, x, 25:4475 (NYO-3554-8)
α-AMYLASE
activity in barley seeds, effects of deuterium oxide on, 25:4464
radiation effects on, in saliva, blood serum, and urine following therapy, γ, 25:4452
ANALYTICAL CHEMISTRY
automation of, uses of computers in, 25:4008 (BNWL-SA-3341)
ANGIOSPERMIDAE
Ananas comosus, radiation effects on roots and shoots of, effects of dose rate on γ, 25:4719
Antirrhinum majus, radioinduced mutations in, effects of dose on γ, 25:4483
Artemisia tridentata, radiation effects on survival of, in desert ecosystems, fallout, 25:4477 (UCLA-12-782, pp 49-81)
Avena sp., radioinduced mutations in diploid and polyploid, review of thermal neutron and x, 25:4484
Beta sp., radiation effects on germination of, effects of infrared, petroleum extract, pyrimidine, and ultrasound on γ, 25:4722
Convolvulaceae sp., radiosensitivity of, ionizing, 25:4717 (NYO-2043-216, pp 1-18)
Crepis capillaris, radioinduced chromatid translocation aberrations in, effects of time postexposure on x, 25:4456
Crepis capillaris, radioinduced chromosome aberrations of, cesium-137 β and γ, 25:4458
Firmiana platanifolia, radiation effects on, following seed exposure, lethal and mutagenic, γ or x, 25:4724
Franseria dumosa, growth and mineral content of, effects of nutrient phosphorus availability on, 25:4477 (UCLA-12-782, pp 49-81)
Glycine sp., radioinduced mutations in populations of, for quantitative traits, review of thermal neutron, 25:4485
Gossypium sp., radioinduced mutations in, effects of pollen exposure on γ, 25:4499
Hibiscus sriacus, radiation effects on, following seed exposure, lethal and mutagenic, γ or x, 25:4724
Hordeum vulgare, activity of α-amylase in seeds of, effects of deuterium oxide on, 25:4464
Hordeum vulgare, radiation effects on frequencies of chlorophyll mutations and chromosome aberrations in, protective effects of anoxia, cysteine, and water against fast neutron and γ, 25:4604
Hordeum vulgare, radioinduced chromosome aberrations in, effects of gibberellic acid on γ, 25:4490
Larrea divaricata, survival in desert ecosystems, physiological characteristics affecting, 25:4477 (UCLA-12-782, pp 49-81)
Leguminosae sp., radiosensitivity of, ionizing, 25:4717 (NYO-2043-216, pp 1-18)
Lycopersicum sp., radioinduced internal disbudding in seedlings of, effects of, on mutations in following generation, γ, 25:4483
Lycopersicum sp., strontium-90 uptake by, effects of ammonium nitrate fertilization and availability of calcium and free calcium carbonates on, 25:4477 (UCLA-12-782, pp 49-81)
Morus sp., radioinduced mutations in, for improved leaf yield and disease resistance, effects of dose on γ, 25:4486
Nicotiana tabacum, radioinduced mutations in, in Italy, review of thermal neutron, 25:4488
Oryza sp., radioinduced mutations in, for culm length and lodging resistance, effects of dose on γ, 25:4487
Phaseolus vulgaris, mutations induced by cycasin in, frequency of chlorophyll and morphological, 25:4717 (NYO-2043-216, pp 1-18)
Phaseolus vulgaris, radioisotope uptake by, effects of availability of nutrient calcium and nitrates and root temperature on cesium-137, sodium-22, and rubidium-86, 25:4477 (UCLA-12-782, pp 49-81)
Phaseolus vulgaris, radiosensitivity of cultured callus tissue, seedlings, and seeds of Phaseolus, comparison of 40 krad cobalt-60 γ, 25:4723
Pisum sativa, radioinduced chromosome aberrations in, following seed exposure, role of free radicals in x, 25:4489
Pisum sativum, radioinduced mutations in, for agricultural improvement, review of x, 25:4488
Ricinus sp., radiation effects on ascorbic acid content and ascorbate oxidase activity in germinating seeds of, 25:4466
Salsola kali, uptake of soil water by, effects of soil moisture content and temperature on, 25:4477 (UCLA-12-782, pp 49-81)
Sorghum sp., radioinduced mutations in seeds of, 25:4495
Trifolium pratense, cesium-137 uptake by leaves and roots of, comparison of concentration factors for plant distribution for, 25:4445
Triticum aestivum, radioinduced mutations in, for quantitative traits, review of x, 25:4488
Triticum durum, radioinduced mutations in, for quantitative traits, review of x, 25:4488
Triticum vulgare, radioinduced inhibition of growth of roots and shoots of, effects of 40 kR dose on γ, 25:4718
Tritium sp., radiation effects on gluten of, effects of dose on, 25:4465
Vicia faba, radioinduced chromatid aberrations in chromosomes of, effects of dose fractionation on x, 25:4497
Vicia faba, radioinduced chromosome aberrations in, x, 25:4494
Vicia faba, radioinduced chromosome aberrations in root tip cells of, effects of dose fractionation on number of x, 25:4492
Vicia sp., radioinduced mutations in, for improved forage, thermal neutron and x, 25:4488
Zea mays, radioinduced mutations in populations of, for quantitative traits, review of thermal neutron, 25:4485
Zea mays, uranyl nitrate effects on production of sucrose in scutellum of, 25:4720
ANGIOTENSINS
radioimmunoassay in blood plasma of rabbits, method for, 25:4419
ANIMALS
radioisotope sorption by aquatic and marine, 25:4479
ANOXIA
effects on γ-radiosensitivity of bacteria and bacteriophages, 25:4549
effects on x-radiosensitivity of cultured Chinese hamster cells, 25:4557
effects on x-radiosensitivity of cultured Chinese hamster cells, 25:4561
effects on x-radiosensitivity of Escherichia coli, 25:4550
effects on x-radiosensitivity of fern spores, 25:4572
effects on x-radiosensitivity of Serratia marcescens, 25:4557
radioprotective effects of, on barley seeds, fast neutron and γ, 25:4604
ANTIGENS
radioimmunoassay in blood serum method for, 25:4417
use of irradiated fetal tissues as, for immunization of mice against virus-induced tumors, 25:4656(R) (ORNL-4615)
ANTIMONY
determination of, use of titanous chloride in rapid quantitative, 25:6239(T) (MLM-1766(TR))
separation from tin by reversed-phase extraction chromatography, 25:4143
ANTIMONY ALLOYS AND SYSTEMS
La--Sb, thermal capacity of LaSb at low temperatures, 25:5218

Pr--Sb, thermal capacity of PrSb at low temperatures, 25:5218
Sb--Tb--Y, magnetic ordering transition, 25:5205
Sb--Tm, thulium-169 NMR in TmSb, 25:5226
Sb--U, enthalpy of formation of intermetallic, direct-reaction calorimetric measurement of, 25:4843
ANTIMONY ISOTOPES Sb-121
energy level of, nuclear magnetic moment of $^{7}/_{2}$, (E), 25:5720
neutron capture by, gamma spectra from resonance and thermal, (E), 25:5724
ANTIMONY ISOTOPES Sb-122
energy levels from antimony-121 neutron capture, spins of, (E), 25:5724
ANTIMONY ISOTOPES Sb-123
neutron capture by, gamma spectra from resonance and thermal, (E), 25:5724
ANTIMONY ISOTOPES Sb-124
energy levels from antimony-124 neutron capture, spins of, (E), 25:5724
ANTIMONY ISOTOPES Sb-125
beta decay of, matrix elements of 437-keV transition in, (E), 25:5730
ANTIMONY ISOTOPES Sb-126
beta decay of isomeric, beta and gamma spectra, branching ratios, and log-ft values for, (E), 25:5693
ANTIPYRINE
complexes with thorium, titanium, uranium, uranyl, zirconium, and zirconyl perchlorates, ir spectra and physical properties of, 25:4087
ARGON
helium-ion reactions at 10 to 30 keV with, cross sections for production of metastable triplet helium atoms by charge exchange in, (E), 25:4569
helium-metastable-atom reactions with, cross sections for ionization in, (E), 25:4569
plasma jets of, diagnostics using Thomson and Rayleigh scattering of laser beams, 25:5078 (CEA-R-3998)
plasma jets of, properties in homopolar devices, 25:5089
plasma of, absorption corrections for optically thick, 25:5088 (AD-710218)
ARGON IONS
reactions with single-crystal germanium, minimum energy for sputtering in, (E), 25:5155
ARGON ISOTOPES Ar-36
alpha elastic scattering at 24.1 MeV, optical-model analysis with l-dependent absorption of angular distributions from, 25:5665
energy levels in quartet scheme, low-lying even-parity, even-spin, (T), 25:5814
lithium-7 reactions (Li-7,t) at 16.6 MeV, triton spectra from, (E), 25:5680 (CEA-N-1232, pp 1-80)
reactions with molybdenum-92 at 137 MeV, gamma spectra from, (E), 25:5688 (UCRL-19961)
ARGON ISOTOPES Ar-38
energy level at 4585 keV from helium-4 (Cl-35,p) reactions at 70 MeV, lifetime of, (E), 25:5664
energy levels from proton resonances in chlorine-37, spreading widths for isobaric analog, (T), 25:5644
energy-level transitions from helium-4 (Cl-35,p) reactions at 70 MeV, intensities of, (E), 25:5664
proton reactions (p,γ) at 1.25 to 2.35 MeV, angular distributions and Q-value for, (E), 25:5631
ARGON ISOTOPES Ar-40
abundance relative to potassium-40 in Pacific Ocean phillipsites, 25:4164
alpha elastic scattering at 24.1 MeV, optical-model analysis with l-dependent absorption of angular distributions from, 25:5665
energy levels from chlorine-40 decay, (E), 25:5614
energy levels from proton inelastic scattering at 5.2 MeV, spin assignments for, (E/T), 25:5667
energy-level transitions from proton inelastic scattering at 5.2 MeV, angular correlations and gamma-ray branching ratios from, (E/T), 25:5667
helium-3 reactions (He-3,t) at 35 MeV, DWBA analysis of angular distributions from, (E/T), 25:5654
reactions (Ar-40,f) with uranium, production cross sections for Z = 42 to 79 isotopes in, (E), 25:5756
ARMY REACTORS (PM-2)
pressure vessel for, radiation effects on ductility of, (E), 25:6146
ARMY REACTORS (SM-1)
pressure vessel for, neutron embrittlement and fluence exposure of, (T), 25:6145 (AD-709858)
ARSENIC
determination of trace amounts of, in silicon nitrides and oxides by neutron activation and γ spectroscopy, 25:4045
determination of, use of titanous chloride in rapid quantitative, 25:6239(T) (MLM-1766(TR))
ARSENIC ISOTOPES As-69
beta decay of, half-life for, (E), 25:5621
ARSENITES
production of radicals of, from γ radiation effects on arsenate-doped calcium tungstate, ESR spectral studies on, 25:4090
ARTERIES
radiation effects on pressure in, of rats following intratracheal and intraperitoneal injection of thorium dioxide, α, 25:4701
ASCORBATE OXIDASE
radiation effects on activity of, in Ricinus seeds, effects of germination on γ, 25:4466
ASCORBIC ACID
radiation effects on content of, in Ricinus seeds, effects of germination on γ, 25:4466
ASPARTATE AMINOTRANSFERASE
content of blood plasma in rats, effects of cysteamine, hypoxia, and pyridoxol on, 25:4594
ASTATINE
sorption from nitric acid on cesium phosphotungstate, 25:4053(T) (ANL-Trans-861)
ASTRON DEVICE
E-layer magnetic field equilibrium in, (T), 25:5119
ASTRONAUTS
radiation dose to, statistical analysis of cosmic, 25:4509 (MDC G-363)
ASTROPHYSICS
book: Spectroscopic Astrophysics, 25:4913
discretization in, (T), 25:4933
ATMOSPHERE
cosmic-ray ionization at balloon altitudes, (E), 25:4990
cosmic-ray phenomena in, (E/T), 25:4984
electron precipitation into upper, production of x rays from, (T), 25:5007
ionization in Cytherean and Martian upper, height-distribution processes of, (E/T), 25:4936
ionization in upper, comparison of ionization by collision of charged particles and photoionization, (E/T), 25:5015
neutron transport at 8,000 to 50,000 ft in, Compton electron currents from photons from 14-MeV, (T), 25:5497
ozone distribution in, solar radiation analysis of vertical, (E), 25:5017
pollution of Chicago, multiple-source dispersion model for studying, 25:4161 (ANL/ES-CC-7)
sulfur content of, performance of californium-252 source for measurement of, 25:4218
ATMOSPHERIC PRECIPITATION
barium-140 content of, in Fayetteville, Arkansas, 25:4163
pollutant scavenging by, mechanisms of, 25:4162 (BNWL-SA-3450)
radioisotope content of, in Faroe Islands during 1969, cesum-137 and strontium-90, 25:4476(R) (RISO-221)
strontium-89 content of, in Fayetteville, Arkansas, 25:4163
strontium-90 content of, 25:4163
ATOMIC ABSORPTION SPECTROMETRY
operation and performance of, in industrial hygiene, review on, 25:4023
ATOMIC BEAMS
deflection by resonance-radiation pressure, 25:4541
ATOMIC ENERGY
transactions of American Nuclear Society 1970 Winter Meeting, 25:6192
ATOMIC ENERGY COMMISSION (USA)
research programs for developing cobalt-60 heat sources, review of, 25:4224
ATOMIC ENERGY, LEGAL ASPECTS
accident liabilities and insurance development, 25:4530
medico-legal claims by personnel following radiation exposure, prevention of, 25:4523
recommendations for control of radiation dose to personnel during diagnostic radiography, 25:4531
recommendations for maximum exposure levels for microwave personnel, 25:4708 (UR-49-1256)
recommendations for radiation standards by FRC, ICRP, and NCRP, 25:4532
recommendations of ICRP for medical examination of personnel at AERE, Harwell, 25:4529 (AERE-R-6523)
safeguards for nuclear materials management, review of Non-Proliferation Treaty, 25:4269
safeguards implementation by US, development of improved methods for, 25:4270
safeguards systems for nuclear materials management, adaptation to Non-Proliferation Treaty of IAEA, 25:4271
safeguards systems for nuclear materials management, development of improved, 25:4272
standards for x-ray emission by television receivers, recommendations for, 25:4522 (BRH/DEP-70-24)
ATOMIC MODELS
equations for statistical, relation to Schroedinger equation, 25:4970
ATOMIC STRUCTURE
theory of, possible effects of concentric-hollow-spheres test of Coulomb law on, 25:4972
ATOMS
electron pair correlation energies in, Gaussian geminals for calculation of, 25:4973
electron scattering by, single-particle formulation of, including strong correlation effects, 25:4966
energy of, matrix elements of second-order relativistic corrections to, 25:4971
energy-level transitions in, correlations between intensity of specific x radiation and nuclear charge, (T), 25:5832
oscillator-strength sums for, calculation of upper and lower bounds for, 25:4946
proton reactions with, angular distribution of fast K-

XUM

and L-shell electrons from, (T), 25:4968
scattering by diatomic molecules, delta-function technique for calculation of inelastic, 25:4962
AUGER ELECTRONS
uses in metallurgical studies, discussion of, 25:4798
AURORAE
characteristics of, for magnetospheric diagnostics, (E/T), 25:5023
charged-particle trajectories during, effect of extraterrestrial ring current on, (T), 25:5032
excitation of atomic nitrogen and oxygen in, correlation with auroral ionization rates, (E/T), 25:5009
proton energy spectra in, ionization rate and electron density height profiles for, 25:5010
AURORAL ZONE
current of electrojet in, spatial extent of return, (E), 25:5003
AUTORADIOGRAPHY
detectors for alpha metallographic, cellulose nitrate track, 25:4344
method for intact germ cells, whole-mount technique for, 25:4421
method for production of microautoradiograms of surface of thermal neutron-irradiated aluminum, 25:4250
nuclear aspects of, suggestions concerning color in, 25:4416
AVES
Gallus sp., content of proteins in serum of, effects of infection with Histomonas (protozoa) on, 25:4692 (COO-1209-13)
Gallus sp., effects of AET on nervous system of, following administration to embryos, 25:4601
Gallus sp., radiation effects on immune reactions of, to allogeneic cells, combined effects of bursectomy or thymectomy on cobalt-60 γ, 25:4468
Gallus sp., radiation effects on uridine incorporation into RNA of nerve tissue of, carbon-14 tracer study of x, 25:4457(R) (UCB-34-P-82-9)
Meleagris sp., radiation effects on pathogenicity of Histomonas (protozoa) for, γ, 25:4692 (COO-1209-13)
radioisotope content of, in Faroe Islands during 1969, cesium-137 and strontium-90, 25:4476(R) (RISO-221)

B

BACTERIOPHAGES
lambda, radioinduced breaks of DNA strands in, effects of triacetoneamine N-oxyl on x, 25:4550
T_4, radiation effects on survival of, protective effects of anoxia and cystamine against γ, 25:4549
T_7, radiation effects on survival of, protective effects of anoxia and cystamine against γ, 25:4549
BARIUM
complexes with 8-quinolinol, structure of, NMR spectral studies on, 25:4081
diffusion in graphite at 1000°C, effects of concentration on, 25:4860
optical constants from reflectance spectra at 1 to 11.6 eV, 25:5188
separation from aqueous solutions by ion exchange using Alamine 336 in thiocyanate solutions, 25:4137 (IS-T-377)
BARIUM FLUORIDES
BaF_2--CaF_2, corrosion by sodium of bearing coatings of, at 1100°F, 25:4185(R) (NYO-3930-8)
BARIUM ISOTOPES Ba-134
energy-level transitions in, M1/E2 multipole mixing of 563- and 569-keV, (E), 25:5706
BARIUM ISOTOPES Ba-137
energy levels of, spectroscopic factors for, (E), 25:5506 (CEA-N-1232, pp 81-159)
mass transfer of metastable, in forced-convection sodium, radiochemical measurement of coefficients of, 25:4774
BARIUM ISOTOPES Ba-138
neutron activation resonance integrals of, thermal, (E), 25:5681 (CNEA-274)
BARIUM ISOTOPES Ba-140
content in rainwater and snow, 25:4163
distribution in troposphere, 25:4163
fission yields for fast reactor spectra, performance of, 25:5973
BARIUM OXIDES
BaO--MoO_3, phase studies of, 25:4873
BARIUM SULFATES
radiation dose to, method using diffuse reflection spectra to measure absorbed γ, 25:4520
BARYONS
decay of $J = {}^3/_2$ and ${}^5/_2$, broken SU(3) x SU(3) chiral algebra for sum rules for coupling constants for, (T), 25:5395
decay of $J = {}^5/_2$, broken SU(3) x SU(3) chiral algebra for F-wave relative to P-wave, (T), 25:5395
decay of, quark model for broken SU(6) sum rules for relation with K decays for, (T), 25:5394
exchange in $K^- + n \rightarrow \Xi^- + K^0$ and $K^- + p \rightarrow \Xi^-(\Xi^0) + K^+(K^0)$ interactions at 1.2 to 2.7 GeV/c in bubble chamber, partial-wave analysis for, (E/T), 25:5384
interactions with 0^- mesons, additive quark model for single and joint decay angular distributions for 0^+, 1^+, and 2^+ meson and ${}^3/_2{}^+$ baryon production in, (T), 25:5375 (TPJU-15/70)
interactions with baryons in ladder approximation, Bethe-Salpeter equation for two-body, (T), 25:5430
BARYONS, RESONANCE
decay in emulsions and hydrogen bubble chamber, (E), 25:5276
decay of ${}^3/_2{}^+$, additive quark model for angular distributions for, (T), 25:5375 (TPJU-15/70)
decay $Y(1327) \rightarrow \Lambda + \pi^0 + \gamma$, spin and parity for probability of, (T), 25:5385
decay $Y(1327) \rightarrow \Lambda + \pi^0$, spin and parity for probability of, (T), 25:5385
decay $Y(1327) \rightarrow \Lambda(I) + \gamma$, spin and parity for probability of, (T), 25:5385
interactions of, resonance width determination from interference of identical particles in, (T), 25:5350 (JINR-P1-5315)
mass of nonstrange $2^+(2050)$, in p + p interactions at 300 to 640 MeV, (T), 25:5388 (JINR-P2-5058)
parity and spin of nonstrange $2^+(2050)$, in p + p interactions at 300 to 640 MeV, (T), 25:5388 (JINR-P2-5058)
parity and spin of Y(1327), (T), 25:5385
production in p + n interactions at 24 GeV in emulsions and hydrogen bubble chamber, (E), 25:5276
production of $\Delta\pi(1425)$ enhancement in $p + p \rightarrow p + p + \pi^+ + \pi^-$ interactions at 7.9 GeV/c, 25:5278
production of exotic, in $K^- + d$ interactions at 3 GeV/c, upper limits for cross sections of, (E), 25:5287
production of nonstrange $2^+(2050)$, in p + p interactions at 300 to 640 MeV, (T), 25:5388 (JINR-P2-5058)
width of, identical particle interference in resonance interactions for determining, (E/T), 25:5350 (JINR-P1-5315)
BARYONS, RESONANCE (N*)
classification in four recurrences of parallel trajectories, 25:5379
coupling constants for Roper octet, broken SU(3) x SU(3) chiral algebra for ratio of weak, (T), 25:5355
mass and width of N(1240) from Z = 0 formalism for composite particles, 25:5417
production of $\Delta^{++}(1236)$ in $\pi^+ + p \rightarrow \pi^+ + p + \pi^+ + \pi^-$ interactions at 11.0 GeV/c, (E), 25:5292
BARYONS, RESONANCE (Y*)
production of $\Lambda(1520)$ in $\pi^+ + d \rightarrow 2p + K^+ + K^-$ interactions at 1.1 to 2.4 GeV/c, (E), 25:5289
production of $\Sigma(1385)$ in $\pi^+ + d \rightarrow n + \Lambda + K^+ + \pi^+$ interactions at 1.1 to 2.4 GeV/c, (E), 25:5289
production of $\Sigma(1385)$ in $\pi^+ + p \rightarrow K^+ + \Sigma(1385)$ interactions at 4 and 5.05 GeV/c, test of SU(3) symmetry from counter and spark chamber study of differential cross sections for, (E), 25:5290
production of $\Sigma(1385)$, $\Lambda(1405)$, and $\Lambda(1520)$ in three-body final states in anti p + p interactions at 2.4 and 2.9 GeV/c, (E), 25:5270
BEARINGS
performance of hydrostatic journal, mathematical analysis of, 25:4185(R) (NYO-3930-8)
testing of liquid sodium-lubricated, design of rig for, 25:4185(R) (NYO-3930-8)
BELGIAN REACTOR-2
carbon transport loop for, testing of graphite in, 25:4835 (DP-Report-448)
BENZENE
benzene--cyclohexane, radiolysis of, effects of composition on hydrogen yields from γ, 25:4121
BENZENE, DIVINYL-
radioinduced cross linking with poly(2-methylpropene), calorimetric studies on effects of dose on γ, 25:4101
BENZENEARSONIC ACID, 2,2'-[(1,8-DIHYDROXY-3,6-DISULFO-2,7-NAPHTHYLENE)BIS(AZO)]DI-
reactions with thorium in biological materials to determine thorium content, 25:4443
BENZENEARSONIC ACID, o-[(2-HYDROXY-3,6-DISULFO-1-NAPHTHYL)AZO]-
use as reagent in automatic colorimetric determination of thorium in aqueous and organic solutions, 25:4014 (NLCO-1072)
BENZOHYDROXAMIC ACID
complexes with divalent and trivalent metals, stability studies on, 25:4083
BERYLLIUM
analysis of, linac facility for photon activation, 25:5472
antiproton absorption at 20 to 65 GeV/c, cross sections for, (E), 25:5295
antiproton absorption cross sections at 20 to 40 GeV/c, (E), 25:5265 (CONF-700314-, Paper 4)
complexes with phenanthrenequinone oxime, potentiometric studies on formation constants of, 25:4080
determination in PuO_2--U_3O_8, effects of ratio of plutonium oxide to uranium oxide on spectrographic, 25:4015 (NUMEC-3524-76)
electron pair correlation energies in, calculation using Gaussian geminals, 25:4973
lattice parameters at 77 to 300°C, effects of impurities on, 25:4795
meson (K^-) absorption at 20 to 65 GeV/c, cross sections for, (E), 25:5295
meson (K^-) absorption cross sections at 20 to 40 GeV/c, (E), 25:5265 (CONF-700314-, Paper 4)
meson (π^-) absorption at 20 to 65 GeV/c, cross sections

for, (E), 25:5295
meson (π^-) absorption cross sections at 20 to 40 GeV/c, (E), 25:5265 (CONF-700314-, Paper 4)
neutron age and fast effect in, sensitivity to cross-section data in moments-method calculation of fission and 14-MeV, 25:5496
neutron spectra in pulsed assembly, thermal, (E), 25:6107
properties for use as encapsulating material for californium-252 sources for neutron capture gamma-ray spectroscopy, 25:4772
radioinduced absorber buildup in, calculation of neutron, 25:4814 (N-70-32313)
BERYLLIUM ISOTOPES Be-8
energy levels from lithium-7 (d,n) reactions at 500 keV, spin--parity assignments for 2.2-MeV, (E), 25:5590
BERYLLIUM ISOTOPES Be-9
deuteron elastic scattering at 28 MeV, optical-model analysis of, (T), 25:5579
deuteron elastic scattering at 9.0 MeV, optical-model analysis of angular distributions of analyzing power from, (E/T), 25:5584
deuteron reactions (d,p) and (d,t) at 9.0 MeV, angular distributions of analyzing power from, (E/T), 25:5584
energy levels from beryllium-10 (d,t) reactions, deformation parameters, spin--parity assignments, spectroscopic factors, and transition probabilities for, (E), 25:5589
helium-3 reactions (He-3,$\gamma\gamma$) at 1.7 to 1.8 MeV, excitations functions for, (E), 25:5573
mesons(μ) depolarization in μ-mesic atoms of, from muon-nucleus magnetic dipole coupling, (E), 25:5576
oxygen-16 reactions (O-16,O-17) at 6 to 22 MeV, excitation functions for, (E), 25:5577
proton elastic and inelastic scattering at 49.4 MeV, angular distributions of cross sections and polarization in, (E), 25:5585
proton elastic scattering at 3.0 to 12.0 MeV, optical-model analysis of angular distributions of analyzing power from, (E/T), 25:5584
proton inelastic scattering at 5.0 to 12.0 MeV, angular distributions of analyzing power from, (E/T), 25:5584
proton reactions (p,d) at 5.0 to 12.0 MeV, angular distributions of analyzing power from, (E/T), 25:5584
proton reactions (p,n) at 20 MeV, neutron spectra from, (E), 25:5557
BERYLLIUM ISOTOPES Be-10
deuteron elastic scattering at 12 and 15 MeV, angular distributions for, (E), 25:5589
deuteron reactions (d,p) and (d,t) at 12 and 15 MeV, angular distributions for, (E), 25:5589
energy levels from proton inelastic scattering, deformation parameters, spin--parity assignments, spectroscopic factors, and transition probabilities for, (E), 25:5589
proton elastic and inelastic scattering at 12 to 16 MeV, angular distributions for, (E), 25:5589
BERYLLIUM ISOTOPES Be-11
energy levels from beryllium-10 (d,p) reactions, deformation parameters, spin--parity assignments, spectroscopic factors, and transition probabilities for, (E), 25:5589
BERYLLIUM ISOTOPES Be-13
energy levels of, compilation of, (E), 25:5567
BERYLLIUM OXIDES
creep strain of, effects of grain-boundary porosity growth on high-temperature, 25:4848
neutron age and fast effect in, sensitivity to cross-section data in moments-method calculation of fission and 14-MeV, 25:5496
pressing behavior of powdered, at 1000 to 1500°C and 1 to 3 tsi, hot, 25:4837
radiation effects on crystal structure of, neutron, 25:4887 (KFK-1215)
radiation effects on, effects of heat treatments on fast neutron, 25:4892
radioinduced boron centers in single crystals of, ESR study of fast-neutron, 25:5162
Al_2C_3--BeO--H_2C--SiO_2, phase studies of subsolidus phase relations of, at 300 to 700°C, 25:4871
BETA DECAY
beta asymmetries from polarized nuclei, technique for precision measurement of, (E), 25:5743
energy of particles in, method for calculation of average kinetic, (T), 25:5846
log ft values for light s--d-shell, nuclei, (T), 25:5599
log ft values from, group-theoretical analysis as test of pairing-force model, (T), 25:5813
transitions in allowed, β--γ correlation measurements for, (E/T), 25:5605 (UCRL-72624)
BETA PARTICLES
detection of, personnel monitoring system for, 25:4335(P)
dose to human tissues during endolymphatic therapy using iodine-131 or phosphorus-32, 25:4512
dose to skin, computer program for fallout, determining, 25:4506 (AD-703266)
dose to spinal cord and body of patients during iodine-131 cisternography, absorbed, 25:4510
effects on plants of, in fallout, protection against, by use of plastic covers, 25:4477 (UCLA-12-782, pp 45-81)
effects on survival of mice, protective effects of adrenochrome monoguanylhydrazone methanesulfonate against, 25:4589
energy of, method for calculation of average kinetic, (T), 25:5846
BETA SPECTROMETERS
development of electron--electron delayed coincidence, for nuclear lifetime measurements, 25:4363
BIBLIOGRAPHIES
on plasma physics and thermonuclear reactors, 25:5067
BIG ROCK POINT POWER REACTOR
operations incident of November 13, 1970, release of noble gases to discharge canal, 25:5892 (DOCKET-50155-53)
BIOLOGICAL MATERIALS
analysis for elements, review on atomic absorption spectrometric, 25:4023
analysis for elements, spectrometric, 25:4016 (UCLA-12-782, pp 83-8)
analysis for radioisotopes in mixtures, spectrometric method for, 25:4031
thorium content of, photometric method for determining, 25:4443
BIOLOGICAL MODELS
development of coaxial cylindrical human spinal cord, for iodine-131 dosimetry, 25:4510
use of silastic as, for blood coagulation studies, 25:4434
BIOLOGICAL STRESS
effects on blood circulation in fetuses of pregnant monkeys, tracer study of, 25:4655 (COO-1762-6)
BIOTITES
cation exchange selectivity of, 25:4160
BIPHENYL, ISOPROPYL-
effects on γ radiolysis of TBP in dodecane solution, 25:4116
BISMUTH
complexes with 8-quinolinol, structure of, NMR spectral studies on, 25:4081
determination of, use of titanous chloride in rapid quantitative, 25:6239(T) (MLM-1766(TR))
neutron elastic scattering at 4 MeV, differential cross sections and polarizing abilities at 150 to 180° from, (E), 25:5762
proton fission at 159 MeV to 18.2 GeV, isomeric yield ratios for indium-117 from, (E), 25:5784
separation from aqueous solutions by ion exchange using Alamine 336 or Amberlyst A-21 in thiocyanate solutions, 25:4137 (IS-T-377)
superconducting energy gap of amorphous, temperature dependence of, (T), 25:5042
superconductivity of thin films of amorphous, far-infrared radiation transmission in, 25:5055
BISMUTH ALLOYS AND SYSTEMS
Bi--In-base, quantum oscillations and order of phase change in microcylinder of, 25:5045
Bi--In-base, quantum oscillations in microcylinder of, 25:5046
Bi--La, thermal capacity of LaBi at low temperatures, 25:5218
Bi--Pb, magnetic flux jumps in superconducting, energy dissipated in, (E/T), 25:5044
Bi--Pr, thermal capacity of PrBi at low temperatures, 25:5218
Bi--U, enthalpy of formation of intermetallic, direct-reaction calorimetric preliminary measurement of, 25:4843
BISMUTH ISOTOPES Bi-200
energy-level transitions from polonium-200 electron-capture decay, (E), 25:5696
BISMUTH ISOTOPES Bi-201
electron-capture decay of, half-lives and gamma intensities for, (E), 25:5696
energy-level transitions from polonium-201 electron-capture decay, (E), 25:5696
BISMUTH ISOTOPES Bi-202
electron-capture decay of, gamma intensities for, (E), 25:5696
energy-level transitions from polonium-202 electron-capture decay, (E), 25:5696
BISMUTH ISOTOPES Bi-203
energy levels from polonium-203 electron-capture decay, (E), 25:5748
energy-level transitions from polonium-203 electron-capture decay, (E), 25:5696
BISMUTH ISOTOPES Bi-204
energy-level transitions from polonium-204 electron-capture decay, (E), 25:5696
BISMUTH ISOTOPES Bi-205
energy levels from polonium-205 electron-capture decay, (E), 25:5748
energy-level transitions from polonium-205 electron-capture decay, (E), 25:5696
BISMUTH ISOTOPES Bi-207
energy levels from polonium-207 electron-capture decay, (E), 25:5748
BISMUTH ISOTOPES Bi-208
energy levels from proton resonances in lead-207, spreading widths of isobaric analog, (T), 25:5644
BISMUTH ISOTOPES Bi-209
isomeric shifts and magnetic hyperfine splitting in μ-mesic, quasi-particle calculation of, (T), 25:5754

XUM

photon reactions (γ,t) at 90 MeV, triton yield in, (E), 25:5678
proton inelastic scattering at 24.5 MeV, differential cross sections, energy splitting, and energy spectra for decuplet excitation from, (E), 25:5745
proton inelastic scattering at 24.5 MeV, proton spectra from, (E), 25:5506 (CEA-N-1232, pp 81-159)

BISMUTH ISOTOPES Bi-210
use as γ source for transmission scanning of bones for measurement of mineral content, 25:4645 (CONF-700515-, pp 263-71)

BISMUTH ISOTOPES Bi-214
determination in air, alpha detection method for, 25:4040

BLOOD
circulation in fetuses, placenta, and uterus of pregnant monkeys and sheep, tracer study of, 25:4655 (COO-1762-6)
circulation in muscles of cats, tracer study of, 25:4429
circulation in patients with organic dementia, xenon-133 clearance method for determining, 25:4681
coagulation, effects of electric charge on, 25:4434
content of glucose, lactate, and pyruvate in, of rats, effects of cysteamine on, 25:4593
determination in feces using chromium-51-labeled erythrocytes, counting method for, 25:4032
distribution of flow in human lungs, measurement using computer data analysis and xenon-133 scanning, 25:4672
distribution of flow of, in lungs of dogs, during ventricular failure, measurement using metastable indium-113 and technetium-99 double scanning, 25:4677
flow of cerebral, to human lungs, methods for measurement of, 25:4669
indium-113 uptake by, of rats, effects of particle size of colloid and pH on, 25:4437
measurement of volume of, in swine using chromium-51- and phosphorus-32-labeled erythrocytes as tracers for, 25:4411 (CEA-R-4031)
radiation effects on circulation of, in lungs of dogs, x, 25:4706
radiation effects on count of autoantibody-forming cells in, of dogs and mice, use of Caningham's method to determine γ, 25:4472
radiation effects on regeneration of granulocytes in, of mice, effects of thymectomy on x, 25:4469
scanning of circulation of, in liver, use of metastable technetium-99-labeled albumin microaggregates or solutions for, 25:4657 (UCLA-12-782, pp 89-125)
toxicity of uranium oxide to peripheral, of dogs following chronic ingestion and low and high dose intratracheal injection, 25:4445

BLOOD PLASMA
activity of enzymes in, of rats, effects of cysteamine, hypoxia, and pyridoxol on, 25:4594
angiotensin II radioimmunoassay in, of rabbits, method for, 25:4419
extraction of insulin iodine-131-labeled insulin from, of man for radioimmunoassay, 25:4420
measurement of volume of, in swine using iodine-131-labeled albumin as tracer for, 25:4411 (CEA-R-4031)
radiation effects on electrolyte content in, of rabbits, x, 25:4698
radioactivity in human, following phosphorus-32 administration, β, 25:4451

BLOOD SERUM
content of culture media, effects of, on x-radiosensitivity of HeLa S3 cells, 25:4606
growth hormone radioimmunoassay content of growth in human, methods for, 25:4422
protein radioimmunoassay in, method for, 25:4417
radiation effects on content of lactate dehydrogenase in, of rats, protective effects of methylene blue against whole-body γ, 25:4605
radiation effects on isoamylases in, from man, γ, 25:4452
radiation effects on isoenzymes of lactate dehydrogenase in, of rats, protective effects of methylene blue against whole-body γ, 25:4605

BOILERS
heat transfer in sodium-heated, relations of critical and Leidenfrost point, 25:4211
leak detectors for steam, development of ion pump-type, 25:4736(R) (ANL/ST-3)
reliability analysis of power reactor, 25:5582 (RISC-214, pp 301-22)
tubes for Dragon reactor, properties of materials for, 25:4748 (DP-Report-537)
tubes for steam, hydrodynamic stability in curved, 25:4208
welds in high temperature gas cooled reactor, corrosion resistance of nickel alloy, 25:5590(R) (ORNL-4589)

BOILING
mechanisms of film and transition, around heated copper spheres in water, 25:4209
model for liquid alkali metal, pressure--temperature, 25:4212

BONE MARROW
count of eosinophils in, of rats, effects of depressant drugs on, in comparison to effects of corticosteroids, 25:4455(R) (ORO-3329-7)
radioprotective effects of transplants of, on dogs, ionizing, 25:4533

BONES
chemical composition and crystal structure of, methods for determination of, 25:4412 (CONF-680211-, pp 5-24)
conference on methods for measurement of mineral content of, 25:4612 (CONF-680211)
conference on methods for measuring mineral content of, 25:4630 (CONF-700515)
density and mineral content of human, effects of age and sex on, methods for measurement of, using radiography, 25:4619 (CONF-680211-, pp 177-91)
density and mineral content of, in man, effects of age, osteoporosis, and sex on, methods for measurement of, using radiography, 25:4618 (CONF-680211-, pp 159-77)
density of human, development of method for determining, using radiography in combination with automatic film calibration, 25:4613 (CONF-680211-, pp 27-80)
gamma attenuation by minerals in, methods for in vitro measurement of, using dipotassium hydrogen phosphate as substitute for bone mineral, 25:4645 (CONF-700515-, pp 263-71)
mineral content of cancellous and compact, of human finger, in patients with osteoporosis, effects of long-term calcium and fluoride therapy on, methods for measurement of, using γ transmission scanning, 25:4636 (CONF-700515-, pp 169-87)
mineral content of dog, methods for measurement of, using γ transmission scanning, 25:4654 (CONF-700515-, pp 424-7)
mineral content of human finger phalanx, effects of age and sex on, γ-transmission scanning method for measurement of, 25:4626 (CONF-680211-, pp 308-19)
mineral content of human vertebra, methods for measurement of, using dual beam γ transmission scanning, 25:4643 (CONF-700515-, pp 243-54)
mineral content of human, effects of age and sex on, methods for measurement of, using radiography, 25:4616 (CONF-680211-, pp 115-35)
mineral content of human, effects of age and sex on, methods for measurement of, using radiography, 25:4617 (CONF-680211-, pp 135-59)
mineral content of human, effects of age, race, and sex on, methods for measuring, using photon transmission scanning, 25:4624 (CONF-680211-, pp 283-96)
mineral content of human, effects of medullary fats on results of measurements of, 25:4644 (CONF-700515-, pp 255-62)
mineral content of human, measurement by γ transmission scanning, 25:4682
mineral content of human, measurement of, using γ transmission scanning, 25:4634 (CONF-700515-, pp 33-47)
mineral content of human, measurement of, using γ transmission scanning, 25:4635 (CONF-700515-, pp 48-57)
mineral content of human, measurement of, using γ transmission scanning, 25:4631 (CONF-700515-, pp 1-21)
mineral content of human, measurements using routine radiographs, 25:4639 (CONF-700515-, pp 199-204)
mineral content of human, method for measurement of, using radiography, 25:4615 (CONF-680211-, pp 95-115)
mineral content of human, methods for measurement of, comparison of results of, using γ transmission scanning or radiography, 25:4651 (CONF-700515-, pp 340-50)
mineral content of human, methods for measurement of, using monoenergetic photon transmission scanning, 25:4623 (CONF-680211-, pp 253-68)
mineral content of human, methods for measurement of, using monoenergetic x-ray transmission scanning, 25:4621 (CONF-680211-, pp 204-15)
mineral content of human, methods for measurement of, using γ transmission scanning and analog computer data processing system, 25:4633 (CONF-700515-, pp 28-32)
mineral content of human, methods for measurement of, 25:4622 (CONF-680211-, pp 216-49)
mineral content of human, methods for measurement of, using computer analysis of line segments of radiographs for, 25:4637 (CONF-700515-, pp 188-94)
mineral content of human, methods for measurement of, using computer analysis of line segments of radiographs for, 25:4638 (CONF-700515-, pp 155-8)
mineral content of human, methods for measurement of, using γ transmission scanning, 25:4653 (CONF-700515-, pp 408-22)
mineral content of human, methods for measurement of, using γ transmission scanning and portable analog computer data processing systems, 25:4632 (CONF-700515-, pp 22-7)
mineral content of human, use of radiographs for measurements of, 25:4640 (CONF-700515-, pp 205-23)
mineral content of human, use of x-ray spectrophotometers for measurement of, 25:4642 (CONF-700515-, pp 237-42)
mineral content of normal and osteoporotic human, methods for measurement of, using dye precipitation method and microradiographs, 25:4629 (CONF-680211-, pp 411-21)
mineral content of, in man, methods for measurement of, using photon transmission scanning, 25:4625 (CONF-680211-, pp 296-308)
mineral content of, in patients with posttraumatic osteopenia, methods for measurement of, using γ transmission scanning, 25:4627 (CONF-680211-, pp 319-

28)
mineral content of, method for measurement of, using polychromatic x-ray images and computer film analysis, 25:4614 (CONF-680211-, pp 80-95)
mineral content of, methods for determination of, 25:4412 (CONF-680211-, pp 5-24)
mineral content of, methods for measurement of, using x-ray transmission scanning, 25:4650 (CONF-700515-, pp 314-31)
mineral content of, methods for measurement of, using x-ray transmission scanning, 25:4647 (CONF-700515-, pp 274-9)
mineral content of, methods for measurement of, using dual beam γ transmission scanning, 25:4645 (CONF-700515-, pp 263-71)
mineral content of, methods for measurement of, using radiography, high-speed densitometers, and computer data analysis, 25:4620 (CONF-680211-, pp 191-203)
mineral content of, methods for measurement of, using γ transmission scanning, 25:4645 (CONF-700515-, pp 308-12)
mineral content of, methods for measurement of, using dual beam γ transmission scanning, 25:4648 (CONF-700515-, pp 291-302)
plutonium-239 retention in, of rats and rabbits, fallout, 25:4478
radioisotope content of human, in Faroe Islands during 1969, cesium-137, strontium-90, 25:4476(R) (RISO-221)
radioisotope metabolism in, effects of circulation, diuretics, oxygen, parathormone, and vitamin D on, 25:4423 (COO-1601-23)
strontium-90 content of, from carp caught in Mecklenburg ponds during 1961 to 1962, 25:4427
strontium-90 content of, from chickens raised during 1965, 25:4427
thorium content of, in rats following intraperitoneal, intramuscular, and oral administration, 25:4441
weight and volume of human skeleton, methods for measurement of, using contact radiography and x-ray densitometry, 25:4652 (CONF-700515-, pp 365-82)
weight of human hand, use of radiographs to measure, 25:4641 (CONF-700515-, pp 224-36)

BORIC ACID
neutron diffusion lengths in solutions of, effects of concentrations on, 25:6183

BORON
analysis of, review on methods for, 25:4009 (TID-25190)
determination in PuO_2--U_3O_8, effects of ratio of plutonium oxide to uranium oxide on spectrographic, 25:4015 (NUMEC-3524-76)
determination of, radiometric method for, 25:4037
determination of, review on methods for, 25:4009 (TID-25190)

BORON ISOTOPES B-9
energy levels at 1.4 and 3.2 MeV from beryllium-9(p,n) reactions, negative results, (E), 25:5557

BORON ISOTOPES B-10
availability of, effects of power reactor growth on, 25:5975
cost of, effects of power reactor growth on, 25:5975
deuteron reactions (d,α) and (d,p) at 2.605 to 2.960 MeV, ratios of excitation functions for, (E), 25:5573
deuteron reactions (d,γγ) at 2.655 to 2.840 MeV, excitation functions for, (E), 25:5573
meson(μ) depolarization in μ-mesic atoms of, from muon-nucleus magnetic dipole coupling, (E), 25:5576
reactions (B-10,Li-6) at 18 and 28 MeV, angular distributions for, (E), 25:5588

BORON ISOTOPES B-11
deuteron elastic scattering at 28 MeV, optical-model analysis of, (T), 25:5579
deuteron reactions (d,n) at 3.5 MeV, DWBA calculation of differential cross sections for, (T), 25:5593
meson(μ) depolarization in μ-mesic atoms of, from muon-nucleus magnetic dipole coupling, (E), 25:5576
nuclear magnetic resonance in transition-metal borides, 25:5229
photodisintegration of, isospin of the giant resonance in, (E/T), 25:5554
proton reactions (p,α) at 2.4 to 3 MeV, α-α coincidence spectra from, (E), 25:5680 (CEA-N-1232, pp 1-80)
spin--lattice relaxation rates in transition-metal diborides, 25:5229

BORON ISOTOPES B-12
deuteron elastic scattering at 28 MeV, optical-model analysis of, (T), 25:5579

BORON ISOTOPES B-13
energy levels of, compilation of, (E), 25:5567

BORON ISOTOPES B-14
energy levels of, compilation of, (E), 25:5567

BORON ISOTOPES B-15
energy levels of, compilation of, (E), 25:5567

BORON SYSTEMS
Al-base--B, microstructure of master alloys of, evaluation of, 25:4780
Al-base--B, properties of master alloys of, evaluation of chemical and physical, 25:4780
Al-base--B--Ti, microstructure of master alloys of, evaluation of, 25:4780
Al-base--B--Ti, properties of master alloys of, evaluation of chemical and physical, 25:4780

BOSONS
interactions of arbitrary-mass spinless, double partial-wave expansion of elastic, (T), 25:5310
interactions of identical, model second-quantized scattering theory for two-body forces in, (T), 25:5431
interactions with external electromagnetic field, formulation of semi-quantized quantum electrodynamics from charged vector, (T), 25:5413
interactions with spinless bosons, lower bounds on threshold charge-exchange amplitude from di-pion mass distributions in final states of, (T), 25:5315
wave function renormalization constant in nonlocal quantum field theory, 25:5411

BOSONS, INTERMEDIATE-VECTOR
production in N + N interactions, cross sections for hadron and γ, γ + 2μ, production relative to cross sections for, (E/T), 25:5266 (IFVE-SEF-ES-81)
production in N + N interactions, feasibility of search for, (E), 25:5267 (IFVE-SEF/STF-69-46)

BRAIN
blood circulation in human, xenon-133 clearance studies of, 25:4681
radiation effects on amino acid content and enzyme activity in, of developing rats, x, 25:4457(R) (UCE-34-P-82-9)
radiation effects on protein content of developing, of rats, effects of age and hypophysectomy on x, 25:4694 (UCLA-12-791)
scanning for tumor localization in, use of metastable technetium-99-labeled pertechnetate for, 25:4657 (UCLA-12-782, pp 89-125)
scanning in patient with Herpes zoster encephalitis using metastable technetium-99-labeled pertechnetate, 25:4660
scanning of, design of collimator for metastable technetium-99, 25:4684
uptake of fatty acids by, of adult mammals, reaction mechanisms for, 25:4458 (UCLA-12-782, pp 1-21)

BREEDING (BIOLOGICAL)
radioinduced mutations for, in rice, effects of dose on γ, 25:4487
radioinduced mutations for, in Soviet Union, review of literature on, 25:4489
radioinduced mutations for, of crop plants in Italy, review of, 25:4488
radioinduced mutations for, of maize and soybeans, review of thermal neutron and x, 25:4485

BREMSSTRAHLUNG
production by electron scattering on nuclei, polarizaton effect of nuclear magnetic moment in, 25:5820
production in strong interactions at high energies in amplitude fast variation region, (T), 25:5357
reactions (γ,2n) with oxygen-16 from threshold to 120 MeV, excitation cross sections for, (E), 25:5557
reactions (γ,f) with plutonium-239, thorium-232, uranium-235, and uranium-238 at 5 to 10 MeV, prompt and delayed neutron yields from, (E), 25:5768
reactions (γ,n) and (γ,2n) with carbon-12 up to 140 MeV, cross sections for, (E), 25:5578
reactions (γ,n) and photoabsorption with europium-151 and -153 and gadolinium-152, -154, -156, and -158, excitation functions for, (E), 25:5778
reactions (γ,n) with lead-208 at 9.8 MeV, differential cross sections for, (E), 25:5795
reactions (γ,n) with magnesium-26 at 19 to 23 MeV, isospin splitting of giant dipole state from neutron spectra from, (E), 25:5671
reactions (γ,n) with oxygen-16 at 15 to 30 MeV, excitation cross sections for, (E), 25:5557
reactions (γ,n) with phosphorus-31 at 26 MeV, photoneutron spectra from, (E), 25:5648
reactions (γ,n) with potassium-39 up to 140 MeV, cross sections for, (E), 25:5578
reactions (γ,np) with calcium-40 up to 140 MeV, cross sections for, (E), 25:5578
reactions (γ,p) and (γ,n) with helium-4 at 20 to 85 MeV, total cross sections and angular distributions from, (E), 25:5544
reactions (γ,p) with helium-3 at 21.5 to 32.5 MeV, angular distributions from, (E), 25:5535
reactions (γ,p) wth helium-3 and -4 at 200 to 500 MeV, meson effects in cross sections for, (E), 25:5547
reactions (γ,p3n) and (γ,4n) with chromium-52 and iron-56 at 150 to 305 MeV, analysis for reaction mechanism in, (E), 25:5679
reactions (γ,pn) and (γ,2n) with chromium-50, iron-54, molybdenum-92, and yttrium-89 at 150 to 305 MeV, analysis for reaction mechanism in, (E), 25:5679
reactions (γ,t) with aluminum-27, bismuth-209, tin, and zinc at 90 MeV, triton yields in, (E), 25:5678
reactions with erbium-167, gold-197, hafnium-175, and iridium-191 at 2.3 to 3.6 MeV, cross sections for, (E), 25:5637

BROMINE ISOTOPES
separation of radioactive, from gas streams by selective filtration and fixation, 25:4145(P)

BROMINE ISOTOPES Br-80
separation of isomers of, on metal surfaces, electrolytic, 25:4127

BROMINE ISOTOPES Br-81
neutron activation resonance integrals of, thermal, (E), 25:5681 (CNEA-274)

XUM

BROMINE ISOTOPES Br-82
exchange between ammonium bromide and bromobutane, electrolyte effect in, 25:4071
BRYOPHYTA
Osmunda regalis, x-radiosensitivity of spores of, effects of acetoacetic acid, anoxia, and indole-2,3-dione on, 25:4573
BUBBLES
binding energy between grain boundaries and, in uranium carbide, 25:4850
diffusion in uranium dioxide, laser image furnace for study of, 25:4853
BUTANE, DODECAFLUORO-
radiation effects on, neutron, 25:4111(R) (ORO-3909-2)
C--dodecafluorobutane, radiation effects on, neutron, 25:4111(R) (ORO-3909-2)
1-BUTANETHIOL, 2-AMINO-3-METHYL-
radioprotective effects of, on membranes in Ehrlich ascites tumor cells in cultures, electron and x, 25:4568
1-BUTANOL
nuclear-spin relaxation times for frozen porphyrexide-doped aqueous solutions of, for polarized proton targets, 25:5463 (RHEL/R-199)
properties of frozen porphyrexide-doped aqueous solutions of, for polarized solutions of, for polarized proton targets, 25:5466 (RPP/A-81)
BUTENE POLYMERS
polybutene--polyethylene, radiolysis at -186°C, ir spectrometric study of, 25:4118
BUTYRALDEHYDE, DIHYDROXY-
erythro, effects on x-radiosensitivity of Ehrlich ascites tumor cells, 25:4564

C

CADMIUM
complexes with hydroxamic acids, stability studies on, 25:4083
complexes with maleic acid, preparation and thermal behavior of, 25:4075
complexes with phenanthrenequinone oxime, potentiometric studies on formation constants of, 25:4080
determination in PuO_2--U_3O_8, effects of ratio of plutonium oxide to uranium oxide on spectrographic, 25:4015 (NUMEC-3524-76)
determination of trace amounts of, in strontium-85, polarographic, 25:4126 (UJV-2431-Ch)
electric conductivity at 1.5 to 300°K, absolute, (E/T), 25:5184
magnetic breakdown from induced-torque measurements, 25:5192
properties for use as encapsulating material for californium-252 sources for neutron capture gamma-ray spectroscopy, 25:4772
separation from aqueous solutions by ion exchange using Alamine 336 or Amberlyst A-21 in thiocyanate solutions, 25:4137 (IS-T-377)
separation from indium by reversed-phase extraction chromatography, 25:4143
superconducting critical field curve of, (E), 25:5057
CADMIUM ALLOYS AND SYSTEMS
electric conductivity at 1.5 to 300°K of dilute, deviations from Matthiessen's rule in, (E/T), 25:5184
Au-base--Cd, phase transformations in, crystallographic calculations for cubic to orthorhombic martensitic, 25:4807
Cd--Mg-base, crystallization of dilute, kinetics of, 25:4808
Cd--Zn, plastic deformation of monocrystalline, 25:4783
CADMIUM FLUORIDES
elastic constants of, pressure derivatives of, 25:5168(R) (COO-623-156)
CADMIUM ISOTOPES Cd-109
gamma spectra of, precision measurements of low-energy, 25:5736
use as γ source for transmission scanning of soft tissues for measurement of lipid content, 25:4646 (CONF-700515-, pp 272-3)
CADMIUM ISOTOPES Cd-110
meson (K) absorption widths in, corrections due to admixtures of excited energy levels, (T), 25:5866
proton elastic and inelastic scattering at 6 to 11 MeV, excitation functions for, (E), 25:5752
CADMIUM ISOTOPES Cd-112
proton elastic and inelastic scattering at 6 to 11 MeV, excitation functions for, (E), 25:5752
CADMIUM ISOTOPES Cd-113
energy levels from silver-113 decay, spin--parity assignments for, (E), 25:5754
neutron resonance scattering at 0.178 eV by cadmium sulfide crystals, reflection and transmission curves and integral reflection coefficients from, (E), 25:5785
nuclear magnetic moments, differential hyperfine structure anomalies, and NMR frequency ratios relative to cadmium-111 for isomeric, measurement using optical pumping, (E/T), 25:5786
CADMIUM ISOTOPES Cd-114
energy levels from phenomenological description of anharmonic quadrupole vibrations, static quadrupole moment of, (T), 25:5782
energy-level transitions from phenomenological description of anharmonic quadrupole vibrations, probabilities for E2, (T), 25:5782
helium-3 reactions (He-3,d) at 18 MeV, angular distributions for, (E), 25:5680 (CEA-N-1232, pp 1-80)
proton elastic and inelastic scattering at 6 to 11 MeV, excitation functions for, (E), 25:5752
CADMIUM ISOTOPES Cd-115
nuclear magnetic moments, differential hyperfine structure anomalies, and NMR frequency ratios relative to cadmium-111 for ground-state and isomeric, measurement using optical pumping, (E/T), 25:5786
CAFFEINE
effects on uv-radiosensitivity of standard HeLa cells and M4 clones, 25:4607
CALCIUM
complexes with 8-quinclinol, structure of, NMR spectral studies on, 25:4081
complexes with maleic acid, preparation and thermal behavior of, 25:4075
determination in human body by neutron activation, 25:4042 (CONF-680211-, pp 496-516)
excretion by man, effects of stable strontium on, 25:4424(R) (TID-25567)
reactions with thorium dioxide, thermodynamics of, 25:4054(T) (IS-Trans-83)
separation from aqueous solutions by ion exchange using Alamine 336 or Amberlyst A-21 in thiocyanate solutions, 25:4137 (IS-T-377)
separation of thorium from, by photochemical precipitation, 25:4026
CALCIUM CARBONATES
leaching behavior of strontium-contaminated solutions of, in vermiculite columns, 25:4265 (ORNL-TM-3130)
$CaCO_3$--$SrCO_3$, diffusion of aqueous solutions of, in soils, use of vermiculite columns for simulation of, 25:4265 (ORNL-TM-3130)
CALCIUM CHLORIDES
effects on stability of exocarp of electron-irradiated cherries, 25:4721
CALCIUM FLUORIDES
diffusion of xenon-133 in fission-recoil-doped monocrystals of, 25:5152(R) (ORO-3508-6)
BaF_2--CaF_2, corrosion by sodium of bearing coatings of, at 1100°F, 25:4185(R) (NYO-3930-8)
CALCIUM GLUCONATE
radiation dose to, method using diffuse reflection spectra to measure absorbed γ, 25:4520
CALCIUM ISOTOPES
energy level transitions in, role of static charge of nucleus in determining probability of E0 pair conversion of, (T), 25:5791
CALCIUM ISOTOPES Ca-40
alpha elastic and inelastic scattering at 29 MeV, differential cross sections and energy spectra for, (E), 25:5643
alpha elastic scattering at 24.1 MeV, optical-model analysis with 1-dependent absorption of angular distributions from, 25:5665
electron elastic scattering at 183 and 250 MeV, Born approximation, charge distributions, and cross sections for, (T), 25:5661
energy levels and transitions in, (E), 25:5680 (CEA-N-1232, pp 1-80)
energy levels from calcium-42 (p,t) reactions, spin--parity assignments for, (E), 25:5677
energy levels from nucleon interaction calculations, spin assignments for odd-parity, (T), 25:5570
energy levels in quartet scheme, low-lying even-parity, even-spin, (T), 25:5814
helium-3 reactions (He-3,d) at 40 MeV, angular distributions for, (E), 25:5617
meson (K) and (π) absorption widths in, corrections due to admixtures of excited energy levels, (T), 25:5866
meson reactions (π^-,γ) with, branching ratios for, (T), 25:5793
nuclear mass excess, (E), 25:5610
nuclear matter densities from Hartree--Fock and Thomas--Fermi calculations using static and velocity-dependent interactions, (T), 25:5873
photon reactions (γ,np) up to 140 MeV, cross sections for, (E), 25:5578
proton inelastic scattering at 20.3 MeV using polarized beams, cross section and asymmetry for, (E), 25:5506 (CEA-N-1232, pp 81-159)
CALCIUM ISOTOPES Ca-41
electron-capture decay of, conversion electron spectra from, (E), 25:5647
CALCIUM ISOTOPES Ca-42
alpha elastic scattering at 24.1 MeV, optical-model analysis with 1-dependent absorption of angular distributions from, 25:5665
deuteron reactions (d,n) with, pseudo-bound-states calculation of angular distributions from, (T), 25:5666
energy level of, lifetime of lowest 6^+, (E), 25:5646
energy levels and transitions in, (E), 25:5680 (CEA-N-1232, pp 1-80)
energy levels from calcium-44 (p,t) reactions, spin--parity assignments for, (E), 25:5677

energy levels of, shell-model calculation of, (T), 25:5611
proton reactions (p,t) at 20 MeV, angular distributions for, (E), 25:5677
CALCIUM ISOTOPES Ca-43
energy levels of, shell-model calculation of, (T), 25:5611
CALCIUM ISOTOPES Ca-44
alpha elastic scattering at 24.1 MeV, optical-model analysis with l-dependent absorption of angular distributions from, 25:5665
energy levels from proton inelastic scattering, (E), 25:5626
energy levels of, shell-model calculation of, (T), 25:5611
proton reactions (p,t) at 20 MeV, angular distributions for, (E), 25:5677
CALCIUM ISOTOPES Ca-45
beta decay of, β spectra and half-life for, (E), 25:5647
distribution in mitochondria of liver of rats, effects of agents for uncoupling oxidative phosphorylation on, 25:4431
energy levels of, shell-model calculation of, (T), 25:5611
sorption in intestinal tract of rats, effects of concentration on, 25:4430
CALCIUM ISOTOPES Ca-46
energy levels from calcium-48 (p,t) reactions, spin--parity assignments for, (E), 25:5677
energy levels of, shell-model calculation of, (T), 25:5611
CALCIUM ISOTOPES Ca-47
energy levels of, shell-model calculation of, (T), 25:5611
retention by man, effects of aluminum phosphate gel on, 25:4424(R) (TID-25567)
sorption by intestine of rats from vascular space, 25:4424(R) (TID-25567)
CALCIUM ISOTOPES Ca-48
alpha reactions (α,t) at 44 MeV, triton spectra from, (E), 25:5506 (CEA-N-1232, pp 81-159)
energy levels at 3.832, 4.284, and 4.507 MeV, spins and parities, decay modes, and lifetimes of, (E), 25:5616
energy levels of, shell-model calculation of, (T), 25:5611
helium-3 reactions (He-3,d) at 18.5 and 30.2 MeV, deuteron spectra from, (E), 25:5506 (CEA-N-1232, pp 81-159)
proton reactions (p,t) at 20 MeV, angular distributions for, (E), 25:5677
CALCIUM ISOTOPES Ca-49
beta decay of, log-ft values for, (T), 25:5658
energy levels of, shell-model calculation of, (T), 25:5611
CALCIUM ISOTOPES Ca-50
energy levels of, shell-model calculation of, (T), 25:5611
CALCIUM TUNGSTATES
radiation effects on arsenate- and vanadate-doped, ESR spectral studies on arsenate and vanadate radicals produced from γ, 25:4090
CALIFORNIUM ISOTOPES Cf-252
availability in 1971, 25:4218
capsules for neutron sources of, properties of construction materials for, 25:4772
evaluation of uses of, 25:4218
fission of, gamma spectra from spontaneous, (E), 25:5687 (UCRL-19949)
fission of, neutron emission in alpha-accompanied spontaneous, (E), 25:5723
fission of, neutron-per-fission ratios from spontaneous, (E), 25:5692
handling, shipping, and storage of sources of, 25:4218
production and encapsulation of purified, design and operation of TURF facility for, 25:4304
radiation effects on tissues of dogs following use as simulated power source for artificial heart, 25:4433
shielding of, materials for, 25:4218
transfer of neutron sources of, between ORNL facilities, design and operation of pneumatic system for, 25:4305
use as neutron source for high-energy calibration of scintillation detectors, 25:4223
CARBAMIC ACID, N-PHENYLDITHIO-
radioprotective effects of, on Escherichia coli, x, 25:4553
CARBON
antiproton absorption at 20 to 65 GeV/c, cross sectons for, (E), 25:5295
antiproton absorption cross sections at 20 to 40 GeV/c, (E), 25:5265 (CONF-700314-, Paper 4)
crystal structure and microstructure of glasslike and polycrystalline artifact, effects of hot pressing to 2500°C and pressures of 700 kg/cm² on, 25:4867
determination by photon activation using NRL Linac, 25:4041 (AD-709901)
determination in boron, 25:4009 (TID-25190)
determination in sodium, development of analytical standards for, 25:4736(R) (ANL/ST-3)
determination in sodium, development of on-line system for, 25:4736(R) (ANL/ST-3)
diffusion in carbon--tungsten alloy, relations with rhenium additions, 25:4746 (AD-710275)
diffusion in rhenium--tungsten alloys and tungsten at 1500 to 1800°C, carbon-14 tracer studies of, 25:4763
diffusion of carbon dioxide--carbon monoxide and hydrogen--water in, at 18 to 900°C, measurement of effective, 25:4856
meson (K^0) reactions at 120 MeV, A^0 and Σ^0 production and total cross sections for, (T), 25:5300
meson (K^-) absorption at 20 to 65 GeV/c, cross sections for, (E), 25:5295
meson (K^-) absorption cross sections at 20 to 40 GeV/c, (E), 25:5265 (CONF-700314-, Paper 4)
meson (π^-) absorption at 20 to 65 GeV/c, cross sections for, (E), 25:5295
meson (π^-) absorption cross sections at 20 to 40 GeV/c, (E), 25:5265 (CONF-700314-, Paper 4)
microstructure of fuel coating of, 25:4863 (DP-Report-574)
neutron total cross sections from 1 to 7 MeV, (E), 25:5598
photon reactions with, vector dominance model for relative phase of rho and ω production, (T), 25:5327
proton elastic and inelastic scattering at 49.4 MeV, angular distributions of cross sections and polarization in, (E), 25:5585
reactions with vanadium pentaoxide, chromatographic study of effects of flowing inert gas on reduction, 25:4842
sorptive properties for oxygen, determination by surface carbon--oxygen complex decomposition measurements, 25:4846
thermal expansion of fluidized bed-produced pyrolytic, at 10 to 1200°C, measurement of lattice, 25:4854
transport between ferritic and austenitic steels in sodium at 500 to 800°C, kinetic and thermodynamic properties of, 25:4755
transport by sodium in stainless steel loops between hot and cold legs, 25:4773
uptake by macrophages and pneumocytes of rat lungs, 25:4410
CARBON DIOXIDES
clearance of carbon-11- and oxygen-15-labeled, from alveolar gas and capillaries of human lungs, comparison of rate of, 25:4667
corrosive effects as impurity in flowing helium on graphite at 600 to 750°C, 25:4835 (DP-Report-448)
corrosive effects of traces of, on graphite under helium-cooled in-pile conditions, 25:4881 (DP-Report-352)
determination in helium by gas chromatography, on-line, 25:4012 (DP-Report-443)
effects of high-temperature, on mechanical properties of austenitic stainless steel, 25:4738 (DP-Report-527)
effects of high-temperature, on mechanical properties of steel, 25:4738 (DP-Report-527)
effects of high-temperature, on properties of Nimonic 75, 25:4738 (DP-Report-527)
hydrogen-atom reactions at 1 to 25 keV with, cross sections for ionization in, (E), 25:4963
proton reactions at 1 to 25 keV with, cross sections for electron capture and total ionization in, (E), 25:4963
CO--CO_2, diffusion in carbons at 18 to 900°C, measurement of effective, 25:4856
CARBON IONS
effects of accelerated, on radiation damage recovery in silicon lattices, 25:4895(P)
CARBON ISOTOPES C-9
mass excess from carbon-12 (He-3,He-6) reactions at 68 to 70 MeV, test of isobaric-multiplet mass equations, (E), 25:5568
CARBON ISOTOPES C-11
clearance of carbon dioxide-incorporated, from alveolar gas into capillaries of human lungs, 25:4667
production in cyclotron of, 25:4664
use for scanning human lungs for perfusion and ventilation, 25:4667
CARBON ISOTOPES C-12
alpha inelastic scattering at 12.5 to 18.0 MeV, angular distributions and total cross sections for, (E), 25:5561
binding energy of, alpha cluster effects in Hartree-Fock solution for, (T), 25:5586
boron-10 reactions (B-10,Li-6) at 18 and 28 MeV, angular distributions for, (E), 25:5588
deuteron elastic and inelastic scattering at 21.8 MeV using polarized beams, asymmetries and differential cross sections for, 25:5506 (CEA-N-1232, pp 81-159)
deuteron reactions (d,α) at 12.1 to 14.1 MeV, angular distributions for, (E), 25:5559
deuteron reactions (d,Li-6) at 51.8 MeV, lithium-6 spectra and differential cross sections for, (E), 25:5562
deuteron reactions (d,p) at 21.8 MeV using polarized beams, asymmetries and differential cross sections for, (E), 25:5506 (CEA-N-1232, pp 81-159)
electron inelastic scattering at 250 MeV, longitudinal and transverse form-factor spectra for, (E), 25:5572
energy level expectation values of, alpha-cluster-model calculation of, (T), 25:5865
energy levels from (p,He-3), (d,α), and (p,d) reactions, spin and parity of, (E), 25:5563
energy levels from beryllium-9 (He-3,γγ) and boron-10 (d,γγ) reactions, lowest T = 2, (E), 25:5573
energy levels from electron inelastic scattering at 250

XUM

MeV, spin--parity assignments for, (E), 25:5572
energy levels in quartet scheme, low-lying even-parity, even-spin, (T), 25:5814
energy levels of, calculation using Faddeev method with three-alpha model, (T), 25:5575
helium-3 reactions (He-3,He-6) at 68 to 70 MeV, Q values for, (E), 25:5568
lithium-6 reactions (Li-6,d) at 25 MeV, peripheral-model analysis of angular distributions from, (T), 25:5601
lithium-6 reactions (Li-6,d) at 29.6 MeV, energy spectra and PWBA analysis of angular distributions from, (E), 25:5592
lithium-6 reactions (Li-6,t) at 20 MeV, angular distributions for, (E), 25:5680 (CEA-N-1232, pp 1-80)
lithium-7 reactions (Li-7,α), (Li-7,d) and (Li-7,t) at 24.4 MeV, energy spectra from, (E), 25:5680 (CEA-N-1232, pp 1-80)
lithium-7 reactions (Li-7,t) at 30 MeV, peripheral-model analysis of angular distributions from, (T), 25:5601
lithium-7 reactions (Li-7,t) at 31.5 MeV, energy spectra and PWBA analysis of angular distributions from, (E), 25:5592
meson reactions (π^-,$2\pi^-$) at 4 GeV/c in propane bubble chamber, upper limits for cross sections of, (E), 25:5293
meson reactions (π^-,$\pi\gamma^0$) at 4 GeV/c in propane bubble chamber, upper limits for cross sections of, (E), 25:5293
neutron elastic scattering in fast region, analysis using extended R-matrix theory, (T), 25:5581
nuclear structure of, α-cluster model of, (E), 25:5562
photon reactions (γ,n) and (γ,2n) up to 140 MeV, cross sections for, (E), 25:5578
proton differential elastic scattering at 185 MeV, DWBA analysis of angular distributions from, (E/T), 25:5552 (ITF-70-56)
proton differential inelastic scattering at 185 MeV, DWBA analysis of angular distributions from, (E/T), 25:5552 (ITF-70-56)
reactions (C-12,f) with uranium, production cross sections for Z = 42 to 79 isotopes in, (E), 25:5756
reactions with carbon-12, two-center shell-model potentials for fast and slow, (T), 25:5841
structure from three-alpha model, (T), 25:5836

CARBON ISOTOPES C-13
energy levels of, compilation of, (E), 25:5567
helium-3 reactions (He-3,n) at 4.2 to 5.7 MeV, neutron polarization from, (E), 25:5574
oxygen-16 reactions (O-16,O-17) at 12 to 25 MeV, excitation functions for, (E), 25:5577
proton reactions (p,d) at 50 MeV, angular distributions for, (E), 25:5563

CARBON ISOTOPES C-14
beta spectra from, shape of, (E), 25:5551
energy levels of, compilation of, (E), 25:5567
uptake in cerebral glycogen of x-irradiated rats, 25:4453
use as tracer to study compatibility of carbide fuels with stainless steel, 25:4739 (JAERI-Memo-4132)

CARBON ISOTOPES C-15
energy levels of, compilation of, (E), 25:5567

CARBON MONOXIDES
clearance of radioactive, from human lungs, 25:4667
determination in helium by gas chromatography, on-line, 25:4012 (DP-Report-443)
effects of high-temperature, on mechanical properties of steel, 25:4738 (DP-Report-527)
effects of high-temperature, on mechanical properties of austenitic stainless steel, 25:4738 (DP-Report-527)
effects of high-temperature, on properties of Nimonic 75, 25:4738 (DP-Report-527)
hydrogen-atom reactions at 1 to 25 keV with, cross sections for ionization in, (E), 25:4563
proton reactions at 1 to 25 keV with, cross sections for electron capture and total ionization in, (E), 25:4963
CO--CO_2, diffusion in carbons at 18 to 900°C, measurement of effective, 25:4856

CARBON SYSTEMS
C--Cr--Fe--Ni, internal friction of austenitic, at 25 to 400°C, effects of defect--interstitial solute reactions on, 25:4786 (COO-1676-13)
C--dodecafluorobutane, radiation effects on, neutron, 25:4111(R) (ORO-3909-2)
C--Fe--Ni, internal friction of austenitic, at 25 to 400°C, effects of defect--interstitial solute reactions on, 25:4786 (COO-1676-13)
C--Fe-base--Ni, internal friction in martensitic, at 20 to 500°C, controlling mechanisms of, 25:4786 (COO-1676-13)
C--C--Zr, crystal structure of fcc, effects of composition on, 25:4877
C--C--Zr, thermodynamic properties of fcc, 25:4877
C--U, preparation of, method for, 25:4747 (AWRE-O-63/70)
C--W, diffusion of carbon in, effects of rhenium additions on, 25:4746 (AD-710275)

CARDIAC PACEMAKERS
development of implantable plutonium-238-fueled, French program for, 25:4239
development of implantable radioisotope-fueled, UK program for, 25:4240
heat sources for, production of high-purity plutonium-238, 25:4227
performance of plutonium-238-fueled, implanted in dogs, 25:4236
power sources for, development of plutonium-238-fueled thermionic, 25:4237
power sources for, development of promethium-147-fueled betavoltaic, 25:4237
safety of plutonium-238-fueled, evaluation of mechanical and radiological, (E/T), 25:4215 (NUMEC-3731-23)

CAROTENE
radiation effects on β, in lipid solvents, 25:4467

CATS
xenon-133 distribution in muscles of, following intramuscular injection in, 25:4429

CATTLE
radioisotope metabolism in dairy, following ingestion of fallout, 25:4436

CAVITIES
radioactive waste disposal in underground nuclear explosion-produced, feasibility studies of gaseous and liquid, 25:4279

CELL PHASE
effects on number of cells with associations of marked chromosomes in x-irradiated cultured leukocytes from monkeys, 25:4493
effects on x-radiosensitivity of carcinoma and sarcoma cells in mice and rats, combined effects of 6-azauridine on, 25:4590

CELLS
autoradiography of intact germ, whole-mount technique for, 25:4421
radiation effects on count of autoantibody-forming, in blood and spleen of dogs and mice, use of Caningham's method to determine γ, 25:4472
radiation effects on sorption of lipids by, of duodenal epithelium of rats, cerium-144 β and γ, 25:4655
radiation effects on survival of Ehrlich ascites tumor, following transplantation into mice, protective effects of oxalic acid against x, 25:4566
radiation effects on, mechanisms of protective effects of sulfur-containing agents against ionizing, 25:4538
radiation effects on, molecular mechanisms of protection against ionizing, 25:4535
radiation effects repopulation of hemopoietic, in mice, effects of estradiol on x, 25:4471
radioinduced chromosome aberrations in human, low dose ionizing, 25:4500
radioinduced degradation of DNA in murine lymphoma, effects of dose, oxygen content, and temperature on repair of x, 25:4536
radiosensitivity of carcinoma and sarcoma, in mice and rats, effects of 6-azauridine on x, 25:4590
radiosensitivity of duodenum crypt, in mice, effects of N-ethylmaleimide, iodoacetamide, and iodoacetic acid on x, 25:4587
radiosensitivity of Ehrlich ascites tumor, combined effects of 5,9-dihydroxypsoralen on γ, 25:4565
radiosensitivity of Ehrlich ascites tumor, following transplantation into mice, effects of methyl hydrazine on x, 25:4567
radiosensitivity of Ehrlich carcinoma, in mice, effects of polyethylenimine on x, 25:4563
radiosensitivity of transplants of Ehrlich ascites tumor, in mice, effects of L-erythro-α,β-dihydroxybutyraldehyde on x, 25:4564
radiosensitivity of, effects of incorporation of halogenated pyrimidine analogues into DNA on, 25:4537
radiosensitivity of, molecular mechanisms of ionizing, 25:4535
thorium dioxide uptake by macrophage and pneumocyte, of rat lungs, 25:4410
uptake of 5-bromodeoxyuridine and 5-iododeoxyuridine by DNA in neoplastic and normal, in mice, tracer study of, 25:4602

CELLS, CULTURED
growth of chemically-radiosensitized, x-irradiated ascites tumor, following transplantation into mice, 25:4562
induction of strand breaks of deoxyribonucleic acid by methyl hydrazine in Ehrlich ascites tumor, 25:4567
metabolism of fatty acids in liver, 25:4458 (UCLA-12-782, pp 1-21)
metabolism of proteins in heart of rats, 25:4458 (UCLA-12-782, pp 1-21)
metabolism of proteins in, from brain, effects of hormones on, 25:4459 (UCLA-12-782, pp 23-47)
radiation effects on membrane permeability of Ehrlich ascites tumor, protective effects of cysteamine and 2-amino-3-methyl-butanethiol against electron and x, 25:4568
radiation effects on reproductive capacity of animal, protective effects of cystamine and cysteamine against x, 25:4560
radiation effects on survival of Chinese hamster, combined effects of ancrie and triacetoneamine-N-oxyl on x, 25:4561
radiation effects on susceptibility of CV-1 mammalian, to infectivity by uv-irradiated herpes simplex virus, uv, 25:4727
radioinduced strand breaks of DNA in Ehrlich ascites tumor, x, 25:4567
radiosensitivity of ascites tumor, effects of

indantrione, menadione,N-ethylmaleimide, and Synkavit on x, 25:4562
radiosensitivity of Chinese hamster, effects of anoxia and phenylglyoxal on x, 25:4557
radiosensitivity of Chinese hamster, effects of dactinomycin and nitrogen mustard on x, 25:4558
radiosensitivity of Chinese hamster, effects of hydroxyurea on x, 25:4559
radiosensitivity of Chinese hamster, protective effects of cysteamine against x, 25:4555
radiosensitivity of Ehrlich ascites tumor, effects of iodine compounds on x, 25:4569
radiosensitivity of membrane permeability of Ehrlich ascites tumor, effects of excess oxygen and Synkavit on electron and x, 25:4568
CELLS, HeLa
radiation effects on reproductivity of, effects of serum content of media on x, 25:4606
radioinduced injuries in, reaction mechanisms for ionizing, 25:4709
radiosensitivity of, effects of caffeine on uv, 25:4607
CEREALS
bread, radioisotope content of, in Faroe Islands during 1969, cesium-137 and strontium-90, 25:4476(R) (RISO-221)
CEREBROSPINAL FLUID
accumulation in cranial cavity, development of implantable americium-241-powered sensor for monitoring, 25:4241
CERIUM
determination in aqueous solution by photochemical precipitation, 25:4026
determination of trace amounts of, in uranium by chemical separation and spectroscopy, 25:4021
properties for use as encapsulating material for californium-252 sources for neutron capture gamma-ray spectroscopy, 25:4772
separation from aqueous chloride solutions by solvent extraction using cyclooctylphenylphosphinic acid or octylphenylphosphinic acid, 25:4147
separation of trace amounts of, from aqueous nitric acid solutions by solvent extraction using D2EHPA in toluene containing trace amounts of uranium, 25:4150
CERIUM ALLOYS AND SYSTEMS
Al--Ce, Kondo effect suppression in $CeAl_2$ by thorium addition, 25:5228
Al--Ce, preparation and properties of Al_4Ce fiber-reinforced, 25:4742(P)
Al--Ce, thermal capacity of $CeAl_2$ at low temperatures, 25:5218
Ce--Ni, thermal capacity of $CeNi_2$ at low temperatures, 25:5218
CERIUM ISOTOPES
energy levels from tin (O-16,xn) reactions and californium-252 spontaneous fission for even, quasi-rotational, (E), 25:5688 (UCRL-19561)
CERIUM ISOTOPES Ce-130
energy levels and transitions from barium (α,xn) reactions, ground-state quasirotational bands in, (E), 25:5711
CERIUM ISOTOPES Ce-132
energy levels and transitions from barium (α,xn) reactions, ground-state quasirctational bands in, (E), 25:5711
CERIUM ISOTOPES Ce-134
energy levels and transitions from barium (α,xn) reactions, ground-state quasirctational bands in, (E), 25:5711
CERIUM ISOTOPES Ce-136
energy levels and transitions from barium (α,xn) reactions, ground-state quasirctational bands in, (E), 25:5711
nuclear charge radius relative to cerium-138, from $Kα_1$ x-ray isotope-shift, (T), 25:5864
CERIUM ISOTOPES Ce-138
energy levels and transitions from barium (α,xn) reactions, ground-state quasirctational bands in, (E), 25:5711
nuclear charge radius relative to cerium-136 and -140, from $Kα_1$ x-ray isotope shift, (T), 25:5864
CERIUM ISOTOPES Ce-139
energy levels of, spectroscopic factors for, (E), 25:5506 (CEA-N-1232, pp 81-159)
CERIUM ISOTOPES Ce-140
energy levels and transitions from barium (α,xn) reactions, ground-state quasirctational bands in, (E), 25:5711
energy levels from proton resonances in lanthanum-139, isobaric analog, (E), 25:5680 (CEA-N-1232, pp 1-80)
neutron activation resonance integrals of, thermal, (E), 25:5681 (CNEA-274)
neutron capture integral in fast region, (E), 25:5656
nuclear charge radius relative to cerium-138 and -142, from $Kα_1$ x-ray isotope shift, (T), 25:5864
CERIUM ISOTOPES Ce-142
neutron activation resonance integrals of, thermal, (E), 25:5681 (CNEA-274)
neutron capture integral in fast region, (E), 25:5656
nuclear charge radius relative to cerium-140, from $Kα_1$ x-ray isotope shift, (T), 25:5864
CERIUM ISOTOPES Ce-143
beta decay of, β--γ angular correlation in, (E), 25:5700
CERIUM ISOTOPES Ce-144
beta decay of, gamma spectra and branching ratios from, (E), 25:5739
beta decay of, gamma spectra, branching ratios, and log-ft values for, (E), 25:5749
determination by β counting using G-M and proportional detectors, efficiency curves for, 25:4029 (CISE-N-119)
effects on sorption of lipids by cells of duodenal epithelium of rats, 25:4695
CERIUM OXIDES
CeO_2--MoO_3, phase studies of, 25:4872
CESIUM
mass transfer in forced-convection sodium, radiochemical measurement of coefficients of, 25:4774
plasma of, ion distribution functions for collisionless surface ionized, (E/T), 25:5098
plasma of, suppression of Kelvin--Helmholtz instability by passive feedback, 25:5111
CESIUM ISOTOPES Cs-133
energy levels from neutron inelastic scattering, (E), 25:5751
neutron inelastic scattering at 0.2 to 2.2 MeV, γ spectra from inelastic, (E), 25:5751
CESIUM ISOTOPES Cs-134
retention in rats, effects of propylthiouracil and L-thyroxine on, 25:4450
CESIUM ISOTOPES Cs-137
content of birds, food, human bones, plants, precipitation, and water in Faroe Islands during 1969, 25:4476(R) (RISO-221)
deposition in relation to total human ingestion from diet in Netherlands, equation for fallout, 25:4515
determination by β counting using G-M and proportional detectors, efficiency curves for, 25:4029 (CISE-N-119)
determination in natural waters by ion exchange and γ counting, use of silica gel as support for inorganic ion exchangers in, 25:4033
effects on chromosomes of Crepis capillaris, aberrant β and γ, 25:4498
fission yields for fast reactor spectra, performance of, 25:5973
radiation dose absorbed by man following 10-year ingestion of fallout, methods for calculation of, 25:4657 (UCLA-12-782, pp 89-125)
release from Triso coated uranium oxide (UO_2) fuel particles, 25:5990(R) (ORNL-4589)
uptake by bean plants, effects of availability of nutrient calcium and nitrates and root temperature on, 25:4477 (UCLA-12-782, pp 49-81)
uptake by leaves and roots of Trifolium pratense, effects of source of contaminant on, following, 25:4449
use as γ source for transmission scanning of human bones for measurement of mineral content, 25:4643 (CONF-700515--, pp 243-54)
CESIUM PHOSPHOTUNGSTATES
sorptive properties for astatine from nitric acid, 25:4053(T) (ANL-Trans-861)
CHALCOPYRITES
copper recovery from, using in-situ nuclear underground leaching, 25:4176
CHALK RIVER AREA (ONTARIO)
radium-226 content of plankton and surface waters of, during 1969, 25:4473 (AECL-3687)
CHARCOAL
pore characteristics of, 25:4856
sorptive properties of filters of, for radioactive iodine and iodomethane, effects of humidity and temperature on, 25:4142
CHARGED-PARTICLE BEAMS
transport of, computer programs for calculations for, 25:5441 (AAEC/TM-544)
transport of, properties of isochronous magnetic optical systems for, 25:5447 (IFVE-OP-69-68)
CHARGED PARTICLES
motion in field of magnetic dipole, (T), 25:5004
motion in linear and toroidal multipole fields, nonadiabatic, (E/T), 25:5091
scattering at high energies, Bethe formula for phase shift for, (T), 25:5334
transport theory of, phase space time evolution method for, 25:5139
CHEMICALS AND REAGENTS
radioprotective effects of, on bacterial spores, 25:4726
CHEMISTRY
research in high-temperature, Kansas Univ, 25:6232(R) (COO-1140-192)
CHERENKOV RADIATION
theory of, 25:4368(T) (AEC-tr-7059(Pt.1))
CHICAGO
atmosphere of, multiple-source dispersion model for studying pollution of, 25:4161 (ANL/ES-CC-7)
CHLORAMPHENICOL
effects on x-radiosensitivity of DNA in Micrococcus radiodurans, 25:4536
CHLORIDES
separation of actinides, rare earths, uranium, and yttrium from aqueous solutions of, by solvent extraction using cyclooctylphenylphosphinic acid or octylphenylphosphinic acid, 25:4147
CHLORINE
determination in human body by neutron activation,

XUM

25:4042 (CONF-680211-, pp 496-516)
meson (K^0) reactions at 120 MeV, Λ^0 and Σ^0 production and total cross sections for, (T), 25:5300
properties for use as encapsulating material for californium-252 sources for neutron capture gamma-ray spectroscopy, 25:4772
CHLORINE ISOTOPES Cl-34
energy levels from sulfur-32 (He-3,p) reactions, spins and gamma mixing and branching ratios for, (E), 25:5627
CHLORINE ISOTOPES Cl-35
reactions (Cl-35,p) with helium-4 at 70 MeV, gamma spectra from, (E), 25:5664
CHLORINE ISOTOPES Cl-40
beta decay of, beta and gamma spectra and log ft value of, (E), 25:5614
CHLOROPHYLL
radioinduced mutations affecting, in shrubs and trees, γ or x, 25:4724
CHLOROPHYTA
Oedogonium cardiacum, radiation effects on survival of, combined effects of hypoxia and potassium cyanide on x, 25:4574
CHOLINE ACETYLTRANSFERASE
radiation effects on activity of, in developing brain of rats, x, 25:4457(R) (UCB-34-P-82-5)
CHROMATES
effects on hydrogen yields from radiolysis of water, 25:4120
CHROMEL
mechanical properties of Type A, effects of explosive shock deformation on, 25:4802
microstructure of Type A, effects of explosive shock deformation on, 25:4802
CHROMIC ACID
acetic acid--H_2CrO_4, effects on electrochemical behavior of uranium, 25:4792
CHROMIUM
determination in boron, 25:4009 (TID-25190)
determination in PuO_2--U_3O_8, effects of ratio of plutonium oxide to uranium oxide on spectrographic, 25:4015 (NUMEC-3524-76)
determination in rocks by neutron activation, 25:4047
determination of trace amounts of, in titanium ore by neutron capture gamma spectroscopy using californium-252 source, 25:4036
effects of alloying additions of, on purification of iron--nickel vacuum melts, relations with composition and reduced pressure, 25:4744
effects of impurities of, on properties of uranium, 25:4747 (AWRE-O-63/70)
magnetic phase transition in, sound propagation near, 25:5186
properties for use as encapsulating material for californium-252 sources for neutron capture gamma-ray spectroscopy, 25:4772
radioinduced helium production in, fission neutron, 25:4822
CHROMIUM ALLOYS AND SYSTEMS
analysis for niobium using 4-(2-pyridylazo)resorcinol, photometric, 25:4018
C--Cr--Fe--Ni, internal friction of austenitic, at 25 to 400°C, effects of defect--interstitial solute reactions on, 25:4786 (COO-1676-13)
Cr--Cr_2O_3, corrosion by sodium of bearing coatings of, at 1100°F, 25:4185(R) (NYO-3930-8)
Cr--Fe-base, phase studies of miscibility gap in, effects of vanadium additions on, 25:4787
Cr--Fe-base--Ni, carburization-decarburization in sodium at 500 to 800°C, effects of carbon content on, 25:4755
Cr--Fe-base--Ni, compatibility with sodium at 800°C, effects of carbon transport on, 25:4736(R) (ANL/ST-3)
Cr--Fe-base--V, phase studies of miscibility gap in, 25:4787
Cr--Mo--steel, mechanical properties of, effects of high-temperature carbon oxides, methane, nitrogen, or water on, 25:4738 (DP-Report-827)
Cr--Ni-base, mechanical properties of, effects of molybdenum and niobium additions on, 25:4782
Cr--Ni-base, microstructure of, effects of molybdenum and niobium additions on, 25:4782
Cr--V-base, reactions with sodium at 550 to 700°C, effects of calcium on activity and distribution of oxygen in, 25:4736(R) (ANL/ST-3)
CHROMIUM BORIDES
Neel temperature of CrB_2, from boron-11 NMR, 25:5229
CHROMIUM CARBIDES
corrosion by sodium of bearing coatings of, at 1100°F, 25:4185(R) (NYO-3930-8)
Cr_3C_2--Cr_2O_3--Nichrome, corrosion by sodium of bearing coatings of, at 1100°F, 25:4185(R) (NYO-3930-8)
Cr_3C_2--Nichrome, corrosion by sodium of bearing coatings of, at 1100°F, 25:4185(R) (NYO-3930-8)
CHROMIUM ISOTOPES Cr-50
photon reactions (γ,pn) and (γ,2n) at 150 to 305 MeV, analysis for reaction mechanism in, (E), 25:5679
CHROMIUM ISOTOPES Cr-51
determination in water phantom containing iron-59, three-gate method for, 25:4513
incorporation in erythrocytes, for measuring volume of whole blood in swine, 25:4411 (CEA-R-4031)
use for diagnosis of pulmonary hemosiderosis in man, 25:4685
CHROMIUM ISOTOPES Cr-52
energy levels from proton resonances in vanadium-51, spreading widths of isobaric analog, (T), 25:5644
neutron reactions using plutonium--beryllium source, gamma production cross section for, (E), 25:5582
photon reactions (γ,p3n) and (γ,4n) at 150 to 305 MeV, analysis for reaction mechanism in, (E), 25:5679
proton elastic and inelastic scattering at 5 to 6.5 MeV, excitation function and proton polarization for, (E), 25:5632
CHROMIUM ISOTOPES Cr-55
beta decay of, weak branching in, (E), 25:5645
CHROMIUM OXIDES
Cr_2O_3--Nichrome, corrosion by sodium of bearing coatings of, at 1100°F, 25:4185(R) (NYO-3930-8)
Cr_3C_2--Cr_2O_3--Nichrome, corrosion by sodium of bearing coatings of, at 1100°F, 25:4185(R) (NYO-3930-8)
Cr--Cr_2O_3, corrosion by sodium of bearing coatings of, at 1100°F, 25:4185(R) (NYO-3930-8)
CHROMOSOMES
aberrations in man, relation between pulmonary hemosiderosis and trisomy 18, 25:4685
associations of marked, in x-irradiated cultured leukocytes from monkeys, effects of cells cycle stage on number of, 25:4493
radiation effects on DNA synthesis in, of Bacillus subtilis and Escherichia coli, uv and x, 25:4456(R) (ORO-3596-15)
radiation effects on frequency of aberrations of, in barley seeds, protective effects of anoxia, cysteine, and water against γ and fast neutron, 25:4604
radioinduced aberrations of chromatids in, of Vicia faba, effects of dose fractionation on x, 25:4497
radioinduced aberrations of chromatids of, in Crepis capillaris, effects of time postexposure on x, 25:4496
radioinduced aberrations of human, low dose ionizing, 25:4500
radioinduced aberrations of, in barley seeds, γ, 25:4490
radioinduced aberrations of, in blood lymphocytes, effects of volume, body weight, and dose on γ, 25:4451
radioinduced aberrations of, in bone marrow in rats, protective effects of serotonin against x, 25:4585
radioinduced aberrations of, in Crepis capillaris, effects of dose on γ, 25:4498
radioinduced aberrations of, in Vicia faba, x, 25:4454
radioinduced aberrations of, of root tip cells of Vicia, effects of dose fractionation on number of x, 25:4492
radioinduced crossover aberrations in, of male Drosophila, comparison of frequency of, with aberrations induced by methylnitroso compounds, x, 25:4481
CLAYS
cation exchange selectivity of soil, 25:4160
COATINGS
removal of reactor containment structure protective, effects of steam, high temperature, and spray solutions on, (E), 25:6034 (ORNL-TM-2412(Pt.5))
COBALT
complexes with 8-quinolinol, structure of, NMR spectral studies on, 25:4081
complexes with maleic acid, preparation and thermal behavior of, 25:4075
complexes with phthalocyanine, radiation effects on alpha- and beta-, thermal annealing of recoil cobalt-60 from neutron, 25:4130
determination by ion exchange in thiocyanate solutions and atomic absorption spectrophotometry, 25:4137 (IS-T-377)
determination in PuO_2--U_3O_8, effects of ratio of plutonium oxide to uranium oxide on spectrographic, 25:4015 (NUMEC-3524-76)
determination in rocks by neutron activation, 25:4047
properties for use as encapsulating material for californium-252 sources for neutron capture gamma-ray spectroscopy, 25:4772
separation from aqueous solutions by ion exchange using Alamine 336 or Amberlyst A-21 in thiocyanate solutions, 25:4137 (IS-T-377)
separation from hard water by ion exchange in thiocyanate solutions using Alamine 336, 25:4137 (IS-T-377)
COBALT ALLOYS AND SYSTEMS
Co--Er, magnetic resonance of Er_2Co_{17} and $ErCo_3$, microwave, 25:5200
Co--Er, magnetic structure of $ErCo_3$, neutron diffraction study, 25:5210
Co--Fe, diffusion in fcc, bcc, and CsCl-type ordered FeCo, isotope effects in, 25:4761
Co--Gd, magnetic properties of Co_2Gd, ferrimagnetism in, 25:5201
Co--Gd--Ni, magnetization and hyperfine field in $Gd(CoNi)_2$, 25:5198
Co--Ho, magnetic resonance of $HoCo_3$, microwave, 25:5200
Co--Ho, magnetic structure of $HoCo_3$, neutron diffraction study, 25:5210
Co--Mo--Pd, electrical and magnetic properties of solid solutions of, temperature dependence of, (E/T), 25:5178
Co--Nd, magnetic resonance of $NdCo_3$, microwave, 25:5200
Co--Nd, magnetic structure of $NdCo_3$, neutron diffraction study, 25:5210

Co--Pd, electric conductivity and short-range order of deformed, 25:4766
Co--Pr, magnetic resonance of $PrCo_3$, microwave, 25:5200
Co--Pr, magnetic structure of $PrCo_3$, neutron diffraction study, 25:5210
Co--Tb, magnetic resonance of $TbCo_3$ and Tb_3Co, microwave, 25:5200
Co--Tb, magnetic structure of $TbCo_3$, neutron diffraction study, 25:5210
Co--WC, corrosion by sodium of bearing coatings of, at 1100°F, 25:4185(R) (NYO-3930-8)
Co--Y, magnetic resonance of Y_2Co_{17} and YCo_3, microwave, 25:5200
COBALT ISOTOPES Co-55
energy levels from iron-54 (d,n) reactions, spin--parity assignments and spectroscopic factors for, (E), 25:5675
COBALT ISOTOPES Co-57
diffusion in fcc, bcc, and ordered FeCo alloy, 25:4761
COBALT ISOTOPES Co-58
energy levels from iron-58(p,n) reactions, (E), 25:5612
energy levels from nickel-58 (n,p) reactions at 14.8 MeV, Q values and spin--parity assignments for, (T), 25:5638
isomeric transitions in, K-conversion coefficients of M3, (E), 25:5608
COBALT ISOTOPES Co-60
isomeric transitions in, K-conversion coefficients of M3, (E), 25:5608
performance as heat source for Maple IB thermoelectric generator, 25:4226
properties for use as heat source, AEC programs for studies of, 25:4224
retention of recoil, in neutron-irradiated alpha- and beta-cobalt phthalocyanine, effects of annealing on, 25:4130
COBALT OXIDES
crystallization of, 25:5221 (AD-710293)
magnetic phase transition in, sound propagation near, 25:5186
COINCIDENCE CIRCUITS
pulse converter for fast, time-to-amplitude, 25:4334
COKE
crystal structure of Santa Maria, effects of heat treatments at 500 to 1500°C on, 25:4840(R) (LA-4526)
pore characteristics of, 25:4856
COLLIMATORS
design for fast neutrons, 25:5477 (UCRL-50857)
design parameters for scintillation cameras, 25:4324
COLLOIDS
structure of thixotropic, effects of exchangeable ions on formation of, 25:6247(T) (ORNL-tr-2395)
COLMONOY NO. 5
corrosion by sodium at 1100°F, 25:4185(R) (NYO-3930-8)
COLMONOY NO. 6
corrosion by sodium at 1100°F, 25:4185(R) (NYO-3930-8)
COLUMBIA RIVER
ecology during 1947 to 1970, effects of, on population of chinook salmon spawning in, 25:4474 (BNWL-1515)
migration of juvenile chinook salmon from, effects of heated effluents from plutonium production reactors on, 25:4504 (BNWL-1472)
COMETS
molecular transitions in, detection by radio emission from, 25:4915 (LA-4542)
COMPOSITE MATERIALS
design and development of filament wound, three dimensional, interlocked, 25:6219 (BDX-613-143)
radioinduced curing of metal--polymer, γ, 25:4108
COMPOSITE PARTICLES
form factor for nucleon, nonrelativistic model for structure function relation with electromagnetic, (T), 25:5372 (CNRS-CPT-70-P-331)
interactions of, second-quantized nonrelativistic time-dependent scattering theory and generalization of in--out formalism for Coulomb potentials for, 25:5431
quantum field theory for spin-1 and $-^3/_2$, Z = 0 formalism in, 25:5417
COMPUTER PROGRAMS
AMASS, for table look-up of nuclidic masses, in FORTRAN, 25:5735
APICS, for predicting diffusion of pollutants in Chicago atmosphere, FORTRAN for IBM 360/75, 25:4161 (ANL/ES-CC-7)
BOPTIC, for beam transport calculations, in FORTRAN IV, 25:5441 (AAEC/TM-544)
BPLOT, for multipurpose plotting using Calcomp plotter, 25:6257 (WHAN-IR-38)
development for aerospace nuclear safety program, 25:4216(R) (SC-PR-70-682)
development for fallout dosimetry, 25:4506 (AD-703266)
FASTER, for calculation of gamma and neutron spectra and intensity, 25:4242
FASTER, for radiation flux mapping around SNAP-27 heat sources, 25:4247
for analysis of bubble chamber particle tracks, 25:4372 (SJC-T-70-3)
for connecting measuring microscopes to Minsk-2 computer for bubble chamber particle track analysis, 25:4369 (IFVE-SPK-69-53)
FORTRAN-IV, for data analysis during γ transmission scanning of bones for mineral content, 25:4648 (CONF-700515-, pp 291-302)
GEM 4, and KENO, for calculation of safe spacing of fissionable materials in water, 25:4285
GIRLS, for indexing x-ray diffraction powder patterns, 25:6240 (NLCO-1066)
HELTOT, for analysis of thorium--uranium-235 fuel cycles in gas cooled reactors, FORTRAN for IBM 7094, 25:6052 (DP-Report-440)
HYLAS, for calculation of heavy element content of irradiated fuels, 25:4815 (RD/B/N-1722)
ISIS, for analysis of fission data, in FORTRAN IV for IBM 360, 25:5790
LEGOK, for analyzing Legendre expansions of angular distributions for negative regions, 25:5476 (ORNL-TM-2903)
MATADOR, for material-balance calculations for molten salt breeder reactor, 25:4138 (ORNL-TM-3053)
RUNKUT, for solving initial value problems for ordinary differential equations, 25:6250 (SC-RR-70-615)
SAMBO, collision analysis package for Monte Carlo codes, 25:5237 (ORNL-TM-3203)
SLADE, for static analysis of thin shells, 25:6249 (SC-RR-69-369)
use for radiation dosimetry in high-energy therapy, 25:4514
WEIGHT, for evaluating weighting functions in small-angle x-ray scattering, in FORTRAN IV, 25:6246 (ORNL-TM-1950(Rev.1))
COMPUTERS
arithmetic of, comprehensive approach to, 25:6238 (LA-4531)
interfaces for, review of design and standardization of, 25:4387 (AEEW-M-986)
use for analysis of data during γ transmission scanning of human bones for measurements of mineral content, 25:4633 (CONF-700515-, pp 28-32)
use for analysis of data during γ transmission scanning of human bones for measurements of mineral content, 25:4632 (CONF-700515-, pp 22-7)
use for analysis of line segments of radiographs of human bones for measurement of mineral content, 25:4638 (CONF-700515-, pp 195-8)
use for analysis of line segments of radiographs of human bones for measurement of mineral content, 25:4637 (CONF-700515-, pp 188-94)
use for processing and display of data on chemical composition of biological materials, 25:4016 (UCLA-12-782, pp 83-8)
use in criticality and safeguard system for plutonium dioxide and uranium dioxide inventory, 25:4255
use of Argonne National Laboratory, for nuclear engineering instruction, 25:6194
uses in analytical chemistry, 25:4008 (BNWL-SA-3341)
uses in nuclear medicine, 25:4392
CONCRETES
creep under prestressed concrete reactor vessel operating conditions, 25:5990(R) (ORNL-4586)
defects in steel-reinforced, design and performance of neutron radiography equipment for detecting, 25:4249
moisture migration in reactor grade, 25:5550(R) (ORNL-4589)
concretes--polymers, physical properties of building blocks of radiation-polymerized, 25:4855
concretes--polymers, preparation and properties of radiation-polymerized for use as structural material, 25:4838
CONNECTICUT YANKEE POWER REACTOR
maintenance of, review of Core 1, 25:5910
operations of, review of Core 1, 25:5910
CONTAMINATION
scavenging of atmospheric, mechanisms of precipitation, 25:4162 (BNWL-SA-3450)
CONTROL SYSTEMS
power supplies for milliwatt electronic, design and performance of plutonium-238-fueled SNAP-19A, 25:4215
COPPER
antiproton absorption at 20 to 65 GeV/c, cross sections for, (E), 25:5295
antiproton absorption cross sections at 20 to 40 GeV/c, (E), 25:5265 (CONF-700314-, Paper 4)
complexes with hydroxamic acids, stability studies on, 25:4083
complexes with phenanthrenequinone oxime, potentiometric studies on formation constants of, 25:4080
complexes, radiation effects on catalytic properties of, in decomposition of hydrogen peroxide, 25:4103
determination by ion exchange in thiocyanate solutions and atomic absorption spectrophotometry, 25:4137 (IS-T-377)
determination in boron, 25:4009 (TID-25190)
determination in skin by neutron activation, 25:4045
determination of trace amounts of, in silicon nitrides and oxides by neutron activation and γ spectroscopy, 25:4045
determination of trace amounts of, in strontium-85, polarographic, 25:4126 (UJV-2431-Ch)
effects on hydrogen yields from radiolysis of water, 25:4120
electron band structure calculations, comparison of standard and modified orthogonalized plane-wave, 25:5231

electron reactions at 400 MeV, energy and angular distribution of photoproduced nucleons and mesons (π) from, 25:5255
heat transfer from spheres of, film and transition boiling mechanisms in, 25:4205
meson (K^0) reactions at 120 MeV, Λ^0 and I^0 production and total cross sections for, (T), 25:5300
meson (K^-) absorption at 20 to 65 GeV/c, cross sections for, (E), 25:5295
meson (K^-) absorption cross sections at 20 to 40 GeV/c, (E), 25:5265 (CONF-700314-, Paper 4)
meson (π^-) absorption at 20 to 65 GeV/c, cross sections for, (E), 25:5295
meson (π^-) absorption cross sections at 20 to 40 GeV/c, (E), 25:5265 (CONF-700314-, Paper 4)
properties for use as encapsulating material for californium-252 sources for neutron capture gamma-ray spectroscopy, 25:4772
radiation effects on dislocation loops in, relations of crystal lattice geometry with fast neutron, 25:4834
radiation effects on lattice parameter and electric conductivity of, annealing recovery of 4.2°K fast-neutron, (E/T), 25:5160
radioinduced helium production in, fission neutron, 25:4822
recovery from chalcopyrite by in-situ nuclear underground leaching, 25:4176
separation from aqueous solutions by ion exchange using Alamine 336 or Amberlyst A-21 in thiocyanate solutions, 25:4137 (IS-T-377)
separation from hard water by ion exchange in thiocyanate solutions using Alamine 336, 25:4137 (IS-T-377)
sintering of dendritic powders of, microstructural changes in, 25:4841(R) (SRO-552-5)
sintering of spherical powders of, microstructural changes in, 25:4841(R) (SRO-552-5)
sputtering by neon ions at 20 keV, relation of channeling to anisotropy in atom ejection patterns from, 25:4939

COPPER ALLOYS AND SYSTEMS
analysis for niobium using 4-(2-pyridylazo)resorcinol, photometric, 25:4018
Al--Cu, superconductivity in ultrarapidly quenched bulk, enhanced, (E/T), 25:5056
Al--Cu-base, deformation of monocrystalline, effects of temperature on, 25:4783
Cu--Mn, magnetization of dilute, 25:6256 (UCSD-34-P-143-33)
Cu--rare earth, antiferromagnetic ordering in RCu compounds, (T), 25:5197

COPPER ISOTOPES Cu-59
energy levels from nickel (p,γ) reactions at 3.45 to 3.60 MeV, analog, (E), 25:5660

COPPER ISOTOPES Cu-63
energy levels from proton resonances in nickel-62, spreading widths of isobaric analog, (T), 25:5644
neutron capture integral in fast region, (E), 25:5656

COPPER ISOTOPES Cu-65
energy levels from proton resonances in nickel-64, spreading widths of isobaric analog, (T), 25:5644

COPPER OXIDES
iron-58 Moessbauer effect in, effects of iron valence in, 25:5221 (AD-710293)

COSMIC PARTICLES
abundance of 150 to 250 MeV/nucleon Z = 16 to 30, elemental, (E), 25:4373
acceleration of primary, (T), 25:4979
charge composition of nuclei, (E/T), 25:4981
charge determination in polycarbonate plastic track detectors, 25:4338
emission from neutron stars, (T), 25:4978
energy spectra of nuclei and protons, (E/T), 25:4981
flux of neutrino and antineutrino, tests of scale invariance model from, (T), 25:5340
interactions above 1 TeV, review of, (E), 25:5274
interactions at very high energies, review of properties of elementary particle interactions from, (E), 25:5245 (CONF-700314-, Paper 5)
mass distribution of, 25:5462 (PPAD-676-E)
mass of primary, (T), 25:4977
meson (π) reactions with nuclei at 50 to 1000 GeV, review of multiparticle production in, (E), 25:5273
monitoring of neutrons by Canadian stations for May--Aug. 1970, (E), 25:4975 (AECL-3736)
origin of primary, (T), 25:4977
origin of primary, (T), 25:4979
properties of primary, (T), 25:4977
proton reactions with nuclei at 50 to 1000 GeV, review of multiparticle production in, (E), 25:5273
research on meson (μ) and quark at California Univ., Oct. 1969 to Sept. 1970, (E), 25:5257(R) (UCI-10-P-19-40)

COSMIC RADIATION
conference on, Budapest Aug.--Sept. 1969, 25:4976
electron--photon components of primary, (E/T), 25:4980
geophysical effects of, (E/T), 25:4984
hazards to astronauts, statistical analysis of proton, 25:4509 (MDC G-363)
ionization profile of intensity at balloon altitudes, (E), 25:4990
meteorological effects of, (E/T), 25:4984
modulation of primary, by solar wind, (E/T), 25:4982
modulation of primary, dynamics of, (E/T), 25:4983

COSMIC RADIO SOURCES
distribution of extragalactic, (E/T), 25:4934
observations at 35 GHz with Algonquin telescope, (E), 25:4918

COSMIC SHOWERS
Cherenkov emission from, (T), 25:4986
experiments on extensive air, summary of results from, (E/T), 25:4985
particle interactions at high energies in EAS, calorimeter study of nuclear-active, (E), 25:5275
radio emission from extensive, (E/T), 25:4987
theory of extensive, (T), 25:4986

COSMOLOGY
cosmic radio source count formula, (E/T), 25:4934
distribution of galaxies, (T), 25:4932

CRATERS
ejecta from Project Sedan, distribution and residence time of tritium in, 25:4181
formation by underground nuclear explosions, effects of water content of surrounding rocks on, 25:4175

CRITICAL ASSEMBLIES
Doppler reactivity in fast ECEL-17 and -18 and ZPR-3 Assembly 48 and 49, (E), 25:6111
Doppler reactivity in plutonium fueled ZPR-9 Assembly 26, (E), 25:6109
Doppler reactivity in ZPR-3 Assembly 53, (E), 25:6110
gamma radiation dose distribution in ZPR-3 Assembly 60, mockup of EBR-2, 25:6125
kinetics of coupled core SHA, (E), 25:6105
neutron flux of fast, effects of irradiation samples reactivity worths on, (E/T), 25:6117
neutron spectra in plutonium fueled FTR-3 core of ZPR-9, measurement of fast and intermediate, 25:6105
perturbation denominator for ZPR-3 Assembly 57 and ZPR-9 Assembly 24, (E/T), 25:6116
physics measurements for fast, normalization of LMFBR parameters from, 25:6114
physics measurements for ZPPR Assembly 2, (E/T), 25:6113
physics measurements for ZPR-3 Assemblies 60 and 61, (E/T), 25:5963
physics measurements of molybdenum reflected fast, (E/T), 25:6140
physics parameters of thermal Argonaut type cores in STEK, (E/T), 25:6053 (RCN-118)
radiation heating rates of internal components in PAX R-1 mockup, (E/T), 25:6126
reactivity of fast liquid sodium cooled, effects of sodium voids on, (E/T), 25:6112
reactivity worth measurements in ZPPR Assembly 2, (E/T), 25:6115
reactivity worths of small samples in ZPR-3 and ZPR-6, integral transport theory analysis of, (E/T), 25:6107
safety aspects of fast liquid sodium cooled, (E/T), 25:6112
shielding for ZPPR, mockup of FTR, 25:6124

CRITICALITY STUDIES
calculation for arrays of fissile materials, Monte Carlo method for, 25:4283
calculation of enriched uranium metal spheres in enriched uranyl nitrate solution, 25:6100
calculation of minimum mass for heavy water reflected enriched uranium metal slab, 25:6101
calculations for arrays of uranium cylinders in water sprays, 25:4282
criticality safety standard N16.1, engineer's evaluation of ANSI, 25:4287
criticality safety standard N16.1, managers' evaluation of ANSI, 25:4289
criticality safety standard N16.1, nuclear specialists evaluation of ANSI, 25:4286
criticality safety standard N16.1, USAEC's evaluation of ANSI, 25:4288

CROSS SECTIONS
charge-exchange and excitation, for production of metastable helium atoms in helium-ion reactions with gases at 10 to 30 keV, (E), 25:4965
charge-exchange, continuum distorted-wave method for calculation of high-energy, 25:4955
de-excitation, for hydrogen 2^2P atoms by collisions with deuterium, helium, hydrogen, and nitrogen gases, (E), 25:4964
electron-capture, for proton reactions with ammonia, carbon dioxide, carbon monoxide, and methane at 1 to 25 keV, 25:4963
excitation, for proton reactions with helium at 25 to 125 keV, (E), 25:4967
ionization, for electron reactions with aluminum, gallium, and indium, (E), 25:4956
ionization, for hydrogen-atom and proton reactions with ammonia, carbon dioxide, carbon monoxide, and methane at 1 to 25 keV, (E)), 25:4963
ionization, for proton reactions with helium at 25 to 125 keV, (E), 25:4967
ionization, for reactions of helium metastable atoms with gases, (E), 25:4969
scattering, for helium by helium, crossed-beam measurement of total relative, as function of velocity, 25:4965
scattering, for protons by helium at 25 to 125 keV, total inelastic, (E), 25:4967

CRYOSTATS
design for polarized proton target, 25:5456 (LA-4465, pp

33.1-2)
design for superconducting magnets, 25:4189 (UCRL-19764)
fabrication of sorption-pumped helium-II, for sustaining temperatures below 1°K, 25:5065
CRYSTAL STRUCTURE
radiation effects on defects in, model for neutron, 25:4887 (KFK-1215)
CRYSTALS
electron energy loss to surface excitations in thin films of, at 25 keV, (T), 25:4937 (IS-T-380)
neutron inelastic scattering by diatomic cubic, containing impurities, (T), 25:5491
neutron scattering by Debye-spectrum, double-differential cross sections for, (T), 25:5494
neutron scattering by lattice vibrations in, (T), 25:5483
photon scattering by, optimal conditions for observation of nuclear coherent, (T), 25:5174
CURIUM
separation from aqueous chloride solutions by solvent extraction using cyclooctylphenylphosphinic acid or octylphenylphosphinic acid, 25:4147
CURIUM ISOTOPES Cm-244
meson (K) absorption widths in, corrections due to admixtures of excited energy levels, (T), 25:5866
use as x-ray source for transmission scanning of bones for measurement of mineral content, 25:4647 (CONF-700515-, pp 274-9)
CURIUM ISOTOPES Cm-248
production of, design and operation of TURF facility for, 25:4304
CURRENT ALGEBRA
covariant and gauge-invariant T products in, 25:5317
current commutators on light cone, formulation of asymptotic chiral symmetry from, 25:5364
current structure from pseudoscalar meson + 2γ decay, model for, 25:5337
decay $K^+ + \gamma + e^+ + \nu$ in on-shell, effects of electromagnetic violations of time reversal invariance in, 25:5342
decay of K and π in on-shell, radiative leptonic, 25:5342
equal-time commutators, Lorentz covariance for constraints on, 25:5308
hadron currents in, dimensionality of operators for, 25:5306 (NYO-4204-1)
models for ultraviolet divergences in electromagnetic radiative corrections to lowest-order weak interactions at arbitrary momentum transfer in, 25:5343
PCAC hypothesis for effective pseudoscalar coupling in μ capture by protons at low energies and threshold cross sections for $e + N \to \pi + N$ and $\gamma + N \to \pi + N$ interactions, 25:5333
PCAC hypothesis in, renormalization of sigma model for consistency with unitarity of, 25:5367
scattering length predictions for $\pi + \pi$ interactions in, sum rules for, 25:5363
SU(2) x SU(2), current-divergence commutators in, implications of Adler zeros on, 25:5316
SU(3) x SU(3) broken chiral, baryon and meson decay mass sum rules and coupling constants in, 25:5395
sum rules for inelastic $\nu + N$ interactions at high energies, 25:5345
sum rules for scattering lengths for $\pi + \pi$ interactions in, 25:5363
CYANIDES
reactions of sodium-dissolved, with molybdenum at 800°C, 25:4736(R) (ANL/ST-3)
CYCLOHEXANE
spectra of, effects of deuterium on Raman, 25:4061
benzene--cyclohexane, radiolysis of, effects of composition on hydrogen yields from γ, 25:4121
5-CYCLOHEXENE-1,2,3,4-TETRONE, 5,6-DIHYDROXY-
sodium salt, complexes with uranium(VI) in perchlorate medium, kinetic studies on, 25:4078
CYCLOHEXIMIDE
effects on γ-radiosensitivity of Saccharomyces cerevisiae, 25:4556
CYCLOTRONS
experimental facilities at Saclay, 25:5506 (CEA-N-1232, pp 81-159)
research and development at Saclay, 25:5550(R) (CEA-N-1232)
use for producing carbon-11, nitrogen-13, and oxygen-15 for use for scanning lungs for function, 25:4664
use in nuclear medicine, 25:4683
CYLINDERS
thermal conductivity of solid right, method for estimating, 25:4203 (DP-Report-578)
CYSTAMINE
effects on oxygen uptake and respiration in tissues in rats, 25:4595
radioprotective effects of, on bacteria and bacteriophages, γ, 25:4549
radioprotective effects of, on cultured animal cells, x, 25:4560
radioprotective effects of, on rats, γ, 25:4581
CYSTEAMINE
copper complexes with, radiation chemistry of, ionizing, 25:4547
effects on activity of enzymes in blood plasma of rats, 25:4594
effects on content of glucose, lactate, and pyruvate in blood of mice, 25:4593
effects on oxygen uptake and respiration in tissues in rats, 25:4595
effects on synthesis of adenosine triphosphate in mitochondria and nuclei in liver and thymus of rats, 25:4597
effects on synthesis of DNA and RNA in thymus gland of rats, tracer study of, 25:4592
effects on synthesis of DNA in spleen and thymus of rats, 25:4596
radioprotective effects of, on cultured animal cells, x, 25:4560
radioprotective effects of, on cultured Chinese hamster cells, x, 25:4559
radioprotective effects of, on DNA of Micrococcus radiodurans, x, 25:4536
radioprotective effects of, on membranes in Ehrlich ascites tumor cells in cultures, electron and x, 25:4568
radioprotective effects of, on mice, combined effects of AET, cysteine, glutathione, and serotonin against x, 25:4582
radioprotective effects of, on mice, x, 25:4676
radioprotective effects of, reaction mechanisms for, 25:4593
radioprotective effects of, reaction mechanisms for, 25:4594
radioprotective effects of, relation of molecular structure to, 25:4548
CYSTEINE
effects as additive on reactions of hydrated radiolytic electrons with biological and food extracts, 25:4117
effects on oxygen uptake and respiration in tissues in rats, 25:4595
effects on synthesis of fatty acids in liver of rats, 25:4600
radioprotective effects of, on barley seeds, fast neutron and γ, 25:4604
radioprotective effects of, on Escherichia coli, x, 25:4554
radioprotective effects of, on Escherichia coli, x, 25:4555
radioprotective effects of, on lysozyme in aqueous solutions, ionizing, 25:4544
radioprotective effects of, on mice, combined effects of AET, cysteamine, glutathione, and serotonin against x, 25:4582
CYSTINE
dihydrochloride, radiation effects on monocrystals of, photochemical conversions of paramagnetic centers in γ, 25:4091
CYTOCHROME OXIDASE
role in metabolism of oxygen and water in lungs, 25:4669
CYTOPLASM
effects on survival of irradiated cells, 25:4651
CZECHOSLOVAKIA
radium-226 content of rivers in uranium mining areas of, 1964 to 1967, 25:4157

D

DACTINOMYCIN
effects on x-radiosensitivity of cultured Chinese hamster cells, 25:4558
effects on x-radiosensitivity of spleen colony formation by bone marrow cells following transplantation into syngenic mice, 25:4570
DATA DISPLAY SYSTEMS
description for on-line computer for nuclear experiments, 25:4390 (HMI-B-100)
development for determination of chemical composition of biological materials, use of computers for, 25:4016 (UCLA-12-782, pp 83-8)
operation of JOSHUA digital computer alphameric, 25:6202
performance of cathode ray tube, for hydrodynamics of collapsing fluid slab fuel elements, 25:6159
performance of graphic, in nuclear physics, 25:6201
DATA PROCESSING SYSTEMS
development for determination of chemical composition of biological materials, use of computers for, 25:4016 (UCLA-12-782, pp 83-8)
development for gallium-67 whole-body scan data, for localization of tumors in man, 25:4656(R) (ORNL-4615)
development for use during γ transmission scanning of human bones, 25:4635 (CONF-700515-, pp 48-57)
development for use during γ transmission scanning of human bones, 25:4634 (CONF-700515-, pp 33-47)
development of analog computer, for data analysis during γ transmission scanning of human bones for measurement of mineral content, 25:4633 (CONF-700515-, pp 28-32)
development of computer, for analysis of xenon-133 scans for measuring distribution of blood flow in lungs, 25:4672
development of computer, for analysis of xenon-133 scan data for measurement of lung ventilation rates, 25:4668
development of computer, for measurement of mineral content of human bones by analysis of line segments of radiographs, 25:4637 (CONF-700515-, pp 188-94)

development of computer, for use during γ transmission scanning of human bones for measurement of mineral content, 25:4648 (CONF-700515-, pp 291-302)
development of modular interactive, for reactor physics calculations, 25:6149
development of portable analog computer, for use during γ transmission scanning of human bones for measurement of mineral content, 25:4632 (CONF-700515-, pp 22-7)
operation of JOSHUA digital computer, 25:6202
use of computer, for analysis of x ray films for measurements of bone mineral content, 25:4613 (CONF-680211-, pp 27-80)
use of computer, for analysis of x ray films for measurement of bone mineral mass, 25:4614 (CONF-680211-, pp 80-95)
use of computer, for analysis of x-ray films for measurements of bone mineral content, 25:4628 (CONF-680211-, pp 331-51)
use of computer, for analysis of x-ray films for measurements of bone mineral content, 25:4620 (CONF-680211-, pp 191-203)
DATA TABULATIONS
decay schemes and characteristics of 105 radioactive atoms, 25:5716
nuclear data sheets for A = 50 through 54 nuclei, 25:5620
DECAY SCHEMES
construction using (n,γ) and (d,p) reaction data, method for, 25:5635
nuclear data sheets for A = 50 through 54 nuclei, 25:5620
nuclear data tables for Z = 1 to 95 nuclei, 25:5716
DECONTAMINATION
methods for NRTS Fuel Cycle Facility hot cells, 25:4299
DENSIMETERS
accuracy of radiometric, for measuring density of flowing slurries, 25:4896
design of radiometric, for measuring apparent density of solids, 25:4764(P)
detectors for radiometric, avalanche semiconductor, 25:4323 (NYO-4028-TA-1)
gamma spectra and density relations for gamma backscatter, 25:4385
response function of beta backscatter, for elements Z = 4 to 82, 25:4386
DEUTERIUM
binding energy and nuclear radius of, calculation using Bolsterli--Feenberg perturbation technique, (T), 25:5537
content in rocks, effects of porosity on, 25:4152(T) (CSIRO-Trans-10083)
deuteron reactions (d,n) at 12 MeV, polarization transfer at 0° in, (E/T), 25:5532
deuteron reactions (d,n) at 4 to 13.5 MeV using polarized beam, neutron polarization in, (E), 25:5514 (LA-4465, pp 13.1-2)
effects on infrared spectra of benzene, 25:4064
effects on ir and Raman spectra of pyrazinium halides, 25:4068
effects on laser effects on gaseous acetylene, 25:4070
effects on matrix-isolation spectra of hydrogen sulfide, 25:4066
effects on Raman spectra of crystalline hydrogen halides, 25:4065
effects on Raman spectra of cyclohexane, 25:4061
effects on Raman spectra of polyethylene, 25:4062
effects on thermodynamic properties of hydrides, 25:4072
exchange between 2,5-di-tert-butyl-3,4-dideuteriothiophene and trifluoroacetic acid, 25:4073
exchange between ferrocene derivatives, effects of substituents on, 25:4069
exchange reactions in laser-irradiated equimolar acetylene--deuteroacetylene mixtures, 25:4070
interactions π⁺ + d at 1.1 to 2.4 GeV/c, total cross sections for, (E), 25:5289
neutron reactions (n,p) at 14.4 MeV, proton spectra for three separable-potential models of, (T), 25:5531
photoinduced production of hot atoms of, at 0.5 to 5 eV, 25:4132
photon reactions with, closure-approximation validity for rho⁰ production in, (T), 25:5336
proton elastic scattering at 3 to 6 MeV, phase shifts, differential cross sections, analyzing power, and proton polarization for, (T), 25:5546
proton elastic scattering at 800 MeV using polarized and unpolarized beams, analysis of, (T), 25:5517 (LA-4465, pp 16.1-2)
proton reactions (p,2p) at 24 MeV using polarized beams, cross-section asymmetry for, (E), 25:5506 (CEA-N-1232, pp 81-159)
proton reactions (p,2p) at 4.5 to 13.0 MeV, excitation functions and energy spectra from, (E), 25:5534
reactions of hot atoms of, comparison of reactions of recoil tritium atoms with, 25:4132
reactions with hydrogen 2^2P atoms of molecular, cross sections for de-excitation in, (E), 25:4964
DEUTERON BEAMS
polarization measurements of, Lamb-shift polarimeter for, 25:4391 (LA-4465, pp 17.1-6)
polarization of, figures of merit in, 25:5455 (LA-4465, pp 23.1-2)
DEUTERONS
form factor from e + d → e + d interactions at low momentum transfers, deuteron-to-proton ratio for electric, (E), 25:5247 (AD-710385)
hydrogen mesic-atom reactions with, isotope exchange in, (T), 25:4952 (JINR-P4-5035)
interactions anti p + d → 2π⁻ + π⁺ + p at rest in deuterium bubble chamber, spectator and anti p S-capture in, (E), 25:5271
interactions anti p + d → 2π⁻ + π⁺ + π + p at rest in deuterium bubble chamber, spectator and anti p S-capture in, (E), 25:5271
interactions anti p + d at 20 to 65 GeV/c, total cross sections for, (E), 25:5295
interactions e + d → e + d at low momentum transfers, neutron-to-proton and deuteron-to-proton electric form factor ratios from, (E), 25:5247 (AD-710385)
interactions e + d → e + d, ratio of neutron--proton electric form factors from, (E), 25:5246 (AD-709522)
interactions e + d, validity of potentials from sensitivity of deuteron form factors to D state in elastic, (T), 25:5830
interactions K⁻ + d → p + Λ + eta'⁻, eta' spin and parity from, (E), 25:5291
interactions K⁻ + d at 20 to 65 GeV/c, total cross sections for, (E), 25:5295
interactions K⁻ + d at 3 GeV/c, upper limits for production cross sections of exotic meson and hyperon resonances in, (E), 25:5287
interactions π + d, two-Regge pole model for dispersion sum rules for, (T), 25:5391
interactions π⁺ + d → 2p + K⁺ + K⁻ at 1.1 to 2.4 GeV/c, phi(1020) and A(1520) production in, (E), 25:5285
interactions π⁺ + d → n + p + K⁺ + π⁺ at 1.1 to 2.4 GeV/c, Σ(1385) production in, (E), 25:5285
interactions π⁺ + d → n + Σ⁺ + K⁰ + π⁺ at 1.1 to 2.4 GeV/c, K⁰* production in, (E), 25:5289
interactions π⁻ + d at 20 to 65 GeV/c, total cross sections for, (E), 25:5295
radius from e + d → e + d interactions at low momentum transfers, (E), 25:5247 (AD-710385)
reactions (d,2p) with hydrogen at 52.2 MeV, angular distribution of n-p interacting pairs from, (E), 25:5548
reactions (d,α) with carbon-12 at 12.1 to 14.1 MeV, angular distributions for, (E), 25:5559
reactions (d,α) with oxygen-16 at 6.875 to 7.415 MeV cms, differential cross sections from, (E), 25:5596
reactions (d,α) with tritium at 51, 76, and 92 keV using polarized beams, analyzing power for, (E), 25:5525 (LA-4465, pp 34.1-2)
reactions (d,Li-6) with carbon-12 at 51.8 MeV, lithium-6 spectra and differential cross sections for, (E), 25:5562
reactions (d,n) and (d,p) with nuclei, formalism for, 25:5803 (LA-4465, pp 20.1-2)
reactions (d,n) with boron-11 at 3.5 MeV, DWBA calculation of differential cross sections for, (T), 25:5593
reactions (d,n) with calcium-42 and neon-20, pseudo-bound-states calculation of angular distributions and spectroscopic factors from, (T), 25:5666
reactions (d,n) with deuterium and hydrogen at 12 MeV, polarization transfer at C⁰ in, (E/T), 25:5532
reactions (d,n) with deuterium at 4 to 13.5 MeV using polarized beam, neutron polarization in, (E), 25:5514 (LA-4465, pp 13.1-2)
reactions (d,n) with iron-54 at 5.8 MeV, differential cross sections for, (E), 25:5675
reactions (d,n) with lithium-7 at 500 keV, neutron angular distributions from, (E), 25:5590
reactions (d,n) with nuclei, analysis of polarization transfer in, (T), 25:5805 (LA-4465, pp 26.1-2)
reactions (d,n) with tritium at 4 to 15 MeV using polarized beam, neutron polarization in, (E), 25:5513 (LA-4465, pp 12.1-2)
reactions (d,n) with tritium at 7 and 11.4 MeV, polarization angular distribution from, (E), 25:5522 (LA-4465, pp 29.1-2)
reactions (d,n) with tritium, quadratic relation between observables in polarization transfer, (T), 25:5519 (LA-4465, pp 22.1-2)
reactions (d,p) and (d,t) with beryllium-10 at 12 and 15 MeV, angular distributions for, 25:5589
reactions (d,p) and (d,t) with beryllium-9 at 9.0 MeV, angular distributions of analyzing power from, (E/T), 25:5584
reactions (d,p) and (d,t) with strontium-86 at 21 MeV, cross sections for, (E), 25:5604 (N-70-25261)
reactions (d,p) with carbon-12 and zirconium-90 at 21.6 MeV using polarized beams, asymmetries and differential cross sections for, (E), 25:5506 (CEA-N-1232, pp 81-159)
reactions (d,p) with helium-3 at 10 MeV using polarized beam, vector and tensor analyzing powers for, (E), 25:5512 (LA-4465, pp 6.1-2)
reactions (d,p) with helium-3 at 10 MeV, reactance matrix analysis of d--³He system in, (T), 25:5509 (LA-4465, pp 2.1-2)
reactions (d,p) with magnesium-26 and silicon-28 at 4.4 and 5.3 MeV, p-γ angular correlations from, (E), 25:5672

reactions (d,p) with neon-20 at 16.4 MeV, angular distributions for, (E), 25:5618
reactions (d,p) with neon-22 at 12.1 MeV, angular distributions for, (E), 25:5618
reactions (d,p) with nuclei, j-dependence of polarization effects in, (T), 25:5828
reactions (d,p) with polarized helium-3, asymmetries in, (E), 25:5524 (LA-4465, pp 32.1-2)
reactions (d,p) with strontium-84 at 21 MeV, cross sections for, (E), 25:5604 (N-70-25281)
reactions (d,p), (d,α), and (d,γγ) with boron-10 at 2.6 to 2.9 MeV, excitation functions for, (E), 25:5573
reactions (d,t) with erbium-170 at 12 MeV, Q-value for, (E), 25:5725
reactions (d,t) with strontium-88 at 21 MeV, cross sections for, (E), 25:5604 (N-70-25281)
reactions (d,t) with thorium-232 and uranium-238 at 17 MeV, tritcn spectra from, (E), 25:5797
reactions with nuclei using polarized beams, method for determination of analyzing tensors in, 25:5802 (LA-4465, pp 11.1-2)
reactions with nuclei using polarized beams, precise method for determination of analyzing tensors for use as secondary standards, 25:5806 (LA-4465, pp 27.1-6)
scattering by beryllium-10 at 12 and 15 MeV, angular distributions for elastic, (E), 25:5589
scattering by beryllium-9 at 9.0 MeV, optical-model analysis of angular distributions of analyzing power from elastic, (E/T), 25:5584
scattering by beryllium-9, boron-11, boron-12, lithium-7, and oxygen-16 at 28 MeV, cptical-model analysis of elastic, (T), 25:5579
scattering by carbon-12 and zirconium-90 at 21.8 MeV using polarized beams, asymmetries and differential cross sections for elastic and inelastic, (E), 25:5506 (CEA-N-1232, pp 81-159)
scattering by helium-3 at 10 and 12 MeV using polarized beams, vector and tensor analyzing powers for elastic, (E), 25:5520 (LA-4465, pp 24.1-2)
scattering by helium-3 at 10 MeV, reactance matrix analysis of d--³He system in, (T), 25:5509 (LA-4465, pp 2.1-2)
scattering by helium-4 at 11.5 MeV, comparisen of double scattering and polarized ion source measurement of polarization in elastic, 25:5510 (LA-4465, pp 3.1-3)
scattering by helium-4 at 12 MeV using polarized beam, vector and tensor analyzing power for elastic, (E), 25:5553 (LA-4465, pp 25.1-2)
scattering by helium-4 at 9.8 MeV using polarized beam, analyzing tensors for, (E), 25:5806 (LA-4465, pp 27.1-6)
scattering by nuclei, formalism for polarization transfer in elastic, (T), 25:5804 (LA-4465, pp 21.1-2)
scattering by nuclei, optical-model parameters for elastic, (T), 25:5854
scattering by polarized helium-3 at 9.9 and 11.9 MeV, asymmetries in, (E), 25:5515 (LA-4465, pp 14.1-2)
scattering by tellurium-124 and neodymium-146 at 12 MeV, excitation energies and differential cross sections for elastic and inelastic, (E), 25:5729
1,2-DICARBADODECABORANE(12)-1-ACETIC ACID
effects on fast neutron- and γ-radiosensitivity of mice, 25:4588
1,2-DICARBADODECABORANE(12)-1-CARBOCYLIC ACID, METHYL-
effects on fast neutron- and γ-radiosensitivity of mice, 25:4588
DIELECTRIC CONSTANTS
determination by substitution method, 25:6225 (COO-623-150)
DIET
radioisotope contamination of, in relation to deposition, equation for cesium-137 and strontium-90, 25:4519
DIETHYLAMINE
complexes with uranium(IV) fluorides, preparation of, 25:4058
DIFFERENTIAL EQUATIONS
energy inequalities in nonlinear initial value, 25:6237 (LA-4525)
DIODES
radiation damage in miniature avalanche, high-energy electron and neutron, 25:4408
DISEASES
radiodiagnosis of human pulmonary, using combined perfusion scanning and radiography, 25:4675
radiodiagnosis of liver, in man, evaluation of indium-113m for, 25:4687
DISEASES, INFECTIOUS
encephalitis, brain scanning in patient with Herpes zoster, use of technetium-99-labeled pertechnetate for, 25:4660
DISEASES, NEOPLASTIC
carcinomas, radiodiagnosis in human kidneys, use of iodine-131-labeled hippuran or mercury-203-labeled chlormerodrin scanning for, 25:4655
carcinomas, radioinduced, in human liver following Thorotrast injection 20 years earlier, 25:4716
carcinomas, radioinduced, in man, effects of high dose on ionizing, 25:4502
carcinomas, radioinduced, in rats following single intratracheal administration of thorium dioxide, 25:4702
carcinomas, radioinduced, in stomach of mice, description of development of whole-body γ, neutron, and x, 25:4703
carcinomas, radiosensitivity of, in mice and rats, effects of 6-azauridine on x, 25:4590
carcinomas, radiosensitivity of, in mice, combined effects of ethylenimine on x, 25:4563
gliomas, radiotherapy of human brain, effects of 5-bromodeoxyuridine on tumor radiosensitivity during, 25:4688
Hodgkin's disease, radiotherapy of human, use of endolymphatic iodine-131 or phosphorus-32 labeled contrast media for, 25:4512
leukemia, radioinduced in rats, protective effects of selenium compounds against ionizing, 25:4545
malignant, radiosensitivity of human head and neck, effects of mixtures of 5-bromodeoxyuridine or 5-iododeoxyuridine with 5-fluorouracil on ionizing, 25:4602
mesotheliomas, radiotherapy of human lung, effects of procarbazine on tumor radiosensitivity during, 25:4689
sarcomas, radioinduced, in rats following single intratracheal administration of thorium dioxide, 25:4702
sarcomas, radiosensitivity of, in mice and rats, effects of 6-azauridine on x, 25:4590
thrombus, radiodiagnosis of tumor, in right heart atrium of patient, use of metastable technetium-99-labeled pertechnetate scanning for, 25:4659
thymomas, radioinduced in mice, replication of DNA in γ, 25:4460
tumors, immunization against virus-induced, in mice, use of transplants of irradiated fetal tissues for, 25:4656(R) (ORNL-4615)
tumors, localization in man, use of whole-body scanning using gallium-67 for, 25:4656(R) (ORNL-4615)
tumors, radiodiagnosis of human brain, evaluation of metastable technetium-99 scanning for, 25:4657 (UCLA-12-782, pp 89-125)
tumors, radioinduced, in lungs of mice, histology of, 25:4699
tumors, spontaneous, in lungs of mice, histology of, 25:4699
DISEASES, PHYSIOLOGICAL
dementia, relation to blood circulation in brain, xenon-133 clearance technique for studying, 25:4681
demineralization, radiodiagnosis of human bone, using γ transmission scanning for, 25:4634 (CONF-700515-, pp 33-47)
embolism, diagnosis of human lung, by radioisotope scanning, effects of perfusion-ventilation relations on, 25:4679
embolism, radiodiagnosis of human lung, using γ scintillation camera with metastable technetium-99 and xenon-133, evaluation of, 25:4676
embolism, radiodiagnosis of human pulmonary, by lung scanning, 25:4680
embolisms, radiodiagnosis of human lung, use of combined inhalation and perfusion scanning for, 25:4657 (UCLA-12-782, pp 89-125)
embolisms, radiodiagnosis of human lung, use of iodine-131-labeled albumin macroaggregate scanning for, 25:4674
emphysema, radiodiagnosis of human, using γ scintillation camera, with metastable technetium-99 and xenon-133, evaluation of, 25:4676
gastritis, radiinduced, in man following therapy of kidney carcinomas, problems in diagnosis of, 25:4712
hemosiderosis, incidence in children, use of chromium-51 and iron-59 to investigate pulmonary, 25:4685
hyperthyroidism, effects on renal clearance of phosphate radioisotopes, 25:4451
hypothyroidism, effects on renal clearance of phosphate radioisotopes, 25:4451
leukopenia, radioinduced in human patients, relation of, to taurine excretion in urine, γ, 25:4603
leukopenia, radioinduced, protection against in human patients, effects of taurine on γ, 25:4603
mitral stenosis, effects on pattern of blood flow in human lungs, 25:4672
osteopenia, effects on bone mineral content of man, methods for determining using γ transmission scanning, 25:4627 (CONF-680211-, pp 319-28)
osteoporosis, effects on bone density and mineral content in man, radiographic methods for measurement of, 25:4618 (CONF-680211-, pp 159-77)
osteoporosis, effects on bone mineral content of man, methods for determining, using dye precipitation and microradiographs, 25:4629 (CONF-680211-, pp 411-21)
osteoporosis, effects on mineral content of human bones, radiographic densitometry method for measurements of, 25:4615 (CONF-680211-, pp 95-115)
osteoporosis, evaluation of effectiveness of long-term calcium and fluoride therapy in human patients, methods using γ transmission scanning of finger bones for measurement of mineral content, 25:4636 (CONF-700515-, pp 169-87)
osteoporosis, incidence in men, relation of, to age, bone mass, bone mineral content, and sex, 25:4651 (CONF-700515-, pp 340-50)
osteoporosis, measurements of bone mineral content in patients with, using routine radiographs, 25:4635

XUM

(CONF-700515-, pp 199-204)
radioinduced, in rats following single intratracheal administration of thorium dioxide, 25:4702
radiotherapy of eye, in man, 25:4650
DISEASES, PLANTS
dwarfism, radioinduced mutations for susceptibility to, in mulberry trees, effects of dose on γ, 25:4486
DISEASES, TRAUMATIC
anaphylaxis, radiation effects on occurrence of, in mice, role of antibody response on proton and x, 25:4470
bone fractures, incidence in man, relation of, to age, bone mass, bone mineral content, occupation, and sex, 25:4651 (CONF-700515-, pp 340-50)
burns, radioinduced, on skin, bone, and cornea of dogs, monkeys, and rabbits, laser, 25:4704
radiation injuries, description of precancerous, in glandular stomach of mice, 25:4703
radiation injuries, treatment in mice, histological evaluation of balneotherapy for γ and neutron, 25:4610
radiation injuries, treatment in personnel, methods for, 25:4524
radiation sickness, protective effects of bone marrow transplants against, in dogs, ionizing, 25:4533
wounds, effects of skin, on survival of mice, combined effects of x radiation on, 25:4576
wounds, radiation effects on healing of, in mice, effects of dose and postirradiation time on recovery from whole-body x, 25:4705
DISPERSION RELATIONS
amplitude for production processes with bound states, superconvergence relations for Omnes equation for, 25:5427
sum rules for π + d interactions, two-Regge pole model for, 25:5391
DIURETICS
effects on radioisotope metabolism in bone, 25:4423 (COO-1601-23)
DODECANE
dodecane--TBP, radiolysis of, effects of isopropylbiphenyl on, 25:4116
DOGS
cardiac pacemakers for, performance of implanted plutonium-238-fueled, 25:4238
design of restraint device for, for use during scanning, 25:4654 (CONF-700515-, pp 424-7)
diffusion of uranium oxides across placental tissues of, following intratracheal and oral administration, 25:4446
distribution of blood flow in lungs of, during ventricular failure, measurement using metastable indium-113 and technetium-99 for double scanning, 25:4677
effects on intrauterine and early extrauterine development of, following maternal ingestion or intratracheal injection of uranium oxide, 25:4446
excretion of uranium oxide by mammary glands of, following intratracheal and oral administration, 25:4446
lanthanum-140 distribution in tissues of beagle, following administration by gavage, inhalation, and injection, effects of chemical form on patterns of, 25:4426
mineral content of bones of, methods for measurement of, using γ transmission scanning, 25:4654 (CONF-700515-, pp 424-7)
radiation dose to, following use of plutonium-238 as power source for artificial heart, γ and neutron, 25:4432
radiation effects on blood cell cytology, blood circulation, bone marrow cytology, and blood transferase activity in, protective effects of AET against x, 25:4599
radiation effects on lungs of, x, 25:4706
radiation effects on physiology of, following implantation of plutonium-238-powered artificial heart, γ and neutron, 25:4432
radiation effects on survival of, protective effects of bacterial endotoxins against x, 25:4586
radiation effects on tissues of, following use of californium-252 and strontium-90 as simulated power sources for artificial heart, 25:4423
radioinduced burn injuries in, laser, 25:4704
radioinduced injuries in, protective effects of bone marrow transplants against ionizing, 25:4533
scanning of lung transplants for function in, 25:4657 (UCLA-12-782, pp 89-125)
toxicity of uranium oxide to organs and tissues of, following acute and chronic intratracheal, oral, and subcutaneous administration, 25:4447
toxicity of uranium oxide to peripheral blood of, following chronic ingestion and low and high dose intratracheal injection, 25:4445
DOUNREAY FAST REACTOR
maintenance requirements of, review of core and cooling system, 25:5908
DRESDEN POWER REACTOR, UNIT 1
operations incident of November 7, 1970, failure of north emergency condenser condensate valve, 25:5890 (DOCKET-50010-71)
radioactive effluents from, minimizing off-gas, 25:5914 (DOCKET-50010-72)
site for, corrections for guide to environmental monitoring and recording requirements for, 25:5915 (DOCKET-50010-73)
DRESDEN POWER REACTOR, UNIT 2
construction of, permit application for, 25:5924 (DOCKET-50237-103)
containment systems for, modifications of standby gas treatment and automatic pressure relief, 25:5922 (DOCKET-50237-98)
fuel elements for, crud deposition test for nose pieces of, 25:5926 (DOCKET-50237-105)
operation of, approval of cobalt-58 irradiation test program for Cycle 1, 25:5925 (DOCKET-50237-108)
operation of, license application for, 25:5924 (DOCKET-50237-103)
operations incident of June 5, 1970, safety analysis of turbine control system trip, 25:5893 (DOCKET-50237-110)
operations incident of October 28, 1970, safety analysis of control rod drives in excess of 7.0 second insertion time, 25:5894 (DOCKET-50237-111)
operations of, review of startup, 25:5911
owners of, financial statements of, 25:5921 (DOCKET-50237-88)
personnel of, retraining program for operation, 25:5923 (DOCKET-50237-101)
DRILL CORES
preparation of samples of radioactive, for radiochemical analysis, design and operation of Los Alamos facility for, 25:4307
DRILL HOLES
neutron distributions in, Monte Carlo calculation of thermal, (T), 25:5493
DRUGS
book: Radiation Protection and Sensitization, 25:4534
radioprotective effects of hypoxia-inducing, on mammals, ionizing, 25:4539
DUSTS
radiation monitoring of, at Research Reactor Institute of Kyoto University during 1968, 25:4608 (KURRI-TR-63)
DYSPROSIUM
determination of trace amounts of, in uranium by chemical separation and spectroscopy, 25:4021
electric conductivity of thin films of, temperature and thickness dependences of, 25:4771
Hall effect in paramagnetic, ferromagnetic, and antiferromagnetic, 25:5182
Hall effect in single crystals of, anomalous magnetization dependence of, 25:5219
magnetic phase transition in, sound propagation near, 25:5186
magnetic properties of single crystals of, (E/T), 25:5194
magnetic transition temperatures of single crystals of, pressure dependence of, (E/T), 25:5195
properties for use as encapsulating material for californium-252 sources for neutron capture gamma-ray spectroscopy, 25:4772
separation by ion exchange using Amberlyst A-21 in aqueous thiocyanate solutions, 25:4137 (IS-T-377)
DYSPROSIUM ALLOYS AND SYSTEMS
Dy--Er-base, magnetic structure of, neutron-diffraction study, 25:5207
Dy--Y, Hall effect in paramagnetic, ferromagnetic, and antiferromagnetic, 25:5182
DYSPROSIUM ISOTOPES Dy-160
energy levels from terbium-160 beta decay, spectroscopic quadrupole moments of 2+, (E), 25:5760
energy-level transitions from terbium-160 beta decay, angular correlation coefficients and attenuation parameters from, (E), 25:5760
DYSPROSIUM ISOTOPES Dy-161
energy levels from terbium-161 decay, (E), 25:5714
Moessbauer effect following Coulomb excitation, 25:5221 (AD-710293)
DYSPROSIUM URANATES
$DyUO_4$--ThO_2, spectra and phase studies of, 25:4084
DYSPROSIUM VANADATES
magnetic properties of $DyVO_4$ at low temperatures, 25:5217

E

EARTHQUAKES
effects on design requirements in Japan of power reactors, 25:5939
effects on piping components and systems, summary of experience on, 25:4188 (TID-25553)
ECONOMICS
course in nuclear power plant financial management, 25:6195
ECOSYSTEMS
distribution of animal and plant populations in, associative factors affecting, 25:4477 (UCLA-12-782, pp 49-81)
factors in Columbia River, affecting spawning of chinook salmon during 1947 to 1970, 25:4474 (BNWL-1515)
radiation effects on survival of animals and plants in desert, research studies at UCLA from July 1965 to July 1970, 25:4425(R) (UCLA-12-782)
radiation effects on survival of animals and plants in

desert, continuous low-dose γ, 25:4477 (UCLA-12-782, pp 49-81)
radioinduced changes in vegetation of desert, fallout, 25:4477 (UCLA-12-782, pp 49-81)
radioisotope transport in freshwater, following nuclear detonation, effects of leaching on fallout, 25:4479
EGGS
radiation effects on development of nematode, effects of dose on x, 25:4692 (COO-1209-13)
radioisotope content of, in Faroe Islands during 1969, cesum-137 and strontium-90, 25:4476(R) (RISO-221)
shell thickness measurements of, beta backscatter gage for, 25:4323 (NYO-4028-TA-1)
ELECTRIC ARCS
properties of high-current free-burning, in air, (E), 25:5093
ELECTRIC DISCHARGE
plasma diagnostics in positive column, using double Langmuir probes, 25:5081 (N-70-32493)
plasma energy distribution in striating, time-resolved measurements of, 25:5077 (AD-710597)
plasma ion heating in Penning, (E), 25:5075
wave propagation in positive column, plasma instabilities from, (E/T), 25:5125(R) (SU-IPR-389)
wave propagation in weakly ionized magnetoplasma, (T), 25:5123 (SU-IPR-366)
ELECTRIC INSULATORS
compaction of ceramic, for sheathed thermocouples, methods for measuring, 25:4402
polarization effects in in-core oxide, 25:4400
resistivity measurements at high temperature, 25:4401
ELECTRIC PROBES
effects on ionization and recombination in partially ionized, 25:5084
performance of double Langmuir, for diagnostics of magnetized positive column, 25:5081 (N-70-32493)
use for plasma diagnostics, conference on, 25:5080(T) (LA-4520-TR)
ELECTRODES
performance of fluoride vapor-deposited tungsten--niobium, thermionic, (E), 25:4993 (TEE-4125-1)
ELECTRODYNAMICS
action principle in vacuum, duality invariant, (T), 25:5403
electromagnetic current density in classical, solution of multipole expansion of, 25:5236 (JINR-P2-5283)
ELECTROJETS
distribution of return current of auroral-zone, during polar substorms, (E), 25:5003
ELECTROLYTIC CELLS
development for reprocessing of MSBR fuel by reductive extraction, 25:4136 (ORNL-TM-3053)
ELECTROMAGNETIC FIELDS
boson field interactions with external, formulation of semi-quantized quantum electrodynamics from charged vector, (T), 25:5413
ELECTROMAGNETIC LENSES
charged-particle beam transport in, transfer matrix calculation of spin aberrations in polarized, 25:5454 (LA-4465, pp 18.1-16)
ELECTROMAGNETIC PUMPS
performance of helical induction, with potassium to 1500°F to simulate lithium at 2200°F, cavitation and hydraulic, 25:4186 (ORNL-TM-2995)
ELECTROMAGNETIC WAVES
absorption cross sections in astrophysical processes, inverse bremsstrahlung process in, (T), 25:5239
interactions with density fluctuations in inhomogeneous magnetized plasma, extraordinary, (T), 25:5126
interactions with magnetospheric homogeneous plasma, nonlinear mechanisms of, (T), 25:5031
propagation of hf, lf, and ultra lf, magnetospheric diagnostics from ground-based measurements of, 25:5030
ELECTROMAGNETISM
current density in classical electrodynamics, solution of multipole expansion of, 25:5236 (JINR-P2-5283)
ELECTRON BEAMS
dosimetry of high-intensity pulsed, calorimeters for, 25:4379 (SC-TM-69-298)
interactions with plasma, ion heating during development of hf instabilities, (E), 25:5073
interactions with plasma, research on, (T), 25:5125(R) (SU-IPR-389)
reactions with metals, fusion reactions from, 25:5118(P)
ELECTRON CAPTURE
Bahcall corrections including Hartree--Fock rearrangement, (T), 25:5837
ELECTRON MICROSCOPY
specimen heating by electron beam in, microthermocouple measurements, (E/T), 25:5163
ELECTRON MULTIPLIER TUBES
efficiency of channel, in magnetic fields, 25:4331
efficiency of Johnston, improvements in, 25:4332
ELECTRON PAIRS
production in photon scattering by nuclear Coulomb field at arbitrary energies and small angles, differential cross sections for, (T), 25:5335
ELECTRON PROBE MICROANALYSIS
equipment and methods for analysis of highly radioactive materials, 25:4011 (CEA-N-1340)
ELECTRON-RING ACCELERATORS
electron beam propagation in, relativistic, 25:5469
ring equilibrium in helical magnetic field, equations for, 25:5448 (JINR-P9-5299)
ELECTRON SOURCES
characteristics of high-current, for electron beam accelerators, (E), 25:5473
ELECTRON TUBES
design of triode-type, for glove box sputtering unit, 25:4259 (BNWL-SA-3609)
ELECTRONIC FILTERS
design of low-pass, 25:4399
ELECTRONS
density of states in fluctuating potential, (T), 25:5240
effects on activity of luciferase system in Photobacterium fischeri, measurement of bioluminescence decay time to determine high dose rate, 25:4730
effects on curing of vinyl-resin paints, 25:4095(P)
effects on DNA in Escherichia coli, protective effects of glycerol, 1,2,3-indantrione, methyl sulfoxide, N-ethyl malemide, and thicurea against, 25:4551
effects on DNA in solutions, effects of incorporation of 5-bromouracil on energy transfer mechanisms of, 25:4542
effects on membrane permeability of Ehrlich ascites tumor cells in cultures, protective effects of cysteamine and 2-amino-3-methyl-butanethiol against, 25:4568
effects on membranes of Ehrlich ascites tumor cells, combined effects of excess oxygen and Synkavit on, 25:4568
effects on miniature avalanche diodes, damage, 25:4408
effects on piezoresistivity of n-type silicon, (E/T), 25:5151 (N-70-35737)
effects on plastically deformed germanium at 3.5 MeV, influence of impurities on photoconductivity spectra from, (E/T), 25:5161
effects on polymerization crosslinking of monomers, 25:4100(P)
effects on polymerization of trioxane for production of polyacetal resin, 25:4098
effects on stability of exocarp of cherries, effects of calcium chloride and storage time on, 25:4721
emission from solar flares, (E/T), 25:4927
emission of exo-, from Apollo 12 samples, thermally stimulated, (E), 25:4935 (ORNL-TM-3131)
energy loss to surface excitations in thin films of ionic crystals and metals at 25 keV, (T), 25:4937 (IS-T-380)
flux in primary cosmic radiation, (E/T), 25:4980
heating effects on metallic films, microthermocouple measurements of, (E/T), 25:5163
interactions at very high energies, scaling laws for particle production in deep inelastic, (T), 25:5319 (CONF-700314-, Paper 8)
interactions e + d → e + d at low momentum transfers, neutron-to-proton and deuteron-to-proton electric form factor ratios from, (E), 25:5247 (AD-710385)
interactions e + d → e + d, ratio of neutron--proton electric form factors from, (E), 25:5246 (AD-709922)
interactions e + d, validity of potentials from sensitivity of deuteron form factors to D state in elastic, (T), 25:5830
interactions e + N → π + N at low energies, PCAC hypothesis for threshold cross sections for, (T), 25:5333
interactions e + p → e + p at 15 and 18 GeV, search for polarization in, (E), 25:5252 (UCRL-20093)
interactions e + p → rho^0 + p, Pomeranchuk decoupling from ordinary Regge trajectories in rho^0 transverse polarization in, (T), 25:5348 (COO-264-562)
interactions e + p at high energies, review of field theoretic models for deep inelastic, (T), 25:5320 (CONF-700314-, Paper 17)
interactions e + p, parton model for structure functions for hadron production in deep inelastic, (T), 25:5330
interactions e + p, search for time reversal invariance violation in inelastic, (E), 25:5400 (UCRL-20041)
interactions e$^+$ + e$^-$, Orsay and Novosibirsk experiments on rho^0, ω, and phi production in, 25:5250 (DNPL/R-7, pp 139-72)
photon scattering cross sections for, Klein--Nishina, (T), 25:5167
propagation in liquid helium, photoejection--pressure study of bubble model of, 25:5034 (TID-25601)
reactions of hydrated radiolytic, with biological tissue and food extracts, effects of acetone, cysteine, and nitrate additives on, 25:4117
reactions with aluminum, gallium, and indium, ionization cross sections for, (E), 25:4956
reactions with copper at 400 MeV, energy and angular distribution of photoproduced nucleons and mesons (π) from, 25:5255
reactions with heavy nuclei, rho + N → rho + N amplitudes and rho photoproduction from Drell--Trefil theory extension for coherent rho^0 production in, (T), 25:5336
reactions with helium at 35 to 150 eV, angular and energy dependence of generalized oscillator strengths for 1^1S--2^1S transition in, (E), 25:4959
reactions with helium-4, calculation of disintegration cross section using translationally invariant particle-hole model, (T), 25:5530
reactions with nuclei, scale-invariant light-cone SU(3) x SU(3) current commutators for universal structure

XUM

functions for particle production in, (T), 25:5328
scattering by aluminum barriers at 0.4 to 2.0 MeV, angular and energy distributions from, (T), 25:4938
scattering by atoms, single-particle formulation of, including strong correlation effects, 25:4966
scattering by calcium-40 at 183 and 250 MeV, Born approximation, cross sections, and charge distributions from elastic, (T), 25:5661
scattering by carbon-12 at 250 MeV, longitudinal and transverse form-factor spectra for inelastic, (E), 25:5572
scattering by erbium-167, gold-197, hafnium-179, and iridium-191 at 2.3 to 3.6 MeV, cross sections for inelastic, (E), 25:5637
scattering by helium, s-wave phase shift near 73.5-eV resonance in elastic, (T), 25:4961
scattering by helium-3 at high energies, charge and magnetic form factors and charge distributions from, (E/T), 25:5535
scattering by liquid helium-4 at low momentum transfer, inelastic, (E), 25:5528
scattering by nuclei with bremsstrahlung production, polarization effect of nuclear magnetic moment in, 25:5820
scattering by oxygen-16 in giant resonance region, electron spectra and matrix elements for inelastic, (E), 25:5558
scattering from nuclei, review of radiative corrections to, (T), 25:5800 (AD-706717)
slowdown in multiplate liquid ionization detectors at 60 keV to 2 MeV, Monte Carlo calculation of, 25:4322 (NP-18433)
transport problems of, modified phase space time evolution method for, 25:5242
use for therapy of eye diseases in man, methods for bilateral fast, 25:4690

ELECTROPLATING
method for metals using high-current rectangular-shaped pulses, 25:4741 (BNWL-CC-491)

ELEMENT 105
fission of, half-life for spontaneous, (E), 25:5757
production in americium-243 neon-22 reactions, (E), 25:5757

ELEMENT 114
research on, review of, 25:5719

ELEMENTARY PARTICLE MODELS
composite, nucleon electromagnetic form factor and form factor for anti N + N + anti N + N interactions in, 25:5372 (CNRS-CPT-70-P-331)
diffraction, for p + p interactions at high energies, review of, 25:5347 (CONF-700314-, Paper 13)
diffraction-dissociation resonance and dual-resonance, for γ + p + π^+ + π^- + p interactions, 25:5323 (DNPL/R-7, pp 3-28)
dual resonance, divergences and renormalization of multiloop planar diagrams in, 25:5409
dual resonance, electrostatic analog for, 25:5353
dual-resonance, allowed spectrum in, 25:5428
hadron decay in quark, broken SU(6) sum rules for, (T), 25:5394
interference, for γ + p + π^+ + π^- + p interactions, 25:5323 (DNPL/R-7, pp 3-28)
multiperipheral, dynamics of, 25:5302 (CONF-700314-, Paper 11)
multiperipheral, phenomenology of hadron strong interactions in, 25:5346 (CONF-700314-, Paper 12)
multiperipheral, scaling behavior for strong interactions in, 25:5351 (NYO-2262-TA-225)
parton, for elementary particle interactions at very high energies, (T), 25:5304 (CONF-700314-, Paper 18)
parton, for ν + N interactions at high energies, 25:5345
parton, for structure functions for hadron production in deep inelastic e + p interactions, 25:5330
peripheral, for π^+ and π^- production in π^- + p interactions near 1 GeV with π and N exchange, 25:5376
Regge-ized absorption, modification for high-energy inelastic scattering, 25:5381
sigma, for consistency of PCAC hypothesis with unitarity, 25:5367
vector dominance, 0^- and 1^- meson radiative decays in broken SU(3) in, 25:5402
vector dominance, for photoproduction of vector mesons, 25:5301 (DNPL/R-7, pp 29-70)
vector dominance, isovector asymmetry in rho production, π photoproduction, and electroproduction for test of, 25:5326
vector dominance, rho^0 coherent production in photon reactions with light nuclei for test of, 25:5336
vector dominance, tests in vector meson production in e^+ + e^- interactions, 25:5250 (DNPL/R-7, pp 139-72)
Veneziano, 0^- and 1^- meson radiative decays in broken SU(3) in, 25:5402
Veneziano, amplitudes for Reggeons and spinning particles in, 25:5440
Veneziano, normalization using dual six-point function for anti p + p + 4π interactions at rest in, 25:5362
Veneziano, pseudoscalar meson interactions in, SU(3) structure for internal symmetry from, 25:5370

ELEMENTARY PARTICLE MODELS (BOOTSTRAP)
theory of, dynamics of multiperipheral model for, 25:5302 (CONF-700314-, Paper 11)

ELEMENTARY PARTICLE MODELS (TRIPLET)
decay angular distributions for 0^+, 1^+, 2^+, and $3/2^+$ resonances in 0$^-$ meson interactions with $1/2^+$ baryons in additive quark, 25:5375 (TPJU-15/70)
hadrons in quark, for ultraviolet divergences in electromagnetic radiative corrections to lowest-order weak interactions at arbitrary momentum transfer, (T), 25:5343
interactions at high energies in quark, mechanisms for strong, 25:5354
quark spin in, 25:5358
quasi-potential equation for relativistic harmonic oscillator for quark, 25:5405 (JINR-E2-5335)

ELEMENTARY PARTICLES
causality for, paradoxes related to full, (T), 25:5307 (RLO-2041-49)
decays of, current algebra commutator ambiguities for radiative corrections to weak semileptonic, 25:5341
electromagnetic interactions at very high energies, scaling laws for, (T), 25:5319 (CONF-700314-, Paper 8)
interactions at high energies in quark model, 25:5358
interactions at high energies, review of field theoretic models for diffraction scattering and dissociation in, (T), 25:5320 (CONF-700314-, Paper 17)
interactions at high energies, theorems for, (T), 25:5303 (CONF-700314-, Paper 16)
interactions at very high energies, conference on, (E/T), 25:5244 (CONF-700314)
interactions at very high energies, parton model for, (T), 25:5304 (CONF-700314-, Paper 18)
interactions at very high energies, review of cosmic particle experiments for study of, (E), 25:5245 (CONF-700314-, Paper 5)
interactions in colliding beams, cross section energy and angular dependence measurement for, (E/T), 25:5360 (RLO-2041-51)
interactions of arbitrary-mass spinless, double partial-wave expansion of elastic, (T), 25:5310
interactions of spin-3/2, with photon, differential and total cross sections for Compton, (T), 25:5329
interactions of, counter experiments with kinematic separation of three-particle final states in, 25:5218
interactions of, Kohn variational principle for two-body s-wave, (T), 25:5430
interactions of, lower bounds for parameters for particle rearrangement in, (T), 25:5425 (JINR-P4-5332)
interactions of, lower bounds on threshold charge-exchange amplitude from di-pion mass distributions in final states of, (T), 25:5315
interactions of, particle number fluctuations in hydrodynamical theory of multiple production in, (T), 25:5309
interactions of, relativistic eikonal approximation for superposition of two, (T), 25:5434
interactions of, second-quantized nonrelativistic time-dependent scattering theory and generalization of in--out formalism for Coulomb potentials for, 25:5431
interactions of, solutions of Faddeev equations for two- and three-body systems in, (T), 25:5429
interactions of, superconvergence relations for Omnes equations for bound states in, 25:5427
polarization density matrix for arbitrary-spin, covariant, (T), 25:5305 (JINR-P2-4931)
production in photon two-body and electron deep inelastic interactions at very high energies, scaling laws for, (T), 25:5319 (CONF-700314-, Paper 8)
production of, particle number fluctuations in hydrodynamical theory for multiple, (T), 25:5309
scattering by nuclei at high energies, Regge-ized absorption model for, (T), 25:5433
scattering on Coulomb and short-range potentials, amplitude for, (T), 25:5438
strong interactions at 5 to 70 GeV/c, review of, (E), 25:5272
strong interactions at high energies in amplitude fast variation region, bremsstrahlung from, (T), 25:5357
strong interactions at high energies, quark model for mechanisms for, (T), 25:5354
strong interactions at high energies, solution of unitary condition for amplitude of arbitrary two-body channel in, (T), 25:5355
strong interactions at high energies, unitarity condition for amplitude behavior for forward, (T), 25:5349 (IFVE-STF-69-74)
strong interactions at very high energies and high momentum transfers, quark production in, (E/T), 25:5281 (CONF-700314-, Paper 15)
strong interactions at very high energies, review of Regge phenomenology for, (T), 25:5347 (CONF-700314-, Paper 13)
strong interactions of, broken SU(3) sum rules for coupling constants of, (T), 25:5394
strong interactions of, local duality in set of coupled reactions with two-body hadron production in, (T), 25:5352 (SU-1206-235)
strong interactions of, phenomenology of multiperipheral models of, (T), 25:5346 (CONF-700314-, Paper 12)
strong interactions of, Pomeranchuk decoupling from ordinary Regge trajectories in, (T), 25:5348 (COO-264-562)
strong interactions of, scaling behavior in multiperipheral models for, (T), 25:5351 (NYO-2262-TA-

225)
strong interactions of, total cross sections for, (E), 25:5265 (CONF-700314-, Paper 4)
symmetry for, unitary representations of conformal group in, (T), 25:5393 (IFVE-STF-69-85)
symmetry group representations for particle--antiparticle doublets, Poincare, 25:5358
weak interactions at arbitrary momentum transfer, current algebra models for ultraviolet divergences in electromagnetic radiative corrections to lowest-order, (T), 25:5343
weak interactions of, broken SU(3) sum rules for coupling constants of, (T), 25:5394
ELEMENTARY PARTICLES (TRIPLET)
interactions of quarks at very high energies and high momentum transfers, (E/T), 25:5281 (CONF-700314-, Paper 15)
production of quarks in hadron strong interactions at very high energies and high momentum transfers, (E/T), 25:5281 (CONF-700314-, Paper 15)
production of quarks in interactions above 1 TeV, review of, (E), 25:5274
research on cosmic quarks at California Univ., Oct. 1969 to Sept. 1970, (E), 25:5257(R) (UCI-10-P-19-40)
ELEMENTS
abundance of cosmic 150- to 250-MeV/nucleon Z = 16 to 30, (E), 25:4373
determination in biological materials, review on atomic absorption spectrometric, 25:4023
determination in biological materials, spectrometric, 25:4016 (UCLA-12-782, pp 83-8)
EMBRYOS
effects of AET on nervous system of chicken, 25:4601
radioinduced malformations in animal and human, low-level ionizing, 25:4713
radioinduced malformations of, in rats, combined effects of iodoacetamide on x, 25:4575
ENDOTOXINS
effects on metabolism in polymorphonuclear leukocytes of x-irradiated guinea pigs, 25:4454 (NYO-3240-55)
radioprotective effects of bacterial, on dogs, mice, and sheep, reaction mechanisms for x, 25:4586
ENVIRONMENT
improvement of, contribution of contained underground nuclear explosions to, 25:4171
EPITHELIUM
phagocytosis in pulmonary alveolar, of rats, 25:4410
ERBIUM
determination of trace amounts of, in uranium by chemical separation and spectroscopy, 25:4021
Hall effect in single crystals of, anomalous magnetization dependence of, 25:5219
magnetic properties and structure of, neutron inelastic scattering study of, 25:5214
magnetic properties of single crystals of, (E/T), 25:5194
magnetoresistance at low temperatures, 25:5175
separation of trace amounts of, from aqueous nitric acid solutions by solvent extraction using D2EHPA in toluene containing trace amounts of uranium, 25:4150
ERBIUM ALLOYS AND SYSTEMS
Al--Er, magnetic structure of ErAl, neutron-diffraction study, 25:5208
Co--Er, magnetic resonance of Er_2Co_{17} and $ErCo_3$, microwave, 25:5200
Co--Er, magnetic structure of $ErCo_3$, neutron diffraction study, 25:5210
Dy--Er-base, magnetic structure of, neutron-diffraction study, 25:5207
Er--Gd, magnetic structure of, 25:5207
Er--Ni, magnetic structure of ErNi, 25:5209
Er-base--Ho, magnetic structure of, neutron-diffraction study, 25:5207
Er-base--Tb, magnetic structure of, neutron-diffraction study, 25:5207
Er-base--Y, magnetoresistance at low temperatures, 25:5175
ERBIUM CHROMATES
metamagnetic properties of single crystals of, 25:5180
ERBIUM ISOTOPES
energy level transitions in, role of static charge of nucleus in determining probability of E0 pair conversion of, (T), 25:5791
ERBIUM ISOTOPES Er-157
energy levels in, ground-state band, (E), 25:5688 (UCRL-19961)
ERBIUM ISOTOPES Er-159
energy levels in, ground-state band, (E), 25:5688 (UCRL-19961)
ERBIUM ISOTOPES Er-166
Moessbauer spectra in erbium oxide at low temperatures, 25:5225
ERBIUM ISOTOPES Er-167
electron inelastic scattering and photo-excitation at 2.3 to 3.6 MeV, cross sections for, (E), 25:5637
energy levels from electron inelastic scattering and photo-excitation at 2.3 to 3.6 MeV, parity assignments for, (E), 25:5637
energy-level transitions from photo-excitation and electron inelastic scattering at 2.3 to 3.6 MeV, multipolarity of, (E), 25:5637
half-life of isomeric, (E), 25:5637
ERBIUM ISOTOPES Er-169
energy levels of, spins and parities of, (E), 25:5725
neutron separation energy for, (E), 25:5725
ERBIUM ISOTOPES Er-170
deuteron reactions (d,t) at 12 MeV, Q-value for, (E), 25:5725
ERBIUM OXIDES
magnetic hyperfine interactions in, Moessbauer study of, 25:5225
magnetic structure of, (T), 25:5215
ERBIUM SILICIDES
magnetic structure of ErSi, (E/T), 25:5212
ERBIUM TUNGSTATES
magnetic structure of Er_6WO_{12}, neutron-diffraction study of, 25:5216
ERYTHROCYTES
labeling with chromium-51 or phosphorus-32, 25:4411 (CEA-R-4031)
labeling with metastable technetium-99, 25:4414
radiation effects on electrolyte content in, of rabbits, x, 25:4698
synthesis of methemoglobin in, in vitro, effects of vitamin K-3 on, 25:4598
ERYTHROPOIESIS
radiation effects on, in bone marrow and spleen of mice, iron-59 tracer study of effects of adrenalectomy on, 25:4696
toxicity of uranium oxide to, in dogs following chronic ingestion and low and high dose intratracheal injection, 25:4445
ETHANE
yields from the gas-phase α radiolysis of propane, 25:4119
ETHANE, 1,2-DICHLORO-
radiolysis of, spectrophotometric studies on rate of formation and subsequent decay of aromatic radical cations produced by pulse, 25:4112
ETHANOL
complexes with thorium and uranium tetrachlorides, formation of crystalline, thermodynamics of, 25:4077
neutron scattering by ordinary and deuterated, total cross sections for cold, (E), 25:5500
ETHANOL, 2-MERCAPTO-
effects on synthesis of DNA and RNA in thymus gland of rats, tracer study of, 25:4592
ETHYL SULFATES
effects on seeds of Sorghum sp., mutagenic, 25:4495
ETHYLENE
radiolysis of, effects of hydrogen sulfide on yields from γ, 25:4122
ETHYLENE POLYMERS
evaluation of borated, as neutron shielding for Project Plowshare explosives, 25:4175
neutron leakage flux for, measurement of cold, (E/T), 25:6203
neutron reactions with, time-dependent coupled neutron--secondary gamma spectra from, (T), 25:5147
radiolysis of high-density, at -180°C, ir spectrometric study of, 25:4118
spectra of, effects of deuterium on Raman, 25:4062
Ni--polyethylene, radiciduced curing of composites of, γ, 25:4108
polybutene--polyethylene, radiolysis at -180°C, ir spectrometric study of, 25:4118
polyethylene--polypropene, radiolysis at -180°C ir spectrometric study of, 25:4118
ETHYLENE, TETRAFLUORO-
radioinduced polymerization with 2-methylpropene, NMR spectral studies on product from γ, 25:4102
ETHYLENIMINE
effects on x-radiosensitivity of transplants of Ehrlich carcinomas in mice, mechanisms for, 25:4563
EUMYCOTA
Saccharomyces cerevisiae, γ-radiosensitivity of, effects of cycloheximide on, 25:4556
Saccharomyces cerevisiae, radioinduced mutations of, effects of methyl methanesulfonate and nitrogen mustard on uv and x, 25:4480
Saccharomyces cerevisiae, radiosterilization of, in fruit juices, γ, 25:4556
EUROPIUM
determination of trace amounts of, in uranium by chemical separation and spectroscopy, 25:4021
magnetic phase transition in, effects on electric conductivity of Neel, 25:5204
magnetic phase transition in, Moessbauer study of hyperfine field in, 25:5203
optical constants from reflectance spectra at 1 to 11.6 eV, 25:5188
separation by ion exchange using Alamine 336 in aqueous thiocyanate solutions, 25:4137 (IS-T-377)
separation from aqueous chloride solutions by solvent extraction using cycloctylphenylphosphinic acid or octylphenylphosphinic acid, 25:4147
separation of trace amounts of, from aqueous nitric acid solutions by solvent extraction using D2EHPA in toluene containing trace amounts of uranium, 25:4150
EUROPIUM CARBIDES
thermal decomposition of, mass spectrometric studies of, 25:4855
thermodynamic properties of, 25:4855

EUROPIUM ISOTOPES Eu-146
- beta and electron-capture decay of, gamma spectra from, (E), 25:5694
- energy levels from gadolinium-146 decay, spin--parity assignments for, (E), 25:5694
- energy-level transitions from gadolinium-146 decay, intensities, multipolarities, and mixing ratios from, (E), 25:5694

EUROPIUM ISOTOPES Eu-151
- energy-level transitions in, conversion electron intensities, multipolarities, and multipole mixing ratios for, (E), 25:5695
- Moessbauer effect following Coulomb excitation, 25:5221 (AD-710293)
- photon reactions (γ,n) and photoabsorption at 8 to 22 MeV, excitation functions for, (E), 25:5778

EUROPIUM ISOTOPES Eu-152
- gamma spectra of, precision measurements of low-energy, 25:5736

EUROPIUM ISOTOPES Eu-153
- photon reactions (γ,n) and photoabsorption at 8 to 22 MeV, excitation functions for, (E), 25:5778
- proton reactions (p,2n) at 14 MeV, gamma and conversion-electron spectra from, (E), 25:5750

EUROPIUM ISOTOPES Eu-154
- gamma spectra of, precision measurements of low-energy, 25:5736

EUROPIUM ISOTOPES Eu-155
- determination by β counting using G-M and proportional detectors, efficiency curves for, 25:4029 (CISE-N-119)
- gamma spectra of, precision measurements of low-energy, 25:5736

EUROPIUM ISOTOPES Eu-156
- gamma spectra of, precision measurements of low-energy, 25:5736

EUROPIUM OXIDES
- magnetic phase transition in, sound propagation near, 25:5186

EXHAUST SYSTEMS
- fires in nuclear facility, equipment and methods for control, detection, and prevention of, 25:4196

EXPERIMENTAL BREEDER REACTOR-II
- cooling system of, maintenance requirements of, 25:5987
- core for, physics measurements of mixed oxide, 25:6031
- fuel element assemblies of, performance of temperature measuring devices for mixed oxide pin type, (E/T), 25:6027
- fuel element meltdown in, energy release calculations for metal and oxide, 25:6082
- fuel element subassembly of, analysis of parallel flow induced vibration of, (T), 25:6030
- fuel elements of, xenon tagging techniques for failure detection of, 25:6025
- fuel elements of, xenon tagging techniques for failure detection of, 25:6026
- fuel pins for, burst tests on irradiated, 25:5950
- gamma radiation dose distribution in, 25:6125
- physics measurements for depleted uranium and nickel reflected cores of, (E/T), 25:5963
- radiation effects testing of Type 316 stainless steel in, 25:5949
- radiation effects testing of Type 316 stainless steel in, 25:5948
- radiation effects testing of uranium oxide (UO_2) fuel elements in, 25:6060

EXPLOSIVES
- shielding for Project Plowshare, evaluation of borated polyethylene as neutron, 25:4175

EXPONENTIAL PILES
- neutron detector response in, diffusion theory calculations for, 25:6118
- neutron spectra in pulsed aluminum, fast, (E/T), 25:6106
- neutron spectra in pulsed beryllium, thermal, (E), 25:6107

EYES
- radiation dosimetry in, of rabbit phantom, 25:4521
- radioinduced cataracts in, of rabbits, review of microwave, 25:4708 (UR-49-1256)
- radioinduced irritation of, of personnel using uv, 25:4710
- radioinduced lenticular opacities in human, review of microwave, 25:4708 (UR-49-1256)
- radiotherapy of diseases of human, methods for bilateral fast electron, 25:4690

F

FALLOUT
- distribution in tissues of swine following ingestion and inhalation of, 25:4435
- effects on infant mortality following nuclear weapons testing, 25:4505 (CONF-691051-, pp 324-35)
- effects on plants in desert ecosystems, lethal, 25:4477 (UCLA-12-782, pp 49-81)
- metabolism in dairy cattle following ingestion of, 25:4436
- protection of plants against, effectiveness of plastic covers for, 25:4477 (UCLA-12-782, pp 49-81)
- radioisotope distribution in, from Project Schooner, 25:4180
- transport in freshwater ecosystems following nuclear detonation, effects of leaching on, 25:4479

FAST FLUX TEST FACILITY
- component design for, effects of neutron-induced metal swelling behavior on, 25:4810 (BNWL-SA-3283)
- fuel pins for, critical parameters in water of, 25:4280
- radiation streaming in, design requirements for γ and neutron, 25:5976

FAST TEST REACTOR
- accidents in, acoustic and inertial constraints for molten fuel and liquid sodium interaction, 25:6099
- cooling system of, corrosion product radioactivity in, 25:5986
- fuel elements for, failure limits for mixed oxide pin type, 25:6096
- shielding requirements for, 25:6124

FATS
- content of human bones, effects of, on results of measurements of mineral content, 25:4644 (CONF-700515-, pp 255-62)

FATTY ACIDS
- metabolism in liver cells in cultures, 25:4458 (UCLA-12-782, pp 1-21)
- radiolysis of in vitro, γ, 25:4458 (UCLA-12-782, pp 1-21)
- synthesis by Bacillus megaterium, 25:4458 (UCLA-12-782, pp 1-21)
- uptake by brain in adult mammals, reaction mechanisms for, 25:4458 (UCLA-12-782, pp 1-21)

FECES
- analysis for blood using chromium-51-labeled erythrocytes, counting method for, 25:4032
- excretion of uranium oxide in, of dogs and rabbits following chronic ingestion, 25:4444
- ratio of strontium-90 content of, to dietary content of man, effects of ingestion in calcium gluconate and milk on, 25:4424(R) (TID-25567)

FERMI FAST BREEDER REACTOR
- cooling system for, request for additional information on service piping for, 25:5916 (DOCKET-50016-87)
- maintenance procedures for, review of zirconium segment removal, 25:5907

FERMIONS
- interactions of spin-3/2, with photon, differential and total cross sections for Compton, (T), 25:5329

FERROMAGNETIC MATERIALS
- model for amorphous, 25:6224 (CALT-822-16)

FERTILIZERS
- effects on growth of plants in desert ecosystems, 25:4477 (UCLA-12-782, pp 49-81)

FETUSES
- blood circulation in, of monkeys and sheep, tracer study of, 25:4655 (COO-1762-6)
- radiation dose to human, following use of radioisotopes for lung scanning of mother, 25:4673

FIELD THEORY
- Born--Infeld theory for small-scale phenomena, 25:5404
- equivalence theorem and observables in, 25:5235 (JINR-P2-5266)

FILICINIDAE
- Osmunda regalis, radiciduced injuries in dry spores of, reaction mechanisms for ionizing, 25:4705

FILMS
- magnetization measurement on thin, apparatus design for, 25:5168(R) (COO-623-156)
- temperature distribution in thin, determination using liquid crystals, 25:5168(R) (COO-623-156)

FILTERS
- design and operation of high-efficiency particulate air, for NRTS hot fuel examination facility, 25:4197
- performance of superheated steam, effects of configuration and material on, 25:5980 (KFK-1183)
- protection of nuclear facility air, equipment and methods for fire, 25:4196
- testing of high efficiency particulate air, for plugging by sprayed water droplets, 25:4190 (UCRL-50523)

FIRES
- control, detection, and prevention of glove box, at Rocky Flats Plant, improved methods for, 25:4195
- control, detection, and prevention of hot cell, equipment and methods for, 25:4193
- control, detection, and prevention of, in nuclear air cleaning systems, equipment and methods for, 25:4196
- protection criteria for nuclear facilities, 25:4194

FISSION
- neutron emission in alpha-accompanied, correlation experiment for measurement of, (E/T), 25:5723
- properties of saddle point and decay widths, comparison with activated complex in chemical kinetics, (T), 25:5810

FISSION FRAGMENTS
- angular distributions of, use in elucidating transition-state properties, (T), 25:5810
- charge distributions from excited heavy nuclei up to Z = 110, (E), 25:5691
- detection and measurement in SNEAK, automatic system for dielectric track detectors for, 25:4343
- detection and measurement using dielectric track detectors, 25:4342
- effects on crystal structure of zirconium ceramics, 25:4887 (KFK-1215)
- effects on sputtering of uranium atoms, 25:4627

XUM

effects on xenon-133 diffusion in calcium fluoride monocrystals, 25:5152(R) (ORO-3508-6)
mass distributions from excited heavy nuclei up to Z = 110, (E), 25:5691
neutron emission from, theory of delayed, 25:5851
FISSION PRODUCTS
decay chain populations and independent yield data for, computer program for calculating, (T), 25:5790
diffusion in graphite, model for effects of concentration on, 25:4860
diffusion in mixed oxide fuels during irradiation, (E), 25:6012
diffusion of gas bubbles and inclusions in mixed oxide fuel elements, (E), 25:6014
distribution in mixed oxide fuel elements, SWELL 2 code for, 25:6013
effects on performance of uranium dioxide fuels, 25:4888 (TRG-Report-1937)
energy-level transitions in californium-252, (E), 25:5687 (UCRL-19949)
production cross sections for, in heavy-ion induced fission, 25:5756
release from coated fuel particles, effects of temperature on, (E), 25:5997
release from high burnup coated particle fuels, 25:5990(R) (ORNL-4589)
release from HTGR type fuel rods, (E), 25:6009
release from mixed oxide gas cooled fuel elements, (E), 25:6015
release from overheated HTGR type fuel elements, (E), 25:6010
separation of noble-gas, from gaseous effluents, methods for, 25:4260 (CEA-Bib-184)
separation of spent uranium from, by nitride precipitation from liquid tin-uranium alloys, 25:4149
transport through graphite barrier in HTGR type fuel elements, effects of transverse flow on, (E/T), 25:6011
FISSIONABLE MATERIAL
analysis for accountability and safeguards, radiometric method for nondestructive, 25:4291
control and inventory of, safeguards methods for, 25:4290
handling and storage of metallic, use of surface density as a parameter for criticality-safe, 25:4284
storage in water, methods for determining safe spacing for, 25:4285
FLUID FLOW
electrohydrodynamic, stability of cylindrical flow, (T), 25:4997
magnetohydrodynamic, around rotating electrically conducting plates, (T), 25:4999
magnetohydrodynamic, Ekman--Hartmann layer solutions on spherical boundary, (T), 25:4998
particle diffusion for Poiseuille and slug, in circular tubes (T), 25:4204 (HASL-238)
pressure effects in time-dependent, high-, (T), 25:5239
velocity of, measurement using temperature variations in vortices behind heated rod obstructing flow stream, 25:4205
FLUIDIZED BEDS
sphere transport in recirculated randomly packed, in cylindrical vessels, (E/T), 25:4182 (AAEC/E-207)
FLUORIDES
content of drinking water, effects of, on bone density in man, methods for determining using γ transmission scanning, 25:4627 (CONF-680211-, pp 319-28)
effects on automatic colorimetric determination of thorium in aqueous and organic solutions, 25:4014 (ALCO-1072)
FLUORINE
determination by photon activation using NRL Linac, 25:4041 (AD-709901)
determination in high-purity tungsten by photon activation, 25:4043 (GA-10125)
meson (K^0) reactions at 120 MeV, Λ^0 and Σ^0 production and total cross sections for, (T), 25:5300
FLUORINE ISOTOPES F-15
energy levels of, compilation of, (E), 25:5567
FLUORINE ISOTOPES F-17
energy levels from nitrogen-15 (He-3,n) reactions, decay properties of $T = {}^3/_2$, (E), 25:5583
FLUORINE ISOTOPES F-19
energy level at 110 keV from oxygen-19 decay, (E), 25:5565
energy levels of, calculation of spin--parity assignments using quadrupole forces, (T), 25:5809
helium-3 reactions (He-3,n) at 4.2 to 5.9 MeV, angular distributions from, (E), 25:5583
neutron capture at 20 to 80 keV, cross sections for, (E), 25:5603 (FOA-4-4440)
FLUORINE ISOTOPES F-20
energy levels from neutron resonances in fluorine-19, radiative widths for, (E), 25:5603 (FOA-4-4440)
FLUOROCARBONS
analysis of radiolytic, research progress on spectrographic, 25:4111(R) (ORO-3909-2)
FORBUSH DECREASES
rigidity dependence and pre-storm increases, (E/T), 25:4983
FORT ST. VRAIN POWER REACTOR, UNIT 1
design parameters of, 25:5884
pressure vessel for, selection of metallic components and thermal barrier for, 25:5883
shielding for, design requirements of, 25:5888
FREE RADICALS
photoreactions of allyl type, from γ-radiolysis of alkenes and alkene--3-methylpentane mixtures, 25:4125
radicinduced in orotic acid, magnetic properties of, 25:4459 (UCLA-12-782, pp 23-47)
radioinduced in potassium permanganate single crystals, ESR study of, 25:4110 (AD-710231)
radioinduced in selencures in aqueous solutions, ionizing, 25:4546
radioinduced, in aqueous solutions of DNA and nucleotides, reactions of, with triacetoneamine-N-oxyl, 25:4541
radioinduced, in bacteria, reactions of, with aminothiols, γ, 25:4548
role in x-radioinduced chromosome aberrations in peas, 25:4489
spectra of, produced in γ-irradiated leucine hydrochloride monocrystals, 25:4092
yields from γ irradiation of monocrystals and polycrystals of orotic acid, 25:4093
FRUITS
cherries, radiation processing of, effects of, on stability of exocarp, electron, 25:4721
radiation processing of juices of, combined effects of cycloheximide on storage life of, γ, 25:4556
FUEL CAPSULES
development and testing for radioisotope-fueled Brayton power systems, 25:4216(R) (SC-PR-70-682)
fabrication and testing of promethium-147 oxide fueled, 25:4217(P)
materials for cobalt-60-containing, selection and testing of, 25:4224
testing of plutonium-238-containing, for cardiac pacemaker, methods for high-temperature, impact, pressure, and ultrasonic microcrack, 25:4215 (NUREG-3731-23)
FURFURYL ALCOHOL
polymers of, infrared spectroscopy of low molecular weight constituents in, 25:4840(R) (LA-4526)
resins of, graphitization of, 25:4840(R) (LA-4526)

G

GADOLINIUM
determination of trace amounts of, in uranium by chemical separation and spectroscopy, 25:4021
magnetic domain structure of single crystals of, (E), 25:5196
magnetic phase transition in, sound propagation near, 25:5186
magnetic properties of single crystals of, (E/T), 25:5194
magnetic transient field in, platinum-isotope ion-implantation perturbed-angular-correlation study of, (E), 25:5189
magnetic transition temperatures of single crystals of, pressure dependence of, (E/T), 25:5195
properties for use as encapsulating material for californium-252 sources for neutron capture gamma-ray spectroscopy, 25:4772
separation of trace amounts of, from aqueous nitric acid solutions by solvent extraction using D2EHPA in toluene containing trace amounts of uranium, 25:4150
thermal capacity near Curie point, 25:5220
GADOLINIUM ALLOYS AND SYSTEMS
Al--Gd, thermal capacity of $GdAl_2$ at low temperatures, 25:5218
Co--Gd, magnetic properties of Co_2Gd, ferrimagnetism in, 25:5201
Co--Gd--Ni, magnetization and hyperfine field in $Gd(CoNi)_2$, 25:5198
Er--Gd, magnetic structure of, 25:5207
Gd--Ni, thermal capacity of $GdNi_5$ at low temperatures, 25:5218
Gd-base--Mg, magnetic ordering and thermoelectric properties of, 25:5169 (IS-T-379)
Gd-base--Th, magnetic ordering and thermoelectric properties of, 25:5169 (IS-T-379)
GADOLINIUM ISOTOPES
energy level transitions in, role of static charge of nucleus in determining probability of EC pair conversion of, (T), 25:5791
GADOLINIUM ISOTOPES Gd-146
electron-capture decay of, gamma spectra from, (E), 25:5694
GADOLINIUM ISOTOPES Gd-152
energy levels from europium-153 (p,2n) reactions at 14 MeV and samarium-150 (α,2n) reactions at 30 MeV, spin--parity assignments and deformation parameters for, (E), 25:5750
energy-level transitions from europium-153 (p,2n) reactions at 14 MeV and samarium-150 (α,2n) reactions at 30 MeV, conversion coefficients and multipolarities for, (E), 25:5750
photon reactions (γ,n) and photoabsorption at 8 to 22 MeV, excitation functions for, (E), 25:5778

XUM

GADOLINIUM ISOTOPES Gd-153
use as γ source for transmission scanning of bones for measurement of mineral content, 25:4649 (CONF-700515-, pp 308-12)
GADOLINIUM ISOTOPES Gd-154
energy-level transitions from erbium-154 beta decay, angular correlation coefficients and attenuation parameters in different liquid sources, (E), 25:5758
photon reactions (γ,n) and photoabsorption at 8 to 22 MeV, excitation functions for, (E), 25:5778
GADOLINIUM ISOTOPES Gd-156
energy levels from terbium-156 decay, (E), 25:5705
energy-level transitions from erbium-156 beta decay, angular correlation coefficients and attenuation parameters in different liquid sources, (E), 25:5758
photon reactions (γ,n) and photoabsorption at 8 to 22 MeV, excitation functions for, (E), 25:5778
GADOLINIUM ISOTOPES Gd-158
photon reactions (γ,n) and photoabsorption at 8 to 22 MeV, excitation functions for, (E), 25:5778
GADOLINIUM ISOTOPES Gd-160
neutron capture integral in fast region, (E), 25:5656
GADOLINIUM URANATES
$GdUO_4$--ThO_2, spectra and phase studies of, 25:4084
GADOLINIUM VANADATES
magnetic properties of $GdVO_4$ at low temperatures, 25:5217
GAGES AND METERS
design parameters of profilometer, for inspection of irradiated liquid metal cooled fuel elements, 25:6033
performance of slow-neutron transmission, for on-stream analysis, review on, 25:4035
GALAXIES
blue objects associated with cD clusters of, detection of faint, (E), 25:4930
diameter--luminosity relation for Virgo cluster, (E/T), 25:4931
distance of Virgo cluster, (E/T), 25:4931
distribution of, (T), 25:4932
evolution of disk, dynamical, (T), 25:4929 (N-70-33057)
luminosity functions for, (T), 25:4932
morphology of, (T), 25:4933
GALLIUM
electron reactions with, ionization cross sections for, (E), 25:4956
separation by ion exchange using Alamine 336 or Amberlyst A-21 in aqueous thiocyanate solutions, 25:4137 (IS-T-377)
separation from aluminum and iron by ion exchange in thiocyanate solutions using Alamine 336, 25:4137 (IS-T-377)
superconductivity of thin films of amorphous, far-infrared radiation transmission in, 25:5059
GALLIUM ALLOYS AND SYSTEMS
Ga--Pu-base, phase studies of, 25:4801
GALLIUM ARSENIDES
vaporization of single crystals of, kinetics of, 25:4074 (UCRL-19685)
GALLIUM ISOTOPES Ga-67
use for whole-body scanning of man for tumor localization, 25:4656(R) (ORNL-4615)
GALLIUM ISOTOPES Ga-70
energy levels from zinc-70(p,n) reactions, (E), 25:5612
GALLIUM ISOTOPES Ga-71
energy levels from proton resonances in zinc-70, spreading widths of isobaric analog, (T), 25:5644
GAMETES
radiation effects on, in pond snails, effects of dose 10,000 on γ, 25:4693
GAMMA CAMERAS
development of, 25:4337
performance for use with metastable technetium-99 and xenon-133, for diagnosis of lung diseases, 25:4676
use in scintiscanning, physical characteristics of, 25:4684
GAMMA RADIATION
angular correlations of, model for statistical perturbation with any correlation time, (T), 25:5874
attenuation in cylindrical concrete structure, Monte Carlo calculation of, (T), 25:4256
detection of, personnel monitoring system for, 25:4335(P)
dose buildup factors in water, 25:5136
dose distribution in ZPR-3 Assembly 60, mockup of EBR-2, 25:6125
dose rates from plutonium dioxide--uranium dioxide fuel rods, method for calculation of, 25:4314
dose to chemical compounds, spectrophotometric method for measuring absorbed, 25:4520
dose to human tissues during endolymphatic therapy using iodine-131, 25:4512
dose to spinal cord and body of patients during iodine-131 cisternography, absorbed, 25:4510
dosimetry in mixed field, response of TLD 700 thermoluminescent dosimeter to reactor neutrons for, 25:4382
dosimetry of, intercomparison of personnel criticality dosimeters for, 25:4377 (AERE-R-6498)
dosimetry of, passive self-reading personnel dosimeter for, 25:4376 (AD-710007)
effects on 2,2-dimethylpropane at 23°C, effects of scavengers on yields from, 25:4113
effects on 2-propanol, 25:4123
effects on amino acid composition of wheat gluten, effects of 10 Mrad dose on, 25:4465
effects on Antirrhinum and tomatoes, effects of dose on mutagenic, 25:4483
effects on arsenate- and vanadate-doped calcium tungstate, ESR spectral studies on radicals produced from, 25:4090
effects on ascorbic acid content and ascorbate oxidase activity in germinating castor seeds, 25:4466
effects on barley seeds, effects of gibberellic acid on injurious and aberrant, 25:4490
effects on benzene--cyclohexane mixtures, effects of composition on yields of hydrogen from, 25:4121
effects on catalytic properties of copper and nickel chelates in decomposition of hydrogen peroxide, 25:4103
effects on chromosomes of lymphocytes in vitro, evaluation of dose-response relationship on aberrant, 25:4491
effects on count of autoantibody-forming cells in blood and spleen of dogs and mice, use of Cavingham's method to determine, 25:4472
effects on crosslinking of poly(2-methylpropene) with acrylonitrile or divinyl benzene, calorimetric studies on, 25:4101
effects on crosslinking of poly(vinyl acetate) solutions, 25:4094
effects on cultured callus tissue, seeds, and seedlings from Phaseolus, cobalt-60 γ, 25:4723
effects on curing of metal--polymer composites, 25:4108
effects on cystine dihydrochloride monocrystals, photochemical conversions of paramagnetic centers in, 25:4091
effects on decomposition of potassium nitrate in potassium bromide matrix, energy transfer in, 25:4056
effects on DNA, nucleosides, nucleotides, and thymine in solutions, lytic, 25:4459 (UCLA-12-782, pp 23-47)
effects on electrical charge and coloration of shielding glasses, (E), 25:5166
effects on Escherichia coli, induction of free radical formation by, 25:4548
effects on ethylene, effects of hydrogen sulfide on yields from, 25:4122
effects on fatty acids in vitro, lytic, 25:4458 (UCLA-12-782, pp 1-21)
effects on frequencies of chlorophyll mutations and chromosome aberrations in barley seeds, protective effects of ancxia, cysteine, and water against, 25:4604
effects on gametogenesis and oviposition of pond snails, effects of dose 10,000 R on, degradatory, 25:4693
effects on germination of sugarbeet seeds, 25:4722
effects on glandular stomach of mice, carcinogenic whole-body, 25:4703
effects on graft polymerization of monomers onto inorganic substrates, 25:4106
effects on growth of Ehrlich ascites tumor cells following transplantation into mice, combined effects of 5,9-dihydroxypsoralen on, 25:4565
effects on growth of pineapples, damaging, 25:4719
effects on growth of wheat, effects of presowing, postexposure treatment with indole acetic acid, tryptophane, and zinc on cobalt-60, 25:4718
effects on hematopoietic system in man, protective effects of taurine against, 25:4603
effects on human isoamylases of parotid saliva, blood serum, and urine following therapy of parotid glands, 25:4452
effects on human lumbar region, functional and morphological studies of nephropathy following cobalt-60, 25:4714
effects on human patients, relation of, to leukopenia and taurine excretion in urine, effects of dose and dose rate on, 25:4603
effects on immune reactions of chickens to skin grafts and spleen cell transplants, combined effects of bursectomy or thymectomy on cobalt-60, 25:4468
effects on immune responses of mice in comparison to 2.2-GeV protons, 25:4470
effects on in vitro growth of Histomonas (protozoa), effects of dose on, 25:4692 (COO-1205-13)
effects on lactic dehydrogenase and lactic dehydrogenase isoenzymes in rats, protective effects of methylene blue against whole-body, 25:4605
effects on leucine hydrochloride monocrystals, EPR spectra of free radicals from, 25:4052
effects on mice, combined effects of barenylacetic acid and methyl-c-barencarboxylic acid on, 25:4588
effects on mice, histological evaluation of balneotherapy for treatment of, 25:4610
effects on mulberry trees, mutagenic, 25:4486
effects on orotic acid, ESR spectral studies on free radicals produced by, 25:4093
effects on ovaries in catfish, combined effects of testosterone on, 25:4591
effects on peas following seed exposure in comparison to effects of EMS and NEM, rate of mutagenic, 25:4485
effects on photographic film, 25:4406 (N-70-25843)
effects on pollen of Gossypium seeds, mutagenic, 25:4459
effects on polymerization of 2-methylpropene with

tetrafluoroethylene, NMR spectral studies on product produced by, 25:4102
effects on polymerization of methyl methacrylate with kaolin clay, energy deposition, kinetics, and mechanism of, 25:4107
effects on polymerization of monomers in wood, comparison of economics of heat, heat--catalyst, and, 25:4109
effects on polymerization of styrene under pressure, 25:4104
effects on potassium bromide at 10°K, thermally stimulated conductivity and luminescence study of annealing of, 25:5158
effects on potassium permanganate single crystals, ESR study of radicals produced in, 25:4110 (AD-710231)
effects on reproductive capacity of coffee leaf miner and Mediterranean fruit fly, 25:4733 (NYO-2043-216, pp 19-48)
effects on reproductive capacity of fall webworm, cobalt-60, 25:4735
effects on rice for culm length and lodging resistance, effects of 20 and 30 KR dose on mutagenic, 25:4487
effects on Saccharomyces, combined effects of cycloheximide on, 25:4556
effects on seeds of sorghum, mutagenic, 25:4495
effects on solid alkenes and alkene--3-methylpentane mixtures, 25:4125
effects on spleen colony formation by stem cells in mice, protective effects of hematoporphyrin against, 25:4572
effects on storage life and acceptability of yellow perch, 25:4734 (TID-25467)
effects on survival of animals and plants in desert ecosystems, continuous low-dose, 25:4477 (UCLA-12-782, pp 49-81)
effects on survival of bacteria and bacteriophages, protective effects of anoxia, cystamine, disulfides, and thiols against, 25:4549
effects on survival of flour beetles, effects of infection with cysticercoids on, 25:4692 (COO-1209-13)
effects on survival of mice, protective effects of adrenochrome monoguanylhydrazone methanesulfonate against, 25:4589
effects on survival of rats, protective effects of AET, cystamine, mexamine, and serotonin against, following dose fractionation, 25:4581
effects on synthesis of DNA and proteins in Escherichia coli, combined effects of iodoacetic acid and vitamin K on, 25:4552
effects on TBP in dodecane solution, effects of isopropylbiphenyl on, 25:4116
effects on thallium-doped potassium chloride crystals at 21°C, color centers induced in, 25:5157
effects on trees, lethal and mutagenic, 25:4724
effects on tryptophan dipeptides, yields from, 25:4114
emission from plutonium dioxide heat sources, spectra of, 25:4245
energy deposition in fast reactors, distribution of, 25:5970
flux of cosmic primary, (E/T), 25:4980
measurement of fission-product, for nondestructive analysis of nuclear materials, 25:4291
mesons (μ) production at sea level by cosmic, (E/T), 25:4974 (AD-710278)
reactions with materials, Klein--Nishina cross sections for scattered electrons from, (T), 25:5167
reflection, albedo distributions for finite media, 25:5146
scattering from barriers of finite thickness, back-, (E), 25:5149
shielding requirements for gas cooled power reactor, 25:5888
shielding requirements for water cooled power reactors, 25:5977
shielding requirements for ZPPR, mockup of FTR, 25:6124
spectra in spacecraft radioisotope heat source, Monte Carlo calculation of, 25:4242
streaming in liquid sodium cooled fast reactors, design requirements for, 25:5976
streaming in two-legged ducts, (E), 25:5138

GAMMA-RAY ASTRONOMY
use in confirmation of theory of nucleosynthesis, (T), 25:4914

GAMMA SOURCES
fabrication of americium-241 oxide, for dosimeter calibration, 25:4248
gamma spectra of, tables of, 25:5685 (KFKI-70-18-NAC)
half-lives of, tables of, 25:5685 (KFKI-70-18-NAC)
radioisotope, use for dual beam transmission scanning of human bones for measurement of mineral content, americium-241 and cesium-137, 25:4643 (CONF-700515-, pp 243-54)
radioisotope, use for dual beam transmission scanning of human bones for measurement of mineral content, americium-241 and iodine-125, 25:4648 (CONF-700515-, pp 291-302)
radioisotope, use for dual beam transmission scanning of bones for measurement of mineral content, americium-241, bismuth-210, and lead-210, 25:4645 (CONF-700515-, pp 263-71)
radioisotope, use for dual beam transmission scanning of soft tissues for measurement of lipid content, americium-241, cadmium-109, and iodine-125, 25:4646 (CONF-700515-, pp 272-3)
radioisotope, use for transmission scanning of bones for measurement of mineral content, gadolinium-153, 25:4649 (CONF-700515-, pp 308-12)
radioisotope, use for transmission scanning of human bones for measurement of mineral content, iodine-125, 25:4624 (CONF-680211-, pp 283-96)
radioisotope, use for transmission scanning of human bones for measurement of mineral content, americium-241 and iodine-125, 25:4682
radioisotope, use for transmission scanning of human bones for measurement of mineral content, iodine-125, 25:4653 (CONF-700515-, pp 408-22)
radioisotope, use for transmission scanning of human bones for measurement of mineral content, iodine-125, 25:4626 (CONF-680211-, pp 308-19)
radioisotope, use for transmission scanning of human bones for measurement of mineral content, americium-241, 25:4627 (CONF-680211-, pp 319-28)
radioisotope, use for transmission scanning of human bones for measurement of mineral content, iodine-125, 25:4625 (CONF-680211-, pp 296-308)
radioisotope, use for transmission scanning of human bones for measurement of mineral content, iodine-125, 25:4636 (CONF-700515-, pp 169-87)
radioisotope, use for transmission scanning of human bones for measurements of mineral content, americium-241 and iodine-125, 25:4634 (CONF-700515-, pp 33-47)
radioisotope, use for transmission scanning of human bones for measurement of mineral content, americium-241 and iodine-125, 25:4635 (CONF-700515-, pp 48-57)
radioisotope, use for transmission scanning of human bones for measurement of mineral content, americium-241 and iodine-125, 25:4631 (CONF-700515-, pp 1-21)
use for transmission scanning of human bones for measurement of mineral content, 25:4623 (CONF-680211-, pp 253-68)

GAMMA SPECTROMETERS
design of three-crystal lithium-drifted germanium, 25:5682 (IS-T-389)

GAS CENTRIFUGES
development for uranium enrichment, effects on world peace, 25:4213 (CONF-691051-, pp 145-53)
development for uranium enrichment, effects on world peace, 25:4214 (CONF-691051-, pp 354-61)

GAS FLOW
electrohydrodynamic, transport equations of unipolar medium with ion oscillations in, 25:4956

GASES
effects of flowing inert, on carbon reduction of vanadium pentaoxide, chromatographic study of, 25:4642
radiation monitoring of, at Research Reactor Institute of Kyoto University during 1968, 25:4508 (KURRI-TR-63)

GENETICS
effects on DNA synthesis in uv-irradiated bacteria, 25:4462
radiation effects on human, ionizing, 25:4502

GEOCHEMISTRY
ionic radii for use in, 25:4085

GEOMAGNETIC FIELDS
characteristics of, for magnetospheric diagnostics, (E/T), 25:5023
cosmic-ray effects in, (E/T), 25:4984
pulsations in, diagnostic tool for magnetospheric research using micro-, (E/T), 25:5028
pulsations in, phase and polarization comparisons between College and Kotzebue, Alaska of Pc1 micro-, (E), 25:5005
pulsations of, determination of magnetospheric parameters from Pc1 micro-, (E/T), 25:5027
relation of magnetospheric, to solar wind, (E), 25:5024
solar-wind interactions with Pi2 pulsations in, (T), 25:5026
variations of, satellite data on sudden impulses and ring current, (E/T), 25:5025

GERMANIUM
properties for use as encapsulating material for californium-252 sources for neutron capture gamma-ray spectroscopy, 25:4772
radiation effects on plastically deformed, influence of impurities on photoconductivity spectra of 3.5-MeV-electron, (E/T), 25:5161
sputtering of single-crystal, by inert-gas ions in low-eV range, (E), 25:5155

GERMINATION
effects on ascorbic acid content and ascorbate oxidase activity in γ-irradiated Ricinus seeds during germination, 25:4466

GLASS
radiinduced electrical charge and coloration of shielding, γ-, (E), 25:5166

GLOVE BOXES
fire protection system for plutonium handling, reliability analysis for, 25:4187 (RISO-214, pp 21-40)
fires in Rocky Flats Plant, methods for control, detection, and prevention of, 25:4195

GLUCOSE
radiation dose to, method using diffuse reflection spectra to measure absorbed γ, 25:4620

β-GLUCURONIDASE
content of blood plasma in rats, effects of cysteamine, hypoxia, and pyridoxol on, 25:4554

XUM

GLUTAMATE DEHYDROGENASE
content of blood plasma in rats, effects of cysteamine, hypoxia, and pyridoxol on, 25:4554
GLUTATHIONE
radioprotective effects of, on mice, combined effects of AET, cysteamine, cysteine, and serotonin against x, 25:4582
GLUTEN
radiation effects on amino acid content of, methods for determining γ, 25:4465
GLYCEROL
effects on electron-radiosensitivity of DNA in Escherichia coli, 25:4551
nuclear-spin relaxation times for frozen porphyrexide-doped aqueous solutions of, for polarized proton targets, 25:5463 (RHEL/R-199)
properties of frozen porphyrexide-doped aqueous solutions of, for polarized solutions of, for polarized proton targets, 25:5466 (RPP/A-81)
GLYCEROLPHOSPHATE DEHYDROGENASE
radiosensitivity of activity of, in solutions, effects of iodine compounds on x, 25:4565
GLYCINE, N-TRYPTOPHYL-
radiolysis of aerated solutions of, yields from γ and x, 25:4114
GLYCOGEN
carbon-14 uptake by cerebral, of x-irradiated rats, 25:4453
GLYCOLYSIS
effects of oxamic acid on, in mice, 25:4566
GLYOXAL, PHENYL-
effects on x-radiosensitivity of cultured Chinese hamster cells, 25:4557
GOLD
gold-197 Moessbauer isomer shift in gelatin-supported microcrystals of, 25:5221 (AD-710293)
heating of films of, by electron microscope beam, (E/T), 25:5163
iodine-ion channeling at 60 MeV in single crystals of, charge-state distribution of emerging, 25:5164
ion penetration into, path lengths for nitrogen-15, (T), 25:4940
properties for use as encapsulating material for californium-252 sources for neutron capture gamma-ray spectroscopy, 25:4772
GOLD ALLOYS AND SYSTEMS
Au-base--Cd, phase transformations in, crystallographic calculations for cubic to orthorhombic martensitic, 25:4807
GOLD ISOTOPES Au-193
energy levels and transitions in, half-lives, transition probabilities, and gamma mixing and branching of, (E), 25:5701
GOLD ISOTOPES Au-194
beta decay of, log ft value of, (E), 25:5728
GOLD ISOTOPES Au-195
energy levels and transitions in, half-lives, transition probabilities, and gamma mixing and branching of, (E), 25:5701
GOLD ISOTOPES Au-197
electron inelastic scattering and photo-excitation at 2.3 to 3.6 MeV, cross sections for, (E), 25:5637
energy levels from electron inelastic scattering and photo-excitation at 2.3 to 3.6 MeV, parity assignments for, (E), 25:5637
energy-level transitions from photo-excitation and electron inelastic scattering at 2.3 to 3.6 MeV, multipolarity of, (E), 25:5637
energy-level transitions in, E2 strength of 191-keV, (E), 25:5709
half-life of isomeric, (E), 25:5637
Moessbauer isomer shift in gold microcrystals in gelatin, 25:5221 (AD-710293)
neutron inelastic scattering at 5, 6.6, and 8.7 MeV, cross sections, gamma spectra, and angular distributions for, (E), 25:5551 (CEA-R-4047)
GOLD ISOTOPES Au-198
beta decay of, β dealignment parameters of first-forbidden, (E), 25:5708
GOLD ISOTOPES Au-199
beta decay of, γ singles and coincidence spectra from, (E), 25:5698
GONIOMETERS
design and operation of automatic neutron diffraction, 25:4394
GRANITES
neutron energy spectra in, calculation of, (T), 25:4374
neutron shielding efficiency of, calculation of, (T), 25:4374
GRAPHITE
corrosion by impurities in flowing helium gas at 600 to 750°C, 25:4835 (DP-Report-448)
crystal structure and microstructure of pyrolytic, effects of hot pressing to 2900°C and pressures of 700 kg/cm² on, 25:4867
crystallite size of artificial, effects of density on, 25:4866
diffusion of barium in, at 1000°C, effects of concentration on, 25:4860
diffusion of fission product metals in, model for effects of concentration on, 25:4860
electric conductivity of heat treated Pocono-type, 25:4840(R) (LA-4526)
failures in thin disks of, apparatus and method for producing thermal-shock, 25:4851
internal friction of, at 900 to 2700°C, effects of graphitization on, 25:4870
microstructure of polycrystalline, effects of preparation method on electron transmission microscopy study of, 25:4868
neutron scattering at 0.004 to 0.12 eV, scattering transport lengths from, (E), 25:5502
neutron slowing down in, (E/T), 25:5160
phase studies of, 25:4865
pore characteristics of, 25:4856
properties for use in liquid-core nuclear rockets, 25:4865
properties in gas cooled reactor core components, chemical and physical, 25:5942(R) (DP-Report-490)
properties of extruded, effects of batch size and binder type on, 25:4840(R) (LA-4526)
properties of hot-molded, effects of calcining temperature on, 25:4840(R) (LA-4526)
properties of, effects of binders and starting powder packing behavior on, 25:4840(R) (LA-4526)
radiation effects on corrosion of, by carbon dioxide traces in helium, in-pile, 25:4881 (DP-Report-352)
radiation effects on dimensions of, at high temperatures, fast neutron, 25:4883 (DP-Report-473)
radiation effects on grain structure of, neutron, 25:4880 (CEA-N-1374)
radiation effects on physical properties and volume shrinkage rate of, at 1200°C, neutron, 25:4885 (DP-Report-556(Pt.2))
radiation effects on physical properties of, fast neutron, 25:4884 (DP-Report-556(Pt.1))
radioinduced graft polymerization of acrylonitrile onto, γ, 25:4106
radioinduced shrinkage at 900 to 1200°C, neutron, 25:4885 (DP-Report-556(Pt.2))
reactions in HTGR type reactor cores, rates of gasification, (T), 25:5985
reactions with uranium dioxide at 1400 to 1756°C, comments and rebuttal on kinetic study of reduction, 25:4849
thermal conductivity of, effects of porosity on, 25:4840(R) (LA-4526)
thermal expansion at 0 to 750°C, effects of high-temperature annealing and prestressing on coefficient of, 25:4852
graphite--ZrC, thermal conductivity of composites of, 25:4840(R) (LA-4526)
GRAVITATIONAL FIELDS
energy--momentum tensor with scale invariance for, 25:5418
GRAVITATIONAL RADIATION
search for astronometrical sources of, (E), 25:5415
GROUP THEORY
conformal group in, unitary representations of, 25:5293 (IFVE-STF-69-85)
Lie algebra in, commutation relations for eigenvalues of operators for fixed representation of, 25:5357
GROWTH
radiation effects on, of shrubs and trees, γ or x, 25:4724
GYMNOSPERMIDAE
Abies holophylla, radiation effects on, following seed exposure, lethal and mutagenic, γ or x, 25:4724
Ephedra vevadensis, radiation effects on seed production and survival of, in desert ecosystems, γ, 25:4477 (UCLA-12-782, pp 49-81)

H

HADRONS
coupling constant for strange vector current for, renormalization of, (T), 25:5356
currents of, dimensionality of operators for, (T), 25:5306 (NYO-4204-1)
decay of, quark model for broken SU(6) sum rules for parity-violating nonleptonic, (T), 25:5294
interactions of, rho - ω interference in strong, 25:5373 (DNPL/R-7, pp 173-205)
interactions with hadrons at 20 to 65 GeV/c, total cross sections for, (E), 25:5265 (CONF-700314-, Paper 4)
interactions with hadrons at 5 to 70 GeV/c, review of, (E), 25:5272
interactions with hadrons at high energies in amplitude fast variation region, bremsstrahlung from, (T), 25:5357
interactions with hadrons at high energies, quark model for mechanisms for, (T), 25:5354
interactions with hadrons at high energies, solution of unitary condition for amplitude of arbitrary two-body channel in, (T), 25:5355
interactions with hadrons at high energies, unitarity condition for amplitude behavior for forward, (T), 25:5349 (IFVE-STF-69-74)
interactions with hadrons at very high energies and high momentum transfers, quark production in, (E/T), 25:5281 (CONF-700314-, Paper 15)
interactions with hadrons at very high energies, review

of Regge phenomenology for, (T), 25:5347 (CONF-700314-, Paper 13)
interactions with hadrons, broken SU(3) sum rules for coupling constants of, (T), 25:5394
interactions with hadrons, local duality in set of coupled reactions with two-body hadron production in, (T), 25:5352 (SU-1206-235)
interactions with hadrons, phenomenology of multiperipheral models for, (T), 25:5346 (CONF-700314-, Paper 12)
interactions with hadrons, Pomeranchuk decoupling from ordinary Regge trajectories in, (T), 25:5348 (COO-264-562)
interactions with hadrons, scaling behavior in multiperipheral models for, (T), 25:5351 (NYO-2262-TA-225)
interactions with leptons, density-matrix formalism for, 25:5331
interactions with neutrinos at high energies, review of, (T), 25:5339 (CONF-700314-, Paper 7)
production at very high energies in colliding beams, scaling laws for, (T), 25:5315 (CONF-700314-, Paper 8)

HAFNIUM
electronic density of states of hcp and bcc, from bremsstrahlung isochromates, 25:5187
radiation effects on mechanical properties of, fast neutron, 25:4813 (IN-1440)
separation by ion exchange using Alamine 336 or Amberlyst A-21 in aqueous thiocyanate solutions, 25:4137 (IS-T-377)
separation from rare earths by anion exchange using nitric acid--methanol system, 25:4139
surface impurities on, use of Auger electron spectroscopy for detection and identification of, 25:4798

HAFNIUM ISOTOPES Hf-171
electron-capture decay of, gamma spectra and log ft of, (E), 25:5699

HAFNIUM ISOTOPES Hf-176
energy levels of, isomer shift and quadrupole moment relative to hafnium-180 of first 2^+, (E), 25:5668
energy-level transitions in, Moessbauer quadrupole hfs spectra of first rotational gamma ray following Coulomb excitation, (E), 25:5668

HAFNIUM ISOTOPES Hf-178
energy levels of, isomer shift and quadrupole moment relative to hafnium-180 of first 2^+, (E), 25:5668

HAFNIUM ISOTOPES Hf-179
electron inelastic scattering and photo-excitation at 2.3 to 3.6 MeV, cross sections for, (E), 25:5637
energy levels from electron inelastic scattering and photo-excitation at 2.3 to 3.6 MeV, parity assignments for, (E), 25:5637
energy levels from photoexcitation of, spin-parity assignments for, (E), 25:5690
energy-level transitions from photo-excitation and electron inelastic scattering at 2.3 to 3.6 MeV, multipolarity of, (E), 25:5637
half-life of isomeric, (E), 25:5637
photoexcitation cross sections for, (E), 25:5690

HAFNIUM ISOTOPES Hf-180
energy levels of, isomer shift and quadrupole moment relative to hafnium-176 and -178 of first 2^+, (E), 25:5668
energy-level transition in, nuclear structure effect in internal conversion of the 57.54-keV E1, (E), 25:5731

HAFNIUM ISOTOPES Hf-181
beta decay of, gamma spectra from, (E/T), 25:5746

HALDEN BOILING REACTOR
control of, developments in computer, 25:5974
operation of, review of development programs in, 25:5946

HANFORD PRODUCTION REACTORS
heated effluents from, effects of, on migration of juvenile chinook salmon from Columbia River, 25:4504 (BNWL-1472)

HARWELL SYNCHROTRON (NIMROD)
development and operation of, April 1--June 30, 1970, 25:5465(R) (RHEL/R-206)

HAYNES STELLITE NO. 6
corrosion by sodium at 1100°F, 25:4185(R) (NYO-3930-8)

HEALTH PHYSICS
program at UKAEA, 25:4088(R) (NP-18528)
programs at radiochemical processing plants, tabulation of, 25:4515

HEART
failure of dog, effects of, on pulmonary blood flow, 25:4677
metabolism of proteins in cell cultures of rat, 25:4458 (UCLA-12-782, pp 1-21)
radiation effects on electrolyte content in muscles of, in rabbits, x, 25:4698
radiation effects on isoenzymes of lactate dehydrogenase in, of rats, protective effects of methylene blue against whole-body γ, 25:4605
scanning for function, use of iodine-131-labeled albumin for, 25:4658
scanning using technetium-99-labeled pertechnetate, 25:4659
use of plutonium-238 as power source for artificial, radiation dose to dogs during, 25:4432
use of radioisotopes as simulated power sources for artificial, pathological effects of, on dogs, 25:4433

HEART, MECHANICAL
heat source for implantable, design of plutonium-238-fueled, 25:4229
power system for implantable, design of plutonium-238-fueled thermoelectric, 25:4235
power system for, design and performance of plutonium-238-fueled Stirling cycle, 25:4233
power system for, design of implantable plutonium-238-fueled vapor cycle, 25:4234
power system for, design of implantable plutonium-238-fueled, 25:4232
power system for, hazards to population from implantable radioisotope-fueled, 25:4236
power systems for, bench model testing of radioisotope-fueled Rankine and Stirling cycle, 25:4231
power systems for, design of radioisotope-fueled Rankine and Stirling cycle, 25:4230

HEAT PIPES
design of, effects of sonic limitations and startup problems on, 25:6236 (LA-4518)

HEAT-RESISTING ALLOYS AND METALS
properties for use in high-temperature gas-cooled reactors, review of, 25:4779
radiation effects on creep, fracture, hardening, and swelling of, review on, 25:4812 (BNWL-SA-3455)

HEAT SOURCES
design of plutonium-238, for powering implantable heart device, 25:4232
design of radioisotope, for Rankine and Stirling cycle engines for powering heart devices, 25:4230
design, fabrication, and testing of high power density and low dose rate promethium-147 oxide, 25:4217(P)
evaluation of Flintnose-1 payload, methods for ballistic, thermal, trajectory, and radiological safety, 25:4216(R) (SC-PR-70-682)
radiation dose rate measurements for plutonium-238, in-phantom, 25:4517
radiation emission from radioisotope, continuous channel electron multiplier detectors for measurement of, 25:4243
radiation spectra of spacecraft radioisotope, gamma and neutron, 25:4242
safety of implantable radioisotope, for heart assist devices, evaluation of population, 25:4236
testing of instrumented Rankine and Stirling cycle, for powering heart devices, results of bench model, 25:4231
testing of Pioneer/Transit, under reentry conditions, 25:4216(R) (SC-PR-70-682)

HEAT TRANSFER
correlation of critical and Leidenfrost point, in sodium-heated steam generators, 25:4211
mechanisms of film and transition boiling, at surfaces of heated copper spheres in water, 25:4209

HEAT TRANSFER SYSTEMS
sodium vapor monitor for, development of, 25:6046

HEATED EFFLUENTS
discharge into Columbia River from plutonium production reactors, effects of, on migration of juvenile chinook salmon, 25:4504 (BNWL-1472)
effects on population of chinook salmon spawning in Columbia River during 1947 to 1970, 25:4474 (BNWL-1515)
use of power reactor, for fog control, 25:5866

HEATERS
design parameters of cartridge type electrical, for simulating liquid sodium cooled fuel elements, 25:6029
performance of cartridge type electrical, for simulating liquid sodium cooled fuel elements, 25:6029

HELIUM
analysis for low level impurities by gas chromatography, on-line, 25:4012 (IP-Report-443)
antiproton absorption at 20 to 65 GeV/c, cross sections for, (E), 25:5295
antiproton absorption cross sections at 20 to 40 GeV/c, (E), 25:5265 (CONF-700314-, Paper 4)
burning in stars, hydrodynamics of flash, (T), 25:4911
diffusion of bubbles of, in Type 20-25 stainless steel, effects of bubble size on, 25:4758
electron behavior in liquid, photoejection--pressure study of bubble model of, 25:5034 (TID-25601)
electron elastic scattering by, s-wave phase shift near 73.5-eV resonance in, (T), 25:4961
electron pair correlation energies in, calculation using Gaussian geminals, 25:4973
electron reactions at 35 to 150 eV with, angular and energy dependence of generalized oscillator strengths for 1^1S--2^1S transition in, (E), 25:4955
energy levels of, radiative lifetime of metastable 2^1S_0 state, (E), 25:4944
energy of ground-state, calculation using correlated wave functions, 25:4948
helium-ion reactions at 10 to 30 keV with, cross sections for production of metastable triplet helium atoms by charge exchange in, (E), 25:4969
helium-metastable-atom reactions with, cross sections for ionization in, (E), 25:4969
meson (K^-) absorption at 20 to 65 GeV/c, cross sections for, (E), 25:5295
meson (K^-) absorption cross sections at 20 to 40 GeV/c, (E), 25:5265 (CONF-700314-, Paper 4)
meson (π^-) absorption at 20 to 65 GeV/c, cross sections

XUM

for, (E), 25:5295
meson (π^-) absorption cross sections at 20 to 40 GeV/c, (E), 25:5265 (CONF-700314-, Paper 4)
oscillator-strength sums for, upper and lower bounds for, 25:4946
penetration into Earth ionosphere, effects of interstellar, 25:5021
photon reactions with liquid, excess electron ejection by, (E), 25:5060 (NP-18484)
plasma jets of, properties in homopolar devices, 25:5089
plasma of, amplification of vacuum uv radiation from, 25:5090
plasma of, line broadening of triplet diffuse series in arcs, (E), 25:5082 (N-70-33122)
plasma of, wave propagation in magnetized column of, (E), 25:5123 (SU-IPR-366)
proton reactions at 25 to 125 keV with, cross sections for excitation, ionization, and total inelastic scattering and energy distributions of electrons ejected from, (E), 25:4967
proton reactions with, continuum distorted-wave method for calculation of electron capture in, 25:4958
radioinduced production in chromium, copper, iron, nickel, and titanium, fission neutron, 25:4822
radioinduced production in nickel, epithermal, fast, and thermal neutron, 25:4821
reactions between metastable atoms of, spin conservation in ionizing, (E), 25:4960
reactions with gases at 10 to 30 keV of metastable triplet atoms of, cross sections for ionization in, (E), 25:4969
reactions with hydrogen 2^2P atoms, cross sections for de-excitation in, (E), 25:4964
reactions with hydrogen molecules, vibrational excitation in, (T), 25:4954
scattering by helium, crossed-beam measurement of total relative cross section as function of velocity, 25:4965

HELIUM IONS
energy-level transitions of He^+, line widths and relative intensities of 6560- and 10124-A, (E), 25:4950
Lamb shifts for 4S, 5S, and 6S levels of, (E), 25:4950
reactions with gases at 10 to 30 keV, cross sections for production of fast metastable triplet helium atoms by charge exchange in, (E), 25:4969
reactions with single-crystal germanium, minimum energy for sputtering in, (E), 25:5155

HELIUM ISOTOPES He-3
charge-asymmetry energy of, relative to tritium, (T), 25:5812
cooling to millidegree temperatures, compressional, 25:6255 (UCSD-34-P-143-27)
deuteron elastic scattering at 10 and 12 MeV using polarized beams, vector and tensor analyzing powers for, (E), 25:5520 (LA-4465, pp 24.1-2)
deuteron reactions (d,p) at 10 MeV using polarized beam, vector and tensor analyzing power for, (E), 25:5512 (LA-4465, pp 6.1-2)
deuteron reactions (d,p) at 10 MeV, reactance matrix analysis of p--^{5}He system in, (T), 25:5509 (LA-4465, pp 2.1-2)
deuteron reactions (d,p) with polarized, asymmetries in, (E), 25:5524 (LA-4465, pp 32.1-2)
deuteron scattering at 10 MeV, reactance matrix analysis of d--^{3}He system in, (T), 25:5505 (LA-4465, pp 2.1-2)
deuteron scattering at 9.9 and 11.9 MeV using polarized target, asymmetries in, (E), 25:5515 (LA-4465, pp 14.1-2)
electron scattering at high energies, charge and magnetic form factors and charge distributions from, (E/T), 25:5535
monitoring in natural gas lines, flowthrough proportional detector for, 25:4352
nuclear radii and charge and magnetic form factors using Faddeev equations and realistic local potentials, ground-state, (T), 25:5833
photon reactions (γ,p) at 200 to 500 MeV, meson effects in cross section for, (E), 25:5547
photon reactions (γ,p) at 21.5 to 32.5 MeV, angular distributions from, (E), 25:5539
proton elastic scattering at 19.5 MeV using polarized beam and target, correlation parameters for, (E), 25:5506 (CEA-N-1232, pp 81-159)
reactions (He-3,α) with lithium-7 at 5 to 8 MeV, PWBA analysis of energy spectra, excitation functions, and angular distributions from, (E/T), 25:5571
reactions (He-3,α) with silicon-28 at 11 MeV, alpha spectrum at 30° from, (E), 25:5602 (ANU-P-501)
reactions (He-3,d) with cadmium-114 at 18 MeV, angular distributions for, (E), 25:5680 (CEA-N-1232, pp 1-80)
reactions (He-3,d) with calcium-40 at 40 MeV, angular distributions for, (E), 25:5617
reactions (He-3,d) with calcium-48 at 18.5 and 30.2 MeV, deuteron spectra from, (E), 25:5506 (CEA-N-1232, pp 81-159)
reactions (He-3,d) with nitrogen-15, pseudo-bound-states calculation of angular distributions and spectroscopic factors from, (T), 25:5666
reactions (He-3,d) with silicon-29 at 15 MeV, DWBA analysis of angular distributions from, (E/T), 25:5670
reactions (He-3,$\gamma\gamma$) with beryllium-9 at 1.7 to 1.8 MeV, excitation functions for, (E), 25:5573
reactions (He-3,He-6) with carbon-12, magnesium-24, and oxygen-16 at 68 to 70 MeV, Q values for, (E), 25:5668
reactions (He-3,He-6) with magnesium-24, neon-20, oxygen-16, and silicon-28 near 65 MeV, test of isobaric-multiplet mass equation, (E), 25:5640
reactions (He-3,n) with carbon-13 at 4.2 to 5.7 MeV, neutron polarization in, (E), 25:5574
reactions (He-3,n) with fluorine-19 at 4.2 to 5.9 MeV, angular distributions from, (E), 25:5583
reactions (He-3,n) with magnesium-24 at 5 and 5.8 MeV, neutron polarization in, (E), 25:5574
reactions (He-3,p) with aluminum-27 and nitrogen-15 at 18 MeV, angular distributions for, (E), 25:5680 (CEA-N-1232, pp 1-80)
reactions (He-3,p) with sulfur-32 at 5.75 MeV, angular correlations for, (E), 25:5627
reactions (He-3,t) with argon-40 and zinc-64 and -66 at 35 MeV, DWBA analysis of angular distributions from, (E/T), 25:5654
reactions (He-3,t) with iron-56 at 30.2 MeV, triton spectra and angular distributions for, (E), 25:5506 (CEA-N-1232, pp 81-159)
scattering by helium-4 at 19.5 to 51.1 MeV, resonance structure in cross section for elastic, (E), 25:5538
scattering by helium-4 at 8.3 and 13 MeV, absolute polarization in elastic, (E), 25:5518 (LA-4465, pp 19.1-2)

HELIUM ISOTOPES He-4
alpha elastic scattering by, unified nuclear reaction theory for, (T), 25:5870
binding energy and nuclear radius of, calculation using Bolsterli--Feenberg perturbation technique, (T), 25:5537
chlorine-35 reactions (Cl-35,p) at 70 MeV, gamma spectra from, (E), 25:5664
deuteron elastic scattering at 11.5 MeV, comparison of double scattering and polarized ion source measurement of polarization in, 25:5510 (LA-4465, pp 3.1-3)
deuteron elastic scattering at 12 MeV using polarized beam, vector and tensor analyzing power for, (E), 25:5553 (LA-4465, pp 25.1-2)
deuteron elastic scattering at 9.8 MeV using polarized beam, analyzing tensors for, (E), 25:5806 (LA-4465, pp 27.1-6)
electrodisintegration of, cross-section calculations using translationally invariant particle-hole model, (T), 25:5530
electron inelastic scattering from liquid, at low momentum transfer, (E), 25:5528
energy levels from electron inelastic scattering at low momentum transfer, spin--parity assignments for, (E), 25:5528
energy levels from helium-4 (p,tp) reactions at 47 MeV, (E/T), 25:5533
helium-3 elastic scattering at 19.5 to 51.1 MeV, resonance structure in cross section for, (E), 25:5538
helium-3 elastic scattering at 8.3 and 13 MeV, absolute polarization in, (E), 25:5518 (LA-4465, pp 19.1-2)
neutron elastic scattering at 17.6, 20.9, and 23.7 MeV, cross sections and phase shifts for, (E), 25:5508 (LA-4465, pp 1.1-2)
neutron elastic scattering at 27.3 and 30.3 MeV using polarized beams, asymmetry in, (E), 25:5523 (LA-4465, pp 30.1-2)
neutron elastic scattering by, unified nuclear reaction theory for, (T), 25:5870
nuclear charge form factor of, calculation using tensor velocity-dependent potential, (T), 25:5529
photon reactions (γ,d) at 1 to 100 MeV, cross-section calculations including d--d final-state interactions, (T), 25:5543
photon reactions (γ,p) and (γ,n) at 20 to 85 MeV, total cross sections and angular distributions from, (E), 25:5544
photon reactions (γ,p) at 200 to 500 MeV, meson effects in cross section for, (E), 25:5547
proton differential elastic scattering at 20 to 40 MeV, contour plot of polarization from, (E), 25:5526 (UCRL-19943)
proton differential elastic scattering at 24 and 26 MeV, angular distributions and cross sections for, (E), 25:5526 (UCRL-19943)
proton reactions (d,p), (p,He-3),(p,pHe-3), (p,tp), and (p,t) at 47 MeV, Watson--Migdal and direct-reaction analysis of spectra and angular distributions from, (E/T), 25:5533
proton reactions (p,He-3p) at 47 MeV, np singlet scattering length from, (E/T), 25:5533
triton elastic scattering at 6 to 12.3 MeV, absolute polarization in, (E), 25:5518 (LA-4465, pp 19.1-2)
triton elastic scattering at 6 to 15 MeV, triton polarization in, (E), 25:5511 (LA-4465, pp 5.1-2)

HEMATITES
Morin spin-flip transition in, search for, 25:5221 (AD-710293)

HEMATOPOIESIS
radiation effects on, in rats following intratracheal injection of thorium dioxide, a, 25:4700

HEMATOPOIETIC SYSTEM
radiation effects on, of mice, effects of dose and postirradiation time on recovery from x, 25:4705

XUM

HEMATCPORPHYRIN
radioprotective effects of, administered immediately prior to exposure, on stem cells in mice, γ, 25:4572
HEPTANE, HEXADECAFLUORO-
separation of isomers of, by gas chromatography, 25:4111(R) (ORO-3905-2)
1-HEPTENE
radiolysis of solid, reversible photoreactions of free radicals of allyl type from γ, 25:4125
1-heptene--3-methylpentane, radiolysis of, reversible photoreactions of free radicals of allyl type from γ, 25:4125
1-HEXENE
radiolysis of solid, reversible photoreactions of free radicals of allyl type from γ, 25:4125
1-hexene--3-methylpentane, radiolysis of, reversible photoreactions of free radicals of allyl type from γ, 25:4125
HEXOKINASE
radiosensitivity of activity of, in solutions, effects of iodine compounds on x, 25:4569
HIGH-ENERGY PHYSICS
conference on very high-energy interactions, (E/T), 25:5244 (CONF-700314)
High Energy Physics Index. Vol. 8, No. 18, 25:5312
High Energy Physics Index. Vol. 8, No. 19, 25:5314
High Energy Physics Index. Vol. 8, No. 20, 25:5313
HIGH-TEMPERATURE GAS-COOLED REACTOR EXPERIMENT
coolant for, heat transfer and gas flow properties of helium, 25:5942(R) (DP-Report-496)
core components in, corrosion and properties of graphite, 25:5942(R) (DP-Report-490)
fuel cycle for, analysis of optimum economic, 25:5942(R) (DP-Report-490)
fuel reprocessing for, equipment and procedures for, 25:5942(R) (DP-Report-490)
fuels for, equipment and methods for post-irradiation testing of, 25:4262 (DP-Report-446)
fuels for, irradiation testing of, 25:5942(R) (DP-Report-490)
fuels for, preparation and properties of pyrolytic carbon coated ceramic particle, 25:5942(R) (DP-Report-490)
instrument development for, 25:5942(R) (DP-Report-490)
neutron spectra in first core of, integral, (E/T), 25:5952 (DP-Report-442)
operation of, review of development programs in, 25:5947
physics parameters of, 25:5942(R) (DP-Report-490)
pipes for, testing of clam-type stainless steel sealing valves in, 25:4183 (DP-Report-484)
power distribution in first core of, radial and axial, (E/T), 25:5952 (DP-Report-442)
steam generator for, development of tube materials for, 25:4748 (DP-Report-537)
temperature measurements in, pulsed ultrasonic thermometer for, 25:4388 (DP-Report-498)
temperature measurements in, resonant probe thermometer for, 25:4389 (DP-Report-590)
transfer function measurements during operation of first core in, (E/T), 25:5953 (DP-Report-445)
HOLMIUM
determination of trace amounts of, in uranium by chemical separation and spectroscopy, 25:4021
Hall effect in single crystals of, anomalous magnetization dependence of, 25:5219
magnetic phase transition in, sound propagation near, 25:5186
magnetic properties and structure of, neutron inelastic scattering study of, 25:5214
magnetic properties of single crystals of, (E/T), 25:5194
oxidation of thin films of, electron microscopic study of, 25:4767
separation of trace amounts of, from aqueous nitric acid solutions by solvent extraction using D2EHPA in toluene containing trace amounts of uranium, 25:4150
HOLMIUM ALLOYS AND SYSTEMS
Al--Ho, magnetic structure of HoAl, neutron-diffraction study, 25:5208
Co--Ho, magnetic resonance of $HoCo_3$, microwave, 25:5200
Co--Ho, magnetic structure of $HoCo_3$, neutron diffraction study, 25:5210
Er-base--Ho, magnetic structure of, neutron-diffraction study, 25:5207
Fe--Ho, magnetic structure of Ho_6Fe_{23} and $HoFe_2$, neutron-diffraction study, 25:5211
Ho--Ni, magnetic structure of HoNi, 25:5209
Ho--Tb, magnetic properties of, magnon energies and exchange interactions, 25:5213
HOLMIUM ISOTOPES Ho-157
energy levels in, ground-state band, (E), 25:5688 (UCRL-19961)
HOLMIUM ISOTOPES Ho-159
energy levels in, ground-state band, (E), 25:5688 (UCRL-19961)
HOLMIUM ISOTOPES Ho-160
energy levels in, ground-state band, (E), 25:5688 (UCRL-19961)
HOLMIUM ISOTOPES Ho-161
energy levels in, ground-state band, (E), 25:5688 (UCRL-19961)
HOLMIUM ISOTOPES Ho-162
energy levels in, ground-state band, (E), 25:5688 (UCRL-19961)
HOLMIUM ISOTOPES Ho-163
electron-capture decay of, Q values and M/L capture ratios from, (E), 25:5748
HOLMIUM ISOTOPES Ho-165
alpha reactions (α,2n) at 21 to 27 MeV, gamma spectra and angular distributions from, (E), 25:5726
energy levels in, ground-state band, (E), 25:5688 (UCRL-19961)
neutron capture integral in fast region, (E), 25:5656
HOLMIUM URANATES
$HoUO_4$--ThO_2, spectra and phase studies of, 25:4084
HORMONES, ADRENAL
corticosteroids, effects on count of eosinophils in bone marrow of rats in comparison to effects of depressant drugs, 25:4455(R) (ORO-3329-7)
HORMONES, PANCREATIC
insulin, extraction of iodine-131-labeled, from human plasma for radioimmunoassay, 25:4420
HORMONES, PARATHYROID
effects on radioisotope metabolism in bone, 25:4423 (COO-1601-23)
HORMONES, PITUITARY
growth hormones, radioimmunoassay in human blood, methods for, 25:4422
HORMONES, PLANT
gibberellic acid, radioprotective effects of, against chromosome aberrations and seed damage in barley, γ, 25:4490
indole-3-acetic acid, effects of growth of γ-irradiated Triticum vulgare, 25:4718
HORMONES, SEX
estradiol, effects on hemopoietic cell growth in spleen of mice, 25:4471
testosterone, effects on γ-radiosensitivity of ovaries in catfish, 25:4591
HORMONES, THYROID
thyroxine, effects on cesium-134 retention in rats, effects of adrenalectomy and temperature on, 25:4450
HOT CELLS
construction of remotely operated high-purity inert-atmosphere mockup of, for chemical analysis of highly radioactive sodium coolants, 25:4310
decontamination of NRTS Fuel Cycle Facility, for entry, methods for, 25:4299
design and operation of TURF, for californium-252 production and source fabrication, 25:4304
design at Research Establishment Risoe, Denmark, 25:4262 (DP-Report-446)
design for postirradiation inspection of fuels at JAERI, 25:4298
equipment for viewing and photographing irradiated samples in, development of stereomacroscopic, 25:4305
equipment maintenance and performance in, after six years of operation, 25:4300
filter system for high-purity argon atmosphere NRTS, design and operation of high-efficiency, 25:4157
fires in, equipment and methods for control, detection, and prevention of, 25:4153
operation of Attila, experience in, 25:4261 (CEA-R-4067)
use in examining EBR-II fuel elements for determining interim performance, 25:4301
HUMBOLDT BAY POWER REACTOR
control elements for, revised withdrawal time limit for, 25:5917 (DOCKET-50133-44)
operations incident of November 27, 1970, safety analysis of reduced off site power, 25:5891 (DOCKET-50133-43)
HYDRAZINE
complexes with uranium(IV) fluorides, preparation of, 25:4058
HYDRAZINE, METHYL-
effects on DNA in Ehrlich ascites tumor cells, induction of strand breaks by, 25:4567
effects on x-radiosensitivity of Ehrlich ascites tumor cells in mice, 25:4567
HYDRIDES
thermodynamic properties of, effects of deuterium on, 25:4072
HYDROCARBONS
analysis for hydrogen, review on neutron absorption method for, 25:4035
HYDROCHLORIC ACID
effects on phosphorescence produced by x radiation effects on indole in polar solution, 25:4085
HYDRODYNAMICS
theory for radiations in, 25:5095 (CEA-R-4057)
HYDROGEN
content in zirconium hydride-coated zirconium, effects of thermal cycling at 298 to 689°K on supercharging of, 25:4756
corrosive effects as impurity in flowing helium on graphite at 600 to 750°C, 25:4835 (DP-Report-448)
determination in boron, 25:4009 (TID-25190)
determination in hydrocarbons, review on slow neutron absorption method for, 25:4035
determination in sodium, development of analytical standards for, 25:4736(R) (ANL/ST-3)
determination in sodium, development of on-line system for, 25:4736(R) (ANL/ST-3)
deuteron reactions (d,n) at 12 MeV, polarization transfer at 0° in, (E/T), 25:5532

XUM

deuteron reactions (d,p) at 52.3 MeV, angular distribution of n-p interacting pairs from, (E), 25:5548
effects on crack growth in aluminum--titanium-base--vanadium alloys at sustained loads, 25:4762
embrittlement of zirconium pressure tubes, analysis of, 25:6191 (RISO-214, pp 255-87)
energy levels of atomic, separation between $2^2S/sub\ ^1/_2/$ and $2^2P/sub\ ^3/_2$, (E), 25:4951
fluorescence of, collisional quenching of Lyman-α, (E), 25:4964
helium-ion reactions at 10 to 30 keV with molecular, cross sections for production of fast metastable triplet helium atoms in, (E), 25:4969
helium-metastable-atom reactions with molecular, cross sections for ionization in, (E), 25:4969
meson (μ) capture at low energies, PCAC hypothesis for effective pseudoscalar coupling in, (T), 25:5333
meson (π^-) capture by, x-ray spectrum from, (E), 25:5288
meson reactions (π^-,γ) at 250 MeV/c, neutron time-of-flight and gamma energy spectra from, (E), 25:5600
neutron differential elastic scattering at 24.0 MeV, phase-shift analysis of angular distributions and cross sections for, (E/T), 25:5540
oscillator-strength sums for atomic, upper and lower bounds for, 25:4946
photoinduced production of hot atoms of, at 0.5 to 5 eV, 25:4132
plasma of, diagnostics during two-phase excitation at cyclotron frequency, 25:5087
plasma of, ion cyclotron heating by two-phase excitation, (E), 25:5076
plasma of, optical measurements of electrostatic turbulence in, (E), 25:5083
polarizability of molecular, calculation of static electric dipole, using nonsymmetrical wave function, 25:4949
proton reactions with atomic, continuum distorted-wave method for calculation of electron capture in, 25:4958
reactions between atomic and molecular, at high and low energies, 25:6223 (CALT-767-P-4-66)
reactions of hot atoms of, comparison of reactions of recoil tritium atoms with, 25:4132
reactions with ammonia, carbon dioxide, carbon monoxide, and methane at 1 to 25 keV of atomic, cross sections for ionization in, (E), 25:4963
reactions with deuterium, helium, hydrogen, and nitrogen gases of 2^2P atoms of, cross sections for de-excitation in, (E), 25:4964
reactions with helium of molecular, vibrational excitation in, (T), 25:4954
scattering by rare gases of atomic, calculation of interaction potentials from elastic, 25:4957
yields from γ radiolysis of 2,2-dimethylpropane, effects of deuterated ammonia and nitrous oxide on, 25:4113
yields from γ radiolysis of benzene--cyclohexane mixture, effects of composition on, 25:4121
yields from radiolysis of water, effects of various ions on, 25:4120
yields from the gas-phase α radiolysis of hydrogen sulfide or propane, 25:4119
H--H_2O, diffusion in carbons at 18 to 900°C, measurement of effective, 25:4856

HYDROGEN IONS (H^-)
energy of ground-state, calculation using correlated wave functions, 25:4948

HYDROGEN IONS (H_2^+)
reactions with molybdenum polycrystals and tungsten monocrystals at 10 to 30 eV, electron yields and energy distributions from, (E), 25:4943

HYDROGEN ISOTOPES
meson (μ^-) reactions with, hyperfine-structure transitions and isotope exchange in, (T), 25:4952 (JINR-P4-5039)

HYDROGEN PEROXIDES
decomposition of, catalytic effects of normal and irradiated semiconductor metal oxides on, 25:4099
decomposition of, radiation effects on catalytic properties of copper and nickel complexes in, 25:4103
effects on hydrogen yields from radiolysis of water, 25:4120
effects on phosphorescence produced by x radiation effects on indole in polar solution, 25:4089

HYDROGEN SULFIDES
effects on yields from radiolysis of ethylene, 25:4122
radiolysis of gaseous, hydrogen yields from α, 25:4119

HYDROGEN SYSTEMS
Fe--H, nonasymptotic structure of 28-keV neutron spectrum near intermediate resonances in, (T), 25:5505
H--Na--D, phase studies of, 25:4736(R) (ANL/ST-3)

HYDROXYL (HO)
radio emission from interstellar, maser action in, (T), 25:4917

HYPERFRAGMENTS
decay in emulsions, proton and neutron stimulation in nonmesonic, (E), 25:5277
production in K⁻ reactions with nuclei at 3.0 GeV/c in emulsions, (E), 25:5277

HYPERONS (Λ)
binding energy in nuclear matter, cluster-expansion methods for, (T), 25:5390
production in final states of anti p + p interactions at 2.4 and 2.9 GeV/c, differential cross sections for, (Σ), 25:5270
production in γ + p → K⁺ + Λ interactions at 1.3 GeV, differential cross sections for, (E), 25:5252
production in meson (K^0) reactions with carbon, chlorine, copper, and fluorine at 120 MeV, cross sections for, (E), 25:5300
trapping probability from production in K⁻ + N interactions in freon bubble chamber, 25:5299

HYPERONS (anti Λ)
production in final states of anti p + p interactions at 2.4 and 2.9 GeV/c, differential cross sections for, (E), 25:5270

HYPERONS (Σ⁻)
conversion rate of Σ → Λ from production in K⁻ + p → Σ⁻ + π^+ in freon, 25:5298
decay Σ⁻ → n + μ + ν in hydrogen bubble chamber, branching ratio for, (E), 25:5265
decay Σ⁻ → n + π^- in hydrogen bubble chamber, parameters for, (E), 25:5260
interactions Σ + N → Λ + N from production in K⁻ + p → Σ⁻ + π^+ interactions in freon, absorption probability of, 25:5298
production in K⁻ + p → Σ⁻ + π^+ interactions at 385 MeV/c in hydrogen bubble chamber, (E), 25:5260
production in K⁻ + p interactions at rest in hydrogen bubble chamber, (E), 25:5269

HYPERONS (Σ^0)
production in γ + p → K⁺ + Σ^0 interactions at 1.45 GeV, differential cross sections for, (E), 25:5253
production in meson (K^0) reactions with carbon, chlorine, copper, and fluorine at 120 MeV, cross sections for, (E), 25:5300

HYPERONS (anti Σ^0)
production in final states of anti p + p interactions at 2.4 and 2.9 GeV/c, differential cross sections for, (E), 25:5270

HYPERONS (Σ⁺)
decay Σ⁺ → n + μ^+ + ν in hydrogen bubble chamber, upper limit for branching ratio for, (E), 25:5265
decay Σ⁺ → n + π^+ in hydrogen bubble chamber, parameters for, (E), 25:5260
decay Σ⁺ → p + π^0 in hydrogen bubble chamber, parameters for, (E), 25:5260
production in K⁻ + p → Σ⁺ + π^- interactions at 385 MeV/c in hydrogen bubble chamber, (E), 25:5260
production in K⁻ + p interactions at rest in hydrogen bubble chamber, (E), 25:5269

HYPERONS (Ξ)
mass of, broken SU(3) x SU(3) chiral algebra and intermediate-mass sum rule for, (T), 25:5395

HYPERONS (Ξ⁻)
production in anti p + p → Ξ⁻ + anti Ξ⁻ interactions at 2.9 GeV/c, total cross sections for, (E), 25:5270

HYPOXIA
effects on activity of enzymes in blood plasma of rats, 25:4594
effects on radiosensitivity of dry fern spores, ionizing, 25:4709
effects on x-radiosensitivity of green algae, 25:4574
radioprotective effects of, on mice, reaction mechanisms for x, 25:4578
radioprotective effects of, reaction mechanisms for, 25:4594

I

IMMUNE REACTIONS
effects of transplants of irradiated fetal tissue on, against virus-induced tumors in mice, 25:4656(R) (ORNL-4615)
radiation effects on primary and secondary antibody, in mice, 2.2-GeV proton, γ, and x, 25:4470
radiation effects on, of chickens to allogeneic cells, combined effects of bursectomy or thymectomy on cobalt-60 γ, 25:4468

IMPACT SHOCK
effects on piping components and systems, summary of experience on, 25:4188 (TID-25552)

INCONEL 600
mechanical properties of, effects of explosive shock deformation on, 25:4802
microstructure of, effects of explosive shock deformation on, 25:4802

1,2,3-INDANTRIONE
effects on electron-radiosensitivity of DNA in Escherichia coli, 25:4551
effects on x-radiosensitivity of ascites tumor cells, 25:4562

INDIAN POINT POWER REACTOR, UNIT 1
fuel shipping cask for, safety analysis of neutron radiation levels for spent, 25:5513 (DOCKET-50003-60)

INDIUM
electric conductivity of single crystals of, anisotropy in, (E/T), 25:5185
electron reactions with, ionization cross sections for, (E), 25:4956
neutron elastic scattering at 4 MeV, differential cross sections and polarizing abilities at 150 to 180° from, (E), 25:5762

separation by ion exchange using Alamine 336 or Amberlyst A-21 in aqueous thiocyanate solutions, 25:4137 (IS-T-377)
separation from cadmium, tellurium, and tin by reversed-phase extraction chromatography, 25:4143
INDIUM ALLOYS AND SYSTEMS
Bi--In-base, quantum oscillations and order of phase charge in microcylinder of, 25:5045
Bi--In-base, quantum oscillations in microcylinder of, 25:5046
In--Pb-base, stress relaxation induced by magnetic field reduction in superconducting, 25:5036(R) (NYO-4060-5)
In-base--Pb, electric conductivity of single crystals of, anisotropy in, (E/T), 25:5185
In-base--Pb, thermal conductivity of normal and superconducting, (E/T), 25:5055
INDIUM CHLORIDES
Coulomb fragmentation of, from electron-capture decay of indium-114m, energy spectra of cadmium fragments from, (E), 25:5153
INDIUM IODIDES
Coulomb fragmentation of, from electron-capture decay of indium-114m, energy spectra of cadmium fragments from, (E), 25:5153
INDIUM ISOTOPES
production from proton fission of uranium at 570 MeV and 18.2 GeV, cross sections for, (E), 25:5784
INDIUM ISOTOPES In-111
energy levels from cadmium-110 proton elastic scattering, spectroscopic factors for isobaric analog, (E), 25:5752
INDIUM ISOTOPES In-113
distribution in tissues of rats, effects of particle size and pH on, 25:4437
energy levels from cadmium-112 proton elastic scattering, spectroscopic factors for isobaric analog, (E), 25:5752
evaluation of metastable, for liver scanning in comparison to gold-198, 25:4687
neutron reactions (n,2n) at 13.1 to 18.2 MeV, excitation functions and isomeric cross-section ratios for, (E), 25:5763
preparation of metastable, from cow generator for use in scanning, effects of pH on particle sizes in, 25:4437
radiation dose from iron hydroxide-incorporated metastable, to man during lung scanning, methods for calculating absorbed, 25:4511
use for scanning human lungs for blood flow during ventricular failure, combined use with technetium-99 for double scanning, 25:4677
use of aerosols of metastable, for lung scanning for function, 25:4657 (UCLA-12-782, pp 89-125)
use of chelate-incorporated, for scanning kidney transplants for function, 25:4657 (UCLA-12-782, pp 89-125)
use of metastable, for lung scanning, 25:4680
use of metastable, for lung scanning during pregnancy, effects of, on fetus, 25:4673
INDIUM ISOTOPES In-114
electron capture decay of isomeric, energy spectra of cadmium fragments from, in indium chloride and indium iodide, (E), 25:5153
INDIUM ISOTOPES In-115
energy levels from cadmium-114 (He-3,d) reactions, (E), 25:5680 (CEA-N-1232, pp 1-80)
energy levels from cadmium-114 proton elastic scattering, spectroscopic factors for isobaric analog, (E), 25:5752
neutron capture by, cross sections for, (E), 25:5789
neutron reactions (n,2n) at 13.1 to 18.2 MeV, excitation functions and isomeric cross-section ratios for, (E), 25:5763
INDIUM ISOTOPES In-116
energy-level transitions from neutron capture by indium-115, strength functions for, (E), 25:5789
INDIUM ISOTOPES In-117
yield ratios from proton fission of bismuth and uranium at 159 MeV to 18.2 GeV, isomeric, (E), 25:5784
INDOLE
effects on x-radiosensitivity of Serratia marcescens, 25:4557
radiation effects on polar solutions of, effects of electron scavengers on phosphorescence produced by x, 25:4089
INDOLE, 3-(2-AMINOETHYL)-5-METHOXY-
radioprotective effects of, on mice, combined effects of AET on x, 25:4583
radioprotective effects of, on rats, γ, 25:4581
INDOLE-2,3-DIONE
effects on x-radiosensitivity of fern spores, 25:4573
INFORMATION CENTERS
operations for Computing Technology Center, 25:6200
INFORMATION RETRIEVAL SYSTEMS
operations of digital computer, 25:6200
INFRARED RADIATION
effects on germination of sugarbeet seeds, 25:4722
effects on physiological reactions in man, high dose, 25:4715
INORGANIC COMPOUNDS
production of labeled, in COMECON states, review on, 25:4128
INSECTA
Ceratitis capitata, radiosterilization of, use of sterile male technique for, 25:4733 (NYO-2043-216, pp 19-48)
Drosophila sp., radioinduced crossover aberrations in chromosomes of male, comparison of frequency of, with aberrations induced by methylnitroso compounds, x, 25:4481
Hyphantria sp., radiation effects on reproductive capacity of, effects of sex on, cobalt-60 γ, 25:4735
Hyphantria sp., radiosensitivity of pupae of, in relation to radiosterilization, cobalt-60 γ, 25:4735
Leucoptera coffeella, radiation effects on longevity of, effects of dose on γ, 25:4733 (NYO-2043-216, pp 19-48)
Leucoptera coffeella, radiosterilization of, use of sterile male technique for, 25:4733 (NYO-2043-216, pp 19-48)
Tribolium confusum, radiation effects on survival of, effects of infection with cysticercoids on γ, 25:4692 (CCO-1209-13)
INSTRUMENTS
description of closed circuit spirometer for obtaining relation between intrapulmonary xenon-133 concentration and external counting rate, 25:4663
radiation effects on spacecraft-borne, radioisotope thermoelectric generator, 25:4409
reliability analysis of mechanical, for reactors, 25:6189 (RISG-214, pp 11-20)
shielding of spacecraft, from radiation by plutonium dioxide heat sources, 25:4246
INTERNAL CONVERSION
higher-order corrections to, (T), 25:5826
theory for, higher approximation effects in, (T), 25:5844
INTERSTELLAR MATERIAL
helium, penetration into Earth ionosphere, 25:5021
protons, penetration into Earth ionosphere, 25:5021
INTESTINES
calcium-45 sorption in, of rats, effects of concentration on, 25:4430
radiography of small, in man using double contrast technique, x, 25:4686
INVARIANCE PRINCIPLES
book: Symmetries and Reflections. Scientific Essays, 25:5396
CP invariance in $K^+ \to 3\pi$ decay in propane bubble chamber, (E), 25:5263
CP violation in radiative and leptonic anti K^0 decays in hydrogen bubble chamber, (E), 25:5262
parity and time reversal conditions in nuclear scattering, derivation from n-matrix elements, 25:5875
time reversal invariance in $K^+ \to \gamma + e^+ + \nu$ decay, on-shell current algebra for effects of electromagnetic violations on, (T), 25:5342
time reversal invariance test using detailed balance in oxygen-16 (d,α) and nitrogen-14 (α,d) reactions, (E), 25:5596
time reversal violation in inelastic $e^- + p$ and $e^+ + p$ interactions, search for, (E), 25:5400 (UCRL-20041)
IODINE
determination of microgram amounts of, by electrochemical isotopic dilution, 25:4027
plasma of, production of quasi-electron-free, 25:5103
recovery from fuel reprocessing plant off-gases, site evaluation of facility for, 25:4155 (DOCKET-50201-53)
IODINE IONS
channeling in gold single crystals at 60 MeV, emergent charge-state distribution, 25:5164
IODINE ISOTOPES
removal from reactor containment air, efficiency of charcoal filter for, 25:4142
IODINE ISOTOPES I-125
energy levels from xenon-125 electron-capture and beta decay, spin--parity assignments for, (E), 25:5764
energy-level transitions from xenon-125 electron-capture and beta decay, angular correlations of, (E), 25:5764
use as γ source for transmission scanning of human bones for measurement of mineral content, 25:4634 (CONF-700515-, pp 33-47)
use as γ source for transmission scanning of human bones for measurement of mineral content, 25:4635 (CONF-700515-, pp 48-57)
use as γ source for transmission scanning of human bones for measurement of mineral content, 25:4648 (CONF-700515-, pp 291-302)
use as γ source for transmission scanning of human bones for measurement of mineral content, 25:4631 (CONF-700515-, pp 1-21)
use as γ source for transmission scanning of human bones for measurement of mineral content, 25:4636 (CONF-700515-, pp 169-87)
use as γ source for transmission scanning of human bones for measurement of mineral content, 25:4653 (CONF-700515-, pp 408-22)
use as γ source for transmission scanning of human bones for measurement of mineral content, 25:4625 (CONF-680211-, pp 296-308)
use as γ source for transmission scanning of human bones for measurement of mineral content, 25:4626 (CONF-680211-, pp 308-19)
use as γ source for transmission scanning of human bones for measurement of mineral content, 25:4624 (CONF-680211-, pp 283-96)

XUM

use as γ source for transmission scanning of soft tissues for measurement of lipid content, 25:4646 (CONF-700515-, pp 272-3)
IODINE ISOTOPES I-127
abundance in meteorites, (E/T), 25:4922
energy levels from tellurium-127 decay, spin and parity of, (E), 25:5734
neutron activation resonance integrals of, thermal, (E), 25:5681 (CNEA-274)
neutron capture by, cross sections for, (E), 25:5789
separation of xenon-128 from, using traps, 25:4129
IODINE ISOTOPES I-128
abundance in meteorites, (E/T), 25:4922
energy-level transitions from neutron capture by iodine-127, strength functions for, (E), 25:5789
IODINE ISOTOPES I-129
abundance in meteorites, (E/T), 25:4922
IODINE ISOTOPES I-131
incorporation in albumin, for measuring volume of blood plasma in swine, 25:4411 (CEA-R-4031)
radiation dose from albumin-incorporated, to man during lung scanning, methods for calculating absorbed, 25:4511
removal from reactor containment air, efficiency of charcoal filter for, 25:4142
use as tracer for thyroid function studies, dose standardization for, 25:4661
use for endolymphatic therapy of Hodgkin's disease, 25:4512
use for heart scanning for function, 25:4658
use for lung scanning, 25:4680
use for lung scanning during pregnancy, effects of, on fetus, 25:4673
use of albumin macroaggregate-incorporated, for lung scanning for localization of embolisms, 25:4674
use of albumin macroaggregate-incorporated, for lung scanning for function, 25:4657 (UCLA-12-782, pp 89-125)
use of albumin-incorporated, for perfusion scans of human lungs, 25:4668
use of albumin-incorporated, for scanning human lungs for perfusion, 25:4665
use of albumin-macroaggregate incorporated, for scanning of human lungs, 25:4670
use of hippuran-incorporated, for kidney scanning, 25:4659
ION BEAMS
interactions with nuclei, formalism for spin-$^3/_2$, 25:5807 (LA-4465, pp 35.1-2)
phase characteristics of, methods for measurement of, 25:5457 (NP-18507)
transport of polarized, transfer matrix method for calculating spin aberrations in, 25:5454 (LA-4465, pp 16.1-16)
ION SOURCES
beam polarization measurement of Lamb-shift, quench ratio method for, 25:5453 (LA-4465, pp 10.1-2)
description of hollow-anode electron-impact, for implantation doping of semiconductors, 25:5165
development of negative, for Van de Graaff accelerators, 25:5680 (CEA-N-1232, pp 1-80)
performance of polarized, for Tandem Van de Graaff accelerator, 25:5452 (LA-4465, pp 9.1-2)
IONOSPHERE
charged-particle motion in field of magnetic dipole, (T), 25:5004
D region, electron energy loss factor calculation for, 25:5001 (AD-710426)
D region, ion chemistry of, (E), 25:5013
D region, oxygen ions in, metastable molecular oxygen source for positive, 25:5011
E region, nitrogen oxide NO and positive nitrogen ions in, metastable nitrogen atoms source for, 25:5011
electron energy loss factors for, calculation of, 25:5001 (AD-710426)
F region, maintenance of winter, correlation to ionization in polar ionosphere, (E/T), 25:5008
F region, nitrogen ions in, metastable positive oxygen ions source for positive, 25:5011
F2 layer, ionization at peak of, correlation of ionic production and transport processes to vertical distribution of, (E/T), 25:5014
interstellar particle penetration into Earth, effects of neutral, 25:5021
ionization in mid-latitude lower, anomalies of, (E/T), 25:5006
ionization in polar, correlation to maintenance of winter F layer, (E/T), 25:5008
metal elements in lower, ionization and loss processes for meteoric, 25:5012
polar cap absorption in, vlf signal-associated, (E), 25:5020
sporadic E, proton precipitation-associated ionization in auroral, 25:5010
x-ray effects on ionization of lower, bremsstrahlung, (E/T), 25:5019
IONS
energy levels of highly ionized, having Z = 6 to 92, calculation of average energies of ground, singly, and doubly excited, 25:4945
energy of, matrix elements of second-order relativistic corrections to, 25:4971
mobility of radioactive, in air, time-of-flight measurement of, 25:4395
penetration of light, into solid bodies, path lengths for, (T), 25:4540
radius of, compilation of, for use in geochemistry, 25:4085
reactions with nuclei, survey on heavy, 25:5617
IRIDIUM
properties for use as encapsulating material for californium-252 sources for neutron capture gamma-ray spectroscopy, 25:4772
IRIDIUM ISOTOPES Ir-191
electron inelastic scattering and photo-excitation at 2.3 to 3.6 MeV, cross sections for, (E), 25:5637
energy levels from electron inelastic scattering and photo-excitation at 2.3 to 3.6 MeV, parity assignments for, (E), 25:5637
energy-level transitions from photo-excitation and electron inelastic scattering at 2.3 to 3.6 MeV, multipolarity of, (E), 25:5637
half-life of isomeric, (E), 25:5637
IRIDIUM ISOTOPES Ir-193
energy-level transition in, analysis for time-reversal invariance in 73-keV, (E), 25:5715
IRON
determination in boron, 25:4009 (TID-25190)
determination in PuO_2--U_3O_8, effects of ratio of plutonium oxide to uranium oxide on spectrographic, 25:4015 (NUMEC-3524-76)
determination in rocks by neutron activation, 25:4047
determination in titanium ore by neutron capture gamma spectroscopy using californium-252 source, 25:4036
determination of, review of modern physical methods for, 25:4010
determination simultaneously with uranium using platinum working electrode, coulometric, 25:4025
effects of impurities of, on properties of uranium, 25:4747 (AWRE-O-63/70)
gamma scattering from, barriers of finite thickness, (E), 25:5149
magnetic transient field in, platinum-isotope ion-implantation perturbed-angular-correlation study of, (E), 25:5189
Moessbauer spectra of thin films of, 25:6231 (COO-623-164)
neutron inelastic scattering at 14 MeV, energy spectra and angular distribution from, (E), 25:5635
neutron spectra in, for assessment of data files, (E), 25:5495
properties for use as encapsulating material for californium-252 sources for neutron capture gamma-ray spectroscopy, 25:4772
radioinduced helium production in, fission neutron, 25:4822
separation by ion exchange using Alamine 336 or Amberlyst A-21 in aqueous thiocyanate solutions, 25:4137 (IS-T-377)
separation from aluminum and gallium by ion exchange in thiocyanate solutions using Alamine 336, 25:4137 (IS-T-377)
separation from hard water by ion exchange in thiocyanate solutions using Alamine 336, 25:4137 (IS-T-377)
separation from rare earths by ion exchange in thiocyanate solutions using Amberlyst A-21, 25:4137 (IS-T-377)
separation of thorium from, by photochemical precipitation, 25:4026
IRON ALLOYS AND SYSTEMS
analysis for niobium using 4-(2-pyridylazo)resorcinol, photometric, 25:4018
Al--Fe-base, K-absorption spectrum edge in, 25:5181
C--Cr--Fe--Ni, internal friction of austenitic, at 25 to 400°C, effects of defect--interstitial solute reactions on, 25:4786 (COO-1676-13)
C--Fe--Ni, internal friction of austenitic, at 25 to 400°C, effects of defect--interstitial solute reactions on, 25:4786 (COO-1676-13)
C--Fe-base--Ni, internal friction in martensitic, at 20 to 500°C, controlling mechanisms of, 25:4786 (COO-1676-13)
Co--Fe, diffusion in fcc, bcc, and CsCl-type ordered FeCo, isotope effects in, 25:4761
Cr--Fe-base, phase studies of miscibility gap in, effects of vanadium additions on, 25:4787
Cr--Fe-base--Ni, carburization-decarburization in sodium at 500 to 800°C, effects of carbon content on, 25:4785
Cr--Fe-base--Ni, compatibility with sodium at 800°C, effects of carbon transport on, 25:4736(R) (ANL/ST-3)
Cr--Fe-base--V, phase studies of miscibility gap in, 25:4787
Fe--H, nonasymptotic structure of 28-keV neutron spectrum near intermediate resonances in, (T), 25:5605
Fe--Ho, magnetic structure of Ho_6Fe_{23} and $HoFe_2$, neutron-diffraction study, 25:5211
Fe--Ni, purification of vacuum melts of, effects of composition, reduced pressure, and alloying additions of aluminum, chromium, molybdenum, titanium, and tungsten on, 25:4744
Fe-base--Mo, K-absorption spectrum edge in, 25:5181
IRON FLUORIDES FeF_2
magnetic phase transition in, sound propagation near,

25:5186
IRON ISOTOPES Fe-54
deuteron reactions (d,n) at 5.8 MeV, differential cross sections for, (E), 25:5675
effects on spectra of ferrocene, 25:4067
energy level of, lifetime of lowest 6^+, (E), 25:5646
energy levels from proton inelastic scattering, lifetimes and spin assignments for, (E), 25:5673
energy levels in, 3h--1p and 4h--2p influence on $J = 0^+$, (T), 25:5669
energy-level transitions from proton inelastic scattering, multipolarities and branching ratios for, (E), 25:5673
lithium-7 reactions (Li-7,He-6) at 24.4 MeV, energy spectra from, (E), 25:5680 (CEA-N-1232, pp 1-80)
photon reactions (γ,pn) and (γ,2n) at 150 to 305 MeV, analysis for reaction mechanism in, (E), 25:5679
proton inelastic scattering at 10 MeV, p--γ angular correlations from, (E), 25:5673
proton inelastic scattering at 19.6 MeV, γ--γ angular correlations and spin-flip probability for, (E), 25:5673
IRON ISOTOPES Fe-56
energy levels from manganese-55 (p,γ) reactions, spin assignments for, (T), 25:5676
helium-3 reactions (He-3,t) at 30.2 MeV, triton spectra and angular distributions for, (E), 25:5506 (CEA-N-1232, pp 81-159)
meson (K) and (π) absorption widths in, corrections due to admixtures of excited energy levels, (T), 25:5866
neutron inelastic scattering at 0.5 to 16 MeV, high-resolution cross section for, (E), 25:5657
neutron reactions using plutonium--beryllium source, gamma production cross section for, (E), 25:5582
photon reactions (γ,p3n) and (γ,4n) at 150 to 305 MeV, analysis for reaction mechanism in, (E), 25:5679
proton inelastic scattering at 19.6 MeV, γ--γ angular correlations and spin-flip probability for, (E), 25:5673
IRON ISOTOPES Fe-57
effects on spectra of ferrocene, 25:4067
energy-level transitions in electron-spin-polarized, internal conversion coefficients and electron intensity differences for, (T), 25:5659
energy-level transitions in, total and K conversion coefficients for, (T), 25:5652
Moessbauer effect in copper oxide, magnesia, and alumina, effects of iron valence, 25:5221 (AD-710293)
proton reactions (p,d) at 17.3 MeV using polarized beams, cross section and asymmetry for, (E), 25:5506 (CEA-N-1232, pp 81-159)
IRON ISOTOPES Fe-59
diffusion in fcc, bcc, and ordered FeCo alloy, 25:4761
use as tracer for determining x radiation effects on erythropoiesis in adrenalectomized mice, 25:4696
use for diagnosis of pulmonary hemosiderosis in man, 25:4685
ISOTOPE DILUTION ANALYSIS
equations for double-spiked, 25:4028
ISOTOPES
decay of highly-unstable, review of research on, 25:5619

J

JAPAN
radioactive waste disposal in, trends in management of, 25:4317
JAPANESE ADVANCED THERMAL REACTOR
components for, fabrication and operation of loop for testing of, 25:4192
JOINTS
design and performance of pipe, summary of experience on, 25:4188 (TID-25553)
design of bonded, for filament wound cylinders, 25:6218 (EDX-613-142)

K

KAOLINS
radioinduced polymerization with methyl methacrylate, energy deposition, kinetics, and mechanism of γ, 25:4107
KIDNEYS
clearance of phosphorus-32-labeled sodium orthophosphate by, of patients with thyroid disease, 25:4451
radioinduced hypertension of, in rabbits, sunlight or uv, 25:4697
radioinduced lesions in, of rats following single intratracheal administration of thorium dioxide, 25:4702
radioinduced lesions of human, following therapy, functional and morphological studies of γ, 25:4714
scanning of transplants of, for function in man, use of metastable indium-113-labeled chelates or metastable technetium-99-labeled DTPA for, 25:4657 (UCLA-12-782, pp 89-125)
scanning using iodine-131-labeled hippuran or mercury-203-labeled chlormerodrin, 25:4655
KRYPTON
helium-ion reactions at 10 to 30 keV with, cross sections for production of metastable triplet helium atoms by charge exchange in, (E), 25:4969
helium-metastable-atom reactions with, cross sections for ionization in, (E), 25:4969
KRYPTON IONS
reactions with single-crystal germanium, minimum energy for sputtering in, (E), 25:5155
KRYPTON ISOTOPES Kr-85
beta decay of isomeric, beta and conversion electron spectra, Q-value, conversion coefficients, and multipolarities of, (E), 25:5634
monitoring in natural gas lines, flowthrough proportional detector for, 25:4352

L

LA CROSSE BOILING-WATER REACTOR
instrumentation for, automatic gain control system for, 25:5912 (DOCKET-1155-85)
LABORATORIES
design and operation of plutonium fuels development, 25:4302
radiation monitoring of, at Research Reactor Institute of Kyoto University during 1968, 25:4508 (KURRI-TR-63)
LACTATE DEHYDROGENASE
content of blood plasma in rats, effects of cysteamine, hypoxia, and pyridoxol on, 25:4594
radiation effects on content of, in blood serum and content of isoenzymes in tissues of rats, protective effects of methylene blue against whole-body γ, 25:4605
radioinduced inactivation of, from heart muscle of rats, neodymium glass laser, 25:4461
radiosensitivity of activity of, in solutions, effects of iodine compounds on x, 25:4569
LACTONES
synthesis of components of, method for, 25:4840(R) (LA-4526)
LAKES
heat dispersion in large, physical modeling of, 25:6217 (ANL-ES-2)
LANTHANUM
compounds with mandelic acid, preparation by reactions of lanthanum alkoxides with mandelic acid, potentiometric studies on, 25:4055
separation by ion exchange using Alamine 336 or Amberlyst A-21 in aqueous thiocyanate solutions, 25:4137 (IS-T-377)
separation of trace amounts of, from aqueous nitric acid solutions by solvent extraction using D2EHPA in toluene containing trace amounts of uranium, 25:4150
superconducting transition in dhcp, effects on nuclear quadrupole resonance frequencies, 25:5058
LANTHANUM ALLOYS AND SYSTEMS
exchange interactions of dilute, review, 25:5232
Al--La, thermal capacity of $LaAl_2$ at low temperatures, 25:5218
Bi--La, thermal capacity of LaBi at low temperatures, 25:5218
La--Sb, thermal capacity of LaSb at low temperatures, 25:5218
La--Sn, electron band structure calculations for $LaSn_3$, comparison of standard and modified orthogonalized plane-wave, 25:5231
La-base--Pu, Kondo effect in, plutonium virtual bound state from, 25:5227
LANTHANUM FLUORIDES
NaF--LaF_3, thermodynamic composition--pressure diagrams of, 25:4857
LANTHANUM ISOTOPES La-139
energy levels from proton resonances in barium-138, spreading widths of isobaric analog, (T), 25:5644
neutron capture integral in fast region, (E), 25:5656
nuclear quadrupole resonance frequencies in dhcp lanthanum, effects of superconducting transition on, 25:5058
LANTHANUM ISOTOPES La-140
distribution in tissues of beagle dogs following administration by gavage, inhalation, and injection, effects of chemical form on patterns of, 25:4426
LASER RADIATION
effects on activity of lactate dehydrogenase from heart muscle of rats, neodymium glass, 25:4461
effects on bones, skin, and eyes of dogs, monkeys, and rabbits, pathological carbon dioxide, 25:4704
scattering on plasma jets, diagnostics from Thomson and Rayleigh, 25:5078 (CEA-R-3998)
LASERS
development for remote position measurement, 25:6222 (BNWL-SA-3335)
performance for plasma temperature, density, and correlation spectrum, 25:5086
use for plasma diagnostics, conference on, 25:5080(T) (LA-4520-TR)
use for plasma production for power generation and space propulsion, 25:5104
LAWRENCIUM
research on, review of, 25:5719
LAWRENCIUM ISOTOPES Lr-256
fission of, half-life for spontaneous, (E), 25:5757

XUM

LAWRENCIUM ISOTOPES Lr-257
fission of, half-life for spontaneous, (E), 25:5757
LEAD
antiproton absorption at 20 to 65 GeV/c, cross sections for, (E), 25:5295
antiproton absorption cross sections at 20 to 40 GeV/c, (E), 25:5265 (CONF-700314-, Paper 4)
complexes with 8-quinolinol, structure of, NMR spectral studies on, 25:4081
complexes with phenanthrenequinone oxime, potentiometric studies on formation constants of, 25:4080
determination in boron, 25:4009 (TID-25190)
determination in PuO_2--U_3O_8, effects of ratio of plutonium oxide to uranium oxide on spectrographic, 25:4015 (NUMEC-3524-76)
determination of trace amounts of, in strontium-85, polarographic, 25:4126 (UJV-2431-Ch)
gamma scattering from, barriers of finite thickness, (E), 25:5149
meson (K-) absorption at 20 to 65 GeV/c, cross sections for, (E), 25:5295
meson (K-) absorption cross sections at 20 to 40 GeV/c, (E), 25:5265 (CONF-700314-, Paper 4)
meson (π^-) absorption at 20 to 65 GeV/c, cross sections for, (E), 25:5295
meson (π^-) absorption cross sections at 20 to 40 GeV/c, (E), 25:5265 (CONF-700314-, Paper 4)
neutron elastic scattering at 4 MeV, differential cross sections and polarizing abilities at 150 to 180° from, (E), 25:5762
separation by ion exchange using Alamine 336 in aqueous thiocyanate solutions, 25:4137 (IS-T-377)
sound velocity measurements in superconducting, 25:5168(R) (COO-623-156)
superconducting films, current-pulse effect in intermediate state, 25:5053
LEAD ALLOYS AND SYSTEMS
Bi--Pb, magnetic flux jumps in superconducting, energy dissipated in, (E/T), 25:5044
In--Pb-base, stress relaxation induced by magnetic field reduction in superconducting, 25:5036(R) (NYO-4060-5)
In-base--Pb, electric conductivity of single crystals of, anisotropy in, (E/T), 25:5185
In-base--Pb, thermal conductivity of normal and superconducting, (E/T), 25:5055
LEAD ISOTOPES Pb-201
energy-level transitions from bismuth-201 electron-capture decay, (E), 25:5696
LEAD ISOTOPES Pb-202
energy-level transitions from bismuth-202 electron-capture decay, (E), 25:5696
LEAD ISOTOPES Pb-206
energy level from mercury-204 (α,2n) reactions, g factor for 7-, (E), 25:5688 (UCRL-19961)
energy levels from 4p--2h shell-model calculation including core excitation, spin--parity assignments for, (T), 25:5737
energy-level transitions from 4p--2h shell-model calculation including core excitation, reduced transition probabilities for, (T), 25:5737
LEAD ISOTOPES Pb-207
energy level at 0.897 MeV from Coulomb excitation, lifetime and magnetic moment of $p_{3/2}^{-1}$ neutron-hole, (E), 25:5710
isomeric shifts and magnetic hyperfine splitting in μ-mesic, quasi-particle calculation of, (T), 25:5794
proton inelastic scattering at 20.2 MeV to $^3/_2^-$ state of, distorted-wave analysis using central, tensor, and core-polarization interactions of differential cross sections from, (T), 25:5780
LEAD ISOTOPES Pb-208
energy levels from lead-208 (γ,n) reactions at 9.8 MeV, resonance parameters for, (E), 25:5795
energy levels in, calculation of particle--hole, (T), 25:5788
energy-level transitions in μ-mesic atoms of, electric quadrupole, (E), 25:4953
energy-level transitions in, calculation of, (T), 25:5788
meson (K) and (π) absorption widths in, corrections due to admixtures of excited energy levels, (T), 25:5866
meson reactions (π^-,γ) with, branching ratios for, (T), 25:5793
nuclear matter and kinetic-energy densities from Hartree--Fock and Thomas--Fermi calculations using static and velocity-dependent interactions, (T), 25:5873
photon reactions (γ,n) at 9.8 MeV, differential cross sections for, (E), 25:5795
proton inelastic scattering at 14.5 to 15.4 MeV using polarized beams, analyzing power for, (E), 25:5506 (CEA-N-1232, pp 81-159)
LEAD ISOTOPES Pb-209
isomeric shifts and magnetic hyperfine splitting in μ-mesic, quasi-particle calculation of, (T), 25:5794
LEAD ISOTOPES Pb-210
use as γ source for transmission scanning of bones for measurement of mineral content, 25:4645 (CONF-700515-, pp 263-71)
LEAD ISOTOPES Pb-214
determination in air, alpha detection method for, 25:4040
LEAD ZIRCONIUM TITANATES
analysis for niobium using sodium butyldithiocarbaminate, spectrophotometric, 25:4017
LEAK DETECTORS
development of ion pump-type, for steam generators, 25:4736(R) (ANL/ST-3)
LEAVES
cesium-137 uptake by, of Trifolium pratense, comparison of concentration factors for plant distribution for, 25:4449
LEPTONS
interactions with hadrons, density-matrix formalism for, 25:5331
LEUCINE
hydrochloride, radiation effects on monocrystals of, EPR spectra of free radicals from γ, 25:4092
LEUCINE, N-TRYPTOPHYL-
radiolysis of aerated solutions of, yields from γ and x, 25:4114
LEUKOCYTES
radiation effects on association of marked chromosomes in cultured, from monkeys, effects of cell cycle stage on x, 25:4493
radiation effects on count of eosinophilic, in intestine of rats in relation to phospholipase B activity, x, 25:4455(R) (ORO-3329-7)
radioinduced biochemical changes in polymorphonuclear, of guinea pigs, effects of endotoxins and poly A-U complexes on x, 25:4454 (NYO-3240-55)
LEUKOPOIESIS
toxicity of uranium oxide to, in dogs following chronic ingestion and low and high dose intratracheal injection, 25:4445
LIGHT
effects on rabbit kidneys, protective effects of stimulation of vagus nerve against hypertension induced by, 25:4697
LIMESTONE
neutron distributions in, Monte Carlo calculation of thermal, (T), 25:5493
LINEAR ACCELERATORS
beam current profile monitor for electron, scanning, 25:5468
development and operation of Saclay 300-MeV electron, 25:5442 (CEA-N-1232, pp 161-212)
experimental facilities for Saclay 300-MeV electron, 25:5442 (CEA-N-1232, pp 161-212)
experimental facility for Livermore, photon activation analysis, 25:5472
experimental facility for ORELA, for simultaneous fast neutron spectra measurements by time-of-flight and pulse-height unfolding, 25:4366
research and development at Saclay, 25:5550(R) (CEA-N-1232)
LINEAR ENERGY TRANSFER
calculations in microorganisms, methods for, 25:4507 (EUR-4506)
LIPIDS
chemical composition of, in bristlemouth fish, 25:4488 (UCLA-12-782, pp 1-21)
content of human tissues, methods for measurement of, using dual beam γ transmission scanning, 25:4646 (CONF-700515-, pp 272-3)
radiation effects on sorption of, by cells of duodenal epithelium of rats, cerium-144 β and γ, 25:4655
LIQUID FLOW
magnetohydrodynamic electroconducting viscous, forced vortex in axial magnetic field in, 25:5000
LIQUID METAL FAST BREEDER REACTOR
accidents in, analysis of coolant flow induced, 25:6070
accidents in, analysis of energy release for, 25:6085
accidents in, analysis of single fuel element subassembly, 25:6068
accidents in, analysis of sodium voiding during, 25:6072
accidents in, comparison with water cooled reactors of core, 25:6077
accidents in, effects of fuel chilling on Doppler feedback control of, 25:6069
accidents in, energy release for molten fuel and liquid sodium interaction, 25:6075
accidents in, energy release for molten uranium oxide (UO_2) and liquid sodium interaction, (E), 25:6076
accidents in, liquid sodium critical point uncertainty for molten fuel and liquid sodium interaction, 25:6074
accidents in, quasi three dimensional analysis of liquid sodium voiding patterns during, 25:6071
accidents in, single bubble model calculations for liquid sodium voiding during, 25:6073
blanket depletion in, analysis of multigroup calculations of, (T), 25:5960
control elements of, reactivity worth of tantalum, (E/T), 25:5964
coolant ejection in, analysis of liquid film thickness for slug type, (E), 25:6067
coolant for, construction and operation of mechanical sodium pump for, 25:4201
coolant of, nozzle system for gas detection in liquid sodium, 25:6047
coolant vapor monitor for, development of, 25:6046
cooling system of 1000 MW(e), corrosion product radioactivity in, 25:5986
core components of, effects of accidents on shock pulse

loading of, 25:6078
core melting in, protection systems for, 25:6088
core of, design parameters for plutonium carbide (PuC)--uranium carbide (UC) fueled, 25:6023
core of, review of AEC programs on safety aspects of, 25:6087
core of, safety aspects of, 25:6086
core performance of, effects of fuel element cladding swelling on, 25:6021
fuel element cladding of, effects of cold wrapper tube technique on swelling of steel, 25:6022
fuel element failure in, development of FEDAL system for determining, 25:4736(R) (ANL/ST-3)
fuel elements for, dual spectrum method for analysis of, 25:4294
fuel elements for, effects of niobium and molybdenum on performance of, (T), 25:6055
fuel elements for, high temperature fast flux irradiation program for mixed oxide, 25:5585 (GA-10264)
fuel elements of, design parameters and performance of cartridge type electrical heater simulators for, 25:6029
fuel elements of, profilometer for inspection of irradiated, 25:6033
physics measurements for, critical assemblies normalization of, 25:6114
safety testing for, operations in Power Burst Facility for, 25:6102
thermodynamics for liquid sodium coolant and molten fuel interaction, 25:6092

LIQUIDS
boiling of, average effective radius of vaporization centers in nucleate, 25:6215(T) (AEC-tr-7202)

LITHIUM
analysis of, linac facility for photon activation, 25:5472
antiproton absorption at 20 to 65 GeV/c, cross sectons for, (E), 25:5295
antiproton absorption cross sections at 20 to 40 GeV/c, (E), 25:5265 (CONF-700314-, Paper 4)
diffusion in silver chloride crystals at 200 to 400°C, isotope effect in, 25:5172
meson (K^-) absorption at 20 to 65 GeV/c, cross sections for, (E), 25:5295
meson (K^-) absorption cross sections at 20 to 40 GeV/c, (E), 25:5265 (CONF-700314-, Paper 4)
meson (π^-) absorption at 20 to 65 GeV/c, cross sections for, (E), 25:5295
meson (π^-) absorption cross sections at 20 to 40 GeV/c, (E), 25:5265 (CONF-700314-, Paper 4)
plasma of, ion heating in Penning discharges, 25:5075
properties for use as encapsulating material for californium-252 sources for neutron capture gamma-ray spectroscopy, 25:4772
pumps for liquid, cavitation and hydraulic performance of electromagnetic, 25:4186 (ORNL-TM-2995)

LITHIUM FLUORIDES
dielectric constant of, low-frequency, 25:6228 (COO-623-153)
dielectric constants of, pressure and temperature dependences of static, 25:5168(R) (COO-623-156)
electron energy loss to surface excitations in thin films of, at 25 keV, (T), 25:4937 (IS-T-380)
neutron binding to F centers in, (T), 25:5154
radiation effects on crystal structure of, neutron, 25:4887 (KFK-1215)
radioinduced V_3 band in pure and magnesium-doped crystals of, identification of x-, (E), 25:5156

LITHIUM IONS
energy of ground-state Li^+, calculation using correlated wave functions, 25:4948

LITHIUM ISOTOPES Li-6
effects on lithium diffusion in silver chloride crystals, 25:5172
energy levels of, correlation structure in, (T), 25:5564
energy levels of, helium-3 + triton cluster structure of ground and second-excited, (E/T), 25:5571
meson(μ) depolarization in μ-mesic atoms of, from muon-nucleus magnetic dipole coupling, (E), 25:5576
polarization of beams of, measurement relative to deuteron beam polarization, (T), 25:5569
reactions (Li-6,d) with carbon-12 and oxygen-16 at 25 MeV, peripheral-model analysis of angular distributions from, (T), 25:5601
reactions (Li-6,d) with carbon-12 at 29.0 MeV, energy spectra and PWBA analysis of angular distributions from, (E), 25:5592
reactions (Li-6,t) with carbon-12 at 20 MeV, angular distributions for, (E), 25:5680 (CEA-N-1232, pp 1-80)

LITHIUM ISOTOPES Li-7
deuteron elastic scattering at 28 MeV, optical-model analysis of, (T), 25:5579
deuteron reactions (d,n) at 500 keV, neutron angular distributions from, (E), 25:5590
effects on lithium diffusion in silver chloride crystals, 25:5172
helium-3 reactions (He-3,α) at 5 to 8 MeV, PWBA analysis of energy spectra, excitation functions, and angular distributions from, (E/T), 25:5571
meson(μ) depolarization in μ-mesic atoms of, from muon-nucleus magnetic dipole coupling, (E), 25:5576
neutron reactions using plutonium--beryllium source, gamma production cross section for, (E), 25:5582
reactions (Li-7,α), (Li-7,d) and (Li-7,t) with carbon-12 at 24.4 MeV, energy spectra from, (E), 25:5680 (CEA-N-1232, pp 1-80)
reactions (Li-7,He-6) with iron-55 at 24.4 MeV, energy spectra from, (E), 25:5680 (CEA-N-1232, pp 1-80)
reactions (Li-7,t) with argon-36 at 16.6 MeV, triton spectra from, (E), 25:5680 (CEA-N-1232, pp 1-80)
reactions (Li-7,t) with carbon-12 and oxygen-16 at 30 MeV, peripheral-model analysis of angular distributions from, (T), 25:5601
reactions (Li-7,t) with carbon-12 at 31.5 MeV, energy spectra and PWBA analysis of angular distributions from, (E), 25:5592

LIVER
indium-113 uptake by, of rats, effects of particle size of colloid and pH on, 25:4437
radiation effects on isoenzymes of lactate dehydrogenase in, of rats, protective effects of methylene blue against whole-body γ, 25:4605
radioinduced lesions in, of rats following single intratracheal administration of thorium dioxide, 25:4702
radioisotope distribution in, of rats, effects of p-dichlorophenol on calcium-45 and strontium-89, 25:4431
scanning in man, evaluation of indium-113m for, 25:4687
scanning of blood circulation in, use of metastable technetium-99-labeled albumin microaggregates or solutions for, 25:4657 (UCLA-12-782, pp 89-125)
scanning using metastable technetium-99-labeled technetium dioxide, 25:4413
synthesis of fatty acids in, of rats, following treatment with carbon chlorides or ethionine, protective effects of cysteine against, 25:4600
thorium content of, in rats following intracardiac administration, 25:4441

LOOPS
design and operation for Japanese sodium test facility, for testing reactor components, 25:4191
fabrication and operation of Japanese ATR, for testing reactor components, 25:4192

LOS ALAMOS OMEGA WEST REACTOR
hazards analysis for, 25:6103

LOW TEMPERATURE PHYSICS
review of possible future developments in ultra-low (<0.3°K), 25:5035 (UCSD-34-P-143-30)

LUCIFERASE
radiation effects on activity of, in Photobacterium fischeri, measurement of bioluminescence decay time to determine high dose rate electron, 25:4730

LUMINESCENCE
mechanisms in bio- and chemo-, research at Johns Hopkins Univ. on, 25:6244(R) (NYO-2802-70)

LUNAR MATERIALS
analysis by α scattering methods on Surveyor missions, 25:4034
analysis of, avalanche semiconductor detectors for x-ray fluorescence, 25:4323 (NYO-4028-TA-1)
electron emission from Apollo 12, thermally stimulated exo-, (E), 25:4935 (ORNL-TM-3131)

LUNGS
book: Pulmonary Investigation with Radionuclides, 25:4662
clearance of carbon-11- and oxygen-15-labeled carbon dioxide from alveolar gas into capillaries of human, comparison of rate of, 25:4667
closure of airways in human, measurement using scintillation counters and xenon-133 as tracer, 25:4428
flow of cerebral blood in human, methods for measurement of, 25:4669
histology of radioinduced and spontaneous tumors in, of mice, 25:4699
indium-113 uptake by, of rats, effects of particle size of colloid and pH on, 25:4437
metabolism of thorium dioxide in, of rat following intratracheal administration, 25:4442
oxygen metabolism in human, measurement using radioactive carbon dioxide and oxygen as tracers, 25:4665
plutonium-239 retention in, of rats and ratbits, fallout, 25:4478
radiation dose to, in patients, during endolymphatic therapy using iodine-131 or phosphorus-32, β and γ, 25:4512
radiation effects on, of dogs, x, 25:4706
radiodiagnosis of diseases of, using combined perfusion scanning and radiography, 25:4675
radioinduced lesions in, of rats following single intratracheal administration of thorium dioxide, 25:4702
relation of perfusion to ventilation in human, methods of determining, 25:4668
scanning for diagnosis of diseases of, evaluation of γ scintillation camera for use with metastable technetium-99 and xenon-133 for, 25:4676
scanning for function of, in patients with embolisms, use of combined metastable technetium-99 or metastable indium-113 aerosol inhalation with iodine-131- or metastable technetium-99-labeled albumin macroaggregate perfusion for, 25:4657 (UCLA-12-782, pp 89-125)
scanning for function, of human, methods using xenon-133

XUM

for, 25:4671
scanning for localization of embolism in, use of iodine-131-labeled albumin macroaggregates for, 25:4674
scanning for measurement of perfusion, residual capacity, ventilation, and vital capacity of human, using xenon-133, 25:4671
scanning for perfusion and ventilation, use of carbon-11, nitrogen-13, and oxygen-15 for, 25:4667
scanning of blood circulation in human, methods using computer data analysis and xenon-133, 25:4672
scanning of distribution of blood flow in, of dogs, during ventricular failure, methods using metastable indium-113 and technetium-99 for double scanning, 25:4677
scanning of human, following embolism, effects of perfusion-ventilation relations on, 25:4679
scanning of human, for diagnosis of embolism using iodine-131, metastable indium-133, or metastable technetium-99 for, 25:4680
scanning of human, for function, use of carbon-11, nitrogen-13, and oxygen-15 for, 25:4664
scanning of human, for function, use of iodine-131-, indium-113-, or technetium-99-labeled macroaggregates or xenon-133 for, 25:4673
scanning of human, for measurement of regional function, use of radioactive gases for, 25:4663
scanning of human, for perfusion and ventilation of human, methods for, 25:4665
scanning of human, using iodine-131-labeled albumin macroaggregate and multiple images, 25:4670
scanning of human, using radioisotope-labeled aerosols, review of equipment and procedures for, 25:4678
scanning of transplants of, for function in dogs, 25:4657 (UCLA-12-782, pp 89-125)
uptake of carbon and thorium by rat, study of phagocytosis and surfactant metabolism following, 25:4410
ventilation of human, measurement of regional, 25:4666

LUTETIUM
determination of trace amounts of, in uranium by chemical separation and spectroscopy, 25:4021
separation by ion exchange using Alamine 336 or Amberlyst A-21 in aqueous thiocyanate solutions, 25:4137 (IS-T-377)
separation of trace amounts of, from aqueous nitric acid solutions by solvent extraction using D2EHPA in toluene containing trace amounts of uranium, 25:4150

LUTETIUM ISOTOPES Lu-171
energy levels from hafnium-171 decay, rotational, (E), 25:5699

LYMPH NODES
radiation dose to, in patients, during endolymphatic therapy using iodine-131 or phosphorus-32, β and γ, 25:4512
retention of thorium dioxide in, of rats following intratracheal administration, 25:4442

LYMPHOCYTES
radioinduced chromosome aberrations in, effects of volume, body weight, and dose on γ, 25:4491

LYSOZYME
radiation effects on, in aqueous solutions, protective effects of cysteine against ionizing, 25:4544

M

MAGNESIUM
complexes with 8-quinolinol, structure of, NMR spectral studies on, 25:4081
complexes with phenanthrenequinone oxime, potentiometric studies on formation constants of, 25:4080
electric conductivity at 1.5 to 300°K, absolute, (E/T), 25:5184
properties for use as encapsulating material for californium-252 sources for neutron capture gamma-ray spectroscopy, 25:4772
separation by ion exchange using Alamine 336 or Amberlyst A-21 in aqueous thiocyanate solutions, 25:4137 (IS-T-377)
separation of thorium from, by photochemical precipitation, 25:4026

MAGNESIUM ALLOYS AND SYSTEMS
electric conductivity at 1.5 to 300°K of dilute, deviations from Matthiessen's rule in, (E/T), 25:5184
Cd--Mg-base, crystallization of dilute, kinetics of, 25:4808
Gd-base--Mg, magnetic ordering and thermoelectric properties of, 25:5169 (IS-T-379)
Mg-base--Zr, crystallization of dilute, kinetics of, 25:4808

MAGNESIUM ISOTOPES Mg-21
mass excess from magnesium-24 (He-3,He-6) reactions, test of isobaric-multiplet equation for, (E), 25:5640
mass excess from magnesium-24 (He-3,He-6) reactions at 68 to 70 MeV, test of isobaric-multiplet mass equation, (E), 25:5568

MAGNESIUM ISOTOPES Mg-24
helium-3 reactions (He-3,He-6) at 68 to 70 MeV, Q values for, (E), 25:5568
helium-3 reactions (He-3,He-6) near 65 MeV, test of isobaric-multiplet mass equation, (E), 25:5640
helium-3 reactions (He-3,n) at 5 and 5.8 MeV, neutron polarization from, (E), 25:5574
neutron capture at 20 to 80 keV, cross sections for, (E), 25:5603 (FOA-4-4440)
neutron capture by, absolute cross section for thermal, (E), 25:5625
proton elastic and inelastic scattering at 5 to 6 MeV, excitation function and proton polarization for, (E), 25:5632
proton inelastic scattering at 20.3 MeV using polarized beams, cross section and asymmetry for, (E), 25:5606 (CEA-N-1232, pp 81-159)

MAGNESIUM ISOTOPES Mg-25
energy levels from neutron resonances in magnesium-24, radiative widths for, (E), 25:5603 (FOA-4-4440)
neutron capture by, absolute cross section for thermal, (E), 25:5625

MAGNESIUM ISOTOPES Mg-26
deuteron reactions (d,p) at 4.4 and 5.3 MeV, p-γ angular correlations from, (E), 25:5672
energy levels from aluminum-27 (n,d) reactions at 14.1 MeV, spectroscopic factors for, (E/T), 25:5662
neutron capture by, gamma spectra and Q-value of thermal, (E), 25:5625
photon reactions (γ,n) at 15 to 23 MeV, isospin splitting of giant dipole state from neutron spectra from, (E), 25:5671
proton reactions (p,n) at 5.2 to 8.0 MeV, excitation function for, (E), 25:5613

MAGNESIUM ISOTOPES Mg-27
energy levels from magnesium-26 (d,p) reactions, (E), 25:5672
energy levels from magnesium-26 neutron capture, (E), 25:5625

MAGNESIUM OXIDES
creep strain of, effects of grain-boundary porosity growth on high-temperature, 25:4848
iron-58 Moessbauer effect in, effects of iron valence in, 25:5221 (AD-710293)
radiation effects on crystal structure of, neutron, 25:4887 (KFK-1215)

MAGNETIC ANALYZERS
field measurements in, probe positioning errors in, 25:5461 (NP-18519)

MAGNETIC FIELDS
measurement of beam analyzer, probe positioning errors in, 25:5461 (NP-18519)

MAGNETIC MIRROR MACHINES
plasma diagnostics in, pressure anisotropy, (E), 25:5085

MAGNETIC MIRRORS
plasma diagnostics during two-phase excitation at cyclotron frequency, 25:5087

MAGNETIC STORMS
effects on ionization in mid-latitude lower ionosphere, anomalous, (E/T), 25:5006
effects on outer radiation belt, (T), 25:5033
electron fluxes in outer-zone magnetosphere following Dec. 17-18, 1962, radial diffusion coefficients and lifetimes from, (E/T), 25:5002 (AD-710604)
occurrences in 1968, correlation with central meridian passages of plages of low or moderate activity, (E), 25:5022

MAGNETISM
storage of, design of superconducting device for, 25:5064(P)

MAGNETOHYDRODYNAMIC GENERATORS
channel characteristics of conduction-type dc, modeling of, 25:4995
design study for, for power system for unmanned nuclear-electric spacecraft, 25:4992(R) (N-70-34006)
properties of Faraday-type, with two-dimensional gas flow, 25:4991 (INR-1199)

MAGNETOSPHERE
diagnostics of, from ground-based measurements of hf, lf, and ultra lf electromagnetic waves, 25:5030
electron radial diffusion from outer-zone, lifetime determination for, (E/T), 25:5002 (AD-710604)
parameters of, determined from Pc1 micropulsations, (E/T), 25:5027
parameters of, using airglow, auroral, and geomagnetic phenomena, (E/T), 25:5023
particle-wave interactions in, nonlinear mechanisms of, (T), 25:5031
plasma studies from ground-based whistler method, thermal, 25:5029
pulsations in, review on micro-, (E/T), 25:5028

MAGNETS
charged-particle beam transport in, transfer matrix calculation of spin aberrations in polarized, 25:5454 (LA-4465, pp 18.1-16)
cryostat for superconducting dipole and quadrupole, design of, 25:4189 (UCRL-19764)
energy losses in pulsed superconducting, calculation of, 25:5459 (NP-18516)
equations for superconducting saddle-coil, 25:5464 (RHEL/R-203)
properties of isochronous beam transport, 25:5447 (IFVE-OP-69-68)

MALATE DEHYDROGENASE
content of blood plasma in rats, effects of cysteamine, hypoxia, and pyridoxol on, 25:4554

MALEIC ACID
complexes with rare earths and other metals, preparation and thermal behavior of, 25:4075
MALEIC ANHYDRIDE
use as catalyst for graphite binders, quantitative optimization for, 25:4840(R) (LA-4526)
MALEIMIDE, N-ETHYL-
effects on electron-radiosensitivity of DNA in Escherichia coli, 25:4551
effects on peas following seed exposure in comparison to effects of γ radiation and EMS, rate of mutagenic, 25:4489
effects on x-radiosensitivity of ascites tumor cells, 25:4562
effects on x-radiosensitivity of ducdenum crypt cells in mice, 25:4587
electron transfer reactions of nucleosides and nucleotides in solutions of, 25:4540
MAMMALIA
radiation effects on, protective effects of amines and hypoxic agents against ionizing, 25:4539
MAMMARY GLANDS
excretion of uranium oxide by, of dogs and rabbits following intratracheal injection or oral ingestion, 25:4446
MAN
analysis of cadavers of, for elements by neutron activation, 25:4042 (CONF-680211-, pp 496-516)
bone mineral content of, effects of osteoporosis on, 25:4629 (CONF-680211-, pp 411-21)
closure of airways in lungs of, measurement using scintillation counters and xenon-133 as tracer, 25:4428
effects of diet on bone density in, methods for measurement using radiography with automatic computer film calibration, 25:4613 (CONF-680211-, pp 27-80)
mineral content of bones in, effects of age and sex on, methods for measurement of, using radiography, 25:4619 (CONF-680211-, pp 177-91)
mineral content of bones in, effects of age and sex on, methods for measurement of, using radiography, 25:4616 (CONF-680211-, pp 115-35)
mineral content of bones in, effects of age on, methods for measurement of, using monoenergetic x-ray transmission scanning, 25:4621 (CONF-680211-, pp 204-15)
mineral content of bones in, effects of age, diseases, estrogen treatment, and sex on, 25:4626 (CONF-680211-, pp 308-19)
mineral content of bones in, effects of age, diseases, and sex on, 25:4617 (CONF-680211-, pp 135-59)
mineral content of bones in, effects of age, osteoporosis, and sex on, methods for measurement of, using radiography, 25:4618 (CONF-680211-, pp 159-77)
mineral content of bones in, effects of age, race, and sex on, 25:4624 (CONF-680211-, pp 283-96)
mineral content of bones in, effects of bed rest on, 25:4653 (CONF-700515-, pp 408-22)
mineral content of bones in, effects of bone disease on, radiographic densitometry methods for determining, 25:4615 (CONF-680211-, pp 95-115)
mineral content of bones in, effects of bone trauma, diseases, sex, and fluoride content of drinking water on, 25:4627 (CONF-680211-, pp 319-28)
mineral content of bones in, effects of various disease conditions and treatments on, 25:4625 (CONF-680211-, pp 296-308)
mineral content of bones of lumbar vertebrae in, development of radiographic method for measurement of, 25:4628 (CONF-680211-, pp 331-51)
mineral content of bones of, relation of, to age, bone mass, race, sex, and incidence of bone fractures and osteoporosis, 25:4651 (CONF-700515-, pp 340-50)
radiation dose absorbed by, during radioisotope scanning of lungs, use of MIRD equations for calculations of, 25:4511
radiation dose absorbed by, following 10-year ingestion of fallout cesium-137, 25:4657 (UCLA-12-782, pp 89-125)
radiation dose to tissues of, during endolymphatic therapy using iodine-131 or phosphorus-32 labeled contrast media, β and γ, 25:4512
radiation dose to, from cosmic radiation and terrestrial radioactivity, 25:4518
radiation dose to, from natural sources at spas of Misasa and Masutomi, Japan, estimation of, 25:4711
radiation effects on human liver 20 years after Thorotrast injection for angiography, neoplastic, 25:4716
radiation effects on mortality of infant, fallout strontium-90, 25:4505 (CONF-691051-, pp 324-35)
radiation effects on skin of, physiological reactions following large dose in, 25:4715
radiation hazards to fetuses of, from scanning of pregnant mother, 25:4673
radiation protection of skin of, effectiveness of sunscreening creams for uv, 25:4608
radioinduced carcinomas in, effects of high dose on ionizing, 25:4502
radioinduced gastritis in, following therapy of kidney carcinomas, 25:4712
radioinduced leukopenia in, protective effects of taurine against γ, 25:4603
radioisotope uptake by, from diet in relation to deposition, equation for fallout cesium-137 and strontium-90, 25:4519
radiosensitivity of neoplasms in, effects of mixtures of 5-bromodeoxyuridine or 5-iododeoxyuridine with 5-fluorouracil on ionizing, 25:4602
radiotherapy of eye diseases in, methods for bilateral fast electron, 25:4690
radiotherapy of gliomas in brain of, effects of mixtures of 5-bromodeoxyuridine with 5-fluorouracil or methotrexate on tumor radiosensitivity during, 25:4688
radiotherapy of lumbar region of, incidence of renal lesions following γ, 25:4714
radiotherapy of mesotheliomas in lungs of, effects of procarbazine on tumor radiosensitivity during, 25:4689
renal clearance of radiophosphate in, with thyroid diseases, effects of medical and surgical treatment on, 25:4451
strontium-90 intake by, following ingestion of fresh water fish as compared to marine fish, and meat, 25:4427
ventilation of lungs of, measurement of regional, 25:4666
weight and volume of bones in skeleton of, methods for measurement of, using contact radiography and x-ray densitometry, 25:4652 (CONF-700515-, pp 365-82)
weight of hand bones of, use of radiographs to measure, 25:4641 (CONF-700515-, pp 224-36)
MANDELIC ACID
compounds with lanthanons, preparation by reaction with alkoxides, potentiometric studies on, 25:4055
reactions with ammonium hydroxide and uranyl nitrate, production of $(NH_4)_2UO_2(O_2C_8H_6)_2$ from, 25:4055
reactions with potassium hydroxide and uranyl nitrate, production of $K_2UO_2(O_2C_8H_6)_2$ from, 25:4055
reactions with sodium hydroxide and uranyl nitrate, production of $Na_2UO_2(O_2C_8H_6)_2$ from, 25:4055
reactions with uranyl nitrate in presence of pyridine, production of $(C_5H_6N)_2UO_2(O_2C_8H_6)_2$ from, 25:4055
MANGANESE
complexes with maleic acid, preparation and thermal behavior of, 25:4075
complexes with phenanthrenequinone oxime, potentiometric studies on formation constants of, 25:4080
determination in boron, 25:4009 (TID-25190)
determination in rocks by neutron activation, 25:4047
determination in skin by neutron activation, 25:4049
determination of trace amounts of, in titanium ore by neutron capture gamma spectroscopy using californium-252 source, 25:4036
properties for use as encapsulating material for californium-252 sources for neutron capture gamma-ray spectroscopy, 25:4772
separation by ion exchange using Alamine 336 or Amberlyst A-21 in aqueous thiocyanate solutions, 25:4137 (IS-T-377)
MANGANESE BORIDES
Curie temperature of MnB_2, from boron-11 NMR, 25:5225
MANGANESE FLUORIDES
magnetic phase transition in, sound propagation near, 25:5186
MANGANESE ISOTOPES Mn-53
energy levels from chromium-53(p,n) reactions, (E), 25:5612
MANGANESE ISOTOPES Mn-55
proton reactions (p,γ) at 1.3 to 1.5 MeV, γ branching ratios from isobaric analog resonances in, (E), 25:5676
MARS (PLANET)
atmosphere of, height-distribution processes of ionization in Martian and Cytherean upper, (E/T), 25:4936
MASERS
radio emission from interstellar hydroxyl and water, (T), 25:4917
MASS SPECTROMETERS
design of non-focusing, 25:4397
MATERIALS TESTING
methods for high-temperature, impact, pressure, and ultrasonic microcrack, of plutonium-238 fuel capsules, 25:4215 (NUMEC-3731-23)
MATERIALS TESTING, NONDESTRUCTIVE
method of testing reactor fuels by neutron transient characteristics in heavy moderators, 25:6204
MEATS
fish, radiation processing of yellow perch, effects of temperature on, 25:4734 (TID-25467)
fish, radioisotope content of, in Faroe Islands during 1969, cesium-137, strontium-90, 25:4476(R) (RISO-221)
fish, strontium-90 content of carp, caught in Mecklenburg ponds during 1961 to 1962, 25:4427
lamb, radioisotope content of, in Faroe Islands during 1969, cesium-137 and strontium-90, 25:4476(R) (RISO-221)
poultry, strontium-90 content of bones and meat from chicken, raised in Mecklenburg area during 1965, 25:4427
reactions of extracts of, with hydrated radiolytic electrons, effects of acetone, cysteine, and nitrate additives on, 25:4117

XUM

MEDICAL PERSONNEL
radiation dose to, in diagnostic radiography, recommendations for control of, 25:4531
radiation protection programs for, 25:4528
MEDICINE
book: Pulmonary Investigation with Radionuclides, 25:4662
research on nuclear, 25:4415
MEMBRANES
radiation effects on permeability of, of Ehrlich ascites tumor cells in cultures, protective effects of cysteamine and 2-amino-3-methyl-butanethiol against electron and x, 25:4568
radiosensitivity of duodenum crypt cell, in mice, x, 25:4587
radiosensitivity of, of Ehrlich ascites tumor cells, effects of excess oxygen and Synkavit on electron and x, 25:4568
MERCURY
complexes with 8-quinolinol, structure of, NMR spectral studies on, 25:4081
determination by neutron activation and other nuclear methods, 25:4133 (NAS-NS-3026(Rev.))
flow in pipes, pressure drop and velocity profile of fully developed, 25:4207
radiochemistry of, review on, 25:4133 (NAS-NS-3026(Rev.))
separation by ion exchange using Alamine 336 in aqueous thiocyanate solutions, 25:4137 (IS-T-377)
separation from other elements by ion exchange, 25:4133 (NAS-NS-3026(Rev.))
MERCURY ISOTOPES Hg-199
energy levels from gold-199 decay, transition probability ratios for, (E), 25:5698
MERCURY ISOTOPES Hg-203
excretion by lungs following use for kidney scanning, 25:4673
use of chlormerodrin-incorporated, for kidney scanning, 25:4659
MERCURY ISOTOPES Hg-206
energy levels from 4p--2h shell-model calculation including core excitation, spin--parity assignments for, (T), 25:5737
MESIC ATOMS
cascade time for K- decay in helium bubble chamber, (E), 25:5254
energy-level transitions in lead-208 μ-, electric quadrupole, (E), 25:4953
hyperfine-structure transitions in deuterium, hydrogen, and tritium μ-, (T), 25:4952 (JINR-P4-5039)
meson(μ) depolarization in beryllium-9, boron-10, boron-11, lithium-6, and lithium-7, from muon-nucleus magnetic dipole coupling, (E), 25:5576
reactions with deuterons and tritons of deuterium and tritium μ-, isotope exchange in, (T), 25:4952 (JINR-P4-5039)
x-ray spectra from π-mesic hydrogen, (E), 25:5288
MESONS
decay of 0- and 1-, vector dominance Veneziano model and sum rules for broken SU(3) symmetry for radiative, (T), 25:5402
decay of J/super P/ = 1+, broken SU(3) x SU(3) chiral algebra for mixing angle, broken SU(3) mass sum rules, and coupling constants for, (T), 25:5395
interactions of pseudoscalar, SU(3) structure for internal symmetry from Veneziano model amplitude for, 25:5370
interactions with $^1/_2$+ baryons, additive quark model for single and joint decay angular distributions for 0+, 1+, and 2+ meson and $^3/_2$+ baryon production in, (T), 25:5375 (TPJU-15/70)
interactions with external electromagnetic field, formulation of semi-quantized quantum electrodynamics from charged vector, (T), 25:5413
interactions with pseudoscalar mesons, perturbation series and O(8) symmetry from SU(3) extension of lambda phi* interactions and kinematic breaking for, (T), 25:5394
interactions with spinless bosons, lower bounds on threshold charge-exchange amplitude from di-pion mass distributions in final states of, (T), 25:5315
mass relation in SU(2) x SU(2) chiral symmetry, modified Weinberg, 25:5364
photoproduction of vector, ω - rho interference in, 25:5325 (DNPL/R-7, pp 115-38)
production of vector, in electromagnetic and strong interactions, 25:5322 (DNPL/R-7)
production of vector, in γ + p interactions, Pomeranchuk decoupling from ordinary Regge trajectories in, (T), 25:5348 (COO-264-562)
MESONS (eta)
decay eta + 2γ, current structure and coupling constants for, 25:5337
interactions π + eta + π + eta in Veneziano model, SU(3) structure for internal symmetry from, 25:5370
production in π- + p + eta + n interactions at 2.9 to 18.2 GeV/c, heavy-plate spark chamber study of differential cross sections for, (E), 25:5279 (CEA-R-4037)
MESONS (K)
decay K + π + l + ν form factors from Veneziano model, 25:5338
decay K + π + l + ν, chiral dynamics for form factors and decay constants for, (T), 25:5395 (JINR-P2-5290)
decay of, K* dominance and K*Kπ coupling in double partial-wave expansion of amplitudes for systematic analysis of semileptonic, (T), 25:5310
decay of, on-shell current algebra for form factors and coupling constants for radiative leptonic, (T), 25:5342
decay of, quark model for broken SU(6) sum rules for relation with baryon decays for, (T), 25:5394
decay of, six-fermion weak interaction in spectra and widths for four-lepton production in, (T), 25:5344
form factor from scattering amplitude in Veneziano model, electric, 25:5338
interactions anti K + K, symmetry-breaking effect on p-wave resonances in, (T), 25:5394
interactions K + anti K + K + anti K in Veneziano model, SU(3) structure for internal symmetry from, 25:5370
interactions K + π + K + eta in Veneziano model, SU(3) structure for internal symmetry from, 25:5370
interactions K + π + K + π in Veneziano model, SU(3) structure for internal symmetry from, 25:5370
interactions π + K, symmetry-breaking effect on p-wave resonances in, (T), 25:5394
width of, broken SU(3) x SU(3) chiral algebra for, (T), 25:5395
MESONS (K-)
absorption by nuclei at 20 to 40 GeV/c, cross sections for, (E), 25:5265 (CONF-700314-, Paper 4)
absorption by nuclei at 20 to 65 GeV/c, cross sections for, (E), 25:5295
decay in helium bubble chamber, cascade time for, (E), 25:5254
decay K- + π- + 2π0, comparison with K+ + π+ + 2π0 decay for partial rates of, (E), 25:5261
interactions K- + d + p + Λ + eta'-, eta' spin and parity from, (E), 25:5291
interactions K- + d at 20 to 65 GeV/c, total cross sections for, (E), 25:5295
interactions K- + d at 3 GeV/c, upper limits for production cross sections of exotic meson and hyperon resonances in, (E), 25:5287
interactions K- + n + Ξ- + K0 at 1.2 to 2.7 GeV/c in bubble chamber, total cross sections, polarization, and partial-wave analysis for baryon exchange in, (E/T), 25:5384
interactions K- + N below 65 GeV, difference of total cross sections for K+ + N and, (E), 25:5294
interactions K+ + N below 65 GeV, differences of total cross sections for K- + N and, (E), 25:5294
interactions K- + N in freon bubble chamber, Λ trapping probability from, (E), 25:5259
interactions K- + p + anti K0 + n at 2 to 20 GeV/c, Regge model with four poles for, (E/T), 25:5371 (CEA-N-1373)
interactions K- + p + anti K0 + n at 400 MeV/c in hydrogen bubble chamber, (E), 25:5262
interactions K- + p + anti K0 + n at high energies, effective Regge trajectories for, (T), 25:5377
interactions K- + p + Λ + eta' at 1.70 to 2.65 GeV/c, cross sections and eta' spin and parity from, (E), 25:5291
interactions K- + p + Σ- + π+ in freon, Σ- reabsorption rate from, 25:5298
interactions K- + p + Σ+(Σ-) + π-(π+) at 385 MeV/c in hydrogen bubble chamber, production of polarized Σ+ and Σ- in, (E), 25:5260
interactions K- + p + X0(960) + Λ on polarized targets, parity and spin of X0(960) from, (T), 25:5361 (TPJU-14/70)
interactions K- + p + Ξ-(Ξ0) + K+(K0) at 1.2 to 2.7 GeV/c in bubble chamber, total cross sections, polarization, and partial-wave analysis for baryon exchange in, (E/T), 25:5384
interactions K- + p at 10 GeV/c, production of (anti pp), (K+K-), and (π+π-) pairs in, (E), 25:5297
interactions K- + p at 20 to 65 GeV/c, total cross sections for, (E), 25:5295
interactions K- + p at rest in hydrogen bubble chamber, Σ- and Σ+production in, (E), 25:5269
reactions with nuclei at 3.0 GeV/c in emulsions, hyperfragment production in, (E), 25:5277
MESONS (K0)
decay K_2^0 + 2π0, branching ratio and amplitude for, (E), 25:5259
reactions with carbon, chlorine, copper, and fluorine at 120 MeV, Λ0 and Σ0 production and total cross sections for, (T), 25:5300
regeneration K_2^0 + K_1^0 in hydrogen at 0°, amplitude of, (T), 25:5294
MESONS (anti K0)
decay in hydrogen bubble chamber, test of ΔS = ΔQ rule and Sachs model of CP violation in leptonic and radiative, (E), 25:5262
production in K- + p + anti K0 + n interactions at 400 MeV/c in hydrogen bubble chamber, (E), 25:5262
MESONS (K+)
decay K+ + 3π at rest in propane bubble chamber, amplitudes and slopes of, (E), 25:5264
decay K+ + 3π in propane bubble chamber, ΔT = $^1/_2$ rule violation and CP invariance in, (E), 25:5263
decay K+ + γ + e+ + ν, on-shell current algebra for

XUM

branching ratio for, 25:5342
decay K+ → γ + e+ + ν, on-shell current algebra for effects of electromagnetic violations of time reversal invariance in, 25:5342
decay K+ → π+ + 2π0, comparison with K- → π- + 2π0 decay for partial rates of, (E), 25:5261
interactions K+ + n → K0 + p at 2 to 20 GeV/c, Regge model with four poles for, (E/T), 25:5371 (CEA-N-1373)
interactions K+ + p at 4.6 GeV/c in bubble chamber, cross section for elastic, (E), 25:5296
interactions K+ + π- → K0 + π0, cross sections for Chew--Low extrapolation of K+ + p → K + π + N interactions, (E/T>, 25:5369
interactions K+ + π- → K+ + π-, cross sections from Chew--Low extrapolation of K+ + p → K + π + N interactions, (E/T), 25:5369
mass difference (K+ - K0), SU(3) symmetry breaking parameters contribution to, (T), 25:5402
production in γ + p → K+ + Λ interactions at 1.3 GeV and γ + p → K+ + Σ+ interactions at 1.45 GeV, differential cross sections for, (E), 25:5253

MESONS (μ)
capture by hydrogen at low energies, PCAC hypothesis for effective pseudoscalar coupling in, (T), 25:5333
charge ratio of cosmic, (E/T), 25:4988
decay of, six-fermion interaction in spectra and widths for five-lepton production in, (T), 25:5344
detection of, produced from neutrinos, (E/T), 25:4989
energy loss in water at 0.5 to 100 GeV/c, Cherenkov detector for measuring, 25:4375
production at sea level by cosmic gamma rays and neutrons, (E/T), 25:4974 (AD-710278)
production of cosmic, (E/T), 25:4988
reactions with nuclei, review of experiments leading to isobaric analog energy levels, (E/T), 25:5580
research on cosmic, at California Univ., Oct. 1969 to Sept. 1970, 25:5257(R) (UCI-10-P-19-40)

MESONS (μ-)
reactions with hydrogen isotopes, hyperfine-structure transitions and isotope exchange in, (T), 25:4952 (JINR-P4-5039)

MESONS (ω)
decay of ω0 in deuterium bubble chamber, quantum numbers from, (E), 25:5271
decay ω → 2π, effect of ω - rho mixing in, 25:5324 (DNPL/R-7, pp 95-114)
decay ω → eta + γ, vector dominance Veneziano model and sum rules for broken SU(3) symmetry for, (T), 25:5402
interference of ω - rho in electromagnetic and strong interactions, 25:5322 (DNPL/R-7)
interference of ω - rho in electromagnetic interactions, (T), 25:5324 (DNPL/R-7, pp 95-114)
interference of ω - rho in strong interactions, 25:5373 (DNPL/R-7, pp 173-205)
interference of ω - rho in vector-meson photoproduction at high energies, 25:5325 (DNPL/R-7, pp 115-38)
parity and spin from ω production and decay in anti p + n → 2π- + π+ + π interactions at rest in deuterium bubble chamber, (E), 25:5271
photoproduction on nuclei, vector dominance model for relative phase of rho and, (T), 25:5327
photoproduction on protons and complex nuclei, review on, 25:5301 (DNPL/R-7, pp 29-70)
production in e+ + e- interactions, Orsay and Novosibirsk experiments on, 25:5250 (DNPL/R-7, pp 139-72)
production in photon reactions with complex nuclei, review of, (E/T), 25:5248 (DNPL/R-7, pp 71-85)
production in photon reactions with nuclei at 5.5 GeV/c, angular distributions for, (E), 25:5249 (DNPL/R-7, pp 87-94)
production in π+ + n interactions in Regge pole model, relative phase of rho and, 25:5374 (DNPL/R-7, pp 207-13)
production of ω0 in anti p + n → 2π- + π+ + π interactions at rest in deuterium bubble chamber, branching ratio and quantum numbers for, (E), 25:5271

MESONS (phi)
decay phi → eta + γ, vector dominance Veneziano model and sum rules for broken SU(3) symmetry for, (T), 25:5402
photoproduction on protons and complex nuclei, review on, 25:5301 (DNPL/R-7, pp 29-70)
production in e+ + e- interactions, Orsay and Novosibirsk experiments on, 25:5250 (DNPL/R-7, pp 139-72)

MESONS (π)
decay of, on-shell current algebra for form factors and coupling constants for radiative leptonic, (T), 25:5342
decay of, six-fermion weak interaction in spectra and widths for four-lepton production in, (T), 25:5344
exchange in π- + p interactions near 1 GeV, peripheral model for, (T), 25:5376
form factor from scattering amplitude in Veneziano model, electric, 25:5338
interactions K + π → K + eta in Veneziano model, SU(3) structure for internal symmetry from, 25:5370
interactions K + π → K + π in Veneziano model, SU(3) structure for internal symmetry from, 25:5370
interactions π + α → π + α, electromagnetic corrections including relativistic terms for, (T), 25:5527
interactions π + d, two-Regge pole model for dispersion sum rules for, (T), 25:5391
interactions π + eta → π + eta in Veneziano model, SU(3) structure for internal symmetry from, 25:5370
interactions π + K, symmetry-breaking effect on p-wave resonances in, (T), 25:5394
interactions π + N, differential cross sections for charge exchange, (T), 25:5294
interactions π + N, review of diffraction for, (E/T), 25:5386 (CONF-700314-, Paper 14)
interactions π + N, sum rules and double partial-wave expansion of amplitudes of, (T), 25:5310
interactions π + p → π + p at low energies, phenomenological Regge trajectories in direct-channel, (T), 25:5382
interactions π + p at 50 to 1000 GeV, review of multiparticle production in, (E), 25:5273
interactions π + p at high energies, Bethe--Salpeter equation for inelastic, 25:5359
interactions π + p at very high energies and high momentum transfers, large-angle and backward, (E/T), 25:5281 (CONF-700314-, Paper 15)
interactions π + π → π + π in Veneziano model, SU(3) structure for internal symmetry from, 25:5370
interactions π + π in minirings and colliding beams, feasibility of, (E), 25:5285 (RLC-2041-40)
interactions π + π, duality and sum rules for scattering lengths in, (T), 25:5363
interactions π + π, symmetry-breaking effect on p-wave resonances in, (T), 25:5394
mass of, PCAC hypothesis consistency with unitarity in sigma model for dependence of amplitudes on, (T), 25:5367
production in e + N → π + N and γ + N → π + N interactions at low energies, PCAC hypothesis for, 25:5333
production in e + N and γ + N interactions, test of vector dominance from asymmetry ratio in, 25:5326
production in electron electromagnetic cascade interactions in copper at 400 MeV, 25:5255
production in p + n interactions at 24 GeV in emulsions and hydrogen bubble chamber, energy spectra and transverse-momentum distributions for, (E), 25:5276
production in particle interaction final states, lower bounds on threshold charge-exchange amplitude from di-pion mass distributions for, (T), 25:5315
production in spinless boson interactions, lower bounds on threshold charge-exchange amplitude from di-pion mass distributions for, (T), 25:5315
production of πrho final state in π reactions with nuclei at high energies, review of diffraction dissociation for, (E/T), 25:5386 (CONF-700314-, Paper 14)
reactions with nuclei at 50 to 1000 GeV, review of multiparticle production in, (E), 25:5273
reactions with nuclei at high energies, diffraction dissociation for πrho final state in, (E/T), 25:5386 (CONF-700314-, Paper 14)
reactions with nuclei, review of experiments leading to isobaric analog energy levels, (E/T), 25:5580

MESONS (π-)
absorption by nuclei at 20 to 60 GeV/c, cross sections for, (E), 25:5265 (CONF-700314-, Paper 4)
absorption by nuclei at 20 to 65 GeV/c, cross sections for, (E), 25:5295
capture by hydrogen, x-ray spectrum from, (E), 25:5268
interactions K+ + π- → K0 + π0, cross sections for Chew--Low extrapolation of K+ + p → K + π + N interactions, (E/T>, 25:5369
interactions K+ + π- → K+ + π-, cross sections from Chew--Low extrapolation of K+ + p → K + π + N interactions, (E/T), 25:5369
interactions π- + d at 20 to 65 GeV/c, total cross sections for, (E), 25:5295
interactions π- + N below 65 GeV, differences of total cross sections for π+ + N and, (E), 25:5294
interactions π- + p → A2- + p at 3.5 to 16 GeV/c in bubble chamber, production mechanism of A2-, 1-daughter production, and cross sections for, (E), 25:5282 (COO-1195-200)
interactions π- + p → eta + n at 2.5 to 18.2 GeV/c, heavy-plate spark chamber study of differential cross sections for, (E), 25:5279 (CEA-R-4037)
interactions π- + p → π0 (eta) + n at 2 to 20 GeV/c, Regge model with four poles for, (E/T), 25:5371 (CEA-N-1373)
interactions π- + p → rho + p in absorption model, cross section for, 25:5381
interactions π- + p → rho0 + n, cross sections and rho spin density matrices in Regge models for, (E/T), 25:5380
interactions π- + p at 17 GeV/c, azimuthal correlations in decays of 1.5- to 2.5-GeV mesonic resonances produced in, (E), 25:5366
interactions π- + p at 20 to 65 GeV/c, total cross sections for, (E), 25:5295
interactions π- + p at 25 GeV/c, multiparticle production in, (E), 25:5260 (CONF-700314-, Paper 10)
interactions π- + p at high energies, effective Regge trajectories for two-body production in, (T), 25:5377
interactions π- + p at infinite momentum, resonance-background interference corrections to finite-energy sum rule estimates of total cross sections for, (T), 25:5378
interactions π- + p near 1 GeV, N and π exchange in

peripheral model for momentum and angular distributions for π^+ and π^- production in, (T), 25:5376
interactions $\pi^+ + \pi^- \to \pi^0(\pi^+) + \pi^0(\pi^-)$ in colliding beams, cross section energy and angular dependence measurement for, (E/T), 25:5360 (RLO-2041-51)
production in $\pi^- + p$ interactions near 1 GeV, peripheral model with N and π exchange for momentum and angular distributions for, (T), 25:5376
reactions $(\pi^-,2\pi^-)$ with carbon-12 at 4 GeV/c in propane bubble chamber, upper limits for cross sections of, (E), 25:5293
reactions (π^-,γ) with hydrogen and oxygen-16 at 250 MeV/c, neutron time-of-flight and gamma energy spectra from, (E), 25:5600
reactions $(\pi^-,\pi\pi^0)$ with carbon-12 at 4 GeV/c in propane bubble chamber, upper limits for cross sectons of, (E), 25:5293

MESONS (π^0)
decay $\pi^0 \to 2\gamma$, current structure and coupling constants for, 25:5337
interactions $\pi^0 + \pi^0$, lower limits for scattering lengths for, 25:5368
production in π^+ reactions with xenon at 2.34 GeV/c in xenon bubble chamber, π^0--π^0 mass spectrum from, (E), 25:5284 (JINR-E1-5085)

MESONS (π^+)
interactions $\pi^+ + d \to 2p + K^+ + K^-$ at 1.1 to 2.4 GeV/c, phi(1020) and Λ(1520) production in, (E), 25:5289
interactions $\pi^+ + d \to n + \Lambda + K^+ + \pi^+$ at 1.1 to 2.4 GeV/c, I(1385) production in, (E), 25:5289
interactions $\pi^+ + d \to n + \Sigma^+ + K^0 + \pi^+$ at 1.1 to 2.4 GeV/c, K^{*+} production in, (E), 25:5289
interactions $\pi^+ + d$ at 1.1 to 2.4 GeV/c, total cross sections for, (E), 25:5289
interactions $\pi^+ + N$ below 65 GeV, differences of total cross sections for $\pi^- + N$ and, (E), 25:5294
interactions $\pi^+ + n$ in Regge pole model, relative phase of rho and ω production in, 25:5374 (DNPL/R-7, pp 207-13)
interactions $\pi^+ + p \to f^0 + \Delta^{++}$ at 13.1 GeV/c in hydrogen bubble chamber, cross sections and dipion mass spectrum for, (E), 25:5283 (COO-1428-238)
interactions $\pi^+ + p \to K^+ + \Sigma(1385)$ at 4 and 5.05 GeV/c, test of SU(3) symmetry from counter and spark chamber study of differential cross sections for, (E), 25:5290
interactions $\pi^+ + p \to \pi^+ + p + \pi^+ + \pi^-$ at 11.0 GeV/c, rho^0, Δ^{++}(1236), and A production in, (E), 25:5292
interactions $\pi^+ + p$ at 8 GeV/c, production of (anti pp), (K^+K^-), and $(\pi^+\pi^-)$ pairs in, (E), 25:5297
interactions $\pi^+ + p$ at high energies, effective Regge trajectories for two-body production in, (T), 25:5377
interactions $\pi^+ + p$ at infinite momentum, resonance-background interference corrections to finite-energy sum rule estimates of total cross sections for, (T), 25:5378
interactions $\pi^+ + \pi^- \to \pi^0(\pi^+) + \pi^0(\pi^-)$ in colliding beams, cross section energy and angular dependence measurement for, (E/T), 25:5360 (RLO-2041-51)
production in $\gamma + p \to \pi^+ + n$ interactions at 2.6 to 16 GeV with linearly polarized photons, spin--parity contributions to cross sections for, (T), 25:5321 (DEMO-70/1)
production in $\gamma + p \to \pi^+ + n$ interactions at 5 and 16 GeV, cross section asymmetry for, (E), 25:5251 (UCRL-15897)
production in $\pi^- + p$ interactions near 1 GeV, peripheral model with N and π exchange for momentum and angular distributions for, (T), 25:5376
reactions with xenon at 2.34 GeV/c in xenon bubble chamber, π^0--π^0 mass spectrum from, (E), 25:5284 (JINR-E1-5085)

MESONS (rho)
decay of rho^0 inside nucleus from photon reactions with nuclei, (T), 25:5336
decay rho $\to$ eta + γ, vector dominance Veneziano model and sum rules for broken SU(3) symmetry for, (T), 25:5402
interactions rho + N $\to$ rho + N, extension of Drell--Trefil theory for rho^0 coherent production in electron reactions with heavy nuclei for amplitudes of, (T), 25:5336
interference of ω - rho in electromagnetic and strong interactions, 25:5322 (DNPL/R-7)
interference of ω - rho in electromagnetic interactions, (T), 25:5324 (DNPL/R-7, pp 95-114)
interference of ω - rho in strong interactions, 25:5373 (DNPL/R-7, pp 173-205)
interference of ω - rho in vector-meson photoproduction at high energies, 25:5325 (DNPL/R-7, pp 115-38)
mass and width from Z = 0 formalism for composite particles, 25:5417
photoproduction on carbon, vector dominance model for relative phase of ω, (T), 25:5327
photoproduction on protons and complex nuclei, review on, 25:5301 (DNPL/R-7, pp 29-70)
polarization of rho^0 in $e + p \to rho^0 + p$ interactions, Pomeranchuk decoupling from ordinary Regge trajectories in transverse, (T), 25:5348 (COO-264-562)
production in anti $p + n \to 2\pi^- + \pi^+ + \pi$ interactions at rest in deuterium bubble chamber, branching ratios for, (E), 25:5271
production in $e^+ + e^-$ interactions, Orsay and Novosibirsk experiments on, 25:5250 (DNPL/R-7, pp 139-72)
production in $\gamma + p \to \pi^+ + \pi^- + p$ interactions, diffraction-dissociation, dual-resonance, and interference models for rho production in, 25:5323 (DNPL/R-7, pp 3-28)
production in photon reactions with complex nuclei, review of, (E/T), 25:5248 (DNPL/R-7, pp 71-85)
production in $\pi + N \to rho + N$ interactions, test of vector dominance from asymmetry ratio in, 25:5326
production in $\pi^+ + n$ interactions in Regge pole model, relative phase of ω and, 25:5374 (DNPL/R-7, pp 207-13)
production in $\pi^- + p \to rho^0 + n$ interactions, cross sections and rho spin density matrices in Regge models for, 25:5380
production of πrho final state in π reactions with nuclei at high energies, review of diffraction dissociation for, (E/T), 25:5386 (CONF-700314-, Paper 14)
production of rho^0 in electron reactions with heavy nuclei, rho + N $\to$ rho + N amplitudes and rho photoproduction from Drell--Trefil theory extension for coherent, (T), 25:5336
production of rho^0 in photon reactions with deuterium, closure approximation validity for, (T), 25:5336
production of rho^0 in photon reactions with heavy nuclei, Drell--Trefil theory extension for rho^0 coherent production in electron reactions with heavy nuclei for amplitudes of, (T), 25:5336
production of rho^0 in photon reactions with light nuclei, coherent, (T), 25:5336
production of rho^0 in $\pi^+ + p \to \pi^+ + p + \pi^+ + \pi^-$ interactions at 11.0 GeV/c, (E), 25:5292
production of rho^0 inside nucleus in photon reactions with nuclei, (T), 25:5336

MESONS (X^0)
decay $X^0 \to 2\gamma$, current structure and coupling constants for, 25:5337
parity and spin of X^0(960) from $K^- + p \to X^0(960) + \Lambda$ interactions on polarized targets, (T), 25:5361 (TFJU-14/70)
production of X^0(960) in $K^- + p \to X^0(960) + \Lambda$ interactions on polarized targets, (T), 25:5361 (TFJU-14/70)

MESONS, RESONANCE
decay $A_2^- \to eta^0 + \pi^-$ in bubble chamber, spin and parity of A_2^- from, (E), 25:5282 (COO-1195-200)
decay eta' $\to \pi^+ + \pi^- + eta(\gamma)$, spin, parity, and branching fraction for, (E), 25:5251
decay eta' $\to \pi^+ + \pi^- + \gamma$, mediation by eta' $\to rho^0 + \gamma$ decay for, (E), 25:5291
decay $K^0 \to K + \gamma$, vector dominance Veneziano model and sum rules for broken SU(3) symmetry for, (T), 25:5402
decay of 0^+, 1^+, 2^+, additive quark model for angular distributions for, (T), 25:5375 (TFJU-15/70)
decay of 1.5- to 2.5-GeV, azimuthal correlations in, (E), 25:5366
interactions of, resonance width determination from interference of identical particles in, (T), 25:5350 (JINR-P1-5315)
isospin of eta'- from $K^- + d \to p + \Lambda +$ eta'- interactions, (E), 25:5291
mass of kappa, SU(3) x SU(3) symmetry breaking parameter relation with Glashow--Weinberg bounds on, (T), 25:5399 (JINR-P2-5250)
parity and spin of A_2^- from $A_2^- \to eta^0 + \pi^-$ decay in bubble chamber, (E), 25:5282 (COO-1195-200)
production of 1.5- to 2.5-GeV, in $\pi^- + p$ interactions at 17 GeV/c, (E), 25:5366
production of Λ in $\pi^+ + p \to \pi^+ + p + \pi^+ + \pi^-$ interactions at 11.0 GeV/c, (E), 25:5292
production of A_2^- and 1^- daughter state in $\pi^- + p \to A_2^- + p$ interactions at 3.9 to 16 GeV/c in bubble chamber, mechanism for, (E), 25:5282 (COO-1195-200)
production of exotic, in $K^- + d$ interactions at 3 GeV/c, upper limits for cross sections of, (E), 25:5287
production of J = 0 $\pi\pi$(1115) in anti $p + n \to 2\pi^- + \pi^+ + \pi$ interactions at rest in deuterium bubble chamber, (E), 25:5271
production of K^{*+} in $\pi^+ + d \to n + \Sigma^+ + K^0 + \pi^+$ interactions at 1.1 to 2.4 GeV/c, (E), 25:5289
production of p-wave, in $\pi + \pi$, $\pi + K$, and K + anti K interactions, symmetry-breaking effect on, (T), 25:5394
production of phi(1020) in $\pi^+ + d \to 2p + K^+ + K^-$ interactions at 1.1 to 2.4 GeV/c, (E), 25:5289
properties of A_2 double-peaked structure, (E), 25:5286
search for eta'- in $K^- + d \to p + \Lambda +$ eta'- interactions, (E), 25:5291
width of, identical particle interference in resonance interactions for determining, (E/T), 25:5350 (JINR-P1-5315)

METALLURGICAL EQUIPMENT
performance of Fisher, for determining particle size of powder compacts and powders, 25:4184(T) (LA-4404-TR)

METALS
abundance in three eclipsing binary stars, (E), 25:4500
electron energy loss to surface excitations in thin films of, at 25 keV, (T), 25:4937 (IS-T-380)
electroplating using high-current rectangular-shaped pulses, 25:4741 (BNWL-CC-491)
occurrences in lower ionosphere, ionization and loss processes for meteoric, 25:5012
radiation effects on creep, fracture, hardening, and

swelling of, review on, 25:4812 (BNWL-SA-3495)
radiation effects on dislocation channeling in, 25:4809 (AD-710358)
radioinduced creep in, loop unfaulting mechanism for neutron, 25:4830
thermoelectric power in, (T), 25:6227 (COC-623-152)
transport properties of, research on, 25:5171(R) (CRO-3087-44)
metal--polymer, radioinduced polymerization of composites of, γ, 25:4108
METEORITES
analysis of Italian, for aluminum and silicon by instrumental pile neutron activation, 25:4048
metal elements in lower ionosphere, ionization and loss processes for, 25:5012
xenon release from heating of neutron-irradiated, (E/T), 25:4922
METHACRYLIC ACID, METHYL ESTER
radioinduced polymerization in wood, comparison of economics of heat, heat--catalyst, and γ, 25:4109
radioinduced polymerization with kaolin clay, energy deposition, kinetics, and mechanism of γ, 25:4107
METHACRYLIC ACID, METHYL ESTER, POLYMERS
radiation-induced optical density fading in, for chemical dosimetry, effects of oxygen on, 25:4384
METHANE
corrosive effects as impurity in flowing helium on graphite at 600 to 750°C, 25:4835 (DP-Report-448)
determination in helium by gas chromatography, on-line, 25:4012 (DP-Report-443)
effects of high-temperature, on mechanical properties of steel, 25:4738 (DP-Report-527)
effects of high-temperature, on mechanical properties of austenitic stainless steel, 25:4738 (DP-Report-527)
effects of high-temperature, on properties of Nimonic 75, 25:4738 (DP-Report-527)
hydrogen-atom reactions at 1 to 25 keV with, cross sections for ionization in, (E), 25:4963
proton reactions at 1 to 25 keV with, cross sections for electron capture and total ionization in, (E), 25:4963
yields from γ radiolysis of 2,2-dimethylpropane, effects of deuterated ammonia and nitrous oxide on, 25:4113
yields from γ radiolysis of 2-propanol, 25:4123
yields from the gas-phase α radiolysis of propane, 25:4119
METHANE, IODO-
effects on x-radiosensitivity of Ehrlich ascites tumor cells in cultures, 25:4569
effects on x-radiosensitivity of enzymes in solutions, 25:4569
removal of labeled, from reactor containment air, efficiency of charcoal filter for, 25:4142
METHANESULFONIC ACID, ETHYL ESTER
effects on peas following seed exposure in comparison to effects of γ radiation and NEM, rate of mutagenic, 25:4489
effects on seeds of Sorghum sp., mutagenic, 25:4495
METHANESULFONIC ACID, METHYL ESTER
effects on seeds of Sorghum sp., mutagenic, 25:4495
effects on uv- and x-radiosensitivity of yeast mutants, 25:4480
METHANOL
complexes with thorium and uranium tetrachlorides, formation of crystalline, thermodynamics of, 25:4077
neutron scattering by ordinary and deuterated, total cross sections for cold, (E), 25:5500
METHEMOGLOBINS
synthesis in erythrocytes in vitro, effects of vitamin K-3 on, 25:4598
METHOTREXATE
effects on radiosensitivity of human brain tumors, combined effects of 5-bromodeoxyuridine on ionizing, 25:4688
METHYL ISOCYANIDE
reactions with recoil tritium atoms, kinetics of, 25:4131
METHYL SULFOXIDE
effects on electron-radiosensitivity of DNA in Escherichia coli, 25:4551
METHYLAMINE
complexes with uranium(IV) fluorides, preparation of, 25:4058
METHYLENE BLUE
radioprotective effects on lactic dehydrogenase and isoenzymes in rats, γ, 25:4605
MICE
content of glucose, lactate, and pyruvate in blood of, effects of cysteamine on, 25:4553
effects of oxamic acid on glycolysis in, 25:4566
effects of skin wounds on survival of, combined effects of x radiation on, 25:4576
growth of γ-irradiated, 5,9-dihydroxypsoralen-treated Ehrlich ascites tumor cells in, 25:4565
growth of oxamic acid-treated, x-irradiated Ehrlich ascites tumor cells following transplantation into, 25:4566
growth of transplants of chemically-radiosensitized x-irradiated, ascites tumor cells in, 25:4562
growth of transplants of x-irradiated, L-erythro-α,β-dihydroxybutraldehyde-treated Ehrlich ascites tumor cells in, 25:4564
immunization against virus-induced tumors, use of transplants of irradiated fetal tissues for, 25:4656(R) (ORNL-4615)
radiation effects on antibody responses in, role of, on susceptibility to anaphylactic shock, 2.2-Gev proton, γ and x, 25:4470
radiation effects on blood of, effects of thymectomy on x, 25:4469
radiation effects on erythropoiesis in bone marrow and spleen of, iron-59 tracer study of effects of adrenalectomy on x, 25:4696
radiation effects on growth of transplants of Erhlich carcinoma in, combined effects of polyethylenimine on x, 25:4563
radiation effects on life span of, in desert ecosystems, γ, 25:4477 (UCLA-12-782, pp 49-81)
radiation effects on repopulation of spleen of, by endogenous hemopoietic cells, effects of estradiol on x, 25:4471
radiation effects on spleen colony formation by stem cells in, protective effects of hematoporphyrin against γ, 25:4572
radiation effects on spleen colony formation by syngenic stem cells in, protective effects of para-aminopropiophenone and propylene glycol against, 25:4571
radiation effects on stomach of, carcinogenic whole-body γ, neutron, and x, 25:4703
radiation effects on survival of, effects of body temperature on protective effects of sodium fluoroacetate against x, 25:4580
radiation effects on survival of, protective effects of mixtures of AET, cysteamine, cysteine, glutathione, and serotonin against x, 25:4582
radiation effects on survival of, protective effects of sodium fluoroacetate against x, 25:4579
radiation effects on survival of, protective effects of hypoxia against x, 25:4578
radiation effects on survival of, protective effects of mixtures of AET and 5-methoxytryptamine against x, 25:4583
radiation effects on survival of, protective effects of serotonin against x, 25:4584
radiation effects on survival of, protective effects of N-substituted AET derivatives against x, 25:4577
radiation effects on survival of, protective effects of adrenochrome monoguanylhydrazone methanesulfonate against internal β and external γ and x, 25:4585
radiation effects on survival of, protective effects of bacterial endotoxins against x, 25:4586
radiation effects on, protective effects of AET and 8-mercaptoquinoline against x, 25:4553
radiation injuries in, histological evaluation of balneotherapy for treatment of γ and neutron, 25:4610
radioinduced injuries in, effects of postirradiation time on recovery from ionizing, 25:4705
radioinduced lung tumors in, histology of, 25:4695
radioinduced mutations in, effects of dose on repair of, ionizing, 25:4501
radiosensitivity of duodenum crypt cells in, effects of N-ethylmaleimide, iodoacetamide, and iodoacetic acid on x, 25:4587
radiosensitivity of, effects of barenylacetic acid and methyl-o-barencarboxylic acid on fast neutron and γ, 25:4588
replication of DNA in thymus cells and γ-radiolinduced thymoma cells in, tracer study, 25:4460
spontaneous lung tumors in, histology of, 25:4695
toxicity of thorium nitrate, thorium chloride, and thorium dioxide in, comparison of, 25:4440
MICROORGANISMS
radiation dosimetry in, methods for, 25:4507 (EUR-4506)
radiation effects on count of, on fish in relation to spoilage, γ, 25:4734 (TID-25467)
MICROWAVE EQUIPMENT
eigenstate change in superconducting rf cavity due to nonlinear response, 25:5063
MICROWAVE SPECTROSCOPY
equipment and method for free-radical rotational, using resonant cavity, 25:6253 (UCRL-50890)
MICROWAVES
effects on animals and man in comparison to effects of γ and x radiation, review of, 25:4708 (UR-45-1256)
interactions with plasma near electron cyclotron harmonics, plasma spreading in, (E), 25:5132
use for plasma diagnostics, conference on, 25:5080(T) (LA-4520-TR)
MILK
radioisotope content of, in Faroe Islands during 1965, cesium-137 and strontium-90, 25:4476(R) (RISO-221)
MILKY WAY
evolution of, development of spiral structure in, (T), 25:4929 (N-70-33057)
nucleosynthesis in, chronology of, (E/T), 25:4922
MILLSTONE POINT POWER REACTOR, UNIT 1
operation of, training of personnel for, 25:5885
personnel for, training program for startup and operation, 25:5887
MINERAL DEPOSITS
prospecting by in situ neutron activation using californium-252 source, 25:4218

XUM

MINERALS
analysis of, use of neutron diffraction in, 25:4151 (CEA-CONF-1500)
conference on methods for measurement of content of, in bones, 25:4630 (CONF-700515)
content of bone, method for measurement of, using polychromatic x ray images and computer film analysis, 25:4614 (CONF-680211-, pp 80-95)
content of bones in dogs, methods for measurement of, using γ transmission scanning, 25:4654 (CONF-700515-, pp 424-7)
content of bones in man, methods for measurement of, using dye precipitation and radiography, 25:4629 (CONF-680211-, pp 411-21)
content of bones, methods for determination of, 25:4412 (CONF-680211-, pp 5-24)
content of bones, methods for measurement of, 25:4612 (CONF-680211)
content of bones, methods for measurement of, using radiography, high-speed densitometers, and computer data analysis, 25:4620 (CONF-680211-, pp 191-203)
content of bones, methods for measurement of, using x-ray transmission scanning, 25:4650 (CONF-700515-, pp 314-31)
content of bones, methods for measurement of, using x-ray transmission scanning, 25:4647 (CONF-700515-, pp 274-9)
content of bones, methods for measurement of, using dual beam γ transmission scanning, 25:4645 (CONF-700515-, pp 263-71)
content of human bones, comparison of results of measurements of, using γ transmission scanning or radiography, 25:4651 (CONF-700515-, pp 340-50)
content of human bones, effects of age and sex on, methods for measurement of, using radiography, 25:4619 (CONF-680211-, pp 177-91)
content of human bones, effects of age and sex on, method for measurement of, using radiography, 25:4616 (CONF-680211-, pp 115-35)
content of human bones, effects of age, race, and sex on, methods for measurement using photon transmission scanning, 25:4624 (CONF-680211-, pp 283-96)
content of human bones, effects of medullary fats on results of measurements of, 25:4644 (CONF-700515-, pp 255-62)
content of human bones, measurement of, using γ transmission scanning, 25:4631 (CONF-700515-, pp 1-21)
content of human bones, measurement of, using γ transmission scanning, 25:4635 (CONF-700515-, pp 48-57)
content of human bones, measurement of, using γ transmission scanning, 25:4634 (CONF-700515-, pp 33-47)
content of human bones, measurements using routine radiographs, 25:4639 (CONF-700515-, pp 199-204)
content of human bones, methods for measurement of, in patients with osteopenia, use of γ transmission scanning for, 25:4627 (CONF-680211-, pp 319-28)
content of human bones, methods for measurement of, using monoenergetic photon transmission scanning, 25:4623 (CONF-680211-, pp 253-68)
content of human bones, methods for measurement of, using photon transmission scanning, 25:4625 (CONF-680211-, pp 296-308)
content of human bones, methods for measurement of, using radiography and computer analysis of data, 25:4628 (CONF-680211-, pp 331-51)
content of human bones, methods for measurement of, using dual beam γ transmission scanning, 25:4648 (CONF-700515-, pp 291-302)
content of human bones, methods for measurement of, using γ transmission scanning, 25:4649 (CONF-700515-, pp 308-12)
content of human bones, methods for measurement of, using monoenergetic x-ray transmission scanning, 25:4621 (CONF-680211-, pp 204-15)
content of human bones, methods for measurement of, radiographic and radiometric, 25:4622 (CONF-680211-, pp 216-49)
content of human bones, methods for measurement of, using γ transmission scanning, 25:4653 (CONF-700515-, pp 408-22)
content of human bones, methods for measurement of, using γ transmission scanning, 25:4632 (CONF-700515-, pp 22-7)
content of human bones, methods for measurement of, using γ transmission scanning, 25:4633 (CONF-700515-, pp 28-32)
content of human bones, methods for measurement of, using computer analysis of radiographs, 25:4637 (CONF-700515-, pp 188-94)
content of human bones, methods for measurement of, using computer analysis of line segments of radiographs for, 25:4638 (CONF-700515-, pp 195-8)
content of human bones, methods for measurement of, using radiography, 25:4617 (CONF-680211-, pp 135-59)
content of human bones, methods for measurement of, using dual beam γ transmission scanning, 25:4643 (CONF-700515-, pp 243-54)
content of human bones, radiographic densitometry methods for measurement of, 25:4615 (CONF-680211-, pp 95-115)
content of human bones, use of radiographs for measurements of, 25:4640 (CONF-700515-, pp 205-23)
content of human bones, use of x-ray spectrophotometers for measurement of, 25:4642 (CONF-700515-, pp 237-42)
content of human finger phalanx, effects of age and sex on, γ-transmission scanning method for measurement of, 25:4626 (CONF-680211-, pp 308-19)
MISSILES
nuclear explosion effects on ballistic, high-altitude, (T), 25:5239
MITOCHONDRIA
radioisotope distribution in liver, of rats, effects of p-dichlorophenol on calcium-45 and strontium-89, 25:4431
radiosensitivity of duodenum crypt cell, in mice, x, 25:4587
MITOMYCINS
effects on x-radiosensitivity of spleen colony formation by bone marrow cells following transplantation into syngenic mice, 25:4670
MITOSIS
radioinduced translocation of chromatids during, in Crepis capillaris, effects of time postexposure on x, 25:4496
MOESSBAUER SPECTROMETERS
design of Van de Graaff accelerator in-beam using Coulomb-excitation gamma source, 25:5467
MOLECULAR BEAMS
scattering on surfaces, interpretation of ionization gage detector signal for studying, 25:4542
MOLECULES
atom inelastic scattering by, delta-function technique for calculation of, 25:4562
dissociation of diatomic, mechanisms in thermal, 25:6252(T) (SC-T-70-4045)
energy-level transitions from, in comets, detection by radio emission from, (E), 25:4916 (LA-4542)
reflection from surfaces, (E/T), 25:6221(T) (BNL-tr-383)
MOLLUSCA
Lymnaea stagnalis, radiation effects on sex cells of, effects of dose 10,000 R on γ, 25:4693
Mytilus edulis, phosphorus-32 uptake, distribution, and excretion by, 25:4448
squid, protein synthesis sites in nerve fibers of, location of, tracer study for, 25:4418
MOLTEN SALT BREEDER REACTOR
fuel reprocessing for, 25:4138 (ORNL-TM-3053)
fuel stream of, computer program for calculation of chemical, nuclear, and physical processes in, 25:4138 (ORNL-TM-3053)
MOLTEN SALT REACTOR EXPERIMENT
maintenance requirements of, 25:6059
MOLYBDENUM
corrosion of borided bearing coatings of, by sodium at 1100°F, 25:4185(R) (NYO-3930-8)
determination in boron, 25:4009 (TID-25190)
dislocation structure of, etching by hot argon flow for visualizing, 25:4796
effects of alloying additions of, on purification of iron--nickel vacuum melts, relations with composition and reduced pressure, 25:4744
effects on mechanical properties and microstructure of chromium--nickel alloy, 25:4782
ion reactions at 10 to 30 eV with polycrystalline, electron yields and energy distributions from, (E), 25:4943
properties for coating niobium thermionic collectors, 25:4750 (TEE-4125-2)
properties for use as encapsulating material for californium-252 sources for neutron capture gamma-ray spectroscopy, 25:4772
properties of electrowon and hydrogen reduction-produced powders and sheets of, 25:4740 (BM-RI-7455)
radiation effects on crystal structure of, neutron, 25:4887 (KFK-1215)
radiation effects on helium release from, alpha particle, 25:4216(R) (SC-PR-70-682)
reactions with cyanide in sodium at 800°C, 25:4736(R) (ANL/ST-3)
separation by ion exchange using Alamine 336 or Amberlyst A-21 in aqueous thiocyanate solutions, 25:4137 (IS-T-377)
structure of work-hardened surface layers of, effects of vacuum annealing on, 25:4797
superconducting critical field curve of, (E), 25:5057
MOLYBDENUM ALLOYS AND SYSTEMS
Co--Mo--Pd, electric and magnetic properties of solid solutions of, temperature dependence of, (E/T), 25:5178
Cr--Mo--steel, mechanical properties of, effects of high-temperature carbon oxides, methane, nitrogen, or water on, 25:4738 (DP-Report-527)
Fe-base--Mo, K-absorption spectrum edge in, 25:5181
Mo--Nb-base, mechanical properties of monocrystalline, at 77 to 475°K, effects of compression on, 25:4800
Mo--Nb-base, mechanical properties of, effects of molybdenum content on, 25:4786 (CCC-1676-13)
Mo--Nb-base, slip in monocrystalline, at 77 to 475°K, effects of compression on, 25:4800
Mo--Pd, electric and magnetic properties of solid solutions of, temperature dependence of, (E/T), 25:5178

MOLYBDENUM ISOTOPES Mo-92
argon-36 reactions at 137 MeV, gamma spectra from, (E), 25:5688 (UCRL-19961)
photon reactions (γ,pn) and (γ,2n) at 150 to 305 MeV, analysis for reaction mechanism in, (E), 25:5679
MOLYBDENUM ISOTOPES Mo-96
energy-level scheme from niobium-96 decay, (E), 25:5718
MOLYBDENUM ISOTOPES Mo-97
energy level at 658 keV from niobium-97 decay, spin and parity of, (E), 25:5732
MOLYBDENUM ISOTOPES Mo-98
neutron capture integral in fast region, (E), 25:5656
MOLYBDENUM ISOTOPES Mo-99
distribution in irradiated plutonium dioxide--uranium dioxide fuel pins, 25:4804
distribution in irradiated plutonium dioxide--uranium dioxide fuel pins, 25:4891
fission yields for fast reactor spectra, performance of, 25:5973
MOLYBDENUM OXIDES
BaO--MoO_3, phase studies of, 25:4873
CeO_2--MoO_3, phase studies of, 25:4872
MONKEYS
blood circulation in fetuses of pregnant, effects of biological stress on, tracer study of, 25:4655 (COO-1762-6)
radioinduced burn injuries in, laser, 25:4704
MONOMERS
radioinduced crosslinking and polymerization of, chain reaction method for, 25:4097
radioinduced crosslinking of, method for electron, 25:4100(P)
radioinduced graft polymerization onto inorganic substrates, γ, 25:4106
radioinduced polymerization in wood, comparison of economics of heat, heat--catalyst, and γ, 25:4109
MONTE CARLO METHOD
computer program package for analysis of collisions using, 25:5237 (ORNL-TM-3203)
MONTMORILLONITES
cation exchange selectivity of, 25:4160
MUSCLES
radiation effects on stimulation threshold of nerve apparatus in, of hind paws of rats following intratracheal and intraperitoneal injection of thorium dioxide, α, 25:4701
xenon-133 distribution in, of cats, following intramuscular injection in, 25:4429
MUSCOVITES
cation exchange selectivity of, 25:4160
MUTAGENS
effects on crop plants in comparison to effects of ionizing radiation, review of literature on aberrant, 25:4489
effects on diploid and polyploid oats, review of, 25:4484
effects on peas and wheat for agricultural improvement, review of, 25:4488
MUTATIONS
induced in beans by cycasin, frequency of chlorophyll and morphological, 25:4717 (NYO-2043-216, pp 1-18)
radiation effects on frequency of chlorophyll, in barley, protective effects of anoxia, cysteine, and water against fast neutron and γ, 25:4604
radioinduced, for culm length and lodging resistance in rice, effects of dose on γ, 25:4487
radioinduced, in agricultural plants in Soviet Union, review of, 25:4489
radioinduced, in agricultural plants, review of literature on, 25:4482
radioinduced, in Antirrhinum and tomatoes, effects of dose on γ, 25:4483
radioinduced, in cotton plants following pollen exposure, γ, 25:4499
radioinduced, in diploid and polyploid oats, review of thermal neutron and x, 25:4484
radioinduced, in maize and soybeans for quantitative traits, review of thermal neutron, 25:4485
radioinduced, in Mediterranean fruit flies, γ, 25:4733 (NYO-2043-216, pp 19-48)
radioinduced, in mice, effects of dose on repair of, ionizing, 25:4501
radioinduced, in mulberry trees for leaf yield and dwarf disease susceptibility, effects of dose on γ, 25:4486
radioinduced, in plants for agricultural improvement in Italy, review of, 25:4488
radioinduced, in seeds of sorghum, 25:4495
radioinduced, in trees for economic or ornamental benefits, γ or x, 25:4724
radioinduced, in yeast, effects of methyl methanesulfonate and nitrogen mustard on uv and x, 25:4480
radioinduced, review of, 25:4524

N

NAPHTHOL
spectra of, correlation of extended Huckel calculations of total electron densities with NMR, 25:4081
NASA RESEARCH REACTOR
reflector for, neutron poison buildup in, 25:4814 (N-70-32313)
NATIONAL ACCELERATOR LABORATORY SYNCHROTRON
design and development of, 25:5445 (CONF-700314-, Paper 3)
experimental facility for, target handling system for, 25:5470
NATURAL BACKGROUND RADIATION
dose to man from cosmic radiation and terrestrial radioactivity, 25:4518
NATURAL GAS
helium-3 and krypton-85 monitoring in, flowthrough proportional detector for, 25:4352
production stimulation using multiple underground nuclear explosions, 25:4173
safety of nuclearly stimulated, for public consumption, evaluation of radiological, 25:4525 (ORNL-TM-3216)
NATURAL WATERS
use of hot spring, for treatment of radiation injuries in mice, histological evaluation of, 25:4610
NEMATODA
Ascaridia galli, radiation effects on development of eggs of, x, 25:4692 (COO-1209-13)
Heterakis gallinarum, radiation effects on development of eggs of, effects of dose on x, 25:4692 (COO-1209-13)
NEODYMIUM
compounds with mandelic acid, preparation by reactions of neodymium alkoxides with mandelic acid, potentiometric studies on, 25:4055
separation of trace amounts of, from aqueous nitric acid solutions by solvent extraction using D2EHPA in toluene containing trace amounts of uranium, 25:4150
NEODYMIUM ALLOYS AND SYSTEMS
Al--Nd, magnetic structure of NdAl, neutron-diffraction study, 25:5208
Co--Nd, magnetic resonance of $NdCo_3$, microwave, 25:5200
Co--Nd, magnetic structure of $NdCo_3$, neutron diffraction study, 25:5210
Nd--Ni, magnetic structure of NdNi, 25:5205
Nd--Ni, thermal capacity of $NdNi_2$ at low temperatures, 25:5218
NEODYMIUM ISOTOPES Nd-141
energy levels of, spectroscopic factors for, (E), 25:5506 (CEA-N-1232, pp 81-159)
NEODYMIUM ISOTOPES Nd-146
deuteron elastic and inelastic scattering at 12 MeV, excitation energies and differential cross sections for, (E), 25:5729
energy levels from deuteron inelastic scattering, (E), 25:5729
NEODYMIUM URANATES
$NdUO_4$--ThO_2, spectra and phase studies of, 25:4084
NEON
electron pair correlation energies in, calculation using Gaussian geminals, 25:4973
helium-ion reactions at 10 to 30 keV with, cross sections for production of metastable triplet helium atoms by charge exchange in, (E), 25:4969
helium-metastable-atom reactions with, cross sections for ionization in, (E), 25:4969
oscillator-strength sums for, upper and lower bounds for, 25:4946
plasma of, energy distribution in striating discharges, 25:5077 (AD-710597)
NEON IONS
effects of accelerated, on radiation damage recovery in silicon lattices, 25:4895(P)
reactions with copper at 20 keV, relation of channeling to anisotropy in atom ejection patterns from, 25:4535
reactions with single-crystal germanium, minimum energy for sputtering in, (E), 25:5155
NEON ISOTOPES Ne-17
mass excess from neon-20 (He-3,He-6) reactions, test of isobaric-multiplet equation for, (E), 25:5640
NEON ISOTOPES Ne-18
energy levels from neon-20 (p,t) reactions, spin--parity assignments and spectroscopic factors for, (E), 25:5587
NEON ISOTOPES Ne-20
binding energy of, alpha cluster effects in Hartree-Fock solution for, (T), 25:5586
deuteron reactions (d,n) with, pseudo-bound-states calculation of angular distributions and spectroscopic factors from, (T), 25:5666
deuteron reactions (d,p) at 16.4 MeV, angular distributions for, (E), 25:5618
energy levels from Coulomb excitation, quadrupole moments and E2 transition probabilities of first excited, (E), 25:5622
energy levels in, calculation of, (T), 25:5559
helium-3 reactions (He-3,He-6) near 65 MeV, test of isobaric-multiplet mass equation, (E), 25:5640
proton reactions (p,t) at 42.6 MeV, angular distributions for, (E), 25:5587
reactions (Ne-20,f) with uranium, production cross sections for Z = 42 to 79 isotopes in, (E), 25:5756
NEON ISOTOPES Ne-21
energy levels from neon-20 (d,p) reactions, (E), 25:5618
NEON ISOTOPES Ne-22
deuteron reactions (d,p) at 12.1 MeV, angular distributions for, (E), 25:5618
energy levels from Coulomb excitation, quadrupole moments

XUM

and E2 transition probabilities of first excited, (E), 25:5622
reactions (Ne-22,f) with uranium, production cross sections for Z = 42 to 79 isotopes in, (E), 25:5756
NEON ISOTOPES Ne-23
energy levels from neon-22 (d,p) reactions, (E), 25:5618
NEPTUNIUM
separation from nitric acid--nitrous acid solutions by solvent extraction using TBP, 25:4135 (CEA-R-4097)
separation from spent fuels or irradiated raw materials by oxidation and solvent extraction, 25:4144(P)
NEPTUNIUM ISOTOPES Np-237
development of polarized neutron targets of, 25:5451 (LA-4465, pp 8.1-2)
neutron fission of, energy integral test of cross section for, (E/T), 25:5773
NERVES
effects of stimulation of vagus, in rabbits, on severity of light- or uv-induced kidney hypertension, 25:4697
protein synthesis in fibers of, in giant squid, tracer study of sites of, 25:4418
radiation effects on stimulation threshold of muscle-, in hind paws of rats following intratracheal and intraperitoneal injection of thorium dioxide, α, 25:4701
NERVOUS SYSTEM
radiosensitivity of central, in mice, effects of serotonin on x, 25:4584
NEUTRINOS
detection of, (E/T), 25:4589
fluxes of cosmic, tests of scale invariance models from, (T), 25:5340
interactions ν + N at high energies, current algebra and parton models for, 25:5345
interactions of, research at California Univ., Oct. 1969 to Sept. 1970, (E), 25:5257(R) (UCI-10-P-19-40)
interactions of, review of, (E), 25:5256 (CONF-700314-, Paper 6)
interactions with hadrons at high energies, review of, (T), 25:5339 (CONF-700314-, Paper 7)
production of natural, (E/T), 25:4589
structure functions for, scale-invariant light-cone SU(3) x SU(3) current commutators for universal, (T), 25:5328
NEUTRINOS (ANTI ν)
fluxes of cosmic, tests of scale invariance models from, (T), 25:5340
structure functions for, scale-invariant light-cone SU(3) x SU(3) current commutators for universal, (T), 25:5328
NEUTRON BEAMS
energy determination of, techniques for accurate, (E), 25:5598
resonance absorption in fast, integral transport theory analysis of, 25:5959
NEUTRON CROSS SECTIONS
compilation of differential, for Z = 1 to 20, (E), 25:5549 (BNL-400(3rd Ed.)(Vol.1))
temperature and multilevel interference effects on resonance, calculations using Quasi-Resonance Triplet Approximation, (T), 25:5666 (TID-25566)
NEUTRON-DIFFRACTION ANALYSIS
use to characterize minerals, 25:4151 (CEA-CONF-1500)
NEUTRON SOURCES
availability of californium-252, in 1971, 25:4218
description of polarized, using underground nuclear explosion, 25:5475 (LA-4465, pp 7.1-2)
evaluation of californium-252, 25:4218
handling, shipping, and storage of californium-252, 25:4218
inspection of beryllium--curium-244, neutron radiographic method for, 25:4253
shielding of californium-252, materials for, 25:4218
target for T(d,n), development of tritium, 25:5503(P)
NEUTRON SPECTROMETERS
design and performance of Bonner activation, for intermediate neutrons, 25:4364
development of simultaneous time-of-flight and pulse-height unfolding, 25:4366
pulse analysis of proton-recoil proportional, analog computer for gamma discrimination in, 25:4362 (CEA-N-1314)
pulse-height spectrum unfolding for NE-213 scintillation, 25:4365
spectra unfolding for, Monte Carlo method for, 25:4367
NEUTRON STARS
cosmic particle emission from, (T), 25:4978
properties of, (T), 25:4978
NEUTRONS
absorption by uranium-233 at 0.02 to 1 eV, eta factor for, (E), 25:5702
attenuation in medium of moving heavy nuclei, velocity spectrum of, (T), 25:5492
beta decay of, review of research on, 25:5536
binding to F centers in lithium fluoride, (T), 25:5154
capture by indium-115, iodine-127, and silver-107 and -109, cross sections for, (E), 25:5789
capture by tantalum-181 and uranium-238 at thermal to 1 MeV energies, energy dependence of γ-ray yields for, (T), 25:5777
capture by uranium-233 at 0.02 to 1 eV, cross section for, (E), 25:5702
capture of resonance, by antimony-121 and antimony-123, (E), 25:5724
collision probabilities for, calculation of asymptotic, (T), 25:5480
decay n → p + e + anti ν, angular correlation between neutron spin and antineutrino momentum in polarized, (E), 25:5258
detection and measurement of, conference on, 25:4320 (KURRI-TR-59)
detection at high counting rates, long proportional detector for, 25:4354
detection of, Monte Carlo calculation of response of silicon detectors for, 25:4351
detection of, performance of liquid helium scintillation detector for, 25:4321 (LA-4465, pp 31.1-2)
diffusion calculations for, simplified eigenvalue problem solutions in, (T), 25:6173
diffusion equation for, solution by space-energy factorization of, (T), 25:6169
diffusion equations for two-group reflected slab reactors, Green's function formulation of Laplace-transformed multigroup, 25:6176
diffusion in infinite media, approximation for synthetic scattering kernel for, (T), 25:5482
diffusion in movable reactor materials, improved spatial differencing for, (T), 25:6177
diffusion in solutions of boric acid, effects of concentrations on, 25:6183
diffusion length measurements in water, effects of source arrangement on foil activation for, (E), 25:6182
diffusion parameters in heavy water spheres, determination using pulsed source technique, (E), 25:5485
distribution in boron-containing media, Monte Carlo model for energy, space, and time, 25:4159
distribution in rocks of varying porosity, Monte Carlo method for calculation of, 25:4152(T) (CSIRO-Trans-10083)
dose rates from plutonium dioxide--uranium dioxide fuel rods, method for calculation of, 25:4314
dosimetry in tissue-equivalent phantom of rabbit eye, 25:4521
dosimetry of, intercomparison of personnel criticality dosimeters for, 25:4377 (AERE-R-6498)
effects on alpha- and beta-cobalt phthalocyanine, behavior of recoil cobalt-60 from, thermal annealing studies on, 25:4130
effects on creep and swelling in uranium dioxide fuel pins, 25:4888 (TRG-Report-1937)
effects on creep in alloys and metals, loop unfaulting mechanism for, 25:4830
effects on creep of uranium dioxide, 25:4853
effects on crystal lattice defects, model for, 25:4887 (KFK-1215)
effects on dodecafluorobutane and carbon--dodecafluorobutane, 25:4111(R) (CRC-3909-2)
effects on embrittlement of A212-B pressure vessel steel, (T), 25:6145 (AD-709898)
effects on embrittlement of pressure vessel steels, damage threshold for, 25:4832
effects on glandular stomach of mice, carcinogenic whole-body, 25:4703
effects on grain structure of graphite, 25:4880 (CEA-N-1374)
effects on mechanical properties of zirconium, 25:6151 (RISO-214, pp 255-87)
effects on mice, histological evaluation of balneotherapy for treatment of, 25:4610
effects on physical properties and volume shrinkage rate of graphites at 1200°C, 25:4885 (DP-Report-856(Pt.2))
effects on shrinkage of graphites at 900 to 1200°C, 25:4885 (DP-Report-856(Pt.2))
emission from plutonium dioxide heat sources, spectra of, 25:4244
fluence measurements in-core, helium accumulating dosimeter for high, 25:4381
flux diffusion theory for, development of collided, (T), 25:6171
flux distributions in reactors during excursions, (T), 25:6161
flux in steel pressure vessels, (E/T), 25:6213
flux monitoring for unattended safeguards applications, dielectric track detector system for, 25:4341
flux monitoring, fission foil--silicon detector for in-core, 25:4353
flux of fast critical assemblies, effects of irradiation samples reactivity worths on, (E/T), 25:6117
flux of fast reactors, analytic model for, (T), 25:5954
flux synthesis methods for, corrections for variational, (T), 25:6170
flux to kerma factors for inorganic and organic materials, 25:6214
form factors from e + d → e + d interactions at low momentum transfers, neutron-to-proton ratio for electric, (E), 25:5247 (AD-710385)
form factors of, e + d → e + d interactions for ratio of neutron--proton electric, (E), 25:5246 (AD-709522)
importance spectra of fast reactors, analytic model for, (T), 25:5954
interactions anti p + n → 2π⁻ + π⁺ + π at rest in deuterium bubble chamber, branching ratios for rho, ω⁰,

and J = 0 $\Sigma^0(1115)$ production in, (E), 25:5271
interactions anti p + n + $2\pi^-$ + π^+ + π at rest in deuterium bubble chamber, branching ratio for, (E), 25:5271
interactions anti p + n + $2\pi^-$ + π^+ at rest in deuterium bubble chamber, branching ratio for, (E), 25:5271
interactions K^- + n + Ξ^- + K^0 at 1.2 to 2.7 GeV/c in bubble chamber, total cross sections, polarization, and partial-wave analysis for baryon exchange in, (E/T), 25:5384
interactions n + p + d + γ, calculation of cross sections using meson exchange currents, (T), 25:5545
interactions p + n at 24 GeV in emulsions and hydrogen bubble chamber, energy spectra and transverse-momentum distributions for π and p and baryon resonance production in, (E), 25:5276
interactions π^+ + n in Regge pole model, relative phase of rho and ω production in, 25:5374 (DNPL/R-7, pp 207-13)
mass energy transfer coefficients for inorganic and organic materials, 25:6214
mesons (μ) production at sea level by cosmic, (E/T), 25:4974 (AD-710278)
monitoring of cosmic, by Canadian stations for May--Aug. 1970, (E), 25:4975 (AECL-3736)
reactions (n,f) with uranium-233 at 0.4 to 2000 eV, ionization detector for cross section measurements of, 25:4333
reactions (n,f) with neptunium-237, plutonium-240, thorium-232, uranium-236, and uranium-238, energy integral tests of cross sections for, (E/T), 25:5773
reactions (n,f) with nuclei, description of near-barrier, 25:5850
reactions (n,f) with plutonium-239, plutonium-242, uranium-233, and uranium-235 at thermal to 3.1 MeV energies, delayed neutron yields from, (E), 25:5769
reactions (n,f) with uranium-233 at 0.02 to 1 eV, cross section for, (E), 25:5702
reactions (n,f) with uranium-235 below 2 MeV, energy dependence of prompt neutron yield in, (E), 25:5755
reactions (n,f) with uranium-235 from 0.009 to 24 eV, cross-sections for resonance, (E), 25:5738
reactions in meteorites, (E/T), 25:4922
reactions with chromium-52, iron-56, lithium-7, nitrogen-14, potassium-39, and zirconium-90 using plutonium--beryllium source, gamma production cross sections for, (E), 25:5582
reactions with nuclei, Z = 1 to 20, compilation of angular distributions and cross sections for, 25:5549 (ENL-400(3rd Ed.)(Vol.1))
resonance absorption in graphite moderated homogeneous reactors, interference effects of thorium-232 and protactinium-233, 25:5958
resonance escape probabilities from Galerkin method solution of neutron slowing down equations, (T), 25:5479
resonance integrals for thorium oxide (ThO_2) rods, (E/T), 25:6205
scattering by cubic diatomic crystals containing impurities, cross sections for inelastic, 25:5491
scattering by helium-4, unified nuclear reaction theory for elastic, (T), 25:5870
scattering by polycrystalline zirconium hydride, cross section calculations for elastic and inelastic coherent, (T), 25:5499
scattering by vanadium, density of phonon eigenstates and cross sections from inelastic, (T), 25:5230
scattering by vibrating lattices with Debye spectra, double-differential cross sections for, (T), 25:5494
scattering by water, water-d_2, and graphite at 0.004 to 0.12 eV, scattering transport lengths from, (E), 25:5502
scattering from crystal lattice vibrations, cross sections for, (T), 25:5483
shielding requirements for gas cooled power reactor, 25:5888
shielding requirements for water cooled power reactors, 25:5977
shielding requirements for ZPPR, mockup of FTR, 25:6124
slowing down in graphite, (E/T), 25:6160
slowing down in homogeneous media, analysis using Green's function method, (T), 25:5484
spectra emerging from fast pulsed moderators, time-focused crystal spectrometer technique for measurement of, 25:6186
spectra in fast reactors, multigroup synthesis methods for, (T), 25:5961
spectra in iron, for assessment of data files, (E), 25:5495
spectra in natural granites, calculation of, 25:4374
spectra in spacecraft radioisotope heat source, Monte Carlo calculation of, 25:4242
spectra in steel pressure vessels, (E/T), 25:6213
spectra in water, time-dependent, (E/T), 25:5489
spectra of fast reactors, (T), 25:6178
streaming in liquid sodium cooled fast reactors, design requirements for, 25:5976
structure functions for, scale-invariant light-cone SU(3) x SU(3) current commutators for, (T), 25:5328
thermalization in finite media, solution of Boltzmann equation for time-dependent nonhomogeneous, (T), 25:5478
thermalization of, asymptotic behavior of generalized Cadilhac model for, (T), 25:5487
thermalization of, corrections to Green-type scattering kernel in model for, (T), 25:5488
transport calculations, energy representations in, 25:5141
transport in finite slab with infinite reflectors, time-dependent noncenergetic, (T), 25:5498
transport in moving water medium, (E), 25:5466
transport in slabs, use of variational methods in, 25:5135 (AAEC/TM-554)
transport in two-dimensional slabs by invariant imbedding, 25:5143
transport of, computer program for analyzing Legendre expansions of angular distributions for negative regions, 25:5476 (CRNL-TM-2903)
transport of, quantum correction for calculations of, (T), 25:6167
transport of, solution of initial-value problem for slab with infinite reflectors using normal-mode expansions, (T), 25:5501
transport theory of, phase space time evolution method for, 25:5139

NEUTRONS, COLD
flux for hydrogenous reactor moderators, measurement of leakage, (E/T), 25:6203
scattering by ordinary and deuterated ethanol and methanol, total cross sections for, (E), 25:5500

NEUTRONS, DELAYED
detector response for, two stage Monte Carlo calculations for, (T), 25:6151
emission from fission fragments, theory for, 25:5851
emission from uranium-233 and -235 neutron fission, relative abundances and half-lives of groups of, (E), 25:5689
energy spectra of, multiplication effects in measurement of, 25:5774
half-lives and abundances in plutonium-242 fast neutron fission, (E), 25:5775

NEUTRONS, EPITHERMAL
capture by uranium-238 above 6 eV, γ spectra from, (E), 25:5776
capture in plate lattice, partial separation of variables for calculation of efficiency of, (T), 25:5490
effects on anomalous helium production in nickel, 25:4821
scattering by cadmium-113 in cadmium sulfide crystals at 0.178 eV, reflection and transmission curves and integral reflection coefficients from resonance, (E), 25:5785

NEUTRONS, FAST
age and fast effect in beryllium and beryllium oxide, sensitivity to cross-section data in moments-method calculation of 14-MeV, 25:5496
attenuation in air at 0.3 to 5.0 MeV, cross sections for, (E), 25:5481
capture by A = 63 to 186 nuclei, reaction integrals for, (E), 25:5656
collimators for, design of, 25:5477 (UCRL-50657)
detection of, gas flow activation detector system for in-core, 25:4355
dosimetry of, track analysis in Makrofol polycarbonate foil for, 25:4339
effects on anomalous helium production in nickel, 25:4821
effects on beryllia single crystals, ESR study of boron centers induced in, 25:5162
effects on beryllium oxide, relations with heat treatments, 25:4892
effects on copper at 4.2°K, annealing of, (E/T), 25:5160
effects on dimensions of graphite at high temperatures, 25:4883 (DP-Report-473)
effects on dislocation loops in copper and nickel, relations with crystal lattice geometry, 25:4834
effects on electric conductivity and mechanical properties of Type Kh 18N22V2T2 steel, 25:4817
effects on electric resistivity of SAP alloys, relations with impurity content, 25:4890
effects on embrittlement of Type A533B steel electroslag weldments at 550°F, 25:4833
effects on frequencies of chlorophyll mutations and chromosome aberrations in barley seeds, protective effects of ancxia, cysteine, and water against, 25:4604
effects on mechanical properties of hafnium, 25:4813 (IN-1440)
effects on metallurgical properties of cold-worked niobium--zirconium alloy pressure tubes, 25:4825
effects on mice, combined effects of barenylacetic acid and methyl-o-barencarboxylic acid on, 25:4888
effects on microstructure of nickel, 25:4811 (BNWL-SA-3300)
effects on microstructure of vanadium, relations with annealing, 25:4828
effects on miniature avalanche diodes, damage, 25:4408
effects on physical properties of graphite, 25:4884 (DP-Report-556(Pt.1))
effects on swelling of Nickel 200 and Types 304 and 316 stainless steel, relations with cold working, 25:4824
effects on swelling of Types 304 and 316 stainless steel, relations with in situ annealing, 25:4823

effects on tensile properties of Types 304 and 316 stainless steel, method for prediction of, 25:4831
effects on thorium oxide (ThO_2)--uranium oxide (UO_2) coated particle fuels, 25:5590(R) (ORNL-4589)
effects on Type 316 stainless steel clad plutonium oxide (PuO_2)--uranium oxide (UO_2) and uranium oxide (UO_2) fuel elements, 25:5990(R) (ORNL-4589)
effects on uniaxial and biaxial creep-rupture of Type 316 stainless steel, 25:4816 (WHAN-FR-19)
effects on void formation in preirradiated high-purity aluminum, 25:4818
moderation of, effects of scattering anisotropy on elastic, (T), 25:6165
production of, development of tritiated target for, (E), 25:5503(P)
reactions (n,2n) with indium-113 and -115 at 13.1 to 18.2 MeV, excitation functions and isomeric cross-section ratios for, (E), 25:5763
reactions (n,α) with aluminum-27 at 14.43 MeV, cross sections for, (E), 25:5641
reactions (n,α), (n,d), (n,γ), (n,p), (n,2n), and (n,n'γ) with nuclei at 3 and 14 MeV cross sections, threshold energies, half-lives, and gamma energies from, (E), 25:5685 (KFKI-70-18-NAC)
reactions (n,d) with aluminum-27 at 14.1 MeV, energy spectra and DWBA analysis of angular distributions from, (E/T), 25:5662
reactions (n,f) with plutonium-239 and uranium-235, fission yields for, (E), 25:5765
reactions (n,f) with plutonium-239, plutonium-242, uranium-233, and uranium-235 at 0.1 to 1.8 MeV, energy dependence of delayed neutron yield from, (E), 25:5770
reactions (n,f) with plutonium-242 at 14.7 MeV, delayed-neutron abundances and half-lives for, (E), 25:5775
reactions (n,f) with uranium-238 at 14 MeV, production of palladium-113, -115, and -116 from, (E), 25:5740
reactions (n,p) with deuterium at 14.4 MeV, proton spectra for three separable-potential models of, (T), 25:5531
reactions (n,p) with nickel-58 at 14.8 MeV, analysis of proton angular distributions from, (T), 25:5638
reactions with carbon and oxygen at 1 to 7 MeV, total cross sections for, (E), 25:5598
scattering by bismuth, indium, lead, tin, and uranium at 4 MeV, differential cross sections and polarizing abilities at 150 to 180° from elastic, (E), 25:5762
scattering by cesium-133 at 0.2 to 2.2 MeV, γ spectra from inelastic, (E), 25:5751
scattering by gold-197, nitrogen-14, oxygen-16, and scandium-45 at 5, 6.6, and 8.7 MeV, cross sections, energy spectra, excitation functions, and angular distributions for, (E), 25:5551 (CEA-R-4047)
scattering by helium-4 at 17.6, 20.9, and 23.7 MeV, cross sections and phase shifts for elastic, (E), 25:5508 (LA-4465, pp 1.1-2)
scattering by helium-4 at 27.3 and 30.3 MeV using polarized beams, asymmetry in elastic, (E), 25:5523 (LA-4465, pp 30.1-2)
scattering by hydrogen at 24.0 MeV, phase-shift analysis of differential cross sections for elastic, (E/T), 25:5540
scattering by iron at 14 MeV, energy spectra and angular distributions from inelastic, (E), 25:5639
scattering by iron-56 at 0.9 to 16 MeV, high-resolution cross section for inelastic, (E), 25:5657
scattering by nuclei, corrections due to finite volume of scatterer for differential cross sections from elastic and inelastic, (T), 25:5504
scattering by praseodymium-141 at 1.2 to 2.2 MeV, γ spectra from inelastic, (E), 25:5751
scattering by thallium-203 and -205 at 0.6 to 1.6 MeV, γ spectra from inelastic, (E), 25:5798
scattering by tritium at 22.1 MeV, polarization in elastic, (E), 25:5516 (LA-4465, pp 15.1-2)
scattering elastically by carbon-12, analysis using extended R-matrix theory, (T), 25:5581
spectra in plutonium fueled fast critical assembly, 25:6105
spectra in pulsed aluminum assembly, (E/T), 25:6106
spectra measurements of, performance of foil activation methods for in-core, 25:4357
spectra of, continuous slowing down models for, (T), 25:5955
transport in atmosphere at 8,000 to 50,000 ft, Compton electron currents from photons from 14-MeV, (T), 25:5497

NEUTRONS, FISSION
age and fast effect in beryllium and beryllium oxide, sensitivity to cross-section data in moments-method calculation of, 25:5496
effects on crystal structure of uranium ceramics, relations with annealing, 25:4887 (KFK-1215)
effects on helium production in chromium, copper, iron, nickel, and titanium, 25:4822

NEUTRONS, FUSION
production in non-cylindrical z-pinches, 25:5116(T) (SC-T-70-4046)

NEUTRONS, INTERMEDIATE
attenuation in two-component retarding medium at 28 keV, nonasymptotic structure of spectrum near intermediate resonances, (T), 25:5505
capture by aluminum-27, fluorine-19, magnesium-24, phosphorus-31, and natural silicon and sulfur, cross sections for, 25:5603 (FCA-4-4440)
capture by uranium-238 at 0.5 to 100 keV, cross section for, (E), 25:5771
capture by uranium-238, γ spectra from, (E), 25:5776
capture-to-fission ratio for plutonium-239, integral measurement of, (E), 25:5772
spectra in plutonium fueled fast critical assembly, 25:6105

NEUTRONS, PILE
effects on corrosion of Zircaloy-2 by steam--water mixtures, 25:4737 (CISE-R-290)
effects on creep strain and yield strength of Type 304 stainless steel, 25:4820
effects on swelling of Types 304 and 316 stainless steel, relations with temperature, 25:4810 (BNWL-SA-3283)
effects on Zircaloy-clad uranium dioxide fuel elements at high burnup, 25:4886(R) (GEAP-10204)
reactions (n,f) with uranium-233 and -235, half-lives and relative abundances of delayed neutron groups from, (E), 25:5689

NEUTRONS, THERMAL
capture by antimony-121 and antimony-123, 25:5724
capture by polarized terbium-159, angular distribution of γ rays from, (E), 25:5717
distributions in hydrogen-containing media, Monte Carlo calculation of, (T), 25:5493
effects on anomalous helium production in nickel, 25:4821
effects on cracking of sodium-bonded Type 316 stainless steel-clad plutonium carbide--uranium carbide fuel pins, 25:4894
effects on diploid and polyploid oats, review of mutagenic, 25:4484
effects on quantitative traits in populations of maize and soybeans, mutagenic, 25:4485
effects on tobacco in Italy, review of mutagenic, 25:4488
flux in strong anisotropic reactor moderators, (E/T), 25:6184
reactions (n,f) with plutonium-239 and -241 and uranium-233 and -235, fission yields for, (E), 25:5765
reactions (n,γ) with magnesium-24 and -25, cross sections for, (E), 25:5625
reactions (n,γ) with magnesium-26, gamma spectra and Q-value of thermal, (E), 25:5625
reactions (n,γ), (n,p), (n,2n), and (n,n'γ) with nuclei, cross sections, threshold energies, half-lives, and gamma energies from, (E), 25:5685 (KFKI-70-18-NAC)
reactions with nuclei, activation resonance integrals for, (E), 25:5681 (CNEA-274)
spectra in pulsed beryllium assembly, (E), 25:6107

NEVADA TEST SITE
chemical and physical properties of desert soils at, 25:4477 (UCLA-12-782, pp 49-81)
radioinduced changes in vegetation of desert ecosystems at, fallout, 25:4477 (UCLA-12-782, pp 49-81)

NEW YORK
radiation monitoring in environs of Brookhaven National Laboratory, Upton, during 1969, 25:4803 (BNL-50196)

NICHROME
Cr_2O_3--Nichrome, corrosion by sodium of bearing coatings of, at 1100°F, 25:4185(R) (NYO-3930-8)
Cr_3C_2--Cr_2O_3--Nichrome, corrosion by sodium of bearing coatings of, at 1100°F, 25:4185(R) (NYO-3930-8)
Cr_3C_2--Nichrome, corrosion by sodium of bearing coatings of, at 1100°F, 25:4185(R) (NYO-3930-8)

NICKEL
complexes with hydroxamic acids, stability studies on, 25:4083
complexes with maleic acid, preparation and thermal behavior of, 25:4075
complexes with phenanthrenequinone oxime, potentiometric studies on formation constants of, 25:4080
complexes, radiation effects on catalytic properties of, in decomposition of hydrogen peroxide, 25:4103
deposition on substrates, 25:5166(R) (COO-623-156)
determination by ion exchange in thiocyanate solutions and atomic absorption spectrophotometry, 25:4137 (IS-T-377)
determination in boron, 25:4009 (TID-25190)
determination in boron, 25:4009 (TID-25190)
determination in PuO_2--U_3O_8, effects of ratio of plutonium oxide to uranium oxide on spectrographic, 25:4015 (NUMEC-3524-76)
determination of trace amounts of, in titanium ore by neutron capture gamma spectroscopy using californium-252 source, 25:4036
diffusion of uranium dioxide in, determination by neutron fission recoil tracks from uranium-235, 25:4845
effects of impurities of, on properties of uranium, 25:4747 (AWRE-O-63/70)
mechanical properties of sintered powder specimens of, 25:4841(R) (SRO-552-5)
mechanical properties of, effects of explosive shock deformation on, 25:4802
microstructure of, effects of explosive shock deformation on, 25:4802
neutron energy loss and straggling in foils of, (E), 25:5598
permeability of sintered powder samples of, relations

XUM

with porosity, 25:4841(R) (SRO-552-5)
preparation of powdered, for quantitative microscopy using image analyzing computers, 25:4841(R) (SRO-552-5)
properties for coating niobium thermionic collectors, 25:4750 (TEE-4125-2)
properties for use as encapsulating material for californium-252 sources for neutron capture gamma-ray spectroscopy, 25:4772
properties for use in electrolytic separation of bromine-80 isomers, 25:4127
radiation effects on dislocation loops in, relations of crystal lattice geometry with fast neutron, 25:4834
radiation effects on microstructure of, fast neutron, 25:4811 (BNWL-SA-3300)
radioinduced anomalous helium production in, epithermal, fast, and thermal neutron, 25:4821
radioinduced helium production in, fission neutron, 25:4822
radioinduced void formation in polycrystalline, 6-MeV selenium ion, 25:4819
radioinduced void formation in, proton, 25:4051(R) (AI-AEC-12972)
separation by ion exchange using Alamine 336 or Amberlyst A-21 in aqueous thiocyanate solutions, 25:4137 (IS-T-377)
separation from vanadium by ion exchange in thiocyanate solutions using Amberlyst A-21, 25:4137 (IS-T-377)

NICKEL 200
radioinduced swelling of, effects of cold working on fast neutron, 25:4824

NICKEL ALLOYS AND SYSTEMS
analysis for niobium using 4-(2-pyridylazo)resorcinol, photometric, 25:4018
corrosion resistance in steam generator welds, 25:5990(R) (ORNL-4589)
fabrication of precision tubes of, equipment and methods for, 25:4745
fatigue cracking in monocrystalline MAR-M200, electron fractrographic study of Stage I, 25:4765
C--Cr--Fe--Ni, internal friction of austenitic, at 25 to 400°C, effects of defect--interstitial solute reactions on, 25:4786 (COO-1676-13)
C--Fe--Ni, internal friction of austenitic, at 25 to 400°C, effects of defect--interstitial solute reactions on, 25:4786 (COO-1676-13)
C--Fe-base--Ni, internal friction in martensitic, at 20 to 500°C, controlling mechanisms of, 25:4786 (COO-1676-13)
Ce--Ni, thermal capacity of $CeNi_2$ at low temperatures, 25:5218
Co--Gd--Ni, magnetization and hyperfine field in $Gd(CoNi)_2$, 25:5198
Cr--Fe-base--Ni, carburization-decarburization in sodium at 500 to 800°C, effects of carbon content on, 25:4755
Cr--Fe-base--Ni, compatibility with sodium at 800°C, effects of carbon transport on, 25:4736(R) (ANL/ST-3)
Cr--Ni-base, mechanical properties of, effects of molybdenum and niobium additions on, 25:4782
Cr--Ni-base, microstructure of, effects of molybdenum and niobium additions on, 25:4782
Er--Ni, magnetic structure of ErNi, 25:5209
Fe--Ni, purification of vacuum melts of, effects of composition, reduced pressure, and alloying additions of aluminum, chromium, molybdenum, titanium, and tungsten on, 25:4744
Gd--Ni, thermal capacity of $GdNi_2$ at low temperatures, 25:5218
Ho--Ni, magnetic structure of HoNi, 25:5209
Nb--Ni--W, phase diagrams at 1800 and 1900°C, isothermal, 25:4788
Nd--Ni, magnetic structure of NdNi, 25:5209
Nd--Ni, thermal capacity of $NdNi_2$ at low temperatures, 25:5218
Ni--nylon, radioinduced curing of composites of, γ, 25:4108
Ni--polyethylene, radioinduced curing of composites of, γ, 25:4108
Ni--Pr, thermal capacity of $PrNi_2$ at low temperatures, 25:5218
Ni--TiC, corrosion by sodium of bearing coatings of, at 1100°F, 25:4185(R) (NYO-3930-8)
Ni--W, electric conductivity and short-range order of deformed, 25:4766
Ni--W, phase diagram at 1400 to 2100°C, 25:4788
Ni-base--W, crystal structure of metastable Ni_3W phase in, 25:4789
Ni-base--W, phase studies of metastable Ni_3W phase in, relations with heat treatments, 25:4794
Ni-base--W, phase studies of metastable Ni_3W phase in, 25:4789

NICKEL IONS
effects of 5-MeV, on microstructure of cold-worked Type 316 stainless steel, 25:4829
effects on microstructure of thermomechanically treated Type 348 stainless steel, 25:4775

NICKEL ISOTOPES Ni-58
alpha elastic scattering at 64 MeV, angular distributions and reflection coefficients from eikonal approximation for, (T), 25:5834
energy levels from proton inelastic scattering, spin--parity assignments for, (E), 25:5642
energy levels from proton inelastic scattering, transition probabilities for, (E), 25:5680 (CEA-N-1232, pp 1-80)
energy-level transitions from proton inelastic scattering, multipole mixing ratios for, (E), 25:5642
neutron reactions (n,p) at 14.8 MeV, analysis of proton angular distributions from, (T), 25:5638
proton elastic and inelastic scattering at 5.88 MeV, proton polarization for, (E), 25:5632
proton inelastic scattering at 12 MeV, proton and γ spectra from, (E), 25:5680 (CEA-N-1232, pp 1-80)
proton inelastic scattering at 8.1 MeV, p--γ angular correlations from, (E), 25:5642
proton reactions (p,γ) at 3.45 to 3.60 MeV, excitation functions for, (E), 25:5660

NICKEL ISOTOPES Ni-60
energy levels in quartet scheme, low-lying even-parity, even-spin, (T), 25:5814

NICKEL ISOTOPES Ni-63
energy level at 11.85 MeV from nickel-64(p,d) reactions, T = 9/2 analog, (E), 25:5609
energy levels from nickel-62 (d,p) reactions, spectroscopic factors for, (E), 25:5680 (CEA-N-1232, pp 1-80)

NICKEL ISOTOPES Ni-64
proton reactions (p,d) at 27.5 MeV, angular distribution for, (E), 25:5609

NICKEL ISOTOPES Ni-65
energy levels from nickel-64 (d,p) reactions, spectroscopic factors for, (E), 25:5680 (CEA-N-1232, pp 1-80)

NICOTINOHYDROXAMIC ACID
complexes with divalent and trivalent metals, stability studies on, 25:4082

NIMONIC 75
mechanical properties of, effects of exposure to high-temperature carbon oxides, methane, nitrogen, or water on, 25:4736 (DP-Report-527)

NINE MILE POINT POWER REACTOR
coolant loss accident conditions in, safety analysis of increased power level, 25:5920 (DOCKET-50220-54)
emergency core cooling system for, performance requirements at increased power level for, 25:5920 (DOCKET-50220-54)
operation of, safety analysis of electrical output oscillations on approach to 510 MW(e), 25:5919 (DOCKET-50220-53)

NINHYDRIN
effects on x-radiosensitivity of Serratia marcescens, 25:4557

NIOBIUM
analysis for nitrogen and oxygen by vacuum fusion, 25:4022
determination in copper-base alloys using 4-(2-pyridylazo)resorcinol, photometric, 25:4018
determination in lead zirconium titanates and titanium dioxide using sodium butyldithiocarbaminate, spectrophotometric, 25:4017
determination using N-cinnamoyl-N-phenylhydroxylamine, spectrophotometric method for, 25:4020
dislocation motion in superconducting, 25:5036(R) (NYO-4060-5)
dislocations in, reactions with solute atoms, 25:4786 (COO-1676-13)
effects on mechanical properties and microstructure of chromium--nickel alloy, 25:4782
internal friction of nitrogen- and oxygen-containing, cold-working maximum of, 25:4778
niobium-93 nuclear acoustic resonance in single crystals of, (E), 25:5223
performance of coated thermionic collectors of, 25:4750 (TEE-4125-2)
performance of collectors of, for thermionic converters, 25:4751 (TEE-4125-3)
properties for coating niobium thermionic collectors, 25:4750 (TEE-4125-2)
properties for use as encapsulating material for californium-252 sources for neutron capture gamma-ray spectroscopy, 25:4772
structure of work-hardened surface layers of, effects of vacuum annealing on, 25:4797
superconducting fluxoid pinning near surfaces in single crystals of, 25:5036(R) (NYO-4060-5)
superconducting, bulk upper critical field of clean Type-II, 25:5054

NIOBIUM ALLOYS AND SYSTEMS
Mo--Nb-base, mechanical properties of monocrystalline, at 77 to 475°K, effects of compression on, 25:4800
Mo--Nb-base, mechanical properties of, effects of molybdenum content on, 25:4786 (COO-1676-13)
Mo--Nb-base, slip in monocrystalline, at 77 to 475°K, effects of compression on, 25:4800
Nb--Ni--W, phase diagrams at 1800 and 1900°C, isothermal, 25:4788
Nb--C, hardness of solid solutions of, factors effecting, 25:4786 (COO-1676-13)
Nb--U-base, corrosion crack initiation in, effects of electrochemical and metallurgical variables on stress, 25:4749 (SC-DR-70-718)
Nb--U-base--Zr, corrosion crack initiation in, effects of electrochemical and metallurgical variables on stress,

25:4749 (SC-DR-70-718)
Nb--Zr-base, radiation effects on metallurgical properties of cold-worked pressure tubes of, fast neutron, 25:4825
NIOBIUM CARBIDES
NbC--TiC, electric conductivity and thermal electromotive forces in homogeneous, temperature effects on, 25:5176
NIOBIUM ISOTOPES Nb-90
beta decay of, gamma spectra and intensities for, (E), 25:5682 (IS-T-389)
NIOBIUM ISOTOPES Nb-91
energy levels from proton resonances in zirconium-90, spreading widths of isobaric analog, (T), 25:5644
NIOBIUM ISOTOPES Nb-93
neutron capture integral in fast region, (E), 25:5656
neutron reactions (n,2n) at 10 to 20 MeV, excitation functions and isomeric cross-section ratios for, (E), 25:5766
nuclear acoustic resonance in niobium single crystals, (E), 25:5223
NIOBIUM ISOTOPES Nb-96
beta decay of, γ singles and coincidence spectra from, (E), 25:5718
NIOBIUM ISOTOPES Nb-97
beta decay of, β-γ circular polarization in, (E), 25:5732
NITRATES
effects as additive on reactions of hydrated radiolytic electrons with biological and food extracts, 25:4117
effects on hydrogen yields from radiolysis of water, 25:4120
NITRIC ACID
separation of trace amounts of rare earths from aqueous solutions of, by solvent extraction using D2EHPA in toluene containing trace amounts of uranium, 25:4150
NITRITES
effects on hydrogen yields from radiolysis of water, 25:4120
NITROGEN
abundance of metastable atomic, source for nitrogen oxide NO and positive nitrogen ions in E region, 25:5011
analysis for nitrogen-15, accuracy and sensitivity of optical method for, 25:4019
determination by photon activation using NRL Linac, 25:4041 (AD-709901)
determination in boron, 25:4009 (TID-25190)
determination in helium by gas chromatography, on-line, 25:4012 (DP-Report-443)
determination in human body by neutron activation, 25:4042 (CONF-680211-, pp 496-516)
determination in niobium and tantalum by vacuum fusion, 25:4022
effects of high-temperature, on mechanical properties of steel, 25:4738 (DP-Report-527)
effects of high-temperature, on mechanical properties of austenitic stainless steel, 25:4738 (DP-Report-527)
effects of high-temperature, on properties of Nimonic 75, 25:4738 (DP-Report-527)
helium-ion reactions at 10 to 30 keV with molecular, cross sections for production of fast metastable triplet helium atoms in, (E), 25:4969
helium-metastable-atom reactions with molecular, cross sections for ionization in, (E), 25:4969
photon transport in liquid, low-energy, 25:5148
plasma of, double Langmuir probe measurements in positive column, 25:5081 (N-70-32493)
proton elastic scattering at 49.4 MeV, angular distributions of cross sections and polarization in, (E), 25:5585
reactions with hydrogen 2^2P atoms of molecular, cross sections for de-excitation in, (E), 25:4964
transport by sodium in stainless steel loops between hot and cold legs, 25:4773
yields of ions and molecules of, from γ radiolysis of 2,2-dimethylpropane, effects of deuterated ammonia and nitrous oxide on, 25:4113
NITROGEN IONS
excitation of auroral, correlation with auroral ionization rates, (E/T), 25:5009
NITROGEN IONS (N^+)
abundance in E region, metastable nitrogen molecule source for, 25:5011
reactions with molybdenum polycrystals and tungsten monocrystals at 10 to 30 eV, electron yields and energy distributions from, (E), 25:4943
NITROGEN IONS (N_2^+)
abundance in F region, metastable positive oxygen ions source for, 25:5011
reactions with molybdenum polycrystals and tungsten monocrystals at 10 to 30 eV, electron yields and energy distributions from, (E), 25:4943
NITROGEN ISOTOPES N-13
energy levels of, compilation of, (E), 25:5567
production in cyclotron of, 25:4664
use for scanning human lungs for function, half-life, γ energy, and solubility coefficient of, 25:4663
use for scanning human lungs for perfusion and ventilation, 25:4667
NITROGEN ISOTOPES N-14
alpha reactions (α,d) at 6.875 to 7.415 MeV cms, differential cross sections from, (E), 25:5596
deuteron reactons (d,α) at 15 and 20 MeV, angular distributions for, (E), 25:5563
energy levels of, compilation of, (E), 25:5567
neutron inelastic scattering at 6.6 MeV and 90°, cross sections, energy spectra, and excitation functions for, (E), 25:5551 (CEA-R-4047)
neutron reactions using plutonium--beryllium source, gamma production cross section for, (E), 25:5582
nitrogen-14 reactions (N-14,N-13) at 16 MeV, effect of form factor on calculations of angular distributions from, (T), 25:5594
proton reactions (p,He-3) at 50 MeV, angular distributions for, (E), 25:5563
scattering by oxygen-16 at 20 to 60 MeV at 70 to 100°, optical-model analysis of excitation functions from, (E/T), 25:5566
NITROGEN ISOTOPES N-15
determination in nitrogen samples, accuracy and sensitivity of optical method for, 25:4019
energy levels of, compilation of, (E), 25:5567
helium-3 reactions (He-3,d) with, pseudo-bound-states calculation of angular distributions and spectroscopic factors from, (T), 25:5666
helium-3 reactions (He-3,p) at 18 MeV, angular distributions for, (E), 25:5680 (CEA-N-1232, pp 1-80)
penetration of ions of, into gold and silver, path lengths for, (T), 25:4940
photon reactions (γ,p) at 5 to 35 MeV, excitation functions for, (T), 25:5595
scattering by oxygen-16 at 20 to 60 MeV at 70 to 100°, optical-model analysis of excitation functions from, (E/T), 25:5566
NITROGEN MUSTARDS
effects on uv- and x-radiosensitivity of yeast mutants, 25:4480
effects on x-radiosensitivity of cultured Chinese hamster cells, 25:4558
NITROGEN OXIDES NO
abundance in E region, metastable nitrogen molecule source for, 25:5011
NITROGEN OXIDES N_2O
effects on ion and molecule yields from γ radiolysis of 2,2-dimethylpropane, 25:4113
NITROSO COMPOUNDS
effects on frequency of crossover aberrations in chromosomes of male Drosophila in comparison to effects of x radiation, 25:4481
NOBELIUM
research on, review of, 25:5719
NOBELIUM ISOTOPES No-255
alpha decay scheme and spectra, (E), 25:5704
half-life, (E), 25:5704
NOBELIUM ISOTOPES No-257
alpha decay scheme and spectra, (E), 25:5704
half-life, (E), 25:5704
NOVAE
distance of Serpentis 1970, (E), 25:4901
light curve for Serpentis 1970, (E), 25:4901
NUCLEAR AUXILIARY POWER SYSTEMS
design and performance of implantable plutonium-238-fueled vapor cycle, for artificial heart, 25:4234
design and performance of plutonium-238-fueled Stirling cycle, for artificial heart, 25:4233
design of 2 to 10 kW(e) radioisotope-fueled organic Rankine cycle, for undersea applications, 25:4225
reentry of small radioisotope-fueled, at superorbital velocities, computer calculations of temperature and trajectories for, 25:4221
NUCLEAR BATTERIES
development of miniature radioisotope-fueled, for implantable cardiac pacemakers, UK program for, 25:4240
development of promethium-147-fueled, for cardiac pacemakers, 25:4237
NUCLEAR EMULSIONS
meson (K^-) reactions with nuclei at 3.0 GeV/c in, hyperfragment production in, (E), 25:5277
NUCLEAR ENGINEERING
training in, fast reactor safety curriculum at UCLA for, 25:6063
training in, use of computer systems for, 25:6194
training in, use of remote computer facilities for, 25:6193
NUCLEAR EXPLOSIONS
blast from, evaluation of underground transportation facilities to protect populations from, 25:4285(R) (ORNL-TM-3016)
dose to man from, estimations by UNSCEAR, 25:4518
fallout deposition from, effects of leaching on radioisotope transport in freshwater ecosystems following, 25:4479
NUCLEAR EXPLOSIONS, HIGH-ALTITUDE
effects on ballistic missiles, (T), 25:5239
NUCLEAR EXPLOSIONS, UNDERGROUND
copper recovery from chalcopyrite using, in-situ leaching method for, 25:4176
crater formation by, effects of water content of surrounding rocks on, 25:4179
debris from, design and operation of small hot cell chemical plant for processing of radioactive, 25:4308
effects on environment, review of beneficial, 25:4171
natural gas production stimulation using multiple,

feasibility study of, 25:4173
petroleum recovery using geothermally heated steam in nuclear cavity, feasibility study of high-viscosity, 25:4174
radiation hazards to man from, method for prediction of, 25:4172
shock wave propagation from contained, in enclosed horizontal tunnel, Marvel studies of, 25:4177
uses in industry in USSR, studies of potential, 25:4169(T) (UCRL-Trans-10477)
uses in USSR industry, review of, 25:4170
NUCLEAR MAGNETIC RESONANCE
line shape asymmetry due to nuclear quadrupole and anisotropic shift interactions, polycrystalline, (T), 25:5222
NUCLEAR MATERIALS MANAGEMENT
accountability and safeguards for, radiometric method for, 25:4292
accountability and safeguards for, radiometric method for, 25:4293
accountability of input to processing plant tanks in, by remote weighing, 25:4296
criticality and safeguards system for, design of computerized, 25:4295
materials balance methods for plutonium, instrument testing for, 25:4297
method using uranium-235 depletion as cross-check on plutonium content of reactor fuels, 25:4257 (BNWL-SA-3304)
methods for Eurochemic fuel processing plant, 25:4266
methods for WAK-type fuel processing plants, 25:4263 (KFK-1102)
safeguards for, nondestructive analysis methods for, 25:4290
safeguards for, radiometric analysis for, 25:4291
safeguards systems for US, development of improved, 25:4270
safeguards systems for, adaptation to Non-Proliferation Treaty of IAEA, 25:4271
safeguards systems for, development of improved, 25:4272
safeguards systems for, in fabrication or reprocessing plants, stochastic model for estimating efficiency of, 25:4273
safeguards systems for, review of Non-Proliferation Treaty requirements for, 25:4269
safeguards systems for, use of burnup data in, 25:4274
NUCLEAR MATTER
binding energy of, dependence on high-energy phase shifts, (T), 25:5862
binding energy per nucleon in, calculation using momentum-dependent potential, (T), 25:5852
energy levels of alpha--nucleon mixture of, cluster-expansion methods for ground-state, (T), 25:5390
energy levels of pure alpha, cluster-expansion methods for ground-state, (T), 25:5390
hyperon (A) binding energy in, cluster-expansion methods for, (T), 25:5390
NUCLEAR MODELS
alpha-particle, binding energies, rms radii, quadrupole moments, excited states, and configuration mixing of 4N nuclei with A = 12 to 28, (T), 25:5855
harmonic oscillator, Coulomb interaction of exterior charge on three-dimensional, (T), 25:5843
optical, derivation of potentials in high-energy approximation, (T), 25:5861
optical, potential parameters for deuteron elastic scattering, (T), 25:5854
pairing, test by group-theoretical analysis of beta decay, (T), 25:5813
quartet, low-lying even-parity, even-spin energy levels of 4n nuclei, (T), 25:5814
shell, effective charges for $f_{7/2}$ neutron and proton in, 25:5646
shell, multiplicity of states in a single shell, (T), 25:5829
shell, potentials for fast and slow heavy-ion collisions in two-center, (T), 25:5841
shell, quasi-potential equation for relativistic harmonic oscillator for, 25:5405 (JINR-E2-5339)
superconducting, proton--neutron correlations in medium and heavy nuclei, (T), 25:5853
NUCLEAR PHYSICS
cross-correlation method in, development of pseudo-random pulse method in, (T), 25:4392 (LYCEN-7032)
research at CEN, 25:5550(R) (CEA-N-1232)
research at UKAEA, 25:4088(R) (NP-18528)
NUCLEAR POWER PLANTS
control of, prospects for automation of, 25:5879
economics of, 25:5878(T) (UCRL-Trans-10495)
economics of, university instruction in, 25:6195
fuel cycle management for, analysis of optimum economic, 25:5897
fuel cycle management for, calculation of optimum economic, 25:5898
fuel supply for Euratom, status of, 25:5880
medical requirements for personnel at AERE, Harwell, assessment of, 25:4529 (AERE-R-6523)
operation of, criteria for optimum economic, 25:5899
operation of, mid-range cost analysis for optimum economic, 25:5904
operation of, power scheduling for optimum, 25:5896
operation of, short-range cost analysis for optimum economic, 25:5905
safety aspects in Japan, 25:5937 (RISO-214, pp 457-75)
seismic design in Japan for, 25:5929
shielding for, design standards and procedures for, 25:5889
siting of, public resistance to, 25:5940
tritium production and release by, levels of, 25:5941
NUCLEAR REACTIONS
book: Nuclear Reactions, 25:5842
Breit--Wigner resonances in, graphical methods for analysis of asymmetric, (T), 25:5868
Faddeev equations for, cluster expansion of, (T), 25:5858
nucleus--nucleus scattering, nuclear-density distribution in, (T), 25:5835
polarization phenomena in, contributions of Los Alamos Scientific Laboratory to conference on, 25:5507 (LA-4465)
production by highly concentrated electron beams, 25:5118(P)
resonances in, analysis of Lane equations for isobaric analog, (T), 25:5818
NUCLEAR REACTIONS (DIRECT)
book: Direct Nuclear Reaction Theories, 25:5823
isobaric analog resonances on even--odd targets, three-body model of, (T), 25:5872
polarization effects in (d,p) stripping, j-dependence of, (T), 25:5828
proton elastic scattering cross sections from three-body model of isobaric analog resonances on even--odd targets, (T), 25:5872
theories for stripping to unbound levels, faithful and pseudo-bound, 25:5869
NUCLEAR STRUCTURE
collective motion in, general formulation of microscopic theory of, (T), 25:5811
description for deformed even-even nuclei using Krutov model, 25:5819
energy levels from resonances in nuclei, spreading widths for isobaric analog, (T), 25:5644
Hartree--Fock calculations of, review of, 25:5855
mechanisms governing interacting systems of nucleons, microscopic theory of, (T), 25:5847
radii, calculations of odd--even staggering of, (T), 25:5856
research using thermal neutron capture and fission at research reactors, 25:5474 (KFK-1157)
rotational bands in deformed even--even nuclei, SL(3,R) symmetry for, 25:5801 (AD-706835)
NUCLEAR THEORY
Bethe--Goldstone equation in, Lennard--Jones approximation for pair correlation amplitude in, 25:5845
book: Nuclear Reactions, 25:5842
calculation of broad three-nucleon resonances for a soft-core two-nucleon potential, 25:5824
Coulomb mixing of analog states in, calculation of centroid energy using Hamada--Johnston potential, 25:5877
forces in low-energy nuclear physics, importance of noncentral, 25:5863
forces in, quadrupole, 25:5809
fractional parentage coefficients for anticommuting creation operators, 25:5822
Hartree--Fock and Thomas--Fermi methods in, comparison of, 25:5873
Hartree--Fock method in, Gaussian overlap approximation for projected, 25:5815
isobaric multiplet mass equation for A = 9, 13, 17, and 21, cubic term in, 25:5840
many body problem in, approximation to Green's function for, 25:5821
multiplicity of states in a single shell, 25:5829
nonlocal potential approach in relativistic nucleon-nucleon scattering, 25:5827
nucleon--nucleon potentials from binding energies and nuclear radii of several nuclei, determination of central, 25:5831
nucleon-nucleon potentials in, off-shell behavior of phase-shift equivalent momentum dependent, 25:5852
potentials in, canonical transformation relating hard-core and velocity-dependent, 25:5867
single-particle operators in, method for calculation of reduced matrix elements for, 25:5808 (N-70-32766)
spin--isospin functions of identical-nucleon system, classification of, 25:5541
Tabakin nucleon--nucleon potential in, 25:5825
two-body interactions in square potentials with soft repulsive cores, variational analysis using harmonic-oscillator states, 25:5849
Yamaguchi equivalent local potentials, comparison with OPEP, 25:5871
NUCLEAR WEAPONS
conference on control of, Sochi, USSR, Oct. 22 to 27, 1969, 25:4165 (CONF-691051)
control of, political and technical problems in, 25:4166 (CONF-691051-, pp 24-8)
development of defensive and offensive, in US and USSR, 25:4167 (CONF-691051-, pp 192-8)
proliferation of, effects of gas centrifuge development for enrichment on worldwide, 25:4214 (CONF-691051-, pp

354-61)
proliferation of, effects of gas centrifuge development for uranium enrichment on worldwide, 25:4213 (CONF-651051-, pp 145-53)
testing of, effects on infant mortality, 25:4505 (CONF-651051-, pp 324-35)
NUCLEI
abundance of cosmic 150- to 250-MeV/nucleon Z = 16 to 30, (E), 25:4373
alpha elastic scattering at 64 MeV, analysis by eikonal approximation, (T), 25:5834
beta decay of light s--d-shell, log-ft values for, (T), 25:5599
binding energy of A = 3, rank-two separable potentials in three-body Faddeev equations for, (T), 25:5830
charge composition of primary, (E/T), 25:4981
Coulomb interference in, relativistic eikonal approximation for superposition of two interactions for, (T), 25:5434
deformation in A = 100 region, evidence for, (E), 25:5687 (UCRL-19949)
deuteron elastic scattering by, formalism for polarization transfer in, (T), 25:5804 (LA-4465, pp 21.1-2)
deuteron elastic scattering by, optical-model parameters for, (T), 25:5854
deuteron reactions (d,n) and (d,p) with, formalism for polarization transfer, (T), 25:5803 (LA-4465, pp 20.1-2)
deuteron reactions (d,n) with, analysis of polarization transfer in, (T), 25:5805 (LA-4465, pp 26.1-2)
deuteron reactions using polarized beams, method for determination of analyzing tensors in, 25:5802 (LA-4465, pp 11.1-2)
deuteron reactions using polarized beams, precise method for determination of analyzing tensors for use as secondary standards, 25:5806 (LA-4465, pp 27.1-6)
electron reactions with heavy, rho + N + rho + N amplitudes and rho photoproduction from Drell--Trefil theory extension for coherent rho^0 production in, (T), 25:5336
electron scattering from, review of radiative corrections to, (T), 25:5800 (AD-706717)
electron scattering with bremsstrahlung production, polarization effect of nuclear magnetic moment in, 25:5820
electrons reactions with, scale-invariant light-cone SU(3) x SU(3) current commutators for universal structure functions for particle production in, (T), 25:5328
energy levels from meson reactions with, review of experiments confirming existence of isobaric analog, (E/T), 25:5580
energy levels in, shells in simple anisotropic harmonic-oscillator picture of, (T), 25:5857
energy levels in, tabulations of spin--parity assignments for, (E), 25:5792
energy levels of deformed, validity of quadrupole force in calculation of, (T), 25:5809
energy levels of even Z = 56 to 62, static quadrupole moments of, (E), 25:5688 (UCRL-19561)
energy levels of even--even, calculation of transition probabilities and static moments for, (T), 25:5816
energy levels of Z = 36 to 62 even--even, lifetimes of, (E), 25:5687 (UCRL-19949)
energy levels of, delayed coincidence electron--electron spectrometer for lifetime measurements of, 25:4363
energy levels of, time-dependent behavior of classical model for reactions involving isobaric analog, (T), 25:5848
energy spectra of primary cosmic, (E/T), 25:4981
energy-level transitions in Z = 36 to 63, (E), 25:5687 (UCRL-19949)
energy-level transitions in, tabulations of lifetimes and spectroscopic and hindrance factors for, (E), 25:5792
ground-state occupation probability in 2s-1d shell, projected Hartree-Fock calculation for, (T), 25:5876
internal conversion of, higher-order corrections to, (T), 25:5826
ion interactions with, formalism for spin-$^3/_2$, 25:5807 (LA-4465, pp 35.1-2)
ion reactions with, survey on heavy, 25:5817
mass equation for A = 9, 13, 17, and 21, cubic term in isobaric multiplet, (T), 25:5840
mass of, computer program for table look-up of, 25:5735
meson (K$^-$) reactions at 3.0 GeV/c in emulsions, hyperfragment production in, (E), 25:5277
meson (π) reactions at 50 to 1000 GeV, review of multiparticle production in, (E), 25:5273
meson (π) reactions at high energies, diffraction dissociation for πrho final state in, (E/T), 25:5386 (CONF-700314-, Paper 14)
neutron differential elastic and inelastic scattering cross sections for, corrections due to finite volume of scatterer for thermal, (T), 25:5504
neutron fission of, description of near-barrier, 25:5850
neutron reactions with Z = 1 to 20, compilation of angular distributions and cross sections for, 25:5549 (ENL-400(3rd Ed.)(Vol.1))
neutron reactions(n,α), (n,γ),(n,n'γ), (n,p), and (n,2n) at 0.025 eV and 3 and 14 MeV, cross sections, threshold energies, half-lives, and gamma energies from, (E), 25:5685 (KFKI-70-18-NAC)
neutron--proton correlations in medium and heavy, (T), 25:5853
nucleon capture at high energies, effective charge factor for E1, (T), 25:5839
nucleon scattering at high energies, diffractional peak width behavior for Gaussian, (T), 25:5424 (IFVE-STF-69-83)
particle scattering at high energies, Reggeized absorption model for, (T), 25:5423
photofission of, description of near-barrier, 25:5850
photon reactions at 5.5 GeV/c, angular distributions for ω production in, (E), 25:5249 (DNPL/R-7, pp 87-94)
photon reactions at high energies, ω - rho interference in, 25:5326 (DNPL/R-7, pp 115-38)
photon reactions with complex, review on rho, ω, and phi production in, 25:5301 (DNPL/R-7, pp 29-70)
photon reactions with heavy, Drell--Trefil theory extension for rho^0 coherent production in electron reactions with heavy nuclei for amplitudes of rho^0 production in, (T), 25:5236
photon reactions with light, model for rho^0 coherent production in, (T), 25:5336
photon reactions with, review of rho and ω production in, (E/T), 25:5248 (DNPL/R-7, pp 71-85)
photon reactions with, rho^0 production and decay inside nucleus from, (T), 25:5336
photon scattering at arbitrary energies and small angles in Coulomb field of, differential cross sections for electron pair and photon production in, (T), 25:5235
polarization of, research on dynamic, 25:5150(R) (UCB-34-P-20-PR-16)
proton elastic scattering by, formalism for polarization transfer in, (T), 25:5804 (LA-4465, pp 21.1-2)
proton reactions (p,2p) at 100 to 500 MeV with Z = 22, 26, and 28, proton spectra, excitation energies, and angular correlations for, (E), 25:5606(R) (UCSB-34-P-144-7)
proton reactions at 50 to 1000 GeV, review of multiparticle production in, (E), 25:5273
radius from rho photoproduction reactions, 25:5301 (DNPL/R-7, pp 29-70)
scattering length of A = 3, rank-two separable potentials in three-body Faddeev equations for doublet, (T), 25:5830
wave functons for ground-state, trial, (T), 25:5838
NUCLEI (CELLS)
effects on survival of irradiated cells, 25:4691
NUCLEIC ACID, DEOXYRIBO-
content of liver cells of amphibians, correlation with x-radiosensitivity, 25:4475 (NYO-3554-8)
effects on radiosensitivity of spores, structures in, 25:4726
effects on x-radiosensitivity of Escherichia coli, 25:4725
incorporation of 5-bromouracil in, effects of, on electron-radiosensitivity of aqueous solutions, 25:4542
incorporation of halogenated pyrimidine analogues into, effects of, on radiosensitivity of cells, 25:4537
induction of strand breaks by methyl hydrazine in, of Ehrlich ascites tumor cells, 25:4567
radiation effects on synthesis of, in chromosomes of Bacillus subtilis and Escherichia coli, uv and x, 25:4456(R) (ORO-3596-15)
radiation effects on, of yeast, gene locus for repair of uv and x, 25:4480
radiation repair of, by temporary blocking of replication, uv, 25:4463
radioinduced breaks of strands of, in Ehrlich ascites tumor cells, x, 25:4567
radioinduced degradation of, in bacteria, review of uv, 25:4462
radioinduced degradation of, in Micrococcus radiodurans, combined effects of chloramphenicol on x, 25:4536
radioinduced degradation of, in Micrococcus radiodurans, protective effects of cysteamine against x, 25:4536
radioinduced degradation of, in Micrococcus radiodurans and murine lymphoma cells, effects of dose, oxygen content, and temperature on repair of x, 25:4536
radioinduced free radicals in aqueous solutions of, reactions of, with triacetoneamine-N-oxyl, 25:4541
radioinduced strand breaks in, in vitro, effects of MEA on frequency of x, 25:4456(R) (ORO-3596-15)
radioinduced strand breaks in, of Escherichia coli, protective effects of glycerol, 1,2,3-indantrione, methyl sulfoxide, N-ethyl malemide, and thiourea against electron, 25:4551
radioinduced strand breaks of, in bacteria and bacteriophages, effects of triacetoneamine N-oxyl on x, 25:4550
radiolysis of, in aqueous solutions, γ, 25:4455 (UCLA-12-782, pp 23-47)
replication in thymus and γ-radioinduced thymomas in mice, tracer study, 25:4460
synthesis in spleen and thymus of rats, effects of AET and cysteamine on, 25:4596
synthesis in thymus gland of rats, effects of AET, cysteamine, 2-mercaptoethanol, and penicillamine on, tracer study of, 25:4592
synthesis in uv-irradiated Escherichia coli, effects of

amino acid starvation on, 25:4731
uptake of 5-bromodeoxyuridine and 5-iododeoxyuridine by, in neoplastic and normal cells in mice, tracer study of, 25:4602
NUCLEIC ACID, RIBO-
radiation effects on uridine incorporation into, of nerve tissue of chickens and rats, carbon-14 tracer study of x, 25:4457(R) (UCB-34-P-82-S)
synthesis in thymus gland of rats, effects of AET, cysteamine, 2-mercaptoethanol, and penicillamine on, tracer study of, 25:4592
NUCLEOGENESIS
chronology of solar and galactic, (E/T), 25:4922
survey of stellar, (T), 25:4914
NUCLEONS
capture by nuclei at high energies, effective charge factor for E1, (T), 25:5829
exchange in π^- + p interactions near 1 GeV, peripheral model for, (T), 25:5376
form factor of composite, nonrelativistic composite model for structure function relation with electromagnetic, (T), 25:5372 (CNRS-CPT-70-P-331)
form factor of, SO(4,2) group for axial vector, (T), 25:5401 (DEMO-70/6)
form factors for, vertex function for, (T), 25:5383
interactions anti N + N + anti N + N, differential cross sections and form factor for, (T), 25:5372 (CNRS-CPT-70-P-331)
interactions e + N + ν + N at low energies, PCAC hypothesis for threshold cross sections for, (T), 25:5333
interactions γ + N + N + l^+ + l^- at high energies, ω - rho interference in, 25:5325 (DNPL/R-7, pp 115-38)
interactions γ + N + ν + N at low energies, PCAC hypothesis for threshold cross sections for, (T), 25:5333
interactions γ + N + ν + N in vector dominance model and Regge model, Δ(1236) trajectory contribution to backward, 25:5332
interactions γ + N, nucleon magnetic moment from, (T), 25:5383
interactions in three-body system of, separable expansions of two-body T-matrix for, (T), 25:5432
interactions K^- + N below 65 GeV, difference of total cross sections for K^+ + N and, (E), 25:5294
interactions K^+ + N below 65 GeV, differences of total cross sections for K^- + N and, (E), 25:5294
interactions K^- + N in freon bubble chamber, Λ trapping probability from, (E), 25:5295
interactions N + N of, Tabakin potential in, 25:5825
interactions N + N, cross sections for hadron and γ, γ + 2μ, production relative to cross sections for hadron and W production in, (E/T), 25:5266 (IFVE-SEF-69-81)
interactions N + N, feasibility of search for W in, (E), 25:5267 (IFVE-SEF/STF-69-46)
interactions N + N, nonlocal potential approach in relativistic, (T), 25:5827
interactions N + N, quasipotential smoothness in eikonal approximation in quantum field theory models for, (T), 25:5387 (JINR-E2-5365)
interactions N + N, separable expansions of two-body T-matrix for, (T), 25:5432
interactions ν + N at high energies, current algebra and parton models for, 25:5345
interactions π + N, differential cross sections for charge exchange, (T), 25:5294
interactions π + N, review of diffraction for, (E/T), 25:5386 (CONF-700314-, Paper 14)
interactions π + N, sum rules and double partial-wave expansion of amplitudes of, (T), 25:5310
interactions π^+ + N below 65 GeV, differences of total cross sections for π^- + N and, (E), 25:5294
interactions π^- + N below 65 GeV, differences of total cross sections for π^+ + N and, (E), 25:5294
interactions rho + N + rho + N, extension of Drell--Trefil theory for rho^0 coherent production in electron reactions with heavy nuclei for amplitudes of, (T), 25:5336
interactions Σ + N + Λ + N from production in K^- + p + Σ^- + π^+ interactions in freon, absorption probability of, 25:5298
magnetic moment of, γ + N interactions for, (T), 25:5383
production in electron electromagnetic cascade interactions in copper at 400 MeV, 25:5255
properties of, relativistic Green function and vertex function for, (T), 25:5383
reactions with polyethylene, time-dependent coupled neutron--gamma spectra from, (T), 25:5147
scattering by nuclei at high energies, diffractional peak width behavior for Gaussian, (T), 25:5424 (IFVE-STF-65-83)
vertex function for, Hartree--Fock approximation for analytical properties of, (T), 25:5383
NUCLEONS (anti N)
interactions anti N + N + anti N + N, differential cross sections and form factor for, (T), 25:5372 (CNRS-CPT-70-P-331)
NUCLEOSIDES
electron transfer reactions of, in solutions of N-ethyl malemide or menadione, 25:4540
radiolysis of, in aqueous solutions, γ, 25:4459 (UCLA-12-782, pp 23-47)
NUCLEOTIDES
electron transfer reactions of, in solutions of N-ethyl malemide or menadione, 25:4540
radioinduced free radicals in aqueous solutions of, reactions of, with triacetoneamine-N-oxyl, 25:4541
radiolysis of, in aqueous solutions, γ, 25:4459 (UCLA-12-782, pp 23-47)

O

OOCYTES
molecular structure of chicken, 25:4459 (UCLA-12-782, pp 23-47)
OPTICAL SYSTEMS
development of stereomacroscopic, for in-hot cell inspection of irradiated fuels and materials, 25:4309
ORES
neutron absorption by boron-containing, space-energy and time distribution parameters for, 25:4159
ORGANIC ACIDS
reactions of carboxylic, with uranium(IV) acetates, preparation of uranium(IV) carboxylates from, 25:4057
reactions with thorium acetate, yields of thorium carboxylates from, 25:4056
ORGANIC COMPOUNDS
production of labeled, in COMECON states, review on, 25:4128
ORGANISMS
radiation effects on, review of protective effects of combinations of compounds against, 25:4609
ORNL HIGH-FLUX ISOTOPE REACTOR
coolant boiling in, experimental procedures for in-core, 25:6048
OROTIC ACID
radiation effects on monocrystals and polycrystals of, ESR spectral studies on γ, 25:4093
radioinduced free radicals in, magnetic properties of, 25:4459 (UCLA-12-782, pp 23-47)
OSMIUM
properties for use as encapsulating material for californium-252 sources for neutron capture gamma-ray spectroscopy, 25:4772
OSMIUM ISOTOPES Os-185
electron-capture decay of, branching ratios for, (E), 25:5741
OSMIUM ISOTOPES Os-191
gamma spectra of, precision measurements of low-energy, 25:5736
OSMIUM ISOTOPES Os-193
gamma spectra of, precision measurements of low-energy, 25:5736
OSTEICHTHYES
Cyclothone acclinidens, chemical composition of lipids in, 25:4458 (UCLA-12-782, pp 1-21)
Cyclothone signata, chemical composition of lipids in, 25:4458 (UCLA-12-782, pp 1-21)
Danaphos occulatus, chemical composition of lipids in, 25:4458 (UCLA-12-782, pp 1-21)
Heteropneustes fossilis, radiosensitivity of ovaries in, effects of testosterone on γ, 25:4591
Oncorhynchus tshawytscha, migration of populations of juvenile, from Columbia River, effects of heated effluents from plutonium production reactors on, 25:4504 (BNWL-1472)
Oncorhynchus tshawytscha, population spawning in Columbia River during 1947 to 1970, effects of ecological factors on, 25:4474 (BNWL-1515)
Vinciguerria lucetia, chemical composition of lipids in, 25:4458 (UCLA-12-782, pp 1-21)
OVARIES
radiosensitivity of fish, effects of testosterone on γ, 25:4591
OVULATION
radiation effects on, in pond snails, effects of dose 10,000 on γ, 25:4693
OXALOHYDROXAMIC ACID
complexes with divalent and trivalent metals, stability studies on, 25:4083
OXAMIC ACID
radioprotective effects of, on Ehrlich ascites tumor cells, mechanisms for x, 25:4566
OXYGEN
abundance of metastable molecular, source for positive molecular oxygen ions in D region, 25:5011
determination by photon activation using NRL Linac, 25:4041 (AD-709901)
determination in boron, 25:4009 (TID-25190)
determination in helium by gas chromatography, on-line, 25:4012 (DP-Report-443)
determination in niobium and tantalum by vacuum fusion, 25:4022
determination in silicon by photon activation, 25:4046
determination in sodium, development of analytical standards for, 25:4736(R) (ANL/ST-2)
determination in sodium, development of on-line system for, 25:4736(R) (ANL/ST-3)
effects on electron- and x-radiosensitivity of membranes of Ehrlich ascites tumor cells in cultures, 25:4566
effects on plutonium segregation in plutonium--titanium and plutonium--zirconium alloys, relations with anneal

XUM

temperature and cooling rate, 25:4790
effects on radioisotope metabolism in bone, 25:4423 (CCO-1601-23)
effects on x-radiosensitivity of DNA in Micrococcus radiodurans and murine lymphoma cells, combined effects of radiation dose and temperature on, 25:4536
metabolism in lungs, measurement using radioactive carbon dioxide and oxygen as tracers, 25:4665
neutron total cross sections from 1 to 7 MeV, (E), 25:5598
proton elastic scattering at 49.4 MeV, angular distributions of cross sections and polarization in, (E), 25:5585
radiation effects on gradient of, in lungs of dogs, x, 25:4706
reactions with thin films of holmium and ytterbium, electron microscopic study of oxidation, 25:4767
solubility in zirconium carbides, 25:4877
sorption by carbon surfaces, determination by decomposition measurements on carbon--oxygen complexes, 25:4846

OXYGEN IONS
abundance of metastable, source for positive molecular nitrogen ions in F region, 25:5011
excitation of auroral, correlation with auroral ionization rates, (E/T), 25:5005

OXYGEN IONS (O_2^+)
abundance in ionospheric D region, metastable molecular oxygen source for, 25:5011

OXYGEN ISOTOPES O-13
energy levels of, compilation of, (E), 25:5567
mass excess from oxygen-16 (He-3,He-6) reactions at 68 to 70 MeV, test of isobaric-multiplet mass equation, (E), 25:5568
mass excess from oxygen-16 (He-3,He-6) reactions, test of isobaric-multiplet equation for, (E), 25:5640

OXYGEN ISOTOPES O-14
energy levels of, compilation of, (E), 25:5567

OXYGEN ISOTOPES O-15
clearance of carbon dioxide-incorporated, from alveolar gas into capillaries of human lungs, 25:4667
energy levels from oxygen-16 (He-3,α) reactions at 11.0 MeV, (E), 25:5602 (ANU-P-501)
production in cyclotron of, 25:4664
use as tracer for measurement of oxygen metabolism in lungs, 25:4669
use for scanning human lungs for function, half-life, γ energy, and solubility coefficient of, 25:4663
use for scanning human lungs for perfusion and ventilation, 25:4667

OXYGEN ISOTOPES O-16
binding energy of, alpha cluster effects in Hartree-Fock solution for, (T), 25:5586
deuteron elastic scattering at 28 MeV, optical-model analysis of, (T), 25:5579
deuteron reactions (d,α) at 6.875 to 7.415 MeV cms, differential cross sections from, (E), 25:5596
electron inelastic scattering in giant resonance region, electron spectra and matrix elements for, (E), 25:5558
energy levels from carbon-12 (B-10,Li-6) reactions, (E), 25:5588
energy levels from carbon-12 (Li-6,d) reactions at 29.0 MeV and (Li-7,t) reactions at 31.5 MeV, evidence for 8+, (E), 25:5592
energy levels from nitrogen-14 (He-3,p) reactions, lifetimes of, (E), 25:5565
energy levels from nucleon interaction calculations, spin assignments for odd-parity, (T), 25:5570
energy levels in quartet scheme, low-lying even-parity, even-spin, (T), 25:5814
energy levels of, many-particle many-hole, (T), 25:5560
helium-3 reactions (He-3,He-6) at 68 to 70 MeV, Q values for, (E), 25:5568
helium-3 reactions (He-3,He-6) near 65 MeV, test of isobaric-multiplet mass equation, (E), 25:5640
lithium-6 reactions (Li-6,d) at 25 MeV, peripheral-model analysis of angular distributions from, (T), 25:5601
lithium-7 reactions (Li-7,t) at 30 MeV, peripheral-model analysis of angular distributions from, (T), 25:5601
meson (K) and (π) absorption widths in, corrections due to admixtures of excited energy levels, (T), 25:5866
meson reactions (π^-,γ) at 250 MeV/c, neutron time-of-flight and gamma energy spectra from, (E), 25:5600
meson reactions (π^-,γ) with, branching ratios for, (T), 25:5793
neutron inelastic scattering at 6.6 MeV, cross sections, energy spectra, and excitation functions for, (E), 25:5551 (CEA-R-4047)
nitrogen-14 and -15 elastic scattering at 20 to 60 MeV at 70 to 100°, optical-model analysis of excitation functions from, (E/T), 25:5566
oxygen-16 and alpha elastic scattering, nuclear density distributions in, (T), 25:5835
photon reactions (γ,2n) from threshold to 120 MeV, excitation cross sections for, (E), 25:5597
photon reactions (γ,n) at 15 to 30 MeV, excitation cross sections for, (E), 25:5597
reactions (O-16,O-17) with beryllium-9 at 6 to 22 MeV, excitation functions for, (E), 25:5577
reactions (O-16,O-17) with carbon-13 at 12 to 25 MeV, excitation functions for, (E), 25:5577
reactions with oxygen-16, two-center shell-model potentials for fast and slow, (T), 25:5841
reactions with tin-112 at 62 and 88 MeV, gamma spectra from, (E), 25:5688 (UCRL-19961)
scattering by oxygen-18 at 20 to 60 MeV at 50 to 100°, optical-model analysis of excitation functions from, (E/T), 25:5566
scattering by samarium-148 at 34 to 50 MeV, angular distributions for inelastic, (E), 25:5702

OXYGEN ISOTOPES O-17
effects on ESR spectra of SO_2^- radicals, 25:4124
energy levels from nitrogen-15 (He-3,p) reactions, (E), 25:5680 (CEA-N-1232, pp 1-80)
energy levels from oxygen-18 (He-3,α) reactions, decay properties of $T = 3/2$, (E), 25:5582
energy levels of, shell-model calculation of even-parity, (T), 25:5556

OXYGEN ISOTOPES O-18
meson (π) absorption widths in, corrections due to admixtures of excited energy levels, (T), 25:5866
oxygen-16 elastic scattering at 20 to 60 MeV at 50 to 100°, optical-model analysis of excitation functions from, (E/T), 25:5566

OXYGEN ISOTOPES O-19
beta decay, (E), 25:5555

OXYGEN SYSTEMS
C--O--Zr, crystal structure of fcc, effects of composition on, 25:4877
C--C--Zr, thermodynamic properties of fcc, 25:4877
H--Na--O, phase studies of, 25:4736(R) (ANL/ST-3)
Nb--O, hardness of solid solutions of, factors affecting, 25:4786 (CCC-1676-13)
O--U, phase studies to 1600°C and 60 kilobars, 25:4753

OYSTER CREEK POWER REACTOR, UNIT 1
instrumentation for, revised operating requirements of protective, 25:5918 (DOCKET-50219-116)
operation of, authorization for 1650 MW(t), 25:5918 (DOCKET-50219-116)
safety evaluation of, Division of Reactor Licensing, 25:5918 (DOCKET-50219-116)

OZONE
distribution of atmospheric, solar radiation analysis of vertical, (E), 25:5017

P

PAINTS
radioinduced curing of vinyl-resin, electron, 25:4095(F)

PALLADIUM
complexes with 8-quinclinol, structure of, NMR spectral studies on, 25:4081
heating of films of, by electron microscope beam, (E/T), 25:5163
properties for use as encapsulating material for californium-252 sources for neutron capture gamma-ray spectroscopy, 25:4772
separation by ion exchange using Alamine 336 in aqueous thiocyanate solutions, 25:4137 (IS-T-377)

PALLADIUM ALLOYS AND SYSTEMS
Co--Mo--Pd, electric and magnetic properties of solid solutions of, temperature dependence of, (E/T), 25:5178
Co--Pd, electric conductivity and short-range order of deformed, 25:4766
Mo--Pd, electric and magnetic properties of solid solutions of, temperature dependence of, (E/T), 25:5178

PALLADIUM ISOTOPES Pd-113
half-life from uranium-238 (n,f) reactions at 14 MeV, (E), 25:5740

PALLADIUM ISOTOPES Pd-115
half-life from uranium-238 (n,f) reactions at 14 MeV, (E), 25:5740

PALLADIUM ISOTOPES Pd-116
half-life from uranium-238 (n,f) reactions at 14 MeV, (E), 25:5740

PANCREAS
radiation effects on human, γ, 25:4452

PAROTID GLANDS
radiation effects on human, γ, 25:4452

PARTICLE TRACKS
analysis of bubble chamber, computer program for microscope system for, 25:4369 (IFVE-SFK-65-53)
analysis of dielectric track detector, automatic system for, 25:4340
analysis of dielectric track detector, for charge determination, 25:4338
analysis of fission fragment, in dielectric track detectors, automatic system for, 25:4343
analysis of fission fragment, in polycarbonate track detectors, 25:4342
etch pit distributions in Makrofol polycarbonate foil, fast neutron-induced, 25:4339

PARTICLES
diffusion of flowing, in circular tubes under Poiseuille and slug flow conditions, (T), 25:4204 (HASL-238)

PEACH BOTTOM POWER REACTOR, UNIT 1
design parameters of, 25:5884
refueling procedures for, 25:5906

PENICILLAMINE
copper complexes with, radiation chemistry of, ionizing,

XUM

25:4547
effects on synthesis of DNA and RNA in thymus gland of rats, tracer study of, 25:4592
PENTANE, 3-METHYL-
1-heptene--3-methylpentane, radiolysis of, reversible photoreactions of free radicals of allyl type from γ, 25:4125
1-hexene--3-methylpentane, radiolysis of, reversible photoreactions of free radicals of allyl type from γ, 25:4125
3-methylpentane--2-pentene, radiolysis of, reversible photoreactions of free radicals of allyl type from γ, 25:4125
2-PENTENE
radiolysis of solid, reversible photoreactions of free radicals of allyl type from γ, 25:4125
3-methylpentane--2-pentene, radiolysis of, reversible photoreactions of free radicals of allyl type from γ, 25:4125
PERSONNEL
licensing of power reactor operator, use of reactor simulators for, 25:6212
medical requirements for, at AERE, Harwell, assessment of, 25:4529 (AERE-R-6523)
radiation effects on, medical supervision following, 25:4523
radiation effects on, methods for protection against, 25:4524
radiation hazards to microwave, review of, 25:4708 (UR-45-1256)
radiation protection program for plutonium production plant, 25:4526
radiation protection programs for radiochemical processing plant, 25:4527
radioinduced irritation of eyes and skin of, using uv light to detect forgeries of bank notes, 25:4710
training of nuclear engineering, use of computers for, 25:6194
training of nuclear engineering, use of remote computer reactor simulator for, 25:6193
training program for boiling power reactor startup and operation, 25:5887
training program for power reactor operators, 25:5895
training program for power reactor startup and operation, 25:6211
PETROLEUM
recovery of high-viscosity, using steam from geothermal heat in nuclear cavity, 25:4174
PHANTOMS
analysis of human, for elements by neutron activation, methods for, 25:4042 (CONF-680211-, pp 496-516)
chromium-51 determination in water, in presence of iron-59, three-gate method for, 25:4513
development of three-dimensional, for evaluation of radioisotope scan images, 25:4657 (UCLA-12-782, pp 89-125)
radiation dosimetry in tissue-equivalent, of rabbit eye, neutron, 25:4521
PHARMACEUTICALS
preparation of new radioisotope-labeled, for use in nuclear medicine, 25:4415
radioactive, radiation dose to man during lung scanning using, methods for calculating absorbed, 25:4511
PHENANTHRENEQUINONE
oxime, complexes with metal ions, potentiometric studies on formation constants of, 25:4080
PHENOL, p-CHLORO-
effects on calcium-45 and strontium-85 distribution in mitochondria of liver of rats, 25:4431
PHENYLENE POLYMERS
properties for use as graphite binders, 25:4840(R) (LA-4526)
PHILLIPSITES
argon-40/potassium-40 ratio in Pacific Ocean, 25:4164
thorium content of Pacific Ocean, 25:4164
uranium content of Pacific Ocean, 25:4164
PHONONS
theory development for, general arbitrary temperature, 25:5483
PHOSPHINIC ACID, CYCLOOCTYLPHENYL-
solvent properties for actinides, rare earths, uranium, and yttrium in aqueous chloride solutions, 25:4147
PHOSPHINIC ACID, OCTYLPHENYL-
solvent properties for actinides, rare earths, uranium, and yttrium in aqueous chloride solutions, 25:4147
PHOSPHOLIPASE B
radiation effects on activity of, in intestine of rats in relation to number of eosinophils, x, 25:4455(R) (ORO-3329-7)
PHOSPHORIC ACID
H_3PO_4--H_2SO_4, effects on electrochemical behavior of uranium, 25:4792
PHOSPHORIC ACID, BIS(2-ETHYLHEXYL) ESTER
solvent properties for trace amounts of rare earths in nitric acid, effects of uranium on, 25:4150
PHOSPHORIC ACID, 2-METHYL-1,4-NAPHTHALENEDIOYL DIESTER
sodium salt, effects on electron- and x-radiosensitivity of membranes of Ehrlich ascites tumor cells in cultures, 25:4568
sodium salt, effects on x-radiosensitivity of ascites tumor cells, 25:4562
PHOSPHORIC ACID, TRIBUTYL ESTER
solvent properties for neptunium, 25:4135 (CEA-R-4097)
dodecane--TBP, radiolysis of, effects of isopropylbiphenyl on, 25:4116
PHOSPHORUS
determination in boron, 25:4009 (TID-25190)
determination in human body by neutron activation, 25:4042 (CONF-680211-, pp 496-516)
PHOSPHORUS ISOTOPES P-29
energy levels from silicon-28 (p,γ) reactions, (E), 25:5633
PHOSPHORUS ISOTOPES P-30
energy levels from silicon-29 (He-3,d) reactions at 15 MeV, spin--parity assignments and spectroscopic factors for, (E/T), 25:5670
PHOSPHORUS ISOTOPES P-31
neutron capture at 20 to 80 keV, cross sections for, (E), 25:5603 (FOA-4-4440)
photon reactions (γ,n) at 26 MeV, photoneutron spectra from, (E), 25:5648
proton reactions (p,γ) at 2.1 MeV, excitation functions and spin-mixing coefficients from, (E), 25:5636
PHOSPHORUS ISOTOPES P-32
clearance of sodium orthophosphate-incorporated from human kidneys, effects of thyroid diseases on, 25:4451
distribution in Mytilus edulis, 25:4448
energy levels from neutron resonances in phosphorus-31, radiative widths for, (E), 25:5603 (FOA-4-4440)
excretion by Mytilus edulis, 25:4448
incorporation in erythrocytes, for measuring volume of whole blood in swine, 25:4411 (CEA-R-4031)
uptake by Mytilus edulis, 25:4448
use for endolymphatic therapy of Hodgkin's disease, 25:4512
PHOTOCHEMISTRY
conference on, of aqueous and polar systems, 25:4060
PHOTOGRAPHIC FILM
radiation effects on ATM, high-energy proton, 25:4407 (N-70-35923)
radiation effects on, gamma and proton, 25:4406 (N-70-35843)
radiation hazards to ATM, space, 25:4405 (N-70-32671)
resolution of radiographic, relations of exposure time and film thickness with, 25:4251
PHOTOMULTIPLIER TUBES
circuit for use in pulse radiolysis, gating, 25:4358
dynode development for fast, silicon transmission secondary electron, 25:6245(R) (NYO-4100-3)
PHOTONS
interactions above 1 TeV, review of, (E), 25:5274
interactions at very high energies, scaling laws for particle production in two-body, (T), 25:5315 (CONF-700314-, Paper 8)
interactions $\gamma + N \rightarrow N + l^+ + l^-$ at high energies, ω - rho interference in, 25:5325 (DNPL/R-7, pp 115-38)
interactions $\gamma + N \rightarrow \pi + N$ at low energies, PCAC hypothesis for threshold cross sections for, (T), 25:5333
interactions $\gamma + N \rightarrow \pi + N$ in vector dominance model and Regge model, Δ(1236) trajectory contribution to backward, 25:5332
interactions γ + N, nucleon magnetic moment from, (T), 25:5383
interactions $\gamma + p \rightarrow K^+ + \Lambda$ at 1.2 GeV, differential cross sections for, (E), 25:5253
interactions $\gamma + p \rightarrow K^+ + \Sigma^0$ at 1.45 GeV, differential cross sections for, (E), 25:5253
interactions $\gamma + p \rightarrow \pi^+ + n$ at 2.6 to 16 GeV with linearly polarized photons, spin--parity contributions to cross sections for, (T), 25:5321 (DEMO-70/1)
interactions $\gamma + p \rightarrow \pi^+ + n$ at 5 and 16 GeV, cross section asymmetry for, (E), 25:5251 (UCRL-19897)
interactions $\gamma + p \rightarrow \pi^+ + \pi^- + p$, diffraction-dissociation, dual-resonance, and interference models for rho production in, 25:5323 (DNPL/R-7, pp 3-28)
interactions γ + p, Pomeranchuk decoupling from ordinary Regge trajectories in vector meson production in, (T), 25:5348 (COO-264-562)
interactions γ + p, review on rho, ω, and phi production in, 25:5301 (DNPL/R-7, pp 29-70)
interactions with spin-3/2 particles, differential and total sections for Compton, (T), 25:5325
production in photon scattering by nuclear Coulomb field at arbitrary energies and small angles, differential cross sections for, (T), 25:5335
production in strong interactions at high energies in amplitude fast variation region, (T), 25:5357
reactions (γ,d) with helium-4 at 1 to 100 MeV, cross-section calculations including d--d final-state interactions, (T), 25:5543
reactions (γ,p) with nitrogen-15 at 5 to 35 MeV, excitation functions for, (T), 25:5595
reactions of 14-MeV-neutron secondary, in atmosphere at 8,000 to 50,000 ft, Compton electron currents from, (T), 25:5497
reactions with boron-11, isospin of the giant resonance in, (E/T), 25:5554
reactions with carbon, vector dominance model for relative phase of rho and ω production in, (T), 25:5327
reactions with complex nuclei, review on rho, ω, and phi production in, 25:5301 (DNPL/R-7, pp 29-70)

XUM

reactions with deuterium, closure-approximation validity for rho^0 production in, (T), 25:5336
reactions with hafnium-179, excitation cross sections for, (E), 25:5690
reactions with heavy nuclei, Drell--Trefil theory extension for rho^0 coherent production in electron reactions with heavy nuclei for amplitudes of rho^0 production in, (T), 25:5336
reactions with helium, excess electron ejection by, (E), 25:5060 (NP-18484)
reactions with light nuclei, model for rho^0 coherent production in, (T), 25:5336
reactions with nuclei at 5.5 GeV/c, angular distributions for w production in, (E), 25:5249 (DNPL/R-7, pp 87-94)
reactions with nuclei at high energies, w - rho interference in, 25:5325 (DNPL/R-7, pp 115-38)
reactions with nuclei, review of rho and w production in, (E/T), 25:5248 (DNPL/R-7, pp 71-85)
reactions with nuclei, rho^0 production and decay inside nucleus from, (T), 25:5336
scattering by nuclear Coulomb field at arbitrary energies and small angles, differential cross sections for electron pair and photon production in, (T), 25:5335
scattering by nuclei in single crystals, optimal conditions for observation of coherent, (T), 25:5174
transport in liquid nitrogen, low-energy, (E/T), 25:5148

PHOTOREACTIVATION
effects on acetone-treated uv-irradiated Escherichia coli, 25:4728

PHTHALOCYANINE
complexes with cobalt, radiation effects on alpha- and beta-, thermal annealing of recoil cobalt-60 from neutron, 25:4130

PIGMENTS
radiosensitivity of plant, 25:4467

PINCH DEVICES
neutron production in non-cylindrical z, 25:5116(T) (SC-T-70-4046)

PINCH EFFECT
radiation losses from dense z-, (E), 25:5092(T) (SC-T-70-4044)

PIPE FITTINGS
design and performance of, summary of experience on, 25:4188 (TID-25553)

4-PIPERIDONE, 2,2,6,6-TETRAMETHYL-, N-OXIDE
effects on x-radiosensitivity of cultured Chinese hamster cells, 25:4561
effects on x-radiosensitivity of DNA in bacteria and bacteriophages, 25:4550
effects on x-radiosensitivity of Escherichia coli, 25:4550
reactions with radioinduced free radicals from DNA and nucleotides in aqueous solutions, 25:4541

PIPES
design of components and systems of, summary of practices in, 25:4188 (TID-25553)
development for components and systems, summary of research on, 25:4188 (TID-25553)
performance in components and systems, summary of service experience in, 25:4188 (TID-25553)
support structures for, summary of experience on design of, 25:4188 (TID-25553)
valves for steam, reliability analysis of isolation, 25:6040 (RISO-214, pp 247-53)
welds in, review of fracture mechanisms in, 25:4781

PLACENTA
radioisotope transfer through human, following diagnostic use or radiation accidents, iodine-131, indium-113, radium-226, technetium-99, thorium-224, and xenon-133, 25:4673

PLACENTAL TISSUES
blood circulation in, of monkeys and sheep, tracer study of, 25:4655 (COO-1762-6)
diffusion of uranium oxide across, of dogs and rabbits following intratracheal injection or oral administration, 25:4446

PLANETS
evolution of, model for, (T), 25:4921

PLANKTON
radium-226 content of, in Chalk River area during 1969, 25:4473 (AECL-3687)

PLANTS
analysis for strontium-90, rapid method for, 25:4039
growth and survival of desert, effects of photosynthetic pathways on, 25:4477 (UCLA-12-782, pp 49-81)
methods for propagation of desert, by root cuttings and seed, 25:4477 (UCLA-12-782, pp 45-81)
plutonium-239 uptake from soil by, effects of DTPA on fallout, 25:4478
radiation effects on reproduction of, in desert ecosystems, fallout, 25:4477 (UCLA-12-782, pp 49-81)
radiation effects on, protection against, by plastic covers, fallout β, 25:4477 (UCLA-12-782, pp 49-81)
radiation lethality for germination and survival of ornamental, LD_{50} for, 25:4724
radioinduced mutations in agricultural, review of literature on, 25:4482
radioisotope content of, in Faroe Islands during 1969, cesium-137 and strontium-90, 25:4476(R) (RISO-221)
radiosensitivity of pigments of, 25:4467
radium content of, in uranium mining areas of Czechoslovakia during 1964 to 1967, 25:4157

PLASMA
bibliography on plasma physics and fusion reactors, 25:5067
charged particle motion in linear and toroidal multipole fields, nonadiabatic, (E/T), 25:5091
confinement in high-field toroidal quadrupole, (T), 25:5070
diagnostics in Tokamak T3-A, density and temperature, (E), 25:5079 (CLM-R-107)
diagnostics of helium arc, using spectroscopic techniques, (E), 25:5082 (N-70-33122)
diagnostics of high-temperature, conference on, 25:5080(T) (LA-4520-TR)
diagnostics of hydrogen, for two-phase excitation at cyclotron frequency, 25:5087
diagnostics of low-power MPD wind tunnel, electron, ion, and neutral-particle, 25:5105
diagnostics of mirror-confined, pressure anisotropy, (E), 25:5085
diagnostics of nitrogen positive column, double Langmuir probe for, 25:5081 (N-70-32453)
diagnostics of striating neon discharge, energy distribution, 25:5077 (AD-710597)
diagnostics of turbulence in, optical measurements of electrostatic, (E), 25:5083
diagnostics using laser scattering, temperature, density, and correlation spectrum, 25:5086
diagnostics using spherical probes, effects on ionization and recombination in, 25:5084
diffusion in Tokamak devices, effects of electrostatic fields on untrapped particle, (T), 25:5071
electron beam interactions with, ion heating during development of hf instabilities, (E), 25:5073
electron beam interactions with, research on, (T), 25:5125(R) (SU-IPR-389)
electron density in circumsolar, from pulsar translucing, (E/T), 25:4920(T) (CSIRO-Trans-9857)
equilibrium calculations for helically symmetric, (T), 25:5106 (NYC-1480-161)
equilibrium in Tokamak discharges, thermal, (T), 25:5117
heating by ion wave turbulence in, electron, (T), 25:5072
heating by trapped-particle modes in, turbulent, (T), 25:5068 (AD-710318)
heating by two-phase excitation, ion cyclotron, (E), 25:5076
heating in beam--plasma system, during development of hf instabilities, (E), 25:5073
heating in Penning discharges, ion, (E), 25:5075
heating of toroidal confined, current-induced turbulent ion, (E), 25:5069
ion burst excitation by grids in, (T), 25:5122 (COO-2059-4)
ion distribution functions for collisionless surface ionized, (E/T), 25:5098
kinetic theory of, difference scheme for Vlasov solutions, 25:5096 (COO-2059-5)
kinetic theory of, numerical integration of Vlasov equation, 25:5097 (COO-2059-6)
production by laser-irradiation, use for power generation and space propulsion, 25:5104
production of quasi-electron-free, using electronic attachment, 25:5103
radiation losses from dense z-pinch, (E), 25:5092(T) (SC-T-70-4044)
radiations from dense decaying helium, amplification of vacuum uv, 25:5090
research at Garching, 1968, 25:5066(R) (NP-18495)
research at UKAEA, 25:4088(R) (NP-18528)
review for teaching purposes, 25:5100
shock wave structure in, finite-Larmor-radius analysis of laminar collisionless, (T), 25:5102
shock wave structure in, theory for radiation hydrodynamics, 25:5095 (CEA-R-4057)
shock waves in, downstream state of collisionless, (T), 25:5099
spectra of optically thick, absorption corrections for, 25:5088 (AE-710218)
stability in Q devices, drift, (E), 25:5112
stability in Tokamak discharges, (T), 25:5117
stability of counterstreaming, electrostatic ion cyclotron, (T), 25:5128
stability of counterstreaming, ordinary-mode electromagnetic, (T), 25:5129
stability of inhomogeneous two-stream, Lyapunov, (T), 25:5108
stability of multi-component, high-frequency flutelike, (T), 25:5110
stability of streaming relativistic, superluminous waves in, (T), 25:5107
stability of, effects of wave interactions on explosive, (T), 25:5109
stabilization of Kelvin--Helmholtz instability in cesium, by passive feedback, 25:5111
thermodynamic equilibrium in, criteria for complete and partial local, (T), 25:5094 (CEA-CONF-1629)
wave excitation by grids in, ion burst, (T), 25:5122 (COO-2059-4)
wave growth and damping in, if electrostatic, (E), 25:5121 (AD-709878)

wave interaction with magnetospheric, nonlinear mechanisms of, (T), 25:5031
wave interactions in warm, Lagrange theory for nonlinear, 25:5124 (SU-IPR-381)
wave interactions in, explosive instabilities from positive and negative energy, (T), 25:5109
wave interactions in, research on, (T), 25:5125(R) (SU-IPR-389)
wave interactions near electron cyclotron harmonics, effects on plasma spreading in, (E), 25:5132
wave interactions with density fluctuations in inhomogeneous magnetized, extraordinary, (T), 25:5126
wave propagation in collisionless, Korteweg--De Vries equation for solitary drift, (T), 25:5127
wave propagation in counterstreaming, ion cyclotron, (T), 25:5128
wave propagation in counterstreaming, ordinary-mode electromagnetic, (T), 25:5129
wave propagation in counterstreaming, ordinary-mode electromagnetic, (T), 25:5128
wave propagation in magnetized column of, low-frequency, (T), 25:5123 (SU-IPR-366)
wave propagation in multicomponent, dispersion relations for plane, (T), 25:5133
wave propagation in positive column, instabilities from, (E/T), 25:5125(R) (SU-IPR-389)
wave propagation in rf electric fields, ion-, (E), 25:5130
wave resonances in hot bounded, ion--electron, 25:5134
wave transformation between electron cyclotron and low hybrid frequencies, (T), 25:5131

PLASMA ACCELERATORS
jet properties in homopolar, 25:5085
neutron production in dense focus, effects of axial magnetic field on, 25:5113 (AD-710606)
neutron production in non-cylindrical z-pinch, 25:5116(T) (SC-T-70-4046)
performance of dense focus, using disk symmetry, 25:5120

PLASMA JETS
diagnostics of argon, using Thomson and Rayleigh scattering of laser beams, 25:5078 (CEA-R-3998)
dielectric permeability of relativistic inhomogeneous, (T), 25:5101
properties of, produced by low-power MPD wind tunnel, 25:5105
spectra of helium arcs, line broadening of triplet diffuse series of, (E), 25:5082 (N-70-33122)

PLASMAPAUSE
position and displacement of, from ground-based whistler method, 25:5029

PLATES
neutron transport in, solution of initial-value problem using normal-mode expansions, (T), 25:5501

PLATINUM
complexes with 8-quinolinol, structure of, NMR spectral studies on, 25:4081
properties for use as encapsulating material for californium-252 sources for neutron capture gamma-ray spectroscopy, 25:4772
structure and intrinsic stress of thin films of, 25:6226 (COO-623-151)

PLATINUM ISOTOPES
use in ion-implantation perturbed-angular-correlation study of transient magnetic fields in iron and gadolinium, (E), 25:5189

PLATINUM ISOTOPES Pt-193
electron-capture decay of, Q values and partial half-lives for L capture from, (E), 25:5748

PLATINUM ISOTOPES Pt-194
energy levels from gold-194 decay, spin and parity of, (E), 25:5728

PLATYHELMINTHES
Raillietina cesticillus, infection of γ-irradiated flour beetles with cysticercoids of, effects of, on survival, 25:4692 (COO-1209-13)

PLOWSHARE PROJECT
airblast from Buggy I Event in, measurements of close-in, 25:4168 (PNE-320)
crater ejecta from Project Sedan in, distribution and residence time of tritium in, 25:4181
fallout from Project Schooner in, distribution of radioisotopes in, 25:4180
natural gas production stimulation in, radiation doses to man from, 25:4525 (ORNL-TM-3216)
rock fracturing in Project Gasbuggy in, postshot measurements of micro-scale, 25:4178
Schooner operation, safety evaluations for, 25:4435
Schooner operation, safety evaluations for, 25:4436
shielding of explosives for, evaluation of borated polyethylene as neutron, 25:4175

PLUTONIUM
analysis for plutonium-240 using fission multiplicity detector, 25:4038
content in spent fuels, determination by uranium-235 depletion, 25:4257 (BNWL-SA-3304)
criticality of arrays of metal spheres of, calculations for, 25:4283
determination in solid wastes, radiometric method for, 25:4293
determination in waste containers, design of counting system for, 25:4292
determination simultaneously with uranium using platinum working electrode, coulometric, 25:4025
development of fuels of, design of laboratory for use in, 25:4302
diffusion in alpha and epsilon phases of, under high pressure, mechanisms of self-, 25:4785 (CEA-R-4052)
diffusion in mixed oxide fuels during irradiation, (E), 25:6012
distribution in sintered plutonium dioxide--uranium dioxide fuels, methods for measurement of, 25:4875
Doppler reactivity effects in plutonium fueled critical assemblies, (E), 25:6109
particle release from thermally stressed, to 1600°C, measurement of rate of, 25:4258 (BNWL-SA-3375)
processing of fuels of, soil studies and foundation design for West Valley Processing Plant for, 25:4154 (DOCKET-50201-52)
radiation effects on distribution between TBP and aqueous nitric acid solutions, effects of isopropyltiphenyl on, 25:4116
recycle in water cooled reactors, economics of, (T), 25:6056
separation from spent fuels or irradiated raw materials by oxidation and solvent extraction, 25:4144(P)

PLUTONIUM ALLOYS AND SYSTEMS
Ga--Pu-base, phase studies of, 25:4801
La-base--Pu, Kondo effect in, plutonium virtual bound state from, 25:5227
Pr-base--Pu, Kondo effect in, plutonium virtual bound state from, 25:5227
Pu--Ti-base, plutonium segregation in, effects of anneal temperature, cooling rate, and oxygen on, 25:4790
Pu--Zr-base, plutonium segregation in, effects of anneal temperature, cooling rate, and oxygen on, 25:4790

PLUTONIUM CARBIDES
PuC--UC, radiation effects on cracking of sodium-bonded Type 316 stainless steel-clad, thermal neutron, 25:4894
PuC--UC, radiation effects on Inconel 800-clad fuel pellets of, in-pile, 25:4889(R) (UNC-5263)
PuC--UC, radiation effects on sodium-bonded clad fuels of, in-pile, 25:4889(R) (UNC-5263)
PuC--UC, radiation effects on stainless steel-clad fuel pellets of, in-pile, 25:4889(R) (UNC-5263)

PLUTONIUM ISOTOPES Pu-238
design of heat sources of, for human implantation, 25:4229
production of high-purity, for radioisotope-powered heart devices, USAEC programs for large-scale, 25:4227
properties of 30-W heat sources of, for human implantation, 25:4228
radiation dose rate measurements for heat sources, in-phantom, 25:4517
radiation dose to dogs following use as power source for artificial heart, γ and neutron, 25:4432
radiation effects on tissues of dogs during use as power source for artificial heart, 25:4433
safety of cardiac pacemaker heat sources of, evaluation of mechanical and radiological, 25:4215 (NUMEC-3731-23)
use as heat source for powering cardiac pacemakers implanted in dogs, 25:4238
use as heat source in betavoltaic batteries and thermionic converters for powering cardiac pacemakers, 25:4237
use as heat source in implanting vapor cycle engine for powering artificial heart, 25:4234
use as heat source in Stirling engine for powering artificial heart, 25:4233
use as heat source in thermal engine for powering implantable heart device, 25:4232
use as heat source in thermoelectric generator for powering implantable artificial heart, 25:4235
use for powering implantable cardiac pacemakers in UK, research program on, 25:4240
use for powering implantable cardiac pacemakers in France, research program on, 25:4239
x-ray emission following alpha disintegration of curium-242, fast coincidence measurements of L-shell fluorescence, 25:4947

PLUTONIUM ISOTOPES Pu-239
neutron capture-to-fission ratio at intermediate energies, integral measurement of, (E), 25:5772
neutron fission at 0.1 to 1.8 MeV, energy dependence of delayed neutron yield from, (E), 25:5770
neutron fission at thermal to 3.1 MeV energies, delayed neutron yield from, (E), 25:5769
neutron fission of, yields for fast and thermal, (E), 25:5765
photofission at 5 to 10 MeV, prompt and delayed neutron yields from, (E), 25:5768
retention in soil, plants, and small mammals, fallout, 25:4478
uptake by plants from soil, effects of DTPA on fallout, 25:4478

PLUTONIUM ISOTOPES Pu-240
determination in plutonium using fission multiplicity detector, 25:4038
energy levels of, deformation-dependence of energy of γ-vibrational, (T), 25:5779
neutron fission of, energy integral test of cross section for, (E/T), 25:5773

XUM

PLUTONIUM ISOTOPES Pu-241
energy levels of, search for long-lived isomeric, (E), 25:5759
neutron fission of, yields for thermal, (E), 25:5765
PLUTONIUM ISOTOPES Pu-242
neutron fission at 0.1 to 1.8 MeV, energy dependence of delayed neutron yield from, (E), 25:5770
neutron fission at 14.7 MeV, delayed-neutron abundances and half-lives for, (E), 25:5775
neutron fission at thermal to 3.1 MeV energies, delayed neutron yield from, (E), 25:5769
PLUTONIUM ISOTOPES Pu-244
abundance in meteorites, (E/T), 25:4922
PLUTONIUM NITRATES
criticality of aqueous solutions of, effects of boron-containing stainless steel Raschig rings on, 25:4281
particle release from thermally stressed, to 1000°C, measurement of rate of, 25:4258 (BNWL-SA-3379)
PLUTONIUM OXIDES PuO_2
criticality, inventory, and safeguards system for, design of computerized, 25:4295
determination in fuel elements, development of instrumentation and material balance methods for, 25:4297
distribution in plutonium dioxide--uranium dioxide fuel pellets, scanning electron microprobe evaluation of, 25:4876
Doppler reactivity effects in critical assemblies, (E), 25:6110
gamma emission spectra from heat sources of, 25:4245
homogeneity in mixed-oxide thermal recycle fuels of, methods for measurement of, 25:4874
neutron emission spectra from heat sources of, 25:4244
particle release from thermally stressed, to 1000°C, measurement of rate of, 25:4258 (BNWL-SA-3379)
preparation and properties of plutonium-238-enriched heat sources of, for human implantation, 25:4228
shielding of plutonium-238-enriched heat sources of, for unmanned spacecraft, 25:4246
PuO_2--U_3O_8, analysis for impurities, effects of ratio of plutonium oxide to uranium oxide on impurity spectral line intensity in spectrographic, 25:4015 (NUMEC-3524-76)
PuO_2--UO_2, critical parameters of FFTF driver fuel pins of, in water, 25:4280
PuO_2--UO_2, fabrication of pellets of, for EBR-II irradiation, 25:4889(R) (UNC-5263)
PuO_2--UO_2, handling of fuel elements of, radiation protection requirements during, 25:4314
PuO_2--UO_2, inspection of fuel elements of, high-resolution neutron radiographic method for, 25:4254
PuO_2--UO_2, microstructure of fuels of, effects of thermal neuron flux on, (E), 25:5993
PuO_2--UO_2, plutonium dioxide homogeneity in fuel pellets of, scanning electron microprobe evaluation of, 25:4876
PuO_2--UO_2, power transient effects on discrete plutonium oxide (PuO_2) particles in fuels of, (E), 25:5995
PuO_2--UO_2, power transient effects on discrete plutonium oxide (PuO_2) particles in pellet fuels of, (E), 25:5994
PuO_2--UO_2, power transient effects on fuels of, (E), 25:5996
PuO_2--UO_2, radiation effects on distribution of fused oxide in, in-pile, 25:4879 (CEA-CONF-1659)
PuO_2--UO_2, radiation effects on partial melting of low-density, in-pile, 25:4879 (CEA-CONF-1659)
PuO_2--UO_2, radiation testing of Type 316 stainless steel clad fuel pellets of, 25:5990(R) (ORNL-4589)
PuO_2--UO_2, reactions with sodium at 400 to 1100°C, calculations of, 25:4736(R) (ANL/ST-3)
PuO_2--UO_2, reprocessing of irradiated, economics of, 25:4134(T) (AEC-tr-7198)
PuO_2--UO_2, thermal conductivity and restructuring of fuels of, in-pile, (E/T), 25:5992
PuO_2--UO_2, thermal conductivity of physically mixed, at 800 to 2400°C, 25:4862
PuO_2--UO_2, thermal conductivity of, effects of burnup on, 25:4839 (KFK-1245)
PuO_2--UO_2-base, creep at 1100 to 1300°C, measurement of compressive, 25:4861
PuO_2--UO_2-base, molybdenum-99 distribution in irradiated fuel pins of, 25:4891
PuO_2--UO_2-base, molybdenum-99 distribution in irradiated fuel pins of, 25:4804
PuO_2--UO_2-base, plutonium homogeneity in sintered, methods for measurement of, 25:4875
PuO_2--UO_2-base, thermal conductivity at 50 to 1000°C, effects of porosity on, 25:4844
PNEUMATIC SYSTEMS
design and operation of, for transfer of radioactive ceramic fuel samples between ANL facilities, 25:4306
design and operation of, for transferring californium-252 sources between ORNL facilities, 25:4305
development for trigger-actuated locking of master--slave manipulators, 25:4312
POLLEN
radiation effects on, of Gossypium sp, 25:4499
POLONIUM
fabrication of heat sources of, design of sputtering unit for, 25:4259 (BNWL-SA-3609)
POLONIUM ISOTOPES Po-200
alpha decay of, alpha energies and half-lives for, (E), 25:5696
electron-capture decay of, half-lives and gamma intensities for, (E), 25:5696
POLONIUM ISOTOPES Po-201
alpha and electron-capture decay of, ratio for, (E), 25:5696
alpha decay of, alpha energies and half-lives for, (E), 25:5696
electron-capture decay of, half-lives and gamma intensities for, (E), 25:5696
POLONIUM ISOTOPES Po-202
alpha and electron-capture decay of, ratio for, (E), 25:5696
alpha decay of, alpha energies and half-lives for, (E), 25:5696
electron-capture decay of, half-lives and gamma intensities for, (E), 25:5696
POLONIUM ISOTOPES Po-203
alpha and electron-capture decay of, ratio for, (E), 25:5696
alpha decay of, alpha energies and half-lives for, (E), 25:5696
electron-capture decay of, gamma and conversion-electron spectra from, (E), 25:5748
electron-capture decay of, half-lives and gamma intensities for, (E), 25:5696
POLONIUM ISOTOPES Po-204
alpha and electron-capture decay of, ratio for, (E), 25:5696
alpha decay of, alpha energies and half-lives for, (E), 25:5696
electron-capture decay of, half-lives and gamma intensities for, (E), 25:5696
POLONIUM ISOTOPES Po-205
alpha and electron-capture decay of, ratio for, (E), 25:5696
alpha decay of, alpha energies and half-lives for, (E), 25:5696
electron-capture decay of, gamma and conversion-electron spectra from, (E), 25:5748
electron-capture decay of, half-lives and gamma intensities for, (E), 25:5696
POLONIUM ISOTOPES Po-207
electron-capture decay of, gamma and conversion-electron spectra from, (E), 25:5748
POLONIUM ISOTOPES Po-210
energy levels from 4p--2h shell-model calculation including core excitation, spin--parity assignments for, (T), 25:5737
energy levels from lead-208 (α,2n) reactions at 30 MeV, time-differential spin-rotation patterns for, (E/T), 25:5742
energy levels of, anomalous orbital magnetism of proton from magnetic moment of 11-, (E/T), 25:5742
energy-level transitions from 4p--2h shell-model calculation including core excitation, reduced transition probabilities for, (T), 25:5737
POLONIUM ISOTOPES Po-218
determination in air, alpha detection method for, 25:4040
POLYMERIZATION
radioinduced, chain reaction method for, 25:4057
POLYMERS
radioinduced crosslinked, method for production of electron, 25:4100(P)
radioinduced graft polymerization of, mechanisms of, 25:4105
concretes--polymers, physical properties of building blocks of radiation-polymerized, 25:4859
concretes--polymers, preparation and properties of radiation-polymerized for use as structural material, 25:4838
metal--polymer, radioinduced polymerization of composites of, γ, 25:4108
POPULATIONS
protection against nuclear explosions, evaluation of underground transportation facilities as shelters for, 25:4255(R) (ORNL-TM-3016)
radiation hazards to human, from underground nuclear explosions, method for prediction of, 25:4172
POROUS MATERIALS
morphology of, determination by microscopic evaluation of particle stacking connectivity, 25:4841(R) (SRO-552-5)
POSITRON CAMERAS
development of, 25:4337
POSITRONS
interactions $e^+ + e^-$, Orsay and Novosibirsk experiments on rho^0, ω, and phi production in, 25:5250 (DNPL/R-7, pp 139-72)
interactions $e^+ + p$, search for time reversal invariance violation in inelastic, (E), 25:5400 (UCRL-20041)
POTASSIUM
pumps for liquid, cavitation and hydraulic performance of electromagnetic, 25:4186 (ORNL-TM-2955)
POTASSIUM ALUMINUM SULFATES
properties of polarized proton targets of, 25:5450 (LA-4465, pp 4.1-2)
POTASSIUM BROMIDES
dielectric constant of, low-frequency, 25:6228 (COO-623-153)

dielectric constants of, pressure and temperature dependences of static, 25:5166(R) (COO-623-156)
luminescence from aqueous solutions of γ-irradiated crystals of, mechanism of, 25:4076
radioinduced defects in crystals of, thermally stimulated conductivity and luminescence study of annealing of 100K γ, 25:5158
KBr--KNO_3, radioinduced decomposition in, energy transfer in, 25:4096
POTASSIUM CHLORIDES
dielectric constant of, low-frequency, 25:6228 (COO-623-153)
dielectric constants of, pressure and temperature dependences of static, 25:5166(R) (COO-623-156)
diffusion of uranium dioxide in, determination by neutron fission recoil tracks from uranium-235, 25:4845
luminescence from aqueous solutions of γ-irradiated crystals of, mechanism of, 25:4076
radioinduced color centers in crystals of pure and thallium-doped, 21°C γ-, 25:5157
radioinduced F centers in crystals of pure and doped, first-stage growth of room-temperature x-, 25:5159
POTASSIUM CYANIDES
effects on x-radiosensitivity of green algae, 25:4574
POTASSIUM HYDROXIDES
reactions with mandelic acid and uranyl nitrate, production of $K_2UO_2(O_3C_8H_6)_2$ from, 25:4055
POTASSIUM ISOTOPES K-39
alpha elastic scattering at 24.1 MeV, optical-model analysis with l-dependent absorption of angular distributions from, 25:5665
energy levels from argon-38 (p,γ) reactions, (E), 25:5631
neutron reactions using plutonium--beryllium source, gamma production cross section for, (E), 25:5582
photon reactions (γ,n) up to 140 MeV, cross sections for, (E), 25:5578
proton reactions (p,n) at threshold to 10.5 MeV, ground-state threshold and total cross section for, (E), 25:5610
POTASSIUM ISOTOPES K-40
abundance relative to argon-40 in Pacific Ocean phillipsites, 25:4164
beta decay of, hindrance of the unique third-forbidden branch of, (E/T), 25:5630
determination by β counting using G-M and proportional detectors, efficiency curves for, 25:4029 (CISE-N-119)
energy levels of, lifetimes of second- and third-excited, (E), 25:5649
energy-level transitions from radiative pion absorption by calcium-40, strengths for, (T), 25:5793
POTASSIUM ISOTOPES K-41
alpha elastic scattering at 24.1 MeV, optical-model analysis with l-dependent absorption of angular distributions from, 25:5665
energy levels from proton resonances in argon-40, spreading widths for isobaric analog, (T), 25:5644
POTASSIUM NITRATES
KBr--KNO_3, radioinduced decomposition in, energy transfer in, 25:4096
POTASSIUM PERMANGANATES
radioinduced radicals in single crystals of, ESR study of γ, 25:4110 (AD-710231)
POTASSIUM PYROSULFITES
radiolysis of solid, effects of oxygen-17 on ESR spectra of SO_2^- radical from, 25:4124
POWDERS
particle size distribution in compacted, use of Fisher equipment for determining, 25:4184(T) (LA-4404-TR)
POWER BURST FACILITY
operations in, LMFBR safety testing, 25:6102
POWER CYCLES
development of organic Rankine, for 2 to 10 kW(e) radioisotope-fueled power systems for undersea applications, 25:4225
development of radioisotope-fueled Brayton, 25:4216(R) (SC-PR-70-682)
POWER PLANTS
design of MHD, for nuclear--electric unmanned spacecraft, 25:4992(R) (N-70-34006)
PRASEODYMIUM
compounds with mandelic acid, preparation by reactions of praseodymium alkoxides with mandelic acid, potentiometric studies on, 25:4055
praseodymium-141 NMR in, 25:5226
PRASEODYMIUM ALLOYS AND SYSTEMS
Al--Pr, thermal capacity of $PrAl_2$ at low temperatures, 25:5218
Bi--Pr, thermal capacity of PrBi at low temperatures, 25:5218
Co--Pr, magnetic resonance of $PrCo_3$, microwave, 25:5200
Co--Pr, magnetic structure of $PrCo_3$, neutron diffraction study, 25:5210
Ni--Pr, thermal capacity of $PrNi_2$ at low temperatures, 25:5218
Pr--Sb, thermal capacity of PrSb at low temperatures, 25:5218
Pr-base--Pu, Kondo effect in, plutonium virtual bound state from, 25:5227
PRASEODYMIUM ARSENIDES
praseodymium-141 NMR in, 25:5226
PRASEODYMIUM ISOTOPES Pr-141
energy levels from neutron inelastic scattering, spin assignments for, (E), 25:5751
neutron capture integral in fast region, (E), 25:5656
neutron inelastic scattering at 1.2 to 2.2 MeV, γ spectra from, (E), 25:5751
nuclear magnetic resonance in praseodymium metal and compounds, 25:5226
PRASEODYMIUM ISOTOPES Pr-144
determination by β counting using G-M and proportional detectors, efficiency curves for, 25:4029 (CISE-N-119)
energy levels from cerium-144 beta decay, spin--parity assignments and lifetimes of, (E), 25:5745
energy levels from cerium-144 decay, spin--parity assignments for, (E), 25:5739
energy-level transitions from cerium-144 decay, intensities, multipolarities, and conversion coefficients for, (E), 25:5739
PRASEODYMIUM PHOSPHIDES
praseodymium-141 NMR in, 25:5226
PRASEODYMIUM SELENIDES
praseodymium-141 NMR in, 25:5226
PRESSURE
physics of extreme temperature and, (T), 25:5239
PRESSURE GAGES
design using dielectric constant of ionic crystal, 25:6230 (COO-623-155)
detectors for beta radiometric, at 20 to 0.02 psi, avalanche semiconductor, 25:4323 (NYO-4028-TA-1)
development of implantable americium-241-fueled, for monitoring intracranial pressures, 25:4241
PRESSURE VESSELS
damage to liquid sodium cooled fast reactor, accident analysis for assessment of, 25:6064
design requirements for prestressed concrete, analysis of limit state, 25:5981 (RISO-214, pp 289-300)
failure of prestressed concrete, model tests on, 25:5990(R) (ORNL-4589)
neutron flux and spectra in steel, (E/T), 25:6213
radiation effects on A212--B steel, effects of neutron fluence on, 25:6145 (AD-709898)
radiation effects on ductility of steel, in-pile, (E), 25:6146
reliability analysis of power reactor, 25:5983 (RISO-214, pp 323-34)
reliability analysis of power reactor, 25:5982 (RISO-214, pp 301-22)
structural characteristics of prestressed concrete, methods for analysis of, 25:5990(R) (ORNL-4589)
welds in, review of fracture mechanisms in, 25:4781
PRINCETON SYNCHROTRON
development for acceleration of heavy ions, 25:5462 (PPAD-676-E)
PROMETHIUM
separation from aqueous chloride solutions by solvent extraction using cyclooctylphenylphosphinic acid or octylphenylphosphinic acid, 25:4147
PROMETHIUM ISOTOPES Pm-143
energy levels from samarium-143 beta and electron-capture decay, spin--parity assignments for, (E), 25:5697
energy-level transitions from samarium-143 beta and electron-capture decay, intensities of, (E), 25:5697
PROMETHIUM ISOTOPES Pm-145
use as x-ray source for transmission scanning of bones for measurement of mineral content, 25:4647 (CONF-700515-, pp 274-9)
PROMETHIUM ISOTOPES Pm-147
determination by β counting using G-M and proportional detectors, efficiency curves for, 25:4029 (CISE-N-119)
use for inducing negative surface charge in silastic used as model for blood coagulation studies, 25:4434
PROMETHIUM OXIDES
fabrication of promethium-147-enriched heat sources of, 25:4217(P)
PROPANE
radiolysis of gaseous, yields from α, 25:4115
PROPANE, 2,2-DIMETHYL-
radiolysis at 23°C, effects of molecular structure on effects of deuterated ammonia and nitrous oxide on yields from γ, 25:4113
1,2-PROPANEDIOL
radioprotective effects of, on mouse stem cells, x, 25:4571
2-PROPANOL
complexes with thorium and uranium tetrachlorides, formation of crystalline, thermodynamics of, 25:4077
radiolysis of, yields of methane from γ, 25:4123
PROPENE, 2-METHYL-
radioinduced polymerization with tetrafluoroethylene, NMR spectral studies on product from γ, 25:4102
PROPENE, 2-METHYL-, POLYMERS
radioinduced cross linking with acrylonitrile or divinylbenzene, calorimetric studies on effects of dose on γ, 25:4101
PROPENE POLYMERS
polyethylene--polypropene, radiolysis at -180°C ir spectrometric study of, 25:4118
PROPIONIC ACID, 3-IODO-
effects on radiosensitivity of alcohol dehydrogenase in aqueous solutions, ionizing, 25:4543
effects on x-radiosensitivity of Ehrlich ascites tumor

XUM

cells in cultures, 25:4569
effects on x-radiosensitivity of enzymes in solutions, 25:4569
PROPICPHENONE, p-AMINO-
radioprotective effects of, on mouse stem cells, x, 25:4571
PROTACTINIUM
solubility in alpha thorium at 25 and 1300°C, 25:4791
PROTACTINIUM ALLOYS AND SYSTEMS
Pa--Th-base, crystal structure of, 25:4791
PROTACTINIUM ISOTOPES Pa-233
neutron resonance absorption interference effects in graphite moderated homogeneous reactors, 25:5958
PROTECTIVE CLOTHING
use by personnel in diagnostic radiography, recommendations for, 25:4531
PROTECTIVE OINTMENTS
effectiveness of sunscreening, for uv-radioprotection of human skin, 25:4608
PROTEINS
metabolism in brain cells in cultures, effects of hormones on, 25:4459 (UCLA-12-782, pp 23-47)
metabolism in rat heart cells in cultures, 25:4458 (UCLA-12-782, pp 1-21)
radiation effects on content of S-100 in developing brain of rats, effects of age and hypophysectomy on x, 25:4654 (UCLA-12-791)
synthesis in nerve fibers of giant squid, tracer study of sites of, 25:4418
PROTON BEAMS
phase density in intense, from duoplasmatron source, redistribution of, 25:5458 (NP-18510)
polarization measurements of, Lamb-shift polarimeter for, 25:4391 (LA-4465, pp 17.1-6)
PROTON SOURCES
beams from duoplasmatron, redistribution of phase density in intense, 25:5458 (NP-18510)
PROTONS
detection of solar, response analysis of system for, 25:4928
detection of, effects of nuclear reactions on silicon detector response for, 25:5606(R) (UCSB-34-P-144-7)
dose from cosmic radiation to astronauts, statistical analysis of hazards of, 25:4569 (MDC G-363)
effects on immune responses of antibodies in mice, 2.2-GeV, 25:4470
effects on photographic film, 25:4406 (N-70-35843)
effects on photographic film at high energies, 25:4407 (N-70-35923)
effects on void formation in nickel, 25:4051(R) (AI-AEC-12972)
energy spectra of auroral, ionization rate and electron density height profiles for, 25:5610
energy spectra of primary cosmic, (E/T), 25:4981
form factor from e + d → e + d interactions at low momentum transfers, deuteron-to-proton ratio for electric, (E), 25:5247 (AD-710385)
form factors from e + d → e + d interactions at low momentum transfers, neutron-to-proton ratio for electric, (E), 25:5247 (AD-710385)
interactions above 1 TeV, review of, (E), 25:5274
interactions anti p + p → 4π at rest, normalization using dual six-point function for, (T), 25:5362
interactions anti p + p → Λ + anti Λ, factorization predictions as test of exotic exchange in, (T), 25:5365
interactions anti p + p → Ξ⁻ + Ξ⁻ at 2.9 GeV/c, total cross sections for, (E), 25:5270
interactions anti p + p at 2.4 and 2.9 GeV/c, differential cross sections for Λanti Λ and Λ anti Σ⁰ final states in, (E), 25:5270
interactions anti p + p at 2.4 and 2.9 GeV/c, Σ(1385), Λ(1405), and Λ(1520) production in three-body final states in, (E), 25:5270
interactions anti p + p at 20 to 65 GeV/c, total cross sections for, (E), 25:5295
interactions e + p → e + p at 15 and 18 GeV, search for polarization in, (E), 25:5252 (UCRL-20093)
interactions e + p → rho⁰ + p, Pomeranchuk decoupling from ordinary Regge trajectories in rho⁰ transverse polarization in, (T), 25:5348 (CCO-264-562)
interactions e + p at high energies, review of field theoretic models for deep inelastic, (T), 25:5320 (CONF-700314-, Paper 17)
interactions e + p, parton model for structure functions for hadron production in deep inelastic, (T), 25:5330
interactions e + p, search for time reversal invariance violation in inelastic, (E), 25:5400 (UCRL-20041)
interactions e⁺ + p, search for time reversal invariance violation in inelastic, (E), 25:5400 (UCRL-20041)
interactions γ + p → K⁺ + Λ at 1.3 GeV, differential cross sections for, (E), 25:5253
interactions γ + p → K⁺ + Σ⁰ at 1.45 GeV, differential cross sections for, (E), 25:5253
interactions γ + p → π⁺ + n at 2.6 to 16 GeV with linearly polarized photons, spin--parity contributions to cross sections for, (T), 25:5321 (DESY-70/1)
interactions γ + p → π⁺ + n at 5 and 16 GeV, cross section asymmetry for, (E), 25:5251 (UCRL-19897)
interactions γ + p → π⁺ + π⁻ + p, diffraction-dissociation, dual-resonance, and interference models for rho production in, 25:5323 (DNPL/R-7, pp 3-28)
interactions γ + p, Pomeranchuk decoupling from ordinary Regge trajectories in vector meson production in, (T), 25:5348 (CCO-264-562)
interactions γ + p, review on rho, ω, and phi production in, 25:5301 (DNPL/R-7, pp 29-70)
interactions K⁻ + p → anti K⁰ + n at 2 to 20 GeV/c, Regge model with four poles for, (E/T), 25:5371 (CEA-N-1373)
interactions K⁻ + p → anti K⁰ + n at 400 MeV/c in hydrogen bubble chamber, (E), 25:5262
interactions K⁻ + p → anti K⁰ + n at high energies, effective Regge trajectories for, (T), 25:5377
interactions K⁻ + p → Λ + eta' at 1.70 to 2.65 GeV/c, cross sections and eta' spin and parity from, (E), 25:5291
interactions K⁻ + p → Σ⁻ + π⁺ in freon, Σ⁻ reabsorption rate from, 25:5298
interactions K⁻ + p → Σ⁺(Σ⁻) + π⁻(π⁺) at 385 MeV/c in hydrogen bubble chamber, production of polarized Σ⁺ and Σ⁻ in, (E), 25:5260
interactions K⁻ + p → X⁰(960) + Λ on polarized targets, parity and spin of X⁰(960) from, (T), 25:5361 (TPJU-14/70)
interactions K⁻ + p → Ξ⁻(Ξ⁰) + K⁺(K⁰) at 1.2 to 2.7 GeV/c in bubble chamber, total cross sections, polarization, and partial-wave analysis for baryon exchange in, (E/T), 25:5384
interactions K⁻ + p at 10 GeV/c, production of (anti pp), (K⁺K⁻), and (π⁺π⁻) pairs in, (E), 25:5297
interactions K⁻ + p at 20 to 65 GeV/c, total cross sections for, (E), 25:5295
interactions K⁺ + p at 4.6 GeV/c in bubble chamber, cross section for elastic, (E), 25:5296
interactions K⁻ + p at rest in hydrogen bubble chamber, Σ⁻ and Σ⁺production in, (E), 25:5269
interactions n + p → d + γ, calculation of cross sections using meson exchange currents, (T), 25:5545
interactions p + n at 24 GeV in emulsions and hydrogen bubble chamber, energy spectra and transverse-momentum distributions for π and p and baryon resonance production in, (E), 25:5276
interactions p + p → p + n + π⁺ at high energies, OPE model for energy behavior and branching ratio of, 25:5392
interactions p + p → p + p + π⁺ + π⁻ at 7.9 GeV/c, Reggeized π exchange for Δπ(1425) enhancement in, 25:5278
interactions p + p → p + p at very high energies and high momentum transfers, large-angle, (E/T), 25:5281 (CONF-700314-, Paper 15)
interactions p + p → p + π⁰ + p, counter experiments for measuring final states in, 25:5318
interactions p + p → p + π⁺ + n, counter experiments for measuring final states in, 25:5318
interactions p + p → π⁺(π⁰) + p + n(p) at 669 MeV, secondary proton polarization in, (E), 25:5268 (JINR-P1-5293)
interactions p + p at 300 to 640 MeV, production of nonstrange 2⁺(2050) resonance in, (T), 25:5368 (JINR-P2-5058)
interactions p + p at 37 MeV, spin correlation coefficients in scattering, (E), 25:5506 (CEA-N-1232, pp 81-159)
interactions p + p at high energies, Bethe--Salpeter equation for fireball production in inelastic, 25:5369
interactions p + p at high energies, review of diffraction models for, (T), 25:5347 (CONF-700314-, Paper 13)
interactions p + p at very high energies and high momentum transfers, secondary production in, (E/T), 25:5281 (CONF-700314-, Paper 15)
interactions p + p below 56 GeV, proposed experiments for, 25:5444 (CONF-700314-, Paper 2)
interactions π + p → π + p at low energies, phenomenological Regge trajectories in direct-channel, (T), 25:5382
interactions π + p at 50 to 1000 GeV, review of multiparticle production in, (E), 25:5273
interactions π + p at high energies, Bethe--Salpeter equation for inelastic, 25:5369
interactions π + p at very high energies and high momentum transfers, large-angle and backward, (E/T), 25:5281 (CONF-700314-, Paper 15)
interactions π⁻ + p → A_2^- + p at 3.9 to 16 GeV/c in bubble chamber, production mechanism of A_2^-, 1-daughter production, and cross sections for, (E), 25:5282 (CCO-1195-200)
interactions π⁻ + p → eta + n at 2.9 to 18.2 GeV/c, heavy-plate spark chamber study of differential cross sections for, (E), 25:5279 (CEA-R-4037)
interactions π⁺ + p → f⁰ + Δ⁺⁺ at 13.1 GeV/c in hydrogen bubble chamber, cross sections and dipion mass spectrum for, (E), 25:5283 (CCO-1428-238)
interactions π⁺ + p → K⁺ + Σ(1385) at 4 and 5.05 GeV/c, test of SU(3) symmetry from counter and spark chamber study of differential cross sections for, (E), 25:5290
interactions π⁻ + p → π⁰ (eta) + n at 2 to 20 GeV/c, Regge model with four poles for, (E/T), 25:5371 (CEA-N-1373)
interactions π⁺ + p → π⁺ + p + π⁺ + π⁻ at 11.0 GeV/c, rho⁰, Δ⁺⁺(1236), and A production in, (E), 25:5252
interactions π⁻ + p → rho + p in absorption model, cross

section for, 25:5381
interactions π^- + p + rho^0 + n, cross sections and rho spin density matrices in Regge models for, (E/T), 25:5380
interactions π^- + p at 17 GeV/c, azimuthal correlations in decays of 1.5- to 2.5-GeV mesonic resonances produced in, (E), 25:5366
interactions π^- + p at 20 to 65 GeV/c, total cross sections for, (E), 25:5295
interactions π^- + p at 25 GeV/c, multiparticle production in, (E), 25:5280 (CONF-700314-, Paper 10)
interactions π^+ + p at 8 GeV/c, production of (anti pp), (K^+K^-), and ($\pi^+\pi^-$) pairs in, (E), 25:5297
interactions π^- + p at high energies, effective Regge trajectories for two-body production in, (T), 25:5377
interactions π^+ + p at high energies, effective Regge trajectories for two-body production in, (T), 25:5377
interactions π^+ + p at infinite momentum, resonance-background interference corrections to finite-energy sum rule estimates of total cross sections for, (T), 25:5378
interactions π^- + p at infinite momentum, resonance-background interference corrections to finite-energy sum rule estimates of total cross sections for, (T), 25:5378
interactions π^- + p near 1 GeV, N and π exchange in peripheral model for momentum and angular distributions for π^+ and π^- production in, (T), 25:5376
penetration into Earth ionosphere, effects of interstellar, 25:5021
penetration into solids, path lengths for, (T), 25:4940
polarization of secondary, in p + p + $\pi^+(\pi^0)$ + p + n(p) interactions at 669 MeV, (E), 25:5268 (JINR-P1-5293)
production in p + n interactions at 24 GeV in emulsions and hydrogen bubble chamber, energy spectra and transverse-momentum distributions for, (E), 25:5276
reactions (γ,f) with nuclei, description of near-barrier, 25:5850
reactions (p,2n) with europium-153 at 14 MeV, gamma and conversion-electron spectra from, (E), 25:5750
reactions (p,2p) and (p,p3n) + (p,4n) with zinc-68 at 10 to 85 MeV, cross sections for, (E), 25:5623
reactions (p,2p) wih deuterium at 24 MeV using polarized beams, cross-section asymmetry for, (E), 25:5506 (CEA-N-1232, pp 81-159)
reactions (p,2p) with deuterium at 4.5 to 13.0 MeV, excitation functions and energy spectra from, (E), 25:5534
reactions (p,2p) with Z = 22, 26, and 28 nuclei at 100 to 500 MeV, proton spectra, excitation energies, and angular correlations for, (E), 25:5606(R) (UCSB-34-P-144-7)
reactions (p,α) with boron-11 at 2.4 to 3 MeV, α-α coincidence spectra from, (E), 25:5680 (CEA-N-1232, pp 1-80)
reactions (p,d) with beryllium-9 at 5.0 to 12.0 MeV, angular distributions of analyzing power from, (E/T), 25:5584
reactions (p,d) with iron-57 at 17.3 MeV using polarized beams, cross section and asymmetry for, (E), 25:5506 (CEA-N-1232, pp 81-159)
reactions (p,d) with nickel-64 at 27.5 MeV, angular distribution for, (E), 25:5609
reactions (p,d) with tin-118 and zirconium-91 at 24.5 MeV using polarized beams, cross sections and asymmetries for, (E), 25:5506 (CEA-N-1232, pp 81-159)
reactions (p,d), (p,He-3), (p,t), (p,He-3p), and (p,tp) with helium-4 at 47 MeV, Watson--Migdal and direct-reaction analysis of spectra and angular distributions from, (E/T), 25:5533
reactions (p,f) with bismuth and uranium at 159 MeV to 18.2 GeV, cross sections for indium isotopes and charge dispersion curves for A = 117 nuclei from, (E), 25:5784
reactions (p,f) with uranium-233 and -238 at 11.5 to 22 MeV, neutron-emission--fission competition and neutron-per-fission ratios from, (E), 25:5692
reactions (p,γ) with argon-38 at 12.5 to 2.35 MeV, angular distributions and Q-value for, (E), 25:5631
reactions (p,γ) with manganese-55 at 1.3 to 1.5 MeV, γ branching ratios for isobaric analog resonances in, (E), 25:5676
reactions (p,γ) with nickel-58 at 3.45 to 3.60 MeV, excitation functions for, (E), 25:5660
reactions (p,γ) with phosphorus-31 at 2.1 MeV, excitation functions and spin-mixing coefficients from, (E), 25:5636
reactions (p,γ) with titanium-50 at 1.3 to 2.7 MeV, excitation functions, angular distributions, and gamma spectra from, (E), 25:5651
reactions (p,He-3p) with helium-4 at 47 MeV, np singlet scattering length from, (E/T), 25:5533
reactions (p,n) with magnesium-26 at 5.2 to 8.0 MeV, excitation function for, (E), 25:5613
reactions (p,n) with potassium-39 at threshold to 10.5 MeV, ground-state threshold and total cross section for, (E), 25:5610
reactions (p,n), (p,2n), (p,pn)(p,3np), and (p,3pn) with scandium-45 at 10 to 85 MeV, cross sections for, (E), 25:5623
reactions (p,t) with calcium-42, -44, and -48 at 20 MeV, angular distributions for, (E), 25:5677
reactions (p,t) with even tin isotopes at 20 MeV, cross sections for, (E), 25:5799
reactions (p,t) with neon-20 at 42.6 MeV, angular distributions for, (E), 25:5587
reactions with ammonia, carbon dioxide, carbon monoxide, and methane at 1 to 25 keV, cross sections for electron capture and total ionization in, (E), 25:4563
reactions with atoms, angular distribution of fast K- and L-shell electrons from, (T), 25:4968
reactions with helium and hydrogen atoms at high energies, continuum distorted-wave method for calculation of electron capture in, 25:4958
reactions with helium at 25 to 125 keV, cross sections for excitation, ionization, and total inelastic scattering and energy distributions of electrons ejected from, (E), 25:4967
reactions with nuclei at 50 to 1000 GeV, review of multiparticle production in, (E), 25:5273
reactions with silicon-28 at 660 MeV, fluorine-18 differential energy distributions from, (E/T), 25:5663
scattering by aluminum-27 at 18 MeV using polarized beam, depolarization parameter for elastic, (E), 25:5506 (CEA-N-1232, pp 81-159)
scattering by beryllium-10 at 12 to 16 MeV, angular distributions for elastic and inelastic, (E), 25:5589
scattering by beryllium-9 and carbon at 49.4 MeV, angular distributions of cross sections and polarizations in elastic and inelastic, (E), 25:5585
scattering by beryllium-9 at 3.0 to 12.0 MeV, optical-model analysis of angular distributions of analyzing power from elastic, (E/T), 25:5584
scattering by beryllium-9 at 5.0 to 12.0 MeV, angular distributions of analyzing power from inelastic, (E/T), 25:5584
scattering by bismuth-209 at 24.5 MeV, differential cross sections and energy spectra for decuplet excitation from inelastic, (E), 25:5745
scattering by cadmium-110, -112, and -114 at 6 to 11 MeV, excitation functions for elastic and inelastic, (E), 25:5752
scattering by calcium-40, magnesium-24, and silicon-28 at 20.3 MeV using polarized beams, cross sections and asymmetries for inelastic, (E), 25:5506 (CEA-N-1232, pp 81-159)
scattering by carbon-12 at 185 MeV, DWBA analysis of differential cross sections from elastic and inelastic, (E/T), 25:5552 (ITF-70-50)
scattering by deuterium at 3 to 6 MeV, phase shifts, differential cross sections, analyzing power, and proton polarization for elastic, (T), 25:5546
scattering by deuterium at 800 MeV using polarized and unpolarized beams, analysis of elastic, (T), 25:5517 (LA-4465, pp 16.1-2)
scattering by helium-4 at 20 to 40 MeV, contour plot of polarization from elastic, (E), 25:5526 (UCRL-19943)
scattering by helium-4 at 24 and 26 MeV, differential cross sections for elastic, (E), 25:5526 (UCRL-19943)
scattering by iron-54 and -56 at 19.6 MeV, γ--γ angular correlations and spin-flip probability for inelastic, (E), 25:5673
scattering by iron-54 at 10 MeV, p--γ angular correlations from inelastic, (E), 25:5673
scattering by lead-207 at 20.2 MeV to $^3/_2^-$ state, distorted-wave analysis using central, tensor, and core-polarization interactions of differential cross sections from inelastic, (T), 25:5780
scattering by lead-208 at 14.5 to 15.4 MeV using polarized beams, analyzing power for inelastic, (E), 25:5506 (CEA-N-1232, pp 81-159)
scattering by magnesium-24, chromium-52, and nickel-58 at 5 to 6 MeV, excitation functions and proton polarization for, (E), 25:5632
scattering by nickel-58 at 12 MeV, proton and γ spectra from inelastic, (E), 25:5680 (CEA-N-1232, pp 1-80)
scattering by nickel-58 at 8.1 MeV, p--γ angular correlations from inelastic, (E), 25:5642
scattering by nitrogen and oxygen at 49.4 MeV, angular distributions of cross sections and polarization in, (E), 25:5585
scattering by nuclei, formalism for polarization transfer in elastic, (T), 25:5804 (LA-4465, pp 21.1-2)
scattering by polarized helium-3 at 19.5 MeV using polarized beam, correlation parameters for elastic, (E), 25:5506 (CEA-N-1232, pp 81-159)
scattering by tritium at 13.6 MeV using polarized beam, asymmetry for elastic, (E), 25:5521 (LA-4465, pp 28.1-2)
spectra of radiation belt, (T), 25:5033
structure functions for, scale-invariant light-cone SU(3) x SU(3) current commutators for, (T), 25:5328

PROTONS (anti p)
absorption by nuclei at 20 to 40 GeV/c, cross sections for, (E), 25:5265 (CONF-700314-, Paper 4)
absorption by nuclei at 20 to 65 GeV/c, cross sections for, (E), 25:5295
interactions anti p + d + $2\pi^-$ + π^+ + p at rest in deuterium bubble chamber, spectator and anti p S-capture in, (E), 25:5271
interactions anti p + d + $2\pi^-$ + π^+ + π + p at rest in deuterium bubble chamber, spectator and anti p S-capture in, (E), 25:5271

XUM

interactions anti p + d at 20 to 65 GeV/c, total cross sections for, (E), 25:5295
interactions anti p + n → 2π⁻ + π⁺ + π at rest in deuterium bubble chamber, branching ratio for, (E), 25:5271
interactions anti p + n → 2π⁻ + π⁺ + π at rest in deuterium bubble chamber, branching ratios for rho, ω⁰, and J = 0 πη(1115) production in, (E), 25:5271
interactions anti p + n → 2π⁻ + π⁺ at rest in deuterium bubble chamber, branching ratio for, (E), 25:5271
interactions anti p + p → 4π at rest, normalization using dual six-point function for, (T), 25:5362
interactions anti p + p → Δ + anti Δ, factorization predictions as test of exctic exchange in, (T), 25:5365
interactions anti p + p → Ξ⁻ + Ξ⁻ at 2.9 GeV/c, total cross sections for, (E), 25:5270
interactions anti p + p at 2.4 and 2.9 GeV/c, differential cross sections for Λanti Λ and Λ anti Σ⁰ final states in, (E), 25:5270
interactions anti p + p at 2.4 and 2.9 GeV/c, Σ(1385), Λ(1405), and Λ(1520) production in three-body final states in, (E), 25:5270
interactions anti p + p at 20 to 65 GeV/c, total cross sections for, (E), 25:5295

PROTOZOA
Histomonas meleagridis, radiation effects on in vitro growth of, effects of dose on γ, 25:4692 (COO-1209-13)

PSORALEN, 5,9-DIHYDROXY-
effects on γ-radiosensitivity of Ehrlich ascites tumor cells, 25:4565

PULSARS
cosmic particle emission from, (T), 25:4978
cosmic-ray origin in, (T), 25:4979
properties of, (T), 25:4978
pulse characteristics of, use in studying circumsolar plasma, (E/T), 25:4920(T) (CSIRO-Trans-9897)

PULSE CONVERTERS
design of time-to-amplitude, for fast coincidence measurements, 25:4334

PUMPS
design for piping components and systems, summary of experience on, 25:4188 (TID-25553)

PUMPS (LIQUID METAL)
construction and operation of mechanical sodium, for liquid-metal-cooled fast breeder reactor, 25:4201

PUREX PROCESS
improvements in, 25:4134(T) (AEC-tr-7158)

PYRIDINE
reactions with mandelic acid and uranyl nitrate, production of $(C_5H_4N)_2UO_2(C_3C_6H_4)_2$ from, 25:4055

PYRIMIDINE
effects on germination of sugarbeet seeds, 25:4722
incorporation of halogenated analogues of, into DNA, effects of, on radiosensitivity of cells, 25:4537

Q

Q DEVICES
ion distribution functions in collisionless surface ionized plasmas in, (E/T), 25:5098
plasma drift instabilities in, collisionless, (E), 25:5112

QUANTUM ELECTRODYNAMICS
constant 2e/h in, determination using ac Josephson effect, 25:5412
formulation of semi-quantized, from charged vector boson field interactions with external electromagnetic field, 25:5413

QUANTUM FIELD THEORY
algebras in relativistic axiomatic, equality of local, 25:5407 (JINR-P2-5330)
Bethe--Salpeter equation for leading trajectory and fireball production processes, 25:5359
charges and generators of symmetry transformations in Wightman, 25:5416
composite particles in, Z = 0 formalism for spin-1 and -3/2, 25:5417
eikonal approximation in models for N + N interactions in, quasipotential smoothness in, 25:5387 (JINR-E2-5365)
Fermi transformation in, criterion for canonical, 25:5415
field matrix element relation with phases of two-channel S-wave scattering, 25:5436
field reduction to Heisenberg operators for interpolating, 25:5431
fields from local observables in axiomatic algebraic theory with superselection rules in, 25:5414
fields in, strong limits of interpolating fields for in--out, 25:5431
mass spectrum in infinite-component local field in, transformation over nonunitary irreducible representation of Sp(4) group for, 25:5406 (JINR-P2-5305)
models for deep inelastic electron scattering at high energies in, 25:5320 (CONF-700314-, Paper 17)
models for diffraction scattering and dissociation in high-energy interactions in, 25:5320 (CONF-700314-, Paper 17)
models for N + N interactions in, quasipotential smoothness in eikonal approximation in, 25:5387 (JINR-E2-5365)
multiloop planar dual diagrams in, divergences and renormalization in, 25:5409
renormalization constant for composite bosons in nonlocal, 25:5411
scattering in, generalization of in--out formalism for Coulomb potentials for, 25:5431
Thirring model in, energy--momentum tensor for locally generated dilatation charge in, 25:5408 (NYO-3829-61)
Yang--Mills gauge transformation in, 25:5410

QUANTUM MECHANICS
approximations deduced from association of Milne and Schroedinger equations, 25:5234 (CEA-R-4007)
causality in, paradoxes related to full, 25:5307 (RLC-2041-49)
discretization in astronomy, (T), 25:4933
energy operators of many-body systems in, invariance of spectrum of, 25:5241
harmonic oscillator in, quasi-potential equation for relativistic, 25:5405 (JINR-E2-5339)
WKB approximation for phase shifts in, modified, 25:5238

QUASARS
photometry of 3C 273, UBV, (E), 25:4916
spectra of, absorption lines in, (E/T), 25:4915

QUINOLINE
spectra of, correlation of extended Huckel calculations of total electron densities with NMR, 25:4081

8-QUINOLINETHIOL
radioprotective effects of, on mice, x, 25:4553

8-QUINOLINOL
complexes with thorium, uranium, and other metals, structure of, NMR spectral studies on, 25:4081
spectra of, correlation of extended Huckel calculations of total electron densities with NMR, 25:4081

R

RABBITS
diffusion of uranium oxides across placental tissues of, following intratracheal and oral administration, 25:4446
effects on intrauterine and early extrauterine development of, following maternal ingestion or intratracheal injection of uranium oxide, 25:4446
excretion of uranium oxide by mammary glands of, following intratracheal and oral administration, 25:4446
plutonium-239 retention in bone and lung tissues of, fallout, 25:4478
radiation effects on content of calcium, potassium, and sodium in blood plasma, erythrocytes, and heart muscle of, x, 25:4698
radioinduced burn injuries in, laser, 25:4704
radioinduced kidney hypertension in, effects of function of vagus nerve on, light or uv, 25:4697
toxicity of uranium oxide to organs and tissues of, following acute and chronic intratracheal, oral, and subcutaneous administration, 25:4447

RADIATION
cytogenetic effects of, on human cells, low dose ionizing, 25:4500
detection and measurement in Pioneer plasma analyzer, performance of equipment for, 25:4243
dose to man from natural sources at spas of Misasa and Masutomi, Japan, estimation of, 25:4711
dosimetry in microorganisms, methods for measuring, 25:4507 (EUR-4506)
effects of pulsed, on 1,2-dichloroethane, spectrophotometric studies on rate of formation and subsequent decay of aromatic radical cations produced by, 25:4112
effects of pulsed, on selenourea, mechanism of, 25:4115
effects on alcohol dehydrogenase in solutions, effects of iodine solutions on ionizing, 25:4543
effects on amino acids in aqueous solutions, protective effects of selenium compounds against ionizing, 25:4545
effects on animal and human embryos, low-level ionizing, 25:4713
effects on bacterial spores, protective effects of chemicals against, 25:4726
effects on biological organisms, protection against, review of, 25:4524
effects on β-carotene in lipid solvents, 25:4467
effects on catalytic properties of semiconductor metal oxides in decomposition of hydrogen peroxide, 25:4095
effects on cells, analysis of two-compartment theory of lethal, 25:4691
effects on cells, effects of incorporation of halogenated pyrimidine analogues into DNA on sensitivity to, 25:4537
effects on cells, mechanisms of protective effects of sulfur-containing agents against ionizing, 25:4538
effects on cells, molecular mechanisms of protection against ionizing, 25:4535
effects on cells, molecular mechanisms of sensitivity to ionizing, 25:4535
effects on Convolvulaceae and Leguminosae species, ionizing, 25:4717 (NYO-2043-216, pp 1-18)

effects on copper complexes with cysteamine and penicillamine, ionizing, 25:4547
effects on dislocation channeling in metals, 25:4809 (AD-710356)
effects on dry fern spores, reaction mechanisms for ionizing, 25:4709
effects on excretion of 17-ketosteroids in rats, comparison of orchiectomy and, 25:4707
effects on HeLa cells, reaction mechanisms for ionizing, 25:4709
effects on hematopoiesis in dogs, protective effects of bone marrow transplants against ionizing, 25:4533
effects on lysozyme in solutions, protective effects of cysteine against ionizing, 25:4544
effects on mammals, protective effects of amines and hypoxic agents against ionizing, 25:4539
effects on man following therapy of kidney carcinomas, pathological, 25:4712
effects on man, effects of high dose ionizing on carcinogenic, 25:4502
effects on mice, carcinogenic, ionizing, 25:4699
effects on mice, effects of dose on repair of mutagenic, ionizing, 25:4501
effects on personnel, medical supervision following, 25:4523
effects on polymerization, chain reaction method for, 25:4097
effects on polyolefins, ir spectrometric study of, 25:4118
effects on rats, protective effects of selenium compounds against ionizing, 25:4545
effects on selenoureа in aqueous solutions, ionizing, 25:4546
effects on water, mechanism of product formation from, 25:4120
fields around SNAP-27 heat sources, mapping of, 25:4247
uses in agriculture, 25:4732(R) (NYO-2043-216)

RADIATION CHEMISTRY
equipment for pulse radiolysis, gated photomultiplier, 25:4398

RADIATION DETECTORS
design for total body monitoring of personnel, 25:4335(P)
performance of continuous channel electron multiplier-type, in measuring radiation in Pioneer plasma analyzer, 25:4243
performance of superfluid relativity gyroscope, for test of Einstein general relativity theory, 25:5422
performance of wide range linear channel neutron flux, 25:6207
radiation effects on spacecraft-borne, radioisotope thermoelectric generator, 25:4409
response in exponential piles of neutron, diffusion theory calculations for, 25:6118
response of delayed neutron, two stage Monte Carlo calculations for, (T), 25:6151

RADIATION DETECTORS, ACTIVATION
calibration in polyethylene spheres for intermediate neutron spectroscopy, 25:4364
design parameters of in-core, for fast breeder reactors, 25:6044
development for in-core fast neutron detection, using beryllium-9 in carrier gas, 25:4355
neutron flux, optimum wire diameter for, 25:6206
performance of multifoil, for in-core fast neutron spectra measurements, 25:4357

RADIATION DETECTORS, BUBBLE CHAMBER
bubble dynamics in liquid hydrogen, in ultrasonic field, 25:4371 (JINR-P13-5327)
meson (K^-) cascade time in liquid helium, 25:5254
particle tracks in, computer program for analysis of, 25:4372 (SJC-T-70-3)
particle tracks in, computer program for microscope system for analysis of, 25:4369 (IFVE-SPK-69-53)

RADIATION DETECTORS, CHERENKOV
development of water, for muons at 0.5 to 100 GeV/c, 25:4375

RADIATION DETECTORS, DIELECTRIC TRACK
development and research on, 25:4345
development for neutron flux monitoring for unattended safeguards applications, 25:4341
image enhancement in thin-film cellulose nitrate, for neutron radiography, 25:4346
image enhancement in thin-film, for neutron radiography, sparking techniques for, 25:4346
particle track analysis in Makrofol polycarbonate, fast neutron-induced, 25:4339
particle track analysis in, automatic system for, 25:4340
particle track counting in polycarbonate, fission fragment, 25:4342
particle tracks in polycarbonate, charge determination of cosmic, 25:4338
particle tracks in, automatic counting system for fission, 25:4343
performance of cellulose nitrate, for alpha metallographic autoradiography, 25:4344
performance of Lexan plastic, for study of elemental abundance of 150 to 250 MeV/nucleon Z = 16 to 30 cosmic nuclei, 25:4373
uses of, 25:4347

RADIATION DETECTORS, FISSION CHAMBER
design for measurement of neutron fission cross sections of uranium-233 at 0.4 to 2000 eV, 25:4333

RADIATION DETECTORS, FISSION FOIL
performance of, analysis of fission yield for fast reactor spectra, 25:5973

RADIATION DETECTORS, GEIGER-MUELLER
operating range of halogen-quenched, count-rate, 25:4361
response to gamma radiation from radioisotope thermoelectric generators, 25:4349

RADIATION DETECTORS, IONIZATION CHAMBER
design of pocket, with audible alarm, 25:4360
development of tissue-equivalent, with quartz fiber electrometer, 25:4330
electron slowdown in multiplate Monte Carlo calculation of, 25:4322 (NP-18433)
performance in cosmic-ray ionization measurements at balloon altitude, (E), 25:4990
performance of dE/dx liquid xenon, 25:4315 (JINR-P13-5403)
windows for, preparation of thin-film parylene, 25:4329

RADIATION DETECTORS, PROPORTIONAL
development of flowthrough, for monitoring helium-3 and krypton-85 in natural gas lines, 25:4352
development of long, for high-rate neutron detection, 25:4354
pulse analysis of proton recoil, for gamma discrimination in neutron spectroscopy, analog computer for, 25:4362 (CEA-N-1314)

RADIATION DETECTORS, SCINTILLATION
book: Current Status of Liquid Scintillation Counting, 25:4358
calibration of sodium iodide, use of californium-252 neutron sources for, 25:4223
design and performance of long, for time-of-flight and position measurements, 25:4318 (JINR-E1-5098)
design for use in analysis of wastes for plutonium, 25:4292
development for gamma scanning inventory of plutonium, 25:4297
performance for γ transmission scanning of human bones, 25:4634 (CONF-700515-, pp 33-47)
performance for γ transmission scanning of human bones, 25:4635 (CONF-700515-, pp 48-57)
performance for xenon-133 scanning of human lungs for lung volume and function, 25:4671
performance of liquid helium, for neutron detection, 25:4321 (LA-4465, pp 31.1-2)
pulse-height spectrum unfolding for NE-213, for neutron spectroscopy, 25:4365
use, with xenon-133, for measuring regional pulmonary ventilation in man, 25:4666

RADIATION DETECTORS, SEMICONDUCTOR
development and uses of avalanche, 25:4323 (NYO-4028-TA-1)
operation of surface-barrier avalanche, 25:4322 (NP-18433)
preparation of, using ion implantation, 25:5506 (CEA-N-1232, pp 81-159)
response analysis for solar flare proton and alpha particles, (E), 25:4928

RADIATION DETECTORS, SEMICONDUCTOR (GERMANIUM)
calibration of, gamma spectra for, 25:5736

RADIATION DETECTORS, SEMICONDUCTOR (SILICON)
design and performance with fission foil for in-core neutron flux monitoring, 25:4353
response of shielded to gamma radiation from radioisotope thermoelectric generator, 25:4350
response of totally depleted and lithium-drifted, to gamma radiation and neutrons from radioisotope thermoelectric generators, 25:4356
response to monoenergetic neutrons, Monte Carlo calculation of, 25:4351
response to protons, nuclear reaction effects on, 25:5606(R) (UCSB-34-P-144-7)

RADIATION DOSE
calculation of absorbed, for man during radioisotope scanning of lungs, use of MIRD equations for, 25:4611
calculation of absorbed, for man following 10-year ingestion of fallout cesium-137, methods using whole-body counting data and MIRD formulas, 25:4657 (UCLA-12-782, pp 89-125)
calculations for human populations from underground nuclear explosions, development of equations for, 25:4172
evaluation for public use of nuclearly stimulated natural gas, 25:4525 (ORNL-TM-3216)
fractionation of, effects on number of chromosome aberrations in root tip cells of Vicia, x, 25:4492
standards for radiography personnel, 25:4531

RADIATION DOSIMETERS
calibration of, fabrication of americium-241 gamma source for, 25:4248
development for gamma dosimetry based on charge generation in dielectrics by Compton and photoelectron scattering, 25:4376 (AD-710007)
development of helium accumulating, for high neutron fluence measurements in-core, 25:4381
intercomparison of personnel nuclear accident, 25:4377 (AERE-R-6498)

RADIATION DOSIMETERS, CALORIMETRIC
development of linear array and total stopping, for high-

XUM

intensity pulsed electron beams, 25:4379 (SC-TM-69-258)
RADIATION DOSIMETERS, CHEMICAL
fading of optical density in PMMA, effects of oxygen on, 25:4384
RADIATION DOSIMETERS, EXOELECTRON
response of beryllium oxide and graphite mixture, at 2 mR to 400 R, 25:4380
RADIATION DOSIMETERS, PHOTOGRAPHIC FILM
performance of Kodak type III, 25:4383
use by personnel in diagnostic radiography, recommendations for, 25:4531
RADIATION DOSIMETERS, THERMOLUMINESCENT
performance evaluation of lithium-7 fluoride, for personnel dosimetry, 25:4378 (BNWL-CC-2633)
response of TLD 700, to reactor neutrons for gamma dosimetry in mixed field, 25:4382
RADIATION DOSIMETRY
calculations for therapy, computer programs for, 25:4514
RADIATION MONITORING
program at Research Reactor Institute of Kyoto University during 1968, 25:4508 (KURRI-TR-63)
programs for environmental, at Brookhaven National Laboratory during 1969, 25:4503 (BNL-50196)
RADIATION PROTECTION
measures for personnel in relation to risk of exposure, 25:4523
mechanisms of cellular and molecular, ionizing, 25:4535
methods for personnel, 25:4524
programs for medical personnel, 25:4528
recommendations for standards of, by FRC, ICRP, and NCRP, 25:4532
requirements for handling plutonium dioxide--uranium dioxide fuel rods, 25:4314
RADIATION SOURCES
dose from moving, (T), 25:5243
production in COMECON states, review on, 25:4128
support films for radioisotope, preparation of thin parylene, 25:4329
RADIATION STANDARDS AND UNITS
recommendation of FRC, ICRP, and NCRP for, 25:4532
RADIATION TARGET CHAMBERS
description of scattering, for high-resolution and angular correlation measurements, 25:5506 (CEA-N-1232, pp 81-159)
RADIATION TARGETS
cryostat for polarized proton, 25:5456 (LA-4465, pp 33.1-2)
development of polarized proton, of frozen porphyrexide-doped aqueous solutions of glycerol, 25:5463 (RHEL/R-159)
development of polarized proton, of frozen porphyrexide-doped aqueous solutions of glycerol, 25:5466 (RPP/A-81)
development of tritium, for fast neutron production, 25:5503(P)
properties of polarized proton, of ammonium aluminum nitrate and potassium aluminum nitrate, 25:5450 (LA-4465, pp 4.1-2)
reactivity worth of, effects on fast neutron flux in critical assemblies of, 25:6117
support films for, preparation of thin parylene, 25:4329
RADIATORS
design of neptunium-237 polarized neutron, 25:5451 (LA-4465, pp 8.1-2)
RADIO GALAXIES
blue objects associated with cD clusters of, detection of faint, (E), 25:4930
RADIO TELESCOPES
performance at 35 GHz of Algonquin, (E), 25:4918
RADIO WAVES
emission from extensive air showers, (E/T), 25:4987
propagation of vlf, effects of PCA events on, July 1966 to December 1968, (E), 25:5020
RADIOACTIVE CONTAMINATION
monitoring of surface, sampling device for, 25:4516(P)
RADIOACTIVE MATERIALS
handling of, fire protection criteria for facilities for, 25:4194
processing of underground nuclear explosion-produced, design and operation of small hot cell chemical plant for, 25:4308
RADIOACTIVE WASTE
analysis for plutonium, design of counting system for, 25:4292
analysis of solid, for plutonium, radiometric method for, 25:4293
book: Clarification and Deactivation of Waste Waters by Frothing Flotation, in Russian, 25:4141
diffusion and movement of calcium--strontium carbonate, in soils, method for simulation of, 25:4265 (ORNL-TM-3130)
disposal in seas around Japan, review of problems of, 25:4316
disposal of gaseous and liquid, in underground nuclear explosion-produced cavities, 25:4279
disposal of gaseous, liquid, and solid, review of methods for underground, 25:4315
disposal of high-level liquid and solid, design and cost estimate for Lyons, Kansas repository for, 25:4277
disposal of high-level solid, feasibility of using salt deposits for, 25:4264 (NP-18527)
disposal of solid, into eastern Atlantic Ocean, European Nuclear Energy Agency program for, 25:4268
disposal of, Japanese trends in, 25:4317
management in US, status of programs for, 25:4275
radiation monitoring of, at Research Reactor Institute of Kyoto University during 1968, 25:4508 (KURRI-TR-63)
separation of noble gas fission products from gaseous, methods for, 25:4260 (CEA-Bib-184)
shipping of calcined solid, design and safety of lead- and water-shielded containers for, 25:4278
solidification of high-level liquid, status of demonstration program for, 25:4276
RADIOACTIVITY
nuclear data tables on α, β, γ, x-ray, and Auger electron emission, 25:5716
RADIOBIOLOGY
research activities at UCLA from July 1969 to July 1970, 25:4425(R) (UCLA-12-782)
RADIOCHEMICAL PROCESSING PLANTS
californium-252 facility for TURF, design and operation of, 25:4304
design and operation of small hot cell, for processing radioactive debris from underground nuclear explosions, 25:4308
design of WAK-type, 25:4263 (KFK-1102)
development and research at Amersham, 25:4088(R) (NP-18528)
development for head-end reprocessing of oxide fuels at Windscale, 25:4146
fissionable material accounting in, remote weighing equipment for use in, 25:4296
handling equipment for TURF, design and operation of in-cell, 25:4303
health physics programs for, tabulation of, 25:4515
hot cell for NTRS Fuel Cycle Facility, equipment maintenance and performance after six years operation in, 25:4300
hot cells for NRTS Fuel Cycle Facility, decontamination methods for, 25:4259
nuclear materials management at Eurochemic, methods for, 25:4266
operation of Eurochemic, safety and radiation protection in, 25:4140
safeguard procedures for WAK-type, development of, 25:4263 (KFK-1102)
safety programs for, 25:4527
safety programs for plutonium, 25:4526
RADIOFREQUENCY SPECTROMETERS
circuit for reducing transmitter ringdown time in pulse NMR, self-switching damping, 25:4356
RADIOGRAPHY, BIOMEDICAL
conference on methods for measurements of bone minerals using measurement, 25:4612 (CONF-680211)
effectiveness, in combination with perfusion scanning, for diagnosis of lung diseases, 25:4675
image resolution for, by mathematical processing, 25:4611 (CEA-R-3920)
methods for estimation of weights of bones of human hands, 25:4641 (CONF-700515-, pp 224-36)
methods for measurement of bone density and mineral content using, 25:4618 (CONF-680211-, pp 159-77)
methods for measurement of bone mineral content, 25:4640 (CONF-700515-, pp 205-23)
methods for measurement of bone mineral content in patients with osteoporosis, 25:4639 (CONF-700515-, pp 199-204)
methods for measurement of bone mineral content in man using, comparison of, to results using radiometric analysis, 25:4622 (CONF-680211-, pp 216-49)
methods for measurement of bone mineral content using, in combination with high-speed densitometers and computer data analysis, 25:4620 (CONF-680211-, pp 151-203)
methods for measurement of bone mineral density mass, and thickness using, 25:4617 (CONF-680211-, pp 125-59)
methods for measurement of bone mineral mass using, with computer film analysis, 25:4614 (CONF-680211-, pp 60-95)
methods for measurement of mineral content of bones of human lumbar vertebrae using, in combination with analog computer data analysis, 25:4628 (CONF-680211-, pp 331-51)
methods for measurement of mineral content of bones using, 25:4616 (CONF-680211-, pp 115-38)
methods for measurement of mineral content of human bones, 25:4637 (CONF-700515-, pp 188-94)
methods for measurement of mineral content of human bones, 25:4638 (CONF-700515-, pp 195-8)
methods for measurement of weight and volumes of bones in human skeleton using, 25:4652 (CONF-700515-, pp 365-82)
methods for measurements of bone density and mineral content using, 25:4619 (CONF-680211-, pp 177-91)
methods for measurements of bone mass using, with automatic computer film calibration, 25:4613 (CONF-680211-, pp 27-80)
methods for measurements of mineral content of human normal and osteoporotic bones using, in combination with dye precipitation, 25:4629 (CONF-680211-, pp 411-21)
methods for measuring mineral content of human bones using, 25:4615 (CONF-680211-, pp 95-115)

XUM

methods for small intestine in man using double contrast technique, x, 25:4686
RADIOGRAPHY, INDUSTRIAL
detectors for neutron, image enhancement in thin-film cellulose nitrate track, 25:4346
detectors for neutron, sparking techniques for image enhancement in thin-film dielectric track, 25:4348
equipment and method for post-irradiation testing of SNAP-8 fuel elements, 25:4252
equipment and method for three-dimensional x-ray holography, 25:4404
equipment for neutron, for detecting defects in steel-reinforced concrete, design and performance of, 25:4249
image recording process in neutron, analytical model for, 25:4251
method for high-resolution neutron, of mixed-oxide fuel elements, 25:4254
method for inspecting beryllium--curium-244 neutron sources, 25:4253
neutron source for, evaluation of californium-252, 25:4218
RADIOIMMUNOASSAY
methods for antigens in blood serum, 25:4417
RADIOISOTOPE SCANNERS
data handling system for pulmonary function studies, 25:4328
data processing systems for image enhancement in, matched and optimum filters for, 25:4359
data processing systems for, development of computer-based, 25:4336
design, operation, and performance of, 25:4325
development of, 25:4337
performance for perfusion-ventilation studies in human lungs using xenon-133, 25:4668
performance of, 25:4326
use of rectilinear, with xenon-133 for measuring human lung perfusion and ventilation, 25:4665
RADIOISOTOPE SCANNING
book: Pulmonary Investigation with Radionuclides, 25:4662
effectiveness for diagnosis of lung disorders following embolism, effects of perfusion-ventilation relations on, 25:4679
effectiveness for diagnosis of pulmonary embolism, 25:4680
effectiveness of multiple images for, of human lungs, 25:4670
effectiveness, in combination with radiography, for diagnosis of lung diseases, 25:4675
evaluation of variables affecting scan image, use of three-dimensional phantoms for, 25:4657 (UCLA-12-782, pp 89-125)
evaluation of xenon-133, for measuring distribution of blood flow in human lungs, 25:4672
image resolution in, by mathematical processing, 25:4611 (CEA-R-3920)
methods using radioisotope-labeled aerosols for inhalation, of lungs, review of equipment and procedures for, 25:4678
preparation of new radioisotope-labeled drugs for use during, 25:4415
radiation dose to man during, of lung, methods for calculation using MIRD equations, 25:4511
research activities at UCLA from July 1969 to July 1970, 25:4425(R) (UCLA-12-782)
RADIOISOTOPES
determination following paper chromatography or paper electrophoresis by elution, electrodeposition, and counting, 25:4030
determination in mixtures in biological materials, spectrometric method for, 25:4031
distribution in fallout from Project Schooner, 25:4180
ion mobility of, time-of-flight measurement of, 25:4395
metabolism in bone, effects of circulation, diuretics, oxygen, parathormone, and vitamin D on, 25:4423 (COO-1601-23)
monitoring in sodium reactor coolants, for detection of fuel element failure, 25:4736(R) (ANL/ST-3)
production cross sections for, in heavy-ion induced fission, 25:5756
production in COMECON states, review on, 25:4128
production in cyclotrons for nuclear medicine, 25:4683
separation from gas streams by selective filtration and fixation, 25:4145(P)
separation from waste waters by frothing flotation, 25:4141
shipping and storage of pharmaceutical, design of shielded container for, 25:4267(P)
shipping of high-specific activity neutron-emitting, design of water-cooled shielded container for, 25:4311
sorption by aquatic and marine animals, fallout, 25:4479
testing of advanced fuels of, methods for ablation and impact, 25:4216(R) (SC-PR-70-682)
use of a emitting, for attitude control system of solar probe space vehicle, 25:4222
uses in agriculture, 25:4732(R) (NYO-2043-216)
RADIOMETRIC ANALYSIS
book: Current Status of Liquid Scintillation Counting, 25:4358
methods for measurement of mineral content of human bones, comparison of results of, to radiographic methods, 25:4622 (CONF-680211-, pp 216-49)
RADIOMIMETIC SUBSTANCES
mutagenic effects of cycasin on beans for chlorophyll and morphology, 25:4717 (NYO-2043-216, pp 1-18)
RADIOPROTECTIVE COMPOUNDS
book: Radiation Protection and Sensitization, 25:4534
effects on cellular radiosensitivity, mechanisms of sulfur-containing, 25:4538
effects on organisms, review of efficiency of combinations of, review of, 25:4605
molecular structure of aminothiols and disulfides, relation of, to protective effects against ionizing radiations, 25:4548
RADIOSENSITIVITY
mechanisms of cellular and molecular, ionizing, 25:4535
RADIOSENSITIZERS
book: Radiation Protection and Sensitization, 25:4534
RADIOTHERAPY
book: Radiation Protection and Sensitization, 25:4534
neutron source for, evaluation of californium-252, 25:4218
planning for high-energy, programs for, 25:4514
RADIUM ISOTOPES Ra-226
content in rivers in uranium mining areas of Czechoslovakia during 1964 to 1967, 25:4157
content of lakes, Ottawa River, plankton, and well water in Chalk River area during 1969, 25:4473 (AECL-3687)
metabolism in man, 25:4424(R) (TID-25567)
placental transfer of decay products of, hazards to fetuses from, 25:4673
RANCHO SECO POWER REACTOR
waste processing at, system for radioactive liquid, 25:5882
RARE EARTH ALLOYS AND SYSTEMS
exchange interactions of, review, 25:5232
lattice distortions in compounds, (E), 25:4803
Ag--rare earth, antiferromagnetic ordering in RAg compounds, (T), 25:5197
Cu--rare earth, antiferromagnetic ordering in RCu compounds, (T), 25:5197
rare earths--transition metals, magnetic properties of R_2M intermetallic compounds, 25:5199
RARE EARTH HYDROXIDES
magnetic properties of, 25:5202
RARE EARTH ISOTOPES
nuclear deformation parameters and quadrupole and hexadecapole moments for, (T), 25:5860
RARE EARTH OXIDES
magnetic structure of cubic, representation analysis, 25:5215
radiation effects on catalytic properties of, in decomposition of hydrogen peroxides, 25:4059
RARE EARTHS
complexes with maleic acid, preparation and thermal behavior of, 25:4075
compounds of, lattice distortions in, (E), 25:4803
conference on, Paris and Grenoble, France, 5/69, Vol. II, 25:5193
determination of trace amounts of, in uranium by chemical separation and spectroscopy, 25:4021
effects on automatic colorimetric determination of thorium in aqueous and organic solutions, 25:4014 (NLCO-1072)
effects on photochemical precipitation of cerium, 25:4026
exchange interactions of, review, 25:5232
magnetic ordering of, (E/T), 25:5205
paramagnetic anisotropy of single crystals of, (T), 25:5206
separation and purification by anion exchange using nitric acid--methanol system, 25:4139
separation from iron and uranium by ion exchange in thiocyanate solutions using Amberlyst A-21, 25:4137 (IS-T-377)
separation from scandium by ion exchange in thiocyanate solutions using Amberlyst A-21, 25:4137 (IS-T-377)
separation from thorium in bismuth solution by fractional crystallization, 25:4138 (ORNL-TM-3053)
separation of thorium from, by photochemical precipitation, 25:4026
thermal capacity of, 25:4760
valence change with pressure or temperature, theoretical model of anomalous, 25:5233
RARE GASES
hydrogen-atom elastic scattering by, calculation of interaction potentials from, 25:4957
separation from fission gases, methods for, 25:4260 (CEA-Bib-184)
RATS
calcium-45 sorption in intestinal tract of, effects of calcium ion content on, 25:4430
carbon-14 uptake by cerebral glycogen in brain of, x, 25:4453
cesium-134 retention in, effects of propythiouracil and L-thyroxine on, 25:4450
distribution of thorium dioxide in tissues of, 25:4442
effects of salt stress on carcinogenesis in, 25:4459 (UCLA-12-782, pp 23-47)
indium-113 distribution in tissues of, effects of particle size and pH on, 25:4437
oxygen uptake and respiration in tissues of, effects of

XUM

cysteamine, cysteamine, and cysteine on, 25:4595
plutonium-239 retention in bone and lung tissues of kangaroo, fallout, 25:4478
radiation effects on amino acid content and enzyme activity in developing brain of, x, 25:4457(R) (UCB-34-P-82-9)
radiation effects on arterial pressure in, following intratracheal and intraperitoneal injection of thorium dioxide, α, 25:4701
radiation effects on blood cell cytology, blood circulation, bone marrow cytology, and blood transferase activity in, protective effects of AET against x, 25:4599
radiation effects on elimination of 17-ketosteroids in, comparison of orchiectomy and, 25:4707
radiation effects on hematopoiesis in, following intratracheal injection of thorium dioxide, 25:4700
radiation effects on lactic dehydrogenase and lactic dehydrogenase isoenzymes in, protective effects of methylene blue against whole-body γ, 25:4605
radiation effects on phospholipase B activity in intestine of, in relation to number of eosinophils, x, 25:4455(R) (ORO-3329-7)
radiation effects on protein content of developing brain of, effects of age and hypophysectomy on x, 25:4694 (UCLA-12-791)
radiation effects on sorption of lipids by cells of duodenal epithelium of, cerium-144 β and γ, 25:4695
radiation effects on stimulation threshold of muscle-nerve apparatus in hind paws of, following intratracheal and intraperitoneal injection of thorium dioxide, α, 25:4701
radiation effects on survival of, protective effects of AET, cystamine, mexamine, and serotonin against γ, 25:4581
radiation effects on survival of, protective effects of selenium compounds against ionizing, 25:4545
radiation effects on uridine incorporation into RNA of nerve tissue of, carbon-14 tracer study of x, 25:4457(R) (UCB-34-P-82-9)
radioinduced aberrations of chromosomes in bone marrow of, protective effects of serotonin against x, 25:4585
radioinduced lesions in kidneys, liver, and lungs of, following single intratracheal administration of thorium dioxide, 25:4702
radioinduced leukemia in, protective effects of selenium compounds against ionizing, 25:4545
radioinduced malformations of embryos of, combined effects of iodoacetamide on x, 25:4575
radioisotope distribution in liver of, effects of p-dichlorophenol on calcium-45 and strontium-89, 25:4431
radioisotope sorption by intestine of, from vascular space, calcium-47 and strontium-85, 25:4424(R) (TID-25567)
retention of thorium dioxide in lungs of, 25:4442
strontium-85 metabolism in bones of, effects of diuretics and parathormone on, 25:4423 (COO-1601-23)
synthesis of adenosine triphosphate in mitochondria and nuclei in liver and thymus of, effects of cysteamine on, 25:4597
synthesis of DNA and RNA in thymus gland of, effects of radioprotective and radiosensitizing drugs on, reaction mechanisms for AET, cysteamine, 2-mercaptoethanol, and penicillamine, 25:4592
synthesis of DNA in spleen and thymus of, effects of AET and cysteamine on, 25:4596
synthesis of fatty acids in liver of, following treatment with carbon chlorides or ethionine, protective effects of cysteine against, 25:4600
thorium metabolism in tissues of, following intraperitoneal, intramuscular, and oral administration, 25:4441
uptake of carbon and thorium by lungs of, electromicroscopic study of, 25:4410

REACTIVITY
Doppler measurements in critical assemblies, (E), 25:6110
Doppler measurements in fast critical assemblies, (E), 25:6111
Doppler measurements in high temperature cavity core gas fueled reactors, 25:5957
Doppler measurements in plutonium fueled critical assemblies, (E), 25:6109
measurement of reactor, noise technique for, 25:6174
perturbation denominator for fast critical assemblies, (E/T), 25:6116
worth measurements for reactor materials, errors in calculation of, (T), 25:6168
worth measurements on small samples, integral transport theory analysis of, (E/T), 25:6127

REACTOR CONTAINMENT STRUCTURES
coatings for, effects of steam, high temperature, and spray solutions on, (E), 25:6034 (ORNL-TM-2412(Pt.5))
leakage tests on, review of criteria for, 25:5938
reliability analysis of, 25:6190 (RISO-214, pp 71-90)
reliability analysis of double shell, 25:6190 (RISO-214, pp 71-90)

REACTOR CONTAINMENT SYSTEMS
contamination control of sodium fires in liquid metal cooled, design requirements for, 25:6049
spray solutions for boiling water, post accident radiolytic gas production and concentration from, (E), 25:6035 (ORNL-TM-2412(Pt.8))

REACTOR CONTROL ELEMENTS
neutron diffusion in movable, improved spatial differencing for, (T), 25:6177
reactivity worth of tantalum, in fast neutron spectra, (E/T), 25:5964

REACTOR CONTROL SYSTEMS
development of computer, international program for, 25:5974

REACTOR FUEL ELEMENTS
analysis for plutonium dioxide, development of instrumentation and materials balance methods for, 25:4297
analysis of LMFBR, dual spectrum method for, 25:4254
assemblies of rod-type, effects of asymmetry on fluid flow and heat transfer in, 25:4206
burnup of, calculations for optimum control of, (T), 25:6172
cladding for LMFBR, mechanical properties of Type 316 stainless steel, 25:4776
cladding for LMFBR, properties of thermomechanically treated Type 348 stainless steel, 25:4775
cladding of liquid sodium cooled, effects of cold wrapper tube technique on swelling of steel, 25:6022
cladding swelling of liquid sodium cooled, effects on core performance of, 25:6021
cycle management during startup of fast breeders, in-core, (T), 25:6054
design of clad carbide rod-type, for in-pile operation at 45 kW/ft, 25:4889(R) (UNC-5263)
design parameters of gas cooled fast, (T), 25:5958
development of spherical, for German pebble bed reactors, 25:6006
dimensional changes of Zircaloy-4 clad thorium oxide (ThO_2)--uranium oxide (UO_2), in-pile progressive, (E), 25:6197
end fittings for, development of control rod guide tube transition joints for, 25:6196
energy loss from viscous damping of pulse, (T), 25:6123
fabrication graphite clad coated particle, for high temperature gas cooled reactors, 25:6005
fabrication of coated particle, 25:5990(R) (ORNL-4585)
fabrication or reprocessing of, stochastic model for estimating efficiency of safeguards operations in, 25:4273
failure detection of liquid metal cooled ceramic, xenon tagging techniques for, 25:6026
failure detection of liquid metal cooled ceramic, xenon tagging techniques for, 25:6025
failure limits for liquid sodium cooled mixed oxide pin type, 25:6096
failure of liquid metal cooled mixed oxide, effects of power transient fission gas pressure on, 25:6098
failure of pin type, effects on coolant flow and fuel assembly deformation of, 25:6017
failure of, development of method for detection of operational, 25:4736(R) (ANL/ST-3)
failure thresholds and mechanisms for liquid sodium cooled fast, (E), 25:6018
fission gas bubbles and inclusions in mixed oxide, diffusion of, (E), 25:6014
fission gas distribution in mixed oxide, SHELL 2 code for, 25:6013
fission gas release from HTGR type, (E), 25:6009
fission gas release from HTGR type, (E), 25:6010
fission gas release from mixed oxide gas cooled, (E), 25:6015
fission gas transport across graphite barrier in HTGR type, effects of transverse flow on, (E/T), 25:6011
fission product release from high burnup coated particle, 25:5990(R) (ORNL-4589)
fission product release from uranium oxide (UC_2) coated particle, 25:5990(R) (ORNL-4585)
heat transfer characteristics of uranium oxide (UO_2), 25:6060
heat transfer characteristics of water cooled rod type, effects of grid and wire wrap spacers on, (E), 25:6028
heat transfer in internally gas cooled annular, 25:5979 (DP-Report-435)
hydrodynamics of collapsing fluid slabs, graphic display methods for, 25:6199
inspection of irradiated liquid metal cooled, design parameters of profilometer for, 25:6033
inspection of mixed-oxide, high-resolution neutron radiographic method for, 25:4254
meltdown of liquid metal cooled metal and oxide, energy release calculations for, 25:6082
meltdown of liquid sodium cooled uranium oxide (UO_2) pin type, 25:6097
neutron resonance integrals for thorium oxide (ThO_2) rod, (E/T), 25:6205
performance of carbide, in TREAT, 25:4885(R) (UNC-5263)
performance of EBR-II experimental, determination by examination in hot cells, 25:4301
performance of fast, computer program for in-core, 25:6032
performance of fast, effects of niobium and molybdenum on, (T), 25:6055
performance of liquid sodium cooled mixed oxide pin type, effects of power transients on, 25:6016
performance of mixed oxide fast, effects of fuel-clad gap

XUM

thermal conductivity on, (E), 25:5999
physics measurements of liquid sodium cooled mixed oxide, 25:6031
pressure drop in internally gas cooled annular, 25:5979 (DP-Report-435)
pressure equalization system for gas cooled fast breeder, 25:6019
radiation effects on fission gas release and swelling of unrestrained carbide, in-pile, 25:4889(R) (UNC-5263)
radiation effects on rod-type carbide, at 70 to 35 kW/ft, in-pile, 25:4889(R) (UNC-5263)
radiation effects on thorium oxide (ThO_2)--uranium oxide (UO_2) coated particle, fast neutron, 25:5990(R) (ORNL-4589)
radiation effects on Type 316 stainless steel clad plutonium oxide (PuO_2)--uranium oxide (UO_2) and uranium oxide (UO_2), fast neutron, 25:5990(R) (ORNL-4589)
radiation effects testing of molybdenum clad uranium oxide (UO_2), 25:6198
radiation testing of stainless steel clad mixed oxide, program for high temperature fast flux, 25:5989 (GA-10264)
reprocessing of HTGR, jaw crusher for head-end, 25:4136 (GAMD-9260(Pt.2))
reprocessing of stainless steel- and zirconium-clad oxide, head-end facility at Windscale for, 25:4146
simulators for liquid sodium cooled, design parameters and performance of cartridge type electrical heater, 25:6029
storage of irradiated, in water, methods for determining safe spacing for, 25:4285
swelling of mixed oxide fast, (E/T), 25:6001
swelling of mixed oxide fast, effects of fuel-clad interaction at startup on, (E/T), 25:6002
swelling of mixed oxide fast, model for initial thermal, (E/T), 25:6000
temperature measuring devices for liquid metal cooled mixed oxide pin type, performance of, (E/T), 25:6027
testing of SNAP-8, neutron radiographic equipment and method for post-irradiation, 25:4252
testing of, application of neutron transient characteristics in heavy moderators for nondestructive, 25:6204
thermal conductivity of annular, method for estimating, 25:4203 (DP-Report-578)
thermal hydraulic testing of hydrogen cooled, (E/T), 25:6141
thermal limits for gas cooled fast breeder, effects on power production economics, 25:5902
vibration of liquid sodium cooled cylinder shaped tube, analysis of parallel flow induced, (T), 25:6030

REACTOR FUELS
analysis and inspection of irradiated, design of JAERI hot cell for use in, 25:4298
analysis of spherical, at 40 atm helium, spectroscopic, 25:4013 (JUL-671-RW)
coating on particulate, structure of pyrocarbon and silicon carbide, 25:4863 (DP-Report-574)
compatibility with Type 304 stainless steel at 650 to 830°C, carbon-14 tracer studies of, 25:4739 (JAERI-Memo-4132)
cycle for fast breeder, accuracy of space collapse techniques for multigroup calculations of, (T), 25:5965
cycle management for gas cooled, statistical analysis of optimum economic, 25:6024
cycle management for power, analysis of optimum economic, 25:5897
cycle management for power, calculation of optimum economic, 25:5898
cycles for gas cooled and water cooled reactors, economic effects of uranium-233 and plutonium recycle on, (T), 25:6056
cycles for gas cooled reactors, effects of uranium-233 recycle on, (T), 25:6057
cycles for high temperature gas cooled systems, economics of high conversion thorium, (T), 25:6051 (DP-Report-434)
cycles in Western Europe, effects of power reactor strategies on, 25:6053
development of coated particle gas cooled, 25:6007
economics of, effects of power reactor types and applications on, 25:5878(T) (UCRL-Trans-10495)
fission gas release from coated particle, effects of temperature on, (E), 25:5997
heavy element content of, method of calculating fission-induced, 25:4815 (RD/B/N-1722)
inspection of irradiated, development of stereomacroscopic equipment for in-hot cell, 25:4309
meltdown of, fragmentation mechanism during, (T), 25:6083
microstructure of mixed oxide, effects of thermal neutron flux on, (E), 25:5993
performance in water cooled systems, performance test code for, 25:5991
plutonium content of spent, determinaton by uranium-235 depletion, 25:4257 (BNWL-SA-3304)
processing of, soil studies and foundation design for West Valley Processing Plant for, 25:4153 (DOCKET-50201-51)
properties of, relations with microstructure and porosity, 25:4841(R) (SRO-552-5)
radiation effects on plutonium and fission product migration in mixed oxide in-pile, (E), 25:6012
radiation effects testing of coated particle gas cooled, 25:6003
radiation effects testing of coated particle gas cooled, 25:6004
radiation effects testing of coated, particle gas cooled, 25:6008
reprocessing in TURF hot cells, design and operation of remote handling equipment for, 25:4303
reprocessing irradiated, Eurochemic experience in, 25:4148
reprocessing of BISO and TRISO, 25:4136 (GAMD-9260(Pt.2))
reprocessing of HTGR, grind-burn-leach processes in, 25:4136 (GAMD-9260(Pt.2))
reprocessing of MSBR, semicontinuous engineering experiments on reductive extraction for, 25:4138 (ORNL-TM-3053)
reprocessing of oxide, economics of, 25:4134(T) (AEC-tr-7198)
reprocessing of spent uranium, by nitride precipitation, 25:4149
reprocessing of, recovery of neptunium, plutonium, and uranium in, 25:4144(P)
safeguards methods for, use of burnup data in, 25:4274
supply for Euratom power plants, status of, 25:5880
testing of clad carbide, incorporating voids for accommodation of swelling, 25:4889(R) (UNC-5263)
testing of Dragon, equipment and methods for post-irradiation, 25:4262 (DP-Report-446)
testing of, application of neutron transient characteristics in heavy moderators for nondestructive, 25:6204
thermal conductivity of oxide, effects of porosity on, 25:4858
thermal performance and restructuring of pellet and sphere-pac mixed oxide, in-pile, (E/T), 25:5992
transfer of radioactive samples of ceramic, between ANL facilities, design and operation of pneumatic system for, 25:4306
transient testing of discrete plutonium oxide (PuO_2) particles in mixed oxide pellets, 25:5994
transient testing of discrete plutonium oxide (PuO_2) particles in mixed oxide, 25:5995
transient testing of mixed oxide, 25:5996

REACTOR LOADING MACHINES
reliability analysis of 300 MW(e) pebble bed, 25:6035 (RISO-214, pp 213-46)

REACTOR MODERATORS
neutron flux in strong anisotropic, measurement of thermal, (E/T), 25:6184
neutron leakage flux for hydrogenous, measurement of cold, (E/T), 25:6203
neutron spectra emerging from fast pulsed, time-focused crystal spectrometer technique for measurement of, 25:6186

REACTOR SAFETY
accident analysis for assessment of damage to liquid sodium cooled fast reactor pressure vessel, 25:6064
accidents in fast reactors, calculations for energy release of, (T), 25:6065
accidents in fast reactors, calculations of energy release of implosion, (T), 25:6066
accidents in liquid sodium cooled fast reactors, acoustic and inertial constraints for molten fuel and liquid sodium interaction, 25:6099
accidents in LMFBR single fuel element subassembly, 25:6068
accidents in LMFBR, analysis of coolant flow induced, 25:6070
accidents in LMFBR, analysis of energy release for, 25:6089
accidents in LMFBR, analysis of sodium voiding during, 25:6072
accidents in LMFBR, effects of fuel chilling on Doppler feedback control of, 25:6069
accidents in LMFBR, energy release for molten fuel and liquid sodium interaction, 25:6075
accidents in LMFBR, energy release for molten uranium oxide (UO_2) and liquid sodium interaction, (E), 25:6076
accidents in LMFBR, liquid sodium critical point uncertainty for molten fuel and liquid sodium interaction, 25:6074
accidents in LMFBR, quasi three dimensional analysis of liquid sodium voiding patterns during, 25:6071
accidents in LMFBR, single bubble model calculations for liquid sodium voiding during, 25:6073
accidents in pressurized water power reactors, energy release for rod ejection, 25:6081
accidents in water cooled and liquid metal cooled reactors, analysis of acoustic wave propagation in two phase media during, 25:6079
accidents in water cooled reactors and LMFBR, comparison of core, 25:6077
AEC program on fast, 25:6087
blowdown in pressurized water reactors, WHAM code evaluation of subcooled, (E/T), 25:6061 (IN-1431)
coolant ejection in LMFBR, analysis of liquid film thickness for slug type, (E), 25:6067

XUM

coolant loss accident conditions in water cooled reactors, heat transfer characteristics for 1.4 MW reverse flow, (E/T), 25:6115
coolant loss accident in pressurized water reactors, coolant flow distribution during, 25:6084
coolant loss accidents in boiling water reactors, radiolytic gas production and concentration following, (E), 25:6035 (ORNL-TM-2412(Pt.8))
coolant loss accidents in water cooled reactors, emergency core cooling system thermodynamics during, 25:6085
core components of LMFBR, effects of accidents on shock pulse loading of, 25:6078
core melting in LMFBR, protection systems for, 25:6088
failure limits for liquid sodium cooled mixed oxide pin type fuel elements, 25:6096
failure of liquid sodium cooled mixed oxide fuel elements, effects of power transient fission gas pressure on, 25:6098
fuel element failure in fast reactors, effects on coolant flow and fuel assembly deformation of pin type, 25:6017
fuel element meltdown in liquid metal cooled reactors, energy release calculations for metal and oxide, 25:6082
fuel meltdown, fragmentation mechanism during, (T), 25:6083
meltdown of liquid sodium cooled uranium oxide (UO_2) pin type fuel elements, 25:6097
operation of pulse research reactors, safety limits for, 25:6121
performance of liquid sodium cooled mixed oxide pin type fuel elements, effects of power transients on, 25:6016
quality assurance criteria for power reactors, 25:6091
reliability analysis of reactors, ELRAFT computer program for fault tree, 25:6090
reliability of components and systems of reactors, conference on, 25:6062 (RISO-214)
sodium void effects on reactivity in fast critical assemblies, 25:6112
thermodynamics for LMFBR liquid sodium coolant and molten fuel interaction, 25:6092

REACTOR SAFETY EXPERIMENTS
design parameters of LOFT, 25:6104
fuel elements in TREAT, effects of power transient fission gas pressure on failure of mixed oxide, 25:6098
fuel elements in TREAT, effects of power transients on performance of liquid sodium cooled mixed oxide pin type, 25:6016
fuel elements in TREAT, failure limits for mixed oxide pin type, 25:6096
fuel elements in TREAT, meltdown of uranium oxide (UO_2) pin type, 25:6097
transient testing of mixed oxide fuels in SPERT, 25:5996

REACTOR SIMULATORS
operation of personnel training, for 600 MW and 800 MW reactors, 25:6208
operation of personnel training, for boiling reactors, 25:6209
operation of personnel training, for power reactor operator license examinations, 25:6212
operation of personnel training, for pressurized water reactors, 25:6210
use of remote computer, for nuclear engineering instruction, 25:6193

REACTORS
control of, nonlinear programming for optimum, (T), 25:6152
criticality of, two group neutron transport equations for, (T), 25:6157
development and research at UKAEA, 25:4088(R) (NP-18528)
dynamics equations for, asymptotic behavior of nonlinear Volterra integral, (T), 25:6180
dynamics of, hybrid computer program analysis of spatial, (T), 25:6179
excursions in, analysis of feedback induced spatial effects during, (T), 25:6161
frequency response of coupled-core, effects of localized oscillation of neutron absorber on spatially dependent, (T), 25:6148
frequency response tests for, comparison of signals for nonlinear effects during, 25:5967
frequency response tests for, optimum discrete level signals for, 25:5968
instrumentation for, performance of wide range linear channel for neutron flux detection, 25:6207
instrumentation for, reliability analysis of mechanical, 25:6189 (RISO-214, pp 11-20)
kinetics of coupled core and zoned core, errors in few group diffusion theory calculations for, (E/T), 25:6162
kinetics of coupled core, (E/T), 25:6185
kinetics of thermionic, multivariable feedback synthesis with cross-coupling for, (T), 25:6163
kinetics of, analysis of point, (T), 25:6150
kinetics of, coarse mesh acceleration of S/sub N/ interactions for, (T), 25:6154
kinetics of, comparison theorem for bounds of nonlinear parabolic equations for negative temperature feedback, (T), 25:6147
kinetics of, comparison theorems for stability domains and solution estimates for point, (T), 25:6153
kinetics of, degenerate thermalization kernel for calculations of, (T), 25:6166
kinetics of, P_3 approximation equations for, (T), 25:6155
kinetics of, spherical harmonics solution of two group linear transport equation for, (T), 25:6156
materials for, radiation effects on properties of metallic, 25:4812 (BNWL-SA-3495)
neutron detector response for, two stage Monte Carlo calculations for delayed, (T), 25:6151
neutron diffusion equations for two-group reflected slab, Green's function formulation of Laplace-transformed multigroup, (T), 25:6176
neutron diffusion in, simplified eigenvalue problem solutions for, 25:6173
neutron flux detectors for, optimum wire diameter for, 25:6206
physics calculations for, computer system for automatic, 25:6149
pressure tubes of, reliability analysis of zirconium, 25:6191 (RISO-214, pp 255-87)
protection systems of, development of integrated, 25:6045
reactivity of, noise technique for measurement of, 25:6174
reliability analysis of, ELRAFT computer program for fault tree, 25:6090
servosystems for, noise reduction in closed loop, (T), 25:6188 (AE-404)
stability analysis of, Mikhailov criteria with time delay for, (T), 25:6164

REACTORS, BERYLLIUM-MODERATED
design concept for rocket, 25:6136

REACTORS, BOILING
containment spray solutions for, post accident radiolytic gas production and concentration from, (E), 25:6035 (ORNL-TM-2412(Pt.8))
containment structures for, design modifications of, 25:5885
cooling system for, design modifications of, 25:5885
power conversion system for, design modifications of, 25:5885
radioactive effluents from power, release rates for, 25:6080
shutdown systems for, availability and reliability analysis of, 25:6036 (RISO-214, pp 41-85)
simulator for, operation of personnel training, 25:6209
steam line isolation valves for, reliability analysis of, 25:6040 (RISO-214, pp 247-53)

REACTORS, BREEDER
core of gas cooled fast power, design modifications for radiation induced swelling of, 25:6020
economics of gas cooled fast power, effects of fuel element thermal limits on, 25:5902
fuel cycle for fast, accuracy of space collapse techniques for multigroup calculations of, (T), 25:5965
fuel element management during startup of, in-core, (T), 25:6054
fuel elements for gas cooled fast, irradiation testing of, 25:5990(R) (ORNL-4589)
fuel elements of gas cooled fast power, pressure equalization system for, 25:6015
materials for, properties of stainless steel and steel, 25:4770
physics calculations for conceptual gas fueled fast power, 25:5971
radiation detectors for fast power, design parameters of in-core activation, 25:6044

REACTORS, CANADA
protection systems for power, reliability analysis of, 25:5936 (RISO-214, pp 127-69)
safety standards for power, 25:5936 (RISO-214, pp 127-69)

REACTORS, FAST
accidents in, calculations for energy release of, (T), 25:6065
accidents in, calculations of energy release of implosion, (T), 25:6066
core of gas cooled breeder power, design modifications for radiation induced swelling of, 25:6020
core of liquid sodium cooled, review of AEC programs on safety aspects of, 25:6087
core of liquid sodium cooled, safety aspects of, 25:6086
dynamics of, neutron spectral synthesis equations for, (T), 25:6178
economics of gas cooled breeder power, effects of fuel element thermal limits on, 25:5902
fuel cycle for breeder, accuracy of space collapse techniques for multigroup calculations of, (T), 25:5965
fuel element management during startup of, in-core, (T), 25:6054
fuel element of, effects on coolant flow and fuel assembly deformation of failed pin type, 25:6017
fuel elements for gas cooled breeder, irradiation testing of, 25:5990(R) (ORNL-4589)
fuel elements for gas cooled, design parameters of, (T), 25:5998
fuel elements for, effects of fuel-clad gap thermal

conductivity on performance of, (E), 25:5999
fuel elements for, effects of fuel-clad interaction at startup on, (E/T), 25:6002
fuel elements for, first startup thermal swelling of mixed oxide, (E/T), 25:6000
fuel elements for, swelling of mixed oxide, (E/T), 25:6001
fuel elements of gas cooled breeder power, pressure equalization system for, 25:6019
fuel elements of liquid metal cooled, failure thresholds and mechanisms for, (E), 25:6018
fuel elements of, LIFE-1 computer program for in-core performance of, 25:6032
fuel elements of, xenon tagging techniques for failure detection of, 25:6025
gamma radiation energy deposition in, distribution of, 25:5970
kinetics of, analysis of discrete ordinate ray effects on, (T), 25:6159
kinetics of, multiple reaction rate weighting for space-energy synthesis of, (T), 25:5966
kinetics of, successive space-energy synthesis method for, (T), 25:5962
materials for, properties of stainless steel and steel, 25:4770
neutron flux and importance spectra of, analytic model for, (T), 25:5954
neutron flux spectra of, performance of fission foils for, 25:5973
neutron moderation in, (T), 25:6165
neutron resonance absorption in, integral transport theory analysis of, 25:5959
neutron spectra in, multigroup synthesis methods for, (T), 25:5961
neutron spectra of, continuous slowing down models for, (T), 25:5955
operation potential of subcritical, as university research facility, 25:6055
physics calculations for conceptual gas fueled breeder power, 25:5971
pressure vessel of liquid sodium cooled, damage assessment method for effects of accidents on, 25:6064
radiation detectors for breeder power, design parameters of in-core activation, 25:6044
radiation streaming in liquid sodium cooled, design requirements for γ and neutron, 25:5976
safety of, UCLA curriculum on, 25:6063

REACTORS, GAS-COOLED
core components in high temperature, gasification reaction rates of graphite, (T), 25:5985
core of fast breeder power, design modifications for radiation induced swelling of, 25:6020
design characteristics of high temperature power, 25:5884
development during October 1969 to March 1970, 25:5990(R) (ORNL-4589)
development of high temperature, status of German program for, 25:5944
economics of fast breeder power, effects of fuel element thermal limits on, 25:5902
fuel cycle for high temperature, statistical analysis of optimum economic, 25:6024
fuel cycles for high temperature, economics of high conversion thorium, (T), 25:6051 (DP-Report-434)
fuel cycles for off-load refueled, HELTOT program system for thorium--uranium-235, 25:6052 (DP-Report-440)
fuel cycles for, effects of uranium-233 recycle on, (T), 25:6057
fuel cycles for, effects of uranium-233 recycle on, (T), 25:6056
fuel elements for fast, design parameters of, (T), 25:5998
fuel elements for high temperature, development and irradiation testing of, 25:5990(R) (ORNL-4589)
fuel elements for high temperature, effects of transverse flow on fission gas transport through, (E/T), 25:6011
fuel elements for high temperature, fabrication of, 25:6005
fuel elements for high temperature, fission gas release from, (E), 25:6009
fuel elements for high temperature, fission gas release from, (E), 25:6010
fuel elements for high temperature, heat transfer and pressure drop in internally cooled annular, (T), 25:5979 (DP-Report-435)
fuel elements of fast breeder power, pressure equalization system for, 25:6019
fuels for high temperature, irradiation testing of coated particle, 25:6008
fuels for high temperature, irradiation testing of coated particle, 25:5990(R) (ORNL-4589)
fuels for, design and irradiation performance of coated particle, 25:6003
fuels for, irradiation performance of coated particle, (E), 25:6004
fuels for, preparation and properties of coated particle, 25:6007
materials for high-temperature, review of properties of heat-resisting, 25:4779
pressure vessels for, development of prestressed concrete, 25:5990(R) (ORNL-4589)
steam generators for high temperature, corrosion resistance of nickel alloy welds in, 25:5990(R) (ORNL-4589)

REACTORS, GAS-FUELED
design concept for gas core, with MHD power plant, 25:6137
Doppler reactivity for high temperature cavity core, 25:5957
kinetics of, analysis of hydrodynamic and neutronic, (T), 25:6175
physics calculations for conceptual fast breeder power, 25:5971
physics parameters of spherical gas core, (E), 25:6133
propellant for gas core, radiant heat transfer in refractory aerosol containing, (T), 25:6135
propellant for gas core, thermal radiation transmission through refractory aerosol containing, (T), 25:6134

REACTORS, GRAPHITE-MODERATED
neutron resonance absorption in heterogeneous, interference effects of thorium-232 and protactinium-233, 25:5958

REACTORS, GREAT BRITAIN
medical requirements for personnel at AERE, Harwell, assessment of, 25:4529 (AERE-R-6523)

REACTORS, HEAVY WATER-MODERATED
physics parameters of cluster lattices in, WIMS code analysis of, (E/T), 25:6181 (AEEW-R-549)
pressure tubes for organic cooled, reliability analysis of SAP, 25:5984 (RISO-214, pp 335-43)
shutdown system for pressure tube, reliability analysis of liquid rod, 25:6037 (RISO-214, pp 57-70)

REACTORS, HETEROGENEOUS
kinetics of, collision probability method for anisotropic scattering, (T), 25:6156

REACTORS, HOMOGENEOUS
neutron resonance absorption in graphite moderated, interference effects of thorium-232 and protactinium-233, 25:5958

REACTORS, JAPAN
design requirements of power, analysis of earthquake resisting, 25:5939
development of power, status of, 25:5945
reliability analysis of power, 25:5937 (RISO-214, pp 457-79)

REACTORS, LIQUID METAL-COOLED
accidents in, analysis of acoustic wave propagation in two phase media during, 25:6079
components for Japanese fast breeder-type, design and operation of sodium loop for testing of, 25:4191
containment systems of, design requirements for contamination control of sodium fires in, 25:6045
coolant cover gases for, method for fission product determination in, 25:4736(R) (ANL/ST-3)
cooling system piping for, effects of inert cell impurities on, 25:5988
core of fast, review of AEC programs on safety aspects of, 25:6087
core of fast, safety aspects of, 25:6086
fuel elements of fast, failure thresholds and mechanisms for, (E), 25:6018
pressure vessel of fast, damage assessment method for effects of accidents on, 25:6064
radiation streaming in fast, design requirements for γ and neutron, 25:5976
sodium boiling in, determination of time-dependent nucleate, 25:4210

REACTORS, ORGANIC-COOLED
pressure tubes for heavy water moderated, reliability analysis of SAP, 25:5984 (RISO-214, pp 335-43)

REACTORS, PEBBLE-BED
development of, status of German program for, 25:5944
fuel elements for, fabrication and performance of, 25:6006
loading machine for 300 MW(e), reliability analysis of, 25:6039 (RISO-214, pp 213-46)
physics calculations for once through uranium oxide (UO_2) fueled, 25:5972

REACTORS, POWER
accidents in pressurized water, energy release for rod ejection, 25:6081
boilers for, reliability analysis of, 25:5982 (RISO-214, pp 301-22)
containment vessels for, criteria for leakage tests on, 25:5938
control elements of, availability and cost of boron-10 for, 25:5975
core of gas cooled fast breeder, design modifications for radiation induced swelling of, 25:6020
design characteristics of high temperature gas cooled, 25:5884
design concept for gas core, with MHD power plant, 25:6137
design evaluation of dual purpose desalination, 25:6144
design parameters in Iran for desalination and agro-industrial complex, analysis of optimum economic, 25:6143
design requirements in Japan of, analysis of earthquake resisting, 25:5939
development in Japan, status of, 25:5945
development of gas cooled, during October 1969 to March 1970, 25:5990(R) (ORNL-4589)
development of gas cooled, status of German program for, 25:5944

XUM

development of ocean based process heat, for offshore industrial complex, 25:5881
development of thermal, review of, 25:5878(T) (UCRL-Trans-10495)
economics for, comparison of operation and maintenance costs, 25:5903
economics of gas cooled fast breeder, effects of fuel element thermal limits on, 25:5902
economics of water cooled, effects of design modifications and fuel cycle management procedures on, 25:5900
emergency core cooling system of water cooled, reliability analysis of, 25:6038 (RISO-214, pp 91-126)
fuel cycle for high temperature gas cooled, statistical analysis of optimum economic, 25:6024
fuel cycles for, effects of Western Europe power strategies on, 25:6053
fuel elements of gas cooled fast breeder, pressure equalization system for, 25:6015
fuel performance in, test code for, 25:5991
loading machine for 300 MW(e) pebble bed, reliability analysis of, 25:6039 (RISO-214, pp 213-46)
operation of pressurized water, refueling and maintenance schedules for optimum economic, 25:5909
performance of, effects of design modifications on, 25:5901
personnel for, training program for startup and operation, 25:6211
physics calculations for conceptual gas fueled fast breeder, 25:5971
pressure vessels for, limit state design requirements for prestressed concrete, 25:5981 (RISO-214, pp 289-300)
pressure vessels for, reliability analysis of, 25:5983 (RISO-214, pp 323-34)
pressure vessels for, reliability analysis of, 25:5982 (RISO-214, pp 301-22)
pressure vessels of, neutron flux and spectra in steel, (E/T), 25:6213
protection systems in Canada for, reliability analysis of, 25:5936 (RISO-214, pp 127-69)
quality assurance criteria for, 25:6091
radiation detectors for fast breeder, design parameters of in-core activation, 25:6044
radioactive effluents from boiling, release rates for, 25:6080
reliability analysis in Japan, 25:5937 (RISO-214, pp 457-79)
safety standards in Canada for, 25:5936 (RISO-214, pp 127-69)
shielding for water cooled, design methods and requirements of, 25:5977
shielding in manned space vehicles, optimization of, (T), 25:6138
simulator for, operation of personnel training, 25:6208
thermal effluents from, fog control by utilization of, 25:5886

REACTORS, PRESSURIZED-WATER
accidents in power, energy release for rod ejection, 25:6081
blowdown in, WHAM code evaluation of semiscale subcooled, (E/T), 25:6061 (IN-1431)
coolant loss accident in, coolant flow distribution during, 25:6084
coolant loss accidents in, LOFT facility for simulation of, 25:6104
coolant of, calculation of local void boiling distribution for, (T), 25:5969
cooling system of 400 MW(t) and 1000 MW(e), corrosion product radioactivity in, 25:5986
emergency core cooling system of, effects of 75 to 100 percent flow blockage on performance of bottom flooding, (E), 25:6042
emergency core cooling system of, effects of flow rates on performance of bottom flooding, (E), 25:6043
emergency core cooling system of, performance requirements of bottom flooding, 25:6041
kinetics of, calculations for feedback in multigroup, (T), 25:5956
operation of power, refueling and maintenance schedules for optimum economic, 25:5909
shielding requirements for, calculations for neutron and thermal, 25:5978
simulation for, operation of personnel training, 25:6210

REACTORS, PROCESS HEAT
design evaluation of dual purpose power and desalination, 25:6144
design parameters in Iran for desalination and agro-industrial complex, analysis of optimum economic, 25:6143
development of ocean based power, for offshore industrial complex, 25:5881

REACTORS, REFLECTOR-MODERATED
design concept for rocket, with beryllium, 25:6136

REACTORS, RESEARCH
development of pulse, 25:6120
fuel elements of pulse, analysis of energy loss from viscous damping of, (T), 25:6123
hazards analysis for urban sited, 25:6103
kinetics of GTRR, analysis of spatial and feedback effects of, (E/T), 25:6108
neutron flux monitoring in KUR, conference on, 25:4320 (KURRI-TR-59)
operation of PULSTAR, review of 1964 to 1970, 25:6122
operation potential of subcritical fast, as university facility, 25:6095
operations of pulse, 25:6120
radiation monitoring of laboratories of, at Kyoto University during 1968, 25:4508 (KURRI-TR-63)
reliability analysis of ESSOR, 25:6054 (RISO-214, pp 597-625)
safety aspects of ESSOR, 25:6094 (RISO-214, pp 557-625)
safety limits for pulse, 25:6121
uses for nuclear structure studies, 25:5474 (KFK-1197)

REACTORS, ROCKET
cooling system of, optimization of heat transfer in, (T), 25:6127
design concept for beryllium reflector moderated, 25:6136
materials for liquid-core, properties of graphite, 25:4865
physics parameters of spherical gas core, (E), 25:6133
propellant for gas core, radiant heat transfer in refractory aerosol containing, (T), 25:6135
propellant for gas core, thermal radiation transmission through refractory aerosol containing, (T), 25:6134
reactivity parameters of uranium-235 fueled solid core, (T), 25:6127

REACTORS, SUPERHEATING
fitters for, testing of configurations and materials for steam coolant, 25:5980 (KFK-1183)

REACTORS, THERMAL
development of power, review of, 25:5878(T) (UCRL-Trans-10495)

REACTORS, WATER-COOLED
accidents in, analysis of acoustic wave propagation in two phase media during, 25:6079
accidents in, comparison with LMFBR of core, 25:6077
containment spray solutions for, post accident radiolytic gas production and concentration from, (E), 25:6035 (ORNL-TM-2412(Pt.8))
containment structures for, effects of blowdown accident conditions on protective coatings for, (E), 25:6034 (ORNL-TM-2412(Pt.5))
coolant loss accidents in, emergency core cooling system thermodynamics during, 25:6085
economics of power, effects of design modifications and fuel cycle management procedures on, 25:5900
emergency core cooling system of, reliability analysis of, 25:6038 (RISO-214, pp 91-126)
fuel cycles for, effects of plutonium recycle on, 25:6056
fuel elements of, effects of grid and wire wrap spacers on heat transfer characteristics of rod type, (E), 25:6028
fuel performance in, test code for, 25:5991
shielding for power, design methods and requirements of, 25:5977

REACTORS, WATER-MODERATED
boiling detection methods for, testing of, 25:6048

REFRIGERATION
design of continuously operating helium-4 evaporation, 25:5061 (UCSD-34-P-143-31)
performance and properties of dilution, 25:5062 (UCSD-34-P-143-32)

REGGE POLE THEORY
conspiracy, cut, and evasion models for $\pi^- + p \rightarrow rho^0 + n$ interactions, (E/T), 25:5380
cuts for factorization relations for amplitudes at $t = 0$, moving two-Reggeon, 25:5435
dual six-point function for normalization of anti $p + p \rightarrow 4\pi$ interactions at rest in Venezians model in, 25:5362
duality for scattering lengths in $\pi + \pi$ interactions, 25:5363
duality in set of coupled strong interactions with two-body hadron production in, local, 25:5352 (SU-1206-235)
duality relation with local unitary equivalence in, 25:5414
hadron strong interactions at very high energies in, review of, 25:5347 (CONF-700314-, Paper 13)
model for dispersion sum rules for $\pi + d$ interactions in, two-Regge pole, 25:5391
model with four poles for $\pi^- + p \rightarrow \pi^0$ (eta) $+ n$, $K^- + p \rightarrow$ anti $K^0 + n$, and $K^+ + n \rightarrow K^0 + p$ interactions in, 25:5371 (CEA-N-1373)
Pomeranchuk decoupling from ordinary trajectories for strong interactions and photoproduction in, 25:5346 (CCO-264-562)
scattering amplitudes in, Reggeized absorption model for, 25:5433
trajectories for two-body production in $\pi^- + p$, $\pi^+ + p$, and $K^- + p \rightarrow$ anti $K^0 + n$ interactions at high energies in, effective, 25:5377
trajectories in direct-channel $\pi + p \rightarrow \pi + p$ interactions at low energies, phenomenological, 25:5362
trajectories in strong interactions and photoproduction in, Pomeranchuk decoupling from ordinary, 25:5348 (CCO-264-562)

RELATIVITY THEORY
book: Relativity Reexamined, 25:5421
Cauchy problem for Einstein-Liouville coupled system in Sobolev spaces in, existence theorem for solution of, 25:5420

discretization in astronomy, (T), 25:4933
test of Einstein general, superfluid relativity gyroscope for, 25:5422
REMOTE-HANDLING EQUIPMENT
description of Attila hot cell, 25:4261 (CEA-R-4067)
design and operation of in-cell TURF, for reprocessing of reactor fuels, 25:4303
design and operation of, for preparing radioactive drill core samples for radiochemical analysis, 25:4307
design for weighing nuclear materials at processing plants, 25:4296
development for maintaining high-energy particle accelerators and for space exploration, 25:4200
development for NAL Synchrotron target, 25:5470
development of low-cost mobile SAM, for industrial and space uses, 25:4198
development of mechanical master--slave-type, review of, 25:4313
locks for master--slave-type, development of pneumatic trigger-actuated, 25:4312
maintenance and performance of, after six years operation in NRTS Fuel Cycle Facility hot cells, 25:4300
performance and use in examining EBR-II fuel elements in hot cells, 25:4301
REPTILIA
Cnedidophorus tigris, radiation effects on survival of, in desert ecosystems, γ, 25:4477 (UCLA-12-782, pp 49-81)
Crotaphytus wislizendii, radiation effects on survival of, in desert ecosystems, γ, 25:4477 (UCLA-12-782, pp 49-81)
RESINS
radioinduced production of polyacetal resin by polymerization of trioxane, electron, 25:4098
RESPIRATORY SYSTEM
protection of human, activities of Leipsig Working Group for, 25:6235(T) (LA-4442-TR)
RHENIUM
effects on carbon diffusion in carbon--tungsten alloy, 25:4746 (AD-710275)
preparation of coated thermionic emitters of, method for, 25:4750 (TEE-4125-2)
properties for use as encapsulating material for californium-252 sources for neutron capture gamma-ray spectroscopy, 25:4772
RHENIUM ALLOYS AND SYSTEMS
Re--Ta-base, mechanical properties of dilute, containing trace nitrogen and oxygen, 25:4786 (COO-1676-13)
Re--W-base, diffusion of carbon in, at 1500 to 1800°C, carbon-14 tracer studies of, 25:4763
RHENIUM ISOTOPES Re-176
beta and electron-capture decay of, half-life, spectra, log ft, and Q of, (E), 25:5733
RHENIUM ISOTOPES Re-177
beta and electron-capture decay of, half-life, spectra, log ft, and Q of, (E), 25:5733
RHENIUM ISOTOPES Re-178
beta and electron-capture decay of, half-life, spectra, log ft, and Q of, (E), 25:5733
RHENIUM ISOTOPES Re-185
energy levels from osmium-185 decay, decoupling parameter for $^1/_2^+$ [411], (E/T), 25:5741
energy levels from osmium-185 electron-capture decay, spin--parity assignments for, (E), 25:5741
energy-level transitions from osmium-185 decay, intensities, multipolarities, and internal conversion coefficients for, (E), 25:5741
RHODIUM
complexes with 8-quinolinol, structure of, NMR spectral studies on, 25:4081
properties for use as encapsulating material for californium-252 sources for neutron capture gamma-ray spectroscopy, 25:4772
RHODIUM ISOTOPES Rh-103
energy levels from ruthenium-103 decay, (E), 25:5714
neutron capture integral in fast region, (E), 25:5656
neutron reactions (n,2n) at 10 to 20 MeV, excitation functions and isomeric cross-section ratios for, (E), 25:5766
neutron reactions (n,3n) at 18 to 20 MeV, excitation functions for, (E), 25:5766
RING CURRENT
effect on charged-particle trajectories responsible for auroral display, extraterrestrial, (T), 25:5032
origin of, (E/T), 25:5025
RIVERS
contamination of Czechoslovak, in uranium mining areas, 1964 to 1967, 25:4157
radium-226 content of, in uranium mining areas of Czechoslovakia during 1964 to 1967, 25:4157
ROBERT E. GINNA POWER REACTOR, UNIT 1
operation of, refueling and maintenance schedules for optimum economic, 25:5909
ROCKET REACTORS (NERVA)
coolant exhaust from, design of low temperature charcoal adsorption beds for fission products in, 25:6142
cooldown of, in-flight coolant management for, (T), 25:6132
engine components of, transport analyses of radiation environment of, 25:6128
fuel elements for, thermal hydraulic testing of, (E/T), 25:6141
nozzle assembly of, Monte Carlo radiation transport analyses of, 25:6129
radiation heating rates of internal components in, (E/T), 25:6126
reactivity feedback effects in, 25:6139
shielding for, neutron and γ radiation levels internal and external to, (E/T), 25:6130
shielding of, requirements for manned and unmanned missions, (T), 25:6131
ROCKS
analysis by α scattering methods, 25:4034
analysis for transition metals by neutron activation, 25:4047
deuterium content of, effects of porosity on, 25:4152(T) (CSIRO-Trans-10083)
fractures in Project Gasbuggy GB-3, postshot measurement of micro-, 25:4178
water content of, surrounding underground nuclear explosions, effects on crater formation, 25:4179
RODS
oscillation at high temperatures, equations for, 25:6251(T) (SC-T-70-4042)
ROOTS
cesium-137 uptake by, of Trifolium pratense, comparison of concentration factors for plant distribution for, 25:4449
radiation effects on growth of, of pineapples, effects of 8,000 to 16,000 rad dose on γ, 25:4719
ROVER REACTORS
coolant exhaust from, design of low temperature charcoal adsorption beds for fission products in, 25:6142
RUBIDIUM
deuteron reactions with, production of strontium-85 by, 25:4126 (UJV-2431-Ch)
RUBIDIUM ISOTOPES Rb-85
x-ray emission rates and fluorescence yields from strontium-85 electron-capture decay, K-, (E), 25:5650
RUBIDIUM ISOTOPES Rb-86
uptake by bean plants, effects of availability of nutrient calcium and nitrates and root temperature on, 25:4477 (UCLA-12-782, pp 49-81)
RUBIDIUM MANGANESE FLUORIDES
magnetic phase transition in, sound propagation near, 25:5186
RUTHENIUM
properties for use as encapsulating material for californium-252 sources for neutron capture gamma-ray spectroscopy, 25:4772
separation by ion exchange using Alamine 336 in aqueous thiocyanate solutions, 25:4137 (IS-T-377)
RUTHENIUM ISOTOPES Ru-95
beta and electron-capture decay of, γ singles and coincidence spectra from, (E), 25:5683 (IS-T-351)
RUTHENIUM ISOTOPES Ru-101
energy levels from ruthenium-102 (γ,n) reactions at 26 MeV, half-lives for isomeric, (E), 25:5761
energy-level transitions from ruthenium-102 (γ,n) reactions at 26 MeV, gamma spectra from, (E), 25:5761
RUTHENIUM ISOTOPES Ru-103
beta decay of, sum coincidence spectra from, (E), 25:5714
energy levels from ruthenium-104 (γ,n) reactions at 26 MeV, half-lives for isomeric, (E), 25:5761
energy levels from technetium-103 decay, (E), 25:5683 (IS-T-391)
energy-level transitions from ruthenium-104 (γ,n) reactions at 26 MeV, gamma spectra from, (E), 25:5761
RUTHENIUM ISOTOPES Ru-104
energy levels from technetium-104 decay, spin--parity assignments for, (E), 25:5796

S

S-MATRIX
element relation with vacuum expectation values of time-ordered products of interpolating fields, 25:5431
expansion in terms of normal-ordered polynomials in in--out fields, 25:5431
field matrix element relation with phases of two-channel S-wave, 25:5436
SAFETY
criticality control in handling and storage of fissile metals, use of surface density as parameter in calculations for, 25:4284
criticality standard N16.1 for, engineer's evaluation of ANSI, 25:4287
criticality standard N16.1 for, managers' evaluation of ANSI, 25:4289
criticality standard N16.1 for, nuclear specialists evaluation of ANSI, 25:4286
criticality standard N16.1 for, USAEC's evaluation of ANSI, 25:4288
evaluation of SNAP-23A system, program for, 25:4220
methods for nuclear fuel reprocessing plants, 25:4527
methods for plutonium production plants, 25:4526
research on aerospace nuclear, 25:4216(R) (SC-PR-70-682)
SAFETY HAZARDS
evaluation of radiological, to population from implantable radioisotope-fueled power systems for heart assist devices, 25:4236

XUM

SALICYLOHYDROXAMIC ACID
complexes with divalent and trivalent metals, stability studies on, 25:4083
SALIVA
radiation effects on isoamylases in, from man, γ, 25:4452
SALT DEPOSITS
radioactive waste disposal in Lyons, Kansas, design and cost estimate for monitor, for, 25:4277
SALTS
radioactive waste disposal in, feasibility study for high-level solid, 25:4264 (NP-1662)
SAMARIUM
determination of trace amounts of, in uranium by chemical separation and spectroscopy, 25:4021
properties for use as encapsulating material for californium-252 sources for neutron capture gamma-ray spectroscopy, 25:4772
SAMARIUM CARBIDES
thermal decomposition of, mass spectrometric studies of, 25:4855
thermodynamic properties of, 25:4855
SAMARIUM ISOTOPES Sm-143
beta and electron-capture decay of, gamma spectra, branching ratios, and log-ft values for, (E), 25:5697
energy levels of, spectroscopic factors for, (E), 25:5506 (CEA-N-1232, pp 81-159)
SAMARIUM ISOTOPES Sm-145
use as x-ray source for transmission scanning of bones for measurement of mineral content, 25:4647 (CONF-700515-, pp 274-9)
SAMARIUM ISOTOPES Sm-146
energy levels from europium-146 decay, spin--parity assignments for, (E), 25:5694
energy-level transitions from europium-146 decay, intensities, multipolarities, and conversion coefficients from, (E), 25:5694
SAMARIUM ISOTOPES Sm-148
alpha inelastic scattering at 10 to 13 MeV, angular distributions for, (E), 25:5703
energy level at 551 keV from Coulomb excitation, transition probability and static electric quadrupole moment of, (E), 25:5703
oxygen-16 inelastic scattering at 34 to 50 MeV, angular distributions for, (E), 25:5703
SAMARIUM ISOTOPES Sm-149
energy-level transitions in, conversion electron intensities, multipolarities, and multipole mixing ratios for, (E), 25:5695
SAMARIUM ISOTOPES Sm-150
alpha reactions (α,2n) at 30 MeV, gamma and conversion-electron spectra from, (E), 25:5750
SAMARIUM ISOTOPES Sm-152
alpha inelastic scattering at 10.38 MeV, quantum-mechanical corrections to probability for double Coulomb excitation, (T), 25:5781
energy-level transitions from argon-40 inelastic scattering with Coulomb excitation, reduced quadrupole moments for, (E), 25:5688 (UCRL-15961)
SAMARIUM ISOTOPES Sm-153
gamma spectra of, precision measurements of low-energy, 25:5736
SAP (SINTERED ALUMINUM POWDERS)
mechanical properties of, analysis of, 25:5984 (RISO-214, pp 335-43)
radiation effects on electric resistivity of, relations of impurity content with fast neutron, 25:4890
SCALERS
control and readout system for group of, design of, 25:4370 (INS-TH-67)
SCANDIUM
determination in rocks by neutron activation, 25:4047
separation by ion exchange using Alamine 336 or Amberlyst A-21 in aqueous thiocyanate solutions, 25:4137 (IS-T-377)
separation of rare earths and thorium from, by ion exchange in thiocyanate solutions using Amberlyst A-21, 25:4137 (IS-T-377)
SCANDIUM FLUORIDES
NaF--ScF_3, thermodynamic composition--pressure diagrams of, 25:4857
SCANDIUM ISOTOPES Sc-41
energy levels from calcium-40(He-3,d) reactions, quasibound, (E), 25:5617
SCANDIUM ISOTOPES Sc-43
energy levels from proton resonances in calcium-42, spreading widths for isobaric analog, (T), 25:5644
SCANDIUM ISOTOPES Sc-45
energy levels from proton and alpha inelastic scattering, (E), 25:5624
energy levels from proton resonances in calcium-44, spreading widths for isobaric analog, (T), 25:5644
neutron inelastic scattering at 6.6 and 8.7 MeV, cross sections, energy spectra, and excitation functions for, (E), 25:5551 (CEA-R-4047)
proton reactions (p,n) and (p,2n) at 10 to 85 MeV, cross sections for, (E), 25:5623
proton reactions (p,pn), (p,3np), and (p,3pn) at 10 to 85 MeV, cross sections for, (E), 25:5623
SCANDIUM ISOTOPES Sc-49
energy levels from calcium-48 (He-3,d) and (α,t) reactions, spectroscopic factors for, (E), 25:5506 (CEA-N-1232, pp 81-159)
energy levels from proton resonances in calcium-48, spreading widths for isobaric analog, (T), 25:5644
energy levels of, spin--parity assignments from calculation of, (T), 25:5658
energy-level transitions in, strengths of M1 analog, (T), 25:5658
SCATTERING
amplitudes at t = 0, saving two-Reggeon cuts for factorization relations for, 25:5438
amplitudes for fast particle scattering on Coulomb and short-range potentials in, 25:5438
amplitudes for Reggeons and spinning particles in Veneziano model, 25:5440
amplitudes for superposition of two interactions in relativistic eikonal approximation, 25:5434
amplitudes of arbitrary-mass spinless-particle elastic, double partial-wave expansion of, 25:5310
amplitudes of high-energy elastic, solution of unitarity equation for, 25:5423 (IFVE-STF-69-65)
amplitudes of relativistic, quasipotential theory for analytical properties of, 25:5437
amplitudes of, Bethe--Salpeter equation for SO(1,2) and SO(1,3) crossed-channel partial-wave analyses of, 25:5426 (NYO-2263-TA-226)
amplitudes of, Reggeized absorption model for, 25:5433
amplitudes of, signature in Berdakci--Ruegg model for, 25:5439
amplitudes of, superconverge relations for Cmnes equations for, 25:5427
bounds for, parameters for lower, 25:5425 (JINR-P4-5232)
Faddeev equations for two- and three-body systems in, solutions of, 25:5429
Faddeev equations for, cluster expansion of, (T), 25:5858
Kohn variational principle for two-body S-wave, 25:5430
parity and time reversal invariance in nuclear, derivation from n-matrix elements, 25:5675
phase shifts for elastic, variational formulation of Harris expansion technique for calculation of, 25:4555
phases of two-channel S-wave, field matrix element relation with, 25:5436
potential for two-body, separable expansions of T-matrix for, 25:5432
potential, generalization of in--out formalism for Coulomb, 25:5431
potentials in, fast particle scattering on Coulomb and short-range, 25:5428
T-matrix for three-body bound-state, separable expansions of two-body, 25:5432
T-matrix for three-body, separable expansions of two-body, 25:5432
theory for, second-quantized nonrelativistic time-dependent, 25:5431
unitary pole approximation for bound- and antibound-state, 25:5432
SCHIZOMYCOTA
Bacillus megaterium, syntheses of fatty acids by, 25:4458 (UCLA-12-782, pp 1-21)
Bacillus subtilis, radiation effects on DNA synthesis in chromosomes of, uv and x, 25:4456(R) (ORO-3556-15)
Escherichia coli, radiation effects on colony forming ability of, photoreactivation of uv, 25:4728
Escherichia coli, radiation effects on DNA synthesis in chromosomes of, uv and x, 25:4456(R) (ORO-3556-15)
Escherichia coli, radiation effects on survival of, protective effects of cysteine against x, 25:4555
Escherichia coli, radiation effects on synthesis of nucleic acids and proteins in, protective effects of cysteine against x, 25:4554
Escherichia coli, radiation effects on, effects of amino acid starvation on DNA repair synthesis and survival following uv, 25:4731
Escherichia coli, radiation effects on, protective effects of N-phenylthiocarbamates and phenylthioacetic acids against x, 25:4553
Escherichia coli, radiation repair in, effects of rate of DNA synthesis on uv, 25:4463
Escherichia coli, radioinduced breaks of DNA strands in, protective effects of glycerol, 1,2,3-indantrione, methyl sulfoxide, N-ethyl salamide, and thiourea against electron, 25:4551
Escherichia coli, radioinduced breaks of DNA strands in, effects of triacetoneamine N-oxyl on x, 25:4550
Escherichia coli, radioinduced free radicals in, reactions of, with aminothiols, γ, 25:4548
Escherichia coli, radiosensitivity of DNA in, protective effects of glycerol, 1,2,3-indantrione, methyl sulfoxide, N-ethyl salamide, and thiourea against electron, 25:4551
Escherichia coli, radiosensitivity of synthesis of DNA and proteins in, combined effects of iodoacetic acid and vitamin K on γ, 25:4552
Escherichia coli, radiosensitivity of, effects of BUdR incubation on uv and x, 25:4725
Escherichia coli, x-radiosensitivity of reproductive capacity of, effects of anoxia and triacetoneamine N-oxyl on, 25:4550
Micrococcus radiodurans, radioinduced degradation of DNA in, effects of dose, oxygen content, and temperature on repair of x, 25:4536

XUM

Micrococcus radiodurans, radioinduced degradation of DNA in, combined effects of chloramphenicol on x, 25:4536
Micrococcus radiodurans, radioinduced degradation of DNA in, protective effects of cysteamine against x, 25:4536
Photobacterium fischeri, radiation effects on activity of luciferase system in, measurement of bioluminescence decay time to determine high dose rate electron, 25:4730
radioinduced degradation of DNA in, critical analysis of, 25:4462
radiosensitivity of spores of, factors affecting, 25:4726
Serratia marcenscens, radiation effects on survival of, protective effects of anoxia and cystamine against γ, 25:4549
Serratia marcescens, x-radiosensitivity of, effects of anoxia, indole, and ninhydrin on, 25:4557
SCINTILLATION CAMERAS
collimators for, design parameters for, 25:4324
data handling system for pulsonary function studies, 25:4328
design, operation, and performance of, 25:4325
development of, 25:4337
performance of Anger, 25:4326
performance of autofluoroscope, 25:4326
performance of magnacamera, for pulmonary function studies, 25:4327
SEALS AND GLANDS
testing of stainless steel clam-type, for reactor pipes, 25:4183 (DP-Report-484)
SEAWATER
radioactive waste disposal in Japanese, review of problems of, 25:4316
SEED
activity of α-amylase in barley, effects of deuterium oxide on, 25:4464
radiation effects on germination of sugarbeet, effects of infrared, petroleum, pyrimidine and ultrasound on γ, 25:4722
radioinduced chromosome aberrations in dormant, of Crepis capillaris, cesium-137 β and γ, 25:4498
radioinduced mutations in, of sorghum, 25:4495
SEIGNETTOELECTRIC MATERIALS
spin-lattice relaxation by quasi-spin waves in order--disorder type, 25:6233 (IJS-575)
SELENIUM
radioprotective effects of compounds of, on amino acids in aqueous solutions, ionizing, 25:4545
radioprotective effects of compounds of, on rats, ionizing, 25:4545
SELENIUM IONS
effects of 8-MeV, on void formation in polycrystalline nickel, 25:4819
SELENIUM ISOTOPES Se-74
neutron activation resonance integrals of, thermal, (E), 25:5681 (CNEA-274)
SELENIUM ISOTOPES Se-75
excretion by lungs following injection of selenate, selenite, cystine-, or methionine-incorporated, 25:4673
SELENIUM ISOTOPES Se-78
effects on spectra of NSe, 25:4063
neutron activation resonance integrals of, thermal, (E), 25:5681 (CNEA-274)
SELENIUM ISOTOPES Se-80
effects on spectra of NSe, 25:4063
neutron activation resonance integrals of, thermal, (E), 25:5681 (CNEA-274)
SEMICONDUCTORS
ion implantation in, electron impact source for, 25:5165
transport properties of, research on, 25:5171(R) (CRO-3087-44)
SEPARATED-ORBIT CYCLOTRONS
beam extraction from ALIS, coupling resonance effects on mechanism of third-resonance, 25:5460 (NP-18517)
SEROTONIN
metabolism and tissue distribution following intracerebral or intraperitoneal injection in mice, tracer studies, 25:4584
radioprotective effects of, against chromosome aberrations in bone marrow of rats, x, 25:4585
radioprotective effects of, on mice, combined effects of AET, cysteamine, cysteine, and glutathione against x, 25:4582
radioprotective effects of, on mice, reaction mechanisms for x, 25:4584
radioprotective effects of, on mice, x, 25:4576
radioprotective effects of, on rats, γ, 25:4581
SERPUKHOV SYNCHROTRON
experimental facilities and research program, description of, 25:5443 (CONF-700314-, Paper 1)
SERVOMECHANISMS
noise reduction in close loop, optimization of, (T), 25:6188 (AE-404)
SF MATERIALS ACCOUNTING
neutron source system for, using fission multiplicity detector, 25:4038
SHEEP
blood circulation in brain of fetuses in pregnant, tracer study of, 25:4655 (COO-1762-6)
radiation effects on survival of, protective effects of bacterial endotoxins against x, 25:4586
SHELTERS
evaluation of underground transportation facilities as blast, program for, 25:4255(R) (ORNL-TM-3016)
SHIELDED CONTAINERS
design and safety of lead- and water-shielded, for shipping calcined solid radioactive wastes, 25:4278
design for shipping and storage of radiopharmaceuticals, 25:4267(P)
design of water-cooled, for shipping high-specific activity neutron-emitting radioisotopes, 25:4311
SHIELDING
design for plutonium dioxide heat sources in spacecraft, 25:4246
design standards and procedures for nuclear power plants, 25:5889
gamma albedo distributions for finite media, 25:5146
gamma scattering from barriers of finite thickness, (E), 25:5149
gamma streaming in two-legged ducts,(E), 25:5138
neutron transport in slabs, use of variational methods in, 25:5135 (AAEC/TM-554)
neutron transport in two-dimensional slabs by invariant imbedding, 25:5143
optimization of, unmanned spacecraft scientific experiments, 25:5137
radiation transfer operators for, multigroup discrete ordinates, 25:5144
requirements for astronauts against cosmic ray proton hazards, 25:4509 (MDC G-363)
transport theory in finite slab geometry, orthogonality in, 25:5140
use by personnel in diagnostic radiography, recommendations for, 25:4531
SHIELDING MATERIALS
radiation effects on electrical charge and coloration of glass, γ-, (E), 25:5166
SHOCK WAVES
propagation in atmosphere of Buggy I Event-generated, measurements of, 25:4168 (PNE-320)
propagation in enclosed horizontal tunnel from contained underground nuclear explosion, Marvel studies of, 25:4177
properties of collisionless, downstream state, (T), 25:5099
structure in plasma, theory for radiation hydrodynamics, 25:5095 (CEA-R-4057)
structure of laminar collisionless, finite-Larmor-radius analysis of, (T), 25:5102
SILICON
analysis for oxygen by photon activation, 25:4046
determination in boron, 25:4009 (TID-25190)
determination in meteorites by instrumental pile neutron activation, 25:4048
determination in PuO_2--U_3O_8, effects of ratio of plutonium oxide to uranium oxide on spectrographic, 25:4015 (NUMEC-3524-76)
determination in titanium ore by neutron capture gamma spectroscopy using californium-252 source, 25:4036
effects of impurities of, on properties of uranium, 25:4747 (AWRE-O-63/70)
precipitation from aluminum--silicon alloy, 25:6242 (NYO-2394-40)
radiation effects on piezoresistivity of n-type, electron, (E/T), 25:5151 (N-70-35737)
radioinduced damage in crystalline, recovery by annealing and bombardment with carbon, neon, or silicon ions, 25:4895(P)
SILICON CARBIDES
microstructure of fuel coating of, 25:4863 (DP-Report-574)
radiation effects on crystal structure of, neutron, 25:4887 (KFK-1215)
SILICON IONS
effects of accelerated, on radiation damage recovery in silicon lattices, 25:4895(P)
SILICON ISOTOPES Si-25
mass excess from silicon-28 (He-3,He-6) reactions, test of isobaric-multiplet equation for, (E), 25:5640
SILICON ISOTOPES Si-27
energy levels from silicon-28 (He-3,α) reactions at 11 MeV, spin--parity assignments for, (E), 25:5602 (ANU-P-501)
SILICON ISOTOPES Si-28
deuteron reactions (d,p) at 4.4 and 5.3 MeV, p-γ angular correlations from, (E), 25:5672
energy levels in quartet scheme, low-lying even-parity, even-spin, (T), 25:5814
energy levels in, calculation of collective correlations of two-phonon, (T), 25:5653
energy levels of, mixing in Hartree-Fock solutions for, (T), 25:5674
helium-3 reactions (He-3,α) at 11 MeV, alpha spectrum at 30° from, (E), 25:5602 (ANU-P-501)
helium-3 reactions (He-3,He-6) near 65 MeV, test of isobaric-multiplet mass equation, (E), 25:5640
neutron capture at 20 to 80 keV, cross sections for, (E), 25:5603 (FCA-4-4440)
proton inelastic scattering at 20.3 MeV using polarized beams, cross section and asymmetry for, (E), 25:5506 (CEA-N-1232, pp 81-159)

XUM

proton reactions at 660 MeV, flucrine-18 differential energy distributions from, (E/T), 25:5663
SILICCN ISOTOPES Si-29
energy levels from neutron resonances in, silicon-28, (E), 25:5603 (FOA-4-4440)
energy levels from silicon-28 (d,p) reactions,(E), 25:5672
helium-3 reactions (He-3,d) at 15 MeV, DWBA analysis of angular distributions from, (E/T), 25:5670
SILICCN ISOTOPES Si-31
energy levels from silicon-30 (d,p) reactions, lifetimes of, (E), 25:5628
SILICCN NITRIDES
analysis of thin layers of, for trace impurities by neutron activation and γ spectroscopy, 25:4045
SILICCN OXIDES
analysis of thin layers of, for trace impurities by neutron activation and γ spectroscopy, 25:4045
properties as support for inorganic ion exchangers in determination of cesium-137 in natural waters, 25:4033
Al_2C_3--BeO--H_2O--SiO_2, phase studies of subsolidus phase relations of, at 300 to 700°C, 25:4871
SILTS
radium-226 content of, in uranium mining areas of Czechoslovakia during 1964 to 1967, 25:4157
SILVER
electric conductivity at 1.5 to 300°K, absolute, (E/T), 25:5184
ion penetration into, path lengths for nitrogen-15, (T), 25:4940
properties for use as encapsulating material for californium-252 sources for neutron capture gamma-ray spectroscopy, 25:4772
SILVER ALLOYS AND SYSTEMS
electric conductivity at 1.5 to 300°K of dilute, deviations from Matthiessen's rule in, (E/T), 25:5184
Ag--rare earth, antiferromagnetic ordering in RAg compounds, (T), 25:5197
SILVER CHLORIDES
diffusion of lithium at 200 to 400°C in crystals of, isotope effect in, 25:5172
SILVER ISOTOPES Ag-107
neutron capture by, cross sections for, (E), 25:5789
SILVER ISOTOPES Ag-108
energy-level transitions from neutron capture by silver-107, strength functions for, (E), 25:5789
SILVER ISOTOPES Ag-109
neutron capture by, cross sections for, (E), 25:5789
SILVER ISOTOPES Ag-110
beta decay of polarized, beta spectra and anisotropy from, (E), 25:5743
energy level at 1.28 +- 0.10 keV from silver-109(n,γ) reactions, (E), 25:5712
energy-level transitions from neutron capture by silver-109, strength functions for, (E), 25:5789
SILVER ISOTOPES Ag-113
beta decay of ground-state and isomeric, β and γ singles and coincidence spectra from, (E), 25:5754
SILVER ORES
analysis of, avalanche semiconductor detectors for x-ray fluorescence, 25:4323 (NYO-4028-TA-1)
SKELETAL SYSTEM
measurements of weight and volume of bones of human, use of contact radiography and x-ray densitometry for, 25:4652 (CONF-700515-, pp 365-82)
SKIN
analysis for copper, manganese and zinc by neutron activation, 25:4049
radiation dose to, computer program for fallout, 25:4506 (AD-703266)
radiation effects on, of man, protective effects of sunscreening creams against uv, 25:4668
radioinduced irritation of, of personnel using uv, 25:4710
SLURRIES
density of flowing, accuracy of radiometric gages for measuring, 25:4896
SODIUM
analysis for impurity carbon, hydrogen, and oxygen, development of analytical standards for, 25:4736(R) (ANL/ST-3)
analysis for impurity carbon, hydrogen, and oxygen, development of on-line systems for, 25:4736(R) (ANL/ST-3)
analysis for trace metallic impurities, development of method for, 25:4736(R) (ANL/ST-3)
analysis of highly radioactive, mockup of remotely operated high-purity inert-atmosphere facility for chemical, 25:4310
barium-137 mass transfer in forced-convection, radiochemical measurement of coefficients of metastable, 25:4774
boiling in reactor cooling systems, determination of time-dependent nucleate, 25:4210
carbon transport by, in stainless steel loops between hot and cold legs, 25:4773
cesium mass transfer in forced-convection, radiochemical measurement of coefficients of, 25:4774
chemistry of nitrogen-bearing species in liquid, 25:4736(R) (ANL/ST-3)
corrosive effects on refractory bearing coatings at 1100°F, 25:4185(R) (NYO-3930-8)
corrosive effects on vanadium at 450 to 600°C, 25:4736(R) (ANL/ST-3)
determination in human body by neutron activation, 25:4042 (CONF-680211-, pp 496-516)
determination of trace amounts of, in silicon nitrides and oxides by neutron activation and γ spectroscopy, 25:4045
excitation in nightglow, mechanism of D-line, (E/T), 25:5018
gas detection in liquid, nozzle system for, 25:6047
nitrogen transport by, in stainless steel loops between hot and cold legs, 25:4773
properties for use as encapsulating material for californium-252 sources for neutron capture gamma-ray spectroscopy, 25:4772
purification of, development of method for, 25:4736(R) (ANL/ST-3)
reaction with molten uranium oxide (UO_2) of liquid, energy release for, (E), 25:6076
reactions with chromium--vanadium alloy at 550 to 700°C, 25:4736(R) (ANL/ST-3)
reactions with plutonium dioxide--uranium dioxide at 400 to 1100°C, 25:4736(R) (ANL/ST-3)
solvent properties of liquid, for xenon, 25:4736(R) (ANL/ST-3)
vapor monitor for heat transfer systems of liquid, 25:6046
SODIUM ALLOYS AND SYSTEMS
H--Na--O, phase studies of, 25:4736(R) (ANL/ST-3)
SODIUM BROMIDES
dielectric constant of, low-frequency, 25:6228 (COO-623-153)
dielectric constants of, pressure and temperature dependences of static, 25:5168(R) (COO-623-156)
luminescence from aqueous solutions of γ-irradiated crystals of, mechanism of, 25:4076
SODIUM CHLORIDES
content of diet, effects of, on carcinogenesis in rats, 25:4459 (UCLA-12-782, pp 23-47)
dielectric constant of, low-frequency, 25:6228 (COO-623-153)
dielectric constants of, pressure and temperature dependences of static, 25:5168(R) (COO-623-156)
luminescence from aqueous solutions of γ-irradiated crystals of, mechanism of, 25:4076
SODIUM DITHIONITES
hydrolysis of, effects of oxygen-17 on ESR spectra of SO_2^- radical from, 25:4124
SODIUM FLUORIDES
dielectric constant of, low-frequency, 25:6228 (COO-623-153)
dielectric constants of, pressure and temperature dependences of static, 25:5168(R) (COO-623-156)
NaF--LaF_3, thermodynamic composition--pressure diagrams of, 25:4857
NaF--ScF_3, thermodynamic composition--pressure diagrams of, 25:4857
NaF--YF_3, thermodynamic composition--pressure diagrams of, 25:4857
SODIUM HYDROXIDES
reactions with mandelic acid and uranyl nitrate, production of $Na_2UO_2(O_3C_8H_6)_2$ from, 25:4088
SODIUM IODIDES
effects on radiosensitivity of alcohol dehydrogenase in aqueous solutions, ionizing, 25:4543
effects on x-radiosensitivity of Ehrlich ascites tumor cells in cultures, 25:4569
effects on x-radiosensitivity of enzymes in solutions, 25:4569
SODIUM ISOTOPES Na-21
energy levels from fluorine-19 (He-3,n) reactions at 4.2 to 5.9 MeV, widths and spin--parity assignments for T = 3/2, (E), 25:5583
energy levels from proton resonances in neon-20, widths and spin--parity assignments for T = 3/2, (E), 25:5583
SODIUM ISOTOPES Na-22
uptake by bean plants, effects of availability of nutrient calcium and nitrates and root temperature on, 25:4477 (UCLA-12-782, pp 49-81)
SODIUM ISOTOPES Na-24
separation from neutron-activated samples by ion exchange, 25:4044
SODIUM NITRATES
effects on phosphorescence produced by x radiation effects on indole in polar solution, 25:4089
SOILS
analysis of, avalanche semiconductor detectors for x-ray fluorescence, 25:4323 (NYO-4028-TA-1)
chemical and physical properties of desert, at Nevada Test Site, 25:4477 (UCLA-12-782, pp 49-81)
chemistry of, tracer studies on, 25:4052 (NYO-2043-216, pp 48-73)
diffusion of calcium--strontium carbonate in, method for simulation of, 25:4265 (ORNL-TM-3130)
moisture content of, evaluation of gamma attenuation method for measurement of, 25:4156
plutonium-239 distribution in, effects of water and wind erosion on fallout, 25:4478
properties of West Valley Processing Plant, studies of geologic, 25:4153 (DOCKET-50201-51)
properties of West Valley Processing Plant, studies of

geologic, 25:4155 (DOCKET-50201-53)
properties of West Valley Processing Plant, studies of geologic, 25:4154 (DOCKET-50201-52)
SOLAR DISTURBANCES
occurrences in 1968, summary of, (E), 25:5022
SOLAR FLARES
occurrences in 1968, summary of, (E), 25:5022
particle emission from, (E/T), 25:4927
particle emission from, detector system for, (E), 25:4928
SOLAR PARTICLES
cosmic-ray modulation by, primary, (E/T), 25:4982
emission from solar flares, (E/T), 25:4927
kinetics of, in solar atmosphere, (E/T), 25:4927
propagation in interplanetary space, (E/T), 25:4927
SOLAR RADIATION
spectrum of extreme ultraviolet, effect of solar cycle on, (E), 25:4925
SOLAR SYSTEM
evolution of, (T), 25:4921
interstellar particle penetration into, effect on Earth ionosphere of neutral, 25:5021
nucleosynthesis in, chronology of, (E/T), 25:4922
origin of, (T), 25:4921
SOLAR WIND
cosmic-ray modulation by, dynamics of primary, (E/T), 25:4983
cosmic-ray modulation by, primary, (E/T), 25:4982
effects on interplanetary field structure, (T), 25:4926
interactions with geomagnetic disturbances and Pi2 pulsations, (T), 25:5026
relation to magnetospheric geomagnetic activity, (E), 25:5024
SOLID STATE PHYSICS
electron band structure calculations, comparison of standard and modified orthogonalized plane-wave, 25:5231
research in, 25:5168(R) (COO-623-156)
research on dynamic nuclear polarization, 25:5150(R) (UCB-34-P-20-PR-16)
SOLIDS
density of, radiometric equipment and method for measurement of apparent, 25:4764(P)
permeability of, method for measurement of, 25:4841(R) (SRO-552-5)
SOUND
propagation near magnetic phase transitions, critical changes in, 25:5186
SOUTHWEST EXPERIMENTAL FAST OXIDE REACTOR
cooling system piping for, effects of inert cell impurities on, 25:5988
core components for, fabrication of extension rods, tightener rods, tightener sleeves, and special rods in, 25:5943 (GEAP-13595)
experimental programs of, review of, 25:6058
operations incident of July 26, 1970, malfunction of emergency electrical system tie breakers, 25:6050 (DOCKET-50231-59)
reactivity coefficients for, 25:5951 (DOCKET-50231-58)
SOVIET UNION
mutation breeding of agricultural plants in, review of literature on, 25:4489
nuclear explosions in, potential industrial uses of underground, 25:4169(T) (UCRL-Trans-10477)
nuclear explosions in, review of industrial uses of, 25:4170
nuclear weapons development in, for defensive and offensive uses, 25:4167 (CONF-691051-, pp 192-8)
SPACE
exploration in, development of remote systems for, 25:4200
magnetic-field structure in interplanetary, (T), 25:4926
SPACE VEHICLES
configuration parameters of manned, with reactor power source, (T), 25:6138
control system of solar probe, use of a emitting radioisotope for attitude, 25:4222
heat sources for unmanned, shielding optimization for plutonium dioxide, 25:4246
power system for nuclear-electric unmanned, MHD, (E), 25:4592(R) (N-70-34006)
power system for Pioneer, radiation field from SNAP-27 heat source in, 25:4243
power systems for unmanned, radiation flux mapping around, 25:4247
power systems for, gamma and neutron spectra of radioisotope thermoelectric, 25:4242
shielding optimization for unmanned scientific experiments, 25:5137
SPECTROMETERS
circuits for nuclear, design of, 25:5506 (CEA-N-1232, pp 81-159)
description of magnetic, for nuclear studies, 25:5506 (CEA-N-1232, pp 81-159)
SPECTROSCOPY
book: Spectroscopic Astrophysics, 25:4913
review of heavy-ion in-beam, (E), 25:5688 (UCRL-19961)
SPHERES
flow in recirculated randomly packed fluidized beds in cylindrical vessels, (E/T), 25:4182 (AAEC/E-207)
SPINAL CORD
scanning using iodine-131-labeled serum albumin, method for calculation of radiation dose to patients during, β and γ, 25:4510
SPLEEN
indium-113 uptake by, of rats, effects of particle size of colloid and pH on, 25:4437
radiation effects on count of autoantibody-forming cells in, of dogs and mice, use of Cuningham's method to determine γ, 25:4472
thorium content of, in rats following intracardiac administration, 25:4441
SPORES
radioinduced injuries in dry, of ferns, effects of oxygen content on, reaction mechanisms for ionizing, 25:4705
radiosensitivity of bacterial, effects of water content on, 25:4726
radiosensitivity of fern, effects of acetoacetic acid, anoxia, and indole-2,3-dione on x, 25:4573
SPUTTERING
equipment for fabrication of radioisotope heat source in glove boxes, 25:4259 (BNWL-SA-3609)
STACK DISPOSAL
sulfur dioxide emission from Chicago power plant, multiple-source dispersion model for studying diffusion of, 25:4161 (ANL/ES-CC-7)
STAINLESS STEEL
compatibility with carbide fuels, carbon-14 tracer studies of, 25:4739 (JAERI-Memo-4132)
corrosion of borided bearing coatings of, by sodium at 1100°F, 25:4185(R) (NYO-3930-8)
diffusion of helium bubbles in Type 20-25, effects of bubble size on, 25:4758
diffusion of tritium in Type 304, 25:5152(R) (CRC-3508-6)
effects of boron-containing Raschig rings of, on criticality of plutonium nitrate solutions, 25:4281
mechanical properties of tubes of Type 316, effects of processing variables on, 25:4776
mechanical properties of Types 304, 321, 347, and 316, effects of high-temperature gases on, 25:4738 (DP-Report-527)
microstructure of tubes of Type 316, effects of processing variables on, 25:4776
properties of thermomechanically treated Type 348, for use as LMFBR cladding, 25:4775
radiation effects on burst strength of Type 304, in-pile, (E), 25:5950
radiation effects on creep strain and yield strength of Type 304, pile neutron, 25:4820
radiation effects on mechanical properties of Type 316, in-pile, (E), 25:5549
radiation effects on microstructure of cold-worked Type 316, 5-MeV nickel ion, 25:4829
radiation effects on microstructure of thermomechanically treated Type 348, nickel on, 25:4775
radiation effects on reactor-grade, review of, 25:4770
radiation effects on stress rupture properties of Type 316, in-pile, (E), 25:5948
radiation effects on swelling of Types 304 and 316, relations of temperature with pile neutron, 25:4810 (BNWL-SA-3283)
radiation effects on tensile properties of Types 304 and 316, method for prediction of fast neutron, 25:4831
radiation effects on uniaxial and biaxial creep-rupture of Type 316, fast neutron, 25:4816 (WHAN-FR-19)
radioinduced swelling of Types 304 and 316, effects of in situ annealing on fast neutron, 25:4822
radioinduced swelling of Types 304 and 316, effects of cold working on fast neutron, 25:4824
strain aging in annealed Type 304, at 1000 to 1600°F, effects of strain rate and temperature on dynamic, 25:4777
STANDARDS
evaluation of ANSI criticality safety N16.1, by criticality specialist, 25:4286
evaluation of ANSI criticality safety N16.1, by managers, 25:4289
evaluation of ANSI criticality safety N16.1, by process engineer, 25:4287
evaluation of ANSI criticality safety N16.1, by USAEC, 25:4288
reactor protection system and safety, in Canada, 25:5936 (RISO-214, pp 127-69)
STARS
book: Spectroscopic Astrophysics, 25:4913
book: Stellar Atmospheres, 25:4912
detection of faint-blue, associated with cD clusters of galaxies, (E), 25:4930
evolution of binary, (T), 25:4897
evolutionary position of BD + 17° 4708, (E), 25:4906
gravitational radiation from, search for, (E), 25:5419
helium core flash in, hydrodynamics of, (T), 25:4911
infrared spectra of VY CMa, near-, (E), 25:4508
light variation of EM Cep, (E), 25:4503
light variation of γ CrB, (E), 25:4907
luminosity criteria for visual binary, comparison of three spectroscopic, (E/T), 25:4910
mass exchange in binary, (T), 25:4897
mass functions of binary, with giant primaries, (E), 25:4905
period of EM Cep, 25:4903
photometry of 36 visual binary, (E), 25:4858

XUM

photometry of IQ Per, UBV, (E), 25:4902
photometry of three eclipsing binary, (E), 25:4900
spectra of AG Carinae, (E), 25:4905
spectra of R And and 19 TX Psa, search for aluminum-26 in, (E), 25:4899
velocity observations of HD 137391, radial, (E), 25:4904
STATISTICS
numerical experiments with a nonlinear chain, 25:6234(T) (LA-4440-TR)
STEAM
production by geothermal heat in nuclear cavity for recovery of high-viscosity petroleum, 25:4174
H_2O--steam, corrosive effects on Zircaloy-2, relations with in-pile radiation, 25:4737 (CISE-R-290)
STEAM POWER PLANTS
operation of, power scheduling for optimum, 25:5896
STEEL
carbon transport between ferritic and austenitic, in sodium at 500 to 800°C, kinetic and thermodynamic properties of, 25:4755
mechanical properties of, effects of exposure to high-temperature carbon oxides, methane, nitrogen, or water on, 25:4738 (DP-Report-527)
properties and structure of 300-grade maraging, effects of thermal cycling on, 25:6254 (UCRL-72099)
properties of heat-resisting, for use in high-temperature gas-cooled reactors, review of, 25:4779
radiation effects on electric conductivity and mechanical properties of Type Kh 18N22V2T2, fast neutron, 25:4817
radiation effects on embrittlement of A212-B pressure vessel, neutron, (T), 25:6145 (AD-709898)
radiation effects on reactor-grade, review of, 25:4770
radioinduced embrittlement of electroslag weldments of Type A533B, at 550°F, fast neutron, 25:4833
radioinduced embrittlement of pressure vessel, damage threshold for neutron, 25:4832
Cr--Mo--steel, mechanical properties of, effects of high-temperature carbon oxides, methane, nitrogen, or water on, 25:4738 (DP-Report-527)
STELLARATORS
magnetic field mapping in, method for, 25:5074
STERILITY
radioinduced, in fall webworm, dose required for cobalt-60 γ, 25:4735
STEROIDS, 17-KETO-
radiation effects on elimination of, in urine of rats, comparison of orchiectomy and fractionated, 25:4707
STOMACH
radiation effects on glandular, of mice, carcinogenic whole-body γ, neutron, and x, 25:4703
STORAGE RINGS
beam luminosity measurements at Adone, 25:5446 (DNPL/R-7, pp 215-43)
experimental facilities and programs at Adone, 25:5446 (DNPL/R-7, pp 215-43)
performance of ISR, 25:5444 (CONF-700314-, Paper 2)
STRANGE PARTICLES
coupling constant for vector current for, renormalization of, (T), 25:5356
STRATOSPHERE
strontium-90 distribution in, 25:4163
STRONTIUM
optical constants from reflectance spectra at 1 to 11.6 eV, 25:5188
separation by ion exchange using Alamine 336 in aqueous thiocyanate solutions, 25:4137 (IS-T-377)
STRONTIUM CARBONATES
$CaCO_3$--$SrCO_3$, diffusion of aqueous solutions of, in soils, use of vermiculite columns for simulation of, 25:4265 (ORNL-TM-3130)
STRONTIUM ISOTOPES Sr-84
deuteron reactions (d,p) at 21 MeV, cross sections for, (E), 25:5604 (N-70-25281)
STRONTIUM ISOTOPES Sr-85
analysis for impurities, polarographic, 25:4126 (UJV-2431-Ch)
electron-capture decay of, K-x-ray emission rates and fluorescence yields from, (E), 25:5650
energy levels from strontium-84 (d,p) and strontium-86 (d,t) reactions, (E), 25:5604 (N-70-25281)
metabolism in bones of rats, effects of diuretics and parathormone on, 25:4423 (COO-1601-23)
production of carrier-free, by deuteron irradiation of rubidium and ion exchange chromatography, 25:4126 (UJV-2431-Ch)
retention by man, effects of aluminum phosphate gel on, 25:4424(R) (TID-25567)
sorption by intestine of rats from vascular space, 25:4424(R) (TID-25567)
STRONTIUM ISOTOPES Sr-86
deuteron reactions (d,p) and (d,t) at 21 MeV, cross sections for, (E), 25:5604 (N-70-25281)
triton reactions (t,p) at 15 MeV, proton spectra and angular distributions for, (E), 25:5615
STRONTIUM ISOTOPES Sr-87
energy levels from strontium-86 (d,p) and strontium-88 (d,t) reactions, (E), 25:5604 (N-70-25281)
STRONTIUM ISOTOPES Sr-88
deuteron reactions (d,t) at 21 MeV, cross sections for, (E), 25:5604 (N-70-25281)
energy levels up to 7 MeV from strontium-86(t,p) reactions, (E), 25:5615
STRONTIUM ISOTOPES Sr-89
content in rainwater and snow, 25:4163
distribution in mitochondria of liver of rats, effects of agents for uncoupling oxidative phosphorylation on, 25:4431
STRONTIUM ISOTOPES Sr-90
content in rainwater and snow, 25:4163
content of birds, food, human bones, plants, precipitation, and water in Faroe Islands during 1969, 25:4476(R) (RISO-221)
content of bones and meat of chickens raised during 1965, 25:4427
content of carp caught in Mecklenburg ponds during 1961 to 1962, 25:4427
deposition in relation to total human ingestion from diet in Netherlands, equation for fallout, 25:4815
determination by β counting using G-M and proportional detectors, efficiency curves for, 25:4029 (CISE-N-119)
determination in plants, rapid method for, 25:4039
distribution in stratosphere and troposphere, 25:4163
effects on infant mortality following nuclear weapons testing, 25:4505 (CONF-691051-, pp 324-35)
metabolism in man, effects of ingestion in calcium gluconate and milk on, 25:4424(R) (TID-25567)
radiation effects on tissues of dogs following use as simulated power source for artificial heart, 25:4423
uptake by tomato plants, effects of ammonium nitrate fertilization and availability of calcium and free calcium carbonates on, 25:4477 (UCLA-12-782, pp 49-81)
use for powering implantable cardiac pacemakers in UK, research program on, 25:4240
STRUCTURES
gamma attenuation in cylindrical concrete, Monte Carlo calculation of, (T), 25:4256
STYRENE
radiinduced polymerization of, under pressure, γ, 25:4104
STYRENE POLYMERS
density of foams of, use of x-ray radiation gauge for measurement of, 25:6220 (BDX-613-180)
SUCROSE
synthesis in corn scutellum, effects of uranyl nitrate on, 25:4720
SULFIDES
radioprotective effects of, on bacteria and bacteriophages, γ, 25:4549
radioprotective effects of, relation of molecular structure to, 25:4548
SULFUR
content in atmosphere, performance of californium-252 source for measurement of, 25:4218
determination in boron, 25:4009 (TID-25190)
SULFUR DIOXIDES
diffusion of stack-released, in Chicago atmosphere, multiple-source dispersion model for predicting, 25:4161 (ANL/ES-CC-7)
SULFUR ISOTOPES S-32
energy levels in quartet scheme, low-lying even-parity, even-spin, (T), 25:5814
helium-3 reactions (He-3,p) at 5.75 MeV, angular correlations for, (E), 25:5627
neutron capture at 20 to 80 keV, cross sections for, (E), 25:5603 (FOA-4-4440)
SULFUR ISOTOPES S-33
energy levels from neutron resonances in sulfur-32, (E), 25:5603 (FOA-4-4440)
SULFURIC ACID
H_3PO_4--H_2SO_4, effects on electrochemical behavior of uranium, 25:4792
SUN
sunrise of, effects on ionization in mid-latitude lower ionosphere, anomalous, (E/T), 25:5006
x-ray emission from, correlation with Hα flares, calcium plages, and microwave emission, (E), 25:4924
x-ray emission from, effects of solar cycle variations on soft, (E), 25:4923
SUNSPOTS
effects on extreme ultraviolet solar spectrum, (E), 25:4925
SUPERCONDUCTORS
critical field curves of molybdenum and cadmium, (E), 25:5057
critical field of clean Type-II, bulk upper, 25:5054
current-pulse effect in intermediate state of lead, 25:5053
dislocation motion in niobium crystals, 25:5036(R) (NYO-4060-5)
electric conductivity above transition temperature in, nonlinear excess, (E/T), 25:5040
energy gap of amorphous bismuth, temperature dependence of, (T), 25:5042
energy spectrum of, with overlapping bands, (T), 25:5041
fluxoid pinning near surfaces in niobium single crystals, 25:5036(R) (NYO-4060-5)
Josephson effect in niobium junction, determination of 2e/h from, (E), 25:5412
Josephson effect in S/N/S point contacts, current steps in V-I characteristic, 25:5037
magnetic flux jumps in, energy dissipated in, (E/T), 25:5044

order parameter healing length in, 25:5049
order parameter motion in Type-II transition-element, in high magnetic field, 25:5050
properties of transition metal, 25:5047
quantum oscillations and order of phase charge in low-kappa Type-II microcylinder, (E), 25:5045
quantum oscillations in low-kappa Type II microcylinder, 25:5046
thermal conductivity of indium--lead alloys, (E/T), 25:5055
thermal properties of, 25:4051(R) (AI-AEC-12972)
transition in dhcp lanthanum, effects on nuclear quadrupole resonance frequencies, 25:5058
transition temperature and normal-state conduction mechanism in oxidized thin films, (E/T), 25:5039
transition temperature of, correlation with empirical pseudopotential from atomic spectra, (T), 25:5048
transition temperatures of ultrarapidly quenched bulk aluminum--copper alloys, (E/T), 25:5056
tunneling in, effect of microwave phonons on, (T), 25:5043
use in rf cavities, change of eigenstate due to nonlinear response in, 25:5063
use of, for storage of magnetic energy, 25:5064(P)
vortex near T/sub c/ in pure, theory of isolated, 25:5051
vortices in neutral and Type-II, boson method for, 25:5052

SURFACE-ACTIVE AGENTS
metabolism in rat lungs, carbon and thorium uptake study of, 25:4410

SURFACE WATERS
radium-226 content of, in Chalk River area during 1969, 25:4473 (AECL-3687)

SURFACES
radioactive contamination on, sampling device for monitoring, 25:4516(P)

SURRY POWER REACTOR, UNIT 1
containment system for, final safety analysis of, 25:5929 (DOCKET-50280-30)
control systems for, final safety analysis of, 25:5930 (DOCKET-50280-31)
cooling system for, final safety analysis of, 25:5929 (DOCKET-50280-30)
electrical systems for, final safety analysis of, 25:5930 (DOCKET-50280-31)
emergency and auxiliary systems for, final safety analysis of, 25:5930 (DOCKET-50280-31)
engineered safeguards for, final safety analysis of, 25:5929 (DOCKET-50280-30)
instrumentation for, final safety analysis of, 25:5930 (DOCKET-50280-31)
operations aspects of, final safety analysis of, 25:5930 (DOCKET-50280-31)
radiation protection system for, final safety analysis of, 25:5930 (DOCKET-50280-31)
radioactive waste disposal system for, final safety analysis of, 25:5930 (DOCKET-50280-31)
site for, environmental survey during May 1968 to June 1970, 25:5928 (DOCKET-50280-29)
site for, final safety analysis of, 25:5929 (DOCKET-50280-30)
steam and power conversion systems for, final safety analysis of, 25:5930 (DOCKET-50280-31)
structures for, lateral load testing of prototype steel piles of support, 25:5927 (DOCKET-50280-28)

SURRY POWER REACTOR, UNIT 2
containment system for, final safety analysis of, 25:5929 (DOCKET-50280-30)
control systems for, final safety analysis of, 25:5930 (DOCKET-50280-31)
cooling system for, final safety analysis of, 25:5929 (DOCKET-50280-30)
electrical systems for, final safety analysis of, 25:5930 (DOCKET-50280-31)
emergency and auxiliary systems for, final safety analysis of, 25:5930 (DOCKET-50280-31)
engineered safeguards for, final safety analysis of, 25:5929 (DOCKET-50280-30)
instrumentation for, final safety analysis of, 25:5930 (DOCKET-50280-31)
operations aspects of, final safety analysis of, 25:5930 (DOCKET-50280-31)
radiation protection system for, final safety analysis of, 25:5930 (DOCKET-50280-31)
radioactive waste disposal system for, final safety analysis of, 25:5930 (DOCKET-50280-31)
site for, environmental survey during May 1968 to June 1970, 25:5928 (DOCKET-50280-29)
site for, final safety analysis of, 25:5929 (DOCKET-50280-30)
steam and power conversion systems for, final safety analysis of, 25:5930 (DOCKET-50280-31)
structures for, lateral load testing of prototype steel piles of support, 25:5927 (DOCKET-50280-28)

SURVIVAL
radiation effects on, of cells, effects of nuclear and cytoplasmic integrity on ionizing, 25:4691

SWINE
measurement of blood and plasma volumes of, tracer methods for, 25:4411 (CEA-R-4031)
radioisotope distribution in tissues of, following ingestion and inhalation of fallout, 25:4435

SYMMETRY GROUPS
breaking effect on p-wave resonances in $\pi + \pi$, $\pi + K$, and $K +$ anti K interactions, 25:5394
chiral dynamics for form factors and decay constants for $K \rightarrow \pi + l + \nu$ decay, 25:5399 (JINR-P2-5290)
O(8), breaking in meson interactions with pseudoscalar mesons, 25:5394
Poincare, particle--antiparticle doublets in representations of full, 25:5398
SO(1,2), crossed-channel partial-wave analysis of scattering amplitude in, Bethe--Salpeter equation for, 25:5426 (NYO-2263-TA-226)
SO(1,3), crossed-channel partial-wave analysis of scattering amplitude in, Bethe--Salpeter equation for, 25:5426 (NYO-2263-TA-226)
SO(4,2), nucleon axial vector form factor from, 25:5401 (DEMO-70/6)
Sp(4), mass spectrum in infinite-component local field transformation over nonunitary irreducible representation of, 25:5406 (JINR-P2-5305)
SU(2) x SU(2) chiral, modified Weinberg sum rules in, 25:5364
SU(3) x SU(3) breaking parameter relation with Glashow--Weinberg bounds on mass of kappa, 25:5399 (JINR-P2-5290)
SU(3) x SU(3), universal structure functions from scale-invariant light-cone current commutators in, 25:5328
transformations in Wightman field theory, generators of, 25:5416

SYMMETRY GROUPS SU(3)
breaking in differential cross sections for $\pi^+ + p \rightarrow K^+ + \Sigma(1385)$ interactions at 4 and 5.05 GeV/c, (E), 25:5290
meson radiative decays in broken, vector dominance Veneziano model and sum rules for 0- and 1-, 25:5402
structure for internal symmetry from Veneziano model for pseudoscalar interactions, 25:5370
sum rules for coupling constants of weak and strong interactions in broken, 25:5394

SYMMETRY GROUPS SU(6)
sum rules for hadron decays in broken, 25:5354

SYNCHROTRONS
design proposals for CERN 300-GeV, 25:5471
operation of JINR, for deuteron acceleration, 25:5445 (JINR-P9-5311)

SYSTEMS FOR NUCLEAR AUXILIARY POWER (SNAP-8)
fuel elements for, neutron radiographic equipment and method for post-irradiation testing of, 25:4252

SYSTEMS FOR NUCLEAR AUXILIARY POWER (SNAP-15)
design and performance of plutonium-238-fueled, for use in electronic control circuits, 25:4219

SYSTEMS FOR NUCLEAR AUXILIARY POWER (SNAP-23)
safety of 23A, program for evaluation of nuclear, 25:4220

SYSTEMS FOR NUCLEAR AUXILIARY POWER (SNAP-27)
fuel capsule for, factors affecting helium pressure buildup in, 25:4216(R) (SC-PR-70-682)
heat sources for, radiation field measurement around, 25:4243
radiation fields around, mapping of, 25:4247

T

T-111 (TANTALUM ALLOY)
performance as structural material for electromagnetic potassium pumps to 1500°F, 25:4186 (ORNL-TM-2555)

TANTALUM
analysis for nitrogen and oxygen by vacuum fusion, 25:4022
determination in boron, 25:4009 (TID-25190)
fabrication of precision tubes of, equipment and methods for, 25:4745
internal friction of nitrogen- and oxygen-containing, cold-working maximum of, 25:4778
lattice vibration spectra of, calculations of, 25:5183
properties for use as encapsulating material for californium-252 sources for neutron capture gamma-ray spectroscopy, 25:4772
reactivity worth of, (E/T), 25:5964
superconducting Josephson effect in point contacts with normal metal, 25:5037
uptake and retention of, in lungs of dogs following use in contrast media for radiography, 25:4657 (UCLA-12-782, pp 89-125)

TANTALUM ALLOYS AND SYSTEMS
Re--Ta-base, mechanical properties of dilute, containing trace nitrogen and oxygen, 25:4786 (COO-1676-13)

TANTALUM ISOTOPES Ta-181
energy-level transitions from hafnium-181 beta decay, anisotropy under combined electric and magnetic interactions, (E/T), 25:5746
neutron capture at thermal to 1 MeV energies, energy dependence of γ-ray yields for, (T), 25:5777
neutron capture integral in fast region, (E), 25:5656

TANTALUM ISOTOPES Ta-182
labeling of Ambystoma with, for studies on breeding migrations, 25:4475 (NYO-3554-8)

TAURINE
radioinduced excretion of, in urine of human patients, relation of, to leukopenia, γ, 25:4603

XUM

radioprotective effects of, on man, γ, 25:4603
TD-NICKEL
fabrication of precision tubes of, equipment and methods for, 25:4745
mechanical properties of, effects of explosive shock deformation on, 25:4802
microstructure of, effects of explosive shock deformation on, 25:4802
TD-NICKEL CHROMIUM
mechanical properties of, effects of explosive shock deformation on, 25:4802
microstructure of, effects of explosive shock deformation on, 25:4802
TECHNETIUM ISOTOPES Tc-93
energy levels from proton resonances in molybdenum-92, spreading widths of isobaric analogs, (T), 25:5644
TECHNETIUM ISOTOPES Tc-95
energy levels from ruthenium-95 decay, spin-parity assignments for, (E), 25:5683 (IS-T-391)
TECHNETIUM ISOTOPES Tc-99
incorporation into erythrocytes, 25:4414
incorporation of metastable, in technetium dioxide, 25:4413
radiation dose from albumin-incorporated metastable, to man during lung scanning, methods for calculating absorbed, 25:4511
use for scanning human lungs for blood flow during ventricular failure, combined use with indium-113 for double scanning, 25:4677
use of aerosols of, combined with albumin-macroaggregate-incorporated-, for inhalation and perfusion scanning of human lungs, 25:4657 (UCLA-12-782, pp 89-125)
use of albumin microaggregate- or solution-incorporated-, for scanning blood circulation in liver, 25:4657 (UCLA-12-782, pp 89-125)
use of DTPA-incorporated, for scanning kidney transplants for function, 25:4657 (UCLA-12-782, pp 89-125)
use of metastable, for lung scanning, 25:4680
use of metastable, for lung scanning during pregnancy, effects of, on fetus, 25:4673
use of metastable, for lung scanning for diagnosis of diseases, 25:4676
use of metastable, for scintigraphy, design of instrumentation for, 25:4684
use of pertechnetate-incorporated metastable, for scanning human heart, 25:4659
use of pertechnetate-incorporated metastable, for brain scanning for tumor, localization, 25:4657 (UCLA-12-782, pp 89-125)
use of pertechnetate-incorporated metastable, for brain scanning in patient with Herpes zoster encephalitis, 25:4660
TECHNETIUM ISOTOPES Tc-101
energy levels from ruthenium-102 (γ,p) reactions at 26 MeV, half-lives for isomeric, (E), 25:5761
energy-level transitions from ruthenium-102 (γ,p) reactions at 26 MeV, gamma spectra from, (E), 25:5761
TECHNETIUM ISOTOPES Tc-103
beta decay of, γ singles and coincidence spectra from, (E), 25:5683 (IS-T-391)
nuclear spin and parity of, (E), 25:5683 (IS-T-391)
TECHNETIUM ISOTOPES Tc-104
beta decay of, β and γ singles and coincidence spectra from, (E), 25:5796
TECHNETIUM OXIDES
labeling with metastable technetium-99, 25:4413
TEETH
enamel density of, beta backscatter gage for measurement of, 25:4323 (NYO-4028-TA-1)
TELEVISION EQUIPMENT
design of computer-controlled mobile, for remote intelligence system, 25:4199
radiation emission by, survey of x, 25:4522 (BRH/DEP-70-24)
TELLURIUM
effects on vaporization of gallium arsenide single crystals, 25:4074 (UCRL-19685)
separaton from indium on tin by reversed-phase extraction chromatography, 25:4143
TELLURIUM ISOTOPES Te-124
deuteron elastic and inelastic scattering at 12 MeV, excitation energies and differential cross sections for, (E), 25:5729
energy levels from deuteron inelastic scattering, (E), 25:5729
TELLURIUM ISOTOPES Te-126
energy levels from isomeric antimony-126 beta decay, spin--parity assignments for, (E), 25:5693
energy-level transitions from isomeric antimony-126 beta decay, (E), 25:5693
TELLURIUM ISOTOPES Te-127
beta decay of ground-state and isomeric, beta and gamma spectra, Q-value, and log ft of, (E), 25:5734
TELLURIUM ISOTOPES Te-130
neutron activation resonance integrals of, thermal, (E), 25:5681 (CNEA-274)
TEMPERATURE
effects on shelf life of fish, 25:4734 (TID-25467)
effects on x-radiosensitivity of DNA in Micrococcus radiodurans and murine lymphoma cells, combined effects of oxygen content and radiation dose on, 25:4536
measurements in vortices behind heated rod obstructing flow stream, determination of fluid flow velocity from, 25:4205
physics of extreme pressure and, (T), 25:5235
TERBIUM
Hall effect in paramagnetic, ferromagnetic, and antiferromagnetic, 25:5182
Hall effect in single crystal of, at 4.2 to 350°K, 25:5177
Hall effect in single crystals of, anomalous magnetization dependence of, 25:5219
magnetic phase transition in, sound propagation near, 25:5186
magnetic properties of single crystals of, (E/T), 25:5194
magnetic properties of, magnon energies and exchange interactions, 25:5213
magnetic transition temperatures of single crystals of, pressure dependence of, (E/T), 25:5195
properties for use as encapsulating material for californium-252 sources for neutron capture gamma-ray spectroscopy, 25:4772
separation of trace amounts of, from aqueous nitric acid solutions by solvent extraction using D2EHPA in toluene containing trace amounts of uranium, 25:4150
TERBIUM ALLOYS AND SYSTEMS
Al--Tb, magnetic structure of TbAl, neutron-diffraction study, 25:5208
Co--Tb, magnetic resonance of $TbCo_3$ and Tb_2Co, microwave, 25:5200
Co--Tb, magnetic structure of $TbCo_2$, neutron diffraction study, 25:5210
Er-base--Tb, magnetic structure of, neutron-diffraction study, 25:5207
Ho--Tb, magnetic properties of, magnon energies and exchange interactions, 25:5213
Sb--Tb--Y, magnetic ordering transition, 25:5205
Tb--Y, Hall effect in paramagnetic, ferromagnetic, and antiferromagnetic, 25:5182
TERBIUM ISOTOPES Tb-155
energy levels from europium-153 (α,2nγ) reactions at 27 MeV and gadolinium-155 (d,2nγ) reactions at 13.5 MeV, Coriolis coupling in anomalous rotational, (E/T), 25:5783
energy-level transitions from europium-153 (α,2nγ) reactions at 27 MeV and gadolinium-155 (d,2nγ) reactions at 13.5 MeV, γ--γ coincidence measurements of, (E/T), 25:5783
TERBIUM ISOTOPES Tb-157
electron-capture decay of, Q values, branching and L_1/K capture ratios from, (E), 25:5748
TERBIUM ISOTOPES Tb-159
energy level at 137 keV, lifetime of, (E), 25:5727
neutron capture by polarized, angular distribution of γ-rays from thermal, (E), 25:5717
TERBIUM ISOTOPES Tb-160
energy levels from terbium-159 thermal neutron capture, spin assignments for, (E), 25:5717
TERBIUM ISOTOPES Tb-161
beta decay of, sum coincidence spectra from, (E), 25:5714
TERBIUM OXIDES
electric conductivity of $TbO_{1.8}$ +y and $TbO_{1.714}$ -z, stable domains from, (E), 25:5179
magnetic structure of, (T), 25:5215
TESTES
radiation effects on isoenzymes of lactate dehydrogenase in, of rats, protective effects of methylene blue against whole-body γ, 25:4605
radiation effects on, of rats, effects of, on elimination of 17-ketosteroids and histological structure, 25:4707
THALLIUM
complexes with 8-quinolinol, structure of, NMR spectral studies on, 25:4081
THALLIUM IONS
radioinduced color centers in potassium chloride crystals doped with, γ-, 25:5157
THALLIUM ISOTOPES Tl-199
energy levels from gold-197 (α,2n) reactions, oblate shape of $^1/_2^-$ isomeric, (E), 25:5707
THALLIUM ISOTOPES Tl-203
energy levels from gamma resonant scattering, (E), 25:5713
energy levels from neutron inelastic scattering, spin--parity assignments for, (E), 25:5798
neutron inelastic scattering at 0.6 to 1.6 MeV, γ spectra from, (E), 25:5798
THALLIUM ISOTOPES Tl-204
determination by β counting using G-M and proportional detectors, efficiency curves for, 25:4029 (CISE-N-119)
THALLIUM ISOTOPES Tl-205
energy levels from neutron inelastic scattering, spin--parity assignments for, (E), 25:5798
neutron inelastic scattering at 0.6 to 1.6 MeV, γ spectra from, (E), 25:5798
THALLIUM ISOTOPES Tl-206
beta decay of, weak branching in, (E), 25:5645
THALLIUM ISOTOPES Tl-207
isomeric shifts and magnetic hyperfine splitting in μ-mesic, quasi-particle calculation of, (T), 25:5794
THALLIUM ISOTOPES Tl-208
energy-level transitions from radiative pion absorption

by lead-208, strengths for, (T), 25:5793
THERMAL STRESSES
effects on piping components and systems, summary of experience on, 25:4188 (TID-25553)
THERMIONIC CONVERTERS
collectors and emitters for, development of coatings for, 25:4750 (TEE-4125-2)
design of, using heat from nuclear reactor, 25:4994(P)
development of plutonium-238-fueled, for cardiac pacemakers, 25:4237
electrode performance for, fluoride vapor-deposited tungsten--niobium, (E), 25:4953 (TEE-4125-1)
emitters for, method for determining temperature of, 25:4752 (TEE-4125-4)
performance of diode-type, incorporating niobium collectors and tungsten emitters, 25:4751 (TEE-4125-3)
THERMOCOUPLES
insulators for sheathed, methods for measuring compaction of ceramic, 25:4402
THERMOELECTRIC CONVERTERS
design and operation of Maple IB cobalt-60-fueled, for terrestrial uses, 25:4226
design of 30W cobalt-60-fueled, for terrestrial power systems, 25:4224
design of cobalt-60-fueled, 25:4224
design of plutonium-238-fueled, for powering implantable artificial heart, 25:4235
development of plutonium-238-fueled, for implantable cardiac pacemakers, French program for, 25:4239
heat sources for, gamma and neutron spectra of radioisotope, 25:4242
radiation from radioisotope, response of silicon detectors to, 25:4356
radiation from radioisotope, sensitivity of G--M detectors to gamma, 25:4349
radiation from radioisotope, sensitivity of shielded silicon detectors to gamma, 25:4350
radiation from spacecraft-borne radioisotope, effects on instruments of, 25:4409
THERMOMETERS
design of pulsed ultrasonic, for high temperatures, 25:4388 (DP-Report-498)
design of resonant probe, for high temperatures, 25:4389 (DP-Report-590)
THERMONUCLEAR REACTIONS
production by highly concentrated electron beams, 25:5118(P)
theory for complete fusion, 25:5115 (JINR-P4-5019)
THERMONUCLEAR REACTORS
bibliography on plasma physics and fusion reactors, 25:5067
ion heating in toroidal, current-induced turbulent, (E), 25:5069
plasma confinement in high-field toroidal quadrupole, (T), 25:5070
radiation damage effects in containment vessel of, 25:5114 (CLM-R-103)
review for teaching purposes, 25:5100
THERMOSPHERE
density variations in, calculations from in situ pulse generation data, (T), 25:5016
THICKNESS GAGES
detectors for radiometric, avalanche semiconductor, 25:4323 (NYO-4028-TA-1)
response function of beta backscatter, for elements Z = 4 to 82, 25:4386
THIOLS
radioprotective effects of amino-, reaction mechanisms for, 25:4592
radioprotective effects of, on bacteria and bacteriophages, γ, 25:4549
radioprotective effects of, relation of molecular structure to, 25:4548
reactions of amino-, with radioinduced free radicals in bacteria, 25:4548
THORIUM
complexes with 8-quinolinol, structure of, NMR spectral studies on, 25:4081
complexes with maleic acid, preparation and thermal behavior of, 25:4075
compounds with carboxylic acids, preparation by reactions of thorium acetate with acids, 25:4056
content in Pacific Ocean phillipsites, 25:4164
content of biological materials, photometric methods for determining, 25:4443
determination in aqueous and organic solutions by colorimetry using Thoron, automatic, 25:4014 (NLCO-1072)
determination in aqueous solution by photochemical precipitation, 25:4026
effects on Kondo effect in $CeAl_2$, 25:5228
metabolism in tissues of rats following intraperitoneal, intramuscular, and oral administration of, 25:4441
properties of, review of physico-chemical and physical, 25:4440
separation by ion exchange using Alamine 336 or Amberlyst A-21 in aqueous thiocyanate solutions, 25:4137 (IS-T-377)
separation from rare earths in bismuth solution by fractional crystallization, 25:4138 (ORNL-TM-3053)
separation from scandium by ion exchange in thiocyanate solutions using Amberlyst A-21, 25:4137 (IS-T-377)
separation from titanium by ion exchange in thiocyanate solutions using Amberlyst A-21, 25:4137 (IS-T-377)
solvent properties of alpha, for protactinium at 25 and 1300°C, 25:4791
uptake by macrophages and pneumocytes of rat lungs, 25:4410
THORIUM ACETATES
reactions with carboxylic acids, yields of thorium carboxylates from, 25:4056
THORIUM ALLOYS AND SYSTEMS
Gd-base--Th, magnetic ordering and thermoelectric properties of, 25:5169 (IS-T-379)
Pa--Th-base, crystal structure of, 25:4791
Th--Y-base, magnetic ordering and thermoelectric properties of, 25:5169 (IS-T-379)
THORIUM CARBIDES
ThC_2--U, fission product retention in carbon-coated fuel particles of, xenon release method for determination of, 25:4882 (DP-Report-436)
ThC_2--UC_2, preparation and properties of coated particle fuels, 25:5942(R) (DP-Report-490)
THORIUM CHLORIDES $ThCl_4$
complexes with alkyl alcohols, formation of crystalline, thermodynamics of, 25:4077
formation of crystalline and gaseous, thermodynamics of, 25:4077
toxicity in mice in comparison with thorium dioxide and thorium nitrate, 25:4440
THORIUM ISOTOPES Th-224
placental transfer of decay products of, hazards to fetuses from, 25:4673
THORIUM ISOTOPES Th-231
energy levels from thorium-232 (d,t) reactions, spin--parity assignments and spectroscopic factors for, (E), 25:5797
THORIUM ISOTOPES Th-232
book: The Toxicology of Radioactive Substances, Volume 4: Thorium-232 and Uranium-238, 25:4438
deuteron reactions (d,t) at 17 MeV, triton spectra from, (E), 25:5797
meson (K) and (π) absorption widths in, corrections due to admixtures of excited energy levels, (T), 25:5866
neutron fission of, energy integral test of cross section for, (E/T), 25:5773
neutron resonance absorption interference effects in graphite moderated homogeneous reactors, 25:5558
photofission at 5 to 10 MeV, prompt and delayed neutron yields from, (E), 25:5768
THORIUM NITRATES
toxicity in mice in comparison with thorium chloride and thorium dioxide, 25:4440
THORIUM OXIDES
book: The Toxicology of Radioactive Substances, Volume 4: Thorium-232 and Uranium-238, 25:4438
THORIUM OXIDES ThO_2
creep strain of, effects of grain-boundary porosity growth on high-temperature, 25:4848
detection of simulated airborne fuels of, pressure sensitive type method for, 25:4216(R) (SC-PR-70-682)
distribution in tissue of rats following intratracheal and intraperitoneal administration, 25:4442
effects on arterial pressure in rats following intratracheal and intraperitoneal injection, 25:4701
effects on hematopoiesis in rats following intratracheal injection, 25:4700
effects on human liver 20 years after use for angiography, neoplastic, 25:4716
effects on stimulation threshold of muscle-nerve apparatus in hind paws of rats following intratracheal and intraperitoneal injection, 25:4701
neutron resonance integrals for rods of, (E/T), 25:6205
pressing of powders of, effects of pressure and temperature on hot, 25:4836
reduction by calcium, thermodynamics of, 25:4054(T) (IS-Trans-83)
toxicity in mice in comparison with thorium chloride and thorium dioxide, 25:4440
toxicity of, review of, 25:4439
$DyUO_4$--ThO_2, spectra and phase studies of, 25:4084
$GdUO_4$--ThO_2, spectra and phase studies of, 25:4084
$HoUO_4$--ThO_2, spectra and phase studies of, 25:4084
$NdUO_4$--ThO_2, spectra and phase studies of, 25:4084
ThO_2--UO_2, radiation testing of coated particle fuels of, 25:5990(R) (ORNL-4589)
ThO_2--$YbUO_4$, spectra and phase studies of, 25:4084
ThO_2--YUO_4, spectra and phase studies of, 25:4084
THORIUM PERCHLORATES
complexes with antipyrine, ir spectra and physical properties of, 25:4087
THULIUM
separation from aqueous chloride solutions by solvent extraction using cyclooctylphenylphosphinic acid or octylphenylphosphinic acid, 25:4147
separation of trace amounts of, from aqueous nitric acid solutions by solvent extraction using D2EHPA in toluene containing trace amounts of uranium, 25:4150
THULIUM ALLOYS AND SYSTEMS
Al--Tm, magnetic structure of TmAl, neutron-diffraction study, 25:5208
Al--Tm, thulium-169 NMR in $TmAl_2$, 25:5226
Sb--Tm, thulium-169 NMR in TmSb, 25:5226

XUM

THULIUM ARSENIDES
thulium-169 NMR in, 25:5226
THULIUM ISOTOPES Tm-167
energy levels from holmium-165 (α,2n) reactions, (E), 25:5726
THULIUM ISOTOPES Tm-169
nuclear magnetic resonance in thulium intermetallic compounds, 25:5226
THULIUM ISOTOPES Tm-170
gamma spectra of, precision measurements of low-energy, 25:5736
THULIUM ISOTOPES Tm-171
half-life of isomeric, (E), 25:5721
THULIUM ISOTOPES Tm-175
beta decay of, gamma spectra for, (E), 25:5747
THULIUM PHOSPHIDES
thulium-169 NMR in, 25:5226
THULIUM SELENIDES
thulium-169 NMR in, 25:5226
THYMINE
radiolysis of, in frozen solutions, γ, 25:4459 (UCLA-12-762, pp 23-47)
THYMUS GLAND
removal of, effects on granulocyte regeneration in blood of x-irradiated mice, 25:4469
replication of DNA in neoplastic and normal tissues of, in mice, 25:4460
surgical removal from chickens, combined effects of cobalt-60 γ radiation and, on cellular immunological reactions, 25:4468
synthesis of DNA and RNA in, of rats, effects of AET, cysteamine, 2-mercaptoethanol, and penicillamine on, 25:4552
THYROID GLAND
content of stable iodine in, measurement by x-ray fluorescence scanning, 25:4682
iodine-131 uptake studies in, of man, dose standardization for, 25:4661
TIN
antiproton absorption at 20 to 65 GeV/c, cross sections for, (E), 25:5295
antiproton absorption cross sections at 20 to 40 GeV/c, (E), 25:5265 (CONF-700314-, Paper 4)
complexes with 8-quinolinol, structure of, NMR spectral studies on, 25:4081
determination in PuO_2--U_3O_8, effects of ratio of plutonium oxide to uranium oxide on spectrographic, 25:4015 (NUMEC-3524-76)
meson (K^-) absorption at 20 to 65 GeV/c, cross sections for, (E), 25:5295
meson (K^-) absorption cross sections at 20 to 40 GeV/c, (E), 25:5265 (CONF-700314-, Paper 4)
meson (π^-) absorption at 20 to 65 GeV/c, cross sections for, (E), 25:5295
meson (π^-) absorption cross sections at 20 to 40 GeV/c, (E), 25:5265 (CONF-700314-, Paper 4)
neutron elastic scattering at 4 MeV, differential cross sections and polarizing abilities at 150 to 180° from, (E), 25:5762
photon reactions (γ,t) at 90 MeV, triton yield in, (E), 25:5678
properties for use as encapsulating material for californium-252 sources for neutron capture gamma-ray spectroscopy, 25:4772
separation by ion exchange using Alamine 336 in aqueous thiocyanate solutions, 25:4137 (IS-T-377)
separation from antimony, indium, and tellurium by reversed-phase extraction chromatography, 25:4143
superconducting Josephson effect in point contacts with normal metal, 25:5037
TIN ALLOYS AND SYSTEMS
La--Sn, electron band structure calculations for $LaSn_3$, comparison of standard and modified orthogonalized plane-wave, 25:5231
TIN ISOTOPES Sn-110
energy levels from (p,t) reactions, (E), 25:5799
mass excess for, (E), 25:5759
TIN ISOTOPES Sn-112
energy levels from (p,t) reactions, (E), 25:5799
oxygen-16 reactions at 62 and 88 MeV, gamma spectra from, (E), 25:5688 (UCRL-15961)
proton reactions (p,t) at 20 MeV, cross section for, (E), 25:5799
TIN ISOTOPES Sn-114
energy levels from (p,t) reactions, (E), 25:5799
proton reactions (p,t) at 20 MeV, cross section for, (E), 25:5799
TIN ISOTOPES Sn-116
energy levels from (p,t) reactions, (E), 25:5799
energy levels from proton inelastic scattering, spin-parity assignments for, (E), 25:5506 (CEA-N-1232, pp 81-159)
proton reactions (p,t) at 20 MeV, cross section for, (E), 25:5799
TIN ISOTOPES Sn-118
energy levels from (p,t) reactions, (E), 25:5799
energy levels from proton inelastic scattering, spin-parity assignments for, (E), 25:5506 (CEA-N-1232, pp 81-159)
proton reactions (p,d) at 24.5 MeV using polarized beams, cross section and asymmetry for, (E), 25:5506 (CEA-N-1232, pp 81-159)
proton reactions (p,t) at 20 MeV, cross section for, (E), 25:5799
TIN ISOTOPES Sn-119
gamma resonance absorption by, interference between photoelectric effect and internal conversion in M1, (E), 25:5787
TIN ISOTOPES Sn-120
energy levels from (p,t) reactions, (E), 25:5799
energy levels from proton inelastic scattering, spin-parity assignments for, (E), 25:5506 (CEA-N-1232, pp 81-159)
proton reactions (p,t) at 20 MeV, cross section for, (E), 25:5799
TIN ISOTOPES Sn-122
energy levels from proton inelastic scattering, spin-parity assignments for, (E), 25:5506 (CEA-N-1232, pp 81-159)
energy levels from tin-124 (p,t) reactions, spin--parity assignments for, (E), 25:5799
proton reactions (p,t) at 20 MeV, cross section for, (E), 25:5799
TIN ISOTOPES Sn-124
energy levels from proton inelastic scattering, spin-parity assignments for, (E), 25:5506 (CEA-N-1232, pp 81-159)
proton reactions (p,t) at 20 MeV, cross section for, (E), 25:5799
TISSUES
lipid content of soft human, methods for measurement of, using dual beam γ transmission scanning, 25:4646 (CONF-700515-, pp 272-3)
radiation effects on cultured callus, from Phaseolus, cobalt-60 γ, 25:4723
surgical removal of bursa of Fabricus, from chickens, effects on immune reactions of γ-irradiated chickens, 25:4468
uranyl nitrate effects on production of sucrose in scutellum, of corn, 25:4720
TITANIUM
determination in boron, 25:4009 (TID-25196)
determination using N-cinnamoyl-N-phenyl- and N-benzoyl-N-p-tolylhydroxylamines, spectrophotometric method for, 25:4020
effects of alloying additions of, on purification of iron--nickel vacuum melts, relations with composition and reduced pressure, 25:4744
effects on automatic colorimetric determination of thorium in aqueous and organic solutions, 25:4014 (NLCO-1072)
electronic density of states of hcp and bcc, from bremsstrahlung isochromates, 25:5187
properties for use as encapsulating material for californium-252 sources for neutron capture gamma-ray spectroscopy, 25:4772
properties for use in electrolytic separation of bromine-80 isomers, 25:4127
radioinduced helium production in, fission neutron, 25:4822
separation by ion exchange using Alamine 336 or Amberlyst A-21 in aqueous thiocyanate solutions, 25:4137 (IS-T-377)
separation from thorium by ion exchange in thiocyanate solutions using Amberlyst A-21, 25:4137 (IS-T-377)
Al--Ti-base--V, fabrication of precision tubes of, equipment and methods for, 25:4745
TITANIUM ALLOYS AND SYSTEMS
analysis for niobium using 4-(2-pyridylazo)resorcinol, photometric, 25:4018
Al--Ti-base--V, crack growth in, at sustained loads, effects of hydrogen on, 25:4762
Al-base--B--Ti, microstructure of master alloys of, evaluation of, 25:4780
Al-base--B--Ti, properties of master alloys of, evaluation of chemical and physical, 25:4780
Al-base--Ti, microstructure of master alloys of, evaluation of, 25:4780
Al-base--Ti, properties of master alloys of, evaluation of chemical and physical, 25:4780
Pu--Ti-base, plutonium segregation in, effects of anneal temperature, cooling rate, and oxygen on, 25:4790
Ti--V, phase transformations in beta isomorphous, 25:4806
Ti--V, phase transformations in beta isomorphous, comments on, 25:4805
TITANIUM CARBIDES
corrosion by sodium of bearing coatings of, at 1100°F, 25:4185(R) (NYO-3930-8)
superconductivity of hypostoichiometric, (E), 25:5038
NbC--TiC, electric conductivity and thermal electromotive forces in homogeneous, temperature effects on, 25:5176
Ni--TiC, corrosion by sodium of bearing coatings of, at 1100°F, 25:4185(R) (NYO-3930-8)
TITANIUM ISOTOPES Ti-47
energy levels of, spins, parities, and angular moments of, (E), 25:5629
TITANIUM ISOTOPES Ti-50
energy level of, lifetime of lowest 6+, (E), 25:5646
proton reactions (p,γ) at 1.3 to 2.7 MeV, excitation functions, angular distributions, and gamma spectra from, (E), 25:5651

TITANIUM ISOTOPES Ti-51
beta decay of, log-ft values for, (T), 25:5658
TITANIUM ORES
analysis for composition by neutron capture gamma spectroscopy using californium-252 source, 25:4036
TITANIUM OXIDES
analysis for niobium using sodium butyldithiocarbaminate, spectrophotometric, 25:4017
determination in titanium ore by neutron capture gamma spectroscopy using californium-252 source, 25:4036
TITANYL PERCHLORATES
complexes with antipyrine, ir spectra and physical properties of, 25:4087
TOKAMAK DEVICES
plasma density and temperatures in T3-A, (E), 25:5079 (CLM-R-107)
plasma drift in, effects of electrostatic fields on untrapped, (T), 25:5071
plasma equilibrium and stability in, thermal, (T), 25:5117
p-TOLUAMIDE, N-ISOPROPYL-α-(2-METHYLHYDRAZINO)-
effects on radiosensitivity of neoplasms in human lungs, ionizing, 25:4689
TOXICITY
book: The Toxicology of Radioactive Substances, Volume 4: Thorium-232 and Uranium-238, 25:4438
review of thorium dioxide and uranic oxide, 25:4439
TRACER TECHNIQUES
book: Pulmonary Investigation with Radionuclides, 25:4662
medicine, use of iodine-131 uptake as test of thyroid function, standardization of tracer for, 25:4661
use of autoradiography in, suggestions concerning, 25:4416
TRANSACTINIDE ELEMENTS
fission fragments of, mass and charge distributions of, (E), 25:5691
properties of, handbook on physical and nuclear, 25:5722
research on, review of, 25:5719
TRANSITION METAL ALLOYS AND SYSTEMS
rare earths--transition metals, magnetic properties of R_2M intermetallic compounds, 25:5199
TRANSITION METAL BORIDES
boron-11 NMR in, 25:5229
TRANSITION METAL OXIDES
radiation effects on catalytic properties of, in decomposition of hydrogen peroxides, 25:4099
TRANSITION METALS
superconducting order-parameter motion in Type-II, in high magnetic field, 25:5050
superconductivity in, Froehlich mechanism for, 25:5047
TRANSPLANTS
scanning of kidney, for function in man, use of metastable indium-113-labeled chelates or metastable technetium-99-labeled DTPA for, 25:4657 (UCLA-12-782, pp 89-125)
scanning of lung, for function in dogs, 25:4657 (UCLA-12-782, pp 89-125)
TRANSPORT THEORY
approximations deduced from association of Milne and Schroedinger equations, 25:5234 (CEA-R-4007)
coefficients in, exact bounds on, 25:6242 (NYO-1480-160)
energy representations in neutron, review of alternatives to direct multigroup treatments of, 25:5141
equations for neutron, quantum correction of, (T), 25:6167
orthogonality in finite slab geometry, 25:5140
phase space time evolution method for, 25:5139
photon--electron, for materials, Klein--Nishina cross sections for scattered electrons from, 25:5167
radiation doses at fixed points from moving source, 25:5243
radiation transfer operators for shielding, multigroup discrete ordinates, 25:5144
radiative transfer, thermal x-ray, 25:5142
solution for electron, modification of phase space time evolution method for, 25:5242
solution of initial-value problem for slab with infinite reflectors using normal-mode expansions, (T), 25:5501
TRANSURANIUM ELEMENTS
energy levels of, calculation using Saxon--Woods potential, (T), 25:5684 (JINR-P4-5221)
nuclear deformation parameters and quadrupole and hexadecapole moments for, (T), 25:5860
TRAPS
design of low temperature charcoal adsorption, for rocket reactor coolant exhaust, 25:6142
as-TRIAZINE-3,5(2H,4H)-DIONE
effects on x-radiosensitivity of cells of carcinomas and sarcomas in mice and rats, 25:4590
s-TRIOXANE
radioinduced polymerization of solid, production of polyacetal resin by electron, 25:4098
TRITIUM
beta decay of, tensor forces and exchange currents in, (T), 25:5542
binding energies, ground-state radii, and charge and magnetic form factors using Faddeev equations and realistic local potentials, (T), 25:5833
binding energy and nuclear radius of, calculation using Bolsterli--Feenberg perturbation technique, (T), 25:5537
charge-asymmetry energy of, relative to helium-3, (T), 25:5812
deuteron reactions (d,α) at 51, 76, and 93 keV using polarized beams, analyzing power for, (E), 25:5525 (LA-4465, pp 34.1-2)
deuteron reactions (d,n) at 4 to 15 MeV using polarized beam, neutron polarization in, (E), 25:5513 (LA-4465, pp 12.1-2)
deuteron reactions (d,n) at 7 and 11.4 MeV, polarization angular distribution from, (E), 25:5522 (LA-4465, pp 29.1-2)
deuteron reactions (d,n) with, quadratic relation between observables in polarization transfer, (T), 25:5519 (LA-4465, pp 22.1-2)
development of targets of, for fast neutron production, 25:5503(P)
diffusion in Type 304 stainless steel, 25:5152(R) (ORO-3508-6)
distribution and residence time of, in Project Sedan crater ejecta, (E), 25:4181
energy losses of recoil atoms of, calculation of mean logarithmic elastic, 25:4957
neutron elastic scattering at 22.1 MeV, polarization in, (E), 25:5516 (LA-4465, pp 15.1-2)
proton elastic scattering at 13.6 MeV using polarized beam, asymmetry for, (E), 25:5521 (LA-4465, pp 28.1-2)
reactions of recoil, comparison of reactions of hot deuterium or hydrogen atoms with, 25:4132
reactions of recoils of, with acetonitrile and methyl isocyanide, kinetics of, 25:4131
release to environment, sources and levels of, 25:5941
TRITONS
binding energy of, lower limit for, (T), 25:5830
binding energy of, t-matrix perturbation theory for, (T), 25:5389
hydrogen mesic-atom reactions with, isotope exchange in, (T), 25:4952 (JINR-P4-5039)
reactions (t,p) with strontium-86 at 15 MeV, proton spectra and angular distributions for, (E), 25:5615
scattering by helium-4 at 6 to 12.3 MeV, absolute polarization in elastic, (E), 25:5518 (LA-4465, pp 19.1-2)
scattering by helium-4 at 6 to 15 MeV, triton polarization in elastic, (E), 25:5511 (LA-4465, pp 5.1-2)
TROPOSPHERE
barium-140 distribution in, 25:4163
strontium-90 distribution in, 25:4163
TRYPTOPHAN
effects on growth of γ-irradiated Triticum vulgare, 25:4718
TRYPTOPHAN, N-TRYPTOPHYL-
radiolysis of aerated solutions of, yields from γ and x, 25:4114
TUBES
mechanical properties of zirconium pressure, effects of hydrogen pickup and neutron radiation on, 25:6151 (RISO-214, pp 255-87)
reliability analysis of SAP pressure, 25:5584 (RISO-214, pp 335-43)
stability in curved steam generator, measurement of hydrodynamic, 25:4208
TUNGSTEN
analysis of high-purity, for fluorine by photon activation, 25:4043 (GA-10125)
crystallization in aluminum--potassium--silicon-doped wire of, at 1400 to 1600°C, effects of porosity on anomalous, 25:4799
determination in boron, 25:4009 (TID-25190)
diffusion of carbon in, at 1500 to 1800°C, carbon-14 tracer studies of, 25:4763
effects of alloying additions of, on purification of iron--nickel vacuum melts, relations with composition and reduced pressure, 25:4744
ion reactions at 10 to 30 eV with single-crystal, electron yields and energy distributions from, (E), 25:4943
performance of emitters of, in fixed-spacing diodes, 25:4750 (TEE-4125-2)
performance of fluoride chemical vapor deposited emitters of, for thermionic converters, 25:4751 (TEE-4125-3)
preparation of coated cesiated thermionic emitters of, method for, 25:4750 (TEE-4125-2)
properties for coating niobium thermionic collectors, 25:4750 (TEE-4125-2)
properties for use as encapsulating material for californium-252 sources for neutron capture gamma-ray spectroscopy, 25:4772
structure of work-hardened surface layers of, effects of vacuum annealing on, 25:4797
temperature of thermionic converter emitters of, method for determination of, 25:4752 (TEE-4125-4)
thermal capacity of, Debye--Waller factor for, 25:5170 (JINR-P14-5358)
TUNGSTEN ALLOYS AND SYSTEMS
C--W, diffusion of carbon in, effects of rhenium additions on, 25:4746 (AD-710275)
Nb--Ni--W, phase diagrams at 1800 and 1900°C, isothermal, 25:4788
Ni--W, electric conductivity and short-range order of deformed, 25:4766

XUM

Ni--W, phase diagram at 1400 to 2100°C, 25:4788
Ni-base--W, crystal structure of metastable Ni_3W phase in, 25:4789
Ni-base--W, phase studies of metastable Ni_3W phase in, 25:4789
Ni-base--W, phase studies of metastable Ni_3W phase in, relations with heat treatments, 25:4794
Re--W-base, diffusion of carbon in, at 1500 to 1800°C, carbon-14 tracer studies of, 25:4763
TUNGSTEN CARBIDES
Co--WC, corrosion by sodium of bearing coatings of, at 1100°F, 25:4185(R) (NYO-3930-8)
TUNGSTEN ISOTOPES W-178
energy levels from rhenium-178 decay, (E), 25:5733
TUNGSTEN ISOTOPES W-181
electron-capture decay of, x-ray singles and x-ray--γ coincidence spectra from, (E), 25:5753
TUNGSTEN ISOTOPES W-186
neutron capture integral in fast region, (E), 25:5656
TUNGSTEN OXIDES
sorptive properties of hydrated, for astatine from nitric acid, 25:4053(T) (ANL-Trans-861)
TYROSINE, N-TRYPTOPHYL-
radiolysis of aerated solutions of, yields from γ and x, 25:4114

U

ULTRASOUND
effects on germination of sugarbeet seeds, 25:4722
ULTRAVIOLET RADIATION
effects on colony forming ability of Escherichia coli, effects of acetone on, 25:4728
effects on DNA in Escherichia coli, role of replication in repair of, 25:4463
effects on DNA synthesis in Schizomycota, species differences in, 25:4462
effects on Escherichia coli, effects of amino acid starvation on DNA repair synthesis and survival following, 25:4731
effects on Escherichia coli, effects of BUdR incubation on, 25:4725
effects on eyes and skin of personnel, during use to detect forgeries of bank notes, 25:4710
effects on human skin, effectiveness of sunscreening creams against, 25:4608
effects on infectivity of herpes simplex virus, effects of uv-irradiated host cells on, 25:4727
effects on mutants of yeast, effects of, on sensitivity to methyl methanesulfonate and nitrogen mustard, 25:4480
effects on rabbit kidneys, protective effects of stimulation of vagus nerve against hypertension induced by, 25:4697
effects on reoviruses, inactivating, 25:4729
effects on survival of HeLa cell strains, effects of caffeine on, 25:4607
spectrum of solar extreme, effect of solar cycle on, (E), 25:4925
UNITED STATES
nuclear weapons development in, for defensive and offensive uses, 25:4167 (CONF-691051-, pp 192-8)
radioactive waste management in, status of programs for, 25:4275
safeguards systems in, development of improved, 25:4270
URACIL, 5-BROMO-
incorporation in DNA, effects of, on electron-radiosensitivity, 25:4542
URACIL, 5-FLUORO-
effects on radiosensitivity of human brain tumors, combined effects of 5-bromodeoxyuridine on ionizing, 25:4688
effects on radiosensitivity of human neoplasms, combined effects of 5-bromodeoxyuridine or 5-iododecxyuridine on ionizing, 25:4602
effects on x-radiosensitivity of spleen colony formation by bone marrow cells following transplantation into syngenic mice, 25:4570
URACIL, 6-PROPYL-2-THIO-
effects on cesium-134 retention in adrenalectomized rats, 25:4450
URANIUM
analysis for trace amounts of rare earths by chemical separation and spectroscopy, 25:4021
antiproton absorption at 20 to 65 GeV/c, cross sectons for, (E), 25:5295
antiproton absorption cross sections at 20 to 40 GeV/c, (E), 25:5265 (CONF-700314-, Paper 4)
argon-40 fission of, production cross sections for Z = 42 to 79 isotopes in, (E), 25:5756
carbon-12 fission of, production cross sections for Z = 42 to 79 isotopes in, (E), 25:5756
complexes of hexavalent, with sodium rhodizonate in perchlorate medium, kinetic studies on, 25:4078
complexes with 8-quinolinol, structure of, NMR spectral studies on, 25:4081
complexes with EDTA, electrochemistry of, 25:4081
complexes with hydroxamic acids, stability studies on, 25:4083
complexes with maleic acid, preparation and thermal behavior of, 25:4075
complexes with phenanthrenequinone oxime, potentiometric studies on formation constants of, 25:4080
compounds with carboxylic acids, preparation of, 25:4057
compounds with mandelic acid, preparation by reactions of uranium alkoxides with mandelic acid, potentiometric studies on, 25:4055
content in Pacific Ocean phillipsites, 25:4164
criticality of arrays of cylinders of, effects of water sprays on, 25:4282
determination simultaneously with iron or plutonium using platinum working electrode, coulometric, 25:4025
effects on separation of trace amounts of rare earths from aqueous solutions of nitric acid by solvent extraction using D2EHPA in toluene, 25:4150
electrochemical behavior in acetic--chromic acid and Mott's solution, 25:4792
enrichment by gas centrifugation, effects on world peace from development of technology for, 25:4213 (CONF-691051-, pp 145-53)
enrichment by gas centrifugation, effects on world peace from development of technology for, 25:4214 (CONF-691051-, pp 354-61)
fabrication of fuels of, since 1955, economics of methods for, 25:4743
meson (K⁻) absorption at 20 to 65 GeV/c, cross sections for, (E), 25:5295
meson (K⁻) absorption cross sections at 20 to 40 GeV/c, (E), 25:5265 (CONF-700314-, Paper 4)
meson (π⁻) absorption at 20 to 65 GeV/c, cross sections for, (E), 25:5295
meson (π⁻) absorption cross sections at 20 to 40 GeV/c, (E), 25:5265 (CONF-700314-, Paper 4)
microstructure of, potentiostatic method for studying, 25:4792
neon-20 fission of, production cross sections for Z = 42 to 79 isotopes in, (E), 25:5756
neon-22 fission of, production cross sections for Z = 42 to 79 isotopes in, (E), 25:5756
neutron elastic scattering at 4 MeV, differential cross sections and polarizing abilities at 150 to 180° from, (E), 25:5762
properties of, effects of impurities of aluminum, chromium, iron, nickel, silicon, and zirconium on, 25:4747 (AWRE-O-63/70)
proton fission at 159 MeV to 18.2 GeV, isomeric yield ratios for indium-117 from, (E), 25:5784
proton fission at 570 MeV and 18.2 GeV, charge dispersion curves for A = 117 nuclei from, (E), 25:5784
proton fission at 570 MeV and 18.2 GeV, cross sections for indium isotope production from, (E), 25:5784
proton fission at 570 MeV and 18.2 GeV, excitation functions for indium-111 production from, (E), 25:5784
radiation effects on sputtering of, fission fragment, 25:4827
separation by ion exchange using Alamine 336 or Amberlyst A-21 in aqueous thiocyanate solutions, 25:4137 (IS-T-377)
separation from aqueous chloride solutions by solvent extraction using cyclooctylphenylphosphinic acid or octylphenylphosphinic acid, 25:4147
separation from rare earths by ion exchange in thiocyanate solutions using Amberlyst A-21, 25:4137 (IS-T-377)
separation from spent fuels or irradiated raw materials by solvent extraction, 25:4144(P)
separation of cerium or thorium from, by photochemical precipitation, 25:4026
separation of spent, from fission products by nitride precipitation from liquid tin-uranium alloys, 25:4149
URANIUM ACETATES
preparation by reactions of acetic acid, uranyl acetate, uranyl chloride, and zinc amalgam, 25:4057
reactions of tetravalent, with carboxylic acids, preparation of uranium(IV) carboxylates from, 25:4057
URANIUM ALLOYS AND SYSTEMS
Bi--U, enthalpy of formation of intermetallic, direct-reaction calorimetric preliminary measurement of, 25:4843
C--U, preparation of, method for, 25:4747 (AWRE-O-63/70)
Nb--U-base, corrosion crack initiation in, effects of electrochemical and metallurgical variables on stress, 25:4749 (SC-DR-70-718)
Nb--U-base--Zr, corrosion crack initiation in, effects of electrochemical and metallurgical variables on stress, 25:4749 (SC-DR-70-718)
O--U, phase studies to 1600°C and 60 kilobars, 25:4753
Sb--U, enthalpy of formation of intermetallic, direct-reaction calorimetric measurement of, 25:4843
ThC_2--U, fission product retention in carbon-coated fuel particles of, xenon release method for determination of, 25:4882 (DP-Report-436)
URANIUM ARSENIDES
enthalpy of formation of, direct-reaction calorimetric measurement of, 25:4843
URANIUM CARBIDES
bubbles and grain boundaries in, binding energy for, 25:4850
radiation effects on crystal structure of, relations of annealing with fission neutron, 25:4887 (KFK-1215)
PuC--UC, radiation effects on cracking of sodium-bonded Type 316 stainless steel-clad, thermal neutron,

25:4894
PuC--UC, radiation effects on Incoloy 800-clad fuel pellets of, in-pile, 25:4889(R) (UNC-5263)
PuC--UC, radiation effects on sodium-bonded clad fuels of, in-pile, 25:4889(R) (UNC-5263)
PuC--UC, radiation effects on stainless steel-clad fuel pellets of, in-pile, 25:4889(R) (UNC-5263)
ThC_2--UC_2, preparation and properties of coated particle fuels, 25:5942(R) (DP-Report-450)
URANIUM CHLORIDES UCl_4
complexes with alkyl alcohols, formation of crystalline, thermodynamics of, 25:4077
formation of crystalline and gaseous, thermodynamics of, 25:4077
URANIUM FLUORIDES UF_4
complexes with diethylamine, hydrazine, methylamine, and tetramethylammonium fluoride, preparation of, 25:4058
vapor pressure of solid, at 555 to 1007°C, 25:4079
URANIUM FORMATES
reactions with ammonium acid fluoride, preparation of uranium ammonium fuoride from, 25:4058
URANIUM ISOTOPES
energy level transitions in, role of static charge of nucleus in determining probability of E0 pair conversion of, (T), 25:5791
URANIUM ISOTOPES U-232
energy levels of, deformation-dependence of energy of γ-vibrational, (T), 25:5779
URANIUM ISOTOPES U-233
neutron absorption at 0.02 to 1 eV, eta factor for, (E), 25:5702
neutron capture at 0.02 to 1 eV, cross section for, (E), 25:5702
neutron fission at 0.02 to 1 eV, cross section for, (E), 25:5702
neutron fission at 0.1 to 1.8 MeV, energy dependence of delayed neutron yield from, (E), 25:5770
neutron fission at thermal to 3.1 MeV energies, delayed neutron yield from, (E), 25:5765
neutron fission of, half-lives and relative abundances of delayed neutron groups from, (E), 25:5689
neutron fission of, yields for thermal, (E), 25:5765
neutron fisson cross sections at 0.4 to 2000 eV, amplifier--discriminator system for ionization detector measurement of, 25:4333
proton fission at 11.5 to 22 MeV, neutron-emission--fission competition and neutron-per-fission ratios from, (E), 25:5692
recycle in gas cooled reactors, economics of, (T), 25:6057
recycle in gas cooled reactors, economics of, (T), 25:6056
URANIUM ISOTOPES U-235
abundance in meteorites, (E/T), 25:4922
burnup in reactor fuels, use in determining plutonium content, 25:4257 (BNWL-SA-3304)
concentration in uranium by ultracentrifugation, effects on world peace from development of technology for, 25:4213 (CONF-691051-, pp 145-53)
concentration in uranium by ultracentrifugation, effects on world peace from development of technology for, 25:4214 (CONF-691051-, pp 354-61)
fission integrals from 0.46 eV to 2.15 keV, shielded, (T), 25:5686 (TID-25566)
fission tracks from, diffusion studies using, 25:4845
neutron capture and fission cross sections below 2.5 keV, Quasi-Resonance Triplet Approximation calculation of, (T), 25:5686 (TID-25566)
neutron fission at 0.1 to 1.8 MeV, energy dependence of delayed neutron yield from, (E), 25:5770
neutron fission at thermal to 3.1 MeV energies, delayed neutron yield from, (E), 25:5765
neutron fission below 2 MeV, energy dependence of prompt neutron yield in, (E), 25:5755
neutron fission cross sections at 0.009 to 24 eV, resonance, (E), 25:5738
neutron fission of, half-lives and relative abundances of delayed neutron groups from, (E), 25:5689
neutron fission of, yields for fast and thermal, (E), 25:5765
photofission at 5 to 10 MeV, prompt and delayed neutron yields from, (E), 25:5768
URANIUM ISOTOPES U-236
energy levels of, deformation-dependence of energy of γ-vibrational, (T), 25:5779
neutron fission of, energy integral test of cross section for, (E/T), 25:5773
URANIUM ISOTOPES U-237
energy levels from uranium-238 (d,t) reactions, spin--parity assignments and spectroscopic factors for, (E), 25:5797
URANIUM ISOTOPES U-238
abundance in meteorites, (E/T), 25:4922
book: The Toxicology of Radioactive Substances, Volume 4: Thorium-232 and Uranium-238, 25:4438
deuteron reactions (d,t) at 17 MeV, triton spectra from, (E), 25:5797
Doppler reactivity effects in plutonium fueled critical assemblies, (E), 25:6109
fission of, decay constant for spontaneous, (E), 25:5767
meson (K) and (π) absorption widths in, corrections due to admixtures of excited energy levels, (T), 25:5866
neutron capture at 0.5 to 100 keV, cross section for, (E), 25:5771
neutron capture at 6 eV to 102 keV, γ spectra from, (E), 25:5776
neutron capture at thermal to 1 MeV energies, energy dependence of γ-ray yields for, (T), 25:5777
neutron fission at 14 MeV, production of palladium-113, -115, and -116 from, (E), 25:5740
neutron fission of, energy integral test of cross section for, (E/T), 25:5773
photofission at 5 to 10 MeV, prompt and delayed neutron yields from, (E), 25:5768
proton fission at 11.5 to 22 MeV, neutron-emission--fission competition and neutron-per-fission ratios from, (E), 25:5692
URANIUM NITRATES
criticality of solutions containing uranium-233 and uranium-235, calculations for, 25:4283
URANIUM NITRIDES
radiation effects on crystal structure of, relations of annealing with fission neutron, 25:4887 (KFK-1215)
radiation effects on swelling of rhenium-clad, at 1600 to 1700°C, relations of grain boundaries with in-pile, 25:4826
URANIUM OXIDES
book: The Toxicology of Radioactive Substances, Volume 4: Thorium-232 and Uranium-238, 25:4438
URANIUM OXIDES UO_2
creep strain of, effects of grain-boundary porosity growth on high-temperature, 25:4848
criticality, inventory, and safeguards system for, design of computerized, 25:4295
crystallization of, effects of temperature and thermal gradients on basaltic, 25:4847
diffusion in nickel, determination by neutron fission recoil tracks from uranium-235, 25:4845
diffusion in potassium chloride, determination by neutron fission recoil tracks from uranium-235, 25:4845
diffusion of bubbles in, laser image furnace for study of, 25:4853
Doppler reactivity effects in critical assemblies, (E), 25:6110
Doppler reactivity effects in fast critical assemblies of, (E), 25:6111
preparation of high-density sintered powder specimens of, method for, 25:4841(R) (SRO-552-5)
radiation effects on creep and swelling in fuel pins of, neutron, 25:4888 (TRG-Report-1937)
radiation effects on creep of, neutron, 25:4893
radiation effects on crystal structure of, relations of annealing with fission neutron, 25:4887 (KFK-1215)
radiation effects on Zircaloy-clad fuel elements of, pile neutron, 25:4886(R) (GEAP-10204)
radiation testing of Type 316 stainless steel clad fuel pellets of, 25:5990(R) (ORNL-4585)
reaction with liquid sodium, energy release for, (E), 25:6076
reduction by graphite at 1400 to 1756°C, comments and rebuttal on kinetic study of, 25:4849
tensile properties of sintered powder cylinders of, 25:4841(R) (SRO-552-5)
thermal conductivity at 50 to 1000°C, effects of porosity on, 25:4844
thermal conductivity of, 25:6060
thermal gradients in, effects of electric current on, 25:4847
PuO_2--UO_2, critical parameters of FFTF driver fuel pins of, in water, 25:4280
PuO_2--UO_2, fabrication of pellets of, for EBR-II irradiation, 25:4889(R) (UNC-5262)
PuO_2--UO_2, handling of fuel elements of, radiation protection requirements during, 25:4314
PuO_2--UO_2, inspection of fuel elements of, high-resolution neutron radiographic method for, 25:4254
PuO_2--UO_2, microstructure of fuels of, effects of thermal neuron flux on, (E), 25:5993
PuO_2--UO_2, plutonium dioxide homogeneity in fuel pellets of, scanning electron microprobe evaluation of, 25:4876
PuO_2--UO_2, power transient effects on discrete plutonium oxide (PuO_2) particles in fuels of, (E), 25:5995
PuO_2--UO_2, power transient effects on discrete plutonium oxide (PuO_2) particles in pellet fuels of, (E), 25:5994
PuO_2--UO_2, power transient effects on fuels of, (E), 25:5996
PuO_2--UO_2, radiation effects on distribution of fused oxide in, in-pile, 25:4879 (CEA-CONF-1659)
PuO_2--UO_2, radiation effects on partial melting of low-density, in-pile, 25:4879 (CEA-CONF-1659)
PuO_2--UO_2, radiation testing of Type 316 stainless steel clad fuel pellets of, 25:5990(R) (ORNL-4585)
PuO_2--UO_2, reactions with sodium at 400 to 1100°C, calculations of, 25:4736(R) (ANL/ST-3)
PuO_2--UO_2, reprocessing of irradiated, economics of, 25:4134(T) (AEC-tr-7198)
PuO_2--UO_2, thermal conductivity and restructuring of fuels of, in-pile, (E/T), 25:5992
PuO_2--UO_2, thermal conductivity of physically mixed, at 800 to 2400°C, 25:4862
PuO_2--UO_2, thermal conductivity of, effects of burnup on,

25:4839 (KFK-1245)
PuO_2--UO_2-base, creep at 1100 to 1300°C, measurement of compressive, 25:4861
PuO_2--UO_2-base, molybdenum-99 distribution in irradiated fuel pins of, 25:4891
PuO_2--UO_2-base, molybdenum-99 distribution in irradiated fuel pins of, 25:4804
PuO_2--UO_2-base, plutonium homogeneity in sintered, methods for measurement of, 25:4675
PuO_2--UO_2-base, thermal conductivity at 50 to 1000°C, effects of porosity on, 25:4844
ThO_2--UO_2, radiation testing of coated particle fuels of, 25:5990(R) (ORNL-4589)
URANIUM OXIDES U_3O_8
diffusion across placental tissues and excretion by mammary glands of dogs and rabbits following intratracheal injection or oral administration, 25:4446
effects on intrauterine and early extrauterine development of dogs and rabbits following maternal ingestion or intratracheal injection, 25:4446
excretion in feces of dogs and rabbits following chronic ingestion, 25:4444
toxicity in dogs and rabbits following chronic ingestion or intratracheal and subcutaneous injection, 25:4444
toxicity of, review of, 25:4439
toxicity to organs and tissues of dogs and rabbits following acute and chronic intratracheal, oral and subcutaneous administration, 25:4447
toxicity to peripheral blood of dogs following chronic ingestion and low and high dose intratracheal injection, 25:4445
PuO_2--U_3O_8, analysis for impurities, effects of ratio of plutonium oxide to uranium oxide on impurity spectral line intensity in spectrographic, 25:4015 (NUMEC-3524-7t)
U_3O_8--ZrO_2, phase studies of, 25:4864
URANIUM PHOSPHIDES
enthalpy of formation of, direct-reaction calorimetric measurement of, 25:4843
URANIUM SELENIDES
enthalpy of formation of, direct-reaction calorimetric measurement of, 25:4843
URANIUM SULFIDES
enthalpy of formation of, direct-reaction calorimetric measurement of, 25:4843
preparation of monocrystals of, 25:4059
transport through gas phase in closed volume, mechanism of, 25:4059
URANIUM TELLURIDES
enthalpy of formation of, direct-reaction calorimetric measurement of, 25:4843
URANYL ACETATES
reactions with acetic acid, uranyl chlorides, and zinc amalgam, preparation of uranium(IV) acetates from, 25:4057
URANYL CHLORIDES
reactions with acetic acid, uranyl acetate, and zinc amalgam, preparation of uranium(IV) acetates from, 25:4057
URANYL COMPOUNDS
preparation of ammonium, dihydropyridyl, potassium, and sodium uranyl mandelates, 25:4055
URANYL IONS
effects on hydrogen yields from radiolysis of water, 25:4120
URANYL NITRATES
effects on production of sucrose in corn scutellum, 25:4720
reactions with mandelic acid in presence of ammonium hydroxide, potassium hydroxide, sodium hydroxide, or pyridine, yields of complex uranyl mandelates from, 25:4055
URANYL PERCHLORATES
activity coefficients in aqueous solutions, 25:4086
complexes with antipyrine, ir spectra and physical properties of, 25:4087
UREA, 1-ETHYL-1-NITROSO-
effects on seeds of Sorghum sp., mutagenic, 25:4495
UREA, HYDROXY-
effects on x-radiosensitivity of cultured Chinese hamster cells, 25:4559
UREA, 1-METHYL-1-NITROSO-
effects on seeds of Sorghum sp., mutagenic, 25:4495
UREA, SELENO-
radiation chemistry of, in aqueous solutions, electrons, 25:4546
radiolysis of, mechanism of pulse, 25:4115
UREA, THIO-
effects on electron-radiosensitivity of DNA in Escherichia coli, 25:4551
URIDINE
radiation effects on incorporation of, into RNA of nerve tissue of chickens and rats, carbon-14 tracer study of x, 25:4457(R) (UCB-34-P-82-9)
URIDINE, 5-BROMO-2'-DEOXY-
effects on radiosensitivity of brain tumor cells, mechanisms for ionizing, 25:4688
effects on radiosensitivity of human neoplasms, combined effects of 5-fluorouracil on ionizing, 25:4602
effects on sensitivity of uv and x-irradiated Escherichia coli, 25:4725
uptake by DNA in neoplastic and normal cells in mice, tracer study on, 25:4602
URIDINE, 2'-DEOXY-5-IODO-
effects on radiosensitivity of human neoplasms, combined effects of 5-fluorouracil on ionizing, 25:4602
uptake by DNA in neoplastic and normal cells in mice, tracer study on, 25:4602
2'-URIDYLIC ACID
polymers, complexes with poly A, effects of, on metabolism in polymorphonuclear leukocytes of x-irradiated guinea pigs, 25:4454 (NYO-3240-55)
URINE
radiation effects on isoamylases in, from man, γ, 25:4452
radioactivity in human, following phosphorus-32 administration, β, 25:4451
ratio of strontium-90 content of, to dietary content of man, effects of ingestion in calcium gluconate and silk on, 25:4424(R) (TID-25567)
UTERUS
blood circulation in, of pregnant monkeys and sheep, tracer study of, 25:4655 (COO-1762-6)

V

VALVES
design for piping components and systems, summary of experience on, 25:4188 (TID-25553)
reliability analysis of boiling water reactor steam line isolation, 25:6040 (RISO-214, pp 247-52)
testing of stainless steel clam-type, for reactor pipes, 25:4183 (DP-Report-484)
VAN ALLEN RADIATION BELTS
electron kinetics in, (T), 25:5033
proton kinetics in, (T), 25:5033
VAN DE GRAAFF ACCELERATORS
experimental facilities at Saclay tandem, development of, 25:5680 (CEA-N-1232, pp 1-80)
experimental facility for, in-beam Moessbauer spectrometer, 25:5467
ion source for Tandem, performance of polarized, 25:5452 (LA-4465, pp 9.1-2)
operation and development at Saclay tandem, 25:5680 (CEA-N-1232, pp 1-80)
research and development at Saclay, 25:5550(R) (CEA-N-1232)
VANADATES
production of radicals of, from γ radiation effects on vanadate-doped calcium tungstate, ESR spectral studies on, 25:4090
VANADIUM
corrosion by sodium at 450 to 600°C, 25:4736(R) (ANL/ST-3)
determination of trace amounts of, in titanium ore by neutron capture gamma spectroscopy using californium-252 source, 25:4036
effects on automatic colorimetric determination of thorium in aqueous and organic solutions, 25:4014 (NLCO-1072)
effects on miscibility gap in chromium--iron alloys, 25:4787
neutron inelastic scattering by, density of phonon eigenstates and cross sections from, (T), 25:5230
properties for use as encapsulating material for californium-252 sources for neutron capture gamma-ray spectroscopy, 25:4772
radiation effects on microstructure of, relations of annealing with fast neutron, 25:4828
separation by ion exchange using Alamine 336 or Amberlyst A-21 in aqueous thiocyanate solutions, 25:4137 (IS-T-377)
separation from nickel by ion exchange in thiocyanate solutions using Amberlyst A-21, 25:4137 (IS-T-377)
superconducting, bulk upper critical field of clean Type-II, 25:5054
Al--Ti-base--V, fabrication of precision tubes of, equipment and methods for, 25:4745
VANADIUM ALLOYS AND SYSTEMS
Al--Ti-base--V, crack growth in, at sustained loads, effects of hydrogen on, 25:4762
Cr--Fe-base--V, phase studies of miscibility gap in, 25:4787
Cr--V-base, reactions with sodium at 550 to 700°C, effects of calcium on activity and distribution of oxygen in, 25:4736(R) (ANL/ST-3)
Ti--V, phase transformations in beta isomorphous, 25:4806
Ti--V, phase transformations in beta isomorphous, comments on, 25:4805
VANADIUM ISOTOPES V-51
energy levels from proton resonances in titanium-50, spreading widths for isobaric analog, (T), 25:5644
energy levels from titanium-50 (p,γ) reactions at 1.371 MeV, spin--parity assignments for, (E), 25:5651
energy-level transitions from titanium-50 (p,γ) reactions at 1.371 MeV, partial widths and mixing and branching ratios from analog, (E), 25:5651
energy-level transitions in, strengths of M1 analog, (T), 25:5658
nuclear magnetic resonance in vanadium(III) oxide at high

pressures and low temperatures, 25:5224
VANADIUM OXIDES
magnetic ordered moment of vanadium in V_2O_3 from nuclear thermal capacity at low temperatures, (E), 25:5191
phase transition in V_2O_3, 4.2°K high-pressure NMR study of metal--insulator, 25:5224
phase transition of V_2O_3, effects of electric field on semiconductor--metal, 25:4759
reduction of V_2O_5, by carbon, chromatographic study of effects of flowing inert gas on, 25:4842
structure of insulating monoclinic V_2O_3 phase, low-temperature, (E), 25:5190
VEGETABLES
potatoes, radioisotope content of, in Faroe Islands during 1969, cesium-137 and strontium-90, 25:4476(R) (RISO-221)
reactions of extracts of, with hydrated radiolytic electrons, effects of acetone, cysteine, and nitrate additives on, 25:4117
VEHICLES
design of computer-controlled, for remote mobile television intelligence system, 25:4159
VENUS (PLANET)
atmosphere of, height-distribution processes of ionization in Martian and Cytherean upper, (E/T), 25:4936
VERMICULITES
cation exchange selectivity of micaceous, 25:4160
VERTEBRAL COLUMN
mineral content of bones of lumbar, in man, development of radiographic method for measurement of, 25:4628 (CONF-680211-, pp 331-51)
VIBRATIONS
effects on piping components and systems, summary of experience on, 25:4188 (TID-25553)
VINYL COMPOUNDS
radioinduced curing of coatings of, electron, 25:4095(P)
VIRUSES
effects on morphology of HeLa cells, effects of antiserum on, 25:4729
Hemophilus influenzae, genetic transformation in, 25:6241 (NYO-1371-63)
herpes simplex, radiation effects on infectivity of, in CV-1 mammalian cells, uv, 25:4727
Herpes zoster, pathology of encephalitis induced by, 25:4660
reovirus 2, radioinduced inactivation of, uv, 25:4729
VITAMIN B GROUP
effects on activity of enzymes in blood plasma of rats, 25:4594
radioprotective effects of, reaction mechanisms for, 25:4594
VITAMIN D GROUP
effects on radioisotope metabolism in bone, 25:4423 (COO-1601-23)
VITAMIN K GROUP
effects on γ-radiosensitivity of Escherichia coli, 25:4552
K-3, effects on synthesis of methemoglobin in erythrocytes in vitro, 25:4598
menadione, effects on x-radiosensitivity of ascites tumor cells, 25:4562
menadione, electron transfer reactions of nucleosides and nucleotides in solutions of, 25:4540

W

WASPALOY
fabrication of precision tubes of, equipment and methods for, 25:4745
WATER
analysis for cesium-137 by ion exchange and γ counting, use of silica gel as support for inorganic ion exchangers in, 25:4033
content in soils, radiometric method for measurement of, 25:4158
corrosive effects as impurity in flowing helium on graphite at 600 to 750°C, 25:4835 (DP-Report-448)
effects of high-temperature, on mechanical properties of steel, 25:4738 (DP-Report-527)
effects of high-temperature, on mechanical properties of austenitic stainless steel, 25:4738 (DP-Report-527)
effects of high-temperature, on properties of Nimonic 75, 25:4738 (DP-Report-527)
effects of irrigation, on growth of plants in desert ecosystems, 25:4477 (UCLA-12-782, pp 49-81)
effects of rock-contained, on crater formation by underground nuclear explosions, 25:4179
effects of sprays of, on criticality of arrays of uranium cylinders, 25:4282
effects on radiosensitivity of bacterial spores, 25:4726
exchange kinetics in labile aquo and substituted aquo transition metal ions, oxygen-17 NMR studies of, 25:6248 (RLO-2221-T-4-3)
filter plugging by sprayed droplets of, testing of high efficiency particulate air, (E), 25:4190 (UCRL-50923)
gamma dose buildup factors in, 25:5136
metabolism in lungs, measurement using radioactive carbon dioxide and oxygen as tracers, 25:4669
neutron diffusion length measurements in, effects of source arrangement on foil activation for, (E), 25:6182
neutron scattering at 0.004 to 0.12 eV, scattering transport lengths from, (E), 25:5502
neutron spectra in, time-dependent, (E/T), 25:5489
neutron transport in moving tube of, (E), 25:5486
polymers, preparation of, attempts at, 25:4051(R) (AI-AEC-12972)
radio emission from interstellar, maser action in, (T), 25:4917
radioisotope content of, in Faroe Islands during 1969, cesium-137 and strontium-90, 25:4476(R) (RISO-221)
radiolysis of, mechanism of product formation in, 25:4120
radioprotective effects of, on barley seeds, fast neutron and γ, 25:4604
separation of cobalt, copper, and iron from, by ion exchange in thiocyanate solutions using Alamine 336, 25:4137 (IS-T-377)
separation of radioisotopes from waste, by frothing flotation, 25:4141
surface tension of, effects of temperature on, 25:6216(T) (AEC-tr-7203)
Al_2O_3--BeO--H_2O--SiO_2, phase studies of subsolidus phase relations of, at 300 to 700°C, 25:4871
H_2O--steam, corrosive effects on Zircaloy-2, relations with in-pile radiation, 25:4737 (CISE-R-290)
H--H_2O, diffusion in carbons at 18 to 900°C, measurement of effective, 25:4856
WATER-d_2
effects on α-amylase activity in barley seeds, effects of gibberellic acid on toxic, 25:4464
neutron diffusion parameters for, determination using pulsed source technique, 25:5485
neutron scattering at 0.004 to 0.12 eV, scattering transport lengths from, (E), 25:5502
WELDS
design and performance of pipe, summary of experience on, 25:4188 (TID-25553)
fracture in pipe and pressure vessel, review of mechanisms of, 25:4781
WELL LOGGING
method for strong neutron-absorbing media using Monte Carlo idealization of neutron energy, space, and time distribution, 25:4159
neutron source for, evaluation of californium-252, 25:4218
WEST VALLEY PROCESSING PLANT
facilities for, topographic map of, 25:4156 (DOCKET-50201-54)
foundation for, site studies and design of, 25:4153 (DOCKET-50201-51)
foundations for, site studies and design of, 25:4154 (DOCKET-50201-52)
iodine recovery building for, soil and foundation studies for, 25:4155 (DOCKET-50201-53)
WHISTLERS
propagation in magnetosphere, thermal plasma study from, (E), 25:5029
WIND TUNNELS
plasma production by low-power MPD engine, 25:5105
WOOD
radioinduced polymerization of monomers in, comparison of economics of heat, heat--catalyst, and γ, 25:4109

X

X RADIATION
effects of reproductive capacity of HeLa S3 cells, effects of serum content of media on, 25:4606
effects on ability of bone marrow stem cells to form spleen colonies following transplantation into syngenic mice, effects of dactinomycin, mitomycin, and 5-fluorouracil on, 25:4570
effects on activity of acetylcholinesterase and choline acetyltransferase in developing brain of rats, 25:4457(R) (UCB-34-P-82-9)
effects on activity of enzymes in solutions, effects of iodine compounds on, 25:4569
effects on ascites tumor cells in cultures, combined effects of indantrione, menadione, N-ethylmaleimide, and Synkavit on, 25:4562
effects on association of marked chromosomes in cultured leukocytes from monkeys, effects of cell cycle stage on, 25:4493
effects on blood cell cytology, blood circulation, bone marrow cytology, and blood transferase activity in dogs and rats, protective effects of AET against, 25:4559
effects on blood flow and oxygen gradient in lungs of dogs, 25:4706
effects on breeding and migration of salamanders, 25:4475 (NYC-3554-8)
effects on carbon-14 uptake by cerebral glycogen of exposed rats, 25:4453
effects on chromatids in chromosomes of Vicia faba, effects of dose fractionation on aberrant, 25:4497
effects on chromatids in root meristems of Crepis capillaris, aberrant, 25:4496
effects on chromosomes in bone marrow of rats, protective effects of serotonin against aberrant, 25:4585
effects on chromosomes of peas following seed exposure,

XUM

role of free radicals in aberrant, 25:4489
effects on chromosomes of Vicia faba, aberrant, 25:4494
effects on content of calcium, potassium, and sodium in blood plasma, erythrocytes, and heart muscle in rabbits, lethal dose whole-body, 25:4698
effects on cultured Chinese hamster cells, combined effects of hydroxyurea on, 25:4559
effects on cultured Chinese hamster cells, combined effects of anoxia and phenylglyoxal on, 25:4557
effects on cultured Chinese hamster cells, effects of dactinomycin and nitrogen mustard on, 25:4558
effects on cultured Chinese hamster cells, protective effects of cysteamine against, 25:4559
effects on development of eggs of Ascaridia (nematode), 25:4692 (COO-1209-13)
effects on development of eggs of Heterakis (nematode), effects of dose on, 25:4692 (COO-1209-13)
effects on diploid and polyploid cells, review of mutagenic, 25:4484
effects on DNA in bacteria and bacteriophages, effects of triacetoneamine N-oxyl on, 25:4550
effects on DNA in Ehrlich ascites tumor cells, induction of strand breaks by, 25:4567
effects on DNA of Micrococcus radiodurans and murine lymphoma cells, effects of dose, oxygen content, and temperature on repair of, 25:4536
effects on DNA of Micrococcus radiodurans, combined effects of chloramphenicol on, 25:4536
effects on DNA of Micrococcus radiodurans, protective effects of cysteamine against, 25:4536
effects on erythropoiesis in bone marrow and spleen of mice, iron-59 tracer study of effects of adrenalectomy on 100 to 300 R, 25:4696
effects on Escherichia coli, effects of BUdR incubation on, 25:4725
effects on Escherichia coli, protective effects of N-phenylthiocarbamates and phenylthioacetic acid against, 25:4553
effects on frequency of crossover aberrations in chromosomes of male Drosophila in comparison to effects of methylnitroso compounds, 25:4481
effects on glandular stomach of mice, carcinogenic whole-body, 25:4703
effects on growth of cells of carcinomas and sarcomas in mice and rats, effects of 6-azauridine on, 25:4590
effects on growth of Ehrlich carcinoma cells following transplantation into mice, combined effects of polyethylenimine on, 25:4563
effects on growth of transplants of Ehrlich ascites tumor cells in mice, combined effects of L-erythro-α,β-dihydroxybutraldehyde on, 25:4564
effects on immune responses of mice in comparison to 2.2-GeV protons, 25:4470
effects on indole in polar solution, effects of electron scavengers on phosphorescence produced by, 25:4089
effects on lithium fluoride, identification of V_3 band induced in, (E), 25:5156
effects on lower ionospheric ionization, bremsstrahlung, (E/T), 25:5019
effects on membrane permeability of Ehrlich ascites tumor cells in cultures, combined effects of iodine compounds on, 25:4569
effects on membrane permeability of Ehrlich ascites tumor cells in cultures, protective effects of cysteamine and 2-amino-3-methyl-butanethiol against, 25:4568
effects on membranes of Ehrlich ascites tumor cells, combined effects of excess oxygen and Synkavit on, 25:4568
effects on metabolism in polymorphonuclear leukocytes of guinea pigs, effects of endotoxins and poly A-U complexes on, 25:4454 (NYO-3240-55)
effects on mice, protective effects of AET and 6-mercaptoquinoline against, 25:4553
effects on mutants of yeast, effects of, on sensitivity to methyl methanesulfonate and nitrogen mustard, 25:4480
effects on peas and wheat for agricultural improvement, review of mutagenic, 25:4488
effects on peripheral blood of mice, effects of thymectomy on lethal, 25:4469
effects on phospholipase B activity in intestine of rats in relation to number of eosinophils, 25:4455(R) (ORO-3329-7)
effects on populations of maize, mutagenic, 25:4485
effects on potassium chloride crystals at room temperature, first-stage growth of F centers induced in, 25:5159
effects on rat embryos, combined effects of iodoacetamide on teratogenic, 25:4575
effects on reproductive capacity of cultured animal cells, protective effects of cystamine and cysteamine against, 25:4560
effects on reproductive capacity of Escherichia coli, effects of anoxia and triacetoneamine N-oxyl on, 25:4550
effects on root tip cell chromosomes of Vicia, effects of dose fractionation on number of aberrant, 25:4492
effects on S-100 protein content of developing brain of rats, effects of age and hypophysectomy on 750 R, 25:4694 (UCLA-12-791)
effects on Serratia marcescens, combined effects of anoxia, indole, and ninhydrin on, 25:4557
effects on spleen colony formation by transplants of stem cells in syngenic mice, protective effects of para-aminopropiophenone and propylene glycol against, 25:4571
effects on spleen of mice, effects of estradiol on hemopoietic stem cells repopulation following whole-body, 25:4471
effects on survival of amphibian species, correlation with DNA content of liver cells, 25:4475 (NYO-3554-8)
effects on survival of cultured Chinese hamster cells, combined effects of triacetoneamine-N-oxyl on, 25:4561
effects on survival of dogs, mice, and sheep, protective effects of bacterial endotoxins against, 25:4586
effects on survival of Ehrlich ascites tumor cells following transplantation into mice, effects of methyl hydrazine on, 25:4567
effects on survival of Ehrlich ascites tumor cells following transplantation into mice, protective effects of oxamic acid against, 25:4566
effects on survival of Escherichia coli, protective effects of cysteine against, 25:4555
effects on survival of fern spores, combined effects of anoxia, acetoacetic acid, and indole-2,3-dione on, 25:4573
effects on survival of green algae, combined effects of hypoxia and potassium cyanide on, 25:4574
effects on survival of mice with skin wounds, protective effects of cysteamine and serotonin against, 25:4576
effects on survival of mice, effects of body temperature on protective effects of sodium fluoroacetate against, 25:4580
effects on survival of mice, protective effects of adrenochrome monoguanylhydrazone methanesulfonate against, 25:4589
effects on survival of mice, protective effects of hypoxia against, reaction mechanisms for, 25:4578
effects on survival of mice, protective effects of mixtures of AET, cysteamine, cysteine, glutathione, and serotonin against, 25:4582
effects on survival of mice, protective effects of mixtures of AET and 5-methoxytryptamine against, 25:4583
effects on survival of mice, protective effects of N-substituted AET derivatives against, 25:4577
effects on survival of mice, protective effects of serotonin against, reaction mechanisms for, 25:4584
effects on survival of mice, protective effects of sodium fluoroacetate against, 25:4579
effects on synthesis of nucleic acids and proteins in Escherichia coli, protective effects of cysteine against, 25:4554
effects on trees, lethal and mutagenic, 25:4724
effects on tryptophan dipeptides, yields from, 25:4114
effects on wound healing and hematopoietic system in mice, effects of dose and postirradiation time on recovery from whole-body, 25:4705
emission from McMath 8207 solar region, effects of solar cycle variations on soft, (E), 25:4923
emission from television receivers, survey of x, 25:4522 (BRH/DEP-70-24)
emission of solar, correlation with Hα flares, calcium plages, and microwave emission, (E), 25:4524
intensity of specific atomic, correlation with nuclear charge, (T), 25:5832
production by electron precipitation into upper atmosphere, (T), 25:5007
spectra from meson (π^-) capture by hydrogen, (E), 25:5288
transport theory, thermal, 25:5142
transport, scattering-angle biasing for deep-penetration, (T), 25:5145

X-RAY BEAMS
use of polychromatic, for transmission scanning of bones for measurement of mineral content, 25:4650 (CONF-700515-, pp 314-31)

X-RAY CAMERAS
design for three-dimensional holography, 25:4404

X-RAY FLUORESCENCE ANALYSIS
book: Quantitative X-ray Spectrofluorescence Analysis, in Russian, 25:4024
detectors for, avalanche semiconductor, 25:4323 (NYO-4028-TA-1)

X-RAY PHOTOMETRY
use for measurements of mineral content of human bones, 25:4642 (CONF-700515-, pp 237-42)

X-RAY SOURCES
radioisotope, use for transmission scanning of bones for measurement of mineral content, curium-244, promethium-145, and samarium-145, 25:4647 (CONF-700515-, pp 274-9)
use for fluorescence scanning of human thyroid for measurement of content of stable iodine, 25:4682
use for transmission scanning of human bones for in vivo measurement of mineral content, 25:4621 (CONF-680211-, pp 204-15)
use for transmission scanning of human bones for measurement of mineral content, 25:4623 (CONF-680211-, pp 253-68)

X-RAY SPECTROMETERS
response spectra for complex geometries, Monte Carlo calculation of, 25:4403

XUM

use for measurements of mineral content of human bones, 25:4642 (CCNF-700515-, pp 237-42)

XENON
helium-ion reactions at 10 to 30 keV with, cross sections for production of metastable triplet helium atoms by charge exchange in, (E), 25:4969
helium-metastable-atom reactions with, cross sections for ionization in, (E), 25:4969
meson (π^+) reactions at 2.34 GeV/c in xenon bubble chamber, π^0--π^0 mass spectrum from, (E), 25:5284 (JINR-E1-5085)
solubility in liquid sodium, 25:4736(R) (ANL/ST-3)

XENON IONS
reactions with single-crystal germanium, minimum energy for sputtering in, (E), 25:5155

XENON ISOTOPES
abundance in meteorites, (E/T), 25:4922

XENON ISOTOPES Xe-125
electron-capture and beta decay of, gamma spectra from, (E), 25:5764

XENON ISOTOPES Xe-128
production by thermal-neutron irradiation of iodine, process development for, 25:4129
separation from iodine-127 using traps, 25:4129

XENON ISOTOPES Xe-129
abundance in meteorites, (E/T), 25:4922

XENON ISOTOPES Xe-133
diffusion from carbon coated thorium carbide--uranium fuel particles, method determination of, 25:4882 (DP-Report-436)
diffusion in fission-recoil-doped calcium fluoride monocrystals, 25:5152(R) (ORO-3508-6)
distribution in muscles following intramuscular injection in cats, 25:4429
radiation dose to man from, during lung scanning, methods for calculating absorbed, 25:4511
uptake by fetus following use for scanning for assessment of uterine blood flow in mother, 25:4673
use as tracer for measurement of airway closure in human lungs, 25:4428
use for cerebral blood circulation studies in patients with organic dementia, multi-detector technique for, 25:4681
use for lung scanning for diagnosis of diseases, 25:4676
use for measuring regional pulmonary function, methods for, 25:4666
use for scanning blood circulation in lungs, 25:4672
use for scanning human lungs for function, 25:4671
use for scanning human lungs for function, 25:4666
use for scanning human lungs for function, half-life, γ energy, and solubility coefficient of, 25:4663
use for scanning human lungs for pulmonary ventilation, 25:4668
use with multicrystal rectilinear scanner, for measuring human lung ventilation, 25:4665
yields from plutonium-239 (n,f) and uranium-235 (n,f) reactions, calculation of, (T), 25:5790

XENON ISOTOPES Xe-135
use for scanning human lungs for function, half-life, γ energy, and solubility coefficient of, 25:4663

p-XYLENE
polymers, preparation of thin films of, for radiation applications, 25:4329

Y

YTTERBIUM
determination of trace amounts of, in uranium by chemical separation and spectroscopy, 25:4021
optical constants from reflectance spectra at 1 to 11.6 eV, 25:5188
oxidation of thin films of, electron microscopic study of, 25:4767

YTTERBIUM ISOTOPES Yb-170
Moessbauer spectra in ytterbium oxide at low teperatures, 25:5225

YTTERBIUM ISOTOPES Yb-171
Moessbauer spectra in ytterbium oxide at low teperatures, 25:5225

YTTERBIUM ISOTOPES Yb-172
energy level transitions from thulium-172 beta decay, angular correlation coefficients and attenuation parameters from, (E), 25:5760
energy levels from neutron capture by ytterbium-171, spin--parity assignments for, (E), 25:5744
energy levels from thulium-172 beta decay, spectroscopic quadrupole moments and quadrupole moment ratios for 2^+ and 3^+, (E), 25:5760
energy-level transitions from neutron capture by ytterbium-171, Mikhailov plots for, (E), 25:5744
meson (K) absorption widths in, corrections due to admixtures of excited energy levels, (T), 25:5866

YTTERBIUM ISOTOPES Yb-175
energy levels from thulium-175 beta decay, spin and parity assignments for, (E), 25:5747
energy-level transitions from thulium-175 beta decay, gamma spectra from, (E), 25:5747

YTTERBIUM OXIDES
magnetic hyperfine interactions in, Moessbauer study of, 25:5225
magnetic structure of, (T), 25:5215
ThO_2--$YbUO_4$, spectra and phase studies of, 25:4084

YTTERBIUM URANATES
ThO_2--YUO_4, spectra and phase studies of, 25:4084

YTTRIUM
complexes with 8-quinolinol, structure of, NMR spectral studies on, 25:4081
complexes with maleic acid, preparation and thermal behavior of, 25:4075
effects on photochemical precipitation of cerium, 25:4026
Hall effect in paramagnetic, ferromagnetic, and antiferromagnetic, 25:5182
separation by ion exchange using Alamine 336 in aqueous thiocyanate solutions, 25:4137 (IS-T-377)
separation from aqueous chloride solutions by solvent extraction using cyclooctylphenylphosphinic acid or octylphenylphosphinic acid, 25:4147
separation of thorium from, by photochemical precipitation, 25:4026

YTTRIUM ALLOYS AND SYSTEMS
exchange interactions of dilute, review, 25:5232
Co--Y, magnetic resonance of Y_2Co_{17} and YCo_3, microwave, 25:5200
Dy--Y, Hall effect in paramagnetic, ferromagnetic, and antiferromagnetic, 25:5182
Er-base--Y, magnetoresistance at low temperatures, 25:5175
Sb--Tb--Y, magnetic ordering transition, 25:5205
Tb--Y, Hall effect in paramagnetic, ferromagnetic, and antiferromagnetic, 25:5182
Th--Y-base, magnetic ordering and thermoelectric properties of, 25:5169 (IS-T-379)

YTTRIUM FLUORIDES
NaF--YF_3, thermodynamic composition--pressure diagrams of, 25:4857

YTTRIUM ISOTOPES Y-89
neutron capture integral in fast region, (E), 25:5656
photon reactions (γ,pn) and (γ,2n) at 150 to 305 MeV, analysis for reaction mechanism in, (E), 25:5675

YTTRIUM ISOTOPES Y-90
determination by β counting using G-M and proportional detectors, efficiency curves for, 25:4029 (CISE-N-119)
energy-level transitions from radiative pion absorption by zirconium-90, partial strengths for, (T), 25:5753

YTTRIUM OXIDES
Y_2O_3--ZrO_2, melting points and phase studies of, 25:4865

Z

ZINC
complexes with 8-quinolinol, structure of, NMR spectral studies on, 25:4081
complexes with maleic acid, preparation and thermal behavior of, 25:4075
complexes with phenanthrenequinone oxime, potentiometric studies on formation constants of, 25:4080
determination in skin by neutron activation, 25:4049
determination of trace amounts of, in strontium-85, polarographic, 25:4126 (UJV-2431-Ch)
effects on growth of γ-irradiated Triticum vulgare, 25:4718
effects on vaporization of gallium arsenide single crystals, 25:4074 (UCRL-19685)
magnetic breakdown from induced-torque measurements, 25:5192
photon reactions (γ,t) at 90 MeV, triton yield in, (E), 25:5678
separation by ion exchange using Alamine 336 or Amberlyst A-21 in aqueous thiocyanate solutions, 25:4137 (IS-T-377)

ZINC ALLOYS AND SYSTEMS
Cd--Zn, plastic deformation of monocrystalline, 25:4783

ZINC ISOTOPES Zn-63
energy levels from copper-63(p,n) reactions, (E), 25:5612

ZINC ISOTOPES Zn-64
helium-3 reactions (He-3,t) at 35 MeV, DWBA analysis of angular distributions from, (E/T), 25:5654

ZINC ISOTOPES Zn-65
electron-capture decay of, x-ray spectra and L/K- and M/L-electron capture ratios from, (E), 25:5655

ZINC ISOTOPES Zn-66
helium-3 reactions (He-3,t) at 35 MeV, DWBA analysis of angular distributions from, (E/T), 25:5654

ZINC ISOTOPES Zn-68
proton reactions (p,2p) and (p,p3n) + (p,4n) at 10 to 85 MeV, cross sections for, (E), 25:5623

ZINC ISOTOPES Zn-70
alpha inelastic scattering at 42 MeV, angular distributions and energy spectra from, (E), 25:5607
energy levels from alpha inelastic scattering at 42 MeV, spin--parity assignments for, (E), 25:5607

ZION POWER REACTOR, UNIT 1
auxiliary systems for, preliminary safety analysis of, 25:5935 (DOCKET-50295-19)
containment system for, preliminary safety analysis of, 25:5933 (DOCKET-50295-17)
control systems for, preliminary safety analysis of, 25:5934 (DOCKET-50295-18)
cooling system for, preliminary safety analysis of,

XUM

25:5933 (DOCKET-50295-17)
design parameters of, preliminary safety analysis of, 25:5932 (DOCKET-50295-16)
electrical systems for, preliminary safety analysis of, 25:5935 (DOCKET-50295-19)
engineered safeguards for, preliminary safety analysis of, 25:5934 (DOCKET-50295-18)
instrumentation for, preliminary safety analysis of, 25:5934 (DOCKET-50295-18)
site for, preliminary safety analysis of, 25:5932 (DOCKET-50295-16)
technical specifications for, proposed complete, 25:5931 (DOCKET-50295-15)
ZION POWER REACTOR, UNIT 2
auxiliary systems for, preliminary safety analysis of, 25:5935 (DOCKET-50295-19)
containment system for, preliminary safety analysis of, 25:5933 (DOCKET-50295-17)
control systems for, preliminary safety analysis of, 25:5934 (DOCKET-50295-18)
cooling system for, preliminary safety analysis of, 25:5933 (DOCKET-50295-17)
design parameters of, preliminary safety analysis of, 25:5932 (DOCKET-50295-16)
electrical systems for, preliminary safety analysis of, 25:5935 (DOCKET-50295-19)
engineered safeguards for, preliminary safety analysis of, 25:5934 (DOCKET-50295-18)
instrumentation for, preliminary safety analysis of, 25:5934 (DOCKET-50295-18)
site for, preliminary safety analysis of, 25:5932 (DOCKET-50295-16)
technical specifications for, proposed complete, 25:5931 (DOCKET-50295-15)
ZIRCALOY-2
fracture mode at 350°C, effects of grain size and strain rate on, 25:4769
mechanical properties of cold-worked tubes of, effects of recovery and recrystallization treatments on, 25:4757
oxide films on, mechanisms for electric conductivity in, 25:5173
radiation effects on corrosion of, by steam--water mixtures, in-pile, 25:4737 (CISE-R-290)
ZIRCONIUM
brittleness of pressure tubes of, effects on reliability, 25:4753
deformation of high-purity monocrystalline, at 4.2 to 293°K, 25:4784
effects of impurities of, on properties of uranium, 25:4747 (AWRE-O-63/70)
effects on automatic colorimetric determination of thorium in aqueous and organic solutions, 25:4014 (NLCO-1072)
electronic density of states of hcp and bcc, from bremsstrahlung isochromates, 25:5187
fracture mode at 350°C, effects of grain size and strain rate on, 25:4769
hydrogen content of zirconium hydride-coated, effects of thermal cycling at 298 to 689°K on supercharging of, 25:4756
mechanical properties of tubes of, effects of hydrogen pickup and neutron radiation on, 25:6191 (RISO-214, pp 255-87)
preparation of high-purity monocrystalline, electron beam zone refiner method for, 25:4784
properties for use as encapsulating material for californium-252 sources for neutron capture gamma-ray spectroscopy, 25:4772
properties for use in electrolytic separation of bromine-80 isomers, 25:4127
radiation effects on distribution between TBP and aqueous nitric acid solutions, effects of isopropylbiphenyl on, 25:4116
separation by ion exchange using Alamine 336 or Amberlyst A-21 in aqueous thiocyanate solutions, 25:4137 (IS-T-377)
separation from rare earths by anion exchange using nitric acid--methanol system, 25:4139
surface impurities on, use of Auger electron spectroscopy for detection and identification of, 25:4758
tensile properties of longitudinal and transverse specimens of polycrystalline, at 4.2°K, 25:4768
ZIRCONIUM ALLOYS AND SYSTEMS
analysis for niobium using 4-(2-pyridylazo)resorcinol, photometric, 25:4018
C--C--Zr, crystal structure of fcc, effects of composition on, 25:4877
C--C--Zr, thermodynamic properties of fcc, 25:4877
Mg-base--Zr, crystallization of dilute, kinetics of, 25:4808
Nb--U-base--Zr, corrosion crack initiation in, effects of electrochemical and metallurgical variables on stress, 25:4749 (SC-DR-70-716)
Nb--Zr-base, radiation effects on metallurgical properties of cold-worked pressure tubes of, fast neutron, 25:4825
Pu--Zr-base, plutonium segregation in, effects of anneal temperature, cooling rate, and oxygen on, 25:4790
ZIRCONIUM CARBIDES
radiation effects on crystal structure of, neutron, 25:4887 (KFK-1215)
radiation effects on crystal structure of, relations of annealing with fission fragment, 25:4887 (KFK-1215)
solvent properties for oxygen, 25:4877
graphite--ZrC, thermal conductivity of composites of, 25:4840(R) (LA-4526)
ZIRCONIUM HYDRIDES
neutron elastic and inelastic scattering cross sections, calculation of various coherent, (T), 25:5455
ZIRCONIUM ISOTOPES Zr-90
deuteron elastic and inelastic scattering at 21.8 MeV using polarized beams, asymmetries and differential cross sections for, 25:5506 (CEA-N-1232, pp 81-159)
deuteron reactions (d,p) at 21.8 MeV using polarized beams, asymmetries and differential cross sections for, (E), 25:5506 (CEA-N-1232, pp 81-159)
energy level transitions from niobium-90 decay, conversion coefficients and multipolarities of, (E), 25:5682 (IS-T-389)
energy levels from niobium-90 decay, (E), 25:5682 (IS-T-389)
meson (K) and (π) absorption widths in, corrections due to admixtures of excited energy levels, (T), 25:5866
meson reactions (π^-,γ) with, transition rates and branching ratios for, (T), 25:5753
neutron reactions using plutonium--beryllium source, gamma production cross section for, (E), 25:5582
ZIRCONIUM ISOTOPES Zr-91
proton reactions (p,d) at 24.5 MeV using polarized beams, cross section and asymmetry for, (E), 25:5506 (CEA-N-1232, pp 81-159)
ZIRCONIUM NITRIDES
radiation effects on crystal structure of, neutron, 25:4887 (KFK-1215)
radiation effects on crystal structure of, relations of annealing with fission fragment, 25:4887 (KFK-1215)
ZIRCONIUM OXIDES
crystal structure of ZrO and Zr_2O, 25:4878
crystal structure of ZrO_2, effects of oxygen activity and temperature on, 25:4878
electric conductivity in films of, on Zircaloy-2, mechanisms for, 25:5173
radiation effects on crystal structure of, neutron, 25:4887 (KFK-1215)
radiation effects on crystal structure of, relations of annealing with fission fragment, 25:4887 (KFK-1215)
U_3O_8--ZrO_2, phase studies of, 25:4864
Y_2O_3--ZrO_2, melting points and phase studies of, 25:4865
ZIRCONIUM PERCHLORATES
complexes with antipyrine, ir spectra and physical properties of, 25:4087
ZIRCONYL PERCHLORATES
complexes with antipyrine, ir spectra and physical properties of, 25:4087

XUM

REPORT NUMBER INDEX

Reports, conference papers and proceedings, numbered translations, and patents are included in this index. Each item is listed by report number; this is followed by the abstract number and a brief notation regarding public availability. The index entries show which reports are on file in the institutions listed on the back of the front cover (Dep.), which reports have been published in open-literature journals (journal citation), and which reports can be purchased (source and price). Whenever a report is identified by more than one number, the availability is given under the primary number, and a cross reference is given under the secondary report number.

The report number codes apply to USAEC reports unless designated otherwise. Non-USAEC reports are identified by parenthetical notes after the report codes; e.g., (non-AEC), (British), (Canadian), (French). The note (Misc.) identifies the codes used for both USAEC and non-USAEC reports. Patents are listed under the heading "PATENTS"; the country of origin is included in parentheses.

A comprehensive list of both USAEC and non-USAEC report codes is contained in the latest revision of TID-85, *Report Number Series Used by the Division of Technical Information in Cataloging Reports.* This information is also included in the Cumulative Report Number Index (issued annually).

Availability of USAEC Reports

All USAEC Reports abstracted in *Nuclear Science Abstracts* are available through one or more of the following sources:

(1) University and public libraries in the United States. A list of these organizations appears on the inside front cover of each issue of *NSA*.

(2) NCR Microcard Editions in Microcard and micronegative form. Orders and inquiries should be sent to: Order Processing Department, 365 South Oak Street, West Salem, Wisconsin 54669.

(3) National Technical Information Service, U. S. Department of Commerce, Springfield, Virginia 22151.

(4) Superintendent of Documents, U. S. Government Printing Office, Washington, D. C. 20402.

(5) National Cash Register Co., P. O. Box 3111, Oak Ridge, Tenn. 37830, in micronegative form. Purchase details available on request.

Availability of Non-USAEC Reports

U. S. Reports. Reports of U. S. Government agencies are available to the public from the National Technical Information Service (NTIS). If specific availability is not shown, inquiries may be directed to NTIS.

Non-U. S. Reports. Reports of atomic energy organizations of other countries are available from NTIS for U. S. sale only. Specific availability in the country of origin is shown, when known, at the report number entry. Otherwise, inquiries should be made to the organizations listed below:

AUSTRALIA

Australian Atomic Energy Commission Research Establishment. Available upon request from the Library, Australian Atomic Research Establishment, Private Mail Bag, Sutherland, New South Wales, Australia.

BELGIUM

Centre d'Étude de l'Energie Nucléaire. Available upon request to individuals and organizations from the Centre d'Etude de l'Energie Nucléaire (C.E.N.), Studiecentrum voor Kernenergie (S.C.K.), Technical Information Dept., MOL-DONK (Belgium).

CERN

CERN European Organization for Nuclear Research. Available without charge from CERN European Organization for Nuclear Research, Geneva 23, Switzerland. Copies are deposited in libraries throughout the world.

FRANCE

Commissariat à l'Energie Atomique. Inquiries for reports numbered 1-2199 should be addressed to Service Central de Documentation du C.E.A., Centre d'Etudes Nucléaires de Saclay, Boîte postale n° 2, 91. GIF-sur-YVETTE, FRANCE. Reports numbered 2200 and above are available from La Documentation Française, 31 quai Voltaire, 75, PARIS (7e), FRANCE.

Service Central de Protection contre les Rayonnements Ionisants. Copies are available from Ministère de la Santé Publique, Service Central de Protection contre les Rayonnements Ionisants, B.P. n° 78 Le Vesinet (France) Telex 25667.

GERMANY

Deutsches Elektronen-Synchrotron DESY. Copies are available from Deutsches Elektronen-Synchrotron DESY, Dokumentation, 2000 Hamburg 52, Notkestieg 1, Germany.

Gesellschaft für Kernforschung mbH (KFK). Copies are available from Gesellschaft für Kernforschung mbH, 75 Karlsruhe, Postfach 947, Germany. Copies are also deposited in many national nuclear centers in the world.

Kernforschungsanlage. Copies may be ordered from Zentralbibliothek der Kernforschungsanlage Jülich, Jülich, Bundesrepublik Deutschland.

Hahn-Meitner-Institute für Kernforschung. Available without charge from Hahn-Meitner-Institute für Kernforschung Ber-

XUM

lin, Bibliothek, Glienicker Strasse 100, 1 Berlin 39, Germany. Copies are deposited in many national nuclear centers in the world.

Johann-Wolfgang-Goethe Universität, Frankfurt Am Main, Institut für Kernphysik, (IKF). Copies are available from Gmelin Institut, 40–42 Varrentrappstrasse, Frankfurt (Main), West Germany.

ISRAEL

Israel Atomic Energy Commission. Available without charge from Israel Atomic Energy Commission, Soreq Nuclear Research Centre, Yavne, Israel.

ITALY

Centro Informazioni Studi Esperienze (CISE). For sale at CISE Press Office, Casella Postale 3986, Milano, Italy. Copies are deposited in the libraries of various nuclear centers in Italy and abroad.

Comitato Nazionale per l'Energia Nucleare. Copies are available from Comitato Nazionale per l'Energia Nucleare, Divisione Affari Internazionali e Studi Economici, Ufficio Pubblicazioni, Via Belisario, 15, Roma, Italy.

JAPAN

Japan Atomic Energy Research Institute (JAERI). Available from the Staff Supply Cooperative of Japan Atomic Energy Research Institute (JAERI), Tokai-mura, Naka-gun, Ibaraki-ken, Japan. Copies are deposited in depositories in Tokyo, Nagoya, and Osaka.

Nagoya University. Copies are available from Research Information Center, Institute of Plasma Physics, Nagoya University, Nagoya, Japan.

University of Tokyo. Available free of charge from Institute for Nuclear Study, University of Tokyo, Tanashi-Machi, Kitatama-gun, Tokyo, Japan.

NETHERLANDS

Reactor Centrum Nederland. For sale by Reactor Centrum Nederland, 112 Scheveningseweg, 's-Gravenhage, The Netherlands. Copies are deposited in university libraries in Holland and in many national nuclear centers in the world.

NEW ZEALAND

Institute of Nuclear Sciences. Copies are available from Librarian, N. Z. Institute of Nuclear Sciences, D.S.I.R., Private Bag, Lower Hutt, New Zealand. Copies are deposited in other countries.

PAKISTAN

Atomic Energy Center. Copies are available from Atomic Energy Center, P. O. Box 658, Lahore, (West Pakistan).

POLAND

Reports of the Polish nuclear institutes are published by the Nuclear Energy Information Center of the Government Commissioner for Use of Nuclear Energy. Copies are available free of charge from Nuclear Energy Information Center, Palace of Culture and Science, Warsaw, Poland.

SPAIN

Junta de Energia Nuclear. "JEN" reports are available without charge from Servicio de Documentation, Junta de Energia Nuclear, Ciudad Universitaria, Madrid (3), España.

SWITZERLAND

Eidgenössisches Institut für Reaktorforschung. "EIR" reports are available from Eidgenössisches Institut für Reaktorforschung, c/o Bibliothek, 5303 Würenlingen/Switzerland.

TURKEY

Turkish Atomic Energy Commission. Copies are available free of charge from T.A.E.C., Çekmece Nuclear Research Center, P. O. Box 1, Airport, Istanbul, Turkey.

Conferences

Published conference proceedings as well as individual unpublished papers from conferences are included in this index. A CONF number is assigned to the conference if published proceedings are received and also if only a single paper is received. The base number used is year-month-sequence. Thus, the number CONF-650101 indicates that the conference was held in 1965, in January, and that this was the first January 1965 conference so received. This number would be assigned to complete published proceedings. If individual papers are received, the base number is extended to include a paper number, e.g., CONF-650101-1. As additional papers are received, they will be assigned consecutive numbers in the series, CONF-650101-1, CONF-650101-2, etc. This numbering system ensures that all papers received from a conference will be associated with that conference in this index.

If published proceedings are received after the receipt of individual papers, the complete proceedings will be abstracted and the abstract number will appear in this index with the base CONF number.

Abbreviations Used in Availability Column

AECL	Reports of the Atomic Energy of Canada Limited are for sale by the Scientific Document Distribution Office, Atomic Energy of Canada Limited, Chalk River, Ontario, Canada.
CFSTI	See NTIS
DENM	Reports of the Atomic Energy Commission Research Establishment, Risö, are available on exchange from the Library, Danish Atomic Energy Commission, Risö, Roskilde, Denmark. Also for sale at the price shown from Jul. Gjellerup, Booksellers, 87 Sölvgade, Kobenhavn K., Denmark. Reports of Danatom are available on loan from Research Establishment, Risö, Roskilde, Denmark. Copies are available from Danatom, Aurehojvej 2, Hellerup, Denmark.
Dep.	AEC reports so designated are maintained in the organizations listed on the inside front cover of *NSA*. Prior to July 1, 1965, reports were deposited either in printed copy form or in microform. After that time, all reports have been in the form of micronegatives. Reports from other countries so designated are available in the United States at the organizations listed on the inside front cover of *NSA*.

XUM

DTIE Available from the U. S. Atomic Energy Commission, Division of Technical Information Extension, P. O. Box 62, Oak Ridge, Tennessee 37830. (Conference papers are available on loan only.)

EM Blueprints of AEC engineering drawings are available from NTIS, U. S. Department of Commerce, Springfield, Virginia 22151. Current prices of the CAPE-packages may be obtained from this address. TID-4100, available from the Division of Technical Information Extension, P. O. Box 62, Oak Ridge, Tennessee 37830, contains information on all the CAPE-packages for sale.

EUR For sale by Centrale de vente des publications des Communautés européennes 37, rue Glesener-Luxembourg.

GPO For sale by the Superintendent of Documents, Government Printing Office, Washington, D. C. 20402.

IAEA Available from the International Atomic Energy Agency, Vienna, Austria, and from its sales agencies in various countries throughout the world. A list of these agencies is found in each STI/DOC and STI/PUB publication.

NORW Reports from Forsvarets Forskningsinstitutt are available from Norwegian Defense Research Establishment, Library, P. O. Box 25, Kjeller, Norway.

"KR" reports are available on an exchange basis from the Library, Institutt for Atomenergi, Box 40, Kjeller, Norway.

Reports of the Norwegian Reactor School are available from the Library, Institutt for Atomenergi, P. O. Box 40, Kjeller, Norway.

NRC For sale by the National Research Council of Canada, Ottawa, Ontario, Canada.

NTIS For sale by the National Technical Information Service (NTIS), U. S. Department of Commerce, Springfield, Virginia 22151 at the following prices for eye legible copy:

1–300 pages	$3.00
301–600 pages	$6.00
601–900 pages	$9.00

Documents over 900 pages have special prices which may be obtained from NTIS. Microfiche copy of each separately bound document can be purchased for $0.95.

Reports issued by organizations outside the United States will be sold by NTIS *only to purchasers within the United States.*

Purchasers outside the United States may acquire such reports from the sources described elsewhere in these columns.

OECD Available from O. E. C. D., Publications 2, rue, André-Pascal, 75 Paris 16^{e}, France, and from its sales agencies in various countries throughout the world. A list of these agencies is found in each OECD publication.

SWED "AE" reports are for sale from Aktiebolaget Atomenergi, Library Section, Box 43041, Stockholm 43, Sweden. Microcopy of these reports is available from the International Documentation Center, Tumba, Sweden.

Reports of the VDDIT-series may be obtained from Aktiebolaget Atomenergi, Information Office, Scientific and Technical Information, Box 43041, Stockholm 43, Sweden.

Other series are not generally available to the public. Organizations in the Atomic Energy field may obtain copies from Aktiebolaget Atomenergi.

UK United Kingdom Atomic Energy Authority reports generally may be purchased from Her Majesty's Stationery Office, P. O. Box 569, London S.E.1. Copies of many UKAEA reports (particularly earlier ones) may be purchased in microcopy form from Micro Methods Ltd., East Ardsley, Wakefield, Yorkshire, England. Copies of UKAEA reports are deposited with the National Lending Library for Science and Technology and 10 public libraries in England; with the USAEC and (through USAEC) with NTIS; and in most national nuclear centers throughout the world. In the USA, UKAEA reports are available on a subscription basis, by subject category, from UNIPUB, Inc., P. O. Box 433, New York, N. Y. 10016, USA.

UN Mail orders should be directed to the Sales Section, Room 1059, United Nations Headquarters, New York, New York 10017.

ZAED Available from Zentralstelle für Atomkernenergie Dokumentation, 6000 Frankfurt/Main 90, P. O. Box 901069, Westendstr. 21, West Germany

XUM

Report No.	Abstract No.	Availability
AAEC/E-	(Australian)	
207	25-4182	Dep. NTIS (U. S. Sales Only)
AAEC/TM-	(Australian)	
544	25-5441	Dep. NTIS (U. S. Sales Only)
554	25-5135	Dep. NTIS (U. S. Sales Only)
ACNP-	(Misc.)	
70503.1	25-5912	See DOCKET-1155-85
AD-	(Misc.)	
703266	25-4506	CFSTI
706717	25-5800	NTIS
706835	25-5801	NTIS
709878	25-5121	NTIS
709898	25-6145	NTIS
709501	25-4041	NTIS
709522	25-5246	NTIS
710007	25-4376	NTIS
710218	25-5088	NTIS
710231	25-4110	NTIS
710275	25-4746	NTIS
710278	25-4974	NTIS
710293	25-5221	NTIS
710318	25-5068	NTIS
710358	25-4809	NTIS
710385	25-5247	NTIS
710426	25-5001	NTIS
710597	25-5077	NTIS
710604	25-5002	NTIS
710606	25-5113	NTIS
AE-	(Non-AEC)	
404	25-6188	Dep. NTIS (U. S. Sales Only)
AEC-tr-		
7095(Pt.1)	25-4368	Dep. NTIS
7198	25-4134	Dep. NTIS
7202	25-6215	Dep. NTIS
7203	25-6216	Dep. NTIS
AECL-	(Canadian)	
3687	25-4473	Dep. NTIS (U. S. Sales Only). AECL $1.00
3736	25-4975	Dep. NTIS (U. S. Sales Only). AECL $1.50
AEEW-M-	(British)	
986	25-4387	Dep. NTIS (U. S. Sales Only)
AEEW-R-	(British)	
549	25-6181	Dep. NTIS (U. S. Sales Only). UK 4s. 6d
AERE-R-	(British)	
6498	25-4377	Dep. NTIS (U. S. Sales Only). UK 4s
6523	25-4529	Dep. NTIS (U. S. Sales Only). UK 1s. 5d
AFOSR-	(Misc.)	
70-1646-TR	25-4974	See AD-710278
70-1828-TR	25-5221	See AD-710293
70-2095-TR	25-5068	See AD-710318
AI-AEC-		
12972	25-4051	Dep. NTIS
ANL/ES-CC-		
7	25-4161	Dep. NTIS
ANL/ST-		
3	25-4736	Dep. NTIS
ANL-ES-		
2	25-6217	Dep. NTIS
ANL-Trans-		
861	25-4053	Dep. NTIS
ANU-P-	(Australian)	
501	25-5602	Dep. CFSTI (U. S. Sales Only)
ARL-	(Misc.)	
70-48	25-5088	See AD-710218
70-79	25-5077	See AD-710597
AROD-	(Misc.)	
4917:5-MC	25-4746	See AD-710275
5325:16-M	25-5121	See AD-709878
AWRE-O-	(British)	
63/70	25-4747	Dep. NTIS (U. S. Sales Only). UK 7s. 0d
BDX-		
613-142	25-6218	Dep. NTIS
613-143	25-6219	Dep. NTIS
613-180	25-6220	Dep. NTIS
BM-RI-	(Misc.)	
7455	25-4740	
BNL-		
400(3rd Ed.)(Vol.1)	25-5549	Dep. CFSTI
50196	25-4503	Dep. CFSTI
BNL-tr-		
365	25-4202	Dep. NTIS
383	25-6221	Dep. NTIS
BNWL-		
1472	25-4504	Dep. NTIS
1515	25-4474	Dep. NTIS
BNWL-CC-		
491	25-4741	Dep. NTIS
2633	25-4378	Dep. NTIS
BNWL-SA-		
3283	25-4810	Dep. NTIS
3300	25-4811	Dep. NTIS
3304	25-4257	Dep. NTIS
3335	25-6222	Dep. NTIS
3341	25-4008	Dep. NTIS
3379	25-4258	Dep. NTIS
3450	25-4162	Dep. NTIS
3495	25-4812	Dep. NTIS
3609	25-4259	Dep. NTIS
BRH/DEP-	(Non-AEC)	
70-24	25-4522	NTIS
BRL-	(Misc.)	
1482	25-4110	See AD-710231
CALT-		
767-P-4-66	25-6223	Dep. NTIS
822-16	25-6224	Dep. NTIS
CEA-Bib-	(French)	
184	25-4260	Dep. NTIS (U. S. Sales Only)
CEA-CONF-	(French)	
1500	25-4151	Dep. CFSTI (U. S. Sales Only)
1629	25-5094	Dep. NTIS (U. S. Sales Only)
1659	25-4879	Dep. NTIS (U. S. Sales Only)
CEA-N-	(French)	
1232	25-5550	Dep. CFSTI (U. S. Sales Only)
1314	25-4362	Dep. NTIS (U. S. Sales Only)
1340	25-4011	Dep. NTIS (U. S. Sales Only)
1373	25-5371	Dep. NTIS (U. S. Sales Only)
1374	25-4880	Dep. NTIS (U. S. Sales Only)
CEA-R-	(French)	
3920	25-4611	Dep. CFSTI (U. S. Sales Only)
3998	25-5078	Dep. NTIS (U. S. Sales Only)
4007	25-5234	Dep. NTIS (U. S. Sales Only)
4031	25-4411	Dep. CFSTI (U. S. Sales Only)
4037	25-5279	Dep. NTIS (U. S. Sales Only)
4047	25-5551	Dep. NTIS (U. S. Sales Only)
4057	25-5095	Dep. NTIS (U. S. Sales Only)
4067	25-4261	Dep. NTIS (U. S. Sales Only)
4092	25-4785	Dep. NTIS (U. S. Sales Only)
4097	25-4135	Dep. NTIS (U. S. Sales Only)
CISE-N-	(Italian)	
119	25-4029	Dep. NTIS (U. S. Sales Only)
CISE-R-	(Italian)	
290	25-4737	Dep. NTIS (U. S. Sales Only)
CLM-R-	(British)	
103	25-5114	Dep. NTIS (U. S. Sales Only). UK 8s. 0d
107	25-5079	Dep. NTIS (U. S. Sales Only). UK 7s. 0d
CNEA-	(Argentinean)	
274	25-5681	Dep. NTIS (U. S. Sales Only)
CNRS-CPT-	(French)	
70-P-331	25-5372	Dep. NTIS (U. S. Sales Only)
CONF-651094-	(Symposium on Basic Research, Harwell, England, Oct. 19-21, 1965)	
1	25-4881	See DP-Report-382
CONF-680211-	(Conference on Progress in Methods of Bone Mineral Measurement, Bethesda, Md., Feb. 15, 1968)	
	25-4612	GPO $4.00
CONF-680824-	(7th Symposium on Gamma Field, Mito, Japan, Aug. 15-16, 1968)	
	25-4482	Gamma Field Symp.; No. 7, 1-136(1968)
CONF-690224-	(2nd Neutron Measurements Symposium, Kyoto, Japan, Feb. 20, 1969)	

Report No.	Abstract No.	Availability
(Absts.)	25-4320	See KURRI-TR-59
CONF-690334-		(1st Annual Seminar on Pulmonary Investigation with Radionuclides, Miami, Fla., Mar. 7-11, 1969)
	25-4662	Springfield, Ill.; Charles C Thomas, Publisher (1970). 384p. $21.50
CONF-690346-		(International Symposium on the Current Status of Liquid Scintillation Counting, Cambridge, Mass., Mar. 31-Apr. 3, 1969)
	25-4358	New York; Grune and Stratton, Inc. (1970). 411p. $19.75
CONF-690517-		(International Symposium on Rare Earths, Paris and Grenoble, France, May 5-10, 1969)
	25-5193	Paris; Centre National de la Recherche Scientifique (1970). 602p
CONF-690525-		(2nd International Symposium on Radiosensitizing and Radioprotective Drugs, Rome, Italy, May 6-8, 1969)
	25-4534	New York; Barnes and Noble, Inc. (1970). 537p. $25.00
CONF-690814-		(11th International Conference on Cosmic Rays, Budapest, Hungary, Aug. 25-Sept. 4, 1969)
	25-4976	Budapest; Central Research Institute for Physics (1969). 620p
CONF-690951-		(Meeting on the Reliability of Mechanical Components and Systems for Nuclear Reactor Safety, Riso, Denmark, Sept. 24-26, 1969)
	25-6062	See RISO-214
CONF-691051-		(19th Pugwash Conference on Science and World Affairs, Sochi, U.S.S.R., Oct. 22-27, 1969)
	25-4165	
CONF-691213-		(Conference on Chemistry of the Solid State, Grenoble, France, Dec. 12, 1969)
1	25-4151	See CEA-CONF-1500
CONF-691221-		(21st Farkas Symposium on Photochemistry of Aqueous and Polar Systems, Jerusalem, Israel, Dec. 29-30, 1969)
	25-4060	Israel J. Chem.; 8: 103-279(1970)
CONF-700204-		(IAEA Meeting on Research Reactor Utilization, Rome, Italy, Feb. 2-6, 1970)
2	25-5474	See KFK-1197
CONF-700305-		(Meeting on Technical Aspects of Peaceful Uses of Nuclear Explosives, Vienna, Austria, Mar. 2-6, 1970)
6	25-4169	See UCRL-Trans-10477
CONF-700314-		(International Conference on Expectations for Particle Reactions at the New Accelerators, Madison, Wis., Mar. 30-Apr. 1, 1970)
	25-5244	Dep. NTIS
CONF-700515-		(Bone Measurement Conference, Chicago, Ill., May 22-23, 1970)
	25-4630	Dep. CFSTI
CONF-700541-		(11th Annual Meeting of the Institute of Nuclear Materials Management, Gatlinburg, Tenn., May 25-27, 1970)
1	25-4257	See BNWL-SA-3304
CONF-700542-		(Conference on Electronic Instrumentation, Moscow, Idaho, May 22, 1970)
1	25-6222	See BNWL-SA-3335
2	25-4008	See BNWL-SA-3341
CONF-700543-		(Conference on Diagnosis of High-Temperature Plasma, Sukhumi, U.S.S.R., May 13-21, 1970)
(Absts.)	25-5080	See LA-4520-TR
CONF-700601-		(Precipitation Scavenging Meeting, Richland, Wash., June 2-4, 1970)
2	25-4162	See BNWL-SA-3450
CONF-700629-		(Daresbury Study Weekend Conference, Daresbury, England, June 12-14, 1970)
	25-5322	See DNPL/R-7
CONF-700630-		(Symposium on Effects of Radiation on Structural Materials, Niagara Falls, Ontario, Canada, June 29-July 2, 1970)
1	25-4816	See WHAN-FR-19
CONF-700706-		(5th Plasma Physics Symposium, Herceg-Novi, Yugoslavia, July 6-16, 1970)
3	25-5094	See CEA-CONF-1629
CONF-700807-		(Conference on Angular Correlations in Nuclear Disintegration, Delft, The Netherlands, Aug. 17-21, 1970)
4	25-5605	See UCRL-72624
CONF-700811-		(3rd International Symposium on Polarization Phenomena in Nuclear Reactions, Madison, Wis., Aug. 31-Sept. 4, 1970)
	25-5507	See LA-4465
1	25-5526	See UCRL-19942
2	25-5466	See RPP/A-81
CONF-700812-		(2nd Inter-American Conference on Materials Technology, Mexico City, Mex., Aug. 24-27, 1970)
2	25-6254	See UCRL-72095
CONF-700815-		(Conference on the Properties of Nuclei Far from the Region of Beta-Stability, Leysin, Switzerland, Aug. 31-Sept. 4, 1970)
2	25-5687	See UCRL-19949
4	25-5688	See UCRL-19961
CONF-700819-		(2nd International Conference on the Strength of Metals and Alloys, Pacific Grove, Calif., Aug. 30-Sept. 4, 1970)
5	25-4812	See BNWL-SA-3495
CONF-700920-		(International Meeting on Fast Reactor Fuel and Fuel Elements, Karlsruhe, Germany, Sept. 28-30, 1970)
2	25-4810	See BNWL-SA-3283
3	25-4879	See CEA-CONF-1659
CONF-701003-		(28th Meeting on Electron Microscopy Society of America, Houston, Tex., Oct. 5-9, 1970)
6	25-4811	See BNWL-SA-3300
CONF-701010-		(Microwave Power Symposium, Scheveningen, Netherlands, Oct. 7-9, 1970)
1	25-4708	See UR-49-1256
CONF-701011-		(17th National Meeting of the American Vacuum Society, Washington, D.C., Oct. 20-23, 1970)
2	25-4259	See BNWL-SA-3605
CONF-701102-		(Meeting of the American Nuclear Society, Washington, D.C., Nov. 15-19, 1970)
	25-6192	Trans. Amer. Nucl. Soc.; 13: 437-888(Nov 1970)
CONF-701106-		(5th Annual Midyear Topical Symposium on Health Physics Aspects of Nuclear Facility Siting, Idaho Falls, Idaho, Nov. 3-6, 1970)
1	25-4258	See BNWL-SA-3379
COO-		
264-562	25-5348	Dep. NTIS
623-150	25-6225	Dep. NTIS
623-151	25-6226	Dep. NTIS
623-152	25-6227	Dep. NTIS
623-153	25-6228	Dep. NTIS
623-154	25-6229	Dep. NTIS
623-155	25-6230	Dep. NTIS
623-156	25-5168	Dep. NTIS
623-164	25-6231	Dep. NTIS
1140-192	25-6232	Dep. NTIS
1195-200	25-5282	Dep. NTIS
1209-13	25-4692	Dep. NTIS
1265-100	25-5538	Phys. Rev. Lett.; 25: 1346-8(9 Nov 1970)
1422-68	25-4631	See CONF-700515-, pp 1-21
1422-69	25-4632	See CONF-700515-, pp 22-7
1422-71	25-4649	See CONF-700515-, pp 308-12
1422-75	25-4644	See CONF-700515-, pp 255-62
1428-238	25-5283	Dep. NTIS
1512-11	25-4485	Gamma Field Symp.; No. 7, 57-77(1968)
1601-23	25-4423	Dep. NTIS
1676-13	25-4786	Dep. NTIS
1762-6	25-4655	Dep. NTIS
2059-4	25-5122	Dep. NTIS
2059-5	25-5096	Dep. NTIS
2059-6	25-5097	Dep. NTIS
CSIRO-Trans-	(Australian)	
9897	25-4920	Dep. NTIS (U. S. Sales Only)
10083	25-4152	Dep. NTIS (U. S. Sales Only)
DDI-	(Non-AEC)	
16-100-1	25-4506	See AD-703266
DEMO-	(Greek)	
70/1	25-5321	Dep. NTIS (U. S. Sales Only)

XUM

Report No.	Abstract No.	Availability
70/6	25-5401	Dep. NTIS (U. S. Sales Only)
DNPL/R-	(British)	
7	25-5322	
DOCKET-1155-	(LaCrosse Boiling Water Reactor) (AEC)	
85	25-5912	Dep. NTIS
DOCKET-50003-	(Indian Point Station; See Also DOCKET-50247, DOCKET-50286) (Non-AEC)	
60	25-5913	Dep. NTIS
DOCKET-50010-	(Dresden Nuclear Power Station; See also DOCKET-50237 and DOCKET-50249) (Non-AEC)	
71	25-5890	Dep. NTIS
72	25-5914	Dep. NTIS
73	25-5915	Dep. NTIS
DOCKET-50016-	(Enrico Fermi Atomic Power Plant) (Non-AEC)	
87	25-5916	Dep. NTIS
DOCKET-50133-	(Humboldt Bay Power Plant) (Non-AEC)	
43	25-5891	Dep. NTIS
44	25-5917	Dep. NTIS
DOCKET-50155-	(Big Rock Point Reactor) (Misc.)	
53	25-5892	Dep. NTIS
DOCKET-50201-	(West Valley Reprocessing Plant--Formerly Spent Fuel Processing Plant) (Misc.)	
51	25-4153	Dep. NTIS
52	25-4154	Dep. NTIS
53	25-4155	Dep. NTIS
54	25-4156	Dep. NTIS
DOCKET-50219-	(Oyster Creek Nuclear Power Plant) (Non-AEC)	
116	25-5918	Dep. NTIS
DOCKET-50220-	(Nine Mile Point Nuclear Station) (Non-AEC)	
53	25-5919	Dep. NTIS
54	25-5920	Dep. NTIS
DOCKET-50231-	(Southwest Experimental Fast Oxide Reactor) (Non-AEC)	
58	25-5951	Dep. NTIS
59	25-6050	Dep. NTIS
DOCKET-50237-	(Dresden Nuclear Power Station, See also DOCKET-50249) (Non-AEC)	
88	25-5921	Dep. NTIS
98	25-5922	Dep. NTIS
101	25-5923	Dep. NTIS
103	25-5924	Dep. NTIS
108	25-5925	Dep. NTIS
109	25-5926	Dep. NTIS
110	25-5893	Dep. NTIS
111	25-5894	Dep. NTIS
DOCKET-50249-	(Dresden Nuclear Power Station; See also DOCKET-50237) (Non-AEC)	
50	25-5922	See DOCKET-50237-98
DOCKET-50280-	(Surry Power Station, See also DOCKET-50281) (Non-AEC)	
28	25-5927	Dep. NTIS
29	25-5928	Dep. NTIS
30	25-5929	Dep. NTIS
31	25-5930	Dep. NTIS
DOCKET-50281-	(Surry Power Station, See also DOCKET-50280) (Non-AEC)	
28	25-5927	See DOCKET-50280-28
29	25-5928	See DOCKET-50280-29
30	25-5929	See DOCKET-50280-30
31	25-5930	See DOCKET-50280-31
DOCKET-50295-	(Zion Station Nuclear Power Plant. See also DOCKET-50304) (Non-AEC)	
15	25-5931	Dep. NTIS
16	25-5932	Dep. NTIS
17	25-5933	Dep. NTIS
18	25-5934	Dep. NTIS
19	25-5935	Dep. NTIS
DOCKET-50304-	(Zion Station Nuclear Power Plant. See also DOCKET-50295) (Non-AEC)	
15	25-5931	See DOCKET-50295-15
16	25-5932	See DOCKET-50295-16
17	25-5933	See DOCKET-50295-17
18	25-5934	See DOCKET-50295-18
19	25-5935	See DOCKET-50295-19
DP-Report-	(British)	
352	25-4881	Dep. NTIS
434	25-6051	Dep. NTIS
435	25-5979	Dep. NTIS
436	25-4882	Dep. NTIS
440	25-6052	Dep. NTIS
442	25-5952	Dep. NTIS
443	25-4012	Dep. NTIS
445	25-5953	Dep. NTIS
446	25-4262	Dep. NTIS

Report No.	Abstract No.	Availability
448	25-4835	Dep. NTIS
473	25-4883	Dep. NTIS
484	25-4183	Dep. NTIS
490	25-5942	Dep. NTIS
498	25-4388	Dep. NTIS
527	25-4738	Dep. NTIS
537	25-4748	Dep. NTIS
556(Pt.1)	25-4884	Dep. NTIS
556(Pt.2)	25-4885	Dep. NTIS
574	25-4863	Dep. NTIS
578	25-4203	Dep. NTIS
590	25-4389	Dep. NTIS
DSR-	(Non-AEC)	
7796	25-5818	Ann. Phys. (N. Y.); 52: 486-506(May 1969)
E-	(Misc.)	
5233	25-5604	See N-70-25281
5366	25-5808	See N-70-32786
5473	25-4814	See N-70-32313
EANDC(US)-	(European-American Nuclear Data Committee)	
138(U)	25-5549	See BNL-400(3rd Ed.)(Vol.1)
EFI-		
70-63	25-5348	See COO-264-562
ER-	(Misc.)	
10725	25-4405	See N-70-32671
EUR-	(European Atomic Energy Community)	
4506	25-4507	Dep. NTIS (U. S. Sales Only). EUR DM 5,10
FOA-	(Swedish)	
4-4440	25-5603	Dep. NTIS (U. S. Sales Only)
GA-	(Misc.)	
10125	25-4043	Dep. NTIS
10264	25-5989	Dep. NTIS
GAMD-	(Misc.)	
9260(Pt.2)	25-4136	Dep. NTIS
GEAP-	(Misc.)	
10204	25-4886	Dep. NTIS
13595	25-5943	Dep. NTIS
GESP-	(Non-AEC)	
7041	25-4992	See N-70-34006
HASL-		
238	25-4204	Dep. NTIS
HEPL-	(Misc.)	
637	25-5247	See AD-710385
HMI-B-	(German)	
100	25-4390	Dep. NTIS (U. S. Sales Only)
IAE-	(Non-AEC)	
2017	25-5116	For translation see SC-T-70-4046
IFVE-OP-	(Russian)	
69-68	25-5447	Dep. NTIS (U. S. Sales Only)
IFVE-SEF-	(Russian)	
69-81	25-5266	Dep. NTIS (U. S. Sales Only)
IFVE-SEF/STF-	(Russian)	
69-46	25-5267	Dep. NTIS (U. S. Sales Only)
IFVE-SPK-	(Russian)	
69-53	25-4369	Dep. NTIS (U. S. Sales Only)
IFVE-STF-	(Russian)	
69-65	25-5423	Dep. NTIS (U. S. Sales Only)
69-74	25-5349	Dep. NTIS (U. S. Sales Only)
69-83	25-5424	Dep. NTIS (U. S. Sales Only)
69-85	25-5393	Dep. NTIS (U. S. Sales Only)
IJS-	(Yugoslavian)	
575	25-6233	Dep. NTIS
IN-		
1431	25-6061	Dep. NTIS
1440	25-4813	Dep. NTIS
INR-	(Non-AEC)	
1199	25-4991	Dep. NTIS (U. S. Sales Only)
INS-TH-	(Japanese)	
67	25-4370	Dep. NTIS (U. S. Sales Only)
IPP-	(Non-AEC)	
1/86	25-5092	For translation see SC-T-70-4044
IPST-Cat.-	(Russian)	

XUM

Report No.	Abstract No.	Availability
5651	25-4368	See AEC-tr-7059(Pt.1)
IS-T-		
377	25-4137	Dep. NTIS
379	25-5169	Dep. NTIS
380	25-4937	Dep. NTIS
389	25-5682	Dep. NTIS
391	25-5683	Dep. NTIS
IS-Trans-		
83	25-4054	Dep. NTIS
ITF-	(Russian)	
70-80	25-5552	Dep. NTIS (U. S. Sales Only)
JAERI-Memo-	(Japanese)	
4132	25-4739	Dep. NTIS (U. S. Sales Only)
JINR-	(Russian)	
E1-5085	25-5284	Dep. NTIS (U. S. Sales Only)
E1-5098	25-4318	Dep. NTIS (U. S. Sales Only)
E2-5339	25-5405	Dep. NTIS (U. S. Sales Only)
E2-5365	25-5387	Dep. NTIS (U. S. Sales Only)
P1-5293	25-5268	Dep. NTIS (U. S. Sales Only)
P1-5315	25-5350	Dep. NTIS (U. S. Sales Only)
P2-4931	25-5305	Dep. NTIS (U. S. Sales Only)
P2-5058	25-5388	Dep. NTIS (U. S. Sales Only)
P2-5266	25-5235	Dep. NTIS (U. S. Sales Only)
P2-5283	25-5236	Dep. NTIS (U. S. Sales Only)
P2-5290	25-5399	Dep. NTIS (U. S. Sales Only)
P2-5305	25-5406	Dep. NTIS (U. S. Sales Only)
P2-5330	25-5407	Dep. NTIS (U. S. Sales Only)
P4-5019	25-5115	Dep. NTIS (U. S. Sales Only)
P4-5039	25-4952	Dep. NTIS (U. S. Sales Only)
P4-5221	25-5684	Dep. CFSTI (U. S. Sales Only)
P4-5332	25-5425	Dep. NTIS (U. S. Sales Only)
P9-5299	25-5448	Dep. NTIS (U. S. Sales Only)
P9-5311	25-5449	Dep. NTIS (U. S. Sales Only)
P13-5327	25-4371	Dep. NTIS (U. S. Sales Only)
P13-5403	25-4319	Dep. NTIS (U. S. Sales Only)
P14-5358	25-5170	Dep. NTIS (U. S. Sales Only)
JUL-	(German)	
671-RW	25-4013	Dep. NTIS (U. S. Sales Only)
KFK-	(German)	
1102	25-4263	Dep. NTIS (U. S. Sales Only)
1183	25-5980	Dep. NTIS (U. S. Sales Only)
1197	25-5474	Dep. NTIS (U. S. Sales Only)
1215	25-4887	Dep. NTIS (U. S. Sales Only)
1245	25-4839	Dep. NTIS (U. S. Sales Only)
KFKI-	(Hungarian)	
70-18-NAC	25-5685	Dep. CFSTI (U. S. Sales Only)
KURRI-TR-	(Non-AEC)	
59	25-4320	Dep. NTIS (U. S. Sales Only)
63	25-4508	Dep. NTIS (U. S. Sales Only)
L-	(Misc.)	
7110	25-4929	See N-70-33057
LA-		
4404-TR	25-4184	Dep. NTIS
4440-TR	25-6234	Dep. NTIS
4442-TR	25-6235	Dep. NTIS
4465	25-5507	Dep. CFSTI
4518	25-6236	Dep. NTIS
4520-TR	25-5080	Dep. NTIS
4525	25-6237	Dep. NTIS
4526	25-4840	Dep. NTIS
4531	25-6238	Dep. NTIS
4542	25-4915	Dep. NTIS
LYCEN-	(French)	
7032	25-4392	Dep. NTIS (U. S. Sales Only)
MDC G-		
363	25-4509	
MIT-	(Misc.)	
2098-497	25-5818	Ann. Phys. (N. Y.); 52: 486-506(May 1969)
MLM-		
1766(TR)	25-6239	Dep. NTIS
MTI-	(Misc.)	
70-TR-64	25-4185	See NYO-3930-8
N-	(Misc.)	
70-25281	25-5604	NTIS
70-32313	25-4814	NTIS
70-32493	25-5081	NTIS
70-32671	25-4405	NTIS
70-32786	25-5808	NTIS
70-33057	25-4929	NTIS
70-33122	25-5082	NTIS
70-34006	25-4992	NTIS
70-35737	25-5151	NTIS
70-35843	25-4406	NTIS
70-35923	25-4407	NTIS
NAS-NS-	(Misc.)	
3026(Rev.)	25-4133	Dep. NTIS
NASA-CR-	(Misc.)	
61329	25-4405	See N-70-32671
66981	25-5151	See N-70-35737
109851	25-4992	See N-70-34006
110646	25-5081	See N-70-32493
NASA-TM-X-	(Misc.)	
2039	25-4814	See N-70-32313
53929	25-4407	See N-70-35923
58050	25-5082	See N-70-33122
64524	25-4406	See N-70-35843
NASA-TN-D-	(Misc.)	
5765	25-5604	See N-70-25281
5879	25-5808	See N-70-32786
NASA-TR-R-	(Non-AEC)	
343	25-4929	See N-70-33057
NLCO-		
1066	25-6240	Dep. NTIS
1072	25-4014	Dep. NTIS
NP-	(AEC File No. for Non-AEC Reports)	
18433	25-4322	Dep. CFSTI (U. S. Sales Only)
18469	25-4515	New York; Atomic Industrial Forum, Inc. (1970). 7p. $5.00
18484	25-5060	Dep. NTIS (U. S. Sales Only)
18495	25-5066	Dep. NTIS (U. S. Sales Only)
18507	25-5457	Dep. NTIS (U. S. Sales Only)
18510	25-5458	Dep. NTIS (U. S. Sales Only)
18516	25-5459	Dep. NTIS (U. S. Sales Only)
18517	25-5460	Dep. NTIS (U. S. Sales Only)
18519	25-5461	Dep. NTIS (U. S. Sales Only)
18527	25-4264	
18528	25-4088	Dep. NTIS (U. S. Sales Only). UK 17s
NRL-	(Misc.)	
7078	25-4809	See AD-710358
7080	25-5800	See AD-706717
7101	25-6145	See AD-709858
7109	25-4041	See AD-709901
NUMEC-		
3524-76	25-4015	Dep. NTIS
3731-23	25-4215	Dep. NTIS
NYO-		
1371-63	25-6241	Dep. NTIS
1480-160	25-6242	Dep. NTIS
1480-161	25-5106	Dep. NTIS
2043-216	25-4732	Dep. CFSTI
2262-TA-225	25-5351	Dep. NTIS
2263-TA-226	25-5426	Dep. NTIS
2394-40	25-6243	Dep. NTIS
2802-70	25-6244	Dep. NTIS
3240-55	25-4454	Dep. NTIS
3399-235	25-5352	See SU-1206-235
3554-8	25-4475	Dep. NTIS
3829-61	25-5408	Dep. NTIS
3930-8	25-4185	Dep. NTIS
4028-TA-1	25-4323	Dep. NTIS
4060-5	25-5036	Dep. NTIS
4100-3	25-6245	Dep. NTIS
4204-1	25-5306	Dep. NTIS
ORNL-		
4589	25-5990	Dep. NTIS
4615	25-4656	Dep. NTIS
ORNL-TM-		
1950(Rev.1)	25-6246	Dep. NTIS
2412(Pt.5)	25-6034	Dep. NTIS
2412(Pt.8)	25-6035	Dep. NTIS
2903	25-5476	Dep. CFSTI
2995	25-4186	Dep. NTIS
3016	25-4255	Dep. NTIS
3053	25-4138	Dep. NTIS
3130	25-4265	Dep. NTIS
3131	25-4935	Dep. CFSTI
3203	25-5237	Dep. NTIS
3216	25-4525	Dep. NTIS
ORNL-tr-		
2395	25-6247	Dep. NTIS
ORO-		
3087-44	25-5171	Dep. NTIS
3329-7	25-4455	Dep. NTIS
3508-6	25-5152	Dep. NTIS
3596-15	25-4456	Dep. CFSTI
3909-2	25-4111	Dep. NTIS
PATENTS	(British)	

XUM

Report No.	Abstract No.	Availability
1,203,688	25-4516	
1,205,359	25-5503	
1,207,838	25-4335	
1,211,467	25-4742	
PATENTS	(French)	
1,569,103	25-4145	
1,569,268	25-4144	
1,571,848	25-4100	
PATENTS	(U. S.)	
3,516,906	25-5118	
3,518,496	25-5064	
3,528,844	25-4095	
3,531,643	25-4764	
3,531,644	25-4267	
3,533,857	25-4895	
3,533,913	25-4217	
3,534,202	25-4994	
PNE-		
320	25-4168	Dep. NTIS
PPAD-		
676-E	25-5462	Dep. NTIS
RCN-	(Dutch)	
118	25-6093	Dep. NTIS (U. S. Sales Only)
RD/B/N-	(British)	
1722	25-4815	Dep. NTIS (U. S. Sales Only)
RHEL/R-	(British)	
199	25-5463	Dep. NTIS (U. S. Sales Only). UK 2s. 6d
203	25-5464	Dep. NTIS (U. S. Sales Only). UK 4s. 6d
206	25-5465	Dep. NTIS (U. S. Sales Only). UK 2s. 6d
RISO-	(Danish)	
214	25-6062	NTIS (U. S. Sales Only)
221	25-4476	Dep. NTIS (U. S. Sales Only)
RLO-		
1388-581	25-5346	See CONF-700314-, Paper 12
2041-40	25-5285	Dep. NTIS
2041-49	25-5307	Dep. NTIS
2041-51	25-5360	Dep. NTIS
2221-T-4-3	25-6248	Dep. NTIS
RPP/A-	(British)	
81	25-5466	Dep. NTIS (U. S. Sales Only)
SAMSO-TR-	(Non-AEC)	
70-277	25-5002	See AD-710604
70-284	25-5113	See AD-710606
SC-DR-		
70-718	25-4749	Dep. NTIS
SC-PR-		
70-682	25-4216	Dep. NTIS
SC-RR-		
69-369	25-6249	Dep. NTIS
70-615	25-6250	Dep. NTIS
SC-T-		
70-4042	25-6251	Dep. NTIS
70-4044	25-5092	Dep. NTIS
70-4045	25-6252	Dep. NTIS
70-4046	25-5116	Dep. NTIS
SC-TM-		
69-298	25-4379	Dep. NTIS
SDL-	(Non-AEC)	
15	25-5151	See N-70-35737
SJC-T-	(Japanese)	
70-3	25-4372	Dep. NTIS (U. S. Sales Only)
SR-	(Misc.)	
356	25-5081	See N-70-32493
SRO-	(Misc.)	
552-5	25-4841	Dep. NTIS
SU-	(Misc.)	
1206-235	25-5352	Dep. NTIS
SU-IPR-		
366	25-5123	Dep. NTIS
381	25-5124	Dep. NTIS
389	25-5125	Dep. NTIS
TE-	(Non-AEC)	

Report No.	Abstract No.	Availability
4109-138-70	25-4376	See AD-710007
4122-2-71	25-4750	See TEE-4125-2
4122-4-71	25-4751	See TEE-4125-3
4122-12-71	25-4993	See TEE-4125-1
4137-27-71	25-4752	See TEE-4125-4
TEE-		
4125-1	25-4993	Dep. NTIS
4125-2	25-4750	Dep. NTIS
4125-3	25-4751	Dep. NTIS
4125-4	25-4752	Dep. NTIS
TID-		
25190	25-4009	Dep. NTIS
25467	25-4734	Dep. CFSTI
25553	25-4188	Dep. NTIS
25566	25-5686	Dep. NTIS
25567	25-4424	Dep. NTIS
25601	25-5034	Dep. NTIS
TPJU-	(Polish)	
14/70	25-5361	Dep. NTIS (U. S. Sales Only)
15/70	25-5375	Dep. NTIS (U. S. Sales Only)
TR-	(Misc.)	
59(6220-50)-2	25-5113	See AD-710606
59(6260-20)-6	25-5002	See AD-710604
TRG-Report-	(British)	
1937	25-4888	Dep. NTIS (U. S. Sales Only). UK 3s
TT-	(Misc.)	
70-50003/1	25-4368	See AEC-tr-7099(Pt.1)
UCB-	(Non-AEC)	
34-P-82-9	25-4457	Dep. CFSTI
34-P-20-PR-16	25-5150	Dep. NTIS
UCI-		
10-P-19-40	25-5257	Dep. NTIS
UCLA-		
12-782	25-4425	Dep. CFSTI
12-791	25-4694	Dep. NTIS
UCRL-		
19685	25-4074	Dep. NTIS
19764	25-4189	Dep. NTIS
19897	25-5251	Dep. NTIS
19943	25-5526	Dep. NTIS
19949	25-5687	Dep. NTIS
19961	25-5688	Dep. NTIS
20041	25-5400	Dep. NTIS
20093	25-5252	Dep. NTIS
50857	25-5477	Dep. NTIS
50890	25-6253	Dep. NTIS
50923	25-4190	Dep. NTIS
72099	25-6254	Dep. NTIS
72624	25-5605	Dep. CFSTI
UCRL-Trans-		
10477	25-4169	Dep. NTIS
10495	25-5878	Dep. NTIS
UCSB-		
34-P-144-7	25-5606	Dep. NTIS
UCSD-		
34-P-143-27	25-6255	Dep. NTIS
34-P-143-30	25-5035	Dep. NTIS
34-P-143-31	25-5061	Dep. NTIS
34-P-143-32	25-5062	Dep. NTIS
34-P-143-33	25-6256	Dep. NTIS
UJV-	(Czechoslovakian)	
2431-Ch	25-4126	Dep. NTIS (U. S. Sales Only)
UNC-	(Misc.)	
5263	25-4889	Dep. NTIS
UNICP-SR-	(Austrian)	
70	25-5068	See AD-710318
UR-		
49-1256	25-4708	Dep. NTIS
WHAN-FR-		
19	25-4816	Dep. NTIS
WHAN-IR-		
38	25-6257	Dep. NTIS

☆U. S. Government Printing Office: 1971—436-210/15

XUM

UNITED STATES
ATOMIC ENERGY COMMISSION
P. O. BOX 62
OAK RIDGE, TENNESSEE 37830

OFFICIAL BUSINESS

POSTAGE AND FEES PAID
U. S. ATOMIC ENERGY COMMISSION

POSTAGE AND FEES PAID
U. S. GOVERNMENT PRINTING OFFICE

UNIVERSITY MICROFILMS
ATTN MRS. MARLENE HURST
MANAGER, PUBLISHER RELATIONS
ANN ARBOR MICHIGAN 48106

1

The U. S. Atomic Energy Commission publishes the

Nuclear Science Series on Radiochemistry and Radiochemical Techniques

Prepared by the National Academy of Sciences–National Research Council

These monographs are prepared not only for radiochemists but also for research workers in other fields, such as physics, biochemistry, and medicine. Copies are available from the National Technical Information Service, U. S. Department of Commerce, Springfield, Virginia 22151. The minimum price is $3.00 for either one, two, or three randomly selected publications. Additional individual copies will be sold in increments of three for $3.00.

RADIOCHEMISTRY OF THE ELEMENTS

Cadmium, NAS-NS-3001 [1960]
Arsenic, NAS-NS-3002(Rev.) [1965]
Francium, NAS-NS-3003 [1960]
Thorium, NAS-NS-3004 [1960]
Fluorine, Chlorine, Bromine, and Iodine, NAS-NS-3005 [1960]
Americium and Curium, NAS-NS-3006 [1960]
Chromium, NAS-NS-3007(Rev.) [1963]
Rhodium, NAS-NS-3008(Rev.) [1965]
Molybdenum, NAS-NS-3009 [1960]
Barium, Calcium, and Strontium, NAS-NS-3010 [1960]
Zirconium and Hafnium, NAS-NS-3011 [1960]
Astatine, NAS-NS-3012 [1960]
Beryllium, NAS-NS-3013 [1960]
Indium, NAS-NS-3014 [1960]
Zinc, NAS-NS-3015 [1960]
Protactinium, NAS-NS-3016 [1959]
Iron, NAS-NS-3017 [1960]
Manganese, NAS-NS-3018 [1960]
Carbon, Nitrogen, and Oxygen, NAS-NS-3019 [1960]
Rare Earths—Scandium, Yttrium, and Actinium, NAS-NS-3020 [1961]
Technetium, NAS-NS-3021 [1960]
Vanadium, NAS-NS-3022 [1960]
Tin, NAS-NS-3023 [1960]
Magnesium, NAS-NS-3024 [1961]
Rare Gases, NAS-NS-3025 [1960]
Mercury, NAS-NS-3026(Rev.) [1970]
Copper, NAS-NS-3027 [1961]
Rhenium, NAS-NS-3028 [1961]
Ruthenium, NAS-NS-3029 [1961]
Selenium, NAS-NS-3030(Rev.) [1965]
Transcurium Elements, NAS-NS-3031 [1960]
Aluminum and Gallium, NAS-NS-3032 [1961]
Antimony, NAS-NS-3033 [1961]
Titanium, NAS-NS-3034 [1961]
Cesium, NAS-NS-3035 [1961]
Gold, NAS-NS-3036 [1961]
Polonium, NAS-NS-3037 [1961]
Tellurium, NAS-NS-3038 [1960]
Niobium and Tantalum, NAS-NS-3039 [1961]
Lead, NAS-NS-3040 [1961]
Cobalt, NAS-NS-3041 [1961]
Tungsten, NAS-NS-3042 [1961]
Germanium, NAS-NS-3043 [1961]
Platinum, NAS-NS-3044 [1961]
Iridium, NAS-NS-3045 [1961]
Osmium, NAS-NS-3046 [1961]
Silver, NAS-NS-3047 [1961]
Potassium, NAS-NS-3048 [1961]
Silicon, NAS-NS-3049(Rev.) [1968]
Uranium, NAS-NS-3050 [1961]
Nickel, NAS-NS-3051 [1961]
Palladium, NAS-NS-3052 [1961]
Rubidium, NAS-NS-3053 [1962]
Sulfur, NAS-NS-3054 [1961]
Sodium, NAS-NS-3055 [1962]
Phosphorus, NAS-NS-3056 [1962]
Radium, NAS-NS-3057 [1964]
Plutonium, NAS-NS-3058 [1965]

RADIOCHEMICAL TECHNIQUES

Liquid-Liquid Extraction with High-Molecular-Weight Amines, NAS-NS-3101 [1960]
Separations by Solvent Extraction with Tri-n-Octylphosphine Oxide, NAS-NS-3102 [1961]
Low-Level Radiochemical Separations, NAS-NS-3103 [1961]
Rapid Radiochemical Separations, NAS-NS-3104 [1961]
Detection and Measurement of Nuclear Radiation, NAS-NS-3105 [1961]
Paper Chromatographic and Electromigration Techniques in Radiochemistry, NAS-NS-3106 [1962]
Applications of Computers to Nuclear and Radiochemistry, NAS-NS-3107 [1962]
Application of Distillation Techniques to Radiochemical Separations, NAS-NS-3108 [1962]
Processing of Counting Data, NAS-NS-3109 [1965]
Activation Analysis with Charged Particles, NAS-NS-3110 [1966]
Chemical Yield Determinations in Radiochemistry, NAS-NS-3111 [1967]
Absolute Measurement of Alpha Emission and Spontaneous Fission, NAS-NS-3112 [1968]

XUM

KUM